Springer Geography

Maria Rădoane
Alfred Vespremeanu-Stroe *Editors*

Landform Dynamics and Evolution in Romania

Springer

Springer Geography

The Springer Geography series seeks to publish a broad portfolio of scientific books, aiming at researchers, students, and everyone interested in geographical research. The series includes peer-reviewed monographs, edited volumes, textbooks, and conference proceedings. It covers the major topics in geography and geographical sciences including, but not limited to; Economic Geography, Landscape and Urban Planning, Urban Geography, Physical Geography and Environmental Geography.

More information about this series at http://www.springer.com/series/10180

Maria Rădoane · Alfred Vespremeanu-Stroe
Editors

Landform Dynamics and Evolution in Romania

Springer

Editors
Maria Rădoane
Geography
Ştefan cel Mare University of Suceava
Suceava
Romania

Alfred Vespremeanu-Stroe
Faculty of Geography
University of Bucharest
Bucharest
Romania

ISSN 2194-315X ISSN 2194-3168 (electronic)
Springer Geography
ISBN 978-3-319-32587-3 ISBN 978-3-319-32589-7 (eBook)
DOI 10.1007/978-3-319-32589-7

Library of Congress Control Number: 2016942904

Printed on acid-free paper

This Springer imprint is published by Springer Nature
The registered company is Springer International Publishing AG Switzerland

Preface

Everybody knows about landforms. They are ubiquitous "beings" which cover the world, even within the landscapes modified by man. We all live in a world made of landforms. Sometimes, they seem to us perennial from the dawns of history as effigies of an eternal world, but other times they look so fresh and young, mobilizing sediments, with versatile configurations. The past and the present come together into the same landform; the evolution and the landscape metamorphosis proceed gradually but the rhythm of change is very different, often incredibly slow surviving to our lives or even to existence of mankind while here and there a "whole" world vanish in a few minutes. All these perceptions that senses bring to us define our imagination and finally build our perspective about the world. Happily the man travels all over wondering how the Earth and landforms exist!

This book tries to present the beautiful and awe-inspiring range of landscape features from the glaciers and their action upon high massifs to coastal dunes or subaqueous landforms of the shoreface. This volume is about the diverse landforms of a country where various environments adjoin. Nevertheless, the laws which govern the way which landforms evolve are the same world-wide, but the infinite influences of the modelling agents create always individual features which remain unique as the human face. Moreover, large-scale landscapes as the Danube Delta or Retezat Massif could look very different from any other delta or mountain so that the understanding of their evolution more than applying general geomorphological principles requires site-specific processes research or even to conceive new research methods.

This volume contains a series of new studies grouped in eight parts mainly depending on the geographical environment.

Part I resumes the most recent knowledge and interpretations of the Romanian Carpathians formation and explains the presence of the large morpho-structural units (Mațenco), whereas their sub-aerial shaping can be more readily understood following the reconstructions of climate conditions (Perşoiu) and vegetation distribution in the last 15,000 years (Feurdean and Tanțău) covering the geographical area of Romania.

Part II brings the newest data and interpretations in the field of glacial and periglacial modelling of the Romanian Carpathians, from the history of deglaciation in the Carpathians (Popescu et al.) to the distribution and characteristics of mountain permafrost (Popescu et al.), the review of knowledge on periglacial processes and deposits (Onaca et al.), thermal weathering of mountain rock slopes (Vasile and Vespremeanu-Stroe) and the morphometrical analysis of glacial cirques (Mîndrescu and Evans). The complex evaluation of glacial and periglacial geomorphosites (Comănescu and Nedelea) closes the part dedicated to mountain geomorphology in this volume.

Part III is dedicated to mass movement processes, with the main focus on landslides. The Romanian contributions to the systematic of mass movements is critically reviewed (Micu), completed by detailed approaches and high-technology inventory and informatics processing of landslides for two different geographical areas (the Moldavian Plateau—Mărgărint and Niculiță; and the Curvature Subcarpathians—Micu) and for debris flow activity in mountain areas (Pop et al.).

Part IV, dealing with soil erosion, combines the researches of agronomists on sheet and rill erosion (monitored for 12 years on experimental plots—Popa) with the ones of geomorphologists in gully erosion rates' assessments (Rădoane and Rădoane) and with the progresses made in the mathematical modelling of soil erosion (Patriche). The applications are set in one of the most highly degraded regions of Romania—the Moldavian Plateau.

Part V (Rivers) discusses fluvial landforms and processes in relation to the time required for essential changes to take place: longitudinal profiles which modify their shape during millions of years with implications in relief evolution (Rădoane et al.); rivers behaviour and the formation of sedimentary complexes of floodplains during the transition from Pleniglacial to Late Glacial (Perşoiu et al.); Holocene fluvial activity highlighting the large floods and their implications in the sedimentary architecture and the formation of river terraces (Perşoiu and Rădoane); adaptation of riverbeds' shape (planform and cross-section) to climate changes and human interventions during the last 150, 100 and 50 years (Rădoane et al.).

Part VI deals with the evolution and present dynamics of the Danube Delta and the Romanian Black Sea coast. A new vision on the formation and the evolution of the Danube Delta is presented, in the light of the newest data gathered by the authors (Vespremeanu-Stroe et al.). Distinct sections are dedicated to coastline evolution during the last 150 years (Vespremeanu-Stroe et al.), cliffs retreat on the southern Romanian coast (Constantinescu) and medium-term (decadal) morphodynamics of the coastal foredunes (Preoteasa and Vespremeanu-Stroe) and deltaic shoreface (Tătui and Vespremeanu-Stroe).

Part VII presents the problem of sediment route in various geomorphologic systems. The succession of erosion–transport–sedimentation geomorphological processes is the key for understanding of sediment transport from the source area (Dumitriu et al.) towards riverbeds (Rădoane et al.). Loess accumulation in the Romanian Plain and Dobrogea (Timar-Gabor et al.) and of fine sediments in small mountain lakes (Mîndrescu et al.) have been used to refine high-resolution

chronologies and to reconstruct palaeoenvironment conditions at the time of these sediments deposition.

Part VIII (Geomorphologic hazards) closes the volume discussing those climatic, hydrologic and geomorphologic processes capable of generating geomorphologic hazards and disasters: snow avalanches—Voiculescu; mass movements—Micu et al.; river floods—Grecu et al.; coastal storms—Zăinescu and Vespremeanu-Stroe. These analyses prove and highlight the necessity of estimating, on a solid basis, the risk associated with these processes, in the benefit of land administration.

Finally, we hope that geoscientists, specialists in environmental planning, practitioners in water and land-use, territorial unit administrators as well as academics will findthis volume valuable concerning the landform dynamics and evolution and necessary for future prediction of landscape changes.

Suceava, Romania — Maria Rădoane
Bucharest, Romania — Alfred Vespremeanu-Stroe

Contents

Contributors

Titu Anghel Faculty of Geography, Babeş-Bolyai University, Cluj-Napoca, Cluj, Romania

Adrian C. Ardelean West University of Timişoara, Timişoara, Timiş, Romania

Florina Ardelean West University of Timişoara, Timişoara, Timiş, Romania

Iuliana Armaş Faculty of Geography, University of Bucharest, Bucharest, Sector 1, Romania

Francisca Chiriloaei Stefan cel Mare University, Suceava, Romania

Zenaida Chiţu National Institute of Hydrology and Water Management, Bucharest, Romania

Roxana Ciurean Department of Geography and Regional Research, University of Vienna, Vienna, Austria

Laura Comănescu Faculty of Geography, University of Bucharest, Bucharest, Romania

Daniela Constantin Faculty of Environmental Science and Engineering, Babeş-Bolyai University, Cluj-Napoca, Romania; Interdisciplinary Research Institute, Bio-Nano-Science of Babeş-Bolyai University, Cluj-Napoca, Romania

Ştefan Constantinescu Faculty of Geography, University of Bucharest, Bucharest, Romania

Ionuț Cristea Stefan cel Mare University, Suceava, Romania

Dan Dumitriu Alexandu Ioan Cuza University, Iaşi, Romania

Ian S. Evans University of Durham, Durham, UK

Angelica Feurdean Senckenberg Research Institute and Natural History Museum, Biodiversity and Climate Research Centre, Frankfurt Am Main, Germany; Emil Racoviţă Institute of Speleology, Romanian Academy, Cluj-Napoca, Cluj, Romania

Gabriela Florescu Cirques and Lakes Research Group, Ştefan Cel Mare University, Suceava, Romania

Ionela-Georgiana Gavrilă Faculty of Geography, Babeş-Bolyai University, Cluj-Napoca, Cluj, Romania

Florina Grecu Faculty of Geography, University of Bucharest, Bucharest, Sector 1, Romania

Ionela Grădinaru Cirques and Lakes Research Group, Ştefan Cel Mare University, Suceava, Romania

Aritina Haliuc Cirques and Lakes Research Group, Ştefan Cel Mare University, Suceava, Romania

Viorel Ilinca Geological Institute of Romania, Bucharest, Sector 5, Romania

Gabriela Ioana-Toroimac Faculty of Geography, University of Bucharest, Bucharest, Sector 1, Romania

Marta Jurchescu Institute of Geography, Romanian Academy, Bucharest, Sector 2, Romania

Liviu Mațenco Department of Earth Sciences, Utrecht University, Utrecht, The Netherlands

Crina Miclăuş Alexandu Ioan Cuza University, Iaşi, Romania

Dana Micu Institute of Geography, Romanian Academy, Bucharest, Sector 2, Romania

Mihai Micu Institute of Geography, Romanian Academy, Bucharest, Sector 2, Romania

Marcel Mîndrescu Ştefan cel Mare University, Suceava, Romania

Mihai Ciprian Mărgărint Department of Geography, Alexandru Ioan Cuza University of Iaşi, Iaşi, Romania

Cristian Necula Faculty of Physics, University of Bucharest, Bucharest, Romania

Alexandru Nedelea Faculty of Geography, University of Bucharest, Bucharest, Romania

Mihai Niculiță Department of Geography, Alexandru Ioan Cuza University of Iaşi, Iaşi, Romania

Alexandru Onaca West University of Timişoara, Timişoara, Timiş, Romania

Cristian Panaiotu Faculty of Physics, University of Bucharest, Bucharest, Romania

Cristian Valeriu Patriche Department of Iaşi, Geography Group, Romanian Academy, Iaşi, Romania

Aurel Perşoiu Emil Racoviţă Institute of Speleology, Romanian Academy, Cluj-Napoca, Cluj, Romania; Stable Isotope Laboratory, Ştefan cel Mare University, Suceava, Romania

Ioana Perşoiu Stefan cel Mare University, Suceava, Romania

Olimpiu Traian Pop Faculty of Geography, Babeş-Bolyai University, Cluj-Napoca, Cluj, Romania

Nelu Popa Research and Development Center for Soil Erosion Control, Perieni, Vaslui County, Romania

Răzvan Popescu University of Bucharest Research Institute, Bucharest, Sector 5, Romania

Luminiţa Preoteasa Faculty of Geography, University of Bucharest, Bucharest, Romania

Delia Robu Stefan cel Mare University, Suceava, Romania

Maria Rădoane Ştefan cel Mare University, Suceava, Romania

Ionuț Şandric Faculty of Geography, University of Bucharest, Bucharest, Sector 1, Romania

Raul Şerban West University of Timişoara, Timişoara, Timiş, Romania

Ioan Tanţău Department of Geology, Babeş-Bolyai University, Cluj-Napoca, Romania; Institute of Biological Research, Cluj-Napoca, Cluj, Romania

Alida Timar-Gabor Faculty of Environmental Science and Engineering, Babeş-Bolyai University, Cluj-Napoca, Romania; Interdisciplinary Research Institute, Bio-Nano-Science of Babeş-Bolyai University, Cluj-Napoca, Romania

Florin Tătui Faculty of Geography, University of Bucharest, Bucharest, Romania

Petru Urdea West University of Timişoara, Timişoara, Timiş, Romania

Mirela Vasile Research Institute of the University of Bucharest, M. Kogălniceanu 36-46, 050107 sector 5, Bucharest, Romania

Daniel Vereş Faculty of Environmental Science and Engineering, Babeş-Bolyai University, Cluj-Napoca, Romania; Institute of Speleology, Romanian Academy, Cluj-Napoca, Romania

Alfred Vespremeanu-Stroe Faculty of Geography, University of Bucharest, Bucharest, Romania

Mircea Voiculescu West University of Timişoara, Timişoara, Timiş, Romania

Liliana Zaharia Faculty of Geography, University of Bucharest, Bucharest, Sector 1, Romania

Florin Zăinescu Faculty of Geography, University of Bucharest, Bucharest, Romania

Chapter 1
Introduction

Maria Rădoane and Alfred Vespremeanu-Stroe

Abstract The central themes of this volume are the dynamics and evolution of Romania's relief. The two aforementioned conceptual frameworks resulted from the different ways in which time was approached in geomorphology: the 'short timeframe' during which landforms change to a small extent; the 'long timeframe' required for 'historical' transformations of the relief. Time scales of interest in this volume range from the shorter time frame (for the more intensive change rate of the landforms—i.e. soil erosion on experimental plots, debris flow, avalanches) to the largest temporal scales (for the glacial landforms, floodplains or longitudinal profiles). The area of interest for the analysis of the dynamics and evolution of landforms in Romania includes landforms ranging between the 4th and the 9th order. Landform assemblages were approached mainly according to genetic criteria (i.e. glacial, periglacial, denudational, coastal and fluvial).

Keywords Time scales · Space scales · Dynamics · Evolution · Romanian geomorphology

The Framework of Current Approaches in Geomorphology

Throughout the history of modern Romanian geomorphology (Ichim and Posea 1993), three landmark contributions were recognised by the scientific community as highly valuable. The earliest work was '*Realizări în Geografia României*' (Progresses in the Romanian Geography 1973). Despite the wide and comprehensive title, the book deals mostly with the Romanian relief. The contributors

M. Rădoane (✉)
Ștefan cel Mare University, Universității 13, 720229 Suceava, Romania
e-mail: radoane@usm.ro; mariaradoane@gmail.com

A. Vespremeanu-Stroe
Faculty of Geography, University of Bucharest, N. Bălcescu 1,
010041 Bucharest, Sector 1, Romania
e-mail: fredi@geo.unibuc.ro

M. Rădoane and A. Vespremeanu-Stroe (eds.), *Landform Dynamics and Evolution in Romania*, Springer Geography,
DOI 10.1007/978-3-319-32589-7_1

approach—centred principally upon (establishing) the age and genesis—tackled various topics of Romanian relief from features such as peneplains to the evolution of hydrographical network, piedmonts and depressions, glacial and periglacial relief. Shortly after, it published the *Relieful României* (Relief of Romania, Posea et al. 1974), an essential and original synthesis of genetic geomorphology which reassesses the main topics of Romania geomorphology. The third work, *Geografia României* (Geography of Romania 1983, 1987, 1992, 2005) consists of four volumes where 23 authors reviewed the relief of the Romanian territory particularly from the perspective of the palaeo-geomorphological evolution of landforms and ranked them into several morphostructure-influenced patterns.

The three aforementioned seminal works tackled the topic of relief transformation through the contribution of geomorphic processes tangentially, without discussing quantitative approaches of the geomorphic event rates. About 40 years later, this volume, '*Landform Dynamics and Evolution in Romania*' proposes a different perspective mainly focused on two central themes: *processes* (*dynamics*) and *evolution*.

In order to motivate these two standpoints in approaching landforms, a brief foray into the history of geomorphological thought is required, which will further substantiate the theoretical context in which the two seemingly complementary concepts were defined. For the role of the dynamics and evolution concepts in geomorphology, we retrospect to the landmark work *Dynamic Basis of Geomorphology* published by Arthur Strahler in 1952. For the first time, the theories of process-based geomorphology are introduced in order to explain the diversity of landforms, and what ensued was described by Roads (2006) as follows: '*As a science, geomorphology has flourished since the turn toward the dynamic basis of geomorphology advocated by* Strahler (1952). *This approach treats geomorphological processes and process-form interactions as manifestations of mechanical stresses and strains acting on earth materials*'.

This perspective on the relief soon became the new brand of geomorphological investigation throughout the international scientific community, and the Romanian geomorphology managed at least in part (despite the limitations of foreign scientific exchanges during the communist era) to remain connected to novel trends.

Specifically, the two aforementioned conceptual frameworks (i.e. dynamics and evolution) resulted from the different ways in which time was approached in geomorphology. In one of the finest geomorphological treatises published by Chorley et al. (1984), the basic conceptual elements were drafted and were later resumed by Ichim et al. (1989) as follows:

(i) the *dynamics of geomorphological processes*, where investigation focuses on the role of various processes in transferring sediments, which in turn affect landforms, i.e. the *functional approach* to the study of relief;
(ii) the *evolution*, where investigation centres around deciphering the main stages of change in landform characteristics under the control of major temporal events (sea-level fluctuations, tectonics, climate changes), i.e. the historical approach to geomorphology;

Historicism and functionalism in geomorphology are based on the 'dual character of time', namely either the 'long timeframe' required for 'historical' transformations of the relief, or the 'short timeframe' during which landforms change to a small extent. During the 'short timeframe', the functional approach is applied to those landforms which clearly show the effects of current processes (e.g. gullies, river reaches, hillslopes, etc.), whereas the 'long time', historicist approach is reserved for landforms whose evolution was slow and provide evidence of the climatic and tectonic influences to which they were subjected (e.g. longitudinal profiles of rivers, floodplains and their respective deposits, piedmonts, mountain ranges, etc.). The time scales according to which the dynamics and evolution of landforms can be interpreted are those defined by Schumm and Lichty (1965): cyclic time ($\sim 10^{5++}$ years); dynamic equilibrium or graded time ($\sim 10^{2+}$ years); stationary time ($\sim 10^{-1}$ years), which were reformulated by Hickin (1983) as geologic, geomorphic and engineering timeframes.

In summary, most geomorphological topics of interest (such as the ones tackled in the present volume) require the use of both the *functionalist*, prediction-oriented approach (deduced from the cause-effect relation), and the *historicist* approach aimed at retrodiction/postdiction. The validity of results yielded by our work was verified based on the accumulation of significant amounts of field (in terms of study area, number of cases, measurement period) and lab data. Based on these, the work hypotheses were tested and conclusions were formulated, many of which had a predictive nature. Special attention was granted to the pressure of global changes and human activity (which are rather difficult to set apart) as controls of landform change intensity. Moreover, the new paradigm gaining ground at a fast pace in the worldwide understanding of geomorphology is related to the manner in which hydrological and sediment cycles are manipulated by unprecedented human intervention (Church 2010).

Temporal and Spatial Scales of the Geomorphological Processes Herein Approached

The matter of knowledge transfer between systems of different magnitude is one of the leading topics in geomorphology and is linked to the temporal and spatial scales (Church 2010). In other words, the geomorphological landscape has distinct properties at differing scales of investigation. Each hierarchic level includes the cumulative effects of lower levels.

In order to frame the investigated geomorphological phenomena within temporal and spatial boundaries, we created the graphic shown in Fig. 1.1, displaying the temporal and spatial scales of interest.

Relative to the *time scale*, the shorter the time frame, the more intensive is the change rate of the landform; this is illustrated by soil erosion on experimental plots where the time required can amount to just minutes (Chap. 15), aeolian

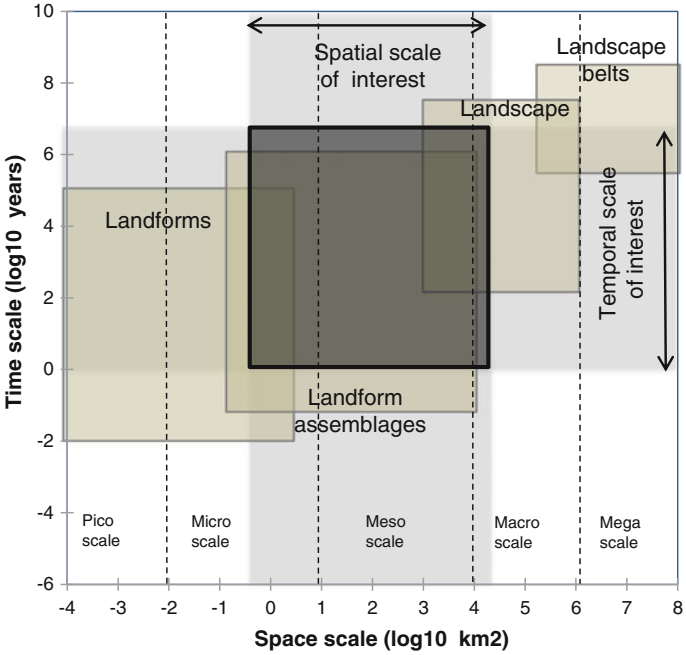

Fig. 1.1 Spatial and temporal scales in geomorphology. In *black* is shown the interest area of researches in the present volume (an adaptation after Slaymaker et al. 2009). Other discussions in the text

micro-features (Chap. 25) or snow avalanches (Chap. 31). Hour-long to day-long time frames are required for the formation of rills (Chap. 15) and sand dunes (Chap. 25) or for debris flows (Chap. 14).

However, the majority of landforms analysed in this volume have change rates ranging from years to hundreds of years, as is the case of hillslopes, river channels (where the rate of channel adjustment was 150 years) or coastal systems. Other processes, such as river channel behaviour and floodplain formation (Chaps. 19 and 20), the genesis and evolution of the Danube Delta (Chap. 22) or lacustrine sediment-inferred palaeoenvironmental processes (Chap. 30), were reconstructed at larger temporal scales (e.g. from 10 to 15,000 years). The largest temporal scales were employed for the analysis of glacial processes (Chap. 5), as well as for modelling the shape of longitudinal profiles whereby the time frame was as ample as 14–15 million years (Chap. 18) in our case.

Relief is a 'continuum', and identifying a suitable *time scale* for its genetic and functional assessment is of utmost necessity. The hierarchy proposed by Chorley et al. (1984) (Table 1.1) is eloquent in this respect.

Such a hierarchy is helpful in attempting to differentiate between distinct conceptual frameworks and highlight certain processes and evolutions. Specifically, the area of interest for the analysis of the dynamics and evolution of landforms in

Table 1.1 Spatial hierarchy of landforms (Chorley et al. 1984). The box frame delineates the area of interest for this volume

Order	Examples
1st	Continents, oceans, plates, convergences zones, divergence zones
2nd	Physiographic provinces, mountain ranges, massifs, plateaus, lowlands, accumulative plains, tectonic depressions (morphostructural units)
3rd	Medium – scale geomorphological units, such as folded mountains, faults blocks, domes and volcanoes
4th	Large-scale erosional/depositional units, such a large valleys, deltas and long continuous beaches
5th	Medium-scale erosional/depositional units; smaller valleys, floodplains, alluvial fans, cirques, moraines
6th	Small-scale erosional/depositional units; small valleys, offshore bars, sand dunes
7th	Hillslopes, reaches of stream channel
8th	Slope and flat facets, pools, riffles, gullies
9th	Stream bed and aeolian sand ripples, slope terracettes
10th	Microroughness represented by the diameter of individual pebbles or sand grains

Romania includes landforms ranging between the 4th and the 9th order. Furthermore, in Fig. 1.1 whereby the spatial scale is measured in square kilometres, we indicated the assemblages of landforms as the area of major interest. Landform assemblages were approached mainly according to genetic criteria (i.e. glacial, periglacial, denudational, fluvial). Whereas in most of these categories the meso-scale was selected as area of interest, in some instances the micro-scales (e.g. erosion plots with areas in the range of square metres) or macro-scales (such as mountain units or drainage basins exceeding 10,000 km^2) were also investigated.

Landmarks in the Development of Modern Romanian Geomorphology

One of the most concise analyses of the evolution of geomorphology in Romania was published by Ichim and Posea (1993) in the referential work edited by Walker and Grabau, *The Evolution of Geomorphology,* which provides a number of valuable ideas. The first and most important regards the fact that Romanian geomorphology was part of the regionalist movement/current. Thus, without disregarding the value of resulting contributions, the input to the general theory of landforms was rather understated. The second idea referred to the synchronicity manifested in applying theoretical concepts highly recognised worldwide, albeit for a long period of time (i.e. the communist era) the scientific exchanges with the international community were restricted.

Whereas we do not aim at carrying out an extensive overview of the history of geomorphological ideas in Romania, it is nevertheless worthwhile highlighting important moments which, in our opinion, marked a change in the knowledge, research methods or the interpretation of landforms, in order to gain a better perspective on the work we set out to accomplish and to find another way of approaching the relief. Therefore, we summarised the landmark moments, ideas and personalities which made a significant contribution to the advancement of modern geomorphology in Romania against the time scale (Fig. 1.2).

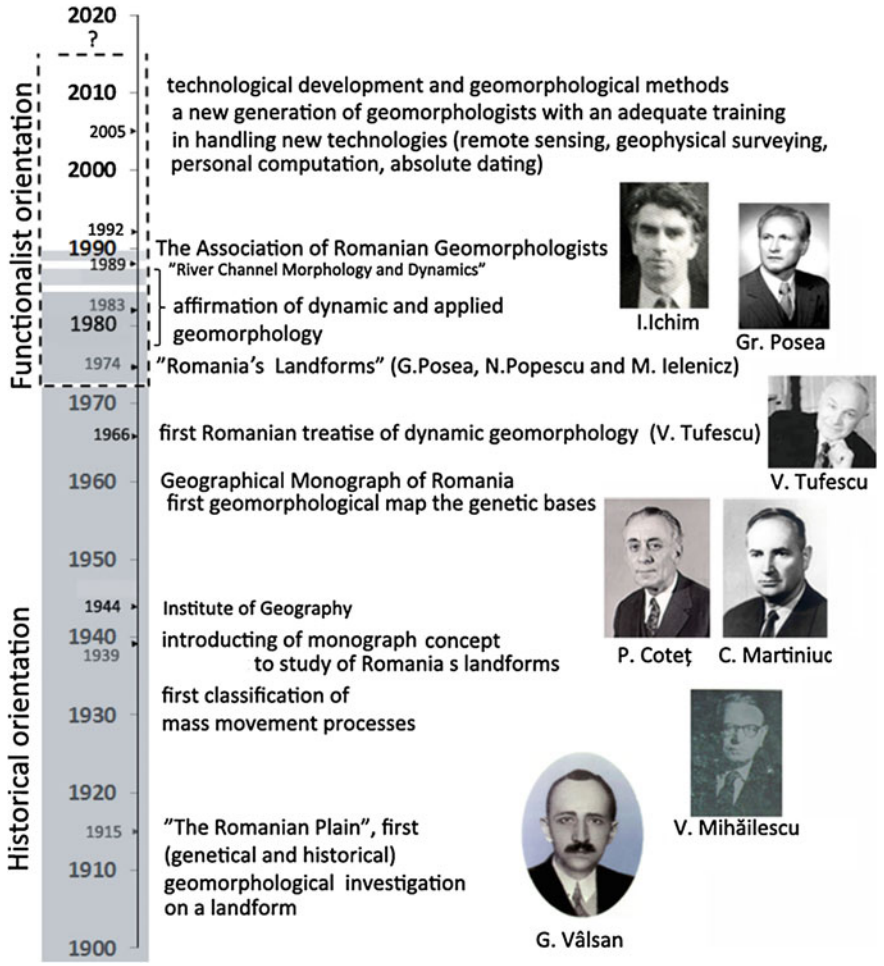

Fig. 1.2 Timeline of the developments made by the modern Romanian geomorphology during the last 100 years (1915–2015). The two fundamental conceptual frameworks utilised in geomorphological analysis, i.e. historicist (derived from the Davisian theory of landform evolution) and functionalist (focused on understanding processes and mechanism underlying relief dynamics) are delineated

Modern Romanian geomorphology was established, in our opinion, with the work of Vâlsan (1885–1935), *Câmpia Română* (1915) (The Romanian Plain), the earliest geomorphological investigation of a landform from a genetic standpoint. The author conducted geomorphological analysis in order to identify the role of neotectonic movements and outlined the relation between endogenous and exogenous factors. The period was propitious for personalities who established themselves as important figures in the evolution of landforms knowledge: Brătescu (1884–1947), who published studies on sea-level oscillations, loess and asymmetry

of fluvial valleys; David (1886–1954), known for highlighting the role of the geological control on morphogenesis, as well as for applying the denudation surface theory in the Carpathians and last, but not least, for his benchmark work in the Subcarpathians; Mihăilescu (1890–1976), reputed for introducing the monograph concept in the study of relief and the first comprehensive classification of mass movement processes, and for publishing the earliest synthesis of landform units in Romania in 1946 (Mihăilescu 1946); Morariu (1905–1982), who investigated denudation surfaces and glaciation in Rodna Mountains. We can further add to the list scientists who also activated during this period and continued throughout the recent decades: Popp (1908–1993), who produced an exemplary work on morphological profiles in the Subcarpathians; Tufescu (1908–2000), who published the first Romanian treatise of dynamic geomorphology (Tufescu 1966).

In the years following WWII, Romanian geomorphology went through two distinct phases:

(i) the reorganisation of research and the elaboration of the first comprehensive synthesis on the Romanian relief, in *Monografia geografică a României* (1960) (the Geographical Monograph of Romania);
(ii) the transition to the systemic research of landforms whereby numerous, very valuable geomorphological monographs investigating landform units, valleys or drainage basins (1963–1990).

The first national geomorphological map (sc. 1:1,000,000, Coteț 1960), as well as the map of geomorphological regions (Martiniuc 1960) were included in *Monografia geografică*. At this stage, the earliest attempts at quantitative and experimental geomorphological approaches were made, particularly at 'Stejarul' Research Station from Pângărați founded by 'Al. I. Cuza' University from Iași (1957), the Pătârlagele Geographical Station (1969) pertaining to the Institute of Geography, and the Central Station for Soil Erosion Control from Perieni founded by the Agricultural and Forestry Academy (1954).

From the 1980s onwards, but especially after the 1990s, the interest of Romanian geomorphologists clearly shifted towards the dynamic and applied (functionalist) side of geomorphology, which was also required by the economic development of the country (e.g. large projects for dam construction throughout drainage systems demanded substantial contributions from dynamic and applied geomorphology). It was a period when Romanian geomorphologists created communication bridges with engineering sciences from the need to engage more effectively in solving problems related to land use, resource exploitation, environmental planning and management. A model of pragmatic mixture of geomorphological and engineering approach styles was provided by the book 'The River Channel Morphology and Dynamics' (Ichim et al. 1989), where a team of geomorphologists and hydraulics engineers have complemented each other in the fluvial knowledge domain. The new orientations involved other work styles for geomorphologists. If the pre-1970 period was the one dominated mostly by individual personalities (highlighted in Fig. 1.2), thereafter research groups or teams became the rule allowing for major

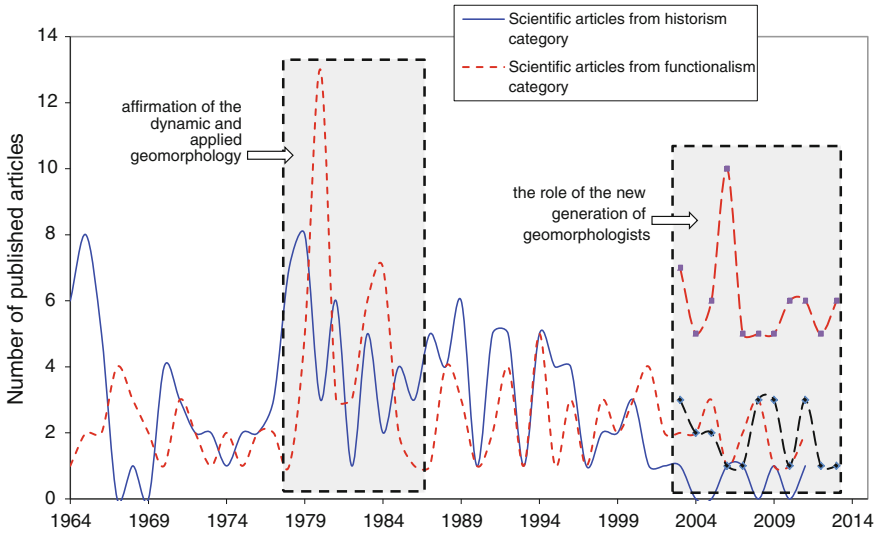

Fig. 1.3 The representativeness of dynamic and historicist geomorphological research according to the number of papers published in *Studii şi cercetări de Geografie, Revue Roumaine de Geographie* (1964–2009) and *Revista de Geomorfologie* (2003–2014)

progresses in many fields, such as the periglacial, fluvial, coastal or sediment dynamics which are all well represented in this volume.

The best evidence in support of these observations is provided by the analysis of the most prestigious Romanian geographical journals prior to 1990 (Revue Roumaine de Geographie—Romanian Journal of Geography, and Studii si Cercetari de Geografie—Studies and Researches in Geography); after the date hereof we also added Revista de Geomorfologie (Journal of Geomorphology). The numbers of scientific articles focusing on landforms from either a historicist or a functionalist perspective were ranked separately for each journal issue (Fig. 1.3). The resulting variation curves are rather self-explanatory in terms of highlighting the conceptual and methodological changes during the 50-year period we monitored. The first observation regards a steady decline in the historicist approach and a significant increase in the interest shown by Romanian geomorphologists to landform adjustments over shorter periods of time. Furthermore, a series of leaps was documented in the variation of the curve, which was outlined in the diagram (Fig. 1.3). For example, the 1978–1988 decade can be regarded as the period of affirmation of dynamic and applied geomorphology, based on the prevalence of articles focusing on such topics; this is the result of the involvement of Romanian geomorphology in tackling a multitude of practical problems, such as land use, resource exploitation and land engineering.

After 1989 (i.e. the year when Romania overthrew the communist political regime), the geomorphology benefitted from the opening and enthusiasm generally manifested during that period (Ichim 1993). The establishment of the Association of

Romanian Geomorphologists in 1990 was an important landmark, albeit previous attempts have been made previously in this regard, in 1972 and 1980 (Posea 1991; Vespremeanu 2005). Throughout this entire period remarkable efforts were made to focus the resources of Romanian geomorphology in order to annually sustain the series of national symposia of geomorphology, now (year 2016) reaching 32 editions.

During the past decades, a new movement synchronous to the worldwide trends in geomorphology became apparent. According to Church (2010), another major leap in the evolution of geomorphology (beginning in the mid-1980s) occurred rapidly post-1990 based on the advancement of technologies employed for landform observation and measurements: '*Dramatic changes have occurred in geomorphology since about 1980, rapidly gathering momentum after about 1990. The bases for these changes are, again, largely technological. The main influences include:* (1) *improved technologies for remote sensing and surveying of Earth's surface;* (2) *the advent of personal computation and of large-scale computation; and* (3) *important developments of absolute dating techniques*'. These technical advancements encouraged two major orientations in geomorphology, namely: opening the way for a renewed consideration of the history of landscape (by reconsidering the role of tectonics in geomorphology) and the ever-increasing degree of recognition of the human factor in the present-day changes of the earth surface. Both research topics have become attractive for the contemporary Romanian geomorphological community (the count of articles published in journals, both Romanian, but most importantly international publications, is yet again proof of this orientation).

Naturally, advancing technologies demand increasingly qualified researchers, of which a large proportion is also oriented towards multidisciplinary. This seems to explain the establishment of several research groups of young geomorphologists (during the past 10–15 years) with education and skills in sciences (geography, physics, mathematics, chemistry, information science) which could successfully implement the novel technologies. This is why within the present volume the contributions of young researchers (<40 years) are prevalent.

Not all branches of geomorphology were equally dynamic throughout time. For example, the hillslope domain retained the interest of Romanian geomorphologists much more frequently prior to 1989 than in recent years (Fig. 1.4). Conversely, other fields of geomorphological investigation (fluvial, coastal, periglacial, Quaternary, soil erosion) underwent remarkable advancements in terms of research methodology, the development of the dynamic and applied side and substantiating conclusions based on processing quantitative data. Furthermore, new fields developed in Romania, such as geomorphometry, boosted by the upgrades in information technology.

We conclude these introductory remarks by observing that the guideline followed in addressing the dynamics and evolution of landforms is related to the concept of geomorphology as system science (Church 2010). As with all environmental sciences (which are essentially system sciences), geomorphology seeks explanations by integrating and superposing the effects of many elements and

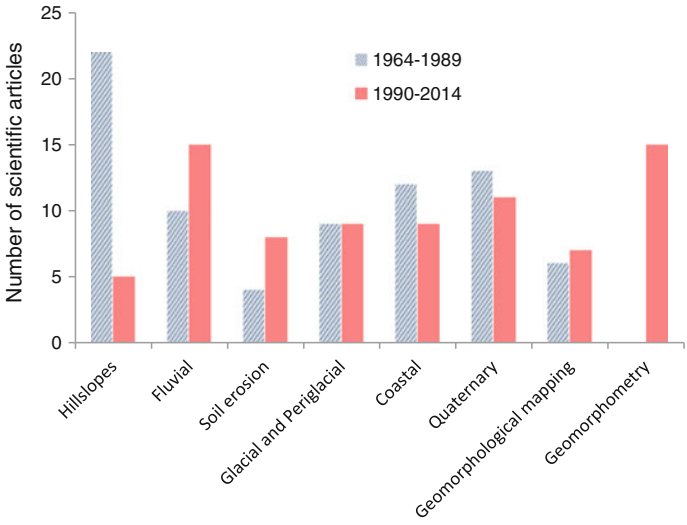

Fig. 1.4 Geomorphological fields covered by articles published in top Romanian journals prior to 1990 and ISI Web of Science journals post-1990

processes acting within a given space during a certain period of time. Thus, in the present volume we demonstrate to a large degree that the central topic—the relief of Romania—is investigated according to thorough concepts and the geomorphological events under scrutiny were analysed based on direct measurements, field experiments, absolute dating and comprehensive databases.

References

Chorley RJ, Schumm SA, Sugden DE (1984) Geomorphology. Methuen, London

Church M (2010) The trajectory of geomorphology. Prog Phys Geogr 34:265

Coteț P (1960) Harta geomorfologică a R.P. Române. In: Monografia geografică a R.P.R., vol. I, Geografia fizică. Editura Academiei Române, Bucureşti (in Romanian)

Geography of Romania (1983) Geografia Romaniei, vol 1, Editura Academiei Române, București

Geography of Romania (1987) Geografia Romaniei, vol. 3, Editura Academiei Române, București

Geography of Romania (1992) Geografia Romaniei, vol. 4, Editura Academiei Române, București

Geography of Romania (2005) Geografia Romaniei, vol. 5, Editura Academiei Române, București

Hickin EJ (1983) River channel changes: retrospect and prospect. Int Assoc Sedimentol Spec Publ 6:61–83

Ichim I (1993) Geomorfologia in pragul Mileniului III. Terra 25(1–4):83–90

Ichim I, Posea G (1993) Geomorphology in Romania. In: Walker HJ, Grabau WE (eds) The evolution of geomorphology. Wiley, Chichester, pp 363–366

Ichim I, Bătucă D, Rădoane M, Duma D (1989) Morfologia și dinamica albiilor de râu. Editura tehnică, Bucureşti (in Romanian)

Martiniuc C (1960) Harta regiunilor geomorfologice ale R.P. Române. In: Monografia geografică a R.P.R., vol. I, Geografia fizică. Editura Academiei Române, Bucureşti (in Romanian)

Mihailescu V (1946) Geografia fizică a României (curs litografiat), Universitatea Bucureşti (in Romanian)
Posea G (1991) Cuvânt inainte. Revista de Geomorfologie 1:1–2 (in Romanian)
Posea G, Popescu N, Ielenicz M (1974) Relieful României. Editura ştiinţifică şi enciclopedică, Bucureşti (in Romanian)
Roads BL (2006) The dynamic basis of geomorphology reenvisioned. Ann Assoc Am Geogr 96 (1):14–30
Schumm SA, Lichty RW (1965) Time, space and causality in geomorphology. Am J Sci 263:110–119
Slaymaker O, Spencer T, Dadson S (2009) Landscape and landscape-scale processes as the unfilled niche in the global environmental change debate: an introduction. In: Slaymaker O, Spencer T, Embleton-Hamann C (eds) Geomorphology and global environmental change. Cambridge University Press, Cambridge, pp 1–36
Strahler AN (1952) Dynamic basis of geomorphology. Geol Soc Am Bull 63(9):23–37
Tufescu V (1966) Modelarea naturală a reliefului și eroziunea accelerată. Editura Academiei RSR (in Romanian)
Vespremeanu E (2005) 40 ani de geomorfologie organizată în România. Revista de Geomorfologie 7:5–7 (in Romanian)

Part I
Background of Landform Evolution

Chapter 2
Tectonics and Exhumation of Romanian Carpathians: Inferences from Kinematic and Thermochronological Studies

Liviu Matenco

Abstract The ultimate topographic expression of intra-continental mountain chains is established during continental collision. The Romanian Carpathians provide a key location for understanding the mechanics of collision during slab retreat because the nappe stacking was not overprinted by back-arc extension, as commonly observed elsewhere. A review of existing kinematic and low-temperature thermochronological data infers that the collisional mechanics is significantly different when compared with high-convergence orogens. The shortening of the orogen at exterior was entirely accommodated by back-arc extension and the area in between simply rotated and moved into the Carpathians embayment. The roll-back collision is driven by foreland-coupling, a process that gradually accretes and exhumes continental material towards the foreland. The topographic expression of the Romanian Carpathians is both inherited from latest Cretaceous—Paleogene times, such as in the Apuseni Mountains or South Carpathians, and overprinted by the Miocene exhumation associated with the roll-back collision, as in the East or the SE Carpathians. The migration of exhumation towards the foreland continued during Pliocene—Quaternary times and is still active modifying the present-day topography in the SE Carpathians. The Transylvanian Basin is one of the best examples available of vertical movements induced by deep mantle processes in what is commonly referred as dynamic topography.

Keywords Kinematics · Thermochronology · Exhumation · Carpathians · Orogenic mechanics

L. Matenco (✉)
Department of Earth Sciences, Utrecht University, P.O. Box 80021, 3508 TA Utrecht, The Netherlands
e-mail: liviu.matenco@uu.nl

M. Rădoane and A. Vespremeanu-Stroe (eds.), *Landform Dynamics and Evolution in Romania*, Springer Geography,
DOI 10.1007/978-3-319-32589-7_2

Introduction

The kinematics and exhumation of collisional orogens have been a constant topic of tectonic studies since the definition of steady-state wedges and associated large-scale hinterland exhumation during the buoyant subduction of continental plates (e.g. Platt 1986; Beaumont et al. 1994; Ring et al. 1999). Continental collision is the moment when out-of-sequence contractional deformation becomes rather the rule than the exception. Understanding its importance is fundamental for a fairy large number of orogenic processes, such as emplacement of metamorphic nappes, exhumation of high pressure rocks, deformation of thin-skinned thrust belts, the interplay between shortening and surface processes, syn-orogenic extension, the geometry of foredeep basins or accretion of continental material (e.g. Marotta et al. 1998; Burov 2007; Doglioni et al. 2007; Burov and Yamato 2008; Haq and Davis 2008; Naylor and Sinclair 2008; Faccenda et al. 2009). When compared with the strain partitioning observed during oceanic subduction stages, the out-of-sequence collision deforms a much wider zone, compressional stresses being transmitted much farther in the orogenic foreland and hinterland (e.g. Ziegler et al. 1998; Roure 2008).

The kinematics, geometry and exhumation of European orogens can be simply divided in two main categories (Fig. 2.1).

High-convergence collisional orogens, such as the Pyrenees or the Alps are characterized by large amounts of contractional exhumation. This exhumation is enhanced in orogenic hinterlands along retro-wedges that display a complex poly-phase deformation with an opposite polarity when compared to the one of the subduction zone (such as the Insubric line, Roure et al. 1989; Schmid et al. 1996; Beaumont et al. 2000). On the contrary, the "Mediterranean"-type of collisional orogens is dominated by subduction processes, resulting in the formation of highly arcuated mountain belts, such as the Apennines, Carpathians, Hellenides and the Betics–Rif system (Fig. 2.1). These orogens evolved rapidly during the retreat (or roll-back) of genetically associated slabs (i.e. Calabrian, Vrancea, Aegean and Gibraltar, respectively) that peaked in almost all situations during Miocene times (e.g. Jolivet and Faccenna 2000; Faccenna et al. 2004; van Hinsbergen et al. 2005; Ismail-Zadeh et al. 2012; Vergés and Fernàndez 2012). The slab retreat is accommodated by coeval extension affecting the hinterland of the upper orogenic plate, which formed large basins floored by either continental or oceanic lithosphere (such as the Pannonian and Aegean Basins, Black Sea or Western Mediterranean). These basins are extensional back-arcs in terms of geodynamic evolution (e.g. Royden 1993; Okay et al. 1994; Jolivet and Faccenna 2000; Horváth et al. 2006; Doglioni et al. 2007) although their relative position behind a magmatic or island-arc (Uyeda and Kanamori 1979; Dewey 1980; Mathisen and Vondra 1983) is not always very clear. In almost all situations, the back-arc extension overprinted and hid the earlier continental accretion, in particular by exhumation along extensional detachments, such as the widely documented core complexes of the

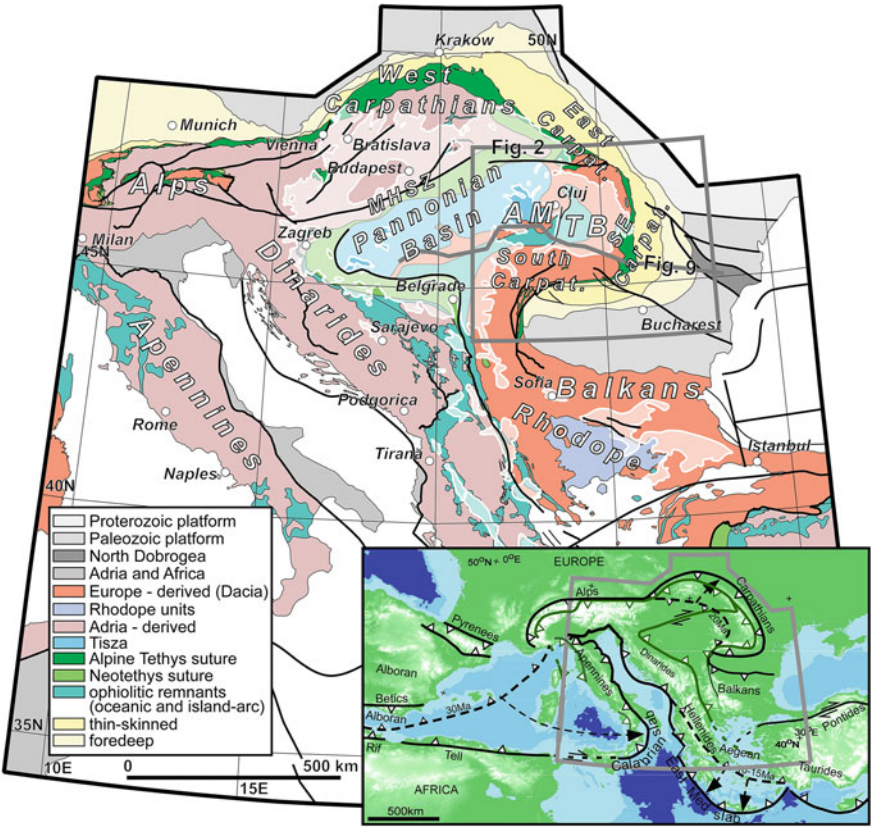

Fig. 2.1 Tectonic map of the Alps–Carpathians–Dinaridic–Hellenidic system (simplified from Schmid et al. 2011) with the extent of the Pannonian and Transylvanian back-arc basins (white transparent background). The *grey rectangle* is the location of Fig. 2.2 *AM*—Apuseni Mountains; *TB*—Transylvanian Basin; *MHSZ*—Mid-Hungarian Shear Zone. The lower inset is the location of the map in the system of European Mesozoic—Cenozoic orogens. *Dashed black line* is the position of the orogenic front prior to the onset of extension associated with the roll-back of the Calabrian, Aegean and Carpathian slabs

Rhodope–Aegean or Betics (Brun and Faccenna 2008; Brun and Sokoutis 2010; Vissers 2012).

An exception is the Romanian segment of the Carpathian Mountains, where the back-arc extension associated with the retreat of a slab kinematically connected with the stable European foreland (e.g. Schmid et al. 2008) took place during Miocene times in the Pannonian Basin, i.e. at far distances from the active subduction. This Miocene extension is rather minor in the areas situated in between, i.e. the eastern Apuseni Mountains, Transylvanian Basin or the East, SE and South Carpathians (e.g. Tiliţă et al. 2013). The clockwise rotation and E-ward translation of these Carpathian units accompanied the W-ward subduction of the Carpathian

embayment (sensu Balla 1986; Ustaszewski et al. 2008). Both processes cannot be accommodated by the dominantly N-S oriented absolute plate motion of Africa relative to Europe (Kreemer et al. 2003; van der Meer et al. 2010; van Hinsbergen and Schmid 2012). The reduced amount of Miocene extension provides a rare opportunity to quantify the crustal accretion processes and associated exhumation during roll-back and continental collision.

The north- to east-ward translations and coeval clockwise rotations during Cretaceous—Tertiary times have resulted in the formation of the characteristic double loop of the Carpathians around their SE corner and the transition from the South Carpathians to the Balkanides (Fig. 2.1, e.g. Csontos and Vörös 2004; Fügenschuh and Schmid 2005). This provides an opportunity to understand kinematic and exhumation processes associated with the formation of such highly arcuated orogens. The absence of studies connecting tectonic exhumation with landform formation in the Carpathians has resulted in long-lasting controversies concerning the age of topography and its links with deformation still taking place at present (e.g. Wohlfarth et al. 2001; Rădoane et al. 2003; Fielitz and Seghedi 2005; Dombrádi et al. 2007; Necea et al. 2013).

In order to derive the quantitative tectonic background required to understand the evolution of landforms in the highly arcuated Romanian Carpathians, this study is reviewing available kinematic and thermochronological data. The study provides critical constraints for understanding the mechanics of crustal accretion of collision in orogens dominated by roll-back. Furthermore, we analyse the link between deep- and near-surface processes acting in the aftermath of continental collision in this tectonically still active segment of the Carpathians.

Main Tectonic Units of the Romanian Carpathians

The Romanian Carpathian Mountains formed in response to a Triassic to Tertiary evolution of tectonic blocks and intervening oceans. In a fairly simplified terminology, four continental blocks [European foreland, Dacia, Tisza and ALCAPA (i.e. ALps–CArpathians–PAnnonia)] were separated by two intervening oceans (Neotethys/Transylvanides and Alpine Tethys/Ceahlău–Severin) closed by subduction and collision (e.g. Săndulescu 1984, 1988; Csontos and Vörös 2004; Schmid et al. 2008).

The European foreland is made up of a collage of units floored by Precambrian, Caledonian or Variscan basement, overlain by Paleozoic, Mesozoic or Cenozoic sediments with variable thicknesses and degrees of deformation. These were observed at depth in wells or defined by various geophysical techniques beneath the thrusting of the Carpathian units (Figs. 2.2 and 2.3, e.g. Săndulescu and Visarion 1988; Visarion et al. 1988). The East European and Scythian platforms are essentially Precambrian units, the latter representing the margin of the former affected by significant deformation during the latest Precambrian—early Paleozoic tectonic events and lower amounts of subsequent reactivations (Săndulescu and

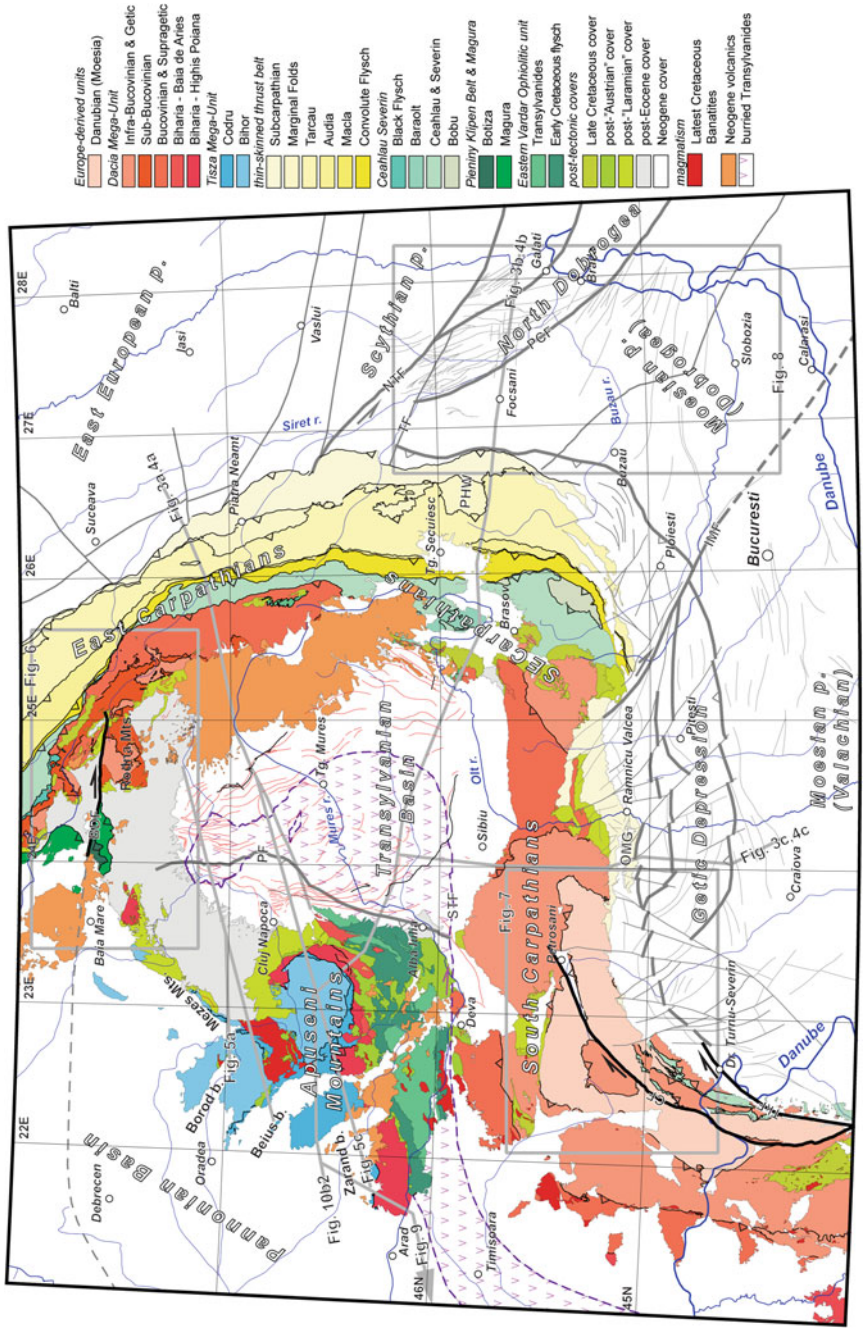

Fig. 2.2 Tectonic map of the Romanian Carpathians (derived by the compilation of 1:50,000 and 1:200,000 maps of the Geological Institute of Romania and Mațenco et al. 2010). *Thick grey lines* are the locations of geological cross sections in Figs. 2.3, 2.4, 2.5 and 2.9. *CF*—Cerna Fault; *BDF*—Bogdan Vodă—Dragoș Vodă fault system; *IMF*—Intramoesian Fault; *TF*—Trotuș Fault; *NTF*—New Trotuș Fault; *OMG*—Ocnele Mari—Govora antiform; *PHW*—Putna half-window

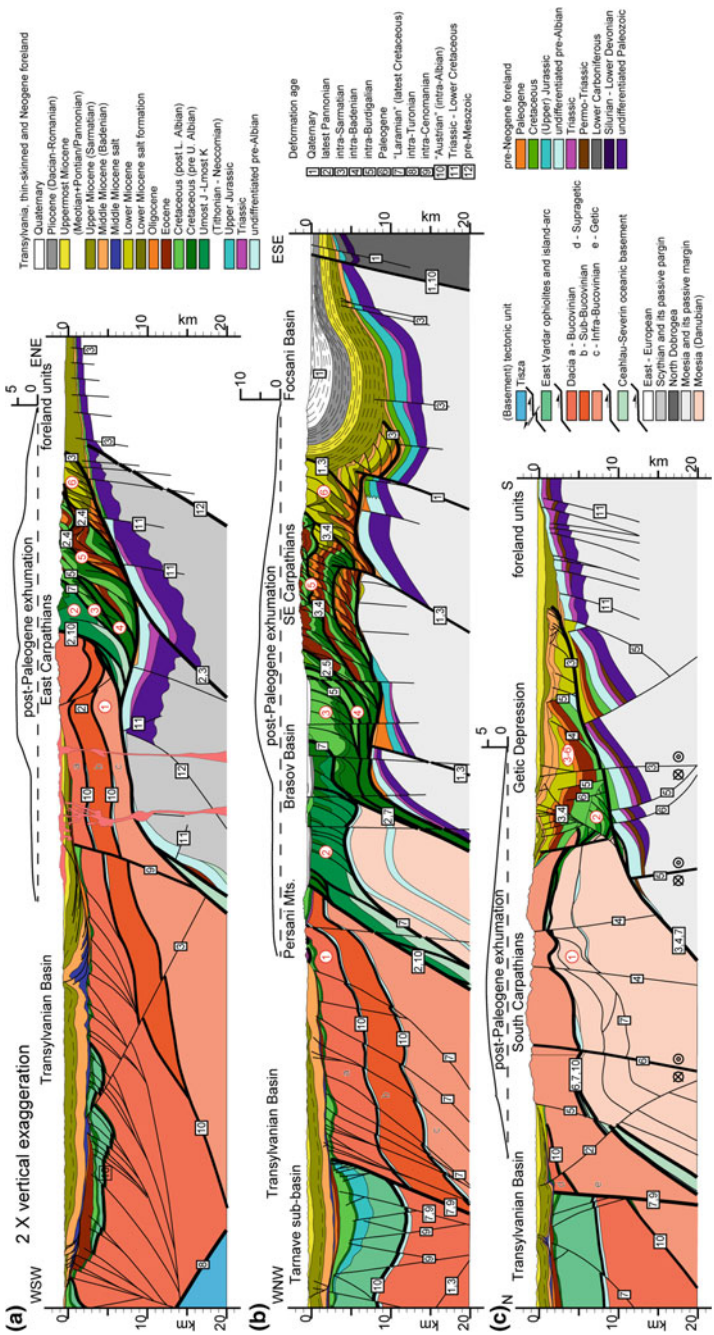

Fig. 2.3 Representative cross sections and corresponding amounts of post-Paleogene exhumation along three transects crossing the (**a**) East, (**b**) SE and (**c**) South Carpathians (modified from Matenco et al. 2010). The location of cross sections is displayed in Fig. 2.2. *Black numbers* indicate deformation ages, *red numbers* indicate tectonic units. Note the 2× vertical exaggeration, for further details see the text

Visarion 1988; Stephenson et al. 2004; Saintot et al. 2006). The SW margin of these units is often described as the prolongation of the NW–SE striking Teisseyre–Tornquist zone, essentially the limit between Proterozoic and Paleozoic European units that was affected by significant deformations during Paleozoic–Cenozoic times (Ziegler Ziegler 1990; Pharaoh 1999; Stănică et al. 1999). The Cretaceous—Paleogene shortening and along-strike displacements have duplicated locally this lineament in the structure of the SE Carpathians (Fig. 2.3, Bocin et al. 2013). To the SW, the Moesian platform (Fig. 2.2) is a Gondwana-derived terrane accreted to the East European/Scythian margin during the Late Carboniferous, subsequently overprinted by significant deformations, such as Permo–Triassic rifting, large-scale Cimmerian (Triassic–Jurassic) contraction and the Miocene Carpathians collision (Visarion et al. 1988; Tari et al. 1997; Seghedi et al. 2005; Vaida et al. 2005).

The Dacia unit makes the bulk of Romanian Carpathians thick-skinned nappes (Figs. 2.1 and 2.2). This unit is a piece of the European continent that split off during the Jurassic opening of the Ceahlău–Severin Ocean (Ştefănescu 1983; Săndulescu 1988; Schmid et al. 2008). The Dacia unit was sutured back to Europe during the Cretaceous closure of this ocean and the subsequent Paleogene—Miocene subduction of its eastern thinned continental passive margin remnant, i.e. the Carpathians embayment. Ultimately, the Miocene collision established the present-day nappe geometry of the East and South Carpathian Mountains (Săndulescu 1984, 1988; Balla 1986; Ustaszewski et al. 2008; Mațenco et al. 2010; Merten et al. 2010). The Dacia unit is made up of a thick-skinned nappe stack with an overall antiformal geometry that is well exposed in the East and South Carpathians (Figs. 2.2 and 2.3). This nappe stack formed during successive events of contraction taking place in late Early to latest Cretaceous times during the closure of the Ceahlău–Severin Ocean and was subsequently deformed during the Paleogene formation of the Danubian extensional dome in the core of the South Carpathians (Figs. 2.2 and 2.3, Schmid et al. 1998; Kräutner and Bindea 2002; Fügenschuh and Schmid 2005; Iancu et al. 2005a). In the East Carpathians, the E-ward facing Bucovinian nappe stack truncates an earlier Variscan thrust system with an opposite vergence during the peak contractional moments of late Early Cretaceous shortening (Fig. 2.3a, Kräutner and Bindea 2002). In the South Carpathians, the Getic/Supragetic nappes contain a medium to high-grade metamorphic Neoproterozoic to early Paleozoic basement and low metamorphic degree Paleozoic, overlain by a latest Paleozoic—Mesozoic sedimentary cover (Fig. 2.3c, Iancu et al. 2005a, b; Balintoni et al. 2010). These basement nappes are largely covered in the connecting area of the SE Carpathians (Fig. 2.3b), but their lateral (Sub-)Bucovinian—Supragetic and Infra-Bucovinian—Getic correlation has been inferred by a combination of surface observations and deep geophysical studies (Visarion et al. 1978; Săndulescu 1984; Bocin et al. 2009, 2013). At the opposite side of the East and South Carpathians, the Biharia nappe of the Apuseni Mountains (Fig. 2.2) has been recently ascribed to the Dacia unit based on its medium to high-grade Middle–Late Jurassic and Early Cretaceous metamorphic overprint (Dallmeyer et al. 1999; Schmid et al. 2008). Its lateral prolongation is inferred from seismic studies combined with well data beneath the Paleogene–Quaternary cover

of Transylvanian and Pannonian Basins (de Broucker et al. 1998; Matenco and Radivojević 2012; Tiliță et al. 2013).

The Tisza unit outcrops in the centre and NW part of the Apuseni Mountains, being covered almost elsewhere by the above-mentioned Paleogene–Miocene sediments of the Pannonian–Transylvania Basins (Fig. 2.2). Tisza is a continental unit with mixed affinities that separated from Europe during Middle Jurassic times. It moved southwards in a position adjacent to the Adriatic continental unit (i.e. that is genetically part of the African plate) and was realigned to European blocks (i.e. Dacia) during the late Early Cretaceous moments of closure and emplacement of the Transylvanides nappes, interpreted as a branch of the Neotethys Ocean (or East Vardar, Săndulescu 1975; Vörös 1977; Csontos and Vörös 2004; Haas and Péró 2004; Schmid et al. 2008). The Tisza continental unit is made up by a medium to high-grade Variscan metamorphic basement that is overlain by a dominant Permian–Triassic Germanic facies with significant lateral variations, including Middle Triassic shallow-water carbonates and Upper Triassic deeper water, i.e. Halstatt facies (Burchfiel and Bleahu 1976; Balintoni 1996; Haas and Péró 2004). A high-temperature Early Cretaceous metamorphic overprint with lower degree retromorphism during enhanced late Cretaceous exhumation has been recently detected in the NE-most corner of the Bihor nappe in the Apuseni Mountains (Fig. 2.2), inferring a tremendous metamorphic gradient across this dome (Kounov and Schmid 2013; Reiser et al. 2014).

The basement and sedimentary cover of ALCAPA continental unit are covered by Miocene sediments in the Romanian Carpathians (Fig. 2.1). The ALCAPA unit is made up of far-travelled Adriatic-derived continental nappes, trusted northwards during the Cretaceous–Paleogene closure of the Alpine Tethys and thick-skinned nappes emplacement of the Alps and Western Carpathians. These units were subsequently affected by counterclockwise rotations and ENE-wards translations during the Miocene extrusion of the Eastern Alps and the coeval extension of the Pannonian Basin. These movements were coeval with the Miocene shortening taking place at the exterior of the Western and Polish–Ukrainian East Carpathians (Ratschbacher et al. 1991; Tari et al. 1992; Csontos 1995; Fodor et al. 1999; Krzywiec 2001). In intra-Carpathians units, the thrusting of the ALCAPA over Dacia took place in Early Miocene times, as inferred by the final emplacement of the Piennides–Măgura nappe system in Maramureș area, and was subsequently followed by large-scale late Miocene sinistral strike-slip motions along the Bogdan– and Dragoș–Vodă faults system situated at their contact (Săndulescu et al. 1993; Tischler et al. 2007, 2008).

The ophiolite-bearing units of the South Apuseni Mountains are commonly grouped with the ones buried beneath the Miocene sediments of the Transylvanian Basin and exposed as the highest tectonic unit of the East Carpathians under the generic name of Transylvanides (Fig. 2.2, Săndulescu and Visarion 1977; Săndulescu 1984). These are thought to be derived from the Neotethys Ocean that was located SE of the Alpine Tethys. After the closure of the Paleotethys Ocean, the Neotethys Ocean started to open during Triassic times. Its northern branch was affected by large-scale Late Jurassic—Earliest Cretaceous obduction (Stampfli and

Borel 2002). The Transylvanides and the genetically associated island-arc volcanics together with their prolongation in eastern Serbia, Macedonia and Greece are interpreted as the part of the Neotethys (or Vardar in the Dinarides–Hellenides) Ocean that became thrusted or obducted over the European margin in late Jurassic times (the Eastern Vardar of Schmid et al. 2008; Mațenco and Radivojević 2012). The initial Late Jurassic emplacement of the Transylvanides was subsequently followed by their large-scale thrusting over Dacia during late Early Cretaceous times over a distance that spans from the Southern Apuseni Mountains to the East Carpathians (Figs. 2.2 and 2.3, e.g. Săndulescu and Visarion 1977; Nicolae and Saccani 2003; Săsăran 2005; Ionescu et al. 2009).

The Ceahlău–Severin unit (Fig. 2.2) contains the relicts of an oceanic embayment that opened between the European foreland and the Dacia unit, interpreted as the eastern prolongation of the Alpine Tethys, kinematically linked with the opening of the Central Atlantic Ocean (Favre and Stampfli 1992; Schmid et al. 2008). The exact moment of Jurassic opening is not fully clear in the Romanian Carpathians, owing to the almost complete subsequent subduction of the underlying oceanic basement (e.g. Săndulescu 1984; Ştefănescu 1995; Iancu et al. 2005a). However, the relationship of the Late Jurassic–Early Cretaceous Sinaia deep-water sediments with their underlying basement is rather obvious in the lateral prolongation of the Carpatho–Balkanides in Serbia and Bulgaria (i.e. the equivalent Kostel and Trojan deep-water formations, Kounov et al. 2010). It indicates that the initial opening of the Ceahlău–Severin Ocean is Middle Jurassic, coeval with the opening of the Alpine Tethys. Deformation of oceanic basement, deep-water sediments and genetically associated contractional trench turbidites combined with the overlying post-tectonic covers (such as Ceahlău conglomerates) indicate that these oceanic relics were emplaced during the late Early Cretaceous (~105 Ma) and latest Cretaceous (~70 Ma) moments of deformation in a system of nappes (Black Flysch, Baraolt, Ceahlău, Severin, Bobu) whose geometry is variable along the strike of the orogen (Fig. 2.2, Săndulescu 1975; Ştefănescu 1976; Săndulescu et al. 1981 and references therein). At the exterior of the Ceahlău–Severin unit, a wide system of nappes form the external Carpathians thin-skinned belt, well exposed in the East and SE Carpathians and buried beneath the latest Miocene–Pliocene cover of the Dacian Basin in the frontal part of the South Carpathians (Figs. 2.2 and 2.3). The various composing nappes (Convolute Flysch, Macla, Audia, Tarcău, Marginal Folds, Fig. 2.2) were emplaced successively in a foreland-breaking sequence during the Miocene subduction of the Carpathians embayment, a thinned continental to possibly oceanic domain formerly connected with the Ceahlău–Severin Ocean (Balla 1986; Săndulescu 1988; Mațenco and Bertotti 2000). The deformation culminated during the final moments of Carpathians collision and emplacement of the frontal Subcarpathian nappe at around 11–8 Ma and was followed by subsidence and differential vertical motions during latest Miocene—Quaternary times, a process that is still active today (e.g. Leever et al. 2006b; Mațenco et al. 2007, 2010; Ismail-Zadeh et al. 2012 and references therein).

The Relationship Between Tectonics and Exhumation in the Romanian Carpathian Mountains

The tectonic units presently exposed in the Romanian Carpathians or buried beneath the Neogene–Quaternary cover of the foreland and back-arc basins have suffered multiple episodes of burial and exhumation during their long poly-phase kinematic history. For instance, the metamorphic basement of the East and South Carpathians retains a dominant latest Proterozoic—Earliest Paleozoic age of metamorphism, but these rocks have been overprinted by numerous other episodes of (re-)burial and exhumation at/from various depths and rates during early or late Paleozoic, Cretaceous, Paleogene or Miocene—Quaternary times, as recorded by both high- and low- temperature thermochonlogical markers (Pană and Erdmer 1994; Medaris et al. 2003; Ciulavu et al. 2008; Balintoni et al. 2009; Merten 2011 and references therein).

We analyse the link between Carpathians exhumation and its present-day topographic expression by describing the effects of last significant tectonic exhumation event. This is obviously a fairly qualitative definition as orogenic burial and exhumation at steady state is a complex concept that assumes continuous exhumation driven by surface processes keeping pace with accretion of continental material in subduction/collision zones (e.g. Willett and Brandon 2002; Braun et al. 2014). In this study, the age of the last significant exhumation event is defined as the cooling age beneath the lowest closure temperature of available thermochronological markers.

The Romanian part of the Carpathians has a high density of low-temperature thermochronological markers that include zircon and apatite fission track (ZFT and AFT, closure temperatures $\sim 230°$ and $\sim 110 \pm 10°$, respectively, Gleadow and Duddy 1981; Brandon and Vance 1992) and apatite U–Th/He (AHe, closure temperature $\sim 75 \pm 5°$, Wolf et al. 1996). These methodologies involve rather complex procedures in orogenic exhumation that are described elsewhere (e.g. Reiners and Brandon 2006 and references therein), including the Romanian Carpathians studies cited below. The individual ages are cooling ages beneath their specific threshold temperatures, which are influences by a multitude of factors, such as the distribution of thermal gradient, surface and tectonic processes, groundwater flow, variations in diffusion controlled by the mineralogy of specific crystals (e.g. Braun et al. 2012). Thermal modelling by using multiple low-temperature thermochronometers and geological markers is constrained by AFT track length analysis (see Ketcham et al. 1999; Farley 2000; Ketcham 2005 for further details). Converting the resulting time—temperature histories into exhumation/denudation estimates has a higher degree of uncertainty than specific ages, because it involves estimating the geothermal gradient at the time of exhumation. Exhumation/burial does not translate directly into vertical movements, as thermochronological markers reflect temperatures (e.g. England and Molnar 1990). In orogenic context, exhumation may be the result of erosion resulting from tectonic uplift, in particular when the rates of exhumation are very high. A direct conclusion can be obtained

only by correlation with all other available geological constraints, including kinematics across the mountain chain. If only low-temperature thermochronological markers are used to derive exhumation, the potential error bar is usually in the order of 1–2 km whenever AHe is available, depending on the geothermal gradient at the time of exhumation (e.g. Ketcham 2005).

Collision of the East Carpathians

A representative East Carpathians profile (Figs. 2.3a and 2.4a) shows large amounts of Miocene exhumation (~6 km) widely distributed over the entire orogenic area

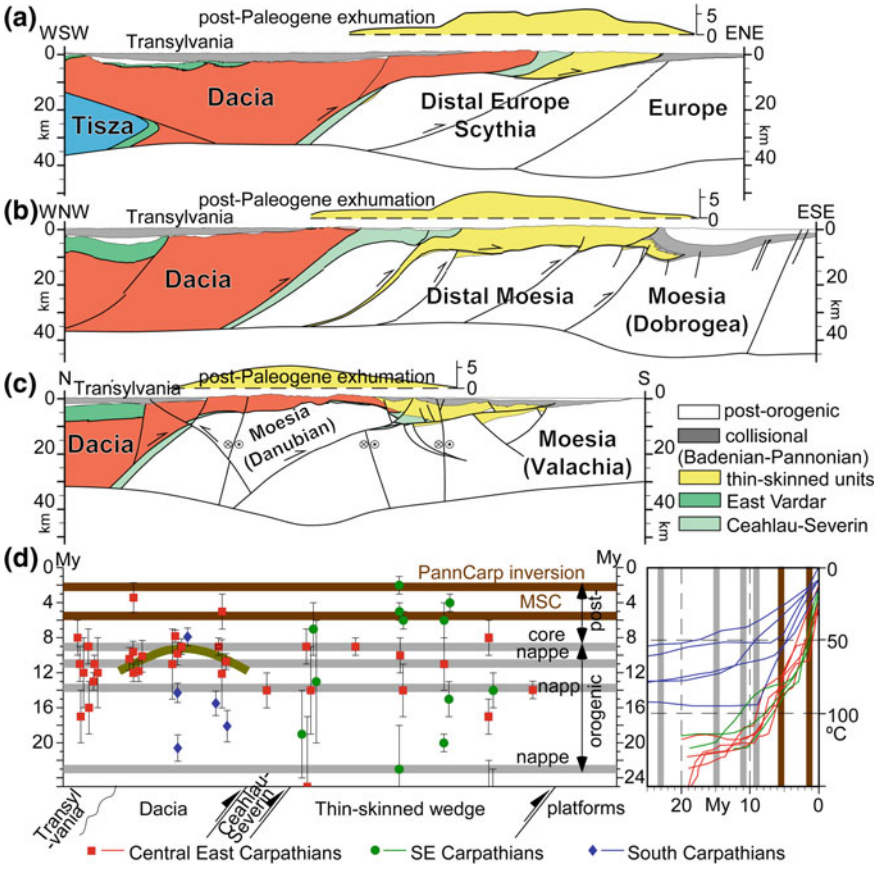

Fig. 2.4 Simplified crustal-scale version of cross sections in Fig. 2.3 by underlying the main tectonic units of the (**a**) East, (**b**) SE and (**c**) South Carpathians and synthetic representation of the apatite fission track data across the three areas an their thermal modelling (**d**) (after Mațenco et al. 2010). Note that only Miocene ages are plotted. For further details, see the text

from the eastern margin of the Transylvanian Basin to the centre of the thin-skinned contractional wedge, which gradually decreases towards the foreland (Matenco et al. 2010).

AFT ages indicate that most of this exhumation took place during the last stages of collision, ~15–11 Ma (Sanders et al. 1999). This overall Middle Miocene exhumation corresponds roughly to the age of emplacement of the frontal Carpathians nappes (Tarcău, Marginal Folds, Subcarpathian), as demonstrated by the study of post-tectonic covers (e.g. Săndulescu et al. 1981; Matenco and Bertotti 2000). The overall distribution of exhumation (Fig. 2.4a) infers that these tectonic events have affected not only the frontal nappes, but was distributed with similar cumulative amplitudes over the entire orogen. In more details (Figs. 2.3a and 2.4a, d) exhumation ages correlated with the main moments of uplift recorded by tectonic sequence stratigraphy studies in the Transylvanian Basin (Fig. 2.5) suggested that

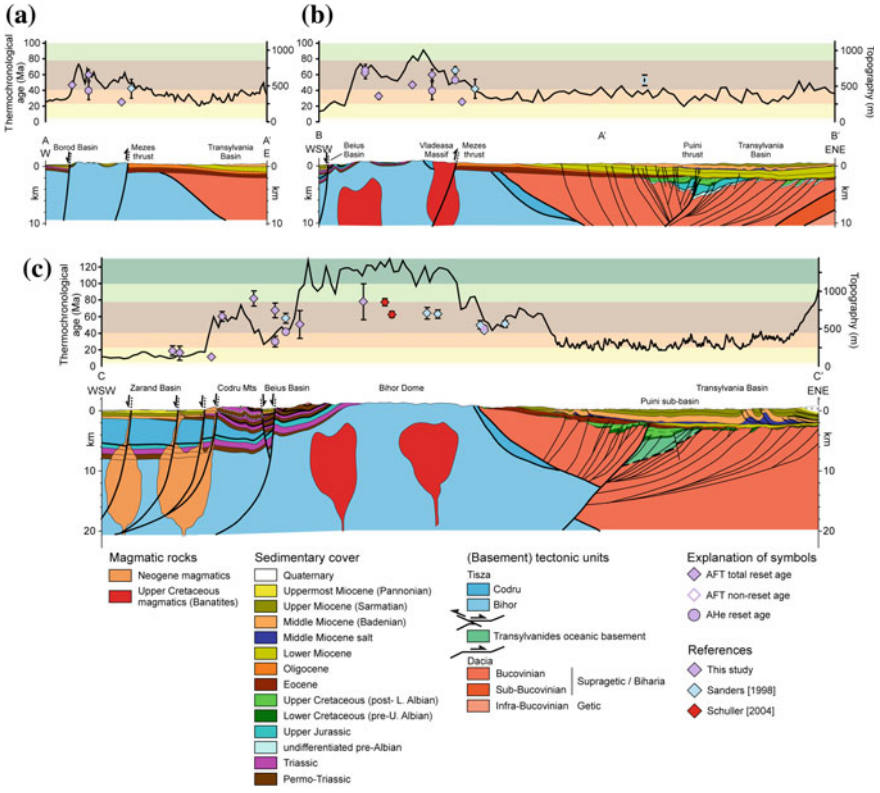

Fig. 2.5 Cross sections over the Apuseni Mountains and neighbouring parts of the Transylvanian and Pannonian Basins, and ages of exhumation derived from apatite fission track and apatite U–Th/He data (modified from Merten et al. 2011). Note the 2× vertical exaggeration. Locations of cross sections are displayed in Fig. 2.2. **a** Cross section over the Mezeș Mountains. **b** Cross section over the Vlădeasa Mountains. **c** Cross section over the Bihor dome

enhanced exhumation took place during 13–8 Ma in two main moments (Mațenco and Bertotti 2000; Krézsek et al. 2010). A first moment of in sequence nappe stacking (~14–10 Ma) deformed the above-mentioned frontal Carpathians nappes and is correlated with three pulses of uplift observed by sequence stratigraphy along the Transylvanian Basin margins (Late Badenian, Middle and Late Sarmatian), which infer a cumulated uplift in the order of 2.7 km of the adjacent East Carpathians. The second moment of out-of-sequence contractional deformation (~10–8 Ma) has resulted in enhanced exhumation of the hinterland and exaggeration of the Bucovinian antiformal nappe stack. This is correlated with two pulses of uplift observed by sequence stratigraphy along the Transylvanian Basin margins (Early and Late Pannonian) that infer a cumulated uplift in the order of 2.3 km in the core of the Bucovinian nappes. This late stage of enhanced exhumation in the orogenic core is genetically linked with a migration of contractional deformation from the former subduction zone to a crustal-scale thrust fault truncating the Scythian lower plate, creating an overall anticlinal ramp structure in the overlying Bucovinian units (Fig. 2.4a).

More recent studies have combined AHe data with existing AFT into a higher resolution exhumation history of the East Carpathians (Merten 2011). This study inferred a more symmetrical distributed Miocene exhumation, estimates ranging from 1.5 to 2.7 km for the Transylvanian Basin to 4.3 km in the centre of the Audia nappe at a rate of $\sim 0.7 \pm 0.1$ mm/year, decreasing gradually to 2 km in more external thin-skinned nappes.

In this overall East Carpathians evolution, localized uplift occurred during Miocene times in the region of Rodna Mountains (Figs. 2.2 and 2.6). Zircon fission track data have demonstrated that the Rodna Mountains was affected by significant amount of cooling during Late Cretaceous times (~85–70 Ma, Santonian–Campanian) coupled with slightly earlier exhumation in the Bucovinian basement located northwards (~99–95 Ma, Cenomanian). This has been interpreted as a large-scale extensional event not yet quantified (Gröger et al. 2013), but most likely a detachment uplifting the core of the Rodna Mountains in its footwall. This exhumation event has been subsequently followed by reburial followed by a Miocene exhumation depicted by AFT and AHe data attributed to deformation near the major Bogdan Vodă–Dragoș Vodă fault system (Fig. 2.6, Gröger et al. 2008). Because the ZFT data were not reset by the reburial and exhumation, the Miocene uplift must have amplitudes in between the AFT and ZFT cooling ages, which translate somewhere between 3–5 and 7–10 km at normal geothermal gradients (Fig. 2.6). This Miocene exhumation spans in the interval 15–10 Ma and is divided into a two-phase deformation history, a first 16–12 Ma thrusting event (exhumation ages 15–13 Ma) being subsequently followed by the exhumation of Rodna Mountains during the sinistral strike-slip transpression taking place at 12–10 Ma (exhumation ages 13–8 Ma). The latter localized 4–5 km exhumation in the Rodna Mountains added to the overall pattern of collisional exhumation, which in this area has values in the order of 1–2 km (Tischler et al. 2007; Gröger et al. 2008; Merten 2011).

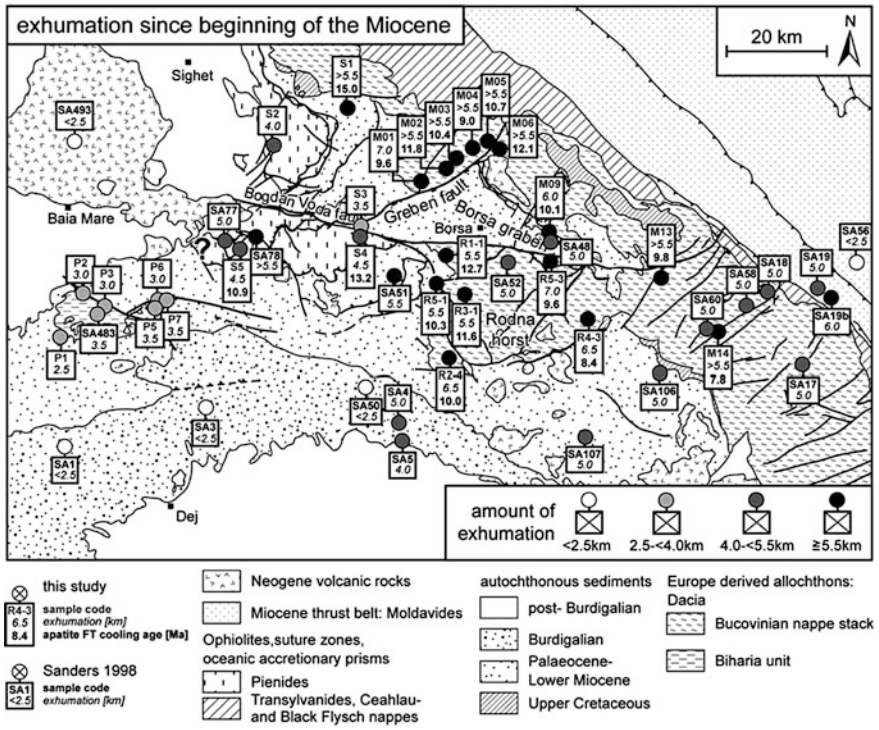

Fig. 2.6 Map showing ages and amounts of exhumation as derived from apatite fission track data in the northern part of the East Carpathians, Rodna Mountains and adjacent areas (Gröger et al. 2008). Location of the map is displayed in Fig. 2.2

Out-of-Sequence Thin- Versus Thick-Skinned Accretion in the SE Carpathians

A representative profile based on AFT data indicates an unusual situation in the SE Carpathians (Fig. 2.4b). The amounts of Miocene exhumation in the Bucovinian nappes and the ophiolitic-bearing Ceahlău unit are fairly low and contrast with the much higher, up to 6 km cumulative exhumation values in more external thin-skinned nappes. This exhumation geometry is at odds with normal critical wedge tapper geometries in collisional orogens, where the maximum amounts of exhumation are recorded in the upper plate hinterland. A number of thick-skinned thrusts truncate the tectonic lower plate (i.e. Moesia) and post-date the emplacement of overlying thin-skinned nappes (Fig. 2.4b). These out-of-sequence thrusts have been inferred by the near-surface geometry of nappes and were confirmed by deep geophysical studies, including reflection/refraction seismics, tomographic inversion, ray-trace analysis and gravity/magnetic modelling (e.g. Hauser et al. 2007; Bocin et al. 2005, 2009, 2013). The thick-skinned thrusting is associated with large

amounts of Quaternary differential subsidence and uplift recorded in the Focșani Basin and the neighbouring external nappes of the SE Carpathians, respectively (Leever et al. 2006b; Matenco et al. 2007). The continuous subsidence creating the exceptionally thick (up-to-13 km) Miocene–Quaternary sediments in Focșani Basin (Fig. 2.4b, Tărăpoancă et al. 2003) is related to the pull exerted by the Vrancea slab of the SE Carpathians (Fig. 2.4b, Tărăpoancă 2004; Matenco et al. 2007, 2010). This pull was explained by a number of different geodynamic models explaining the deep mantle structure of the SE Carpathians (see the review of Ismail-Zadeh et al. 2012 and references therein).

More recent AFT and AHe data have inferred a higher resolution exhumation history of the SE Carpathians (Merten et al. 2010; Necea 2010). The results indicate that exhumation migrated towards the foreland, ages degreasing from Cretaceous in internal basement nappes to Miocene–Quaternary in the external part of the thin-skinned wedge (Merten et al. 2010). The Miocene nappe thrusting exhumation occurred at rates of around 0.8 mm/year, which is the same order of magnitude when compared to the East Carpathians. However, in the SE Carpathians this deformation has been overprinted by two subsequent events of out-of-sequence thick-skinned thrusting, possibly enhanced by the sea-level drop that took place near the Miocene—Pliocene limit in the Paratethys during the Messinian Salinity Crisis. These latest Miocene—Early Pliocene and Pleistocene exhumation events had much higher rates in the order of 1.6–1.7 mm/year (Merten et al. 2010). These rates have been confirmed by a high-resolution profile located in the northern part of the SE Carpathians (Putna Valley, Necea 2010). In this area, similar migration of exhumation from Cretaceous to Quaternary from the internal to the external part of the orogen has been observed, the Quaternary exhumation being overly exaggerated in the area of the Putna half-window (Fig. 2.2). Here, the youngest 1 Ma AHe exhumation age from the entire Carpathian Mountains has been recorded, inferring peak Quaternary exhumation in the order of 5 km (Necea 2010).

The total amount of Miocene shortening recorded by the thin-skinned thrust wedge of the East and SE Carpathians is laterally variable along the strike of the orogen. It increases northwards from 140 to 160 km in the northern part of the SE Carpathians to around 220–240 km in the Polish segment of the East Carpathians (Roure et al. 1993; Ellouz and Roca 1994; Ellouz et al. 1994; Morley 1996).

Nappe Stacking, Orogen Parallel Extension and Transcurrent Movements in the South Carpathians

Available exhumation data in the South Carpathians indicate that the bulk of their last event of tectonic exhumation took place during (Late) Cretaceous—Paleogene times (Bojar et al. 1998; Sanders 1998; Schmid et al. 1998; Sanders et al. 2002; Fügenschuh and Schmid 2005; Merten 2011), significantly predating the main Miocene–Quaternary exhumation recorded by the East and SE Carpathians.

The main tectonic processes was the closure of the Ceahlău–Severin Ocean that took place coeval and was subsequently followed by large-scale ~90° clockwise rotations accompanying the N- to E-ward translations of the Tisza–Dacia unit around the Moesian promontory (e.g. Ratschbacher et al. 1993; Csontos 1995). This process started with the late Early Cretaceous (intra-Albian, ~105 Ma) onset of closure of the Ceahlău–Severin Ocean accompanied by the thrusting of the Supragetic over the Getic units. This was subsequently followed by coupling of the Moesian margin, over-thrusting of the Getic–Supragetic system and the formation of the Danubian nappes (Fig. 2.2) during late Cretaceous (late Campanian—Early Maastrichtian, ~80–68 Ma) times (e.g. Berza et al. 1983; Săndulescu 1984; Iancu et al. 2005a and references therein). The latter led to burial of the Danubian nappes that were affected by an overall sub-greenschists facies metamorphism (Ciulavu et al. 2008). These events are in agreement with the distribution of ZFT and AFT data that indicate dominantly a Cretaceous background in terms of exhumation ages in the Getic–Supragetic system (Fig. 2.7).

At the end of these contractional deformations, the clockwise rotations have brought the South Carpathians strike in a position that was likely sub-parallel with the Moesian margin (Fügenschuh and Schmid 2005), which is also parallel with the direction of subsequent translations into the Carpathian embayment. The continuation of deformation with such an orogenic geometry resulted in the elongation of

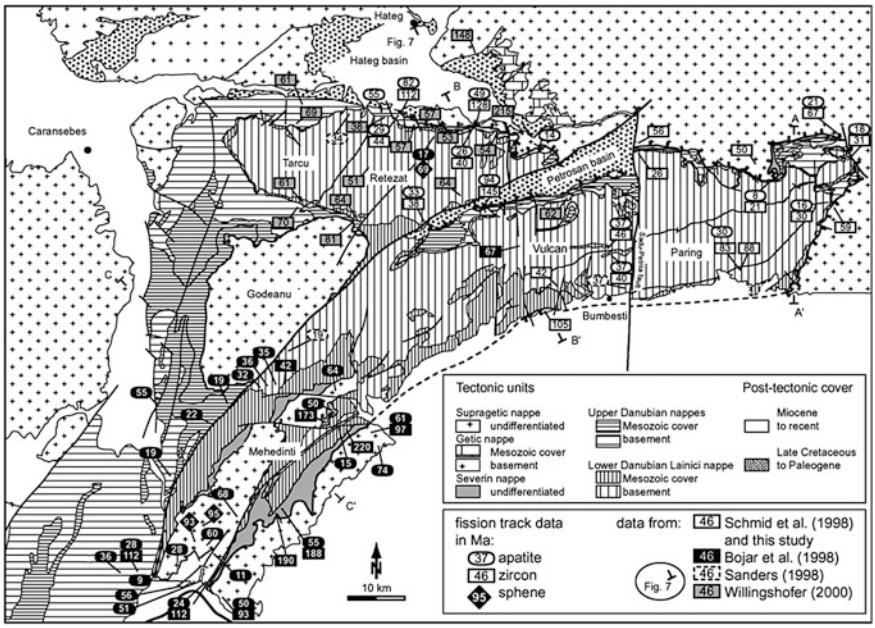

Fig. 2.7 Map compilation showing ages of exhumation in the Danubian nappes and adjacent Getic units of the South Carpathians, as derived from thermochronological studies (Fügenschuh and Schmid 2005)

the South Carpathians (i.e. orogen—parallel extension) and the initiation of large-scale transcurrent motions in respect to the Moesian margin. In a first stage, the orogen parallel extension formed an elongated extensional dome that exhumed the previously buried Danubian nappes (Schmid et al. 1998; Mațenco and Schmid 1999). This overall process culminated during Late Eocene times with the formation of the presently top to E–NE Getic detachment that reactivated the earlier late Cretaceous Getic–Danubian thrust. The gradual erosion of the Cretaceous orogen coupled with the mechanical variability of the orogen—parallel extensional in relationship with segmenting strike-slip and normal faults created a pattern of exhumation where the ZFT and AFT ages are widely distributed throughout the latest Cretaceous—Eocene times in the Danubian nappes, but are generally younger E-wards (Fig. 2.7, Willingshofer et al. 2001; Fügenschuh and Schmid 2005).

The N to NE translations and rotations of the South Carpathians accommodated initially by the orogen parallel extension continued during Oligocene—Lower Miocene times by the activation of the Cerna–Timok system of large-offset curved strike-slip faults cumulating ~100 km total dextral offset (Fig. 2.2). The Cerna Fault accommodate ~35 km of Early Oligocene dextral offset (Berza and Drăgănescu 1988), its rotational kinematic resulting in transtension, most relevant by the formation of the Petroșani Basin (Fig. 2.2, Ratschbacher et al. 1993). This was subsequently followed by the activation of the curved dextral Timok Fault that cumulates one of the largest offsets (~65 km) observed in continental Europe (e.g. Krautner and Krstic 2003). The age of this fault is still uncertain, but is likely late Oligocene—Early Miocene. To the S, the Timok offset is gradually transferred to the thrusting of the Srednogorie and Western Balkans units (Fig. 2.1). To the ENE and E, the Timok offset was significantly overprinted by the subsequent Miocene deformation of the Getic Depression characterized by strike-slip (mostly dextral) and thrusting of the South Carpathians over the Moesian platform (Răbăgia and Mațenco 1999; Tărăpoancă et al. 2007; Răbăgia et al. 2011; Krézsek et al. 2013). The Timok Fault is the likely precursor of the modern contact between the Carpathian units and the Moesian platform (the S Călimănești–Tg. Jiu Fault of Visarion et al. 1988). It was connected during Oligocene—Early Miocene times with the Carpathians embayment by transferring its dextral offsets to the thrusting of internal Moldavides (Audia, Macla and Curbicortical Flysch nappes, Fig. 2.2) in the East and SE Carpathians (Schmid et al. 2008; Krézsek et al. 2013).

These events were followed by the Middle–Late Miocene transpressional docking of the South Carpathians against the Moesian platform and thrusting emplacement of thin-skinned sediments of the Getic Depression. A regional profile crossing roughly the central part of the South Carpathians (Fig. 2.3c, see also a more recent interpretation based on modern wide angle reflection data of Krézsek et al. 2013) indicates a roughly symmetric geometry of the Miocene exhumation that reached maximum values of ~5 km in the centre of the orogen, decreasing rapidly elsewhere. This is in agreement with the much lower amounts of thrusting of the Getic Depression (up to ~35 km) when compared with East and SE Carpathians, and with exhumattion data, only few AFT Miocene ages as young as ~8 Ma being obtained in the centre of exhumation (Fig. 2.4c, d). A larger

number of AFT exhumation ages distributed throughout the Miocene have been obtained in the western part of the Danubian nappes (Bojar et al. 1998), near the connecting area with the Serbian Carpathians and the Balkanides (Figs. 2.1 and 2.2). These are likely the result of higher amounts of tectonic uplift driven by the combination between Miocene thrusting and transpression.

Higher resolution exhumation studies based on AFT and AHe data suggest that the exhumation of the South Carpathians was a more continuous process that started already in Paleogene times with the formation of the core complex and gradually decreased with lower values into the Miocene as a combination between tectonic induced uplift with low values and the gradual erosional breakdown of an earlier built orogen (Merten 2011). This uplift gradually increases E-wards towards the connection with the SE Carpathians, where what was thought to be Miocene tectonic exhumation started already during late Oligocene times (Merten et al. 2010; Necea 2010), confirming the connection with the Timok fault and the continuity of deformation.

The Orogenic Evolution and Subsequent Stability of the Apuseni Mountains

Owing to their high structural complexity, the Apuseni Mountains have the most distributed exhumation history in the entire Romanian Carpathians. The multi-phase deformation at the contact between Tisza and Dacia combined with poor outcrops exposures and widespread covering by post-tectonic Cretaceous, Paleogene and Miocene–Quaternary sediments or volcanics makes them also the least understood mountains in the entire chain. On the overall, the results of low-temperature thermochronology studies (Sanders 1998; Sanders et al. 2002; Schuller and Frisch 2006; Schuller et al. 2009; Merten et al. 2011; Kounov and Schmid 2013; Reiser et al. 2014) agree that the exhumation of the Apuseni Mountains took place during two main periods.

The first late Jurassic—late Cretaceous (Early Campanian) exhumation period was driven by multi-phase large-offset structures, often with opposite polarities and mechanics (contraction vs. extension). Following their Middle Jurassic separation, the onset of the contractional deformation at the contact between Tisza and Dacia started during the late Jurassic (~Tithonian) emplacement of the East Vardar ophiolites and island-arc volcanics, presently exposed in the Southern Apuseni Mountains, over the Dacia margin (Schmid et al. 2008). This was possibly driven by obduction (emplacement of oceanic lithosphere over a continent) or island-arc collision, as the coeval emplacement of similar ophiolites is documented all along the European-derived margin, from Romania to Greece (Fig. 2.1). This event is associated with the deposition of a shallow-water Late Jurassic—Early Cretaceous carbonatic sequence directly over the Transylvanides ophiolitic sequence in the Southern Apuseni Mountains and their continuation beneath the Transylvanian

Basin and East Carpathians (e.g. Săsăran 2005). However, differently from elsewhere, the final emplacement by thrusting of the Transylvanides over the top of the Bucovinian nappe pile took place much later, during late Early Cretaceous times (Săndulescu and Visarion 1977; Săndulescu 1984). In the Apuseni Mountains, these events are recorded by burial in high-T thermochronology and by exhumation recorded by ZFT data in the Biharia nappes, Transylvanides and their sedimentary cover (Schuller 2004; Kounov and Schmid 2013; Reiser et al. 2014). Given the widespread ages from latest Jurassic to late Early Cretaceous (~140–100 Ma), it is rather unclear if these were two separate events or just one continuous process leading to the ~150 km inferred thrusting of the Transylvanides up to the East Carpathians. This complex deformation was followed by the main intra-Turonian deformation that created the Biharia/Codru/Bihor nappe stack of the Apuseni Mountains with a presently top-NW transport direction. This event has no reasonable attached mechanism in Romanian literature, as is not observed in the East, SE and South Carpathians. Interestingly, the restoration of latest Cretaceous—Miocene ~90° clockwise rotations and Miocene extension of the Pannonian Basin (e.g. Ustaszewski et al. 2008) indicate that this deformation has the required SW vergence, timing and proximity to be driven by a Dinarides event during the closure of the Neotethys (Dimitrijević 1997).

The second exhumation period was driven by a long-wavelength contractional uplift of the Bihor dome during latest Cretaceous—Eocene times and by lower offset Oligocene (possibly also Earliest Miocene) thrusting that took place at the contact with the Transylvanian Basin sediments in the area of the Mezeș Mountains, Puini thrust and its southern prolongation (Figs. 2.2 and 2.5). These events are observed in AFT and AHe thermochronology combined with field kinematics (Fig. 2.5, Merten et al. 2011).

In contrast with the East, SE and South Carpathians, the Miocene tectonics did not created any significant exhumation in the Apuseni Mountains. The few low-temperature thermochronological ages obtained are related to the magmatic cooling of Neogene volcanics (Fig. 2.5, Merten et al. 2011). The relative Miocene stability at AHe resolution of the Apuseni Mountains (~1 km given the high geothermal gradients) is in sharp contrast with the coeval large amounts of subsidence recorded by the Pannonian and Transylvanian Basins, and with the large uplift of the East, SE and South Carpathians. In fact, the Apuseni Mountains are a relic of a much wider and continuous mountain chain that occupied the space between the Dinarides and the Carpathians at the end of Paleogene times.

Dynamic Topography in the Transylvanian Basin

One of the most striking European examples of dynamic topography is the Miocene formation and evolution of the Transylvanian Basin (Fig. 2.2). The up to 3.5 km thick Middle–Upper Miocene sedimentary cover has an apparent symmetric geometry both in cross sections and in map views (Figs. 2.2 and 2.3). It overlies an

earlier basement and cover affected by large-scale tectonic movements that include the late Early Cretaceous emplacement of the ophiolite-bearing Transylvanides nappes drilled by exploration wells and inferred from the magnetic and gravity anomalies in the central and western part of the basin (Figs. 2.2 and 2.3, e.g. Ciupagea et al. 1970; Săndulescu and Visarion 1977; de Broucker et al. 1998; Ionescu et al. 2009; Tiliţă et al. 2013). This was followed by the extensional formation of two main late Cretaceous sub-basins (Târnave and Puini, Figs. 2.3b and 2.5c) that was likely connected with the coeval extensional exhumation of the Rodna Mountains (Gröger et al. 2008). These two sub-basins were inverted in two subsequent contractional episodes that took place during the latest Cretaceous and latest Eocene, which affected the entire Transylvanian Basin (de Broucker et al. 1998; Krézsek and Bally 2006). This contraction resulted in the formation of an orogenic area that was subsequently affected by large-scale erosion (the pre-Paratethys buried denudational surface of Paraschiv 1997). The deposition of a foredeep wedge in the northern part of the basin took place in response to the thrusting of ALCAPA over Dacia during late Oligocene—Early Miocene times (Krézsek and Bally 2006; Tischler et al. 2008). The onset of regional subsidence in the Transylvanian Basin took place during Middle Miocene times (Badenian), continuing with accelerated pulses throughout the Middle–Late Miocene (Filipescu and Gîrbacea 1997; Krézsek and Filipescu 2005; Tiliţă et al. 2013). The subsidence started near the East and SE Carpathians and gradually extended over the entire basin (Tiliţă et al. 2013). In parallel, the exhumation of the neighbouring Carpathians during Middle–Late Miocene uplifted the margins of the Transylvanian Basin in several pulses of movement and created forced regressive sequences with coarse deltaic deposition (Krézsek and Filipescu 2005; Krézsek et al. 2010; Matenco et al. 2010). These vertical tectonic movements were interrupted by an eustatic sea-level drop during Middle Badenian times, which lead to the deposition of thick salt and other evaporitic sequences throughout the basin (Peryt 2006; de Leeuw et al. 2010). These evaporites migrated during the latest Middle–Late Miocene and created locally large exaggerated diapirs due to the overburden, contractional stresses and volcanic sagging (Krézsek and Bally 2006; Szakacs and Krezsek 2006; Tiliţă et al. 2013). Towards the end of the late Miocene times ($\sim$8 Ma) the entire Transylvanian Basin was uplifted to the $\sim$600 m maximum topographic elevations of the sedimentary fill, being subsequently affected by significant erosion and local deposition of Pliocene–Quaternary continental sediments (Matenco et al. 2010).

None of these substantial Miocene vertical movements can be explained by the few low-offset faults observed in the Transylvanian Basin (Fig. 2.3). Both the initial subsidence and the subsequent regional exhumation are dynamic topography processes, i.e. related to the deep mantle evolution during the roll-back of the Carpathians slab. It is rather unclear which dynamic topography process may be responsible from the wide variety inferred, although some are more likely, such as mantle thinning during extension and its subsequent response (for a review see Tiliţă et al. 2013). Furthermore, the evolution of the adjacent intra-mountain Pliocene–Quaternary Braşov and Tg-Secuiesc Basins (Figs. 2.2 and 2.3b) and the

associated alkaline and adakitic volcanism is also driven by dynamic topography processes. The formation of these extensional grabens with sediments averaging few hundreds to few tens of metres is related to the rise of the astenospheric mantle in the hinterland of the rapidly sinking Vrancea slab, as inferred by a wide array of deep geophysical observations and numerical modelling (Seghedi et al. 2011; Ismail-Zadeh et al. 2012 and references therein).

In fact, the postulation of Transylvania as a back-arc basin behind the volcanic arc of the East Carpathians is highly questionable. In mechanical terms, the Pannonian Basin is the typical back-arc driven by the Miocene roll-back of the Carpathians slab (e.g. Horváth et al. 2006). Given the coeval stability of the Apuseni Mountains and the pre-Miocene continuity of the orogen in the entire intra-Carpathians region, the Transylvanian Basin can be alternatively interpreted as an unusual large fore-arc basin overlying the frontal part of a wide orogen, as commonly discussed elsewhere (e.g. Fuller et al. 2006). In other words, the current dilemma is: can the Transylvanian Basin be considered a small back-arc or a large fore-arc basin? A response would be eventually important for deciphering the underlying mechanisms driving its evolution.

Mechanisms Driving the Miocene–Quaternary Evolution of the Carpathians Foredeep and Foreland Platforms

Typical models of orogenic mechanics (e.g. Beaumont 1981; Platt 1986; Naylor and Sinclair 2008; Cawood et al. 2009 and references therein) assume that foredeeps form in response to flexure of the continental lower plate involved in subduction and collision under load exerted by the coeval orogenic nappe stacking. This mechanism creates syn-kinematic foredeep wedges that record the moments of thrust loading and are locally involved in thrusting. In the Carpathians, this mechanism should have controlled the deposition of the undeformed foredeep and the thrusting of the Subcarpathian molasse sequence. The same mechanics assumes that the flexural isostatic rebound associated with the ceasure of contractional stresses should have created a limited amount of uplift in post-orogenic times. Along the strike of the Romanian Carpathians, only the East Carpathians segment underlain by the East European/Schythian platform units respects these general rules of foredeep evolution and post-orogenic rebound. The SE and South Carpathians segments underlined by the various units of the Moesian Platform show atypical foredeep evolution and post-collisional geometries (Mațenco et al. 1997; Bertotti et al. 2003; Leever et al. 2006a).

The external East Carpathians displays typical wedge-shaped foredeep geometries of the Miocene sediments overlying the East European/Scythian platform units (Fig. 2.3a). These deposits show a clear syn-kinematic character with lateral transitions of sedimentological facies, such as from shallow-water clastic and carbonates at far distances from the orogen to coarse clastic deep-water molasse overlying

the earlier turbiditic/flysch deposition in its proximity. The latter was involved in thrusting by the final emplacement of the Subcarpathian nappe (Ionesi 1994; Miclăuș et al. 2009, 2011). This foredeep displays a characteristic transgressive–regressive cyclicity driven by the Miocene moments of thrust loading. Post-dating these moments of deformation, the entire East Carpathians—foredeep—East European/Scythian transect underwent exhumation and uplift to continental conditions. The rather high present-day topographic elevations of the foreland East European/Scythian units (Fig. 2.2) of around 300–400 m are associated with ongoing uplift (van der Hoeven et al. 2005; Schmitt et al. 2007) and suggest that the flexural rebound was associated with a process such as slab detachment in the East Carpathians after the Miocene collision (Wortel and Spakman 2000; Sperner et al. 2001).

In contrast, the external parts of the SE and South Carpathians display atypical foredeep geometries (Fig. 2.3b, c). Foredeep wedges are observed in Upper Miocene (Middle–Upper Sarmatian) sediments in the frontal part of the Getic Depression and at high depths beneath the Focșani Basin (e.g. Fig. 2.3c, see also Tărăpoancă et al. 2003; Krézsek et al. 2013 and references therein). These wedges are overlain by a thick latest Miocene–Quaternary mostly post-tectonic sedimentation. This sedimentation is part of a large basin that overlies the Moesian Platform and segments of the thin-skinned nappes of the SE Carpathians and Getic Depression (Fig. 2.2, the Dacian Basin of Jipa and Olariu 2009) and was driven by the continuous subsidence of the Moesian platform in post-collisional times (Matenco et al. 2003, 2007). This subsidence is responsible for the low and flat topography that presently dominates the relief in most of the Dacian Basin.

The driving mechanisms of this subsidence cannot be, yet again, quantified by the study of the upper crustal structural geometries of the Moesian platform, but it is certainly driven by the evolution of the Vrancea slab. Modern high-resolution local tomography and modelling studies (Martin and Wenzel 2006) have demonstrated that the high-velocity anomaly often associated with the Vrancea slab is much larger, extending from the SE Carpathians in a SW-ward direction well beneath the Moesian platform, and can be divided in two segments. While the Vrancea segment is (bearly) still attached, the anomaly beneath the Moesian platform is apparently detached from the Moesian lithosphere (Heidbach et al. 2007). This is a typical geometry that in other similar collisional settings has been interpreted as a STEP (subduction-transform edge propagator) fault. Such lithospheric-scale structures have been often invoked in highly arcuated orogenic systems, such as in the formation of the Apennines (Govers and Wortel 2005). In the case of the South and SE Carpathians, this mechanism implies that a lithospheric tear in the Carpathians subducting slab propagated along the South Carpathians during Miocene—Quaternary times, eventually arriving in the present-day configuration. Such a hypothesis is still speculative and requires a better understanding of the coupling between mantle dynamics and near-surface deformation (Ismail-Zadeh et al. 2012).

Limited to the SE Carpathians area located between the Intramoesian and Trotuș faults and their WNW-ward prolongation (Fig. 2.2), one other mechanism is juxtaposed over the longer term pattern of subsidence, the latter reaching extreme

values in the centre of the Focșani Basin (~6 km of Upper Miocene–Quaternary sediments, Fig. 2.3b). Large-scale differential vertical motions were recorded during late Pliocene—Quaternary times by ~5 km of uplift of the external Carpathians nappes and up to 2 km of subsidence in the neighbouring Focșani Basin, which accommodated a total amount of shortening in the order of 5 km (Leever et al. 2006b; Mațenco et al. 2007; Necea 2010). This process is still active today: outside the well-known intermediate mantle Vrancea earthquakes (Ismail-Zadeh et al. 2012 and references therein), there is a direct correlation between crustal seismicity and activity of recent faults derived from geophysical or neotectonic studies. Crustal seismicity correlates with thick-skinned thrusting beneath the external nappes of the SE Carpathians (Bocin et al. 2009) and with the activation of the large array of normal faults farther in the foreland (Mațenco et al. 2007), most likely genetically related with the 2013 seismicity of the Galați area.

These studies are important for prediction of natural hazards, such as seismicity or flooding. For instance, the correlation of active faulting with the vertical movements derived from GPS studies resulted in predicting the evolution of areas threatened by flooding in the foreland of the SE Carpathians (Fig. 2.8). This prediction infers a clear pattern of acceleration of flooding and rivers instability, which is in agreement with existing geomorphological studies (Rădoane et al. 2003).

The Extension and Inversion of the Pannonian Basin

The Pannonian Basin is made up of a large number of Miocene (half-)grabens distributed in a wide area, from the Apuseni Mountains to the Alps in the west, Western Carpathians in the north and Dinarides in the south. A transect connecting the Apuseni Mountains with the SE part of the basin (Fig. 2.9) indicates that the extensional mechanics was asymmetric and the deformation migrated in space and time across the basin, from Early Miocene to early Pontian (20 Ma or older to ~8.5 Ma, Mațenco and Radivojević 2012). The asymmetry is reflected by the formation of large-scale crustal detachments that accommodated the local formation of core complexes with significant footwall exhumation These structures are well documented near the Dinarides (Ustaszewski et al. 2010; Stojadinovic et al. 2013; Toljić et al. 2013) or speculated near the South Carpathians and Apuseni Mountains (such as the Makó–Tomnatec trough, Fig. 2.9, or the Békés Basin, Tari et al. 1999; Magyar et al. 2006; Balázs et al. 2016). In this area, the extension started near the Dinarides during Early Miocene times, continued everywhere in the basin during the Middle Miocene and finished in the area close to the Apuseni Mountains and South Carpathians during the late Miocene (Fig. 2.9).

The first and last stages of extension were associated with the formation of detachments and half-grabens, while the second Middle Miocene stage of extension was more symmetric, resulting in the widespread formation of grabens across the

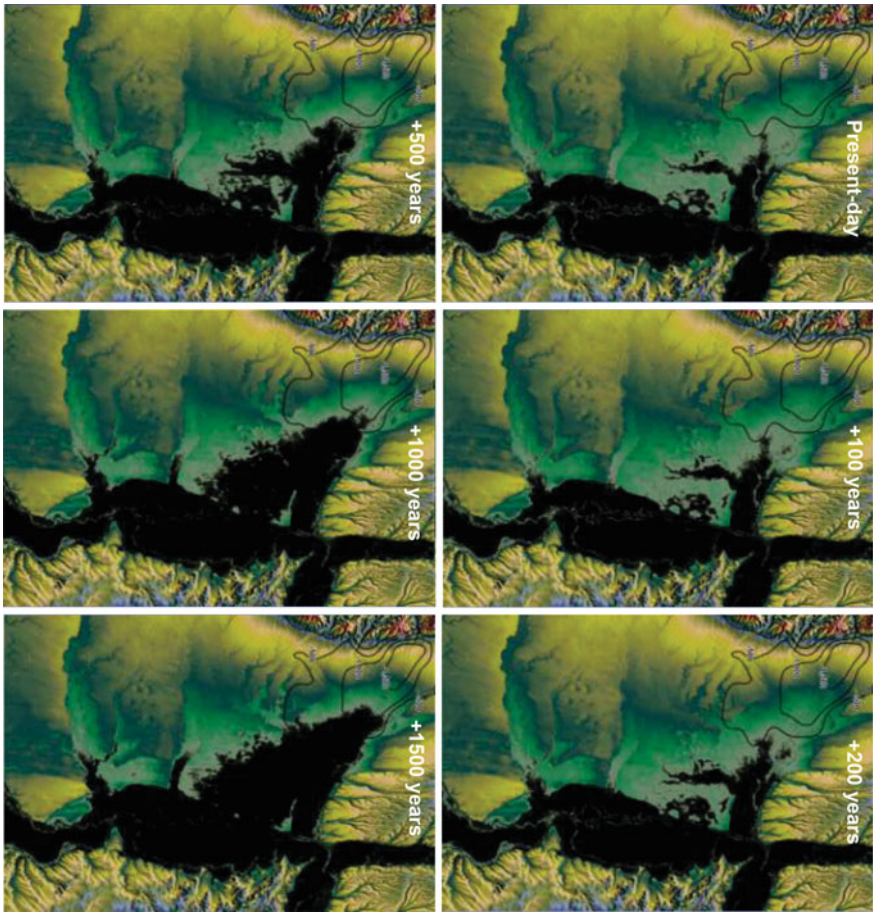

Fig. 2.8 Model prediction of the evolution of areas threatened by flooding in the SE Carpathians by correlating vertical movements derived from GPS studies in the Carpathians foreland (van der Hoeven et al. 2005) with active faulting patterns (see Matenco et al. 2007 for further details)

basin (Matenco and Radivojević 2012). The last, late Miocene (Pannonian–Early Pontian) stage of extension was associated with the large-scale mantle lithospheric thinning and the formation of the astenospheric upraise that is presently still observed beneath the Pannonian Basin (Horváth et al. 2006, 2015). The variability of the Miocene extensional mechanics is observed in the Miocene extensional basin cross-cutting the western margin of the Apuseni Basin and their W-ward prolongation (Fig. 2.2): the Middle Miocene Beiuș Basin is a roughly symmetric graben, while the Borod, Zarand Basins and Tomnatec Depression are highly asymmetric and are associated with footwall uplift during extension (Dinu et al. 1991; Răbăgia 2009; Matenco and Radivojević 2012).

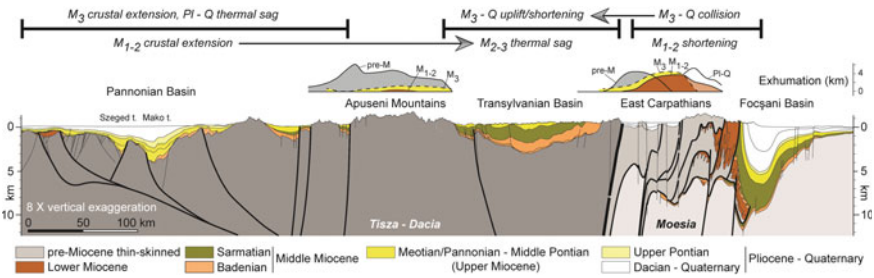

Fig. 2.9 Simplified geological cross section across the SE part of the Pannonian Basin, Apuseni Mountains, Transylvanian Basin and SE Carpathians and amounts of exhumation over the Apuseni Mountains and SE Carpathians derived from low-temperature thermochronology (modified from Matenco and Radivojević 2012). The geological cross section displays only Miocene–Quaternary sediments geometries and faults patterns. All pre-Miocene structures were ignored. The location of the cross section is displayed in Fig. 2.1. pre-*M* = pre-Miocene; M_1 = Early Miocene; M_2 = Middle Miocene; M_3 = Late Miocene; Pl = Pliocene; *Q* = Quaternary

The latest Miocene–Quaternary inversion of the Pannonian Basin driven by the indentation/subduction of the Adriatic promontory has created thrusting near the Dinaridic margin, associated with transcurrent (both transpressional and transtensional) deformation observed in the basin centre and to the NE (Fodor et al. 2005; Pinter et al. 2005; Bada et al. 2007). The effects of this inversion are fairly reduced in the eastern Dinarides near the South Carpathians and Apuseni Mountains, being limited to the formation of either positive flower structures with uplift in the order of few hundred metres (e.g. Fruska Gora on the flank of the city of Novi Sad in Serbia, Toljić et al. 2013), or small-scale transtensional structures with similar offsets (such as the Derecske Trough west of the Apuseni Mountains, Windhoffer and Bada 2005). Quaternary uplift of the Apuseni Mountains is suggested by deep river incisions with highly elevated terrace systems (such as on the NE flank of the Borod Basin) and non-equilibrated river network (Dombrádi et al. 2007), but this uplift must be below the resolution of AHe thermochronometer ($\sim$1 km given the high geothermal gradient).

Mechanics of Continental Collision and Large-Scale Evolution of Topography

All available studies suggest that the Miocene slab retreat/roll-back of the Carpathians slab was accommodated by extension in the Pannonian Basin. The extension was accompanied by different translational and rotational kinematics in the two intra-Carpathians ALCAPA and Tisza–Dacia blocks during Paleogene—Miocene times (counterclockwise and clockwise, respectively, Csontos 1995; Ustaszewski et al. 2008). The Miocene roll-back of the Romanian Carpathians was accommodated almost entirely in the Tisza–Dacia sector of the chain, the contact

with ALCAPA being somewhere in the Maramureş Piennides and the Bogdan Vodă—Dragoş Vodă fault system, Figs. 2.1 and 2.2). In this Tisza–Dacia sector of the chain, balanced cross sections and various reconstructions have inferred a total amount of shortening in the external Carpathians in the order of 120–160 km, increasing from north to south (Roure et al. 1993; Ellouz et al. 1994; Morley 1996). The amount of back-arc extension in the Tisza–Dacia sector of the Pannonian Basin is variable due to coeval clockwise rotational kinematics, decreasing from the contact with ALCAPA along the Mid-Hungarian Shear Zone towards the SE junction between the South Carpathians and Dinarides (Fig. 2.1). Available estimates indicate total amount of extension in the order of 140–180 km near the Mid-Hungarian Shear Zone (Lenkey 1999; Ustaszewski et al. 2008). These estimates of coeval Miocene extension and contraction are similar, which means that there was no large-scale absolute plate motion involved in the Carpathians shortening. In other words, the continental unit composed by the Apuseni Mountains, Transylvanian Basin, East, SE and South Carpathians simply rotated clockwise and moved E-wards into the Carpathian embayment, driven solely by pull and sink of the slab roll-back, collapsing the Pannonian Basin in the back and shortening the Carpathians in front (Fig. 2.9). There was no other driving force pushing or otherwise moving this continental unit E-wards, in agreement with the overall N-wards movement of Africa relative to Europe during Miocene times. Or, otherwise said, the mantle lithosphere of the Carpathians embayment simply sank into the asthenosphere and pulled the Romanian Carpathians E-wards.

Such a simple translation process of continental units, collapsing by extension the back-arc and shortening the foreland, is not unique. It is also interpreted in most of other highly curved Mediterranean orogens. For instance, the W-wards movement of the Betics–Rif system was accommodated by Miocene shortening at the exterior and coeval extensional collapse of the Alboran Domain, driven by the roll-back of the Gibraltar slab, while Africa–Iberia convergence was N–S to NE–SW oriented (Vergés and Fernàndez 2012). The W-wards movement of the Calabrian slab was accommodated by Oligocene—Quaternary shortening at the exterior of the Apennines and coeval back-arc extension and opening of the oceanic Liguro–Provencal and Tyrrhenian domains of the Western Mediterranean. In both situations, the velocity of roll-back was almost one order of magnitude higher than the slow N–S approach of Africa relative to Europe/Iberia (Faccenna et al. 2005, 2014). One other much larger example is the ~900 km of S-ward translation of Aegean units that was accompanied by ~500 km of N–S Europe—Africa convergence, while the amount of subducted material in the mantle is in the order of 1500 km (van Hinsbergen et al. 2005; Jolivet and Brun 2010).

Mechanics of Collision in the Romanian Carpathians

What is unique in the Romanian Carpathians is the location of the Miocene extensional back-arc, situated at far distances from the contractional plate margin.

Therefore, the successive amounts of shortening and associated exhumation are preserved and can be quantified to derive the mechanics of collision during roll-back. The link between exhumation and kinematics can be analysed along a transect from the Pannonian Basin to the SE Carpathians, i.e. towards the place where the slab is still preserved beneath the orogen in the Vrancea area (Fig. 2.9). Note that this transect is based only on the latest Cretaceous—Quaternary AFT and AHe data (Merten et al. 2010, 2011) and, therefore, indicate only low-temperature exhumation. This transect excludes strain partitioning at transcurrent structures, such as in the South Carpathians or Bogdan Vodă—Dragoș Vodă fault system of the East Carpathians. It also excludes the exhumation associated with intra-Carpathians deformation, such as the late Oligocene—Early Miocene thrusting of ALCAPA over Tisza–Dacia or the late Early Cretaceous collision between Tisza and Dacia and the emplacement of the Transylvanides nappes. However, it does not exclude reactivations of the latter contacts.

The distribution of pre-Miocene (latest Cretaceous–Paleogene) values (Fig. 2.9) indicates large-scale exhumation of the Apuseni Mountains and more reduced values at the western termination of the SE Carpathians, in the Bucovinian nappes and neighbouring Ceahlău–Severin units. Although such data are missing in the Transylvanian Basin, the overall pattern indicates a gradual increase of exhumation values towards the hinterland. All available kinematic data in the Apuseni Mountains, Transylvania Basin and East/SE Carpathians generally agree that the successive latest Cretaceous–Paleogene deformation events have the same kinematics and therefore are driven by the subduction that took place at the exterior of the Carpathians. This points towards large-scale exhumation increasing towards the Carpathians hinterland during the pre-Miocene, i.e. pre-roll-back times.

The pattern of exhumation changed once the roll-back started during the Early Miocene by the onset of simple translations and rotations of the Romanian Carpathians (Fig. 2.9). The Apuseni Mountains stopped their enhanced tectonic uplift and remained relatively stable and the low amounts of exhumation recorded are likely related to the erosional breakdown of an elevated topography. The entire Miocene exhumation took place in the external Carpathians thin-skinned nappes (or Moldavides, sensu Săndulescu 1988). The combination between low-temperature thermochronology and kinematics infers that individual moments of nappe accretion created exhumation in their immediate hinterland, but the overall Miocene exhumation migrated foreland-wards (Fig. 2.10b). The involvement of buoyant non-thinned platform units in the subduction zone during the late Miocene, possibly accompanied by slab detachment, stopped this process in the East Carpathians, exhumation being shifted backwards in the orogenic core between 11 and 8 Ma. By contrast, the foreland-ward exhumation migration continued in the SE Carpathians, driven by the thick-skinned accretion of blocks from the lower Moesian plate. The transition from thin- to thick-skinned enhanced the exhumation as the $\sim$5 km recorded during the Pliocene–Quaternary has the highest rate in the post-Paleogene history.

A comparison of Carpathians kinematics with a “standard” double-vergent orogen helps to understand the significance of this orogenic mechanics (Fig. 2.10).

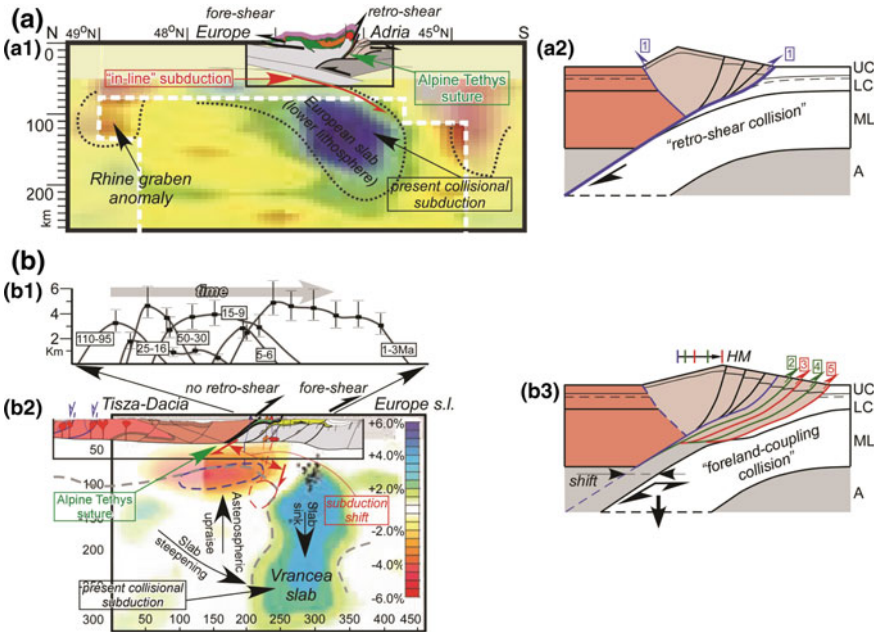

Fig. 2.10 Illustration of the concept of orogenic collision in two types of end-members orogens. **a** Tectonic cross section overlain by teleseismic mantle tomography (*a1*) along a transect crossing the Central Alps (simplified from Lippitsch et al. 2003; Schmid et al. 2004) and cartoon (*a2*) of the envisaged mechanical model of double-vergent orogenic collision (adapted from Willett and Brandon 2002). **b** Tectonic cross section overlain by teleseismic mantle tomography (*a2*) along a transect crossing the Apuseni Mountains and SE Carpathians (modified from Martin and Wenzel 2006; Matenco et al. 2010) and cartoon (*a3*) of the envisaged mechanical model of foreland-coupling collision (adapted from Matenco et al. 2010). The graph above the orogenic transect (*a1*) represents exhumation values and ages derived from thermochronology (compiled and simplified from Merten 2011). The exhumation data infer that exhumation migrates in time towards the foreland in the foreland-coupling collision of the Carpathians. This is in contrast with nested exhumation ages that characterize double-vergent orogens at steady state

The N–S Europe—Africa convergences have created one of the most studied orogens in the world, the Alps (Fig. 2.10a). The Middle Jurassic opening of the Alpine Tethys was followed by a prolonged history of oceanic subduction during Cretaceous—Eocene times, including the accretion of intervening Brianconnais domain (Schmid et al. 2004 and references therein). The beginning of collision with the European lower plate starting with Oligocene times is marked by the onset of deformation in the Southern Alps retro-wedge (such as illustrated in the NFP20 East profile, simplified in Fig. 2.10a1, Schmid et al. 1996). The onset of collision enhanced the exhumation along the Periadriatic lineament (the Insubric segment in Fig. 2.10a1), while the exhumation is reduced N-wards (e.g. Rosenberg and Berger 2009). The subsequent Miocene–Quaternary deformation takes place dominantly in the Southern Alps, including the lower crustal indentation of Adria (Fig. 2.10a1).

This illustrates a typical retro-wedge collision where continental material entering collision zone is exhumed by retro-shears in the hinterland by an opposite polarity deformation (Fig. 2.10b, Schmid et al. 1996; Willett et al. 2006). The resulting position of the subducted slab shows almost perfect alignment with the crustal geometry of subducted Europe (Fig. 2.10a1, Lippitsch et al. 2003).

At the other extreme, there is no retro-wedge deformation in the Romanian Carpathians during the Miocene collision (Fig. 2.10b2). Exhumation is localized over the thin-skinned wedge and shows a general pattern of migration in time towards the foreland (Fig. 2.10b1). The high-velocity anomaly of the Vrancea slab is shifted with 70–100 km towards the foreland from the correct position of the oceanic suture zone between Dacia and Moesia. This shift is the result of the thick-skinned accretion of continental blocks during the Miocene–Quaternary collision. In mechanical terms, this means that material is gradually accreted from the lower plate during collision (Fig. 2.10b3), but the rapid roll-back does not allow large-scale exhumation in upper crustal retro-shears and remains at depth. Such a process creates mechanical decoupling and migration of the slab towards the foreland, which may be associated with processes such as lithospheric delamination or lithospheric instability (Cloetingh et al. 2004; Duretz and Gerya 2013). The continental accretion of material in the lowed plate during roll-back collision is called foreland-coupling collision, as defined in the Romanian Carpathians (Mațenco et al. 2010).

Inferences for the Tectonic Age of Romanian Carpathians Topography

The mode of collision has direct implication for the present-day distribution of topography in orogens such as the Romanian Carpathians. As explained above, defining tectonic topographic ages is highly qualitative, but helps understanding the last significant tectonic event responsible for the creation of present-day relief. Such a map was defined for the Romanian Carpathians in a landmark study (Fig. 2.11, Merten 2011). This map ignores exhumation processes at higher resolution than AHe closure temperature, which is in the order of 1 km for the Miocene evolution of the Apuseni Mountains and $\sim$2 km elsewhere.

The overall topography of the Apuseni Mountains is the result of latest Cretaceous–Paleogene shortening moments that locally reactivated the inherited Tisza–Dacia contact (Fig. 2.11). This is expressed by the formation of the large Bihor dome and deformation along the Puini Fault system during latest Cretaceous —Middle Eocene times in the Apuseni Mountains and the NW part of the Transylvanian Basin. Renewed Middle Eocene–Oligocene contraction reactivated the Puini thrust and exhumed its hanging-wall at the eastern margin of the Apuseni Mountains. This is coeval with the thrusting of the Mezeș Mountains and their southern prolongation over sediments of the Transylvanian Basin (Fig. 2.11).

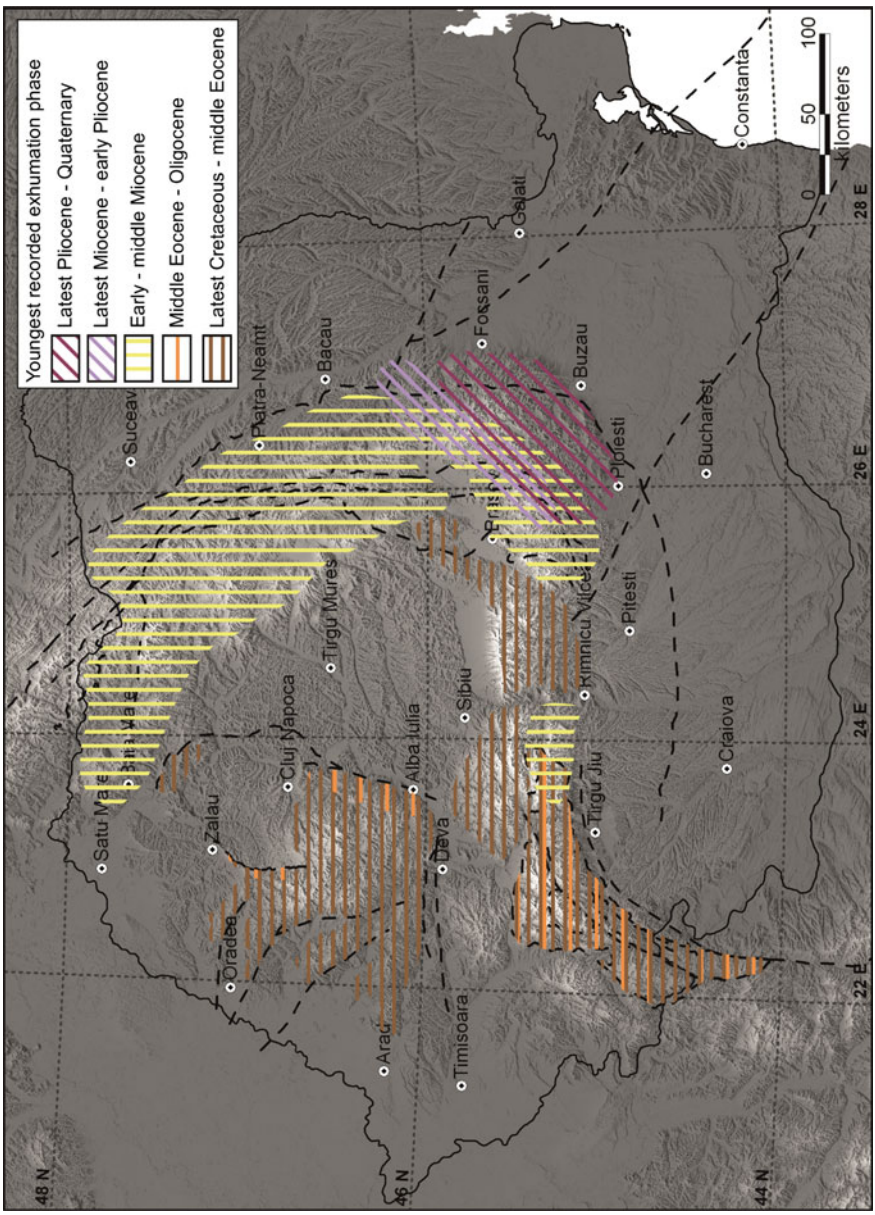

Fig. 2.11 Topographic map of Romanian Carpathians showing the age of the youngest tectonic exhumation phase (after Merten 2011), inferring the tectonic age of topographic relief. The bulk of the present-day topography in the areas of the Apuseni Mountains and South Carpathians were formed during latest Cretaceous—Paleogene times. Only a limited area in the centre of the South Carpathians indicates enhanced Miocene exhumation. The present-day topography of the entire East and SE Carpathians is the result of post-Paleogene exhumation events. The bulk of this exhumation is Miocene, being overprinted by a younger latest Miocene–Quaternary exhumation event that was restricted to the external areas of the SE Carpathians

The South Carpathians topography reflects dominantly the Latest Cretaceous—Paleogene moments of (Supra-)Getic/Danubian nappe stacking and the subsequent orogen parallel extension and transcurrent deformation along the Cerna fault (Figs. 2.2 and 2.11). Most of the Getic–Supragetic nappes in the eastern hanging-wall of the extensional detachment have a topography that is inherited from the latest Cretaceous nappe stacking and subsequent erosional breakdown. The western part of the South Carpathians displays mixed latest Cretaceous—Paleogene topography ages. Note that the overprinting Miocene exhumation in this western area is too localized to be visible in the map in Fig. 2.11. However, the Miocene exhumation has overprinted the central—southern part of the South Carpathians, most likely coeval with the formation of the Ocnele Mari–Govora anticline (Figs. 2.2 and 2.3c, Răbăgia et al. 2011). The present-day topography of the Transylvanian Basin was influenced by the Miocene moments of uplift in the neighbouring mountain chains and was ultimately established towards the end of the Miocene times by the exhumation of the basin at the ~600 m maximum present elevation of Pannonian sediments. It is one of the most spectacular examples of dynamic topography in Europe.

The topography in the East and SE Carpathians is certainly inherited from Miocene times, where 4–6 km of total exhumation has overprinted all earlier events (Fig. 2.11). The topography in the external part of the SE Carpathians has been subsequently established during the two latest Miocene–Early Pliocene and latest Pliocene–Quaternary exhumation events. The overall migration of this exhumation in a foreland direction is visible in topography by the migration of the water divides, deflection of rivers and high topographic non-equilibrium (Rădoane et al. 2003; Leever 2007; ter Borgh 2013).

Conclusions

Deriving the mechanics of continental collision is of fundamental importance to understand processes driving the topographic expression of orogens. Romanian Carpathians provide a key location for understanding mechanics of collision during slab retreat because the genetically associated back-arc extension is situated at far distances and did not overprinted the nappe stacking, which is often observed elsewhere. Our review of available kinematic and low-temperature thermochronological data infers that collisional mechanics during roll-back is significantly different when compared with high-convergence orogens, such as the Alps or the Pyrenees. In most roll-back orogens, the large amount of subducted material observed by high-velocity anomalies in teleseismic tomography studies is derived from the passive translation of the upper plate accommodated by back-arc extension. In our studied case, there were no absolute plate motions during Miocene—Quaternary times, the entire subduction and accretion at the exterior of the orogen was accommodated by back-arc extension and the continental block of the Romanian Carpathians simply rotated clockwise and translated E-wards into the

Carpathians embayment. The exhumation pattern changed with time, from enhanced in hinterland during pre-roll-back times to focused near or in the thin-skinned wedge during roll-back. The latter is characterized by gradual accretion of sediments or continental basement derived from the lower subducting plate. This material was not exhumed in retro-wedges as is the common case of double-vergent orogens, but remained at high depths and, therefore, shifted the location of the main subduction zone towards the foreland. This process is called foreland-coupling collision and near the topographic surface induces exhumation that migrates towards the foreland with gradually increased values due to the transition from thin-skinned to thick-skinned thrusting.

This type of collision has significant inferences for the topographic evolution of the Romanian Carpathians. The present topographic expression of Apuseni Mountains is inherited from pre-roll-back times, when the exhumation was higher at farther distances in the hinterland of the subduction zone. The topography of the East and SE Carpathians is inherited from the moments of roll-back collision that shifted exhumation to the vicinity of the main subduction zone. The migration of exhumation towards the foreland continued during Pliocene—Quaternary times and is still active, modifying the present-day topography in the SE Carpathians. The Transylvanian Basin is one of the best examples of dynamic topography, i.e. near-surface movements induced by deep mantle processes, both during its initial Middle–Late Miocene subsidence and during the exhumation of the basin towards the end of Miocene times. The kinematics and exhumation of the South Carpathians were driven by the coupled rotational–translational movements of the Tisza–Dacia unit into the Carpathians embayment.

All these findings demonstrate the strong coupling between deep-Earth and near-surface processes. Their understanding is of fundamental importance for the evolution of continental topography and mitigation of geo-hazards.

Acknowledgments This review study is based on the long-term commitment of the Netherlands Research Centre for Integrated Solid Earth Science (ISES) for understanding the kinematics and exhumation in the Romanian Carpathians. Numerous PhD students and postdoctoral fellows have worked in this line of research, among which relevant for this study are Carlo Sanders, Mihai Tărăpoancă, Csaba Krezsek, Traian Răbăgia, Karen Leever, Andrei Bocin, Sandra Merten, Marten ter Borgh and Ioan Munteanu. In particular, Sandra Merten has a fundamental contribution in understanding the exhumation of such an orogen with low amounts of exhumation. Paul Andriessen and Sierd Cloetingh are acknowledged for their long-term collaboration and involvement.

References

Bada G, Horváth F, Dövényi P, Szafián P, Windhoffer G, Cloetingh S (2007) Present-day stress field and tectonic inversion in the Pannonian basin. Global Planet Change 58(1–4):165–180

Balázs A, Matenco L, Magyar I, Horváth F, Cloetingh S (2016) The link between tectonics and sedimentation in back-arc basins: new genetic constraints from the analysis of the Pannonian Basin. Tectonics 35(6):1526–1559. doi:10.1002/2015TC004109

Balintoni I (1996) Transilvanidele vestice, comentarii structurale. Studia Universitas Babeş-Bolyai Seria Geologia XLI(1):95–100 (in Romanian)

Balintoni I, Balica C, Ducea MN, Chen FK, Hann HP, Sabliovschi V (2009) Late Cambrian-Early Ordovician Gondwanan terranes in the Romanian Carpathians: a zircon U-Pb provenance study. Gondwana Res 16(1):119–133. doi:10.1016/j.gr.2009.01.007

Balintoni I, Balica C, Ducea MN, Hann HP, Sabliovschi V (2010) The anatomy of a Gondwanan terrane: the neoproterozoic-Ordovician basement of the pre-Alpine Sebeş-Lotru composite terrane (South Carpathians, Romania). Gondwana Res 17(2–3):561–572. doi:10.1016/j.gr.2009.08.003

Balla Z (1986) Palaeotectonic reconstruction of the central Alpine-Mediterranean belt for the Neogene. Tectonophysics 127(3–4):213–243

Beaumont C (1981) Foreland basins. Geophys J Roy Astron Soc 65:291–329

Beaumont C, Fullsack PH, Hamilton J (1994) Styles of crustal deformation in compressional orogens caused by subduction of the underlying lithosphere. Tectonophysics 232:119–132

Beaumont C, Munoz JA, Hamilton J, Fullsack P (2000) Factors controlling the Alpine evolution of the central Pyrenees inferred from a comparison of observations and geodynamical models. J Geophys Res 105(B4):8121–8145

Bertotti G, Matenco L, Cloetingh S (2003) Vertical movements in and around the SE Carpathian foredeep: lithospheric memory and stress field control. Terra Nova 15:299–305

Berza T, Drăgănescu A (1988) The Cerna-Jiu fault system (South Carpathians, Romania), a major Tertiary transcurrent lineament. DS Inst Geol Geofiz 72–73:43–57

Berza T, Kräutner HG, Dimitrescu R (1983) Nappe structure of the Danubian window of the central South Carpathians. An Inst Geol Geofiz 60:31–34

Bocin A, Stephenson R, Tryggvason A, Panea I, Mocanu V, Hauser F, Matenco L (2005) 2.5D seismic velocity modelling in the south-eastern Romanian Carpathians Orogen and its foreland. Tectonophysics 410(1–4):273–291

Bocin A, Stephenson R, Mocanu V, Matenco L (2009) Architecture of the south-eastern Carpathians nappes and Focşani basin (Romania) from 2D ray tracing of densely-spaced refraction data. Tectonophysics 476(3–4):512–527

Bocin A, Stephenson R, Matenco L, Mocanu V (2013) Gravity and magnetic modelling in the Vrancea zone, south-eastern Carpathians: redefinition of the edge of the East European Craton beneath the south-eastern Carpathians. J Geodyn 71:52–64. doi:10.1016/j.jog.2013.08.003

Bojar AV, Neubauer F, Fritz H (1998) Jurassic to Cenozoic thermal evolution of the southwestern South Carpathians: evidence from fission-track thermochronology. Tectonophysics 297(1–4):229–249

Brandon MT, Vance JA (1992) Tectonic evolution of the Cenozoic Olympic subduction complex, Washington State, as deduced from fission track ages for detrital zircons. Am J Sci 292(8):565–636

Braun J, van der Beek P, Batt G (2012) Quantitative thermochronology numerical methods for the interpretation of thermochronological data. Cambrige University Press, London

Braun J, Simon-Labric T, Murray KE, Reiners PW (2014) Topographic relief driven by variations in surface rock density. Nat Geosci 7(7):534–540. doi:10.1038/ngeo2171

Brun J-P, Faccenna C (2008) Exhumation of high-pressure rocks driven by slab rollback. Earth Planet Sci Lett 272(1–2):1–7

Brun J-P, Sokoutis D (2010) 45 m.y. of Aegean crust and mantle flow driven by trench retreat. Geology 38(9):815–818

Burchfiel BC, Bleahu M (1976) Geology of Romania. Geological Society of America Special Paper, vol 158

Burov E (2007) Coupled lithosphere-surface processes in collision context. In: Lacombe O, Lave J, Roure F, Verges J (eds) Thrust belts and Foreland Basins. From fold kinematics to hydrocarbon systems. Springer, Berlin, pp 3–40

Burov E, Yamato P (2008) Continental plate collision, P-T-t-z conditions and unstable vs. stable plate dynamics: insights from thermo-mechanical modelling. Lithos 103(1–2):178–204

Cawood PA, Kroner A, Collins WJ, Kusky TM, Mooney WD, Windley BF (2009) Accretionary orogens through Earth history. Geol Soc London Spec Publ 318(1):1–36

Ciulavu M, Mahlmann RF, Schmid SM, Hofmann H, Seghedi A, Frey M (2008) Metamorphic evolution of a very low- to low-grade metamorphic core complex (Danubian window) in the South Carpathians. Geol Soc London Spec Publ 298(1):281–315

Ciupagea D, Pauca M, Ichmir T (1970) Geologia bazinului Transilvaniei. Bucureşti (in Romanian)

Cloetingh SAPL, Burov E, Maţenco L, Toussaint G, Bertotti G, Andriessen PAM, Wortel MJR, Spakman W (2004) Thermo-mechanical controls on the mode of continental collision in the SE Carpathians (Romania). Earth Planet Sci Lett 218(1–2):57–76

Csontos L (1995) Tertiary tectonic evolution of the Intra-Carpathian area: a review. Acta Vulcanol 7:1–13

Csontos L, Vörös A (2004) Mesozoic plate tectonic reconstruction of the Carpathian region. Palaeogeogr Palaeoclimatol Palaeoecol 210(1):1–56

Dallmeyer DR, Pana DI, Neubauer F, Erdmer P (1999) Tectonothermal evolution of the Apuseni mountains, Romania: resolution of Variscan versus Alpine events with $^{40}Ar/^{39}Ar$ ages. J Geol 107:329–352

de Broucker G, Mellin A, Duindam P (1998) Tectono-stratigraphic evolution of the Transylvanian basin, pre-salt sequence, Romania. In: Dinu C, Mocanu V (eds) Geological structure and hydrocarbon potential of the Romanian areas, vol 1. BGF Special Volume no. 1. Bucharest, pp 36–69

de Leeuw A, Bukowski K, Krijgsman W, Kuiper KF (2010) Age of the Badenian salinity crisis; impact of Miocene climate variability on the circum-Mediterranean region. Geology 38 (8):715–718

Dewey JF (1980) Episodicity, sequence and style at convergent plate boundaries. In: Strangway DW (ed) The continental crust and its mineral deposits, vol Special Paper 20. Geological Association Canada, Waterloo, Ontario, pp 553–573

Dimitrijević MD (1997) Geology of Yugoslavia, 2nd edn. Geoinstitute, Belgrade, Belgrade

Dinu C, Calotă C, Mocanu V, Ciulavu D (1991) Geotectonic setting and the particular structural features of the Beius basin, on the basis of geological and geophysical data systhesis. Revue Roumaine de Geophysique 35:77–87

Doglioni C, Carminati E, Cuffaro M, Scrocca D (2007) Subduction kinematics and dynamic constraints. Earth Sci Rev 83(3–4):125–175

Dombrádi E, Timár G, Bada G, Cloetingh S, Horváth F (2007) Fractal dimension estimations of drainage network in the Carpathian-Pannonian system. Global Planet Change 58(1–4):197–213

Duretz T, Gerya TV (2013) Slab detachment during continental collision: influence of crustal rheology and interaction with lithospheric delamination. Tectonophysics 602:124–140. doi:10.1016/j.tecto.2012.12.024

Ellouz N, Roca E (1994) Palinspastic reconstructions of the Carpathians and adjacent areas since the Cretaceous: a quantitative approach. In: Roure F (ed) Peri-Tethyan platforms. Editions Technip, Paris, pp 51–78

Ellouz N, Roure F, Săndulescu M, Badescu D (1994) Balanced cross sections in the Eastern Carpathians (Romania): a tool to quantify Neogene dynamics. In: Roure F, Ellouz N, Shein VS, Skvortsov I (eds) Geodynamic evolution of sedimentary basins, International symposium Moskow 1992 Proceedings. Technip, Paris, pp 305–325

England P, Molnar P (1990) Surface uplift, uplift of rocks, and exhumation of rocks. Geology 18 (12):1173–1177

Faccenda M, Minelli G, Gerya TV (2009) Coupled and decoupled regimes of continental collision: numerical modeling. Earth Planet Sci Lett 278(3–4):337–349

Faccenna C, Piromallo C, Crespo-Blanc A, Jolivet L, Rosetti F (2004) Lateral slab deformation and the origin of the western Mediterranean arcs. Tectonics 23:TC1012. doi:10.1029/2002TC001488

Faccenna C, Civetta L, D'Antonio M, Funiciello F, Margheriti L, Piromallo C (2005) Constraints on mantle circulation around the deforming Calabrian slab. Geophys Res Lett 32:L06311. doi:10.01029/02004GL021874

Faccenna C, Becker TW, Miller MS, Serpelloni E, Willett SD (2014) Isostasy, dynamic topography, and the elevation of the Apennines of Italy. Earth Planet Sci Lett 407:163–174. doi:10.1016/j.epsl.2014.09.027

Farley KA (2000) Helium diffusion from apatite: general behavior as illustrated by Durango fluorapatite. J Geophys Res Solid Earth 105(B2):2903–2914

Favre P, Stampfli GM (1992) From rifting to passive margin: the examples of the Red Sea, Central Atlantic and Alpine Tethys. Tectonophysics 215(1–2):69–97. doi:10.1016/0040-1951(92)90075-H

Fielitz W, Seghedi I (2005) Late Miocene-quaternary volcanism, tectonics and drainage system evolution in the East Carpathians, Romania. Tectonophysics 410(1–4):111–136

Filipescu S, Gîrbacea R (1997) Lower Badenian sea-level drop on the western border of the Transylvanian basin: foraminiferal paleobathymetry and stratigraphy. Geol Carpath 48(5): 325–334

Fodor L, Csontos L, Bada G, Györfi I, Benkovics L (1999) Tertiary tectonic evolution of the Pannonian basin system and neighbouring orogens: a new synthesis of paleostress data. In: Durand B, Jolivet L, Horvath F, Seranne M (eds) The Mediteranean basins: tertiary extension within the Alpine orogen. The Geological Society, London, pp 295–334 (Geological Society, London, Special Publications no. 156)

Fodor L, Bada G, Csillag G, Horvath E, Ruszkiczay-Rudiger Z, Palotas K, Sikhegyi F, Timar G, Cloetingh S (2005) An outline of neotectonic structures and morphotectonics of the western and central Pannonian Basin. Tectonophysics 410(1–4):15–41

Fügenschuh B, Schmid SM (2005) Age and significance of core complex formation in a very curved orogen: evidence from fission track studies in the South Carpathians (Romania). Tectonophyiscs 404:33–53

Fuller CW, Willett SD, Brandon MT (2006) Formation of forearc basins and their influence on subduction zone earthquakes. Geology 34(2):65–68

Gleadow AJW, Duddy IR (1981) A natural long-term track annealing experiment for apatite. Nucl Tracks 5(1–2):169–174. doi:10.1016/0191-278X(81)90039-1

Govers R, Wortel MJR (2005) Lithospheric tearing at STEP faults: response to edges of subduction zones. Earth Planet Sci Lett 236:505–523

Gröger HR, Fugenschuh B, Tischler M, Schmid SM, Foeken JPT (2008) Tertiary cooling and exhumation history in the Maramures area (internal eastern Carpathians, northern Romania): thermochronology and structural data. Geol Soc London Spec Publ 298(1):169–195

Gröger HR, Tischler M, Fugenschuh B, Schmid SM (2013) Thermal history of the Maramureş area (Northern Romania) constrained by zircon fission track analysis: Cretaceous metamorphism and Late Cretaceous to Paleocene exhumation. Geol Carpath 64(5):383–398. doi:10.2478/geoca-2013-0026

Haas J, Péró C (2004) Mesozoic evolution of the Tisza Mega-unit. Int J Earth Sci V 93(2):297–313

Haq SSB, Davis DM (2008) Extension during active collision in thin-skinned wedges: insights from laboratory experiments. Geology 36(6):475–478

Hauser F, Raileanu V, Fielitz W, Dinu C, Landes M, Bala A, Prodehl C (2007) Seismic crustal structure between the Transylvanian Basin and the Black Sea, Romania. Tectonophysics 430 (1–4):1–25

Heidbach O, Ledermann P, Kurfeß D, Peters G, Buchmann T, Mațenco L, Negut M, Sperner B, Müller B, Nuckelt A, Schmitt G (2007) (Romanian Carpathians) Attached or not attached: slab dynamics beneath Vrancea, Romania. In: International Symposium on Strong Vrancea Earthquakes and Risk Mitigation, Bucharest, Romania, 4–6 Oct 2007, pp 4–20

Horváth F, Bada G, Szafian P, Tari G, Adam A, Cloetingh S (2006) Formation and deformation of the Pannonian Basin: constraints from observational data. Geol Soc London Mem 32(1): 191–206

Horváth F, Musitz B, Balázs A, Végh A, Uhrin A, Nádor A, Koroknai B, Pap N, Tóth T, Wórum G (2015) Evolution of the Pannonian basin and its geothermal resources. Geothermics 53:328–352. doi:10.1016/j.geothermics.2014.07.009

Iancu V, Berza T, Seghedi A, Gheuca I, Hann H-P (2005a) Alpine polyphase tectono-metamorphic evolution of the South Carpathians: a new overview. Tectonophysics 410(1–4):337–365

Iancu V, Berza T, Seghedi A, Maruntiu M (2005b) Palaeozoic rock assemblages incorporated in the South Carpathian Alpine thrust belt (Romania and Serbia): a review. Geologica Belgica 8 (4):48–68

Ionescu C, Hoeck V, Tomek C, Koller F, Balintoni I, Besutiu L (2009) New insights into the basement of the Transylvanian depression (Romania). Lithos 108(1–4):172–191

Ionesi L (1994) Geologia unităților de platformă și a orogenului Nord-Dobrogean. Ed. Tehnică, București (in Romanian)

Ismail-Zadeh A, Matenco L, Radulian M, Cloetingh S, Panza G (2012) Geodynamics and intermediate-depth seismicity in Vrancea (the south-eastern Carpathians): current state-of-the art. Tectonophysics 530–531:50–79. doi:10.1016/j.tecto.2012.01.016

Jipa DC, Olariu C (2009) Dacian basin: depositional architecture and sedimentary history of a Paratethys Sea. Geo-Eco-Marina Special publication no. 3. National Institute of Marine Geology and Geo-ecology, Bucharest

Jolivet L, Brun J-P (2010) Cenozoic geodynamic evolution of the Aegean. Int J Earth Sci 99 (1):109–138

Jolivet L, Faccenna C (2000) Mediterranean extension and the Africa-Eurasia collision. Tectonics 19(6):1095–1106. doi:10.1029/2000tc900018

Ketcham RA (2005) Forward and inverse modeling of low-temperature thermochronometry data. Rev Mineral Geochem 58:275–314

Ketcham RA, Donelick RA, Carlson WD (1999) Variability of apatite fission-track annealing kinetics; III, extrapolation to geological time scales. Am Miner 84(9):1235–1255

Kounov A, Schmid S (2013) Fission-track constraints on the thermal and tectonic evolution of the Apuseni Mountains (Romania). Int J Earth Sci 102(1):207–233. doi:10.1007/s00531-012-0800-5

Kounov A, Seward D, Burg J-P, Bernoulli D, Ivanov Z, Handler R (2010) Geochronological and structural constraints on the Cretaceous thermotectonic evolution of the Kraishte zone, western Bulgaria. Tectonics 29(2):TC2002. doi:10.1029/2009tc002509

Kräutner HG, Bindea G (2002) Structural units in the pre-Alpine basement of the Eastern Carpathians. Geol Carpath 53:143–146

Krautner HG, Krstic B (2003) Geological map of the Carpatho-Balkanides between Oravita-Nis and Sofia. Geoinstitut, Belgrade

Kreemer C, Holt WE, Haines AJ (2003) An integrated global model of present-day plate motions and plate boundary deformation. Geophys J Int 154(1):8–34. doi:10.1046/j.1365-246X.2003.01917.x

Krézsek C, Bally AW (2006) The Transylvanian Basin (Romania) and its relation to the Carpathian fold and thrust belt: insights in gravitational salt tectonics. Mar Pet Geol 23(4): 405–442

Krézsek C, Filipescu S (2005) Middle to late Miocene sequence stratigraphy of the Transylvanian Basin (Romania). Tectonophysics 410(1–4):437–463

Krézsek C, Filipescu S, Silye L, Matenco L, Doust H (2010) Miocene facies associations and sedimentary evolution of the Southern Transylvanian Basin (Romania): implications for hydrocarbon exploration. Mar Pet Geol 27(1):191–214

Krézsek C, Lăpădat A, Matenco L, Arnberger K, Barbu V, Olaru R (2013) Strain partitioning at orogenic contacts during rotation, strike–slip and oblique convergence: Paleogene-Early Miocene evolution of the contact between the South Carpathians and Moesia. Global Planet Change 103:63–81. doi:10.1016/j.gloplacha.2012.11.009

Krzywiec P (2001) Contrasting tectonic and sedimentary history of the central and eastern parts of the Polish Carpathian foredeep basin—results of seismic data interpretation. Mar Pet Geol 18:13–38

Leever KA (2007) Foreland of the Romanian Carpathians, controls on late orogenic sedimentary basin evolution and Paratethys paleogeography. PhD, VU University Amsterdam, Amsterdam

Leever KA, Bertotti G, Zoetemeijer R, Maenco L, Cloetingh SAPL (2006a) The effects of a lateral variation in lithospheric strength on foredeep evolution: implications for the East Carpathian foredeep. Tectonophysics 421(3–4):251–267

Leever KA, Matenco L, Bertotti G, Cloetingh S, Drijkoningen GG (2006b) Late orogenic vertical movements in the Carpathian Bend Zone—seismic constraints on the transition zone from orogen to foredeep. Basin Res 18(4):521–545. doi:10.1111/j.1365-2117.2006.00306.x

Lenkey L (1999) Geothermics of the Pannonian basin and its bearing on the tectonics of basin evolution. PhD, Vrije Universiteit, Amsterdam

Lippitsch R, Kissling E, Ansorge J (2003) Upper mantle structure beneath the Alpine orogen from high-resolution teleseismic tomography. J Geophys Res 108(B8). doi:10.1029/2002JB002016

Magyar I, Fogarasi A, Vakarcs G, Buko L, Tari G (2006) The largest hydrocarbon field discovered to date in Hungary: Algyo. In: Golonka J, Picha FJ (eds) The Carphathians and their foreland: geology and hydrocarbon resources, vol 84. AAPGMemoir, pp 619–632

Marotta AM, Fernandez M, Sabadini R (1998) Mantle unrooting in collisional settings. Tectonophysics 296(1–2):31–46

Martin M, Wenzel F (2006) High-resolution teleseismic body wave tomography beneath SE-Romania—II. Imaging of a slab detachment scenario. Geophys J Int 164(3):579–595

Maţenco L, Bertotti G (2000) Tertiary tectonic evolution of the external East Carpathians (Romania). Tectonophysics 316:255–286

Maţenco L, Radivojević D (2012) On the formation and evolution of the Pannonian Basin: constraints derived from the structure of the junction area between the Carpathians and Dinarides. Tectonics 31(6):TC6007. doi:10.1029/2012tc003206

Maţenco L, Schmid S (1999) Exhumation of the Danubian nappes system (South Carpathians) during the early tertiary: inferences from kinematic and paleostress analysis at the Getic/Danubian nappes contact. Tectonophysics 314:401–422

Maţenco L, Zoetemeijer R, Cloetingh S, Dinu C (1997) Lateral variations in mechanical properties of the Romanian external Carpathians: inferences of flexure and gravity modelling. Tectonophysics 282:147–166

Maţenco L, Bertotti G, Cloetingh S, Dinu C (2003) Subsidence analysis and tectonic evolution of the external Carpathian-Moesian platform region during Neogene times. Sed Geol 156(1–4):71–94

Maţenco L, Bertotti G, Leever K, Cloetingh S, Schmid S, Tărăpoancă M, Dinu C (2007) Large-scale deformation in a locked collisional boundary: interplay between subsidence and uplift, intraplate stress, and inherited lithospheric structure in the late stage of the SE Carpathians evolution. Tectonics 26(4):TC4011. doi:10.1029/2006TC001951

Maţenco L, Krézsek C, Merten S, Schmid S, Cloetingh S, Andriessen P (2010) Characteristics of collisional orogens with low topographic build-up: an example from the Carpathians. Terra Nova 22(3):155–165

Mathisen ME, Vondra CF (1983) The fluvial and pyroclastic deposits of the Cagayan Basin, Northern Luzon, Philippines—an example of non-marine volcaniclastic sedimentation in an Interarc Basin. Sedimentology 30(3):369–392

Medaris G, Ducea M, Ghent E, Iancu V (2003) Conditions and timing of high-pressure Variscan metamorphism in the South Carpathians, Romania. Lithos 70(3–4):141–161. doi:10.1016/s0024-4937(03)00096-3

Merten S (2011) Thermo-tectonic evolution of a convergent orogen with low-topographic build-up: exhumation and kinematic patterns in the Romanian Carpathians derived from thermochronology. VU University Amsterdam, Faculty of Earth and Life Sciences, Amsterdam

Merten S, Maţenco L, Foeken JPT, Stuart FM, Andriessen PAM (2010) From nappe stacking to out-of-sequence postcollisional deformations: cretaceous to quaternary exhumation history of the SE Carpathians assessed by low-temperature thermochronology. Tectonics 29(3):TC3013. doi:10.1029/2009tc002550

Merten S, Maţenco L, Foeken JPT, Andriessen PAM (2011) Toward understanding the post-collisional evolution of an orogen influenced by convergence at adjacent plate margins:

late Cretaceous—tertiary thermotectonic history of the Apuseni Mountains. Tectonics 30(6): TC6008. doi:10.1029/2011tc002887
Miclăuş C, Loiacono F, Puglisi D, Baciu D (2009) Eocene-Oligocene sedimentation in the external areas of the Moldavide basin (Marginal Folds Nappe, Eastern Carpathians, Romania): sedimentological, paleontological and petrographic approaches. Geol Carpath 60(5):397–417
Miclăuş C, Grasu C, Juravle A (2011) Sarmatian (Middle Miocene) Coastal deposits in the wedge-top depozone of the Eastern Carpathian Foreland basin system. A case study. Analele Stiintifice ale Universitatii "Al I Cuza" din Iasi Seria Geologie 57(1):75–90
Morley CK (1996) Models for relative motion of crustal blocks within the Carpathian region, based on restorations of the outer Carpathian thrust sheets. Tectonics 15(4):885–904
Naylor M, Sinclair HD (2008) Pro- vs. retro-foreland basins. Basin Res 20(3):285–303
Necea D (2010) High-resolution morpho-tectonic profiling across an orogen: tectonic-controled geomorphology and multiple dating approach in the SE Carpathians. PhD Thesis, VU University Amsterdam, Amsterdam
Necea D, Fielitz W, Kadereit A, Andriessen PAM, Dinu C (2013) Middle Pleistocene to Holocene fluvial terrace development and uplift-driven valley incision in the SE Carpathians, Romania. Tectonophysics 602:332–354. doi:10.1016/j.tecto.2013.02.039
Nicolae I, Saccani E (2003) Petrology and geochemistry of the Late Jurassic calc-alkaline series associated to Middle Jurassic ophiolites in the South Apuseni Mountains (Romania). Schweiz Mineral Petrogr Mitt 83:81–96
Okay AI, Sengor AMC, Gorur N (1994) Kinematic history of the opening of the Black Sea and its effect on the surrounding regions. Geology 22(3):267–270
Pană D, Erdmer P (1994) Alpine crustal shear zones and pre-Alpine basement terranes in the Romanian Carpathians and Apuseni Mountains. Geology 22(9):807–810
Paraschiv D (1997) The pre-Paratethys buried denudational surface in Romanian territory. Revue Roumaine de Géographie 41:21–32
Peryt TM (2006) The beginning, development and termination of the Middle Miocene Badenian salinity crisis in Central Paratethys. Sed Geol 188–189:379–396
Pharaoh TC (1999) Palaeozoic terranes and their lithospheric boundaries within the Trans-European Suture Zone (TESZ): a review. Tectonophysics 314:17–41
Pinter N, Grenerczy G, Weber J, Stein S, Medak D (2005) The Adria microplate: GPS geodesy, tectonics and hazards (Nato Science Series: IV: Earth and Environmental Sciences). Springer, Berlin
Platt JP (1986) Dynamics of orogenic wedges and the uplift of high-pressure metamorphic rocks. Geol Soc Am Bull 97(9):1037–1053
Răbăgia A-M (2009) Sequential Stratigraphic studies in the northern part of the Pannonian basin for deriving the tectono-stratigraphic evolution. PhD, University of Bucharest, Faculty of Geology and Geophysics, Bucharest
Răbăgia T, Matenco L (1999) Tertiary tectonic and sedimentological evolution of the South Carpathians foredeep: tectonic versus eustatic control. Mar Pet Geol 16(7):719–740
Răbăgia T, Matenco L, Cloetingh S (2011) The interplay between eustacy, tectonics and surface processes during the growth of a fault-related structure as derived from sequence stratigraphy: the Govora-Ocnele Mari antiform, South Carpathians. Tectonophysics 502(1–2):196–220. doi:10.1016/j.tecto.2009.09.017
Rădoane M, Rădoane N, Dumitriu D (2003) Geomorphological evolution of longitudinal river profiles in the Carpathians. Geomorphology 50(4):293–306
Ratschbacher L, Frisch W, Linzer HG, Merle O (1991) Lateral extrusion in the Eastern Alps; part 2, structural analysis. Tectonics 10(2):257–271
Ratschbacher L, Linzer HG, Moser F, Strusievicz RO, Bedelean H, Har N, Mogos PA (1993) Cretaceous to Miocene thrusting and wrenching along the central South Carpathians due to a corner effect during collision and orocline formation. Tectonics 12:855–873
Reiners PW, Brandon MT (2006) Using Thermochronology to understand orogenic erosion. Annu Rev Earth Planet Sci 34:419–466. doi:10.1146/annurev.earth.1134.031405.125202

Reiser MK, Schuster R, Spikings R, Tropper P, Fugenschuh B (2014) New age data and geothermobaric estimates from the Apuseni Mountains (Romania); evidence for Cretaceous amphibolite-facies metamorphism. Int J Earth Sci (submitted)

Ring U, Brandon MT, Willett SD, Lister GS (1999) Exhumation processes. In: Ring U, Brandon MT, Willett SD, Lister GS (eds) Exhumation processes, vol 154, pp 1–27 (Geological Society, London, Special Publications)

Rosenberg CL, Berger A (2009) On the causes and modes of exhumation and lateral growth of the Alps. Tectonics 28:doi:10.1029/2008tc002442

Roure F (2008) Foreland and Hinterland basins: what controls their evolution? Swiss J Geosci 101:5–29

Roure F, Choukroune P, Berastegui X, Munoz JA, Villien A, Matheron P, Bareyt M, Seguret M, Camara P, Deramond J (1989) Ecors deep seismic data and balanced cross sections: geometric constraints on the evolution of the Pyrenees. Tectonics 8(1):41–50. doi:10.1029/TC008i001p00041

Roure F, Roca E, Sassi W (1993) The Neogene evolution of the outer Carpathian flysch units (Poland, Ukraine and Romania); kinematics of a foreland/fold-and-thrust belt system. Sed Geol 86:177–201

Royden LH (1993) Evolution of retreating subduction boundaries formed during continental collision. Tectonics 12(3):629–638

Saintot A, Stephenson RA, Stovba S, Brunet M-F, Yegorova T, Starostenko V (2006) The evolution of the southern margin of Eastern Europe (Eastern European and Scythian platforms) from the Latest Precambrian-early palaeozoic to the early cretaceous. Geol Soc London Mem 32(1):481–505

Sanders C (1998) Tectonics and erosion, competitive forces in a compressive orogen: a fission track study of the Romanian Carpathians. PhD, Vrije Universiteit, Amsterdam

Sanders C, Andriessen P, Cloetingh S (1999) Life cycle of the East Carpathian Orogen: erosion history of a doubly vergent critical wedge assessed by fission track thermochronology. J Geophys Res 104(095–029):112

Sanders C, Huismans R, van Wees JD, Andriessen P (2002) The Neogene history of the Transylvanian basin in relation to its surrounding mountains. In: Cloetingh S, Horvath F, Bada G, Lankreijer A (eds) Neotectonics and surface processes: the Pannonian Basin and Alpine/Carpathian System, vol 3. EGU Special Publication, pp 121–133

Săndulescu M (1975) Essai de synthese structurale des Carpathes. Bull Soc Geol France XVII:299

Săndulescu M (1984) Geotectonica României (translated title: Geotectonics of Romania). Ed. Tehnică, Bucharest

Săndulescu M (1988) Cenozoic tectonic history of the Carpathians. In: Royden LH, Horvath F (eds) The Pannonian basin, a study in basin evolution, vol 45. AAPG Memoir, pp 17–25

Săndulescu M, Visarion M (1977) Considerations sur la structure tectonique du soubassement de la depression de Transylvanie. Dări de seamă ale şedinţelor, Inst Geo Geofiz LXIV:153–173

Săndulescu M, Visarion M (1988) La structure des plate-formes situées dans l´avant-pays et au-dessous des nappes du flysch des Carpathes orientales. St tehn econ, Geofiz 15:62–67

Săndulescu M, Krautner HG, Balintoni I, Russo-Săndulescu D, Micu M (1981) (Romanian Carpathians) The structure of the East Carpathians (Moldavia-Maramureş area). In: Carp.-Balc. Assoc., XII Congr

Săndulescu M, Visarion M, Stănică D, Stănică M, Atanasiu L (1993) Deep structure of the Inner Carpathians in the Maramureş-Tisa zone (East Carpathians). Rom J Geophys 16:67–76

Săsăran EF (2005) Upper Jurassic - Lower Cretaceous carbonates sedimentation from Bedeleu nappe (Apuseni Mountains): facies, biostratigraphy and sedimentary evolution. PhD, Babeş-Bolyai University of Cluj Napoca, Cluj Napoca

Schmid SM, Pfiffner OA, Froitzheim N, Schonborn G, Kissling E (1996) Geophysical-geological transect and tectonic evolution of the Swiss-Italian Alps. Tectonics 15(5):1036–1064

Schmid SM, Berza T, Diaconescu V, Froitzheim N, Fuegenschuh B (1998) Orogen-parallel extension in the South Carpathians during the Paleogene. Tectonophysics 297:209–228

Schmid SM, Fugenschuh B, Kissling E, Schuster R (2004) Tectonic map and overall architecture of the Alpine orogen. Eclogae Geologicae Hervetiae 97:92–117

Schmid S, Bernoulli D, Fügenschuh B, Matenco L, Schefer S, Schuster R, Tischler M, Ustaszewski K (2008) The Alpine-Carpathian-Dinaridic orogenic system: correlation and evolution of tectonic units. Swiss J Geosci 101(1):139–183

Schmid SM, Bernoulli D, Fügenschuh B, Matenco L, Schefer S, Oberhänsli R, Ustaszewski K (2011) Tracing the closure of Neotethys from the Alps to Western Turkey II: similarities and differences between Dinarides, Hellenides and Anatolides-Taurides. Geophysical Research Abstracts 13:EGU2011–4000

Schmitt G, Nuckelt A, Knöpfler A, Marcu C (2007) (Romanian Carpathians) Three dimensional plate kinematics in Romania. In: International symposium on strong Vrancea earthquakes and risk mitigation, Bucharest, Romania, pp 34–45

Schuller V (2004) Evolution and geodynamic significance of the upper cretaceous Gosau basin in the Apuseni Mountains, Romania. PhD thesis, Universitat Tubingen, Institut fur Geowissenschaften, Tubingen

Schuller V, Frisch W (2006) Heavy mineral provenance and paleocurrent data of the Upper Cretaceous Gosau succession of the Apuseni mountains (Romania). Geol Carpath 57(1):29–39

Schuller V, Frisch W, Danisik M, Dunkl I, Melinte MC (2009) Upper cretaceous Gosau deposits of the Apuseni mountains (Romania)—similarities and differences to the Eastern Alps. Austrian J Earth Sci (102):133–145

Seghedi A, Berza T, Iancu V, Maruntiu M, Oaie G (2005) Neoproterozoic terranes in the Moesian basement and in the Alpine Danubian nappes of the South Carpathians. Geologica Belgica 8 (4):4–19

Seghedi I, Matenco L, Downes H, Mason PRD, Szakács A, Pécskay Z (2011) Tectonic significance of changes in post-subduction Pliocene-quaternary magmatism in the south east part of the Carpathian-Pannonian region. Tectonophysics 502(1–2):146–157. doi:10.1016/j.tecto.2009.12.003

Sperner B, Lorenz F, Bonjer K, Hettel S, Muller B, Wenzel F (2001) Slab break-off-abrupt cut or gradual detachment? New insights from the Vrancea Region (SE Carpathians, Romania). Terra Nova 13:172–179

Stampfli GM, Borel GD (2002) A plate tectonic model for the Paleozoic and Mesozoic constrained by dynamic plate boundaries and restored synthetic oceanic isochrons. Earth Planet Sci Lett 196(1–2):17–33. doi:10.1016/S0012-821X(01)00588-X

Stănică M, Stănică D, Marin-Furnică C (1999) The placement of the trans-European suture zone on the Romanian territory by electromagnetic arguments. Earth Planets Space 51:1073–1078

Ştefănescu M (1976) O noua imagine a structurii flişului intern din regiunea de curbură a Carpaţilor. DS Inst Geol Geofiz LXII 5:257–259 (in Romanian)

Ştefănescu M (1983) General remarks on the Eastern Carpathians flysch and its depositional environment. Revue Roumaine de Geologie, Geophysique et Géographie 27:59–64

Ştefănescu M (1995) Stratigraphy and structure of Cretaceous and Palaeogene flysch deposits between Prahova and Ialomiţa valleys. Rom J Tectonics Reg Geol 76:1–49

Stephenson RA, Mart Y, Okay A, Robertson A, Saintot A, Stovba S, Khriachtchevskaia O (2004) TRANSMED Section VIII; East-European Craton-Crimea-Black Sea-Anatolia-Cyprus-Levant Sea-Sinai-Red Sea. In: Cavazza W, Roure F, Spakman W, Stampfli GM, Ziegler PA (eds) The TRANSMED Atlas: the Mediterranean region from Crust to Mantle. Springer, Berlin

Stojadinovic U, Matenco L, Andriessen PAM, Toljić M, Foeken JPT (2013) The balance between orogenic building and subsequent extension during the tertiary evolution of the NE Dinarides: constraints from low-temperature thermochronology. Global Planet Change 103:19–38. doi:10.1016/j.gloplacha.2012.08.004

Szakacs A, Krezsek C (2006) Volcano-basement interaction in the Eastern Carpathians: explaining unusual tectonic features in the Eastern Transylvanian Basin, Romania. J Volcanol Geoth Res 158(1–2):6–20

Tărăpoancă M (2004) Architecture, 3D geometry and tectonic evolution of the Carpathians foreland basin. PhD, VU University Amsterdam, Amsterdam

Tărăpoancă M, Bertotti G, Maţenco L, Dinu C, Cloetingh S (2003) Architecture of the Focsani depression: A 13 km deep basin in the Carpathians bend zone (Romania). Tectonics 22 (6):1074. doi:10.1029/2002TC001486

Tărăpoancă M, Ţambrea D, Avram V, Popescu BM (2007) The geometry of the South carpathians sole thrust and the Moesia boundary: the role of inherited structures in establishing a transcurrent contact on the concave side of the Carpathians. In: Lacombe O, Lave J, Roure F, Verges J (eds) Thrust Belts and Foreland basins: from fold kinematics to hydrocarbon systems. Springer, Berlin, pp 492–508

Tari G, Horváth F, Rumpler J (1992) Styles of extension in the Pannonian basin. Tectonophysics 208:203–219

Tari G, Dicea O, Faulkerson J, Georgiev G, Popov S, Ştefănescu M, Weir G (1997) Cimmerian and Alpine stratigraphy and structural evolution of the Moesian platform (Romania/Bulgaria). In: Robinson AG (ed) Regional and petroleum geology of the Black Sea and surrounding regions, vol 68. AAPG Memoir, pp 63–90

Tari G, Dovenyi P, Dunkl I, Horvath F, Lenkey L, Ştefănescu M, Szafian P, Toth T (1999) Lithospheric structure of the Pannonian basin derived from seismic, gravity and geothermal data. In: Durand B, Jolivet L, Horvath F, Serrane M (eds) The Mediterranean basins: extension within the Alpine Orogen, vol 156, pp 215–250 (Geological Society, London, Special Publications)

ter Borgh M (2013) Connections between sedimentary basins during continental collision: how tectonic, surface and sedimentary processes shaped the Paratethys. PhD, Utrecht University, PhD Thesis, Utrecht

Tiliţă M, Maţenco L, Dinu C, Ionescu L, Cloetingh S (2013) Understanding the kinematic evolution and genesis of a back-arc continental "sag" basin: the Neogene evolution of the Transylvanian basin. Tectonophysics 602:237–258. doi:10.1016/j.tecto.2012.12.029

Tischler M, Gröger HR, Fügenschuh B, Schmid SM (2007) Miocene tectonics of the Maramures area (Northern Romania): implications for the Mid-Hungarian fault zone. Int J Earth Sci 96:473–496. doi:10.1007/s00531-00006-00110-x

Tischler M, Maţenco L, Filipescu S, Groger HR, Wetzel A, Fugenschuh B (2008) Tectonics and sedimentation during convergence of the ALCAPA and Tisza-Dacia continental blocks: the Pienide nappe emplacement and its foredeep (N. Romania). Geol Soc London Spec Publ 298 (1):317–334

Toljić M, Maţenco L, Ducea MN, Stojadinović U, Milivojević J, Đerić N (2013) The evolution of a key segment in the Europe-Adria collision: the Fruška Gora of northern Serbia. Global Planet Change 103:39–62. doi:10.1016/j.gloplacha.2012.10.009

Ustaszewski K, Schmid S, Fügenschuh B, Tischler M, Kissling E, Spakman W (2008) A map-view restoration of the Alpine-Carpathian-Dinaridic system for the Early Miocene. Swiss J Geosci 101:273–294

Ustaszewski K, Kounov A, Schmid SM, Schaltegger U, Krenn E, Frank W, Fügenschuh B (2010) Evolution of the Adria-Europe plate boundary in the northern Dinarides: from continent-continent collision to back-arc extension. Tectonics 29(6):TC6017. doi:10.1029/2010tc002668

Uyeda S, Kanamori H (1979) Back-arc opening and the mode of subduction. J Geophys Res 84:1049–1061

Vaida M, Seghedi A, Verniers J (2005) Northern Gondwanan affinity of the East Moesian Terrane based on chitinozoans. Tectonophysics 410(1–4):379–387

van der Hoeven AGA, Mocanu V, Spakman W, Nutto M, Nuckelt A, Maţenco L, Munteanu L, Marcu C, Ambrosius BAC (2005) Observation of present-day tectonic motions in the Southeastern Carpathians: results of the ISES/CRC-461 GPS measurements. Earth Planet Sci Lett 239(3–4):177–184

van der Meer DG, Spakman W, van Hinsbergen DJJ, Amaru ML, Torsvik TH (2010) Towards absolute plate motions constrained by lower-mantle slab remnants. Nat Geosci 3(1):36–40

van Hinsbergen DJJ, Schmid SM (2012) Map view restoration of Aegean—West Anatolian accretion and extension since the Eocene. Tectonics 31(5):TC5005. doi:10.1029/2012tc003132

van Hinsbergen DJJ, Hafkenscheid E, Spakman W, Meulenkamp JE, Wortel R (2005) Nappe stacking resulting from subduction of oceanic and continental lithosphere below Greece. Geology 33(4):325–328

Vergés J, Fernàndez M (2012) Tethys-Atlantic interaction along the Iberia-Africa plate boundary: the Betic-Rif orogenic system. Tectonophysics 579:144–172. doi:10.1016/j.tecto.2012.08.032

Visarion M, Veliciu S, Ștefănescu M (1978) Thermal field in the Romanian Carpathian Bend and some aspects of its interpretation. Studia Geophys et Geod 22:196–200

Visarion M, Săndulescu M, Stănică D, Veliciu S (1988) Contributions á la connaissance de la structure profonde de la plate-forme Moésienne en Roumanie. St Tehn Econ Geofiz 15:68–92

Vissers RLM (2012) Extension in a convergent tectonic setting: a lithospheric view on the Alboran system of SW Europe. Geologica Belgica 15(1–2):53–72

Vörös A (1977) Provinciality of the Mediterranean Lower Jurassic brachiopod fauna: causes and plate-tectonic implications. Paleogeogr Paleoclimatol Paleoecol 21:1–16

Willett SD, Brandon MT (2002) On steady states in mountain belts. Geology 30(2):175–178

Willett SD, Schlunegger F, Picotti V (2006) Messinian climate change and erosional destruction of the central European Alps. Geology 34(8):613–616

Willingshofer E, Andriessen P, Cloetingh S, Neubauer F (2001) Detrital fission track thermochronology of Upper cretaceous syn-orogenic sediments in the South Carpathians (Romania): inferences on the tectonic evolution of a collisional hinterland. Basin Res 13: 379–395

Windhoffer G, Bada G (2005) Formation and deformation of the Derecske Trough, Pannonian basin: insights from analogue modeling. Acta Geol Hung 48(4):351–369

Wohlfarth B, Hannon G, Feurdean A, Ghergari L, Onac BP, Possnert G (2001) Reconstruction of climatic and environmental changes in NW Romania during the early part of the last deglaciation ($\sim$15,000–13,600 cal yr BP). Quatern Sci Rev 20(18):1897–1914

Wolf RA, Farley KA, Silver LT (1996) Helium diffusion and low-temperature thermochronometry of apatite. Geochim Cosmochim Acta 60(21):4231–4240. doi:10.1016/S0016-7037(96)00192-5

Wortel MJR, Spakman W (2000) Subduction and Slab Detachment in the Mediteranean-Carpathian Region. Science 290:1910–1917

Ziegler PA (1990) Geological Atlas of Western and Central Europe, 2nd edn. Shell International and Geol. Soc. London

Ziegler PA, van Wees J-D, Cloetingh S (1998) Mechanical controls on collision-related compressional intraplate deformation. Tectonophysics 300(1–4):103–129

Chapter 3
Climate Evolution During the Late Glacial and the Holocene

Aurel Perşoiu

Abstract The Late Glacial and Holocene dynamics of fluvial and slope erosion in Romania cannot be understood in the absence of well-dated, continuous, and spatially homogenous records of past climate changes. In this chapter, we provide the scientific community with the first compilation of past climate changes during this period in Romania (Central-East Europe). The lack of climate reconstructions from the Eastern and Southern parts of the country restricts our synthesis to the western half of the country, with an emphasis on the high and mid-altitudes (between 200 and 2000 m a.s.l.), where most of the studied sites are located. We are using a combination of speleothem and diatom $\delta^{18}O$ and $\delta^{13}C$ values, chironomid-inferred July temperatures, tree ring width, and pollen-based quantitative reconstructions to infer the main climatic changes during the last ca. 15,000 years. The data we are using show that, although synchronous within dating uncertainties with similar changes elsewhere in Europe, those in NW and SW Romania were generally less dramatic, with reduced amplitude of air temperature changes. These changes were mostly expressed during the cold season, suggesting frequent changes in seasonality. Precipitation amount decreased markedly at the onset of cold periods (GS–1, 8.2 and 3.2 ka events etc.) suggesting increased continentality. Warming at the end of the Last Glacial was abruptly interrupted by the onset of the cooling at ca. 12,800 cal BP, cooling that lasted until ca. 11,700–11,600 cal BP. The Early Holocene was generally dry and warm, especially in NW Romania, the warmer than present conditions prevailing until the mid-Holocene. After ca. 5000 cal BP, a slow cooling trend towards the present prevailed, punc-

A. Perşoiu (✉)
Emil Racoviţă Institute of Speleology, Romanian Academy, Clinicilor 5, 400006 Cluj-Napoca, Cluj, Romania
e-mail: aurel.persoiu@gmail.com

A. Perşoiu
Stable Isotope Laboratory, Ştefan cel Mare University, Universităţii 13, 720229 Suceava, Romania

M. Rădoane and A. Vespremeanu-Stroe (eds.), *Landform Dynamics and Evolution in Romania*, Springer Geography,
DOI 10.1007/978-3-319-32589-7_3

tuated by shorter (ca. 200 years) and longer (>500 years) periods of enhanced cooling, mostly expressed in NW Romania, and not evident in the SW. Also, after 5000 cal BP, a slow increase in the influence of the Mediterranean climate is detectable in SW Romania, possibly expanding towards the NW. The last 1000 years are characterized by a generally warm and dry period lasting until ~ 1300 AD, followed by an erratic (with rapid swings from cold and wet to warm and dry and back) Little Ice Age, between 1300 and 1900 AD.

Keywords Eastern Europe · Holocene · Palaeoclimate · Temperature · Stable isotopes

Introduction

The dynamics of Earth's surface processes is intrinsically linked to (inter alia) climatic changes at various time scales (e.g., Schumm and Licthy 1965). Deciphering these links requires a detailed knowledge of the geomorphologic processes to be investigated and of the climatic changes during the lifetime of these processes, as well as a clear understanding of the mechanisms linking the two.

These topics have earned an important place in the scientific discourse in Romania recently (see the chapters in this volume), but their investigation was generally hampered by the lack of palaeoclimatic reconstructions focusing on *climatic changes* rather than on the *impact of climatic changes* (e.g., Feurdean et al. 2014). In this context, the aim of this chapter is to briefly present the main climate changes that affected the territory of Romania during the past ca. 15,000 years, highlighting the changes in temperature and precipitation amount as one of the drivers of geomorphologic processes (Fig. 3.1). Our study thus *presents* the data, rather than *interpreting it* or *describing the mechanisms behind the observed changes*, in order to offer a tool in the hand of geomorphologists studying the changes in Earth surface processes during the present interglacial.

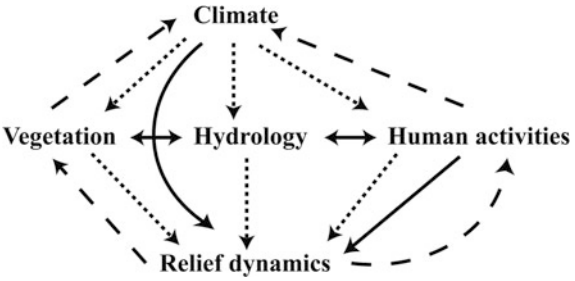

Fig. 3.1 Schematic view of the factors controlling the dynamics of relief during the Holocene (direct control—*filled arrows*, indirect control—*dotted arrows*, feedback mechanisms—*dashed arrows*)

Sources of Palaeoclimate Data

This review is based on a compilation of data (Fig. 3.2) derived from various archives (speleothems, peat bogs, lakes, and tree rings) and climate proxies (speleothem stable isotopes, pollen counts, tree ring width, bat guano $\delta^{13}C$), each with its own advantages and limitations, outlined below.

Speleothems

Oxygen and carbon stable isotopes in speleothems have been used by Onac et al. (2002), Tămaş et al. (2005), Constantin et al. (2007) and Drăguşin et al. (2014) to constrain past changes in temperature, precipitation source(s), and vegetation in NW and SW Romania (Fig. 3.2). These authors have found that calcite $\delta^{18}O$ in caves from Romania reflects changes in mean annual temperature, showing a positive correlation with air temperature, but also a possible influence of shifts in the source of precipitation from the North Atlantic region toward the Mediterranean, both in NW (Onac et al. 2002) and SW Romania (Drăguşin et al. 2014). Interpretation of $\delta^{13}C$ variability in speleothems is less straightforward, being related to changes in vegetation and soil microbial activity (e.g., Dorale et al. 1998) or kinetic processes

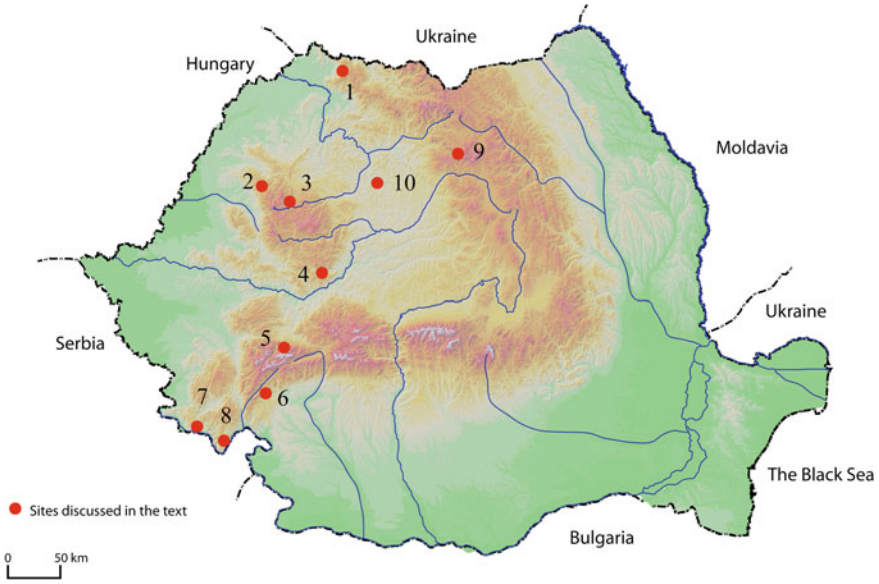

Fig. 3.2 Main sites discussed in the text: 1—Steregoiu and Preluca Ţiganului peat bogs (Feurdean et al. 2008), 2—Urşilor Cave (Onac et al. 2002), 3—V11 Cave (Tămaş et al. 2005), 4—Zidită Cave (Forray et al. 2015), 5—Brazi Lake (Toth et al. 2012), 6—Ascunsă Cave (Drăguşin et al. 2014), 7—Poleva Cave (Constantin et al. 2007), 8—Gaura cu Muscă Cave (Onac et al. 2015), 9—Călimani Mts. (Popa and Kern 2009), 10—Ştiucii Lake (Feurdean et al. 2013)

during calcite precipitation (Genty et al. 2003). In NW Romania (Fig. 3.2), Onac et al. (2002) linked variation in $\delta^{13}C$ in speleothem calcite to changes in rainfall intensity, with lighter values corresponding to wetter periods, while for the same region Tămaş et al. (2005) have shown that heavier $\delta^{13}C$ values correspond to drier/colder periods, due to increased participation of (isotopically heavier) atmospheric-derived CO_2 to the overall budget of soil CO_2. In SW Romania (Fig. 3.2), Drăguşin et al. (2014) have shown that increasing $\delta^{13}C$ values are probably linked to drier conditions during the mid-Holocene, possibly due to the northward expansion of the Mediterranean climatic conditions around that time.

Peat bogs and Lakes

Peat bogs and lakes are the most frequently probed archives of past climate and vegetation history in Romania. While they host a wide range of potential proxies for reconstructing past climate changes, only a few of them have been investigated: pollen, chironomids, and charcoal abundance (e.g., Feurdean et al. 2008, 2013). Pollen records have been used generally to understand past changes in vegetation (an overview of these changes is presented by Feurdean et al., Chap. 4 this volume and Mîndrescu et al., Chap. 30 this volume). However, in NW Romania (Fig. 3.2), Feurdean et al. (2008) have used modern analogue (MAA) and weighted averaging partial least squares regression (WA–PLS) methods to infer quantitative temperature (mean annual, coldest month and warmest month) and precipitation amount changes through the Late Glacial and the Holocene. These techniques rely on the assumptions that vegetation type and changes are controlled by climate, that present-day climate–vegetation relationships were similar in the past and that they can be transferred back in time. Lake sediments provide two more proxies of summer air temperatures during the Holocene in Romania: Toth et al. (2012) used chironomids to infer July air temperatures from the Late Glacial through the early Holocene in SW Romania (Fig. 3.2), while Feurdean et al. (2013) used charcoal from lake sediments in central Transylvania (Fig. 3.2) to infer past fire regimes and subsequently changes in summer soil moisture and air temperature (with high charcoal content being associated to higher temperatures and consequently drier soils). Further, Magyari et al. (2013) have used diatom $\delta^{18}O$ values to reconstruct winter temperature changes in SW Romania and showed a possible link between drier winter precipitation amount and the positive phase of the North Atlantic Oscillation.

Tree Rings

Over the past decade, tree rings have been increasingly used to reconstruct past climatic condition during the last few centuries. Thus, Popa and Kern (2009) have

used tree ring width (TRW) from stone pine (*Pinus cembra* L.) in NE Romania (Fig. 3.2) to reconstruct summer air temperature variability during the last 1000 years, while Levanic et al. (2012) have used TRW measured on black pine (*Pinus nigra*) from SW Romania (Fig. 3.2) to reconstruct July precipitation amount during the last ca. 300 years.

Guano

Bat guano deposits in caves host several potential climate and environmental proxies: plant and insect macroremains, pollen, $\delta^{13}C$ etc. (Forray et al. 2015; Onac et al. 2015). While pollen and macroremains are interpreted in a similar manner as those found in lake and peat bog sediments, disentangling between climatic and biotic (in-bat) factors controlling $\delta^{13}C$ in bat guano is less straightforward. Using a combination of present-day observations and bat ecology studies, Onac et al. (2015) have shown that $\delta^{13}C$ in bat guano is indicative of changes in hydrologic conditions, higher (more positive) values corresponding to drier conditions.

Past Climate Reconstructions

Late Glacial

Temperatures around the globe started to increase at ca. 19,000 years ago, following orbitally induced changes in the amount and distribution of solar radiation and increased concentrations of CO_2. The increase accelerated in the Northern Hemisphere after 14,692 b2k (years before AD 2000, Blockley et al. 2012), as seen in the $\delta^{18}O$ record in Greenland ice cores. In NW Romania, Tămaş et al. (2005) observed a synchronous (within dating uncertainty) increase in mean annual temperatures, while Feurdean et al. (2008) have found a small increase in mean annual temperatures, possibly a result of a warming trend in winter temperatures, as summer ones stayed roughly unchanged. Contrary, Toth et al. (2012) have found a small increase in summer temperatures in SE Romania, based on chironomid data; the discrepancy between the two regions being possibly due to the more southerly (and at higher elevation) location of the lake analyzed by Toth et al. (or differences in the way the two proxies—pollen and chironomids reflect changes in air temperature). Between ~14,000 and 12,800 cal BP (GI–1d through GI–1a) conditions were more stable than in the wider North Atlantic realm (Fig. 3.3), with two possible cooling episodes during GI–1d and GI–1b (Feurdean et al. 2014). Generally, the climatic conditions in NW Romania were characterized by summer temperatures close to present-day values (Feurdean et al. 2008), while those during winter were lower. These thermal characteristics must have induced stronger seasonal amplitudes, thus enhancing the continentality of the climate around this time.

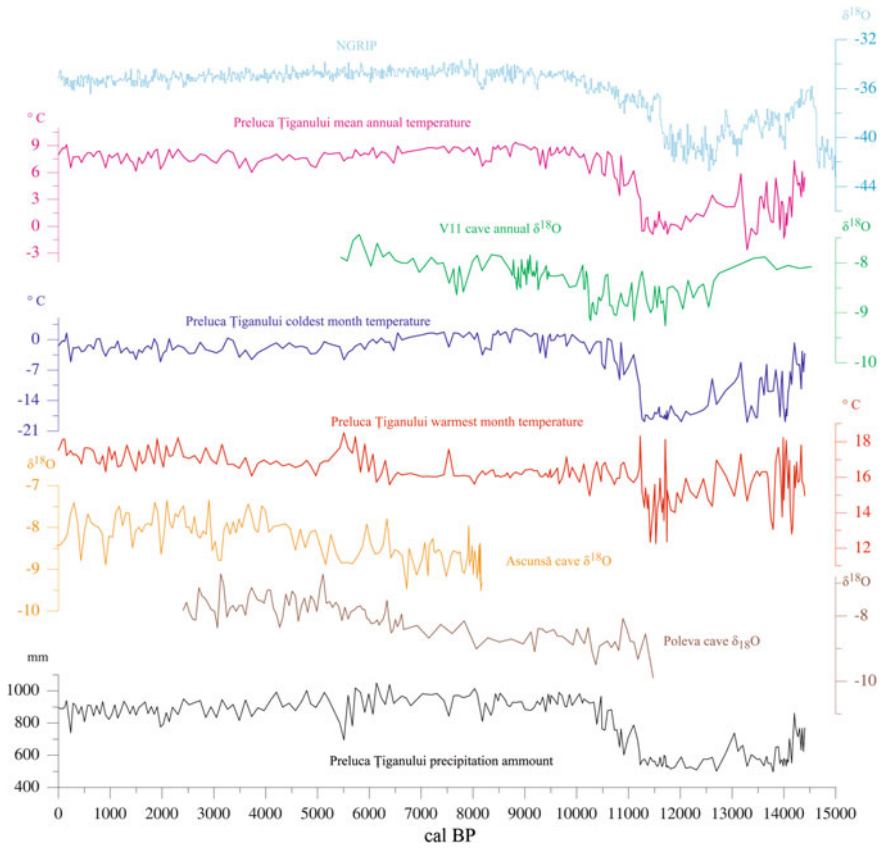

Fig. 3.3 Reconstructed climatic parameters and proxy records from Romania, plotted against the NGRIP $\delta^{18}O$

Pollen data from NW Romania (Feurdean et al. 2008) also suggests reduced precipitation around this time, both in summer and winter, conditions which, coupled with high summer temperatures, could have led to decreased soil moisture conditions and increase in the occurrence of wild fires (Feurdean et al. 2012, 2013).

The cooling after 12,800 cal BP (Fig. 3.3) was roughly synchronous with the Younger Dryas (GS–1) period, and was recorded by both speleothem $\delta^{18}O$ and $\delta^{13}C$ and pollen in NW Romania, and chironomids in SW Romania. However, the magnitude of the change during the summer was higher in the southern part of Romania (2 °C), as compared to the northern one (1 °C), while winters saw a drop in temperature of about 8 °C and a further decrease in precipitation amount. Rather than being stable, temperature and precipitation values continued to decrease during the GS–1, indicating a progressive drying, while the more pronounced decrease in winter temperature than in summer showed increasingly continental climate conditions.

The Holocene

The warming at the end of GS–1 (11,700 b2k) occurred within a few decades, with summer temperatures increasing by about 4 °C, while precipitation values remained relatively low (Fig. 3.3), following the early Holocene peak in summer insolation. Reduced precipitation and increased summer temperatures (leading to enhanced evaporation) are also reflected in the reduction of soil moisture and lake levels (Magyari et al. 2009; Buczkó et al. 2012; Feurdean et al. 2013). Following the rapid increase at the end of GS–1, air temperatures were relatively unstable for ca. 1000 years, then resumed their abrupt increase toward 10,000 cal BP, peaking around this time (Fig. 3.3, Feurdean et al. 2008). The pollen-based derived increase in summer temperatures is similar to those recorded by the $\delta^{18}O$ records from speleothems in NW (Tămaş et al. 2005) and SW Romania (Constantin et al. 2007). The precipitation regime was generally unstable in the early Holocene (prior to ca. 10,000 cal BP), with a gradual shift toward wetter conditions after the arid GS–1. The early Holocene warming was interrupted by two colder intervals, centered on 10,200 cal BP and 8200 cal BP (Feurdean et al. 2008; Tămaş et al. 2005; Schnitchen et al. 2006), both showing a reduction in annual and winter air temperatures, as well as an increase in precipitation amount (Fig. 3.3).

Mean annual temperatures continued to increase toward the mid-Holocene (~5500 cal BP) as indicated by $\delta^{18}O$ records from NW and SW Romania (see below). Interestingly, while Constantin et al. (2007) and Drăguşin et al. (2014) report a continuous increase in mean annual temperatures over the mid-Holocene in SW Romania, data from speleothems in NW Romania, in a region directly facing frontal systems from the North Atlantic, show more stable conditions, with pollen-based reconstruction from further north (Fig. 3.3, Feurdean et al. 2008) supporting the climatic stability in N Romania, as opposed to S Romania. This discrepancy could be the result of the northward expansion of Mediterranean climatic conditions (Rohling et al. 2002), engulfing SW Romania, while the more northern regions remained under the dominance of westerly circulation and more Atlantic climatic conditions. Alternatively, variations recorded by the $\delta^{18}O$ of speleothem calcite in SW Romania could be indicative of shifts between the two moisture sources: the North Atlantic and the Mediterranean (Rozanski et al. 1993), each with a different isotopic composition related to variation in evaporation (the later enhanced in the warmer Mediterranean, thus resulting in higher isotopic values, that could be interpreted as "warming").

Following the peak in summer temperature conditions at around 5000 cal BP (Fig. 3.3), temperatures started to decrease toward present day, while precipitation amount increased, as suggested by pollen data from NW Romania (Feurdean et al. 2008) and guano-derived $\delta^{13}C$ from SW Romania (Onac et al. 2015). These general trends of cooling and wetting were interrupted by dryer and possibly warmer conditions at 3300, 2400, 1800, and 1500 cal BP, as indicated by increased fire activity and decreased lake levels in records from central Transylvania (Feurdean et al. 2013). Winter temperatures show a decreasing trend after ca. 3200 cal BP, as

indicated by $\delta^{18}O$ of diatoms from a lake in SW Romania (Magyari et al. 2013), while precipitation amount decreased, possibly as a result of a shift toward more positive values of the North Atlantic Oscillation index (Magyari et al. 2013). A general feature of the climate during the past ca. 3000 years was the occurrence of rapid and generally short-lived (50–200 years) cooling periods, that punctuated the overall cooling trend, the later mainly expressed in NW Romania, while SW Romania experiencing rather stable temperature conditions.

The Last 1000 Years

On the long term, on the possibly orbitally driven late-Holocene cooling (Fig. 3.3), two warming periods have been superimposed, between ~0 and 400 AD (Roman Warm Period) and between ~900 and 1200 AD (Medieval Warm Period, MWP). While the former is poorly represented in pollen and speleothem records, the MWP has been seen in pollen and macrofossils recovered from ice caves (Feurdean et al. 2011), $\delta^{13}C$ in bat guano (Forray et al. 2015; Onac et al. 2015) and in tree ring width (Popa and Kern 2009). The MWP was generally dry and warm in western Romania; and was ended by a cooling trend that started after ca 1200 AD and continued (with a higher degree of instability than during the preceding MWP) until ca. 1850 AD (Feurdean et al. 2011; Forray et al. 2015). In NE Romania, tree rings tell a slightly different story, the cooling being initiated after ca. 1370 and lasting until 1630, followed by a rather abrupt warming, interrupted in 1820–1840 (Popa and Kern 2009). Further, while the MWP was generally characterized by stable temperatures and low variability in precipitation amount (Forray et al. 2015; Feurdean et al. 2011), during the LIA, the climate had a more erratic behavior, with rapid swings from cold to warm periods, sometimes within a decade (Popa and Kern 2009; Onac et al. 2015). After ca. 1850, climate started to warm gradually and became drier, with decades-long period of small amplitude cooling (centered on 1940 AD and 1975 AD).

Acknowledgements AP acknowledges support from project PN-II-RU-TE-2014-4-1993 "Crossing the Carpathians: environmental and cultural controls of the expansion of Neolithic cultures in SE Europe".

References

Blockley SPE, Lane CS, Hardiman M, Rasmussen SO, Seierstad IK, Steffensen JP, Svensson A, Lotter AF, Turney CSM, Ramsey CB (2012) Synchronisation of palaeoenvironmental records over the last 60,000 years, and an extended INTIMATE event stratigraphy to 48,000 b2k. Quatern Sci Rev 36:2–10

Buczkó K, Magyari E, Hübener T, Braun M, Balint M, Toth M, Lotter AF (2012) Responses of diatoms to the Younger Dryas climatic reversal in a South Carpathian mountain lake (Romania). J Paleolimnol 48:417–431

Constantin S, Bojar AV, Lauritzen SE, Lundberg J (2007) Holocene and Late Pleistocene climate in the sub-Mediterranean continental environment: a speleothem record from Poleva Cave (Southern Carpathians, Romania). Palaeogeogr Palaeoclimatol Palaeoecol 243:322–338

Dorale JA, Edwards RL, Ito E, Gonzales LA (1998) Climate and vegetation history of the Midcontinent from 75 to 25 ka: a speleothem record from Crevice Cave, Missouri, USA. Science 282:1871–1874

Drăguşin V, Staubwasser M, Hoffmann DL, Ersek V, Onac BP, Vereş D (2014) Constraining Holocene hydrological changes in the Carpathian-Balkan region using speleothem $\delta^{18}O$ and pollen-based temperature reconstructions. Clim Past 10:381–427

Feurdean A, Klotz S, Mosbrugger V, Wohlfarth B (2008) Pollen-based quantitative reconstruction of Holocene climate variability in NW Romania. Palaeogeogr Palaeoclimatol Palaeoecol 260:494–504

Feurdean A, Perşoiu A, Pazdur A, Onac BP (2011) Evaluating the palaeoecological potential of pollen recovered from ice in caves: a case study from Scărişoara Ice Cave, Romania. Rev Palaeobot Palynol 165:1–10

Feurdean A, Liakka J, Vanniere B, Marinova E, Hutchinson SM, Mosburgger V, Hickler T (2013) 12,000-years of fire regime drivers in the lowlands of Transylvania (Central-Eastern Europe): a data-model approach. Quatern Sci Rev 81:48–61

Feurdean A, Spessa A, Magyari EK, Veres D, Hickler T (2012) Trends in biomass burning in the Carpathian region over the last 15,000 years. Quat Sci Rev 45, 111e125

Feurdean A, Perşoiu A, Tanţău I, Stevens T, Markovic, Magyari EK, Onac BP, Andric M, Connor S, Galka M, Hoek WZ, Lamentowicz M, Sümegi P, Perşoiu I, Kolaczek P, Kunes P, Marinova E, Slowinski M, Michczynska D, Stancikaite M, Svensson A, Veski S, Fărcaş S, Tămaş T, Zernitskaya V, Timar A, Tonkov S, Toth M, Willis KJ, Plóciennik M, Gaudeny T (2014) Climate variability and associated vegetation response throughout Central and Eastern Europe (CEE) between 8 and 60 kyrs ago. Quat Sci Rev 106:206–224.

Forray FL, Onac BP, Tanţău I, Wynn JG, Tămaş T, Coroiu I, Giurgiu AM (2015) A late Holocene environmental history of a bat guano deposit from Romania: an isotopic, pollen and microcharcoal study. Quatern Sci Rev 127:141–154

Genty D, Blamart D, Ouahdi R, Gilmour M, Baker A, Jouzel J, Van-Exter S (2003) Precise dating of Dansgaard–Oeschger climate oscillations in western Europe from stalagmite data. Nature 421:833–837

Levanič T, Popa I, Poljanšek S, Nechita C (2012) A 323-year long reconstruction of drought for SW Romania based on black pine (Pinus nigra) tree-ring widths. Int J Biometeorol, 1–12. doi:10.1007/s00484-012-0596-9. Online ISSN: 1432-1254

Magyari EK, Buczko K, Jakab G, Braun M, Pal Z, Karatson D, Papp P (2009) Palaeolimnology of the last crater lake in the Eastern Carpathian Mountains—a multiproxy study of Holocene hydrological changes. Hydrobiologia 631:29–63

Magyari EK, Demény A, Buczkó K, Kern Z, Vennemann T, Fórizs I, Vincze I, Braun M, Kovács JI, Udvardi B, Veres D (2013) A 13,600-year diatom oxygen isotope record from the South Carpathians (Romania): reflection of winter conditions and possible links with North Atlantic circulation changes. Quatern Int 293:136–149

Onac BP, Constantin S, Lundberg J, Lauritzen S-E (2002) Isotopic climate record in a Holocene stalagmite from Urşilor Cave (Romania). J Quat Sci 17:319–327

Onac BP, Hutchinson SM, Geantă A, Forray FL, Wynn JG, Giurgiu AM, Coroiu I (2015) A 2500-year late Holocene multi-proxy record of vegetation and hydrologic changes from a cave guano-clay sequence in SW Romania. Quatern Res 83:437–448

Popa I, Kern Z (2009) Long-term summer temperature reconstruction inferred from tree-ring records from the Eastern Carpathians. Clim Dyn 32:1107–1117

Rohling EJ, Mayewski PA, Abu-Zied RH, Casford JSL, Hayes A (2002) Holocene atmosphere-ocean interactions: records from Greenland and the Aegean Sea. Clim Dyn 18:587–593

Rozanski K, Araguás-Araguás L, Gonfiantini R (1993) Isotopic patterns in modern global precipitation. In: Swart PK, Lohmann KC, McKenzie J, Savin S (eds) Climate change in continental isotopic records. Geophysical monograph series, vol 78, pp 1–36

Schnitchen C, Charman DJ, Magyari E, Braun M, Grigorszky I, Tóthmérész B, Molnár M, Szántó Z (2006) Reconstructing hydrological variability from testate amoebae analysis in Carpathian peatlands. J Paleolimnol 36:1–17

Schumm SA, Lichty RW (1965) Time, space, and causality in geomorphology. Am J Sci 263 (2):110–119

Tămaş T, Onac BP, Bojar AV (2005) Lateglacial-middle Holocene stable isotope records in two coeval stalagmites from the Bihor Mountains, NW Romania. Geol Q 49:154–194

Toth M, Magyari EK, Brooks SJ, Braun M, Buczko K, Balint M, Heiri O (2012) A chironomid-based reconstruction of late glacial summer temperatures in the southern Carpathians (Romania). Quatern Res 77:122–131

Chapter 4
The Evolution of Vegetation from the Last Glacial Maximum Until the Present

Angelica Feurdean and Ioan Tanţău

Abstract High-resolution records of past vegetation dynamics have been recently available from Romania. This chapter represents a compilation of up to date, high-resolution palaeoecological records (pollen, plant macrofossil and charcoal) from Romania and provides an overview of broad-scale vegetation dynamics and diversity from the Last Glacial Maximum (LGM) to the present. Specifically, we discuss: (i) temporal and spatial variations in the magnitude of vegetation responses to abrupt climate changes for the LGM and Lateglacial; (ii) pattern of changes in the Holocene tree species distribution and diversity with implication on their current status in the Romanian forests; and (iii) the imprint of various types of human activities (fire, pastoralism, agriculture) on the vegetation composition and dynamics. Finally, this synthesis provides an opportunity to reflect on the status of palaeovegetation research and to identify future critical research subjects in this region.

Keywords Palaeoecological records · Vegetation dynamics · Human activities · LGM · Holocene · Romania

A. Feurdean (✉)
Senckenberg Research Institute and Natural History Museum, Biodiversity and Climate Research Centre, Frankfurt Am Main, Germany
e-mail: angelica.feurdean@gmail.com

A. Feurdean
Emil Racoviţă Institute of Speleology, Romanian Academy, Clinicilor 5, 400006 Cluj-Napoca, Cluj, Romania

I. Tanţău
Department of Geology, Babeş-Bolyai University, M. Kogălniceanu, 1, 400084 Cluj-Napoca, Romania

I. Tanţău
Institute of Biological Research, Cluj-Napoca, Cluj, Romania

M. Rădoane and A. Vespremeanu-Stroe (eds.), *Landform Dynamics and Evolution in Romania*, Springer Geography,
DOI 10.1007/978-3-319-32589-7_4

Introduction

Palaeoecological studies (pollen, plant macrofossils, stomata, charred remains, fungi) are a rich source of information of changes in the vegetation composition and dynamics over long time scales (Willis and Birks 2006). They also provide significant insights into the magnitude and timing of land cover change brought by human use of land (Behre 1988; Brun 2009).

Geographically, Romania is situated at the convergence of three biogeographical regions: southern (Balkans), central and eastern Europe. This and Romania's heterogeneous landscapes with steep climatic and topographic gradients have resulted in high levels of floristic diversity, one of the highest in Europe. These include areas containing a mixture of Eurasiatic, central European, Circumpolar, Atlantic, Mediterranean and sub-Mediterranean species, and many endemic and sub-endemic species (Doniţa 1962; Cristea 1993). A number of coniferous and deciduous tree species survived in glacial refugia in Romania during the Pleistocene ice ages (Feurdean et al. 2007a), thus it is an excellent key region to study and understand present-day distribution and diversity of European trees. Large parts of Romanian forests are still considered as undisturbed or old-growth forests. The status of largely undisturbed forests of Romania, however, contradicts some of the archaeological evidences for a progressive human impact starting with the Early Neolithic (ca. 8 ka). It also contrasts with palaeoecological research, indicating that many forests have had undergone prehistoric and historic clearance and burning (Fărcaş et al. 2003, 2013; Tanţău et al. 2003, 2006, 2011a, b; Feurdean and Willis 2008a; Feurdean et al. 2009; Magyari et al. 2009), and thus have deep human imprints.

Here, we review published high-resolution palaeoecological records from Romania (Fig. 4.1) and provide an overview of the broad-scale vegetation dynamics and diversity from the Last Glacial Maximum (LGM) to the present. Specific issues to discuss include: (i) vegetation responses to abrupt climate changes for the LGM and Lateglacial; (ii) pattern of changes in the Holocene tree species distribution and diversity; and (iii) the imprint of human activities on the vegetation composition and dynamics.

Palaeoecological Indicators in the Sedimentary Archives

The most common indicators of past vegetation composition and associated climate conditions as well as human activities are listed below:

(i) Dry to arid conditions are indicated by the occurrence of pollen of xerophytes and halophytes (saline) plants such as *Artemisia, Ephedra,* Chenopodiaceae and *Juniperus*;
(ii) Moist conditions are suggested by the presence of pollen of hydrophytes (Cyperaceae, *Typha, Sparganium, Myriophyllum, Potamogeton, Alisma,*

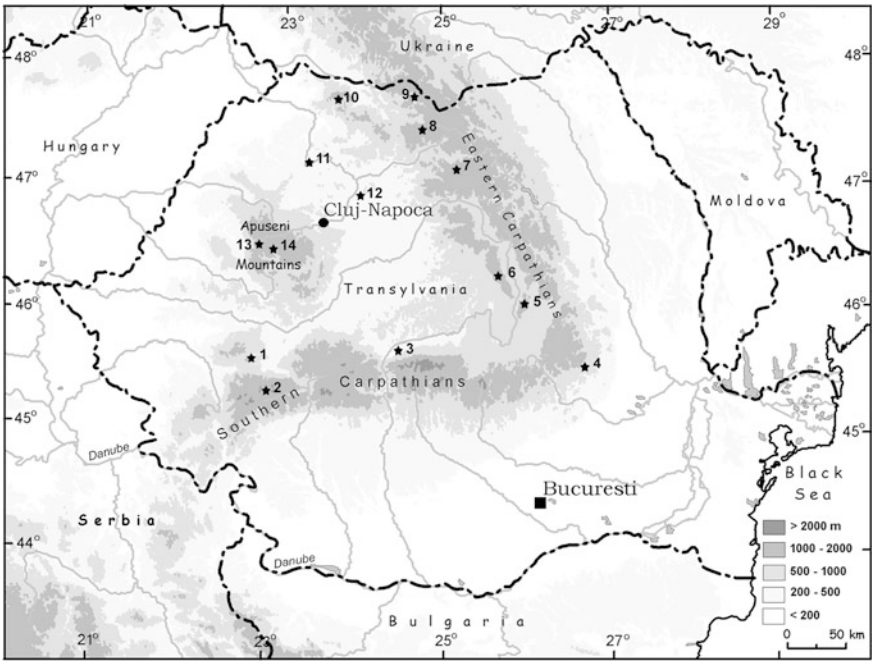

Fig. 4.1 Location map of the study area in the Romanian Carpathians and sites mentioned in the text: *1* Peşteana (Fărcaş and Tanţău 2012); *2* Tăul Zănoguţii (Fărcaş et al. 1999), Lake Galeş (Magyari et al. 2012); *3* Avrig (Tanţău et al. 2006); *4* Bisoca (Tanţău et al. 2009); *5* Mohoş (Tanţău et al. 2003), Sfânta Ana (Magyari et al. 2009); *6* Luci (Tanţău et al. 2014a); *7* Iezeru Călimani (Fărcaş et al. 1999); *8* Poiana Ştiol (Tanţău et al. 2011a), Gărgălău (Tanţău et al. 2014b); *9* Bardău, Cristina (Fărcaş et al. 2013); *10* Steregoiu (Björkman et al. 2003), Preluca Ţiganilor (Feurdean 2005); *11* Turbuţa (Feurdean et al. 2007a, b); *12* Ştiucii Lake (Feurdean et al. 2015); *13–14* Ic Ponor, Padiş (Bodnariuc et al. 2002), Molhasul Mare, Călineasa (Feurdean et al. 2009)

Nuphar, Lemna), spores of ferns and mosses (*Equisetum, Botrychium, Ophioglossum*, *Sphagnum*) and algae (*Pediastrum*);

(iii) Agriculture is documented by the presence of pollen types of cultivated plants and associated weeds (*Cerealia*-type, *Secale, Triticum*-type, *Hordeum*-type, *Avena*-type, *Zea, Centaurea cyanus, Agrostemma githago*); and arboriculture (*Juglans, Castanea, Vitis, Prunus, Malus, Pyrus*), generally known as primary anthropogenic indicators;

(iv) Ruderal/pastures/meadows are indicated by the increase in herbs pollen types such as *Plantago media/major, P. lanceolata*, *Artemisia*, Asteraceae, *Cannabis*-type, *Urtica*-type, *Rumex, Polygonum aviculare*-type, commonly known as secondary anthropogenic indicators (Behre 1981; Tanţău 2006; Brun 2011; Marinova et al. 2012; Feurdean et al. 2013a). Other accepted grazing indicators are fungal spores of *Chaetomium, Sordaria, Podospora, Sporormiella* (van Geel et al. 1980; Bakker et al. 2013);

(v) Fire activity is documented through the identification of macroscopic (larger than 150 μm) and microscopic charcoal particles (smaller than 150 μm) (Whitlock and Larsen 2001). In temperate regions, natural fire occurrences are associated to warm and dry climate conditions, in particular during summers (Feurdean et al. 2013b). However, increased fire activity in the late Holocene can also be associated to human ignition and its use as a tool to clear the landscapes for grazing or arable agriculture (Marlon et al. 2013);
(vi) Soil erosion is typically identified by the presence of fungi of *Cenococum geophilus* thought routine plant macrofossil counting.

Vegetation Responses from LGM to Early Holocene Abrupt Climatic Change

In order to better visualise changes in the main vegetation types throughout time, the pollen taxa at selected sequences were grouped into five main ecological types following the methodology outlined in Feurdean et al. (2014) and Tanţău et al. (2014a). These vegetation types are: coniferous (*Picea abies, Pinus, Abies alba, Larix decidua, Juniperus)*, cold deciduous tree/shrubs taxa (*Alnus, Betula, Salix, Populus)*, temperate deciduous tree taxa (*Ulmus, Quercus, Tilia, Corylus avellana, Acer, Fraxinus, Carpinus betulus, Hedera, Ilex, Fagus sylvatica, Viscum*, *Sambucus, Viburnum, Cornus, Frangula, Myrica, Prunus, Sorbus*), warm and dry steppe elements (Ericaceae, *Calluna, Hippophäe,* Poaceae, Cyperaceae, etc.) and grasses and dry shrubs (*Artemisia* and Chenopodiaceae/Amaranthaceae).

General Trends

Only a few sequences from Romania are older than the Lateglacial (>14.7 ka), and most of these only cover the terminal part of the Last Glacial (18–14.7 ka). These pollen records suggest that the landscapes in the Carpathian region were likely covered by open forest mixed with steppe–tundra vegetation (Figs. 4.2 and 4.3).

The tree taxa were mainly of boreal (*Picea abies, Pinus, Juniperus*) and cool temperate type (*Alnus, Betula, Salix*). Scattered pollen percentages of temperate deciduous trees (*Ulmus, Quercus, Fraxinus, Corylus avellana*) were also recorded (Tanţău et al. 2006, 2014a; Feurdean et al. 2007a, 2012b, 2014; Fărcaş and Tanţău 2012; Magyari et al. 2014). However, plant macrofossils and charcolised remains of these taxa have not been reported at these sequences. Nevertheless tree remains have been found in sequences collected from archaeological sites (Haesaerts et al. 1998). The steppe–tundra assemblages represent a vegetation type that has no analogue to modern vegetation. These consisted of steppic plants composed of herbs growing in open landscape under dry conditions, and tundra elements

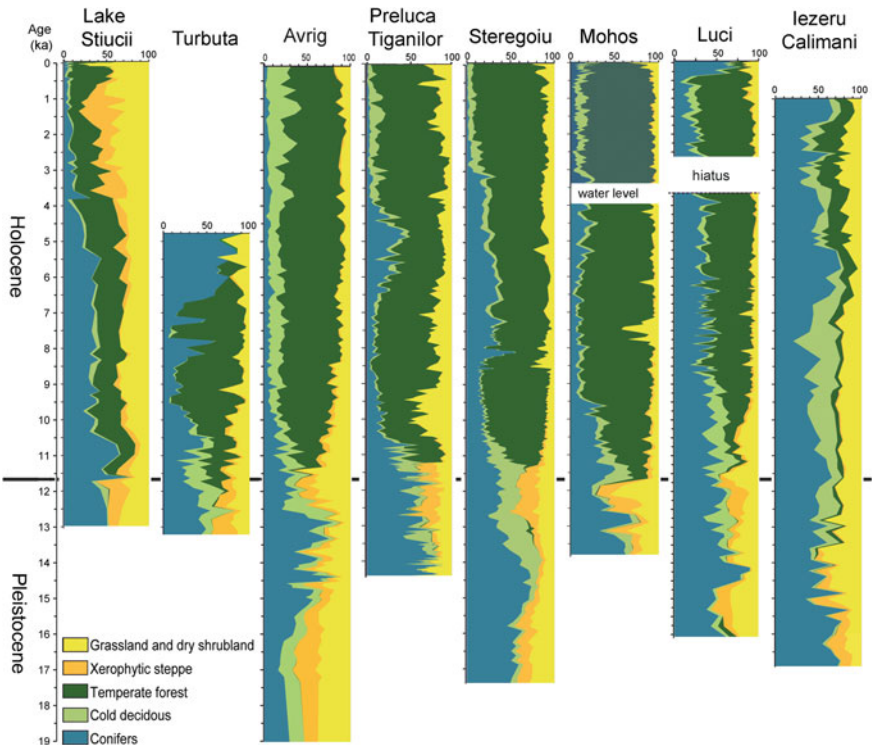

Fig. 4.2 Vegetation changes over the last 18 ka in high-resolution terrestrial pollen records from Romania. The taxa are grouped into a summary percentage diagram where each pollen type was assigned to a major vegetation type following a simple biome scheme

composed of arctic herbs and shrubs that occur where the conditions are too cold for trees to grow (Fig. 4.4). Such a mixture of vegetation assemblages was possible during the glacial times due to the overlap of extreme cold and dry conditions (Fig. 4.4).

Box 1. Pollen records from Romania covering the end of the Last Glacial indicate the occurrence of open boreal forest, principally needle-leaved and cold deciduous trees. Small populations of temperate deciduous trees may have been also present in the region.

A considerable expansion of boreal forests took place in response to temperature increase at the onset of the Lateglacial (14.7 ka) in the region (Figs. 4.2 and 4.3), with a slight elevational distinctiveness in the vegetation composition (Fărcaş et al. 1999; Björkman et al. 2002; Tanţău et al. 2003, 2006, 2014a; Feurdean et al. 2007a, b, 2012b, 2014; Fărcaş and Tanţău 2012; Magyari et al. 2012, 2014). Specifically,

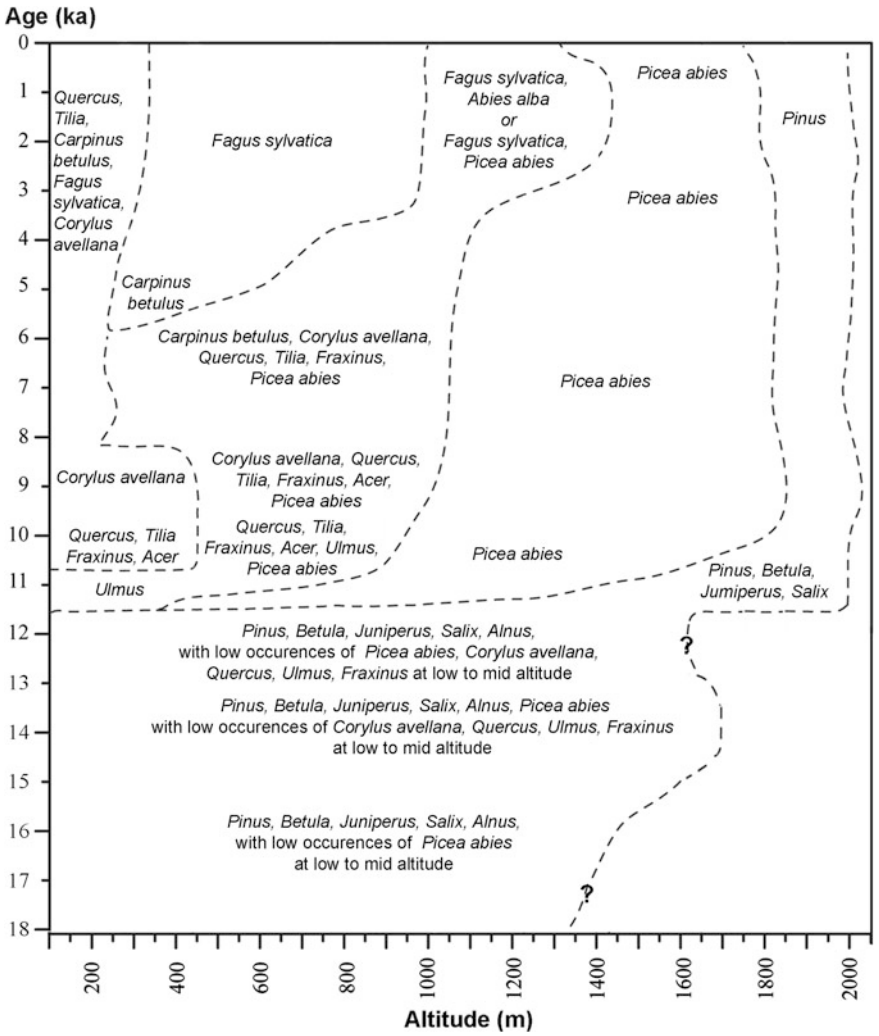

Fig. 4.3 Schematic representation of trends in the main forest constituents in Romania over the past 18 ka. *Dashed line* represents the spatial and temporal limits of the main tree taxa

the pollen records from lowlands indicate the presence of open woodlands composed of needle-leaved taxa (*Pinus, Picea abies, Larix decidua*), cold deciduous species (*Betula, Alnus Salix*), and a greater extent of open habitats including grasses (Poaceae) and forbs (*Artemisia*, Chenopodiaceae, Asteraceae). Conversely, records from uplands contained more extensive boreal forests (Fig. 4.2). This inference is supported by the findings of macro-remains of *Pinus sylvestris, P. cembra, P. mugo*, *Betula* (*B. pubescens, B. pendula*) and *Salix* (Wohlfarth et al. 2001; Feurdean and Bennike 2004; Feurdean et al. 2007a, b; Magyari et al. 2012).

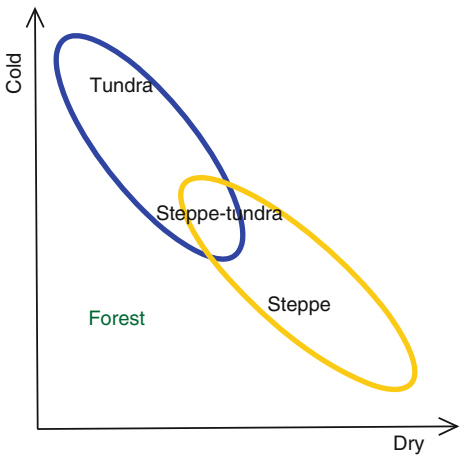

Fig. 4.4 Climatic niche of steppe–tundra vegetation. Tundra vegetation occurs under cold climatic conditions, while steppe vegetation prevails under too dry conditions for tree growth. The prevalence of mixt cold and dry conditions during the glacial time led to the formation of this non-analogue vegetation type

After the retreat or the halt in the forest development between 14.2 and 13.8 ka, there is a further expansion of forest associated to temperature and precipitation increase during the Allerød (GI–1c-1a) from 13.8 to 12.7 ka (Figs. 4.2 and 4.3). There is also a change in the forest composition from one dominated by *Pinus* and *Betula* to mixed forests with *Picea abies, Pinus,* and *Betula.* During this time interval, diversity and proportion of cold deciduous taxa (*Salix, Sambucus, Alnus, Populus tremula, Prunus padus*) as well as more warmth-demanding temperate tree species such as *Ulmus, Quercus, Tilia, Fraxinus excelsior* and *Corylus avellana* became enriched (Figs. 4.2 and 4.3).

Box 2. The response of vegetation to the Lateglacial warming is characterised by: (i) The expansion of forest cover and tree diversity; and (ii) The expansion of *Picea abies* and to some extend of warmth-demanding temperate trees (*Ulmus, Quercus, Fraxinus, Corylus avellana*).

Vegetation assemblages reacted sensitively to the cold and dry conditions of the Younger Dryas (YD)/GS–1 (12.7–11.7 ka). There is a fragmentation of the forest cover and reduced tree diversity, which paralleled an expansion of grasslands and steppe–tundra vegetation (Fărcaş et al. 1999; Björkman et al. 2002; Tanţău et al. 2003, 2006, 2014a; Feurdean et al. 2007a, b, 2012b, 2015; Fărcaş and Tanţău 2012; Magyari et al. 2012, 2014). The most evident change in the tree species composition is that dry-adapted, needle-leaved taxa (*Pinus* and *Larix decidua)* as well as *Betula* have replaced *Picea abies* and the deciduous species further diminished their population size (Fig. 4.2).

Following the cold and dry YD period, the pollen and plant macrofossil records indicate a marked vegetation response to the temperature and precipitation increase at the YD/Holocene transition (11.7 ka). This was manifested as a retraction of

steppe–tundra vegetation and an advancement of tree cover (Figs. 4.2 and 4.3). Initially, the woodlands were primary composed of cold deciduous temperate taxa (*Betula, Alnus, Salix*). This was followed (11.3 ka) by the expansion of temperate forests dominated by *Ulmus*, whereas from 10.7 ka also of *Quercus, Tilia, Acer, Fraxinus excelsior, Corylus avellana* (Figs. 4.2 and 4.3). In addition, the plant macrofossil records at these sites indicate that *Larix decidua* was a significant component of the early Holocene forests (Feurdean and Bennike 2004; Magyari et al. 2012).

Box 3. The drop in temperature and precipitation during the Younger Dryas led to the fragmentation of the boreal forest cover and a re-expansion of steppe–tundra habitats. Conversely, the steppe–tundra retracted quickly at the onset of the Holocene warming. Rapid forest advancement initially composed of needle-leaved taxa and cold deciduous tree taxa (11.7 ka) were followed by the expansion of temperate deciduous taxa (11.3 ka).

Ecosystem Responses to Repeated Climatic Shifts of the Lateglacial

The pollen and macrofossils records indicate that each abrupt climatic cooling event of the Lateglacial (Older Dryas, Younger Dryas) caused a rapid modification in the ecosystem composition, manifested as the reduction of the abundance or local extinction of many tree taxa alongside the development of plant communities with no modern analogue such as the steppe–tundra (Fig. 4.5).

However, forests were capable of recovering during each subsequent warm period (Bølling, Allerød, early Holocene). Taxa that expanded at the beginning of each warm period (*Pinus, Betula, Alnus, Salix,* and *Juniperus*) were those that have biological traits which enable a rapid response to climate change including fast life history strategies (i.e. rapid establishment probability, lower sum of minimum growing degree days, high relative growth rate, lower minimum seed-bearing age) and high stress tolerance rates (i.e. to drought, temperature fluctuations). Tree taxa that needed longer to expand (*Picea abies, Ulmus, Quercus, Tilia, Fraxinus excelsior, Acer,* and *Corylus avellana*) have slower life history traits (i.e. a longer life span, slower recruitment and reproductive maturity, larger sum of minimum growing degree days) and lower stress tolerance (Bhagwat and Willis 2008; Feurdean et al. 2012b).

Statistical examination of temporal changes in vegetation assemblages indicates that the major vegetation shifts occurred around 11.7 ka, but other transitions were also visible around 14.7, 13.8 and 12.7 ka (Feurdean et al. 2012b; Tanţău et al. 2014a). The Younger Dryas/Holocene transition features the strongest

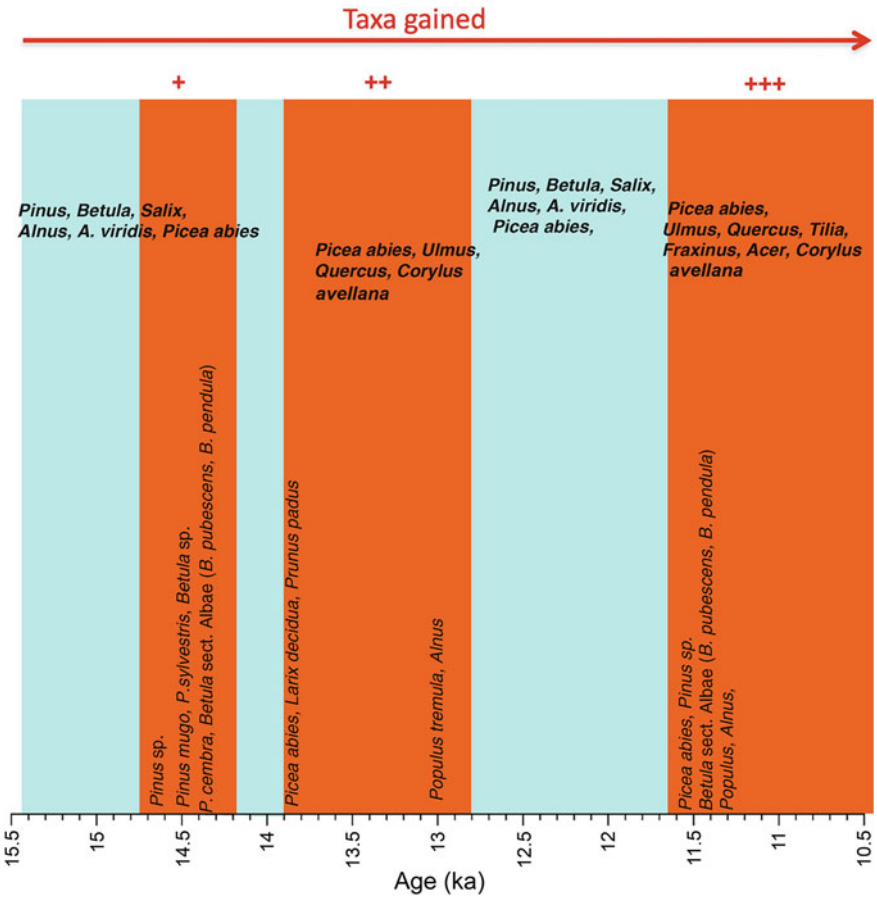

Fig. 4.5 Tree succession during the Lateglacial showing stages of tree recovery during the warm interstadials (*orange rectangle*) and their reduction during cold stadials (*blue rectangle*)

compositional change (turnover), when about 70 % of the early Holocene vegetation assemblages were different compared to those of the cold Younger Dryas (Feurdean et al. 2012b). Results from numerical modelling show that sites at mid-elevations show the greatest compositional changes (Fig. 4.6). This implies that mid-elevations were more sensitive to past climate fluctuations.

Box 4. Changes in vegetation assemblages were strongest at the YD/Holocene transition (11.7 ka) and mid-elevations (700–1000 m) appear to have been the most sensitive to abrupt climate shifts.

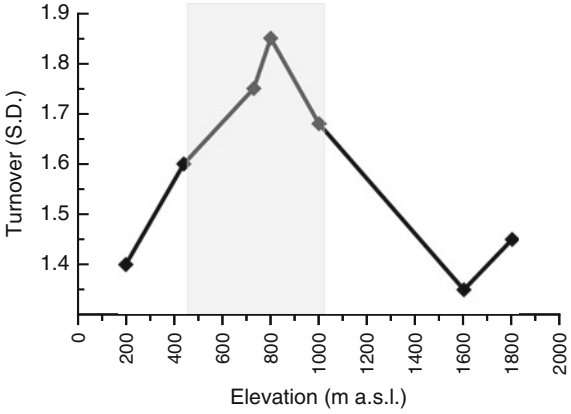

Fig. 4.6 Estimated compositional turnover plotted against an elevation gradient (redrawn from Feurdean et al. 2012b; *SD* = standard deviation)

Patterns in the Main Tree Taxa Dynamics During the Holocene

The pollen records indicate that the forest composition has been dynamic throughout the Holocene with changes in tree diversity and distribution that can be grouped into five temporal categories: taxa that expanded at the onset of the Holocene (*Betula, Larix decidua, Pinus, Picea abies, Ulmus*); taxa that peaked during the early Holocene (*Ulmus*, *Quercus, Tilia, Fraxinus excelsior, Acer*); taxa that were the abundant during the early Holocene (*Corylus avellana* and *P. abies*); taxa that expanded during the late Holocene (*Carpinus betulus, Fagus sylvatica* and *Abies alba*); and taxa that show re-increasing values during last centuries e.g. *P. abies, Pinus, Alnus, Betula, C. avellana, Salix, Pinus, F. excelsior*, *Sambucus, Sorbus,* and *Viburnum* (Fig. 4.3).

Picea abies, a species with widespread glacial refugia in Romania, expanded at the onset of the postglacial (11.7 ka) and has maintained its abundance throughout the Holocene (Fig. 4.3). *P. abies* shows a second population expansion during mid-Holocene (at ca. 8 ka). The main driver of its expansion was found to be climate-mediated competition (Björkman et al. 2003; Feurdean et al. 2011; Tanţău et al. 2014a). The recent increased proportion in *P. abies* was, however, documented to be a result of active management that includes forest exploitation and plantation for timber production (Fărcaş et al. 2003; Feurdean and Willis 2008a; Feurdean et al. 2011). These pollen records also show that *P. abies* is the native dominant forest species at mid-high and high elevation mountain belts (1200–1800 m a.s.l.) in Romania.

Pinus had the most extensive distribution during glacial time and between 11.7 and 11 ka (Fig. 4.3). It was documented to decrease significantly between 11 and 10 ka at low to mid-elevation as a result of competitive replacement by deciduous taxa (Björkman et al. 2003; Feurdean et al. 2011; Tanţău et al. 2014a). Its small,

recent return was found to be the consequence of active forest management, including plantation (Fig. 4.3).

The expansion of *Ulmus* has occurred synchronously across Romania at the onset of the Holocene (ca. 11.3 ka), due to its local survival in glacial refugia. It was then followed (11–10.7 ka) by *Quercus, Tilia, Fraxinus excelsior,* and *Acer,* species that had more restricted refugia (Fig. 4.3). Their extensive distribution between 10.7 and 8.6 ka resulted in a large replacement of needle-leaved (*Larix decidua, Pinus, Picea abies*) and cold deciduous species (*Betula, Alnus*) particularly at low and mid-elevations (Fărcaş et al. 1999, 2013; Tanţău et al. 2003, 2006, 2009, 2014a; Feurdean 2005; Feurdean et al. 2007b, 2009, 2010). The palaeoecological results indicate that *Ulmus, Tilia, F. excelsior* and *Acer* proportion declined at all sites already during the early Holocene (8.5–7.5 ka). Their marked reduction in the forests of Romania has occurred between 4 and 1.5 ka and these taxa never regained the former importance (Fărcaş et al. 1999, 2013; Tanţău et al. 2003, 2006, 2009, 2011a, b, 2014a, b; Feurdean 2005; Feurdean et al. 2007b, 2009, 2010). Their decline was linked with human impact on these forests (Figs. 4.3 and 4.7). *Quercus*, on the other hand, has been able to maintain its abundance throughout the Holocene

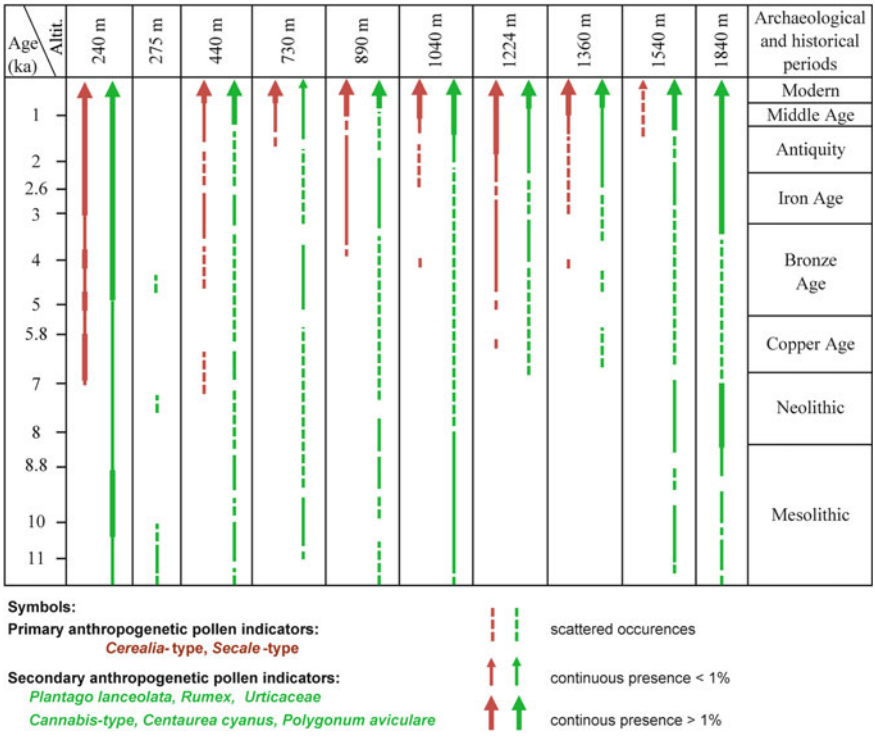

Fig. 4.7 Schematic representation of the occurrence of cultivated (primary) and ruderal/pastoral (secondary) anthropogenic pollen indicators at selected sites from Romania. Archaeological and historical periods are also indicated

(Feurdean et al. 2009, 2011; Tanţău et al. 2014a). In combination with increased light demanding species and anthropogenic indicators in the pollen records, it appears that *Quercus* has benefited from increasing light following the opening up of the primeval forests and from forest management as humans have protected *Quercus* forests for their acorn value for pigs (Carrión et al. 2001; Feurdean et al. 2009).

The *Corylus avellana* spread was an asynchronous process within Romania, occurring from about 10.3 ka at western sites and around 9.3 ka in the eastern Carpathians (Fărcaş et al. 1999, 2007, 2013; Rösch and Fischer 2000; Bodnariuc et al. 2002; Tanţău et al. 2003, 2006, 2009, 2011a, 2014a, b; Feurdean 2005; Feurdean et al. 2007b, 2009, 2010; Magyari et al. 2009). *C. avellana* appears to have been a co-dominant forest component with *P. abies,* a forest association with no modern analogue in the current forests of Romania (Fig. 4.3). Its decline has occurred at around 5.5 ka, when it was largely replaced by *Carpinus betulus.*

Carpinus betulus expanded from ca. 6.5 ka and was an important forest constituent between 5.5 and 3.5 ka (Fărcaş et al. 1999, 2007, 2013; Rösch and Fischer 2000; Bodnariuc et al. 2002; Tanţău et al. 2003, 2006, 2009, 2011a, 2014a, b; Feurdean 2005; Feurdean et al. 2007b, 2009, 2010; Magyari et al. 2009). It probably grew in mixed forest stands with *Tilia, Quercus, Ulmus, Acer*, *Fraxinus excelsior* at low elevation, and with *Fagus sylvatica* in the low mountain belt (probably up to 600 m a.s.l). The abundance of *Carpinus betulus* in the Romanian forests was of rather short duration and it was replaced by *F. sylvatica,* firstly in the western parts (at ca. 5 ka), followed by the eastern part (ca. 3 ka). *Carpinus betulus* proportion became significantly reduced from ca. 2 ka. Its decline was assigned to increased human pressure, although climate mediated competitive exclusion cannot be ruled out (Feurdean et al. 2009; Tanţău et al. 2011a, 2014a). Anthropogenic-induced disturbances have also facilitated the recent extension of other early successional species or those with fast recruitment and regeneration rates, i.e. *Alnus, Betula, Corylus avellana, Salix, Pinus, F. excelsior*, *Sambucus, Sorbus,* and *Viburnum* (Fig. 4.3).

Fagus sylvatica, a late successional, shade tolerant species, has been continuously present in the sub-montane and mid-altitudinal forest belts of Romania from ca. 5 ka onwards (Fig. 4.3). The highest amount was recorded at mid-elevations, in agreement with its present-day altitudinal distribution. *F. sylvatica* proportion became slightly reduced from 500 years ago, and the reasons for its decline were clearance and selective logging and plantation with conifers (Fărcaş et al. 1999, 2007, 2013; Tanţău et al. 2003, 2006, 2009, 2011a, 2014a, b; Feurdean 2005; Feurdean et al. 2007b, 2009, 2010; Magyari et al. 2009; Geantă et al. 2014). Currently, *F. sylvatica* is the dominant forest species in lower mountain belts (600–800 m a.s.l.), and the second abundant after *Picea abies* in the upper mountain forests (Toader and Dumitru 2004).

Abies alba, a late successional slow growing species is the youngest tree species in the Romanian forests. It first expanded in the western Carpathians (ca. 5 ka), then in the eastern part around ca. 3 ka. *A. alba* is sensitive to forest grazing and disturbance by fire (Feurdean and Willis 2008b) and hence forests characterized by high abundance of this taxon became strongly reduced or fragmented over the last

few centuries due to overexploitation (Feurdean and Willis 2008b; Tanţău et al. 2011a; Geantă et al. 2014).

Box 5. Climate, location of the glacial refugia, and a reduced inter-specific competition were important in shaping tree distribution and diversity patterns during the early to mid-Holocene. Distribution and abundance of tree species during the late Holocene were more dependent on human impact. There is also variability in the relative abundance of major functional tree types (broadleaved/needle-leaved tree cover) throughout the Holocene. The early-mid Holocene extension of needle-leaved forest (*Picea abies*, *Pinus, Larix decidua*) appears to have been driven by natural causes, whilst their late Holocene extension has been favoured by forest clearance followed by plantation. Thus, many of today's forests are compositionally and proportionally different from the original forests.

The Influence of Human Impact on the Vegetation

Results from vegetation modelling in Europe suggest that due to the technological limitations, a high area per capita (ca. 6.5 ha) was needed by Neolithic populations until about 2500 years ago. A smaller area was used thereafter due to the technological improvements (Kaplan et al. 2009, 2011).

A common feature in our Holocene pollen records is the discontinuous presence of pollen types associated to ruderal places, pastures and meadows (secondary anthropogenic pollen indicators) from the early Holocene (Fig. 4.7). There is also an isolated occurrence of pollen of cultivated plants at most of these sites from 7.5 ka (Fig. 4.7). Nevertheless, evidence of cultivated fields is particularly apparent in the lowland records, with Lake Ştiucii sequence in the Transylvanian Plain revealing the most continuous and sustained impact of humans on the vegetation (Feurdean et al. 2015). It has been suggested that wild plants such as *Cornus mas, Corylus avellana, Sambucus nigra/ebulus, Vitis, Prunus type (Prunus, Malus, Pyrus*) were used as food resources by the Mesolithic and Neolithic communities (Marinova et al. 2013). Their continuous presence in the Holocene pollen diagrams may indicate that humans may have used these plants in their diet (Feurdean et al. 2013a).

A more continuous and abundant occurrence of secondary anthropogenic pollen indicators (particularly *Plantago lanceolata* and *Rumex*) and of herbs diversity is noted from about 4–3 ka, corresponding to the Bronze Age/early Iron Age (Fig. 4.7 Geantă et al. 2014). This feature is also pronounced at pollen sites from mountainous area. Therefore the main signal in terms of a change in land use strategies is the increasing use of higher mountain areas for seasonal pastoral activities. Because

the increased pasture area was also associated to a rise in charcoal abundance, it appear that fire was used to create and enlarge pastures (Feurdean et al. 2012a). The next distinct rise in the abundance of both primary and secondary anthropogenic indicators is evident at the beginning of the Roman Period (2000 years). This paralleled a decrease in forest cover in particular of *Fagus sylvatica* and *Abies alba* (Figs. 4.3 and 4.7). Key changes in the land use during the Roman period were the spread of intensive agriculture at a larger scale, and the increased demand for wood for construction, fortifications and mining (Cârciumaru 1995/1996; Wollmann 1996).

From the Middle Age onwards (from 1 ka) the occurrence of pollen types of cultivated land (*Secale, Hordeum, Triticum*, *Zea, Centaurea cyanus, Polygonum aviculare, Agrostemma githago*) and pastoral activities became continuous at all sites, regardless of elevation (Fig. 4.7). However, the magnitude of forest clearance, animal husbandry and agricultural farming appears more extensive and sustained in the lowlands. For example, the pollen record from Lake Ştiucii (Transylvania Depression) indicates that human activities have been continuous for almost four millennia and led to profound ecological changes on the landscape in this region, i.e. transition from woodlands to forest steppe biome (Feurdean et al. 2013b, 2015). In agreement with our pollen records from the upland areas, simulations of the rate of deforestation obtained by Kaplan et al. (2009) indicate that mountain areas in Eastern Europe appear to have retained large tracts of their natural forests until at least ca. 1000 years ago. In contrast, the pollen-based finding of significant land transformation by humans already four millennia ago in the lowlands was much earlier than modelled for this region. The mismatch between the pollen-based land cover reconstruction and modelled land cover indicates that regional natural variations in environmental factors and shifting socio-economic boundaries are not always captured by the models.

Box 6. The pollen records show signs of arable agriculture from early Neolithic, i.e. 7.5 ka. A more continuous and abundant presence of pastoral indicators occurred in the late Bronze Age/early Iron Age (3.5 ka), during the Roman Age (2 ka), and with the onset of Middle Age (the last 1 ka). Lowlands, however, appeared earlier and stronger impacted than the high elevations. Heavily exploited ecosystems have led to irreversible ecosystem changes in this region.

Acknowledgements We acknowledge financial support from the Romanian National Authority for Scientific Research, CNCS – UEFISCDI PN-II-RU-TE-2011-3-0145, PN-II-RU-TE-2014-4-2445.

References

Bakker J, Paulissen E, Kaniewski D, Poblome J, De Laet V, Verstraeten G, Waelkens M (2013) Climate, people, fire and vegetation: new insights into vegetation dynamics in the eastern Mediterranean since the first century AD. Climate Past 9:57–87

Behre KE (1981) The interpretation of anthropogenic indicators in pollen dia-grams. Pollen Spores 23:225–245

Behre KE (1988) The role of man in European vegetation history. In: Huntley B, Webb T (eds) Vegetation history. Kluwer Academic Publishers, London, pp 633–672

Bhagwat SA, Willis KJ (2008) Species persistence in northerly glacial refugia of Europe: a matter of change or biogeographical traits? J Biogeogr 35:464–482

Björkman S, Feurdean A, Cinthio K, Wohlfarth B, Possnert G (2002) Late Glacial and early Holocene vegetation development in the Gutâiului Mountains, northwestern Romania. Quatern Sci Rev 21:1039–1059

Björkman S, Feurdean A, Wohlfarth B (2003) Late glacial and Holocene forest dynamics at Steregoiu in the Gutâiului Mts., Northwest Romania. Rev Palaeobot Palynol 124:79–111

Bodnariuc A, Bouchette A, Dedoubat JJ, Otto T, Fontugne M, Jalut G (2002) Holocene vegetational history of the Apuseni Mountains, central Romania. Quatern Sci Rev 21:1465–1488

Brun C (2009) Biodiversity changes in highly anthropogenic environments (cultivated and ruderal) from the Neolithic to present day in the eastern part of France. Holocene 19:861–871

Brun C (2011) Anthropogenic indicators in pollen diagrams in eastern France: A critical review. Veg Hist Archaeobotany 20:135–142

Cârciumaru M (1995/1996) Paleoethnobotanica. Studii în preistoria şi protoistoria României. Istoria agriculturii din România. Bucureşti (in Romanian)

Carrión JS, Andrade A, Bennett KD, Munuera M, Navarro C (2001) Crossing forest thresholds. Inertia and collapse in a Holocene sequence from south-central Spain. Holocene 11:635–653

Cristea V (1993) Fitosociologie şi vegetaţia României. Babeş-Bolyai University, Cluj (in Romanian)

Doniţa N (1962) Elemente pentru interpretarea zonalităţii vegetaţiei din RPR. Acta Horti Botanici Bucurestiensis, pp 919–935 (in Romanian)

Fărcaş S, Tanţău I (2012) Poiana Ruscă Mountains (Romania). Peşteana peat bog. Grana 51:249–251

Fărcaş S, de Beaulieu JL, Reille M, Coldea G, Diaconeasa B, Goeury C, Goslar T, Jull T (1999) First 14C datings of late Glacial and Holocene pollen sequences from Romanian Carpathes. Comptes Rendus de l'Académie des Sciences de Paris 322:799–807

Fărcaş S, Tanţău I, Bodnariuc A (2003) The Holocene human presence in Romanian Carpathians, revealed by the palynological analysis. Wurzburger Geographische Manuskripte 63:111–128

Fărcaş S, Tanţău I, Bodnariuc A, Feurdean A (2007) L'histoire des forets et du paléoclimat Holocène dans les Monts Apuseni. Contribuţii Botanice 42:115–126

Fărcaş S, Tanţău I, Mîndrescu M, Hurdu B (2013) Holocene vegetation history in the Maramureş Mountains (Northern Romanian Carpathians). Quatern Int 293:92–104

Feurdean A (2005) Holocene forest dynamics in northwestern Romania. Holocene 13:435–446

Feurdean A, Bennike O (2004) Late Quaternary palaeoecological and palaeoclimatological reconstructions in the Gutâiului Mountains, northwest Romania. J Quat Sci 19:809–827

Feurdean A, Willis KJ (2008a) The usefulness of a long-term perspective in assessing current forest conservation management in the Apuseni Natural Park, Romania. For Ecol Manage 256:421–430

Feurdean A, Willis KJ (2008b) Long-term variability of Abies alba (Mill.) populations in the NW Romanian forests implications for its conservation management. Divers Distrib 14:1004–1017

Feurdean A, Wohlfarth B, Björkman S, Tanţău I, Bennike O, Willis KJ, Fărcaş S, Robertsson AM (2007a) The influence of refugial population on Lateglacial and early Holocene vegetational changes in Romania. Rev Palaeobot Palynol 145:305–320

Feurdean A, Mosbrugger V, Onac B, Polyak V, Vereş D (2007b) Younger Dryas to mid-Holocene environmental history of the lowlands of NW Transylvania, Romania. Quat Res 68:364–378

Feurdean A, Willis KJ, Astaloş C (2009) Legacy of the past land use changes and management on the 'natural' upland forests composition in the Apuseni Natural Park, Romania. Holocene 19:1–15

Feurdean A, Willis KJ, Parr C, Tanţău I, Fărcaş S (2010) Postglacial patterns in vegetation dynamics in Romania: homogenization or differentiation? J Biogeogr 37:2197–2208

Feurdean A, Tanţău I, Fărcaş S (2011) Temporal variability in the geographical range and abundance of *Pinus, Picea abies*, and *Quercus* in Romania. Quat Sci Rev 30:3060–3075

Feurdean A, Spessa A, Magyari EK, Willis KJ, Veres D, Hickler T (2012a) Trends in biomass burning in the Carpathian region over the last 15,000 years. Quat Sci Rev 45:111–125

Feurdean A, Tămaş T, Tanţău I, Fărcaş S (2012b) Elevational variation in the biotic response to repeated climate changes in the Carpathians as revealed by the pollen records. J Biogeogr 39:258–271

Feurdean A, Parr C, Tanţău I, Fărcaş S, Marinova E, Perşoiu I (2013a) Biodiversity variability across elevations in the Carpathians: parallel change with landscape openness and land use. Holocene 23:869–881

Feurdean A, Liakka J, Vanniere B, Marinova E, Mossbruger V, Hickler T (2013b) Holocene fire regime drivers in the lowlands of Transylvania (Central-Eastern Europe): a data-model approach. Quat Sci Rev 81:48–61

Feurdean A, Perşoiu A, Tanţău I, Stevens T, Markovic S, Magyari EK, Onac BP, Andric M, Connor S, Galka M, Hoek WZ, Lamentowicz M, Sümegi P, Perşoiu I, Kolaczek P, Kuneš P, Marinova E, Slowinski M, Michczyńska D, Stancikaite M, Svensson A, Veski S, Fărcaş S, Tămaş T, Zernitskaya V, Timar A, Tonkov S, Toth M, Willis KJ, Płóciennik M, Gaudeny T (2014) Climate variability and associated vegetation response throughout Central and Eastern Europe (CEE) between 8 and 60 kyrs ago. Quat Sci Rev 15:204–244

Feurdean A, Marinova E, Nielsen AB, Liakka J, Veres D, Hutchinson SM, Braun M, Timar-Gabor A, Astalos C, Mossbruger V, Hickler T (2015) Origin of the forest steppe and exceptional grassland diversity in Transylvania (central-eastern Europe). J Biogeogr 42:951–963

Geantă A, Gałka M, Tanţău I, Hutchinson SM, Mîndrescu M, Feurdean A (2014) High mountain region of the Northern Romanian Carpathians responded sensitively to Holocene climate and land use changes: a multi-proxy analysis. Holocene 23(6):869–881

Haesaerts P, Borziak I, van der Plicht I, Damblon F (1998) Climatic events and upper Paleolithic chronology in the Dniester basin: New 14C results from Cosautsi. Radiocarbon 40:649–657

Kaplan JO, Krumhardt KM, Zimmermann N (2009) The prehistoric and preindustrial deforestation of Europe. Quat Sci Rev 28:3016–3034

Kaplan JO, Krumhardt KM, Ellis EC, Ruddiman WF, Lemmen C, Goldewijk KK (2011) Holocene carbon emis-sions as a result of anthropogenic land cover change. Holocene 21:775–791

Magyari EK, Buczkó K, Jakab G, Braun M, Pál Z, Karátson D, Papp P (2009) Palaeolimnology of the last crater lake in the Eastern Carpathian Mountains—a multiproxy study of Holocene hydrological changes. Hydrobiologia 631:29–63

Magyari EK, Jakab G, Balint M, Kern Z, Buczkó K, Braun M (2012) Rapid vegetation response to Lateglacial and early Holocene climatic fluctuation in the South Carpathian Mountains (Romania). Quatern Sci Rev 35:116–130

Magyari EK, Kuneš P, Jakab G, Sümegi P, Pelánková B, Schäbitz F, Braun M, Chytrý M (2014) Last glacial maximum vegetation in East Central Europe: are there true analogues in Siberia? Quatern Sci Rev 95:60–79

Marinova E, Tonkov S, Bozilova E, Vajsov I (2012) Holocene anthropogenic land-scapes in the Balkans: The paleobotanical evidence from southwestern Bul-garia. Veget Hist Archaeobotany 21:413–427

Marlon JR, Bartlein PJ, Daniau AL, Harrison SP, Maezumi SY, Power MJ, Tinner W, Vanniére B (2013) Global biomass burning: a synthesis and review of Holocene paleofire records and their controls. Quatern Sci Rev 65:5–25

Rösch M, Fischer E (2000) A radiocarbon dated Holocene pollen profile from the Banat Mountains (southwestern Carpathians, Romania). Flora 195:277–286

Tanţău I (2006) Histoire de la végétation tardiglaciaire et holocène dans les Carpates Orientales (Roumanie). Ed. Presa Universitară Clujeană, Cluj-Napoca, pp 200

Tanţău I, Reille M, de Beaulieu JL, Fărcaş S, Goslar T, Paterne M (2003) Vegetation history in the eastern Romanian Carpathians: pollen analysis of two sequences from the Mohoş crater. Veget Hist Archaeobotany 12:113–125

Tanţău I, Reille M, de Beaulieu JL, Fărcaş S (2006) Late Glacial and Holocene vegetation history in the southern part of Transylvania (Romania): pollen analysis of two sequences from Avrig. J Quat Sci 21:49–61

Tanţău I, Reille M, de Beaulieu JL, Fărcaş S, Brewer S (2009) Holocene vegetation history in Romanian Subcarpathians. Quat Res 72:164–173

Tanţău I, Feurdean A, de Beaulieu JL, Reille M, Fărcaş S (2011a) Holocene vegetation history in the upper forest belt of the Eastern Romanian Carpathians. Palaeogeogr Palaeoclimatol Palaeoecol 309:281–290

Tanţău I, Fărcaş S, Beldean C, Geantă A, Ştefănescu L (2011b) Late Holocene paleoenvironments and human impact in Făgăraş Depression (Southern Transylvania, Romania). Carpathian J Earth Environ Sci 6:101–108

Tanţău I, Feurdean A, de Beaulieu JL, Reille M, Fărcaş S (2014a) Vegetation sensitivity to climate changes and human impact in the Harghita Mountains (Eastern Romanian Carpathians) over the past 15,000 years. J Quat Sci 29:141–152

Tanţău I, Geantă A, Feurdean A, Tămaş T (2014b) Pollen analysis from a high altitude site in Rodna Mountains (Romania). Carpathian J Earth Environ Sci 9(2):23–30

Toader T, Dumitru I (2004) Romanian Forests. National parks and natural parks. National Forest Administration ROMSILVA, Bucharest

Van Geel B, Bohncke SJP, Dee H (1980) A palaeoecological study of an upper Late Glacial and Holocene sequence from "De Borchert", The Netherlands. Rev Palaeobot Palynol 31:367–448

Whitlock C, Larsen CPS (2001) Charcoal as a fire proxy. In: Smol JS, Birks HJB, Last WM (eds) Tracking environmental change using lake sediments. Kluwer Academic Publishers, Dordrecht, pp 75–97

Willis KJ, Birks HJB (2006) What is natural? The need for a long-term perspective in biodiversity conservation. Science 314:1261–1265

Wohlfarth B, Hannon G, Feurdean A, Ghergari L, Onac BP (2001) Reconstruction of climatic and environmental changes in NW Romania during the early part of the last deglaciation ($\sim$15,000–13,600 cal year BP). Quat Sci Rev 20:1897–1914

Wollmann V (1996) Mineritul metalifer, extragerea sării şi carierele de piatră în Dacia Romană. Bibliotheca Musei Napocensis XIII, Cluj-Napoca

Part II
Glacial and Periglacial Landforms

Chapter 5
Deglaciation History of High Massifs from the Romanian Carpathians: Towards an Integrated View

Răzvan Popescu, Petru Urdea and Alfred Vespremeanu-Stroe

Abstract The study of past glaciations extent and chronology in the Romanian Carpathians has been of great interest for scientists in the last 135 years. In the last decade, in addition to the geomorphologic investigations, several studies presented numerous absolute age datings of the glacial deposits that improved considerably the knowledge on the last glaciation chronology. Moreover, much progress was achieved in understanding the palaeoclimate oscillations during the last glacial cycle and Holocene. This paper summarizes the recent results and offers a unitary discussion of the deglaciation chronology of the highest massifs from the Romanian Carpathians (Retezat, Parâng, Făgăraș and Rodnei Massifs). The glacial oscillations in Southern Carpathians seem to be in good agreement with the Alpine chronology: a maximum extent during the global Last Glacial Maximum (LGM) with a preference for the LGM late phase (20–21 ka), up to three glacial readvances during the Oldest Dryas (18.6, 16.3 and 15.0 ka), one possible glacial advance during the Older Dryas (around 13.5 ka), a Younger Dryas glacial advance at 12.9–12.1 ka and a last possible glacial phase with isolated small glaciers and glacierets occurrence during the early Holocene cold events. Rodnei Massif seems to have a slightly different deglaciation pattern with an earlier local LGM (37–26 ka) and a different altitudinal moraine distribution. At their maximum phase, glaciers reached altitudes below 1200 and 900 m above sea level (a.s.l.) in Southern Carpathians and north of Eastern Romanian Carpathians, respectively, and their equilibrium line altitudes (ELAs) were below 1700 m a.s.l. During the warm phases of Late Glacial (Bølling/Allerød), the glaciers retreated dramatically or even disappeared

R. Popescu (✉)
Research Institute of the University of Bucharest, M. Kogălniceanu Bd. 36-46, 050107 Bucharest, 5th District, Romania
e-mail: razvan.popescu@geo.unibuc.ro

P. Urdea
West University of Timișoara, V. Pârvan 4, 300223 Timișoara, Timiș, Romania

A. Vespremeanu-Stroe
Faculty of Geography, University of Bucharest, N. Bălcescu 1, Sector 1, 010041 Bucharest, Romania

M. Rădoane and A. Vespremeanu-Stroe (eds.), *Landform Dynamics and Evolution in Romania*, Springer Geography,
DOI 10.1007/978-3-319-32589-7_5

completely from most of the glacial cirques. With all the new data and knowledge improvements, some uncertainties and contradictions appear and they need to be properly addressed in the coming years in order to understand in-depth the past evolution of the Romanian Carpathians.

Keywords Last glacial maximum · Lateglacial · Deglaciation · Cosmogenic nuclides · Glacial landforms · Romanian Carpathians

Introduction

The Carpathians represent a key region for the understanding of the spatial link between the eastern part of the Scandinavian Ice Sheet and Alpine glaciers (Urdea 2004). Romanian Carpathians are nowadays glacier-free mountain ranges exposed only to periglacial environment (cold climate) modeling at altitudes above the natural timberline. While glacierets or even perennial snow banks are absent in the Romanian Carpathians, the sporadic alpine permafrost and several ice caves are composing today the only perennially frozen deposits (Urdea 1993; Perşoiu and Pazdur 2011; Popescu et al. Chap. 6, this volume).

Pleistocene glaciers presence in the Romanian Carpathians is widely acknowledged and it was inferred for more than a century ago (Tietze 1878; Lehmann 1881, 1885). However, little progress was achieved in establishing a complete chronology of the glaciations timing and extent. This was mainly determined by the pale morphology of moraines—advance state of erosion and fossilization by post glacial deposits—and thus, difficult to observe in the field and identify on the topographical maps. Often, debris flow, landslide, and fluvial deposits may be mistakenly interpreted as terminal moraines (Urdea et al. 2011). As a result, the Quaternary glaciers extension and glacial chronology from the Romanian Carpathians was long time controversially discussed (Mihăilescu 1966; Posea et al. 1974; Niculescu et al. 1983; Urdea 2004), even on the first syntheses the opinions were very different (e.g. Puchleitner 1901; de Martonne 1904; Sawicki 1912). A better geomorphological situation exists in higher mountain ranges like the Alps subjected to heavier glaciations in the past and presenting much more expressive and better preserved glacial moraines.

In order to assign moraines to different time periods, a set of approaches can be used: determination of relative topographic and stratigraphic position, morphology analyses (shape, freshness, boulder size), determining the glaciological characteristics of palaeoglaciers, determining equilibrium line altitude (ELA) in the catchments and comparing it with the ELA of similar glaciers in the vicinity (Ivy-Ochs et al. 2009). More recently, quantitative determinations of glaciations chronologies started to be established based on absolute dating using terrestrial cosmogenic radionuclide technique (Kohl and Nishiizumi 1992).

In recent years, large scale glacial cirques inventories (Mîndrescu and Evans 2014) and several absolute moraine datings in the highest massifs of the Romanian

Carpathians (Reuther et al. 2007; Urdea and Reuther 2009; Gheorghiu 2012; Kuhlemann et al. 2013; Gheorghiu et al. 2015; Ruszkiczay-Rüdiger et al. 2015) changed the view upon glaciations extent and chronology in the Romanian Carpathians. Also, major progress in late Quaternary palaeoclimate and paleoenvironmental reconstructions was achieved in the last decade by investigating different climatic archives like speleothems (Onac et al. 2002; Tămaș et al. 2005; Constantin et al. 2007; Drăguşin et al. 2014) and alpine glacial lake sediments (Magyari et al. 2009, 2012, 2014).

The aim of the present paper is to summarize the major progresses that have been achieved (especially in the last decade) in the knowledge of the deglaciation history of the highest massifs of the Romanian Carpathians covered by the largest Pleistocene glaciers: Retezat, Făgăraș and Parâng Mountains from Southern Carpathians (SC) and Rodnei Mountains from Eastern Romanian Carpathians (ERC) (Fig. 5.1). We also aim to discuss all the results in relation with the palaeoclimatological information recently obtained. A special attention is paid to the transition from glacial to periglacial processes (and their interaction) in the Late Glacial and at the Pleistocene—Holocene boundary phase that brought the alpine relief close to the shape that we see today.

Regional Settings

Romanian Carpathians occupy c. 65,000 km^2 with more than 1/3 higher than 1500 m a.s.l. Southern Carpathians is the highest and the most massive sector of the Romanian Carpathians with 11 peaks above 2500 m a.s.l. The highest altitude is reached in the Moldoveanu Peak from Făgăraș Massif (2544 m). The upper limit of natural timberline is located at about 1800 m a.s.l. here and 1600 m in Rodnei Mountains.

The 0 °C mean annual air temperature (MAAT) isotherm is located at about 2050 m altitude in SC, respectively, at about 1850 m altitude in ERC. At Vârful Omu meteorological station (2504 m a.s.l.; Bucegi Mountains), the mean multiannual air temperature (1941–2014 interval) is −2.3 °C. Precipitations are greater than 1000 mm/year above 2000 m altitudes with northern slopes slightly wetter [c. 1200 mm/year at Bâlea Lake meteorological station (2037 m a.s.l.) from Făgăraș Mountains] (Sandu et al. 2008).

The Pleistocene glaciation affected only the valleys and cirques from massifs higher than 1800 m a.s.l. and did not reach the foreland (Posea et al. 1974; Urdea 2004). The most evident and widespread geomorphological signs of past glaciations are encountered in Southern Carpathians where 547 glacial cirques (87 % of all glacial cirques from Romanian Carpathians) were formed (Mîndrescu et al. 2010). In the SC, The Făgăraș and Retezat Massifs have the most extensive subalpine and alpine domains (>1800 m) with 238 and 116 km^2, respectively, while the other

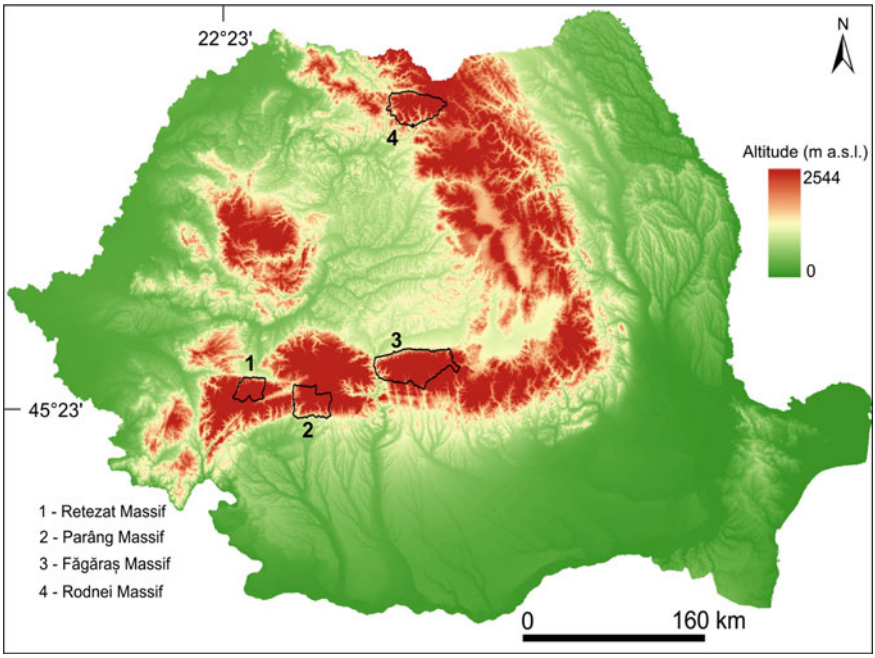

Fig. 5.1 Location of the four massifs from the Romanian Carpathians where recent investigations (discussed in the present paper) on deglaciation chronology were performed

ranges (Parâng, Bucegi, Iezer–Păpuşa etc.) are smaller than 75 km^2. The second sector of glaciation in Romanian Carpathians was located in the north (within ERC), in the Rodna, Maramureş and Călimani ranges, where the regional lower air temperatures compensated a slightly more reduced altitude (Mîndrescu et al. 2010), the maximum altitude is 2303 m a.s.l. in the Pietrosu Peak from the Rodnei Mountains).

Sculptural glacial landforms (cirques and U–shape valleys), well represented in the high mountains, can also be distinguished in middle altitude massifs. The glacial deposits, especially the terminal and lateral moraines from the lower altitudes were partially eroded or reworked by streams and covered by soil and forests while at higher altitudes, they were covered by newer materials resulted from the adjacent slopes erosion during the Holocene. However, the latter can still be distinguishable and are easier to map (Urdea and Reuther 2009).

Major glaciations (discussed herein) affected the four massifs composed by granitic rocks (Retezat, Parâng) and crystalline schists (Făgăraş and Rodnei) which permitted fairly uniform cirque erosion (Mîndrescu et al. 2010).

Deglaciation Chronology of the Romanian Carpathians

The research of the Romanian Carpathians glacial relief has known four major phases (Urdea and Reuther 2009). The first two (1880–1960 interval) consisted mostly in discovering and describing the glacial features from high massifs of SC and ERC leading to the first syntheses made either for a regional range (Puchleitner 1901; de Martonne 1907 for Southern Carpathians and Kräutner 1930 for the Eastern and Southern Carpathians) or for the entire Carpathian range (Sawicki 1912; Pawłowski 1936).

In a third phase, the Romanian geomorphologists attributed the glacial landforms to two major Pleistocene glacial cycles (Riss and Würm) for the Southern Carpathians (Niculescu et al. 1960, 1983; Posea et al. 1974) and even a third glacial phase (Mindel) for Rodnei Massif in the northern part of ERC (Sîrcu 1964, 1978). Some studies, however, indicate only one glacial phase in the Romanian Carpathians with several stadials than can explain the glacial relief (Posea 1981). These studies were influenced by the seminal work of Penk and Brückner (1909) who introduced the concept of four glaciation cycles during the Pleistocene (Günz, Mindel, Riss and Würm). This system is still maintained in an extended version in the forelands of the Eastern Alps (Feibig et al. 2011) while in other parts of the Alps, like in the Swiss sector, it was abandoned (Ivy-Ochs 2015). Instead, 15 independent glaciations are suggested to have occurred in this region (Schlüchter 2004).

In the fourth phase, geomorphologists offered a greater attention to glacial deposits (moraines) in regional studies (Nedelea 2006; Szepesi 2007; Andra 2008; Simoni 2011) and more recently it started the absolute dating of these landforms. For example Urdea (1993, 2000) performed a detailed mapping of several series of moraines in the Retezat Massif located between 1035 and 2150 m a.s.l. and correlated them with several glacial advances during Riss and Würm. In the last decade, absolute dating using the technique shed a new light upon the glaciation history in different massifs of the Romanian Carpathians and especially on the late Pleistocene period since the Last Glacial Maximum (LGM) to the Holocene when glaciers disappeared.

Glaciations during the early and middle Pleistocene were improbable in the Romanian Carpathians because of their low altitudes at that time (Badea et al. 1983; Reuther et al. 2007). The currently preserved glacial cirques may have developed in the last 360 ka with probable glacial conditions in marine isotopic stage (MIS) 2, 4, 6, 8, and 10 and with a lower probability in the MIS 12, the latter extending the time span of their formation to 470 ka (Mîndrescu et al. 2010).

Retezat Massif

Retezat Massif exhibits a rich and complex alpine morphology mainly shaped by glacial and periglacial processes which transformed this massif in the best studied alpine region (by mountain geomorphologists) from the Romanian Carpathians (Urdea 2000; Vespremeanu-Stroe et al. 2012; Onaca et al. 2015). Here, after early studies, Emm. de Martonne considered that at their maximum stage, the glaciers descended to about 1300 m on the northern slope, in Pietrele valley, and down to 1400 m on the southern slope in the Lăpușnicu Mare Valley (de Martonne 1907). In the same study, the author assumed that the longest glaciers reached 6–8 km and the perennial snow limit was below 1900 m a.s.l. In more recent and detailed studies, there were recognized several moraine generations initially attributed to ten glacial advances (Urdea 2000) that correspond to three or four major glacial episodes termed M1–M4 (Fig. 5.2).

The lowest moraines (M1 glacial advance) that can be identified in the Retezat Massif are situated at 1060 m a.s.l. on the southern slope (Lăpușnicu mare valley) and 1035 m a.s.l. on northern slope (Pietrele–Nucșoara glacial complex). They were deposited by glaciers reaching maximum lengths of 18 km (Lăpușnicu mare was the longest glacier from Retezat) and 7 km on the north side (Urdea 2000). While first estimations (Urdea 2000, 2004) attributed this maximum glacial advance to MIS 6 cold period (180–135 ka, Roucoux et al. 2011) based on the former glacial chronologies from the Alps and Tatra Mountains, Reuther et al. (2007) appreciated that the moraine would have been completely eroded if it was deposited over 130 ka and, based on pedological investigations, indicated an early Würmian age (70–50 ka). Surprisingly, the cosmogenic datings of boulders located on the lateral moraine of the same M1 moraines complex, indicated an age of only $21^{+0.8}_{-1.5}$ ka (Ruszkiczay-Rüdiger et al. 2015). This age corresponds with the late LGM which occurred between 30 and 19 ka BP in the European Alps and corresponds to MIS 2 stage (Ivy-Ochs 2015). During this period the palaeo ELA of glaciers was calculated to be at 1725 m a.s.l. using the accumulation–area ratio (AAR) (0.75) method (Reuther et al. 2004, 2007).

The medium altitude moraines complex (M2 glacial advance) mapped on Nucșoara–Pietrele (Urdea 2000) comprises two moraine sets, one reaching 1200 m a.s.l. corresponding to a major glacial advance down to the confluence of Stânișoara, Pietrele, Valea Rea, and Galeșu valleys (M2a), and another moraines set at 1600–1750 m a.s.l. corresponding to a smaller glacial readvance (M2b) (Ruszkiczay-Rüdiger et al. 2015) (Fig. 5.2). First age datings on 15 moraine boulders and one bedrock surface corresponding to M2 glacial advance located on 6 sites from Pietrele and Stânișoara valleys indicated that M2 glacial advance took place at 16–17 ka (Reuther et al. 2007). This advance was initially attributed to a local last glacial maximum (LLGM) delayed relative to global LGM because of the high aridity caused by the Black Sea low level at that time (Reuther et al. 2007); this interpretation was also encouraged by the assumed pre LGM age of the M1 moraine. However, new dated samples indicated older ages for M2a moraines

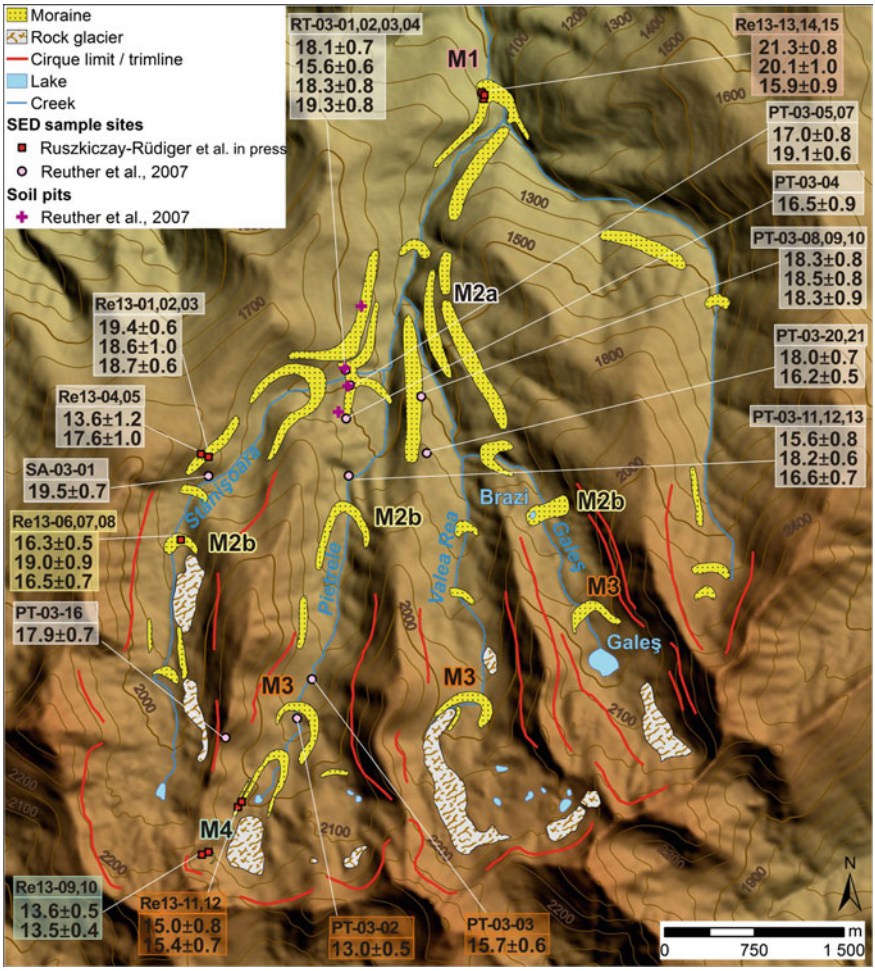

Fig. 5.2 The position of moraines and rock glaciers within the glacial complex of Nucşoara–Pietrele from the northern side of the Retezat Massif along with the ^{10}Be ages obtained by Ruszkiczay-Rüdiger et al. (2015) and the recalculated ages of Reuther et al. (2007) (from Ruszkiczay-Rüdiger et al. 2015)

($18.6^{+0.9}_{-0.8}$ ka) and M2b moraines (16.3 ± 0.6) (Ruszkiczay-Rüdiger et al. 2015). Also, recalculation of the ages published by Reuther et al. 2007 using new half-life and production rate of ^{10}Be (Korschinek et al. 2010) indicated they are in fact ca. 14 % older than the former estimation (19.5–18.0 ka for M2a moraines and 17.0–15.5 ka for M2b moraines) and fit well with the newly obtained ages (Ruszkiczay-Rüdiger et al. 2015). The ELA during the M2a glacial advance was calculated at 1770 m a.s.l. (Reuther et al. 2007) (Fig. 5.3).

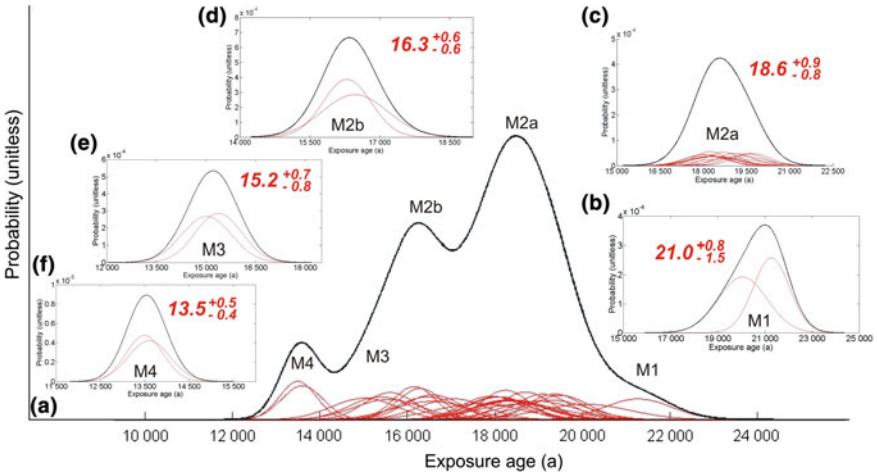

Fig. 5.3 Probability distribution functions of the ^{10}Be exposure ages obtained for several moraines corresponding to the main glacial advances on the Nucșoara–Pietrele glacial complex (Retezat Massif). The red curves represent individual boulder exposure ages and error with assumed Gaussian distributions while the bold black curves represents sum of individual distributions (from Ruszkiczay-Rüdiger et al. 2015)

The high altitude moraine set (M3 phase) comprise a well evidenced lateral moraine composed of blocky material, located in the Pietrele cirque at altitudes between 2000 and 2030 m a.s.l. and another end moraine located at a lower altitude of 1850–1950 m a.s.l. (Urdea 2000). Also, a prominent erratic block, called Bordul Tomii, from 1902 m a.s.l. is located between the two M3 moraines. The original ages obtained on two blocks related to M3 moraines were 13.6–11.4 ka (Reuther et al. 2007). However, the new samples from the higher M3 lateral moraine and age recalculation of the two boulders corresponding to the lower one by Ruszkiczay-Rüdiger et al. (2015) indicated older ages, of 15.4–15.0 and 15.7–13 ka, respectively; the unexpected young age of the Bordul Tomii erratic block (13.0 ka) determined the authors to consider it as an outlier and to exclude it from interpretation. The M3 moraine generation was attributed to a glaciers stabilization phase occurring at a mean age of $15.2^{+0.7}_{-0.8}$. The ELA at that time was calculated to about 2030 m a.s.l. (Reuther et al. 2007).

A last glacial readvance (M4) was inferred by geomorphological evidences in the small glacial cirque from western Pietrele valley (Ruszkiczay-Rüdiger et al. 2015). In this small cirque, the blocky deposit interpreted as a lateral-terminal moraine yielded a ^{10}Be age of $13.5^{+0.5}_{-0.4}$ ka based on samples from two different blocks.

Parâng Massif

This mountainous area gained early attention of geologists and geographers (e.g., Lehmann 1885; Mrazec 1898; de Martonne 1899). Their attention materialized in the identification of several glacial landforms at different altitudes, which were interpreted as tracers of distinct glacial phases. In addition, the first cartographic glaciers reconstructions for Southern Carpathians were performed by de Martonne (1907) and Schréter (1908) for Mija and Jieț basin respectively located in the Parâng Mountains. These glaciers reached lengths of about 6 km and altitudes of about 1300 m a.s.l., or slightly below (Grozescu 1920). The perennial snow limit —calculated using the Penck method—was at c. 1950 m a.s.l. (de Martonne 1907). Nevertheless, in comparison with the Retezat Massif, less information is available on Late Pleistocene glacial deposits (morphology, distribution and age) from Parâng massif. However, geomorphologic investigations along with exposure age datings were performed recently on Jieț and Lotrului valley (Urdea and Reuther 2009; Gheorghiu et al. 2015). The five samples located in the Groapa Seacă area from the Jieț valley, indicated ages of 17.9 ± 1.6–16.7 ± 1.5 ka for erratic boulders situated at 1197–1235 m a.s.l. (Urdea and Reuther 2009) but if we assume that these ages are ca. 14 % younger than in reality as recently indicated for the Retezat Massif (Ruszkiczay-Rüdiger et al. 2015), than their ages would increase to 20.6–19 ka. The older ages cluster would correspond well to the end of LGM, respectively, to M1 glacial phase from Retezat, while the youngest ages cluster to M2a glacial advance. Taking into consideration the close distance between Parâng and Retezat massifs (≈50 km) it is likely they would share a similar glacial chronology as well. Thus, they would correspond both to M1 and M2 moraines.

Gheorghiu et al. (2015) mapped and analyzed the glacial features from the crystalline upper sector of the Lotru river between 1400 and 2365 m a.s.l. comprising four distinct glacial cirques and valleys (from East to West: North Mohoru, Zănoaga Pietroasă, Gâlcescu and Zănoaga Mare) and dated 24 moraine boulders using ^{10}Be cosmogenic nuclides technique. The main results presented by Gheorghiu et al. (2015) will be summarized in the followings. First, their ages address the deglaciation history post 14 ka. No moraines were found below 1700 m a.s.l. because of the river incision in its middle sector (around 1400 m a.s.l.). Several lateral moraines, some of them parallel to each other reflecting different glacier thickness levels, and other terminal moraines with more reduced surfaces were mapped in the study area (Fig. 5.4). High altitude recessional moraines, located at the slope bottom are topographically evidenced.

The authors assume the presence of an indented glacier composed of several branches corresponding to each valley of the study area (Lotru glacial complex) which entered a downwasting phase because of the climate warming after 14 ka. The main body of the complex glacier melted at that time and the remaining branches entered a retreating phase at different speeds. The Gâlcescu and North Mohoru glaciers retreated slowly because of their narrower cirque topography and associated colder microclimates which determined thicker ice bodies to be formed

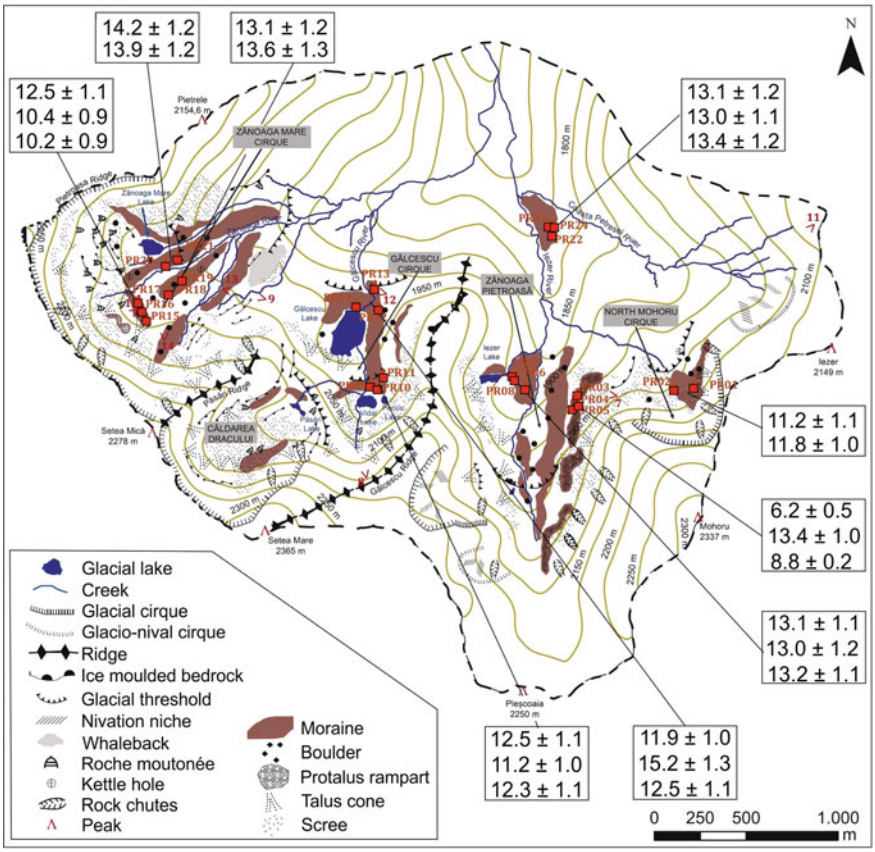

Fig. 5.4 Geomorphological map and glacial landforms of the upper sector of Lotrului Valley (Parâng Massif) (after Gheorghiu et al. 2015)

and slower ice degradation. Also, Gâlcescu cirque was fed by ice from the upper cirque of Căldarea Dracului. As a consequence, Gâlcescu glacier was reaching altitudes of 1930 m at 12.5 ka and North Mohoru glacier reached 1765 m a.s.l. at 13–13.4 ka. In opposition, the Zănoaga Mare glacier retreated much faster because of its well-opened cirque and related warmer microclimate which determined thin glacier morphology and faster ice degradation. Thus, it was already retreated at 2030 m a.s.l. at 14.2–13.9 ka. An intermediate behavior was revealed at Zănoaga Pietroasă glacier which retreated at about 1900 m at 13.4–13.2 ka. Here (in the upper Iezer Valley) it deposited a terminal moraine that blocked the Iezer stream and formed a lake but also a lateral moraine left in place after its thinning. For the Zănoaga Mare cirque, the post 13.9 ka phase consisted in further glacier down-wasting and formation of two ice flows that deposited two distinct probably ground moraines with numerous large boulders still visible. These ice flows retreated about 300 m upwards on the low declivity cirque floor from 2040 m to about 2047 m

between 13.6 ka and 12.5 ka. The slow retreat continued towards the cirque headwalls where some small glaciers and glacierets with snouts at 2045–2060 m a.s.l. finally disappeared at 12.5–10.2 ka. In North Mohoru cirque the most retreated moraine with the front at 2055 m a.s.l. was dated at 11.8 ka indicating glacier melting at that time.

Using the AAR method with a value of 0.65 as the percentage of a glacier accumulation area above ELA, the ELA was calculated to be at 1990 and 2027 m a.s.l.in Iezer and Gâlcescu cirques at 13 ka for the Zănoaga Mare cirque (Gheorghiu et al. 2015).

Făgăraș Massif

Although for the Southern Carpathian Făgăraş Mountains are the area where glacial landforms have been identified for the first time by Lehmann (1881), we are far from knowing their full glacial history. Even from the first studies, it was assumed that at their maximum extent, glaciers descended down to 1100 m a.s.l. especially on the northern side, (e.g., de Martonne 1907; Lucerna 1908).

In some parts of the Făgăraș Massif glacial deposits are in a relatively good state of conservation. Capra, Bâlea and Doamnei valleys from central Făgăraș along with Dejani valley from eastern Făgăraș were recently investigated producing the first ages necessary for the initiation of a regional glaciation chronology (Urdea and Reuther 2009; Kuhlemann et al. 2013). Geomorphological mapping of moraines and also absolute age datings using cosmogenic nuclides were performed on the afore-mentioned valleys.

The U-shape profile specific to formerly glaciated valleys extends down to about 1100 m a.s.l. on both north and south slopes (e.g., Capra and Dejani valleys) but no moraines can be found at this altitude indicating a long time span that passed since that glacial advance maybe during Riss glaciation (Kuhlemann et al. 2013). Instead, between 1200 and 1500 m a.s.l. large groups of latero-terminal moraines occur (Fig. 5.6). The lowest moraines were initially attributed to early Würm (Urdea 2004) or LGM periods (Urdea and Reuther 2009) whilst the recently determined exposure ages confirmed the LGM origin of the lowest moraine from Capra valley (1306 m a.s.l.) of 17.4 ± 3.2 (Kuhlemann et al. 2013). The authors suggest that in spite of this age being centered at 17.4 ka which would rather correspond to Late Glacial, it actually belongs to LGM depositional age within error between 24 and 18 ka (Bard et al. 2000 cited in Kuhlemann et al. 2013). The early Würmian age (~60 ka) is also infirmed by the reduced Capra creek incision of only 5 m in the moraine material and 1–2 m in the solid rock compared with the estimated 28 m supposed that would have eroded in the 60 ka period taking into consideration the 0.2 mm/a incision rate supported by thermo-chronological data (Kuhlemann et al. 2013).

A second group of small moraines encountered on Capra valley at 1600–1700 a.s.l. which were dated to 15.1 ± 2.4 ka (Fig. 5.6). No moraines at this altitude were mentioned for the Dejani valley.

Upper moraine sets, between 1850 and 2050 m a.s.l., are accommodated by most of the valleys from Făgăraș Massif. The undulated topography with a chaotic distribution pattern of moraines and often rock glaciers shows well preserved traces of the last episode of the complex deglaciation history and interaction between glacial and periglacial processes. In Dejani cirque there were recognized four stadial moraines between 1860 and 2010 m a.s.l. that were attributed to the Late Glacial end (Urdea and Reuther 2009). One steep horizontal moraine ridge was found in the Arpaşu Mic cirque surrounding a depression almost filled with a rock glacier. The age of this moraine located at 2063 m a.s.l. was found to be 12.8 ± 2.0 ka. Similarly, a roche moutonnée from Doamnei valley (2065 m a.s.l.), yielded an age of 13.1 ± 2.3 ka. These two ages were attributed to Younger Dryas glacial readvance (Kuhlemann et al. 2013).

Above 2100 m Kuhlemann et al. (2013) indicate the occurrence of small moraines, nivation hollows and rock glaciers and the former two were related to the early Holocene cold spell like the 8.2 ka. Urdea and Reuther (2009) mention several small moraines in the Dejani west cirque up to 2130 m a.s.l. that were attributed to three cold episodes from the Younger Dryas—Preboreal interval discovered in the Avrig marsh sediments by Tanţău et al. (2005).

ELA calculation using the AAR of 0.67 indicated significant spatial and temporal differences. In LGM the ELA was higher on northern slopes (1800 m a.s.l.) in comparison to southern slopes (1700 m a.s.l.), it equalized during the Oldest Dryas (1950 m a.s.l.) and then reversed during Younger Dryas (2050–2130 m a.s.l. for the northern/southern slopes) and accentuated this asymmetry in the Early Holocene (2250–2499 m a.s.l. for the northern/southern slopes; Kuhlemann et al. 2013). The LGM inversion with the southern valleys keeping more ice (lower ELA positions) than the northern valleys was related to the prevalent south-west direction of the palaeowinds. Following LGM, the main direction of mass air advection shifted from south-west to west which allowed for a symmetrical supply of the two opposing slopes. Towards the Early Holocene the solar radiation increase determined the higher ELA on the southern slopes. Also, it was inferred an ELA increase of 200 m from the west to the east of the massif during Holocene.

Rodnei Massif

Rodnei is the highest massif from the ERC with a well preserved sculptural glacial relief and glacial deposits. As in the case of the Southern Carpathians, in the Rodnei Mountains the morphological tracks of the Quaternary glaciations were identified and powerfully sustained in the late XIX century by Lehmann (1881) and Czirbusz (1896). Their ideas were confirmed later for the entire massif by Sîrcu (1978). The latter argued that this massif was affected by three glacial phases (Mindel, Riss

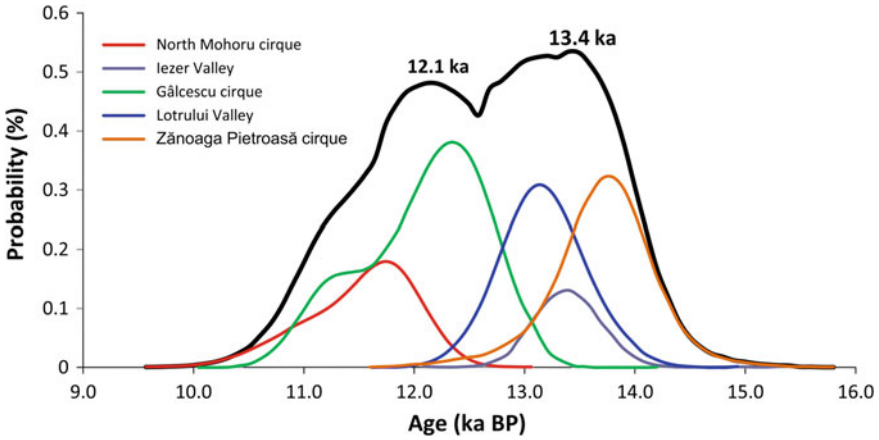

Fig. 5.5 Cumulated probability distribution functions of the ^{10}Be exposure ages with assumed errors in a Gaussian distribution obtained for the five sampled sites from Lotrului Valley, Parâng Massif (*colored lines*) and the sum of the mean individual distribution (built with data from Gheorghiu et al. 2015)

and Würm) and that the perennial snow limit at the glacial maximum stage was at 1500–1550 m a.s.l. Several moraines, distant erratic blocks and striated bedrock surfaces are the main evidences of the past glaciers presence. Gheorghiu (2012) performed detailed geomorphological investigations and surface exposure datings using in situ produced ^{10}Be cosmogenic nuclides in the north-western area of the Rodnei Massif. The spatial pattern of glacial traces is consistently different in comparison to the Southern Carpathians. The study area focuses on the two main glacial valleys of Pietroasa and Buhăiescu (the first includes the tributary valley of Șarampin as well) which were investigated down to 700 m a.s.l. Their upper basins comprise the Iezer and Zănoaga Mare cirques along with the four cirques from Buhăiescu cirque complex (Tăuri, Curmătura, Rebra and Buhăiescu Mare). The main results of the study (Gheorghiu 2012) will be presented in the following.

The lowest preserved glacial deposits are erratic block spreads between 1350 m and 700 m a.s.l. in the Șarampin and Pietroasă Valleys and 950–830 m a.s.l. in the Repede Valley (Figs. 5.5 and 5.6). The ages obtained in the former two valleys indicate maximum values of 37.2 ± 3.4 ka at 868 m a.s.l. decreasing to 36.6 ± 3.3, 33.3 ± 3.0 and 26.6 ± 2.4 ka at 970–1000 m a.s.l. and to 18.3 ± 1.6 ka at about 1100 m. The 36.6 ka old boulder partially composed of red limestone is located 1 km north of its source rockwall, *i.e.,* the upper Turnu Roșu ridge. At higher altitudes, a medial moraine 500 m long located between Șarampin and Pietroasa valleys at altitudes of 1170–1360 m a.s.l. yielded a mean age of 16.7 ka. A spectacular 4 km long lateral moraine stretching on the western part of the two valleys from 1550 to 800 m a.s.l. starts as a very shallow ridge bellow the Turnu Roșu and becomes narrower (<100 m) and higher (5–20 m) in the lower part. Openings in both moraines by anthropic activities revealed a matrix supported

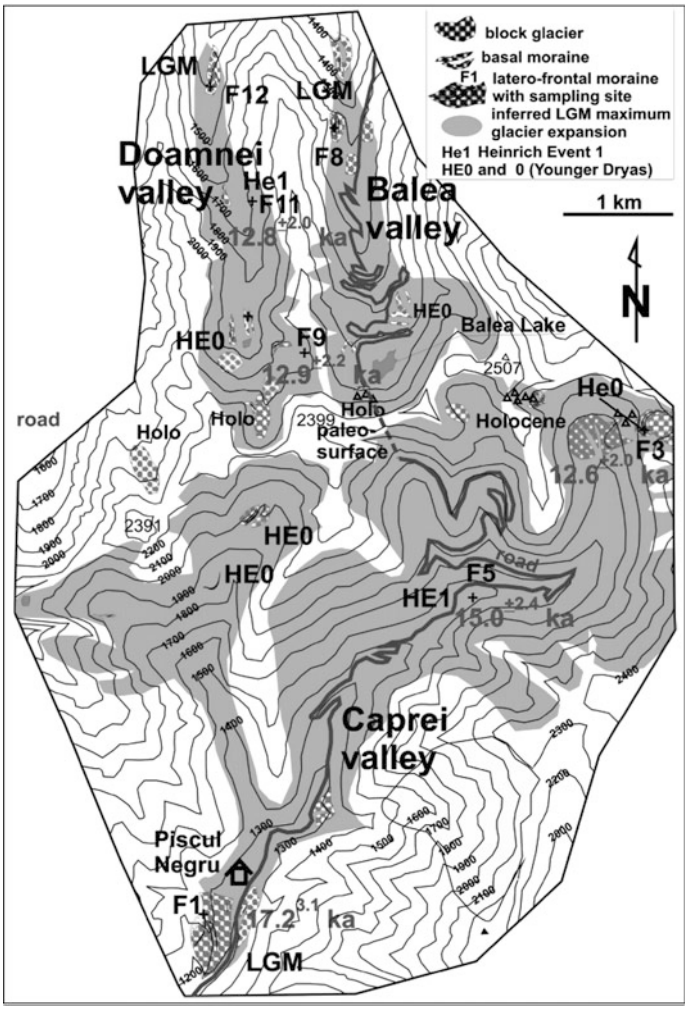

Fig. 5.6 LGM glaciers extension and moraine locations on the Capra, Doamnei and Bâlea valleys from Făgăraș Massif (from Kuhlemann et al. 2013)

diamicton of various sizes and shapes. In the Buhăiescu Valley (tributary of Repede Valley), immediately bellow the glacial cirques (~1600 m a.s.l.) a flat topped till deposit (several tens of meters thick) was dated at 15.8 ± 1.4 ka. Two neighboring upslope moraines are found at 1650–1750 m a.s.l. one of them yielding an age of 13 ± 1.1 ka (average value of the three sampled blocks).

In the six glacial cirques several types of moraines were recognized: ablation moraines in Iezer and Buhăiescu Mare cirques, ground moraine in the Zănoaga Mare cirque and several recessional moraines in all the cirques most of them with a good state of conservation. The best preserved moraine in the study area lays in the

Rebra cirque at 1940 m a.s.l. (not dated) while the largest moraine was found in the Curmătura cirque. Several meltwater channels were also recognized between Buhăiescu Mare and Rebra and in the Buhăiescu Mare and Curmătura cirques. Several moraines present kettle holes on their surfaces. Besides moraines, several bedrock surfaces were used for dating. Zănoaga Mare and Buhăiescu Mare cirques revealed contrasting deglaciation chronology. The former presented low altitude moraines (1670–1760 m a.s.l.) of relatively young ages (12.1 ± 1.1–11.2 ± 1.0 ka) while in the latter the striated bedrock from higher altitudes (1820–1970 m a.s.l.) yielded relatively older ages (14.1 ± 1.3–14.3 ± 1.3 ka). These differences could be determined by different morphometric characteristics of the cirques, Zănoaga Mare being deep and narrow allowing for a limited sun exposure and consequently for a prolonged ice presence in opposition to larger and shallower Buhăiescu Mare cirque which determined a faster ice retreat as previously mentioned for the Parâng Massif. Iezer, Tăuri and Curmătura cirques share a common deglaciation pattern chronologically situated between the two mentioned extremes. Their lower moraines and bedrock surfaces from about 1800–1930 m a.s.l. showed ages between 13.4 ± 1.2 ka and 12.4 ± 1.1 ka.

ELA in Rodnei Mountains was calculated using accumulation area ratio (AAR) and area altitude balance ratio (AABR) methods for the local last glacial maximum (LLGM) and for Younger Dryas (YD). The average calculated LLGM ELA for Pietroasa valley was 1200 m a.s.l. (AAR method) or 1290 m a.s.l. (AABR method). For Buhăiescu Valley the LLGM ELA was 918 m a.s.l. (AAR method) and 1383 m a.s.l. (AABR). During the Younger Dryas period the averaged estimated ELA for the Buhăiescu cirque complex range between 1790 m a.s.l. (Zănoaga Mare) and 1955 m a.s.l. (Curmătura), using the AAR method and between 1846 m a.s.l. (Zănoaga Mare) and 1944 m a.s.l (Tăuri) using the AABR method (Gheorghiu 2012).

Towards an Integrated View of the Deglaciation History of the Romanian Carpathians

Glaciers Extent During the Local Last Glacial Maximum (36?, 26–19 Ka)

While the major sculptural landforms (glacial cirques) from the highest massifs of the Romanian Carpathians were probably formed in the last 360 or even 470 ka (Mîndrescu et al. 2010), the present-day recognizable accumulation landforms of glacial origin (moraines) are much younger (<40 ka) usually from LGM or newer. In fact, the moraines from different altitudes can be used in reconstructing glacial fluctuations and gradual retreat only after major glacial advances. Such major glacial advance during and after which the currently depositional glacial edifice (moraines and erratic blocks) was created, is the so called global LGM. Even

though the LGM could not be imposed as a chronozone (Hughes et al. 2013) because significant time differences in glacial maximum timing occur around the world mountains, it is widely acknowledged that a major glacial advance happened in MIS 2 (29–12 ka). The LGM period was inferred by reconstructing the position of the continental ice sheets which started to grow from 33 ka and were already at their maximum (LGM) positions in 26.5–20 (to 19) ka time interval (Clark et al. 2009). Also, World Ocean level oscillations registered rapid decrease in 30–29 ka time interval and a slower but constant decrease in 29–21 ka interval (Lambeck et al. 2014). However, it is possible that LGM was not the most extensive glacial advance during the last glacial cycle (Würm); some studies suggest comparable or even heavier glaciations in MIS 5d (100 ka) and MIS 4 (70 ka) (Ivy-Ochs et al. 2008; Ehlers et al. 2011). On the other hand, since the highstand of MIS 5e (≈120 ka: 2–6 m a.s.l.) till present the sea level reached the lowest position at the end of LGM (20–19 ka: 125–130 m below the present sea level; Waelbroeck et al. 2002; Lambeck et al. 2014), but other comparable lowstands (less than 100 m below the present sea level) during Late Pleistocene (Siddall et al. 2003; Martínez-Botí et al. 2015) were reached in MIS 6 (155–135 ka) equivalent to Riss maximum glaciation, MIS 8 (270–246 ka) equivalent to Mindel glaciation and MIS 10 (350–336 ka) equivalent to Günz glaciation.

The numerous studies dealing with the glacial history of the Alps indicate that glaciers advanced beyond the Alpine front at around 30 ka, they reached their maximum LGM extent at c. 24 ka (Rhine and Rhone glaciers) or were at their maximum positions between 27 and 21 ka (Tagliamento moraine amphitheater) or 28.5–22.9 ka (Ticino and Adda glaciers) (Ivy-Ochs 2015 and references therein). Two or three LGM stadials and stepwise retreat with still-stands and several minor readvances were proved to have occurred in the Alps (Monegato et al. 2007; Keller and Krayss 2005).

In the Southern Carpathians, the absolute age datings of the lowest moraines from Retezat, Parâng and Făgăraș massifs indicated that the largest glacial advance most likely occurred simultaneously at the end of the global LGM. Thus, the end moraine of Nucșoara–Pietrele palaeoglacier (Retezat Massif) located as low as 1035 m a.s.l. was dated to 21.0 ka (Ruszkiczay-Rüdiger et al. 2015) while those from Jieț valley (Parâng Massif) located in the Groapa Seacă–Jieț Valley, where, in a vast area at 1190–1260 m a.s.l., morainic deposits, initially considered as fluvial–glacial deposits by de Martonne (1907) are associated with large erratic blocks, of 20.6 ± 1.6 ka age (recalculated ages from Urdea and Reuther 2009, see Section "Deglaciation Chronology of the Romanian Carpathians - Parâng Massif") (Table 5.1). In the Făgăraș Massif, the lowest moraine from Capra Valley (1300 m a.s.l.) dated to 17.4 ± 3.2 ka was considered to be of LGM age (≈19–20 ka) because of the high uncertainty range (Kuhlemann et al. 2013). Nevertheless, it is possible that LGM has not been the greatest glacial extent ever recorded in the Southern Carpathians as several previous cold phases (from early and mid-Würm, Riss and Mindel glaciations: MIS 4, MIS5d, MIS 6, MIS 8, MIS 10) were equally favorable to the growth of glaciers. For the Făgăraș Massif Kuhlemann et al. (2013) indicate that bellow the lowest moraines from 1200 to 1300 m a.s.l. of the Capra

Table 5.1 Mean altitudes and ages of the moraine generations from the four studied massifs

Cold phases	Retezat		Parâng		Făgăraș		Rodnei	
	Reuther et al. (2007), Ruszkiczay-Rüdiger et al. 2015		Urdea and Reuther (2009), Gheorghiu et al. (2015)		Urdea and Reuther (2009), Kuhlemann et al. (2013)		Gheorghiu (2012)	
	Alt. (m)	Age (ka)	Alt. (m)	Age (ka)	Alt. (m)	Age (ka)	Alt. (m)	Age (ka)
Pre LGM	–	–	–		–	–	870–1000	37.2–26.6
Global LGM	1035	$21^{+0.8}_{-1.5}$	1197	20.6 ± 1.6[a]	1306	17.4 ± 3.2[b]	–	–
Oldest dryas	1200	$18.6^{+0.9}_{-0.8}$	1235	19 ± 1.5[a]			–	–
	1600–1750	16.3 ± 0.6	–	–	–	–	1170–1360[c]/ 1600[d]	16.7[c]/ 15.8[d]
	1850–1950	$15^{+0.7}_{-0.8}$	–	–	1600–1700	15.1 ± 2.4	–	–
Older dryas	2145	$13.5^{+0.5}_{-0.4}$	1880–2040	13.4	–	–	1750, 1930	14.2–14.1
Younger dryas	–	–	~2015	12.1	1850–2070	12.8 ± 2.0–13.1 ± 2.3	1670–1971	14.3–12.1
Early Holocene	–	–	2055	10.3	–	–	1760	11.2

[a]The presented ages are the corrected values from Urdea and Reuther (2009) (+14 % cf. Ruszkiczay-Rüdiger et al. 2015)
[b]The authors state that this age rather corresponds to LGM depositional age within error between 24 and 18 ka (Bard et al. 2000 cited in Kuhlemann et al. 2013)
[c]Pietroasa Valley
[d]Buhăiescu Valley

valley, the specific U-shape glacial trough continues down to 1100 m where there are no currently recognizable moraines.

A different situation was found in the Rodnei Massif where no LGM–related moraines were found on the investigated north-western valleys. Instead, several erratic boulder spreads in the 700–1350 m altitudinal level, at 4–6 km distance from the glacial cirques rockwalls, were dated to 37.2 ka (<900 m a.s.l.), 36–26 ka (970–1000 m a.s.l.) and 18.3 ka (1100 m a.s.l.) (Table 5.1) (Gheorghiu 2012). Even though the geomorphological context of their deposition is unclear, the glacial transport involvement is highly probable. However, the major age differences in such short distances and altitudinal ranges raise some questions regarding the method (if all the ages reflect or not the boulder deposition) or the mapping accuracy of the glacial features. The author suggests the hypothesis of a local LGM occurring before the global LGM. This hypothesis is indeed supported by a recent palaeoclimatic study (Constantin et al. 2007) based on cave speleothem isotopic records from south-west Romania which indicated a marked cold interval at ~40–35 ka and by the likely presence of the Scandinavian Ice at 200–300 km to the north, reaching a maximum extension since 30 ka, which could have influenced the regional climate of Rodnei massif.

Large glacial advance in the LGM was possible because of the major decrease of MAAT estimated at −14…−15 °C in comparison to the present for the Alpine foreland (Keller and Krayss 2005). The same authors indicate precipitation decrease with 20 % compared with the present values. The ELA lowered with about 1700 m in the Alps. For the Southern Carpathians the LGM ELA was estimated at about 1700 m a.s.l. which is 1200 m lower in comparison to the theoretical present ELA (Reuther et al. 2007). In these conditions many of the highest massifs developed transection glaciers with transfluences passes between neighboring and opposed valleys and also ice caps and plateau glaciers like it was hypothesized for several massifs in the Southern Carpathians, especially in the area on the Borăscu peneplein (Urdea 2004), well documented on Godeanu Mountains (Ignéczi and Nagy 2015) or Făgăraş (Nedelea and Comănescu 2012). For Rodnei Massif, the ELA during the local LGM was estimated to be at 1250 m a.s.l. (Pietroasa Valley) and 900–1300 m a.s.l. for Buhăiescu valley depending on the calculation method (Gheorghiu 2012).

Glaciers Still-Stands and Readvances During the Cold Phases of the Late Glacial (19–13 Ka Period)

The worldwide deglaciation started at ~21–20 ka as indicated by a relatively short and reduced sea level rise of 10–15 m until 18 ka (Lambeck et al. 2014). This was determined by an increase in northern summer insolation (Clark et al. 2009) that marked the transition from LGM to Late Glacial period. In the Alps, the Late Glacial (19–11.6 ka) began when glaciers receded back behind the mountain front after piedmont glacial lobes collapse in the north and glaciers retreat from the amphitheaters in the south (Ivy-Ochs 2015). The post LGM warming phase had a

major impact on mountain glaciers in the Alps which reduced with more than 80 % their LGM volumes at 18 ka (Ivy-Ochs et al. 2008).

Late Glacial is often divided into Oldest Dryas, Bølling, Older Dryas, Allerød and Younger Dryas time intervals (van Raden et al. 2013) and this chronology was also used in Romanian palaeoreconstruction studies (e.g. Feurdean et al. 2012). Two relatively longer cold intervals (Oldest and Younger Dryas) and a shorter one (Older Dryas) are separated by two milder intervals of similar lengths (Bølling and Allerød). In the Alps there were deposited the Gschnitz stadial moraines (two to four moraine ridges) with ages of 17–16 ka which are related to the H1 Heinrich event occurring at c. 16.8 ka (Ivy-Ochs et al. 2006; Ivy-Ochs 2015). The summer temperatures at that time were 8–10 °C colder than today with precipitation reduced by 25–50 % (Ivy-Ochs 2015 and references therein). Makos (2015) indicated for the Tatra Mountains two early Late Glacial (Oldest Dryas) advances at 17–16 and 15 ka.

Oldest Dryas climatic characteristics are the less documented of a Late Glacial interval in the Romanian Carpathians because records unluckily missed from long term speleothem based reconstructions (Tămaş et al. 2005; Constantin et al. 2007) and because the glacial lakes sediment archives used so far were mostly covered with ice at most of its time (Magyari et al. 2012).

At the beginning of the Oldest Dryas a major glacial advance occurred in both Retezat and Parâng Massifs at $18.6^{+0.9}_{-0.8}$ ka (Retezat) (Ruszkiczay-Rüdiger et al. 2015) and 19 ± 1.5 ka (Parâng) (the recalculated ages from Urdea and Reuther 2009). The corresponding moraines from Retezat (belonging to M2a phase) reached very low altitudes (1200 m) while those from Parâng reached 1180–1200 m close to the LGM extent. However, in the Lotrului Valley from Parâng Massif no Oldest Dryas moraines could be found (Gheorghiu et al. 2015). In Făgăraş Mountains the lowest moraine from 1306 m a.s.l. which yielded an age of 17.4 ± 3.2 initially attributed to LGM (Kuhlemann et al. 2013) could also be the first generation of Oldest Dryas moraines but it is difficult to say for sure because of the high uncertainty of the age determination.

A second glacial advance and a final glacial stabilization in Oldest Dryas were recorded in Retezat in moraines from 1600 to 1750 m a.s.l. ($16.3^{+0.6}_{-0.6}$ ka) and 1850–1950 m a.s.l. ($15.2^{+0.7}_{-0.8}$), respectively, (Ruszkiczay-Rüdiger et al. 2015) (Table 5.1). In Făgăraş Massif the second set of moraines from 1600 to 1700 m a.s.l. which yielded an age of 15.1 ± 2.4 (Kuhlemann et al. 2013) might be related to the late Oldest Dryas glacial stabilization. In Rodnei Massif, towards the end of the Oldest Dryas (16.7 and 15.8 ka), the lateral moraine between Pietroasa and Şarampin valleys (1170–1360 m a.s.l.) and the flat topped till deposit from Buhăiescu Valley (1600 m a.s.l.) were deposited. This means that later cold stages did not allow any glacier to descend down here.

At Tăul dintre Brazi lake (1740 m a.s.l.) the glacier retreated at 15.7 as proved by the sedimentation initiation in 15.7–15.1 ka time interval (Magyari et al. 2009). At 14.8 ka climate entered a rapid warming phase and a relatively warm interval occurred between 14.5 and 13.9 ka which was attributed to the Bølling warm

interstadial (Tămaş et al. 2005). Similarly, Magyari et al. (2012) found a climate warming trend at 14.5 ka which determined a rapid uphill migration of tree line to 1800 m a.s.l. on the northern valleys. Taking into consideration that this is similar to the present tree line we can assume comparable climate conditions with the present climate during late Bølling (14.2–13.9 ka) which fostered either the complete disappearance of the glaciers or their dramatic retreat surviving only a few small glaciers (probably as debris-covered glaciers) and glacierets in the most favorable glacial cirques.

A similar conclusion was drawn for the Alps where already "by the beginning of the Bølling interstadial much of the mountains were free of ice" (Ivy-Ochs 2015).

Older Dryas was a short cold period in the Alps, rather like a cold event of about a century, between 14.04 and 13.9 ka (van Raden et al. 2013). In Romanian Carpathians a cold event after Bølling warm period that could represent the local Older Dryas was detected by Tămaş et al. (2005) around 13.9 ka. This cold period could have determined a small glacial advance in the highest cirques from Retezat Mountains above 2100 m a.s.l. as their corresponding moraines left in place after glaciers retreat were dated to a mean age of 13.5 ka (Ruszkiczay-Rüdiger et al. 2015). In Parâng, several boulders produced surface exposure ages of 14.2–13.4 ka at 1880–2040 m in the Lotrului glacial complex so that they could be related to recessional moraines deposited during the Older Dryas (Gheorghiu et al. 2015). In Rodnei Massif, a few boulders were dated slightly before or during the Older Dryas, at 14.1–14.2 and 13.4 ka but interpreted as located in recessional and not advancing glacial deposits (Gheorghiu 2012) (Table 5.1).

Between 13.6 and 12.6 ka a warm phase occurred in the northern Romanian Carpathians that was related to the international Allerød climatic interval (Björck et al. 1998) with a cold and wet period at 13.2–12.8 ka (Tămaş et al. 2005). Besides, the GRIP ice core oxygen profile (Rasmussen et al. 2006) indicates that Allerød was slightly colder than Bølling and thus it could have allowed the persistence of the Older Dryas glaciers at shaded locations in the Carpathians. In Retezat massif no traces of Allerød age moraines were found while in Parâng, Făgăraş and Rodnei Mountains the uncertainty range of the several Allerød related ages is usually higher than the period itself and cannot allow for an Allerød glacial oscillation interpretation. However, the hypothetical Allerød moraines would have been erased by the following severe cold period and associated glacial advance.

Younger Dryas: From Glaciers to Rock Glaciers (12.9–11.6 Ka)

The last cold period of the last glacial cycle which was favorable to small glacial advance was Younger Dryas. This cold phase is known to have started at 12.8–12.7 ka from Greenland ice records (Björck et al. 1998). In the Alps, the Younger Dryas cold stage determined glacial advances and deposition of the

Egesen stadial moraines, easily recognizable and with a blocky composition (Ivy-Ochs 2015). Three or four Egesen moraine generations were deposited in early Younger Dryas (12.2 ± 1.0 ka which is the Egesen maximum) and late Younger Dryas (11.3 ± 0.9) (Ivy-Ochs et al. 2009). The interpretation of the glacial records and glacier-climate models in terms of summer temperature change (ΔTs) and precipitation change (ΔP) indicate that during the Egesen maximum the thermal offset was of −3.5…−5 °C in terms of mean annual air temperature compared to present climate while the pluvial offsets significantly differed from a region to another: 0 to +15 % (Northern Eastern Alps), −20…−30 % (central valleys) or −15…−50 %, respectively (Kerschner and Ivy-Ochs 2008). At a larger scale, it was assumed a precipitation reduction towards the end of the Younger Dryas of up to 30 % of the present values (Ivy-Ochs 2015).

Palaeoclimate reconstruction from the Romanian Carpathians indicate Younger Dryas cooling after 12.6 ka (Tămaş et al. 2005) or 12.8 ka (Magyari et al. 2012). The temperature change during summer was −2 °C in Southern Carpathians and −1 °C in Northern Romanian Carpathians while the winter temperatures dropped with about 8 °C (Perşoiu, Chap. 3 this volume and references therein). Thus, several moraines located in glacial cirques from Parâng and Făgăraş between 1900 and 2070 m a.s.l. were dated to Younger Dryas age (Gheorghiu et al. 2015; Kuhlemann et al. 2013). In Parâng Massif, several erratic blocks from Zănoaga Mare and Gâlcescu cirque from 1940 to 2045 m a.s.l. were dated to 11.9–12.5 ka while in Făgăraş Massif the moraine from Arpaşu Mic cirque (2063 m) yielded an age of 12.8 ± 2.0 ka (Figs. 5.4 and 5.5; Table 5.1). In Rodnei Massif several moraines and bedrock surfaces from glacial cirques yielded ages between 13.1 and 12.1 ka in the Zănoaga Mare, Iezer, Tăuri and Curmătura glacial cirques that can be attributed to Younger Dryas (Fig. 5.7). Closer north (ca. 130 km) in Pozhezhevs'ka Valley (in Ukrainian Carpathians, 48°09′ lat. N) the glaciers advanced at lower altitude than in Rodnei Massif down to 1400 m a.s.l. at 12.9 ± 0.3–12.4 ± 0.3 ^{10}Be ka (Rinterknecht et al. 2012). Also, on the Southern slope of the Tatra Mountains, on Malá Studená valley, the last glaciers persisted at 2046–2190 m a.s.l. during 10.7–11.1 ka (Engel et al. 2015). An interesting case was encountered in the Retezat Massif in Pietrele and Stânişoara valleys, where Ruszkiczay-Rüdiger et al. (2015) found no evidences of Younger Dryas glaciers existence. Therefore, the authors assume that either there were no glaciers in Younger Dryas in Retezat, or they developed in glacial valleys with a colder microclimate. In Făgăraş Masif, it is highly probable that in hanging cirques above 2200 m there were lens glaciers or horseshoe type glaciers valleys like Hârtegu, Căldarea Corabiei (oriented to N) or Podu Giurgiului cirque (oriented to ENE).

Besides small glaciers development during the Younger Dryas the climate was much more favorable to permafrost aggradation and rock glaciers intense activity, enhanced by the cold conditions (Magyari et al. 2012) and increased climate continentality (Perşoiu, Chap. 3 this volume). The cold conditions allowed for intense rock fall activity and coarse debris supply (Sass and Krautblatter 2007) while the decreased precipitations inhibited large glaciers to reach lower altitudes at least after the early Oldest Dryas. Thus, rock glaciers developed progressively

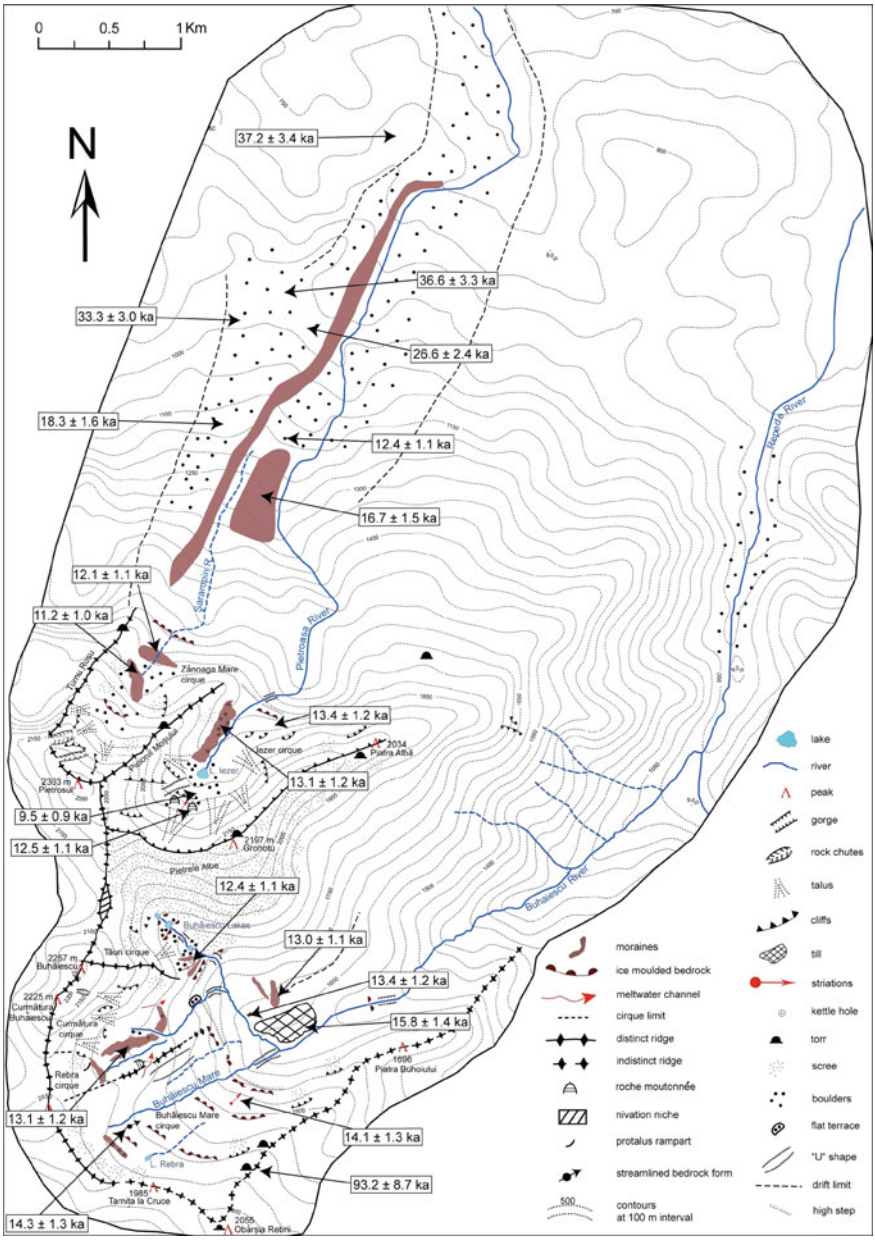

Fig. 5.7 Geomorphological sketch of Pietroasa and Repede Valleys (Rodnei Massif) with evidenced glacial landform and the ontained ^{10}Be exposure ages

beginning with the late Oldest Dryas until the beginning of the Holocene. According to Ivy-Ochs (2015) the rock glaciers could have developed during Late Glacial in the glacial cirques or rockwall niches which floors were bellow the regional ELA. For the Eastern Alps, Kellerer-Pirklbauer et al. (2012) appreciate that currently relict rock glaciers appeared during the Late Glacial and assume a rock glacier age-slope thermal state relation with older rock glaciers having emerged on warmer slopes in opposition to younger rock glaciers developing later on colder slopes. This conditioning is related to the local deglaciation timing and it is highly probable to have determined a progressive development of rock glaciers from low to high altitudes. We may assume that rock glaciers developed both during the colder phases of the Late Glacial (periglacial rock glaciers) and during the transitional periods towards warmer intervals when burial of glacial ice allowed continuous ice lenses to form inside rock glaciers (rock glaciers with both glacial and periglacial ice; Onaca et al. 2013). The evolution from glaciers to rock glaciers passed by following morphogenetic series: glaciers → ablation complex → debris-covered glaciers → ice-cored rock glaciers → debris rock glaciers (Urdea 2004), a good example being Pietrele rock glaciers from Retezat Mountains, or Doamnei (Căldarea Pietroasă) rock glaciers, from Făgăraş Mountains. Kern et al. (2004) assumed by geomorphological analysis on the upper part of the Lăpuşnicu Mare glacial valley (Retezat Massif) that rock glaciers replaced the corrie glaciers near the Ana Lake and beneath the Judele peak at the end of Preboreal and Boreal respectively. Based on rock glaciers creep rates and rock wall denudation rates calculations, Vespremeanu-Stroe et al. (2012) supported the idea of an early Holocene rock glaciers developments in the glacial cirques and also the 8.2 ka cold climate event as the ideal enlargement phase of Retezat rock glaciers and even small glaciers or glacierets development at the sites of currently probable active rock glaciers like Judele and Ştirbu (Retezat).

Rock glaciers density differs from massif to massif and is greater in Retezat in comparison to Parâng and Făgăraş while in Rodnei they do not exist at all. The higher abundance of rock glaciers is an indicator of heavy periglacial debris supply during Late Glacial and Holocene.

The climate conditions at the end of the Younger Dryas and early Holocene are still in debate as several palaeoclimate signals and moraine ages constraints show different results. Some studies (Magyari et al. 2012; Tóth et al. 2012) indicate the end of Younger Dryas at 11.6 ka and warmer than present climate during early Holocene. Fărcaş et al. (1999) suggested that organic sedimentation in a glacial lake from 1840 m a.s.l. started before 11.1 ka. Magyari et al. (2009, 2012) showed from pollen spectra analysis that Pinus mugo vegetation was already at the level of Galeşu Lake (1990 m a.s.l.) in Retezat Massif at 11.6 ka and that summer temperatures were +2.8 °C in comparison to the present values during 10.6–10.3 ka interval. Similarly, Tóth et al. (2012) found summer temperature increment at 11.5 ka and warmer than present summer temperatures between 10.2 and 8.5 ka. Constantin et al. (2007) indicate two thermal maxima at 11 and 10.3 ka.

On the other hand, Tămaş et al. (2005) indicate still relatively cold climate conditions during the Preboreal at 11–10.6 ka and 10.5–10.2 ka time intervals.

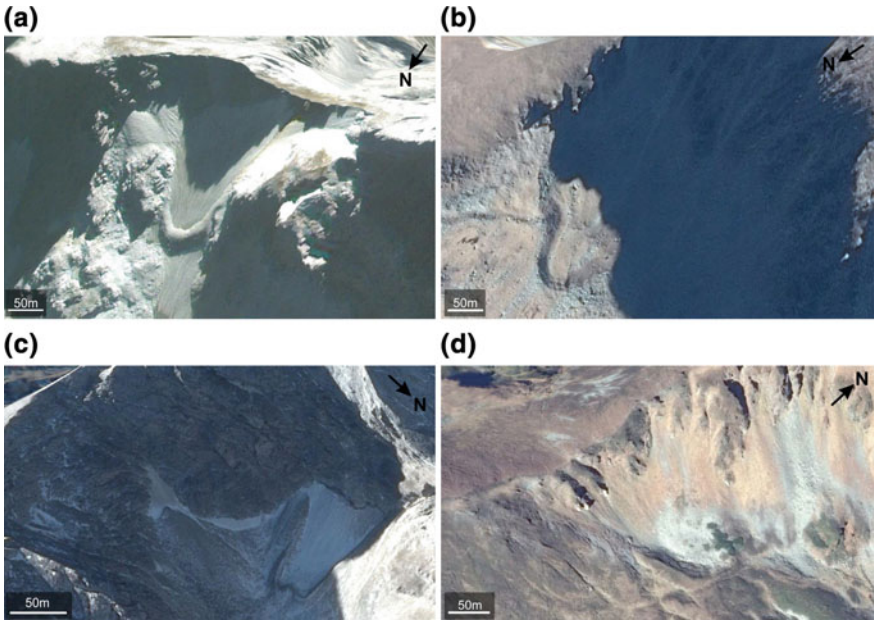

Fig. 5.8 Contemporary ice bodies from the Balkan Peninsula Mountains with small moraines at their fronts: Mertur glacier (Prokletije Mountains) (**a**) and Snezhnika glacieret (Pirin Mountains) (**c**) (Gachev et al. 2009; Gachev and Stoyanov 2012) similar with the last glaciers (Younger Dryas or early Holocene) from the Romanian Carpathians which created the highest moraines like those from North Mohoru cirque (Parâng Mountains; **b**) and Rebra cirque (Rodnei Massif; **d**)

Perșoiu (Chap. 3 this volume) describes a rapid temperature increase towards 11 ka and major oscillations in the following millennium (11–10 ka). As a consequence, the cold events (decades to centuries in length) from the Early Holocene could explain the formation of small glaciers and glacierets at the base of some glacial cirques headwalls taking into consideration that such glaciers can form in years if climate conditions are favorable. Their morphology was similar to that of the current small glaciers and glacierets from the Balkans (Gachev et al. 2009; Gachev and Stoyanov 2012) (Fig. 5.8). The geomorphological evidences from the higher part of the Zănoaga Mare cirque (Parâng Mountains) and the obtained exposure ages of 10.3 ka from 2055 m a.s.l. support the idea of small glacierets in the early Holocene at this site. Similarly, the chaotic appearance of moraines in the highest parts of some glacial cirques from Făgăraș Massif (Dejani West) at altitudes above 2100 m a.s.l. could be related to small glaciers fluctuations during the early Holocene (Urdea and Reuther 2009). In fact, Kuhlemann et al. (2013) calculated an early Holocene ELA of 2250 m a.s.l. on the northern slopes of the Făgăraș massif. However, in Rodnei massif, the 11.2 ka moraine from Zănoaga Mare cirque (~1800 m a.s.l.) could be related to the final stabilization of moraines from Younger Dryas period which had a more sever character in 11.8–11.4 ka interval in the northern Romanian Carpathians (Tămaș et al. 2005).

The hypothesis of early Holocene isolated small glaciers presence in the Romanian Carpathians is also supported by the evidences from some valleys of the Alps where an individualized moraine located between Egesen and LIA moraine positions marked a different glacial advance in the early Holocene, at 10.5 ka (Ivy-Ochs 2015).

Concluding Remarks and Open Questions

Major progresses concerning the last deglaciation chronology of the Romanian Carpathians were brought in the several studies published in the last decade (2007–present). They were facilitated by geomorphological means (detailed mapping of the glacial landforms, glacial moraines investigation) and by the application of modern techniques of absolute age determinations. The main findings can be summarized as follows:

i. The glacial fluctuations since the LGM until the beginning of the Holocene seem to be similar with those from the Alps and the Tatra Mountains and in agreement with both local and worldwide palaeoclimate reconstruction studies: the greatest glacial extent during the LGM period with a regional preference towards the end of LGM ($21^{+0.8}_{-1.5}$ in Retezat–20.6 ± 1.6 in Parâng) and several moderate to minor glacial advances in Late Glacial and possibly early Holocene: two glacial advances at 19 ± 1.5 ka (Parâng)—$18.6^{+0.9}_{-0.8}$ (Retezat) and 16.3 ± 0.6 (Retezat) and glaciers stabilization at $15.2^{+0.7}_{-0.8}$ (Retezat)—15.1 ± 2.4 (Făgăraş) during the Oldest Dryas cold period, a probable glacial advance during the Older Dryas at $13.5^{+0.5}_{-0.4}$ ka in Retezat and 13.4 ka in Parâng, a glacial advance during the Younger Dryas at 12.9–12.1 ka and a possible minor glacial phase during the cold events of the Early Holocene;
ii. Several moraine generations are found between 1035 m and 2200 a.s.l. the former corresponding to the LGM (M1 phase in Retezat) while the latter are related to the Younger Dryas and early Holocene last minor glacial advance. Between these altitudes, other five moraine generations can be found belonging to Late Glacial advances. The estimated ELA fluctuated between 1725 m a.s.l. during the LGM and 2200 m a.s.l. during the early Holocene in comparison to a present theoretical ELA of 2900 m a.s.l. The mean temperatures were much lower than today: −14 to −15 °C (LGM), −9 to −10 °C (Oldest Dryas) and −3.5 to −5 °C (Younger Dryas), while the precipitation were generally lower than in the present;
iii. Rodnei Massif seems to have a different and a more complex deglaciation pattern in comparison to the Southern Carpathians: a local LGM occurring well before the Global LGM between 37.2 ± 3.4 and 26.6 ± 2.4 and a greater intrasite altitudinal fluctuations of moraines with similar ages.

Nevertheless, numerous inadvertences exist between the obtained results across the studied sites mainly because little is known so far about the past geomorphological evolution of glaciers from the Romanian Carpathians and the landscape changes during Holocene under periglacial conditions. The main questions that arise are:

i. Was there any local glacial maximum before the global LGM which surpassed the extension of the M1 moraines from 1035 to 1300 m a.s.l. from SC?
ii. Were there Younger Dryas and early Holocene glaciers or glacierets in all of the highest massifs of the Romanian Carpathians? If not, how can be explained their lack from Retezat Massif?
iii. Did the glaciers disappeared completely in some warm phases of the Late Glacial like the Bølling or they just retreated at higher ground?

Above all the glacial depositional edifice with its several moraine generations and their specific stratigraphy is still poorly understood along with their recognition and intercorrelation from massif to massif which is still fragmentary. Thus, more detailed paleoenvironmental (both geomorphology, landscape and climate evolution) research and at a greater spatial scale is needed to fill the knowledge gaps. Not at last, more absolute age datings should be performed not only in the highest massifs but also in the middle altitude mountains in order to provide less ambiguous and unitary chronologies.

Another direction that needs further research is related to the quantitative information related to past glacial conditions (ELA, climatic conditions), morphometric characteristics of paleo glaciers and their sculptural traces (e.g., glacial cirques and rounded peneplains).

Acknowledgements This study was supported by a postdoctoral scholarship offered by the University of Bucharest Research Institute (ICUB) to RP in 2015.

References

Andra AD (2008) Bazinul hidrografic Topolog: studiu geomorfologic. PhD Thesis (Manuscript), Bucureşti (in Romanian)

Badea L, Gâştescu P, Velcea V, Bogdan O, Donisă I, Dragomirescu S, Florea N, Niculescu G, Popova-Cucu A, Roşu A, Sencu V (1983) Geografia României I Geografia fizică. Editura Academiei Republicii Socialiste România, Bucureşti (in Romanian)

Björck S, Walker MJC, Cwynar C, Johnsen S, Knudsen KL, Lowe JJ, Wohlfarth B, INTIMATE members (1998) An event stratigraphy for the last termination in the North Atlantic region based on the Greenland ice-core record: a proposal by the INTIMATE group. J Quat Sci 13:283–292

Clark PU, Dyke AS, Shakun JD, Carlson AE, Clark J, Wohlfarth B, Mitrovica JX, Hostetler SW, McCabe AM (2009) The last glacial maximum. Science 325:710–714

Constantin S, Bojar AV, Lauritzen SE, Lundberg J (2007) Holocene and late pleistocene climate in the sub-Mediterranean continental environment: a speleothem record from Poleva Cave (Southern Carpathians, Romania). Palaeogeogr Palaeoclimatol Palaeoecol 243(3):322–338

Czirbusz G (1896) Hegyen-völgön. A Radnai havasokon, Erdély V:10–12
de Martonne E (1899) Sur la période glaciaire dans les Karpates méridionales. Comptes Rendus de l'Académie de Science Paris CXXIX:894–897
de Martonne E (1904) La période glaciaire dans les Karpates méridionales. Comptes Rendus de la IX^{ieme} Session de Congres Géologique International (Vienne 1903):691–702
de Martonne E (1907) Recherches sur l'évolution mor-phologique des Alpes de Transylvanie (Karpates méri-dionales). Revue de géographie annuelle I (1906–1907)
Drăguşin V, Staubwasser M, Hoffmann DL, Ersek V, Onac BP, Vereş D (2014) Constraining holocene hydrological changes in the Carpathian–Balkan region using speleothem δ 18 O and pollen-based temperature reconstructions. Clim Past 10(4):1363–1380
Ehlers J, Gibbard PL, Hughes PD (2011) Introduction. In: Ehlers J, Gibbard PL, Hughes PD (eds) Quaternary glaciations—extent and chronology: a closer look. Developments in quaternary science, vol 15. Elsevier, Amsterdam
Engel Z, Mentlik P, Braucher R, Minar J, Leanni L, Team Aster (2015) Geomorphological evidence and ^{10}Be exposure ages for the last glacial maximum and deglaciation of the Velka and Mala Studena dolina valleys in the High Tatra Mountains, Central Europe. Quater Sci Rev 124:106–123
Fărcaş S, de Beaulieu JL, Reille M, Coldea G, Diaconeasa B, Goeury C, Goslar T, Jull T (1999) First ^{14}C datings of late glacial and Holocene pollen sequences from Romanian Carpathians. Comptes Rendus de l'Académie de Science de la Vie Paris 322:799–807
Feibig M, Ellwanger D, Doppler G (2011) Pleistocene glaciations of Southern Germany. Developments in Quaternary Science 15:1–11. In: Ehlers J, Gibbard PL, Hughes PD (eds) Quaternary Glaciatrions-Extent and Chronology: A Closer Look. Elsevier, Amsterdam, pp 163–173
Feurdean A, Tămaş T, Tanţău I, Fărcaş S (2012) Elevational variation in regional vegetation responses to late-glacial climate changes in the Carpathians. J Biogeogr 39:258–271
Gachev E, Stoyanov K (2012) Present day small perennial firn-ice patches in the mountains of the Western Balkan Peninsula XLVI:51–70
Gachev E, Gikov A, Zlatinova C, Blagoev B (2009) Present state of Bulgarian glacierets. Land Anal 11:1–24
Gheorghiu D (2012) Testing climate synchronicity since the last glacial maximum between Scotland and Romania. PhD thesis, University of Glasgow
Gheorghiu DM, Hosu M, Corpade C, Xu S (2015) Deglaciation constraints in the Parâng Mountains, Southern Romania, using surface exposure dating. Quat Int 388:156–167
Grozescu MH (1919–1920) Morphologie de la valée du Lotru. Comptes-Rendus des Séances, Institut Géologique de Roumanie VIII:178–181
Hughes PD, Gibbard PL, Ehlers J (2013) Timing of glaciation during the last glacial cycle: evaluating the concept of the "Last Glacial Maximum" (LGM). Earth Sci Rev 125:171–198
Ignéczi A, Nagy B (2015) Former plateau ice fields in the Godeanu Mountains, Southern Carpathians; providing the first evidence on glaciated peneplains in the Carpathians. Quat Int. doi:10.1016/j.quaint.2015.09.058
Ivy-Ochs S (2015) Glaciers variations in the European Alps at the end of the last glaciation. Cuadernos de investigación Geográfica 41(1):295–315
Ivy-Ochs S, Kerschner H, Kubik PW, Schlüchter C (2006) Glacier response in the European Alps to Heinrich event 1 cooling: the Gschnitz stadial. J Quat Sci 21:115–130
Ivy-Ochs S, Kerschner H, Reuther A, Preusser F, Heine K, Maisch M, Kubik PW, Schlüchter C (2008) Chronology of the last glacial cycle in the European Alps. J Quat Sci 23:559–573
Ivy-Ochs S, Kerschner H, Maisch M, Christl M, Kubik PW, Schlüchter C (2009) Latest Pleistocene and Holocene glacier variations in the European Alps. Quat Sci Rev 28(21):2137–2149
Keller O, Krayss E (2005) Der Rhein-Linth Gletscher im letzten Hochglazial. 2. Teil: Datierung und Modelle der Rhein-Linth-Vergletscherung, Klimarekonstructionen. Vierteljahresschrift der Naturforschended Gesselschaft in Zürich 150:69–85
Kellerer-Pirklbauer A, Lieb GK, Kleinferchner H (2012) A new rock glacier inventory of the eastern European Alps. Austrian J Earth Sci 105(2):78–93

Kern Z, Balogh D, Nagy B (2004) Investigations for the actual elevation of the mountain permafrost zone on postglacial landforms in the head of Lăpuşnicu Mare Valley, and the history of deglaciation of Ana Lake—Judele Peak region, Retezat Mountains, Romania. Analele Universităţii de Vest din Timişoara, GEOGRAFIE 14:119–132

Kerschner H, Ivy-Ochs S (2008) Palaeoclimate from glaciers: examples from the Eastern Alps during the Alpine lateglacial and early Holocene. Glob Planet Change 60:58–71

Kohl CP, Nishiizumi K (1992) Chemical isolation of quartz for measurement of in-situ-produced cosmogenic nuclides. Geochim Cosmochim Acta 56(9):3583–3587

Korschinek G, Bergmaier A, Faestermann T, Gerstmann UC, Knie K, Rugel G, Wallner A, Dillmann I, Dollinger G, von Gostomski CL, Lierse Ch, Kossert K, Maitia M, Poutivtsev M, Remmert A (2010) A new value for the half-life of ^{10}Be by heavy-ion elastic recoil detection and liquid scintillation counting. Nucl Instrum Methods Phys Res B 268(2):189–191

Kräutner Th (1930) Die Spuren der Eiszeit in den Ost- und Süd-Karpathen, Geologisch-Morphologische Studie, Verhandlungen und Mitteilungen des Siebenbürg. Vereins für Naturwissenschaften zu Hermannstadt LXXIX–LXXX:10–85

Kuhlemann J, Dobre F, Urdea P, Krumrei I, Gachev E, Kubik P, Rahn M (2013) Last glacial maximum glaciation of the Central South Carpathian range (Romania). Austrian J Earth Sci 106:83–95

Lambeck K, Rouby H, Purcell A, Sun Y, Sambridge M (2014) Sea level and global ice volumes from the last glacial maximum to the Holocene. Proc Natl Acad Sci 111:15296–15303

Lehmann PW (1881) Beobachtungen über Tektonik und Gletscherspuren im Fogaraschen Gebirge. Zeitschrift der Deutschen Geogischen Gesellschaft XXXIII:109–117

Lehmann PW (1885) Die Südkarpaten zwischen Retjezat und Königstein. Zeitschrift der Geseellschaft Für Erdkun-de Berlin XX 325–336:346–364

Lucerna R (1908) Einige Gletscherspuren aus dem Fogarascher Gebirge, (südliches Siebenbürgen). Zeitschrift für Gletscherkunde II 1907–1908:67–71

Magyari E, Braun M, Buczkó K, Kern Z, László P, Hubay K, Bálint M (2009) Radiocarbon chronology of glacial lake sediments in the Retezat Mts (South Carpathians, Romania): a window to late glacial and Holocene climatic and paleoenvironmental changes. Central Eur Geol 52(3–4):225–248

Magyari EK, Jakab G, Bálint M, Kern Z, Buczkó K, Braun M (2012) Rapid vegetation response to lateglacial and early Holocene climatic fluctuation in the South Carpathian Mountains (Romania). Quat Sci Rev 35:116–130

Magyari EK, Veres D, Wennrich V, Wagner B, Braun M, Jakab G, Schäbitz F (2014) Vegetation and environmental responses to climate forcing during the last glacial maximum and deglaciation in the East Carpathians: attenuated response to maximum cooling and increased biomass burning. Quat Sci Rev 106:278–298

Makos (2015) Deglaciation of the High Tatra Mountains Cuadernos de investigación Geográfica 41(2):317–335

Martínez-Botí MA, Foster GL, Chalk TB, Rohling EJ, Sexton PF, Lunt DJ, Pancost RD, Badger MP, Schmidt DN (2015) Plio-Pleistocene climate sensitivity evaluated using high-resolution CO_2 records. Nature 519:49–54

Mihăilescu V (1966) L'État actuel de nos connaissances sur le relief des Carpates roumaines pendant le Quaternaire. Geographica Polonica Geomorphological Problems Carpathians II 10:9–36

Mîndrescu M, Evans IS (2014) Cirque form and development in Romania: allometry and the buzzsaw hypothesis. Geomorphology 208:117–136

Mîndrescu M, Evans IS, Cox NJ (2010) Climatic implications of cirque distribution in the Romanian Carpathians: palaeowind directions during glacial periods. J Quat Sci 25(6): 875–888

Monegato G, Ravazzi C, Donagana M, Pini R, Calderoni G, Wick L (2007) Evidence of a two-fold glacial advance during the last glacial maximum in the Tagliamento end moraine system (Eastern Alps). Quat Res 68:284–302

Mrazec L (1898) Sur l'existence d'anciens glaciers sur le versant Sud des Karpathes Méridionales. Buletinul Soceietății de Ştiințe VIII(2):466–468
Nedelea A (2006) Valea Argeşului în sectorul montan—studiu geomorfologic. PhD Thesis, Editura Universitară, București (in Romanian)
Nedelea A, Comănescu L (2012) Types of glacial landforms on Capra Valley (The Făgăraș Mountains-Romania). Adv Appl Sci Res 3(6):3970–3980
Niculescu G, Nedelcu E, Iancu S (1960) Nouvelle contribution a l'étude de la morphologie glaciaire des Carpates roumaines. In: Recueil'études géographi ques concernant le territoire de la République Populaire Roumaine. Editura Academiei, Bucureşti, p 29–43
Niculescu G, Nedelcu E, Iancu S (1983) Glaciația şi relieful glaciar. Geografia României I, Geografia fizică. Editura Academiei Republicii Socialiste România, Bucureşti, p 136–141 (in Romanian)
Onac BP, Constantin S, Lundberg J, Lauritzen SE (2002) Isotopic climate record in a Holocene stalagmite from Ursilor Cave (Romania). J Quat Sci 17(4):319–327
Onaca A, Urdea P, Ardelean C (2013) Internal structure and permafrost characteristics of the rock glaciers of Southern Carpathians (Romania) assessed by geoelectrical soundings and thermal monitoring. Geogr Annaler Ser A Phys Geogr 95(3):249–266
Onaca A, Ardelean AC, Urdea P, Ardelean F, Sîrbu F (2015) Detection of mountain permafrost by combining conventional geophysical methods and thermal monitoring in the Retezat Mountains, Romania. Cold Reg Sci Technol 119:111–123
Pawłowski S (1936) Les Karpates á l'époque glaciaire. Comptes Rendus de Congres Géologique International (Varsovie 1934), Section II, p 89–141
Penk A, Brückner E (1901–1909) Die Alpen im Eiszeitalter. Tauchnitz, Leipzig
Perşoiu A (this volume) Climate evolution during the Late Glacial and the Holocene. In: Rădoane M, Vespremeanu-Stroe A (eds) Landform dynamics and evolution in Romania
Perşoiu A, Pazdur A (2011) Ice genesis and its long-term mass balance and dynamics in Scarişoara Ice Cave Romania. Cryosphere 5(1):45
Popescu R, Onaca A, Urdea P, Vespremeanu-Stroe A (this volume) Spatial distribution and main characteristics of alpine permafrost from Romanian Carpathians. In: Rădoane M, Vespremeanu-Stroe A (eds) Landform dynamics and evolution in Romania
Posea G, Popescu N, Ielenicz M (1974) Relieful României. Editura Ştiințifică, București (in Romanian)
Posea G (1981) O singură glaciațiune în Carpați. Studii şi Cercetări de Geologie, Geofizică, Geografie. Geografie 28:369–391 (in Romanian)
Puchleitner S (1901) Die Eiszeit Gletscherspuren in den Südkarpathen. Mitt. d. k.k. Geogr. Gesellschaft Wien, LII:124–139
Rasmussen SO, Andersen KK, Svensson AM, Steffensen JP, Vinther BM, Clausen HB, Siggaard-Andersen ML, Johnsen SJ, Larsen LB, Dahl-Jensen D, Bigler M, Rothlisberger R, Fischer H, Goto-Azuma K, Hansson ME, Ruth U (2006) A new Greenland ice core chronology for the last glacial termination. J Geophys Res 111:D06102
Reuther AU, Geiger C, Urdea P, Heine K (2004) Determining the glacial equilibrium line altitude (ELA) for the Northern Retezat Mountains, Southern Carpathians and resulting paleoclimatic implications for the last glacial cycle. Analele Universității de Vest din Timişoara, Geografie 16:9–32
Reuther A, Urdea P, Geiger C, Ivy-Ochs S, Niller HP, Kubik P, Heine K (2007) Late Pleistocene glacial chronology of the Pietrele Valley, Retezat Mountains, Southern Carpathians, Constrained by ^{10}Be exposure ages and pedological investigations. Quat Int 164–165:151–159
Rinterknecht V, Matoshko A, Gorokhovich Y, Fabel D, Xue S (2012) Expression of the younger dryas cold event in the Carpathian Mountains, Ukraine? Quat Sci Rev 39:106–114
Roucoux KH, Tzedakis PC, Lawson IT, Margari V (2011) Vegetation history of the penultimate glacial period (Marine isotope stage 6) at Ioannina, North-West Greece. J Quat Sci 26(6):616–626

Ruszkiczay-Rüdiger Z, Kern Z, Urdea P, Braucher R, Madarász B, Schimmelpfennig I, ASTER team (2015) Late Pleistocene glacial chronology of the Retezat Mts, Southern Carpathians, using ^{10}Be exposure ages. Quat Int

Sandu I, Pescaru V, Poiană I, Geicu A, Cândea I, Ţâştea D (2008) Clima României. Editura Academiei Române, Bucureşti (in Romanian)

Sass O, Krautblatter M (2007) Debris flow-dominated and rockfall-dominated talus slopes: genetic models derived from GPR measurements. Geomorphology 86:176–192

Sawicki L (1912) Les études glaciaire dans les Karpates. Apercu historique et critique. Annales de Géographie, Paris XXI:230–250

Schlüchter C (2004) The Swiss glacial record: a schematic summary. In: Ehlers J, Gibbard PL (eds) Quaternary glaciations: extent and chronology part 1: Europe. Elsevier, London

Schréter Z (1908) A Páreng-hegység orográfiai és glaciologiai viszonyairól. Földrajzi Közlemények XXXVI:135–150

Siddall M, Rohling EJ, Almogi-Labin A, Hemleben C, Meischner D, Schmelzer I, Smeed DA (2003) Sea-level fluctuations during the last glacial cycle. Nature 423:853–858

Simoni S (2011) Studiu geomorfologic al bazinului Râului Doamnei. Editura Universităţii din Piteşti, Piteşti (in Romanian)

Sîrcu I (1964) Cîteva precizări în legătură cu glaciaţia cuaternară din Carpaţii Orientali Româneşti. Nat Ser Geol Geogr 3:24–31 (in Romanian)

Sîrcu I (1978) Munţii Rodnei. Studiu morfogeografic. Editura Academiei, Bucureşti (in Romanian)

Szepesi A (2007) Masivul Iezer. Elemente de geografie fizică. Editura Universitară, Bucureşti (in Romanian)

Tămaş T, Onac BP, Bojar AV (2005) Lateglacial-middle Holocene stable isotope records in two coeval stalagmites from the Bihor Mountains, NW Romania. Geol Quart 49(2):185–194

Tanţău I, Reille M, de Beaulieu JL, Fărcaş S (2005) Late Holocene vegetation history in the southern part of Transylvania (Romania): pollen analysis of two sequence from Avrig. J Quat Sci 21(1):49–61

Tietze K (1878) Über das Vorkommnis der Eiszeitspuren in den Ostkarpathen. Verhandlungen der geologische Reichsanstalt, Wien, pp 142–146

Tóth M, Magyari EK, Brooks SJ, Braun M, Buczkó K, Bálint M, Heiri O (2012) A chironomid-based reconstruction of late glacial summer temperatures in the southern Carpathians (Romania). Quat Res 77:122–131

Urdea P (1993) Permafrost and periglacial forms in the Romanian Carpathians. In: Proceedings of sixth international conference on permafrost, vol 1. University of Technology Press, Beijing, p 631–637

Urdea P (2000) Munţii Retezat. Studiu geomorfologic. Edit. Academiei Române, Bucureşti (in Romanian)

Urdea P (2004) The Pleistocene glaciation of the Romanian Carpathians. In: Ehlers J, Gibbard PL (eds) Quaternary glaciations—extent and chronology, Part 1: Europe. Elsevier, Amsterdam, pp 301–308

Urdea P, Reuther A (2009) Some new data concerning the Quaternary glaciation in the Romanian Carpathians. Geogr Pannonica 13(2):41–52

Urdea P, Onaca A, Ardelean F, Ardelean M (2011) New evidence on the quaternary glaciation in the Romanian Carpathians. Dev Quat Sci 15:305–322

van Raden UJ, Colombaroli D, Gilli A, Schwander J, Bernasconi SM, van Leeuwen J, Leuenberger M, Eicher U (2013) High-resolution late-glacial chronology for the Gerzensee lake record (Switzerland): δ^{18}O correlation between a Gerzensee-stack and NGRIP. Palaeogeogr Palaeoclimatol Palaeoecol 391:13–24

Vespremeanu-Stroe A, Urdea P, Popescu R, Vasile M (2012) Rock glacier activity in the Retezat Mountains, Southern Carpathians, Romania. Permafrost Periglac Processes 23:127–137

Waelbroeck C, Labeyrie L, Michel E, Duplessy JC, Lambeck K, McManus JF, Balbon E, Labracherie M (2002) Sea-level and deep water temperature changes derived from benthic foraminifera isotopic records. Quat Sci Rev 21:295–305

Chapter 6
Spatial Distribution and Main Characteristics of Alpine Permafrost from Southern Carpathians, Romania

Răzvan Popescu, Alexandru Onaca, Petru Urdea and Alfred Vespremeanu-Stroe

Abstract The sporadic permafrost specific to the Southern Carpathians is accommodated in three main features at sites with commonly low solar radiation—(i) rock glaciers (>1950 m altitude), (ii) talus slopes, and (iii) shaded rock walls (>2400 m)—with a net prevalence of the former category. Due to its marginal character, the alpine permafrost in Southern Carpathians develops only in the most favorable conditions which consist in cold microclimates imposed by topography (low solar radiation, high altitude), but also in specific ground surface characteristics which promote ground overcooling. Among all, coarse openwork debris is the most favorable land cover type for permafrost development because of the cooling effect it exerts on the underground, especially via air ventilation during cold snow free interval (fall and early winter) and air stratification (low conductivity) under thick snow cover. Because of the large surfaces covered by coarse debris at high altitudes, the granitic massifs of Retezat and Parâng present the most extensive areas with probable permafrost from the Southern Carpathians. Instead, the fine debris specific to crystalline ranges of Făgăraș and Iezer—Păpușa or the small and thin conglomeratic debris of Bucegi massif inhibit nowadays the permafrost formation with very few exceptions. Although most rock glaciers prove to be relict, the present-day climate supports the existence of permafrost into thick and coarse debris (intact rock glaciers and lower sectors of the talus slopes) especially at altitudes higher than 2000 m. The geophysical surveys from granitic rock glaciers situated at 1950–2100 m indicate a thin (<10 m) undersaturated permafrost layer located under a thick (8–10 m) active layer. At altitudes higher than 2100 m, permafrost seems to be thicker (>10–20 m) and sometime supersaturated in ice.

R. Popescu (✉)
Research Institute of the University of Bucharest,
M. Kogălniceanu Bd. 36-46, 050107 Bucharest, 5th District, Romania
e-mail: razvan.popescu@geo.unibuc.ro

A. Onaca · P. Urdea
West University of Timișoara, V. Pârvan 4, 300223 Timișoara, Timiș, Romania

A. Vespremeanu-Stroe
Faculty of Geography, University of Bucharest, N. Bălcescu 1,
010041 Bucharest, Sector 1, Romania

M. Rădoane and A. Vespremeanu-Stroe (eds.), *Landform Dynamics and Evolution in Romania*, Springer Geography,
DOI 10.1007/978-3-319-32589-7_6

Keywords Alpine permafrost · Debris porosity · Thermal measurements · Geophysical soundings · Southern Carpathians

Introduction

Mountain permafrost has been intensely studied during the last decades across the European mountain ranges with climatic conditions varying from very cold like, e.g., Scandinavian Mountains (Humlum 1996; Etzelmüller et al. 2003; Juliussen and Humlum 2007) to marginal periglacial environments like, e.g., Sierra Nevada (Tanarro et al. 2001; Gómez-Ortiz et al. 2014) and the Pyrenees (Lugon et al. 2004; Serrano et al. 1999; Julián and Chueca 2007). Numerous investigations were performed especially in the Alps where transport infrastructure is well developed in the high altitude permafrost zone (Bommer et al. 2010). The recent documented climate change in the alpine areas (Harris et al. 2009) which determined major glaciers retreat during the last 150 years and accelerating trends in the last three decades (Paul et al. 2007), was shown to exert a considerable influence on alpine permafrost as well (Isaksen et al. 2007; Gądek 2014).

Permafrost distribution in the alpine environments is characterized by high fragmentation because of the extreme variability of thermal conditions across short distances (Gubler et al. 2011). These are caused by highly variable topography which causes the uneven repartition of the solar radiation (Gruber and Haeberli 2009) and debris deposits. The local microclimatic effects are of great importance especially at the lower boundary of the discontinuous permafrost where frozen ground develops only in the most favorable conditions. The typical permafrost hosting landforms are rock glaciers, talus slopes and rockwalls, the former (rock glaciers and talus slopes) allowing for permafrost presence at much lower elevation because of the cooling effect of the coarse debris acting as a "thermal diode" (Harris and Pedersen 1998; Gruber and Hoelzle 2008). Also, permafrost preservation at very low elevations located in much warmer conditions could be determined by atypical thermal processes like ground air circulation known as "chimney effect" (Kneisel et al. 2000; Delaloye et al. 2003; Morard et al. 2008; Stiegler et al. 2014).

In mapping alpine permafrost distribution, rock glaciers and their typology play a central role because, according to most scientific opinions, they represent ice/debris deposits deformed by downslope creep movement under permafrost conditions (Haeberli et al. 2006; Berthling 2011). When climate warms, the active rock glaciers experience partial permafrost thawing and the increase of active layer depth up to 10 m (Ikeda and Matsuoka 2002) whilst creep cessation turns the state of the rock glacier into inactive. If located on steep slopes, the warming active rock glaciers experience accelerated movement (destabilization) for a relatively shorter period of time until complete inactivation (Delaloye et al. 2013; Sorg et al. 2015). When permafrost thaws completely, the rock glaciers become relict. The altitudinal transition from active to inactive rock glaciers marks the limit between discontinuous and sporadic permafrost zone (Barsch 1996).

Several studies regarding permafrost distribution in presently unglaciated mountains from central-eastern European mountains like the Carpathians, Rila and Pirin were done in the last years. In the high Tatra Mountains, sporadic permafrost was proved to exist after applying several thermal and geophysical methods (Dobiński 1997; Gądek and Kędzia 2008). Active rock glaciers occurrence is improbable as revealed by lichenometric studies (Kędzia 2014) and most of them formed in the Late Glacial period (Kłapyta 2013). Recent rock glaciers inventories were carried out in the Rila and Pirin Massifs (Balkan Peninsula), indicating that all of the rock glaciers are relict (Gikov and Dimitrov 2010; Dimitrov and Gikov 2011).

Rock glaciers from the Romanian Carpathians, including the Parâng and Retezat Massifs were described by Sîrcu and Sficlea (1956), Sîrcu (1971), Ichim (1978) and Urdea (1985). Urdea (1992) does the first rock glaciers inventory in the three highest massifs of Southern Carpathians and applies the first thermal measurements which indicated the presence of the perennially frozen ground. Permafrost occurrence in a rock glacier from Retezat Massif (Judele) was also supported by Kern et al. (2004) based on field observations and spring water temperature measurements. Recently, geophysical methods (electrical resistivity tomography and ground penetrating radar) and continuous ground surface temperature monitoring confirmed the permafrost presence (Vespremeanu-Stroe et al. 2012; Onaca et al. 2013, 2015; Popescu et al. 2015).

In this study we summarize the present state of knowledge on permafrost distribution patterns and characteristics, permafrost associated landforms and factors contributing to its development and preservation in Southern Carpathians, Romania. A major importance is attributed to rock glaciers as the main landforms accommodating permafrost, but we also present the results from measurements applied on other permafrost hosting landforms like talus slopes and rockwalls.

Regional Settings

Two major areas from the Southern Carpathians are of great importance for permafrost study because of the widespread occurrence of rock glaciers and intensive geomorphological investigations performed so far: (i) the granitic areas of Retezat and Parâng Massifs and (ii) the crystalline schist area of Făgăraș and Iezer—Păpușa Mountains which are found in the western and eastern parts of the Southern Carpathians (Fig. 6.1).

These two units comprise massifs that are characterized by high altitudes (their maximum values range between 2469 and 2544 m above sea level—a.s.l.), a well developed glacial relief and a relatively widespread occurrence of debris deposits, both of glacial and periglacial origin, and rockwalls. The 0 °C mean annual air temperature (MAAT) is located at around 2050 m a.s.l. and the natural upper level of timberline is at around 1800 m a.s.l. The lowest MAAT is around −2.3 °C (2504 m a.s.l., Vârful Omu meteorological station, Bucegi Mountains). The total amount of annual precipitation is around 1000 mm on the highest crests above

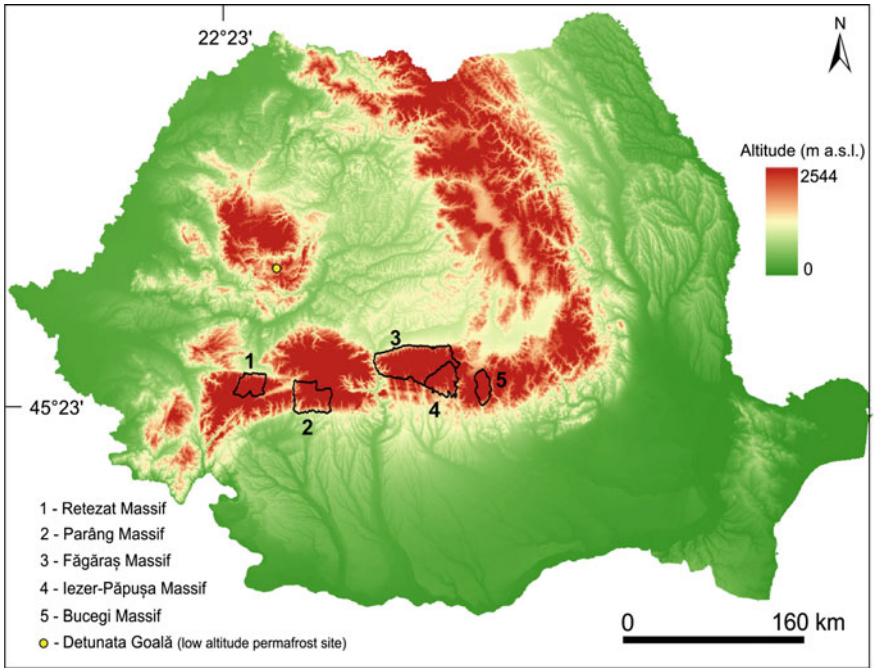

Fig. 6.1 Location of the permafrost susceptible massifs from the Romanian Carpathians

2500 m altitude while on northern glacial cirques above 2000 m a.s.l. they reach c. 1200 mm (Sandu et al. 2008). About half of the annual precipitation falls as rain. Both the MAAT and altitude of timberline are currently in a slightly increasing trend. Above the forest limit the land cover is represented by alpine meadows, debris deposits and rockwalls. The debris deposits including rock glaciers are more or less covered with alpine shrubs, especially *Pinus mugo*, up to 2100 m in altitude. Above this limit the debris deposits are covered only sparsely by herbaceous vegetation. Debris flow processes are quite active even in the alpine areas as witnessed by the erosional channels from steep talus slopes and fine sediments gathered in small elongated fans on the slope foot and sometimes on rock glaciers root (upper) zones.

A visible topographic asymmetry exists between north and south tectonic slopes which is pronounced especially in the Parâng and Făgăraş Massifs. The northern slopes are steeper and shorter and present a greater cover of debris surfaces and rockwalls in opposition to the southern ones. In the Southern Carpathians, the glacial cirque floors rise eastward while cirque aspect tends east-north-east confirming the importance of winds from westerly directions in the period of their formation (Mîndrescu et al. 2010). The lowest preserved moraines from Retezat Massif are located to elevations slightly below 1100 m and were deposited in the Last Glacial Maximum (Ruszkiczay-Rüdiger et al. 2015).

A marked geomorphologic contrast between granitic and crystalline massifs was observed in the Southern Carpathians. On one side the granitic area of the Retezat and Parâng Massifs presents major surfaces of openwork screes including a greater density of rock glaciers (Urdea 1998), larger valleys with shorter and less inclined adjacent slopes and a lower surface of rockwalls while the crystalline area is characterized by a smaller proportion of debris deposits, most of them fossilized (filled in with fine sediments), a greater slope energy and a larger rockwall surface (only the Făgăraș Massif).

An additional study area was in the Bucegi Mountains where calcareous and conglomerate rockwalls presents a large development between 2000 and 2500 m a.s.l. in altitude, making it a good study area for rockwall permafrost research.

Other areas with rock glaciers occurrence but with lower altitudes are represented by Țarcu and Godeanu Massifs located in the vicinity of Retezat. Țarcu Mountains, by Bloju Massif, can be included in the granitic zone of Retezat and Parâng, comprising large areas of well developed rock glaciers but located usually below 2050 m a.s.l., while Godeanu Mountains belong to the crystalline schist group where the few rock glaciers located below 2100 m altitude are mostly fossilized.

The Key Factors for Permafrost Development

General Presentation

Permafrost development and distribution is controlled by factors acting at three different spatial scales (from large to small): climate, topography, and ground conditions (Gruber 2005). Hence, cold climate is the most important prerequisite for permafrost formation. A MAAT of −3 °C is the isotherm above which widespread permafrost occurs in the European Alps even though this limit is subjected to many exceptions (Gruber and Haeberli 2009). However, most of the studies performed in the last decades are concentrated on the discontinuous mountain permafrost belt where climate changes can determine not only ground temperature rise but also phase change, from frozen to unfrozen, that can trigger natural hazards. The lower limit of the discontinuous permafrost zone varies considerably with the climate characteristics corresponding to MAATs of −1 to −1.6 °C in the more continental regions of the Alps like in, e.g., Upper Engadin and Mater Valley from the Swiss Alps (Ikeda and Matsuoka 2002; Gruber and Hoelzle 2001) and to MAATs from −0.5 to +2 °C in the more humid areas, like, e.g., Maritime and Bernese Alps (Ribolini and Fabre 2006; Imhof 1996). Thus, the great role of precipitation upon mountain permafrost distribution at a large scale is also evidenced. The warmer inferior limits of active rock glaciers in the more humid periglacial environments might be determined by a more ice supersaturated permafrost frequently related to former glacier ice (evolving into debris covered glaciers). In opposition, the great

majority of the permafrost ice from rock glaciers accommodated in more continental regions is of periglacial origin which could explain the colder inferior limits of active rock glaciers. From another point of view, a major influence of precipitation upon permafrost is played by the summer rainfall which is one of the few and most aggressive heat sources that reaches directly to the permafrost table by infiltration through the permeable active layer. Even though it's local scale variability imposed by slope, aspect and topography was proved (Buytaert et al. 2006), the effects on alpine permafrost distribution are still poorly understood.

Snow cover is another factor with major influence on the ground thermal conditions and permafrost development through its control upon heat fluxes at the ground-atmosphere interface during the cold season. Alpine snow cover is characterized by extreme heterogeneity because of the preferential snowfalls deposition but mostly because of the wind redistribution (Mott et al. 2010). In similar topographic and climatic conditions, permafrost presence or absence can be dictated by snow cover timing and thickness in the mid-latitude high mountain regions (Ishikawa 2003). The snow thickness was shown to exert a great influence upon annual depth of the cold wave, which can be twice as deep in winters with a snow height below 0.8 m in comparison to winters with snow thickness greater than 0.8 m (Rödder and Kneisel 2012). The same authors found that interannual variability of the snow cover persistence through the summer does not determine any changes on the active layer thickness. Besides, especially autumn thin snow cover plays a major role in ground cooling mechanisms, i.e., it allows an efficient warm air evacuation from rock glaciers through snow funnels (Bernhard et al. 1998) and also contributes substantially to heat conduction out of the ground by strong temperature gradients between snow and ground caused by long wave emissivity increase and short wave absorption decrease (Keller and Tamás 2003).

The strength of the relation between solar radiation and potential permafrost distribution assessed by BTS measurements (bottom temperature of late winter snow cover) (Haeberli 1973) is variable across different mountainous areas. Some statistical analyses indicate a rather weak relation for example in the Scandinavian Mountains (Isaksen et al. 2002) or Swiss Alps (Gruber and Hoelzle 2001) while in other studies from Central Pyrenees (Julián and Chueca 2007) a good relation was found.

The topographic effects on alpine permafrost distribution are mostly reflected in the local distribution of the solar radiation income and air temperature altitudinal variation (vertical lapse rate) whilst the interplay between these two factors should mainly be taken into account when trying to determine the local limits of discontinuous permafrost. For example, on the south exposed slopes where solar radiation is much higher, the permafrost limits are also higher with 200 m for Upper Engadin area (Ikeda and Matsuoka 2002). The aspect effect on permafrost limits is much more pronounced for the rockwalls conditions where, in the absence of long-lasting snow cover, the thermal differences between north and south aspects reach up to 1000 m (Gruber 2005). In the sporadic and discontinuous permafrost zone, the microclimate created by topography is of great importance for permafrost development as well. For example, glacial cirques with very high rockwalls

(>300–400 m) have a lowering effect of local MAAT or compensate the high MAAT with extremely reduced solar radiation, which allows for perennially frozen ground, small surface glacierets to develop (Moscicki and Kędzia 2001) or even active rock glaciers to occurr (Serrano et al. 2006).

Grain Size of Debris Deposits—The Key Factor for Permafrost Development in Marginal Periglacial Environment

At MAATs above −1 or 0 °C, the permafrost areas are restricted only to the most favorable sites which are usually imposed by the land cover type. The cooling effect of the coarse blocky surfaces upon underground thermal state has been recently evidenced (Harris and Pedersen 1998) in comparison to other surface types like alpine meadows, fine sediments and rocky slopes. Ikeda and Matsuoka (2006) showed that bouldery rock glaciers characterized by openwork active layer made out of large boulders have the potential to extend at lower altitudes and in warmer MAAT conditions compared to the pebbly rock glaciers made of small clasts (usually below 20 cm).

In the highest massifs of Southern Carpathians, the predominantly vegetation free debris deposits (rock glaciers and talus slopes) are located between c. 1900 and 2300 m altitude roughly corresponding to MAATs between +1 and −1 °C. These climatic conditions are specific only to marginal permafrost conditions (see above) in which debris grain size is expected to play a major role for permafrost distribution patterns. The question of the role played by debris grain size was raised by the major differences of the ground thermal conditions encountered between crystalline schist rock glaciers from Făgăraș Massif and the granitic rock glaciers from Retezat and Parâng Massifs. The cold microclimatic conditions corresponding to the Văiuga rock glacier (Făgăraș) did not trigger nowadays the permafrost development in comparison to the slightly warmer microclimate from Retezat glacial cirques of, e.g., Judele and Berbecilor, where rock glaciers contain permafrost on almost their entire surfaces (Table 6.1).

Table 6.1 The main characteristics of two contrasting rock glaciers from Făgăraș and Retezat, evidencing the role of grain size and porosity in determining permafrost presence

RG	Rock type	Altitude (m)	Aspect	MAAT (°C)	PISR (kWh/m^2)	RG type	Mean clast volume (m^3)
Văiuga	Schists	2230	N	−0.8	607	**Relict**	0.01
Berbecilor	Granodiorites	2145	N	−0.3	716	**Intact**	0.1

The bold is used to evidence the unexpected difference in rock glacier status, intact and relict
RG rock glacier; *MAAT* estimated mean annual air temperature at the rock glacier front; *PISR* potential incoming solar radiation

Our direct measurements of clasts size revealed major textural differences inter-sites. The three axis of each clast (length, width and depth) was measured in situ on several 4 × 4 m^2 sample plots and the volume of each clast was computed using the equation: $V = 0.6 \times a \times b \times c$ cf. Matsuoka and Sakai (1999). The mean volume of the 606 measured clasts from Văiuga rock glacier (two sample plots) was found to be as low as 0.01 m^3 while the mean volume of the 179 clasts from Berbecilor rock glacier (three sample plots) is ten times larger (Table 6.1). Also, a major difference in relative frequency distribution on volume clasts can be observed (Fig. 6.2a). Besides lower grain size, the crystalline debris clasts present a fine interstitial matrix in comparison to the granitic screes which are mostly openwork (Fig. 6.2b).

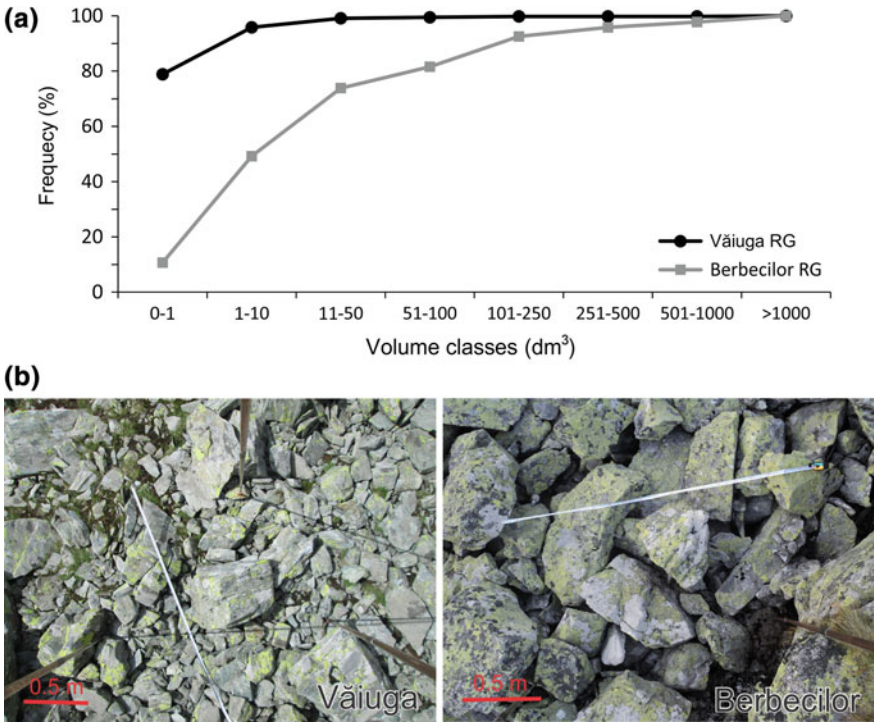

Fig. 6.2 The grain size contrast between Văiuga crystalline rock glacier and Berbecilor granodiorite rock glacier. **a** Cumulative relative frequency distribution of rock glacier gelifracts on volume classes measured in 4 × 4 m sample plots; **b** Vertical photographs from 2 m height used to measure the clasts size

Ground Overcooling Processes in Southern Carpathians

Several studies performed during the last two decades revealed different mechanisms often acting complementary, that contribute to negative ground thermal anomalies and permafrost development in mountain environments. They can be summarized as follows:

- Underground air circulation in active rock glaciers (Bernhard et al. 1998), low altitude talus slopes (Wakonigg 1996; Delaloye et al. 2003; Gude et al. 2003; Sawada et al. 2003; Morard et al. 2008; Stiegler et al. 2014) and high altitude talus slopes (Delaloye and Lambiel 2005; Lambiel and Pieracci 2008) is proved to be one of the main reasons for ground overcooling and permafrost development in coarse debris deposits. This mechanism called "chimney effect" is determined by the density differences between warm and cold air and consists in warm air exit and cold air absorption into the debris through a dense network of snow funnels, especially at the beginning of the winter for rock glaciers, and during almost the entire winter for talus slopes where snow melt "windows" form in their upper parts. Warm air replacement with colder air occurring on flat debris deposits (mainly vertical air movement) is known as "Balch-effect" (Balch 1900). Besides air ventilation, the seasonal production of ice is another factor for permafrost occurrence in high alpine regions (Schneider et al. 2012);
- The inhibition of underground warming effect caused by snow cover onset (Gruber and Hoelzle 2008). This is a purely conductive mechanism and it is based on the low conductivity of the coarse blocks under the snow layer;
- The shading effect imposed by the surface roughness which reduces the solar radiation up to 40 % in a coarse debris deposit from the sporadic permafrost alpine zone in comparison to fine sediments areas (Otto et al. 2012).

Ground surface thermal regimes were found to vary significantly on different temporal and spatial scales in the Southern Carpathians. The former is evidenced by the great oscillations of mean BTS values from one year to another in the same sites of the same rock glacier (Fig. 6.3a). This applies on both crystalline and granitic rock glaciers (Fig. 6.3b). The mean BTS is a relevant indicator of the thermal balance because it responds only to significant variability in climatic and ground conditions that have the potential to modify the underground thermal state down to greater depths. "Normal" mean BTS values were recorded in 2009–2011 and 2013–2014 winters in comparison to 2012 when a significantly lower value was encountered in all of the investigated rock glaciers. Mean BTS values in the typical years varied between −2 and −4.5 °C in the granitic rock glaciers (Pietrele and Berbecilor) indicating possible and probable permafrost occurrence, while crystalline rock glaciers (Văiuga) displayed near 0 °C average BTS specific only to seasonally frozen ground. In contrast, in the exceptionally cold year of 2011–2012, the mean BTS values reached −2.6 °C in Văiuga rock glacier and −5.6 and −7.8 °C in Pietrele and Berbecilor rock glaciers (Fig. 6.3b).

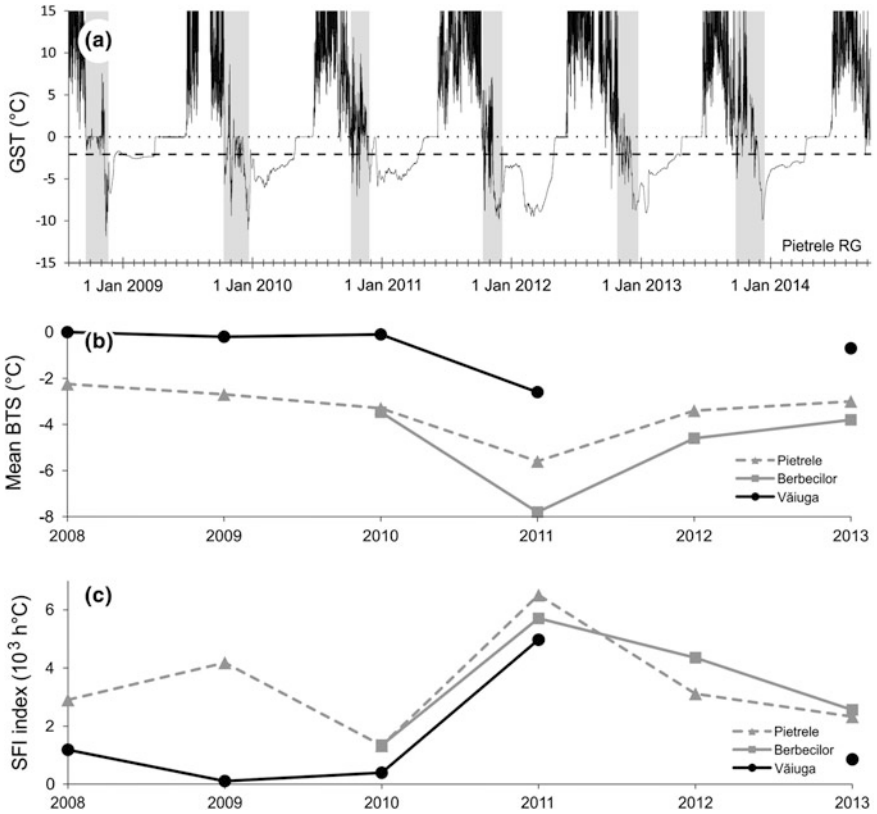

Fig. 6.3 Intersite and interannual variability of the rock glaciers thermal regimes explained by the ground overcooling intensity during autumn and early winter. **a** Six-years ground surface thermal regime of Pietrele rock glacier with the cold snow free interval (CSFI) evidenced with light grey (2008–2014); **b** The contrasting intersite variability of thermal regime reflected in mean BTS values. Note the possible and probable permafrost related BTS values of granitic Pietrele and Berbecilor rock glaciers in opposition with the non permafrost BTS values specific to crystalline Văiuga rock glacier. **c** Interannual variability of ground overcooling intensity quantified by CSFI index. Note the (i) unusual overcooling during 2011 and the (ii) higher potential of granitic rock glaciers to lose heat during CSFI

The primary factor which determines ground cooling with different intensities from year to year is of course climate, through the interplay between cold atmospheric temperatures and the timing of snow cover onset. When surpassing 60, 80 or 100 cm according to different authors (Hanson and Hoelzle 2004; Ikeda and Matsuoka 2002; Brenning et al. 2005), the snow mantle is in power to isolate the ground from short-term atmospheric oscillations. Thus, the air temperature during the cold snow free interval (CSFI) and its duration dictates the amount of heat lost by the ground. This cooling degree was quantified through the CSFI index by summing up all the negative Celsius degrees hours (h °C) during autumn and early

winter until snow cover onset. For the calculus, in situ ground surface temperature data were used. Usually, in Văiuga rock glacier the SFI index is below 1200 negative h °C while in Pietrele and Berbecilor it oscillates between 1300 and 4400 negative h °C (Fig. 6.3c). In the exceptional cold and relatively dry autumn of 2011, the SFI index raised strongly in all of the studied rock glaciers, to almost 5000 negative h °C in Văiuga and around 6000 negative h °C in Pietrele and Berbecilor rock glaciers, thus explaining the great disturbance in mean BTS registered in March 2012. These results indicate that granitic rock glaciers are subjected to much more intense ground overcooling in comparison to the crystalline rock glaciers. This fact can be related to the larger grain size and associated voids of the granites that allows for a better cold air penetration and a longer period of CSFI caused by the later snow induced insulation. In opposition, the small clasts and the matrix developed in the crystalline rock glaciers usually inhibit the ground overcooling.

Other factors than climate can influence mean BTS values as well. These can be related to the internal structure and especially to the volume of permafrost and its ice percentage. For example, Berbecilor rock glacier suffers greater oscillation of mean BTS in nearly the same CSFI index conditions (Fig. 6.3) probably because of the smaller permafrost surface (c. 2000 m^2) in comparison to Pietrele rock glacier, which has a more than double probable permafrost area (c. 5000 m^2). This mechanism which implies that seasonally frozen ground loses heat much faster than permafrost could also explain the greater sensitivity of relict rock glaciers like Văiuga to SFI index.

Air movement inside rock glaciers was proved to take place in Retezat and Parâng Massifs. Besides efficient cold air penetration replacing warmer inside air in rock glaciers during the early winter when thin snow cover occurs (Vespremeanu-Stroe et al. 2012; Popescu et al. 2015), a continuous air exchange between ground and atmosphere (Ishikawa 2003) was also proved to exist (Onaca et al. 2015). In situ thermal measurements indicate that during the cold air fronts, the thermistors located in relatively higher positions of rock glaciers, usually ridges, registered minor warming trends (Fig. 6.4a). This usually happens until the end of the winter, when melt water penetration at the snow bottom takes place (initiation of the 0 curtain period). Other studies in the Alps (e.g. Delaloye and Lambiel 2005) indicated that cold air can be absorbed directly through a thick and porous snow layer in rock glaciers while warm air (with slightly positive temperatures) could be expelled in the upper parts of the talus slopes. Given the position (inside rock glaciers surface) and temperatures (negative values) found in "warm" locations from Retezat rock glaciers, we do not exclude the idea of air stratification under an insulating snow cover. We assume that this mechanism of air movement and stratification inside debris deposits is restricted only to openwork and porous debris deposits.

Similar results were found in the steep talus slopes from Retezat Massif (Fig. 6.4b) where "warm" (same negative temperatures) air evacuation was registered at the beginning of the winter in the upper part of Știrbu talus slope. Here, the air stratification hypothesis determined by air density contrast is supported by the

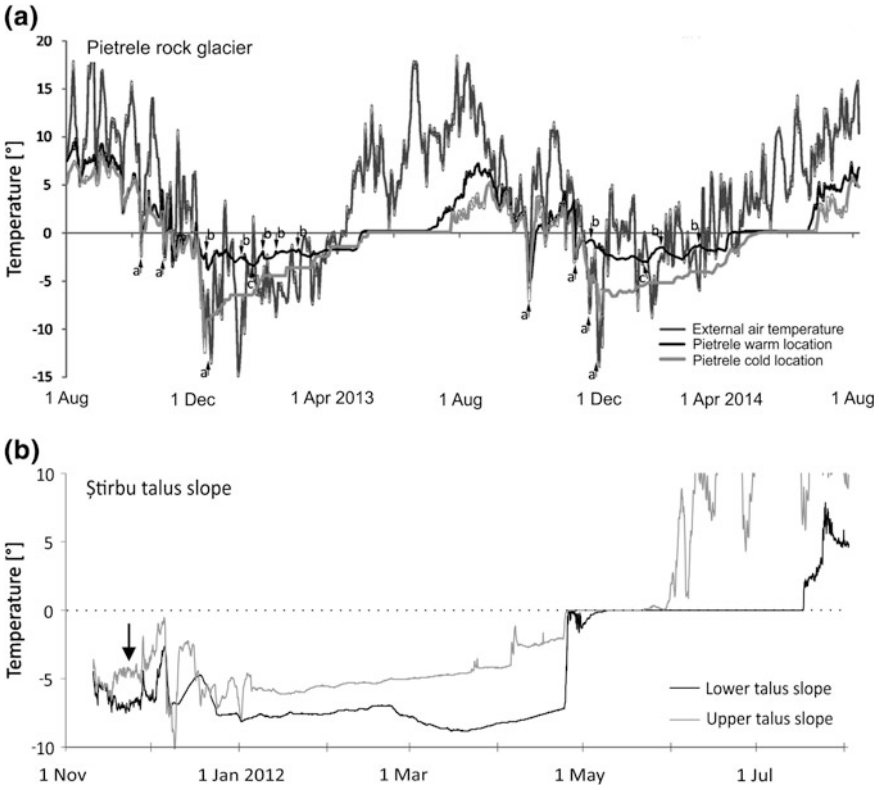

Fig. 6.4 Ground thermal regime from Pietrele rock glacier (**a**) and Ştirbu talus slope (**b**) along air temperature revealing internal air movement inside coarse debris deposits. In plot **a** it is shown the efficient ground overcooling (*a* events) at a cold location and warm air ascent (*b* events) inside rock glaciers at the warm location. Warm air ascent is enhanced during intense frost episodes as revealed by reversed thermal relationship between air and ground surface (Onaca et al. 2015). Plot **b** shows the warm air evacuation during November (marked by *black arrow*) and air stratification below thick and insulating snow cover during January–April time interval in a talus slope, by comparing the thermal regimes from lower and upper talus slopes

accentuating temperature contrast between up and down locations which increases towards the winter's end in opposition with rock glaciers, where temperatures tend to homogenize.

At the same time, the furrows formed by the permafrost compressive flow, characteristic for the largest rock glaciers in the Southern Carpathians (e.g., Pietrele, Valea Rea, Galeşu) have a thermally protective influence, by preserving cold air that isolates the active layer from the warmer atmospheric air, because during the strong cooling of air temperatures in the first part of the winter, cold, denser air is trapped in the furrows on both sides of the ridge and isolates the interior of the ridge from the warmer atmospheric air (Hanson and Hoelzle 2004). The topographical

configuration of the mentioned rock glaciers is almost identical to the Murtèl rock glacier, where the 'chimney effect' is not present (Hanson and Hoelzle 2004).

The other two mechanisms of ground overcooling in coarse blocks, i.e., snow cover warming inhibition and the shading effect of large boulders are possible in the granitic massifs of Southern Carpathians but they cannot be easily detected through temperature monitoring.

Permafrost Distribution Patterns in the Southern Carpathians

Background

At its lower limit, discontinuous permafrost is highly fragmented and restricted in only the most favorable conditions. These conditions are normally offered by coarse debris which causes negative thermal anomalies in the underground (see Section "The Key Factors for Permafrost Development"). Debris deposits can be of periglacial origin (talus slopes and block fields) or of glacial origin (moraines and glacial till). The former result from rock falls and develop permafrost by both glacial (incorporation of perennial snow banks or small firn fields) and periglacial (refreeze of percolating water and ice segregation) processes. Under the effect of slope declivity, the debris containing permafrost creep downslope creating rock glaciers with specific ridges and furrows topography (talus rock glaciers). Glacial moraines and glacial till develop permafrost after the glacier retreat and evolve into debris rock glaciers under permafrost creep conditions. In their young stages, rock glaciers present only one frontal ridge that detaches from the perennially frozen talus slope (Scapozza et al. 2011). These landforms, called protalus ramparts, are embryonic rock glaciers (Haeberli 1973; Fukui 2003). However, there are many landforms with only one terminal ridge that were considered to be of glacial origin (e.g., Ballantyne and Kirkbride 1986) involving fragments of rocks from above rockwalls sliding on former small glacierets or perennially snow banks. After ice melting, the terminal arcuate ridge remains prominently above the ground. We assume that both scenarios of protalus rampart formation are possible in alpine environments and these landforms can be of both glacial/nival and periglacial origin. One great difference between the two types of protalus ramparts is represented by the surface topography which is smoother in periglacial protalus ramparts in contrast with glacial protalus ramparts which are characterized by a large hollow between frontal ridge and talus slope. A distinct case is represented by debris deposits underlain by permafrost that do not evolve into rock glaciers. These block fields are located on quasi-horizontal surfaces where creep processes are inhibited (dynamic inactivity cf. Barsch 1996). Such a case we assume to be found in Mândra glacial cirques from Parâng Massif.

Perennially frozen rockwalls develop usually where mean annual rock surface temperature (MARST) is below 0 °C (Noetzli et al. 2007), a few hundred meters above the rock glaciers permafrost (Gruber 2005). However, local thermal offsets must be taken into account when dealing with rockwall permafrost distribution (Hasler et al. 2011). In general, MARST vary greatly with aspect and interannual variations are larger in comparison to rock glaciers MAGST (Gruber 2005). Rock jointing degree has a major influence on thermal regime of the top 3–4 m of the rockwalls allowing air ventilation and overcooling during the cold season (Magnin et al. 2015).

Rock Glaciers (RG) Permafrost

Rock glaciers are widely distributed across the highest sectors of Retezat, Parâng, and Făgăraș Massifs (Urdea 1992). In lower altitude Massifs like Țarcu (2190 m), Godeanu (2291 m) and Iezer—Păpușa (2469 m) rock glaciers have a sporadic presence while in even lower altitude massifs they do not appear at all. A notable exception is represented by the Bucegi Massif which despite its high altitude (2504 m) and glacial sculpted valleys, it presents no rock glaciers. A major discrepancy in rock glaciers distribution and characteristics exists between granitic (Retezat and Parâng) and crystalline (Făgăraș) mountains. The former present a higher rock glaciers density (Urdea 1998) and an openwork structure of the active layer. Moreover, expressive morphologies, steep terminal fronts with sparse vegetation distribution indicate that rock glaciers above 2050–2100 m altitude could be at least inactive in Retezat and Parâng mountain ranges. In opposition, the rock glaciers from Făgăraș Massif, extending even at higher altitudes, are characterized by less inclined fronts, a surface debris mantle filled with fine sediments and a relatively uniform vegetation distribution across their surfaces which indicates their contemporary relict state (Fig. 6.5).

BTS (bottom temperature of winter snow cover) measurements were applied experimentally on Pietrele rock glacier from the Retezat Massif in the early 1990s (Urdea 1993) and intensely in several sites from the highest massifs of Southern Carpathians beginning with the year of 2008 (Vespremeanu-Stroe et al. 2012). This method relies on the late winter (March) thermal stability at the snow-ground interface, which reflects the thermal conditions from the underground. Usually, a temperature colder than −2 and −3 °C is associated with possible and probable permafrost occurrence in the Alps (Haeberli 1973). BTS methods is often used in mapping the potential permafrost distributions in various mountain ranges (Ikeda and Matsuoka 2002; Lewkowicz and Ednie 2004; Julián and Chueca 2007).

BTS measurements applied on rock glaciers from the Southern Carpathians show usually mixed thermal conditions across their surfaces with both areas of maximum overcooling and relatively warm state. In Retezat and Parâng Massifs, sporadic patches of probable permafrost can be encountered in the rock glaciers from the 2000–2100 m altitudinal floor as revealed by BTS maps. Between 2100

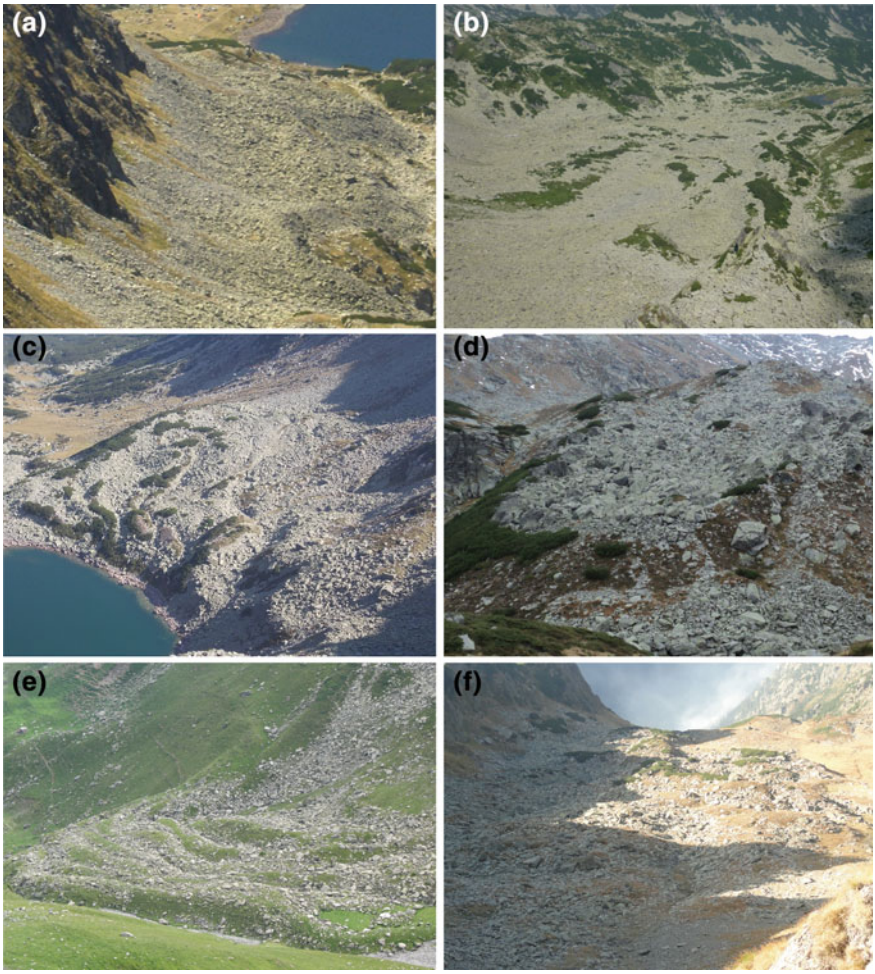

Fig. 6.5 The main typologies of rock glaciers from the Southern Carpathians: Berbecilor lobate rock glacier probably active (**a**), Pietrele tongue shape inactive rock glacier (**b**) from Retezat Massif; inactive tongue shape rock glaciers Roşiile 2 (**c**) and Gemănarea (**d**) from Parâng Massif; relict rock glaciers Capra (**e**) and Lăiţel (**f**) from Făgăraş Massif

and 2200 m a.s.l. the permafrost coverage enlarges significantly especially for the most sheltered rock glaciers like Judele (Retezat), and Roşiile 1 (Parâng) (Fig. 6.6). No great difference was found between lobate and tongue shape rock glaciers in what concerns permafrost favorability. Below 2000 m a.s.l., only a few thermal anomalies can be found on blocky surfaces. The BTS values were always close to 0 °C on alpine meadows confirming the absence of permafrost on this land cover type no matter the altitude.

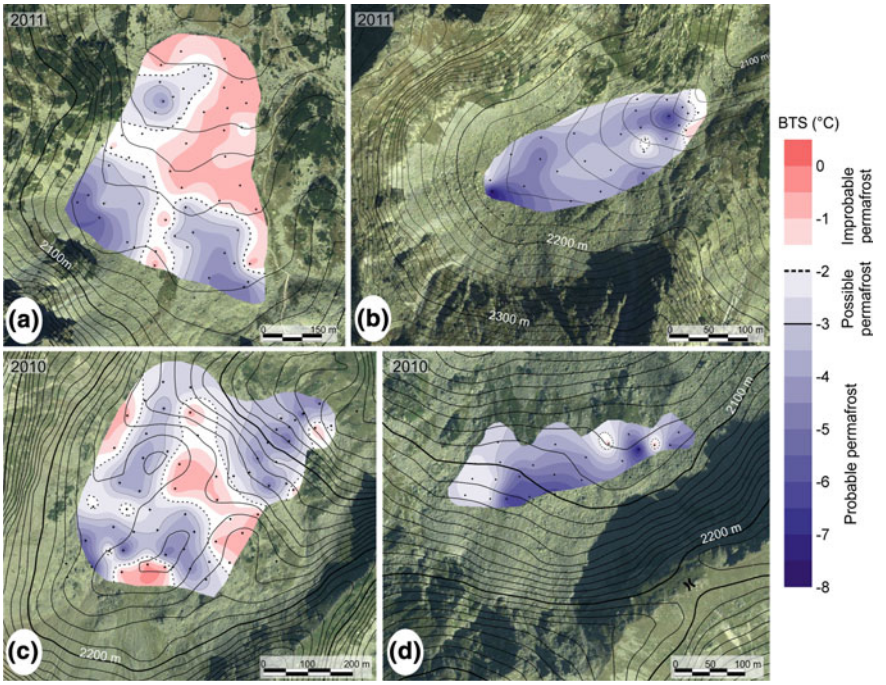

Fig. 6.6 BTS maps of granitic rock glaciers from Retezat and Parâng Massifs. Pietrele rock glacier (**a**) and Gemănarea (**c**) reveal isolated areas with permafrost related BTS values in comparison to Judele (**b**) and Roşiile 1 (**d**) rock glaciers where negative thermal anomalies ($T < -3$ °C), characteristic to probable permafrost, cover almost their entire surface

The BTS measurements on rock glaciers from Făgăraş and Iezer—Păpuşa Massifs indicate the absence of permafrost in most of the investigated RG. The most notable exceptions belong to the upper part of Doamnei rock glacier (Făgăraş) and to the debris deposits below the Tambura peak (Iezer—Păpuşa) where minimum BTS values indicate a high probability of frozen ground.

Continuous ground surface temperature (GST) measurements were performed on several rock glaciers from the Southern Carpathians often in remote locations that cannot be easily accessible for BTS monitoring. The method consists in continuous temperature monitoring at a fixed interval (two and a half hours) using miniature digital data loggers (Hoelzle et al. 1999). We used iButtons loggers (model DS 1922L) with less than 0.2 °C accuracy at near 0 °C temperatures (Gubler et al. 2011).

More than twenty rock glaciers from the Southern Carpathians, most of them from Retezat Massif, were monitored at least one year in the 2008–2014 period. These data generally confirm the BTS measurements in terms of permafrost probability in rock glaciers even though GSTs are slightly warmer than BTS points measured in the same day and the same location. Delaloye (2004) indicated that

GSTs are usually 1–1.5 °C warmer than BTS because the data loggers are located deeper in the ground while BTS probes reach only the exposed and overcooled surface of gelifracts.

Interannual amplitudes of temperatures during the thermal stability periods are similar in all of the investigated rock glaciers. Very low temperatures were registered in March 2012 and relatively warm temperatures during March 2009, but these differences do not usually surpass 5 °C.

In the granitic rock glaciers, the GST curves indicate the lack of permafrost below 2000 m in Upper Ana (Retezat) and Roșiile 3 rock glacier (Parâng), and possible and probable permafrost above these altitudes. The lowest GST during the late winter are registered at 2100–2200 m a.s.l., in rock glaciers located in shaded cirques like Judele, Galeșu, and Știrbu (Retezat) and Roșiile 1 (Parâng), indicating a high probability of permafrost presence.

In the crystalline rock glaciers, the results show near 0 °C GST at the end of the winter not only in rock glaciers below 2050 m (Capra and Bâlea) but also at 2300 m a.s.l. (Văiuga rock glacier). An exception is represented by Doamnei rock glacier, where GST measurements confirm probable permafrost in its upper part in accordance with the BTS survey. Moreover, the GST indicates possible permafrost also in its lower sector, into an isolated area of the rock glacier, which should be put in relation with the site-specific enormous unconsolidated blocks, quite unusual for the Făgăraș Massif. In Iezer—Păpușa, the GST curves from 2012 to 2014 period indicate boundary conditions for possible permafrost presence in the blocky surface under the Tambura peak.

A synthetic thermal indicator is represented by the mean annual ground surface temperature (MAGST) (Fig. 6.7). Usually, the GST is measured at 0–20 cm in the ground and the sensors are covered by small fragments of rock (e.g., Ribolini and Fabre 2006). However, in the Southern Carpathians we measured GST in two manners: iButtons were hung at 40–80 cm between the gelifracts (near surface GST

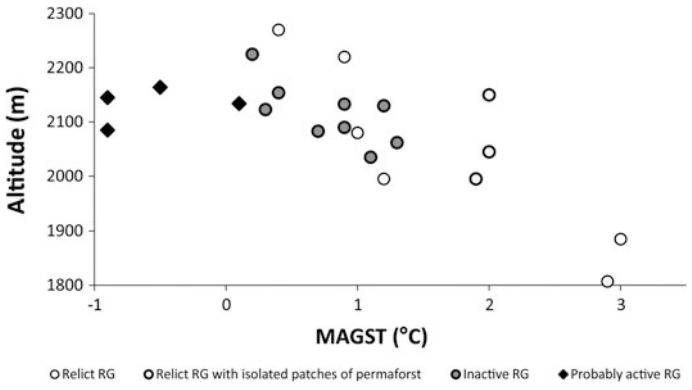

Fig. 6.7 Homogenized MAGST values for Southern Carpathians rock glaciers (averaged from multiple years and multiple sites in the same rock glacier where available) (Popescu et al. submited)

in order to avoid exposure to solar radiation) or they were placed in 2 cm drilled holes (skin GST) in surface blocks and then covered with a 10 cm thick gelifract. The near surface average MAGST range from +1 °C in 2000–2100 m a.s.l. to 0 °C at 2100–2200 m a.s.l. only on northern, northeastern and northwestern rock glaciers. In comparison, the skin MAGST is in average 1 °C warmer. In Retezat Massif, negative MAGST were encountered in Judele, Știrbu and Galeșu rock glaciers, while in Parâng Massif the only negative MAGST was encountered in Roșiile 1 rock glacier.

In the crystalline massifs, the MAGSTs are usually positive, with an exception of the upper part of Doamnei rock glacier. In Iezer—Păpușa Massif, the MAGST values were between 1.5 and 2.1 °C in the 2012–2014 time interval.

In all of the investigated massifs, MAGST showed no great difference from probable permafrost sites to non permafrost sites which indicates that caution is needed when using MAGST as a permafrost predictor.

The late summer (August and September) spring water temperature is another indicator of permafrost presence in alpine environments including the Southern Carpathians (Urdea 1993). The probable permafrost limit is at 1 °C (Haeberli and Patzelt 1982; Frauenfelder et al. 1998) while permafrost is still possible between 1 and 2 °C (Warhaftig and Cox 1959; Haeberli and Patzelt 1982). Itinerant temperature measurements confirmed the possible and probable permafrost occurrence in several rock glaciers (Fig. 6.8) from Retezat, Parâng and Făgăraș Massifs where

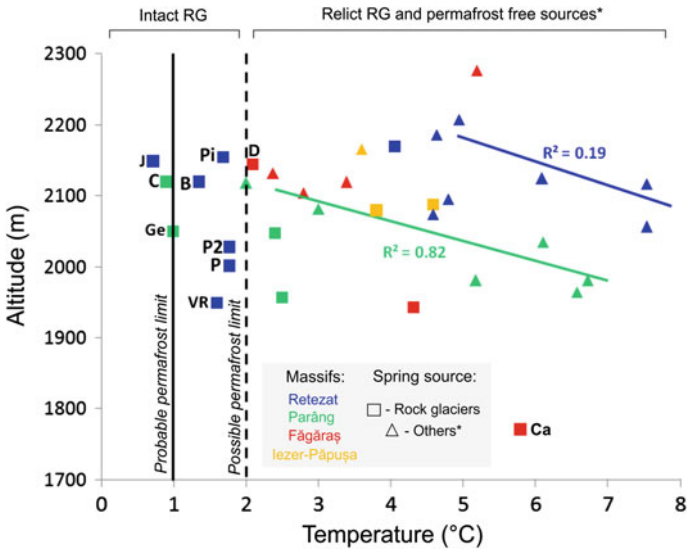

Fig. 6.8 Itinerant measurements of spring water temperature from Retezat, Parâng, Făgăraș, and Iezer—Păpușa Mountains. *Asterisk* other sources imply talus cones, alpine meadows and rockwalls. The acronyms stand for: J—Judele, Pi—Pietricele, B—Berbecilor, P2—Pietrele 2, P—Pietrele and VR—Valea Rea (Retezat); C—Cârja and Ge-Gemănarea (Parâng); D—Doamnei and Ca—Capra (Făgăraș) (Popescu et al. submited)

values are below 2 °C. In contrast, the springs with other sources than rock glaciers revealed values above 2 °C which decrease with altitude (Vespremeanu-Stroe et al. 2012). The continuous monitoring of several rock glacier springs during summer revealed the typical pattern related to intact and relict rock glaciers. The former are characterized by cold (0.7–1.8 °C) and isothermal regime while the latter are warm (above 5 °C) and oscillating in accordance with the monthly air temperatures. By measuring the temperature of Gemănarea and Judele rock glacier creeks several hundred meters downstream from the spring point, we found a rapid increase rate of 0.1 °C at 17 and 10 m, respectively, on horizontal distance (Popescu et al. 2015). This increasing rate could explain the temperatures between 1 and 2 °C associated with intact rock glaciers springs, if we take into consideration that most of them were intercepted at distances of 60–200 m from the frozen source.

Talus Slope Permafrost

The BTS measurements on talus slopes from Retezat Massif were performed in 2011 (within average climatic conditions; Fig. 6.9). All the investigated talus slopes are connected downwards to lobate rock glaciers (Pietrele 2 and Pietricele) or tongue shape rock glaciers (Pietrele and Lower Ana) and present very cold values only in the lower half. An exception is represented by Pietricele talus slopes where the Northeastern BTS profile indicated cold values up to the rockwall base. In the case of Pietrele 2 and Lower Ana, the BTS values from their lower parts are even lower in comparison to those from rock glaciers indicating that permafrost may be present even in the talus slopes located next to relict rock glaciers like Lower Ana.

The BTS measurements performed in Parâng Massif indicated similar results with those obtained in the Retezat Massif (Popescu et al. 2015). Low temperatures in the basal part (1/2–2/3) of the talus slopes were obtained in the Roşiile 1 cirque. Shorter BTS profiles in Făgăraș and Iezer—Păpușa Mountains indicated a predisposition for colder temperatures at the lower parts of the talus slopes close to Doamnei rock glacier and Tambura talus slope.

The continuous thermal monitoring of talus slopes from Retezat Massif confirmed the temperature contrast between the lower and the upper parts. In Știrbu lower talus slope the temperature is colder than in the upper part during almost the entire winter (to see Fig. 6.4b). Increasing temperatures in the upper part concomitantly with temperature decreases in the lower parts during several days in November suggests the warm air evacuation at the beginning of the cold season, and the efficiency of the chimney effect acting into these well-inclined (>20°) features, respectively. Under a thick snow cover, the smooth thermal regime and the mean temperature offset of 2 °C, increasing to 5 °C in late winter, indicate rather snow isolated conditions and an underground stratification of warm air in the upper parts and the cold air in the lower parts of the cavernous system of openwork debris.

The GST measurements in Văiuga talus slope (Făgăraș) revealed a different, mostly conductive thermal regime. During the first part of the winter the upper and

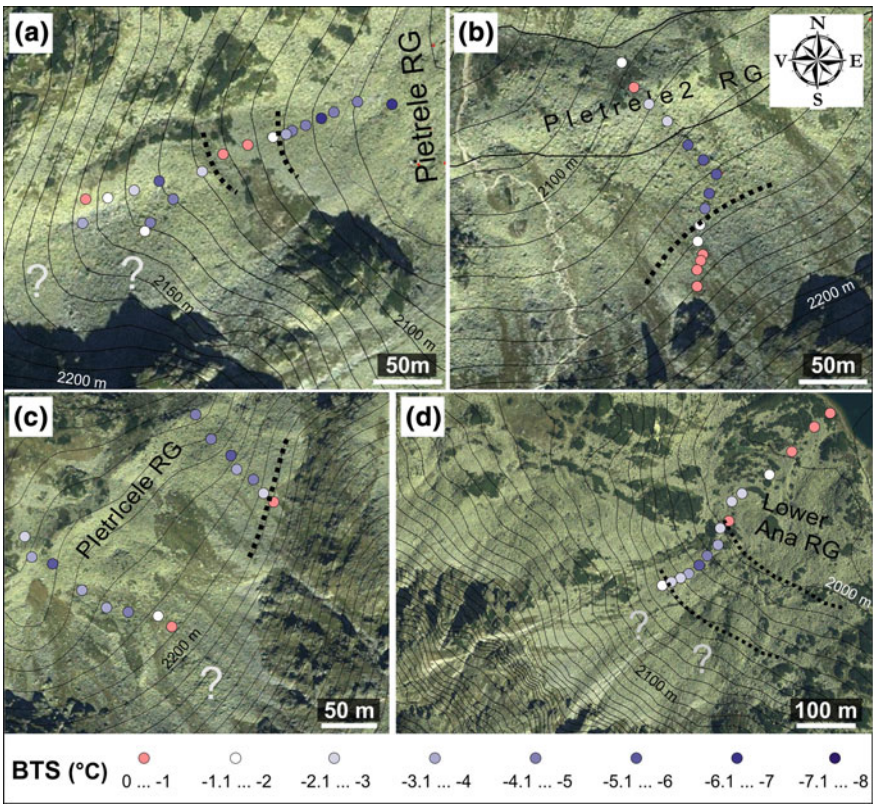

Fig. 6.9 BTS measurements on talus slopes from Retezat Massif indicating negative thermal anomalies in their lower sectors (Popescu et al. submitted)

lower parts present a relatively similar thermal regime, while between December and February the temperature is lower in the upper part. Towards the 0 curtain period, the temperature distribution becomes "normal", with colder regimes in the lower parts and warmer in the upper parts. However, the differences are much smaller (1–1.5 °C) in comparison to those obtained in the Retezat Massif. The data suggest that here the underground air circulation in the almost consolidated fine debris is rather absent. The low temperatures from the lower talus composed by coarser grain size could be related to the purely conductive cooling mechanism proposed by Gruber and Hoelzle (2008).

Rockwall Permafrost Probability

Continuous monitoring of steep rockwall thermal regimes was performed at different altitudinal levels and slope aspects from Romanian Carpathians. Usually, the rock temperature is exposed to cold atmospheric temperatures during the entire winter because snow cover cannot settle. Freeze-thaw cycles frequency was found to be much greater on southern slopes (Vasile et al. 2014). In opposition, on northern slopes the short-term freeze-thaw cycles frequency is much lower but seasonal frost penetration reaches greater depths. Using the Berggren equation modified by Matsuoka and Sakai (1999), the maximum potential frost depth in the highest north exposed rockwalls of Southern Carpathians rockwall surpasses 7 m (Vasile et al. 2014). In Parâng Massif, at 2190 m a.s.l., using the annual rock surface temperature data and the mentioned equation, an annual frost penetration depth of more than 5 m was calculated and it was estimated that above 2350–2400 m, the northern rockwalls could maintain perennially frozen areas (Popescu et al. 2015). On northern rocky slopes, mean annual rock surface temperatures (MARST) varied between 0.7 and 2 °C at altitudes between 2140 and 2270 m. At 2490 m, MART was found to be slightly negative in the Retezat Massif during one year of measurement (−0.2 °C in 2010–2011). On southern and eastern slopes, MARST is higher than 3 °C even at altitudes between 2200 and 2450 m (Fig. 6.10).

Taking into consideration the thermal regime, it is probable for rockwalls to present only patches of perennially frozen areas in their most shaded zones. Moreover, considering the warmer air temperatures from the last decade, it seems plausible that during the eighth and ninth decade of the last century, rockwall permafrost was more widespread (Popescu et al. submitted).

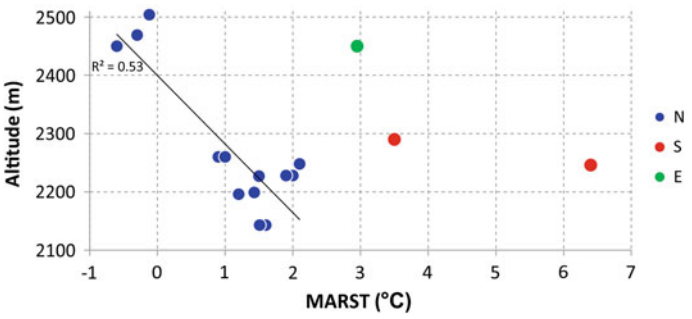

Fig. 6.10 Mean annual rock surface temperature (MARST) variations with altitude on rockwalls with different aspects from Făgăraș, Bucegi, Parâng, and Retezat Mountains (Popescu et al. submitted)

Internal Structure and Characteristics of Permafrost

In order to determine the permafrost thickness and composition, the borehole drillings in rock glaciers, talus slopes and rockwalls provide the most accurate results (Haeberli 1985; Arenson et al. 2002; Gruber et al. 2004; Scapozza et al. 2011). However, this operation is very expensive in the remote mountainous areas and also very difficult from a technical point of view (steep slopes and blocky materials that have to be cored). In this context, geoelectric techniques like electrical resistivity tomography (ERT) can be used to determine the subsurface conditions (Maurer and Hauck 2007; Kneisel et al. 2008). Ground penetrating radar (GPR) investigations are also useful for this purpose (e.g., Sass and Krautblatter 2007). According to Scapozza et al. (2011) who compared in detail the ERT data with physical evidences of permafrost internal structure (recovered from borehole drillings), resistivity values between 10–20 and 50 kΩm are specific for porous sediments or low resistivity permafrost with temperate ice, values between 50 and 200 kΩm are characteristic to frozen sediments undersaturated or saturated with ice while values >200 kΩm are related to supersaturated permafrost with active creep processes. For GPR investigations, Otto et al. (2012) interpreted the dense reflection patterns and the electromagnetic propagation velocities of more than 0.15 and less than 0.12 m/ns as indicating the presence and absence of permafrost, respectively.

Both ERT and GPR methods were applied on several sites from the Southern Carpathians in the last years, in order to sound the internal composition of rock glaciers and talus slopes and to detect permafrost (Vespremeanu-Stroe et al. 2012; Onaca et al. 2013, 2015; Popescu et al. 2015). Results confirm significantly more extensive permafrost in Retezat and Parâng in comparison to Făgăraș Massif.

Pietrele rock glacier revealed a high resistivity layer (25–240 kΩm) that can be interpreted as permafrost under a thick active layer of c. 10 m in its Southeastern sector (Onaca et al. 2013) (Fig. 6.11). Further investigations revealed permafrost presence in the lower part of the frontal talus slope feeding the Pietrele rock glacier (Onaca et al. 2015). Here, the high resistivity layer (35–140 kΩm), probably permafrost, is found at a 7–8 m depth and has a thickness of about 10–12 m. GPR profiles also confirmed the patchy permafrost presence in the southeastern sector of Pietrele rock glacier and the lower part of the talus slope. The ERT profiles on Pietricele rock glacier also revealed a fragmented high resistivity layer at 5–7 and 8–10 m depth with values of 45–120 and 20–65 kΩm respectively in the western and eastern part of the rock glacier which, most probably, is permafrost. These areas are separated by a vegetation covered debris flow deposit. In the lower part of the talus slope located above Pietricele rock glacier, a high resistivity layer of 30–170 kΩm and a thickness of 8–12 m was found under an active layer of about 5–7 m (Onaca et al. 2015) (Fig. 6.11). Raw ERT data indicated an isolated high resistivity core (several hundreds of kΩm) in the central sector of Lower Ana rock glacier which is most probably related to a permafrost core associated with boulders presence (Vespremeanu-Stroe et al. 2012).

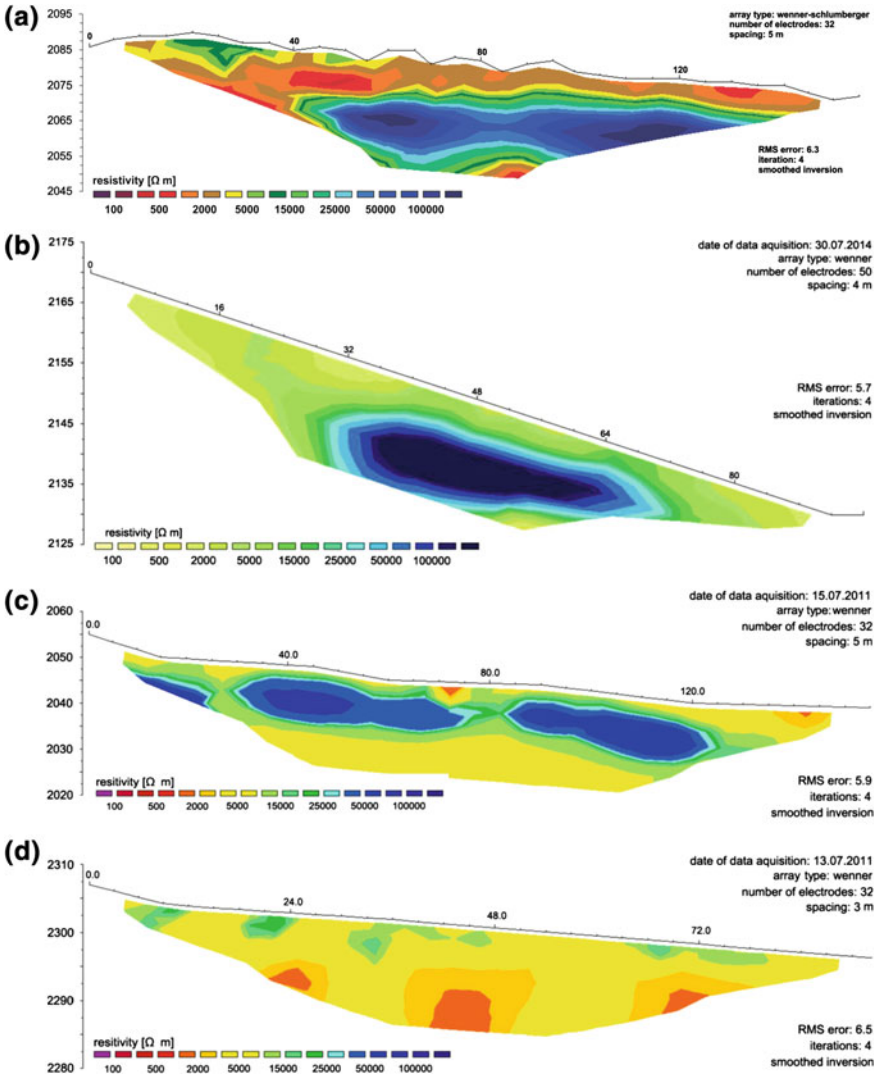

Fig. 6.11 ERT profiles from Roşiile 1 rock glacier (Parâng) (**a**), a talus slope feeding Pietricele rock glacier (Retezat) (**b**), Doamnei rock glacier (Făgăraş) (**c**), and Văiuga rock glacier (Făgăraş) (**d**) (data compiled from Onaca et al. (2013, 2015) (profiles **b**, **c** and **d**) and Popescu et al. (2015) (profile **a**)

High resistivity pockets of more than 100 kΩm were encountered in Berbecilor and Judele rock glaciers but the high resistivity of the dry and extremely coarse active layer (consisting of metric boulders) did not allow identifying the active layer—permafrost limit (Popescu 2015). However, several transversal GPR profiles on Judele rock glacier (Onaca et al. 2015) revealed a widespread distribution of the dense reflection pattern with electromagnetic propagation velocities of more

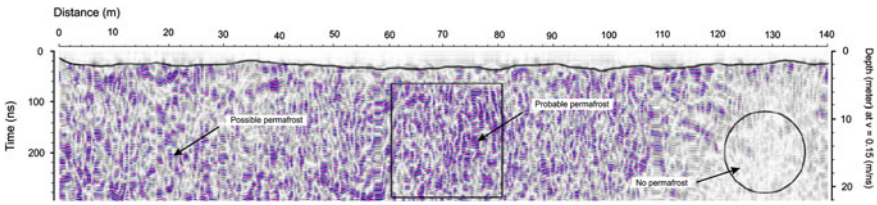

Fig. 6.12 Transversal GPR profile from the upper part of Judele rock glacier revealing dense reflection pattern characteristic to permafrost on almost the entire length of the profile

0.13 m/ns along almost the entire length of the profiles (Fig. 6.12). This suggests a wider permafrost presence in this rock glacier at least in its upper part.

In Parâng Massif, the ERT profiles performed on Roşiile 1 rock glacier revealed a high resistivity layer of 20–175 kΩm that can be interpreted as permafrost (Fig. 6.11a). The thickness of this layer is about 15–20 m and develops under an active layer of 6–12 m (Popescu et al. 2015). At lower altitudes, the Roşiile 2 (Ieşu) rock glacier displays a high resistivity layer of 30–85 kΩm at a depth increasing from 3 m in the upper part to 8 m towards the middle sector of the rock glacier (Onaca et al. 2013). Also, its thickness decreases from 15 to 5 m.

In Făgăraş Massif, the ERT investigations revealed probable permafrost only in Doamnei (Pietroasa) rock glacier (Onaca et al. 2013) (Fig. 6.11c). In its upper part, two ERT profiles indicated a high resistivity layer of 7–10 m thickness and resistivity values of 25–140 kΩm under an active layer of 3–5 m. However, the active layer did not reach its maximum thickness at the date of measurements, the end on July. In Văiuga rock glacier, even at higher altitude (2280 m) the resistivity values were lower, ranging between 5 and 20 kΩm (Fig. 6.11d) indicating the presence of either low resistivity permafrost or porous sediments layer. Even lower resistivity values (<10 kΩm) confirm the relict state of Capra and Bâlea rock glaciers.

According to all presented geophysical results, we assume that thin (<10 m) and undersaturated permafrost prevails in the Southern Carpathians (mostly in the granitic massifs) located under a thick (8–10 m) active layer. The latter also suggests a probable disequilibrium relation of permafrost with the present climate. In colder conditions, at altitudes between 2100 and 2200 m in the granitic massifs, especially in Retezat, permafrost seems to be thicker (>10–20 m) and supersaturated in ice at least on certain sectors of the rock glaciers and in the lower part of the talus slopes.

Conclusions

Alpine permafrost in the Southern Carpathians has a marginal character developing only in the most favorable conditions. These consist in cold microclimates imposed by topography, but also in specific ground surface characteristics. Among all, coarse openwork debris is the most favorable land cover type for permafrost development because of the cooling effect it exerts on the underground. Because of

the large surfaces of coarse blocks and of the high altitudes, Retezat and Parâng Massifs present the largest areas of permafrost from the Southern Carpathians.

The main mechanism responsible for the ground overcooling of coarse blocks, i.e. the internal warm air evacuation and cold air infiltration at the beginning of the cold season, was proved to exist in the Southern Carpathians. Grain size and (related) porosity of the debris deposits were found to be the driving factors for the efficiency of such thermal processes.

The permafrost creep related landforms, i.e., rock glaciers and protalus ramparts are mostly relict and therefore a component of a rather inherited periglacial landscape. Nevertheless, the present-day climatic conditions of Southern Carpathians are cold enough to allow patches of permafrost to maintain in inactive rock glaciers within the 1950–2100 m altitudinal level, located on shaded northern slopes of Retezat and Parâng Massifs. This permafrost is rather thin, it is undersaturated in ice and it has a well developed active layer. At higher altitudes, between 2100 and 2200 m a.s.l., the coldest microclimatic conditions determine a more widespread permafrost distribution in some rock glaciers. This situation is characterized by greater thicknesses, higher ice content and smaller active layer depth of permafrost that could be subjected to creep related movement. Also, the lower sectors of northern talus slopes above 2050–2100 m are as well underlain with permafrost in granitic massifs. Air circulation and stratification in their interior also develop and are enhanced by their steep topography.

The MAGST registered in permafrost containing debris deposits (both rock glaciers and talus slopes) are usually positive in the Southern Carpathians indicating permafrost degradation conditions. However, a few sites with 0 °C or slightly negative MAGST indicate local conditions for permafrost equilibrium with the present climate.

In crystalline schists massifs, the scree deposits are usually fossilized at all altitudinal levels. Both rock glaciers and talus slopes are mostly consolidated by interstitial matrix and covered by vegetation. Permafrost is absent at most investigated sites. The matrix provenience was related to the less resistant rock, which disintegrates in situ. Moreover, the grain size was proved to be statistically much smaller than for granites and the lower pore space volume is much easier to be filled up with fine sediments. Atypical areas of coarse blocks deposits like Doamnei rock glacier still have some chances for permafrost preservation in the present, but such situations are scarce in crystalline massifs like Făgăraș and Iezer—Păpușa.

Rockwall permafrost probability was inferred based on negative MART occurring at the top of the northern rockwalls at 2500 m a.s.l. Thus, theoretically, perennially frozen rockwalls could occurr even above 2350–2400 m in the most shaded sites with negative MARST. Besides the highest massifs cited so far (Făgăraș, Parâng, Retezat, and Iezer Păpușa) we assume that Bucegi Massif could also host some patches of rockwall permafrost because of its high altitudes and rockwalls.

For the vast number of remaining massifs from the Southern Carpathians, especially the calcareous ones, we assume the potential to be subjected only to atypical and azonal low altitude permafrost conditions in porous debris deposits down to MAAT isotherms of 2–5 °C, corresponding roughly to altitudes of 1600–1250 m.

Acknowledgments This study was supported by a postdoctoral scholarship offered by the University of Bucharest Research Institute (ICUB) to RP in 2015. The contribution of colleagues from both University of Bucharest and West University of Timişoara is greatly appreciated. Many thanks go to Mirela Vasile and Nicolae Cruceru for their valuable scientific assistance, data processing and long-term fieldwork involvement. The effort of Loredana Bîzgan and Monica Voinea in thermal and grain size data processing and also in fieldwork assistance was of great help. The colleagues Florin Tătui, Luminița Preoteasa, Alexandru Manoliu, Sabin Rotaru and Florin Zăinescu had an important contribution in fieldwork campaigns. Adrian Ardelean, Flavius Sîrbu, Raul Şerban and Patrick Chiroiu from the West University of Timişoara had a major role in obtaining and processing of the GPR and ERT data presented.

References

Arenson LU, Hoelzle M, Springman SM (2002) Borehole deformation measurements and internal structure of some rock glaciers in Switzerland. Permafrost Periglac Process 13:117–135

Balch ES (1900) Glaciers or freezing caverns. Allen, Lane & Scott, Philadelphia

Ballantyne CK, Kirkbride MP (1986) The characteristics and significance of some Lateglacial protalus ramparts in upland Britain. Earth Surf Proc Land 11(6):659–671

Barsch D (1996) Rockglaciers: indicators for the present and former geoecology in high mountain environments. Springer Series in Physical Environment 16. Springer, New York

Bernhard L, Sutter F, Haeberli W, Keller F (1998) Processes of snow/permafrost interactions at a high mountain site, Murtèl/Corvatsch, Eastern Swiss Alps. In: Proceedings of the seventh international conference on permafrost, vol 55, Yellowknife, Collection Nordicana, pp 35–41

Berthling I (2011) Beyond confusion: rock glaciers as cryo-conditioned landforms. Geomorphology 131:98–106

Bommer C, Phillips M, Arenson LU (2010) Practical recommendations for planning, constructing and maintaining infrastructure in mountain permafrost. Permafrost Periglac Process 21:97–104

Brenning A, Gruber S, Hoelzle M (2005) Sampling and statistical analysis of BTS measurements. Permafrost Periglac Process 16(3):231–240

Buytaert W, Celleri R, Willems P, De Bièvre B, Wyseure G (2006) Spatial and temporal rainfall variability in mountainous areas: a case study from the south Ecuadorian Andes. J Hydrol 329 (3–4):413–421

Delaloye R (2004) Contribution à l'étude du pergélisol de montagne en zone marginale. PhD thesis, University of Fribourg, GeoFocus 10

Delaloye R, Lambiel C (2005) Evidence of winter ascending air circulation throughout talus slopes and rock glaciers situated in the lower belt of alpine discontinuous permafrost (Swiss Alps). Nor Geogr Tidsskr 59:194–203

Delaloye R, Reynard E, Lambiel C, Marescot L, Monnet R (2003) Thermal anomaly in a cold scree slope (Creux du Van, Switzerland). In: Phillips M, Springman SM, Arenson LU (eds) Proceedings of eight international conference of permafrost, Zürich, 1. Balkema, Lisse, pp 175–180

Delaloye R, Morard S, Barboux C, Abbet D, Gruber V, Riedo M, Gachet S (2013) Rapidly moving rock glaciers in Mattertal. In: Graf C (ed) Mattertal—ein Tal in Bewegung. Publikation zur Jahrestagung der Schweizerischen Geomorphologischen Gesellschaft 29. Juni–1. Juli 2011, St. Niklaus. Birmensdorf, Eidg. Forschungsanstalt WSL, pp 21–31

Dimitrov P, Gikov A (2011) Relict rock glaciers identification and mapping in Pirin mountain using aerial and satellite images. In: Proceedings of the seventh scientific conference: space, ecology, safety, Sofia, pp 206–263

Dobiński W (1997) Distribution on mountain permafrost in the high Tatra based on freezing and thawing indices. Biul Peryglac 36:29–36

Etzelmüller B, Berthling I, Sollid JL (2003) Aspects and concepts on the geomorphological significance of Holocene permafrost in southern Norway. Geomorphology 52:87–104

Frauenfelder R, Allgöver B, Haeberli W, Hoelzle M (1998) Permafrost investigations with GIS—a case study in the Fletschhorn area, Wallis, Swiss Alps. In: Proceedings of seventh international conference on permafrost, vol 55, Yellowknife, Canada, Collection Nordicana, pp 291–295

Fukui K (2003) Permafrost and surface movement of an active protalus rampart in the Kuranosuke Cirque, the northern Japanese Alps. In: Phillips M, Springman SM, Arenson LU (eds), Proceedings of Eight International Conference of Permafrost, vol 1, Zürich, Balkema, Lisse, pp 265–270

Gądek B (2014) Climatic sensitivity of the non-glaciated mountains cryosphere (Tatra Mts., Poland and Slovakia). Global Planet Change 121:1–8

Gądek B, Kędzia S (2008) Winter ground surface temperature regimes in the zone of sporadic discontinuous permafrost, Tatra Mountains (Poland and Slovakia). Permafrost Periglac Process 19:315–321

Gikov A, Dimitrov P (2010) Identification and mapping of the relict rock glaciers in the Rila Mountain using aerial and satellite images. In: Proceedings of the sixth scientific conference: space, ecology, safety, Sofia, pp 252–259

Gómez-Ortiz A, Oliva M, Salvador-Franch F, Salvà-Catarineu M, Palacios D, de Sanjosé-Blasco JJ, Tanarro-García LM, Galindo-Zaldívar J, de Galdeano CS (2014) Degradation of buried ice and permafrost in the Veleta cirque (Sierra Nevada, Spain) from 2006 to 2013 as a response to recent climate trends. Solid Earth 5:979–993

Gruber S (2005) Mountain permafrost: transient spatial modeling, model verification and the use of remote sensing. PhD thesis, University of Zürich

Gruber S, Haeberli W (2009) Mountain permafrost. In: Margesin R (ed) Permafrost soils biology series. Springer, Berlin

Gruber S, Hoelzle M (2001) Statistical modelling of mountain permafrost distribution: local calibration and incorporation of remotely sensed data. Permafrost Periglac Process 12:69–77

Gruber S, Hoelzle M (2008) The cooling effect of coarse blocks revisited: a modeling study of a purely conductive mechanism. In: Kane DL, Hinkel K (eds) Proceedings of the ninth international conference on permafrost, Institute of Northern Engineering, University of Alaska, Fairbanks, pp 557–561

Gruber S, King L, Kohl T, Herz T, Haeberli W, Hoelzle M (2004) Interpretation of geothermal profiles perturbed by topography: the alpine permafrost boreholes at Stockhorn Plateau, Switzerland. Permafrost Periglac Process 15:349–357

Gubler S, Fiddes J, Keller M, Gruber S (2011) Scale-dependent measurement and analysis of ground surface temperature variability in alpine terrain. The Cryosphere 5:431–443

Gude M, Dietrich S, Mäusbacher R, Hauck C, Molenda R, Ruzicka V, Zacharda M (2003) Probable occurrence of sporadic permafrost in non-alpine scree slopes in central Europe. In: Phillips M, Springman SM, Arenson LU (eds) Proceedings of the eighth international conference on permafrost, Zürich, Balkema, Lisse, pp 331–336

Haeberli W (1973) Die basis-temperature der winterlichen Schneedecke als möglicher Indikator für die Verbreitung von Permafrost in den Alpen. Zeitschrift für Gletcherkunde und Glazialgeologie 9:221–227

Haeberli W (1985) Creep of mountain permafrost: internal structure and flow of alpine rock glaciers, Versuchanst. Mitteilungen der Versuchsanstalt für Wasserbau, Hydrologie und Glaziologie der ETH Zürich 77:142

Haeberli W, Patzelt G (1982) Permafrostkartierung im gebiet der Hochenbenkar-Blockgletscher, Obergurgl, Ötztaler Alpen. Z Gletscherk Glazialgeol 18(2):127–150

Haeberli W, Hallet B, Arenson L, Elconin R, Humlum O, Kääb A, Kaufmann V, Ladanyi B, Matsuoka N, Springman S, Vonder Mühll D (2006) Permafrost creep and rock glacier dynamics. Permafrost Periglac Process 17(3):189–214

Hanson S, Hoelzle M (2004) The thermal regime of the active layer at the Murtèl rock glacier based on data from 2002. Permafrost Periglac Process 15(3):273–282

Harris SA, Pedersen DE (1998) Thermal regime beneath coarse blocky materials. Permafrost Periglac Process 9:107–120

Harris C, Arenson LU, Christiansen HH, Etzelmüller B, Frauenfelder R, Gruber S, Haeberli W, Hauck C, Hölzle M, Humlum O, Isaksen K, Kääb A, Kern-Lütschg MA, Lehning M, Matsuoka N, Murton JB, Nötzli J, Phillips M, Ross N, Seppälä M, Springman SM, Mühll DV (2009) Permafrost and climate in Europe: monitoring and modeling thermal, geomorphological and geotechnical responses. Earth Sci Rev 92:117–171

Hasler A, Gruber S, Haeberli W (2011) Temperature variability and offset in steep alpine rock and ice faces. The Cryosphere 5(4):977–988

Hoelzle M, Wegmann M, Krummenacher B (1999) Miniature temperature dataloggers for mapping and monitoring of permafrost in high mountain areas: first experience from the Swiss Alps. Permafrost Periglac Process 10:113–124

Humlum O (1996) Origin of rock glaciers: observations from Mellemfjord, Disko Island, central West Greenland. Permafrost Periglac Process 7:361–380

Ichim I (1978) Preliminary observations on the rock glacier phenomenon in the Romanian Carpathians. Revue Roumaine de Géologie, Géophysique et Géographie 23(2):295–299

Ikeda A, Matsuoka N (2002) Degradation of talus-derived rock glaciers in the Upper Engadin, Swiss Alps. Permafrost Periglac Process 13:145–161

Ikeda A, Matsuoka N (2006) Pebbly versus bouldery rock glaciers: morphology, structure and processes. Geomorphology 73:279–296

Imhof M (1996) Modelling and verification of the permafrost distribution in the Bernese Alps (Western Switzerland). Permafrost Periglac Process 7:267–280

Isaksen K, Hauck C, Gudevang E, Ødegård RS, Sollid JL (2002) Mountain permafrost distribution in Dovrefjell and Jotunheimen, southern Norway, based on BTS and DC resistivity tomography data. Nor Geogr Tidsskr 56(2):122–136

Isaksen K, Sollid JL, Holmlund P, Harris C (2007) Recent warming of mountain permafrost in Svalbard and Scandinavia. J Geophys Res 112:F02S04. doi:10.1029/2006JF000522

Ishikawa M (2003) Thermal regimes at the snow-ground interface and their implication for permafrost investigation. Geomorphology 52:105–120

Julián A, Chueca J (2007) Permafrost distribution from BTS measurements (Sierra de Telera, Central Pyrenees, Spain): assessing the importance of solar radiation in a middle elevation shaded mountainous area. Permafrost Periglac Process 18:137–149

Juliussen H, Humlum O (2007) Towards a TTOP ground temperature model for mountainous terrain in central-eastern Norway. Permafrost Periglac Process 18:161–184

Kędzia S (2014) Are there any active rock glaciers in the Tatra Mountains? Studia Geomorphologica Carpatho Balcanica XLVIII:5–16

Keller G, Tamás M (2003) Enhanced ground cooling in periods with thin snow cover in the Swiss National Park. In: Phillips M, Springman SM, Arenson LU (eds) Proceedings of eight international conference of permafrost Zürich, 1. Balkema, Lisse, pp 531–536

Kern Z, Balogh D, Nagy B (2004) Investigations for the actual elevation of the mountain permafrost zone on postglacial landforms in the head of Lăpuşnicu Mare Valley, and the history of deglaciation of Ana Lake—Judele Peak region, Retezat Mountains, Romania. Analele Universităţii de Vest din Timişoara, GEOGRAFIE 14:119–132

Kłapyta P (2013) Application of Schmidt hammer relative age dating to Late Pleistocene moraines and rock glaciers in the Western Tatra Mountains, Slovakia. Catena 111:104–121

Kneisel C, Hauck C, Vonder Mühll D (2000) Permafrost below the timberline confirmed and characterized by geoelectrical resistivity measurements, Beaver Valley, Eastern Swiss Alps. Permafrost Periglac Process 11:295–304

Kneisel C, Hauck C, Fortier R, Moorman B (2008) Advances in geophysical methods for permafrost investigations. Permafrost Periglac Process 19:157–178

Lambiel C, Pieracci K (2008) Permafrost distribution in talus slopes located within the alpine periglacial belt, Swiss Alps. Permafrost Periglac Process 19:293–304

Lewkowicz AG, Ednie M (2004) Probability mapping of mountain permafrost using the BTS method, Wolf Creek, Yukon Territory, Canada. Permafrost Periglac Process 15:67–80

Lugon R, Delaloye R, Serrano E, Reynard E, Lambiel C, González Trueba JJ (2004) Permafrost and little ice age relationships, Posets massif, Central Pyrenees, Spain. Permafrost Periglac Process 15:207–220

Magnin F, Deline P, Ravanel L, Noetzli J, Pogliotti P (2015) Thermal characteristics of permafrost in the steep alpine rock walls of the Aiguille du Midi (Mont Blanc Massif, 3842 m asl). The Cryosphere 9(1):109–121

Matsuoka N, Sakai H (1999) Rockfall activity from an alpine cliff during thawing periods. Geomorphology 28:309–328

Maurer H, Hauck C (2007) Instruments and methods geophysical imaging of alpine rock glaciers. J Glaciol 53(180):110–120

Mîndrescu M, Evans IS, Cox NJ (2010) Climatic implications of cirque distribution in the Romanian Carpathians: palaeowind directions during glacial periods. J Quat Sci 25(6): 875–888

Morard S, Delaloye R, Dorthe J (2008) Seasonal thermal regime of a mid-latitude ventilated debris accumulation. In: Proceedings of the ninth international conference on permafrost, Fairbanks, pp 1233–1238

Moscicki J, Kędzia S (2001) Investigation of mountain permafrost in the Kozia Dolinka valley, Tatra Mountains, Poland. Nor Geogr Tidsskr 55:1–6

Mott R, Schirmer M, Bavay M, Grünewald T, Lehning M (2010) Understanding snow-transport processes shaping the mountain snow-cover. The Cryosphere 4:545–559

Noetzli J, Gruber S, Kohl T, Salzmann N, Haeberli W (2007) Three-dimensional distribution and evolution of permafrost temperatures in idealized high-mountain topography. J Geophysical Research: Earth Surf 112(F2)

Onaca A, Urdea P, Ardelean C (2013) Internal structure and permafrost characteristics of the rock glaciers of Southern Carpathians (Romania) assessed by geoelectrical soundings and thermal monitoring. Geogr Ann Ser A Phys Geogr 95(3):249–266

Onaca A, Ardelean AC, Urdea P, Ardelean F, Sîrbu F (2015) Detection of mountain permafrost by combining conventional geophysical methods and thermal monitoring in the Retezat Mountains, Romania. Cold Reg Sci Technol 119:111–123

Otto J-C, Keuschnig M, Götz J, Marbach M, Schrott L (2012) Detection of mountain permafrost by combining high resolution surface and subsurface information—an example from the Glatzbach catchment, Austrian Alps. Geogr Ann Ser A Phys Geogr 94:43–57

Paul F, Kääb A, Haeberli W (2007) Recent glacier changes in the Alps observed by satellite: consequences for future monitoring strategies. Geomorphology 56:111–122

Popescu (2015) Fenomenologia permafrostului din Carpații Românești. PhD thesis, University of Bucharest (in Romanian)

Popescu R, Vespremeanu-Stroe A, Onaca A, Cruceru N (2015) Permafrost research in the granitic massifs of Southern Carpathians (Parâng Mountains). Z Geomorphol 59(1):1–20

Popescu R, Vespremeanu-Stroe A, Vasile M, Nedelea A, Cruceru N (submited) Permafrost state in the marginal periglacial conditions of Southern Carpathians, Romania. The Cryosphere

Ribolini A, Fabre D (2006) Permafrost existence in rock glaciers of the Argentera Massif, Maritime Alps, Italy. Permafrost Periglac Process 17:49–63

Rödder T, Kneisel C (2012) Influence of snow cover and grain size on the ground thermal regime in the discontinuous permafrost zone, Swiss Alps. Geomorphology 175:176–189

Ruszkiczay-Rüdiger S, Kern Z, Urdea P, Braucher R, Madarász B, Schimmelpfennig I, ASTER Team (2015) Revised deglaciation history of the Pietrele-Stânișoara glacial complex, Retezat Mts, Southern Carpathians, Romania. Quat Int. doi:10.1016/j.quaint.2015.10.085

Sandu I, Pescaru V, Poiană I, Geicu A, Cândea I, Ţâştea D (2008) Clima României. Editura Academiei Române, Bucharest (in Romanian)

Sass O, Krautblatter M (2007) Debris flow-dominated and rockfall-dominated talus slopes: genetic models derived from GPR measurements. Geomorphology 86:176–192

Sawada Y, Ishikawa M, Ono Y (2003) Thermal regime of sporadic permafrost in a block slope on Mt. Nishi-Nupukaushinupuri, Hokkaido Island, Northern Japan. Geomorphology 52:121–130

Scapozza C, Lambiel C, Baron L, Marescot L, Reynard E (2011) Internal structure and permafrost distribution in two alpine periglacial talus slopes, Valais, Swiss Alps. Geomorphology 132(3–4):208–221

Schneider S, Hoelzle M, Hauck C (2012) Influence of surface and subsurface heterogeneity on observed borehole temperatures at a mountain permafrost site in the Upper Engadine, Swiss Alps. The Cryosphere 6:517–531

Serrano E, Agudo C, de Pison EM (1999) Rock glaciers in the Pyrenees. Permafrost Periglac Process 10:101–106

Serrano E, San José JJ, Agudo C (2006) Rock glacier dynamics in a marginal periglacial high mountain environment: flow, movement (1991–2000) and structure of the Argualas rock glacier, the Pyrenees. Geomorphology 74:285–296

Sîrcu I (1971) Geografia fizică a R.S.România. Editura Didactică şi Pedagogică, Bucureşti (in Romanian)

Sîrcu I, Sficlea V (1956) Cîteva observaţii geomorfologice în munţii Parîngului şi ai Şureanului. Analele Ştiinţifice ale Universităţii "Al. I. Cuza" din Iaşi, II- Ştiinţe Naturale-Geografie 2:387–402 (in Romanian)

Sorg A, Kääb A, Roesch A, Bigler C, Stoffel M (2015) Contrasting responses of Central Asian rock glaciers to global warming. Sci Rep 5:1–6

Stiegler C, Rode M, Sass O, Otto JC (2014) An undercooled scree slope detected by geophysical investigations in sporadic permafrost below 1000 m ASL, central Austria. Permafrost Periglac Process 25(3):194–207

Tanarro LM, Hoelzle M, Garcia A, Ramos A, Gruber S, Gómez Ortiz A, Piquer M, Palacios D (2001) Permafrost distribution modelling in the mountains of the Mediterranean: Corral del Veleta, Sierra Nevada, Spain. Nor Geogr Tidsskr 55:253–260

Urdea P (1985) Câteva aspecte ale reliefului periglaciar din Munţii Retezat. Analele Ştiinţifice ale Universităţii "Al. I. Cuza" din Iaşi, Secţ. IIb. Geol Geogr 31:73–76 (in Romanian)

Urdea P (1992) Rock glaciers and periglacial phenomena in the Southern Carpathians. Permafrost Periglac Process 3:267–273

Urdea P (1993) Permafrost and periglacial forms in the Romanian Carpathians. In: Proceedings of sixth international conference on permafrost, Beijing, University of Technology Press 1, pp 631–637

Urdea P (1998) Rock glaciers and permafrost reconstruction in the Southern Carpathians Mountains, Romania. In: Proceedings of seventh international conference on permafrost, Yellowknife, Canada, Collection Nordicana 57, pp 1063–1069

Vasile M, Vespremeanu-Stroe A, Popescu R (2014) Air versus ground temperature data in the evaluation of frost weathering and ground freezing. Examples from the Romanian Carpathians. Rev Geomorfologie 16:61–70

Vespremeanu-Stroe A, Urdea P, Popescu R, Vasile M (2012) Rock glacier activity in the Retezat Mountains, Southern Carpathians, Romania. Permafrost Periglac Process 23:127–137

Wakonigg H (1996) Unterkühlte Schutthalden. Arbeiten aus dem Institut für Geographie der Karl-Franzens-Universität Graz (Beiträge zur Permafrostforschung in Österreich) 33:209–223

Warhaftig C, Cox A (1959) Rock glaciers in the Alaska Range. Bull Geol Soc Am 70:383–436

Chapter 7
Present-Day Periglacial Processes in the Alpine Zone

Alexandru Onaca, Petru Urdea, Adrian C. Ardelean, Raul Şerban and Florina Ardelean

Abstract This chapter reviews the existing knowledge concerning the current state of the main frost-driven processes in the Romanian Carpathians. Since permafrost has a patchy distribution and occurs in marginal conditions only in few massifs from the Romanian Carpathians, the key periglacial processes are those associated with seasonal frost, which are widespread above the tree line. The present-day amplitude of solifluction, frost heaving or frost creep is generally lower than in other periglacial environments ranging from few mm to tens of centimetres/year. The results revealed that mass wasting and frost weathering in the alpine environment of the Romanian Carpathians are strongly controlled by ground freezing, which depends on several factors, such as ground materials, topography, vegetation cover, snow cover, water content and incoming solar radiation. Major progress has been achieved in the last few years, when comprehensive monitoring of several periglacial processes (e.g. solifluction, frost heaving, frost creep) has started. The outcomes improved the understanding of current periglaciation in the Romanian Carpathians, but many uncertainties still exist regarding several periglacial processes (e.g. frost weathering) and the role of the environmental controlling factors. The periglacial deposits have a central, but not a defining position within the alpine landscape, occupying a greater extent than glacial or fluvial deposits. Based on the estimated volume of sediments within the alpine sector of a small alpine catchment in the Southern Carpathians, a post-glacial mean denudation rate of 0.26 mm/year was calculated.

Keywords Periglacial processes · Deposits · Denudation rates · Alpine environment · Romanian Carpathians

A. Onaca (✉) · P. Urdea · A.C. Ardelean · R. Şerban · F. Ardelean
West University of Timişoara, V. Pârvan 4, 300223 Timişoara, Timiş, Romania
e-mail: alexandru.onaca@e-uvt.ro; ducuonaca@yahoo.com

M. Rădoane and A. Vespremeanu-Stroe (eds.), *Landform Dynamics and Evolution in Romania*, Springer Geography,
DOI 10.1007/978-3-319-32589-7_7

Background

Approximately 25 % of the Earth's land surface qualifies currently as periglacial (French 2007). In modern usage, periglacial refers to the conditions, processes and landforms associated with cold, non-glacial environments (Harris et al. 1988). In Romania, periglacial conditions occur generally in high-altitude alpine zones, located above 1700 m which roughly correspond with the tree line (Onaca 2013). The largest extension of the alpine periglacial environment occurs in the Southern Carpathians, where approximately 1566 km^2, from a total of 1783 km^2 in the Romanian Carpathians, experience periglacial conditions.

A remarkable variety of both active and inactive periglacial forms were described in the last 150 years (Urdea et al. 2008a) in the alpine zone of the Romanian Carpathians. However, since most of the conducted studies were purely descriptive, the scientific evidences concerning the amplitude of the actual frost-induced processes are scarce. The lack of knowledge was determined mainly by the absence of necessary observational data regarding frost action in the historically recent times and nowadays. Consequently, erroneous assumptions concerning the conceptual framing of the periglacial features from the Romanian Carpathians contributed to a delayed scientific progress in this direction. Hypnotised by the Łoziński (1909) meaning of the periglacial term (French 2000), many autochthonous geomorphologists hesitated to embrace the modern meaning of the 'periglacial', by denying the capacity of frost-induced processes to produce current distinctive landforms and deposits in the alpine zone of the Romanian Carpathians. The excessive dissemination of the unfamiliar "cryo-nival" to designate the role of frost and snow in shaping the Pleistocene periglacial features contributed decisively to the scientific isolation of the Romanian periglacial geomorphology.

As it often happens in science, in the last 50–60 years of the twentieth century, the studies of periglacial phenomena have become "scientific fashionable subjects" in Romania too. Although few studies provided a good description of periglacial landforms (e.g. Niculescu and Nedelcu 1961; Niculescu 1965), the analysis of contemporary periglacial processes is characterised by inconsistency, since the quantitative benchmarks are lacking. The cryo-nival concept was obsessively used to designate periglacial processes, such as: frost weathering, solifluction and pipkrake, avalanches and nivation (Micalevich-Velcea 1961; Sîrcu 1978; Bălteanu and Posea 1983; Ielenicz 1984; Murătoreanu 2009). Only few authors admit the existence of nowadays periglacial processes (e.g. Florea 1998; Rusu 2002; Lesenciuc 2006), whereas the majority prefer the expression "cryo-nival morphogenesis" to designate the current periglaciation (Schreiber 1994; Simoni 2011). In the article about the present-day periglacial processes in the mountains between Ialomiţa and Olt, Nedelcu (1964) performed for the first time a brief analysis of the morphogenetic conditions, together with a detailed presentation of the specific periglacial processes. A forward step in the understanding of the current frost-derived processes in the Carpathians highlands was offered by Posea et al. (1974), who realised

an extremely useful analysis of the morphoclimatic conditions of the so called "cryo-nival belt".

The need for detailed information concerning high mountain systems and implicitly the behaviour of periglacial processes has grown substantially in the last two decades, due to increased awareness related to the delicate nature of alpine environments (Barsch 1993). On the one hand, human activity in alpine regions has increased constantly endangering the natural evolution of this sensible environment (Urdea et al. 2009). On the other hand, the contemporary atmosphere warming poses as a fundamental threat for the geomorphologic stability of the cold environments, both at a continental and at a local scale (Anisimov and Nelson 1996). In this context, the pioneering studies of Urdea (1989, 2000), have served to change the flawed assumptions concerning the current frost action in the alpine zone of the Romanian Carpathians. Gradually, the new beliefs were embraced by the younger geomorphologists, which took advantage by the recent developments in the field of shallow geophysics, geographic information systems, remote sensing and statistical techniques to provide new insights into the frost-driven processes—periglacial landforms—alpine environment relationships (Urdea et al. 2003, 2008b; Vespremeanu-Stroe et al. 2012; Onaca 2013; Onaca et al. 2013a, b; Popescu et al. 2015; Ardelean 2015).

Despite recent findings provided by previous studies, gaps in the understanding of this "exotic" problem for the Romanian Carpathians still exist. This chapter aims to present a comprehensive picture of the existing knowledge concerning the current state of the main frost-induced processes and to highlight the current uncertainties. In addition, the role of the environmental factors in controlling the evolution of periglacial processes and landforms is assessed.

Romanian Carpathians Periglacial Phenomena

Periglacial environments are dominated by typical processes associated with seasonal and perennial frost (French 2007). The variety and distribution of the periglacial features highlight the importance of frost driven processes in the alpine zone of the Romanian Carpathians, both in the Pleistocene period, during the Holocene and nowadays (Urdea et al. 2008a). Based on previous regional studies and personal geomorphological observations, the periglacial features from Romanian Carpathians were classified based on the landform criteria (Table 7.1). We adjusted the classification of Ballantyne and Harris (1994) for Upland Britain, by adding a sixth main group, entitled permafrost and ground ice.

The present-day zonal periglacial processes described in the alpine zone of the Romanian Carpathians could be classified in two main categories: frost weathering (frost action) and mass movement (mass wasting). The former category includes frost shattering, frost cracking and frost heave, whereas the later class is related to various mass movement processes, such as: frost creep, solifluction (gelifluction), rockfalls, rock avalanches and debris flows. In many cases, these processes operate

Table 7.1 The classification system of present-day periglacial phenomena in the Southern Carpathians (adapted after Ballantyne and Harris 1994)

Main division	Periglacial landforms
Permafrost and ground ice	Rock glaciers
Patterned ground	Circles, polygons, hummocks, nets, stripes
Solifluction landforms	Solifluction lobes, steps, terraces and sheets, ploughing boulders
Frost weathering	Tors, block fields, slopes, block streams debris-mantled slope
Talus slope and related landforms	Talus cones, sheets, avalanche cones, tongues and tracks, debris cones and flows, protalus ramparts
Snow melt effects, fluvial and eolian features	Nivation hollows, cryoplanation terraces, stratified slope deposits, deflation surfaces and pavements

collectively and in practice are often impossible to be differentiated by field measurements (e.g. frost creep and gelifluction). Furthermore, these processes are strongly interrelated, if we consider that the loose material available for transport by mass movement processes is the result of the rock disintegration by frost weathering.

Besides the periglacial processes mentioned above, other azonal processes (e.g. fluvial and eolian processes) take part in shaping the periglacial landscape. In the alpine area of the Romanian Carpathians one of the main contributors to slopewash activity is the so called "snow bank hydrology" (sensu French 2007), since the controversial "nivation" was abandoned due to its vagueness. This conceptual change occurred after different studies have revealed that the "nivation morphology" is the result of the collective action of several erosional processes, such as: frost shattering, gelifluction and slopewash (French 2007).

Periglacial Deposits and Post-glacial Denudation Rates

Within the alpine environment, the sediment flux plays a major role in landform evolution (Otto 2006). The complex processes that lead to the accumulation, storage and redistribution of sediment, in mountain areas affected by glaciation, act on various time and spatial scales (Ballantyne 2002). However, the impact of the past glaciation on landscape evolution seems to be highly variable, leading to several approaches to the problem of paraglacial landscape evolution (Ballantyne 2003; Dadson and Church 2005; Harbor and Warburton 1993), based on the general idea that glacier retreat increases the instability within the adjacent valley slopes, stimulating the collapse of steep flanks, thus generating an increase in sediment input (Davies et al. 2001).

Sediment storage specific landforms are generally assembled in a nested manner, underneath overhanging rock walls, indicating the existence of complex sediment transport systems (Otto et al. 2009). Thus, the estimation of sediment volumes plays

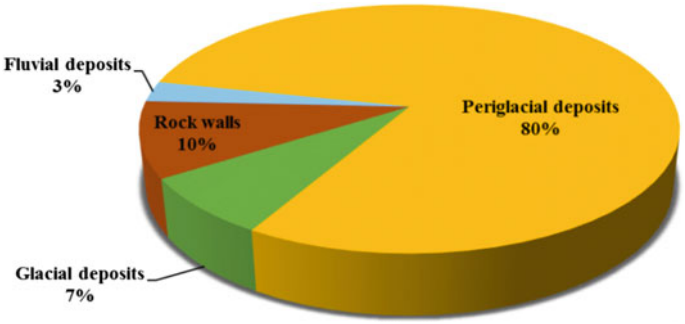

Fig. 7.1 Distribution of main types of deposits within the Doamnei Valley (Ardelean 2015)

a major role in sediment budget quantification, a key factor in understanding the post-glacial evolution of the alpine environment (Caine 1974).

Despite the fact that there is still very few knowledge available on current denudation rates for the Romanian Carpathians, we assume that during the Lateglacial and early Holocene these rates were considerably higher than today (Onaca 2013). However, rough estimations of post-glacial denudation rates in the alpine environments were only recently assessed (Vespremeanu-Stroe et al. 2012; Ardelean 2015). Ardelean's study (Ardelean 2015) proved to be the first approach of quantifying the sediment budget within the alpine sector of one small catchment (Doamnei, Făgăraş Mountains, 45°36′N, 24°35′E) in the Romanian Carpathians. The study revealed that periglacial landforms cover 2.92 km^2 (80 %) from a total of 3.6 km^2 (Fig. 7.1), adding up to a total volume of 4.4×10^6 m^3.

Denudation rates quantify surface lowering of complex geomorphic systems, being thus one of the main factors in determining the recent evolution of alpine environments. Based on the estimated volume of sediments within the alpine sector of the Doamnei valley a mean denudation rate of 0.26 mm/year was determined by Ardelean (2015) for the entire investigated area of 3.6 km^2. The calculated value is lower than those estimated in previous studies deployed in Romania, showing a good fit to the current values for the European Alps (Table 7.2).

Based on the overall sediment volume, a mean sediment yield value of 52.8 t/km^2/year was obtained for the last 10 k years for the entire investigated area. An increase in sediment redistribution values is observed when considering mean sediment yield value within the hanging valleys of over 1140 t/km^2/year. In a more detailed overview regarding sediment flux values within the investigated area, it is clear that periglacial process move up to 77 % of the material stored within the hanging valleys and over 70 % of the material stored within the main valley. Thus, talus sheets dominate the sediment flux system, gravitational processes on slopes moving up to 396 t/km^2/year only within the hanging valleys, followed closely by periglacial creep within the rock glacier, responsible for a mean redistribution rate of over 336 t/km^2/year sector (Fig. 7.2).

Table 7.2 Mean denudation rates in the Romanian Carpathians and European Alps

Location	Mean denudation rate (mm/year)	Time period	Source
Doamnei Valley (Romanian Carpahians)	0.26	10 ka	Ardelean (2015)
Retezat Mountains (Romanian Carpathians)	0.90	10 ka	Vespremeanu-Stroe et al. (2012)
Turtmann Valley (Swiss Alps)	0.62	10 ka	Otto et al. (2009)
Langental (Dolomites)	1.10	Post-glacial	Schrott and Adams (2002)
Rhone/Brig (Swiss Alps)	0.35	Present-day	Sclunegger and Hinderer (2003)

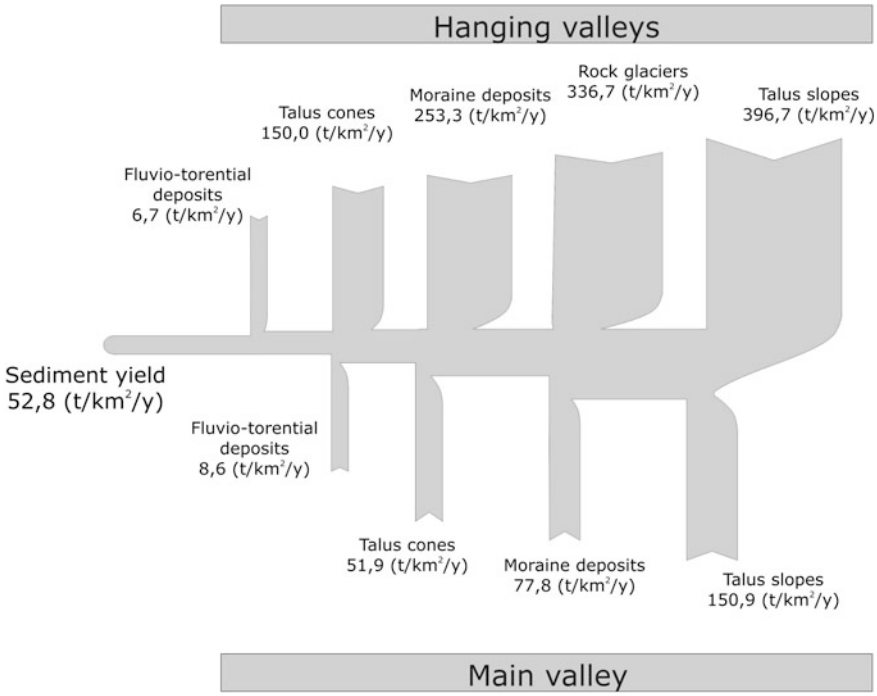

Fig. 7.2 Sediment flux within the Doamnei Valley and its subdivisions

The lithological heterogeneity of the Carpathian alpine domain determines different behaviours of frost weathering. In areas occupied by igneous intrusive rocks (granite, granodiorite), exfoliation and granular disaggregation are evident processes, marked by the appearance of rock slabs and cavernous surfaces (Fig. 7.3b). The position of in situ split blocks (Fig. 7.3a) and rockwall fresh scars are in connection with accumulation deposits and prove the actuality of frost weathering.

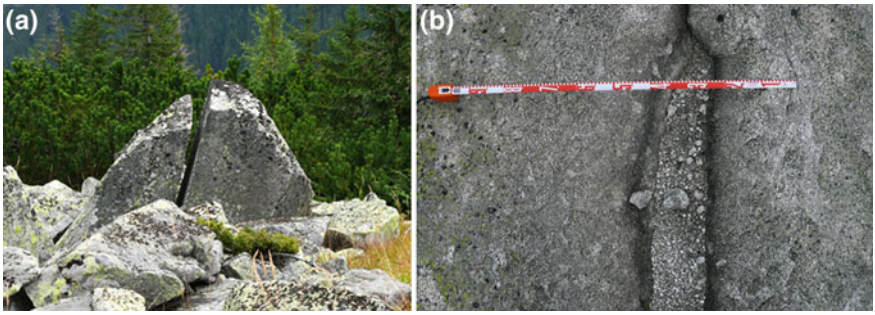

Fig. 7.3 Frost splitting (**a**) and granular disaggregation (**b**) in the granodiorites in the Retezat Mountains

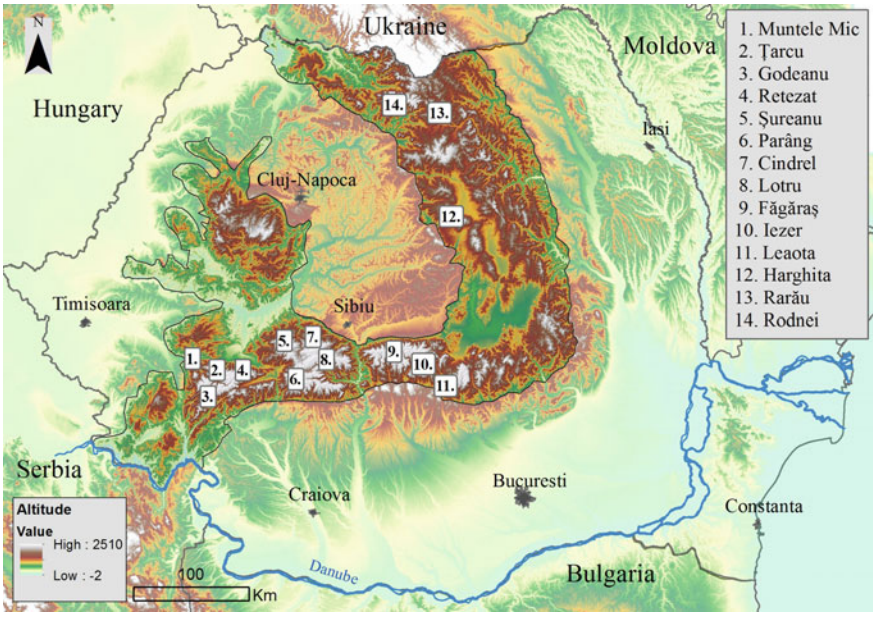

Fig. 7.4 The location of the investigation sites within the Romanian Carpathians

A recent lichenometric approach has provided the first ages of different periglacial deposits (Puțan 2015). For the block streams in the central part of the Făgăraș Mountains (Fig. 7.4), the mean age of lichens covering the uppermost boulders is between 130 and 400 years (Puțan 2015). In case of the investigated scree slopes, the mean ages of the uppermost boulders range between 100–150 years and 60–70 years, whereas the maximum ages exceed 400 years (Puțan 2015). These results are consistent with the assumption that during the last cold phase, known as the "Little Ice Age", intense rockfall occurred.

Frost Heaving

The major cause of frost heaving is the formation of ice lenses in soils (Penner 1986), as it was pointed out since 1929 by Taber (1929). The surface of the ground is thus raised by the volumetric expansion of water as it freeze (French 2007), which is capable to induce rapidly heaving pressure of 100–300 kPa (Williams and Smith 1989). Frost heaving involves frost pull, frost push and needle ice formation (Fig. 7.5a) and may cause both the predominantly upward displacement of soil and/or clasts and the size sorting (Fig. 7.5b) of the heterogeneous materials. This complex process is often associated with patterned ground formation (stripes, circles, polygons, earth hummocks) and mass wasting through solifluction and creep (lobes, sheets, terraces). In spring, the melting of segregation ice within the soil causes thaw subsidence of ground surface.

In the Romanian Carpathians, Sîrcu (1976) has described firstly this process, assuming that nowadays this mechanism is no longer active in the alpine domain. Urdea's (2000) measurements performed in the 1986–1987 cold season in Retezat Mountains showed that the ground heaved significantly (approximately 20 mm) between December and March, due to lower than −15 °C temperatures of the external air, high moisture within the soil and more than 40 freeze-thaw cycles. Recent contributions by Urdea et al. (2003, 2010, 2012) revealed that the frost heave associated with earth hummocks in Muntele Mic Massif (1759 m; 45°22′N, 22°28′E) has higher amplitudes than the heave of the flat terrain nearby (Fig. 7.6a). This finding was explained by the higher efficiency of freezing within the investigated frost-induced mound, compared with the flat terrain (Urdea et al. 2003; Onaca 2013).

Earth hummocks are miniature cryogenic mounds (Grab 2005a) which may occur in permafrost-free periglacial environments, such as the alpine zones. These features represent widespread phenomena in the arctic and subarctic lowlands too and were classified as non-sorted patterned ground. In the Muntele Mic Massif, a

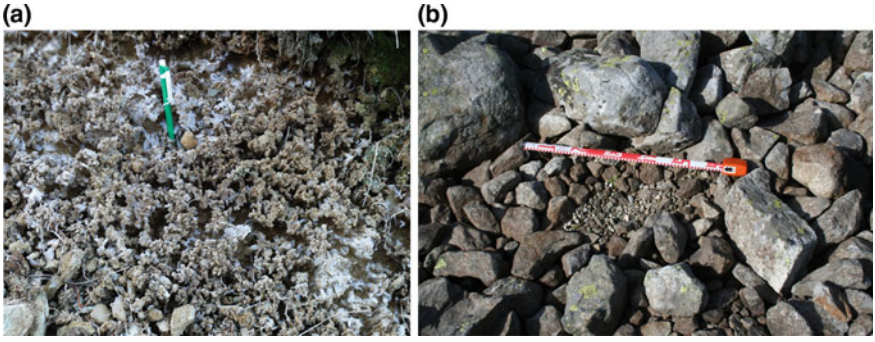

Fig. 7.5 Needle ice and consequent uplift of pebbles in Țarcu Mountains (**a**) and frost sorting on the shore of Ana Lake in the Retezat Mountains (**b**)

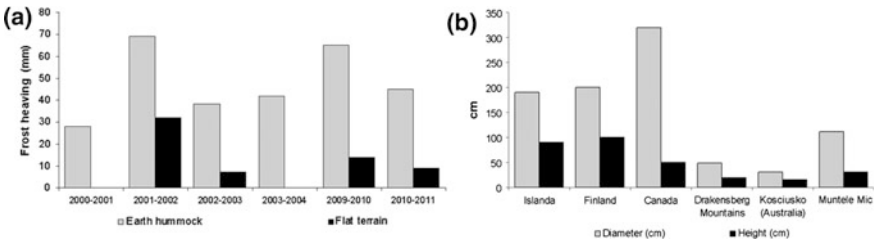

Fig. 7.6 Main parameters of earth hummocks; **a** annual frost heaving rates recorded in Muntele Mic Massif (*data source* Urdea et al. 2003; Onaca 2013) and **b** dimensions around the world (*source of the data* Gerrard 1992; Seppälä 1998; Tarnocai and Zoltai 1978; Grab 1998; Costin and Wimbush 1973; Onaca 2013)

survey of 100 periglacial hummocks was undertaken, revealing that the majority of the mounds are elongated to the north. In the Harghita Mountains, the described mounds range between 15 and 50 cm in height and between 30 and 60 cm in diameter and have a spatial density of 60–65 hummocks/100 m^2 (Schreiber 1994). Their height and diameter are considerably smaller than the corresponding of similar landforms in Scandinavia or Canada, but greater than reported findings in South Africa or Australia (Fig. 7.6b).

Due to particular textural characteristics, the higher moisture within the earth hummocks allows a longer and deeper seasonal frost. Local differences in surface conditions (soil physical characteristics, snow cover depth and duration, vegetation, slope, aspect, etc.) may also produce significant differences in the pattern of seasonal ice lenses formation. The temperatures recorded within the earth hummock at different depths suggest that the intensity of frost heave mainly depends on the soil moisture content, rather than the number of freeze-thaw cycles. Significant differences were noted between the ground thermal regime within the earth hummock and the flat terrain in the 2010–2011 cold season (Onaca 2013) (Table 7.3). Based on both ground temperature records and geophysical investigations, we found that the complete disappearance of ice occurs approximately at the middle of May. The

Table 7.3 Characteristics of the ground thermal regime (°C) of earth hummock (EH) (1759 m) and flat terrain (FT) (1777 m) in Muntele Mic at different depths in 2010–2011 season

Depths	10 cm		20 cm		30 cm		40 cm	
Site	EH	FT	EH	FT	EH	FT	EH	FT
Mean annual ground temperature	5.1	5.1	5	5.2	4.9	5.3	4.8	5.2
Mean winter temperature	−0.6	0.1	0	0.6	0.2	1.1	0.7	1.2
Days with temperature below 0 °C	152	88	116	0	110	0	0	0
No. of freeze-thaw cycles	17	11	4	–	4	–	–	–
Ground freezing index (GFI)	−147	−18	−70	–	-23	–	–	–
First day with negative temperatures	27.11	3.01	3.01	–	26.01	–	–	–
Last day with negative temperatures	26.04	2.04	28.04	–	11.05	–	–	–

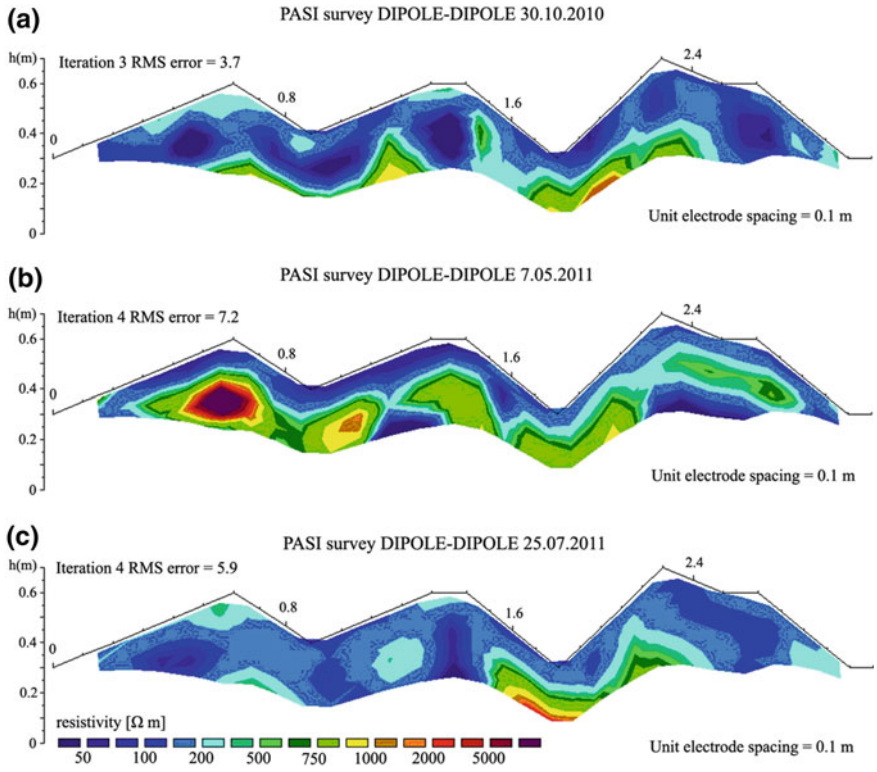

Fig. 7.7 The 2-D geoelectric sections of earth hummocks in the Muntele Mic Massif at different dates during 2010–2011 season (date of investigation: (**a**) 30.10.2010, (**b**) 7.05.2011 and (**c**) 25.07.2011). The *red colour* in the middle picture indicates a patch of frozen materials recorded on 7 May 2011 (Onaca 2013)

frozen soil starts to thaw from the surface beginning with the second part of April but, at 30 cm deep, the ice lenses could maintain for 2–3 weeks more (Table 7.3). The 2-D resistivity profiling was used to assess the changing physical properties of the subsurface material, in case of three neighbour mounds. In Figs. 7.7a, c the resistivity values suggest that the subsurface is unfrozen, whereas in Fig. 7.7b a frozen core is visible within the left mound as revealed by very high resistivity values (>5 kΩm), whereas the surrounding area was completely thawed.

Recently, the aspect controlled temperature variations on the north and south flanks of the mounds was analysed (Onaca 2013). The recordings showed that the miniature mound remained frozen for a longer period (for 5 days more) on its northern aspect compared with its southern aspect. Based on this finding we assume that on the northern flank of the hummock both the ice segregation development and frost heave amplitudes are higher. This could explain why the majority of the mounds from Muntele Mic site are elongated in a northerly direction, irrespective of slope orientation. According to Grab (2005b) the tendency of hummocks to elongate

Table 7.4 Frost heave annual rates recorded in various periglacial environments

Region	Total heave, per year (cm)	Source
Alaska	1–20	Romanovsky et al. (2008)
Colorado Front Range	25–29.5	Fahey (1973)
Alberta Rockies	2–4.5	Smith (1987)
Tibet Plateau	4.3-7.7	Wang and French (1995)
Muntele Mic	0.28–0.69	Onaca (2013)

in a particular direction, could be explained by the coalescence of closely spaced mounds. The elongation is enhanced on the northern aspect of the hummocks where, due to topographic shading, the freeze intensity is higher (Onaca 2013). Compared with other cold, but non-glacial regions of the world, the annual frost heave measured in Muntele Mic Massif revealed considerably lower values (Tables 7.4).

Solifluction

Since solifluction-derived landforms and deposits occur in a wide climatic range (in regions with MAAT from +7 to −20 °C) (Matsuoka 2011), these features have a widespread distribution on the alpine slopes of the Romanian Carpathians, too. The slow downslope soil movement indicate only the occurrence of freeze-thaw action (Ballantyne and Harris 1994), regardless the presence of permafrost. The process operates with high efficiency in moist fine-grained soils, involving the cumulative action of frost creep, needle ice creep and gelifluction, whereas plug-like flow is restricted only to slopes underlain by permafrost (Matsuoka 2001).

In the alpine domain of the Romanain Carpathians this process could be considered the dominant mechanism of sediment transport (Onaca 2013). Solifluction features show a range of morphologies in the alpine environment of the Romanian Carpathians, such as: lobes, benches, terraces, sheets, streams and ploughing boulders (Fig. 7.8). The recent measurements performed in the Southern Carpathians revealed surface displacement rates ranging from several millimetres to tens of millimetres per year (Urdea 2000; Onaca 2013). According to Matsuoka (2001), the rates of surface displacements strongly depend on climate, hydrology, geology and topography. As a result, a great variety of surface velocities were reported from different mid-latitude or tropical mountain ranges (Fig. 7.9).

The displacements measured at the surface of 19 solifluction lobes in Făgăraș, Iezer, Cindrel, Muntele Mic, Parâng and Șureanu during one season (2013–2014) confirm the low rates (between 3.6 and 39.3 mm year^{-1}) of slow dynamics in the alpine environment of the Southern Carpathians. Recent contributions (Onaca 2013) revealed that the greatest deformations occur at 20 cm depth in case of a turf-banked solifluction lobe in Făgăraș Mountains (2380 m; 45°35′N, 24°36′E). Due to strong lateral heterogeneity of surface characteristics and microtopography,

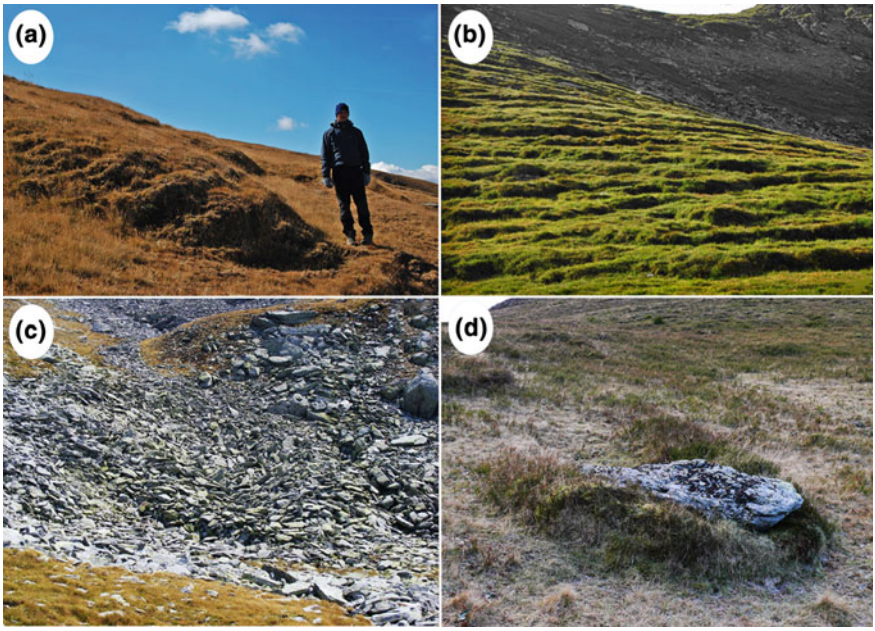

Fig. 7.8 Solifluction landforms in Southern Carpathians: **a** turf-banked solifluction lobe in Cindrel Moutains (45°34′ N, 23°46′E); **b** turf-banked terraces in Făgăraș Mountains (45°35′N, 24° 36′E; **c** stone-banked lobe in Parâng Mountains (45°21′N, 23°31′E); **d** ploughing boulder in Țarcu Mountains (45°20′N, 22°39′E)

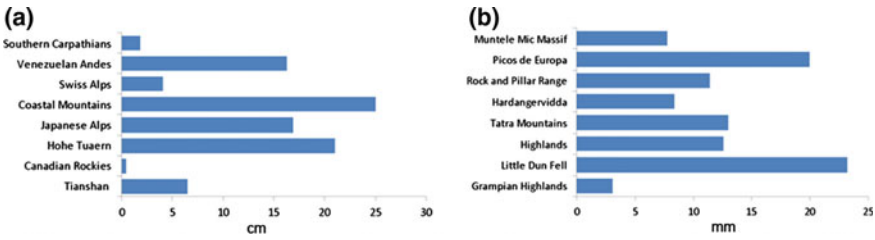

Fig. 7.9 Comparison of the velocity rates of solifluction landforms from Southern Carpathians and other alpine areas; **a** Surface velocity (cm year^{-1}) of solifluction features in mid-latitude to tropical mountains (*data source* Pérez 1987; Gamper 1983; Mackay and Mathews 1974; Matsuoka 1998; Jaesche et al. 1997; Smith 1988, 1992; Gorbunov and Seversky 1999). **b** Measured velocity rates (mm year^{-1}) of ploughing boulders (*data source* Onaca 2013; Serrano et al. 2011; Grab et al. 2008; Berthling et al. 2001a; Kotarba 1976; Ballantyne 2001; Tufnell 1972, 1976; Chattopadhyay 1983)

significant variations in the displacement rates occur. Our observations confirm that the surface velocity of few stakes stacked in a solifluction lobe range between <1 cm and 15 cm per year. In Șureanu Mountains, the measurements revealed that higher displacements characterise the lower part of the solifluction lobes where

more freeze-thaw cycles were recorded, compared with the upslope part of a 20 m long solifluction lobe (Onaca 2013).

The importance of ground temperature regime on the active frost-induced processes has been widely described (Hoelzle et al. 1999). It is well known that in areas with seasonal frost, the most favourable period for solifluction movements is during the snowmelt season (Matsuoka 2005). To capture the relationships between ground freezing and solifluction movements a combined study of both surface motion and thermal ground conditions was recently started. On 12 August 2013, miniature thermistors were installed within three active turf-banked solifluction lobes in Făgăraș (F1: 2380 m; 45°35′N, 24°36′E) and Cindrel (C1: 2119 m, 45°35′N, 23°47′E; C2: 2116 m, 45°34′N, 23°46′E) Mountains at different depths to record temperature values every 4 h (Table 7.5). The measurements reveal that in all the cases a frozen layer of at least 50 cm thick began to develop between November and January. The frozen layer persisted until June 2014, maintaining for around 130–200 days/season. In contrast to other sites in Southern Carpathians where the ground surface temperature (GST) regime was observed in different seasons (Onaca 2013), we noticed the almost complete absence of daily freeze-thaw cycles at these sites. In case of C2 site there was a greater number of days with negative temperatures at 50 cm depth, than at 5 cm depth since the first frost was strong enough to penetrate deep into the ground, and the thawing of the soil occurred at 50 cm one month later than at 5 cm depth. Considering the short-term variation of thermal regime during the winter we assume that the snow depth was not thick enough here to insulate the soil and to prevent further penetration of the freezing front. Since C2 lobe was extremely rocky compared with the other two, the differential thermal conductivity of the clasts and surrounding soils would have enhanced the ice lens growth beneath these boulders.

To establish possible controls on surface velocity of the turf-banked solifluction lobes, we performed bivariate statistics and one-way analysis of variance (ANOVA) on one season (2013–2014) movement rates of 19 solifluction lobes from Southern Carpathians against possible controlling factors, such as: lobes dimensions, tread and riser angle, altitude, slope, azimuth and texture. For variables without a normal distribution (Shapiro–Wilk and Kolmogorov–Smirnov tests) a logarithmic in base 10 transformation was applied for achieving the normal distributions.

The Pearson correlation coefficients revealed significant negative relationships of the lobes surface velocity with altitude and slope (Table 7.6). These relationships are explained in a proportion of 20–42 % by these variables. Significant correlations were observed also between lobes tread angle and riser angle and altitude, slope and coarse material content. These relationships are explained in a proportion of 25–66 %. Additionally, it appears that the length of the solifluction lobes increases when the amount of coarse particles decreases. ANOVA and post hoc tests revealed significant differences in the length, altitude, slope, riser angle and tread angle between the lobes facing N, S and W direction. Significant differences in the lobes surface velocity between S and NW slopes were also observed.

Following the procedures of Hugenholtz and Lewkowicz (2002), we measured the main morphometric characteristics of 69 turf-banked lobes from six different

Table 7.5 Ground thermal regime at different depths in case of three solifluction lobes in Southern Carpathians

Depths	5 cm			10 cm			20 cm			50 cm		
Site	F1	C1	C2	F1	C1	C2	F1	C1	C2	F1	C1	C2
MAGT	2.17	2.77	2.29	2.81	2.26	2.26	2.34	2.71	2.21	2.37	2.62	1.48
Winter temperature	−1.23	−2.05	−3.40	−0.92	−1.56	−3.32	−0.53	−0.98	−3.25	0.13	−0.10	−2.28
Days with $T \leq 0$ °C	201	154	136	196	127	136	183	162	148	144	160	195
Daily freeze-thaw cycles	1	1	1	1	0	0	0	0	0	0	0	0
GFI	−153	−239	−365	−104	−185	−354	−65	−133	−351	−13	−55	−378
First day with $T \leq 0$ °C	11/15/2013	11/18/2013	11/18/2013	11/17/2013	11/30/2013	11/23/2013	11/20/2013	12/7/2013	11/22/2013	1/8/2014	12/31/2013	11/18/2013
Last day with $T \leq 0$ °C	6/5/2014	5/17/2014	5/13/2014	6/5/2014	5/17/2014	5/23/2014	6/5/2014	5/19/2014	5/24/2014	6/20/2014	6/11/2014	6/2/2014

Table 7.6 Correlation coefficients and coefficient of determination R^2 (in brackets) between variables which are significant correlated at the 0.05 level

	Altitude (m)	Slope (°)	Coarse material[a] (>2 mm)	Fine material[a] (<2 mm)	Riser angle (°)	Tread angle (°)	Surface velocity (mm/year)	Length (m)
Riser angle (°)	0.511 (0.261)	0.496 (0.246)	–	–	–	–	–	–
Tread angle (°)	0.543 (0.294)	0.766 (0.587)	0.818 (0.668)	−0.804 (0.647)	0.774 (0.600)	–	–	–
Surface velocity	−0.507 (0.200)	−0.591 (0.419)	–	–	–	–	–	–
Length	–	–	−0.789 (0.622)	–	–	–	–	–

[a]Sediments were collected from turf-banked solifluction lobes at 20 cm depth. Sediments were dried, weighed and sieved with a 2 mm mesh size. Sediments weight for both classes are expressed in percentages

– No correlation

mountain ranges: Făgăraş, Iezer, Cindrel, Muntele Mic, Parâng, Şureanu. In addition, the mean velocity and soil grain size were determined (Table 7.7). The average values of turf-banked lobes morphometric characteristics from Southern Carpathians revealed smaller landforms, but with greater angles of riser and tread than reported in Scandinavia (Ridefelt and Boelhouwers 2006), or Canada (Hugenholtz and Lewkowicz 2002).

The analysis reveals that complex processes are involved in the evolution and downslope movement of solifluction lobes, resulting from the interaction of multiple factors (e.g. topographic, climatic, soil moisture, uppermost layer texture, snow cover, freeze-thaw action, vegetation cover etc.).

Ploughing Blocks

Ploughing blocks are mass wasting features (Tufnell 1972) widespread on vegetation covered slopes in the alpine domain of the Romanian Carpathians (Fig. 7.8d). The large clasts move downslope faster than their surroundings (Washburn 1973) and form a characteristic microrelief, consisting in a marked furrow upslope behind the block and a mound on the downslope side of the boulders (Chattopadhyay 1983). These small-scale landforms are considered reliable indicators of the lower limit of the current periglacial activity and usually their distribution corresponds to that of active solifluction sheets and lobes (Ballantyne 2001). Gelifluction, frost creep and frost heave (Berthling et al. 2001b; Ballantyne 2001) are the processes involved in the mechanism of ploughing boulder movement.

In Romania, they were reported in different mountain ranges in the Southern Carpathians (Niculescu and Nedelcu 1961), between 1600 m and nearly the highest elevations in Retezat (Urdea 2000), Parâng (Iancu 1961; Urdea and Vuia 2000; Onaca 2013), Şureanu (Urdea and Drăguţ 2000), Făgăraş (Florea 1998; Urdea et al. 2010; Onaca 2013), Ţarcu (Niculescu and Nedelcu 1961), Lotru (Onaca 2013), Godeanu (Niculescu 1965) and Leaota (Murătoreanu 2009). In the Eastern Carpathians, the presence of the ploughing blocks was reported in the Rodnei Mountains by Donisă (1968) and Sîrcu (1978) and in the Rarău Massif by Rusu (2002). In the majority of these studies, the authors focused on the description of the morphology of these features and little attention was paid to the analysis of the environmental factors controlling the movement of the ploughing blocks. Urdea (1989) performed the first measurements on the downslope movement of ploughing boulders in Retezat, whereas over the last few years the authors started to monitor the recent activity of ploughing blocks at several sites in the Southern Carpathians.

For one site (Muntele Mic Massif), measurements of the horizontal movement of the ploughing boulders are available for a period of 12 years (between 2000 and 2012). The downslope displacement rates, for eight of the initial twenty-six boulders monitored, range between 2.3 and 25.8 mm/year, with an annual average downslope displacement of just under 10 mm/year. The movement rates presented

Table 7.7 Main characteristics of turf-banked lobes in Southern Carpathians

Mountain range	Nr.	Mean riser height (cm)	Mean riser angle (°)	Mean tread angle (°)	Mean tread length (m)	Mean tread width (m)	Mean velocity at the surface (mm)/year	Soil grain size (%) >25 cm depth		Textural group
								Coarse >2 mm	Fine <2 mm	
Făgăraş	49	52	62	22	4.9	5.2	14.1	11	89	Fine sand
Iezer	7	47	51	17	4.2	5.7	9.7	23	77	Fine sand
Cindrel	8	35	32	8	5.2	5.2	17.4	12	88	Coarse sand
Muntele Mic	2	45	53	11	3.7	5.4	–	28	72	Fine sand
Parâng	2	32	49	14	10.5	13.5	9	24	76	Fine sand
Şureanu	1	54	39	7	25	7	33	56	44	Coarse sand

Table 7.8 Rates of ploughing blocks downslope movement in Southern Carpathians

Region	Period (years)	No. of boulders	Elevation (m)	Slope	Average rate (mm/year)		
					Min.	Mean	Max.
Făgăraș	1	9	2274–2305	12–25	3.0	11.1	25.0
Parâng	3	11	2149–2181	5–23	2.3	6.6	15.2
Lotru	3	6	2011–2099	14–31	1.6	8.1	17.0
Muntele Mic	2	19	1633–1750	9–29	2.0	10.4	32.0

in this study are comparable with the previous results reported in Scandinavia, Great Britain, Tatra Mountains or New Zeeland (Fig. 7.9b).

Between the monitoring sites, the mean annual displacement rates are highly variable. During the last few years (between 2011 and 2014) the downslope movement of 45 new boulders from Făgăraș, Parâng, Lotru and Țarcu Mountains was monitored, showing mean annual rates between 6 and 11 mm/year (Table 7.8). Thus, our measurements revealed significant interannual displacement variations, such as in other sites (Tufnell 1976; Berthling et al. 2001a). In many cases we observed that boulders located on the same slope, in similar topographical and pedological conditions moved completely different within the same season. For example, in the Muntele Mic site, one boulder moved downslope more rapidly (30 mm/year) compared to others situated nearby, which remained static, or moved slowly (2–5 mm/year). Previous studies assumed that variations in rates of displacements are likely to be controlled by one of the following factors: block size, slope, the depth to which boulders are embedded into the soil (Ballantyne 2001) and snow cover characteristics (Grab et al. 2008) (Table 7.8).

To establish possible controls on the movement rates of ploughing boulders, we performed bivariate statistics and one-way ANOVA on the one season (2013–2014 season) movement rates of 101 boulders from Muntele Mic against possible controlling factors, such as: boulders dimensions and volume, altitude, slope and aspect. Two ploughing blocks with extreme annual movement rates (56 and 104 mm) were considered outliers and removed from the statistical analysis. Considering the relationships between quantitative parameters, ploughing boulders dimensions correlates negatively with altitude and positively with downslope movement, as revealed by the Pearson correlation values (Table 7.9). Thereby, the boulders with large size are situated at lower altitudes and appear to record greater movement rates. Although the positive correlations between boulders dimensions and the downslope movement are statistically significant at $p < 0.05$, the weight of these variables is rather poor, indicating that the downslope movement is explained in a proportion of only 10 % by the boulders size.

ANOVA and post hoc tests (Bonferroni and Tamhane) show statistically significant differences between the dimensions (height and volume) of boulders facing south-east and ones with western orientation. The boulders height and volume are larger on the southern exposed slopes (0.70 m and 3.65 m^3) than the boulders

Table 7.9 Correlation coefficients and coefficient of determination R^2 (in brackets) between variables which are significant correlated at the 0.05 level

	Altitude	Width	Height	Volume
Length	–	–	–	–
Width	−0.267 (0.071)	–	–	–
Height	−0.311 (0.119)	–	–	–
Volume	−0.215 (0.056)	–	–	–
Surface velocity	−0.306 (0.119)	0.230 (0.053)	0.305 (0.093)	0.244 (0.061)

situated on slopes with a north-western (0.43 m and 0.54 m^3), western (0.34 m and 0.65 m^3) or eastern (0.33 m and 0.72 m^3) aspect. Also, the south facing boulders are situated at a lower mean altitude (1620 m) than the boulders with a western (1679 m) or north-western (1690 m) orientation.

Based on these findings we assume that different rates of movement could be strongly controlled by the local pattern of freezing and thawing. In the alpine zone, the ground freezing regime shows extreme spatial variability because of the influence of rugged topography (Onaca 2013). Because variations in surface characteristics, snow cover depth and duration and soil moisture may occur within short distances, as the energy fluxes at the ground surface are often extremely complicated (Ishikawa 2003).

Frost Creep and Other Periglacial Processes

Frost heaving, frost creep and thaw settlement have been attributed to the slow downslope movement of block streams, debris cones, scree slope, stone-banked lobes. Urdea (2000) recorded horizontal motion of individual decimeteric boulders between few cm and 18 cm/year in Retezat Mountains on steep slopes (20–33°). In Rarău Mountains, in 100 cm deep soils, at an altitude of 1350 m and a slope of 25°, the creep of soil and solifluction recorded values of 3–5 cm/year (Rusu 2002). More recently, Onaca (2013) using a high-precision Leica TPS 1200 total station examined the annual rates of movement of six block streams in the Southern Carpathians. The measurements revealed very low annual movement rates in the range of the level of noise of the method (<1 cm). Several boulders recorded displacements of few tens of centimetres or even more, but it was considered that other processes were responsible for this accelerated motion (e.g. snow avalanches, rockfalls). The same conclusion was formulated by Onaca (2013), after analysing extremely heterogeneous annual rates of displacements recorded in case of a debris cone located in the Făgăraș Mountains (2320 m; 45°36′N, 24°37′E). Displacement rates ranging from 1 to >100 mm/year were measured, but in few cases the painted boulders were found at the foot of the slopes, suggesting that wet snow avalanches have transported them downslope (Voiculescu 2004).

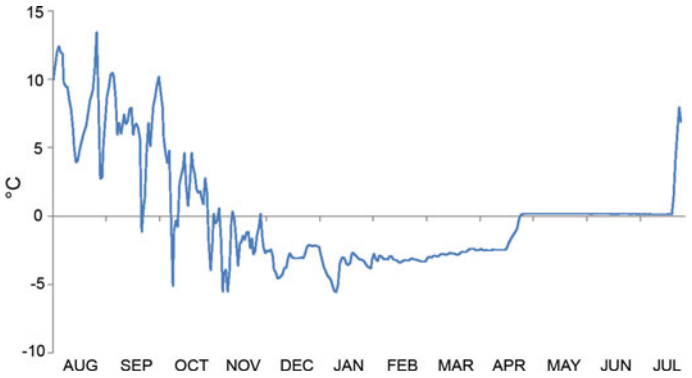

Fig. 7.10 Mean daily ground surface temperature evolution during one season (2012–2013) corresponding to a stone-banked lobe in Parâng Mountains

Annual horizontal displacement rates ranging from 1 to 4 cm were reported by Urdea et al. (2004) for a stone-banked lobe in Parâng Mountains (2380 m) (Fig. 7.7c). Analysing the GST regime of this stone-banked lobe for one season (2012–2013) (Fig. 7.10) we found that, coarse blocks have a cooling influence on ground temperatures compared with fine-grained soils (Juliussen and Humlum 2008). At this site the average GST in the interval without short-term variation (known also as the 'BTS window') was −2.8 °C, whereas the mean annual ground surface temperature (MAGST) was 0 °C, despite that permafrost is unlikely to occur here (Onaca 2013).

Creep of Permafrost

Rock glaciers represent creeping bodies of rock–ice mixture flowing downslope due to deformation of the ice within (Haeberli et al. 2006). A recent inventory (Onaca et al. in press) of the rock glaciers from Southern Carpathians revealed that the vast majority (74 %) of the 306 identified rock glaciers are relict. More than 60 % of all the intact rock glaciers are located in Retezat Mountains, where the mean terminal elevation of intact rock glaciers occurs at 2089 m (Onaca et al. in press).

A recent approach (Necşoiu et al. 2016) based on a combination of optical and radar remote sensing techniques (coherence analysis, correlation analysis and multitemporal InSAR techniques, such as SBAS), allowed the evaluation of the displacement rates of the rock glaciers from the central part of the Retezat Mountains. Due to very thin deforming frozen layers, the velocity of these landforms is very low compared with other active rock glaciers located in other parts of the world. Displacement rates of few centimetres/year were recorded in case of Pietrele, Judele and Valea Rea rock glaciers. The analysis stretched over 46 years, revealing an unexpected increase in the kinematics of the Pietrele rock glacier

between 2007 and 2014, probably as a consequence of consecutive warmer years and higher amount of liquid water within this rock glacier (Delaloye et al. 2008). The study was the first to document also intra-annual/seasonal variations in rock glaciers dynamics with the highest rates of horizontal velocities occurring in late summer and autumn (Necşoiu et al. 2016).

Environmental Control on the Periglacial Phenomena

Mass wasting and frost weathering in the alpine environment of the Romanian Carpathians are strongly controlled by ground freezing, which depends on local factors (ground materials, topography, vegetation cover, snow cover, water content, incoming solar radiation, etc.).

Recent studies have shown that the overall magnitude of the effect of microclimatic, topographic conditions and ground materials on the MAGST in alpine environments can be as high as 15 °C within less than 1 km distance (Haeberli et al. 2010). In similar studies carried out in the Alps, the measured MAGST values showed variations of up to 9 °C (Gubler et al. 2011), or 4.3 °C as revealed by other cases (Rödder and Kneisel 2012). These variations are linked to the main factors controlling the GST regime, which are the incoming solar radiation, the presence or absences of coarse blocks, along with the snow cover characteristics (Brenning et al. 2005; Luetschg et al. 2008). The main problem is that all the controlling factors show a strong lateral heterogeneity, mainly due to variable topography, causing important small-scale variations of GST values (Nelson et al. 1998). Therefore, the reactions to environmental changes are likewise extremely heterogeneous in space, since particular sites where favourable conditions occur are expected to have little or even reverse reaction to air temperature rising, while in other cases, fast and intense reactions are expected (Gisnås et al. 2014).

To fully understand near surface energy exchange fluxes and snow/ground/atmosphere interactions within high mountain regions, accurate determination of the factors controlling the GST regime are needed. Figure 7.11 depicts the temperature regime of the soil at a depth of 5 cm, exhibiting important differences between two turf-banked solifluction lobes, one facing south and the other facing north, located only a few tens of metres away in the Făgăraş Mountains, at 2370 m.

The site of the solifluction lobe facing south was probably snow free or covered by a thin snow cover, since important variation in the GST regime occurred during the winter. Despite that significant interannual changes are expected in relation with the freezing efficiency at these sites, recent measurements confirmed maximum surface displacement rates of more than 20 mm/year in case of the southern exposed site, whereas at the north-facing lobe, the recorded surface motion was below 1 cm/year. Previous studies revealed that certain lithologies are more prone to mechanical weathering and as a consequence the frost action is more productive in regions dominated by frost-susceptible rocks. The inventory of the Southern Carpathian rock glaciers revealed that the uneven distribution of these creeping

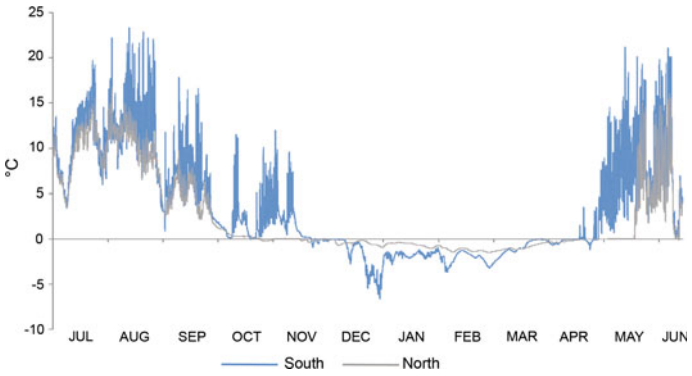

Fig. 7.11 GST evolution during one season (2010–2011) recorded at 5 cm depth in case of two solifluction lobes in the Făgăraș Mountains

permafrost bodies (Haeberli et al. 2006) is determined by topography, lithology and debris availability (Onaca et al. in press). According to Urdea (1998), the lithology seems to have a great influence on the distribution, density, mean size of rock glaciers and the distribution of intact rock glaciers. Thus, the highest values of rock glaciers density are encountered in mountain units where the dominant lithology consists of granodiorites and granites, whereas the rock glaciers developed here are considerably larger and therefore have higher specific areas (Onaca et al. in press). Since large joint spacing occurs frequently in granodiorite and granite intrusive magmatic bodies favouring the production of large boulders (Fig. 7.12), the porosity of rock glaciers from Retezat and Parâng Mountains is considerably higher, allowing air ventilation through the porous material (chimney effect), contributing thus to permafrost preservation (Delaloye and Lambiel 2005). In addition, 77 % of the total intact rock glaciers occur in zones related to granites and granodiorites (Onaca et al. in press).

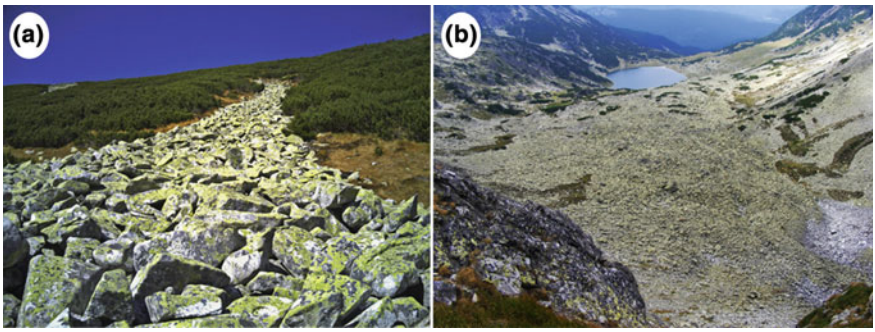

Fig. 7.12 Large granodiorite boulders forming a block stream (**a**) and a rock glacier (**b**) in the Retezat Mountains

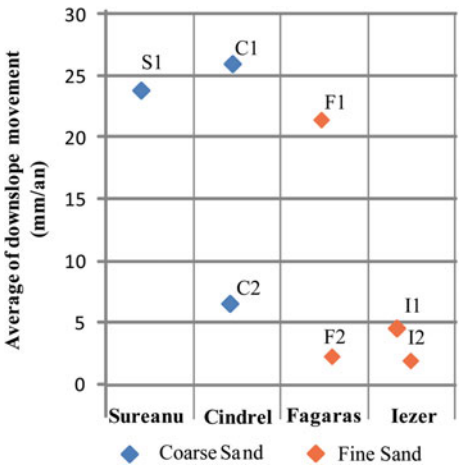

Fig. 7.13 The mean annual downslope movement of solifluction lobes in different materials

Similar results were reported by Şerban et al. (2015) by analysing the largest existing inventory of block streams, consisting in 2056 landforms located within the Retezat–Godeanu mountain group. Thus, the largest block streams occur on granodiorites and granites (Fig. 7.12a), whereas at sites where weak rocks, which disintegrate into fine and platy debris (paragneisses, schists, sandstones occur), the size of block streams is considerably smaller.

In a similar manner, in finer-grained materials the rate at which soil freezes is dependent upon its physical characteristics, such as: size of particles, thermal conductivity, moisture content, density, porosity, etc. The most frost-susceptible soils are considered coarse silts with more than 50 % of particles smaller than 0.2 mm, more than 12 % of grains smaller than 0.02 mm and not more than 40 % of particles smaller than 0.002 mm (Knutson 1993). Our recent analysis showed that in case of coarse sands the movement of solifluction lobes is slightly greater than in fine sands (Fig. 7.13).

The distribution of both rock glaciers and block streams has proved to be strongly controlled by slope orientation. Thus, the southern quadrant (59 %) was more preferred for block streams formation than the northern quadrant (18.5 %). Additionally, the longest block streams occur on slopes facing south, whereas on northern slopes the rock streams are extremely short. Based on this observation, it appears that these landforms developed in the Lateglacial, when most of the northern slopes were still occupied by glaciers, whereas the majority of the southern flanks were free of ice. In contrast, in case of Southern Carpathians rock glaciers, more than half of them face north, north-east and east, whereas only 9 from a total of 306 face south (Onaca et al. in press). Talus derived rock glaciers seem to be more evenly distributed across aspect categories, since their distribution is mainly controlled by the debris availability. In contrast, debris rock glaciers are the typical expression of aspect-dependent landforms, since they originate from the last glaciers that survived during the Late Glacial in northern exposed valleys (Onaca et al. in press).

Concluding Remarks: Towards Improving the Understanding of the Present-Day Periglacial Processes in the Romanian Carpathians

High mountain systems are among the environments most sensitive to global climatic changes, reacting rapidly to air temperature rising (Kääb et al. 2005). The modifications induced by contemporary atmosphere warming generates irreversible changes in the dynamic of the ecosystems and in the local hydrological system (Jorgenson et al. 2006). The current results have confirmed that freeze-thaw driven processes have a relatively low intensity nowadays. Therefore, current periglacial processes are mainly limited to the remodelling of landforms within the alpine environment, rarely leading to the initiation of new landforms. Within the current climate warming conditions, the intensity of periglacial processes will most probably decline, leading to severe ecological changes above the alpine timberline.

Unfortunately, our understanding of the alpine environment and its vulnerability to global changes is still very limited for at least two main reasons: (i) the high complexity of the relations between the elements which compound these geosystems and (ii) the high spatial variability of the conditions and factors controlling the energy balance at the ground surface.

Thus, for a better understanding of the behaviour of the current frost-induced processes in the Romanian Carpathians, and the changes induced by air temperature rising in alpine environments, it is outmost important to:

- continue the monitoring of the periglacial processes and to extend the field monitoring to other processes, such as the poorly understood disintegration of exposed rocks, by either mechanical or biochemical processes.
- perform the monitoring using high resolution techniques (e.g. InSAR, Terrestrial Laser Scanner, Structure for Motion, etc.) to capture the current reduced dynamic of periglacial processes, since the displacement rates are in most of the cases extremely small;
- gain more insight on the relation between the controlling factors and the periglacial processes. We have to improve our understanding of the role of soil moisture, snow cover, surface characteristics (e.g. soil texture, thermal conductivity of materials, etc.) and vegetation on periglacial processes;
- increase our knowledge concerning the interaction between frost action, periglacial processes and periglacial landforms. The periglacial morphology within the Romanian Carpathians is not fully known; therefore, inventories of specific frost-derived landforms would be extremely useful in order to assess the impact of the environmental variables on the spatial distribution of landforms. Since these landforms are valuable diagnostic features for past and present environmental conditions, their spatial distribution is an extremely effective way to model the past and present amplitude of periglaciation;
- better understand the azonal processes in the alpine environment associated with wind, snow and running water. There is a lack of studies concerning the

geomorphic impact of snow avalanches, debris flows, wind abrasion and deflation or gully erosion in the alpine environment of the Romanian Carpathians;
– examine the reaction of these processes to a warming climate and to model future changes in periglacial activity in the Romanian Carpathians.

Acknowledgements This work has been supported from the strategic grant POSDRU/159/1.5/S/133391, Project "Doctoral and Post-doctoral programs of excellence for highly qualified human resources training for research in the field of Life sciences, Environment and Earth Science" cofinanced by the European Social Fund within the Sectorial Operational Program Human Resources Development 2007–2013.

References

Anisimov OA, Nelson FE (1996) Permafrost distribution in the Northern Hemisphere under scenarios of climatic change. Global Planet Change 14(1):59–72

Ardelean AC (2015) Cuantificarea bugetului de sedimente și determinarea ratelor de denudație în Valea Doamnei, Munții Făgăraș. Unpublished PhD Thesis, Universitatea de Vest Timișoara (in Romanian)

Ballantyne CK (2001) Measurement and theory of ploughing boulder movement. Permafrost Periglac Process 12:267–288

Ballantyne CK (2002) Paraglacial geomorphology. Quatern Sci Rev 21:1935–2017

Ballantyne CK (2003) Paraglacial landform succession and sediment storage in deglaciated mountain valleys: theory and approaches to calibration. Zeitschrift für Geomorphologie Suppl. 132:1–18

Ballantyne CK, Harris C (1994) The Periglacial of Great Britain. Cambridge University Press, Cambridge

Bălteanu D, Posea G (1983) Procese actuale de modelare a reliefului. In: Geografia României, I, Geografia fizică. Edit. Academiei, Bucureşti, pp 171–181 (in Romanian)

Barsch D (1993) Periglacial geomorphology în the 21st century. Geomorphology 7:141–163

Berthling I, Eiken T, Madsen H, Sollid JL (2001a) Downslope displacement rates of ploughing boulders in a mid-alpine environment: Finse, southern Norway. Geografiska Annaller 83A (3):103–116

Berthling I, Eiken T, Sollid JL (2001b) Frost heave and thaw consolidation of ploughing boulders in a mid-alpine environment, Finse, southern Norway. Permafrost Periglac Process 12:165–177

Brenning A, Gruber S, Hoelzle M (2005) Sampling and statistical analyses of BTS measurements. Permafrost Periglac Process 16:383–393

Caine N (1974) The geomorphic processes of the alpine environment. In: Ives JD, Barry RG (eds) Arctic and Alpine environments. Methuen, London, pp 721–748

Chattopadhyay GP (1983) Ploughing blocks on the Drumochter Hills in the Grampian Highlands, Scotland: a quantitative report. Geogr J 149(2):211–215

Costin AB, Wimbush DJ (1973) Frost cracks and earth hummocks at Kosciusko, Snowy Mountains, Australia. Arct Alp Res 5:111–120

Dadson SJ, Church M (2005) Postglacial topographic evolution of glaciated valleys: a stochastic landscape evolution model. Earth Surf Proc Land 30:1387–1403

Davies MC, Hamza O, Harris C (2001) The effect of rise in mean annual temperature on the stability of rock slopes containing ice-filled discontinuities. Permafrost Periglac Process 12:137–144

Delaloye R, Lambiel C (2005) Evidence of winter ascending air circulation throughout talus slopes and rock glaciers situated in the lower belt of alpine discontinuous permafrost (Swiss Alps). Norsk Geografisk Tidsskrift-Norwegian J Geogr 59:194–203

Delaloye R, Perruchoud E, Avian M, Kaufmann V, Bodin X, Hausmann H, Ikeda A, Kääb A, Kellerer-Pirklbauer A, Krainer K, Lambiel C, Mihajlovic D, Staub B, Roer I, Thibert E (2008) Recent interannual variations of rock glacier creep in the European Alps. In: Kane DL, Hinkel KM (eds) Proceedings of the 9th international conference on permafrost, June 29–July 3, 2008, Fairbanks, Alaska, 1, pp 343–348

Donisă I (1968) Geomorfologia Văii Bistriței. Editura Academiei Republicii Socialiste România (in Romanian)

Fahey BD (1973) An analysis of diurnal freeze–thaw and frost heave cycles in the Indian Peaks region of the Colorado Front Range. Arct Alp Res 5:269–281

Florea M (1998) Munţii Făgăraşului. Studiu geomorfologic, Edit. Foton, Braşov (in Romanian)

French HM (2000) Does Lozinski's periglacial realm exist today? A discussion relevant to modern usage of the term 'periglacial'. Permafrost Periglac Process 11:35–42

French HM (2007) The periglacial environment, 3rd edn. Wiley, Chichester

Gamper WM (1983) Controls and rates of movement of solifluction lobes in the eastern Swiss Alps. In: Proceedings of the 4th international conference permafrost (Fairbanks, Alaska). Natl. Acad. Sci., Washington, DC pp 433–438

Gerrard AJ (1992) The nature and geomorphological relationships of earth hummocks (thufur) in Iceland. Zeitschrift für Geomorphologie Supplement Bd 86:173–182

Gisnås K, Westermann S, Schuler T, Litherland T, Isaksen K, Boike J, Etzelmüller B (2014) A statistical approach to represent small-scale variability of permafrost temperatures due to snow cover. The Cryosphere 8:509–536

Gorbunov AP, Seversky EV (1999) Solifluction in the mountains of Central Asia: distribution, morphology, processes. Permafrost Periglac Process 10:81–89

Grab SW (1998) Non-sorted patterned ground in the high Drakensberg, southern Africa: some new data. Geogr J 164:19–31

Grab S (2005a) Aspects of the geomorphology, genesis and environmental significance of earth hummocks (thúfur, pounus): miniature cryogenic mounds. Prog Phys Geogr 29(2):139–155

Grab S (2005b) Eath hummocks (thufur): new insights to their thermal characteristics and development in eastern Southern Lesotho, southern Africa. Earth Surf Proc Land 30:541–555

Grab SW, Dickinson KJM, Mark AF, Maegli T (2008) Ploughing boulders on the Rock and Pillar Range, south-central New Zeeland: their geomorphology and alpine plant associations. J R Soc NZ 38(1):51–70

Gubler S, Fiddes J, Gruber S, Keller M (2011) Scale-dependent measurement and analysis of ground surface temperature variability in alpine terrain. The Cryosphere Discussions 5:307–338

Haeberli W, Hallet B, Arenson L, Elconin R, Humlum O, Kääb A, Kaufmann V, Ladanyi B, Matsuoka N, Springman S, Vonder Mühll D (2006) Permafrost creep and rock glacier dynamics. Permafrost Periglac Process 17:189–214. doi:10.1002/ppp.561

Haeberli W, Noetzli J, Arenson L, Delaloye R, Gärtner-Roer I, Gruber S, Isaksen K, Kneisel C, Krautblatter M, Phillips M (2010) Mountain permafrost: development and challenges of a young research field. J Glaciol 56:1043–1058

Harbor J, Warburton J (1993) Relative rates of glacial and nonglacial erosion in alpine environments. Arct Alp Res 25:1–7

Harris SA, French HM, Heginbottom JA, Johnston GH, Ladanyi B, Sego DC, van Everdingen RO (1988) Glossary of permafrost and related ground-ice terms. National Research Council of Canada, Ottawa

Hoelzle M, Wegmann M, Krummenacher B (1999) Miniature temperature dataloggers for mapping and monitoring of permafrost in high mountain areas: first experience from the Swiss Alps. Permafrost Periglac Process 10:113–124

Hugenholtz CH, Lewkowicz AG (2002) Morphometry and environmental characteristics of turf-banked solifluction lobes, Kluane Range, Yukon Territory, Canada. Permafrost Periglac Process 13:301–313
Iancu S (1961) Elemente periglaciare în masivul Parângului. Probleme de geografie, vol VIII, pp 191–203 (in Romanian)
Ielenicz I (1984) Munţii Ciucaş-Buzău. Studiu geomorfologic. Edit, Academiei, Bucureşti (in Romanian)
Ishikawa M (2003) Thermal regime at the snow–ground interface and their implications for permafrost investigation. Geomorphology 52:105–120
Jaesche P, Veit H, Stingl H, Huwe B (1997) Influence of water and heat dynamics on solifluction movements in a periglacial environment in the Eastern Alps (Austria). In: Iskandar IK (ed) Proceedings international symposium, physics, chemistry and ecology of seasonally frozen soils (Fairbanks, Alaska). CREL Spec. Rep pp 80–86
Jorgenson MT, Shur YL, Pullman ER (2006) Abrupt increase in permafrost degradation in Arctic Alaska. Geophys Res Lett 33:L02503
Juliussen H, Humlum O (2008) Thermal regime of openwork block fields on the mountains Elgåhogna and Sølen, central-eastern Norway. Permafrost Periglac Process 19:1–18
Kääb A, Reynolds J, Haeberli W (2005) Glacier and permafrost hazards in high mountains. In: Huber U, Bugmann HM, Reasoner M (eds) Global change and mountain regions. Springer, Dordrecht p, pp 225–234
Knutson A (1993) Frost action in soils. Norwegian Road Research Laboratory, Oslo
Kotarba A (1976) Wspólczesne modelowanie weglanowych stoków wysokogórskich (The role of morphogenetic processes in modelling high mountain slopes). Instytut Geografii i Przestrzennego Zagospodarowania. Prace Geograficzne, Polska Akademia Nauk, pp 120–128
Lesenciuc C-D (2006) Masivul Giumalău. Edit, TehnoPress, Iaşi (in Romanian), Studiu geomorfologic
Łoziński MW (1909) Über die mechanische Verwitterung der Sandsteine im gemässigten Klima. Acad Sci Cracovie Bull Internat Cl Sci Math et Nat 1:1–25
Luetschg M, Lehning M, Haeberli W (2008) A sensitivity study of factors influencing warm/thin permafrost in the Swiss Alps. J Glaciol 54:696–704
Mackay JR, Mathews WE (1974) Movement of sorted stripes, the cinder cone, Garibaldi Park, BC, Canada. Arct Alp Res 6:347–359
Matsuoka N (1998) Modelling frost creep rates in an alpine environment. Permafrost Periglac Process 9:121–133
Matsuoka N (2001) Solifluction rates, processes and landforms: a global review. Earth Sci Rev 55:107–133
Matsuoka N (2005) Temporal and spatial variations in periglacial soil movements on alpine crest slopes. Earth Surf Proc Land 30(1):41–58
Matsuoka N (2011) Climate and material controls on periglacial soil processes: toward improving periglacial climate indicators. Quatern Res 75:356–365
Micalevich-Velcea V (1961) Masivul Bucegi. Studiu geomorfologic. Edit, Academiei, Bucureşti (in Romanian)
Murătoreanu G (2009) Munţii Leaota. Studiu de geomorfologie. Edit, Transversal, Târgovişte (in Romanian)
Necşoiu M, Onaca A, Wigginton S, Urdea P (2016) Rock glacier dynamics in Southern Carpathian Mountains from high-resolution optical and multi-temporal SAR satellite imagery. Remote Sens Environ 177:21–36
Nedelcu E (1964) Sur la cryo-nivation actuelle dans les Carpates Méridionales entre les rivieres Ialomiţa et Olt. Rev. roum. géol., géophys., géogr. Géographie 8:121–128
Nelson F, Hinkel K, Shiklomanov N, Mueller G, Miller L, Walker D (1998) Active-layer thickness in north central Alaska: systematic sampling, scale and spatial autocorrelation. J Geophys Res Atmos (1984–2012) 103:28963–28973
Niculescu G (1965) Munţii Godeanu. Studiu geomorfologic. Edit, Academiei, Bucureşti (in Romanian)

Niculescu G, Nedelcu E (1961) Contribuţii la studiul microreliefului crionival din zona înaltă a munţilor Retezat–Godeanu–Ţarcu şi Făgăraş–Iezer. Probleme de geografie VIII:87–121
Onaca A (2013) Procese şi forme periglaciare din Carpaţii Meridionali. Abordare geomorfologică şi geofizică [Periglacial processes and landforms from the Southern Carpathians. A geomorphological and geophisical approach]. Unipublished PhD Thesis, Universitatea de Vest Timişoara, Romania (in Romanian)
Onaca A, Urdea P, Ardelean A (2013a) Internal structure and permafrost characteristics of the rock glaciers of Southern Carpathians (Romania) assessed by geoelectrical soundings and thermal monitoring. Geografiska Annaler, Series A, Phys Geogr 95(3):249–266
Onaca A, Urdea P, Ardelean A, Şerban R (2013b) Assessment of internal structure of periglacial landforms from Southern Carpathians (Romania) using DC resistivity tomography. Carpathian J Earth Environ Sci 8(2):113–122
Onaca A, Ardelean F, Urdea P, Magori B (in press) Southern Carpathian rock glaciers: Inventory, distribution and environmental controlling factors. Geomorphology
Otto JC (2006) Paraglacial sediment storage quantification in the Turtmann Valley, Swiss Alps. Unpublished PhD Thesis., Rheinischen Friedrich-Wilhelms-Universität Bonn, Germany
Otto JC, Schrott L, Jaboyedoff M, Dikau R (2009) Quantifying sediment storage in a high alpine valley (Turtmanntal, Switzerland). Earth Surf Proc Land 34:1726–1742
Penner E (1986) Aspects of ice lens growth in soils. Cold Reg Sci Technol 13:91–100
Pérez FL (1987) Downslope stone transport by needle ice in a High Andean area (Venezuela). Rev Geomorphol Dyn 36:33–51
Popescu R, Vespremeanu-Stroe A, Onaca A, Cruceru N (2015) Permafrost research in the granitic massifs of Southern Carpathians (Parâng Mountains). Zeitschrift für Geomorphologie 59(1):1–20
Posea G, Popescu N, Ielenicz M (1974) Relieful României. Edit, Ştiinţifică, Bucureşti (in Romanian)
Puţan R (2015) Analiza unor procese şi forme periglaciare din bazinul superior al văii Capra din Munţii Făgăraş. Unpublised PhD Thesis, Universitatea de Vest din Timişoara, Romania (in Romanian)
Ridefelt H, Boelhouwers J (2006) Observations on regional variation in solifluction landform morphology and environment in the Abisko Region, Northern Sweden. Permafrost Periglac Process 17:253–266
Rödder T, Kneisel C (2012) Influence of snow cover and grain size on the ground thermal regime in the discontinuous permafrost zone, Swiss Alps. Geomorphology 175:176–189
Romanovsky VE, Marchenko SS, Daanen R, Sergeev DO, Walker DA (2008) Soil climate and frost heave along the permafrost/ecological North American arctic transect. In: Kane DL, Hinkel K (eds) Ninth international conference on permafrost. Institute of Northern Engineering, University of Alaska, Fairbanks, pp 1519–1525
Rusu C (2002) Masivul Rarău. Studiu de geografie fizică. Edit, Academiei Române, Bucureşti (in Romanian)
Schreiber WE (1994) Munţii Harghita. Studiu geomorfologic. Edit, Academiei, Bucureşti (in Romanian)
Schrott L, Adams T (2002) Quantifying sediment storage and Holocene denudation in an Alpine basin, Dolomites, Italy. Zeitschrift fur Geomorfologie Supplementband, pp 129–145
Sclunegger F, Hinderer M (2003) Pleistocen/Holocene climate change, re-establishment of fluvial drainage network and increase in relief in the Swiss Alps. Terra Nova 15:88–95
Seppälä M (1998) New permafrost formed in peat hummocks (pounus), Finnish Lapland. Permafrost Periglac Process 9:367–373
Şerban R, Popescu M, Urdea P, Onaca A (2015) Influence of lithology and geomorphometric parameters on block streams morphology from Retezat-Godeanu Mountains Group, Southern Carpathians. Methodological challenges in geography, 15–16 May 2015, Timişoara
Serrano E, Sanjosé JJ, González JJ, Del Río M, Ruiz P, Atkinson A, Martín R, Rico I, Fernández A (2011) Análisis y control de indicadores geomorfológicos en el Parque Nacional Picos de Europa. In: Ramirez L, Benigno A (eds) Proyectos de investigación en parques nacionales: 2007–2010, ICONA, pp 7–32

Simoni S (2011) Studiu geomorfologic al bazinului Râului Doamnei. Edit. Univ. din Piteşti, Piteşti (in Romanian)
Sîrcu I (1976) Frost heaving stones in the Godeanu Mountains. Anal. şt. Univ."Al. I. Cuza" Iaşi, secţ. II, Geologie-Geografie, XXI:126
Sîrcu I (1978) Munţii Rodnei. Studiu morfogeografic. Edit, Academiei, Bucureşti (in Romanian)
Smith DJ (1987) Frost-heave activity in the Mount Rae Area, Canadian Rocky Mountains. Arct Alp Res 19:155–166
Smith DJ (1988) Rates and controls of soil movement on a solifluction slope in the Mount Rae area, Canadian Rocky Mountains. Zeitschrift für Geomorphologie, N.F. Suppl. 71:25–44
Smith DJ (1992) Long term rates of contemporary solifluction in the Canadian Rocky Mountains. In: Dixon JC, Abrahams AD (eds) Periglacial geomorphology. Wiley, Chichester p, pp 203–221
Taber S (1929) Frost heaving. J Geol 37:428–461
Tarnocai C, Zoltai SC (1978) Earth hummocks of the Canadian Arctic and Subarctic. Arct Alp Res 10:581–594
Tufnell L (1972) Ploughing blocks with special reference to north-west England. Biul Peryglac 21:237–270
Tufnell L (1976) Ploughing block movements on the Moor House Reserve (England) 1965–75. Biul Peryglac 26:313–317
Urdea P (1989) Munţii Retezat. Studiu geomorfologic Universitatea "Al. I. Cuza" Iaşi, Facultatea de Biologie-Geografie-Geologie. PhD thesis manuscript (in Romanian)
Urdea P (1998) Rock glaciers and permafrost reconstruction in the Southern Carpathians Mountains, Romania. In: Permafrost—seventh international conference proceedings, Yellowjnife, Canada. Collection Nordicana, 57, Univ. Laval, pp 1063–1069
Urdea P (2000) Munţii Retezat. Studiu geomorfologic. Edit, Academiei Române, Bucureşti (in Romanian)
Urdea P, Drăguţ L (2000) Noi date asupra reliefului glaciar si periglaciar din Munţii Şureanu. Studii şi cercetări de geografie 47:40–53
Urdea P, Vuia F (2000) Aspects of the periglacial relief in the Parâng Mountains. Revista de Geomorfologie 2:35–39
Urdea P, Vuia F, Ardelean M, Voiculescu M, Török-Oance M (2003) Consideraţii preliminare asupra elevaţiei periglaciare în etajul alpin al Carpaţilor Meridionali. Revista de Geomorfologie 4–5:5–13
Urdea P, Vuia F, Ardelean M, Voiculescu M, Török-Oance M (2004) Investigations of some present-day geomorphological processes in the alpine area of Southern Carpathians (Transylvanian Alps). Geomorphologia Slovaca 4(1):5–11
Urdea P, Ardelean M, Onaca A, Ardelean F (2008a) An outlook on periglacial of the Romanian Carpathians. Analele Universităţii de Vest din Timişoara, Geografie XVIII, pp 5–30
Urdea P, Ardelean M, Onaca A, Ardelean F, Török-Oance M (2008b) Application of DC resistivity tomography in the alpine area of Southern Carpathians (Romania). In: Kane DL, Hinkel K (eds) Proceedings of the ninth international conference on permafrost. University of Alaska, Fairbanks p, Institute of Northern Engineering, pp 323–333
Urdea P, Török-Oance M, Ardelean M, Vuia F, Voiculescu M (2009) Geomorphological aspects of the human impact in the alpine area of Southern Carpathians (Romania). Hrvatski geografski glasnik 71(1):19–32
Urdea P, Onaca A, Ardelean M, Ardelean F, Török-Oance M (2010) Geomorphological mapping and characteristics of some periglacial landforms from Southern Carpathains Romania. Third European Conference on Permafrost, 13–17 June 2010, Longyearbyen, Svalbard
Urdea P, Onaca A, Ardelean F, Ardelean M, Török-Oance M (2012) Aspects of the Thermal Regime on the Periglacial Belt of Southern Carpathians (Romania). Tenth international conference on permafrost 4:605–606
Vespremeanu-Stroe A, Urdea P, Popescu R, Vasile M (2012) Rock glacier activity in the Retezat Mountains, Southern Carpathians, Romania. Permafrost Periglac Process 23:127–137
Voiculescu M (2004) Types of avalanches and their morphogenetic impact in Făgăraş Massif – Southern Carpathians (Romania). Geomorphologia Slovaca 4(1):72–81

Wang B, French HM (1995) Frost heave and its implications for patterned ground, Tibet Plateau, China. Arct Alp Res 27:337–344
Washburn AL (1973) Periglacial processes and environments. Edward Arnold, London
Williams PJ, Smith MW (1989) The Frozen Earth. Fundamentals of geocryology. Cambridge University Press, Cambridge

Chapter 8
Thermal Weathering and Distribution of Mountain Rockwalls

Mirela Vasile and Alfred Vespremeanu-Stroe

Abstract Thermal weathering assessment is essential in establishing present and past rock surfaces dynamics in mountain areas. Though for the Romanian Carpathians most studies rely on air temperature when estimating the intensity of freeze-thaw cycles, comparative analysis of in situ ground thermal measurements shows that important differences occur in the thermal behaviour of mountain sectors and landforms. Specifically, air temperature fails to account seasonal frost cycles and the duration of snow cover, which, in most situations leads to a misleading evaluation of freeze-thaw magnitude. Virtually snow-free surfaces such as steep rockwalls would thus be subject to intense manifestation of freeze-thaw weathering. Based on intensive rock temperature measurements performed above 1800 m elevations in the Southern Carpathians, we here describe the occurrence patterns of both diurnal and seasonal frost in different topographic conditions (exposure, altitude) as a first step in evaluating frost weathering susceptibility. Important differences are noticed between north and south-facing rock surfaces, as the first experiences deep continuous freezing throughout most of the cold season whereas the latter is subject to high day–night thermal amplitudes and up to 120 diurnal freeze-thaw cycles per year. This reflects into the characteristics of weathered rock fragments, the rate of weathering and into the resultant long-term configuration of the slope. In order to report these patterns to the present distribution of rockwalls in the Romanian Carpathians, an inventory was obtained comprising 788 rock surfaces mapped in the Eastern and Southern Carpathians, by the use of available satellite imagery. Both frequency and coverage of rock surfaces highlight their development mainly on the northern slopes of the Southern Carpathians (above 2000 m) in the detriment of the southern ones (5:1 ratio in terms of total area). This could, in part, reflect the differences of frost propagation intensity (mainly

M. Vasile (✉)
Research Institute of the University of Bucharest, 36-46 M. Kogalniceanu Blv., 050107 sector 5, Bucharest, Romania
e-mail: mirelavsl@yahoo.com; mirela.vasile@geo.unibuc.ro

A. Vespremeanu-Stroe
Faculty of Geography, University of Bucharest, 1st, N. Balcescu Blv., 010041 sector 1, Bucharest, Romania

M. Rădoane and A. Vespremeanu-Stroe (eds.), *Landform Dynamics and Evolution in Romania*, Springer Geography,
DOI 10.1007/978-3-319-32589-7_8

expressed in the size of the removed particles and of the resulting debris) and implicitly of freeze-thaw weathering magnitude, but should also integrate the control of lithology and structural imprint on a local scale.

Keywords Frost weathering · Mountain rockwalls · Topography control · Lithology · Romanian Carpathians

Background

Weathering is one of the key processes in temperate mountain environments that contribute to the ongoing landforms and landscape transformation, in response to medium to long-term climatic variations (Summerfield 1991; Goudie 2004; Hales and Roering 2005). The influence of thermal weathering upon rock surfaces through freezing and thawing of contained water is still considered by many authors as the exclusive formation mechanism of angular rock fragments that compose periglacial deposits (Peltier 1950; Tricart 1972; Posea et al. 1974). Most often, the high frequency of thermal oscillations through the freezing point is presumed to determine the enlargement of joints and cracks networks, finally leading to rock fragments detachment (Washburn 1979; French 2007). Nevertheless, the reliability of these assumptions is recently being argued (André 2003; Hall and Thorn 2011; Hall et al. 2013) given the great amount and diversity of field and laboratory data provided by dedicated studies over the last three decades.

Acknowledging the complexity of weathering (Viles 2013), much more attention is presently being paid to the freeze-thaw process itself and to real-time field investigations, trying to establish weathering triggering thresholds and rates, by using quantitative data. Thus, completing and/or correcting initial weathering assessment by visual observation of gelifracts within the framework of climatic geomorphology (Tricart 1972) and of early experimental laboratory studies (Collins 1944; Lautridou 1971; Fukuda 1971; Walder and Hallet 1985), joint and interdisciplinary research projects and continuous field monitoring are now expanding, focusing not only on climatic parameters, but mostly on frost propagation, rock thermal behaviour, mechanical reaction to frost as a basis for short to medium weathering rates and rock surfaces evolution (Matsuoka and Sakai 1999; Matsuoka 2008; Draebing et al. 2014). This multi-parameter approach enables the improvement of thermal weathering models and creates a standardized and detailed perspective on rock surfaces dynamics and reaction to thermal processes on wide scale and in various state conditions (Gruber et al. 2004; Hales and Roering 2005; Pogliotti et al. 2008).

Romanian geomorphologists reported most frequently to the qualitative (and relative) assessment of weathering, invoking high frequency of frost cycles and using air temperature values as a proxy to express its intensity (Micalevich-Velcea 1961; Tufescu 1966; Posea et al. 1970). Moreover, most of the works on mountain geomorphology discuss only briefly about the impact of frost weathering in alpine areas, very few contributing to the development of the topic (Stoenescu 1951; Posea

et al. 1974). This trend continued until the early 2000's, when more specific climatic indexes were proposed in the context of periglacial studies (Urdea 2000) and the potential frequency of freeze-thaw oscillations was firstly discussed in relation to specific mountain sectors in the Carpathians (Vespremeanu-Stroe et al. 2004). There is still a quite high reticence towards the novel scientifically-based concepts on weathering, which might explain the weak interest towards developing dedicated studies, or accounting it in other applied geomorphology studies, which also resume to the climatic approach of the process.

Following the methods applied in the European or Japanese Alps, a in situ network of continuous soil and rock temperature monitoring was set in 2008 in over 40 locations from the Southern and Eastern Romanian Carpathians (Vespremeanu-Stroe and Vasile 2010; Vasile et al. 2014), with the purpose of evaluating effective frost weathering potential on a wide range of altitudes and in multiple topographic conditions in this mountain area.

We here present a synthesis of the thermal monitoring results, in order to provide a more comprehensive perspective of rock thermal behaviour and to assess the field conditions of freeze-thaw weathering occurrence within the periglacial belt of the Romanian Carpathians. The discussion is made on both frequency and intensity of freeze-thaw oscillations with the distinction of diurnal and seasonal cycles. The morphologic response of surfaces exposed to frost action, i.e., rockwalls and intact rock faces, can also reflect the intensity of the cryogenic process or different patterns of frost propagation and, implicitly, of frost weathering. In this context, the present distribution and morphometry of free rockwalls in the Romanian Carpathians were assessed using satellite imagery (Vasile et al. 2015; Vasile et al. in progress). Based on the resulting rockwalls inventory and on the thermal database obtained so far, the question is in what degree rockwall morphometry correlates with both high-frequency short-term freeze-thaw oscillation and to intense long-term constant freezing.

Models and Concepts in Thermal Weathering

The very different thermal and mechanical characteristics of water and rocks lead to specific behaviours and interactions during freezing (Draebing et al. 2014), imposing distinct frost propagation patterns which eventually determine the dimensions, shape and total volume of the gelifraction products (i.e. of the resulting rock fragments). On the other hand, although rock temperature indicates the ideal conditions of freezing and thawing, it cannot certify the actual rock damage occurrence. Having in view that the 0 °C water freezing threshold is being influenced by natural factors (salt concentration in water, rock porosity, permeability, thermal conductivity, hydraulic pressure) which have been shown to lower this temperature commonly to −2…−5 °C and exceptionally up to −8 °C (detailed in Matsuoka 2001; Hall 2007), additional (unequivocal) methods have been proposed and successfully applied: acoustic emissions detection, rock cracks dynamics monitoring, exotherms detection.

There has been a general acceptance of the 9 % volumetric expansion of water during freezing in rock discontinuities as the driving force of rock breakdown, under the pressure exerted within fissures and fractures in rocks (up to 100 atm/cm^2, Şeclăman and Anastasiu 1983). This model was associated with macrogelivation caused by ice bursting during diurnal freezing (Matsuoka 2001), and has been documented by simultaneous fissures expansion (Matsuoka 1994, 2008) and the in situ detection of acoustic emissions produced through rock cracking during freezing (Amitrano et al. 2012; Girard et al. 2013). However, controlled conditions in laboratory experiments draw attention to the importance of water saturation level in rock which controls the properties of the ice–water–rock system. Acoustic emissions detection during freezing in controlled environments (Hallet et al. 1991; Murton et al. 2006; Duca et al. 2014) highlights the formation of new cracks in compact rock samples and the enlargement of existing ones due to water movement towards an existing freezing front. This leads to interstitial ice segregation and consequently induces additional pressure into the rock body. Although this model has been shown to be effective in constant low temperature conditions, similar to seasonal frost cycles in mountain areas, the formation of ice lenses through interstitial ice growth has also been detected during diurnal freezing in natural conditions, by means of high resolution geophysical survey (Sass 2004, 2005).

Despite the significant progress made in the real-time assessment of frost damage in rock, a unitary model of the process is not yet fully considered. Taking into account the above mentioned findings, we assume ice segregation to promote intense damage in rock during seasonal freezing. The cumulated effect of this process would lead to the detachment of medium-large rock fragments due to its in-depth action. In comparison, we consider that diurnal freeze-thaw cycles continuously contribute to rock strength weakening but, independently, would result in only small-sized gelifraction products as their impact is limited to the first tens of centimeters of the rock mass (Matsuoka 2008). As the data comprised here are limited to rock temperature, we only present the thermal dimension/context of freeze-thaw weathering. In this purpose, we determined the surface freezing index (8.1) for each type of frost cycle (after Matsuoka 1994; Matsuoka and Sakai 1999).

$$F_i = t \times \Delta T \,(\text{h } ^\circ\text{C} - \text{hours degrees}) \tag{8.1}$$

where F_i = surface freezing index, t = frost duration (in hours) and ΔT = thermal amplitude of the freezing phase of the freeze-thaw cycle (in °C).

We further distinguish between diurnal and seasonal frost cycles taking into account their frequency, intensity, and persistence as follows:

– *diurnal (daily) freeze-thaw cycles* are imposed by day–night thermal variations, with a reduced persistence of the freezing phase (less than 24 h) which leads to a low value of F_i (see Section "Freeze-Thaw Regime of Mountain Rockwalls and Magnitude Assessment") and a virtually reduced frost penetration depth, from several millimeters (surficial frost) up to 20–40 cm (Matsuoka 2008; Sass 2005).

High frequency of such oscillations within this layer impacts the rock by weakening it through the cumulated effect, theoretically resulting in small-size fragments;

– *seasonal (annual) frost* is characterized by negative rock temperature persistence over an extended time interval (from several weeks to 3–4 months). Compared to day–night oscillations, in the case of which frequency is a top indicator, duration is essential in setting seasonal freezing magnitude. Very low temperatures are usually achieved during this phase in rockwalls or rock masses unaffected by an isolating snow layer. Consequently, in comparison to diurnal freezing, considerably higher F_i values are typical, favoring segregation ice growth through the development, maintenance and propagation of ice lenses and freezing fronts. We assume this freezing pattern to enable both micro- and macrogelivation given the extended rock layer in which frost propagates, the potential frost depth reaching several meters (Matsuoka 2008; Magnin et al. 2011).

Daily air temperature values available from meteorological stations above 1800 m above sea level (a.s.l.) in the Romanian Carpathians (Vf. Omu—Bucegi Mountains, 2504 m a.s.l., Babele—Bucegi Mountains, 2206 m and Ţarcu—Ţarcu Mountains, 2180 m) were used to compare the previous assessments (Posea et al. 1974; Vespremeanu-Stroe et al. 2004) with the results of field thermal monitoring (detailed in Vasile et al. 2014).

Topography and Ground Cover Control on Freeze-Thaw Weathering

As discussed above, the complexity of frost weathering triggering processes is imposed by multiple parameters (thermal regime, water content, rock properties) while the assessment of its impact at local or regional scale should not be generalized, as it accounts specific relief characteristics (i.e. landform type, altitude, exposure, slope, surface cover) and climatic conditions. Reporting to the Romanian Carpathians, previous studies (Vespremeanu-Stroe et al. 2004) indicate a maximum mean annual number of freeze-thaw days [Ng in (8.2)] in intra-mountain depressions (>100 days), followed by high-altitude (>2000 m) mountain plateaus, peaks, and crests (80–110 days). This analysis was based on long-term daily air temperature records from 27 meteorological stations covering the altitudinal range between 314 and 2504 m a.s.l. and is limited to diurnal freeze-thaw assessment.

$$\mathrm{Ng} = N(T\mathrm{min}) - N(T\mathrm{max}) \tag{8.2}$$

where $N(T\mathrm{min})$ = number of days with minimum temperature ≤ 0 °C, and $N(T\mathrm{max})$ = number of days with maximum temperature < 0 °C.

A similar mountain units typology was followed in the recent work of Vasile et al. (2014), which evaluates the annual ground thermal regime of flat surfaces

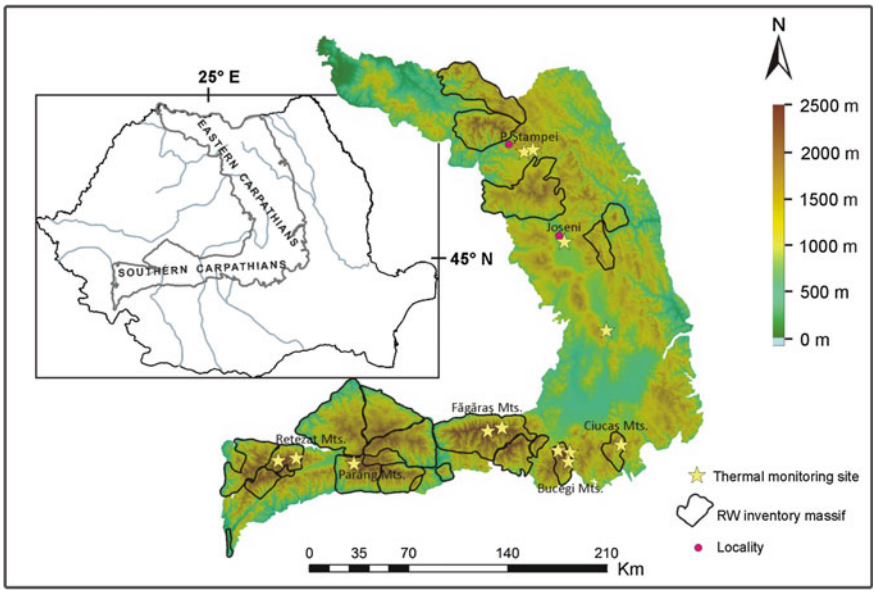

Fig. 8.1 Localisation of ground thermal monitoring sites and mountain massifs for which rockwall mapping was performed in the Eastern and Southern Carpathians

(generally affected by long-lasting snow cover) and of steep rock surfaces (partially or completely snow-free during winter). Air, soil, and near-surface rock temperatures were continuously registered for one to three years between 2008 and 2013 in intra-mountain depressions and valley couloirs (Poiana Stampei, Joseni), mean-high interfluves and plateaus in the Bucegi Mountains and in compact rock surfaces in Ciucaş, Bucegi, Făgăraş, Parâng and Retezat Mountains (Fig. 8.1).

Distinct patterns of ground thermal regime have been identified in relation to air temperature (Table 8.1). Thus, in intra-mountain depressions the simultaneous measurements indicated a significant number of days with freeze-thaw potential (97 in winter season 2009–2010, based on air temperature values) which do not materialize as frost cycles in the ground. The flat soil-covered areas show very few frost oscillation, most of the winter maintaining a constant near 0 °C temperature, indicator of the insulating effect of a thick snow layer which prevents ground cooling or warming. The snow-free rock outcrop monitored in the same period and area exhibits less than half of the cycles registered in air, which most probably reflects the influence of rock properties (Vasile et al. 2014). Therefore, although showing the highest potential of diurnal freeze-thaw action, the morphometric characteristics of low altitude mountain depression areas (such as Poiana Stampei, in Dornelor Depression, Eastern Carpathians) where flat soil-covered surfaces and forested slopes prevail, actually restrain the effectiveness of thermal weathering. This trend changes with altitude, as the number of diurnal oscillations in soil and rock within mountain depressions slightly increases. Also, seasonal frost enlarges duration and becomes

Table 8.1 Diurnal frost cycles assessment based on daily air temperature values and in situ continuous measurements in air, soil and rock at the selected locations

Location	Landform type	Alt. (m)	Meteorologic stations air temperature data		Number of diurnal frost cycles based on in situ temperature data		
			Diurnal cycles	Mean annual	Air	Rock	Soil 3 cm
Poiana Stampei	Depression	900	124	5	97	44	7
Vf. Omu (Bucegi Mts.)	High alt. interfluve	2500	104	−2.4	–	80	22
Baba Mare (Bucegi Mts.)	High alt. plateau and rockwall	2260	96	0.1	–	130	23
Doamnei[a] (Bucegi Mts.)	Rockwall	1900	–	–	41	84	–
Turnul Porţii[b] (Retezat Mts.)	Rockwall	2335	81	−0.6	21	24	–

[a]Thermistors functional from December to August; exposed to South
[b]Thermistors functional from November to September; exposed to North (after Vasile et al. 2014)

more active on mean-high altitude interfluves (Fig. 8.2), which are subject to lower mean annual temperatures and more variable winter conditions.

Consequently, in the case of mountain depressions, valley couloirs and other soil-covered near-horizontal surfaces in the Carpathians (mountain interfluves and plateaus), air temperature is not a confident parameter in estimating the effect of freeze-thaw weathering as it overestimates the dimensions of the process (in this case, the frequency of diurnal freeze-thaw oscillations). Therefore, air measurements or meteorological data offer a good estimate only for the overall interval in which, thermally, frost can occur. At ground level, this interval is not only characterized by diurnal oscillations, but can also reflect seasonal frost or the persistence of snow cover.

The ratio of each process could be considered constant for similar settings, but it modifies with altitude increase or depending on the type of surface (soil or rock showing distinct thermal properties; Williams and Smith 2008), exposure and slope value. For example, freeze-thaw cycles cover 2 % of the winter season duration in mountain depression environments (Poiana Stampei location), in the rest of the time the ground exhibiting the influence of snow cover (persistent and constant near 0 °C temperature, no variations). The report changes to 20–30/80–70 % on mean-high altitude (1300–2000 m) mountain interfluves and plateaus (Fig. 8.2; Vasile et al. 2014). Additionally, at the highest altitudes on soil-covered horizontal surfaces (mountain interfluves >2000 m a.s.l.), seasonal frost occurrs most of the time (about 3 months per year), implicitly reducing the frequency of diurnal cycles.

The compared analysis of steep rockwalls thermal regime and air temperature measurements highlights the strong control of exposure over the frost weathering

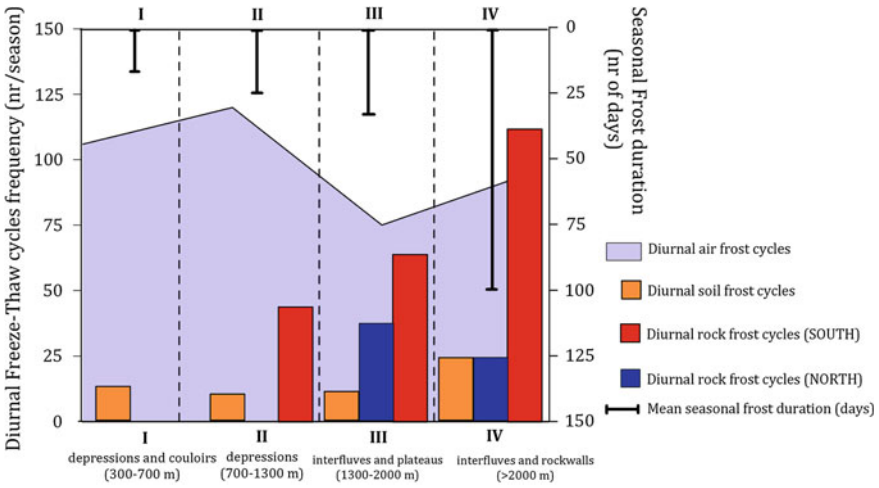

Fig. 8.2 Mean annual values of diurnal freeze-thaw cycles number and seasonal frost duration based on air, soil and rock temperature field measurements and meteorological air temperature values (after Vasile et al. 2014). Rock temperature was assessed for north and south-exposed vertical and compact slopes. Note that air frost cycles are very different by the rock frost cycles in most of the cases (excepting the diurnal cycles on the northern slopes >1300 m altitude) which makes them unreliable for using into morphodynamics approaches

patterns in rock [also highlighted by Gruber et al. (2004), Magnin et al. (2011), Matsuoka (2008)]. In the case of north-exposed vertical rockwalls, exemplified by the Turnul Porţii location (2335 m a.s.l.) from the central sector of the Retezat Mountains, rock and air temperatures have a similar evolution during the monitoring period (Table 8.1). On such shadowed surfaces, thermal variations in rock are basically imposed only by the surrounding air temperature. Thus, above 2000 m, following the general decrease of air temperature values due to altitude and in the absence of direct solar radiation, rock temperature variations generate a virtually low frequency of diurnal frost cycles (24 at Turnul Porţii, from November 2011 to September 2012), but lead to the most extended seasonal frost within the monitored types of landforms (as detailed in Section "Freeze-Thaw Regime of Mountain Rockwalls and Magnitude Assessment"). Oppositely, the south-facing rockwalls experience intense thermal variation expressed by high diurnal thermal amplitudes (average winter rock ΔT reaches 25–30 °C compared to air ΔT of 8–10 °C at Doamnei location, Bucegi Mountains, Vasile et al. 2014) which lead to an intense activity of diurnal freezing and thawing that covers most of the winter interval (Fig. 8.2), and to a very weak manifestation of seasonal freezing.

Comparison with in situ measurements in various conditions proves that consideration of air temperature alone in the evaluation of frost processes can be misleading, as the dynamics of specific mountain sectors turns to be only slightly affected by thermal weathering (namely by freeze-thaw processes), although climatic conditions indicate a very high potential. Furthermore, the integration of

specific characteristics of the surface and topographic details are required for a reliable result. The conversion or calibration of meteorological data based on in situ data from a wide range of altitudes, exposures and landforms (when such data are available and accurate) can be applied in estimating weathering magnitude.

Flat surfaces or with low inclination such as depressions, interfluves sectors and large plateau areas present a typically stable winter ground regime, dominated by prolonged snow cover which makes these mountain areas easier to investigate. When addressing steep surfaces with diverse exposures, air temperatures fail to comprise the effects of solar radiation and the influence of rock properties. Thermal weathering evaluation requires detailed rock surface measurements for the assessment of the snow effect and of the typology, frequency/duration and intensity of daily and seasonal freeze-thaw cycles. This aspect is utterly important in determining frost weathering susceptibility of rock surfaces which can further be integrated into mountain hazard assessments.

Freeze-Thaw Regime of Mountain Rockwalls and Magnitude Assessment

Mountain areas are characterized by the high variability of relief on relatively short distances. Consequently, local and large-scale estimations of thermal weathering influence on alpine rockwalls and rock surfaces dynamics require the consideration of topographic parameters (altitude, exposure, slope, shadow effects, fragmentation degree) along with the weighting of active freeze-thaw patterns (predominance and effectiveness of frost types). In order to determine freeze-thaw regime and potential thermal weathering of rockwalls in various topographic conditions, up to 20 locations in the Southern Carpathians were monitored for two to five years (near-surface—3 cm—temperature recording at every two hours).

Landforms exposure is particularly important when discussing thermal processes because it controls the insolation degree and, implicitly, the incoming solar radiation and caloric energy budget (Stocker-Mittaz et al. 2002). The freeze-thaw regime of rockwalls with different exposures was addressed above 1800 m a.s.l. in Bucegi, Făgăraş and Retezat Mountains, with special attention on the North–South differences.

At the Baba Mare location (limestone outcrop on Bucegi Mountains plateau area, 2260 m a.s.l.), vertical rock slopes oriented towards all the four main cardinal directions could been monitored on a distance range of 80 m during three years (2011–2014). Averaged values of daily cycles frequency for the three seasons clearly indicate an intense activity on the south-exposed rockwalls (80 cycles) compared to the opposite north-exposed ones (35–38 frost cycles) (Fig. 8.3a). East and West oriented rockwalls show a relatively similar behaviour, with about 50 diurnal cycles per season. F_i index values during diurnal cycles are similar on East,

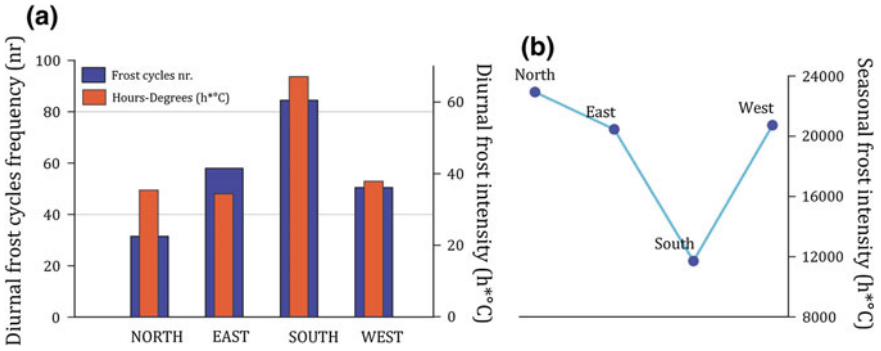

Fig. 8.3 Diurnal frost cycles frequency and intensity expressed by F_i freezing index (**a**) and seasonal frost intensity (**b**), in vertical rock faces disposed on the main four exposures (Baba Mare limestone outcrop, Bucegi mountains, 2260 m a.s.l.). The values represent three-years averages (2011–2014)

West and North (45–50 h °C) but are almost twice higher on the south facets, especially due to the intense amplitudes that occur during winter days under the effect of direct insolation.

Further on, it is noticeable that seasonal frost presents a different distribution pattern (Fig. 8.3b). At this location, seasonal frost occurs on each side of the rock outcrop, with the highest intensity on the North facet (22.5×10^3 h °C), and the lowest on the South, where the duration of the seasonal cycle is almost 70 % shorter. East and West again present close F_i values during the seasonal frost, with a frost intensity only 10 % lower than on the North. This indicates an intermediate radiative input for eastern and western rockwalls which translates through a medium to high impact of both daily and annual freeze-thaw oscillations.

The compared analysis of north and south-exposed rockwalls was performed using multiple data series from the Southern Carpathians (see Figs. 8.5 and 8.6). Data obtained in the locations with the longest temporal cover (3–5 years) also correspond to three different lithologies: limestone (Baba Mare site, Bucegi Mountains); granite (Turnul Porţii site, Retezat Mountains); schist (Căldarea Pietroasă site, Făgăraş Mountains) (Fig. 8.5). Disparities do arise between sites, most probably induced by different rock sensitivity to frost given by specific thermal and mechanical properties (Pogliotti et al. 2008). This aspect is partially discussed in Section "Rockwalls Distribution and Thermal Weathering Potential", and detailed elsewhere (Vasile et al. 2015; Vasile et al. in progress). The general trend is similar, irrespective of the rock type. In each context, the south-exposed rockwall shows about 2.5–3 times more diurnal cycles than the corresponding north-exposed location. The intensity distribution follows a similar pattern, with larger amplitudes imposed by site-specific conditions (especially the microclimate) with 2–3.5 times higher intensities for diurnal frost cycles that occur on the South in comparison with the North rockwalls. The differences become larger (3–3.5) when the northern slopes are into a negative macro-feature (i.e. a glacial cirque) and

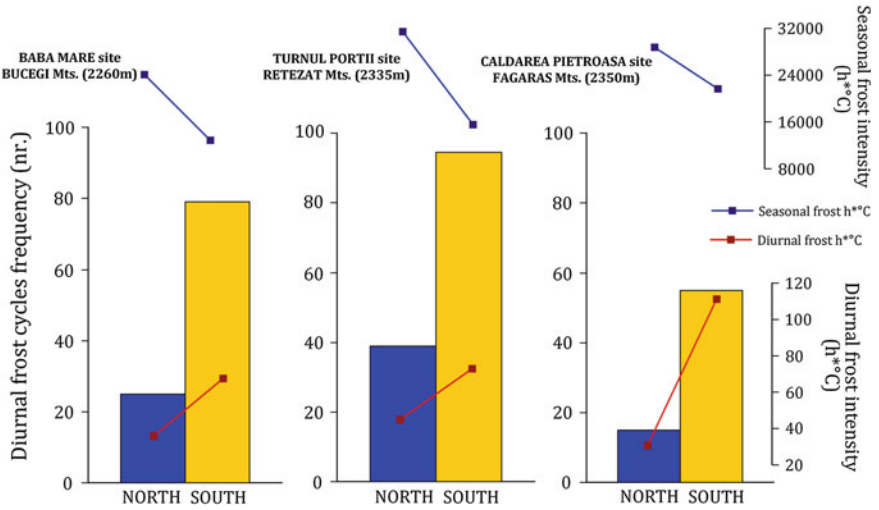

Fig. 8.4 North-South patterns of diurnal and seasonal frost magnitude on different lithologies: limestone (Baba Mare site, Bucegi mountains), granite (Turnul Porţii site, central area of Retezat mountains) and metamorphic schist (Căldarea Pietroasă site, central area of Făgăraş mountains) (Fig. 8.1). Please note the discrepancy between North and South rockwalls exposure to frost cycles both in terms of frequency and magnitude

smaller when the rockwalls are positive features (i.e. towers, inselbergs, rock needles, tors).

The occurrence pattern of seasonal frost once more highlights the reversed intensity ratio (Fig. 8.3), showing that northern rock surfaces are much more affected by persistent gelivation than the southern ones. In all three locations, the seasonal frost average F_i index is of 10×10^3 h °C on South and of about 25×10^3 h °C on North (Fig. 8.4). Our assumption is that these differences generate major implications in what concerns freeze-thaw weathering manifestation and contribution to the modeling process of this type of rockwalls. If we consider the combined action of both diurnal and seasonal frost, one may argue that, although affecting a relatively shallow rock layer, it is expected that the frost weathering process is overall more accentuated and diverse on the south-exposed alpine rockwalls, given the high magnitude (intensity and frequency) of daily cycles and the occurrence of the annual one (though on a short time span). We consequently presume that the common action of the two freeze-thaw patterns can result in various forms of weathering products with small grain-size (usually centimetric fragments) on the southern rockwalls, while the persistent frost on the opposite north facing walls will usually lead to the detachment of medium to large blocks (decimeters to meters). These marked differences in grain-size of the removed particles are generating debris features (talus slopes, rock glaciers, protalus ramparts) with very distinct characteristics on the antagonic slope exposures and further determine the in situ weathering. Therefore, most of the high altitude southern

slopes in the area exhibit weathering mantles with fine (frequently soil-covered) debris matrix, whereas the northern ones are generally coarser, predominantly with openworked debris deposits and exposed rockwalls.

Expanding the North–South comparison to a wider altitudinal range (1900–2500 m a.s.l.) which comprises all the field monitoring locations in the Southern Carpathians (Fig. 8.5), the same ratio maintains in the number of diurnal frost cycles, which is not too visibly influenced by altitude increase. On the other hand, seasonal freezing intensity shows an ascending trend on both exposures, almost doubling on a range of 400 m. This proves the predilection of high-altitude rockwalls (>2100 m) to produce abundant rock fragments (in relation to the high intensity of diurnal cycles) with larger sizes due to seasonal frost deep penetration.

Another aspect that should be discussed is rock adaptability and resistance to the pressures determined by frost propagation and thawing. It has been shown that thermal homogeneity is characteristic to north-exposed rockwalls in the absence of direct solar radiation (Vasile et al. 2014). Keeping this in mind, seasonal phase change should promote slowly within a rock body, which would adapt more easily to the change of pressure and would ultimately induce a slow propagation of damage in rock. On the other hand, the south-exposed surfaces are frequently affected by lack of water in the first few centimeters (Girard et al. 2013; Sass 2005) due to intense incoming solar radiation, which would turn freeze-thaw cycles inefficient. These are only two examples of conditioning factors that may interfere, thus caution is required when evaluating freeze-thaw action in rock. Finally, the results of rock thermal monitoring indicate that, referring to vertical rockwalls in the Southern Carpathians, shallow weathering caused by freeze-thaw action seems to be very active on southern exposures, it has a moderate effect on eastern and western rock faces and it is very reduced on North, where deep rock fracturing is more probable to occur, under the action of ice segregation.

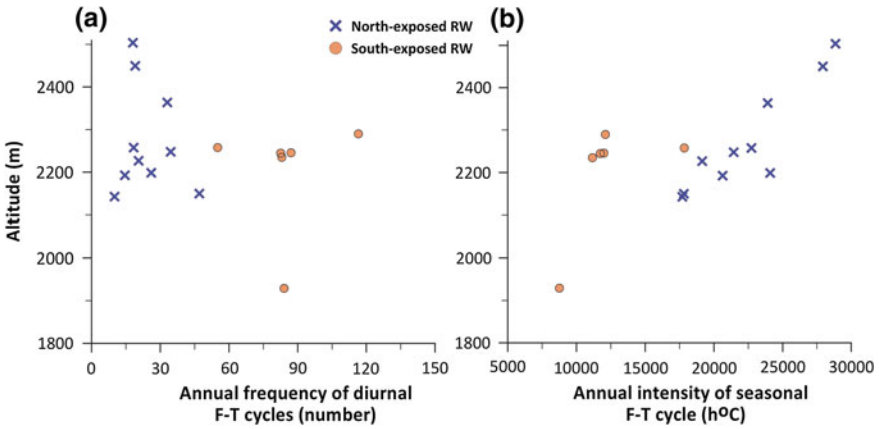

Fig. 8.5 Altitudinal distribution of diurnal freeze-thaw cycles frequency (**a**) and seasonal frost intensity (by F_i) (**b**) in multiple north and south-exposed vertical rockwalls monitored in the Southern Carpathians, in the 1900–2500 m a.s.l. altitudinal range

Rockwalls Distribution and Thermal Weathering Potential

It is acknowledged that the evolution of mountain landforms can be highly controlled by weathering and erosive processes of surfaces, the effect of which can accurately be quantified over short time spans (Hovius et al. 2004; Cain 2004). In the same time, lithology and structure can also impose the extent and morphometry of presently exposed rock surfaces (Burbank and Anderson 2001; Hugget 2007). In this section, we present an inventory of the rockwalls in the Eastern and Southern Carpathians following their morphometric characteristics and main lithology, in order to present the extent/spreading of rock surfaces exposed to weathering in relation to the distribution of freeze-thaw patterns (described above). Preliminary data were discussed in Vasile et al. (2015), while the topic is widely presented in Vasile et al. (in progress).

Rockwalls mapping was made by visual assessment of rock surfaces on available satellite images and orthophotoplans (Google Earth imagery), resulting a total number of 788 surfaces, from which 88 % in the Southern Carpathians. This method could been applied (i.e. rockwalls could been identified) in 23 mountain massifs (17 in the Southern Carpathians and 6 in the Eastern Carpathians, marked in Fig. 8.1). For each vectorized surface the mean area, orientation, slope, relative height and altitude were determined on the 25 m resolution EU digital elevation model (available at the European Environmental Agency) in Global Mapper® and SAGA GIS® softwares (based on average value of raster pixels). The term rockwall (or rock slope) refers herein to steep exposed rock faces, with angles usually higher than 37–40° (Gruber and Haeberli 2007; French 2007). In addition, the vectorized geological map of Romania (scale 1: 200 000) was used to determine the main rock type of mapped rockwalls.

Each surface comprised in the inventory was plotted in relation to its exposure and mean altitude (Fig. 8.6a, c). In the Southern Carpathians, the highest concentration of rockwalls (RW) corresponds to the North slopes (NW, N, NE—from 315° to 45°, Fig. 8.6a) in the altitudinal range of 2000–2500 m. This area corresponds to the maximum-intensity sector of both diurnal and seasonal freezing as shown by field data, which allows us to state that most of the steep rock slopes (i.e., with low influence of snow cover) are presently affected by thermal weathering. Comparatively, the surfaces mapped in the Eastern Carpathians are more widespread in terms of exposition (with a slightly higher density of the eastern rock faces) and concentrated at altitudes between 1500 and 2000 m a.s.l. (Figure 8.6b), basically due to the general lower elevation of the 6 massifs investigated here.

The distribution of RW cumulated area reflects the overwhelming RW cumulated surface on the north facing slopes of the Southern Carpathians in report to the south-facing ones (a ratio of 5:1; Fig. 8.6b). Similarly, the Eastern Carpathians show a net predominance of western RW compared to the eastern ones, and their modest extension on North and South (Fig. 8.6d), probably as an influence of the NW-SE main ridge general orientation (see Fig. 8.1) and of the tectonics imprints

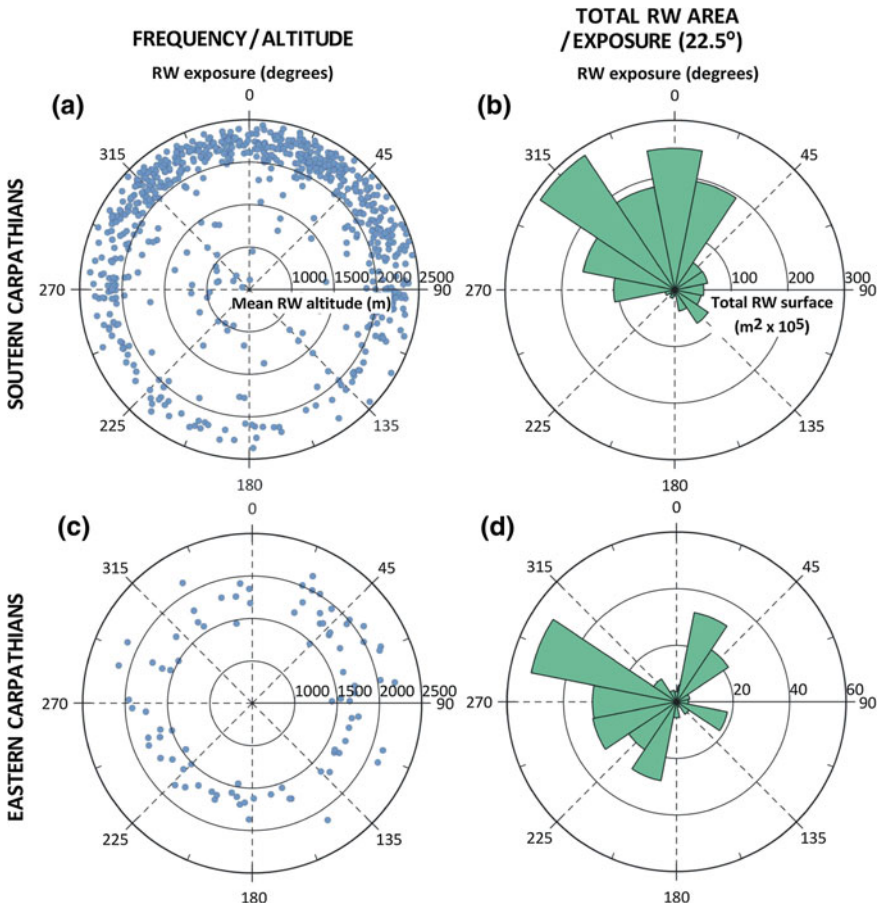

Fig. 8.6 The altitudinal distribution and exposure of inventoried rockwalls in the Southern (**a**) and Eastern Carpathians (**c**). Cumulated area of identified rockwalls in the Southern (**b**) and Eastern Carpathians (**d**) on 25° exposure bins (modified after Vasile et al. 2015)

which favored an initial topography with higher and steeper slopes towards the Transylvanian Plate.

In the first case (Southern Carpathians), the range inherits a general North–South structural asymmetry, which imposed a higher steepness on North. Despite this influence, the high frequency of north-exposed rock surfaces compared to the south-exposed ones is a good indicator of the differential modeling of the mountain slopes and fits well with the distinction between freeze-thaw manifestation patterns described above. We consider that the steep rock surfaces facing South suffer an intense but low magnitude (i.e. shallow) weathering-imposed modeling. Considering the reduced extension of both compact rock slopes and blocky deposits, the weathering of small and medium-size fragments could be the

prevailing pattern, as a consequence of intense action of the diurnal freeze-thaw cycles combined with the reduced magnitude of seasonal frost.

Rock surfaces are much more numerous and extended (we may say "well preserved") on the North side of the mountain massifs in the Southern Carpathians (Fig. 8.6b), where it has been shown that seasonal frost prevails during most of the cold season. Large boulders accumulations are visible at the basis of most north facing rock surfaces in the periglacial sector of the Southern Carpathians feeding the talus slopes, rock glaciers and protalus ramparts. Having in view their present extension, we assume that profound long-lasting freezing typical for these rock slopes promotes a slow-rate weathering of mean and large-size rock fragments.

The exposure-related frequency and surface distribution differences between the Southern and Eastern Carpathians may find their explanation in the general orientation and structural characteristics of these units. Nevertheless, we consider that the general constant morphotectonic evolution of the slopes over the last 10 ka (Săndulescu 1984) allows for the estimation of thermal weathering patterns and impact when discussing this process at local scale and comparing rockwalls developed on similar lithologies.

Figure 8.7 shows the averaged values of RW frequency, mean altitude, height and area for all the 788 inventory records, differentiated on exposure and on five prevalent rock categories (limestones, conglomerates, schists, granitic, and volcanic rocks). Given the reduced statistic population of volcanic rocks (5 RW), only the first four lithologies are discussed. The overall frequency and expansion of the rockwalls sustain the presumption that south-exposed rock surfaces are the most affected by surficial weathering processes on all rock types (Fig. 8.7a, d). On the other hand, the detailed perspective on morphometric parameters reflects a significant control of lithology and its connection to weathering efficiency.

The altitudinal RW distribution (mean altitude, Fig. 8.7b) shows the high elevation of rockwalls accommodated on granites and metamorphic schists (>2150 m a.s.l. on all exposures) that are generally associated with peaks, high crests or headwalls compared to sedimentary rocks (1600–1800 m a.s.l.) which generally reflect a strong structural control. On the other hand, metamorphic, and igneous rock surfaces have the lowest individual mean height (45–50 m) and area ($<10 \times 10^3$ m^2) on each exposure (Fig. 8.7c, d), in comparison to sedimentary rocks. Limestone and conglomerate RW in the Carpathians typically occur in tectonic uplift areas (Săndulescu 1984) which explains their significantly higher mean height (150–180 m) and size (7 times larger than on schists and granites). Also, the frequent occurence of sedimentary walls in mountain ranges with low to medium elevations explains their lower average altitude.

The distribution and morphometry of RW in relation to exposure and rock types reflects on one hand the predisposition of hard rocks to weathering due to (i) influence of schistosity planes in the case of schists, which are characterized by numerous but small rock surfaces and frequently produce small-size fragments (Fig. 8.8a, b) and (ii) large networks of joints and fractures (typical to granites) which determine the detachment of large boulders accumulated as debris deposits at the base of the slope (Fig. 8.8c, d). On the other hand, limestones and

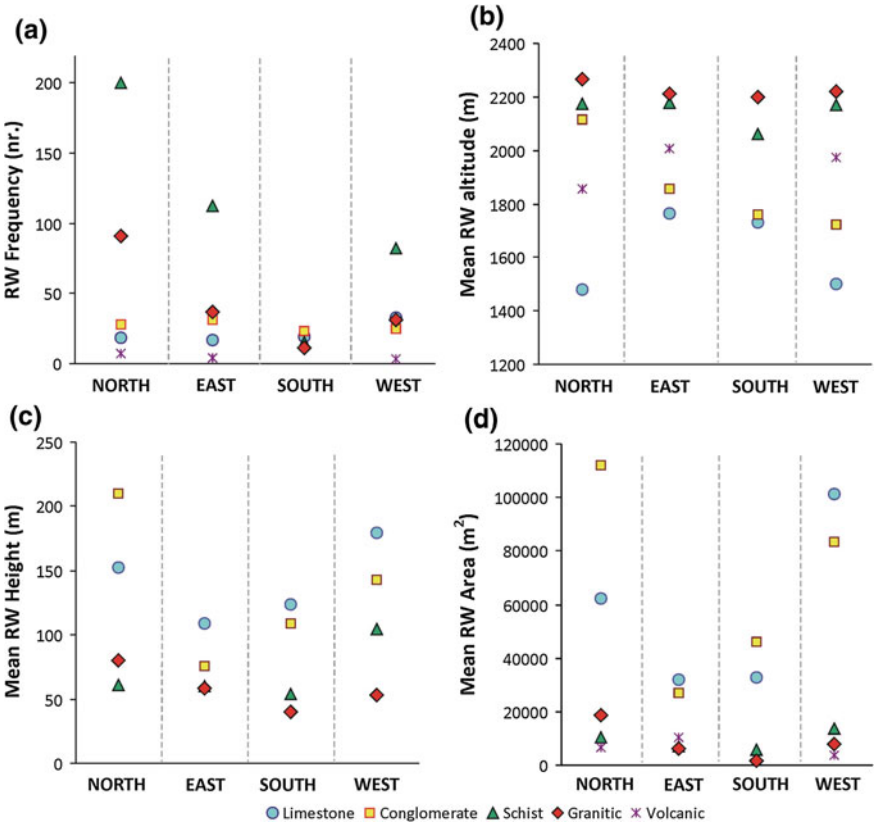

Fig. 8.7 Lithological influence on rockwalls frequency (**a**) and morphometry (mean altitude—**b**, height—**c**, and area—**d**) (Vasile et al. in progress)

conglomerates exhibit medium-high porosity values (10–20 %) compared, for example to granites (1–3 %). This characteristic enables microgelivation (Matsuoka 2001) (i.e. small-scale weathering) which would be intense in a diurnal freeze-thaw regime, argumenting the absence of large-size boulders deposits in many of the investigated sedimentary massifs.

Finally, these results show that rock properties and exposure control over thermal weathering magnitude have a meaningful contribution to RW distribution in the Romanian Carpathians which should be considered in more detailed researches along with the inherited structural control. Additional data on the mechanical properties of each lithology should be added to the thermal database, and debris deposits distribution information should complete the morphometric data on the adjacent rock slopes. Such an approach would allow a much better estimation on weathering, along with the determination of medium- to long-term retreat rates, which would give a thorough perspective on rockwalls dynamics in the Romanian Carpathians.

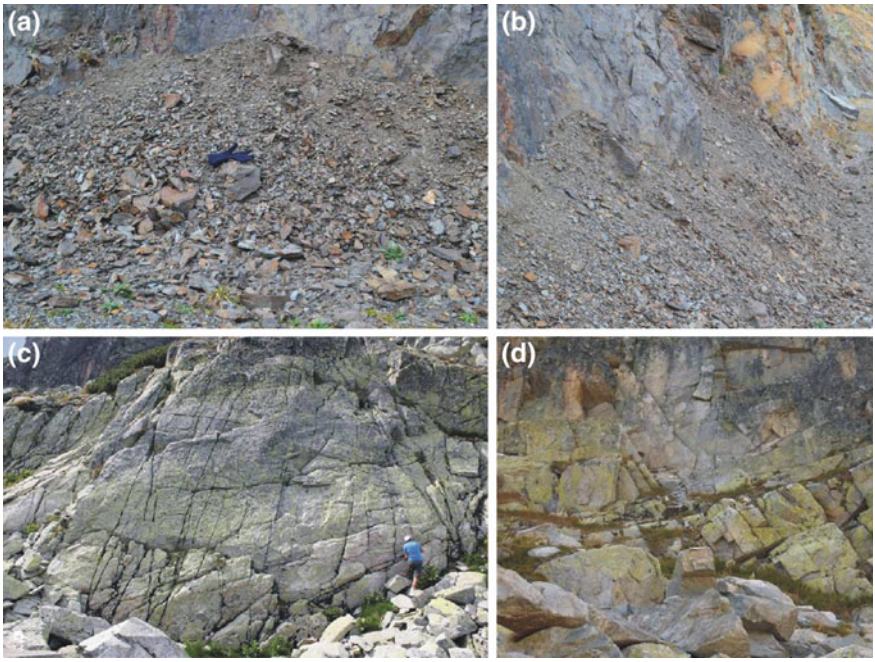

Fig. 8.8 Examples of small-size debris resulted from the weathering of schists (Capra valley, Făgăraş mountains) (**a**, **b**) and intensely jointed RW developed on granitic rocks (Judele cirque, Retezat mountains) (**c**, **d**) (*photos* by M. Vasile)

Conclusions

Thermal weathering patterns in depressions, medium-high interfluves and steep rockwalls in the Romanian Carpathians were determined based on field measurements of near-surface ground temperature in variated topographic conditions. This approach covers only one dimension in evaluating weathering potential and magnitude in the Carpathian mountain environment.

It is shown that air temperature oscillations can set only the potential (thermally "ideal") period for freeze-thaw oscillations to effectively produce in soil or rock. A good example are the depression areas (e.g. Poiana Stampei, Eastern Carpathians) which, although showing a maximum potential, present a constant ground thermal behaviour with few oscillations, due to persisting snow cover. The impact of seasonal frost is highlighted, as its intensity increases with altitude, enhancing deep freezing of soil-covered or rock surfaces which reflects into the intensity of present periglacial processes, including rock weathering patterns.

High altitude (>2100 m a.s.l.) vertical or steep rockwalls are virtually less affected by the insulating effect of the snow cover. Their thermal behaviour on various exposures and altitudinal settings allowed the distinction of the high

frequency and intensity of diurnal freeze-thaw oscillations on the insolated south-exposed rock facets, compared to the more thermally homogeneous north-exposed surfaces, where few diurnal cycles are recorded but the seasonal frost magnitude is maximum. The rockwalls exposed on East and West present a similar annual thermal evolution, with intensities more close to the northern slopes.

Freeze-thaw regime on the northern and southern rock surfaces indicates that shallow weathering caused by diurnal freeze-thaw action is very active on southern exposures and reduced on North, where deep rock fracturing is more probable to occur, under the action of ice segregation. This correlates with the present distribution and morphometry of compact rock surfaces in the Eastern and Southern Carpathians which, although preserving lithological and structural control at local scale or at the level of the entire range, reflect the action of thermal weathering in steady-state tectonic conditions. Thus, RW high frequency and total covered surface on the northern slopes and their reduced extension on South in relation to the general configuration of these opposite slopes (frequent boulders deposits vs. wide soil-covered surfaces) are indicators of the distinct patterns of thermal weathering which contribute to the medium and long-term rockwalls dynamics.

Acknowledgments The commitment of Răzvan Popescu and Nicolae Cruceru during field campaigns is highly acknowledged. This work was partially supported by the strategic grant POSDRU/159/1.5/S/133391, Project "*Doctoral and Post-doctoral programs of excellence for highly qualified human resources training for research in the field of Life Sciences, Environment and Earth Science*" cofinanced by the European Social Fund within the Sectorial Operational Program Human Resources Development 2007–2013, and by Mirela Vasile's Fellowship for Young Researchers at the Research Institute of the University of Bucharest (ICUB).

References

Amitrano D, Gruber S, Girard L (2012) Evidence of frost-cracking inferred from acoustic emissions in a high-alpine rock-wall. Earth Planet Sci Lett 341–342:86–93

André MF (2003) Do periglacial areas evolve under periglacial conditions? Geomorphology 52:149–164

Burbank DW, Anderson RS (2001) Tectonic geomorphology. Blackwell Science Ltd., 274 pp

Cain N (2004) Mechanical and chemical denudation in mountain systems. In: Owens PN, Slaymaker O (eds) Mountain geomorphology. Arnold, London, pp 132–152

Collins AR (1944) The destruction of concrete by frost. J Inst Civil Eng 23:29–41

Draebing D, Krautblatter M, Dikau R (2014) Interaction of thermal and mechanical processes in steep permafrost rock walls: a conceptual approach. Geomorphology 226:226–235

Duca S, Occhiena C, Mattone M, Sambuelli L, Scavia C (2014) Feasibility of ice segregation location by acoustic emission detection: a laboratory test in gneiss. Permafrost Periglac Process 25:208–219. doi:10.1002/ppp.1814

French H (2007) The periglacial environment, 3rd edn. Wiley

Fukuda M (1971) Freezing-thawing process of water in pore space of rocks. Low Temp Sci Ser A 29:225–229

Girard L, Gruber S, Weber S, Beutel J (2013) Environmental controls of frost cracking revealed through in-situ acoustic emission measurements in steep bedrock. Geophys Res Lett 40:1748–1753. doi:10.1002/grl.50384

Goudie A (ed) (2004) Encyclopaedia of geomorphology, vol I. Routledge, London
Gruber S, Haeberli W (2007) Permafrost in steep bedrock slopes and its temperature-related destabilization following climate change. J Geophys Res 112:F02S18, 10. doi:10.1029/2006JF000547
Gruber S, Hoelzle M, Haeberli W (2004) Rock-wall temperatures in the Alps: modelling their topographic distribution and regional differences. Permafrost Periglac Process 15:299–307. doi:10.1002/ppp.501
Hales TC, Roering JJ (2005) Climate-controlled variations in scree production, Southern Alps, New Zealand. Geology 33(9):701–704
Hall K (2007) Evidence for freeze-thaw events and their implications for rock weathering in northern Canada: II. The temperature at which water freezes in rock. Earth Surf Proc Land 32:249–259. doi:10.1002/esp.1389
Hall K, Thorn C (2011) The historical legacy of spatial scales in cold region weathering: misrepresentation and resulting misdirection. Geomorphology 130:83–90
Hall K, Thorn C, Sumner P (2013) On the persistence of 'weathering'. Geomorphology 149–150:1–10. doi:10.1016/j.geomorph.2011.12.024
Hallet B, Walder JS, Stubbs CW (1991) Weathering by segregation ice growth in microcracks at sustained sub-zero temperatures. Verification from an experimental study using acoustic emissions. Permafrost Periglac Process 2:283–300
Hovius N, Lague D, Dadson S (2004) Processes, rates and patterns of mountain-belt erosion. In: Owens PN, Slaymaker O (eds) Mountain geomorphology. Arnold, London, pp 109–131
Hugget RJ (2007) Fundamentals of geomorphology, 2nd edn. Routledge
Lautridou JP (1971) Conclusions générales des recherches de gélifraction expérimentale. Centre National des Recherches Scientifique, Centre de Géomorphologie de Caen, Bulletin 10:65–79
Magnin F, Deline P, Ravanel L, Noetzli J, Pogliotti P (2011) Thermal characteristics of permafrost in the steep alpine rock walls of the Aiguille du Midi (Mont Blanc Massif, 3842 m a.s.l.). The Cryosphere Discuss 8(3):2831–2866
Matsuoka N (1994) Diurnal freeze-thaw depth in rockwalls: field measurements and theoretical considerations. Earth Surf Proc Land 19:423–435
Matsuoka N (2001) Microgelivation versus macrogelivation: towards bridging the gap between laboratory and field frost weathering. Permafrost Periglac Process 12:299–312. doi:10.1002/ppp.393
Matsuoka N (2008) Frost weathering and rockwall erosion in the south-eastern Swiss Alps: long-term (1994–2006) observations. Geomorphology 99:353–368. doi:10.1016/j.geomorph.2007.11.013
Matsuoka N, Sakai H (1999) Rockfall activity from an alpine cliff during thawing periods. Geomorphology 28:309–328
Micalevich-Velcea V (1961) Masivul Bucegi: studiu geomorfologic. Editura R.P.R, Bucureşti (in Romanian)
Murton JB, Peterson R, Ozouf JC (2006) Bedrock fracture by ice segregation in cold regions. Science 314:1127–1129
Peltier LC (1950) The geographic cycle in periglacial regions as it is related to climatic geomorphology. Ann Assoc Am Geogr 40:214–236
Pogliotti P, Cremonese E, Morra di Cella U, Gruber S, Giardino M (2008) Thermal diffusivity variability in alpine permafrost rock walls. In: Proceeding of the ninth international conference on permafrost, Fairbanks, Alaska, USA, pp 1427–1432
Posea G, Ilie I, Grigore M, Popescu N (1970) Geomorfologie generală. Editura Didactică şi Pedagogică, Bucureşti (in Romanian)
Posea G, Popescu N, Ielenicz M (1974) Relieful României. Editura Ştiinţifică, Bucureşti (in Romanian)
Săndulescu M (1984) Geotectonica României. Editura Tehnică, Bucureşti (in Romanian)
Sass O (2004) Rock moisture fluctuations during freeze-thaw cycles: preliminary results from electrical resistivity measurements. Polar Geogr 28:13–31

Sass O (2005) Rock moisture measurements: techniques, results and implications for weathering. Earth Surf Proc Land 30:359–374. doi:10.1002/esp.1214

Şeclăman M, Anastasiu N (1983) Petrografie. Universitatea din Bucureşti, Note de curs (in Romanian)

Stocker-Mittaz C, Hoelzle M, Haeberli W (2002) Modelling alpine permafrost distribution based on energy-balance data: a first step. Permafrost and Periglac Process 13:271–282. doi:10.1002/ppp.426

Stoenescu M (1951) Clima Munţilor Bucegi. Editura Tehnică, Bucureşti (in Romanian)

Summerfield MA (1991) Global geomorphology: an introduction to the study of landforms. Longman Scientific & Technical, Harlow, UK

Tricart J (1972) Geomorphology of cold regions. Trans. Watson E. McMillan, London

Tufescu V (1966) Modelarea naturală a reliefului şi eroziunea accelerată. Editura Academiei Republicii Socialiste România (in Romanian)

Urdea P (2000) Munţii Retezat. Studiu geomorfologic. Editura Academiei, Bucureşti (in Romanian)

Vasile M, Pleşoianu A, Vespremeanu-Stroe A (in progress) Rockwalls morphometry and distribution in the Romanian Carpathians

Vasile M, Vespremeanu-Stroe A, Popescu R (2014) Air versus ground temperature data in the evaluation of frost weathering and ground freezing. Examples from the Romanian Carpathians. Rev Geomorfol 16:61–70

Vasile M, Pleşoianu A, Vespremeanu-Stroe A (2015) Distribuţia şi morfometria pereţilor stâncoşi din Carpaţii Româneşti. Influenţa caracteristicilor litologice şi a dezagregării. Simpozionul Naţional de Geomorfologie, Sf. Gheorghe, 21–24 May 2015

Vespremeanu-Stroe A, Vasile M (2010) Rock surface freeze-thaw and thermal stress assessment in two extreme mountain massifs: Bucegi and Măcin Mts. Rev Geomorfol 12:33–44

Vespremeanu-Stroe A, Mihai B, Cruceru N, Preoteasa L (2004) The freeze-thaw cycles frequency in the Romanian Carpathians. Rev Roum Géogr 48:147–155

Viles HA (2013) Linking weathering and rock slope instability: non-linear perspectives. Earth Surf Proc Land 38:62–70. doi:10.1002/esp.3294

Walder J, Hallet B (1985) A theoretical-model of the fracture of rock during freezing. Geol Soc Am Bull 96:336–346

Washburn AL (1979) Geocryology. A survey of periglacial processes and environments. Arnold, London

Williams PJ, Smith MW (2008) The frozen Earth. Fundamentals of geocryology. Cambridge University Press, Cambridge

Chapter 9
Glacial Cirques in the Romanian Carpathians and Their Climatic Implications

Marcel Mîndrescu and Ian S. Evans

Abstract This section summarizes a morphometric analysis of glacial cirques from the Romanian Carpathians, further inferring climatic information from spatial patterns of morphometric traits. Results derived from the detailed statistical analysis of a comprehensive database of glacial cirques are presented briefly. The distribution of cirques by altitude, aspect, size, classification (cirque grade), and geology is presented and related to controlling factors. New contributions concerning the palaeoglaciation level during Late Pleistocene in the Romanian Carpathians, and the direction of prevailing winds during glaciation are provided. Statistical distributions of cirque size and shape are outlined and illustrated. A comprehensive data base of all glacial cirques in the Romanian Carpathians is now available to guide or substantiate further comparative or/and interdisciplinary studies. It is also possible to rank the mountain ranges by the degree of glacial modification.

Keywords Glacial cirques · Controlling factors · Morphometric analysis · Romanian carpathians

Carpathian Glaciation: Background

The Carpathians are a young, mid-latitude mountain system. In Romania they are between 45° and 48° North, sheltered from Atlantic maritime influences but a long way from the arid interior of Asia. Romania has a remarkable variety of mountain ranges that rise high enough to have supported glaciers in the last extensive glaciation and probably in several previous glaciations. Erosive glaciers persisted long enough to erode cirques and troughs at many valley heads. Glaciated ranges

M. Mîndrescu (✉)
Ștefan cel Mare University, Universității 13, 720229 Suceava, Romania
e-mail: marcel.mindrescu@gmail.com

I.S. Evans
University of Durham, Durham, UK
e-mail: i.s.evans@durham.ac.uk

M. Rădoane and A. Vespremeanu-Stroe (eds.), *Landform Dynamics and Evolution in Romania*, Springer Geography,
DOI 10.1007/978-3-319-32589-7_9

currently have over 1400 mm of precipitation per year, and less than 1800 h of sunshine (Mîndrescu et al. 2010).

Although the tectonics of the Romanian Carpathians are complex and varied, many mountain ranges reach altitudes between 1800 and 2500 m and three just exceed 2500 m. This has been sufficient to produce cirque and valley glaciers during the colder periods of the Late Quaternary, but not to produce extensive ice caps. Urdea et al. (2011) estimated Equilibrium Line Altitudes (ELAs) of former glaciers for 17 regions of minor glaciation as between 1497 and 1719 m, averaging 1610 m. These low values reflect conditions at maximum glaciation (lowest ELA) and can be related to the altitudes of the lowest cirque floors, not the average.

The early work of Urdea (2004) on degrees of weathering, and of Reuther et al. (2007) and Urdea and Reuther (2009) on cosmogenic exposure ages in the Transylvanian Alps (Southern Carpathians) has recently been revised by Ruszkiczay-Rüdiger et al. (2015). It now seems that glaciation in Romania was in phase with that elsewhere in Europe: there were at least two major glaciations in the Late Quaternary, including the Last Glacial Maximum (Würmian: Marine Isotope Stage 2). Furthermore, it has increasingly become evident that some cirques in three of the ranges with valley glaciers (Retezat, Făgăraş and Rodna) sheltered small glaciers in the Late Glacial Younger Dryas stage (Gheorghiu et al. 2015).

Distribution of Cirques

All summits rising above 2000 m altitude supported glaciers. Valley glaciers were produced in the highest mountains: Făgăraş (reaching 2544 m), Retezat (2509 m) and Parâng (2518 m), and in the Rodna Mountains of northern Romania (2303 m). Retezat and Făgăraş, respectively, have 238 and 116 km^2 above 1800 m; all other ranges have less than 75 km^2. Each valley glacier had its source in a cluster of cirques. Numerous cirques cluster around the plateaux of the Bucegi (2505 m), Iezer (2470 m) and Godeanu Mountains (2291 m). Cirques are found in all the major ranges of the Transylvanian Alps (TA). Many other ranges, not quite so high, produced isolated cirques: the Maramureş ranges, Tibleş, Călimani, Leaota, Cindrel, Lotru, Latoriţei, Căpăţânii, Şureanu, Ţarcu, Muntele Mic, and Bihor, each reaching between 1800 and 2250 m. A single (but well-developed) cirque is found on Malaia (1662 m) in the Siriu Mountains of the 'Carpathian Bend'.

It is estimated that altogether at least 631 cirques formed, 547 in the Transylvanian Alps, 81 in northern Romania (we include 14 on the Ukrainian side of the border ridge as it is best to cover all slopes of a mountain) and three in Bihor Mountains (Apuseni) in the west (Fig. 9.1). Recognition of a landform inevitably involves a subjective element, and there may be some revision of these numbers, but Ardelean et al. (2013) show that convergence is achieved for cirques once a precise operational definition is applied. Urdea et al. (2011) tabulated numerous further small glaciers (mainly niche glaciers and 'ice aprons') which do not appear

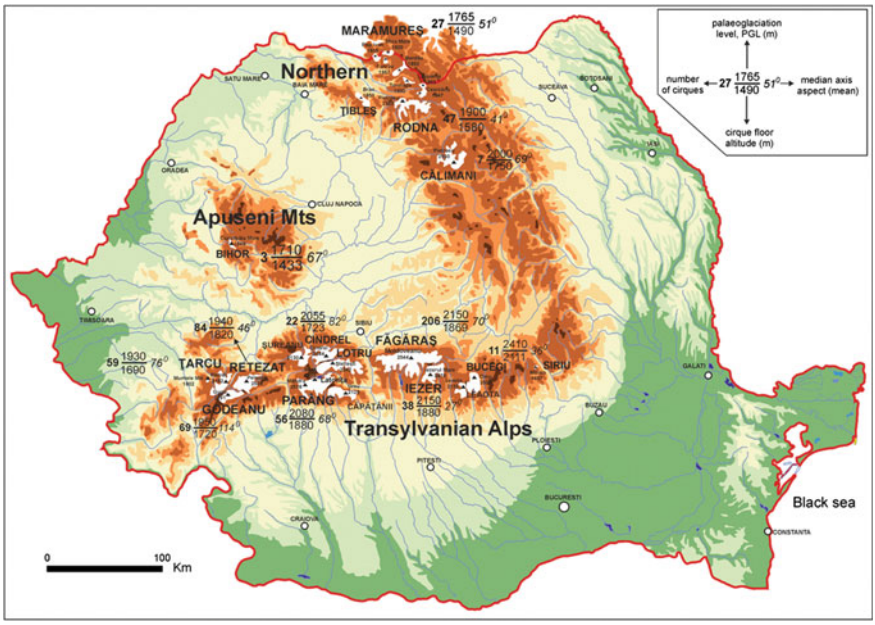

Fig. 9.1 Distribution of the glacial cirques in the Romanian Carpathians (clockwise ordering): Maramureş (*27*), Rodna and Ţibleş (*47*), Călimani (*7*), Siriu (*1*), Bucegi (*11*), Leaota (*1*), Iezer (*38*), Făgăraş (*206*), Lotru and Cindrel and Şureanu (*22*), Parâng and Latoriţa and Căpăţânii (*56*), Retezat (*84*), Godeanu (*69*), Ţarcu and Muntele Mic (*59*) and Bihor (*3*)

to have developed cirques, probably because they were too short-lived. These had Equilibrium Line Altitudes as low as 1544 m.

The distance between the northernmost Carpathian cirque, Dezeskul Grun (Northern Maramureş Mts) and the southernmost, Groapa Olanului Mare (Godeanu Mts) is 302 km, whereas the longitudinal span of the cirque population is 286 km between La Blid (Muntele Mic) and Malaia (Siriu Mts). Carpathian cirques are located in 14 major drainage basins and distributed as follows: Olt (153), Strei (151), Argeş (110), Tisa (48), Jiu (39), Timiş (30), Cerna (28), Dâmboviţa (28), Bistriţa (22), Someş (8), Ialomiţa (8), Arieş (3), Prut (2) and Buzău (1). While cirques are found in 19 Carpathian massifs, 87 % of the cirque population pertains to just 7 mountain groups: Rodna, Iezer, Făgăraş, Parâng, Retezat, Godeanu, and Ţarcu. Of these, Făgăraş and Retezat Mts hold the highest density of cirques, and these alone contain 46 % of the 631 cirques. It may therefore be concluded that cirque glaciers formed especially in the highest massifs, as well as the westernmost mountain areas.

The general eastward layout of main ridges resulted in an uneven distribution of cirques on the two slopes/mountainsides, i.e. northern and southern: 57 versus 42 %. At this broad scale, it would appear that Carpathian cirques exhibit only moderate glacial asymmetry; however, this varies regionally with Northern

Romania (NR: Northern Romanian Carpathians) having 83 % of cirques formed on northern slopes and just 16 % on southern slopes. Conversely, the cirque population of the Transylvanian Alps is overall rather evenly spread on the two mountain sides (northern—52.5 %, southern—47.5 %), albeit distributions vary significantly depending on the massif.

Ranges Apparently Lacking Cirques

One peculiar aspect of glaciation in the Romanian Carpathians regards the small number, or absence, of cirques in mountain areas similar in altitude, morphology, or position with clearly glaciated ranges. How can this be explained? Such instances are frequent, particularly in the Eastern Carpathians (EC), but are not absent from the Transylvanian Alps (e.g. Piatra Craiului, Căpăţânii, Şureanu/Vârful lui Pătru, Vâlcan Mts), either. In the EC (e.g. Suhard, Bistriței, Ceahlău Mts) this situation can be explained partly by local structural or topographic conditions, but largely by the triad of controls forming the so-called *ice cube* (Mîndrescu 2006): latitude, altitude and distance eastward (from the western edge of the EC mountain chain, and thus from oceanic climatic influences). As expected, in the Eastern Carpathians cirques are clustered in the northern part of the range (NR) which is also the highest. Continentality increases eastward in the EC, so that susceptibility to glaciation also decreases eastward. Coincidentally, the peak elevation line is located in the western extremity of the EC range, acting as a major orographic barrier and effectively reducing the precipitation and susceptibility to glaciation eastward. Thus, eastward location combined with altitude can best explain the absence of active cirque glaciers from major ranges such as Suhard, Giumalău, Bistriţei, Ceahlău and Baiu Mts, as well as the scarcity of cirques in Siriu and Leaota Mts.

Two additional controls, both related to the geological structure, had lasting effects on the forms of glaciation, mainly in the Eastern Carpathians: suspended synclines and Neogene volcanic and subvolcanic bodies. Two ranges rising above 1900 m a.s.l. consist of suspended synclines, i.e. Ceahlău, Ciucaş (EC) and Piatra Craiului (TA); in these cases, the high gradients typical for syncline flanks likely prevented the formation of cirque glaciers. Furthermore, the occurrence of young volcanic structures (as in Ţibleş, Călimani or Gurghiu Mts) or subvolcanic bodies (Toroiaga in Maramureş Mts) also interfered with the formation or full development of cirque glaciers due to steep slopes and the lack of preexisting topography with hollows facilitating ice accumulation.

Altitude

Cirque floor altitudes range between 1330 and 2360 m, and average 1938 m (median 1960 m). They are lower in Northern Romanian Carpathians and in Bihor: the 81 cirques in the north, in Maramureş, Ţibleş, Rodna, and Călimani have floor modal altitudes averaging 1696 m, while the three cirques in Bihor (central western Romania) average 1473 m. The 1030 m range in altitudes reflects firstly climatic and secondly topographic differences between mountain ranges. Floor altitudes vary considerably within each range, due to local topographic conditions and the variation in snowline (ELA) as climate varied during the Late Pleistocene. Altogether, in the majority of cirques from the Romanian Carpathians the floor altitudes range from 1800 to 2000 m (which is rated as the most intensely glaciated level).

In the Transylvanian Alps from Ţarcu to Bucegi, there are 546 cirques with a mean floor altitude of 1978 m: the range is from 1470 to 2360 m. There is broad variation within each range, but in general they are higher to the east, rising at 0.755 m/km, over 235 km (Fig. 9.2). Temperature differences being small, this trend is attributed to a reduction in precipitation, implying that snow was brought by winds from the west. The trend is greatest for south and east facing cirques (1.075 and 1.004 m/km, respectively, by 90° quadrant); it is only 0.360 and 0.395 m/km for north- and for west-facing cirques. Cirque floors in Lotru, Cindrel, and Şureanu) are over 100 m lower than those farther south in Parâng, sheltered from northwest winds. Variations of floor altitude with aspect are significant only when this eastward trend is allowed for. Averages are 1966 m for the North quadrant, 1979 m for the East, 1973 m for the South and 2010 m for the West.

In Northern Romania cirques formed mainly near the western edge of the EC mountain chain on crystalline and volcanic rocks, where ranges exceed at least 1800 m a.s.l., particularly in the northern sector. For example, the northernmost cirques in the Romanian Carpathians, known as the Mica Mare group, occur just below summits with altitudes between 1820 and 1713 m. Cirque floor altitudes in

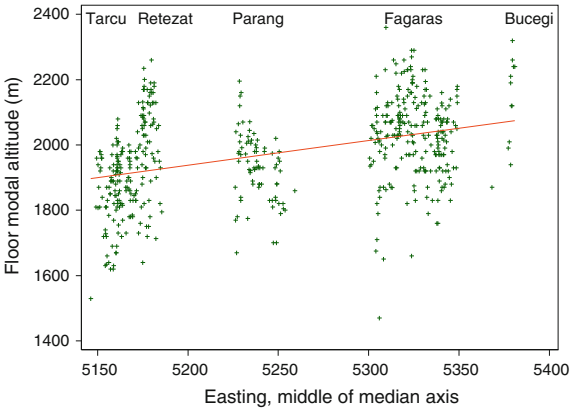

Fig. 9.2 Cirque floor altitudes in the Transylvanian Alps, from Ţarcu to Bucegi

Northern Romania decrease with latitude (northward), and increase eastward, such that the floors are higher in the ranges on the Moldavian side.

The highest Carpathian cirques are in the Transylvanian Alps (Southern Carpathians), with an average floor altitude 280 m higher than in Northern Romanian cirques. In 70 % of South Carpathian cirques the floor altitude ranges between 1800 and 2100 m. While cirque glaciers could fully develop wherever the peak altitude was at least 1900 m, the average altitude of summits which support cirques in the Transylvanian Alps is 2275 m; some of the floor altitudes compare with altitudes of the highest peaks in Rodna Mts. Furthermore, floor altitudes span over 800 m, significantly larger compared to Northern Romania. Cirque floor altitudes in the Transylvanian Alps were determined mainly by summit altitudes and the longitudinal position of mountain ranges within this sector of the Carpathians; the highest cirques are found in the '2500 elevation group' (i.e. massifs rising above 2500 m a.s.l.) or in the easternmost ranges, farthest removed from oceanic climate influences.

The overall southeastward rise of cirque floors in Romania should be regarded as the resultant of two components: an eastward rise of 204 m along the Transylvanian Alps, related to diminishing precipitation; and a southward rise of 283 m in northern Romania, due partly to rising temperatures but also to diminishing precipitation. Cirques are thus lowest in the north and west of Romania (Mîndrescu et al. 2010).

Aspect and Wind

The tendency to face north (poleward: solar radiation and shade effect) is combined with an eastward tendency (mainly because of snow drifted to leeward slopes by wind) which is strongest in the Transylvanian Alps, where it increases westward (Fig. 9.3). The mean axial aspect is 063° overall, but 042° for northern Romania and 069° for the Southern Carpathians. A mean of 093° for Godeanu–Ţarcu implies formative wind from north of west, as does the greater wind effect in Făgăraş than in Iezer, which lies southeast of Făgăraş (Mîndrescu et al. 2010), plus the cirques in Parâng being lower than those to its north. Retezat and Făgăraş are the most dissected ranges, with the sharpest ridges; this is because of their more symmetrical glaciation (lower vector strengths), related to higher summit altitudes. Although Parâng is also high, extensive summit plateaux have been preserved there and in Lotru and Cindrel, permitting a greater wind-drifting effect.

55 % of Carpathian cirques face north, northeast, and east. Of the 8 aspect classes, east-facing cirques are the most numerous (130); 68 % of cirques have aspects between 0° and 180° (eastward components), and just 32 % have aspects from 180° to 360° (westward). Moreover, northward cirques are more frequent (59 %) compared to southward ones (41 %). Based on these ratios, an eastward tendency of Carpathian cirques appears to be prevalent, especially for the Southern Carpathians (TA), despite the northward and southward orientation of the main

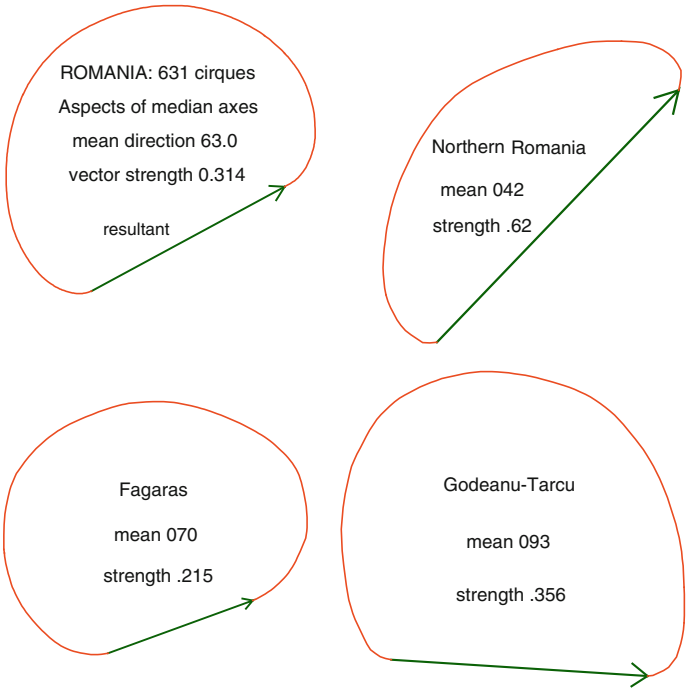

Fig. 9.3 Mean axial aspect of cirques in the Romanian Carpathians (*upper-left*), Northern Romania (*upper-right*), Făgăraş Mts (*bottom left*) and Godeanu–Ţarcu Mts (*bottom-right*)

slopes of glaciated ranges. The two main tendencies in terms of aspect, eastward and northward, are more balanced in northern Romania (NR).

Selective glacial asymmetry is derived from the analysis of well-defined cirque populations in terms of location and degree of development. Main crest asymmetry is the most relevant type we encountered and is applicable solely to glacial cirques tangent to the main crests. The most outstanding main crest asymmetry documented in the Romanian Carpathians is in the Făgăraş range which hosts the largest cirque population in Carpathian arc (206). The total mountain area measured above the 1500 m a.s.l. contour line is 649 km^2, of which the northern slope accounts for just 188.5 km^2 (29.5 %) and the southern slope for 451.5 km^2 (70.5 %). A measure of asymmetry computed from the number of cirques located on the two slopes is the north/south ratio, yielding 0.75 for Făgăraş (88 cirques on north slope/118 cirques on south slope: inverse asymmetry). However, when solely cirques tangent to the main crest are considered, the asymmetry is 1.36 (68 on north slope/50 cirques on south slope: normal asymmetry). Thus, the main crest asymmetry is normal and suggests that glaciation was more intense on the northern slope of Făgăraş Mts (Mîndrescu 2009).

The eastward tendency is strongest for the highest Romanian Carpathian cirques (104 with floors above 2100 m a.s.l., with a vector mean direction of 115°).

The 414 cirques with floors between 1800 and 2100 m (inclusive) have a vector mean direction of 055°. The lowest cirques (112 with floors below 1800 m a.s.l.) typically have NE aspects (mean 053°). This impacted on cirque size; thus, north-, northeast- and southeast-facing cirques are the largest and best-developed among Carpathian cirques. Thus, while the lee effect acted as the main control in western and/or higher altitude ranges, the shade effect was determinant in northern and lower mountains.

The northward and eastward tendencies are only slightly evident in cirque floor altitudes. In northern Romania, cirques facing 037° have floors 117 m lower than those of opposite aspects; and in the Făgăraş, those facing 346° are 113 m lower than opposite. Elsewhere, however, there is less variation with aspect.

The palaeo-ELA estimates tabulated by Urdea et al. (2011) show remarkably little variation between north-facing and south-facing glaciers, with the latter usually less than 100 m higher. Kuhlemann et al. (2013) corrected their palaeo-ELA estimates for 17 valleys in the central Făgăraş Mountains to give values between 1631 and 1900 m. The lower values are for southward aspects, which they attributed to moisture brought by winds from the southwest. This contradicts the cirque evidence mentioned above, as well as the trend of aeolian features in the Pannonian and Oltenian plains. An alternative explanation is that that plateau remnants on the north–south ridges between the south-flowing Făgăraş glaciers provided further sources of wind-blown snow, even from northwest winds, and that increased accumulation there (see also Mîndrescu 2004).

Size

Romanian cirques are comparable in size to those elsewhere (Barr and Spagnolo 2015; Evans and Cox 2015), and generally intermediate between those measured in Britain and in British Columbia. Width, length and height range are centred around median values of 596, 650 and 260 m respectively (Fig. 9.4), and mean values are rather higher. Distributions are skewed, with small cirques more frequent than large ones: thus Mîndrescu and Evans (2014) provided analyses on logarithmic scales. Cirques around the highest mountains are somewhat larger than lower or isolated cirques. Size varies over one (decimal) order of magnitude, with length and width always between 180 and 2230 m, and height range between 115 and 870 m (Fig. 9.4). Cirque areas vary between 4 and 377 ha, averaging 44 but with a median of 32 ha.

Based on the ratio of horizontal axes (W/L), a large number of cirques from Romanian Carpathians (47 %) rank as circular (W/L = 0.80–1.20) (i.e. developed evenly along the two horizontal axes), of which 12 % are nearly perfectly balanced. Of the remainder, 37 % rank as broad cirques (W/L > 1.20), whereas just 16 % are long cirques (W/L < 0.80) (i.e. developed more along the median axis). In just 4 cirques the length is twice as great as the width, whereas in another 16 this ratio is reversed (width = 2 × length); in 98 instances the width is 1.5 the size of the length

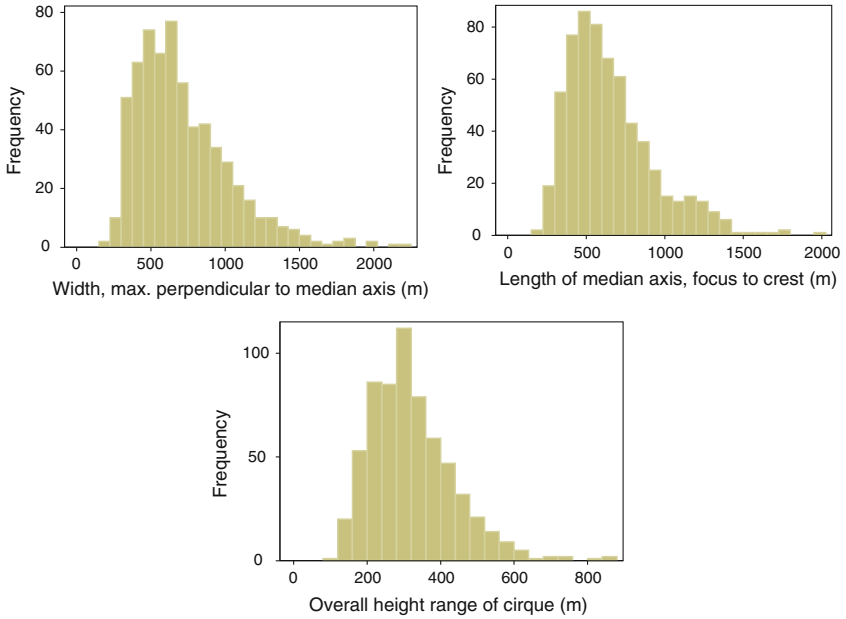

Fig. 9.4 Romanian cirque sizes: length, width and height

(broad cirques), while in 41 the ratio is inverse (length = 1.5 × width; trough cirques). The greater occurrence of broad cirques compared to trough cirques indicates a typical pattern of development for Carpathian cirques by lateral-regressive glacial erosion in the rock mass. Moreover, morphometric values help distinguish between glacial cirques and non-glacial (fluvial) valley heads.

Headwall height values are an additional criterion for cirque classification, according to which in many cirques (47 %) headwall height is in the average (100–199 m) range, defining the typical headwall for Carpathian cirques, whereas only 4 % (26 cirques) have low headwalls (under 100 m). 35 % have tall headwalls (200–300 m inclusive), and a distinctive type includes cirques with very tall headwalls exceeding 300 m in height, accounting for 14 % of all cirques. Six of these have headwalls over 500 m high, none of which are classic cirques; some may possibly be glacial trough-heads instead of actual cirques. The morphometric range of the headwall points toward a minimum value (threshold) of headwall height, below which gradients become inadequate for cirque glaciers to be erosive. This equals 60 m in Northern Romania, 70 m in the Transylvanian Alps and 80 m in Bihor Mts.

As regards the variation of cirque size with aspect, differences exist between north facing and south-facing slopes, with the latter being comparatively smaller in general. However, in terms of area ratios, south-facing cirques have floors better calibrated (adjusted) to overall cirque dimension, which could arise from the nature of less rigid, southern glaciers: the increased intensity of insolation ‘fuelling’

south-facing glaciers resulted in 'warmer', more dynamic bodies of ice. Albeit not as productive as north-facing glaciers in terms of cirque area enlargement, they were more effective in shaping floors than headwalls.

By region, the largest cirques are in Rodna: median length 742 m, width 729 m and amplitude 310 m. It is followed by Făgăraş in vertical dimensions, but by Bucegi in horizontal: in fact, median width (734 m) is slightly greater for Bucegi although means are much greater for Rodna (816 cf. 727 m for length and 868 cf. 780 m for width). With both smaller and larger cirques than Bucegi, Rodna has much higher standard deviations. Maramureş and Călimani have the smallest cirques in width and length, but Bihor and Ţarcu have the smallest in vertical dimensions (Mîndrescu and Evans 2014).

Shape

Cirque shape was most often described when defining glacial cirques as 'hollow spaces' of various sizes, enclosed on three sides and open downstream. In fact, the shape of the cirque is given by headwall curvature around the floor. The plan closure of the cirque best defines both the shape and the erosion process exerted by cirque glaciers. Depending on their degree of maturity, they increasingly eroded into the mountain, becoming enclosed. Unlike other evidence of glacial erosion, cirque plan closure was the least altered following deglaciation.

To assess the plan shape of cirques from the Romanian Carpathians the plan closure was determined, according to which the cirque population was ranked in 6 shape classes: very open (below 90°), open (90°–130°), slightly open (130°–170°), troughs (170°–190°), slightly closed (190°–230°), and closed (above 230°). This variable illustrates the degree of downstream opening of glacial cirques. The vast majority of Carpathian cirques are open or slightly open (80 % are between 85° and 188°), whereas very open cirques are more numerous than troughs. Just 7 % are slightly closed and 2 % are closed. Considering the low percentage of cirques with lake basins (20 %), regarded as an indication of glacial maturity, it may be assumed that approximately 3/4 of the cirques were developing during the late stages of glaciation and just 1/4 had reached maturity, as suggested by their plan closure. Surely, cirque shape was influenced by several factors aside from the intensity of glaciation, which either accelerated or slowed their evolution, among which altitude, continental climate and geology (lithology and structure) are notable.

Plan closure averages 137°, and varies between 37° and 283° (Fig. 9.5). The analysis of plan closure revealed the existence of three types of cirques with different shapes: (i) cirques with values ranging from 92° to 122°, typical for glacial areas with few cirques (under 8, with the exception of Ţarcu); (ii) cirques between 125° and 143°, common for glacial areas from the extremities of Transylvanian Alps and Northern Carpathians; and (iii) cirques above 143° which are most frequent in massifs peaking above 2500 m a.s.l. or those with average cirque populations (Cindrel and Lotru).

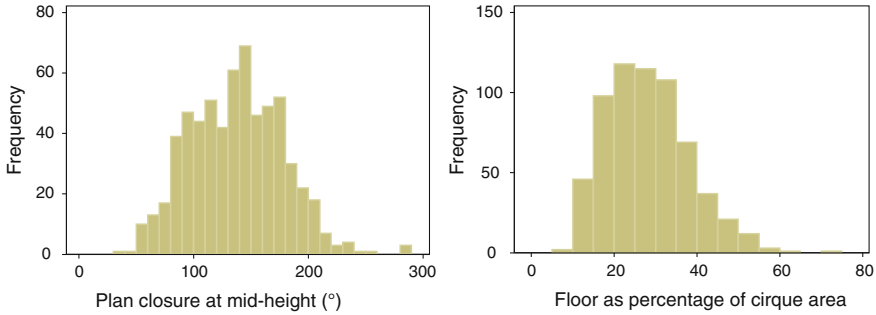

Fig. 9.5 Shape (plan closure) and floor area coverage of Romanian cirques

Plan closure varies with aspect, such that north-facing cirques from Retezat or Făgăraş have greater closure compared to opposing slopes. North, northeast, east and southeast-facing cirques typically have the most developed, mature shapes, consequent both on reduced insolation on north and northeast-facing slopes and on deflation of snow which favoured nival build up on east- and southeast-facing slopes. Lower insolation, in particular, favoured north-facing slopes (especially in inner sectors) of more massive mountain ranges (i.e. Făgăraş, Parâng, Retezat, Rodna), whereas deflation occurred mainly onto sheltered slopes of Maramureş, Godeanu, Ţarcu or southern Făgăraş.

Low floor gradients together with high headwall gradients define the degree of evolution of glacial cirques; thus the most advanced cirques, with gently sloping or even counter-slope floors and steep headwalls (profile closure above 50°) are those of Făgăraş, Retezat, Godeanu, Parâng, and Rodna, which are either high altitude mountain areas or the northern and western extremities of the Romanian Carpathians. Based on headwall height and gradient, cirques were ranked into several classes, of which deep cirques (with headwalls over 300 m high and gradients above 50°) are the most spectacular. In the Romanian Carpathians 11.4 % (75 cirques) rank as deep cirques; half of these are in the Făgăraş Mts (50 %), but they are present also in other major glacial areas such as Maramureş, Rodna, Iezer, Bucegi (1), Parâng, Retezat and Godeanu.

The minimum floor gradient in the Romanian Carpathians averages 8.4°, ranges between 0° and 20° and is bimodal, with 101 cirques having flat floors or lakes, recorded as 0°. Only 10 % of cirques have minima above 15.1°. In terms of maximum headwall gradient, values range from 36° to 75°, albeit 80 % are between 40° and 64°. Maximum gradient averages 51°. Cirques with low gradient headwalls (below 40°) indicate poor development and primitive cirque shape, and account for 10 % of all cirques (63). Conversely, headwall gradients exceeding 60° (in 122 cirques) indicate advanced, well-developed cirques on strong rocks and are typical for higher grade cirques.

The most important component of cirque shape is the overall gradient along the median axis, from crest to threshold. This averages 24°, and in 90 % of cirques it is

between 15° and 33°, providing ideal conditions for rotational flow in a glacier that fills the cirque up to the centre of the crest. Cirques on higher mountains tend to have steeper headwalls and larger, flatter floors, and to bite more deeply into the mountains (to have greater closure in plan). Larger cirques tend to be better developed, with greater plan closure and maximum gradient, and lower minimum gradients. As cirques develop, they enlarge in length and width much more than in vertical dimensions.

Only 41 % of cirques have significant cols (depressions of more than 30 m in their crests). Multiple cols are found mainly in the Făgăraş, Retezat and Rodna mountains. In almost all cirques, floors cover between 10 and 55 % of the cirque map area (range 8–71 %: Fig. 7.5). A larger, flatter floor is indicative of better cirque development and greater glacial erosion.

Regionally, cirques in Călimani are much poorer than elsewhere, with easily the worst plan and profile closure, Grade and maximum gradient, as well as the lowest relative floor area and number of cols and the highest minimum gradient. Bihor generally scores poorly and Maramureş, Iezer and Ţarcu also have poor scores. Maximum gradient is highest for Făgăraş, Retezat and Parâng, while minimum gradient is lowest for Retezat, Parâng and Lotru–Cindrel. The three latter have the highest overall Grade and all four together with Bucegi have the highest plan closures (mean 140°). Cols are most frequent in Rodna, Retezat and Făgăraş and floors are proportionately larger in Ţarcu and Retezat (Mîndrescu and Evans 2014).

Classification

Cirques may be graded into five classes of degree of development and clarity of definition and delimitation (Evans 2006). This reflects plan closure, maximum gradient, minimum gradient, roundness of headwall in plan, sharpness of crest and more subjective assessments such as presence of a clear down-valley limit (threshold) and simplicity of concavity in plan and profile. The first three of these are the more reliably quantifiable and, in combination, can provide a good estimate of cirque Grade, but the subjective assessment is also important. Of the 631 cirques, 62 are recognized as ‘classic’, 216 are ‘well-defined’, 249 ‘definite’, 76 ‘poor’ and 28 ‘marginal’ (debatable): see illustrations in Mîndrescu et al. (2010). Larger and higher cirques are more likely to have a better Grade. Higher grade cirques tend to be larger in horizontal more than in vertical dimensions. The steady variation of size and shape variables with Grade is illustrated in Mîndrescu and Evans (2014).

The vast majority of Carpathian cirques rank as well-defined and definite (74 % of the total cirque population); the remaining 26 % are classic cirques (10 %) and poor or marginal (16 %). Figure 9.6 shows examples of each Grade. Based on this distribution the high intensity of cirque glaciation in the Romanian Carpathians may be inferred, as well as the short-life of glaciers during glaciation in the Romanian Carpathians.

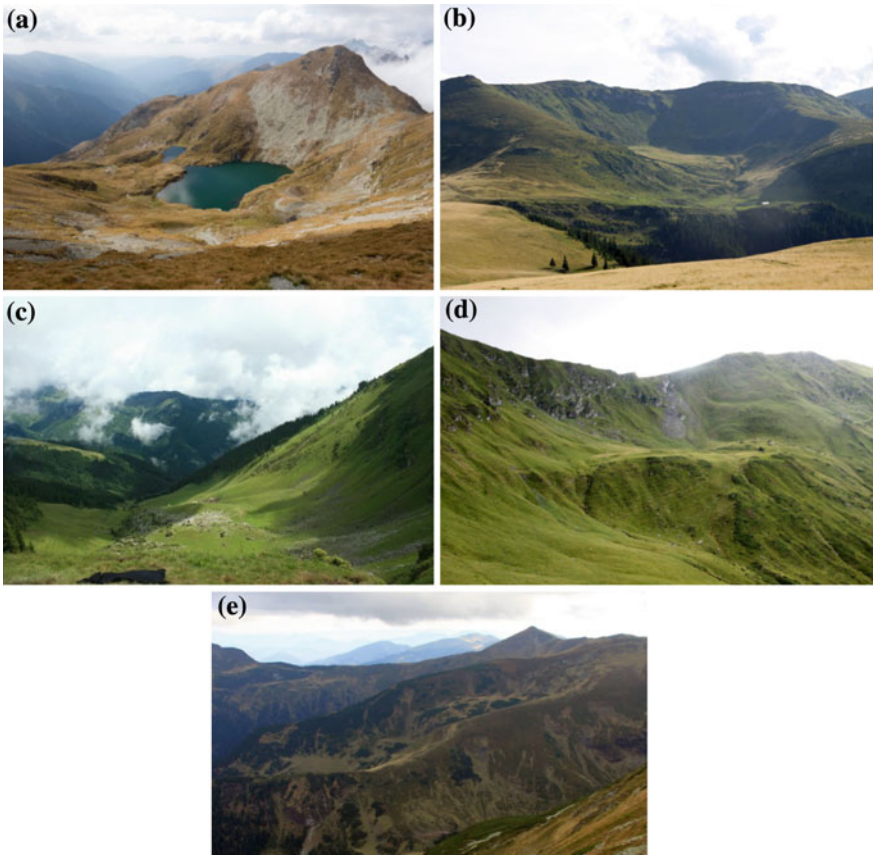

Fig. 9.6 Examples of cirque development in five grades. **a** Capra in the Făgăraș, a *classic* cirque with a large rock basin divided into two lakes. **b** Izvorul Cailor, a *well-defined* cirque in the Rodna Mts with a well-developed headwall and floor, but no lake. **c** Groapa Julii, a *definite* cirque in the Maramureș Mts with a moderate headwall curved around an outsloping floor. **d** Putredu Superior in the Rodna Mts, a *poor* cirque because of the gentle headwall and irregular floor. **e** Buhăiescu Mic in the Rodna Mts, a *marginal* cirque because of a very poor headwall and floor

Classic cirques are the best-developed and have all the features of ideal cirques, albeit most are lacking ample glacial basins such as Bucura or many in the High Tatras. These cirques have a longer history of glaciation (i.e. were glaciated during several glacial periods), therefore are more evolved and larger in size.

As regards poor and marginal cirques, doubts have been expressed about their origin. Whereas they were most likely subjected to the action of ice in the shape of cirque glaciers (the most common glacier type in the Romanian Carpathians), in some instances cirque-like landforms may have resulted from other processes. The genetic processes which could best emulate the cirque shape are deep-seated rock

slope failures, which can produce hollows (scars) resembling poor cirques (Turnbull and Davies 2006), although those in deglaciated ranges are commonly on trough-sides and only a few are likely to form cirques (Jarman 2006; Wilson and Jarman 2015).

The development of nested cirques is relatively common in the Romanian Carpathians, resulting from the succession of several glacial phases acting on a less than resilient yet structurally complex geological substrate. 73 large cirques contain one or more inner, higher cirques. These are found especially on the higher and more heavily glaciated mountains, rising 450 m above former Equilibrium Line Altitude: 63 of them are in five ranges: Făgăraş, Retezat, Godeanu, Parâng and Rodna.

Geology

According to the geological distribution, the most numerous cirques formed on gneiss and paragneiss (43.3 %), particularly those in Făgăraş and Godeanu ranges. This mapped lithology includes small extents of various other types of rocks, and ranks among the most mixed compared to the other mapped categories. The second largest group of cirques formed on granite (mainly in Retezat, Ţarcu and Parâng), followed by those on epimetamorphic schists (all cirques from Iezer, Jupania in Maramureş, Muntele Mic, and Bihor) and micaschists (Rodna and Parâng). Other cirques (albeit in small numbers) are on flysch and arkose (Maramureş and Godeanu), crystalline limestone (Făgăraş) and conglomerate (Bucegi, and Bardău cirques in Maramureş), diabase and diabase tuff (Maramureş and Godeanu) and andesite (Călimani, Ţibleş, and Toroiaga in Maramureş).

The higher mountains are on granite and gneiss and these have well-formed cirques, with a disproportionate number of large lakes, generally basins eroded into bedrock. Major lake basins are found in 11 % of cirques, but 26 % of granite cirques. The largest and best-developed cirques, however, are on mica-schist. The poorest and narrowest cirques are on andesite, which includes all those in the Călimani and Tibleş Ranges.

Geological structure (i.e. the disposition of strata) is another control of cirque development. Depending on the median axis of the cirque glacier and the main structural lines, two major tendencies are manifest in the development of cirques: either parallel or transverse to bedding. In the former case, cirque length increased significantly through headwall collapse leading to the formation of trough cirques with near horizontal floors which often lack evident cirque lips. Conversely, transverse cirques evolved more towards the sides of the headwall, thus increasing the plan closure.

Discussion: Origins

Turnbull and Davies (2006) suggested that many cirques formed by deep-seated rock slope failure, especially from earthquakes as these tend to produce failure on the upper part of a hillslope, whereas rainstorm-related failures tend to be lower on slopes. In Romania, earthquakes are most frequent around the Carpathian Bend, the southern end of the Eastern Carpathians. This, however, is a region with no cirques. Cirques are confined to higher mountains, and their strong correlation with evidence of glaciation (moraines, striations, facetted stones) supports the traditional interpretation, that they are formed by glacial erosion.

Cirques are formed by glaciers, not only cirque glaciers but also at the heads of valley glaciers with fairly steep surface gradients. The existence of cirques also encourages the formation and endurance of glaciers. Erosion of valley-head and valley-side concavities provides sheltered localities where wind-blown snow comes to rest, and shade that reduces melting from solar radiation. It is this positive feedback that makes cirques such distinctive landforms, and enduring evidence of the presence of erosional glaciers.

Conclusions

Cirque glaciation is characteristic of many mountain ranges in Romania. Some were just high enough to support small glaciers forming isolated cirques, but the highest ranges generated larger glaciers around whose sources many cirques developed. Cirques on higher mountains developed further, probably because the glaciers occupying them lasted longer. These cirques are larger, better developed and more complicated (more inner cirques nested within large outer cirques). They cover a broader range of aspects and are often back-to-back, producing sharp ridges with cols. Nearby, however, fragments of summit plateaux survive, showing that summits have not been lowered much by glaciation (i.e. by cirque development). Summit plateaux in the Godeanu, Ţarcu, Parâng, Lotru and Cindrel Mountains have clearly not been lowered by glaciation.

The distribution of glaciers and thus of cirques was influenced by differential solar radiation and by wind. The effect of winds from the west was considerably greater in the Transylvanian Alps (Southern Carpathians) than in northern Romania. At least in the west (e.g. Godeanu Mountains), there is evidence of winds from north of west. The variation of cirque floor altitudes, over some 1000 m, suggests that higher and lower cirques may have developed in different climates, and it is possible that the direction of snow-bearing winds varied.

Romanian cirques are believed to have been eroded by glaciers in the last few glaciations of the Late Quaternary. Analysis and combination of seven measures of degree of glacial modification and cirque development, by region, led Mîndrescu and Evans (2014) to conclude that Retezat is easily the ‘most glaciated’, followed

by Parâng and Făgăraş. Next come Bucegi, Rodna, Lotru–Cindrel and Godeanu. Glacial modification is much less in Maramureş, Iezer, Ţarcu and Bihor. Easily the least modified, with the poorest cirques, is Călimani.

References

Ardelean F, Drăguţ L, Urdea P, Török-Oance M (2013) Variations in landform definition: a quantitative assessment of differences between five maps of glacial cirques in the Ţarcu Mountains (Southern Carpathians, Romania). Area 45:348–357

Barr ID, Spagnolo M (2015) Glacial cirques: origins, characteristics and palaeoenvironmental implications. Earth Sci Rev 151:48–78

Evans IS (2006) Allometric development of glacial cirque form: geological, relief and regional effects on the cirques of Wales. Geomorphology 80(3–4):245–266

Evans IS, Cox NJ (2015) Size and shape of glacial cirques. In: Jasiewicz J, Zwoliński Z, Mitasova H, Hengl T (eds) Geomorphometry for geosciences. Adam Mickiewicz University in Poznań Institute of Geoecology and Geoinformation, International Society for Geomorphometry, Poznań, pp 79–82. http://geomorphometry.org/EvansCox2015

Gheorghiu DM, Hosu M, Corpade C, Xu S (2015) Deglaciation constraints in the Parâng Mountains, Southern Romania, using surface exposure dating. Quat Int (in press)

Jarman D (2006) Large rock slope failures in the Highlands of Scotland: characterisation, causes and spatial distribution. Eng Geol 83(1–3):161–182

Kuhlemann J, Dobre F, Urdea P, Krumrei I, Gachev E, Kubik P, Rahn M (2013) Last glacial maximum glaciation of the central South Carpathian range (Romania). Austrian J Earth Sci 106:83–95

Mîndrescu M (2004) Topographic and climate conditions required for glacier formations in cirques. Ann Univ Kharkov, Geogr ser 620:88–95

Mîndrescu M (2006) Geomorfometria circurilor glaciare din Carpaţii româneşti. PhD thesis, University of Iaşi, Romania (in Romanian)

Mîndrescu M (2009) Asimetria glaciară din masivul Făgăraş. Analele univ. Ştefan cel Mare din Suceava, seria Geografie 18:25–34 (in Romanian)

Mîndrescu M, Evans IS (2014) Cirque form and development in Romania: allometry and the buzz-saw hypothesis. Geomorphology 208:117–136

Mîndrescu M, Evans IS, Cox NJ (2010) Climatic implications of cirque distribution in the Romanian Carpathians: palaeowind directions during glacial periods. J Quat Res 25(6):875–888

Reuther AU, Urdea P, Geiger C, Ivy-Ochs S, Niller HP, Kubik PW, Heine K (2007) Late Pleistocene glacial chronology of the Pietrele Valley, Retezat Mountains, Southern Carpathians constrained by ^{10}Be exposure ages and pedological investigations. Quat Int 164–165:151–169

Ruszkiczay-Rüdiger Z, Kern Z, Urdea P, Braucher R, Madarász B, Schimmelpfennig I, ASTER Team (2015) Revised deglaciation history of the Pietrele-Stânişoara glacial complex, Retezat Mts, Southern Carpathians, Romania. Quaternary International (accepted)

Turnbull JM, Davies TRH (2006) A mass movement origin for cirques. Earth Surf Proc Land 31:1129–1148

Urdea P (2004) The Pleistocene glaciation of the Romanian Carpathians. In: Ehlers J, Gibbard PL (eds) Quaternary glaciations—extent and chronology, part 1: Europe. Elsevier, Amsterdam, pp 301–308

Urdea P, Reuther AU (2009) Some new data concerning the quaternary glaciation in the Romanian Carpathians. Geographica Pannonica 13(2):41–52

Urdea P, Onaca A, Ardelean F, Ardelean M (2011) New Evidence on the quaternary glaciation in the Romanian Carpathians. In: Ehlers J, Gibbard PL, Hughes PD (eds) Quaternary glaciations—

extent and chronology, a closer look. Developments in quaternary science, vol 15. Elsevier, Amsterdam, pp 305–332
Wilson P, Jarman D (2015) Rock slope failure in the Lake District. In: McDougall DA, Evans DJA (eds) The Quaternary of the lake district: field guide. Quaternary Research Association, London, pp 83–95

Chapter 10
Geomorphosites Assessments of the Glacial and Periglacial Landforms from Southern Carpathians

Laura Comănescu and Alexandru Nedelea

Abstract Geomorphosites are landforms that in time have received a certain value due to human perception. This value can be scientific, ecological, aesthetic, cultural-historical and economic. *The Southern Carpathians* present numerous and various glacial and periglacial geomorphosites. In order to obtain an overall image of this area, the authors calculated indexes for glacial, periglacial and global geomorphic diversity. Geomorphic diversity is a dimensionless parameter that shows the number and diversity of geomorphosites within the study area. Global geomorphic diversity (glacial and periglacial) has a medium value of 0.365, with differences between glacial and periglacial. The values for glacial geomorphic diversity varied between 0 and 0.90 with a medium value of 0.30. The periglacial geomorphic diversity had higher values, ranging between 0.10 and 0.95 with a medium value of 0.43. In the *Southern Carpathians*, *The Viştea basin* (*Făgăraş Mts.*) *was chosen as study area* for an evaluation of geomorphosites. Several methods amongst the most widely used in the literature (Pralong in Géomorphol Relief Processus Environ 3:189–196, 2005; Coratza and Giusti in Il Quaternario 18(1):307–313, 2005; Bruschi and Cendrero in Il Quaternario 18(1):293–306, 2005; Serrano and Gonzalez-Trueba in Géomorphol Relief Processus Environ 3:197–208, 2005; Reynard et al. in Geogr Helv 62 3:148–158, 2007; Pereira et al. in Geogr Helv 62 (3):159–169, 2007; Zouros in Geogr Helv 62 3: 169–180, 2007; Comănescu et al. in Forum Geografic. Studii şi cercetări de geografie şi protecţia mediului XI:54–61, 2012) were applied and their results were subsequently compared. Each of the above-mentioned methods has their strong and weak points and the resulted global values vary on a large scale. The hierarchy obtained for each method in particular shows much smaller differences. By adding all the resulted ranks, the authors can conclude that the Viştea Valley glacial geomorphosite is the most important one from the Viştea basin.

L. Comănescu (✉) · A. Nedelea
Faculty of Geography, University of Bucharest,
1st N. Bălcescu Blv., sector 1, 010041 Bucharest, Romania
e-mail: lauracomanescu@yahoo.com

M. Radoane and A. Vespremeanu-Stroe (eds.), *Landform Dynamics and Evolution in Romania*, Springer Geography,
DOI 10.1007/978-3-319-32589-7_10

Keywords Geomorphic diversity · Inventory · Glacial and periglacial geomorphosites · Southern Carpathians

Introduction

The current, unanimously accepted, definition considers geomorphosites to be landforms which, in time, have acquired a certain value due to human perception (Panizza 2001). Reynard (2005) argued that geomorphosites need to have several attributes and, as such, besides the scientific component (around which the focus should gravitate) additional values are also important (ecological, cultural, aesthetic and economic). Geomorphosites are multifunctional entities and a main component of the geomorphic landscape (Reynard 2005) . They can acquire different values, which may change over time depending on the way human society perceives and uses them.

Starting with this definition, Fig. 10.1 reveals the interconnection established between the human society and geomorphosites and the four fundamental attributes this relation relies on: knowledge, research, positive impact and use.

In time, the study of geomorphosites developed the following directions: defining, inventorying, establishing an assessment methodology and mapping.

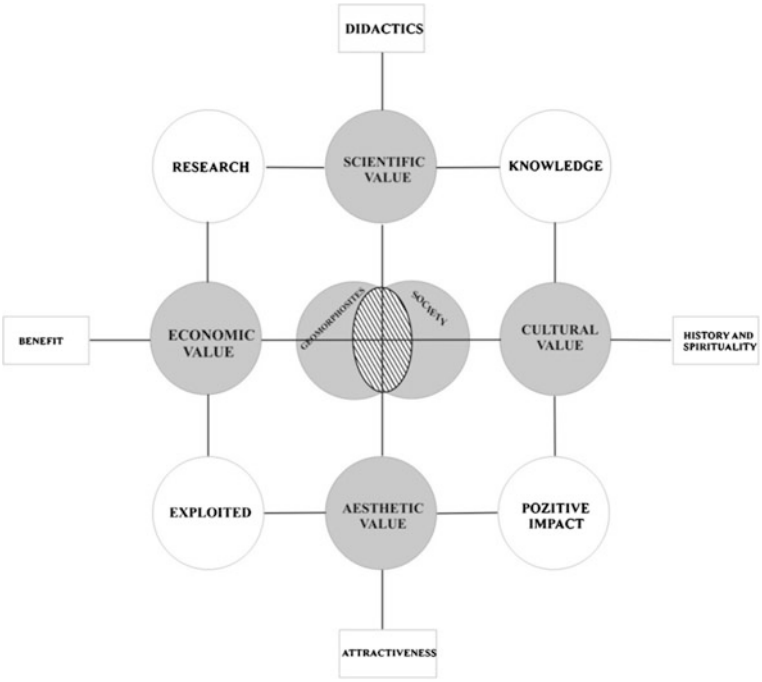

Fig. 10.1 Interrelations between geomorphosites and the human factor

Evaluating geomorphosites has been a constant concern for the scientific community, first in the larger framework of geosites and then in the individual class of geomorphosites. Though, at the level of the inventory methodologies there is no unitary methodology, due to the final purposes of the respective demarches, but also due to different regions of applying the methodologies.

Grandgirard (1999) formulates the first effective criteria of geomorphosites assessment, many of them residing directly or indirectly in the methods worldwide operating now (integrity, representativeness, rarity, paleogeographic value).

Wimbledon et al. (2000), within the Geosites project, establishes a set of criteria, which were embraced at that time by the international community, namely: representativeness, complexity, geodiversity and the site's potential for multidisciplinary studies. This method made it possible for the inventories realized within the project, but in different countries, to be more homogenous.

After the year 2000, the efforts for creating an evaluation method for geomorphosites become evident in the international geographical literature. As such, depending on the school that presented them and the areas they were used in, several methods have been developed.

A first synthesis of these methods was proposed by Reynard et al. (2009), as they tried to establish a series of common characteristics for these classifications (taking the scientific value as a central point of the assessment), and subsequently divided them into direct evaluations (subjective, done by researchers using their own grids) and indirect ones (objective, by clear quantifications). In the same paper (Reynard et al. 2009), the authors pay a particular attention to the purpose and the context in which some of the methods mentioned above were applied, as well as to the main criteria and sub-criteria employed for the assessment.

The study of geomorphosites in the Romanian literature started in 2004 at the University of Oradea (focusing mostly on the geomorphosites from the Apuseni Mountains) (Ilieş and Josan 2007, 2009, Ilieş et al. 2011; Ilieş 2014), continued in 2008 at the University of Bucharest (studying areas from the Southern Carpathians and the Dobrogea Plateau) (Comănescu and Dobre 2009; Comănescu and Nedelea 2010; Comănescu et al. 2009, 2011a, b, 2012, 2014) and after 2011 the Babeş-Bolyai University in Cluj (with studies on the Trascău Mountains, the Transylvania Depression and the western parts of the Northern Carpathians) (Cocean 2011; Cocean and Surdeanu 2011; Irimus et al. 2011; Irimia and Toma 2012; Gavrilă and Anghel 2013). All the resulted papers aimed for: inventorying geomorphosites from different areas, evaluating them using different methods existing in the specialized literature and constructing geotourism maps of areas representative for Romania.

The Inventory of the Geomorphosites

An inventory aims to review all geomorphosites located within specific boundaries, as a first step in their evaluation. In the specialized literature, there is no generally accepted methodology for inventorying geomorphosites because of the diverse

finality that the inventorying approaches had over time and the different areas with particular features where they were applied, each area requiring specific criteria (Cocean 2011). The most widely known and used inventorying fiche is the one elaborated by Pralong (2005) and by Reynard et al. (2007) which consider both the quantitative and the qualitative analysis, the same fiche that we used in this study. A very important step in the inventorying process is classifying the geomorphosites, and this can be done following several criteria. Here is an exemplification of these criteria using geomorphosites from the Southern Carpathians.

The Temporal–Functional Criterion

- *Active geomorphosites* represent geomorphosites with an important educational value because they help the understanding of the present-day morphology; are key-features in reconstructing the paleo-geographical conditions, and in turn cause the development of passive geomorphosites (Reynard et al. 2009) (e.g. the Stonerivers in the Retezat Mountains, the Rockglaciers in the Făgăraş Mountains).
- *Passive geomorphosites* constitute archives of the paleo-environmental conditions in which the respective landforms formed and developed, and enable the study of the genesis (inclusive the age) and evolution of the relief (Reynard et al. 2009) (e.g. glacial steps, the generations of moraines in the Făgăraş Mountains).

The Genetic Criterion

- *Glacial geomorphosites*—valleys, cirques, steps, thresholds, roche moutonnée, moraines, (e.g. Bâlea cirque, Bâlea Valley, the threshold on which the Bâlea Waterfall developed, the moraine from the Capra Chalet in the Făgăraş Mountains);
- *Periglacial geomorphosites*—nivation cirques, nivation hollows, nivation horseshoes, disaggregation ridge, escarpment slopes, needles, towers, slide rocks, rocks stream, rock glaciers, blockfields (present in the Făgăraş, Retezat, Parâng, Cindrel, Şureanu and other Mountains).

The Tourism Relevance Criterion

- *Local and regional interest geomorphosites*—Pleşcoaia, Setea Mare, Ieşu, Căldarea lui Murgoci cirques located in Parâng Mountains, Iezerul Podul Giurgiului cirque located in Făgăraş Mountains, the Tărtărău nival cirque located in Parâng Mountains;

– *National interest geomorphosites*—Mălăeşti valley in Bucegi Mountains, Zănoaga, and Bucura cirques in Retezat Mountains, Câlcescu, Mija, Roşiile cirques in Parâng Mountains, the Judele, Râul Bărbat, Lăpuşnicul Mare glacial complexes in Retezat Mountains;
– *International interest geomorphosites*—Bâlea Valley, Bâlea Cirque, Capra Valley, in Făgăraş Mountains.

The Surface Criterion

– *Punctual geomorphosites*: Cleopatra's Needle in Făgăraş Mountains, Morarului Crags in Bucegi Mountains;
– *Linear geomorphosites*: the Arpaş, Viştea and Podragu glacial valleys in Făgăraş Mountains; the Mălăeşti, Cerbului and Morarului glacial valleys in Bucegi Mountains;
– *Areal geomorphosites*: Mioarele cirque in Făgăraş Mountains, Iezeru Şureanu cirque in Şureanu Mountains, the moraines in Parâng Mountains.

There are numerous glacial and periglacial geomorphosites within the study area and they vary in terms of functionality, genesis, tourism relevance and surface (Fig. 10.2). Table 10.1 shows a selection and inventory of different categories of geomorphosites located in the Southern Carpathians.

Because of the large extension of the study area, the authors propose a generalized approach with the specific aim to determine the geomorphic diversity for each massif according to the two types of landforms (glacial and periglacial) by only considering the geomorphosites in these categories (Table 10.2).

The concept of geomorphodiversity was introduced in the specialized literature in order to express the overall value of the geomorphosites for particular areas, usually large-sized, as well as the multitude/diversity and types of landforms (Panizza 2009; Demek et al. 2011; Kostrzewski 2011).

The coefficient of geomorphic diversity was calculated based on the formula

$$\mathrm{Gmd} = \left(\sum \mathrm{Eg}Xn + \mathrm{Gm}\right)/s \tag{10.1}$$

where Gmd is the geomorphodiversity coefficient; Eg—the number of landforms; *n*—the number of genetic relief types; Gm—the number of geomorphosites, and *S*—surface (km^2) (Comănescu et al. 2014).

"A special attention was given to geomorphosites, which are practically calculated twice, both in the first category and in the second category, in order to give a plus value to those" (Comănescu et al. 2014). The result is a total dimensionless value that indicates the quantity and degree of geomorphic diversity within the considered area. The disadvantage of this parameter lies in the fact that it does not convey the total, effective value of the geomorphosites (Comănescu et al. 2014).

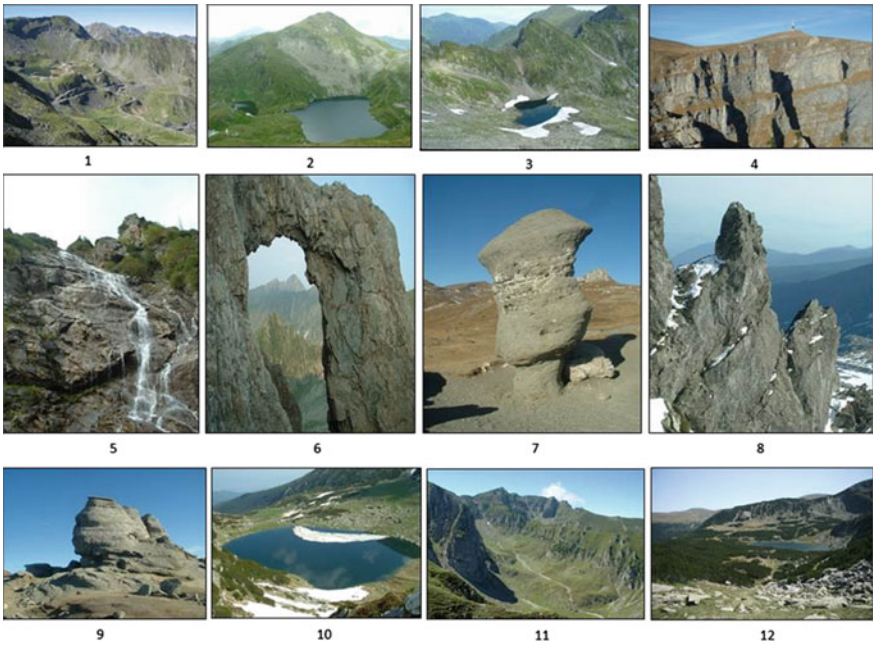

Fig. 10.2 Representative glacial and periglacial geomorphosites from the Southern Carpathians: *1* Bâlea glacial complex (Făgăraș Mts.), *2* Capra glacial complex (Făgăraș Mts.), *3* Podul Giurgiului glacial complex (Făgăraș Mts.), *4* Coștilei slope (Bucegi Mts.), *5* Capra waterfall (Făgăraș Mts.), *6* Ogres' window (Făgăraș Mts.), *7* Babe (Bucegi Mts.), *8* Pelegii Cliffs (Retezat Mts.), *9* Sphinx (Bucegi Mts.), *10* Galeșu glacial complex (Retezat Mts.), *11* Glacial Valley Mălăiești (Bucegi Mts.), *12* Câlcescu glacial complex (Parâng Mts.)

The global value of geomorphodiversity was computed as an average between the glacial and periglacial geomorphodiversity, since other genetic types of topography are not being considered by this scientific approach.

The global geomorphic diversity (glacial and periglacial) registers a mean value of 0.365 but presents marked differences between the glacial and the periglacial (Table 10.2; Fig. 10.3). For example, the periglacial geomorphosites are more numerous and varied while the glacial ones have a superior intrinsic value even if they cover a more reduced surface. The highest values register in the Făgăraș and Retezat massifs (0.925) and the lowest in Ghițu, Frunți, Cernei and Mehedinți massifs (0.05).

The values for geomorphic diversity of the glacial landforms vary from 0 (Ghițu, Frunți, Cozia, Vâlcan, Cernei and Mehedinți) to 0.9 (Făgăraș, Retezat). The median value of this parameter is the highest registered in all Romanian Carpathians (Table 10.2; Fig. 10.4).

The values reflecting the geomorphic diversity of the periglacial landforms are higher than those obtained for the glacial ones due to their stronger presence within the study area. The Southern Carpathians present many periglacial landforms some

Table 10.1 Synthesis of the glacial and periglacial geomorphosites from the Southern Carpathians

No	Name	Location (mountain)	Functionality	Genesis	Tourism relevance	Surface
1	Ialomiţa Valley	Bucegi	Passive	Glacial	National	Linear
2	Doamnei Valley	Bucegi	Passive	Glacial	Regional/local	Linear
3	Morarului Valley	Bucegi	Passive	Glacial	National	Linear
4	Cerbului Valley	Bucegi	Passive	Glacial	National	Linear
5	Mălăieşti Valley	Bucegi	Passive	Glacial	National	Linear
6	Mălăieşti! Cirque	Bucegi	Passive	Glacial	National	Areal
7	Ţigăneşti Cirque	Bucegi	Passive	Glacial	Regional/local	Areal
8	Caraiman Scree	Bucegi	Active	Periglacial	Regional/local	Areal
9	Mitarca Cirque	Leaota	Passive	Glacial	Regional/local	Areal
10	afl. Mitarca Cirque	Leaota	Active	Periglacial	Regional/local	Areal
11	Great Scree	Piatra Craiului	Active	Periglacial	National	Areal
12	Hornul Găinii Scree	Piatra Craiului	Active	Periglacial	Regional/local	Areal
13	Iezerul Mare Cirque	Iezer	Passive	Glacial	National	Areal
14	Pişcanul nival Cirque	Iezer	Active	Periglacial	Regional/local	Areal
15	Bâlea Cirque	Făgăraş	Passive	Glacial	International	Areal
16	Buda Cirque	Făgăraş	Passive	Glacial	Regional/local	Areal
17	Capra Cirque	Făgăraş	Passive	Glacial	National	Areal
18	Capra Valley	Făgăraş	Passive	Glacial	International	Linear
19	Bâlea Valley	Făgăraş	Passive	Glacial	International	Linear
20	Morena Capra	Făgăraş	Passive	Glacial	Regional/local	Areal
21	Orzăneaua erratic block	Făgăraş	Passive	Glacial	Regional/local	Punctual
22	Podragu Cirque	Făgăraş	Passive	Glacial	National	Areal
23	Turnu Steep	Cozia	Passive	Periglacial	Regional/local	Areal
24	Piatra Şoimului erosion outlier	Cozia	Passive	Periglacial	Regional/local	Punctual
25	Căldarea Dracului Cirque	Parâng	Passive	Glacial	Regional/local	Areal
26	Găuri Cirque	Parâng	Passive	Glacial	Regional/local	Areal
27	Mija Cirque	Parâng	Passive	Glacial	National	Areal
28	Mija Mare debris cone	Parâng	Active	Periglacial	Regional/local	Areal
29	Piciorul Tecanului Scree	Parâng	Active	Periglacial	Regional/local	Areal
30	Zănoaga Mare—Câlcescu stone see	Parâng	Active	Periglacial	Regional/local	Areal

(continued)

Table 10.1 (continued)

No	Name	Location (mountain)	Functionality	Genesis	Tourism relevance	Surface
31	Stone pavements on the main ridge (west of Setea Mare)	Parâng	Active	Periglacial	Regional/local	Areal
32	Grassy mounds in the Mohoru—Setea Mare saddle	Parâng	Active	Periglacial	Regional/local	Areal
33	Iezerele Cindrelului Cirque	Cindrel	Passive	Glacial	National	Areal
34	Gropata Cirque	Cindrel	Passive	Glacial	Regional/local	Areal
35	Balindru Cirque	Lotru	Passive	Glacial	Regional/local	Areal
36	Șteflești Cirque	Lotru	Passive	Glacial	National	Areal
37	Negovanu Scree	Căpăţânii	Active	Periglacial	Regional/local	Areal
38	Coşana Scree	Căpăţânii	Active	Periglacial	Regional/local	Areal
39	Şureanu Cirque	Şureanu	Passive	Glacial	National	Areal
40	Cârpa Cirque	Şureanu	Passive	Glacial	Regional/local	Areal
41	Pătru Cirque	Şureanu	Passive	Glacial	Regional/local	Areal
42	Gropşoare Cirque	Şureanu	Passive	Glacial	Regional/local	Areal
43	Lăpuşnicul Mare Valley	Retezat	Passive	Glacial	National	Linear
44	Nucşoara Valley	Retezat	Passive	Glacial	National	Linear
45	Judele Valley	Retezat	Passive	Glacial	National	Linear
46	Păpuşii Stitch	Retezat	Passive	Glacial	Regional/local	Linear
47	Zănoaga Cirque	Retezat	Passive	Glacial	National	Areal
48	Bucura Cirque	Retezat	Passive	Glacial	National	Areal
49	Gemenele Cirque	Retezat	Passive	Glacial	Regional/local	Areal
50	Galeş Cirque	Retezat	Passive	Glacial	Regional/local	Areal
51	Cârnea Valley	Godeanu	Passive	Glacial	Regional/local	Linear
52	Mâţulu Valley	Godeanu	Passive	Glacial	Regional/local	Linear
53	Bulzu Valley	Godeanu	Passive	Glacial	Regional/local	Linear
54	Groapa Balmoşului Valley	Godeanu	Passive	Glacial	Regional/local	Linear
55	Hidegului Valley	Ţarcu	Passive	Glacial	National	Linear
56	Custurii Cirque	Ţarcu	Passive	Glacial	Regional/local	Areal
57	Bloju Cirque	Ţarcu	Passive	Glacial	Regional/local	Areal
58	Petreanu Cirque	Ţarcu	Passive	Glacial	Regional/local	Areal

Table 10.2 Values for geomorphic diversity of the mountains in the Southern Carpathians

No	Mountain	Geomorphic diversity of the glacial relief	Geomorphic diversity of the periglacial relief	Global geomorphic diversity
1	Bucegi	0.20	0.50	0.35
2	Leaota	0.10	0.35	0.225
3	Piatra Craiului	0.05	0.35	0.20
4	Făgăraş	0.90	0.95	0.925
5	Iezer–Păpuşa	0.25	0.45	0.35
6	Ghiţu	0	0.10	0.05
7	Frunţi	0	0.10	0.05
8	Cozia	0	0.15	0.075
9	Parâng	0.85	0.90	0.875
10	Şureanu	0.45	0.50	0.475
11	Cindrel	0.35	0.40	0.375
12	Lotru	0.30	0.40	0.35
13	Căpăţânii	0.25	0.30	0.275
14	Retezat	0.90	0.95	0.925
15	Godeanu	0.45	0.60	0.525
16	Ţarcu	0.65	0.80	0.725
17	Vâlcan	0	0.25	0.125
18	Cernei	0	0.10	0.05
19	Mehedinţi	0	0.10	0.05
20	**Global**	**0.30**	**0.43**	**0.365**

actual other relict (e.g. dating from Pleistocene) and many of them are geomorphosites. The obtained values vary between 0.10 (Ghiţu, Frunţi, Cernei, Mehedinţi) to 0.95 (Făgăraş, Retezat), and the medium value (0.43) is the highest registered in all Romanian Carpathians (Table 10.2; Fig. 10.5).

Evaluating Geomorphosites

The geomorphosites were evaluated using international literature's most known and utilized methods developed by: Pralong (2005), Coratza and Giusti (2005), Bruschi and Cendrero (2005), Serrano and Gonzales Trueba (2005), Reynard et al. (2007), Pereira et al. (2007), Zouros (2007), Comănescu et al. (2012).

The introductory part of each method, including geomorphosite identification and description, was removed consequently, only the qualitative, objective body of these methods was considered. All the evaluation processes, regardless their

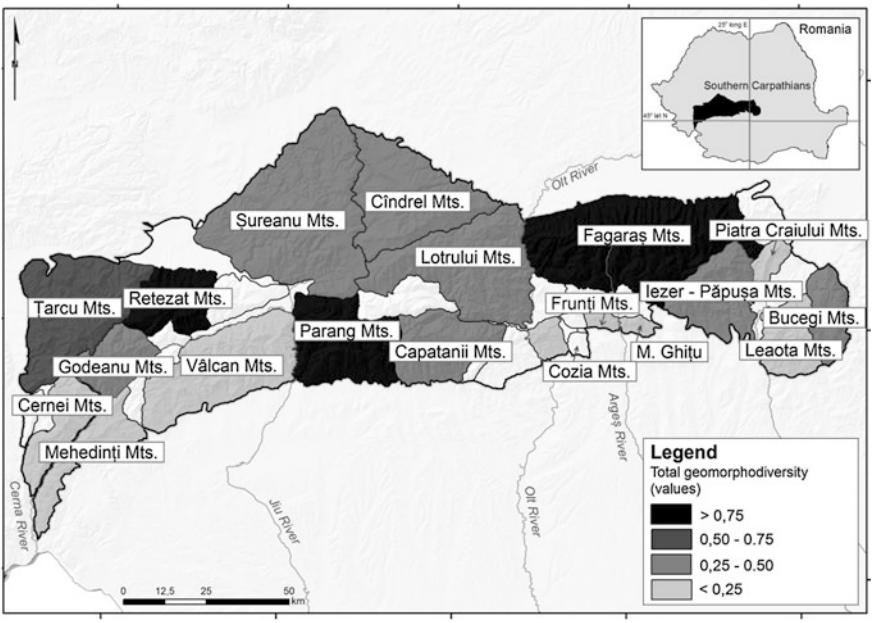

Fig. 10.3 Global geomorphic diversity in the Southern Carpathians

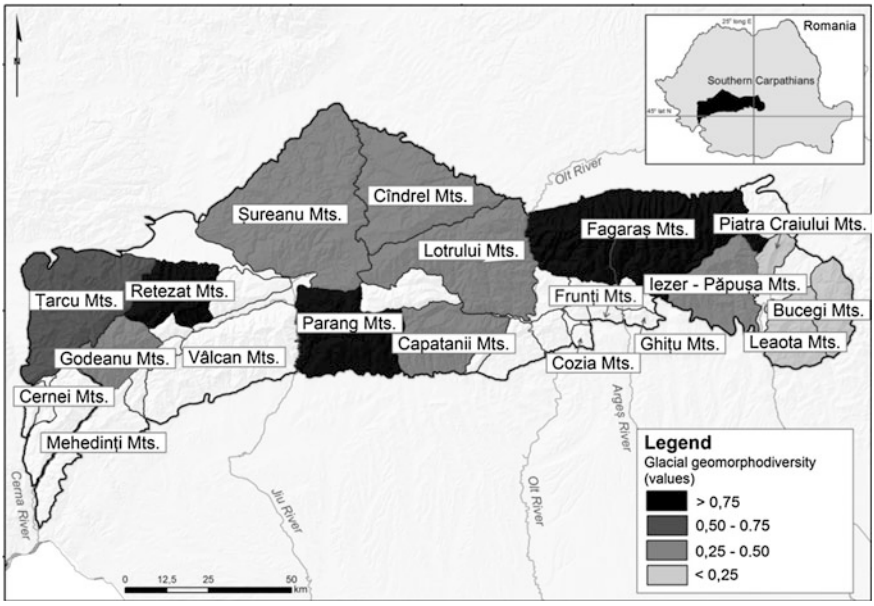

Fig. 10.4 Glacial geomorphic diversity in the Southern Carpathians

Table 10.3 Synthesis of the geomorphosites evaluation methods

No	Method	Scientific value	Additional values	Management	Use
1	Method developed by Pralong (A)	Yes	Yes	Yes	Implicit
2	Method developed by Coratza and Giusti (B)	Yes	No	No	No
3	Method developed by Bruschi and Cendrero (C)	Yes	Implicit	Yes	Yes
4	Method developed by Serrano and Gonzales Trueba (D)	Yes	Yes	Yes	Yes
5	Method developed by Reynard et al. (E)	Yes	Yes	No	No
6	Method developed by Pereira et al. (F)	Yes	Yes	Yes	Yes
7	Method developed by Zouros (G)	Yes	Yes	Yes	Yes
8	Method developed by the authors (H)	Yes	Yes	Yes	Yes

objective, focus on the scientific value, even if its weight is different for each of them and it takes a secondary role for the methods that aim to quantify the touristic value of that geomorphosite (Table 10.3).

For the evaluation of geomorphosites, the authors chose as case study the Vişţea basin from the Făgăraş Mountains because this basin reproduces at a micro-scale the most important characteristics of the study area, where glacial and periglacial geomorphosites were inventoried (Table 10.4; Figs. 10.6 and 10.7). The results were compared, for each method the total value (reduction to a unit were made where necessary) and rank (place) that the respective geomorphosite has in each evaluation, were calculated.

Evaluation Using Pralong (2005) Method

This method was developed in 2005 by J.P. Pralong and covers two aspects: qualitative (geomorphosite's description spreadsheet) and quantitative evaluation. The purpose of this method is to establish tourism attraction value of geomorphosites also considering tourism infrastructure and the means and possibilities available to exploit them.

The tourism attraction value is calculated as an average of four distinct criteria according to the formula

Table 10.4 Geomorphosites in the Vişţea basin

No	Name	Genesis	Type	Code
1	Galaşea Mare–Vişţea Mare Ridge	Periglacial	Linear	BVper01
2	Vişţea Mare Ridge	Periglacial	Linear	BVper02
3	Zănoaga Glacial Saddle	Glacial	Areal	BVgla01
4	Drăguşului Ridge	Periglacial	Linear	BVper03
5	Hârtopu Mare Cirque	Glacial	Areal	BVgla02
6	Vişţea Mare Waterfall	Glacial	Punctual	BVgla03
7	Vişţişoara Cirque	Glacial	Areal	BVgla04
8	Vişţea Mare Peak	Periglacial	Punctual	BVper04
9	Portiţa Vişţei Saddle	Glacial	Areal	BVgla05
10	Vişţea Needle	Periglacial	Punctual	BVper05
11	Vişţea Valley	Glacial	Linear	BVgla06
12	Hârtopu Ursului Cirque	Glacial	Areal	BVgla07
13	Vişţişoara Glacial Valley	Glacial	Linear	BVgla08
14	Saddle between Vişţişoara and Iezerul Galben cirques	Glacial	Areal	BVgla09
15	Vişţea Mare debris	Periglacial	Areal	BVper06

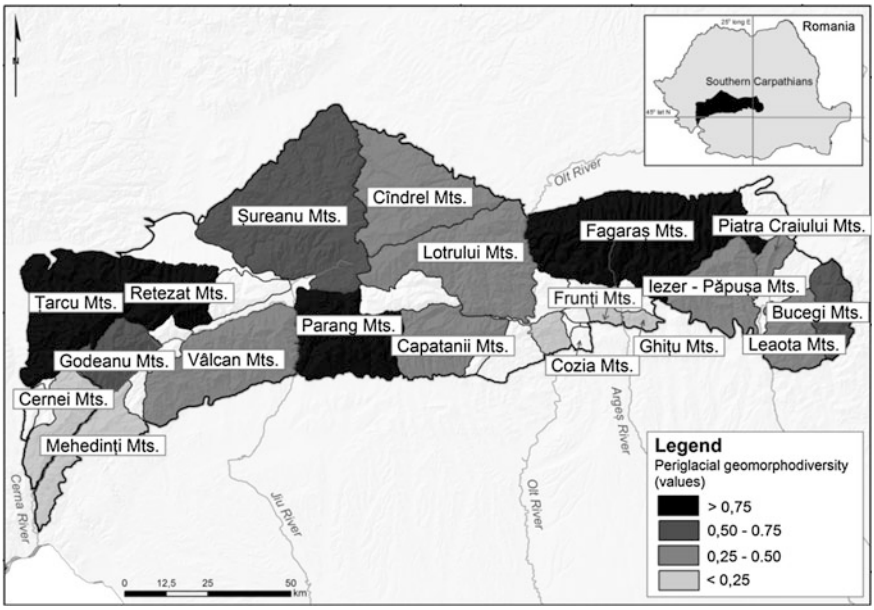

Fig. 10.5 Periglacial geomorphic diversity in the Southern Carpathians

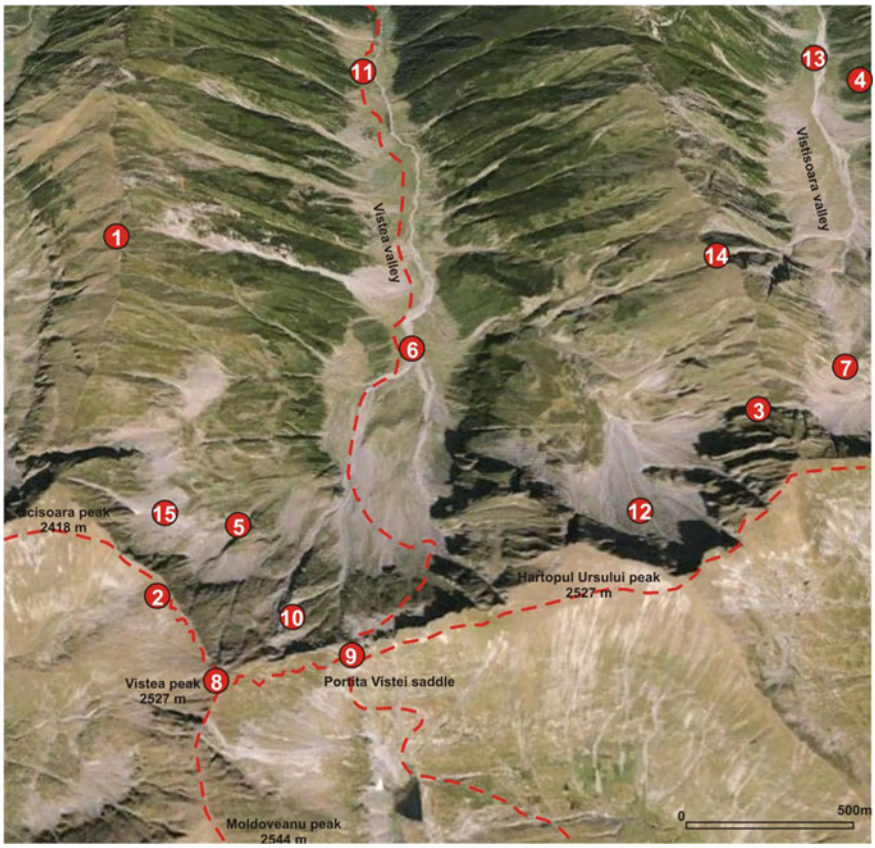

Fig. 10.6 Geographic location of the geomorphosites in the Vişţea basin (modified after Comănescu et al. 2011b)

$$\text{Vtour} = (\text{Vsce} + \text{Vsci} + \text{Vcult} + \text{Veco})/4 \tag{10.2}$$

where: Vtour stands for tourism attraction value, Vsce for aesthetic value, Vsci for scientific value, Vcult for cultural-historical value and Veco for economic value.

The author of this formula considers all criteria equally important in assessing the tourism attraction value of geomorphosites, which explains why each criterion is given 100 % importance within the formula. The criteria considered were awarded scores ranging on a 0–1 scale (Pralong 2005) .

The considered criteria are: for the scientific value: paleogeographic interest, representativeness, surface (percentage), integrity and ecological interest; for the aesthetic value: number of lookout points, average distance between lookout points, slope, impact of colour against the surroundings; for the cultural-historical value: cultural and historical features presented in iconographic representations and/or in different writings, historical and archaeological relevance, religious and symbolic

Fig. 10.7 The analyzed geomorphosites from the Vișteа basin

relevance, art and cultural events; for the economic value: accessibility, natural hazards, annual number of visitors, official level of protection (Pralong 2005) .

"The *total* (*global*) *value* ranges from a low 0.187 for Zănoaga Glacial Saddle to scores as high as 0.375 for Vișteișoara Cirque or 0.40 for Vișteа Valley. This low amplitude indicates a similar genesis and low economic and cultural value" (Table 10.5) (Comănescu et al. 2011b).

"*The scientific value* scores well too as these geomorphosites are vital in understanding the genesis and evolution of the glacial relief in this area" (Comănescu et al. 2011b). The scores vary within a limited amplitude (0.5) with a maximum (0.75) for the Vișteа Valley, Vișteișoara Cirque and Portiţa Vișteі Saddle and a minimum (0.25) for Drăguşului Ridge, Hârtopu Mare Cirque, Galaşea Mare-Vișteа Mare Ridge and Vișteа Mare Ridge (Table 10.5).

"*The aesthetic value* definitely scores highest. The numerous lookout points, the good colour contrast and spectacular drop offs contribute greatly to these scores. The debris accumulations along Vișteа Mare Valley score the lowest value (0.25) while Galaşea Mare–Vișteа Mare Ridge, Vișteа Mare Peak, Vișteа Needle and Vișteа Valley scored the highest (0.75). These geomorphosites are spectacular landforms and are included in their trekking itineraries by numerous tourists" (Comănescu et al. 2011b) (Table 10.5).

"The scores for the *cultural value* are very low as the region's cultural component is little advertised; no dedicated promotional materials or any other iconographic

Table 10.5 Evaluating the Vişţea basin geomorphosites using the method developed by Pralong (modified after Comănescu et al. 2011b)

No	Name	Scientific value	Aesthetic value	Cultural value	Economic value	Global value
1	Galaşea Mare–Vişţea Mare Ridge	0.25	0.75	0	0.05	0.262
2	Vişţea Mare Ridge	0.25	0.5	0	0.05	0.20
3	Zănoaga Glacial Saddle	0.5	0.20	0	0.05	0.187
4	Drăguşului Ridge	0.25	0.65	0	0.05	0.237
5	Hârtopu Mare Cirque	0.25	0.55	0	0.05	0.212
6	Vişţea Mare Waterfall	0.5	0.55	0.05	0.05	0.287
7	Vişţişoara Cirque	0.75	0.65	0.05	0.05	0.375
8	Vişţea Mare Peak	0.5	0.75	0	0.05	0.325
9	Portiţa Vişţei Saddle	0.75	0.65	0	0.05	0.362
10	Vişţea Needle	0.5	0.75	0	0.05	0.325
11	Vişţea Valley	0.75	0.75	0.05	0.05	0.40
12	Hârtopu Ursului Cirque	0.5	0.65	0	0.05	0.30
13	Vişţişoara Glacial Valley	0.5	0.5	0	0.05	0.262
14	Saddle between Vişţişoara and Iezerul Galben Cirques	0.5	0.5	0	0.05	0.262
15	Vişţea Mare debris	0.5	0.25	0	0.05	0.20

representations were edited. The region under study is not awarded with any particular historical, religious or mythological importance as a matter of fact, there are only three geomorphosites that do align to this criterion (Vişţea Mare Waterfall, Vişţişoara Cirque, Vişţea Valley)" (Comănescu et al. 2011b) (Table 10.5).

"The scores for the *economic value* are low and homogeneous (0.05) given that the region's economic life and tourism infrastructure (except for hiking trails) are almost inexistent" (Comănescu et al. 2011b) (Table 10.5).

This is the most used evaluation method for geomorphosites and was applied in different areas, including the Alps. When comparing the geomorphosites located in the study area with those found in the Alps for example, it is clear that those in the Alps are better known scientifically and as tourism assets, and the differences result from their cultural and economic value. The comparison shows where differences come from, namely: for the scenic value, all geomorphosites have the same value

(0.4–0.75); for the scientific value, there are no significant differences (0.45–0.85); the cultural value has got significant differences (between 0 and 0.42), and the economic value registers most differences (0.05–0.85).

The main cause for the Carpathians' geomorphosites scoring so low in comparison with the Alps is related to the deficient infrastructure, the reduced number of tourists (geomorphosites under study in Făgăraş are located in areas accessible only to fit experienced trekkers) and the lack of defining elements in terms of cultural value (there are no iconographic representations of symbolic, mystical or religious relevance).

The strengths of the method are the following: the method covers the most important points of a geomorphosite assessment (both in what concerns the scientific value and the additional values). The weaknesses are as follows: elements regarding the management, promotion or natural and anthropic risks which could affect such an element are present. The method is also somehow subjective by the use of some attributes which are unclearly defined, as: large scale, medium scale, small scale (for representativeness) which leaves space to multiple interpretations depending on the expertise of the person who makes the evaluation.

Coratza and Giusti (2005) Method

This method was used for obtaining an inventory of the geomorphosites in the Emilia—Romagna Province and is applied for determining environmental impact and for territorial planning purposes. Only the scientific value of geomorphosites is calculated based on the following formula:

$$Q = sS + dD + aA + rR + eE + zZ \tag{10.3}$$

where Q is the scientific value; *s, d, a, r, c, e, z*—are multiplication factors depending on different assessment purposes; *S, D, A, R, C, E, Z*—considered values: scientific value (*S*) and didactical value (*D*) of the geomorphosite, A—surface (% of the total surface), rarity—*R*, state of preservation—*C*, exposure—*E*, added value(s)—*Z*. By introducing the professional experience of the expert (scientific and didactical value) the subjectivity is increased according to each person that constructs the evaluation (Coratza and Giusti 2005).

This method introduces a uniformity in the obtained values (that vary between 0.19 and 0.64 with 80.00 % varying between 0.4 and 0.6) because of its parameters (additional values are brought to a common denominator with the sub-criteria included in the scientific value), because the values of the *professional experience of the expert* (*CE*) includes the *scientific research* (*S*) and the *didactical value* (*D*) and because no multiplication factors are used.

The Vişlea Valley registers the highest score (0.64) thanks to additional value elements (for tourism importance, as it is the marked trail leading up in a few minutes to the Moldoveanu Peak—2544 m, the highest in the Romanian Carpathians).

Table 10.6 Evaluating the Vişţea basin geomorphosites using the method developed by Coratza and Giusti

No	Name	Global value	No	Name	Global value	No	Name	Global value
1	Galaşea Mare–Vişţea Mare Ridge	0.58	6	Vişţea Mare Waterfall	0.58	11	Vişţea Valley	0.64
2	Vişţea Mare Ridge	0.58	7	Vişţişoara Cirque	0.42	12	Hârtopu Ursului Cirque	0.42
3	Zănoaga Glacial Saddle	0.58	8	Vişţea Mare Peak	0.50	13	Vişţişoara Glacial Valley	0.50
4	Drăguşului Ridge	0.33	9	Portiţa Vişţei Saddle	0.50	14	Saddle between Vişţişoara and Iezerul Galben Cirques	0.50
5	Hârtopu Mare Cirque	0.42	10	Vişţea Needle	0.58	15	Vişţea Mare debris	0.19

The same additional value elements (for tourism use) are present for the Vişţea Waterfall (0.58) and Vişţea Needle (0.58). The Galaşea Mare—Vişţea Mare Ridge, Vişţea Mare Ridge and Zănoaga Gacial Saddle geomorphosites have the same value (0.58) with criteria such as professional experience of the expert, visibility and additional value, standing out (Table 10.6). The lowest value (0.19) was calculated for the debris located at the base of the Vişţea Mare ridge which does not score for criteria such as rarity (uniqueness), visibility or added value (Table 10.6).

The method can be used for evaluating the scientific value, but it cannot be applied in case of a demarche which would regard the touristic exploitation of geomorphosites due to the reduced weight which is given to additional values. This is the main drawback of the method. Besides, it is rather difficult to apply, because it requires strong expertise and experience, as some of the quality parameters employed for the assessment are subjective. For the scientific value, which is the central value of the geomorphosites, this is the most comprehensive and complex method.

Bruschi and Cendrero (2005) Method

This method was developed at the University of Cantabria (Spain) (Bruschi and Cendrero 2005; Bruschi and Cendrero 2009; Bruschi et al. 2011) and it aims to be an assessment method for the evaluation of geosites but can also be used in the case

of geomorphosites and it is useful both for the inventory and evaluation of environmental impact, which makes it very practical.

It is so far the most complex method in use, as the formula for weighting of the final value considers the following: the intrinsic quality (rarity, importance for scientific research, use in didactic purposes, diversity, age, significance as part of the historical, artistic, archaeological heritage, relation to other items of the natural heritage, state of preservation), the potential risks and protection measures (number of inhabitants in the areas, active natural hazards, possibility of collecting samples, the interrelation with planning policies, existing interests in mineral extraction, ownership status) and the potential use (activities, preservation measures, accessibility, surface, proximity of infrastructure, socio-economic features of the region). The final value is calculated with the help of a series of formulas used to determine the intrinsic value of geomorphosites, the state of preservation and potential use (Bruschi and Cendrero 2005).

However, a series of weak points can be noticed, namely: the degree of knowledge is introduced at intrinsic values, recreational activities at possible threatening and not at the potential of use of the site (Reynard et al. 2009). Also, we can notice that additional values have got a quite reduced importance in the final evaluation, decreasing from the immediate practical usability. The strength of the method consists in its practical applicability (the method holds clear practicality and it has been used for a number of coastal geomorphosites in Cantabria and The Basque Country and also for carrying out environmental impact assessments for building a new motorway) (Reynard et al. 2009)

The values obtained for the geomorphosites in the Vișstea basin range within a low set of values (0.19) due to the high number of parameters considered and the homogeneity of the values these parameters register (which frequently revolve around 0). This is also supported by the presence of only three classes of values that hold the following percentages: 0.30–0.40 (13.33 %), 0.40–0.50 (66.66 %), and above 0.50 (20.00 %).

The maximum value of 0.56 is held by Vișstea Valley (Table 10.7), a complex linear geomorphosite that integrates a series of smaller more simple geomorphosites, and which scores highly in terms of: degree of scientific knowledge, use in didactical purposes, diversity of elements, degree of preservation, possibility of sample collection, relation with planning policies, manners in which observation is possible, accessibility. The lowest value (0.37) was calculated for debris located at the base of the Vișstea Mare ridge (Table 10.7), because this geomorphosite is vulnerable to subjective hazards for tourism activities due to its mobility and for Drăgușului Ridge.

Table 10.7 Evaluating the Vişţea basin geomorphosites using the method developed by Bruschi and Cendrero

No	Name	Global value	No	Name	Global value	No	Name	Global value
1	Galaşea Mare–Vişţea Mare Ridge	0.45	6	Vişţea Mare Waterfall	0.49	11	Vişţea Valley	0.56
2	Vişţea Mare Ridge	0.48	7	Vişţişoara Cirque	0.47	12	Hârtopu Ursului Cirque	0.47
3	Zănoaga Glacial Saddle	0.43	8	Vişţea Mare Peak	0.48	13	Vişţişoara Glacial Valley	0.53
4	Drăguşului Ridge	0.37	9	Portiţa Vişţei Saddle	0.42	14	Saddle between Vişţişoara and Iezerul Galben Cirques	0.42
5	Hârtopu Mare Cirque	0.52	10	Vişţea Needle	0.50	15	Vişţea Mare debris	0.37

Serrano and Gonzalez-Trueba (2005) Method

The method was applied for 22 geomorphosites located in a Natural Protected Area (Picos de Europa). It approaches geomorphosites as multifunctional elements that can act as cultural, economic, tourism and educational resources therefore require a complex, multi-purpose evaluation. The following are considered: scientific value (genesis, morphology, dynamics, chronology, lithology, geologic structure), additional value (aesthetic, cultural, educational value and representativeness, tourism attraction), geomorphosite use and management (accessibility, fragility, vulnerability, intensity of use, degradation risks, state of preservation, impact, visibility, limits of acceptable changes). The evaluation is objective (as it only includes a quantitative analysis) and is fairly easy to do. Scores range between 0 and 100 points but, in order to facilitate comparison with other methods these were reduced by a factor of 100 (Serrano and Gonzales-Trueba 2005).

A weak point of this method is the lack of some clearly quantified criteria, especially in the case of scientific value, a fact which favours the subjectivity of the person who accomplishes the evaluation. The final result is not general, but only a qualitative transposing, this way groups on classes with similar value being accomplished and not a clear classification. The entire method is led to establishing some priorities in preserving the heritage of a region and less for a scientific inventory or for touristic use (Cocean 2011).

This method considers a high number of parameters and many of the geomorphosites scored values close to zero which explains the small differences (amplitude

Table 10.8 Evaluating the Vişţea basin geomorphosites using the method developed by Serrano and Gonzales-Trueba

No	Name	Global value	No	Name	Global value	No	Name	Global value
1	Galaşea Mare–Vişţea Mare Ridge	0.36	6	Vişţea Mare Waterfall	0.42	11	Vişţea Valley	0.51
2	Vişţea Mare Ridge	0.39	7	Vişţişoara Cirque	0.44	12	Hârtopu Ursului Cirque	0.44
3	Zănoaga Glacial Saddle	0.38	8	Vişţea Mare Peak	0.44	13	Vişţişoara Glacial Valley	0.47
4	Drăguşului Ridge	0.34	9	Portiţa Vişţei Saddle	0.38	14	Saddle between Vişţişoara and Iezerul Galben Cirques	0.40
5	Hârtopu Mare Cirque	0.45	10	Vişţea Needle	0.44	15	Vişţea Mare debris	0.29

of 0.22) between the maximum value (Vişţea Valley −0.51) and the minimum (debris field located at the base of the Vişţea Mare ridge −0.29).

This is also supported by the fact that the method grants an increased importance to additional values; more than 50 % of calculated values range between 0.40 and 0.50, because the studied geomorphosites share a relatively common genesis, morphology, dynamics and geology. Also, when considering the parameters related to additional values, the use and management, no significant differences are present. A relative homogeneity can be observed in terms of genetic categories (Galaşea Mare—Vişţea Mare ridge, Vişţea Mare Ridge, Zănoaga Glacial Saddle, Drăguşului Ridge score values between 0.34 and 0.39; Hârtopu Mare Cirque, Vişţişoara Cirque, Hârtopu Ursului Cirque between 0.44 and 0.45; Portiţa Vişţei Saddle and the Saddle between Vişţişoara and Iezerul Galben cirques between 0.38 and 0.40) (Table 10.8).

Reynard et al. (2007) Method

It was developed by Reynard et al. (2007) and focuses on quantifying the scientific value and the additional (cultural, economic, aesthetic, ecological) of geomorphosites. It focuses on quantifying the (main) scientific value (rarity, integrity, representativeness, paleogeographic importance) and the additional ones: cultural (religious, historical and artistic importance, geohistorical), economic (economic profit), aesthetic (lookout points, altitudinal distribution and spatial structure) and

ecological (ecological impact, protected sites). The qualitative aspects deals with general data, description and morphogenesis, as well as with the synthesis (global and educational value, risks and threats, management measures) (Reynard et al. 2007).

The method is intended to inventory local geomorphosites and its main purpose is to correlate human perception of these to their scientific value. Further, we left out all qualitative aspects related to general data, description, morphogenesis or synthesis (global value, educational value, risks, threats and management measures).

The author considers that a geomorphosite is impossible to comprise all the values; this is the reason why in accomplishing the final calculation, the highest value is considered (for cultural value) and the average between these values (for other values). The method is interdisciplinary and it seeks to assess the geomorphosites at various scales for the management of protected areas and the conservation of natural heritage. This is relatively easy to apply, being designed for students.

The total value varies between 0.71 (Vişţea Valley) and 0.27 (Vişţea Mare waterfall). The Vişţea Mare Waterfall geomorphosite as well as Vişţea Needle score 0 for ecological value because they cannot constitute themselves a support platform for valuable ecosystems for the alpine and subalpine area. Although the studied area is not included in the Făgăraş Mountains Alpine Gap National Park, it scores due to the presence of protected species of flora and fauna, as some of the evaluated geomorphosites constitute their natural habitat (Table 10.9).

Both the *cultural component* and the *economic* one scored 0 for all the studied geomorphosites (Table 10.9). In terms of *economic value,* activities such as grazing and tourism are present, but this method strictly quantifies only directly obtained profit.

The scientific value, which for this method has an important percentage, scores values between 0.85 (Vişţea Valley, Portiţa Vişţei Saddle, Vişţea Mare Peak) and 0.25 (Vişţea Mare Ridge), reflecting the importance these geomorphosites have for determining the stages and phases of glacial and periglacial sculpting.

The aesthetic component is the most subjective one, and it scores value ranging between 0.75 for Vişţea Needle and Vişţea Mare Peak that stands out with its level difference, space structure, sightseeing possibilities, and 0.10 for the debris field located at the base of the Vişţea Mare ridge for which these parameters register low values (Table 10.9).

Table 10.9 Evaluating the Vişţea basin geomorphosites using the method developed by Reynard et al. (2007)

No	Name	Scientific value	Scenic value	Cultural value	Economic value	Ecological value	Global value
1	Galaşea Mare–Vişţea Mare Ridge	0.47	0.66	0	0	0.5	0.38
2	Vişţea Mare Ridge	0.25	0.50	0	0	0.5	0.37
3	Zănoaga Glacial Saddle	0.65	0.66	0	0	0.5	0.47
4	Drăguşului Ridge	0.45	0.33	0	0	0.5	0.33
5	Hârtopu Mare Cirque	0.65	0.66	0	0	0.5	0.47
6	Vişţea Mare Waterfall	0.38	0.66	0	0	0	0.27
7	Vişţişoara Cirque	0.65	0.66	0	0	0.5	0.47
8	Vişţea Mare Peak	0.85	0.75	0	0	0.5	0.58
9	Portiţa Vişţei Saddle	0.85	0.58	0	0	0.5	0.58
10	Vişţea Needle	0.75	0.75	0	0	0	0.47
11	Vişţea Valley	0.85	0.66	0	0	0.5	0.71
12	Hârtopu Ursului Cirque	0.65	0.66	0	0	0.5	0.47
13	Vişţişoara Glacial Valley	0.75	0.50	0	0	0.5	0.58
14	Saddle between Vişţişoara and Iezerul Galben Cirques	0.75	0.50	0	0	0.5	0.58
15	Vişţea Mare debris	0.59	0.10	0	0	0.5	0.37

Pereira et al. (2007) Method

The method was initially developed in the Natural Protected Area—Montesinho Natural Park in Portugal (Pereira et al. 2007). This method is part of the studies meant to assess the natural heritage on a regional scale.

The study follows a *series of steps*: geomorphosite inventory (identifying potential geomorphosites, qualitative analysis, selection and description), quantification and hierarchy. In order to obtain this evaluation, the following are considered: scientific value (rarity within the area, integrity, representativeness, pedagogic

importance, diversity, other geological features with patrimony value, importance for scientific research, national coverage), additional values (cultural value, aesthetic value, ecologic value) and management values (accessibility, visibility, current use of any geomorphologic interests, current use of any other natural and cultural features, protection measures and limitations in use, the presence of improvements to the trails, integrity, vulnerability to being used as geomorphosite). The total value is calculated as sum of the scores achieved for each criterion, and for the purpose of classification the corresponding rank is also calculated (the sum of all ranks occupied per criterion) (Pereira et al. 2007).

The main advantage of this method is the early use of a quantitative evaluation, as early as the selection phase which, before, relied exclusively on a qualitative, therefore subjective, evaluation. Among the weak points of this method we mention: the inclusion of integrity (as criterion) both at scientific and protection value.

In the selection stage the intrinsic value, potential use and level of protection are established. Generally, geomorphosites scoring high in terms of scientific value are selected regardless of the scores they get for other criteria, the same goes for geomorphosites-awarded great scores in terms of potential use.

The values obtained for Vişţea basin show that the geomorphosites within this area score high for scientific value and some of them for management elements (legal status, usage limitations, integrity and vulnerability to being used as geomorphosite) and low for additional (cultural) value and some for the aesthetic value as well (debris field allocated at the base of the Vişţea Mare ridge) (Table 10.10).

The highest value (0.553) was registered by the Vişţea Valley scoring for integrity, representativeness, pedagogic importance, diversity, other geological

Table 10.10 Evaluating the Vişţea basin geomorphosites using the method developed by Pereira et al. (2007)

No	Name	Global value	No	Name	Global value	No	Name	Global value
1	Galaşea Mare–Vişţea Mare Ridge	0.412	6	Vişţea Mare Waterfall	0.443	11	Vişţea Valley	0.553
2	Vişţea Mare Ridge	0.408	7	Vişţişoara Cirque	0.495	12	Hârtopu Ursului Cirque	0.487
3	Zănoaga Glacial Saddle	0.309	8	Vişţea Mare Peak	0.487	13	Vişţişoara Glacial Valley	0.491
4	Drăguşului Ridge	0.295	9	Portiţa Vişţei Saddle	0.444	14	Saddle between Vişţişoara and Iezerul Galben Cirques	0.436
5	Hârtopu Mare Cirque	0.471	10	Vişţea Needle	0.527	15	Vişţea Mare debris	0.387

features with patrimony value, importance for scientific research, aesthetic value, ecologic value, accessibility, visibility, current use of any geomorphologic interests, protection measures and limitations in use, integrity, vulnerability to being used as geomorphosite.

The lowest value (0.295) was registered by Drăguşului Ridge, which unlike other similar geomorphosites has a reduced accessibility and visibility, lacks any kind of improvements and has no cultural value (Table 10.10).

Zouros (2007) Method

The method was applied in 2007 for the evaluation of geomorphosites located in various geoparks from the Aegean area (Zouros 2007). The method considers: scientific and educational value: integrity, rarity, representativeness, exemplarity; geodiversity; aesthetic and ecologic value; cultural value; potential risk and prevention: legal protection; vulnerability; potential use: recognisability; geographic distribution; accessibility; economic potential. For each criterion, sub-criteria were defined and the established score range varies between 0 and 5 or 10, respectively. The final total per criteria can be as high as 100 (Zouros 2007). This method can also be used to make a comparison between attribute distribution and their contribution to the resulting geomorphosite value. The strength of the assessment is its immediate practical applicability in the management of the natural heritage of the geoparks, while its weakness refers to the existence of subjective assessment criteria.

The method proposed by Zouros for evaluating geomorphosites offered values ranging between 0.58 (Vişţea Valley) and 0.35 (the debris field located at the base of the Vişţea Mare ridge). Vişţea Valley scored for integrity, representativeness, geodiversity, aesthetic and ecologic value, vulnerability, potential use, recognisability, accessibility, economic potential (in terms of tourism). The debris field located at the base of the Vişţea Mare Ridge scored low for rarity, representativeness, exemplarity, geodiversity, aesthetic and ecologic value, cultural value, legal protection, vulnerability, accessibility, economic potential (Table 10.11).

The introduction of geodiversity as an evaluation parameter favours geomorphosites with a complex morphology, genesis and dynamic (Vişţea Valley, Vişţea Needle, Vişţea Mare Waterfall, Vişţişoara Cirque, Vişţişoara Valley, Vişţea Mare Peak) that stand out as important components even when calculating geodiversity and geomorphic diversity for large areas. They represent interest points for a large scale of geographers, geomorphologists, geologists, ecologists, pedologists, etc. Because the territories evaluated by this method are not a part of a protected natural area, the values obtained are uniform and the class distribution is as it follows: 0.30–0.40–20.00 %; 0.40–0.50–46.66 %; above 0.50–33.33 % (Table 10.11).

Table 10.11 Evaluating the Vişţea basin geomorphosites using the method developed by Zouros

No	Name	Global value	No	Name	Global value	No	Name	Global value
1	Galaşea Mare–Vişţea Mare Ridge	0.42	6	Vişţea Mare Waterfall	0.51	11	Vişţea Valley	0.58
2	Vişţea Mare Ridge	0.41	7	Vişţişoara Cirque	0.51	12	Hârtopu Ursului Cirque	0.48
3	Zănoaga Glacial Saddle	0.39	8	Vişţea Mare Peak	0.56	13	Vişţişoara Glacial Valley	0.49
4	Drăguşului Ridge	0.38	9	Portiţa Vişţei Saddle	0.44	14	Saddle between Vişţişoara and Iezerul Galben Cirques	0.44
5	Hârtopu Mare Cirque	0.48	10	Vişţea Needle	0.54	15	Vişţea Mare debris	0.35

Comănescu et al. (2012) Method

The proposed method gives equal importance to all values when evaluating geomorphosites: scientific (includes the ecological value), aesthetic, cultural and economic as well as management and use of the geomorphosites (Comănescu et al. 2012). The method was applied for some protected areas, its purpose is to achieve an inventory of geomorphosites, their superior capitalization and establishing the most appropriate management system.

The total value is calculated based on the formula

$$\mathrm{Vtot} = (\mathrm{Vsci} + \mathrm{Vsce} + \mathrm{Vcult} + \mathrm{Veco} + \mathrm{Mg})/100 \tag{10.4}$$

where, Vsci—scientific value (paleogeographic interest; representativeness; rarity; integrity; degree of scientific knowledge; use in educational purposes; ecologic value; diversity), Vsce—aesthetic value (visibility; spatial structuring; colour contrast; level difference; landscape framing), Vcult—cultural value (cultural features; historic features; religious features; iconographic/literary representations; festivals or cultural manifestations; symbolic value), Veco—economic value (accessibility; infrastructure; yearly visitors; number of types and forms of usage (including tourism); economic potential—incomes), Mg—management and use (preservation degree; protected sites; vulnerability/natural risks; intensity of use, the use of aesthetic, cultural and economic value, relations with planning policies) (Comănescu et al. 2012).

The results presented in Table 10.12 prove that any correlation between the scientific value and the additional ones is not possible. A high scientific value

Table 10.12 Evaluating the Vişţea basin geomorphosites using the method developed by Comănescu et al. (2012)

No	Name	Global value	No	Name	Global value	No	Name	Global value
1	Galaşea Mare–Vişţea Mare Ridge	0.33	6	Vişţea Mare Waterfall	0.43	11	Vişţea Valley	0.50
2	Vişţea Mare Ridge	0.36	7	Vişţişoara Cirque	0.39	12	Hârtopu Ursului Cirque	0.40
3	Zănoaga Glacial Saddle	0.31	8	Vişţea Mare Peak	0.46	13	Vişţişoara Glacial Valley	0.42
4	Drăguşului Ridge	0.34	9	Portiţa Vişţei Saddle	0.31	14	Saddle between Vişţişoara and Iezerul Galben Cirques	0.30
5	Hârtopu Mare Cirque	0.39	10	Vişţea Needle	0.42	15	Vişţea Mare debris	0.19

usually means similar values for management and use. The amplitude between the obtained values is 0.31, with most geomorphosites scoring values between 0.3 and 0.4 (53.33 %). The relatively low values compared with other evaluation methods result from the high score (20 p) of the cultural value, given that the main elements used for this value are not represented in the study area (Table 10.12).

The highest total value is registered by the Vişţea Valley (0.50) that scores for all criteria except the cultural value, and the lowest total value is registered by the debris field located at the base of the Vişţea Mare Ridge (0.19), that has no cultural value, and almost zero aesthetic value, management and use value. It is clear that geomorphosites with similar genesis (ridges, cirques, saddles, glacial valleys) score relatively similar values, with the differences resulting most of the times from the aesthetic criterion or accessibility and the different types in which it (the geomorphosite) is used for tourism activities (Table 10.12).

Discussions

Although the above-mentioned methods target different objectives, they all consider the following criteria: rarity, representativeness and entirety (Comănescu et al. 2012). Some methods emphasize on the environmental impact (Coratza and Giusti 2005), while for the others the main objective is establishing an inventory of geomorphosites (Serrano and Gonzales-Trueba 2005), to promote geomorphosites for tourism (Pralong 2005); the method developed Zourous (2007) as the one

proposed by Pereira et al. (2007) focuses on evaluating geomorphosites for the management of natural parks (Comănescu et al. 2012). An increased importance is given to potential hazards and use of geomorphosites for touristic purposes, which explains taking into account for the first time a criterion referring to the geomorphosite prestige.

The additional values of geomorphosites are evaluated explicitly in the methods proposed by Pralong (2005), Reynard et al. (2007) and Pereira et al. (2007), while the method proposed by Serrano and Gonzales-Trueba (2005) only considers the cultural value. These methods include the economic value in the evaluation process (the first two directly, and the third implicitly as it is more restrictive and only scores those geomorphosites that produce revenues) (Erhartic 2010).

Pralong (2005) analyzes in clear the economic value of geomorphosites whereas the other methods only present it as default information deriving from the type of use (Serrano and Gonzales Truebo 2005 and Pereira et al. 2007). Except the approach taken by Reynard et al. (2007), all the others concern with management and use of geomorphosites. As we will see, the listed methods share a few features and differ in some others as they were developed to meet different objectives and means of assessment (Grandgirard 1999). The criteria considered in determining geomorphosite value depend very much on the purpose and objectives of the evaluation (Reynard et al. 2007).

Although all of these methods rely on a quantitative system, a certain level of subjectivity cannot be prevented, as all of these parameters are rated by an evaluator based on his perception and experience; objectivity is particularly difficult to achieve in the case of the aesthetic value. Therefore, the method proposed by Pralong (2005) is the most complex and the most accurate one—some of the elements introduced in his method are descriptive (didactic value, risks, use) instead of quantifiable as such, comparison of similar geomorphosites is not possible (Erhartic 2010).

Also, most methods have a major scientific component whereas, in the case of Reynard's method, the scientific assessment only serves as grounds for carrying out a geomorphosite inventory and establishing environmental impact. This method does not place particular importance on the utilization of a particular geomorphosite, but takes into account especially the scientific value, which makes it more transparent and accessible.

The method proposed by Zouros (2007), describes geodiversity in detail, a quite different approach, considering the format of all other methods, yet understandable given that this method was first used within geoparks. Potential risks and use of geomorphosites are given much importance and, for the first time, the recognisability criterion was included in such an assessment, an extremely important factor in analyzing large-scale tourism activities.

Table 10.13 presents a synthesis of the scores obtained with the eight evaluation methods presented above (Fig. 10.8). The total rank results from the sum for each evaluation method and offers a general image of the value of each geomorphosite. Because the subjectivity of each author cannot be eliminated, we consider the rank hierarchy as very important for minimizing it (Comănescu et al. 2012).

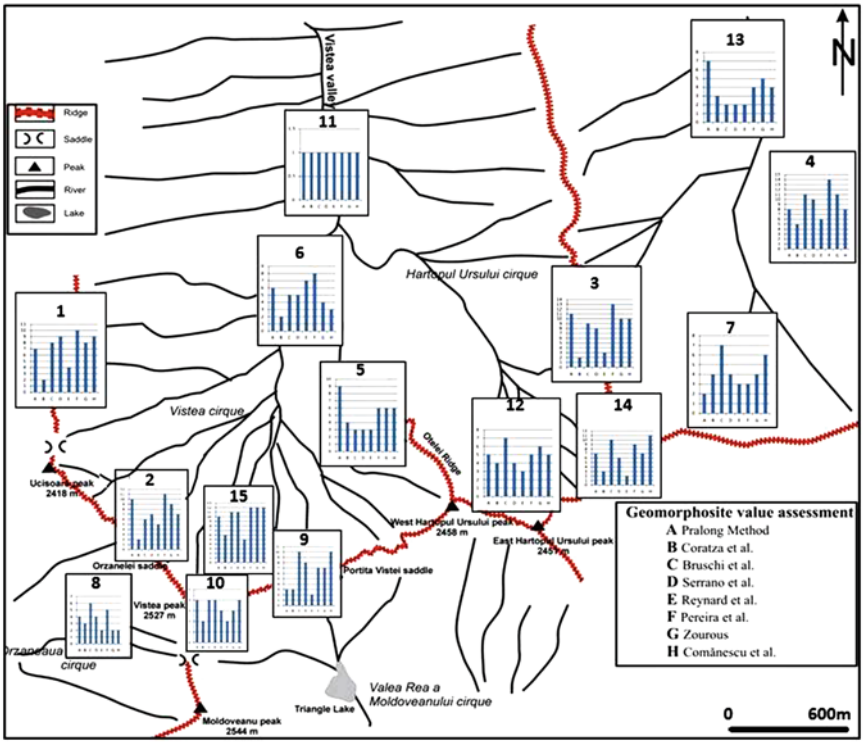

Fig. 10.8 Geomorphosite assessment methods—comparative summary

We computed the average value rank, which is inversely related to the effective value of the investigated geomorphosites.

The values obtained by the different evaluation methods differ according to the variables analyzed, but the upper part of the hierarchy remains mostly the same. Vișstea Valley occupies the first position in all evaluations due to its outstanding scientific features, aesthetic and use value, relatively good accessibility and the fact that this geomorphosite includes additional smaller ones. It has the smallest added rank (8).

On the second place with an added rank of 26 (at a remarkable distance from the first place) stands the Vișstea Needle that occupies places between second and fourth for all the evaluation methods. The Vișstea Needle as well as other residual landforms from the Făgăraș Mountains attracts through its uniqueness, level difference, special structure and geologic and geomorphologic scientific value mainly for specialists.

The third place in terms of value (with an added rank of 28) is occupied by the Vișstea Mare Peak, and with the exception of the Bruschi et al. method it stands between second and fifth.

The highest added rank (79) (translated into the lowest values) was achieved by the debris field located at the base of the Vișstea Mare Ridge which, with the

Table 10.13 Evaluating the Vişţea basin geomorphosites with different methods—rank hierarchy synthesis table

No	Name	Pralong (A)	Coratza et al. (B)	Bruschi et al. (C)	Serrano et al. (D)	Reynard et al. (E)	Pereira et al. (F)	Zourous (G)	Comanescu et al. (H)	Rank	Mean of rank
1	Vişţea Valley	1	1	1	1	1	1	1	1	8	1.000
2	Vişţea Needle	4	2	4	4	3	2	3	4	26	3.250
3	Vişţea Mare Peak	4	3	6	4	2	5	2	2	28	3.500
4	Vişţişoara Glacial Valley	7	3	2	2	2	4	5	4	29	3.625
5	Vişţişoara Cirque	2	4	7	4	3	3	4	6	33	4.125
6	Hârtopu Ursului Cirque	5	4	7	4	3	5	6	5	39	4.875
7	Hârtopu Mare Cirque	9	4	3	3	3	6	6	6	40	5.000
8	Vişţea Mare Waterfall	6	2	5	5	7	8	4	3	40	5.000
9	Portiţa Vişţei Saddle	3	3	10	8	2	7	7	10	50	6.250
10	Saddle between Vişţişoara and Iezerul Galben Cirques	7	3	10	6	2	9	7	11	55	6.875
11	Galaşea Mare–Vişţea Mare Ridge	7	2	8	9	4	10	8	9	57	7.125
12	Vişţea Mare Ridge	10	2	6	7	5	11	9	7	57	7.125
13	Zănoaga Glacial Saddle	11	2	9	8	3	13	10	10	66	8.250
14	Drăguşului Ridge	8	5	11	10	6	14	11	8	73	9.125
15	Vişţea Mare debris	10	6	11	11	5	12	12	12	79	9.875

exception of the methods that emphasize the scientific value (Coratza et al. and Reynard et al.) where it placed 5–6th, has ranked between 10 and 13 due to its low additional values.

The added ranks of geomorphosites with the same genesis, morphology and similar dynamic have comparable values (all ridge type geomorphosites have values between 57 and 73; cirques between 33 and 40; and saddles between 50 and 55). This proves that even though the ranks of similar type geomorphosites are different from one method to another (according to the specific criteria and multitude of objectives) a sum of these ranks will provide a reliable hierarchy.

Conclusions

Geomorphosite assessment is an instrument that allows understanding of the role these could play in the development of regions, as well as in the evolution of tourist activities of different types. Reynard et al. (2009) remarks about the analyzed methods (with the exception of the Zouros method) that they have an inevitable degree of subjectivism, as the real value of these components of environment cannot be measured. The scientific value is evaluated in absolutely all methods, this being the main characteristic of geomorphosites, its lack determining the absence of the quality of geomorphosite. Additional values are differently exemplified, depending on the purpose of evaluation (in most cases protection or promotion of geomorphosites), the potential of use and the measures which impose for superior protection.

With all the clear differences which appear between the methods analyzed as regards numerical values, it must be underlined that the ranks of geomorphosites remain generally the same, which proves that in order to accomplish their classification, all methods are viable.

The area analyzed in detail, namely the Viștea watershed in the Făgăraș Mountains, displays a wide range of glacial and periglacial geomorphosites, with a high degree of representativeness both at the massif scale and at the level of the Southern Carpathians. These landscapes have a high scientific value, as they can offer important information concerning the genesis, evolution and dynamics of the glacial and periglacial topography. The other specific features (ecological, economic, cultural and aesthetic) have different values from method to method, but they are generally lower in comparison with other areas belonging to the Southern Carpathians.

References

Bruschi VM, Cendrero A (2005) Geosite evaluation; can we measure intangible values? Il Quaternario 18(1):293–306

Bruschi VM, Cendrero A (2009) Direct and parametric methods for the assessment of geosites and geomorphosites. In: Reynard E, Coratza P, Regolini-Bissig G (eds) Geomorphosites. Verlag Dr. Friedrich Pfeil, Munchen, pp 73–89

Bruschi VM, Cendrero A, Albertos JAC (2011) A statistical approach to the validation and optimisation of geoheritage assessment procedures. Geoheritage 3:131–149
Cocean G (2011) Munţii Trascău. Relief, Geomorfosituri, Turism. Edit. Presa Universitară Clujeană, Cluj-Napoca (in Romanian)
Cocean G, Surdeanu V (2011) The assessment of geomorphosites of tourist interest in the Trascău Mountains. Studia Universitatis Babeş-Bolyai, Geographia 2:67–81
Comănescu L, Dobre R (2009) Inventorying, evaluating and tourism valuating the geomorphosites from the Central sector of the Ceahlău National Park. GeoJ Tourism Geosites 1(3):86–96
Comănescu L, Nedelea A, Dobre R (2009) Inventoring and Evaluation of geomorphosites in the Bucegi Mountains. Geogr Forum Geogr Stud Environ Prot Res 8:38–44
Comănescu L, Nedelea A (2010) Analysis of some representative geomorphosites in the Bucegi Mountains: between scientific evaluation and tourist perception. Area 4:406–416
Comănescu L, Dobre R, Nedelea A (2011a) The identification of geomorphosites in different cartographic materials. The study case—Bucegi Mts (Romania). Egypt J Environ Change 3(1):25–33
Comănescu L, Nedelea A, Dobre R (2011b) Evaluation of geomorphosites in Vistea Valley (Fagaras Mountains-Carpathians, Romania). Int J Phys Sci 6(5):1161–1168
Comănescu L, Nedelea A, Dobre R (2012) The evaluation of Geomorphosites from the Ponoare protected area. Geogr Forum Geogr Stud Environ Prot Res 9:54–61
Comănescu L, Nedelea A, Dobre R, Bandoc G (2014) Inventoring the principal geomorphosites for determining geomorphodiversity. Case Study—the central sector of the Bucegi Mountains (The Carpathians, Romania). J Environ Prot Ecol 15(4):1849–1857
Coratza P, Giusti C (2005) Methodological proposal for the assessment of the scientific quality of geomorphosites. Il Quaternario 18(1):307–313
Demek J, Kirchner K, Mackovcin P, Slavik P (2011) Geomorphodiversity derived by a GIS-based geomorphological map: case study the Czech Republic. Zeitschrift für Geomorphologie 55:415–435
Erhartic B (2010) Geomorphosite assessment. Acta Geographica Slovenica 50(2):295–319
Gavrilă I, Anghel T (2013) Geomorphosites inventory in the Măcin Mountains (South-Eastern Romania). GeoJ Tourism Geosites 11(1):42–53
Grandgirard V (1999) L' evaluation des geotopes. Geol Insubr 4(1):59-66
Ilieş D (2014) Tourism planning and management for natural heritage. Edit. Bernardinum, Poland
Ilieş D, Josan N (2007) Preliminary contribution to the investigation of the geosites from Apuseni Mountains (Romania). Revista de geomorfologie 9:53–59
Ilieş D, Josan N (2009) Geosituri şi geopeisaje. Edit. Universităţii din Oradea (in Romanian)
Ilieş D, Ilieş A, Herman G, Baias Ş, Morar C (2011) Geotourist map of Baile Felix-Băile 1 Mai-Betfia (Bihor County, Romania). GeoJ Tourism Geosites IV(8):219–227
Irimia D, Toma B (2012) The identification of the geomorphosites in Buzău Subcarpathians. Tourism capitalization options. Studia Universitatis Babeş-Bolyai—Geographia LVII 2: 161–171
Irimuş IA, Petrea D, Vescan I, Toma B, Vieru I (2011) Vulnerability of touristic geomorphosites in Transylvanian saliferous areas (Romania). GeoJ Tourism Geosites 2(8):212–219
Kostrzewski A (2011) The role of relief geodiversity in geomorphology. Geographia Pol 84(2): 69–74
Panizza M (2001) Geomorphosites: concepts, methods and examples of geomorphological survey. Chin Sci Bull 46:4–6
Panizza M (2009) The geomorphodiversity of the Dolomites (Italy): a key of geoheritage assessment. Geoheritage 1:33–42
Pereira P, Pereira D, Caetano Alves M (2007) Geomorphosite assessment in Montesinho Natural Park (Portugalia). Geogr Helv 62(3):159–169
Pralong JP (2005) A method for assessing tourist potential and use of geomorphological sites. Géomorphol Relief Processus Environ 3:189–196
Reynard E (2005) Géomorphosites et paysages. Géomorphol Relief Processus Environ 3:181–188

Reynard E, Fontana G, Kozlik L, Scapozza C (2007) A method for assessing "scientific" and "additional values" of geomorphosites. Geogr Helv 62(3):148–158

Reynard E, Coratza P, Regolini-Bissig G (2009) Geomorphosites. Verlag Dr. Friedrich Pfeil, Munchen

Serrano E, Gonzalez-Trueba JJ (2005) Assessment of geomorphosites in natural protected areas: the Pico de Europa National Park (Spain). Géomorphol Relief Processus Environ 3:197–208

Wimbledon WAP, Ishchenko AA, Gerasimenko NP, Karis LO, Suominen V, Johansson CE, Freden C (2000) Geosites-an iugs initiative: science supported by conservations. In: Barettino D, Wimbledon WAP, Gallego E (eds) Geological heritage: its conservation and management

Zouros N (2007) Geomorphosite assessment and management in protected areas of Greece. Case study of Lesvos island—coastal geomorphistes. Geogr Helv 62(3):169–180

Part III
Hillslope Evolution by Mass Movement Processes

Chapter 11
The Systematic of Landslide Processes in the Conditions of Romania's Relief

Mihai Micu

Abstract Landslides are extremely active slope-shaping processes. Their broad spectrum of processes and forms, alongside different types of displaced material is conditioned by a wide range of predisposing, preparing, and triggering factors. There are numerous attempts to classify them homogeneously, but quite often, the heterogeneity of the phenomenon imposes different criteria, depending on regions or scientific schools and approaches. Criteria like morphology and morphogenesis always found a common usage; meanwhile others like age or morphodynamic behavior are still debated. In Romania, the wide range of processes and forms, as well as the potential consequences inflicted to the socio-economic environment is well reflected within an extended geomorphologic literature, dealing with both fundamental and applied considerations. If for a long period of time, landslide systematic in Romanian geomorphology was predominantly descriptive, during the last two decades, one faces an almost completely shifted approach, changing from fundamental aspects to predictive studies, in the form of susceptibility, hazard, and risk. Through an in-depth review of the most important outcomes of the last 100 years' literature in the field of landslide systematic, several milestones might be set up. The relationship between geomorphology and other geonomic sciences, as well as the connections between national and international literature are discussed in terms of common or uncommon criteria of classification. A concise description of the main types of landslides (according to modern literature) throughout Romania is given in terms of synthetic regional descriptions.

Keywords Landslides Romania · Classification

M. Micu (✉)
Institute of Geography, Romanian Academy, Dimitrie Racoviță 12,
023993 Bucharest, Sector 2, Romania
e-mail: mikkutu@yahoo.com

M. Rădoane and A. Vespremeanu-Stroe (eds.), *Landform Dynamics and Evolution in Romania*, Springer Geography,
DOI 10.1007/978-3-319-32589-7_11

A Short History

The international literature on mass movements is rich in landslide classification, given by the wide range of processes, forms, or displaced material. Mass movement classifications are given by Sharpe (1938), Hutchinson (1988), Zaruba and Mencl (1969), McCalpin (1984), Cruden and Varnes (1996), Dikau et al. (1996), Cruden and Fell (1997), Lee and Jones, (2004) or Hungr et al. (2013), but the most used classification is the one given by DJ Varnes in 1978 and later on, in 1984.

The wide range of processes, forms, and potential consequences is well reflected in the extended Romanian geomorphologic literature, focusing on both fundamental and applied considerations regarding slope mass movements. Several milestones can be set up along the last 100 years of researches. The following selective analysis emphasizes different patterns within the research, conditioned by the fundamental knowledge requirements, end-user demands or access to measurement tools and new, updated research methods, as detailed in the brief attempt below.

1910–1960: Pioneering and Fundaments

From its early beginnings, the Romanian literature follows and sometimes even anticipates, the international framework, while the litho-structural environment extremely prone to landslides allows the very first studies to be traced back towards the early twentieth century. The geomorphologic literature of the 2–5th decades of the twentieth century was strongly marked by geologic studies focused especially on the mass movements' classifications (e.g., Mrazec 1923; Munteanu-Murgoci 1923; Macovei and Botez 1923; Mihăilescu 1939; Dragoş 1957).

The first studies dealing with landslides as active morphodynamic processes, coupling slope and channel environments, date back in the 1920s and belong to Macovei and Botez (a study realized in 1915, but published due to the conditions imposed by the First World War only in 1923), Mrazec (1923) or Munteanu-Murgoci (1923). A very interesting overview on the variety of forms and processes offered by the Curvature Subcarpathians of Romania is given in March 1915 by Macovei and Botez, which studied the numerous *falls* and *slides that* occurred during the first trimester of that year. They differentiate (maybe for the first time in the Romanian literature) several types of processes and associated forms: *slides stricto*-sensu (affecting areas up to 140 ha and occurring *…only when the topographic slope is according to the strata inclination…*), *flows* (completely different process, described as developing along three main morphodynamic sectors—the torrential origin area, the flowing track and the terminal accumulative fan—which involves a fluid displacement of oversaturated, fine material, *looking more like a glacier in terms of morphology*), *debris slides* (affecting anaclinal strata), and *falls* (associated mainly with river undercut). Besides giving a brief description of the causes of such processes, the article outlines the importance of serious land

reclamation works among which are transversal torrential dams and reforestations (with a role in diminishing the process, not stopping it completely).

A more detailed geomorphologic description is given by Mihăilescu in 1939, who, in its *Geomorphology Course* given at the Faculty of Sciences in Bucharest makes a correlation with the Italian term *frana* (which is even used by the author in 1927 as neologism), citing the work of Almagia (1910). He suggests the term, relatively translated as *displacement* (in Romanian *pornitură*) and divides the process in two main categories: *dry displacements* (falls, topples) and *wet displacements* (slides, flows). The author emphasizes the morphology and morphometry of such processes (as seen in Fig. 11.1a), which may affect *entire mountains* (Fig. 11.1b). Later on, in 1939, the same author uses the morphogenetic criterion (initial stage of the material, displacement mechanism, resulted form) in order to classify the slope mass movements into *topples and rolling* (Fig. 11.2a), *humid and wet slides* (Fig. 11.2b), *dry and wet falls* (Fig. 11.2c, d).

Later on, in 1946, he classifies them only into *dry* (topples and compaction) and *humid* (solifluxion, earth flows, debris torrents and slides) displacements. In 1957, Dragoş divides them according to the environment into *subaerial*—falls, flowing sands, strata bending, solifluxion, slides—*submarine* and *tectonic*) (Dragoş 1957). Towards the end of this time period appear the first attempts to provide national distributions of landslides. In 1959, Rădulescu was claiming that "…the landslide studies in Romania have been done in a way which is not well systematized… therefore, even though we have well-fundamented papers, synthesis works cannot be realized yet…" (Rădulescu 1959a, b). The author provides a map with the distribution of different landslide types (slides, flows, and falls) and even gives a rough estimation (at a national scale) of 116,000–900,000 ha affected by these processes.

By looking at the above-mentioned contributions, we may notice that the morphologic and morphodynamic criteria which were used by these landslide-geomorphology pioneers get their classifications extremely close to the

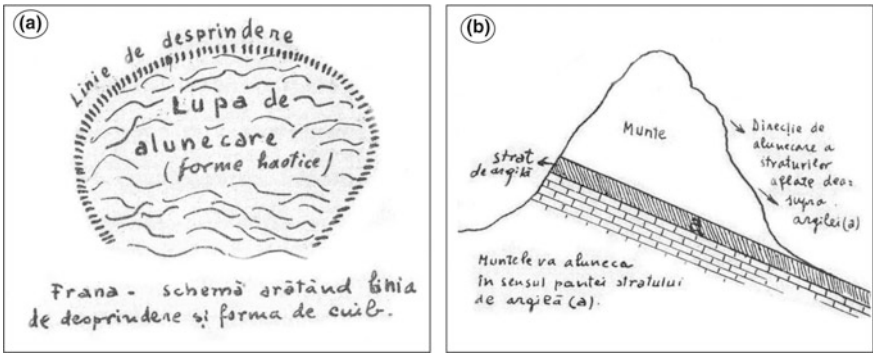

Fig. 11.1 The morphology of *pornituri* (slope displacements) according to Mihăilescu (1927): *frana* "typical" slide (**a**), displacement sketch across a mountain (**b**)

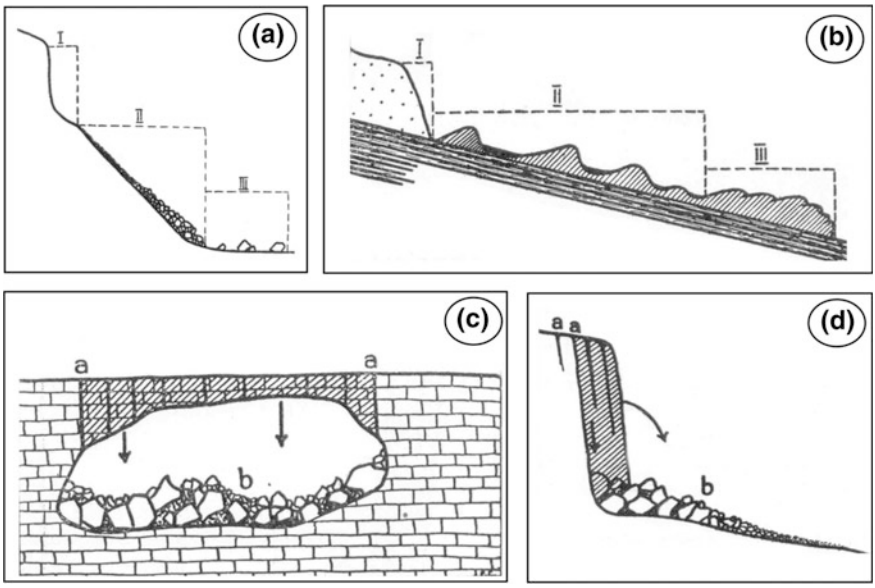

Fig. 11.2 The classification of Mihăilescu (1939): falls and rollings (**a**), humid mound-like slide (**b**), endo-karst dry falls (**c**), coastal wet falls (**d**)

ones used worldwide at that moment (Almagia 1910; Sharpe 1938), even anticipating those given by Hutchinson (1988) or Zaruba and Mencl (1969).

1960–1990: Forms, Processes, and Remediation Suggestions

During the following three decades, the landslide systematic studies went in parallel, in two main directions: a fundamental research one (in the attempt of offering explanations in terms of forms and processes and their predisposing and preparing/triggering factors) and a newly-born but fast growing applied approach (enhanced by the economical framework, which was focusing on finding the optimal land-use strategies or enhancing land reclamations (Morariu and Tufescu 1964; Ichim and Lupaşcu 1975).

The interest was oriented towards mass movement morphodynamics (e.g., Cioacă 1967; Ielenicz 1970; Ichim 1972; Posea 1972; Surdeanu 1975; Bălteanu 1970; Grecu 1982), litho-structural predisposition (e.g., Donisă 1968; Badea 1972; Grecu 1983; Ichim 1972; Ielenicz 1984), age (Morariu et al. 1964) regional patterns of their morphology (e.g., Băcăuanu 1977; Ielenicz 1981; Bălteanu 1983; Grecu 1985), typological mapping (Grigore and Ielenicz 1972; General Geomorphological Map of Romania 1:200,000, Institute of Geography, Romanian Academy) and towards the major interactions between slope and channel processes (e.g.,

Dragomirescu and Gâştescu 1960; Posea 1969; Popescu and Popescu 1978; Bălteanu 1974; Surdeanu 1975). All throughout the period, the shy and not that numerous translations to/from English introduced into the Romanian geomorphologic language, a mistake that was carried out up to recent times by many authors: the term *landslides* was associated to the Romanian correspondent of *alunecări*, which actually correspond only to the subtype of *slides*.

These decades are rich in systematic studies, among which the most important might be those of: Martiniuc and Băcăuanu (1961; the authors adapt a landslide classification to the structural conditioning of the Moldavian Plateau, a typical homocline area—Fig. 11.3); Tufescu (1964; according to the causes, he separates between mechanical: *topples*, *falls*, *piping*, *strata bending*, *compaction*, *creep*, and water-driven: *flowing sands*, *earth flows*, *solifluxion*, *slides*; Fig. 11.4); Coteţ (1969; according to the water content, he separates among *dry*—falls, rollings, compaction, *humid*—slides, solifluxions, and *mixed*—combination between gravitational and erosional processes—displacements); Bălteanu and Mateescu (1975; are providing a first unitary, national-scale map of present-day modeling processes); Bally and Stănescu (1977; provides a geological—both lithologic and structural—insight and finds inspiration in the classifications of Sharpe and Hutchinson).

Among the landslide types, the deep-seated ones (considered by all authors as displacing more than 10 m thick deposits) raise a particular interest, due to the high morphogenetic complexity and large magnitude. There are numerous studies

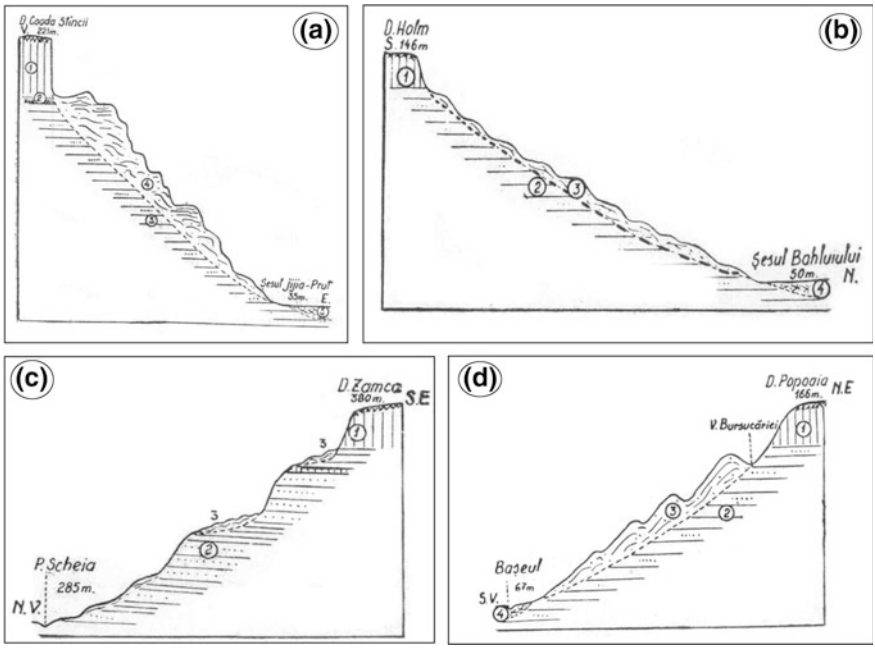

Fig. 11.3 The classification of slides according to Martiniuc and Băcăuanu (1961): mixed-fragmentation slides (**a**), monticule-like slide, step-like slide (**c**), wave-like slide (**d**)

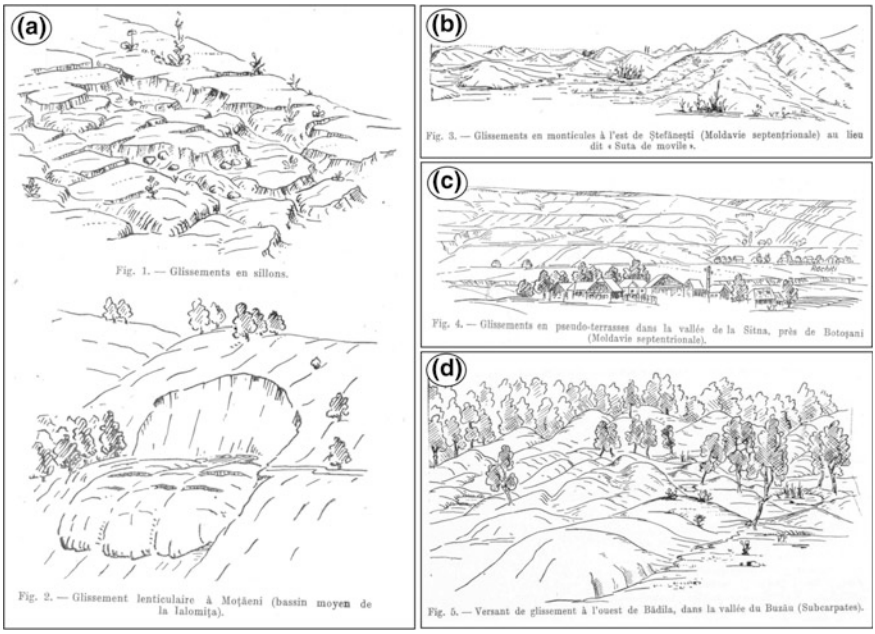

Fig. 11.4 The classification of slides, according to Tufescu (1964): furrow-like slides (**a**), monticule-like slide (**b**), pseudo-terraces like slide (**c**), entirely landslide-affected slope (**d**)

aiming at establishing the causes of such processes, mainly in the neotectonically active area of the Curvature Carpathians (for which area, Posea and Ielenicz (1970, 1976) and Posea (1972) are using terms like *massive zonal slope slide*, *profound massive slope slide*, *profound massive valley slide*, or *landslide valleys*; Posea and Popescu 1976; Bălteanu 1970, 1971), the Eastern Carpathians (Sârcu 1962; Surdeanu 1975, 1976; Surdeanu and Rădoane 1976) or the Transylvanian Depression, where a particular type of landslides, called in Romanian *glimee*, finding its most representative morpho-litho-structural occurrence environment, tried to made its way in the nomenclature (suggested as a landslide type during the 1964 XIth International Geographical Congress). Studied by Morariu and Gârbacea (1968) and later on by Josan and Grecu (1981), Grecu (1982, 1983, 1985), Gîrbacea and Grecu (1983) and Gârbacea (1992, 1997, 2013) these old (even Wurm), large (Şaeş complex extending across 1500 ha), deep-seated (frequently affecting the regolith and the bedrock together) particular processes barely find a correspondent in international classifications. While their genesis is still largely debated, their morphology gets them sometimes close to lateral spreads and sometimes can only include them inside the very general *complex* type.

Other interesting classifications are given by Mamulea (1975; mass movements without an own displacement subsurface, mass movements with an undetermined displacement subsurface, mass movements with a determined displacement subsurface), Băcăuanu (1977; classifies the landslides according to the homocline

landforms of the Moldavian Plateau), Ielenicz (1970; gives a national-scale evaluation of landslide distribution and outlines the common morphological traits according to the main morphostructural units) and Bălteanu (1983; adapts for the Curvature Subcarpathians the classification of Varnes 1978). A particular interest is raised by mudflows, acknowledged as showing a high frequency but low-magnitude dynamic pattern (Tufescu 1964; Bălteanu 1976, 1983).

1990–2000: New Horizons

After 1990, the interest towards landslide classification diminished and such approaches could be found in wide synthesis works, which outline the large number of criteria used for such purposes: the relationship between the sliding surface and the geological structure, evolutive direction, type of movement, thickness, shape, etc. (Josan et al. 1996; Posea 2002). Instead of systemic studies, over the last two decades of the twentieth century there was a growing concern for applied studies, focusing on landslides as land degradation processes (e.g., Surdeanu 1998; Sandu 1998), the dynamics of conditioning factors (e.g., Bălteanu and Cioacă 1997; Cioacă 1996; Dinu 1997; Posea and Vespremeanu 1985; Surdeanu 1992) or on the triggering factors and their spatial and temporal patterns (e.g., Dinu and Cioacă 1997; Cioacă and Dinu 1998). The technological (computers, software) and methodological (the interdisciplinary character of applied statistics or remote sensing imagery) developments, together with the highly increasing opening towards new, easily accessible state-of-the-art information, marked the geomorphological literature in terms of both quantity and quality.

Since the end of the twentieth century, the interest was shifted steadily towards the analysis of slope mass movements as hazards and subsequently induced risks, as these processes were started to be related through evolutive models with the potential consequences that they might inflict (e.g., Surdeanu 1985; Bălteanu 1992; Rădoane et al. 1995; Bălteanu et al. 1989, 1996; Grecu 1992; Loghin and Păunescu 2002; Armaş et al. 2003, Surdeanu et al. 2010). A detailed review of modern approaches concerning landslide susceptibility, hazard or risk, at either local, regional or national scales using both qualitative and quantitative methods is given by Bălteanu et al. 2012 and by Micu et al. Chap. 32, this volume.

Landslide Typology in Romania: An Updated Picture

For terminology-harmonization reasons, in this chapter the most widely used classification available in the specialist literature, i.e. the one of Cruden and Varnes (1996, improved by Hungr et al. 2013) was used, in order to outline the most widespread landslide types in Romania.

Slides

In Romania, the large slide typology reflects the wide complexity of predisposing, preparing, and triggering factors. The Carpathian Mountains, Subcarpathian Hills and Depressions, Transylvanian or Moldavian Plateaus show extremely prone settings for slide occurrence, being in the mean time among the country's regions featuring a high concentration of elements at risk.

The mountainous flysch sector is characterized by the existence of large, dormant (partially relict) slides (rock slides, debris slides, or complex) (Fig. 11.5a). Showing a low-frequency high-magnitude pattern, these slide types present a lot of sectors with recent reactivations, either at their toe or scarp. The hilly or tableland areas developed on molasse deposits are featuring very frequent but low-magnitude slides, in form of earth slides and flows, rock slides and rarely debris slides (Fig. 11.5b). In these areas, the slides are forming large complex areas in which they associate with (either as conditioning or being induced by) erosion processes, especially in the form of rill and inter-rill erosion and rarely gullies.

There are two main triggers of the wide variety of slides, either in form of single or multiple slide events: precipitation and earthquakes. Torrential rainfalls during summer are causing earth flow pulsations that are enhancing slope instability in the main sources' area in the form of retrogressive slides. The spring showers (overlapping snowmelt in the mountains or high hills) and autumn rainfalls are frequently causing deep-seated earth or rock slides in the flysch Carpathians, as well as a wide spectrum of shallow slides in the Subcarpathians or plateaus. Even though not fully explicitly outlined, the earthquakes are determining both co-seismic and post-seismic failures such as rock slides combined with rockfalls or debris flows (e.g., Bălteanu 1979; Mândrescu 1981, 1982; Radu and Spânoche 1977; Micu et al. 2015). Due to the long-lasting habitation, the hilly areas of the Subcarpathians were marked by an intense human impact on the environment. The large deforestations throughout the second half of the nineteenth century, the large development of communication networks along the second half of the twentieth century or the changes occurred in land ownership after the fall on the communist regime (1990 onwards), acted as preparing factors for slides occurrence and reactivation.

Fig. 11.5 Deep-seated rock slide in the Buzău Carpathians (Şeţu, **a**) and shallow translational earth slides in the Buzău Subcarpathians (Bălăneasa catchment; **b**) (*Photos* M. Micu)

Flows

Fast moving and extremely dangerous from the point of view of potential damages, the flows may frequently affect the debris and soils/earth and less likely the rocks. The morphometrical variables and the litho-structural conditions of the Carpathians are making them less prone to rock or debris flows if compared to the Alps or the Pyrenees. A detailed description of their occurrence conditions and further development framework is provided in this volume by Pop et al., Chap. 14.

The very folded and faulted structure of the Subcarpathians, the loose sandy, marly or clayey formations that are forming the molasse deposits on which they are built makes this hilly region extremely prone to such processes, especially in the form of earth flows. Under specific conditions (amount of water content especially), flows can range within the same process from hyperconcentrated flows to earth flows or debris flows. Small nonchanneled and superficial earth flows, small channeled earth or debris flows or deeper earth/debris flows are preconditioned also by the thick sand or gravel unconsolidated deposits that correspond to the Upper Pliocene–Quaternary period (frequent in the Moldavian, Curvature or Getic Subcarpathians, Central Moldavian and Someş Plateaus, Western Hills). Their pulsatory behavior is imprinted by the summer torrential rainfalls. The rich content of clay minerals (illite, montmorillonite) contributes to successive overpasses of Atterberg limits and, depending on the regional and seasonal precipitation patterns, the processes can shift from a viscous to a plastic displacement, like frequently happens in the Curvature Subcarpathians (e.g., Chirleşti mudflow, described in detail by Bălteanu and Micu in 2012 (Fig. 11.6). Known in the Romanian specialized literature as "*alunecări curgătoare*", this processes found a correspondence within the classification of Hungr et al. (2013) as flowslides.

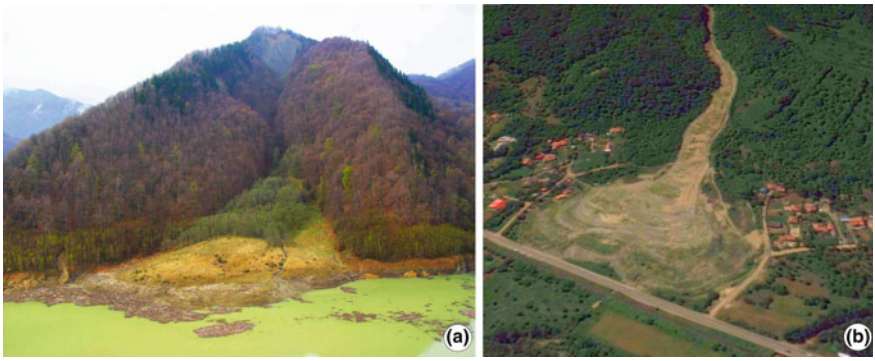

Fig. 11.6 Debris flow (Siriu; **a**; *Photos* M. Micu) and earth flow (Chirleşti; **b**; GeoEye aerial photo, 2013) in the Buzău Carpathians

Falls

According to Ilinca (2010), in the Carpathians, these processes occur in the high mountain area, mainly in form of rockfalls, where the predisposition given by the presence of natural rock slopes exists. In the mean time, preparing and triggering factors for rock fall occurrence are enhanced along the roads that cross the Carpathians (Fig. 11.7), situation in which the sources might be both natural and anthropic (undercut slopes).

A recent estimation of rock surfaces in the Carpathians (Vasile et al. 2015), shows that the area covered by rock walls reaches about 17 km^2, approximately 3 % of the total surface of the mountain range. This area is theoretically more prone to rockfalls. As described by Ilinca (2010), these events are generally reported mainly in hard jointed rock formations. The joints or discontinuities in the rocks appear due to several tectonic, stratigraphical, mechanical, climatic, and anthropogenic factors. As Hencher (1987) pointed out, a rock slope can be affected by many types of discontinuities like tectonic joints, faults, lithological boundaries, sheeting joints, bedding planes, fissures, cooling joints, and metamorphic fabrics. Along these discontinuity planes the shear strength is looser, especially where groundwater infiltration exists. The relationships between joints and slope face define the type of rock detachment which can be planar, wedge, topple, overhang, or complex (Hencher 1987; Hantz et al. 2003).

Spreads

Moving with a much slowly speed compared to the previous mass movement categories, the lateral spreads (Fig. 11.8) are characterizing the areas in which more-or-less cohesive rock formations are overlaying and slowly moving onto much finer materials, without featuring an obvious ruptural surface. Even though

Fig. 11.7 Rockfalls in the Buzău Carpathians, along National Road nr. 10 (*Photos* M. Micu)

Fig. 11.8 *Glimee* at Şaeş (Transylvanian Tableland, **a**; *Photo* M. Micu) and lateral spread at Seimeni (Dobrogea Tableland, **b**; GeoEye aerial photo, 2014)

not that common, lateral spreads can be found in Romania along the large flood plains of rivers crossing the Eastern (flysch) Carpathians, in the low-altitude Moldavian or Transylvanian plateaus or along the Danube, at its contact with the Dobrogea Plateau. In Transylvania, a rather resembling process (at least from a morphologic point of view, since the morphogenesis should be better assessed in terms of failure mechanisms) is known in the Romanian specialist literature under the name of *glimee* (Fig. 11.8a; a comprehensive literature has been provided in the above text).

Interesting cases of such processes are encountered along the Danube, at Seimeni, Dunărea, Topalu. Due to the lithology (loess-like deposits), the high level of the underground waters, the compaction caused sometimes (like in the case of the city of Galaţi) by slope overload and the lateral erosion caused by the Danube in its seasonal level shifting leads to the slow occurrence of cracks and spreads that may affect houses, blocks of flats, or almost entire neighborhoods or villages. Such an example is the village of Seimeni, which was affected in 1999, 2005, and 2010 by such processes that endangered more then 20 households (Cazacu and Drăghici 2011).

Topples

Less widespread in comparison with the other mass movement processes, topples are affecting fissured cohesive rocks overlaying marly or clayey slipping strata. This alternation may be encountered throughout the flysch chain of the Eastern Carpathians, where the intense folding is often bringing to vertical fissured sandstone packs which may later end up on topple on top of the schistose intercalations. In this region, topples are quite often combined with falls, making them more difficult to be distinguished. Another prone environment is the one of the Pliocene formations of the outer Curvature Subcarpathians, where loess-like deposits overlaying clay lens lead to topple occurrence but with a smaller magnitude (Fig. 11.9).

Fig. 11.9 Gravel/sand topple at Muscel (Buzău Subcarpathians; *Photos* M. Micu) before and after the collapse

Creep

As either shallow (seasonal; Fig. 11.10a) or deep-seated (without depending on seasonal variability; Fig. 11.10b), the creep is a common process all throughout the Carpathians and Subcarpathians.

Fig. 11.10 Soil creep at Valea Viei (Buzău Subcarpathians; **a**) and rock slope deformation (rock creep) at Cătiaşu (Buzău Carpathians; **b**) (*Photos* M. Micu)

In the flysch sector of the Eastern Carpathians, it is quite often that the creep represents the incipient stage of large, deep-seated landslides. Rarely described in the literature (Bălteanu 1983; Băcăinţan 1983; Rădoane 1995), the creep itself barely poses threats to society, but an enhancement of its displacement speed may be associated with potential slide initiation.

Compound/Complex

The presence, especially in the Subcarpathians (very common in the Curvature sector, but encountered also in the Moldavian and Getic units), of large areas affected by compound or complex landslides (Fig. 11.11), is conditioned from a morphological or morphodynamic point of view mainly by the combination of gravitational and hydrological processes.

Gully erosion has contributed to the enhancement in landslide typology, their morphodynamic patterns, their frequency, and more often magnitude. Previous studies (Bălteanu 1983) showed for the region of the Buzău Carpathians and Subcarpathians that, if gully-affected slopes represent only 1.5 % out of the entire area, the slopes across which the gully erosion—less present, apparently playing a reduced role, but actually conditioning and enhancing slope mass movements—increases in proportion to 38 %.

Fig. 11.11 Complex landslide at Siriu (Buzău Carpathians) (*Photo* M. Micu)

Conclusions

The complexity of predisposing (litho-structural conditions, neotectonics), preparing (land-use changes as a result of human intervention on the environment), and triggering (spatial and temporal patterns in precipitation or temperature distribution, seismicity) factors that are characterizing the Romanian territory makes it prone to a wide variety of slope and channel present-day modeling processes, among which the landslides are playing a determinant role in numerous physiographic units. This variety, expressed in terms of morphogenesis (agents, processes, and induced forms) or morphodynamics (as response to lithological constrains, structural conditioning, morphometry, or specific triggers) requested numerous calls to find the most suitable classification. While the first attempts (1910–1960) to provide eloquent classifications were following a bottom-up approach, starting with single scattered cases meant to allow regional generalizations, the latter (1960–1990) studies aimed at establishing not only regional descriptions but also national evaluations. This allowed the contemporary (2000 onwards) studies to follow top-down approaches, supported by more accurate statistic or probabilistic models of future slope evolution, focused on homogeneous morphostructural units, representative catchments, or different-level administrative units.

The dawn of Romanian geomorphologic literature on landslide systemic shows significant imports from geology, as actually registered worldwide. The first classifications are not only in agreement with the international ones, but they even precede them sometimes. The lithological predisposition, the structural constraining and, as a result, the landslides' morphology represented long time the main criteria taken into consideration in landslide classifications. In this way, the geomorphological school gained a strong ability to perform different-scale mappings, but for a long period it did not make significant progresses towards morphodynamic evaluations. The opening of new research centers (Pângăraţi, Pătârlagele, Perieni, Aldeni) during the 6–7th decades of the twentieth century created propitious conditions for more in-depth studies, which provided an important insight into the succession of agents-processes-forms, allowing the first empiric quantitative evaluations on landslide morphodynamics.

For a long period of time, landslide geomorphology in Romania was predominantly descriptive. Regional classifications were only taking into consideration such criteria as morphology or morphography, while elements such as depth, age or degree of activity were only subsidiary. This is the main reason for which, for a long period, terms like mound, step, nest, wave, tongue were prioritarily used in landslide description. Slowly but steadily, considerable progresses are being achieved along the fundamental direction, Romanian geomorphologists providing more accurate and in-depth morphogenetic explanations on numerous scattered cases, allowing a better regionalization of similar processes. On the other hand, the socio-economic environment, focusing increasingly more on land reclamations and on the assessment of optimal land use for an increased economical productivity, enhanced the interdisciplinarity in landslide studies. This process helped the

geomorphologists to improve systematic landslide by taking into consideration criteria coming still from geology (including engineering geology) or newly-developed fields like remote sensing and aerial photo interpretation. As a result, criteria such as age, morphodynamic patterns, multitemporal distribution appeared in landslide classification alongside more detailed descriptions of their reasoning.

Encouraged by the increased accessibility and opening towards the modern literature registered after 1990 and supported by the technological (hardware and software, in situ or remote measurements devices) progresses, the landslide geomorphology of the last two decades almost completely shifted approaches, changing from fundamental aspects to predictive studies, in form of susceptibility, hazard, and risk. In the attempt to align itself to the mainstream, the classifications used nowadays are following those used in the state-of-the-art international literature, allowing a common language extremely useful in the international and interdisciplinary modern risk management and communication frameworks.

An overview on Romania's territory is showing several areas (Fig. 11.12) which are differently affected by specific landslide types. Favored by the lithology, conditioned by structure and morphometric traits, prepared by the different patterns in land use and land management and triggered by precipitation and earthquakes, the landslides may be clustered into several representative units, as follows:

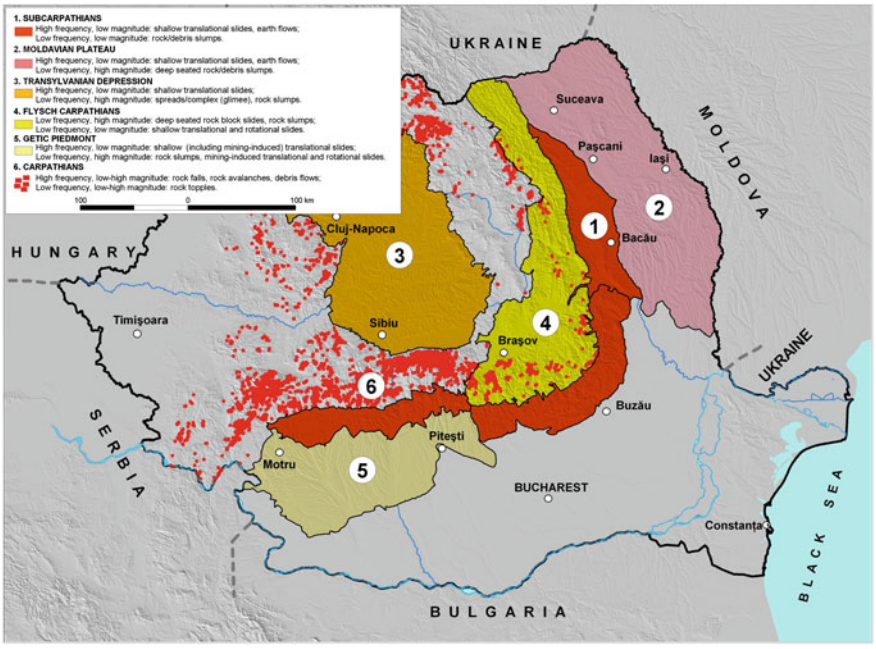

Fig. 11.12 The distribution of most landslide-affected physiographic units of Romania (to see the text for other explanations)

1. **The Subcarpathians**. Presenting heights of up to 900 m, the hilly Subcarpathian chain is featuring morphometrical traits induced by the loose Neogene (Mio–Pliocene) molasse deposits (dominated by schistose marls and clays in association with sands and gravels), highly folded, and densely faulted. Besides the litho-structural and morphometrical favorability, the intense neotectonic movements (uplift rates of 3–5 mm/year) and high sub-crustal seismicity (characterizing especially the Curvature sector) augment the overall denudation potential, inside which landslides plays by far the most important role. The most widespread types are the shallow translational (seldom rotational, either caused by river undercut or by clayey lens inside thick sands and gravels deposits) slides, affecting the soil and partially the upper part of the regolith. Together with the earth flows, they show a very high frequency but low magnitude, still affecting, as single processes, areas up to 5–10 ha. The slides occur mainly during the spring (rain showers overlapping snowmelt) and autumn (long-lasting rains), while the earth flows show a pulsatory behavior, answering rather fast to torrential summer rains. Conditioned by the illite/montmorillonite/smectite rich clays, the earth flows are featuring a visco-plastic behavior and high speed (up to 20 m/h) displacements. The other landslide types are less represented; however, they may be encountered throughout the entire unit due to the extremely heterogeneous lithology, structure, and morphometric traits. Flash floods are characteristic of the contact area with the Carpathians and meanwhile, the presence of large depressions with extended flood plains alternating with narrowing river sectors contribute to increasing flood potential. Both situations are leading to the occurrence of a large number of riparian landslides (in the form of shallow translational earth and debris slides or rock slumps). Large deforestations are enhancing the potential of slope failure.
2. **The Moldavian Plateau**. The typical plateau homocline structure imprints the main morphological characteristics of the large number of landslides recorded here, mainly as a result of the lithological favorability (an alternance of consolidated—schistose sandstones and limestones—and unconsolidated—clays, marls, sands, silts—rocks). The predominant NW-SE homocline inclination (inside which several subunits may be separated) is conditioning landslide typology: along the north and west-facing cuesta escarpments occur numerous shallow and deep-seated rock slumps (frequently combined into complex landslides, potentially-affecting the entire slope), while along the dip slope are registered mainly shallow and medium-seated slides and less often earth flows. To this situation contributed significantly, the land-use changes throughout the time, in one of Romania's most important agricultural regions: deforestations, lack of extended, and well-maintained agro-technical and land reclamation works, property fragmentation. A detailed insight is provided within Chap. 12, this volume.
3. **Transylvanian Depression**. The region is representative for a particular type of landslides, i.e., *glimee* (in Romanian). This type of landslides appears also in other regions of Romania (for example, Moldavian Plateau) but found in several plateau subunits of the Transylvanian Depression the optimal occurrence

environment. Placed somewhere at the border between spreads and complex, *glimee* are usually displaced as parallel successive rows throughout the upper half of the slope, rarely reaching the valley bottom. Showing a high magnitude (deep-seated and extended across hundreds and thousands of hectares) pattern, these old (almost entirely dormant or relict) landslides are associated with shallow translational slides (either as first time failures or subsequent reactivations) and rock slumps. The latter are characterizing the cuesta escarpments that are bordering the major rivers crossing the plateau, playing a major role in the evolution of such lineaments. The presence of salt deposits adds dissolution as an enhancing factor of slope instability.

4. **The Flysch Carpathians**. Especially throughout the Eastern Carpathians, built on Cretaceous and Palaeogene flysch deposits, one may encounter a large number of deep-seated landslides, mainly in the form of translational rock block slides and rock slumps. Showing a high magnitude (frequently above 1–3 mil. m^3) but low frequency (tens of years), these processes are characterizing mainly the outer (Paleogene) flysch units, built on looser formations (alternation of less cohesive sandstones with schistose marly and clayey intercalations). Today present in the form of relict and dormant deposits (almost entirely covered by old forests), these deep-seated landslides are marked by numerous reactivations, especially due to river undercut, since the large accumulation deposits frequently reached the valley bottom, causing river blockages and forming landslide dams. The morphology of numerous such landslides is showing a potential seismic implication and may rank them as co- or post-seismic landslides. The presence of large scarps in the immediate vicinity of ridge-tops and crests, close to fault line lineaments and the accumulation sector showing no primary interaction with the river network are standing as potential proofs for earthquake-induced landslides. The overall potential of such slope failures is enhanced by the active deforestations that are characterizing the period of the last 20 years.
5. **The Getic Piedmont**. The relatively large number of landslides inside this unit may be related as well to both natural and human conditions. On one hand, shallow and medium-seated translational slides occur frequently in the higher part of the piedmont, on clay and marl deposits which are containing sand and gravel intercalations. Usually, they are associated also with erosion forms and processes. On the other hand, high densities of landslides may also be found in the coal-mining fields, on the artificial slopes of quarries and sterile heaps or caused by the presence of underground mining galleries or old ventilation shafts. Deep-seated rock slides (mainly rotational) have a large development along the cuesta scarp slopes bordering the main rivers.
6. **High (mainly crystalline) Carpathians**. Widely scattered above 1800–2000 m a.s.l., the steep slope of the Carpathians Mountains (built on crystalline rocks, conglomerates, limestones—sone ridges even below 1800 m, and cohesive sandstones) are prone to a wide range of fast-moving landslides like rockfalls, rock avalanches, debris flows, or rock topples. Additional processes like snow avalanches and flash floods are sometimes interacting with landslides,

causing severe damages. Especially rockfalls are representing a continuous threat along the main transportation corridors crossing the Carpathians. More detailed information on the predisposition, preparing, and triggering factors of such processes are provided in Part II of this volume.

References

Almagia R (1910) Studi geografici sulle frani in Italia. Rome, Mem. Soc. geogr. Italiana 13(1):1–342

Armaş I, Damian R, Şandric I, Osaci–Costache G (2003) Vulnerabilitatea versanţilor la alunecări de teren în sectorul subcarpatic al Văii Prahova. Editura Fundaţiei România de Mâine, Bucureşti (in Romanian)

Badea L (1972) Observaţii asupra unor alunecari de teren din bazinul Buzăului. Probl. geogr., V, Bucureşti

Bally RJ, Stănescu P (1977) Alunecări de teren. Prevenire şi combatere. Edit. Ceres, Bucureşti (in Romanian)

Băcăinţan N (1983) Mesurages sur le creep dans certains sols des montagnes de Baraolt, RRGGG-Geogr 27

Băcăuanu V (1977) Processus et formes actuelles de relief dans le Plateau Moldave. An. Şt. Univ. "Al.I.Cuza" Iaşi, sec. II-c, tom XII

Bălteanu D (1970) Morfodinamica porniturilor de teren pe Valea Apostului (Munţii Buzăului). SCGGG-Geogr., XVII(2) (in Romanian)

Bălteanu D (1971) Preliminary observations on present-day slope modeling processes in the perimeter of Pătârlagele research station, Geogr. Jud. Buzău, Bucharest, 71–79

Bălteanu D (1974) Relaţii între curgerile de noroi şi eroziune torenţială în modelarea versanţilor din Subcarpaţii Buzăului. SCGGG-Geogr., XXI(1) (in Romanian)

Bălteanu D (1976) Some investigations on the present-day mass movements in the Buzău Subcarpathians. RRGGG-Geogr 20:53–61

Bălteanu D (1979) Procese de modelare a versanţilor declanşate de cutremurul din 4 martie 1977 în Carpaţii şi Subcarpaţii Buzăului. SCGGG-Geogr, XXVI (in Romanian)

Bălteanu D (1983) Experimentul de teren în geomorfologie. Edit. Academiei Române, Bucureşti (in Romanian)

Bălteanu D (1992) Natural Hazards in Romania. RRG, 36

Bălteanu D, Mateescu F (1975) Harta proceselor actuale de modelare a reliefului. In: Atlas, Republica Socialistă România, Edit. Academiei, Bucureşti (in Romanian)

Bălteanu D, Cioacă A (1997) Mass movements in the Vrancea seismogenic region. Studia Universitatis Babeş-Bolyai, Cluj-Napoca, ser. Geographia, XLII, 1–2:83–86

Bălteanu D, Micu M (2012) Morphodynamics of the Chirleşti mudflow (Buzău Mountains). Rom J Geogr 56(2)

Bălteanu D, Dinu M, Cioaca A (1989) Hărţile de risc geomorphologic. SCGGG-Geogr XXXV (in Romanian)

Bălteanu D, Cioacă A, Dinu M, Sandu M (1996) Some case studies of geomorphological risk in the Curvature Carpathians and Subcarpathians. RRG, 40

Bălteanu D, Jurchescu M, Surdeanu V, Ioniţă I, Goran C, Urdea P, Rădoane M, Rădoane N, Sima M (2012) Recent landform evolution in the Romanian Carpathians and pericarpathian region. In Loczy D et al. (eds) Recent landform evolution: the Carpatho-Balkan-Dinaric region. Springer Geography, Berlin, pp 249–286

Cazacu GB, Draghici G (2011) Identificarea şi determinarea hazardelor naturale – alunecarea de la Seimeni. Revista Română de inginerie civilă, 2 (in Romanian)

Cioacă A (1967) Alunecările de teren de la Baia Verde (Slănic) şi morfodinamica lor. SCGGG-Geografie, 2, Bucureşti (in Romanian)
Cioacă A (1996) Landslides in the Carpathian Curvature Paleogene Flysch. Particularities. Geogr. Fis.e Dinam. Quatern., 19
Cioacă A, Dinu M (1998) Landslides triggered by precipitation in the Subcarpthians, in November 1996–March 1998 interval. Simpozionul Geomofologic Româno-Italian, Oradea, pp 68–75
Coteţ P (1969) Geomorfologie cu elemente de geologie. Edit. Didactică şi Pedagogică, Bucureşti (in Romanian)
Cruden DM, Fell R (1997) Landslide risk assessment. AA Balkema, Rotterdam Brookfield
Cruden DM, Varnes DJ (1996) Landslide types and processes. In: Turner AK, Schuster RL (eds) Landslides: investigation and mitigation. National Academey Press, Washington, DC, pp 36–75
Dikau R, Brunsden D, Schrott L, Ibsen ML (eds) (1996) Landslide recognition. Identification, movement and causes. Wiley, Chichester
Dinu M (1997) The relationship between landslides and slope evolution in the Vâlcea Subcarpathians, Rumania. Geografia Fisica e Dinamica Quaternaria, 19, Torino, p 227–232
Dinu M, Cioacă A (1997) Precipitation-induced landslides in the Moldavian Plateau (1996–1997). RRG, 41, Bucureşti
Donisă I (1968) Geomorfologia Văii Bistriţei. Edit. Academiei RSR, Bucureşti (in Romanian)
Dragomirescu S, Gâştescu P (1960) The forming of Betis lake through a natural dam. Probl. Geogr., VIII p 275–281
Dragoş V (1957) Deplasările de teren. Edit. Ştiinţifică, Bucureşti (in Romanian)
Gârbacea V (1992) Harta glimeelor din Câmpia Transilvaniei. SUBB-G 37(1–2):21–24 (in Romanian)
Gârbacea V (1997) Remarques sur le relief de "glimee" en Roumanie. Geografia Fisica e Dinamica Quaternaria 19:219–221
Gârbacea V, Grecu F (1983) Relieful de tip glimee din Podişul Transilvaniei şi potenţialul său economic. Mem. Secţ. Şt. Acad. Română, IV(2/1982):305–312 (in Romanian)
Gârbacea V (2013) Relieful de glimee. Edit. Presa Universitară Clujeană, Cluj (in Romanian)
Grecu F (1982) Consideraţii asupra glimeelor din bazinul hidrografic Hârtibaciu. BSSGR, VI:185–188 (in Romanian)
Grecu F (1983) Alunecările de teren de la Movile (Podişul Hârtibaciului). ONMI, XXVII(2):112–117 (in Romanian)
Grecu F (1985) Clasificări şi tipuri de alunecări din depresiunea Transilvaniei. Terra 3:15–17 (in Romanian)
Grecu F (1992) Bazinul Hârtibaciului. Elemente de morfohidrografie. Edit. Academiei, Bucureşti (in Romanian)
Grigore M, Ielenicz M (1972) Cartografierea porniturilor. BSSG, II:235–242
Hantz D, Vengeon JM, Dussauge-Peisser C (2003) An historical, geomechanical and probabilistic approach to rock-fall hazard assessment. Nat Hazards and Earth Syst Sci 3:693–701
Hencher SR (1987) The implications of joints and structures for slope stability. In: Anderson MG, Richards KS (eds) Slope stability. Wiley, New York
Hungr O, Laroueil S, Picarelli L (2013) The Varnes classification of landslide types, an update. Landslides 11(2):167–194
Hutchinson JN (1988) General Report: Morphological and geotechnical parameters of landslides in relation to geology and hydrogeology. In: Bonnard C (ed) Proceedings of fifth international symposium on landslides, Rotterdam, Balkema, pp 3–35
Ichim I (1972) Le role des processus de mouvement de masse dans le modelage des monts du flysch (Carpathes Orientales). Acta geographica Debrecina, t. X:209–223
Ichim I, Lupaşcu Gh (1975) Degradările de teren din regiunea subcarpatică cuprinsă între valea Nechit şi valea lui Ion, cu privire specială asupra raporturilor dintre alunecări şi unele procese pedogenetice. Lucrările colocviului naţional de geomorfologie aplicată şi cartografiere geomorfologică, 26-28 octombrie 1973, Iaşi (in Romanian)
Ielenicz M (1970) Zonele cu alunecări de teren din ţara noastră. Terra 2(1):31–40 (in Romanian)

Ielenicz M (1981) Procese actuale în Carpaţii de Curbură. Terra, 4 (in Romanian)
Ielenicz M (1984) Munţii Ciucaş-Buzău. Studiu geomorfologic. Edit. Academiei RSR, Bucureşti (in Romanian)
Ilinca V (2010) Valea Lotrului. Studiu de geomorfolgie aplicată. PhD Thesis, University of Bucharest (in Romanian)
Josan N, Grecu F (1981) Contribution a la connaissance des processus de versant du Plateau du Hârtibaciu (Depression de Transylvanie). RRGGG-Geogr., t.25:255–260
Josan N, Petrea R, Petrea D (1996) Geomorfologie generală. Edit. Univ. Din Oradea (in Romanian)
Lee EM, Jones DKC (2004) Landslide risk assessment. Thomas Telford, London
Loghin V, Păunescu E (2002) Tipizarea, clasificarea şi caracterizarea alunecărilor de teren din Subcarpaţii dintre Dâmboviţa şi Prahova în vederea alcătuirii unei baze de date. AUB, Vol. LI (in Romanian)
Macovei G, Botez G, (1923) Comunicare asupra fenomeneor de alunecări şi prăbuşiri de teren din judeţul Râmnicul Sărat. D.S. ale Inst. Geol. Român (1914–1915), Bucureşti (in Romanian)
Mamulea M (1975) O propunere de clasificare a porniturilor de teren. SCGGG, Geografie, vol. 20 (in Romanian)
Martiniuc C, Băcăuanu V (1961) Porniturile de teren şi modul cum pot fi prevenite sau stabilizate. Natura, XIII:25–35 (in Romanian)
Mândrescu N (1981) The Romanian earthquake of March 4, 1977: aspects of soil behavior. Rev. Roum. Geophysique, 25, Edit. Acad Rom
Mândrescu N (1982) The Romanian earthquake of March 4, 1977: damage distribution. Rev. Roum. Geophysique, 26–27, Edit. Acad Rom
McCalpin JP (1984) Prelminary age classification of landslides for inventory mpping. Selected Works. Utah State University
Micu M, Bălteanu D, Ionescu C, Havenith HB, Radulian M, van Westen C, Damen M, Jurchescu M (2015) A preliminary regional assessment of earthquake-induced landslide susceptibility for Vrancea Seismic Region. Geophys Res Abstr 17(EGU2015-12524):2015
Mihăilescu V (1927) Despre frane şi alte forme rezultate prin activitatea agenţilor externi – o sugestie. Bul. S.R.R. geogr., 1927 (in Romanian)
Mihăilescu V (1939) Porniturile de teren din regiune Nehoiaş. BSRRG, LVIII (in Romanian)
Morariu T, Gârbacea V (1968) Deplacements massifs de terrain de type glimee en Roumanie. RRGGG, XII:13–18
Morariu T, Tufescu V (1964) Problemes de geomorphologie appliquee en Roumanie. RRGGG, VIII:213–218
Morariu T, Diaconeasa B, Gârbacea V (1964) Age of land-slidings in the Transylvanian Tableland. RRGGG, VIII:149–157
Mrazec L (1923) Cauza alunecărilor de strate. Dări de seamă, Institutul Geologic, tom VI (in Romanian)
Munteanu-Murgoci G (1923) Propuneri de terminologie pentru alunecări şi curgeri de teren. Dări de seamă, Institutul Geologic, tom VI (in Romanian)
Popescu N, Popescu G (1978) Contribuţii la studiul alunecărilor de teren din Subcarpaţii de la Curbură. SCGGG, Geografie, tom XXV (in Romanian)
Posea G (1969) Glissments, meandres et voies de communications dans la valle de Buzău. Travaux du symposium international de geomorphologie appliquee, Bucarest, 1967
Posea G (1972) Alunecarea de la Nehoiu-Borcea. AUB, Geogr, XXI
Posea G (2002) Geomorfologia României. Edit. Fundaţiei România de Mâine, Bucureşti (in Romanian)
Posea G, Ielenicz M (1970) Alunecările de teren de pe Valea Buzăului. AUB, Geogr., XIX (in Romanian)
Posea G, Ielenicz M (1976) Types de glissements dans les Carpates de la Courbure. RRGGG, XX:63–72
Posea G, Popescu N (1976) Les glissements masifs dans les piemonts pericarpatiques. RRGGG, XX:45–52

Posea G, Vespremeanu E (1985) Unele experimente asupra alunecărilor mari din România. Cercet. Geomorf. pentru îmbunătăţiri funciare, Bucureşti (in Romanian)
Radu C, Spânoche E (1977) On geological phenomena associated with the 10 November 1940 earthquake. Revue Roumaine de Geologie, Geophysique et Geographie. – Geophysique, 21:159–165
Rădoane M, Rădoane N, Ichim I (1995) Folosirea metodei cubului matricial în evaluarea susceptibilităţii la alunecări de teren. Studiu de caz: judeţul Neamţ. Studii si cercetări de geografie, 40:111–118 (in Romanian)
Rădoane N (1995) Posibilităţi de abordare a procesului de creep. Studii caz din zona văii Bistriţei Moldoveneşti. Analele Universităţii "Ştefan cel Mare", Suceava (in Romanian)
Rădulescu NA (1959a) Distribuţia alunecărilor de teren în România. Probl. De Geogr., VI, 21
Rădulescu NA (1959b) The distribution of landslides in Romania. Probl. De Geogr., VI
Sandu M (1998) Culoarul depresionar Sibiu-Apold. Studiu geomorfologic. Edit. Academiei Române, Bucureşti (in Romanian)
Sârcu I (1962) Rolul alunecărilor şi prăbuşirilor de mase de roci în formarea munţilor cristalini ai Rodnei. AUAIC, VIII (in Romanian)
Sharpe CFS (1938) Landslides and related phenomena. Columbia University Press, New York
Surdeanu V. (1975) Consideraţii asupra alunecărilor de teren din Valea Bistriţei în sectorul Bicaz-Piatra Neamţ. Lucr. Stat. Stejarul, Pângăraţi (in Romanian)
Surdeanu V (1976) Le glissement de terrain de Ticos. Anuar. Muz. St. Nat, III, Piatra-Neamţ
Surdeanu V (1985) Consideraţii asupra inventarierii alunecărilor de teren în vederea întocmirii hărţilor de risc. Lucr. Semin. D. Cantemir, 5, Iaşi (in Romanian)
Surdeanu V (1992) Corelations between landslides and other denudation processes. SUBB, XXXVII, pp 1–2
Surdeanu V (1998) Geografia terenurilor degradate, Editura Presa Universitară Clujeană, Cluj-Napoca (in Romanian)
Surdeanu V, Rădoane N (1976) Relation entre les plans de mouvement et les indices physiques des depots de versant dans la zone du lac Izvorul Muntelui. Anuar. Muz. St. Nat, III, Piatra-Neamţ
Surdeanu V, Pop O, Chiaburu M, Dulgheru M, Anghel T (2010) La dendrogéomorphologie appliquée a l'étude des processus géomorphologiques des zones minières dans le Massif du Călimani (Carpates Orientales, Roumanie). In: Surdeanu V, Stoffel M, Pop O (eds) Dendrogéomorphologie et dendroclimatologie – méthodes de reconstitution des milieux géomorphologiques et climatiques des régions montagneuses. Presa Universitară Clujeană, Cluj-Napoca, pp 107–124
Tufescu V (1964) Typologie des glissements de Roumanie RRGGG-Geogr., VIII Tufescu V (1968) Coulees boueuses dans les Carpates dy Flysch et les Subcarpathes de Roumanie. RRGGG, XII:19–25
Varnes DJ (1978) Slope movement types and processes. In: Schuster RL, Krizek RJ (eds) Special report 176: landslides: analysis and control. Transportation and Road Research Board, National Academy of Science, Washington, DC, pp 11–33
Vasile M, Pleşoianu A, Vespremeanu-Store A (2015) Distribuţia şi morfometria pereţilor stâncoşi din Carpaţii Româneşti. Influenţa caracteristicilor litologice şi a dezagregării. Simpozionul Naţional de Geomorfologie, Sf. Gheorghe, 21–24 May 2015 (in Romanian)
Zaruba Q, Mencl V (1969) Landslides and their control. Elsevier, Amsterdam

Chapter 12
Landslide Type and Pattern in Moldavian Plateau, NE Romania

Mihai Ciprian Mărgărint and Mihai Niculiță

Abstract This study proposes a regional scale approach of landslide typology and patterns for the Moldavian Plateau, one of the Romanian regions most affected by mass movement processes. A regional historical landslide inventory was carried out, using remote sensing imagery, resulting a number of 24,263 polygons, which cover 18.3 % of the whole study area (24,803 km^2). Preconditioning, preparatory, and triggering factors were revised and the following types of landslides were identified and attributed in the inventory: rotational, translational, lateral spread, flows, and complex landslides. The statistic interpretations of the geomorphometric variables of the polygons that define the areas affected by landslides, reveal a strong relation between the landslide phenomenon and the lithology, the morphostructure and the topography. The general pattern of landslide distribution emphasizes a repetitive model along cuesta scarp slopes; this is mainly related to the lithology dominated by limestones, sandstones, and volcanic consolidated tuffs at the upper part of the slopes, with friable clayey and sandy strata intercalations. The landslide inventory and the revealed types and patterns of landslides are an essential step for a better understanding of landslide phenomenon, landslide risk assessment, and landslide management in the Moldavian Plateau.

Introduction

Landslides are widespread geomorphologic processes which nowadays, and also in the past, shape the earth surface in any climatic zone. The occurrence and the spatial distribution of the landslides are linked to a large range of triggering factors, in a general geographical setting given by certain preconditioning and preparatory

M.C. Mărgărint (✉) · M. Niculiță
Department of Geography, Alexandru Ioan Cuza University of Iași,
Carol I Av 11, 700506 Iași, Romania
e-mail: margarint.ciprian@yahoo.com

M. Niculiță
e-mail: mihai.niculita@uaic.ro

M. Rădoane and A. Vespremeanu-Stroe (eds.), *Landform Dynamics and Evolution in Romania*, Springer Geography,
DOI 10.1007/978-3-319-32589-7_12

factors. The spatial distribution and the types of landslide mechanism over a certain area are unique to every land surface, from local to regional extent, and constitute a specific pattern. The intepretation of these patterns and the analysis of the distribution, conditions, and morphology of the past, present and future landslides is analysed for the study area in the present study.

One of the most important tools in the analysis of the spatial and temporal patterns of mass movement processes and their consequences on environmental or social systems are landslide inventories (McKean and Roering 2004; Van Westen et al. 2008; Guzzetti et al. 2012; Conforti et al. 2014; Komac and Hribernik 2015). Currently, we can see a continuous increase of new remote sensing data and techniques and consequently a general increase in the accuracy of the landslides inventories, which allow a better use in the management of risk induced by these processes (Şandric and Chiţu 2009; Guzzetti et al. 2012; Kavzoglu et al. 2015). The high quality of remote sensing data is also essential for the interpretation of the relation between the morphology of the landslides, the local setting and consequently, their typology (Tarolli et al. 2012; Lin et al. 2013; Mondini et al. 2014).

The international literature provides several studies regarding the spatial patterns of landslides controlled by geologic structure and lithology (Guzzetti et al. 1996; Jäger et al. 2013), as response to land-use changes (Glade 2003), induced by earthquakes (Yin et al. 2010; Meunier et al. 2013; Tonini et al. 2014), extreme meteorological events (Hovius et al. 2000; Bucknam et al. 2001; Ardizzone et al. 2007; Mondini et al. 2014), and also for a general distribution of these processes (Korup 2005a, b; Van den Eeckhaut et al. 2007; Guzzetti et al. 2008).

A landslide inventory for the Moldavian Plateau (24,803 km^2) was created, with a total of 24,263 polygons. In this study, the inventory was used as the base for deciphering the spatial patterns of the landslides, and it is seen as a milestone for the further regional hazard and risk assessment (Guzzetti et al. 1999; Micu 2011; Pourghasemi et al. 2014; Talaei 2014; Zhao et al. 2015; Ciampalini et al. 2015).

Study Area

The General Framework

The Moldavian Plateau is situated in the northeastern part of Romania, as a part of a larger unit that continues over the country borders, to the North and East. The study area is bordered by the Prut Valley to the East and North and by Siret and Moldova valleys to the West (Fig. 12.1). To the northwest, the study area was delineated using the Subcarpathians nappe limit with the undeformed foredeep deposits of the Moldavian Platform (Mațenco and Bertotti 2000), according to the Geologic Map of Romania at scale 1:200,000. The southwest extreme part, dominated by fluvial terraces and Holocene alluvial deposits, known as Tecuci Plain, was not included in the studied area, being considered a part of the Romanian Plain (Posea 2005). The

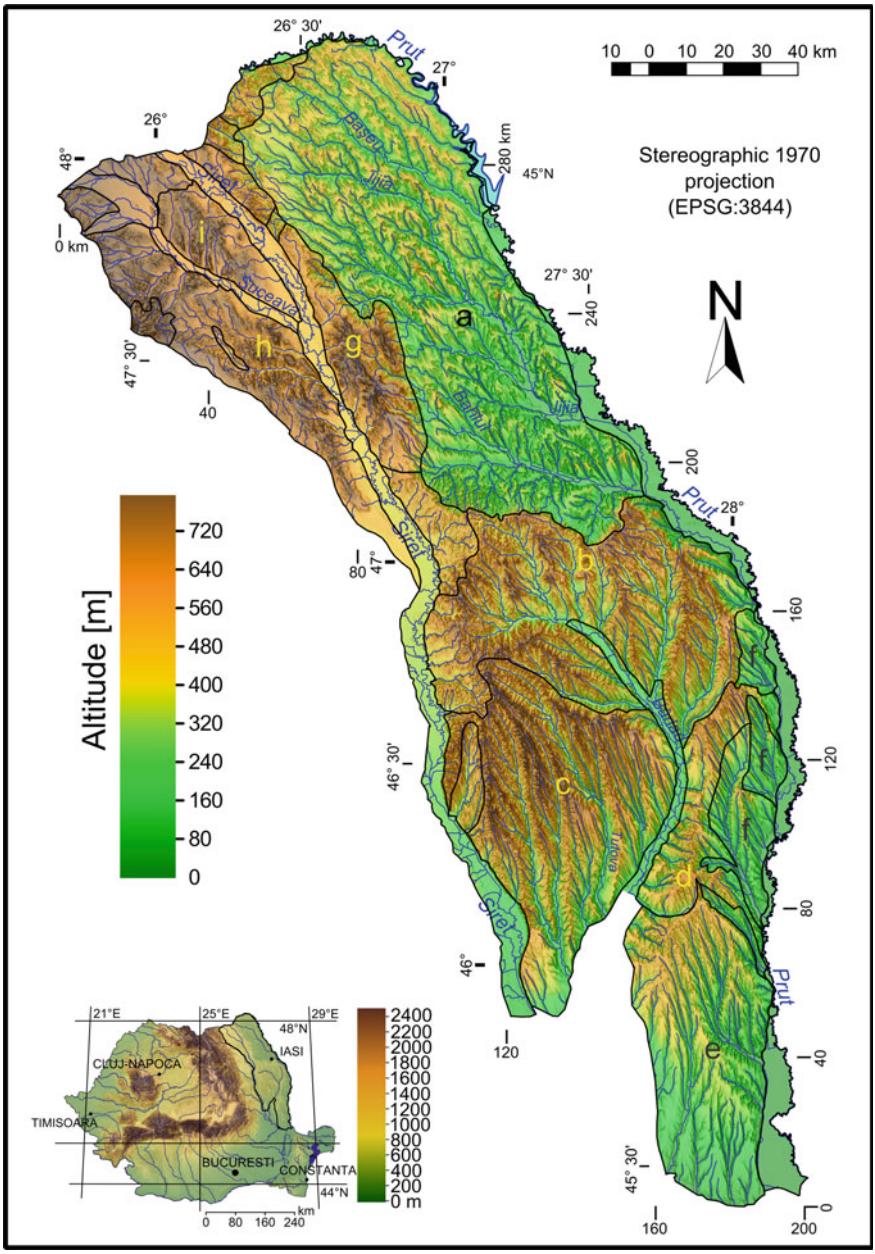

Fig. 12.1 Geographic location, physiographic subdivisions, and elevation of the Moldavian Plateau, based on SRTM data; the *letters* indicate the geomorphologic regions: **a** the Jijia Hills, the Bârlad Plateau with the subunits: **b** Central Moldavian Plateau, **c** Tutova Hills, **d** Fălciu Hills, **e** Covurlui Plateau, **f** Huşi–Sărata–Elan–Horincea Hills, and the Suceava Plateau composed of: **g** Siret Hills, **h** Fălticeni Plateau, **i** Dragomirnei Plateau

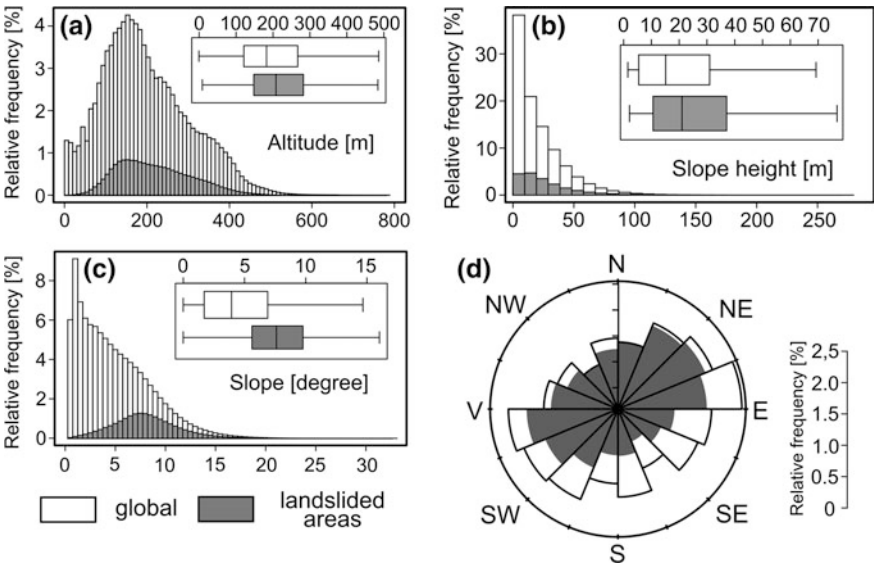

Fig. 12.2 The distributions of altitude (**a**), slope height (**b**) slope angle (**c**), and slope aspect (**d**) for the Moldavian Plateau and for the landslide areas

study area has a surface of 24,803 km^2, with an altitudinal range of 3–794 m above sea level (a.s.l.) (Fig. 12.2). The landforms overlay on a monoclinic sedimentary structure, which leans with 4–12 m/km from northwest to south-east, while the crystalline basement of the East–European Platform sinks toward west, under the Carpathian Orogene (Ionesi et al. 2005).

The monoclinic structure influenced the development of a repetitive pattern of valleys and ridges (Niculiţă 2011), and it was reflected in many other geographic features (the climate, the land use patterns, the main transport corridors, the settlement network, etc.).

The outcropping geologic formations have newer ages from north (Cretaceous rocks in Prut valley side) to south (quaternary gravel, sands, and loess from lower Bârlad and Siret valleys) (Fig. 12.3) (Ionesi et al. 2005). The lithology of the sedimentary outcropping layers is constituted from an alternation of sandstones, limestones, tuffs, and micro-conglomerates appearing on the ridges and at the upper part of the hillslopes, and an alternation of clays, silts, and sands occurring beneath the median and basal part of the hillslopes. At the contact of these two main alternations of rocks, morphologic alignments have been individualized through erosion. These alignments which generally constitute the limits between the geographic subunits (the Bârlad Plateau, the Suceava Plateau and the Jijia Hills—Fig. 12.1) are dominated by old and extensive landslide complexes (Grozavu et al. 2012; Mărgărint and Niculiţă 2014).

Landslide Causal Factors

A large range of the environmental settings and human activities can produce optimum conditions for the occurrence of landslides which combine either the displacement itself and/or the reduction of the shear resistance of the slope. The large variety of slope movements reflects the diversity of factors that may disturb the slope stability (Popescu 1994). Also, it is well known that seldom, if ever, a landslide can be attributed to a single causal factor, this issue emphasizing the complex behavior of mass movement processes.

According to the scale of analysis, the knowledge of landslide causal factors (as in the general case of landslide investigation) has two main scalar approaches: (i) local scale analysis, focused on the investigation of particular sites and computation of safety factor ratio; this type of approach divides the following main classes of causal factors: ground conditions, geomorphological processes, physical processes and man-made processes (Popescu 2002), and (ii) regional (medium to small scale) analysis, approach that uses geographical criterion, and a consequent terminology for the control factors: geology, geomorphology, climate, hydrology (considered as static factors, Capecchi et al. 2015), hydrogeology, and land cover/use (Fell et al. 2008; Guzzetti et al. 2008). Due to the scopes of the present study, the second approach will be followed. The actual distribution of landslides in the Moldavian Plateau is a natural consequence of the spatiotemporal combinations of these causal factors. This essential aspect of landslides occurrence in this region is proved by the large extension of complex landslides that spread for many kilometers, especially along the cuesta fronts (Fig. 12.3).

According to their influence in the timing and the development of slope displacements, and subsequently by their spatial coverage, these factors can be divided in: (i) preconditioning, (ii) preparatory, and (iii) triggering factors (Schmidt and Dikau 2005; Broothaerts et al. 2012).

Preconditioning Factors

The preconditioning factors are those that generally increase the degree of the instability of slopes. Their spatial distribution mainly influences the general patterns of landslide distribution at a regional scale. Among these, for the Moldavian Plateau we can also include the following factors: the morphostructural features, the topography (viewed as geomorphometric variables), the lithology, the climate, and the land use.

Morphostructure. The geologic structure has influenced landform morphology and river network configuration. The geologic structure of strata is monoclinic, ranging from 2 to 12 m/km dip and WWS–EEN strike (Jeanreanud 1971; Ionesi 1994; Ionesi et al. 2005). The incision of river network has created the following structural valleys and cuestas: (i) the NW–SE oriented valleys that are consequent, with cuesta scarps (steep hillslopes, corresponding to the up-dip of the strata) on the

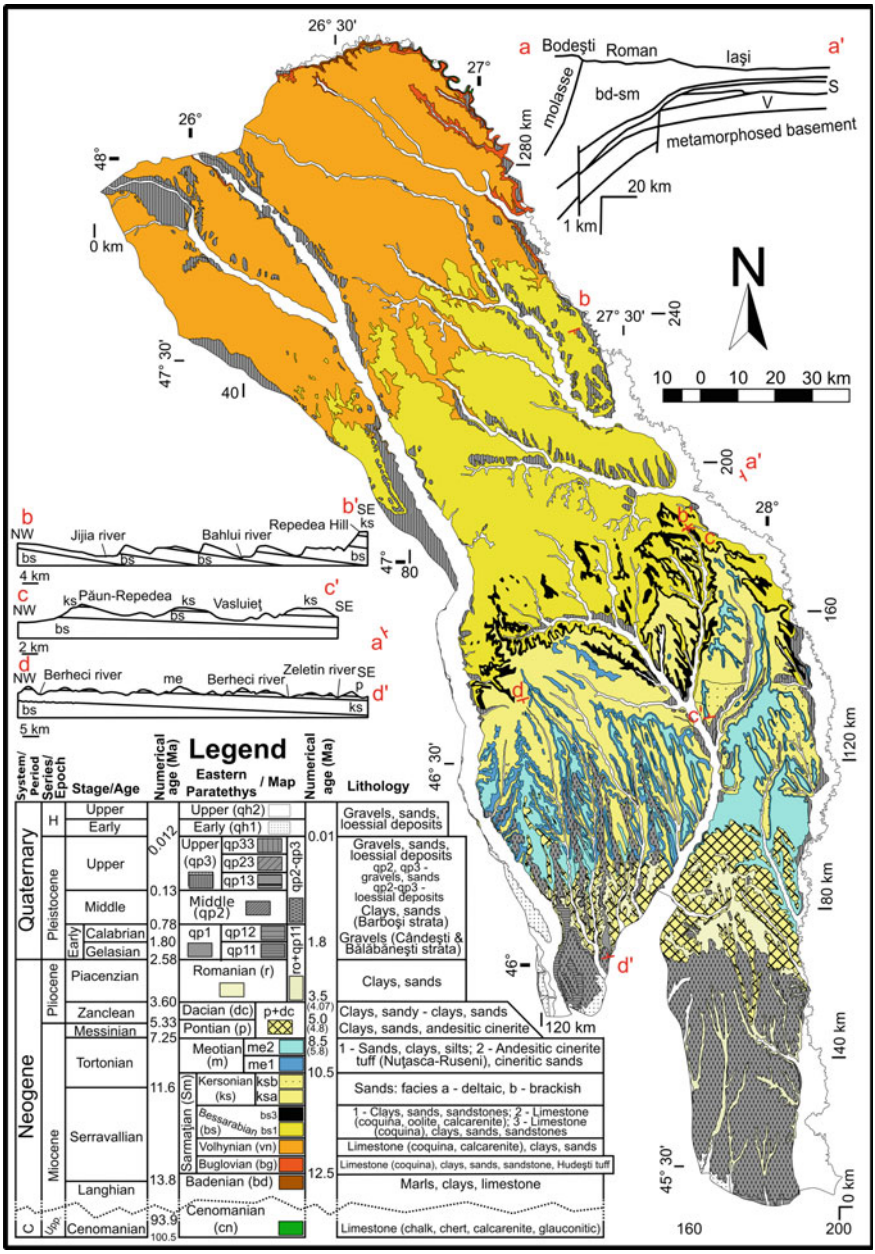

Fig. 12.3 Geological setting of the Moldavian Plateau: **a** Geological map, compiled from Romanian Geological Institute, 1968 1:200,000 scale geological maps, Jeanrenaud 1971, and reshaped to match the surface shape of SRTM data; the geo-chronological scale is taken from Maţenco et al. (2007), with the Sarmatian taken from Ionesi (1994) and updated with the latest information from International Chronostratigraphic Chart v. 2014/02; Cross sections directions are figured on the main map and are reproduced after: **b** Pătruţ and Dăneţ (1987); **c** Băcăuanu (1968); **d** and **e** Jeanreanud (1971)

left side, and cuesta dip slopes (gentle hillslopes corresponding to the dip of the strata) on the right side; (ii) the SW–NE oriented valleys that are subsequent, with cuesta scarps on the right side and cuesta dip slopes on the left side; (iii) SE–NW oriented valleys that are obsequent, and developed on cuesta scarp slopes (Ioniță 2000; Niculiță 2011).

These landforms are characterized by homoclinal shifting (Selby 1985), with a general tendency of the river network to migrate towards south and east. Thus, this migration maintains the steep slope of the cuesta scarp by fluvial erosion of slope toe. A strong evidence of post-depositional faults, generated by the Pliocene to Pleistocene subsidence of the Focşani basin has been revealed in the southern part of the Moldavian Plateau (Maţenco et al. 2007; Pohrib et al. 2012). Three types of faults have been identified in this region: (i) the normal faults, oriented from NW to SE, and from NNW to SSE, (ii) W–E transfer faults, and (iii) strike-slip faults, sinistral, linked to the New Trotuş Fault (Maţenco et al. 2007). Usually, the vertical displacement is below 20 m, and the horizontal offset is comprised between 20 and 200 m (Maţenco et al. 2007).

Lithology. Overall, the surface lithology of the Moldavian Plateau is dominated by clays, and subsequently by sands (mainly in the Tutovei and the Fălciu Hills), and by thin loess cover spread on a large part of the area (Haase et al. 2007), with higher depths in the Covurlui Hills and Jijia Hills. Sandstones and limestones occur especially in the Suceava Plateau (with thickness less than 100 m) and the Central Moldavian Plateau (with thickness comprised between 5 and 30 m), meanwhile tuffs and sandstones outcrop as thick strata (under 20 m) in the Central Moldavian Plateau, the Tutova, and the Fălciu Hills. The relations between the lithology and the geochronologic units scale, as well as their spatial distribution can be followed in Fig. 12.3.

The surficial deposits have similar textural characteristics as the predominantly clayey and sandy surface lithology. On the ridges, the depth of surficial deposits is less than 20 m. On the hillslopes, the depth is comprised between 3 and 5 m (Minea 2012; Stângă 2012), but in certain situations it can go up to 20 m (the cases of rotational deep-seated landslides). The loess deposits cover the ridges and plateaus and have depths less than 5 m, with exception of the southern part of the Tutova Hills, the Covurlui Hills, and Jijia Hills, in which case the depths could exceed 20 m (Institutul Geologic al României 1968; Haesaerts et al. 2003). The alluvial deposits depth ranges generally from 10 to 30 m, and presents two clear distinguished layers: a first gravel-sandy layer, right over the geologic strata, and a second one, clayey-silty above (Minea 2012; Stângă 2012).

Soils are represented by chernozems under 200 m a.s.l., luvisols over 200 m a.s.l., on ridges, plateaus and cuesta dip slopes, with variations to phaeozems (especially in the Suceava Plateau) (Băcăuanu et al. 1980). The regosols occur along the cuesta scarp slopes, while the floodplains are characterized by alluvial soils and chernozems.

Topography (geomorphometric variables). This factor is controlled by the large extension of the asymmetric hills (cuestas) and the wide floodplains. The altitude ranges from 3 m a.s.l. (in the south part of the plateau, along the Prut floodplain) to

794 m a.s.l., in the northwest part of the Moldavian Plateau, along the contact with the Carpathian mountainous area. The mean altitude of the Moldavian Plateau is 199 m. At subunit level, the altitudes are comprised as follows: Suceava Plateau—200 to 794 m a.s.l., Jijia Hills—30 to 250 m a.s.l., Central Moldavian Plateau, Tutovei Hills and Fălciu Hills—70 to 550 m a.s.l., and Covurlui Plateau—6 to 250 m a.s.l.

For the hilly units, the elevation amplitude between main ridges and valleys is usually bigger than 100 m (Fig. 12.1). For the hills sustained by consolidated lithological layers (limestones and sandstones), the plateau-like ridges are well developed. Usually, because of the monoclinic structure with WWS–EEN strike, the north and west exposed hillslopes are cuesta scarp slopes, with slope angle ranging between 5° and 32°, while the south and east exposed hillslopes are cuesta dip slopes, with slope angle ranging between 1° and 5°. The mean slope of the entire area of the Moldavian Plateau is 4.7°.

Cuesta scarp slopes are characterized by lengths less than 1 km, while cuesta dip slopes have lengths between 1 and 5 km. Hillslopes have usually planar curvature for cuesta dip slopes and mixed (concave-convex) curvature for cuesta scarps.

Climate. The climate of the Moldavian Plateau is temperate continental, with hot-dry summers, and cold-dry winters. The values of the annual mean precipitations are decreasing from north (640 mm), to south (480 mm) (Croitoru and Minea 2014). These quantities are recorded especially in the summer and spring seasons (20–45 % from the annual quantity for each season). Snowfall occurs every year, from November till March.

Land cover/land use. Forests cover 14 % of the area (Corine Land Cover 2006), being located either on the ridges and plateaus (natural forests) or on steep cuesta scarp hillslopes (most of them are reforested areas). The arable terrains cover 50 % from the entire area of the Moldavian Plateau; these are spread especially on cuesta dip slopes and drained floodplains, but small patches of agricultural terrains appear also on the cuesta scarp slopes. The pastures cover 12 % (mainly along cuesta scarp slopes and floodplains). Build-up areas (urban and rural) cover approximately 10 % of the studied area; cities are situated on floodplains and surrounding hills, while rural settlements are located either on the hillslopes, or on the floodplains.

Preparatory Factors

The preparatory factors act both at regional and local scale and influence the landslide patterns. They have the role to induce an unstable equilibrium through modifications in slope geometry or creating hotspots of moisture by modifications of subsurface drainage. Among these factors, the most important are represented by successions of *rainy years*, the *changes of land use,* and the *existing landslides* themselves. By analyzing the historical documents of the last 170 years, Pujină and

Ioniţă (1996) have concluded that new landslides generally occur once in 40 years, the reactivations of existing landslides having a 15 years interval of recurrence. This periodization is closely linked with series of at least two years with higher precipitations during the entire year, like 1969–1973 time period (Pujină 2008). Land use changes influence on mass movement processes is given by: lack of slope stabilization and erosion control measures, deforestation of slopes and especially of dormant landslides, without other major interventions (Mihai et al. 2014), poor forest management (Rotaru et al. 2007), vegetation removal, excavation of slope at its toe.

Other factors with local influence in preparation of slope displacements are the following: the modifications of slope geometry due to *anthropic interventions*, the occurrence of *moisture hotspots* due to phreatic nappes discontinuities, and the distribution of *springs* and *lakes*.

Triggering Factors

The triggering factors are represented by events with a very short duration (minutes or days) or by the exceeding of certain physical thresholds of slope stability. These thresholds are linked both to the events themselves but also to the cumulative effects of the preparatory factors.

For the study area, the meteorological events with effects in landslide triggering are: *intense rainstorms*, *heavy rainfall,* and *rapid melt of thick snow*. For the 1969–2000 interval, the reactivation of landsliding processes was recorded mainly for the spring season, when a threshold of 50 mm in 24 h was reached, coupled with preexistent moisture conditions. For the summer season, under conditions of a deficit of moisture, this threshold was estimated to be of approximately 100 mm in 24 h (Pujină 2008). The effects of the heavy rainfalls are significant at the lower parts of the slopes (Densmore and Hovius 2000), being amplified by the existence of old displaced masses, gully activity, and fluvial erosion of slope toe. Associated with these rainy events, and also with rapid melting of deep snow, are rivers and lakes level fluctuations that cause hotspots of moisture, responsible for initiation or reactivating of slope processes.

Due to the vicinity of the Moldavian Plateau with the seismic Vrancea region, shocks induced by *strong earthquakes* (magnitude over 7 M on the Richter scale and return period of 35–40 years) have represented an important triggering factor (Bălteanu et al. 2010, 2012). Because of the lack of multi-temporal analysis of landslides, it is difficult to consider a spatial pattern of landslides linked with this factor, as in other seismic active regions cited by the international literature (Yin et al. 2010; Meunier et al. 2013; Tonini et al. 2014).

Materials and Methods

Data Acquisition and Preparation

For the identification and the delineation of landslides, the optical satellite imagery and high resolution DEMs available in the Google Earth® and Bing Maps archives (SPOT, Formosat, WorldView, GeoEye, Pleiades, QuickBird, KOMPSAT, IKONOS), and national orthorectified imagery were used. The digitization was performed in Google Earth® and Quantum GIS software. The altitude data used for the geomorphometric analysis is SRTM3 resampled to 30 m (SRTM 2014). Slope angle and aspect were computed with the maximum gradient method (Travis et al. 1975).

The geometric characteristics of the areas affected by landslides (like width and length) were computed by method of Niculiță (2015), using the direction of the mass flow, because there are many situations where the landslide bounding box width is longer than the landslide bounding box length. These situations appear mainly on cuesta scarp slopes, which can be extended on several kilometers along valleys. Landslides with width longer than the length of the bounding box can be seen in Fig. 12.5a, 12.5g, while those with a length longer than the width are shown in Fig. 12.5e, f. The landslide height has been obtained by the subtraction of the maximum and the minimum slope height. For each pixel, the slope height is computed as difference in altitude between the pixel and the local channel (Böhner and Selige 2006). Slope and aspect angles of landslides were estimated by considering the mean value of all the pixels inside the landslide polygon. The general slope was computed as the ratio between the landslide height and length. For the assessment of the relation between structural landforms (cuesta scarp and dip slopes) and landslides, we have used the cuesta extents delineated by Niculiţă (2011).

Landslide Inventory

Using remote sensing imagery and field work, a geomorphological historical landslide inventory (Malamud et al. 2004b; Guzzetti et al. 2012) was created for the Moldavian Plateau (Niculiţă and Mărgărint 2014). Five elements of landslides morphology (the crown, the scarp, the rough displaced mass, the flanks, and the toe) have been used to identify the occurrence and to delineate the extension of landslides. The areas situated in between these landslide elements were digitized as polygons, and some mapping generalization methods have been applied: simplification, amalgamation, and refinement (Slocum et al. 2009).

The landslide inventory presented in this study can be classified as a geomorphologic and historic one. The inventory is geomorphologic because the remote sensing data sources and the field reality do not always allow the precise delineation and identification of the event-based landslides. The landslides are recognized by

their morphologic signatures and usually larger landslides contain also event-based landslides. In this way, the inventory is a historical one, because we consider different generations of landslides, with different ages. The used methodology is consistent with methodologies cited in the literature (Van den Eeckhaut et al. 2005; Ardizzone et al. 2007).

For every landslide polygon, using field experience, the geomorphometric analysis and the geomorphologic and the environmental setting, the type according to Varnes (1978) and Cruden and Varnes (1996) classifications was assigned. A statistical synthesis of geomorphometric descriptors of landslide types is presented in Table 12.1, and the spatial distribution of the landslides, is displayed in Fig. 12.4.

Statistical Analysis

The statistical analysis was performed with R software and its base packages (R Development Core Team 2008). Circular statistics were computed with circular package (Agostinelli and Lund 2013). For fitting Inverse Gamma, Pareto and Weibull distributions *MASS*, (Venables and Ripley 2002), *stats*, and *actuar* packages were used (Dutang et al. 2008). All the plots were realized in R software.

The landslide frequency density, magnitude and magnitude curves were obtained by applying in R the methodology described by Malamud et al. (2004a). The Weibull distributions were computed in R following the methodology explained in Donnarumma et al. (2013).

Results and Discussions

Landslide Types

A landslide is the movement of a mass of rock, debris, or earth down a slope (Cruden 1991). In this study, the landslides will be discussed following the widespread typology created by Varnes (1978), completed by Cruden and Varnes (1996) and recently updated and discussed by Hungr et al. (2014). These classification systems are mainly based on the dominant type of movement and the types of material before displacement and they have the qualities to be simple and flexible, being applicable at global scale. In Romania, for the Moldavian Plateau, based especially on the shape of the deformed slopes, which can often reveal the complexity of the causal factors of these gravitational processes, Băcăuanu et al. (1980) have distinguished a wide range of landslides: mound, step-like, wave-like, flows, and complex landslides. These types appear in a wide range of spatial combinations, often with a remarkable continuity, especially along the cuesta scarp slopes.

Table 12.1 Descriptive statistics of the landslides geomorphometry

Variables	Total	1*	2*	3*	41*	42*
Number of landslides	24,263	520	16,030	1057	4947	1709
Total landslide area [km^2]	4535.4	115.3	551.7	10.21	2845.7	1012.5
Proportion from study area [%]	18.3	0.45	2.2	0.05	11.5	4.1
Smallest landslide area [m^2]	123	100,200	123.2	625.9	121,100	62,720
Largest landslide [km^2]	13.3	0.6	0.9	0.02	13.3	12.0
Mean landslide area [km^2]	0.19	0.22	0.034	0.01	0.57	0.59
Median landslide area [km^2]	0.04	0.18	0.02	0.01	0.29	0.36
Std. dev. of landslide area [km^2]	0.51	0.12	0.03	0.005	0.89	0.75
Area of most freq. landslide [km^2]	0.0025	0.10	0.005	0.049	0.15	0.25
Smallest landslide length [m]	23.1	296.3	23.1	30.6	154.5	294.7
Largest landslide length [m]	13,690	1029	1445	567.3	13,690	4921
Mean landslide length [m]	455.2	526.6	239.3	152.5	1055	909.1
Median landslide length [m]	272.8	489.0	191	133.5	734.7	810.1
Std. dev. of landslide length [m]	615.7	148.9	169.9	81.3	1041.9	462.0
Length of most freq. landslide [m]	95.0	445.0	90.0	92.5	350	475.0
Smallest landslide width [m]	8.2	308.1	8.2	20.1	144.3	203.0
Largest landslide width [m]	14,750	991.0	1303.0	472.5	14,750	6225
Mean landslide width [m]	395.9	526.9	198.1	102.3	917.5	883.4
Median landslide width [m]	225.7	487.8	156.0	86.8	656.3	777.6
Std. dev. of landslide width [m]	548.3	150.9	149.8	56.6	889.1	557.2
Width of most freq. landslide [m]	55	402.5	55	57.5	300	475
Smallest landslide height [m]	0	15.1	0	0	13.2	24.2
Largest landslide height [m]	326	197.3	176.1	58.0	326	317.3
Mean landslide height [m]	41.1	72.6	24.0	10.3	82.0	92.6

(continued)

Table 12.1 (continued)

Variables	Total	1*	2*	3*	41*	42*
Median landslide height [m]	29.1	66.9	20.2	8.5	70.8	82.3
Std. dev. of landslide height [m]	39.1	28.2	18	7.9	43	42.8
Height of most freq. landslide [m]	7.5	57	7	4.8	47.5	62.5
Smallest mean landslide slope [°]	0.0	2.3	0.0	0.0	2.0	2.6
Largest mean landslide slope [°]	24.9	16.3	24.9	19.1	20.6	16.6
Mean of mean landslide slope [°]	7.7	8.5	7.8	5.1	8.1	7.8
Median mean landslide slope[°]	7.5	8.1	7.5	4.7	7.8	7.8
Std. dev. of mean landslide slope [°]	2.7	2.3	2.9	2.7	2.2	1.9
Most freq. mean slope of landslides [°]	7.3	7.6	7.3	3.7	7.5	8.15
Smallest general landslide slope [%]	0	2.1	0	0	0.1	1.3
Largest general landslide slope [%]	140.7	32.9	140.7	55.2	42.1	38.1
Mean of general landslide slope [%]	7.6	10.5	7.8	3.7	7.4	7.5
Median general landslide slope[%]	6.4	9.6	6.4	2.5	6.7	7.1
Std. dev. of general landslide slope [%]	6.3	4.8	6.9	4.3	4.9	3.7
Most freq. general slope of landslides [%]	3	7.8	3	0.8	2.3	4.3

*The columns 3–7 represent the landslide type code according to the Sect. 12.4.1

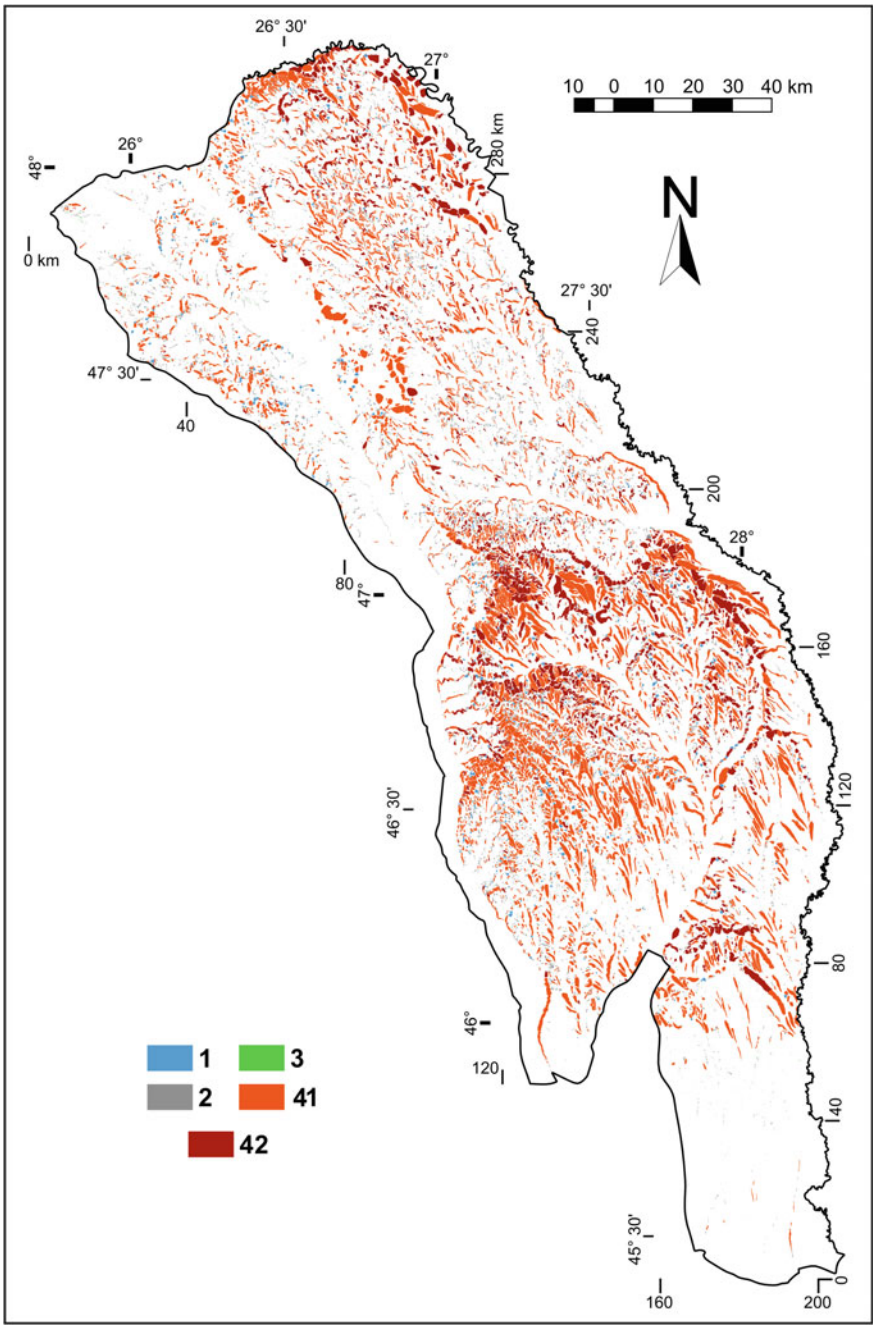

Fig. 12.4 The spatial distribution of landslides in the Moldavian Plateau: *1* rotational slides; *2* translational slides; *3* earth flows; *4* lateral spreads; 41 and 42 complex landslides

Table 12.2 The absolute frequency of landslide types from the physiographic units of the Moldavian Plateau

Physiographic units	1*	2*	3*	41*	42*	Total**
Covurlui Hills	5	733	139	118	3	998
Fălciu Hills	12	580	45	114	106	857
Tutova Hills	129	4179	288	1251	72	5919
Central Moldavian Plateau	124	2925	107	92	811	4059
Jijia Hills	92	4271	90	1427	660	6540
Siret Hills	61	950	64	479	23	1577
Suceava Plateau	89	1874	301	464	31	2759
Huşi-Elan-Sărata-Horincea Hills	4	353	13	104	1	475
Total**	516	15,865	1047	4049	1707	23,184

*The columns 3–7 represent the landslide type code according to the Sect. 12.4.1
**The inconsistency of the row and column total surface and proportion is due to the multiple superposing of landslide polygons along regions borders, and the inclusion of some landslides to Siret, Prut and Bârlad rivers valleys (Fig. 12.1)

The landslide inventory has 24,263 polygons, the density of landslides in the study area being 1.02 landslides per km^2. The surface covered by landslides is 18.3 % from the study area (4534.7 km^2, without adding the area of overlapping landslides), the density of landslide area per km^2 being 0.19.

In the study area, we have identified the following types of landslides: 1—rotational, 2—translational, 3—lateral spread, 4.1—rotational–translational complexes, and 4.2—rotational–translational-flow complexes. The absolute frequency of these types for the physiographic regions of the Moldavian Plateau (Fig. 12.1) is presented in Table 12.2.

Rotational Slides (Slumps)

A rotational landslide is the downward and outward movement of a mass on top of a concave upward failure surface (Abbott 2004). For the Moldavian Plateau, as in many others regions, purely rotational slumps with a cylindrical or ellipsoidal shape of the sliding surface are difficult to find, being probably more common in soil mechanics textbooks than in nature (Hungr et al. 2014).

In the presented inventory, a number of 520 polygons belong to this class. Also, a number of 6656 polygons were identified as complex landslides, with an important, but not exclusive rotational behavior of sliding (Table 12.1). For simple rotational slides, the area of polygons ranges between 123 m^2 and 13.32 km^2, with a mean value of 0.1869 km^2.

In this region, the rotational slides occur chiefly at the upper part of the slopes with cohesive rocks like sandstones, limestones, and volcanic tuffs placed above clayey, silty, or sandy formations. This is the classic case of the Iaşi Cuesta Scarp, where the Bessarabian succession begins with clays, which have more than 300 m

in thickness, followed by marls with sands intercalations, and two sandstone–limestone hard horizons at the upper part. This lithological succession, with a slow inclination to the southeast, has led to one of the most impressive morphological alignment of the study region (Figs. 12.1 and 12.7).

Rotational slides are almost linearly aligned for dozens of kilometers, and the succession of old, stabilized, circular main scarps, constitute a real pattern of these gravitational processes (Fig. 12.7). The evolution of these rotational slides seems to be controlled by a regional generalized event (prolonged rainy periods and/or earthquakes), preceded and followed by long-term shallow translational slides. This is the reason why these landslides are found as complex landslide polygons in the inventory, as presented above. This kind of alternation in the slopes affected by rotational slides was reported in many other geological and geographical settings (Petley et al. 2002; Van den Eeckhaut et al. 2009, 2010; Poiraud and Defive 2011; Massey et al. 2013). The permanent reactivations of these landslides are related with a wide range of preparatory and triggering factors, like meteorological events, land cover/use changes, and fluctuation of hydrogeological level. The multi-temporal successions of translational movements in the bottom part of the slopes are clearly expressed in Fig. 12.7.

A similar situation to Iaşi Cuesta Scarp occurs along outcrops of sandstones in the eastern part of the Suceava Plateau—the well-known "Moldavian Scarp" (Ungureanu 1993), and along the outcrops of the volcanic tuffs, in the southern part of the Central Moldavian Plateau and the northern parts of the Fălciu and Tutova Hills (Mărgărint et al. 2013b). In the latter case, rotational behavior is present mainly at the upper part of the slopes but also at medium and lower levels (Figs. 12.5a, 12.6a).

Translational Slides

Translational slides are defined as a displacement of a mass of rocks, debris or earth along a planar or undulating surface of rupture, sliding out over the original ground surface (Cruden and Varnes 1996). Their occurrence is linked to the large extension of sensitive clays and silts in the Moldavian Plateau. They are generally spread all over the study area. Their area is generally reduced, with values comprised between 123.2 m^2 and 0.98 km^2, with a mean value of 0.034 km^2. It is noteworthy that individual translational bodies have small areas (see mean and median in Table 12.1), with an obvious exception represented by a large number of slides prepared by the consistent number of anthropic lakes and pounds, especially in the northeast part of the region—the Jijia Hills (Figs. 12.5c, and 12.6c). Individual translational slides are spread all over the length of the hillslopes.

An important factor for the decreasing of cohesiveness of the materials along the slope is represented by the continuous sliding of the complex landslides throughout the time. The great thickness of the rotational landslide deposits from the upper levels of the slopes, permanently eroded and cut by the incipient hydrographic network, has constituted to major preparatory factor for these reactivations,

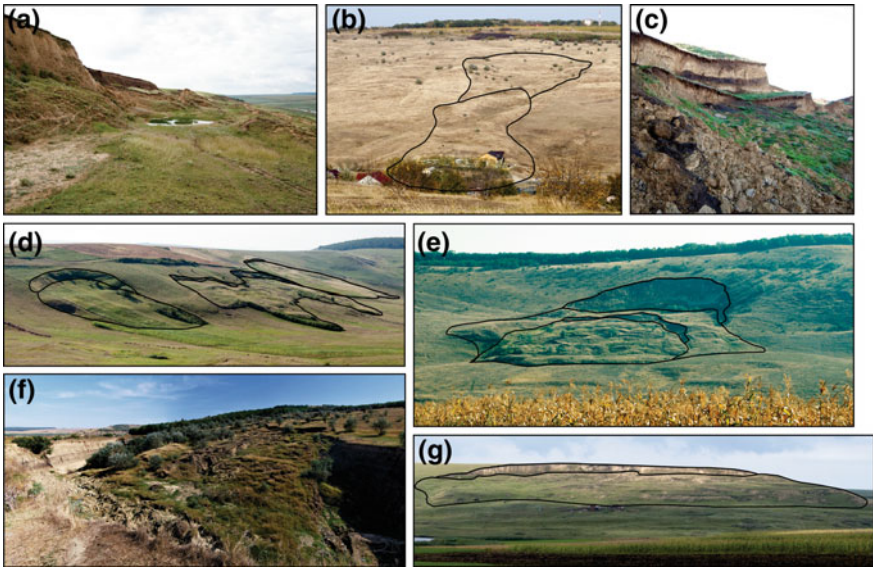

Fig. 12.5 Representative types of landslides from Moldavian Plateau: **a**, **e** rotational, **f** lateral spread, **c** translational, **d** translational and flow like, **b** flow, **g** succession of translational slides affected by a recent rotational one

classified as complex slides. This important issue was well emphasized by other landslide regional approaches (Klimeš 2008), and recently discussed in geomorphometric terms (Goetz et al. 2014). The occurrence of sands and sandy silts intercalations in the Bessarabian to Romanian formations (Fig. 12.3) constitutes favorable condition for mixing the translational movement with flows.

Earth Flows

A flow is a spatially continuous movement in which surfaces of shear are short-lived, closely spaced, and not usually preserved (Cruden 2011). In the Moldavian Plateau, the occurrence of individual flows is very low compared with the other types; that is why we did not create a distinct class. As a mechanism, the flows do occur, but in mixture with other types of movements (rotational and translational), so we will find this genetic type included in the rotational–translational-flow complexes (Figs. 12.5f, and 12.6f; Table 12.1).

Lateral Spreads

Cruden (2011) defines a spread as an extension of a cohesive soil or rock mass combined with a general subsidence of the fractured mass of cohesive material into

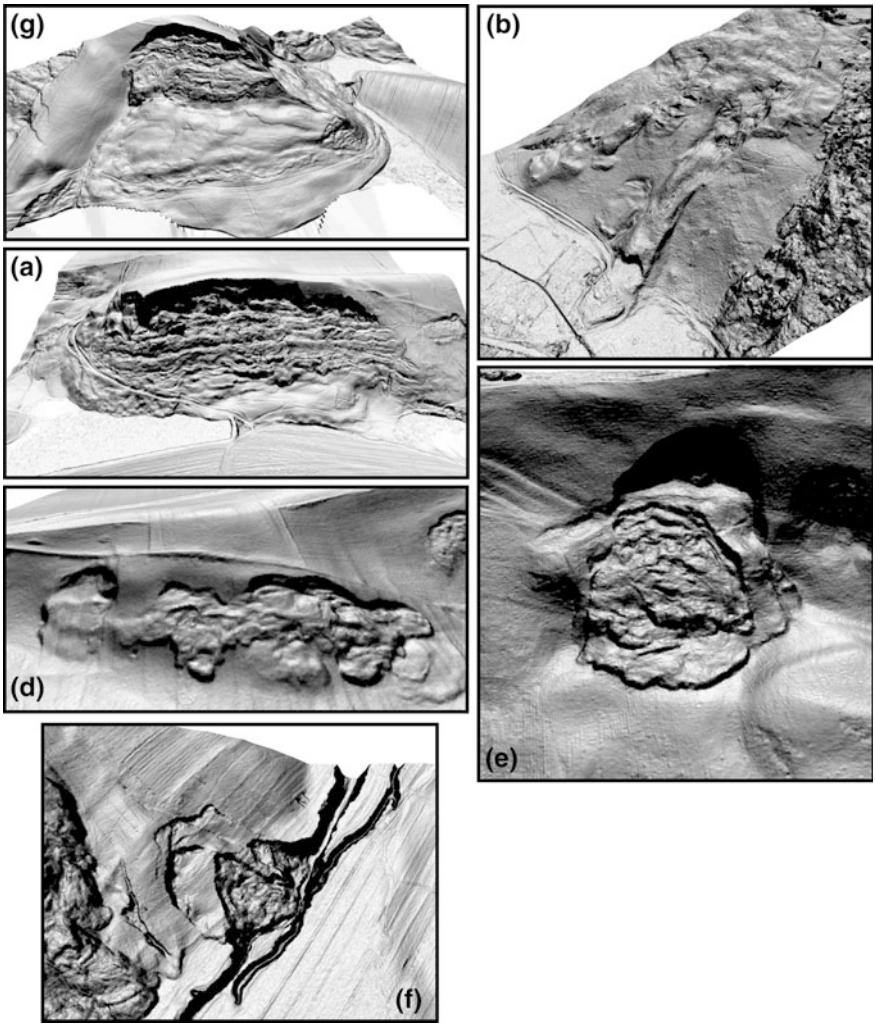

Fig. 12.6 3D perspectives of LIDAR shading for typical landslides (the photos of the same landslides are shown in Fig. 12.5, and the notation is consistent with the photos)

softer underlying material. For the Moldavian Plateau, such similar features occur, but have some differences, being linked with the river and gully dissection of hillslope toe or channel heads. We have called this type of spreads, lateral spreads, because the spread mechanism is controlled by the incision, which does not allow a typical rotational movement, but also limits the material subsidence at the base (Figs. 12.5f, and 12.6f).

Complex Landslides

In many cases, a single type of movement is impossible to be assigned to a slope mass delimited and mapped in a polygonal manner. For these situations, Varnes (1978) introduced the term of complex landslides, which can be detailed using a composite terminology (Hungr et al. 2014).

Remarkable for the Moldavian Plateau is the large extension of landslides which cannot be attributed to a single genetic mechanism. The different types of movements can be recognized through the abundance of a large variety of micro-morphologic details of landslides (secondary scarps, lateral cracks, various roughness, micro-depressions, mounds). This morphological complexity is related to a long-term evolution of cuesta scarps. Generally, a fresh morphology is associated with the translational slides and flows and this issue emphasizes a clear differentiation between present and past processes and created landforms (Dikau and Schmidt 2001; Damm and Terhorst 2010).

A large part of these complex landslides, but also some event-based landslides are more wide than long, and this is due to the structural landforms, respectively elongated cuesta scarps, which can be followed on tens of kilometers (Figs. 12.4, and 12.7). The development of landslides along the fronts of cuesta diminishes the possibilities for an individual treatment of landslides at this scale of analysis, being probably one of the major limitations of the inventory.

Two subclasses have been differentiated for the complex landslides: (i) polygons with obvious rotational and translational movements, and (ii) polygons with rotational, translational, and clearly distinguished parts with flows. In the first subclass, a particular type of slope morphology was included, regionally known as "*hârtoape*". These are large mono- or poly-amphitheater like basins, associated with old, dormant landslides which have thicknesses of 10–20 m, and are affected by recent processes, such as shallow landslides, slumps, and surface erosion (Mărgărint et al. 2013a). These areas also can present a very dense incipient drainage network, which directly controls the permanent evolution of landslide processes (Figs. 12.5d, 12.6d, and 12.7).

The regional grouping of polygons with complex landslides which include flows, especially in the Bârlad Plateau, can be a reason to individualize a distinctive subclass, related to important occurrence of sandy formations (Fig. 12.7).

Spatial and Morphometric Patterns of the Landslides

Analyzing the distributions of the geomorphometric variables of the landslide polygons, we can summarize that the most frequent landslide area interval is 2500–3500 m^2, totalizing 1044 counts. This shows the prevalence of small landslides, but these landslides represents only a small part of the total area covered by landslides (0.6 %) and of the total number of landslides (landslides with areas lower than 10,000 m^2 are only 22.2 % from the total number of landslides). Although

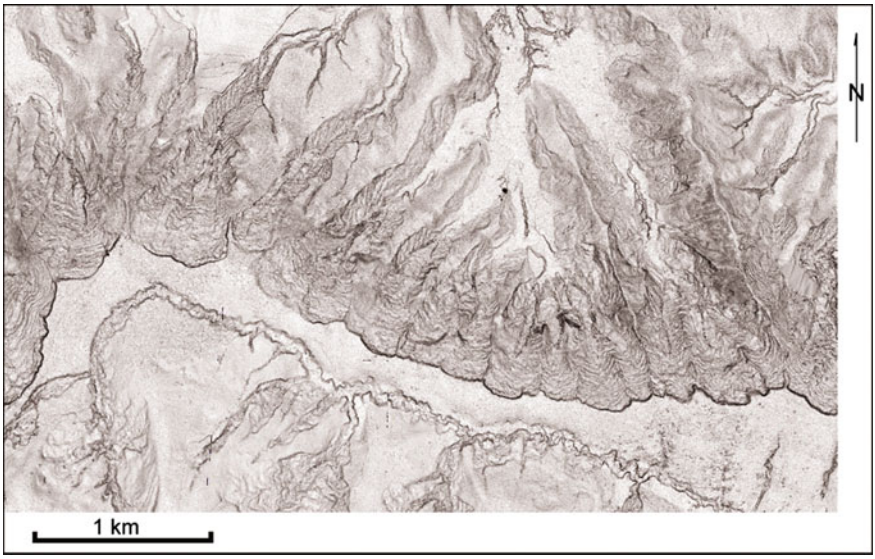

Fig. 12.7 LIDAR DEM image of Iaşi Cuesta Scarp Slope, dominated by continuous complex landslides

representing 44.5 % from the total number of landslides, medium-sized landslides (area between 10,000 and 100,000 m^2) cover only 9.5 % from the total landslide area. Big landslides, with area between 100,000 m^2 and 1 km^2 cover 49.4 %, while numbering 29.8 % from the total number of landslides. The very big landslides (with area bigger than 1 km^2) represent 3.5 % from the total number of landslides.

The distribution of landslide area is consistent with the results from other regions over the Globe (Korup 2005b; Van den Eeckhaut et al. 2007; Guzzeti et al. 2008). The probability density function of landslide areas is studied, because there is a strong support of the idea that landslide areas have a double pareto/inverse gamma like distribution, with small landslides very frequent, showing a gradual increase of the density, and as the big landslides are not quite frequent, the density decreases rapidly along a power-law tail. Because our inventory is historical, and consequently not complete, we could not fit an inverse gamma or pareto distribution to our data, we only simulated inverse gamma distributions with different order of magnitude (Fig. 12.8). Also, frequency density was estimated, and not probability density function (Korup 2005b; Van den Eckhaut et al. 2007; Trigila et al. 2010).

The tail for the frequency density (Fig. 12.8) has a slope of—1.4, which is smoother than the values given in the literature (−2 to−2.4) by Malamud et al. (2004a, b). The reasons for this smoothness is the fact that by delineating complex landslides and event-generated landslides, certain event-based landslides of the population which are comprised by the complex landslides, are not present in the distribution of our inventory. Our tail distribution slope values are close to those obtained by Korup (2005b). This does not imply that the inventory is not usable,

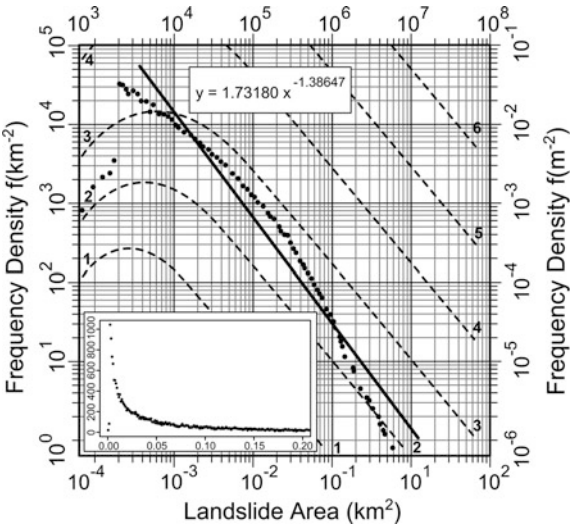

Fig. 12.8 The frequency density distribution of landslide area in log-log scales

but rather incomplete, by not taking into account certain landslides as individuals of the distribution. In the same time, the complex landslides are usable because it represents areas where instability and reactivations can occur.

The majority of the missing individual landslides usually appear clustered on top of the delineated surfaces affected by landslides (Ardizzone et al. 2007). Because of this clustering we believe that the total surface affected by landslides, which we obtained, is close to the real total projected surface, and the future inclusion of the event-based landslides will not modify significantly the total landslide area. Because the landslide inventory is not event-based, and thus incomplete, the magnitude cannot be assessed properly, but applying the formula given by Malamud et al. (2004b), the magnitude of the power-law tails is 4.38. About the magnitude, we can only remark that, as others mention (Korup 2005b; Van Den Eeckhaut et al. 2007; Guzzeti et al. 2008) the frequency density spans across two orders of magnitude, showing again the incompleteness state of the inventory, and the fact that is a geomorphologic one, containing landslides with different ages and magnitudes. The theoretical number of real landslides, from which the ones with small area are lost due to erosion, can be estimated to 40,415; the corresponding theoretical total area is 8154 km^2. These values were obtained applying the methodology of Malamud et al. (2004b), by considering the count of landslides with areas bigger than 0.1 km^2, which represent 44.5 % of the total number of landslides, their cumulative area, and extrapolating to 100 %. We expect the real projected surface to be bigger, but close to the actual surface, because the 8154 km^2 is the cumulative surface, including the overlapping of small landslides.

A good way to analyze the landslide distribution in a spatial way is to compute the landslide index, as the proportion of surface of 1 × 1 km rectangles covered by landslides (Trigila et al. 2010). This index is represented in Fig. 12.9 and shows the

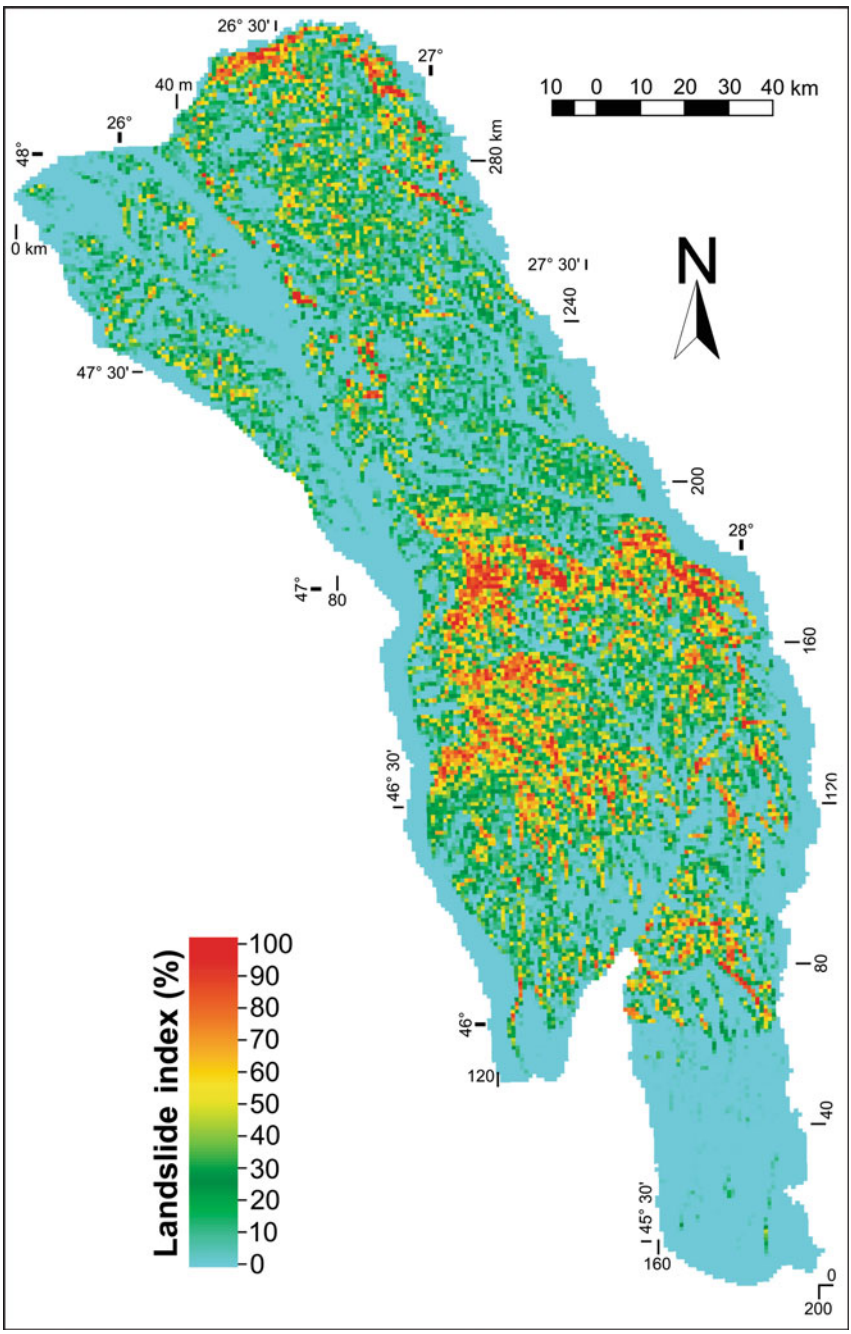

Fig. 12.9 Landslide area patterns in the Moldavian Plateau: the landslide index for 1 × 1 km (1 km^2) grid

areas where landslides have a higher density: Central Moldavian Plateau, the north part of Tutovei Hills, the northern part of Jijia Hills, the Siret Hills, and the contact between Fălciului Hills and Covurlui Plateau.

Landslides have an altitudinal distribution which has a different shape than the general distribution of altitude in the study area (Fig. 12.2), but the tendency of the distributions are similar, with an abrupt increase of the frequency of altitudes affected by landslides, and general altitudes toward 170–180 m a.s.l., when a maximum is reached, and then a gradual decrease with a flattening after 420 m a.s.l. for landslides, and 540 m a.s.l. for the entire study area (Fig. 12.10). The slope of

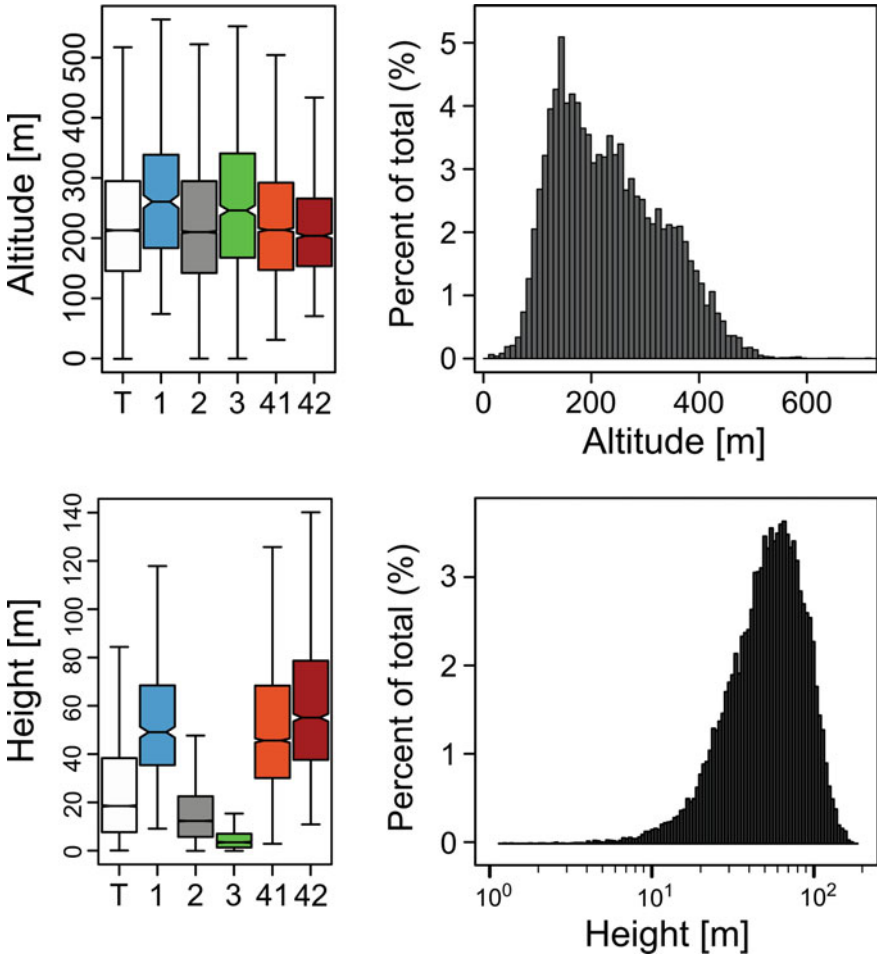

Fig. 12.10 Descriptive statistics graphics for landslide inventory geomorphometry: altitude and height shown in boxplots and histogram, the boxplots representing the totals (*T*) and landslide types (1, 2, 3, 41, and 42), according to the Sect. 12.4.1. The colors are the same with those used in Fig. 12.4

the terrain affected by landslides show a Weibull distribution, asymmetric to the left, the maximum frequency being centered on 7 degrees (Fig. 12.2).

This value is close to the modal value of slope, 8.6 degrees, which has been shown to be the characteristic slope angle at failure (Ohmori and Sugai 1995; Iwahashi et al. 2003; Korup 2005b; Guzzeti et al. 2008; Donnarumma et al. 2013).

Comparing the results with the conclusions of Korup (2005b) and Guzzeti et al. (2008), who point out that in their study area (mountainous areas) landslides have modified the slope modal value of topography with up to 3 degrees, the data for Moldavian Plateau show an insignificant difference in slope modal value, between landslides and undisplaced areas. Considering the fact that landslides do not change the slope distribution we can state that this pattern is related to the general evolution of hillslopes, mass movement processes, and river incision of the toe, which sustain the slope of cuesta scarp slopes. For the cuesta dip slopes, landslides change the slope distribution, by creating steep portions, which reduce the general asymmetry of cuestas. Only lateral spreads do not follow this pattern, because these landslides appear in specific conditions of landform-channel network relations.

The general slope (slope height/length), which can be seen as the slope of the original hillslope (before the landslide) shows an exponential distribution, mainly because of the influence of the landslide height. Also, the descriptive statistics of the landslide types show the presence of a similar slope threshold for the hillslopes affected by landslides (Table 12.1). According to their typology, only rotational and lateral spread types have different general slope characteristics, compared with the general slope of translational and complex types, which show similar characteristics with the general slope of the overall landslides. Thus, the mean general slope of the landslides is 6 %, with the spread of majority of the values between 4 and 10 % (Fig. 12.11).

Slope height (Figs. 12.2, and 12.10) shows the large variety of landslide locations on hillslopes. The typology of landslides shows distinctive features of hillslope locations, translational and complex landslides being distributed all over the length of the hillslopes with great amplitudes; the translational and lateral spread landslides have a smaller amplitude, and are located in the lower half of the slopes.

Landslide length and width are correlated, since the landslides from the Moldavian Plateau show complementary length–width relations (Fig. 12.12). The rotational landslides are either circular or elongated, with length bigger than width. Translational landslides and flows have clearly elongated shape, with length several times bigger than width. Complex landslides, especially those situated on cuesta scarp slope, and lateral spreads have the width bigger than the length.

Slope aspect (Fig. 12.2) of the terrain of both all the areas and of the areas affected by landslides show that the most frequent pixels are those with NE, E, SW, W aspect, related to the general pattern of cuesta landforms, cuesta dip slopes having the largest surfaces. If the number of landslides is compared with the cuesta landforms delineated by Niculiţă (2011), the same pattern is well emphasized (Fig. 12.13a). In reality, the pattern introduced by the large complexes, which occurred mainly on cuesta scarp slopes, can be shown only if we analyze the surface of landslides on each cuesta hillslope type (Fig. 12.13b). Generally, N and

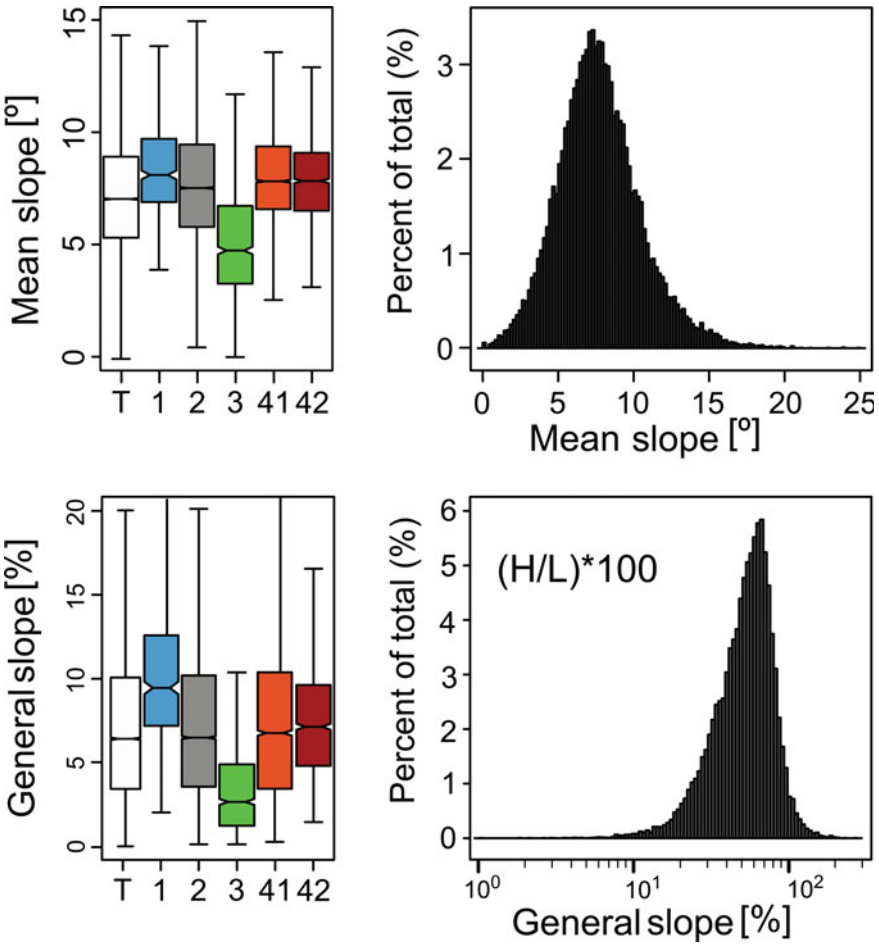

Fig. 12.11 Descriptive statistics graphics for landslide inventory geomorphometry: mean slope and general slope shown in boxplots and histogram, the boxplots representing the totals (*T*) and landslide types (*1*, *2*, *3*, *41*, and *42*), according to the Sect. 12.4.1. The colors are the same with those used in Fig. 12.4

W oriented hillslopes represent cuesta scarp slopes while E and S hillslopes represent cuesta dip slopes. Although cuesta scarp slopes cover a smaller proportion of the study area than the dips slopes (as it can be seen in Fig. 12.2), the first have a larger surface of landslides than the latter ones.

By landslide type, the most frequent are rotational–translational complexes (62.8 %), followed by rotational–translational-flow complexes (22.3 %), translational (12.2 %), rotational landslides (2.5 %), and river induced (0.2 %).

The physiogeographic regions with the biggest areas occupied by landslides (as proportion from the total landslide area) are the Central Moldavian Plateau with

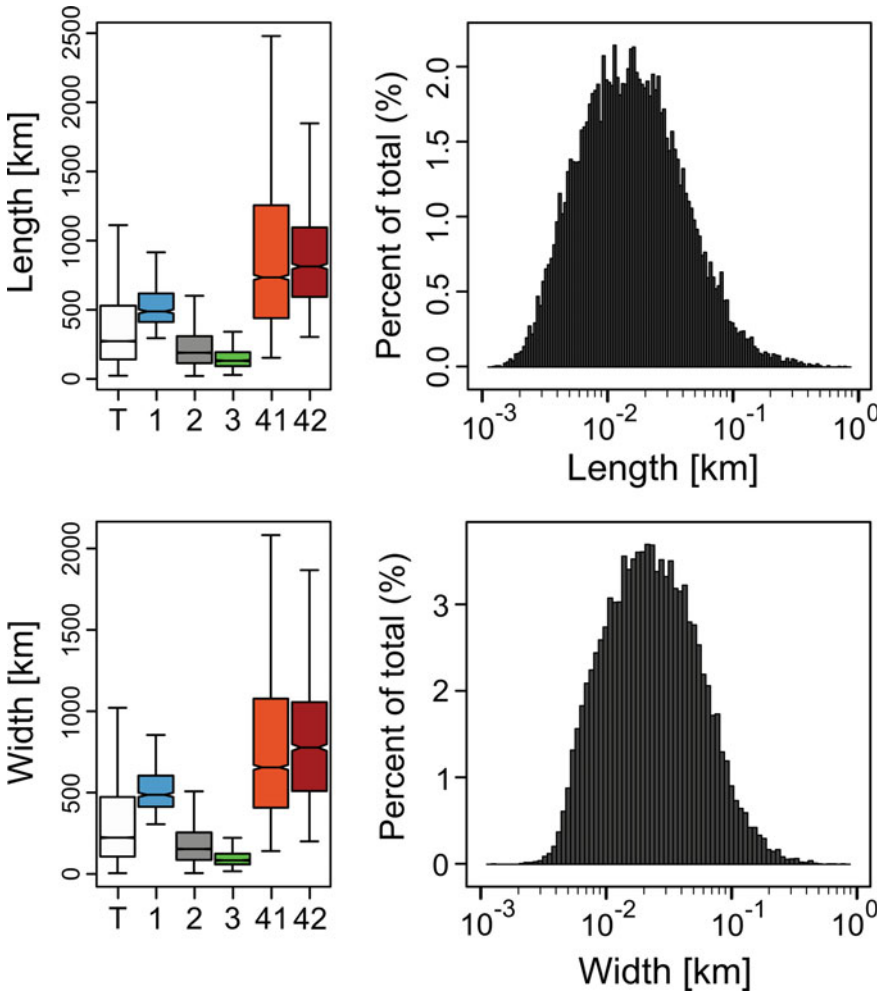

Fig. 12.12 Descriptive statistics graphics for landslide inventory geomorphometry: mean length and width shown in boxplots and histogram, the boxplots representing the totals (*T*) and landslide types (*1*, *2*, *3*, *41*, and *42*), according to the Sect. 12.4.1. The colors are the same with those used in Fig. 12.4

30.4 %, Jijia Plateau with 26.5 %, Tutovei Hills with 20.3 %, the others having smaller proportions: Siret Hills (7 %), Suceava Plateau (6.2 %), Fălciu Hills (4.1 %), Covurlui Plateau (2.3 %), Huşi–Sărata–Elan–Horincea Hills (2.3 %).

Considering the proportion of the landslide area from the total area of the physiogeographic regions, the situation is close to that of the whole study area, the Central Moldavian Plateau having 38.2 %, Suceava Plateau 33.6 %, Tutova Hills 29.1 %, Huşi–Sărata–Elan–Horincea Hills 26.5 %, Fălciu Hills 21.8 %, Jijia Plateau 19.3 %, Siret Hills 17.9 %, only Covurlui Plateau having 4.5 %.

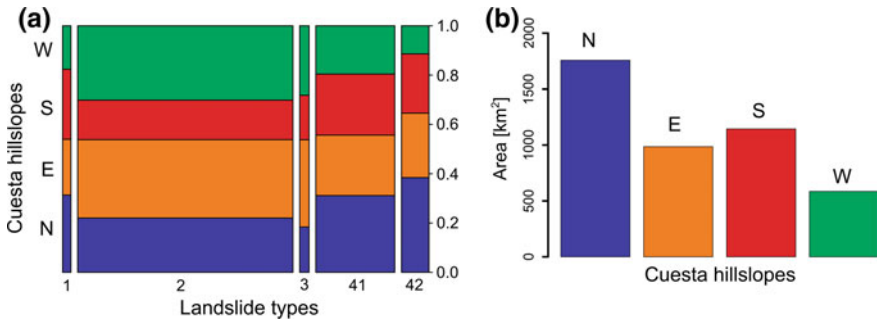

Fig. 2.13 Descriptive statistics graphics for landslide inventory geomorphometry **a** mosaic plot of landslide types and cuesta hillslopes class (Niculiță 2011), **b** barplot for absolute values of areas of landslides for cuesta hillslopes class (Niculiță 2011). The numbers of landslide types (**a**) are the same with those used in Fig. 12.4. The colors are the same with those used in Fig. 12.4

The rotational landslides are the most frequent in Tutova Hills (24.8 % from the total rotational population), Central Moldavian Plateau (23.8), Jijia Hills (17.7 %), Suceava Plateau (17.1 %), and Siret Hills (11.7 %), in relation with the occurrence of consolidated geological formations (Fig. 12.3). The translational landslides are the most frequent in Jijia Hills (26.7 %), Tutova Hills (26.1 %), Central Moldavian Plateau (18.3 %), in relation with the clayey deposits extension. The lateral spread are the most frequent in Suceava Plateau (28.7 %), Tutova Hills (27.5 %), Covurlui Plateau (13.3 %), being related to the channel network and gully density. The rotational–translational complexes are the most frequent in Jijia Plateau (34.9 %), Tutova Hills (30.6 %), Siret Hills (11.7 %), and Suceava Plateau (11.3 %). The rotational–translational-flow complexes are the most frequent in Central Moldavian Plateau (47.5 %), Jijia Hills (38.6 %), Fălciu Hills (6.2 %), Tutova Hills (4.2 %). These complex categories distribution is consistent with the mentioned patterns of lithology, incipient drainage network and main characteristics of landslide type discussed above.

Regarding the surface lithology, 25.1 % of landslide area is present on Bessarabian rocks, with 17.1 % on clay member (*bs1*—abbreviations according to the legend of Fig. 12.3), and 8.3 % on the limestone-sand-sandstone member (*bs3*), 17.2 % on Meotian rocks, with 10.4 % on the sand-clay (me1) and 6.8 % on the cineritic member (*me2*), 16.5 % on the Kersonian rocks, with 14.5 % on the deltaic facies (*ksa*) and 2 % on the brackish facies (*ksb*), 13.3 % on Holocene deposits, 12.4 % on Volhynian rocks, 4.1 % on Pontian and Dacian rocks, 3.4 % on Upper Pleistocene rocks (*qp3*) and 2.9 % on Romanian rocks (*ro*). The other geologic formations have all landslide areas lower than 2 % of landslide total area.

General Remarks

The large complexity of landslides from the Moldavian Plateau can determine us to affirm that nature of triggering factors has recorded a real historical variability. The largest scarps of complex landslides are now smoothed, and in many cases covered by well-developed forest vegetation. Therefore, for the assessment of current and future activity of landslides, an important issue is represented by the interaction of landslides history with current and future triggering factors (Schmidt and Dikau 2005).

The knowledge of landslide types and patterns is an important issue of the assessment of their spatial probability of occurrence. A special characteristic of landslides in the Moldavian Plateau are some patterns which link the landslides with human concentrations and activities. Many settlements are spread along cuesta scarp slopes or "*hârtoape*" complex amphitheaters, due to their microclimatic, hydrogeologic, and historic conditions (Mărgărint et al. 2010). But regarding vulnerability and risk assessment perspective, these locations play an important role, leveraging these issues. In the recent decades (especially the '70 and '80), the terrains affected by landslides have constituted the object for many local projects in order to mitigate the negative effects of landslides for settlements, along roads or in diminishing agricultural potential of the terrain (Pujină 2008). After the social changes of 1989, unusual patterns of the agricultural lands were extended as a consequence of serious legislative lacks, as we can see in Fig. 12.14. The fragmentation of new agricultural parcels resulted from recent appropriation (Popovici et al. 2013) makes possible the delineation of the landslides. A similar pattern, but much older, is given by integral extension of settlements on the stabilized landslides along cuesta scarp fronts (Fig. 12.14b).

The alignment of large complexes of landslides of landslides which border almost the entire Jijia Hills constantly have put serious problems along railways and roads that cross-neighboring units (Bârlad and Suceava Plateaus). Every year, slope displacements are reported and sometimes affect with severe damages these important lifelines. More than that, the design of future ways of communication must take into consideration the new maps of the spatial distribution of mass movements achieved through new mapping techniques, like LIDAR DEM and high-resolution satellite remote sensing imagery, which were not available until now (Mărgărint et al. 2013b). The future steps of regional scale approaches of landslides, like susceptibility, hazard, and risk assessments, will benefit successfully from statistical outputs of relations between landslide occurrence and lithology, morphostructure, geomorphometric variables, landuse, etc.

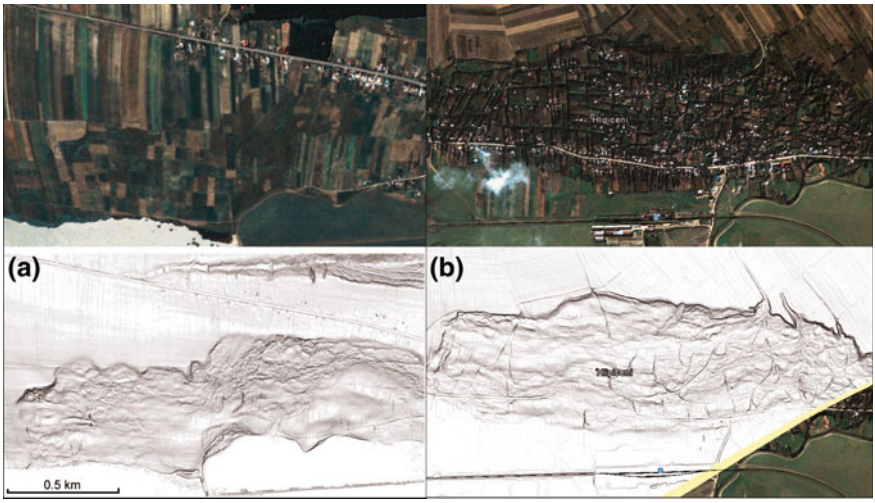

Fig. 12.14 Specific patterns of land use associated with landslides: **a** the fragmentation of new agricultural parcels (after 1989) delineating a landslide induced by lakes, **b** extension of Hlipiceni village (Northern Jijia Hills) amazingly fits an elongated cuesta scarp landslide

Conclusions

The present paper has analyzed the causal factors, landslide patterns distributions, and types in the Moldavian Plateau, using as a base a historical landslide inventory, containing 24,263 landslide polygons and created from the interpretation of remote sensing images. The inventory is geomorphologic and incomplete, as shown by the low frequencies of the small landslides, but its validity is given by the shape of the distribution tail, which fits the literature information. Further expansions of this inventory will require the introduction of age, the separation of more event-based landslides and the delineation of the scarp from the landslide body.

The landslide spatial distribution indicates the hotspots inside the study area, and although only 18.3 % is covered by landslides and despite a relative lifelessness is recorded in the rates of mass movement processes in the last decades, landslides are a chronic phenomenon, able to reactivate if the causal factors allow it.

Considering the data from the landslide inventory and field experience we have generalized the following types of landslides: rotational, translational, lateral spread, flow, and complex landslides.

In the present analysis, we conclude that the geological conditions (the monoclinic structure with a succession of clays and silts with limestone and sandstone intercalation) and morphostructure create a strong control in the spatial distribution of landslides. While landslides occur on all lithological classes and occupy the entire range of slope positions (upper, middle, lower), there are differences depending on their type. Using spatial and geomorphometric analysis of the

landslides we argued a link between mass movement processes and the geologic, morphostructural, and topographic setting. The general presented pattern is completed by local situations, which are generated by a large range of local preparatory factors.

The landslide inventory needs to be further extended by the inclusion of age, event-based landslides and multi-temporal attributes to complete the general image of landslide types and patterns in the Moldavian Plateau. This will contribute to a better understanding of landslide phenomenon, to the ability to estimate the associated risk, and to the assessment and sustainable management of landscape resources in the Moldavian Plateau.

Acknowledgments The authors gratefully acknowledge partial support of Mihai Niculiţă by the European Social Fund in Romania, under the responsibility of the Managing Authority for the Sectoral Operational Program for Human Resources Development 2007–2013 [grant POSDRU/159/1.5/S/133391]. We are grateful to Prut–Bârlad Water Administration who provided us with the LIDAR data. We have used the computational facilities given by the infrastructure provided through the POSCCE-O 2.2.1, SMIS-CSNR 13984-901, No. 257/28.09.2010 Project, CERNESIM (L4).

References

Abbott PL (2004) Natural disasters. McGraw-Hill Companies Inc., New York

Agostinelli C, Lund U (2013) R package 'circular': circular statistics (version 0.4-7). https://r-forge.r-project.org/projects/circular/

Ardizzone F, Cardinali M, Galli M, Guzzetti F, Reichenbach P (2007) Identification and mapping of recent rainfall-induced landslides using elevation data. Nat Hazards Earth Syst Sci 7: 637–650

Băcăuanu V (1968) Campia Moldovei. Studiu geomorfologic. Editura Academiei (in Romanian)

Băcăuanu V, Barbu N, Pantazică M, Ungureanu A, Chiriac D (1980) Podișul Moldovei. Natură, om, economie. Editura științifică și enciclopedică, București (in Romanian)

Bălteanu D, Chendeş V, Sima M, Enciu P (2010) A country-wide spatial assessment of landslide susceptibility in Romania. Geomorphology 124:102–112

Bălteanu D, Jurchescu M, Surdeanu V, Ioniță I, Goran C, Urdea P, Rădoane M, Rădoane N, Sima M (2012) Recent landform evolution in the Romanian Carpathians and Pericarpathian Region. In: Loczy D, Stankoviansky M, Kotarba A (eds) Recent Landform Evolution, pp 249–286

Böhner J, Selige T (2006) Spatial prediction of soil attributes using terrain analysis and climate regionalisation. In: Böhner J, McCloy KR, Strobl J (eds) SAGA—analysis and modelling applications. Göttinger Geographische Abhandlungen, p 115

Broothaerts N, Kissi E, Poesen J, Van Rompaey A, Getahun K, Van Ranst E, Diels J (2012) Spatial patterns, causes and consequences of landslides in the Gilgel Gibe catchment, SW Ethiopia. Catena 97:127–136

Bucknam RC, Coe JA, Chavarria MM, Godt JW, Tarr AC, Bradley L-A, Rafferty S, Hancock D, Dart RL, Johnson ML (2001) Landslides triggered by Hurricane Mitch in Guatemala—inventory and discussion. US Geological Survey Open File Report 01–443

Capecchi V, Perna M, Crisci A (2015) Statistical modeling of rainfall-induced shallow landsliding using static predictors and numerical weather predictions: preliminary results. Nat Hazards Earth Syst Sci 15:75–95

Ciampalini A, Raspini F, Bianchini S, Frodella W, Bardi F, Lagomarsino D, Di Traglia F, Moretti S, Proietti C, Pagliara P, Onori R, Corazza A, Duro A, Basile G, Casagli N (2015) Remote sensing as tool for development of landslide database: the case of the Messina Province (Italy) geodatabase. Geomorphology. doi:10.1016/j.geomorph.2015.01.029

Conforti M, Muto F, Rago V, Critelli S (2014) Landslide inventory map for north-eastern Calabria (South Italy). J Maps 10:90–102

Corine Land Cover 2006 seamless vector data v. 17 (2013) http://www.eea.europa.eu/data-and-maps/data/clc-2006-vector-data-version-3

Croitoru AE, Minea I (2014) The impact of climate changes on rivers discharge in Eastern Romania. Theor Appl Climatol. doi:10.1007/s00704-014-1194-z

Cruden DM (1991) A simple definition of a landslide. Bull Internat Assoc Eng Geol 43:27–29

Cruden DM (2011) The working classification of landslides: material matters. In: 2011 Pan-Am CGS geotechnical conference

Cruden DM, Varnes DJ (1996) Landslide types and processes. In: Turner AK, Schuster RL (eds) Landslides investigation and mitigation. Transportation research board, US National Council, Special Report 247, Washington, DC, Chapter 3:36–75

Damm B, Terhorst B (2010) A model slope formation related to landslide activity in the Eastern Prealps, Austria. Geomorphology 122:338–350

Densmore AL, Hovius N (2000) A fingerprints of bedrock landslides. Geology 28:371–374

Dikau R, Schmidt K-H (2001) Mass movements in South, West and Central Germany—objectives and main results of the MABIS project. Z Geomorphol Suppl 125:1–12

Donnarumma A, Revellino P, Guerriero L, Grelle G, Guadagno FM (2013) Failure analysis of shallow landslides using a three parameter Weibull distribution of slope angle. Rend Online Soc Geol It 24:110–112

Dutang C, Goulet V, Pigeon M (2008) Actuar: an R package for actuarial science. J Stat Softw 25:1–37

Fell R, Corominas J, Bonnard C, Cascini L, Leroi E, Savage WY (2008) Guidelines for landslide susceptibility, hazard and risk zoning for land-use planning. Eng Geol 102:99–111

Glade T (2003) Landslide occurrence as a response to land use change: a review of evidence from New Zealand. Catena 51:297–314

Goetz JN, Bell R, Brenning A (2014) Could surface roughness be a poor proxy for landslide age? Results from the Swabian Alb, Germany. Earth Surf Proc Landf 39(12):1697–1704

Grozavu A, Mărgărint MC, Patriche CV (2012) Landslide susceptibility assessment in the Brăieşti-Sineşti sector of Iaşi cuesta. Carpath J Earth Environ Sci 7:39–46

Guzzetti F, Cardinali M, Reichenbach P (1996) The influence of structural setting and lithology on landslide type and pattern. Environ Eng Geosci 2:531–555

Guzzetti F, Carrara A, Cardinali M, Reichenbach P (1999) Landslide hazard evaluation: a review of current techniques and their application in a multi-scale study, Central Italy. Austria 31: 181–216

Guzzetti F, Ardizzone F, Cardinali M, Galli M, Reichenbach P, Rossi M (2008) Distribution of landslides in the Upper Tiber River basin, central Italy. Geomorphology 96:105–122

Guzzetti F, Mondini AC, Cardinali M, Fiorucci F, Santangelo M, Chang K-T (2012) Landslide inventory map: New tools for an old problem. Earth Sci Rev 112:42–66

Haase D, Fink J, Haase G, Ruske R, Pécsi M, Richter H, Altermann M, Jäger K-D (2007) Loess in Europe–its spatial distribution based on a European Loess Map, scale 1:2,500,000. Quatern Sci Rev 26:1301–1312

Haesaerts P, Borziak I, Chirica V, Damblon F, Koulakovska L, van der Plicht J (2003) The East Carpathian loess record: a reference for the middle and late pleniglacial stratigraphy in Central Europe. Quaternaire 14(3):163–188

Hovius N, Stark CP, Hao-Tsu C, Jiun-Chuan L (2000) Supply and removal of sediment in a landslide-dominated mountain belt: Central Range. Taiwan. J Geol 108:73–89

Hungr O, Leroueil S, Picarelli L (2014) The Varnes classification of landslide types, an update. Landslides 11:167–194

Institutul Geologic al României (1968) Harta geologică a României, scara 1:200 000, foile şi notele explicative: 1 (Dărăbani), 5 (Rădăuţi), 6 (Suceava), 7 (Ştefăneşti), 13 (Piatra Neamţ), 14 (Iaşi), 22 (Bârlad), 30 (Focşani)
International Commission on Stratigraphy (2014) International Chronostratigraphic Chart v. 2014/02. http://www.stratigraphy.org/index.php/ics-chart-timescale
Ionesi L (1994) Geologia unităților de platformă și a Orogenului Nord-Dobrogean. Editura Tehnică, Bucureşti (in Romanian)
Ionesi L, Ionesi B, Roşca V, Lungu A, Ionesi V (2005) Sarmaţianul mediu şi superior de pe Platforma Moldovenească. Editura Academiei Române, Bucureşti (in Romanian)
Ioniță I (2000) Relieful de cueste din Podișul Moldovei. Corson, Iași (in Romanian)
Iwahashi J, Watanabe S, Furuya T (2003) Mean slope-angle frequency distribution and size frequency distribution of landslide masses in Higashikubiki area. Jpn Geomorphol 50:349–364
Jäger D, Sandmeier C, Schwindt D, Terhorst B (2013) Geomorphological and geophysical analyses in a landslide area near Ebermannstadt, Northern Bavaria. Quatern Sci J 62:150–161
Jeanreanud P (1971) Harta geologică a Moldovei Centrale dintre Siret și Prut. Analele Științifice ale Universității "Alex. I. Cuza" din Iași, sec. II, XVII:65–78 (in Romanian)
Kavzoglu T, Sahin EK, Colkesen I (2015) Selecting optimal conditioning factors in shallow translational landslide susceptibility mapping using genetic algorithm. Eng Geol 192:101–112
Klimeš J (2008) Analysis of preparatory factors of landslides, VsetínskéVrchy Highland, Czech Republic. Acta Res Reports 17:47–53
Komac M, Hribernik K (2015) Slovenian national landslide database as a basis for statistical assessment of landslide phenomena in Slovenia. Geomorphology. doi:10.1016/j.geomorph.2015.02.005
Korup O (2005a) Distribution of landslides in south-west New Zeeland. Landslides 2:43–51
Korup O (2005b) Geomorphic imprint of landslides on alpine rivers system, southwest New Zeeland. Earth Surf Proc Landf 30:783–800
Lin CW, Tseng CM, Tseng YH, Fei LY, Hsieh YC, Tarolli P (2013) Recognition of large scale deep-seated landslides in forest areas of Taiwan using high resolution topography. J Asian Earth Sci 62:389–400
Malamud BD, Turcotte DL, Guzzetti F, Reichenbach P (2004a) Landslides, earthquake, and erosion. Earth Planet Sci Lett 229:45–59
Malamud BD, Turcotte DL, Guzzetti F, Reichenbach P (2004b) Landslide inventories and their statistical properties. Earth Surf Proc Landf 29:687–711
Massey CI, Petley DN, McSaveney M (2013) Patterns of movement in reactivated landslides. Eng Geol 159:1–19
Maţenco L, Bertotti G (2000) Tertiary tectonic evolution of the external East Carpathians (Romania). Tectonophysics 316:255–286
Maţenco L, Bertotti G, Leever K, Clouting S, Schmid SM, Tărăpoancă M, Dinu C (2007) Large-scale deformation in a locked collisional boundary: interplay between subsidence and uplift, intraplate stress, and inherited lithospheric structure in the late stage of the SE Carphatian evolution. Tectonics 26, TC4011. doi:10.1029/2006TC001951
Mărgărint MC, Niculiţă M (2014) Comparison and validation of Logistic Regression and Analytic Hierarchy Process models of landslide susceptibility assessment in monoclinic regions. A case study in Moldavian Plateau, N-E Romania. Geophys Research Abstracts 16, EGU 2014–6371
Mărgărint MC, Grozavu A, Condorachi D, Pleşcan S, Boamfă I (2010) Geomorphometric features of the built areas of the localities along Iaşi cuesta. Geographia Technica 2:79–89
Mărgărint MC, Grozavu A, Patriche CV (2013a) Assessing the spatial variability of coefficients of landslide predictors in different regions of Romania using logistic regression. Nat Hazards Earth Syst Sci 13:3339–3355
Mărgărint MC, Juravle DT, Grozavu A, Patriche CV, Pohrib M, Stângă IC (2013b) Large landslide risk assessment in hilly areas. A case study of Huşi town region. It J Eng Geol Environ Book Series 6:275–286
McKean J, Roering J (2004) Objective landslide detection and surface morphology mapping using high-resolution airborne laser altimetry. Geomorphology 57:331–351

Meunier P, Uchida T, Hovius N (2013) Landslide patterns reveal the sources of large earthquakes. Earth Planet Sci Lett 363:27–33
Micu M (2011) Landslide assessment: from field mapping to risk management. A case-study in the Buzău Subcarpathians. Forum Geografic 10:70–77
Mihai B, Săvulescu I, Şandric I, Chiţu Z (2014) Integration of landslide susceptibility assessment in urban development: a case study in Predeal town, Romanian Carpathians. Area. doi:10.1111/area.12123
Minea I (2012) The Bahlui hydrographic basin. Hydrological study. "Alex. I. Cuza" Univ. Press, Iaşi (in Romanian)
Mondini AC, Viero A, Cavalli M, Marchi L, Herrera G, Guzzetti F (2014) Comparison of event landslide inventories: the Poliaschina catchment test case, Italy. Nat Hazards Earth Syst Sci 14:1749–1759
Niculiţă M (2011) A landform classification schema for structural landforms of the Moldavian platform (Romania). In: Hengl T, Evans IS, Wilson JP, Gould M (eds) Geomorphometry 2011. Redlands, CA, pp 129–132
Niculiţă M (2015) Automatic extraction of landslide flow direction using geometric processing and DEMs. In: Jasiewicz J, Zwoliński Z, Mitasova H, Hengl T (eds) Geomorphometry for Geosciences. Poznań, Poland: Bogucki Wydawnictwo Naukowe, Adam Mickiewicz University in Poznań—Institute of Geoecology and Geoinformation, pp 201–203
Niculiţă M, Mărgărint MC (2014) Landslide inventory for the Moldavian Plateau. In: Proceedings of international conference analysis and management of changing risks for natural hazards, 18–19 Nov 2014, Padua, Italy. http://www.changes-itn.eu/Portals/0/Content/2014/Final%20conference/ abstracts/AP3_Abstract_Niculita.pdf
Ohmori H, Sugai T (1995) Toward geomorphometric models for estimating landslide dynamics and forecasting landslide occurrence in Japanese mountains. Z Geomorphology Suppl.-Bd. 101:149–164
Pătruţ I, Dăneţ T (1987) Le Pre-cambrien (Vendien) et le Cambrien dans la Plate-forme Moldave, Analele Ştiinţifice ale Universităţii "Alex. I. Cuza" din Iaşi (Serie Nouă), s. II-b, XXXIII:26–30
Petley DN, Bulmer MH, Murphy W (2002) Patterns of movement in rotational and translational landslides. Geology 30:719–722
Pohrib MD, Juravle DT, Niacşu L, Ursu A, Stanciu A, Plătică D (2012) Paleogeography of the chersonian to meotian in the north of Fălciu Hills (Moldavian Platform) based on sedimentological data. Carpath J Earth Environ Sci 7:23–26
Poiraud A, Define E (2011) Morphology and geomorphological significance of relict landslides in the Tertiary basin of Puy-en-Velay (Massif Central, France). Géomorphologie: relief, processus, environnement 3:247–260
Popescu ME (1994) A suggested method for reporting landslide causes. Bull IAEG 50:71–74
Popescu ME (2002) Landslide causal factors and landslide remedial options, keynote lecture. In: Proceedings of the third international conference on landslides, slope stability and safety of infra-structures, Singapore 61–81
Popovici EA, Bălteanu D, Kucsicsa Gh (2013) Assessment of changes in land-use and land-cover pattern in Romania using Corine Land Cover database. Carpath Journ Earth Env Sci 8:195–208
Posea G (2005) Geomorfologia României: reliefuri, tipuri, geneză, evoluţie, regionare. Editura Fundaţiei "România de Mâine" (in Romanian)
Pourghasemi HR, Moradi HR, Fatemi Aghda SM, Sezer EA, Goli Jirandeh A, Pradhan B (2014) Assessment of fractal dimension and geometric characteristics of the landslides identified in North of Tehran. Iran. Environ Earth Sci 71:3617–3626
Pujină D (2008) Alunecările de teren din Podişul Moldovei. Editura Performantica, Iaşi (in Romanian)
Pujină D, Ioniţă I (1996) Present-day variability and intensity of the sliding processes in the Bârlad Tableland. Proc Internat Con Disaster Mitigation, Madras A4:35–40
R Development Core Team (2008) R: A language and environment for statistical computing. R Foundation for Statistical Computing, Vienna, Austria. ISBN 3-900051-07-0, URL http://www.R-project.org

Rotaru A, Oajdea D, Răileanu P (2007) Analysis of the landslide movements. Inter J Geol 1:70–79
Schmidt J, Dikau R (2005) Preparatory and triggering factors for slope failure: analyses for two landslides in Bonn, Germany. Z Geomorph NF 49:121–138
Selby MJ (1985) Earth's changing surface: An Introduction to geomorphology. Claredon Press
Slocum TA, McMaster RB, Kessler FC, Howard HH (2009) Thematic Cartography and Geovisualization. Pearson Education Inc
Shuttle Radar Topography Mission (SRTM) 1 Arc-Second Global (2014) https://lta.cr.usgs.gov/SRTM1Arc
Stângă IC (2012) Bazinul Tutovei. Riscurile naturale şi vulnerabilitatea teritoriului, "Editura Universităţii "Alex. I. Cuza" din Iaşi (in Romanian)
Şandric I, Chiţu Z (2009) Landslide inventory for the administrative area of Breaza, Curvature Subcarpathians. Romania. J Maps 7:75–86. doi:10.4113/jom.2009.1051
Talaei R (2014) Landslide risk assessment using a multi-method approach in Hashtchin region (NW of Iran). Acta Geod Geophys 49:381–401
Tarolli P, Sofia G, Dalla Fontana G (2012) Geomorphic features extraction from high-resolution topography: landslide crowns and bank erosion. Nat Hazards 61:65–83
Tonini M, Pedrazzini A, Penna I, Jaboyedoff M (2014) Spatial pattern of landslides in Swiss Rhone Valley. Nat Hazards 73:97–110
Travis MR, Elsner GH, Iverson WD, Johnson CG (1975) VIEWIT: computation of seen areas, slope and aspect for land-use planning. USDA F.S. Gen. Tech. Rep. PSW-11/1975, p 70, Berkeley, California, USA
Trigila A, Iadanza C, Spizzichino D (2010) Quality assessment of the Italian Landslide Inventory using GIS processing. Landslides 7:455–470
Ungureanu A (1993) Geografia podişurilor şi câmpiilor României. Editura Universităţii "Alex. I. Cuza" din Iaşi (in Romanian)
Van Den Eeckhaut M, Poesen J, Verstraeten G, Vanacker V, Moyersons J, Nyssen J, Van Beek LPH (2005) The effectiveness of hillshade maps and expert knowledge in mapping old deep-seated landslides. Geomorphology 67:351–363
Van Den Eeckhaut M, Poesen J, Govers G, Verstraeten G, Demoulin A (2007) Characteristics of the size distribution of recent and historical landslides in a populated hilly region. Earth Planet Sci Lett 256:588–603
Van Den Eeckhaut M, Reicchenbach P, Guzzetti F, Rossi M, Poesen J (2009) Combined landslide inventory and susceptibility assessment based on different mapping units: an example from the Flemish Ardennes Belgium. Nat Hazards Earth Syst Sci 9:507–521
Van Den Eeckhaut M, Marre A, Poesen J (2010) Comparison of two landslide susceptibility assessment in the Champagne-Ardenne region (France). Geomorphology 115:141–155
Van Westen CJ, Castellanos E, Kuriakose SL (2008) Spatial data for landslide susceptibility, hazard, and vulnerability assessment: an overview. Eng Geol 102:112–131
Varnes DJ (1978) Slope movement types and processes. In: Schuster RL, Krizek RJ (eds) Landslides, analysis and control, special report 176: transportation research board. National Academy of Sciences, Washington, DC, pp 11–33
Venables WN, Ripley BD (2002) Modern applied statistics with S, 4th edn. Springer, New York
Yin J, Chen J, Xu X, Wang X, Zheng Y (2010) The characteristics of the landslides triggered by the Wenchuan M_s 8.0 earthquake from Anxian to Beichuan. J Asian Earth Sci 37:452–459
Zhao C, Chen W, Wang Q, Wu Y, Yang B (2015) A comparative study of statistical index and certainty factor models in landslide susceptibility mapping: a case study for the Shangzhou District, Shaanxi Province, China. Arab J Geosci 11:9079–9088

Chapter 13
Landslide Types and Spatial Pattern in the Subcarpathian Area

Mihai Micu

Abstract The Romanian Subcarpathians are the most representative landslide-prone areas of Romania in terms of typological complexity. Conditioned by a wide range of predisposing, preparing, and triggering factors, landslides are playing a determinant role among the present-day geomorphic processes, posing in the mean time a major threat to a large number of elements at risk throughout one of Romania's most densely inhabited regions. Within this chapter, the landslides characterizing the main morphostructural and physiographic subunits of the Subcarpathians are discussed in terms of typology imposed by the litho-structural predisposition, anthropic preparatory factors and climatic and seismic triggers. Based on the above-mentioned considerations, a regional distribution reflecting their spatial pattern is attempted through a synthetic map.

Keywords Landslides · Subcarpathians · Typology · Areal distribution · Romania

Introduction

As a physiographic unit, the Subcarpathians act as a passageway between the Carpathian Mountains and the other Carpathian foredeep units. The entire unit features a very young and extremely dynamic relief formed by an association of hilly massifs and large depressions, offering an environment propitious to settlements, reflected by the high density of population and localities. Overall, it represents a fragile environment, with vastly degraded surfaces as a result of the intense human intervention in the landscape. Slope and channel processes are often interacting through connectivity, a general process enhanced by the active neotectonics and seismicity. Among the present-day geomorphic processes, the land-

M. Micu (✉)
Institute of Geography, Romanian Academy, Dimitrie Racoviță 12, 023993 Bucharest, Sector 2, Romania
e-mail: mikkutu@yahoo.com

M. Rădoane and A. Vespremeanu-Stroe (eds.), *Landform Dynamics and Evolution in Romania*, Springer Geography,
DOI 10.1007/978-3-319-32589-7_13

slides hold an important share. The complex Subcarpathian morphogenetic environment is reflected in a wide typology of landslide forms and processes, adapted to a large number of preconditioning, preparing and triggering factors. Yearly, the landslides are causing large damages to a wide variety of elements at risk (households, roads, electricity lines, oil wells) hence imposing appropriate risk management strategies.

Study Area

Developed across some 16,600 km^2, the Romanian Subcarpathians represent around 6.9 % out of the national territorial surface. In terms of genesis, structure and orography, the Romanian Subcarpathians are the most recent Carpathian orogeny wave. As described by Badea (2008), the formation of the Subcarpathian structure started to take place during the final orogenic phases of the Alpine cycle (Paleogene–Mid Miocene), when the Carpathian foredeep molasse was subjected to an active and intensity-growing process of tectonisation extended towards the end of Pliocene and the beginning of Quaternary. As a result, the entire Subcarpathian unit consists of Mio–Pliocene molasse deposits that are locally including older Paleogene flysch formations (and even older Cretaceous deposits in the fundament). The active neotectonic movements (uplifts of 3–4 mm/year, according to Zugrăvescu et al. 1998) led to an enhanced fragmentation harnessed by the rhythmical deepening of the valley, increasing the overall denudation conditions. The general movement, showing regional and local disparities in terms of tectonic structures and lines, led to the deformation of landforms, often revealed within comparative studies of deposits and terraces (Badea and Bălteanu 1977).

Bordering the Carpathian chain toward the exterior between Moldova and Motru Valleys, and divided into three main subunits (Moldavian, Curvature and Getic, separated by Dâmboviţa and Trotuş Valleys; Fig. 13.1), the Subcarpathian chain is formed out of a number of differently extended longitudinal morphostructural areas, individualized in terms of age, lithology and tectonics. The inner one consists of a relief generally conformable with the Miocene (and locally pre-Miocene) structure (with anticline hills and syncline depressions and hills underlain by monocline flanks, alongside depressions underlain by a monocline structure) and subsidiary, inverted relief (syncline hills and buttonhole depressions). The middle strip shows a relief also conformable with the structure (with only seldom relief inversions) and consists of hills and depressions carved in large, simple, faulted, and folded Pliocene formations. Towards the exterior, the discontinuous outer strip shows often a piedmont-like structure built on Upper Pliocene–Quaternary alluvial deposits. Nowadays, the Subcarpathian relief undergoes a phase of structural, lithological and neotectonic adaptation, as the modeling follows different patterns across catchments or tectonic compartments (Bălteanu 1983).

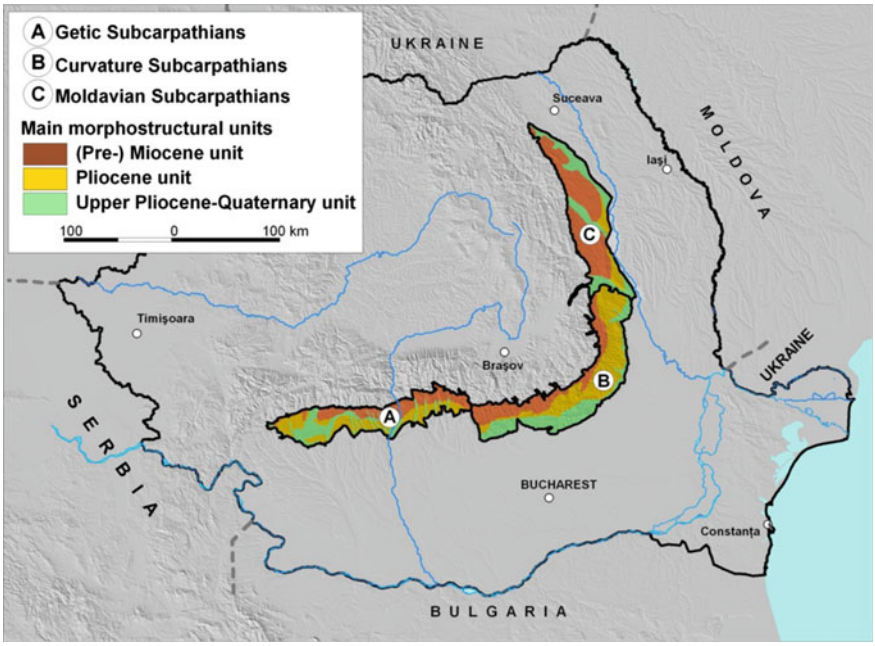

Fig. 13.1 The Subcarpathian chain with its subunits

Altitudes range between 200 m (Motru, Jiu, Dâmboviţa, Buzău, Trotuş, Moldova transversal valleys or transversal and diagonal depressions like Târgu–Jiu—Câmpu Mare, Tismana, Dumitreşti, etc.) and 1000–1200 m (the highest altitudes being registered at the border with the Carpathians, in peaks like Chiciura 1218 m, Măţău 1018 m, Odobeşti 996 m or Manta 967 m). Generally, precipitation show two peak periods, namely April–June and October–November. The mean yearly quantities of precipitation exceed 1000 mm in the Getic unit, decreasing around 600–700 mm in the Curvature–Moldavian area. Mediterranean retrogressive cyclones are responsible for the abundant precipitation that may be registered throughout the summer (e.g., 177.8 mm in July 1975, registered in 24 h) (Dragotă 2006).

The favorable conditions (accessible relief, sheltered topo-climate, rich salt deposits and potential for trading activities) allowed the appearance and the development (especially along the main river valleys) of human activities since the antiquity and Middle Ages. Presently, the average value of population density is around 90 inh./km^2, while along the main valleys (Bistriţa, Trotuş, Râmnicul Sărat, Buzău, Prahova, Olt, Jiu) and inside the large, extended depressions (Târgu–Jiu Câmpu Mare, Horezu, Tismana, Olăneşti–Călimăneşti, Curtea de Argeş, Pătârlagele, Dumitreşti) the value rises towards 150–200 in./km^2 (Romania: Space, Society, Environment 2006).

Landslides Typology and Spatial Patterns

Predisposing Factors

All throughout the hilly and depressionary unit of the Subcarpathians, the litho-structural conditions and the neotectonic features represent the most important predisposing factors in landslide occurrence.

The nature of the rocks (predominance of heterogeneous and low cohesive associations of clays, marls, sands, and schistose sandstones) is enhancing the shaping activity of external agents, overlapping the general internal active dynamics (Badea 2008). The structural features (intensely faulted and tightly folded strata, largely extended homocline sub-sectors) are imposing a wide landslide typology in terms of morphology, morphometry and morphodynamics. As a result of the Vrancea intracontinental collision area, the active neotectonic movements (general uplift and local subsidence, frequent earthquakes) are imprinting an increased denudation potential through fast valley deepening, especially to the middle sector (Curvature Subcarpathians).

The litho-structural conditions are generally imposing three main morphostructural subunits, differently extended throughout the Subcarpathian chain and characterized by different patterns of landslide types. Toward the interior, at the contact with the Carpathians it develops the subunit of strongly tectonised preMiocene–Miocene structures (consisting of asymmetrical and fractured folds, forming often monocline surfaces), while in the median sector it extends the larger subunit of Upper Miocene–Pliocene structures with simple, large, sometimes slightly faulted and almost symmetrical folds. The Subcarpathians are generally ending towards the exterior with a more-or-less continuous stripe of Upper Pliocene–Quaternary piedmont deposits, generally imposing a well-developed homocline relief. The most complex situation is in the Curvature sector of the Subcarpathians, between Buzău and Teleajen Valleys, where Paleogene flysch spurs penetrates the Mio–Pliocene unit, complicating the contact between the two major structural units.

The landslides show obvious adaptations to these litho-structural conditions, representing discontinuous temporal and spatial modeling processes which play an important role in changing the equilibrium on slope (Sandu and Micu 2008). Along the inner Mio–Pliocene unit, their spatial distribution, typology and magnitude within various smaller subunits (or small drainage basins) reflects the stage of relief evolution and also the land-use practices. The slopes developed on intensely folded structures are featuring mainly shallow and medium-seated translational earth and debris slides of a high frequency but low magnitude. The steep slopes carved in less cohesive clays, marls or loose schistose sandstones with clayey-marly intercalations are subjected to numerous earth flows, which extends throughout areas lacking a proper forest cover. Shallow to medium-seated slumps are characterizing mainly the lower sector of the slopes, caused by the intense river undercut during the frequent flash-flood episodes. The thick layers of less cohesive schistose sandstones that are

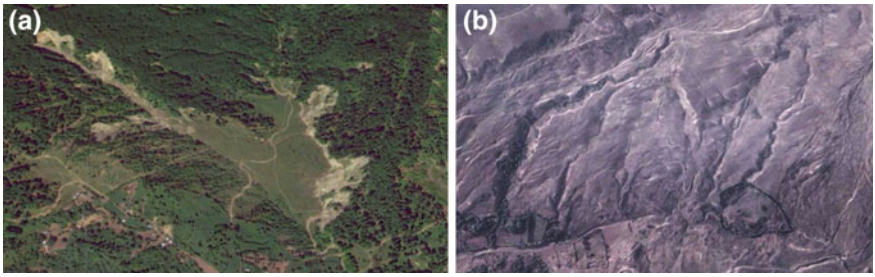

Fig. 13.2 Landslide typology adapted to structural conditioning (homocline, Râmna catchment; **a**) and combined gravitational and erosional processes causing complex landslides (Slănic catchment; **b**)

emerging toward the contact with the Carpathians are marked by deep-seated rock block slides that show a high magnitude but a rather low frequency. There are numerous slope sectors showing a polycyclic evolution and accumulation of landslide deposits, which make their individual inventory extremely difficult. Dormant (and even relict, in the highest hilly areas) landslides suffer many reactivations, especially due to river undercut or retrogressive scarp evolution. The numerous faults are also conditioning landslide occurrence. Even though the number of old faults largely prevails in front of the neotectonic ones, they are nevertheless acting as structural weaknesses enhanced by earthquakes. In the outer Pliocene–Quaternary units, the widely developed homocline relief imposes a different landslide typology, adapted in terms of morphology and morphodynamics (Fig. 13.2a). Along the north, north-west and west-facing cuesta escarpments one may individualize numerous shallow–to–deep-seated rotational rock and debris slides (frequently combined with earth flows into widespread complex landslide areas), while along the dip slope mainly shallow and medium-seated earth and debris translational slides and earth flows are developing. In the mean time, the presence (especially towards the external border) of homocline sectors built on thick packages of Quaternary sands and gravels containing clay lenticular intercalations increases the occurrence potential of erosional processes, which mix with landslides shaping complex formations. The increasingly-larger presence of deep gullies witnesses the wide extent of land degradation. These processes, particularly intense on the Sarmatian and Romanian sands and gravels, affect all the vegetation-free steep slopes (Fig. 13.2b).

Another factor that predisposes the overall Subcarpathian chain to a high proneness to landslides is the presence of salt and salt breccia formations (upper Oligocene and mid Miocene) which is leading to an increase of slope instability due to the chemical properties of the material. Processes like dissolution and piping are developing very fast within such formations, leading to the occurrence of a very dense network of rills which may transform into gullies (sometimes due to the successive collapse of piping holes). In the mean time, besides the fast infiltration, piping is also responsible of the fast drainage, resulting in complex landslide areas.

Preparatory and Triggering Factors

As a propitious region for human habitation, the Romanian Subcarpathians were marked by an intense anthropic pressure on the natural environment. Starting with salt exploitation during the Antiquity and passing through increasingly higher deforestation that lasted throughout the Middle Ages up to the modern times, human activities brought their share to landslide morphogenesis.

Started in the Middle Ages and enhanced throughout several social and economic frameworks (like, for example, the Adrianople Peace Treaty in 1829 that removed the Turkish Ottoman trading monopoly on wood, leading to intense deforestations in the Carpathians and Subcarpathians thus resulting in the loss of almost 4 million ha of forest until 1939; Giurescu 1975), deforestation played a major role in preparing the slopes for gravitational processes (as a fact worthy to be reminded, Iorgulescu mentions in 1891 the existence in the 3000 inhabitants' small town of Nehoiu, in the Curvature Carpathians, of 58 timber mills). Several changes in property (following the Second World War or following the fall of communism in 1989) either improved (large reforestations during 1960–1980 period) or deteriorated (1990 to present-day deforestations) the forest coverage.

Road cuts represent another important activity that leads to the occurrence of such processes. As a result of settlements' enlargement, the road network grown in density and numerous slopes already undergoing a dynamic equilibrium were turned into landslide-prepared areas. The roads which are following the main transversal valleys are up-to-date still threatened by medium and deep-seated landslides. Such an eloquent example is the National Road no. 10, along Buzău Valley (Curvature Carpathians), annually affected by landslide reactivations in the Unguriu–Ciuta–Măgura, Viperești, Pătârlagele–Valea Lupului sectors.

Trigger: Precipitation

As described in the worldwide literature (van Westen et al. 2006, 2008; van Asch 1997; Crozier 1986; Corominas and Moya 2008 among many others), precipitation represents the most important landslide-triggering factor and the Romanian Subcarpathians make no exception of that. Several studies (Bălteanu 1970, 1983; Bălteanu and Constantin 1998; Bălteanu and Micu 2009; Dragotă et al. 2008; Micu 2008; Şandric 2008; Chiţu 2010; Jurchescu 2012) emphasize the role of precipitation in landslide initiation or reactivation, providing either smaller scale (seasonally, annually) estimations or more in-depth assessments (triggering thresholds). A more detailed description of precipitation-induced landslides is provided by Micu et al. in Chap. 33, this volume.

The short term (24–72 h) and long-term (monthly, seasonal) precipitation distribution finds a good correlation in landslide occurrence in the Romanian Subcarpathians. Two general frameworks may be separated: shallow landslide and deep-seated landslide occurrence.

Shallow landslides usually appear during early spring–early summer, and their occurrence is generally subjected to early spring showers which may overlap snowmelt or spring–early summer showers. Rarely, the occurrence interval may be fastened by sudden temperature increases like it happened in February 18–21, 2010 (Micu et al. 2013), when a rapid warming caused by a Mediterranean frontal air mass moving northwards and crossing the Curvature Subcarpathians caused a rapid raise of maximum temperatures from −0.2 to 18.9 °C. The same weather conditions are enhancing earth flow pulsations, like it happened in the Buzău (Micu 2008; Bălteanu and Micu 2012), Vrancea (Prefac 2006, 2009) or Ialomiţa (Chiţu 2010) Subcarpathians. The spring and early summer months of the years 1970, 1974–1976, 1984, 1990, 1992, 1996, 2001, 2005, 2006, 2010, and 2015 were marked by such processes, usually developing shallow and medium-seated translational earth slides. Successive mappings after each rainy event allowed in some cases even some triggering thresholds (Bălteanu 1970; Bălteanu and Constantin 1998; Dragotă et al. 2008; Micu 2008; Micu et al. 2013; Şandric 2008): above 35 mm/24 h, 50 mm in 48 h, above 120 mm in 72 h or above 200 mm/month (twice the monthly average), all values showing less than 5 years recurrence intervals.

Deep-seated landslides are more complex in terms of trigger and quite often we may barely speak of only one. They occur either as reactivation of old, dormant early Holocene landslide deposits or first-time failures, and their complexity (in terms of both forms and processes) reflects the intense correlation between human actions on the environment (especially massive deforestations, reservoirs construction or road cuts), earthquakes and precipitation.

They might occur throughout almost the entire year (except for the winter) but the highest frequency is recorded at the end of spring–beginning of summer, when the groundwater accumulation reaches the maximum due to snowmelt and precipitation. The studies performed on some deep-seated landslides (Micu et al. 2013; Fig. 13.3) in the Curvature Subcarpathians outlined several precipitation quantities reliable to trigger deep-seated landslides, in the mean time emphasizing the importance, in this case, of antecedent wet intervals: >50 mm (1–3 days), with a return period of 100 years; 60–140 mm (10–30 days), with a return period of 10–35 years and above 250 mm (1–60 days), with a return period of 30 years.

Trigger: Earthquakes

In seismically active regions like Vrancea (Curvature Carpathians), earthquakes are known as having the potential to trigger numerous co- or post-seismic landslides (Keefer 1984, 2002; Jibson and Keefer 1993). As the most active intermediate (focal depth >50 km) earthquake province of Europe, Vrancea seismic region represents the main seismic energy source throughout Romania, with significant transboundary effects recorded as far as Ukraine, Russia or Bulgaria. During the last 300 years, the region featured 14 earthquakes with $M > 7$, among which seven events with magnitude above 7.5 and three between 7.7 and 7.9 (ROMPLUS catalog, INFP). Apart from the direct damages and possible landslide occurrences

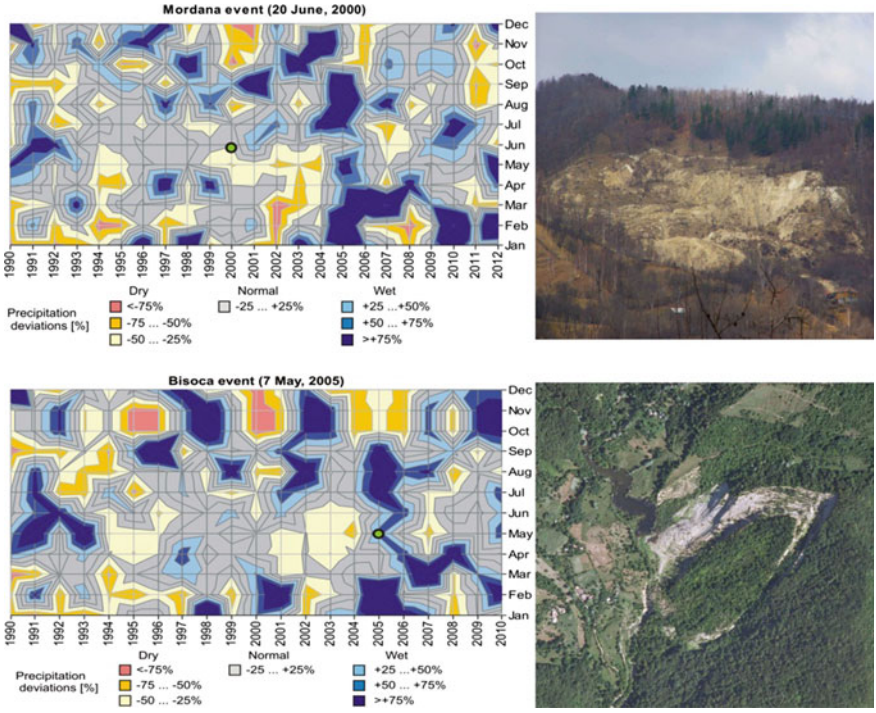

Fig. 13.3 The deep-seated landslides of Mordana and Bisoca brought into the pluvial preparing-triggering framework (after Micu et al. 2013)

(rock slumps, rock block slides, rockfalls, rock avalanches), the earthquakes are also responsible for causing numerous other associated geohazards among which ground fracturing, fault line reactivations, groundwater level disturbances, springs, or mud-volcanoes emergences.

Within a multi-temporal inventory, the separation of rainfall from earthquake-induced landslides (except witnessed cases; Bălteanu 1979a) is an extremely challenging task. There are some morphological aspects at a landslide that should be regarded as signs of a seismic trigger (Havenith and Bourdeau 2010): occurrence in the upper sector of steep slopes, in the immediate vicinity of ridges, anti-dip slope, convex morphography, no apparent initial connection with the river network, fault line (hanging wall) vicinity (Fig. 13.4a). These co-seismic landslide occurrence conditions are matching more the Curvature Carpathian environment, whilst the Subcarpathians look more prone to post-seismic failures. An outline of this assumption is given by Fig. 13.4b, showing the distribution of Newark displacement (ND, cm) values in a boundary sector of the Curvature (Buzău) Carpathians–Subcarpathians. Computed by H. Havenith for 1940 $M = 7.7$ earthquake, taking into account topographic amplification (factor of 1.5 for convex areas) and using the empirical Newmark displacement assessment law by Jibson et al. (1998), the

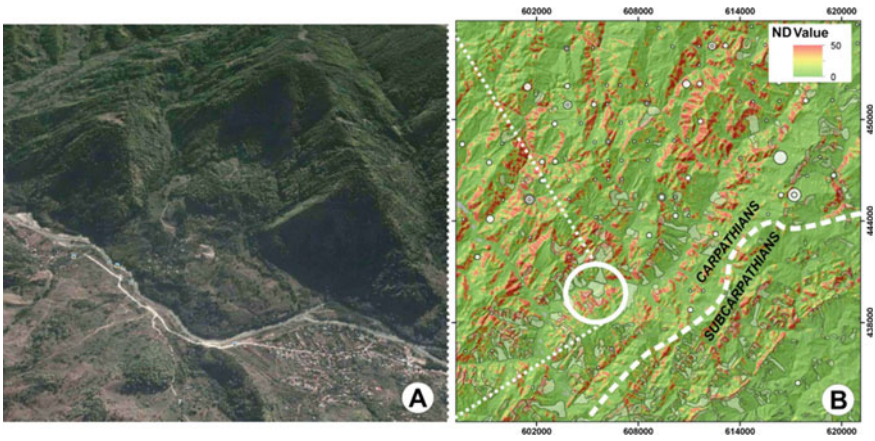

Fig. 13.4 The typical morphology of an earthquake-induced landslide (Balta landslide, Buzău Curvature Carpathians; **a)** brought in the context of a comparative Newmark displacement map in a sector of the Curvature Carpathians and Subcarpathians (**b**) (after Micu et al. 2015)

resulting map shows that significant displacement values (more extended in the Carpathians if compared with the Subcarpathians) may be obtained for the $M = 7.7$ earthquake scenario considering topographic amplification effects.

The more gentle topography (lower slope inclinations, shorter slopes, lower presence of narrow convex ridges) and the lithology (visco-plastic clays and marls) make the overall area of the Subcarpathians more prone to precipitation-induced landslides, at least as first-time failures (according to Keefer 2002, earthquakes are less susceptible to cause landslide deposit reactivations). However, the earthquakes of 1940 ($M = 7.7$, 150 km focal depth, 7–8 MSK intensity) and 1977 ($M = 7.4$, 94 km focal depth, 8–9 MSK intensity) have been confirmed to trigger rockfalls and rock slides as well as to prepare rock slides and earth flows (Bălteanu 1979b; Radu and Spânoche 1977; Mândrescu 1981, 1982).

In conclusion, intermediate-focus earthquakes registered in the Vrancea seismic area may trigger massive slope failures (rock slumps and block slides, rockfalls/avalanches) within a relatively smooth relief (only if we compare the Carpathians to the high mountain regions in Central Asia, where this correlation has been proven effective; Abdrakhmatov et al. 2003; Havenith et al. 2002, 2003), especially considering possible geologic (fault typology, lithology, structural traits, bedding orientation, thick regolith, dominant seismic wave propagation direction) and topographic (convex morphology, high inclinations in the slope's upper third, hanging walls, scarps far from valley bottoms) site-effects (Bourdeau and Havenith 2008). Smaller deep-focus earthquakes ($M < 7.7$) would only accidentally trigger (minor and individual) landslides (Micu et al. 2014a), while widespread slope instability phenomena could be induced by larger ($M > 7.7$, even $M >= 8$) earthquakes, especially under wet conditions (Micu et al. 2015).

Landslide Typology in the Subcarpathians

Slides

The most widespread landslide type is represented by shallow (to medium-seated) translational earth (less debris) slides (Fig. 13.5). They occur mainly during spring, as a result of snowmelt and early spring showers, showing a high frequency but low magnitude and affecting the soil layer and the uppermost part of the regolith. All throughout the Subcarpathians, these processes characterize the entire slope profile (both as first-time failures and subsequent reactivations), in the upper and middle sectors being caused predominantly by precipitation water infiltration, while the lower sector is showing an increased connectivity due to the lateral erosion and river undercut along both major rivers and tributaries. While the major movement mechanism is translational, the rotational slides appear also with a large share in sectors with active river undercut or in areas in which clayey or marly lens appear inside thick sand or gravel deposits (Romanian–Villafranchian Cândeşti gravels). The resulted material is often reaching valley bottom, increasing the alluvia budget, or it remains along the slope in a stage of dynamic equilibrium, being covered by grass or bushes during the summer and autumn. Generally, their morphometry reveals lengths below 100–150 m, widths extending to 20–50 m and scarps usually between 1 and 5 m. The main morphodynamic changes, in both depletion and accumulation (speeds up to 2–5 m/h), are recorded between March and June. Similar processes are described by Costin (1959), Brânduş and Cojocaru (1975), Brânduş (1979), Muică (1986), Surdeanu and Ichim (1991), Cioacă and Dinu (1995, 2000a), Dinu (1997, 1999), Muică and Bălteanu (1995), Ichim et al. (1998), Popescu (1998), Prefac (2001), Loghin (2002) or Rădoane et al. (2006).

The deep-seated slides (displacing more than 10 m thick deposits) are not that common as the shallow ones, but are still holding a large share. Characterizing slopes with 15° to 20° inclinations, they usually appear as dormant (and even relict) forms, affected by different-size reactivations, more developed at the slope-channel interface. Affecting both the regolith and the bedrock, they usually show complex

Fig. 13.5 Shallow translational earth slides in the Curvature (Buzău) Subcarpathians

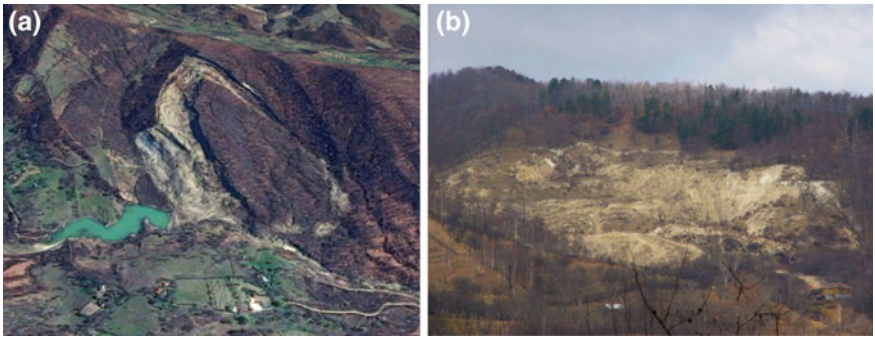

Fig. 13.6 Deep-seated rock block slide at Bisoca (**a**) and deep seated rock slump at Mordana (**b**) in the Curvature (Buzău) Subcarpathians

mechanism, in which translational displacements in form of rock block slides (especially inside homocline areas) may alternate with rock slumps or scattered compression and local compaction perimeters.

They are generally triggered by extreme weather events (early spring showers overlaying sudden early snowmelts) and such an example is Mordana landslide (Curvature Subcarpathians; Fig. 13.6), triggered during the spring of 2000.

Extended across a 9 ha surface, the landslide displaced a 20–25 m thick package of Miocene marls and loose marly sandstones with narrow salt breccia intercalations. It also shows a typical morphology: multiple movement mechanisms (rotational and translational), numerous associated processes (salt dissolution, erosion) and a rich micro-morphology across the scarp and body (ponds, cracks, rills, gullies, mounds). Sometimes, the polycyclic evolution leads in this landslide-prone area of the Subcarpathians to the formation of landslide valleys ('văi de alunecare' as they are known in the Romanian literature), i.e., small catchments completely covered with landslide deposits.

Similar processes are described by Grujinschi et al. (1975), Zamfirescu et al. (1975), Cioacă (1987), Dinu and Cioacă (1987, 1997), Grumăzescu (1973), Ielenicz (1998), Sandu (1999), Cioacă and Dinu (2000b), Ene et al. (2008, 2009) or Niculescu (2008).

Flows

Highly predominant in form of earth flows, these visco-plastic processes take a large share among the landslide types characterizing the Subcarpathians. Due to lithological (predominantly loose, fine granular and low cohesive deposits) constrains, debris flows are extremely rare while rock flows are missing completely, finding a proper morphogenetic environment in the high Carpathians. Since they usually affect rather small areas, detailed studies have been focused on the larger processes, like Chirleşti earth flow, situated at the contact between the Curvature Carpathians and Subcarpathians.

As described by Bălteanu and Micu (2012), previous studies conducted in the Curvature Carpathians and Subcarpathians of Romania (Bălteanu 1974, 1976, 1983; Ielenicz 1984; Vespremeanu-Stroe et al. 2006) outlined the important role played by flow-like processes in the shaping of steep slopes developed on Palaeogene flysch and Neogene molasse deposits.

Depending on factors like water quantity, available material in the source-areas, rocks petrographic properties or the morphology of pre-existent relief, the movement takes on a visco-plastic behavior, shaping the relief through an intense, pulsatory activity. The above-mentioned studies also showed the presence of three main types of earth flows: (i) with fixed source-areas (undergoing a dynamic equilibrium stage, with small retrogressive reactivations throughout the main scarp); (ii) partially reactivated earth flows (large reactivations during excess rain intervals); and (iii) active flows (showing quasi-continuous movements throughout all three main functional sectors). Previous detailed studies (Bălteanu 1974, 1976, 1983) showed that the earth flows are making the transition between slope modeling imposed by fluvial erosion and landslides, depending on the water quantity, the morphological configuration and the geotechnical properties of the sedimentary deposits.

The earth flows are characteristic for steep slopes with low forest coverage, built on deposits predominantly of marls, clays and sands. They usually measure less than 200–300 m in length (featuring one main source-areas and several other secondary ones), but may exceed 1.5 km (like Chirleşti and Rotarea earth flows; Fig. 13.7) and show a fast-moving displacement (25–30 to 100 m/h; Bălteanu 1983; Bălteanu and Micu 2012).

Falls

Conditioned mainly by the general lithological traits, falls and topples are not among the most widespread landslide types in the Subcarpathians, appearing only as very local manifestations.

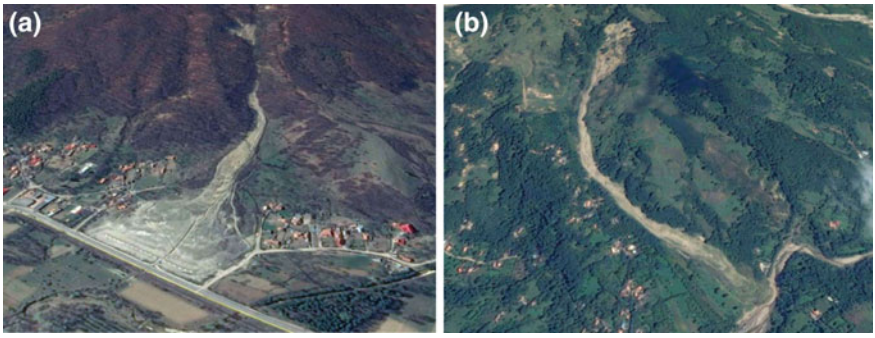

Fig. 13.7 Earth flows at Chirleşti (**a**) and Rotarea (**b**) in the Curvature (Buzău) Subcarpathians

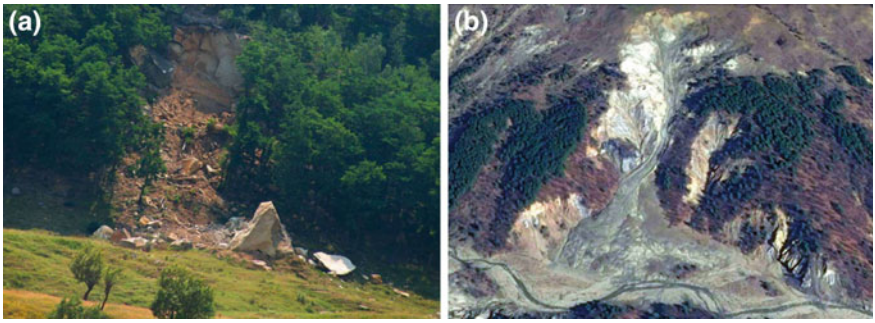

Fig. 13.8 Rockfall in sandstone outcrops at Chiojdu (**a**) and collapses induced by salt dissolution at Pleşi (**b**) in the Curvature (Buzău) Subcarpathians

Nevertheless, there are at least three frameworks which enhance falls occurrence: (i) the presence of Palaeogene flysch (Ivăneţu, Homorâciu, Văleni) spurs in the Curvature sector of the Subcarpathians (thicker packages of massive or schistose sandstones appear in the middle of looser, molasse deposits, leading to a differentiated denudation; Fig. 13.8a); (ii) the presence of salt breccia formations (falls are combined with dissolution sink holes and cave sealing collapses; Fig. 13.8b); (iii) the presence of thick upper Pliocene–Quaternary gravel deposits along the contact with the exterior units (differently extended terrace formations may be affected by such processes due to active river undercut).

Complex

Complex landslides occur across the Subcarpathians mainly as a result of inter-connected fluvial (gullying) and gravitational (sliding) processes. For example, previous studies (Bălteanu 1983) showed for the Buzău sector of the Curvature Subcarpathians that, if gully-affected slopes represent only 1.5 %, the slopes across which gully erosion, less present and though apparently playing a reduced role, is actually conditioning and enhancing slope mass movements, increase in proportion to 38 %. Sometimes, gully erosion represents the main cause of landslides (as described for example by Bălteanu and Micu in 2012 when discussing Chirleşti earth flow; the main responsibility within this case falls onto the lithology and subsequently, structure). As shown in Fig. 13.9, gullies that are incising the thick Romanian gravels are outlining the presence of numerous inner clay lenses responsible for the development of rotational landslides.

In the mean time, gully erosion and landslides may take place simultaneously and this is the case of salt breccia formations, where gullies and piping are associated with flows and slides. Also, the same framework is represented by the slopes developed on clays and sandstones, where gullies are alternating with mud or debris flows. Here, the shift from erosion to viscous and further on, plastic displacement

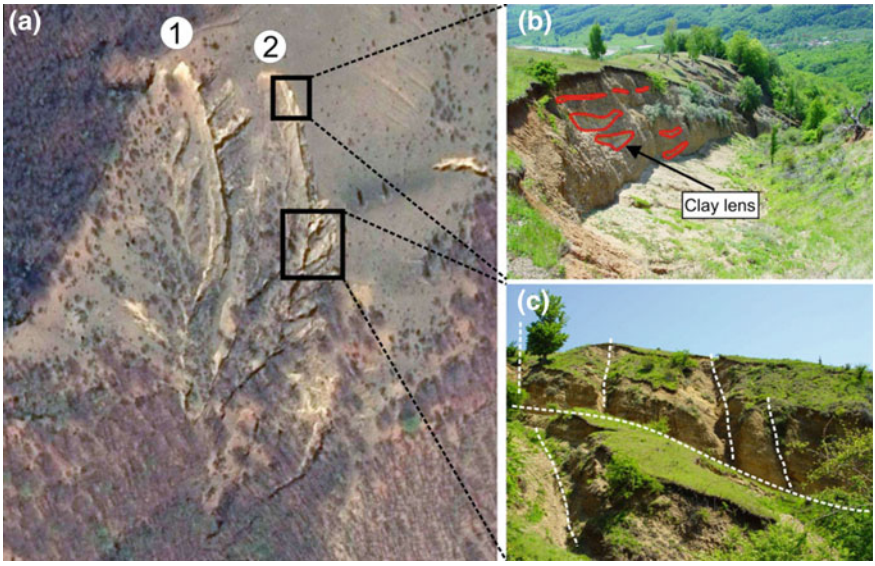

Fig. 13.9 The formation of complex landslides at Zeletin (Curvature Buzău Subcarpathians): younger (**a**, *1*) and older (**a**, *2*) gullies reveal clay lens (**b**) responsible for rotational slides (**c**)

depends especially on the topography and the potential content of moving material. A third general framework that leads to complex landslides occurrence is registered when gully erosion stands among the direct consequences of landslides. Across slopes developed on marls and clays, severely affected by dormant or active landslides, gullies are occurring and developing (usually between the landslide deposit and the bedrock) after the main landslide movement, reflecting the last one's major morphological and morphometrical traits.

Landslide Spatial Pattern in the Subcarpathians

In an attempt to offer a more accurate (still relative though) image on the spatial patterns of landslides in the Romanian Subcarpathians, an excerpt of the first national landslide inventory of Micu et al. (2014b) has been extracted (Fig. 13.10).

This point-based (uppermost part of the source area) regional inventory consists of 5624 landslides, having different sources (thus, different degrees of reliability): PhD. theses (Şandric 2008; Micu 2008; Chiţu 2010; Jurchescu 2012), research projects (FP 7 MC ITN CHANGES; Zumpano et al. 2014), literature review (more than 40 titles), County Inspectorates for Emergency Situations (Vrancea, Buzău, Prahova, Dâmboviţa, Argeş, Vâlcea, Gorj) reports. The typology of processes (slides, flows, or falls) has not been defined entirely due to the lack of harmonization among different sources and also to the different mapping densities

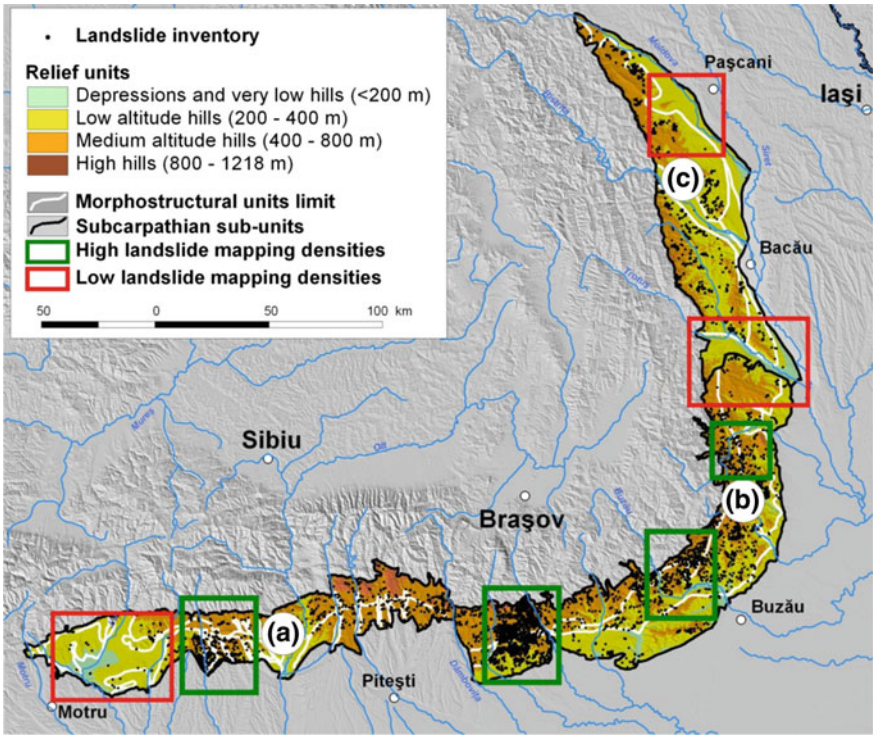

Fig. 13.10 Landslide inventory (after Micu et al. 2014b) in the Romanian Subcarpathians: potential statistic overestimation caused by high landslide mapping densities and potential underestimation induced by low landslide mapping densities

(introducing a certain but accepted bias in the statistical interpretation), therefore the inventory, at this scale, defines its composing items only as landslides.

Despite the above-mentioned drawbacks, this first partial inventory is considered as still giving an appropriate and representative image onto the landslide distribution due to several reasons: it contains the largest number of landslides taken into consideration so far for a regional assessment, covers the entire area rather homogeneously and it largely has an appropriate scientific background. Based on this inventory, a first-time regional quantitative relative correlation of landslides with different conditional factors (100 m SRTM DEM derivatives, Institute of Geology 1:200,000 map scale geological map, CORINE land cover 2006 map) has been established (Fig. 13.11).

The spatial pattern of landslides derived out of the correlation properly reflects the results of previous larger scale studies. Generally, in terms of main morphostructural units, the largest concentration of landslides (slides and flows) characterizes the widely extended inner Miocene (and pre-Miocene) sector, consisting of highly folded and faulted molasse deposits. The relief consists of high and very high hills (600–1200 m) separated by tectonic or fluvial depressions.

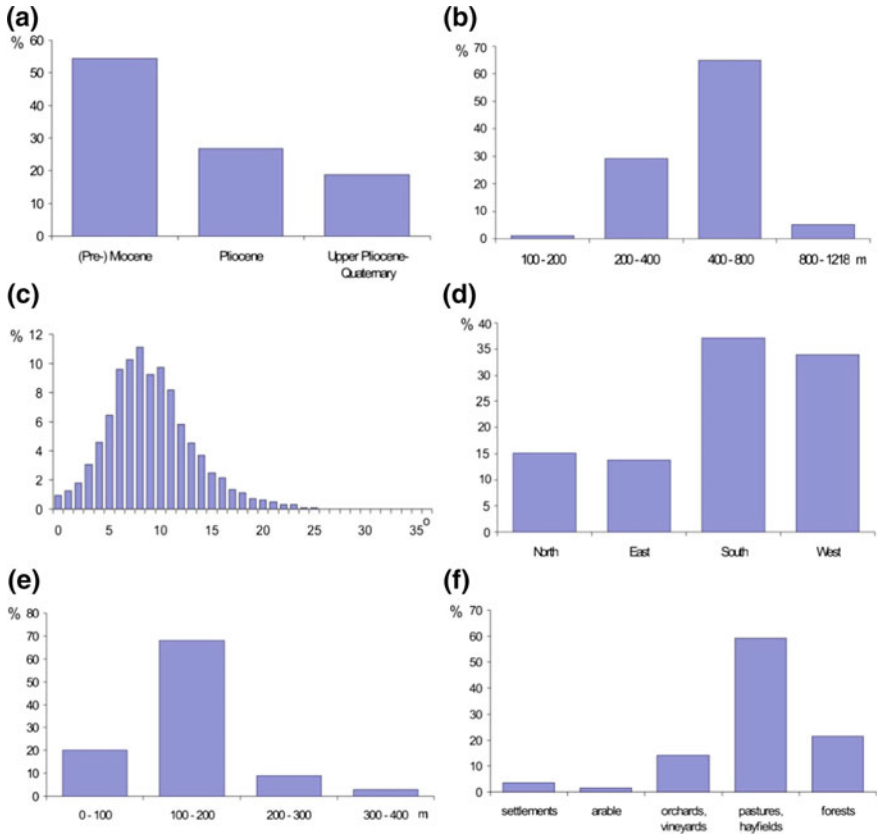

Fig. 13.11 The distribution of landslides (%) on: main morphostructural units (**a**), altitude (meters; **b**), slope inclinations (degrees; **c**), slope aspect (radians; **d**), internal relief (m/km^2; **e**), main land-use categories (**f**)

The upper Oligocene (Aquitanian) and Miocene (especially Helvetian–Sarmatian) formations mainly consists of schistose loose sandstones and clayey schists with salt, tuff and gypsum intercalations, all showing a high proneness towards shallow–to–deep-seated slides and shallow-medium-seated earth and debris flows. While the steeper slopes (above 15°) show a decreasing favorability to such processes (reflecting more cohesive rocks or being much better covered with forests), the largest majority of landslides are clustering inside the 5° to 15° interval. This inclination is characterizing the middle and lower sectors of the slopes, often covered by extended landslide deposits (sometimes developed in form of large glacis-like surfaces) reactivated by precipitation water infiltration of lateral fluvial erosion. The middle Pliocene sector, consisting of large and symmetrical conformal structures (especially Meotian–Pontian age) is characterized by medium and high altitude hills, developed on very loose sandstones, marls and clays with an increased sandy content. Together with the Upper Pliocene–Quaternary sector (the

least extended), it matches the proportion of landslides within the first unit. The large extensions of gentle (5° to 15°) slopes largely covered by pastures and hayfields, especially across slopes with a southern and western orientation (already containing a thicker regolith) form the most landslide-prone environments. Advancing more toward the exterior, the landslides are combining more and more with erosional processes, being almost replaced by the latter throughout the Quaternary deposits.

Conclusions

Alongside the Moldavian Plateau and parts of the Transylvanian Depression, the Subcarpathians are ranked among the most important landslide hotspots in Romania. Due to the intense tectonics (reflected in the strongly folded and faulted strata), favorable lithology (heterogeneous Neogene molasse), intensely fragmented relief, long-term human intervention on the environment, precipitation pattern and high seismicity, the Subcarpathians are featuring a wide range of landslides. Among the most widespread are shallow translational (subsidiary rotational) and medium-seated earth and debris slides, followed by earth flows and deep-seated rock block slides or rock slumps.

Obtaining a complete landslide inventory for the Subcarpathians is an extremely challenging task, due to numerous uncertainties in landslide mapping and interpretation. There are numerous cases of reactivations of smaller areas inside large, glacis-like landslide deposit accumulations, as well as inside individual dormant or relict landslides. Due to petrographic properties, the rheology changes quite often between viscous and plastic, thus inducing problems in the correct and final typological classification. Under these circumstances, the large majority of the slopes undergo (and whiteness) a long polycyclic landslide evolution that leads to difficult individualizations. In order to cope with these uncertainties, local and regional multi-temporal inventories are requested in order to allow top-down analyses or bottom-up generalizations.

Among the three sectors, the Curvature Subcarpathians show the largest morphogenetic complexity. More numerous and accurate correlations between different landslide types occurrences and combined seismo-tectonic and climatic factors are needed since this represents a vital step in supporting a regional multi-hazard risk assessment.

References

Abdrakhmatov K, Havenith HB, Delvaux D, Jongmans D, Trefois P (2003) Probabilistic PGA and arias intensity maps of Kyrgyzstan (Central Asia). J Seism 7:203–220

Badea L (2008) Unităţile de relief din România: dealurile pericarpatice. Edit. Ars Docendi (in Romanian)

Badea L, Bălteanu D (1977) Terasele Buzăului în sectorul subcarpatic. SCGGG-Geogr XIV, 2 (in Romanian)
Bălteanu D (1970) Morfodinamica porniturilor de teren pe Valea Apostului (Munţii Buzăului). SCGGG-Geogr XVII, 2 (in Romanian)
Bălteanu D (1974) The relationship between mudflows and torrential erosion in the modeling of Buzău Subcarpathians slopes. SCGGG-Geogr XXI, 1
Bălteanu D (1976) Two case studies of mudflows in the Buzău Subcarpathians. Geografiska Annaler 58 A, Stockholm
Bălteanu D (1979a) Effects of the March 4, 1977 earthquake on slope modeling in the surroundings of the Pătârlagele research station (Buzău Carpathians and Subcarpathians). Studia Geomorphologica Carpatho-Balcanica XIII:175–189
Bălteanu D (1979b) Slope modeling processes triggered by March 4, 1977 earthquake in Buzău Carpathians and Subcarpathians. SCGGG-Geogr XXVI
Bălteanu D (1983) Experimentul de teren în geomorfologie. Edit. Academiei Române, Bucureşti (in Romanian)
Bălteanu D, Constantin M (1998) Valley damming by landslides in the Buzău Subcarpathians. Analele Universităţii din Oradea, Ser. Geografie-Geomorfologie VIII–A:33–38
Bălteanu D, Micu M (2009) Landslide investigation: from morphodynamic mapping to hazard assessment. A case study in the Romanian Subcarpathians, Muscel catchment. In: Malet J-Ph, Remaitre A, Bogaard T (eds) Landslide processes. From geomorphologic mapping to dynamic modeling. CERG Editions, Strasbourg, p 235–241
Bălteanu D, Micu M (2012) Morphodynamics of the Chirleşti mudflow (Buzău Mountains). Rom J Geogr 56(2)
Bourdeau C, Havenith HB (2008) Site effects modelling applied to the slope affected by the Suusamyr earthquake (Kyrgyzstan, 1992). Eng Geol 97:126–145
Brânduş C (1979) Subcarpaţii Tazlăului. Studiu geomorphologic. Ed. Acad., Bucureşti (in Romanian)
Brânduş C, Cojocaru E (1975) Observaţii geomorfologice asupra alunecărilor de teren ce afectează unele şosele din judeţul Bacău. Lucr. Colocv. nat. de geomor. -aplic. si cartogr. geomorf., Iaşi (in Romanian)
Chiţu Z (2010) Predicţia spaţio-temporală a hazardului la alunecări de teren utilizând tehnici S.I.G. Studiu de caz arealul subcarpatic dintre Valea Prahovei şi Valea Ialomiţei. Manuscript PhD thesis, University of Bucharest (in Romanian)
Cioacă A (1987) Consideraţii asupra reliefului structural din Subcarpaţii Vrancei. SCGGG—Geogr XXIV, 1 (in Romanian)
Cioacă A, Dinu M (1995) Geomorphological hazards. Lignite mining and the newly-built relief in the North of Oltenia (Romania). Geografia Fisica e Dinamica Quaternaria, Comitato Glaciologico Italiano, Torino 18:3–6, 1996, Italia. IT ISSN 0391-9838
Cioacă A, Dinu M (2000a) Telega-Meliceşti landslide. In: Bălteanu D, Ielenicz M (eds) Geomorfological processes in the tectonic active areas. The Fifth Romanian-Italian Workshop on geomorphology, p 13–19 Bucureşti
Cioacă A, Dinu M (2000b) The impact of exploiting natural subsoil resurces on Subcarpathian relief (Romania). Geografia Fisica e Dinamica Quaternaria. Comitato Glaciologico Italiano, Torino, 22:3–14, Italia, IT ISSN 0391-9838
Corominas J, Moya J (2008) A review of assessing landslide frequency for hazard zoning purposes. Eng Geol 102:193–213
Costin E (1959) The study of degraded lands in Vrancea and their reforestations. INCEF, II, Edit. Agro—Silvică, Bucureşti (in Romanian)
Crozier MJ (1986) Climatic triggering of landslide episodes. In: Landslides: causes, consequences and environment, Croom Helm, p 169–192
Dinu M (1997) The relationship between landslides and slope evolution in the Vâlcea Subcarpathians. Geogr. Fis. e Dinam. Quat., Comit. Glaciol. Italiano, Torino 19
Dinu M (1999) The Subcarpathians between Topolog and Bistriţa Vâlcii: present-day slope modeling processes. Edit. Academiei Române

Dinu M, Cioacă A (1987) The morphotectonics of Vâlcea and Vrancea Subcarpathians. Lucr. Sem. Geogr. "D. Cantemir", 7, Univ. "Al. I Cuza", Iaşi (in Romanian)

Dinu M, Cioacă A (1997) Some geomorphological risk factors in the Curvature Carpathians and Subcarpathians. Geografia Fisica e Dinamica Quaternaria. Comitato Glaciologico Italiano, Torino, 19:233–238, Italia, IT ISSN 0391–9838

Dragotă CS (2006) Precipitaţiile excedentare din România. Edit. Academiei Române (in Romanian)

Dragotă C, Micu M, Micu D (2008) The relevance of pluvial regime for landslide genesis and evolution. Case study: Muscel basin (Buzău Subcarpathians, Romania). In: Present environment & sustainable development. 2. Edit. Universităţii "Al. I. Cuza", Iaşi, p 242–257

Ene M, Tîrlă L, Osaci-Costache G (2008) Collapses of Ocnele Mari, Vâlcea Subcarpathians, Romania. In: Ecology and environment rom Carpathians to Taurus Mountains. Proceeding of the 5th Turkey–Romania Geographical Academic Seminar, June 5–15, 2007, Antalya—Turkey

Ene M, Osaci-Costache G, Târlă L (2009) The Caving at Ocnele Mari in the Vâlcea Subcarpathians, Romania. Geografia Fisica e Dinamica Cuaternaria 32:67–72, Comitato Glaciologico Italiano–Torino

Giurescu C (1975) Istoria pădurilor româneşti din cele mai vechi timpuri până astăzi. Edit Ceres, Bucharest (in Romanian)

Grujinschi C, Zamfirescu Fl, Dinu C, Fodoreanu D, Georgescu O, Nicolau E, Hossu G, Imon A, Drumen C, Ulian A (1975) Alunecările de teren—factor activ în formarea şi menţinerea cuestelor din bazinul văii Râmna. Lucr. Colocv. Naţ. de geomorf. apl. şi cartogr. geomorf., Iaşi (in Romanian)

Grumăzescu H (1973) Subcarpaţii dintre Câlnău şi Şuşiţa. Studiu geomorfologic. Edit. Academiei R.S.R, Bucureşti (in Romanian)

Havenith HB, Bourdeau C (2010) Earthquake-induced landslide hazards in mountain regions: a review of case histories from Central Asia. Geol Belg 13(3):137–152

Havenith HB, Jongmans D, Faccioli E, Abdrakhmatov K, Bard PY (2002) Site effects analysis around the seismically induced Ananevo rockslide, Kyrgyzstan. Bull Seism Soc Am 92:3190–3209

Havenith HB, Strom A, Jongmans D, Abdrakhmatov K, Delvaux D, Trefois P (2003) Seismic triggering of landslides. Part A: field evidence from the Northern Tien Shan. Nat Hazard Earth Syst Sci 3:135–149

Ichim I, Rădoane M, Rădoane N, Grasu C, Miclăuş C (1998) Dinamica sedimentelor. Aplicaţie la râul Putna. Ed. Tehnică, Bucureşti (in Romanian)

Ielenicz M (1984) Munţii Ciucaş-Buzău. Studiu geomorfologic. Edit. Academiei RSR, Bucureşti (in Romanian)

Ielenicz M (1998) Sisteme de modelare a versanţilor în Subcarpaţii de Curbură şi impactul manifestării lor asupra peisajului. Com geogr II, Bucureşti (in Romanian)

Iorgulescu B (1891) Dicţionarul geografic, statistic, economic şi istoric al jud. Buzău. Stabiliment grafic I.V.Socec (in Romanian)

Jibson RW, Keefer DK (1993) Analysis of the seismic origin of landslides: examples from the New Madrid seismic zone. Geol Soc Am Bull 105:521–536

Jibson RW, Harp EL, Michael JA (1998) A method for producing digital probabilistic seismic landslide hazard maps: an example from the Los Angeles, California, area. US Geological Survey Open-File Report 98–113

Jurchescu M (2012) Bazinul morfohidrografic al Olteţului. Studiu de geomorfologie aplicată. Manuscript PhD thesis, University of Bucharest (in Romanian)

Keefer DK (1984) Landslides caused by earthquakes. Geol Soc Am Bull 95:406–421

Keefer DK (2002) Investigating landslides caused by earthquakes—a historical review. Surv Geophys 23:473–510

Loghin V (2002) Modelarea actuală a reliefului şi degradarea terenurilor în bazinul Ialomiţei. Edit. Cetatea de Scaun, Târgovişte (in Romanian)

Mândrescu N (1981) The Romanian earthquake of March 4, 1977: aspects of soil behavior. Rev Roum Geophys 25, Edit. Acad Rom

Mândrescu N (1982) The Romanian earthquake of March 4, 1977: damage distribution. Rev Roum Geophys 26, Edit. Acad Rom. Rev Roum Geophys 27, Edit. Acad. Rom

Micu M (2008) Evaluarea hazardului legat de alunecări de teren în Subcarpaţii dintre Buzău şi Teleajen. Manuscript PhD thesis, Institute of Geography, Bucharest (in Romanian)

Micu M, Bălteanu D, Micu D, Zarea R, Ruţă R (2013) 2010-landslides in the Romanian Curvature Carpathians. In: Loczy D (ed) Extreme weather and geomorphology. Springer, p 251–265. doi:10.1007/978-94-007-6301-2

Micu M, Jurchescu M, Micu D, Zarea R, Zumpano V, Bălteanu D (2014a) A morphogenetic insight into a multi-hazard analysis: Bâsca Mare landslide dam. Landslides. doi:10.1007/s10346-014-0519-4

Micu M, Malet JP, Bălteanu D, Mărgărint C, Niculiţă M, Jurchescu M, Chiţu Z, Şandric I, Simota C, Mathieu A (2014b) Typologically-differentiated landslide susceptibility assessment for Romania. Geophysical Research Abstracts vol 16. EGU2014, p 13315

Micu M, Bălteanu D, Ionescu C, Havenith HB, Radulian M, van Westen C, Damen M, Jurchescu M (2015) A preliminary regional assessment of earthquake-induced landslide susceptibility for Vrancea Seismic Region. In: Geophysical Research Abstracts, vol 17. EGU2015, p 12524

Muică N (1986) Observaţii privind degradarea terenurilor în împrejurimile Pătârlagelor. In: Cercetări geografice asupra mediului înconjurător în judeţul Buzău, Inst. Geogr. Bucureşti (in Romania)

Muică C, Bălteanu D (1995) Relations between landslide dynamics and plant cover in the Buzău Subcarpathians. RRGGG-Géogr 39

Niculescu G (2008) Subcarpaţii dintre Prahova şi Buzău. Studiu geomorfologic sintetic. Edit. Academiei Române (in Romanian)

Popescu N (1998) Modelarea versanţilor prin alunecări de teren într-o regiune Subcarpatică cu strucura monoclinalăV. Câlnăului în sectorul Modreni—Racoviţeni, Vol. II. Comunicări de geografie, Bucureşti (in Romanian)

Prefac Z (2001) Procese geomorfologice actual în bazinul Strâmbei, vol VI. Comunicări de Geografie, Editura Universităţii din Bucureşti (in Romanian)

Prefac Z (2006) Raportul dintre degradarea şi utilizarea terenurilor în bazinul Strâmbei, vol V. Forum Geografic, Edit. Universitaria, Craiova (in Romanian)

Prefac Z (2009) Dinamica versanţilor din bazinul hidrografic al Râmnei. Phd Thesis, University of Bucharest (in Romanian)

Rădoane N, Rădoane M, Olaru P, Dumitriu D (2006) Efectele geomorfologice ale inundaţiilor din 28–29 iulie 2004 în bazine hidrografice mici din valea Trotuşului. Geografia in contextul dezvoltarii durabile, Cluj Napoca (in Romanian)

Radu C, Spânoche E (1977) On geological phenomena associated with the 10 November 1940 earthquake. Rev Roum Geophys 21, Edit. Acad. Rom

Romania: Space, Society, Environment (2006) Edit Academiei Române

Şandric I (2008) Sistem informaţional geografic temporal pentru analiza hazardelor naturale. O abordare bayesiană cu propagare a erorilor. Manuscript PhD thesis, University of Bucharest (in Romanian)

Sandu M (1999) Alunecarea de la Lacul lui Baban. Stadiu de evoluţie, Revista Geografică, t. V, Bucureşti (in Romanian)

Sandu M, Micu M (2008) Morphostructure and Morphology in the Bend Carpathians and Subcarpathians. Trotuş—Teleajen Sector. Rev Roum Geogr, Tomes 49–52, 2005–2008

Surdeanu V, Ichim I (1991) Alunecări de teren din bazinele subcarpatice ale râurilor Râmnicu Sărat şi Râmna ca surse de aluviuni. Terra, anul XXIII (XLIII)(2) (in Romanian)

Van Asch TWJ (1997) The temporal activity of landslides and its climatological signals. In: Matthews JA, Brunsden D, Frenzel B, Gläser B, Weiß MM (eds) Rapid mass movement as a source of climatic evidence for the Holocene. Palaeoclimate Research. Gustav Fischer. Stuttgart 19:7–16

Van Westen C, Van Asch TJ, Soeters R (2006) Landslide hazard and risk zonation—why is it still so difficult? Bull Eng Geol Environ 65:167–184

Van Westen CJ, Castellanos E, Kuriakose SL (2008) Spatial data for landslide susceptibility, hazard, and vulnerability assessement: an overview. Eng Geol 102:112–131

Vespremeanu-Stroe A, Micu M, Cruceru N (2006) The 3D analysis of Valea Viei mudflow morphodynamics, Buzău Subcarpathians. Revista de Geomorfologie 8:95–109

Zamfirescu F, Grujinschi C, Dinu C, Fodoreanu D, Georgescu O, Nicolau E, Hossu G, Simon A, Drumen C, Ulian A (1975) Procesele de sufoziune-factor principal în declanşarea alunecărilor de mare amploare din bazinul văii Râmna, Lucr. Colocv. Naţ. de geomorf. apl. şi cartogr. geomorf., Iaşi (in Romanian)

Zugrăvescu D, Polonic G, Horomnea M, Dragomir V (1998) Recent vertical movements on the Romanian territory, major tectonic compartments and their relative dynamics, Rev Roum Géophys, seria Geofizică 42

Zumpano V, Hussin H, Reichenbach P, Bălteanu D, Micu M, Sterlacchini S (2014) A landslide susceptibility analysis for Buzău County, Romania. Revue Roumaine de Geographie/Rom J Geogr 58(1)

Chapter 14
Debris Flows in Călimani Mountains and Lotrului Valley

Olimpiu Traian Pop, Viorel Ilinca, Titu Anghel, Ionela-Georgiana Gavrilă and Răzvan Popescu

Abstract Debris flows (DF) are one of the dominant geomorphic processes and play an important role in the present-day morphodynamics of the steep slopes and stream channels in the Romanian Carpathians. A large number of studies describe the characteristics, dynamics, and site occurrence of various types of active present-day mass movement processes affecting the steep slopes in Romania, but only in the last two decades few of them were addressed particularly to DF dynamics and related landforms. Geomorphic and sedimentologic criteria used worldwide to recognize DF activity and related landforms are presented here to correct identification of their presence and to assess the behavior of this specific process in several Carpathian massifs. Several causative factors (geological, geomorphological, topographic, climatic, phytogeographic, and anthropic factors) are responsible for the occurrence of DFs mainly in the high mountain areas of Romanian Carpathians, but also at lower altitudes. Both natural and human-induced DFs severely affect forest vegetation giving therefore the possibility to reconstruct past geomorphic activity by using dendrogeomorphic methods. The case studies conducted until present day in different areas of the Romanian Carpathians and based on the dendrogeomorphic approach proved to be reliable solution to reconstruct spatiotemporal frequency of DFs. In the present-day context of increasing human pressure on DF affected areas in Romanian Carpathians, more fundamental

O.T. Pop (✉) · T. Anghel · I.-G. Gavrilă
Faculty of Geography, Babeş-Bolyai University, Clinicilor 7-5, 400006 Cluj-Napoca, Cluj, Romania
e-mail: olimpiu_p@yahoo.com

V. Ilinca
Geological Institute of Romania, Caransebeş 1, Bucharest, Sector 5, Romania
e-mail: ilincaviorel@yahoo.com

R. Popescu
University of Bucharest Research Institute, M. Kogălniceanu 36-46, 050107 Bucharest, Sector 5, Romania
e-mail: rzv_popescu@yahoo.com

M. Rădoane and A. Vespremeanu-Stroe (eds.), *Landform Dynamics and Evolution in Romania*, Springer Geography,
DOI 10.1007/978-3-319-32589-7_14

and applied studies are needed in order to gather a better understanding of the characteristics of DF processes and their mechanisms, leading to a more accurate geomorphic hazard assessment.

Keywords Debris flow · Spatial distribution · Dendrogeomorphology · Calimani and Lotrului Mountains

Introduction

Many mountain areas are prone to debris flow (DF) activity, which represent a real threat for local communities, causing frequent losses of human lives and damages to properties or infrastructure (houses, roads, bridges, etc.). Indirect damages are produced by damming the mountain streams or by providing a rapid fill of river beds with sediments transported from upslope areas (Montgomery et al. 2003). The term debris flow (DF) refers here to a rapid mass movement on the steep slopes, or along the preexisting channels, of a mixture having in composition a variable proportion of solid materials (debris, soil, organic fragments as wood or barks, etc.), air and a small percent of water. Debris material consists in a mixture of silt, sand, gravel, cobbles and boulders with air, water and small traces of clay; a variable proportion of organic material (logs, stumps, and mulch) can also be incorporated in the mixture during the flow. The debris is commonly unsorted and has a low plasticity, being produced by mass-wasting processes (colluvium), weathering (residual clasts and soil), glacier transport (till), volcanism (pyroclastic deposits), or human activity (e.g., mine spoil) (Hungr et al. 2001; Hungr 2005). The initiation and dynamic characteristics of DF led to consider it as a particular mass movement process intermediate between hyperconcentrated flows and landslides (Pierson and Costa 1987; Coussot and Meunier 1996). A revision of discriminating criteria (sediment concentration, rheological behavior, grain size distribution, and grain density in the flow, etc.) used to classify sediment–water flow types on hillslopes was thoroughly described by Innes (1983), Costa (1988) and Pierson (2005), as well as in a recent paper by Germain and Ouellet (2013).

For a given torrent, during different rainfall events, a variety of physical processes and dynamic characteristics may occur (Arattano and Franzi 2004). The variation of the flow processes occurring especially in the channels of the small mountainous watersheds are strongly controlled by the character and content of materials involved. Flow processes can be identified in the field based on geomorphic and sedimentologic evidence. A sediment concentration of 47–77 % by volume and of 70–90 % by weight into the sediment–water mixture characterizes the mechanism of sediment transport by DF (Costa 1988). The clay-size sediment content influences the type of DF, which can be cohesive (higher content of clay) or non-cohesive (Scott et al. 1995). It is now largely accepted that a clear distinction can be done between DFs that occur on slope surfaces and those following the preexisting channels, such as the torrent or stream beds channels.

The geomorphic and sedimentologic evidences described by Costa (1984, 1988) are commonly used in order to identify areas dominated by DF activity and to differentiate them from other hydrogeomorphic activity, especially floods and debris floods (hyperconcentrated flows). In terms of hazard and risk assessment, a better understanding of flow processes is needed, in order to establish an accurate hazard zonation and to adopt a proper design of mitigation measures. It is important because appropriate mitigation strategies applied for one process may not be efficient for another (Germain and Ouellet 2013).

The great variety of conditions and factors that support DF activity produce a wide range of debris volume involved in the flow. Debris volume influences the distance and the covered surfaces in the runout area. Therefore, DF size can vary considerably from one region to other. Moreover, DFs of different size classes and having different return periods may affect the same basin. Based on the total volume of material accumulated at the surface of the debris cone, the peak discharge and the area inundated by debris, a 10-fold classification of DF size was proposed by Jakob (2005). Class 1 refers to DF having 10–102 m^3 volume that occurs in small channels or gullies. For the class 10, the author indicates a DF total volume >109 m^3, these events being considered to have the most destructive effects. The above-mentioned classification finds its applicability for hazard assessment when designing different active and/or passive DF mitigation measures within debris basins.

DF Activity and Resulting Landforms

Geomorphic Evidences Used to Recognize DF Deposits

Recently Wilford et al. (2004) proved that elementary watershed morphometric measurements can be used to differentiate hydrogeomorphic processes that affect alluvial and colluvial fans. Their model is based on a combination of watershed length with the Melton ratio (watershed relief divided by the square root of watershed) area and can be successfully used to predict DF and debris-flood-prone watersheds.

The distinctive geomorphic features resulted from DF activity include erosional and depositional forms. In the source area, the flow commonly initiates on steep slope areas ranging between 25° and 45° (Hungr 2005), where bare rock or poorly consolidated debris surfaces exist. It creates here an erosional scar that extends downslope in the transport zone with a U-shaped, rectangular, or wide trapezoidal channel in cross section (Costa 1984; Corominas et al. 1996). The channel is flanked by marginal *levées* resulted mainly by deposition of poorly sorted and large size clasts. In the depositional zone, which commonly corresponds to the lower slope sector and a flatter area, debris flow reduces its momentum and then stops its movement. It therefore spreads out and forms a terminal lobate deposit on the

surface of a debris fan, reshaping its previous morphology. Terminal deposit extends on the debris cone from its apex and has a similar unsorted structure as the *levées* deposits.

Sedimentologic Evidence Used to Recognize DF Deposits

DF deposits consist of unsorted materials distributed in a wide variety of size particle classes, ranging from clays to large boulders of few meters in diameter. A clear distinction exists between DF and hyperconcentrated flow processes and the associated deposits, as the former are single-phase flows, meanwhile the latter ones are two-phase flows (Coussot and Meunier 1996).

In contrast to the structural features of deposits resulted from water floods and hyperconcentrated flow that show clear stratification, cross-bedding and imbrication, those resulted by DF processes have a non-stratified structure with no imbrication and a very poor sorting of materials having an extreme range of particle sizes from clays to boulders. Large clasts are supported by a DF matrix composed by clay (<5 % after Corominas et al. 1996) to sand particle size, as well as organic materials, such as wood and bark fragments. The long-axis (*A*-axis) orientation of clasts is dominantly parallel to the flow (Wilford et al. 2004).

DF Assessment in Romanian Carpathians

A large number of publications describe the characteristics, dynamics, and site of various types of active present-day mass movement processes affecting the steep slopes in Romania, but few addressed DF dynamics and related landforms. Until a few years ago, only mudflows and earthflows were studied among this particular kind of landslides, called flows. Most studies concerning the mudflows were carried out in the Carpathian and Subcarpathian Bend (Badea and Posea 1953; Tufescu 1970; Bălteanu 1974, 1976; Vespremeanu-Stroe et al. 2006; Micu and Bălteanu 2009; Bălteanu and Micu 2012). An example of study describing an earth flow-like event in the Eastern Carpathians was presented by Surdeanu et al. (1989).

The DF process and landforms started to be conceptualized in Romania only recently, for less than a decade. Up to that moment, both DFs and hyperconcentrated flows were treated together as torrential processes, without considering the distinction between them. This ambiguous classification influences and creates problems also in the present-day Romanian geomorphological literature. For example, authorities use the term *viitură* (flash flood) for all flow-type processes that occur along slopes, without taking into account the distinctions which could be made between DFs and hyperconcentrated flows (Ilinca 2014). In the Eastern Carpathians, hydrogeomorphic processes, including DFs and debris floods that occur in small drainage basins and their effects on sediment transfer were also

described as flash floods or floods (Rădoane et al. 2005). In Romanian geomorphologic literature a first reference to DF processes as a particular flow process was made by Rădoane et al. (2001). The authors explained the Varnes classification of mass movements giving short explanation of the DF processes main characteristics.

Despite the fact that, in the Romanian Carpathians, DF is one of the most widespread types of mass movement that affects the steep slopes and plays an important role in the present-day morphodynamics on talus slope formation, so far there is a lack of studies focused on this process and the associated morphology. Recently, a small number of case studies addressing this topic were conducted in the mountain areas, e.g., in Călimani Mountains (Pop 2012; Pop et al. 2009, 2010, 2013, 2014; Surdeanu et al. 2011), Lotrului Valley (Ilinca 2010, 2014) and Retezat Mountains (Văidean et al. 2014). Field observations and the analysis of existing ortophotoplans point out that numerous mountain areas are affected by present-day DF activity but still unstudied (e.g., Bucegi, Piatra Craiului, Făgăraş, Iezer–Păpuşa, Parâng, Retezat, Godeanu, and Ţarcu massifs in the Southern Carpathians, Rodna, and Ţibleş Mountains in the Eastern Carpathians).

Inventory of DF Affected Areas in Călimani Mountains and Lotrului Valley

In the Romanian Carpathians, an inventory of DF areas is still expected to be realized. At a regional scale, studies focused on mapping DF affected areas were conducted only in Călimani Mountains and Lotrului Valley (Fig. 14.1) (Ilinca 2010; Pop 2012; Pop et al. 2010). In Călimani Mountains (Fig. 14.2), the feasibility of the systematic inventory of DF affected areas was tested firstly in its central part (Pop et al. 2010) and then extended to entire surface of the massif (Pop 2012). The affected areas were first mapped on existing orthophotoplans (mission 2003–2005) and the location of DF tracks was then checked in the field. In this way, a total number of 350 DF tracks were identified and their spatial distribution represented on the map (Fig. 14.3). A simple analysis of DF distribution in Călimani Mountains allows us to conclude that DFs initiate mainly on steep slope sectors above the treeline belt and affect the forest belt downslope. Figure 14.4 gives an example of a DF track monitored during 5 years (between 2007 and 2012). Between 2007 and 2012, the 9 m incision depth created by DF channel erosion within the slope deposits (Fig. 14.5) suggests that under present-day morphological conditions, changes occur rapidly. Practically, after each event DFs scours the channel by reworking the debris deposit of periglacial origins. Nowadays, the hiking trail that crosses the DF track became impracticable due to its continuous enlargement and channel deepening.

A widespread DF activity occurring at lower altitudes has also been inventoried on forested steep slopes of Lotrului valley (Ilinca 2010). These findings prove that the occurrence of DFs is not limited in the high mountain areas of Romanian Carpathians, but similar processes may produce wherever the triggering factors combine.

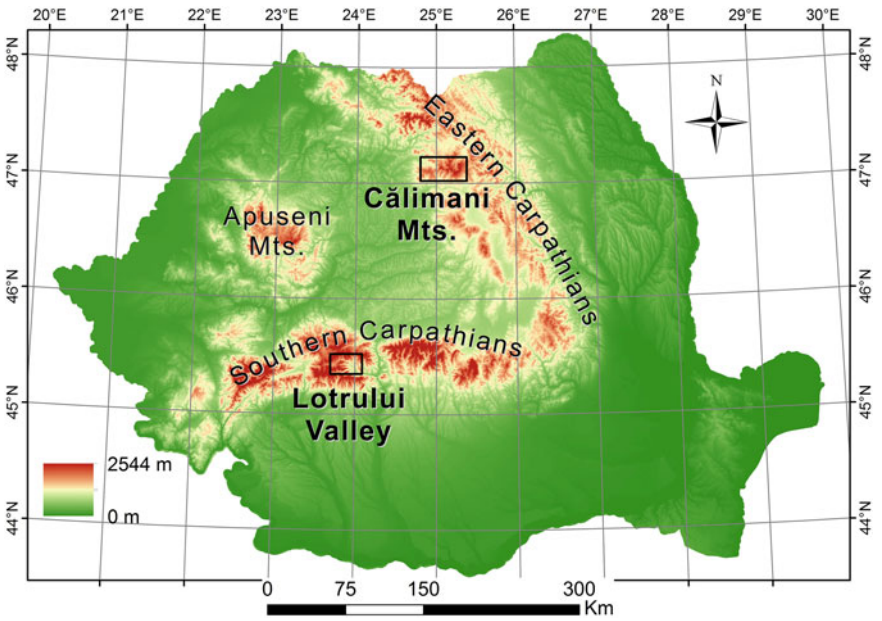

Fig. 14.1 The study areas and their location in Romania

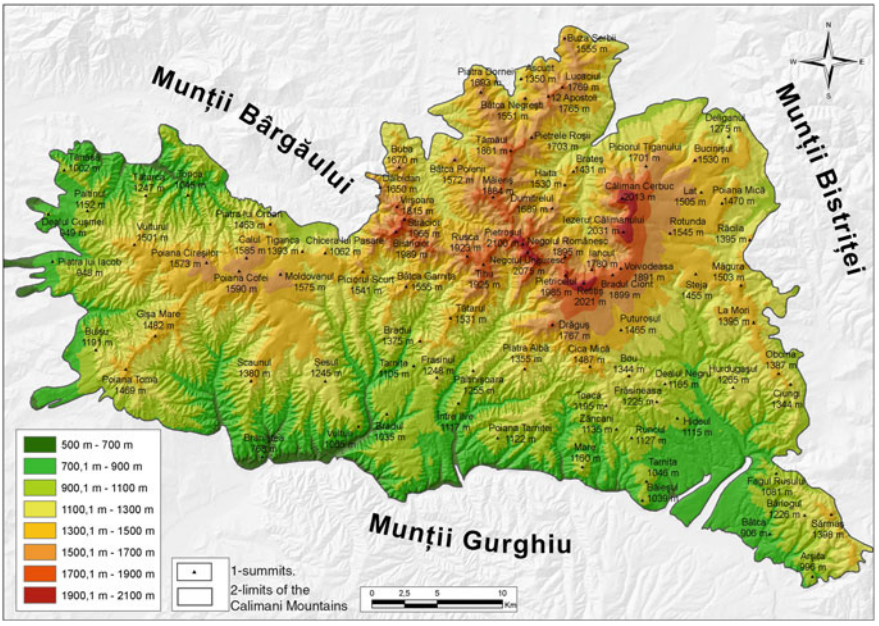

Fig. 14.2 Location map of Călimani Mountains

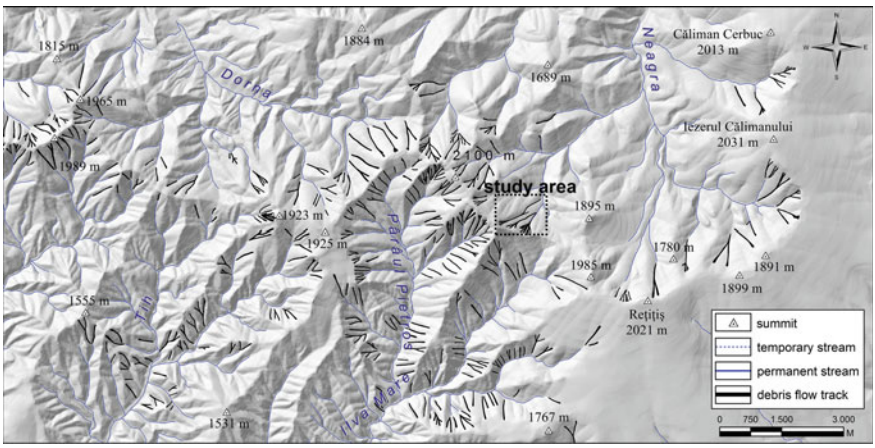

Fig. 14.3 Spatial distribution of DF in Călimani Mountains (data from Pop 2012)

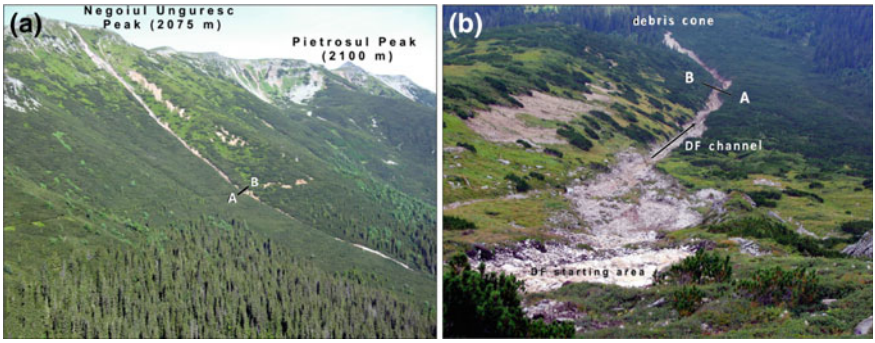

Fig. 14.4 **a** An example of DF path monitored on the steep slopes of Călimani Mountains. **b** The starting area is located roughly at the contact between subalpine grassland belt and shrub belt (the photos are taken in summer 2007 by O. Pop)

Causative Factors Explaining Spatial Distribution and DF Occurrence

Geological, Geomorphological and Topographic Factors

In the Romanian Carpathians, most of the DF source areas are located on slopes below the zone of bedrock, as described by Becht and Rieger (1997) in the Eastern Alps. Many debris flow sites located above 2000–2200 m altitude have the source area on slopes dominated by bedrock. In this case only small debris can occur,

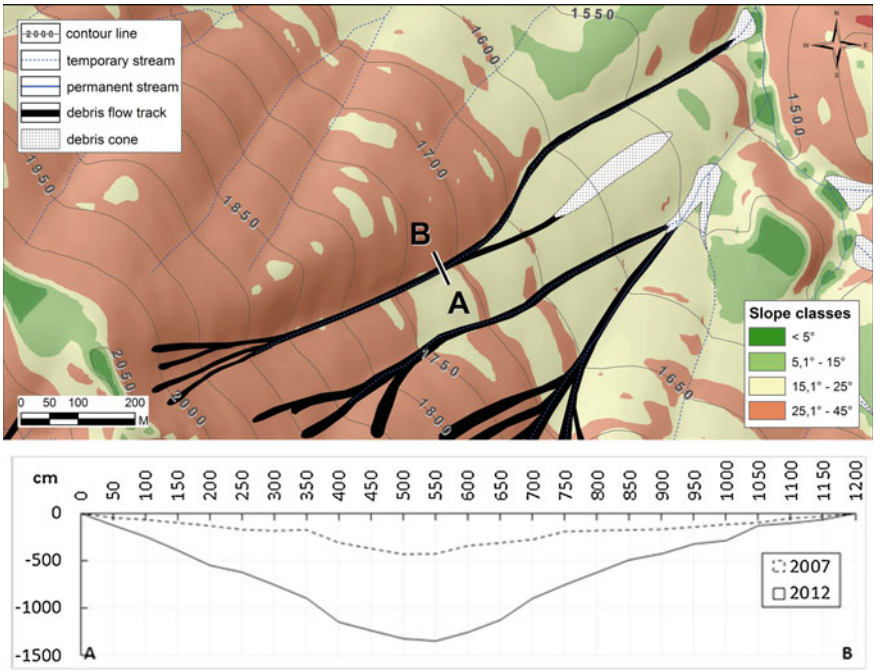

Fig. 14.5 Surveys of a middle sector of DF channel cross section—an example taken from Călimani volcanic Massif, Eastern Carpathians: dashed line indicates cross section channel measurements in 2007, meanwhile **b** indicates the measurements repeated in 2012 in the same cross section channel sector (Pop 2012)

whereas the material consists in rock fragments and boulders and no or small quantity of clay.

DF deposits include materials mainly reworked from colluvium. Large blocks are derived from the rockfall slope deposits or from the cirque walls. In some cases, large blocks are scoured from the channel bedrock. Materials originating from active, inactive, relict rock glaciers, or moraines are also entrained by DF (Fig. 14.6). A particular origin of large blocks is in the case of those derived from the spoil heaps located in the mining areas, e.g., in the Călimani Mountains.

In forested areas, the flow mixture contains high amounts of organic material, including timber (tree trunks, branches, or roots). This is frequent in some areas with active logging, in which case woody debris can form, known also as debris torrents by the Canadian authors (Slaymaker 1988; Van Dine 1985). In the case of DFs occurring at low altitudes in the Carpathians, and implicitly in the forest area, the thickness of surficial deposits increases significantly. This increases the amount of available material, which is commonly entrained by landslides and followed by DFs along channels (Fig. 14.7). It is the case of some sites affected by DFs from lower Lotru hydrographic basin (Ilinca 2010). Hydrogeological characteristics of

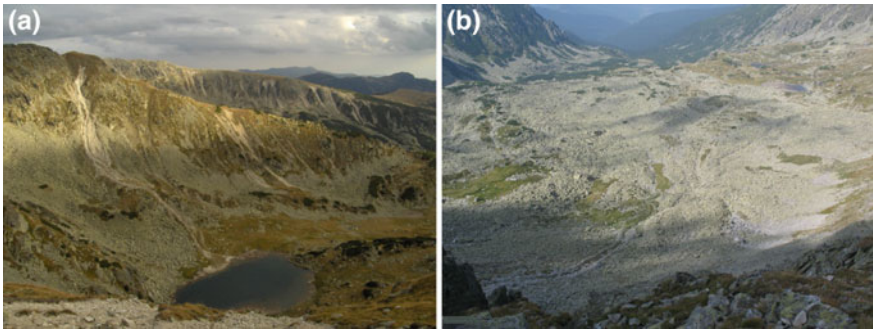

Fig. 14.6 Cirque walls in granitic bedrock (**a**) and rock glacier deposits (**b**) dissected by DF paths in Retezat Mountains, Southern Carpathians (photo taken in summer 2014 by R. Popescu)

Fig. 14.7 A DF source area with large amount of sediments in the channel (photo taken in May, 2014 by V. Ilinca)

the unconsolidated substratum (surficial deposits) could also explain the spatial pattern distribution and size of a large number of DF initiation areas.

DF failure angles range typically from 25° to 40° as described by Hungr (2005). Slope degrees below 25° are too gentle to generate DFs, while on slopes greater than 45° cannot accumulate enough debris. Observations made on many small basins from Lotru and Căpăţânii Mountains show a total length generally less than

150 m. For example, from 14 sites located in lower Lotru hydrographic basin, only one site barely exceeds 1000 m length, while the shortest reach only 151 m (Ilinca 2014).

Climatic Factors

Heavy rainfall and rapid snow melting episodes are the main causes of triggering DFs. For the Romanian Carpathians, there are yet no studies to determine a rainfall threshold above which a DF can occur. However, observations made on events from Lotrului Valley indicate that DFs are usually triggered when daily rainfall exceeds 40 mm/24 h (Ilinca 2010, 2014). In the case of DFs occurring in Călimani mining areas, field observations point out that a minimum of 25 mm precipitations daily recorded at Reţiţiş meteorological Station (2023 m a.s.l.) is enough to produce water accumulation on the spoil heap surface that subsequently produces DF release on its talus slopes. The unconsolidated material is reworked from the spoil heap talus and deposed along stream channels.

Anthropic Factors

Frequency, magnitude and geographic extent of DFs can be influenced by forest logging practices (Sidle 2005). Exposed or degraded land replaces the forest and may increase the amount of both sediment and wood supply. The woody material is important because it can create small dams behind which debris accumulates and can subsequently be removed by other debris surge (Văidean et al. 2014). However, DFs can occur in forested basins (without logging activity), as observed in the Lotru Valley during the last decades (Ilinca 2014). Here, some forested basins (almost 100 % covered with forest) generated debris flow that damaged the national road 7A and other local roads (Fig. 14.8). Forest roads themselves are another source of sediments especially where they are cut on slopes with thick colluviums.

Man-made landforms (e.g., spoil heaps) are commonly build up with erodible material and therefore may favor an intense DF activity. The results obtained from studies conducted in the mining areas from Călimani Mountains (Eastern Carpathians) show that human-induced DF can be extremely active and affect both the new surfaces created by mining activities and the preexisting channels of hydrographic network (Pop et al. 2009, 2012; Surdeanu et al. 2011). The reservoirs constructed downstream in the riverbed and designed to stop sediments transported by hydrogeomorphic processes allow estimating values of a sediment accumulation rate that range between 1430 and 3250 m^3/year (Pop et al. 2009). During the 1980s, after the occurrence of several spoil heaps sliding events, new landforms resulted which were later intensely reworked by hydrogeomorphic processes, including DFs (Fig. 14.9). A detailed geomorphological mapping of these affected areas (Fig. 14.10) was performed using ArcGIS 9 software, based on topographical maps,

Fig. 14.8 County Road covered by debris. The image shows the state after authorities' intervention which cut a breach in the debris deposit (photo taken in July 2014 by V. Ilinca)

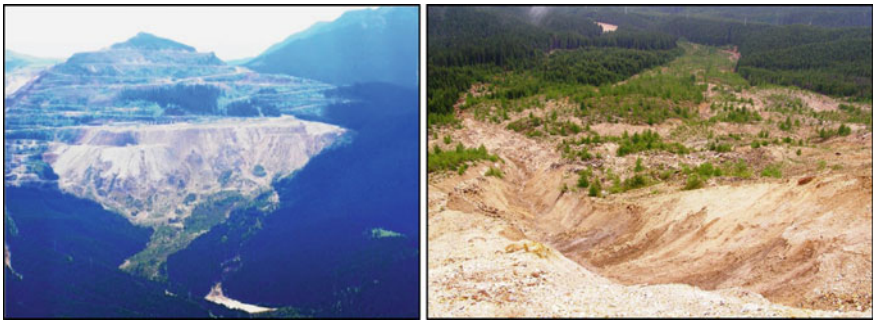

Fig. 14.9 Spoil heaps on northern flank of Negoiul Românesc sulpr mining area (Călimani Mountains, Eastern Carpathians) affected by repeated landsliding and DF activity; the unstable deposits below the spoil heap talus slopes (*left side photo*) are colonized by trees (*right side photo*) (photos taken in summer 2007 by O. Pop)

orthophotoplans and field observations (Surdeanu et al. 2011). By using the same geomorphological mapping method in the further studies, a better understanding of newly created landforms could be reached.

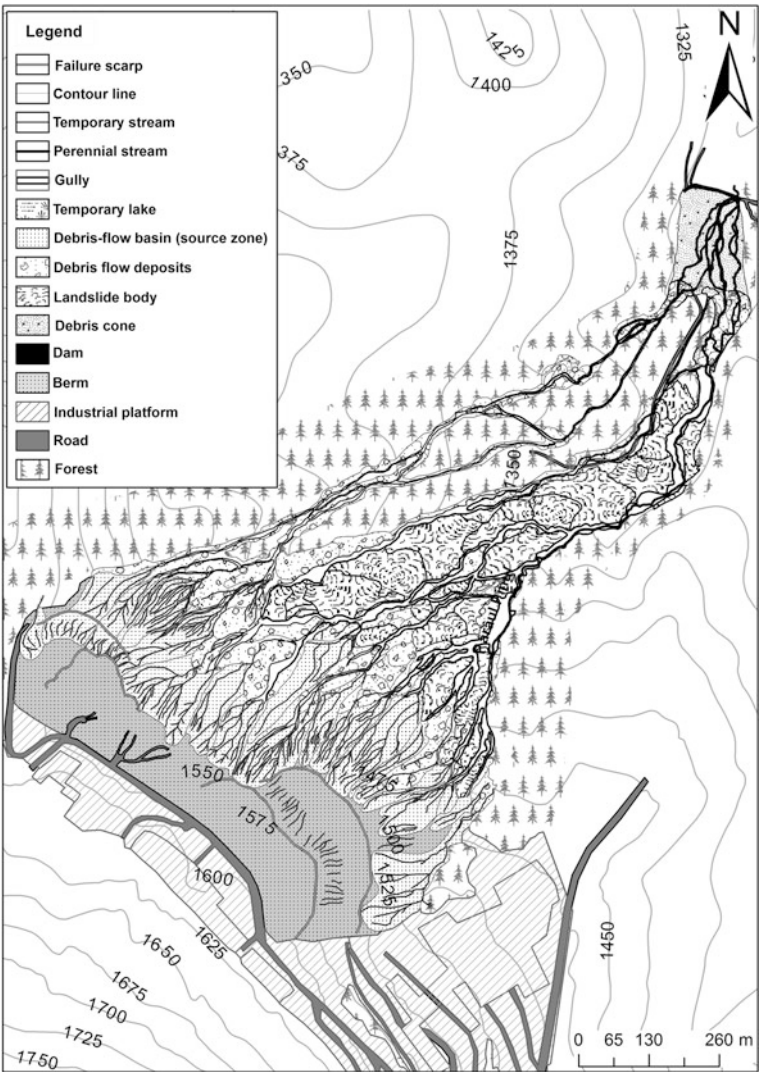

Fig. 14.10 Detailed geomorphological map of a spoil heap area from Călimani Mountains (from Surdeanu et al. 2011)

Reconstructing Past Debris Flow Activity

Several studies conducted in High Tatra Mountains belonging to the Carpathian Range widely recognize the role of past and present-day DF activity on the steep slope morphology (Kotarba 1992, 1997; Kotarba and Stromquist 1984). Because of the short and subjective collective memory and the lack of archival records,

generally little is known about the spatial and temporal frequency of DFs. Remote mountain areas are rarely long-term monitored, the data regarding past debris flow activity are scarce. Indirect methods might be a solution to identify the areas affected by such phenomena in the past. In Tatra Mountains, lichenometric methods were applied to date DF frequency and allow reconstruction of past activity back to LIA period (Kotarba 1991). Such lichenometric approaches that aim at estimating recent DF activity in the Romanian Carpathians are totally absent and could therefore be envisaged by future studies.

DF material often affects trees growing along channels or on depositional cones and may even modify the structure of forest stands (Butler and Walsh 1994; Butler 2001). As veritable natural archives, trees are able to record the signs of past events in their annual ring structure. Dendrogeomorphic methods are based on the identification of the growth anomalies produced by trees due to mechanical impact of DFs, proving that they can be an useful tool in reconstructing spatiotemporal frequency of DF with annual or even seasonal resolution (Stoffel and Bollschweiler 2008; Bollschweiler and Stoffel 2010). An increasing number of publications prove that dendrogeomorphic methods are widely applied in other mountain areas in order to reconstruct past DF activity, meanwhile in the Carpathians similar studies are lacking, despite the great potential that forested areas have for such approaches.

In areas unaffected by human activities from Retezat Mountains, a dendrogeomorphic reconstruction of DF history study was conducted by Văidean and Petrea (2014). According to the authors of this study, tree-ring analysis covers the period of the last century, allowing the reconstruction of a minimum 12 DF events that occurred since 1929 until present.

In Călimani mining areas, the impact of DF activity on riparian forests was also assessed by tree-ring analysis (Pop 2012; Pop et al. 2014). In this case, Norway spruce trees (*Picea abies* (L) Karst.) buried by sulfur-rich toxic sediments reacted by producing severe growth suppression (GS) and the formation of tangential rows of traumatic resin ducts (TRD) shortly after a major DF and debris flood event (Fig. 14.11). Moreover, it has been proved that the intensity and persistence of growth anomalies in trees are positively correlated with local depths and granulometry of sediments.

In both cases, the analyzed Norway spruce trees (*P. abies* (L) Karst.) proved to be a suitable tree species that records valuable information about the past DF activity. Further dendrogeomorphological studies in other parts of the Romanian Carpathian Range applied on various coniferous or broadleaved tree species will confirm their potential in reconstructing the DF history.

In the Călimani mining area, tree-age determination was also applied to date colonization period of surfaces resulted by spoil heap slidings and DF activity (Surdeanu et al. 2011). As confirmed in this study, natural reforestation of the new resulted surfaces was not uniform (Fig. 14.12). The different ages of colonizing trees on these newly formed surfaces proves that geomorphic instability is still present in the area. A combination of various restrictive conditions and factors (presence of toxic, sulfr-rich material, lack of soil, the frequency of DF, presence of large blocks at the surface of deposits, etc.) which inhibit tree germination and

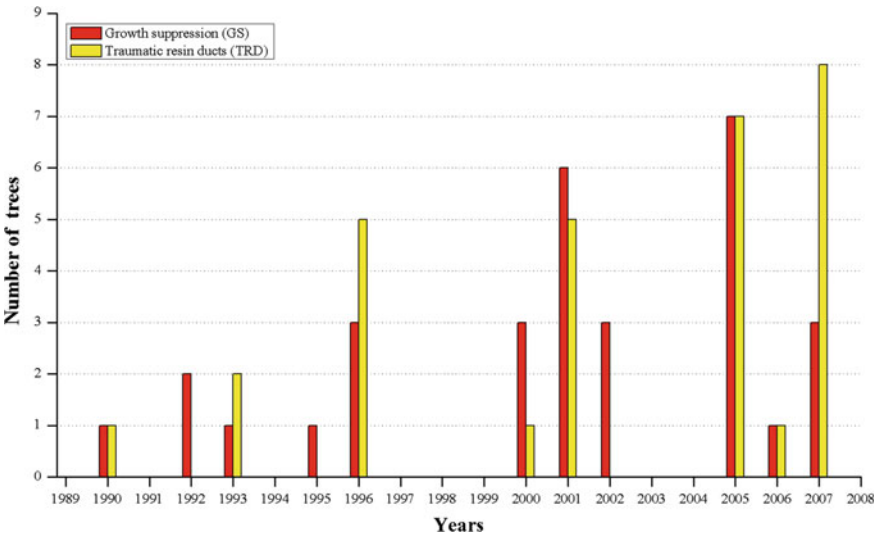

Fig. 14.11 Temporal frequency of growth suppression (*GS*) and traumatic resin duct (*TRD*) occurrences in the growth-ring records of the trees sampled in Călimani mining area (from Pop et al. 2014)

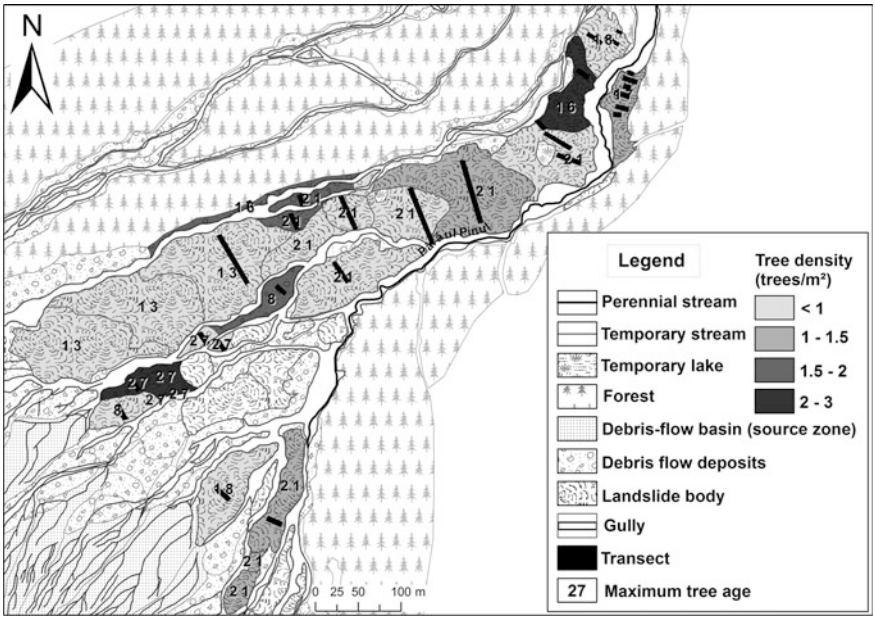

Fig. 14.12 Map of the tree density and maximum tree age

growth could explain the differences between the colonization rates of the new surfaces resulted after the major spoil heap sliding. In this geomorphologically unstable environment, the sparse natural forest growing on the new surfaces created by sliding and DF activity will not be able to stabilize them.

As regards the estimation of DF velocity and peak discharge, some attempts were used separately. Ilinca (2010, 2014) estimates the DF velocity and peak discharge based on Johnson and Rodine equation (Johnson and Rodine 1984). Four cross sections were investigated along the second largest DF site from Lotru Valley with a basin area of 0.17 km^2 and a total length of 996 m. The estimated peak velocity and peak discharge range from 1.31 to 2.64 m/s, and 4.0 to 10.03 m^3 respectively. For other sites few empiric equations were used (Ilinca 2010), but due to the large differences they exhibit for the same site, the results are not reliable. This might be due to the equations which were initially developed for areas with different geological and morphometric characteristics.

DF Hazard Management

In the Romanian Carpathians, hazard management policy has not a long-established tradition, as it is the case of the alpine countries. The strategies rarely include actions for prevention (e.g., controlling erosion in the starting area and flow redirection). The main engineering works are applied especially in the areas with affected local communities and are oriented to secure inhabitants in the DF activity area or to clean up the affected infrastructure after a DF event occurred. The exposed infrastructure is mainly protected by works that include construction of deflection debris dams, channelization, bridge reinforcement, or (re)construction and debris removal from the roads.

Some problems related to small and steep basins derived from misunderstanding of the process and incorrect remedial measures practice (Costa 1988). In areas described above, as well as in other areas from the Romanian Carpathians, many DF destroy or block the main roads. This is a consequence of the culverts property that is designed for water flow. Taking into account that DF material incorporates boulders and tree trunks, the culverts lack the ability of all debris discharge, reason why clogging culverts result in debris deposition on roads. Other problems are related to DF source areas. For example, small basins that generate DF along a transport corridor have engineering works only at the mouth, neglecting the source area. It is the case of the DF from Brădișor dam (Fig. 14.13) that has large source area with thick surficial deposit, partly mobilized by DF which blocks the Lotru river course at almost each event (Ilinca 2014).

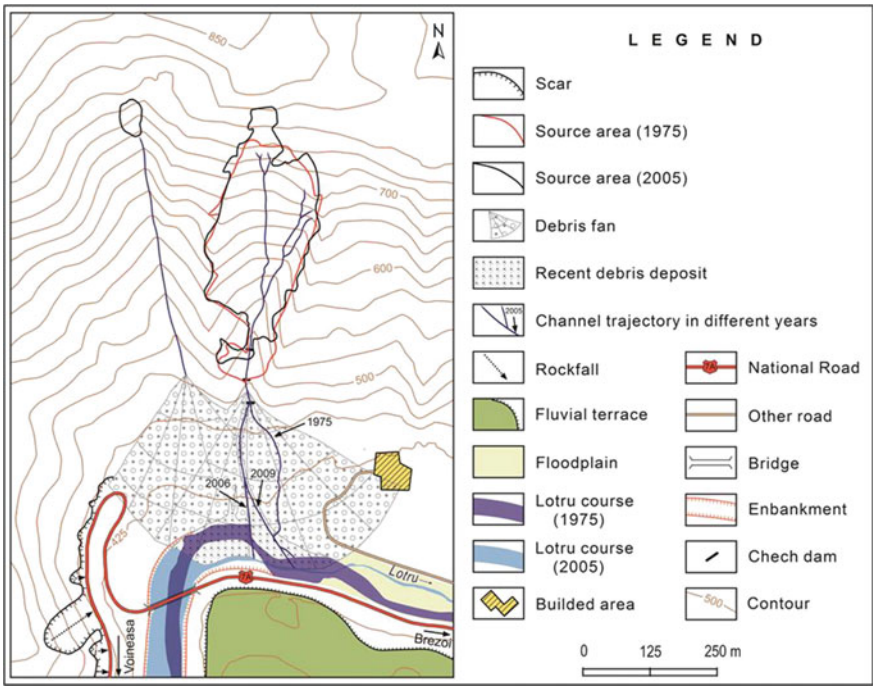

Fig. 14.13 Map of Brădişor DF affected areas, Lotru Valley (from Ilinca 2014)

Concluding Remarks

Understanding the characteristics of DF processes and their mechanisms is necessary in Romania, due to the present-day context of increasing human pressure on DF affected areas, especially in the mountainous areas. More fundamental studies are needed in order to assess the characteristics of spatial distribution and DF dynamics.

In Romania, DF is almost an exclusive mountain geomorphic process which occurs in both forested and unforested areas. The process is widespread from the alpine ranges (above 2000 m altitude) to the mountain base (even below 500 m altitude). Observations made in various massifs of the Carpathians show that DFs occur on moderate to steep slopes in different geologic environments. Man-made landforms, e.g., spoil heaps are also prone to an intense reworking of materials by DF processes.

Correct identification of landslide types from mountain areas can eventually lead to a more accurate assessment of hazard. Mapping DF affected areas could be implemented in management decisions in order to considerably reduce losses induced by this geomorphic hazard.

References

Arattano M, Franzi L (2004) Analysis of different water-sediment flow processes in a mountain torrent. Nat Hazards Earth Syst Sci 4:783–791

Badea L, Posea G (1953) Mudflow from Chirileşti (in Romanian). Natura V(6):109–112

Bălteanu D (1974) Relations between mudflows and ephemeral stream erosion in the modelling of the Buzău Subcarpathians (in Romanian). Stud Cercet Geol Geofiz Geogr Ser Geogr XXI (1):109–116

Bălteanu D (1976) Two case studies of Mudflows in the Buzău Subcarpathians. Geografiska Annaler Ser A Phys Geogr 58(3):165–171

Bălteanu D, Micu M. (2012) Morphodynamics of the Chirileşti mudflow (Buzău Mountains). Rev Roum Géogr/Rom Journ Geogr 56(2):117–125

Becht M, Rieger D (1997) Debris flows on alpine slopes (eastern Alps). Géomorphologie: relief, processus, environnement 3(1):33–41

Bollschweiler M, Stoffel M (2010) Tree rings and debris-flow: recent developments, future directions. Prog Phys Geogr 34(5):625–645

Butler DR (2001) Geomorphic process–disturbance corridors-a variation on a principle of landscape ecology. Prog Phys Geogr 25(2):237–248

Butler DR, Walsh SJ (1994) Site characteristics of debris flows and their relationship to alpine treeline. Phys Geogr 15(2):181–199

Corominas J, Remondo J, Farias P, Estevao M, Zézere J, de Terán Díaz, Dikau R, Schrott R, Moya J, González A (1996) Debris flow. In: Dikau R, Brunsden L, Schrott R, Ibsen M-L (eds) Landslide recognition—identification, movement and causes. Wiley, Chichester, pp 161–180

Costa JE (1984) Physical geomorphology of debris flows. In: Costa JE, Fleisher PJ (eds) Developments and applications of geomorphology. Springer, Berlin, pp 268–317

Costa JE (1988) Rheologic, geomorphic and sedimentologic differentiation of water floods, hyperconcentrated flows and debris flows. In: Baker VR, Kochel RC, Patton PC (eds) Flood geomorphology. Wiley, New York, pp 112–122

Coussot P, Meunier M (1996) Recognition, classification and mechanical description of debris flows. Earth Sci Rev 40:209–227

Germain D, Ouellet MA (2013) Subaerial sediment-water flows on hillslopes: Essential research questions and classification. Prog Phys Geogr 37:813–833

Hungr O (2005) Debris-flows: classification and terminology. In: Jakob M, Hungr O (eds) Debris-flow and related phenomena. Springer-Praxis, Berlin, pp 9–21

Hungr O, Evans SG, Bovis M, Hutchinson JN (2001) Review of the classification of landslides of the flow type. Environ Eng Geosci 7:221–238

Ilinca V (2010) Valea Lotrului – studiu de geomorfologie aplicată. PhD thesis, University of Bucharest (in Romanian)

Ilinca V (2014) Characteristics of debris flows from the lower part of the Lotru River basin (South Carpathians, Romania). Landslides 11:505–512

Innes JL (1983) Debris flows. Prog Phys Geogr 7(4):469–501

Jakob M (2005) A size classification for debris flows. Eng Geol 79:151–161

Johnson A, Rodine JR (1984) Debris flows. In: Brunsden D, Prior DB (eds) Slope instability. Wiley, Chichester, pp 257–361

Kotarba A (1991) On the age and magnitude of debris flows in the Polish Tatra Mountains. Bull Pol Acad Earth Sci 39(2):129–135

Kotarba A (1992) Mountain slope dynamics due to debris-flows activity in the High Tatra Mountains, Poland. Bulletin de l'Association des Géographes Français 3:257–259

Kotarba A (1997) Formation of high-mountain talus slopes related to debris-flow activity in the High Tatra Mountains. Permafrost Periglac Process 8:191–204

Kotarba A, Stromquist L (1984) Transport, sorting and deposition processes of alpine debris slope deposits in the Polish Tatra Mountains. Geogr Ann 66(4):285–294

Micu M, Bălteanu D (2009) Landslide hazard assessment in the Curvature Carpathians and Subcarpathians, Romania. Zeitschrift für Geomorphologie, Supplementbände 53(2):31–47
Montgomery DR, Massong TM, Hawley SCS (2003) Influence of debris flows and log jams on the location of pools and alluvial channel reaches, Oregon Coast Range. Geol Soc Am Bull 115:78–88
Pierson TC (2005) Hyperconcentrated flow – transitional process between water flow and debris flow. In: Debris flow hazards and related phenomena, Jakob M, Hungr O (eds.) Praxis, UK, pp. 159–202
Pierson TC, Costa JE (1987) A rheologic classification of subaerial sediment-water flows. Rev Eng Geol 7:1–12
Pop OT (2012) Etude comparative des processus géomorphologiques contemporains dans les massifs volcaniques du Sancy (France) et du Călimani (Roumanie). PhD Thesis, Babeş-Bolyai University, Faculty of Geography, Cluj-Napoca, Romania
Pop OT, Hodor N, Surdeanu V, Irimuş I-A (2009) Conséquences de l'instabilité morphodynamique liée à l'exploitation du soufre dans le massif volcanique du Călimani (Roumanie). Revue Géographique de l'Est, 49, URL:http://rge.revues.org/955
Pop OT, Surdeanu V, Irimuş I-A, Guitton M (2010) Distribution spatiale des coulées de débris contemporaines dans le Massif du Călimani (Roumanie). Studia Universitatis Babeş-Bolyai Geographia 1:33–44
Pop OT, Buimagă-Iarinca Ş, Stoffel M, Anghel T (2013) Réponse des épicéas (*Picea abies* (L.) Karst.) à l'accumulation des sédiments dans le bassin de rétention Dumitrelul (massif du Călimani, Roumanie). In: Decaulne A (ed) Arbres et Dynamiques. Presses Universitaires Blaise Pascal, Clermont-Ferrand, France, pp 73–87
Pop OT, Buimagă-Iarinca Ş, Anghel T, Stoffel M (2014) Effects of open-cast sulphur mining on sediment transfers and toxification of riparian forests. Geografiska Annaler: Ser A, Physic Geogr 96(4):485–496. doi:10.1111/geoa.12077 (Special Issue: Sedimentary fluxes and budgets in different climatic environments)
Rădoane M, Dumitriu D, Ichim I (2001) Geomorfologie, vol II. Editura Universităţii Suceava
Rădoane N, Olariu P, Dumitriu D (2005) Bazinele hidrografice mici, unităţi fundamentale de interpretare a dinamicii reliefului. In: Surdeanu V (ed) Geography within the contemporary development, Presa Universitară Clujeană, pp 43–52 (in Romanian)
Scott KM, Vallance JW, Pringle PT 1995. Sedimentology, behavior, and hazards of debris flows at Mount Rainier. Washington, USGS Professional Paper 1547, pp 1–56
Sidle RC (2005) Influence of forest harvesting activities on debris avalanches and flows. In: Jakob M, Hungr O (eds) Debris-flow hazards and related phenomena. Springer, Berlin
Slaymaker O (1988) The distinctive attributes of debris torrents. Hydrol Sci J 33:567–573
Stoffel M, Bollschweiler M (2008) Tree-ring analysis in natural hazards research—an overview. Nat Hazards Earth Syst Sci 8:187–202
Surdeanu V, Rădoane N, Catană C (1989) Le glissement de terrain de Taşbuga (Carpates Orientales). Studia-Geomorphologica Carpato-Balcanica 23:123–136
Surdeanu V, Pop OT, Dulgheru M, Anghel T, Chiaburu M (2011) Relationship between trees colonization, landslide and debris-flow activity in the sulphur mining area of Călimani Mountains (Romania). Revista de Geomorfologie 13:39–48
Tufescu V (1970) Mudflows in the Flysch Carpathians and Bend Sub-Carpathians of Romania. Z Geomorphol Supplbd 9:146–156
Văidean R, Petrea D (2014) Dendrogeomorphological reconstruction of past debris flow activity along a forested torrent (Retezat Mountains). Revista de Geomorfologie 16:17-24
Văidean R, Arghiuş V, Pop OT (2015) Dendrogeomorphic reconstruction of past debris-flood activity along a torrential channel: an example from Negoiul basin (Apuseni Mountains, Romanian Carpathians). Zeitschrift für Geomorphologie 59 (3):319–335
Van Dine DF (1985) Debris flows and debris torrents in the southern Canadian Cordillera. Can Geotech J 22:44–68
Vespremeanu-Stroe A, Micu M, Cruceru N (2006) The 3D analysis of Valea Viei mudflow morphodynamics, Buzău Subcarpathians. Revista de Geomorfologie 8:95–108
Wilford DJ, Sakals ME, Innes JL, Sidle RC, Bergerud WA (2004) Recognition of debris flow, debris flood and flood hazard through watershed morphometrics. Landslides 1:61–66

Part IV
Soil Erosion

Chapter 15
Sheet and Rill Erosion

Nelu Popa

Abstract In this chapter, we intend to summarize the methodology and the most important results obtained in surface erosion monitoring and degraded lands improvement in the Moldavian Plateau, based on the experience of over six decades of the Perieni Research—Development Center for Soil Erosion Control, Romania. Considering that a high-quality database on erosion plots in Romania is not available (only very limited for some areas and short periods of time) we believe that extensive analysis on the results obtained in the Moldavian Plateau would have more scientific importance than estimates approximated at the level of Romanian territory. The main problems discussed include, among others: the analysis of the relationships between precipitation, runoff and soil erosion; verification of the soil conservation measures effectiveness in the conditions of extreme rainfall events; assessment of soil water storage in anti-erosion equipped areas by forest belts; estimation of surface erosion in small catchments by conventional and unconventional methods.

Keywords Sheet erosion · Rill erosion · Runoff plots · Conservation practices · Romania

Introduction

Definitions. There are many definitions dealing with erosion, each of them seen from the viewpoint of the specialist (geologist, geomorphologist, hydrologist, pedologist, or territorial planning experts). As this chapter is written by a specialist in land improvements, we here refer to definitions given by experts from the United States Department of Agriculture (Schwab et al. 1966).

Sheet erosion is the removal of surface soil in thin layers by raindrop impact and shallow flows of water on ground surface. Sheet erosion occurs in areas between

N. Popa (✉)
Research and Development Center for Soil Erosion Control, 737405 Perieni, Vaslui County, Romania
e-mail: nelu_c_popa@yahoo.com

M. Rădoane and A. Vespremeanu-Stroe (eds.), *Landform Dynamics and Evolution in Romania*, Springer Geography,
DOI 10.1007/978-3-319-32589-7_15

rills, the eroded sediment moves to rills and then gets transported downslope if sufficient sediment transport capacity is available.

Rill erosion is usually linked with sheet erosion as the shallow flows of water driving sheet erosion tend to merge. Rill erosion occurs in small channels (1–200 mm in depth and width) that can be easily smoothed out or obliterated by normal tillage. Rill erosion is common in bare agricultural land, particularly in freshly seeded soil where the soil structure has been loosened.

Brief research history. Over time, there were significant concerns in Romania regarding the study of erosion and associated processes. Particularly, the problem was initially in the attention of foresters from which, most notably was Antonescu (cited by Ionescu-Sișești and Staicu 1958) through his work at the end of the nineteenth century. At that time, erosion control regulations were contained only in the forestry code. Ionescu-Sișești (1925) extends the studies on agricultural land and manages to draw the attention of officials on major damages that erosion inflicts on agriculture. Thus, in 1930 the first law for improving degraded lands is promulgated, aiming at three purposes: soil protection, enhancement of degraded lands and regulation of the water regime. Although it provided some significantly positive measures, the law did not produced the expected effects because soils improvement works had to be carried out with the consent of at least two-thirds of the land owners and funds allocated by the State were very small.

Scientific activity for the study of erosion began in 1940 with the establishment of the Soil Erosion Laboratory at the Institute of Agronomic Research in Romania which passed afterwards under the authority of the Research Institute for Soil Science and Agrochemistry in Bucharest. Among the most important works produced here, we highlight the Soil Erosion Map of Romania, scale 1:500,000 (Florea et al. 1976), Erodability Map of Romania and Zoning Map of Runoff Standard Coefficient, scale 1:500,000 (Vătau et al. 1993a, b).

In 1954, the Research Station for Soil Erosion Control was funded at Perieni on the recommendation of two Romanian academicians: M. Moţoc and T. Săvulescu. Located in a representative area (the Moldavian Plateau), Perieni Station has developed an ambitious concept of soil conservation on sloping farmland that spread in the 1980s by completion of 35 standard perimeters to combat soil erosion on a total area of 62,400 ha, located in most counties of Romania with hilly relief. Simultaneously, this approach was adopted on larger areas, so at the end of 1989 an area of approximately 2.2 million ha of agricultural land was equipped with anti-erosion measures. In the next period, by introducing the Law no. 18 in 1991 and by its subsequent updates, most of the anti-erosion works were taken out of service due to some provisions that have led to the division of land into small parcels, delivered to targeted small hill-valley direction, which favored accentuation of degradation processes by soil erosion.

Perieni Station was transformed in 1970 into Central Station and in 2006 became Research and Development Center for Soil Erosion Control Perieni. The above-mentioned methodology had a significant role in approaching a new strategy regarding the decrease of the erosion processes. Thus, the experiments carried out in the Moldavian Plateau and in other perimeters with hilly relief in Romania led to

original results, with an important theoretical and practical resonance (Nistor and Nistor 1979, 1981; Popa 1977; Popa et al. 1984; Neamțu 1998).

The researches made on standard unit plots, occupied with different cultures, allowed the accumulation of relevant data reflecting the link between the erosion phenomenon and factors influencing it (Moţoc and Ioniță 1983; Ioniță and Ouatu 1985). Water and soil losses were monitored in relation to the major climatic parameters (precipitation and temperature), soil parameters, relief, vegetation, agricultural machinery works, etc. The studies, which had the ultimate goal the arrangement and rational use of agricultural land, aimed the full range of slope and channel processes that contribute to slopes' surface modification or to supply solid material to the hydrographic network.

In the following, we intend to summarize the operating mode used and the most important results obtained in surface erosion monitoring and degraded lands improvement in the Moldavian Plateau, based on the experience of over six decades of the Research and Development Center for Soil Erosion Control Perieni.

A high-quality database on erosion plots is not available in Romania (only very limited for some areas and short periods, cf. Table 15.3). Therefore, we believe that extensive analysis on the results obtained in the Moldavian Plateau would have more scientific importance than estimates approximated at the level of the entire Romanian territory.

Our approach on the subject takes into account the following structure:

(i) Description of experimental sites and working methods;
(ii) Analysis of the relations between precipitation, runoff, and soil erosion;
(iii) Evaluation of soil conservation measures effectiveness in the conditions of extreme rainfall events;
(iv) Assessment of soil water storage in anti-erosion areas equipped by forest belts;
(v) Estimation of surface erosion in small catchments by conventional and unconventional methods.

Description of Experimental Sites and Working Methods

The study area is located in eastern Romania, Tutova Rolling Hills, and is shown in Fig. 15.1 and Table 15.1.

Ţărnii Valley (Fig. 15.2a) *and Crâng sites*. In the early 1950s, the agricultural land presented an accentuated division in small plots of 1–2 ha arranged with the long side on the up-and-down hill direction. Since 1954, the land passed into administration of RDCSEC Perieni and was completely reorganized in terms of soil conservation. Table 15.2 schematically shows the main actions of surface erosion control that have been applied at Perieni Center. These were aimed to achieve the following objectives: (a) Decreasing soil losses to a tolerable level (4–6 t ha^{-1} $year^{-1}$); (b) Regularization of water flow on slopes that contribute to: (b1) maintaining and increasing the storage of water in dry areas; (b2) draining water excess

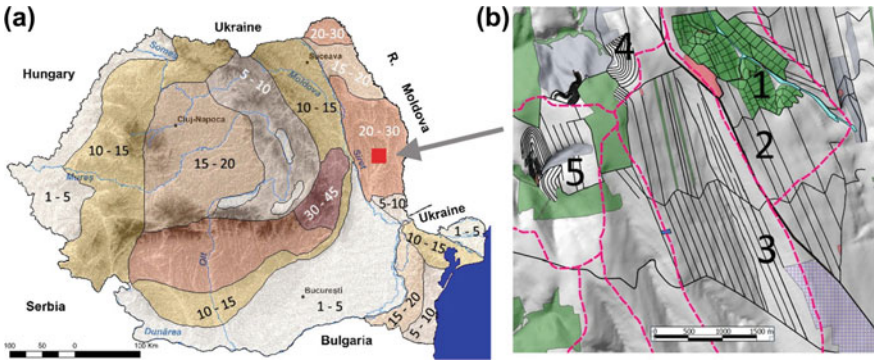

Fig. 15.1 Map of total erosion (t ha^{-1} year^{-1}) in Romania (Moțoc 1983) (**a**). Location of the experimental sites from RDCSEC Perieni (**b**)

Table 15.1 The main characteristics of the experimental sites

No.	Site	Surface (ha)	Slope (%)	Type of ownership	Soil type
1	Headquarters RDCSEC Perieni	12.70	0	The public domain, in the administration of RDCSEC Perieni	
2	Site with the standard plots for controlling runoff and erosion	0.77	12		Cambic Chernozem, slightly eroded
3	Țărnii Valley microcatchment	500.00	10–13		Cambic Chernozem, slightly eroded
4	Crâng microcatchment	30.00	5–22		Forest gray soil, moderately eroded and Erodisol
5	Ghelțag microcatchment	100.00	5–20	Private	Forest gray soil, moderately eroded and Erodisol

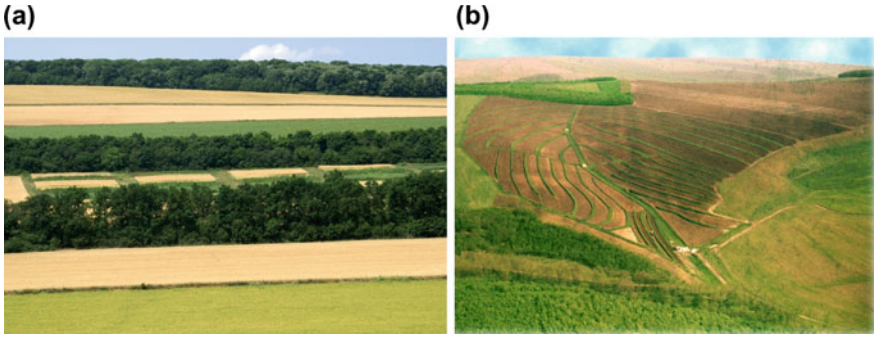

Fig. 15.2 Small catchments with soil conservation measures **a** Țărnii Valley. **b** Ghelțag

Table 15.2 Soil conservation measures applied in Țărnii Valley and Crâng microcatchments

Type of measures	Measures
Agrophytotechnical	Restructuring and relocation land use categories Organization of agricultural land Establishing crop assortments Establishing crop structure Crop rotation; Crop systems (contour tillage and planting, strip cropping, grass strips, terraces) Soil tillage (plowing, minimum tillage) Restoring fertility of eroded soils
Soil erosion control	Modeling–leveling land surface Designing and construction of farming road network Terracing Drainage of excess moisture from subsurface Interception and discharge of flows on slopes
Forestry	Forest belts Massive forest plantations

in wetlands; (c) Ensuring optimal land use conditions to increase crop yields; (d) Ensuring quality protection of soil and water resources; (e) Reduction of water pollution by fertilizers and other chemicals used in agriculture; (f) Ensuring conditions for an increased biodiversity; (g) Improving aesthetics of the landscape.

Țărnii Valley and Crâng sites are constantly improved and they represent models for farmers concerning the development and exploitation of agricultural lands from the hilly area of eastern Romania.

Ghelțag site. Ghelțag microcatchment (Fig. 15.2b) has been arranged between 1975 and 1977 and was correctly exploited for nearly 20 years. After the promulgation of Law 18 in 1991, the land passed into the private ownership of approximately 80 people. The restitution of land was made on the old locations which meant disposing of the plots on up-and-down hill direction. The narrow-width strips made impossible to perform contour tillage system which led to the decommissioning of soil conservation measures. Besides, this situation was found everywhere in the hilly areas of Romania. In the last decade, the land was leased by RDCSEC Perieni and the agricultural exploitation was performed using modern agricultural technologies and with the reintroduction of soil conservation measures as follows: contour tillage, contour planting, strip cropping, crop ration, bench terraces, grassed waterway, etc.

Climatic parameters were recorded at two different locations. The first is the inside RDCSEC Perieni, where an automatic weather station is placed. The later is provided with sensors for measuring, automatically registering and transmitting of the following climatic parameters: rainfall quantity, wind speed and direction, air temperature outside and inside the building where the data reception console is installed, outdoor humidity and indoor temperature and humidity soil at depths of 20, 40, 60 and 100 cm, solar radiation, ultraviolet radiation. The station was located

in a fenced enclosure, together with other classical devices for recording climatic parameters (a rain gauge and a pluviograph) for data security in case of emergencies and for calibration. The second location is in the neighborhood of the runoff plots, where three types of rain gauges and a pluviograph are placed.

The researches regarding runoff, soil and nutrient losses were performed on standard runoff plots located on the left side of the Țărnii Valley microcatchment. The system for collecting runoff from these plots allows the retention of water and soil in covered tanks. Each plot is equipped with three tanks of 1000, 200, and 50 L; the first tanks being equipped with a device for reducing of 4:5 volume of drained water. The plots have 100 m^2 area (4 m × 25 m), which are exploited in the conventional system and are cultivated with maize, winter wheat, Bromus, beans, and soybeans, respecting the principle of crop rotation.

The way that Ghelţag and Țărnii Valley microcatchments have behaved during heavy rains has been determined by conducting some measurements of erosion on slopes by topographic methods, as well as measurements of runoff in control sections located on the torrential network. Control sections are triangular weirs, constructed of concrete, the shape and structure of cross sections being consistent with those used by one of the most representative research units in the field of hydrotechnical engineering, namely the Department of Agriculture of Soil Conservation Service from United States (Brakensiek et al. 1979). The measurements consisted of recording water level on the weir and then calculating the water flow which crossed the section, according to the specific mathematical relationships of each section. Also, in Țărnii Valley monitoring of soil moisture variation in the soil was also taken into account, in the soil profile to a depth of 100 cm at 10 cm intervals, for various crops. To do this, monthly soil sampling has been planned in handmade boreholes, and soil moisture has been determined by the gravimetric method. The drillings, accounting 20, were placed on an alignment that crossed the upper Țărnii Valley, on the East–West direction. Estimation of surface erosion in small catchments was made both by conventional methods such as RUSLE models (Renard 1997) and ROMSEM (Moțoc and Sevastel 2002), but also through unconventional methods such as radionuclides technique. Estimation of water erosion rates in European countries was done using several models of which the most utilized still remains USLE (Wischmeier et al. 1959) and later releases as RUSLE. The Romanian model ROMSEM respects the form of the universal soil loss equation (USLE) but has a few changes in some parameters that have been adapted to the conditions in Romania. This model has been very extensively utilized during the years 1970s–1980s, when measures to control soil erosion were widely extended, so in late 1989 an area of about 2.2 million ha of agricultural land was arranged by anti-erosion works. The second approach to estimate the rates of erosion and sedimentation inventory was based on measuring Caesium–137 isotopes over the four alignments that cross the study field and comparing with those recorded in a reference site where neither erosion nor sedimentation processes were observed (Popa et al. 2011). Demonstration of a minus or plus of radioactivity at the site of interest compared with that of the reference site, indicates a certain level of erosion or sedimentation. Caesium–137 was deposited first to the ground surface

during the 1950s–1960s as a result of nuclear weapons experimentation, performed in the terrestrial atmosphere. These isotopes were absorbed by soil particles and their movement in the horizontal plane due to erosion is reflected in the subsequent redistribution of the radionuclide inventory (Zapata 2002). In order to determine the inventory of Caesium–137 in Țărnii Valley, 153 manual drillings have been executed, arranged in four parallel alignments crossing the basin. From each drill one, two or more soil samples have been taken, depending on the thickness of the alluvial layer, each sample weighing 800–1000 g. The samples were sent for analysis to the National Research and Development Institute for Physics and Nuclear Engineering, Magurele to determine the level of radioactivity of the isotopes of Caesium–137. Further, data on spatial variation of soil radioactivity levels were transformed into data on erosion and sedimentation in the study area by using a conversion model (Mass Balance Model 3) developed by Walling (2007).

Analysis of the Relation Between Precipitation, Surface Runoff and Soil Erosion

From the long-term measurements made at RDCSEC Perieni concerning runoff and erosion, we selected the most significant data from standard plots referring to: winter wheat, maize, beans, perennial grasses (Bromus) and continuous fallow (check plot). The results emphasize how different crops protect the soil against water erosion. The study period comprised 28 years (1985–2012), a period long enough for the number of rain events that triggered soil erosion to ensure an acceptable statistical population. Frequency analysis of runoff and soil loss values for main crops (Fig. 15.3) indicates, as expected, maximum values for the plot with continuous fallow (Popa et al. 2012a). To note that the most significant water losses (over 60 % of the total) by runoff, is due to the rains included in the first three categories, meaning the rainfalls with values below 30 mm. Also, major overland flows were recorded for torrential rains that exceeded 50 mm. As regards the soil losses, they are largely associated with runoff, but their weight greatly increases for the rains with values greater than 50 mm. For maize, the overall look is changing as, although runoff remains significant, soil losses are reduced to less than half compared to the previous case.

At beans, the large number of rainfalls in the category below 30 mm made the runoff and soil losses to represent approximately a third of the total, while rainfalls exceeding 50 mm are causing runoff and soil erosion of more than 50 % of the total.

Finally, at winter wheat the situation was totally different from the previous ones. The maximum values of runoff and erosion have been registered for the category of rainfalls between 20 and 30 mm, which were the most frequent.

Comparatively analyzing the four examined cases, it can be observed that runoff and soil losses in relation with rainfall frequency are greatest for fallow, lower for maize and beans and very uneven for winter wheat. This is due to the influence of vegetation cover which is zero for continuous fallow and maximum for winter

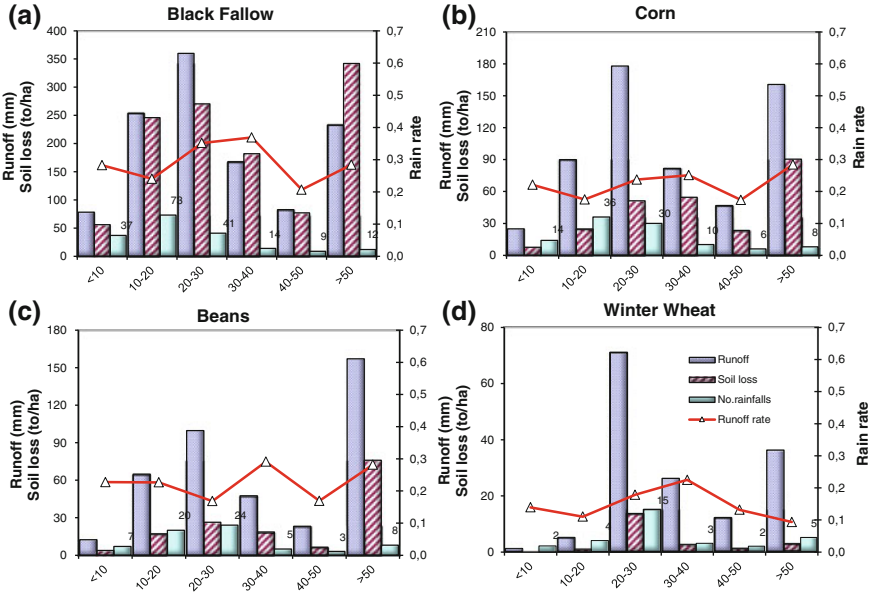

Fig. 15.3 Frequency of runoff, soil losses and rainfalls that triggered runoff between 1985 and 2012 **a** Continuous fallow. **b** Maize. **c** Bean. **d** Winter wheat

wheat. The winter wheat crop is vulnerable to erosion during sowing, in late October and early November and best protects the soil against erosion in June, before the harvest, when the vegetative mass reaches the maximum value. After harvest, although the degree of protection of stubble is low, only the large number of rainfalls in July and August makes the runoff to have higher values, while soil losses are insignificant.

The graphs in Fig. 15.4a–c show dynamic values of runoff, erosion and drainage coefficient, recorded on the standard runoff plots during the growing season (April to November) and calculated as multiannual average values for the 1985–2012 period. It is found that the maximum values of runoff and erosion correspond to June for continuous fallow, maize and beans, while for winter wheat maximum runoff was recorded in July after harvesting (on stubble) and erosion reaches the highest value in September when any significant rain finds the land freshly prepared to sowing.

Evolution of the discharge coefficient (the ratio between the amount of water drained at the soil surface and the intensity of the rainfall which caused the runoff) during the warm season is distinctly different for the analyzed cases. Thus, at fallow, it is noticed a gradual increase to a maximum of 0.19 in August, followed by a decrease in the coming months, while at maize and beans a peak is distinguished in June, followed by a fall in July and a secondary maximum in August. Finally, the graph evolution of the discharge coefficient for winter wheat shows three significant levels: very low, in May and June (0.005–0.007), medium, in July

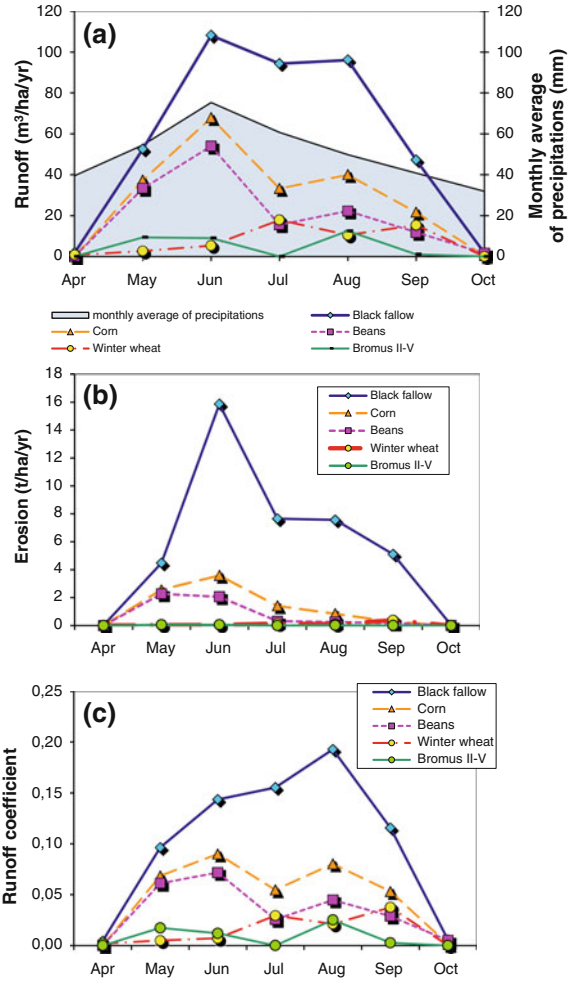

Fig. 15.4 Distributions of monthly average of runoff (**a**), erosion (**b**) and the discharge coefficient (**c**) during 1985–2012 on standard runoff plots occupied by the continuous fallow, maize, winter wheat, beans, and Bromus

and August (0.03) when the land is covered by stubble and most prominent in September (0.04), when the land is practically unprotected against the action of the rainfalls in autumn. For Bromus, the discharge coefficient has very low values during the entire year, a sign that the soil is highly protected against runoff and erosion.

Figure 15.5 shows the multiannual averages of runoff and erosion for a 28 years period. The highest erosion of 40.7 t ha^{-1} $year^{-1}$ was determined for continuous fallow, mean values of 5.1 and 8.73 t ha^{-1} $year^{-1}$ for beans and maize, respectively, and minimum values of 0.7 and 0.3 t ha^{-1} $year^{-1}$ for winter wheat and Bromus. Runoff generally reflects the same allure of graphs, except the culture of year I Bromus where somewhat higher values of runoff are due to vegetation cover insufficiently developed in the first part of the year to protect the soil.

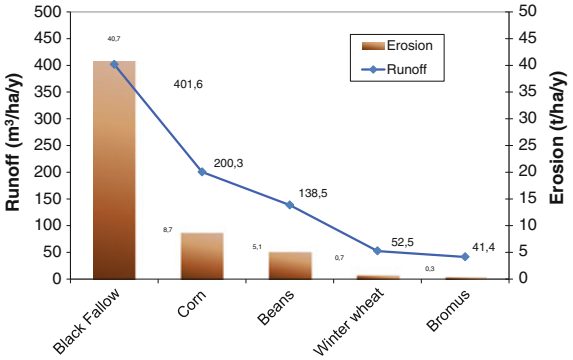

Fig. 15.5 Annual average values of runoff and erosion over the period 1985–2012

Data processing for the entire observation period of runoff and erosion processes on plots highlighted another trend of decreasing of the amount of eroded soil in time, regardless of the use of plots (Fig. 15.6). 28 years of measurements were grouped in two periods: 1985–1999 and 2000–2012, for which the statistical distributions of histograms were determined. The result clearly indicates the negative

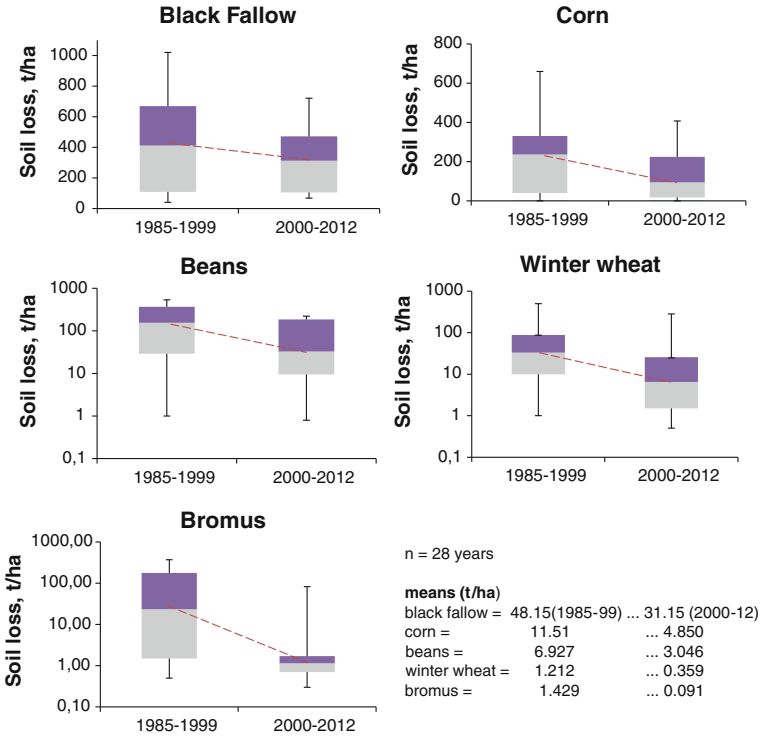

Fig. 15.6 The trend of reducing soil erosion measured on experimental plots with different uses

Table 15.3 Variation of the rainfall and drainage processes on plots in successive periods of time

Plot land use → Process↓	Periods	Black fallow	Maize	Beans	Winter wheat	Bromus
Precipitations (mm)	1985–1999 2000–2012	441.7 497.9 **+ 11.3 %**				
Precipitation which have triggered erosion (mm)	1985–1999 2000–2012	143.4 122.8–**14.4 %**	100.0 66.2	83.8 39.7	39.5 31.6	60.0 17.0–**71.7 %**
Runoff (mm)	1985–1999 2000–2012	43.2 32.9–**23.8 %**	23.6 13.3	18.4 8.2	6.6 4.1	10.6 1.2–**88.6 %**
Runoff coefficient	1985–1999 2000–2012	0.30 0.27–**11.1 %**	0.24 0.20	0.22 0.21	0.17 0.13	0.18 0.07–**59.7 %**

trend of soil erosion. The gap is smaller for black and much larger for field plots with different crops. To explain this phenomenon, we processed the results of runoff on the plots in the same manner, as well as the atmospheric rainfall. The annual rainfall in the considered period registered a slightly positive trend, the increase reaching 11.3 %. Instead, for all runoff parameters, the decline was increasingly higher for the plots with fallow compared to those with Bromus. It follows that over time the capacity of infiltration of rainwater was higher, the layer of drained water being in almost dramatic decline according to the five types of uses of the plots. It seems that the source of this paradoxical state (higher amounts of precipitations over time, but lower runoff at the same time) is the type of precipitation, namely those that trigger runoff. The records showed that in the second time interval considered (2000–2012), rainfalls triggering runoff were less by 14.4 % compared to the first part of the period (1985–1999). And this is just for fallow plot, which is the most sensitive to erosion. In the case of the other types of uses, reduction of these types of rainfall exceeded 80 %, as shown in Table 15.3.

Evaluation of Soil Conservation Measures Effectiveness in the Conditions of Extreme Rainfall Events

The studies from Ghelţag Basin refer to three of the most significant rainfalls recorded in the past two decades: 76.3 mm of rain in August 29, 2004 with the insurance of 5 % for maximum rainfall in 24 h, calculated on a dataset of 73 years, recorded at the Bârlad weather station, 53.5 mm in May 7, 2005 (insurance of 30 %) and 88.5 mm in September 5th 2007 (insurance 3 %). In the first case, the situation of the area occupied by crops was as follows: 24 ha of the total of 100 ha had been freshly plowed after the mash culture (Fig. 15.7a), 52 ha with the stubble of winter wheat, 12 ha cultivated with maize, 12 ha cultivated with soybeans (Fig. 15.7b).

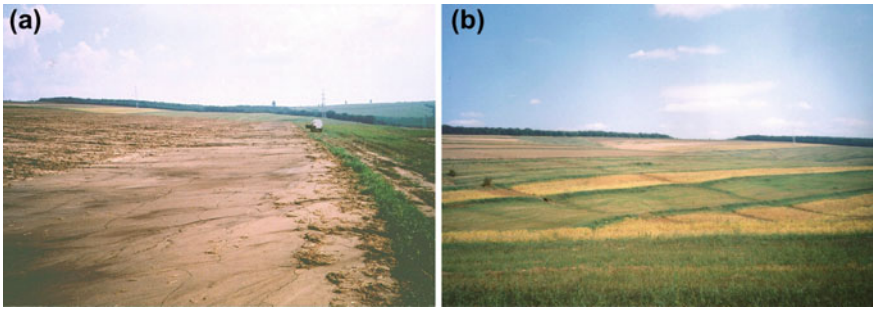

Fig. 15.7 The effects of August 29, 2004 rainfall (H = 53.5 mm) in Ghelţag: **a** Parcel freshly prepared for sowing. **b** Parcels with maize, soybeans and winter wheat stubble

The worst situation regarding intensity of erosion processes was observed on plots not covered by vegetation where the land has been worked by plowing and prepared for sowing. The measurements showed an average of the soil losses comprised between 20 and 24.5 t/ha. These values were significantly lower than those recorded on some plots in the neighborhood, cultivated up-and-down hill direction (35–45 t/ha), under similar conditions of soil and relief. In the whole basin, estimated average erosion has a relatively low value (7.4 t/ha) proving that applying strips culture system where crops were intercalated with the well-developed plant mass assured significant protection against erosion. Thus, at maize we noted a loss of soil between 1.0 and 1.5 t/ha, while on the stubble of winter wheat, plant residues have constituted a very good protection and soil losses were insignificant (<0.1 t/ha). Grassed waterway behaved well and quickly discharged excess of water drained from the slopes without triggering forms of deep erosion (rills). The maximum values of recorded runoff on the triangular weir were of 4.14 m^3/s for cultivated land and 2.81 m^3/s for pasture, respectively. Through the weir section corresponding to cultivated land about 9,100 m^3 have passed, which is approx. 12 % of the total amount of precipitation which triggered runoff and erosion. On May 7, 2005 when 53.5 mm were recorded in 80 min, the situation of crops in the studied basin was as follows: 48 ha with winter wheat and 52 ha crops freshly sown (peas 11 ha, soybeans 19 ha, mustard 16 ha and maize 6 ha). It appears that at that time more than half of the land surface was freshly worked so favorable conditions for triggering erosion processes were created. The estimates have shown that the losses of soil varied between 15 and 35 t/ha, depending on the slope. On the whole basin, the average erosion has been much lower (11 t/ha), given the influence of stripcropping system, where recently sown plots alternated with those cultivated with winter wheat. The maximum values of recorded runoff on the triangular weir were 4.63 m^3/s for the cultivated land and 3.17 m^3/s for the pasture. Through the section of weir corresponding to cultivated land have passed about 5300 m^3, which is approx. 9.8 % of the total amount of precipitation which triggered runoff and erosion.

Fig. 15.8 The effect of rain on September 5, 2007 (H = 88.5 mm) in Ghelțag Microcatchment: **a** Negligible erosion on winter wheat stubble. **b** Erosion on a parcel freshly prepared for sowing rape

In the third analyzed case, the crop structure before the rain from September 5, 2007 was as follows: 30 of the total 100 ha were just prepared for sowing rape, 58 ha with stubble of winter wheat and soybeans, 12 ha cultivated with maize. The erosion was estimated under 0.5 t/ha for winter wheat and soybean stubble (Fig. 15.8a), 15–35 t/ha (Fig. 15.8b) for the land freshly prepared for sowing rape and the average erosion for the entire basin was estimated at 22 t/ha.

In the sections for runoff control on the grassed waterway, maximum runoff values of 6.25 m^3/s were recorded for cultivated land and 4.05 m^3/s for pasture. Through the section of the weir corresponding to cultivated land have passed about 13,000 m^3, which is approx. 14.7 % of the total amount of precipitation.

Figure 15.9 shows how some of the soil conservation measures from Țărnii Valley reacted during the rain from September 9, 2007. The first two images show deposition of sediments in microdepressions created by executing the contour plowing and on the platform of agro-terraces, where the slope is reduced to almost zero. It also shows how shelter belts favor flow dissipation and how the grassy embankment of a road protected it against runoff.

An important factor that favored increasing soil losses through water erosion, was the microrelief formed in the previous period of the 1960 when tillage were executed on up-and-down hill direction (Fig. 15.10a, b). Even today, where contour cropping and strip cropping systems are applied (Fig. 15.10c), the former micro-waves still exist, practically overlapping the old land properties and favoring concentrated flows caused by the rainfall from September 9, 2007 (Fig. 15.10d).

Compared to the situation described above, soil losses through surface erosion on privately owned land, plowed on up-and-down hill direction, varied between 47 and 110 t/ha, depending on the terrain and soil parameters, values that are about three times higher than those recorded in the microcatchments where soil conservation measures have been applied (Fig. 15.11a, b).

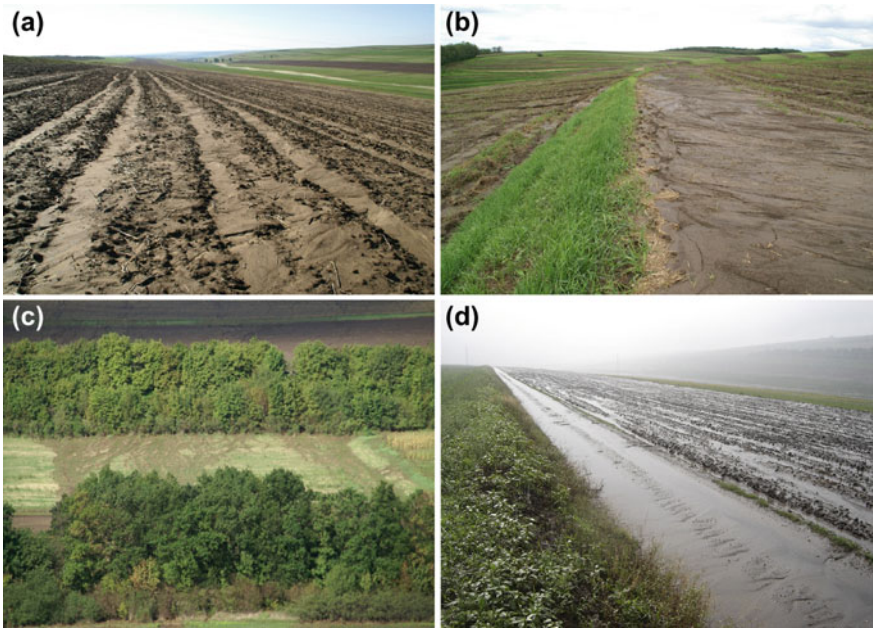

Fig. 15.9 Behavior of anti-erosion measures and works during heavy rainfalls: **a** Retaining sediments on the contour plowing paths. **b** Retaining sediments on the platform of an agroterrace. **c** Flow dissipation by the shelter belts. **d** Camp road protected by a grassy embankment

Assessment of Soil Water Storage in Anti-erosion Areas Equipped with Forest Belts

Influence of the forest belts on soil moisture is most evident during dry periods. One of these was the period September 2006–July 2007 when the deficit of rainfall, compared to the annual average (493 mm) was 218 mm. Data on soil water reserves for different crops, on plots under the influence of forest belts, were compared with those obtained on the neighboring parcels, uninfluenced by these forest belts (Fig. 15.12a, b). The greatest difference of soil water reserve calculated for the depths of 30 and 100 cm were registered for peas and winter wheat. Thus, for peas at the depth of 30 cm, the difference in water reserve has increased from 16 % in June to 26 % in July, while at the depth of 100 cm, the difference was 7 % in June to 42 % in July. For the rest of the period the differences were insignificant.

On winter wheat crop, the differences between the two studied cases are more evident on a longer period of the year, compared with peas. Most notable are the comparative results from April, May and June when the water storage is higher at the plot under the influence of forest belts with values between 36 and 67 % for the depth of 30 cm and values between 27 and 38 % for the depth of 100 cm.

Figure 15.13 shows two suggestive images of drought in July 2007 with two plots of maize: the first in the area of influence of forest belts and the second in an

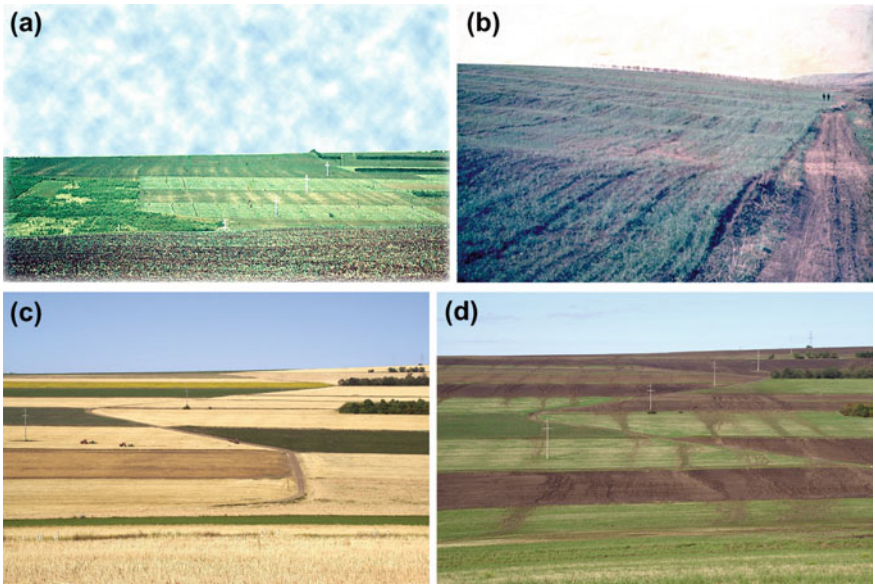

Fig. 15.10 Right side of Țărnii Valley: **a** Image from 1966 when individual plots were disposed on up-and-down hill direction. **b** microrelief formed by plowing up-and-down hill direction by overturning furrows laterally. **c** Image from July 2007 with the terrain arranged by soil conservation measures. **d** Surface and rill erosion during the rain from September 9, 2007

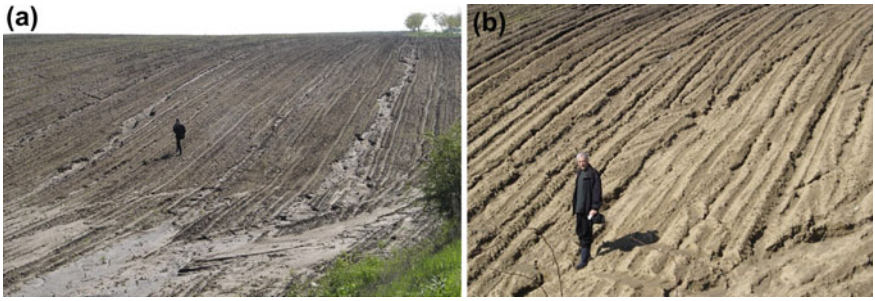

Fig. 15.11 Surface erosion caused by the rainfall from September 9, 2007, on the privately owned farm plots, worked on up-and-down hill direction (**a**, **b**)

area outside of this influence. The first case highlights the good condition of vegetation, compared to the other case, where the crop is totally compromised.

The results clearly demonstrate that forest belts contributed not only to reducing runoff and soil losses by water erosion but also to limit the effects of drought by ensuring more favorable microclimate for plant growth. Analysis of distribution in the basin of soil losses calculated by RUSLE method (Fig. 15.14e) showed that the right hillside is more affected by erosion than the left (it has a greater length, in some places exceeding 1000 m).

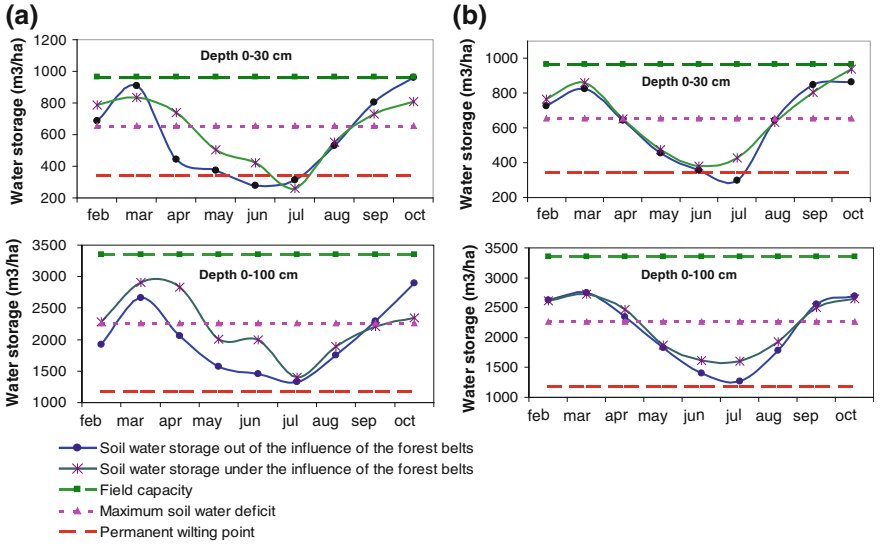

Fig. 15.12 Soil water storage in Ţărnii Valley in 2007, at depth intervals of 0–30 and 0–100 cm for the following crops: **a** Winter wheat. **b** Peas

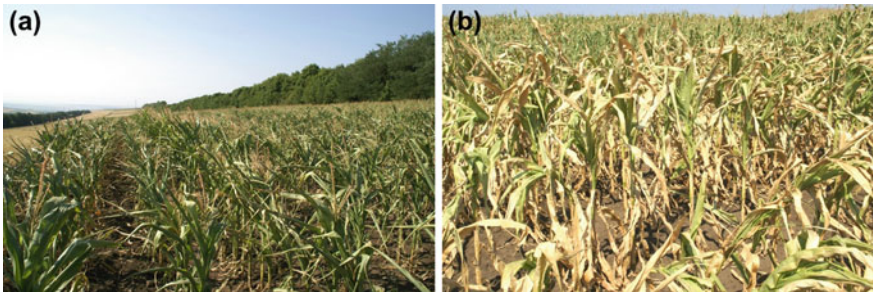

Fig. 15.13 Images from July 2007 of maize plots located: **a** between forest belts. **b** outside the influence of forest belts

Estimating Surface Erosion in Small Catchments by Conventional and Unconventional Methods

Application of RUSLE model required calculation of each factor of the equation. Rain erosivity factor for the period of 2004–2011 had the value of 796 MJ mm/ha h. The analysis of soil studies regarding Ţărnii Valley showed that 81.4 % of the area was covered by medium loamy soil, 9.5 % by clayey loamy soil, 6.7 % by clay and 2.4 % was silty-sandy. For each of these types of soil, the K factor was calculated and plotted on a map together with P factor, digital elevation

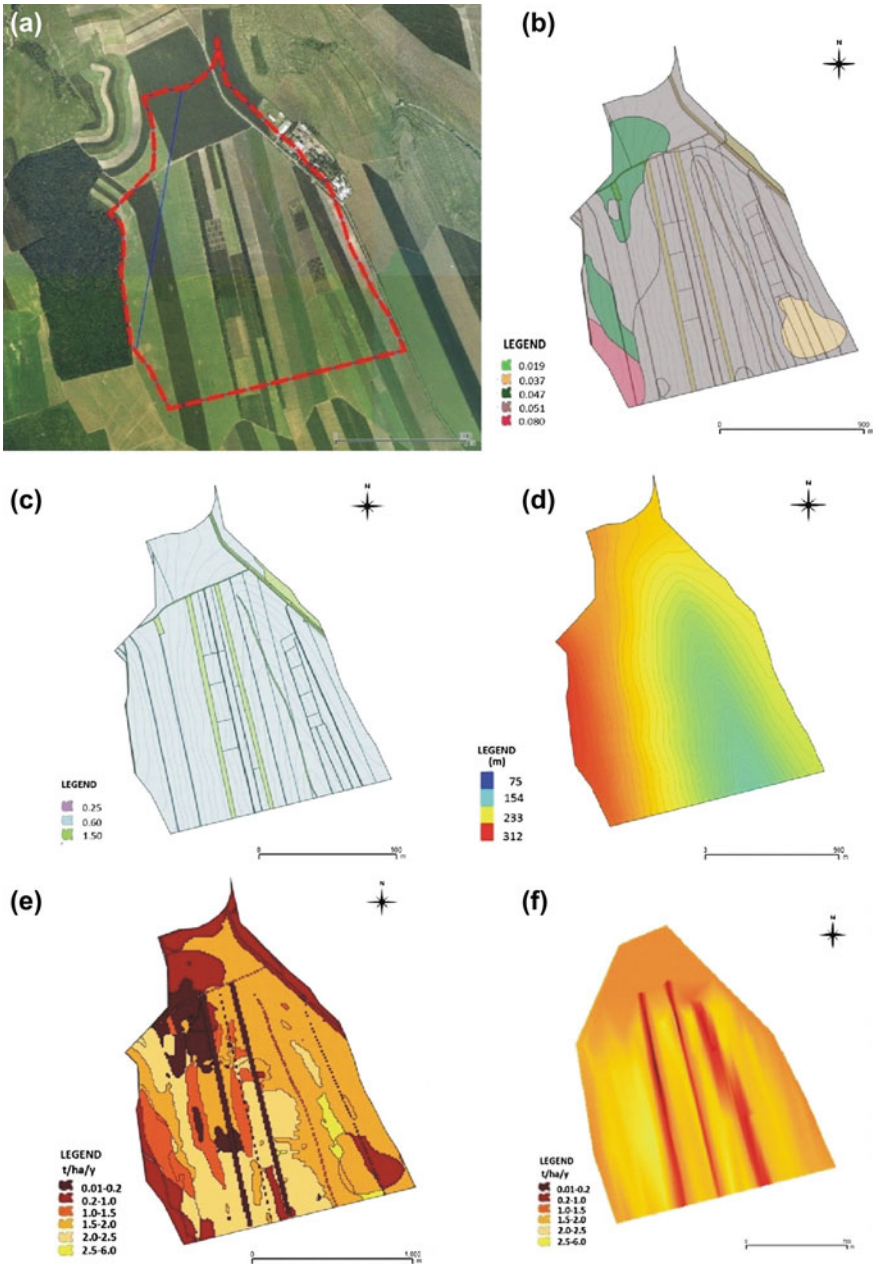

Fig. 15.14 **a** The orthophotomap of Ţărnii Valley. **b** The distribution map of *K* factor. **c** The distribution map of C factor. **d** The numerical elevation model of the land. **e** The distribution of soil loss calculated by RUSLE model included in the program of Idrisi Andes. **f** Distribution of soil loss determined by Caesium–137 technique

Table 15.4 Comparative calculation of soil losses in Țărnii Valley by RUSLE method and by Caesium–137 isotopes technique

Soil loss categories (t ha^{-1} year^{-1})	RUSLE				Cs–137 technique			
	Area (ha)	% from total	Soil loss		Area (ha)	% from total	Soil loss	
			Total (t year^{-1})	Avg. (t ha ^{1} year^{-1})			Total (t year^{-1})	Avg. (t ha^{-1} year^{-1})
0.01–0.20	24.3	10.7	0.77	0.032	1.3	0.6	0.04	0.032
0.20–1.00	35.6	15.7	24.05	0.675	12.7	5.6	11.11	0.875
1.00–1.50	20.1	8.9	24.31	1.206	33.6	14.8	48.72	1.450
1.50–2.00	93.3	41.2	161.53	1.730	105.4	46.5	203.00	1.926
2.00–2.50	50.0	22.1	123.69	2.474	68.2	30.1	169.14	2.480
2.50–6.00	3.1	1.4	8.65	2.736	5.4	2.4	24.03	4.450
Total	226.6	100.0	342.99	1.513	226.6	100.0	456.04	2.013

model (which includes *L* and *S* factors) and soil loss distribution (Fig. 15.14a–d). Depending on land use and crop structure, *C* factor values of 0.003 for shelter breaks, 0.02 for camp roads and 0.35 for arable land were noted. P factor values ranged between 0.6 and 1.0 depending on the extent of soil conservation measures implemented in the basin. Table 15.4 illustrates the results obtained on soil erosion by RUSLE method and by the Caesium–137 radionuclides technique.

In the middle of the hillside an erosion of 2.5 t ha^{-1} year^{-1} was estimated, while on the left side, values between 1.5 and 2.0 t ha^{-1} year^{-1} can be found on most of the surface except some small areas where erosion reaches values of 2.5–6.0 t ha^{-1} year^{-1}.

Also noteworthy is the influence of forest belts, on an area of approx. 10 ha, where erosion did not exceed 0.02 t ha^{-1} year^{-1}. The annual average of soil losses in the study area was 1.513 t ha^{-1} year^{-1}, significantly below the allowable amount of 4–6 t ha^{-1} year^{-1} and showed that soil conservation measures auctioned very well. The results obtained by the radionuclides technique showed that on about 21 % of the studied area soil losses were insignificant. Figure 15.14f reveals that this is the case especially in the forest belts and on bottom of the basin where the slope is greatly diminished.

The largest area representing approx. 77 % of the total is affected by erosion processes with values between 1.5 and 2.5 t ha^{-1} year^{-1}, while on small areas, erosion reached up to 6.5 t ha^{-1} year^{-1}. Similar to the results of the first method, it is found that the right hillside is more affected by erosion, particularly in the upstream parts of the forest belts. The annual erosion average for the entire studied area had the value of 2.013 t ha^{-1} year^{-1}.

Comparing the results obtained by these two methods, it is concluded that

- In areas with erosion below 1.0 t ha^{-1} year^{-1}, the method of radionuclides provided slightly underestimated data compared to those calculated by RUSLE;
- The general aspect of the distribution of soil losses obtained by the method of radionuclides is closer to that achieved by direct field observations made in the recent decades;

– The two methods were complementary one to another in that the method of isotopes provided more relevant results concerning the current state of land degradation by erosion and sedimentation whereas the RUSLE method allowed designing scenarios for the future evolution of erosion given the current and perspective influence of soil conservation measures.

Discussions and General Conclusions

Consistent results obtained by experimental research at RDCSEC Perieni were compared in short time and some very old measurements made in several areas in Romania (Table 15.5). These data, along with other estimates in Romania (Ioniță et al. 2006) show that surface and rill erosion summarize 61.8×10^6 t and represent 54.5 % of the processes that contribute to soil loss (ravination, landslides, polymorphic erosion).

Bare lands, without vegetation protection, had the highest rate of sheet and rill erosion (40.7 t ha^{-1} $year^{-1}$) which exceeded by far the value obtained on the same type of plots in Mediterranean environment (32 t ha^{-1} $year^{-1}$, according to Cerdan et al. 2006, 2010). Instead, on the parcels with different crops, values measured in Tutova Rolling Hills were less or comparable to those reported at European level. Cited authors consider that the distinction between the Mediterranean area and the rest of Europe consists in the type of soil subject to sheet erosion (e.g., the greater amount of skeletal fragments in Mediterranean soil), but also in the differences of vegetation density for these two types of regions. Evolution for a long time period (28 years) of soil erosion measured on the plots cultivated with different crops showed a diminution of the process (between 35 and 94 %) for all categories of land use. At the same time, a diminution of runoff was observed (consequently a greater capacity for infiltration of water from precipitation) and this given that the trend of total rainfall was positive in the same period of study.

Measurements on sloping farmland from the northern half of the Moldavian Plateau have registered a decrease of erosion by up to 16 % after only four years of crop rotation. Thus, the loss of soil was reduced to below the allowable limit of 3–4 t ha^{-1} $year^{-1}$. A decrease of total erosion in small catchments from the Moldavian Plateau was observed after 25 years of ameliorative interventions. By the use of crop systems (contour tillage and planting, strip cropping, grass strips and crop rotation of 3 and 4 years with an adequate crop structure (30 % winter wheat, 30 % maize, 30 % leguminous plants for grains and 10 % perennial grasses) soil losses were diminished by 79 %, in comparison with unarranged terrains (Ailincăi et al. 2012). Using evaluations for Europe (Cerdan et al. 2006, 2010), arable land contributes by more than 70 % to total soil losses. The average value of sheet and rill erosion for Europe is about 1.2 t ha^{-1} $year^{-1}$ for the entire area and about 3.6 t ha^{-1} $year^{-1}$ for arable land. Compared to these, erosion rates for Romania should be 4.2 t ha^{-1} $year^{-1}$, based on estimations made by Ioniță et al. (2006).

Table 15.5 Runoff plot data in Romania

Location	Measuring period	Plot land use	Slope (%)	Length (m)	Mean annual precipitation (mm)	Runoff rate (mm $year^{-1}$)	Erosion rate (t ha^{-1} $year^{-1}$)	Soil type	Source
Aldeni, Buzau	1975–81	Winter wheat	18	40	523.1	31.1	7.0		Ioniță (2006)
		Maize				66.2	26.6		
		Fallow				93.5	44.8		
Bilcesti, Arges	1968–85	Orchard on hillslope without terraces	25	20	737.5	36.9	13.80	Brown luvic, loamy-sandy	
				40		39.7	27.30		
		Orchard on terraces		20		27.0	5.10		
				40		14.0	2.80		
CeanTurda, Cluj	1950–59	Winter wheat	7	25	542.3		0.67	Mollisol loamy-clayey	
		Maize					7.90		
		Winter wheat	12				0.90		
		Maize					12.4		
Podu Iloaei, Iasi	1983–2012	Fallow	16	25	532.9	59.7	18.24	Mollisol loamy-clayey	Ailincăi et al. (2012)
		Sunflower				35.4	8.97		
		I^{st} year perennial grasses				18.7	1.91		
		Perennial grasses				6.3	0.25		
		Maize				29.6	8.42		
		Peas				21.3	3.79		
		Winter wheat				11.4	1.66		

(continued)

Table 15.5 (continued)

Location	Measuring period	Plot land use	Slope (%)	Length (m)	Mean annual precipitation (mm)	Runoff rate (mm $year^{-1}$)	Erosion rate (t ha^{-1} $year^{-1}$)	Soil type	Source
Perieni, Vaslui	1985–2012	Fallow	12	25	492.0	38.4	40.71	Mollisol loamy	Popa et al. (2012a, b)
		Maize				19.1	8.67		
		Beans				13.5	5.08		
		Winter wheat				5.4	0.71		
		Perennial grasses				3.2	0.33		

Table 15.6 Soil quality limiting factors and size of affected area (Bălteanu and Popovici 2010)

Soil quality limiting factors	Affected area		
	1992	2002	
	Thousands ha	Thousands ha	% of total agricultural land
Frequent droughts	3900	7100	48
Water erosion	4065	6300	43
Frequent moisture excess	900	3781	26
Landslides	700	702	5

Analyzing data published by the National Statistics Institute, (Bălteanu and Popovici 2010) show that the factors that exert the greatest impact on soil quality are different forms of erosion, together with the drought, excess moisture and all this nearly doubled in 2002 compared to 1992 (Table 15.6).

Land degradation and expansion of affected areas during the 1990–2007 time period are consequences of two important factors: human impact and climate and hydrological extreme events. By political and administrative decisions, arable lands were excessively fragmented (less than 2 ha) and precarious financial resources of the owners impeded the application of sustainable technologies of exploitation. Among the natural factors involved in soil quality degradation and thus in the accentuation of erosion processes were particularly the extreme hydro-climatic phenomena from the recent decades. In south eastern Romania (Dobrogea, The Bărăgan Plain and south of the Moldavian Plateau) desertification phenomena were registered. On the other hand, the severe floods in 1991, 2004, 2005, 2008, and 2010 destroyed a large surface of farmland. On sloping farmland (Subcarpathians, Moldavian and Transylvanian Depression Plateau Lands) landslides were reactivated in many areas (Bălteanu and Popovici 2010).

Acknowledgments The research leading to these results received partial funding from the Research Project ADER 1.1.2.(2011–2014) (Ministry of Agriculture and Rural Development), "Development of soil erosion control models at 1:1 scale, in small basins, in order to extend soil conservation measures."

References

Ailincăi C, Jitareanu G, Bucur D, Ailincăi D (2012) Soil erosion and conservation measures in Moldavian Plateau. Cerc. Agron. în Moldova XLV(4):29–42

Balteanu D, Popovici EA (2010) Land use changes and land degradation in Romania. Rev Roum Géogr/Rom J Geogr 54(2):95–105

Brakensiek DL, Osborn HB, Rawls WJ (1979) Field manual for research in agricultural hydrology. USDA handbook, vol 224. U.S. Department of Agriculture, Washington, DC

Cerdan O, Poesen J, Govers G et al (2006) Sheet and rill erosion. In: Boardman J, Poesen J (eds) Soil Erosion in Europe. Wiley, Chicester, pp 501–515

Cerdan O, Govers G, Le Bissonnais Y et al (2010) Rates and spatial variations of soil erosion in Europe: a study based on erosion plot data. Geomorphology 122:167–177

Florea N, Orleanu C, Ghitulescu N (1976) Harta eroziunii solurilor în România, sc 1:500,000. ICPA, Bucureşti (in Romanian)
Ionescu-Şişeşti G (1925) Fenomene de distrugere şi de reconstruire a solului. Publicaţia. Ministerului Agriculturii şi Domeniilor, Bucureşti (in Romanian
Ionescu-Şişeşti G, Staicu I (1958) Eroziunea şi lupta contra ei. Agrotehnica, Vol.II(X), Ed Agro-silvică de Stat, Bucureşti (in Romanian)
Ioniţă I, Ouatu O (1985) Contribuţii la studiul eroziunii solurilor din Colinele Tutovei. Cerc. Agr. în Moldova 3:58–62 (in Romanian)
Ioniţă I, Radoane M, Sevastel M (2006) – Romania, In: Boardman J, Poesen J (eds) Soil Erosion in Europe. Wiley, Amsterdam-London-New York-Oxford-Paris-Tokyo, pp 155–166
Moţoc M (1983) Ritmul mediu de degradare erozională a solului în R.S. România. Bul. Inf. ASAS Bucuresti 12 (in Romanian)
Moţoc M, Ioniţă I (1983) Unele probleme privind metoda de stabilire a indexului ploaie şi vegetaţie pentru ploi singulare la intervale scurte. Bul. inf. ASAS Bucureşti 12 (in Romanian)
Moţoc M, Sevastel M (2002) Evaluarea factorilor care determină riscul eroziunii hidrice în suprafaţă. Ed Bren, Bucureşti (in Romanian)
Neamţu T (1998) Ecologie, Eroziune şi Agrotehnică Antierozională. Ed Ceres, Bucureşti (in Romanian)
Nistor D, Nistor D (1979) Sistemul de lucrări minime ale solului pe terenurile în pantă erodate; Producţia vegetală - Cereale şi Plante Tehnice 1 (in Romanian)
Nistor D, Nistor D (1981) Aspecte economice şi energetice ale folosirii îndelungate a îngrăşămintelor la porumb. Producţia vegetală - Cereale şi plante tehnice 4 (in Romanian)
Popa A (1977) Cercetări privind eroziunea şi măsurile de combatere a acesteia pe terenurile arabile din Podişul Central Moldovenesc. MAIA, Bucureşti (in Romanian)
Popa A, Stoian G, Popa G et al (1984) Combaterea eroziunii solului pe terenurile arabile. Ed Ceres, Bucureşti (in Romanian)
Popa N, Filiche E, Petrovici G et al (2011) Using caesium-137 techniques to estimate soil erosion and deposition rates on agricultural fields with specific conservation measures in the Tutova rolling hills, Romania. IAEA-TECDOC-1665. Viena:259–278
Popa N, Nistor D, Filiche E et al (2012a) Studies on runoff and erosion rates in eastern Romania. In: Abstracts of the 1st CIGR inter-regional conference on land and water challenge, Bari, Italy, 10–14 Sept 2012
Popa N, Nistor D, Mărgineanu R (2012b) Soil erosion estimates in a small agricultural watershed. In: Abstracts of the international conference on land conservation—Landcon 1209, University of Belgrade, Faculty of Forestry, Belgrade, Serbia, 17–21 Sept 2012
Renard KG (1997) Predicting soil erosion by water: a guide to conservation planning with the revised universal soil losses equation (RUSLE). ARS, USDA
Schwab GO, Frevert RK, Edminster TW (1966) Soil and water engineering. Willey, New York
Vătau A, Teodorescu V, Ionescu V (1993a) Harta coeficienţilor de scurgere standard – România, sc. 1:500.000, ICPA Bucureşti, Ed. Direcţia Topografică Militară (in Romanian)
Vătau A, Teodorescu V, Ionescu V (1993b) Harta erodabilităţii solurilor–România, sc. 1:500,000. ICPA Bucureşti, Ed. Direcţia Topografică Militară (in Romanian)
Walling DE (2007) Models for converting radionuclide (137Cs, Excess 210Pb, and 7Be) measurements to estimates of soil erosion and deposition rates (Incl Software for Model Implementation). http://www-naweb.iaea.org/nafa/swmn/swmcn-databases.html
Wischmeier WH (1959) A rainfall erosion index for a universal soil-loss equation. Soil Sci Soc Am J 23(3):246–249
Zapata F (2002) Handbook for the assessment of soil erosion and sedimentation using environmental radionuclides. Kluwer Academic Publishers, Dordrecht

Chapter 16
Gully Erosion

Maria Rădoane and Nicolae Rădoane

Abstract Gullies are an important part of the soil erosion process and their occurrence and development may cause serious problems to a region's economy. Most types of gullies occur in Romania, but the majority are relatively small, discontinuous, valley-side gullies. To obtain some consistent observations on gully initiation and development in Romania's physiographic conditions, we sampled a large spectrum of gully types (i.e., over 9000 gullies were inventoried and 12 were surveyed in detail). The case studies from the Moldavian Plateau reveal that gully development occurs in accordance with allometric principles which are characteristic to a variety of natural phenomena; sidewall processes are 5–10 times more effective in dislodging soil and rock compared to downcutting and are highly dependent on the silt-clay content in the gully perimeter; and the hydraulic efficiency of gullies is substantially lower compared to streams, and thereby the transport of debris along the gully is essentially a pulsating process. The rate of gully head cutting is over 1.5 m/year for gullies cut in sandy deposits and under 1 m/year for the gullies cut in marls and clays. A model of gully development is proposed which shows an accelerated rate of gully development immediately downstream after their initiation and a reduced progress and even cessation of advance when attaining an equilibrium length.

Keywords Typology · Areal distribution · Morphometric analysis · Advancement rates · Moldavian Tableland

M. Rădoane (✉) · N. Rădoane
Ștefan cel Mare University, Universității 13, 720229 Suceava, Romania
e-mail: radoane@usm.ro; mariaradoane@gmail.com

N. Rădoane
e-mail: nicolrad@yahoo.com

M. Rădoane and A. Vespremeanu-Stroe (eds.), *Landform Dynamics and Evolution in Romania*, Springer Geography,
DOI 10.1007/978-3-319-32589-7_16

Introduction

Gully erosion is one of the most destructive soil/land erosion processes; within a short period of time the topsoil and the underlying unconsolidated rock substrate are removed by runoff, resulting in the formation of a steep-sided channel deeper than 2 m, with an abrupt gully headcut and numerous thresholds in the channel thalweg. This landform is commonly known as a ravine (gully), albeit it bears different names across the Globe (e.g., *arroyo* or *coulee* in USA, *uvrag* in Russia, *burone* or *fosco* in Italy, *ravin* in France, *donga* in South Africa, *lavaka* in Madagascar, *nullah* in India, etc.).

Due to the typically high gully development rates, these landforms have significant impact on vast farmland areas. Furthermore, they deliver large amounts of sediments to rivers and reservoirs. Gully erosion is regarded as an indicator of desertification (UNEP 1994); the main causes of which are allegedly global climate changes and anthropogenic pressure (Torri and Poesen 2014). However, experimental studies on gully erosion commonly lacked the ampleness of those dedicated to surface sheet erosion, even in Europe (Poesen et al. 2006). Gully erosion rate estimates showed that gullying is responsible for a large extent of the topsoil loss in small catchments, ranging to as high as 90 % or above in numerous instances (Poesen et al. 2003).

The contribution of research on gully erosion in Romania stemmed from several research topics, such as gully erosion as a sediment source (Moţoc et al. 1979; Mihaiu et al. 1979; Moţoc 1983, 1984; Gaşpar and Cristescu 1987; Moţoc and Sevastel 2002; Rădoane 2002), farmland degradation and fragmentation (Ioniţă and Ouatu 1985; Rădoane et al. 1995, 1999; Ioniţă 2000, 2003, 2008), forest domain soils (Traci 1985; Traci et al. 1981; Clinciu et al. 2010) and the behavior of gully erosion landforms as a response to erosion control works (Giurma 2000; Mircea 2002).

Defining gully erosion landforms was always a controversial topic, depending on the scientific field approaching the subject. Whereas agronomists and land improvement professionals were mainly focused on landforms occurring in non-cohesive rocks (i.e., *ravines*), foresters and forest soil preservation professionals were more invested in gullies occurring in cohesive rocks (i.e., *torrents*). According to Heede (1980), this is precisely the main distinction between the two terms. In a separate paper (Rădoane et al. 1999), we reviewed the various arguments and viewpoints regarding the two types of landforms; therefore, in the present study we dedicate this chapter to the former category of gully erosion forms, i.e., ravines (gullies).

The objectives we pursued in tackling this topic are structured as follows: (i) Gully typology; (ii) Gully distribution and analysis of regional control factors; (iii) Investigations on the shape and processes occurring in gully systems by means of study cases; (iv) Gully development rates and determining gully advancement rates; and (v) Gully erosion control and prevention.

Gully Typology

Gullies are ranked and classified according to a variety of criteria reflecting both the diversity of control factors and the genetic processes and evolution of these landforms; thus, we believe it is necessary to discuss first the most relevant aspects regarding gully classification. The following classes of gullies were identified as typical for the Romanian territory (cf. Bălteanu and Taloiescu 1978; Rădoane et al. 1999; Ioniță 2000): *continuous gullies*[1] and *discontinuous gullies*[2] are types of landforms which indicate the stage and pace of gully evolution; the gully *planform* may provide clues regarding their origin and the relation to the type of rock deposit whereby they were incised (Fig. 16.1 shows a summarized classification with short comments provided for each type); the location of gullies within drainage basins/catchments is relevant when determining the type of ephemeral runoff, the role of drainage upstream of the gully headcut or the occurrence of piping conditions. According to these criteria, several types of gullies were established: *valley floor gullies*, whereby the evolution is linked to the valley concentrating the runoff/discharge; *valley origin gullies* which develop headwards along the channel of the valley and may evolve into valley gullies; *hillside gullies* located on the hillslopes, independent of the valley channel. Furthermore, gullies can be ranked according to their *cross-section* ranging from U-shaped gullies to V-shaped gullies, with many intermediate types. The shape of the cross-section is related to the resilience of rock deposits to erosion and the nature of geomorphic processes (Rădoane 2002).

Gully Distribution

The distribution of gullying processes was studied in Romania mainly based on the inventory of gully erosion landforms from the Moldavian Plateau (Ichim et al. 1990; Rădoane et al. 1999; Stângă 2011), Buzău Subcarpathians (Mihaiu et al. 1979; Mircea 1999), Southern Subcarpathians and Getic Piedmont (Otlacan-Nedelcu 2001; Jurchescu 2012), Braşov Depression (Clinciu et al. 2010), etc. One of the most elaborate investigations of this kind was conducted by Rădoane and Rădoane (1992),

[1]The incision of continuous gullies is generated by the presence of numerous rills branching out in the gully headcut area. They rapidly become increasingly deep downstream and retain an approximately constant depth throughout the length of the gully. In the vast majority of instances continuous gullies form gully systems (networks). Albeit they occur under various climate conditions, they are prevalent in arid and semiarid regions.

[2]The evolution of discontinuous gullies is initiated by a knick point anywhere on the hillside profile, and their depth decreases towards the gully mouth. A discontinuous gully will evolve into a continuous one as the gully head migrates towards the upper edge of the watershed and the channel deepens. Several discontinuous gullies developing on a hillside can merge and form a continuous gully if the in situ rock does not interfere with or restrict this process.

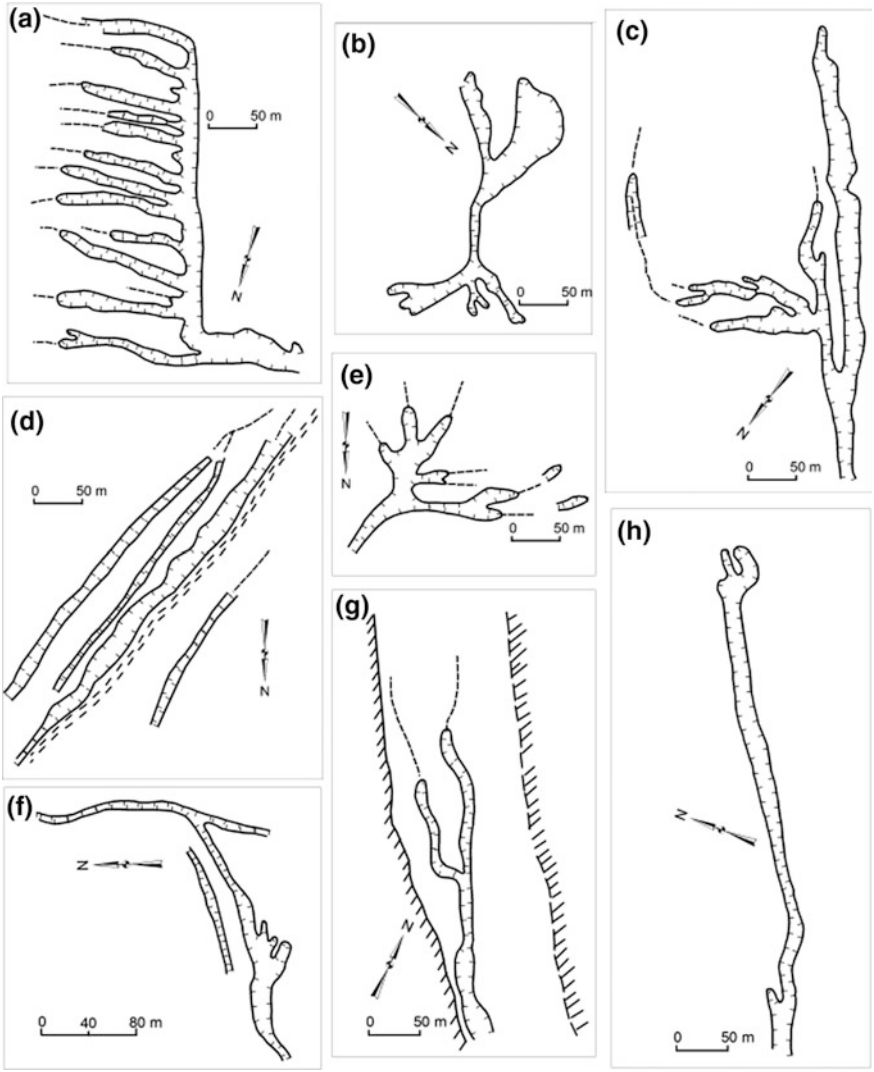

Fig. 16.1 Gully planform configurations representative for Podișul Moldovenesc (the Moldavian Plateau): **a** Trellis-type gully in Deleni area, Iași, with depths ranging between 2 and 3 m, which initially formed along an old trail and eventually evolved on the bottom of a dell. **b** Gully bulb type in Crăiești, Tg. Bujor area, incised in predominantly sandy deposits which boosted processes such as suffusion/piping and collapse in the gully headcut area. **c** Gully composed of discontinuous secondary gullies and linear continuous gully. **d** Parallel gullies which developed as a result of cart trail relocation in Todireni area, Iași. **e** Dendritic gully. **f** Hillside confluence gully forming at cart trail intersections. **g** Gully developed in Bahlueț river floodplain, in Ceplenița. **h** Linear gully in Sulița, Botoșani

and was further enhanced by employing advanced research techniques, albeit on a smaller scale, by Stângă (2011).

The Moldavian Plateau, delimited roughly by Siret and Prut watercourses, amounts to approximately 25,000 km^2 and comprises the most extensive areas affected by polymorphic land degradation processes.

According to official reports from 2010, of the 3,372,916 ha of land undergoing severe erosion in Romania, this region accounts for no less than 33.5 % (www.anpm.ro), which can be attributed to the mixed action of control factors, namely:

The *regional geology* consists mainly of poorly consolidated Sarmatian rock formations, as well as Pliocene deposits in the southern sector of the Plateau. The following sequence of main lithological complexes unfolds southward: Buglovian–Bessarabian, composed predominantly of *loamy marls*; Kersonian, comprising of *marly clays* and *sands*; Meotian, consisting of *clay* and *sands interbedded with sands and tuff*; Pontian–Romanian, comprising of *gravel* and *sands* (Fig. 16.2, the location of these lithological entities is shown in the inset). The *relief* shaped on this substrate consists of numerous consequent river valleys whereby the hillsides often exceed 300 m up to 500 m in length and their gradients typically range between 20 and 30 %.

The *climate elements* which control gullying processes are temperature and precipitation quantized in the shape of the *hydrothermal coefficient* (Zachar 1982). When this coefficient assumes value between 1.25 and 2.50, the most favorable conditions for gullying are met, and the Moldavian Plateau ranks within this interval.

The dynamics of *land use/land cover* in Moldova throughout the past two centuries indicates that forested areas decreased from 75 % to as little as 25 %. Currently, forests account for just 15 % of the total study area (EEA 2007). Agricultural uses are prevalent, with an "*atomization*" of the agricultural farms amounting to about 45,000 parcels, with an average surface of 0.7 ha, and the frequently up- and down-slope farming (Stângă 2011).

Over 9000 gullies were inventoried in this region, such that 36 % of the 1 km^2 squares each contain at least one gully. Whereas the number of gullies per unit area (1 km^2) commonly ranges between 2 and 4, in some instances it can be as high as 20. The map in Fig. 16.2 indicate several clusters of areas with high gully density per 1 km^2, mainly in Jijia basin, upper Bahluieț basin and Bârlad middle basin. The density values range from 0.1 to 3 km/km^2, with an average value between 0.1 and 1 km/km^2. The highest susceptibility to gully erosion was documented in Bârlad middle basin.

Figure 16.3 shows how lithology and landform configuration can act as controls in the gully erosion process, indicating that:

In terms of the *geological structure and slope aspect* the largest number, as well as the highest density of gullies, occur on the hillsides of consequent valleys on the NE and SW slopes (Fig. 16.3a), whereby 50 % of the total numbers of inventoried gullies are located, ensued by the NW slopes, i.e., the cuesta escarpments (15 % frequency). In terms of the *hillslope energy*, the peak frequency of gullies was documented on slopes whereby the energy ranges from 50 to 100 m (average 53 m;

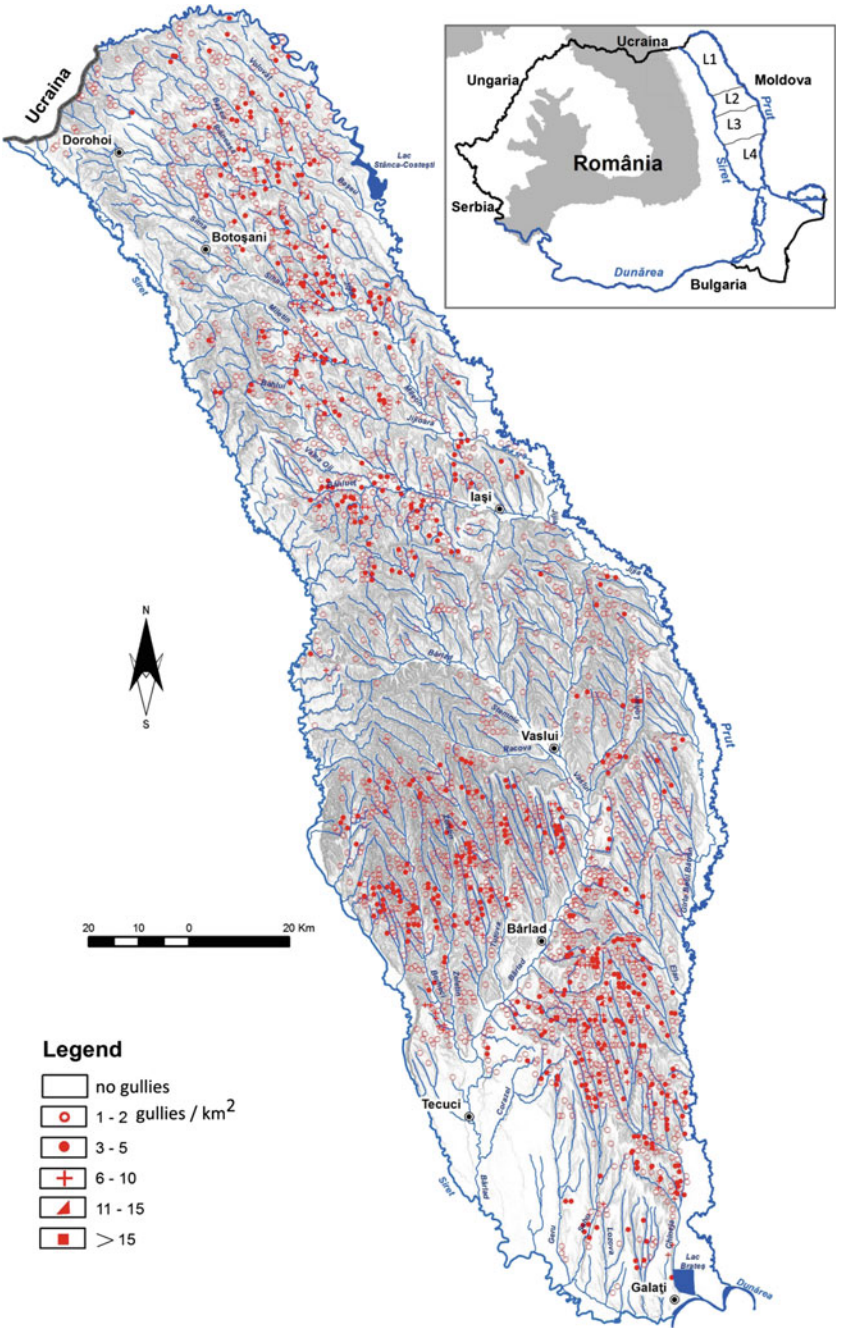

Fig. 16.2 Map of gully density per km^2 within the region delimited by Siret River to the west and Prut River to the east. In the inset: L1–silt-clay lithology; L4–predominantly sandy lithology; L2 and L3–intermediate types of lithology

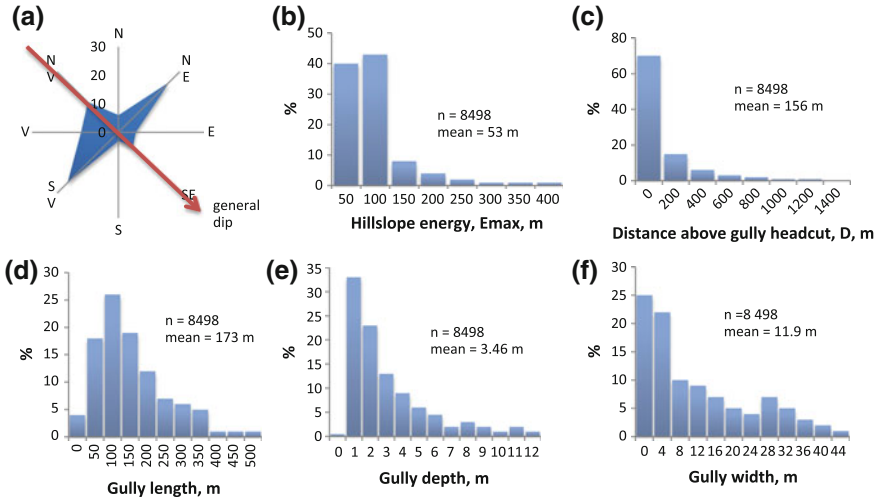

Fig. 16.3 Number of gullies related to: **a** slope aspect and direction of geological strata; **b** hillslope energy; and **c** distance from the gully headcut to the watershed. Frequency distributions of: **d** gully length; **e** gully depth; and **f** gully width in the Moldavian Plateau

Fig. 16.3b). In relation to *the slope gradient*, the gully frequency is distributed as follows: gradients ranging from 16 to 32 m/100 m correspond to 60 % of gullied hillsides. As regards the distribution related to *slope length,* the largest number of gullies occurs on slopes ranging between 250 and 500 m, regardless of the lithology of deposits. Another parameter relevant to understanding this process is the distance from the gully headcut to the watershed, also known as critical distance of gullying (Graf 1977), as it provides an indication of the stage of the gullying process. The peak frequency of this parameter ranges from 0 to 200 m, with an average of 170 m (Fig. 16.3c).

The variables describing the geometry of inventoried gullies are gully *depth, width, and length.* Distribution histograms (Fig. 16.3d–f) indicate a general right-side asymmetry (particularly in terms of depth), whereas the width exhibits a slight bimodality. The depth increases southwards within the study area according to the distribution of deposits lithology as follows: 2 m in most gullies developed on loamy marls (L1), 3–4 m on marly clays and sands (L2 and L3) and 4–5 m on rocks with greater sand content (L4). The gully width varies in a similar manner, from 8 m in L1 to 12–16 m in L2–L4. The width frequency distribution is highly bimodal in L3 and L4; the clustering of values in two groups (i.e., between 0 and 16 m, and 20 and 40 m, respectively) is determined by the type of gully: the former group comprises mainly hillslope gullies, whereas the latter includes valley gullies which are generally wider. As regards the gully length, the average value for the entire study area ranges from 100 to 150 m with a slight decrease depending on the lithological grade from L1 to L4 (see also Fig. 16.2 to locate areas with variable lithology).

To conclude, the amount of soil and rock removed by gully erosion from the area located between Siret and Prut Rivers was evaluated at 274 million m^3. If this amount were converted to a layer of topsoil and rock and distributed evenly across the study area, the thickness of the resulting layer would amount to 10.9 m. While this figure is undoubtedly impressive, it is, however, justified by the aggressiveness of this destructive process spanning a long period of time (100–450 years), affecting mostly agricultural lands. Unlike other forms of erosion, gully erosion displaces massive quantities of soil and rock which cannot be restored in a foreseeable timeframe.

Case Study Investigations on Forms and Processes in a Gully System

Detailed research conducted on a variable number of (i.e., 12–19) gullies (Table 16.1) in eastern Romania included topographical surveying, sampling rock material within the gully perimeter and measuring repeatedly the morphology of

Table 16.1 Morphometric characteristics of investigated gullies (Rădoane et al. 1999)

No.	Name	Length (m)	Active surface area (m^2)	Average depth (m)	Average width (m)	Average cross-section area (m^2)	Volume of materials removed (m^3)
1	Suliţa	1536.0	51,266	4.41	33.71	108.44	166,502
2	Gurguiata	704.5	35,205	6.30	43.34	186.97	131,648
3	Coada Gâştii	158.8	720,000	6.70	53.00	195.20	31,005
4	Roşcani I	881.3	9969	4.35	12.36	30.82	27,311
5	Roşcani II	338.0	3803	4.58	11.92	31.51	10,650
6	Poiana I	351.0	5102	5.03	14.58	52.00	18,252
7	Poaiana II	247.5	5367	5.46	21.55	74.39	5334
8	Poiana III	87.7	787,000	3.35	8.00	16.30	1429
9	Fântânele I	399.0	9789	5.02	22.75	76.68	30,595
10	Fântânele II	85.7	787,000	5.54	24.71	85.21	1426
11	Bâzanu	873.8	11,829	4.64	13.82	54.54	47,633
12	Meria	290.0	6267	6.67	22.88	81.52	23,641
13	Secăreşti I	424.0	8807				22,453
14	Secăreşti II	414.0	5809				15,108
15	Cepleniţa	410.0	20,076				55,368
16	Gurguiata Mică	145.0	1493				7088
17	Deleni	262.0	3902				4371
18	Ungureanu	263.0					7298
19	Giurgeni	428.0	6269				26,228

Table 16.2 Morpho-sedimentological variables describing investigated gullies (Rădoane et al. 1999)

Variable	Symbol	Measuring unit	Variation amplitude
Gully length from gully headcut	*L*	m	1536.0–89.75
Gully relief	*E*	m	80.3–24.10
Gully planform area	SA	m^2	51,266.0–786.90
Maximum depth	HX	m	11.75–0.30
Average depth	HD	m	7.74–0.14
Width	*B*	m	53.20–1.10
Cross-section perimeter	*P*	m	68.00–3.40
Gully floor width	LFR	m	12.60–0.10
Width/depth ratio	$F = B/HX$	–	4.53–3.67
Hydraulic radius	$RH = SS/B$	m	7.89–0.44
Cross-section area	SS	m^2	419.20–0.48
Shape factor (Heede 1974)	SF = HX/HD	–	1.52–2.14
Cumulative volume of removed material: – By sidewall processes – By downcutting processes	*W* WM WA	mł/m mł/m mł/m	99,519.0–4.00 39,983.0–0.10 42,330.0–0.10
Average diameter of material: – From gully floor – From gully walls	DA DT	mm mm	0.35–0.0008 0.24–0.0016
Silt-clay percentage of material: – From gully floor – From gully walls	FA FT	% %	95–1 93–9
Weight mean of silt-clay percentage in the gully cross-section	$M = [(SC \times B) + (SB \times 2D)]/B \times 2D$	–	92.78–7.86

gully headcuts. Thus, for each gully we determined a set of morphometric and sedimentological variables listed in Table 16.2.

The geomorphometric and sedimentological aspects selected for a brief presentation are connected to: (i) allometric gully development; (ii) the effect of particle size composition of gully deposits; (iii) the nature of geomorphic processes occurring in the gully system; (iv) the shape factor and hydraulic efficiency in gully development.

(i) Allometric gully development

The hydraulic geometry concept, as defined and developed by Leopold and Maddock (1953) is, according to Woldenberg (1966), one of the clearest examples of allometry in geomorphology. Many authors regard gullies as "valley embryos/buds" (as Vâlsan poetically stated in 1945; in fact, his statement referred to "torrents as valley embryos", but we may extend his assertion to gullies, as well); therefore the allometric growth model also applies to a similar extent to gullies.

The independent variable employed to demonstrate gully allometry was the *distance from gully head to mouth* (DVF); its selection was motivated by the fact that the gully headcut changes very rapidly, thus resulting in changes of all downstream geometric parameters (Seginer 1966; Rădoane et al. 1999). Depending on this variable, the variation patterns of all parameters describing gully shape were determined (listed in Table 16.2). Results showed that these are positively related to DVF and depend on it to a variable extent (50–90 %); the only exception is the slope gradient along the gully which is independent of the gully length variation.

We illustrate Cepleniţa Gully (Fig. 16.4a), whereby the planform and in-depth development are quantized in the equation in Fig. 16.4b. The "b" exponents of the power equation measure the proportional changes of the active area (AA) and cross-section area (CS) in relation to the distance from the headcut (DVF). According to Church and Mark (1980), if $b = 1$, the ratio is constant and no change occurs in terms of relative proportion or shape (i.e., the non-allometric or isometric case). Allometry occurs and is positive if $b > 1$, and negative if $b < 1$. The greater the b value, the faster the change in the value of the morphometric variable of the gully. Not all geometric parameters have the same change rate along the gully. The highest change rate pertains to the volume of deposits displaced from the gully (W) with the highest growth ($b > 3$); the planform development of the gully ($b > 1.852$) is faster compared to the in-depth development ($b > 1.258$).

In the investigated gullies from the Moldavian Plateau we documented a common tendency of increase in size to a much faster rate in Cepleniţa and Giurgeni gullies compared to Gurguiata, Secăreşti and Coada Gâştii, which share a slower development rate.

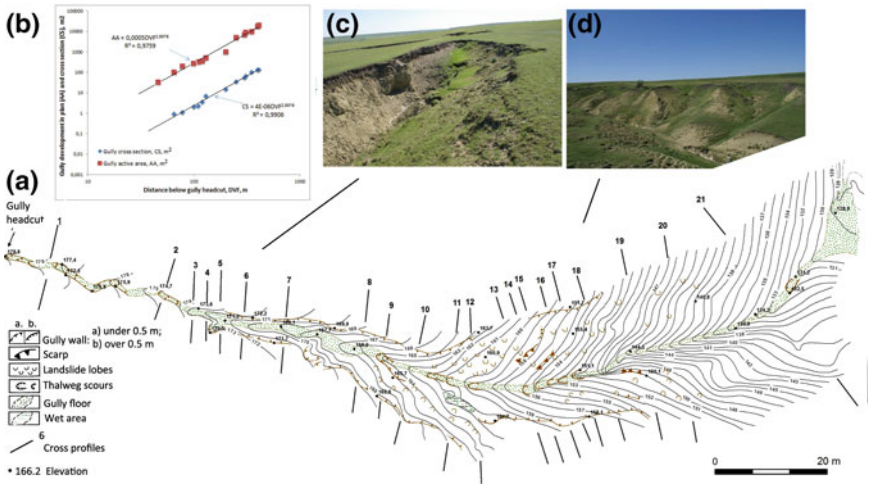

Fig. 16.4 **a** Cepleniţa Gully, located in the vicinity of Hârlău (see Fig. 16.2). **b** Planform and in-depth allometry curves of gully development (**c**, **d**)

(ii) The effects of gully deposits grain size

Similar to the lithological influence exerted on gully distribution within the Moldavian Plateau, particle size appears to have a significant influence on gully morphometry. Grain size analyses of superficial deposits within the gully perimeters resulted in the diagrams in Fig. 16.5, based on which we came to the following conclusions.

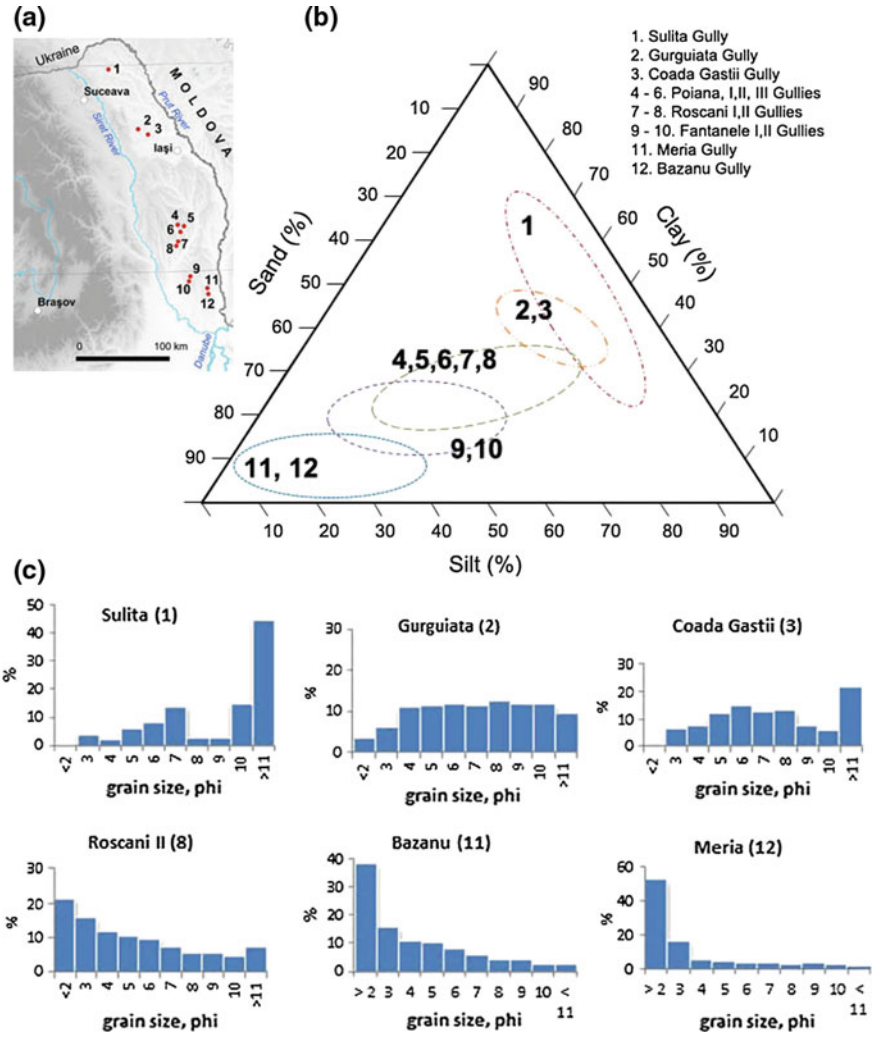

Fig. 16.5 Grain size distribution in gully deposits from the Moldavian Plateau (numbers according to Table 16.1). **a** Gully location within the study area. **b** Clay, silt and sand content in gully deposits from the Moldavian Plateau. **c** Histogram of average grain size distribution in gully deposits

In terms of particle size, gully deposits are grouped in three areas: (i) *clayey-silty,* characteristic for gullies from the northern half of the study area (Sulița, Gurguiata, Coada Gâștii), overlying middle ald lower Sarmatian marls and clays. The grain size distributions typical for these deposits have in common a right-side asymmetry (Sulița gully) generated by the prevalence of fine-grained fractions, above 10 %; (ii) *silty,* comprising gullies from the middle sector of the investigated area, which marks the transition from upper Sarmatian marls and clays to Meotian sands with intercalations of sandstones and clays (Roșcani and Poiana gullies). In this case, grain size distributions are either unimodal, symmetrical (around 4–8 phi), or bimodal, well represented at the extremities of histograms, i.e., >10 phi; (iii) *sandy*, in the southern sector of the study area (Fântânele, Bâzanu, Meria gullies) where the substrate is predominantly composed of Meotian, Pontian, and Romanian deposits (sands and clays with intercalations of tuffs and sandstones). Histograms indicate high percentages of diameters below 2 phi.

Processing a large number of morphometric and sedimentological variables for each gully required the use of multivariate analysis methods in order to capture the degree of sensitivity to creating the most "efficient" landform. We were able to emphasize the role of the *M parameter* which aggregates the characteristics of the cross-section geometry and those of particle size composition. This parameter is in fact called the *weighted average of the silt-clay percentage in the gully perimeter*.

In his study on river channels, Schumm (1960) employed this parameter as a factor which could explain the shape and stability of the alluvial channel cross-section and reached the following conclusion: as the silt-clay percentage in the channel perimeter increases, the channel becomes narrower, deeper and more stable; conversely, the lower the silt-clay percentage, the wider, more superficial and unstable becomes the channel.

In gullies, the weighted average of the silt-clay percentage controls the cross-section shape; albeit, the relationship is reversed, such that a low value of the M parameter is usually typical for deep, narrow, steep-walled gullies. When the perimeter is composed of deposits with high percentage of silt-clay, the gullies tend to be broad and less deep. The significance of this gully morphology is related to the nature of geomorphic processes in gully systems (which will be discussed in the following section of the chapter).

In the case of gullies from the Moldavian Plateau, the diagram in Fig. 16.6 supports the observation concerning the role of the M parameter in generating groups of gullies in the investigated area. Thus, three classes of values can be distinguished: class III ($M < 20$), in the southern Moldavian Plateau whereby gullies are deep and narrow, with large headcut thresholds and walls withdrawal occurs by undermining the wall bottom (e.g., Meria, Bâzanu, Poiana); class II (M ranges from 20 to 60), characteristic for the middle sector of the study area, where gullies tend to broaden their cross-sections by means of landsliding (e.g., Roșcani, Fântânele); class I ($M > 60$), characteristic for the northern sector of the Moldavian Plateau, whereby the evolution of gullies is controlled mainly by landsliding in the area located immediately downstream of the gully headcut (e.g., Ungureanu, Deleni, Gurguiata, Coada Gâștii, Sulița).

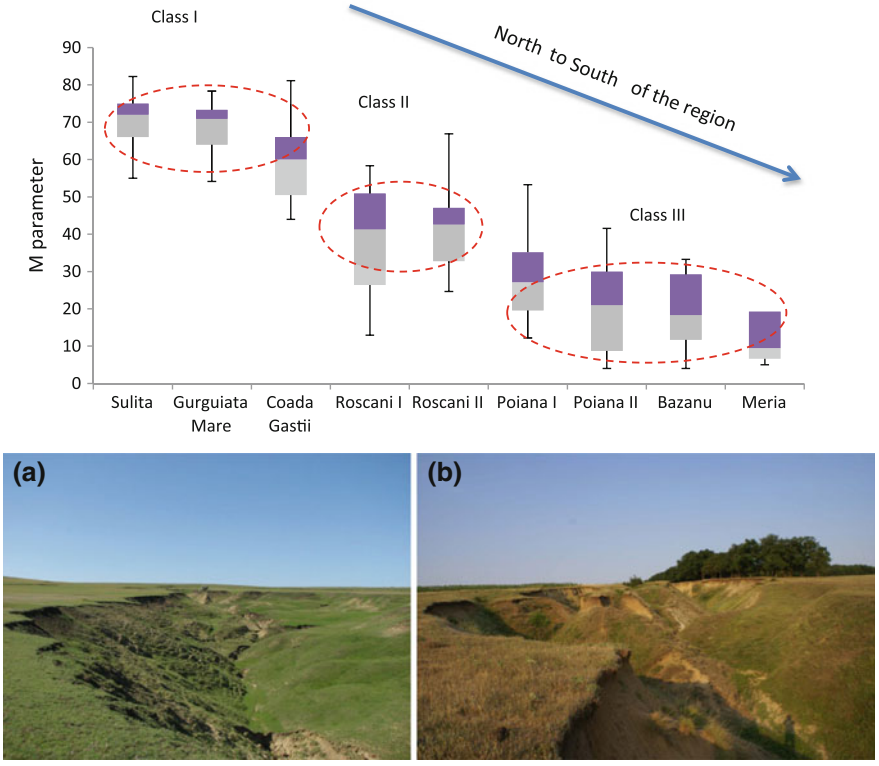

Fig. 16.6 Groups of gullies from the Moldavian Plateau according to the value of the *M* parameter (further discussion in text). **a** Gurguiata Mare Gully, incised in clayey-silty deposits, with broad cross-section and landsliding just downstream of the gully headcut. **b** Bâzanu Gully, incised in predominantly sandy deposits, with steep walls and frequent rock failures

To sum up, the weighted average of the silt-clay percentage in the gully perimeter is a valuable indicator for further defining categories of erosion control interventions. In the following sections we will find that the grain size composition of deposits not only controls the shape of the cross-section, but also the nature of geomorphic processes in the gully system is also strongly influenced by the type of deposit on which the gully develops.

(iii) The nature of geomorphic processes in the gully system

The processes occurring in a gully pertain to two types (Bradford and Piest 1980; Roloff et al. 1981): *sidewall processes* (mass-wasting, rills, badlands) and *longitudinal transport processes*. In order to assess the share of each category of processes, the indirect method introduced by Veness (1980) was employed. In building the plot (Fig. 16.7a), we hypothesized that the two sources of sediments are equivalent (Wa, the volume of debris resulting from downcutting processes = Ww, the volume of debris yielded by sidewall processes), such that the result is a straight

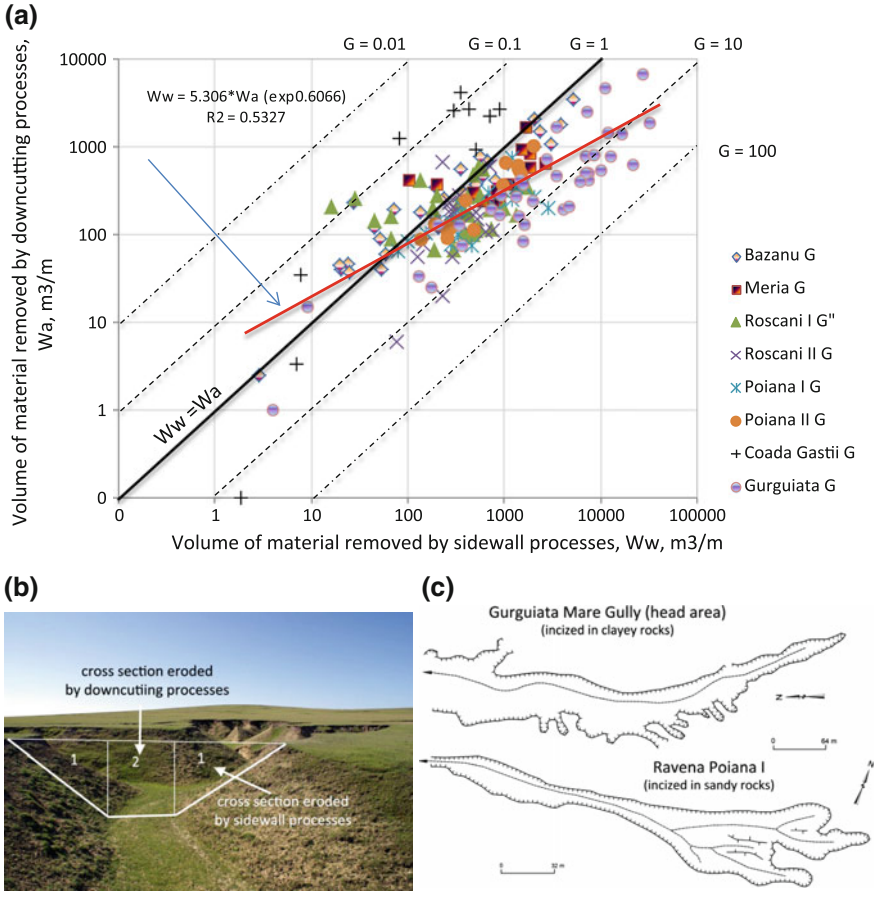

Fig. 16.7 **a** Relationship between the amounts of material removed from the gully cross-section by downcutting and sidewall processes, respectively, in investigated gullies from the Moldavian Plateau. **b** Method of assessment of the two types of processes occurring in a gully (Gurguiata Mică Gully). **c** Illustration of gully planforms depending on the dominant erosion processes: wedge-shaped Gurguiata Mare gully incised in clayey rocks versus lobate-shaped Poiana I gully incised in rocks with increased sand content

line and the ratio between the two variables is $G = 1$. The gullies in the study area were positioned depending on this line; with few exceptions, the G ratio ranges between 0.1 and 10, albeit the G value ranges from 1 to 10 in over 65 % of the instances. Based on these data, further conclusions can be drawn

- overall, sidewall erosion processes can account for up to $1 \div 5$ times as much as downcutting in terms of gully erosion;
- gullies incised in rocks with high silt-clay contents have G ratio values below 1 (i.e., downcutting is prevalent) in the upper third of the gully, and above 1 up to as high as 10 in the lower sector of the gully (whereby lateral withdrawal

through sidewall erosion processes is prevalent). In this case, the gully has a wedge-shaped planform (as illustrated by Gurguiata gully, Fig. 16.7c);
– gullies incised in rocks with high sand contents often have lobate (or pear shaped) planforms (e.g., Poiana gully, Fig. 16.7c, or Meria), due to sidewall processes being dominant in the upper third of the gully, whereas incision is prevalent in the lower sector.

According to researches conducted by Rădoane (2002) and Ioniță (2000), the two dominant types of processes in gully systems are also being controlled by climate seasonality: i.e., sidewall processes are more active during the cold season due to the successive freeze-thaw cycles and provide 57 % of the displaceable material from the gully, whereas downcutting is active particularly during the warm season, when runoff can concentrate in the gully thalweg and thus evacuate the displaced material.

(vi) The shape factor and hydraulic efficiency in gully development

The shape factor (i.e., the ratio between maximum depth and average depth) as introduced by Heede (1974) is another relevant parameter whereby the value becomes significant in relation to river channels. The gully shape factor is commonly above 2, which indicates that the cross-section has a broad "wet" perimeter, which in turn conveys the hydraulic inefficiency of gullies. Conversely, rivers in a state of dynamic equilibrium have average shape factors below 2, thus indicating high hydraulic efficiency. The 2.0 value of the shape factor was defined by Heede (1974) as the *hydraulic efficiency threshold*.

By applying this concept to the investigated gullies (specifically longer ones) from the Moldavian Plateau (Fig. 16.8), we determined that most cross-sections

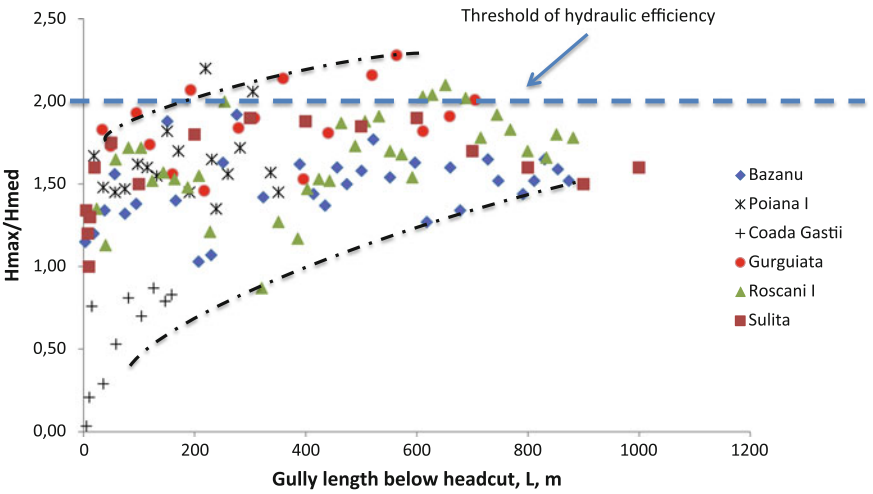

Fig. 16.8 Threshold of hydraulic efficiency in continuous gullies from the Moldavian Plateau highlighted through the relationship between the shape factor (see Table 16.2) and gully length

rank below the hydraulic efficiency threshold. The general trend is the rapid increase along the first 100 m of the gully length, ensued by stagnation and even decrease in the hydraulic efficiency as the gully unfolds in terms of length. The reason lies in the fact that displaced material is to a large extent relented on the gully floor, mainly in the lower sector. Ioniță (2000, 2003, 2006) elaborated on this phenomenon in the case of discontinuous gullies, where the Heede factor is not applicable. Therefore, Ioniță (2003) proposed the $Sp/Sf = 1$ ratio as a threshold for hydraulic efficiency in discontinuous gullies (where Sp = area of actual cross-section, Sf = area of silted cross-section). Thus, the pulsating activity of erosion and accumulation processes along discontinuous gullies may be assessed.

To conclude, the case studies from the Moldavian Plateau reveal that gully development occurs in accordance with allometric principles which are characteristic to a variety of natural phenomena; sidewall processes are 5–10 times more effective in dislodging soil and rock compared to downcutting and are highly dependent on the silt-clay content in the gully perimeter; and the hydraulic efficiency of gullies is substantially lower compared to streams, and thereby the transport of debris along the gully is essentially a pulsating process.

Gully Advancement Rates

Surveys on gully advancement rates and surface development rates were carried out by Rădoane et al. (1995, 1999, 2009) on test gullies from the Moldavian Plateau (Table 16.3). Ioniță (2000, 2003, 2006) and Hurjui et al. (2008) also conducted surveys on several gullies from Colinele Tutovei. The methods applied included the usage of topographical equipment and/or series of large-scale maps (1/5000), orthophotos and GPS measurements.

Table 16.3 Surface growth and headcut advancement rates for some gullies from the Moldavian Plateau

Gully	Initial survey	Second survey	Third survey	Area development (m^2)	Annual rate of development		Headcut advancement (m/years)
					m^2	%	
Suliţa	1987		2008	0	0	0	0
Gurguiata Mare	1986	NA	2008	0	0	0	0
Gurguiata Mică	1986	1998	2008	439 355	45.0 35.5	1.45 1.27	1.10 0.82
Coada Gâştii	1986	NA	2008	36,000	1636	0.23	0.45
Poiana I	1991	1998	NA	207	29.6	1.04	0.86
Poiana II	1991	1998	NA	254	36.3	1.00	1.00
Bâzanu	1991	1998	NA	2219	317.0	4.07	1.00
Meria	1991	1998	NA	158	22.6	0.61	1.10

Large gullies, such as Sulița and Gurguiata Mare, have reached an extinguishment stage and are thus converted into elementary valleys. Smaller gullies from the southern Moldavian Plateau, however, are still in the active stage, advancing at rates of 1 m/year or above. Moreover, investigated gullies from the southern sector are also expanding at faster rates in terms of surface growth.

Within the study area, we observed that in large gullies the only active feature is the development of an aggressive affluent/tributary (as is the case with Gurguiata Mică), which can destabilize the entire gully system. We illustrate the headcut advancement of Gurguiata Mică gully (see Table 16.1 for size data) in order to understand the nature of processes occurring within the gully during a 22-year period (Fig. 16.9). The headcut area and the adjacent downstream channel sector

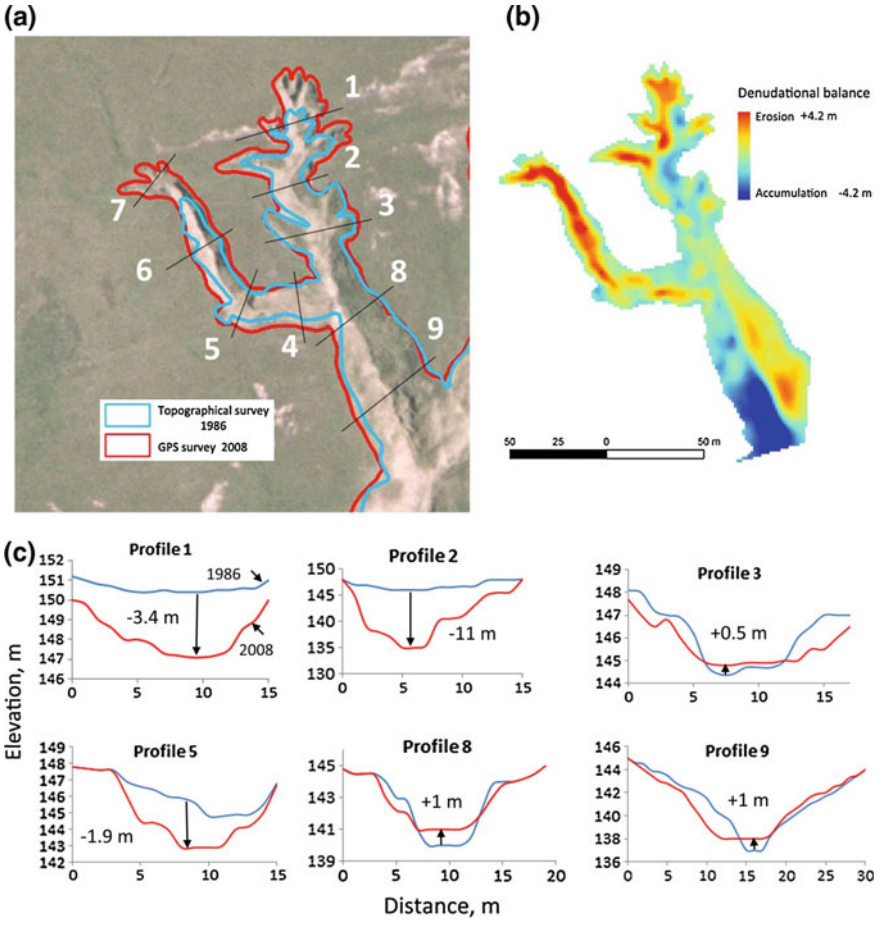

Fig. 16.9 Advancement of Gurguiata Mică Gully between 1986 and 2008 **a** Two successive gully shape measurements on orthophotos. **b** Denudational balance of the gully: erosion zones versus accumulation zones. **c** Cross-sections along the gully

are the most dynamic portions of the gully (whereby incision was as high as 11 m in the 22-year period). Downcutting is replaced downstream by gully floor aggradation, which indicates that displaced material was distributed along the gully. The highest aggradation occurs at the confluence with Gurguiata Mare gully, where sidewall processes are also significant in terms of the global denudational balance of the gully.

Long-term direct surveys (over 30 years) on discontinuous gully advancement in Colinele Tutovei (Ioniță 2000, 2003, 2006) revealed that the average advancement rate was 0.92 m/year (ranging from 0.42 to 1.83 m/year). The mean surface growth was 17 m^2 (ranging between 3.2 and 34.3 m/year). Over 60 % of the total gully development occurred in just 5 years (1980, 1981, 1988, 1991 and 1996). The age of discontinuous gullies ranges between 23 and 48 years.

The advancement rate was considerably higher in continuous gullies (i.e., 12.5 m/year on average) and a similar decline was documented between 1961 and 1990. Headcut advancement occurred with an increase in gully area by 366.8 m^2/year. Just 4 years (1981, 1988, 1991 and 1996) accounted for 66 % of the total gully growth, due to larger amounts of precipitation (Ioniță 2006).

Measurements on the development of continuous gullies from Colinele Tutovei conducted by Hurjui et al. (2008) indicated that gullies (both valley and hillside gullies) account for 3.6 % of the total area of a stream drainage basin/catchment (such as Studinet catchment, A = 96.8 km^2) (Fig. 16.10). In the second catchment, Simila (A = 265.21 km^2), 122 gullies were inventoried, of which only 10 %

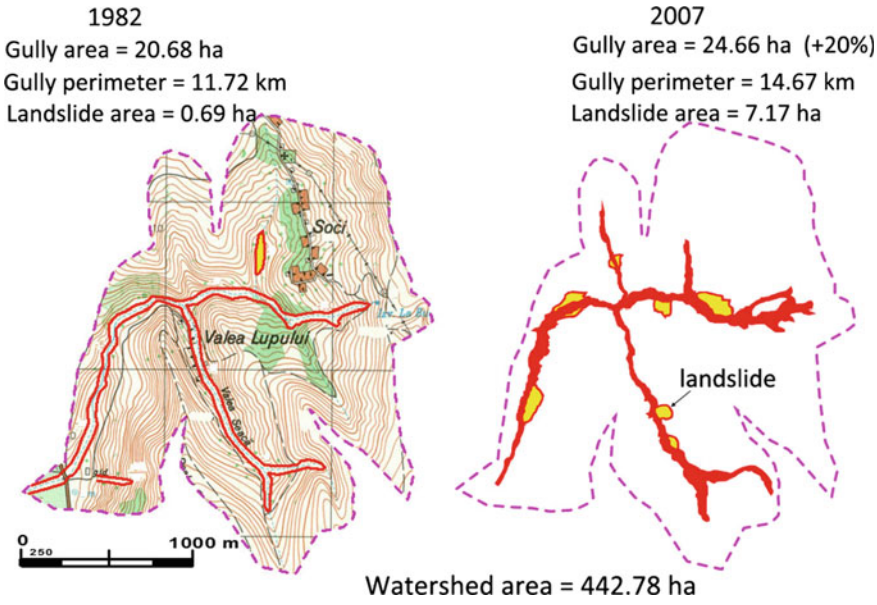

Fig. 16.10 Evolution of a valley gully system and landsliding dynamics in Simila catchment, Colinele Tutovei (Hurjui et al. 2008)

underwent any surface growth between 1982 and 2007. In the third catchment, Lohan (A = 110.4 km^2), surface growth of existing gullies was slower, due in part to erosion control works within gully perimeters.

Mean annual gully growth rates were around 2500 m^2/year, i.e., 10 times higher than the growth rates reported by Ioniță (2006) for the 1961–1990 timeframe. This significant disparity could be accounted for by the different measurement methods (conventional survey techniques versus RTK GPS equipment and topo surveys ed. 1982), as well as the increasing climate aggressiveness post-1990 (with excessive precipitation in 1991, 2005, and 2007).

Gully Advancement Time

During the past several decades, literature on gully dynamics has become abundant, based on which we can discern the most important factors in gully formation and growth. For instance, Nordström (1988) listed no less than 25 factors controlling a gully erosion cycle, of which 12 are more significant/have a larger share. In most instances detecting that a certain factor is present is insufficient; instead, it is necessary to appreciate which combination of factors is capable of reaching and exceeding the gully initiation threshold (Patton and Schumm 1975). Quantizing these factors and determining the threshold is a truly difficult task.

In attempting to find a solution for this problem, we assumed that hillslope morphology and superficial deposits are a result of the long-term variability of hydrological and climate conditions in that particular region. For example, the catchment size is directly related to runoff/discharge, such that the latter may be replaced with another equally significant variable, but easier to determine. This explains why in empirical models developed so far (Beer and Johnson 1963; Thompson 1964; Poesen and Govers 1990), predictors are mostly derived from slope morphology and small catchment morphology, such as: drainage area upstream of gully headcut; gully relief energy; height of thresholds in gully thalweg; drainage density; gully slope gradient; soil parameters (clay, silt, sand, organic matter, and calcium carbonate contents, saturation, etc.); precipitation (amount of precipitation in 24 h). Together, these variables account for 80 % of the variation in both gully growth rate and sediment yield by evacuation from the gully cross-section.

In order to predict the development rates for gullies from the Moldavian Plateau, we used a multivariate statistical model employing survey data on gully headcut advancement from 1986 to 1992 and 2008.

The selection of independent variables was based on two criteria: they were relatively easily acquired from the field or topographical maps and orthophotos, and able to explain to a high degree the variability in the gully advancement rate.

The statistical model chosen for assessing gully advancement rates in the Moldavian Plateau is according to Eq. (16.1):

$$\log Y = a + b \times \log X_1 + c \times \log X_2 + \cdots + n \times \log X_n \tag{16.1}$$

where Y = gully head advancement rate, Ra (m/year); X_1 = gully length, L (m); X_2 = catchment area upstream of gully headcut, A (ha); X_3 = catchment slope gradient upstream of gully headcut, P (%); X_4 = relief energy upstream of gully headcut, E (m).

This multiple regression model was used to estimate the time of gully advancement in the study area; according to it, as the catchment area upstream of the gully headcut increases, the time required for advancement diminishes. Variations in the advancement time are generated by the differing lithology (in this case, either marly-clayey or sandy).

The model is illustrated in Figs. 16.11 and 16.12, which show how the average gully lengths increase as the ages of the respective gullies augment, in the two main lithological zones of the Moldavian Plateau located between Siret and Prut Rivers.

In the northern sector of the study area (approximately north of Vaslui), whereby the lithology is dominated by marls and clays, the mean gully length is 188 m (averaged for 3577 gullies). It can increase at an accelerated pace during the first 25–30 years after which the advancement rate diminishes until reaching an equilibrium length at approximately 50–70 years.

In the southern sector, where the sand content increases in the substrate, the average parameters computed for the 2864 inventoried gullies are: mean length =

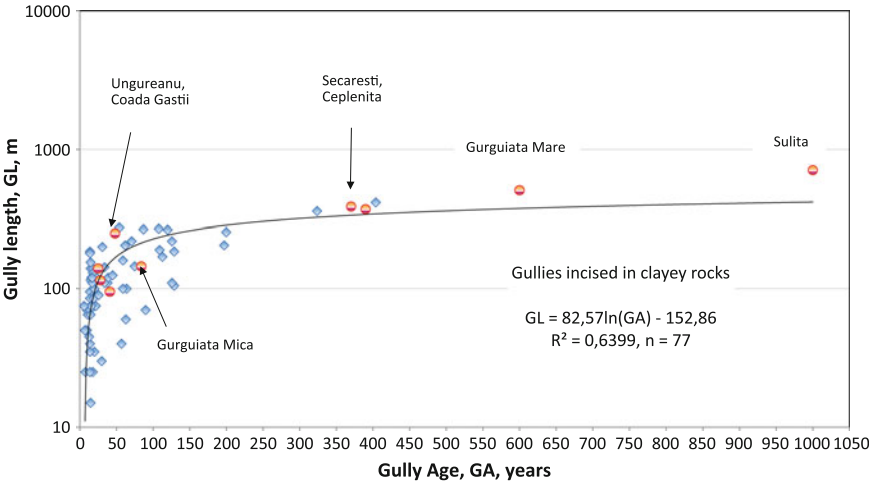

Fig. 16.11 Gully age determined based on the multiple regression model recalibrated for the northern sector of the Moldavian Plateau

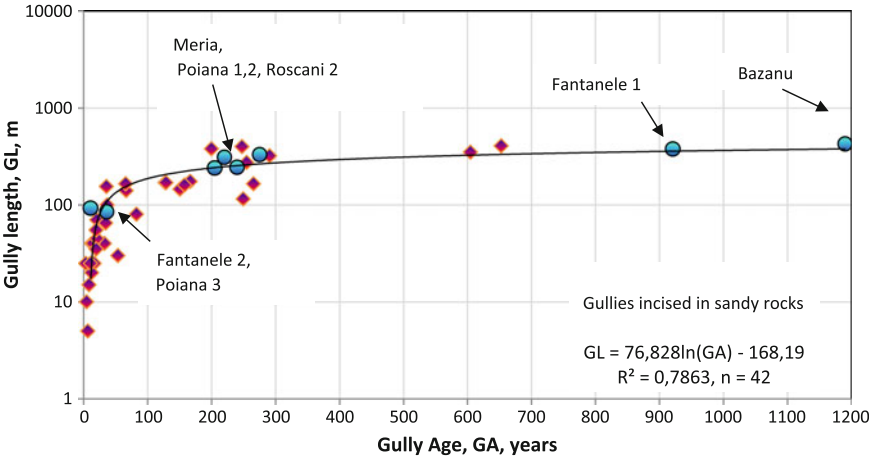

Fig. 16.12 Gully age determined based on the multiple regression model recalibrated for the southern sector of the Moldavian Plateau

141 m, mean depth = 4.6 m, and mean width = 17 m. The accelerated growth rate stage spans a longer period of time, of up to 100 years, after which an equilibrium length is reached. The most recent measurements on test gullies–Poiana, Roşcani, Meria, and Bâzanu–fall into the general variation trend, such that the new equation was greatly improved (Fig. 16.12).

The conclusions which should be drawn concerning the dynamics of gully landforms from the Moldavian Plateau regard two coordinates of analysis: spatial and temporal.

Spatially, we demonstrated that throughout a large portion of the Romanian territory (which, in addition, is characterized by high erodability), sediment-yielding landforms and processes through gullying are strongly controlled by the quality of the rock substrate whereby gullies are incised. Undoubtedly, other factors exert some control to various degrees on these landforms; however, thus far in Romania the monitoring of gully erosion was not rigorous enough to allow for detailed assessment of all controls.

On a temporal scale, we documented that the active phase of the gullying process occurs during the first 25–30 years after incision, ensued by a long stagnation and extinction which can last up to 300–450 years. Therefore, 50 % of the gully length (as well as the corresponding active surface and the volume of dislodged material) is produced in less than 20 % of the expected lifespan of the respective gully. All of these parameters are valid under natural conditions of evolution, excluding any sort of intervention for improvement of recovery of affected land.

Gully Erosion Prevention and Control

Due to the particular mixture of topography, soil and climate aggressiveness specific to the Romanian territory, soil erosion on sloping lands results in significant loss in both agriculture and other sectors of the economy. The structure of land use in Romania is dominated by agricultural land, which accounts for over 60 % of the total area. Scientific studies have shown that nearly 50 % of the agricultural land is affected by sheet erosion, gully erosion, or landsliding in various stages of evolution. Thus, of the total area 7.4 million ha of agricultural land subjected to these processes, 46 % are undergoing slight erosion, 42 % moderate erosion, and 12 % are affected by severe and excessive erosion.

In 1991, a new legislative act (Law no 18) regarding the reconstitution of property over agricultural land came into effect, thus marking an unfortunate era for sloping farmlands, which suffered disastrous consequences to a large extent. Thus, 9 million ha of agricultural land were divided into over 48 million individual plots, ranging from 1.8 to 2.5 ha each.

In these areas (Fig. 16.13), preexisting erosion control works were disabled or fell into disrepair and the land was mostly used for subsistence farming employing

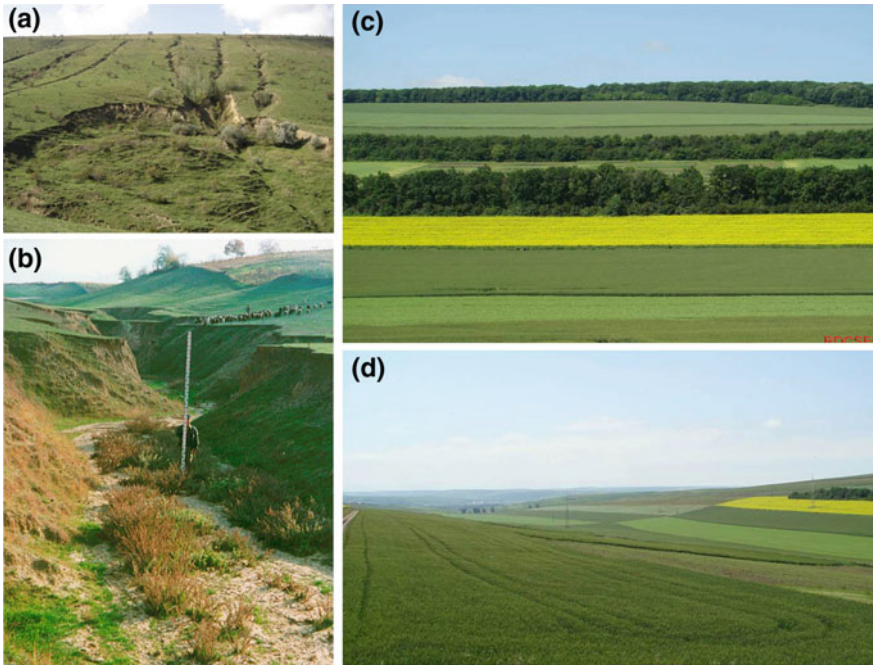

Fig. 16.13 Degraded lands versus improved lands in Colinele Tutovei (*photo* C. Hurjui): **a** degraded hillslope with rills and gullies in Tunseşti area, Simila catchment. **b** Roşcani valley gully (Perieni area, nearby Bârlad). **c**, **d** Tărna valley hillslopes improved by terraces and tree strips

rudimentary agrotechnics and crops which boost erosion. From 1990 to 1991, nearly 70 % of the national agricultural land fund was restored to private ownership; by 1990, approx. 90 % was private property. Needless to say, the fastest rate of change in terms of ownership pertained to arable land, vineyards, and orchards. Thus, arable lands tend to diminish, as they are replaced by pastures and meadows, and built-up land. However, orchards have undergone the most dramatic decrease, by as high as 25 % in 15 years.

Land improvement works are applied and managed mostly by the National Administration of Land Reclamation. Based on a government report published in 2010 (www.anmp.ro), we may produce a general assessment regarding the manner in which sloping lands are protected from erosion. The agricultural area endowed with various improvement works in 2010 amounted to 8,406,117 ha, which is less by 252,141 ha compared to 1999. However, we documented certain betterment in terms of several erosion control indicators post-2009 (irrigation facilities, drainage works, erosion control works). In the course of just one year (between 2009 and 2010), the area endowed with erosion control works increased by 914 ha. The manner in which these prevention and erosion control works operate in order to reduce sheet erosion and rill erosion was also presented in Chap. 15—this volume.

Conclusions

The Moldavian Plateau, delimited roughly by Siret and Prut watercourses, amounts to approximately 25,000 km^2 and comprises the most extensive areas affected by polymorphic land degradation processes. According to official reports from 2010 of the 3,372,916 ha of land undergoing severe erosion in Romania, this region accounts for no less than 33.5 %, which can be attributed to the mixed action of control factors. The amount of soil and rock removed by gully erosion from the area located between Siret and Prut Rivers was evaluated at 274 million m^3. If this amount were converted to a layer of topsoil and rock and distributed evenly across the study area, the thickness of the resulting layer would amount to 10.9 m. While this figure is undoubtedly impressive, it is however justified by the aggressiveness of this destructive process spanning a long period of time (100–450 years), affecting mostly agricultural lands. Unlike other forms of erosion, gully erosion displaces massive quantities of soil and rock which cannot be restored in a foreseeable timeframe.

Spatially, we demonstrated that throughout a large portion of the Romanian territory (which, in addition, is characterized by high erodability), sediment-yielding landforms and processes through gullying are strongly controlled by the quality of the rock substrate whereby gullies are incised. Undoubtedly, other factors exert some control to various degrees on these landforms; however, thus far in Romania the monitoring of gully erosion was not rigorous enough to allow for detailed assessment of all controls.

On a temporal scale, we documented that the active phase of the gullying process occurs during the first 25–30 years after incision, ensued by a long stagnation and extinction which can last up to 300–450 years. Therefore, 50 % of the gully length (as well as the corresponding active surface and the volume of dislodged material) is produced in less than 20 % of the expected lifespan of the respective gully. All of these parameters are valid under natural conditions of evolution, excluding any sort of intervention for improvement of recovery of affected land.

Acknowledgments The research leading to these results also has received partial funding from the Research Projects ADER 12.4.1 (Ministry of Agriculture and Rural Development): "Soluţii de organizare a teritoriului agricol şi de exploatare agricolă durabilă bazate pe inventarierea alunecărilor de teren şi ravenelor (Solutions of the agricultural land organization and sustainable farming-based inventory of landslides and gullies)."

References

Bălteanu D, Taloescu I (1978) Asupra evoluţiei ravenelor. Exemplificări din dealurile şi podişurile de la exteriorul Carpaţilor. Studii şi cercetări G.G.G., Geography series, XXV, Bucureşti (in Romanian)

Beer CE, Johnson HP (1963) Factors related to gully growth in the deep loess area of Western Iowa. Trans ASAE 6:237–240

Bradford JM, Piest RF (1980) Erosional development of valley bottom gullies in the upper midwestern United States. In: Coates DR, Vitek JD (eds) Thresholds in geomorphology. Allen and Unwin, pp 75–101

Church M, Mark DM (1980) On size and scale in geomorphology. Prog Phys Geogr 4:342–390

Clinciu I, Petriţan C, Niţă MD (2010) Monitoring of the hydrotechnical torrent control structures: a statistical approach. Environ Eng Manage J 9:1699–1707

EEA (2007) CLC2006 technical guidelines. European Environmental Agency 70, Copenhagen

Gaşpar R, Cristescu C (1987) Cercetări hidrologice în bazine hidrografice torenţiale mici. ICAS, Bucureşti (in Romanian)

Giurma I (2000) Soluţii constructive pentru amenajarea formaţiunilor torenţiale. Performantica Press, Iaşi (in Romanian)

Graf WJ (1977) The rate law in fluvial geomorphology. Am J Sci 277:178–191

Heede BH (1974) Stage of development of gullies in Western United States of America. Z Geomorphol NF 18(3):260–271

Heede BH (1980) Gully erosion–soil failure: possibilities and limits of control. In: Aulitzky H, Grubinger H, Nemecek E (eds) International symposium, Interpraevent 1980, watershed analyses to prevent catastrophes through engineering structures and land use planning, vol 1. Forschungsgesellschaft far vorbeugende Hochwasserbekampfung (Research Association for the Prevention of Floods), Klagenfurt, pp 317–330

Hurjui C, Nistor D, Petrovici G (2008) The evolution of catchment gullies in Studinet and Simila watersheds, Eastern Romania, during the last 25 years. the 15th Congress of ISCO, Budapest

Ichim I, Mihaiu G, Surdeanu V, Rădoane M, Rădoane N (1990) Gully erosion in agricultural lands in Romania. In: Boardman J, Foster IL, Dearing J (eds) Soil erosion on agricultural land. Willey, London, pp 55–69

Ioniţă I (2000) Formarea şi evoluţia ravenelor din Podişul Bârladului. Corson Press, Iaşi (in Romanian)

Ioniță I (2003) Hydraulic efficiency of the discontinuous gullies. In: Poesen J, Valentin C (eds) Gully erosion and global change, vol 50(2–4). Catena, pp 369–379
Ioniță I (2006) Gully development in the Moldavian Plateau of Romania. Catena 68:133–140
Ioniță I (2008) Sediment movement from small catchments within the Moldavian Plateau of Eastern Romania. In: Schmidt J, Cochrane T, Phillips C, Elliot S, Davies T, Basher L (eds) Sediment dynamics in changing environments, International Association of Hydrological Sciences Publication 325, IAHS Press, Wallingford, Oxfordshire, pp 316–320
Ioniță I, Ouatu O (1985) Contribuții la studiul eroziunii solurilor din Colinele Tutovei. Rev. Cercet. Agron, Iași, 3(71):58–62 (in Romanian)
Jurchescu M (2012) Bazinul morfohidrografic al Olteţului. Studiu de geomorfologie aplicată. PhD thesis, University of Bucharest (in Romanian)
Leopold LB, Maddock T (1953) The Hydraulic geometry of stream channels and some physiographic implications. Geological Survey Proffesional Paper 252, Washington
Mihaiu G, Taloiescu I, Negut N (1979) Influența lucrărilor transversale asupra evoluției ravenelor formate pe alternanțe de orizonturi permeabile și impermeabile. Bul Inf ASAS 8:103–105 (in Romanian)
Mircea S (1999) Study concerning gully erosion evolution in natural and managed watersheds in Buzau region. PhD Thesis, University of Agricultural Sciences and Veterinary Medicine, Bucharest
Mircea S (2002) Formarea, evoluția și strategia de amenajare a ravenelor, BREN Press, Bucureşti (in Romanian)
Moțoc M (1983) Ritmul mediu de degradare erozională a solului în RSR, Buletinul Inf. ASAS, Nr.2, Bucureşti (in Romanian)
Moțoc M (1984) Participarea proceselor de eroziune și a folosințelor terenului la diferențierea transportului de aluviuni în suspensie pe râurile din România. In: Buletinul Info. ASAS, 13, Bucureşti (in Romanian)
Moțoc M, Sevastel M (2002) Evaluarea factorilor care determină riscul eroziunii hidrice în suprafată, Bren Press, Bucureşti (in Romanian)
Moțoc M, Stănescu P, Taloiescu I (1979) Actual conceptions regarding erosional phenomenon and it control. Institute for Soil Science and Agrochemistry. Agriculture Library. Bucharest, pp 77–86
National Environmental Protection Agency (2015) Ministry of environment, water and forests. http://www.anpm.ro. Accessed 21 Feb 2015
Nordström K (1988) Gully erosion in the Lesotho lowlands—a geomorphological study of the interactions between intrinsic and extrinsic variables. Department of Physical Geography, Uppsala University, UNGI Report 69, Uppsala
Otlacan-Nedelcu L (2001) The uselfulness of a new model for the gully control structures effect prediction. In: Stott DE, Mohtar RH, Steinhart GC (eds) Sustaining the global farm, proceedings of Purdue University, pp 1000–1007
Patton PC, Schumm SA (1975) Gully erosion, north western Colorado: a threshold phenomenon. Geology 3(2):88–90
Poesen J, Govers G (1990) Gully erosion in the loam belt of Belgium. Typology and control measures. In: Boardman J, Foster IDL, Dearing JA (eds) Soil erosion on agricultural land. Wiley, New York, pp 513–536
Poesen J, Nachtergaele J, Verstraeten G, Valentin C (2003) Gully erosion and environmental change: importance and research needs. Catena 50:91–133
Poesen J, Vanwalleghem T, de Vente J, Knapen A, Verstraeten G, Martınez-Casasnovas JA (2006) Gully erosion in Europe. In: Boardman J and Poesen J (eds) Soil erosion in Europe. Wiley, New York, pp 515–536
Rădoane N (2002) Geomorfologia bazinelor hidrografice mici. "Ștefan cel Mare" University Press, Suceava (in Romanian)
Rădoane M, Rădoane N (1992) Areal distribution of gullies by the grid square method. Case study: Siret and Prut interfluve. Rev Roum Geogr 36:95–98

Rădoane M, Ichim I, Rădoane N (1995) Gully distribution and development in Moldavia, Romania. Catena 24:127–146
Rădoane M, Rădoane N, Ichim I, Surdeanu V (1999) Ravene. Forme, procese şi evoluţie. Cluj University Press, Cluj-Napoca (in Romanian)
Rădoane M, Rădoane N, Cristea I, Popescu L, Barnoaiea I, Budui V, Chiriloaei F (2009) Monitorizarea evoluției ravenelor test din Podișul Moldovei în Perioada 1986–2008. Ann "Ștefan cel Mare" Univ 18(1):5–18
Roloff G, Bradford JM, Scrivner CL (1981) Gully development in the deep loess hills region of Central Missouri. Soil Sci Am J 45(1):119–123
Schumm SA (1960) The shape of alluvial channels in relation to sediment type. U.S. Geological Survey Professional Paper 352B, pp 17–30
Seginer I (1966) Gully development and sediment yield. J Hydrol 4:236–253
Stângă CI (2011) Gully erosion and associated risks in the Tutova basin–Moldavian Plateau. Land Anal 17:193–197
Thompson JR (1964) Quantitative effect of watershed variables on rate of gully head advancement. Trans ASAE 7(1):54–55
Torri D, Poesen J (2014) A review of topographic threshold conditions for gully head development in different environments. Earth Sci Rev 130:73–85
Traci C (1985) Împădurirea terenurilor degradate. Ceres Press, Bucureşti (in Romanian)
Traci C, Gaşpar R, Munteanu SA (1981) Efectul lucrărilor de amenajare a unor bazine hidrografice torenţiale mici. ICAS, 2, Bucureşti (in Romanian)
United Nations Environment Programme – UNEP (1994) United nations conventions to combat desertification in those countries experiencing serious drought and/or desertification, particularly in Africa, Geneva. http://www.unep.org/environmentalgovernance/. Accessed 20 Feb 2015
Vâlsan G (1945) Procese elementare în modelarea scoarţei terestre. SRG, Bucureşti (in Romanian)
Veness JA (1980) The role of fluting in gully extensions. J Soil Conserv NSW 36(2):100–107
Woldenberg M (1966) Horton's laws justified in terms of allometric growth and steady state in open systems. Geol Soc Am Bull 77:431–434
Zachar D (1982) Soil Erosion. Developments in Soil Science 10. Elsevier Scientific Press, Amsterdam, Oxford, New York

Chapter 17
Soil Erosion Modelling

Cristian Valeriu Patriche

Abstract Surface soil erosion modelling has benefited and continues to benefit from the progress in information technology area and statistical and mathematical processing of spatial data. In Romania, quantitative studies concerning soil erosion have a tradition of over 70 years, beginning with the establishment of experimental runoff plots. An important step in the history of soil erosion research in Romania is the adaptation of the universal soil loss equation (USLE) to the specific environmental and anthropogenic conditions form our country (ROMSEM). This has led to the achievement of a first quantitative zonation of soil erosion at national scale. During the past decade, it is to be noticed a multiplication of local and regional scales applications, attempting mainly the 3-dimensional implementation of ROMSEM model in GIS environment, and also the application of other models such as USLE, RUSLE, USPED and PESERA. A common problematic issue is the lack of measured erosion data for hydrographic basins or other geographical units, which are necessary for the validation of models. The model adapted for Romania (ROMSEM) differs substantially from the original one (USLE), mainly by the different manners of quantifying rainfall erosivity and soil erodibility. This hampers the comparison between the roles played by erosion factors in ROMSEM model, on the one hand, and USLE or RUSLE models, on the other hand. An application carried out for an average size hydrographic basin from eastern Romania has shown that ROMSEM model produces realistic results, comparable with erosion values measured in similar environmental settings.

Keywords Surface erosion · Erosion modelling · USLE · RUSLE · GIS application · Romania

C.V. Patriche (✉)
Department of Iaşi, Geography Group, Romanian Academy,
Carol I Av 8, 700505 Iaşi, Romania
e-mail: pvcristi@yahoo.com

M. Rădoane and A. Vespremeanu-Stroe (eds.), *Landform Dynamics and Evolution in Romania*, Springer Geography,
DOI 10.1007/978-3-319-32589-7_17

Introduction

The scientific approach of soil erosion was initiated in the early 1930s by American specialists in soil science and agronomy (Cook 1936). The research focused on identifying and quantifying the control factors of erosion process, leading to the development of the universal soil loss equation (USLE) (Wischmeier and Smith 1978). Most of the following studies focused on calibration of the different parameters included in the equation, aiming to improve its accuracy, to simplify its application and to adapt it for different environmental settings. Such calibrations were carried out in Romania as well by Moţoc et al. (1975, 1979), resulting in the development of a specific soil erosion model (ROMSEM), which was adopted by the National Research and Development Institute for Soil Science, Agrochemistry and Environment (ICPA 1987) within the methodology for elaboration of soil studies.

Besides these calibrations, some studies also focused on revising the universal soil loss equation. Williams (1975) proposed a modified equation (MUSLE) to predict sediment yield per rainfall event and Renard et al. (1991, 1997) proposed a revised form of USLE, more complex and computerized (RUSLE). Starting in the 1980s, the use of computers and statistical methods in soil erosion research increased substantially, leading to the formulation of more complex models, integrated in software packages, such as EPIC, WEPP, which have been successfully applied in Romania as well, within the Perieni Research and Development Centre for Soil Erosion Control (Popa 2010).

Complex GIS software (e.g. ArcGIS, TNTmips, IDRISI, GRASS, SAGA–GIS, TAS–GIS, ILWIS etc.) generally include modules for computing various topographical indices, including the *LS* factor form RUSLE based on flow accumulation. IDRISI includes also a module for soil erosion estimation according to RUSLE methodology.

Apart from these complex GIS software, a series of specialized programs for soil erosion assessment are to be noticed: USLE2D (Desmet and Govers 1996), designed for computation of flow accumulation and *LS* factor through several algorithms; WATEMSEDEM (Van Rompaey et al. 2001), allowing erosion computation based on USLE or RUSLE; WEPP (Laflen et al. 1991) and RUSLE2D (USDA-ARS 2008), which apply RUSLE locally (e.g., slope profile, farm); LISEMWIN/OPENLISEM (http://blogs.itc.nl/lisem/). WEPP and RUSLE2D are based on highly detailed databases regarding the USA territory. However, they cannot be directly applied in other regions, mainly because of the difficulty in changing the climate data, the creation of new files being a very demanding operation.

Some of these specialized programs were coupled with GIS software in order to extend their spatial analysis capacity. For instance, an ArcGIS module was created for WEPP (named GeoWEPP), OPENLISEM was coupled with PCRASTER.

Summary information regarding the various erosion models are found in several research papers (Morgan 2010; Merritt et al. 2003; Grimm et al. 2002). ROMSEM model has been successfully applied in different regions of Romania (Biali and Popovici 2003; Patriche et al. 2006, 2012; Prefac 2008; Bilaşco et al. 2009;

Dumitru et al. 2010; Arghiuş and Arghiuş 2011). Other studies focused on reformulation of USLE model (Cârdei 2009; Cârdei et al. 2009), or the elaboration of physical models (Domniţa 2012).

The main achievements in soil erosion modelling, with emphasis on Romanian territory, are presented according to the following structure: (a) a brief scan of used soil erosion models and the comparative analysis of the main results; (b) comparative presentation of the quantifying manners of soil erosion factors in USLE, RUSLE and ROMSEM; (c) a study case showing the application of ROMSEM for soil erosion estimation within specific environmental conditions from our country.

Erosion Models Applied in Romania

In Romania, soil erosion modelling has begun in the 1940s with the establishment of runoff plots within agricultural research stations (Perieni—Vaslui County, Podu Iloaiei—Iaşi County, Aldeni—Buzău County, Bilcești—Argeş County, Cean–Turda—Cluj County), with the recording, storing and processing of erosion data. At the same time, soil mapping, carried out by ICPA, resulted in the achievement of an inventory of terrains affected by various erosion degrees, leading further to the publishing of the soil erosion map in Romania at scale 1:500,000 (Florea et al. 1977). This qualitative map illustrates the areas affected by water and wind erosion, as well as areas exposed to flooding risk, showing that 45.6 % of agricultural lands are affected by water erosion and only 1.4 % by wind erosion (Ioniță et al. 2006).

The next important stage in soil erosion modelling in Romania is the adaptation of USLE model (Wischmeier and Smith 1978) by Moţoc et al. (1975, 1979). The model is based on correlations between experimental data and erosion factors. Starting from the outcomes of this model, as well as accounting many other information provided by different institutions (Ioniță et al. 2006), Motoc (1983) accomplishes the first quantitative zoning of total erosion on agricultural lands in Romania.

According to this zoning, the highest total erosion rates are specific to the Curvature Subcarpathians (30–45 t ha^{-1} $year^{-1}$), due mainly to the loose lithology, and also to the Getic Subcarpathians, Bârlad Plateau and northern Jijia Plain (20–30 t ha^{-1} $year^{-1}$). The total water erosion in Romania is an estimated 126 million t $year^{-1}$ of which 61.8 million t $year^{-1}$ results from surface erosion. On agricultural land, mean annual soil loss is about 106.6 million t $year^{-1}$, the greatest contribution coming from degraded pastures (45 million t $year^{-1}$), unproductive, abandoned lands (29.8 million t $year^{-1}$) and arable lands (28 million t $year^{-1}$) (Moţoc et al. 2010).

Other national scale evaluations are the standard soil loss map and soil erodibility map (Vătău et al. 1993a, b) at scale 1:500,000 and erosion, landslides and flooding map (Munteanu et al. 2000) at scale 1:1000,000.

A series of models developed abroad and integrated in software packages (EPIC, WEPP) were tested in Romania as well, within the research station of Perieni

(Popa 2010). For WEPP model application, due to the difficulty of modifying the climate data, the North–Plate Nebraska station was selected out of the 1079 US meteorological stations from CLIGEN module, which presented similar characteristics to Bârlad meteorological station. Simulations on different plots, for the 1989–1993 time period reveal significant correlations between WEPP simulated erosion and measured erosion, the values of correlations coefficients ranging from 0.564 to 0.943, with an average of 0.808.

During the past 15 years, there has been a progressive increase in GIS applications for soil erosion modelling. Most of them focus on ROMSEM model application at local or regional scales. Some studies experiment the implementation of other models such as RUSLE, USPED, WEPP, vector or hydrological models. Table 17.1 presents synthetically the main applications of this type, while the positioning of study areas is displayed in Fig. 17.1.

The resolution of models varies from 10 × 10 m to 100 × 100 m, while the size of study areas ranges from small hydrographic basins (0.29–2.72 km^2) to major geographical units (Someşan Plateau—2625 km^2). Generally, the applications are based on digital terrain models computed by vectorization of elevation data from topographic maps. The information regarding soil characteristics are extracted either from fine scale soil maps (1:5000, 1:10,000) or from more generalized soil maps (1:200,000). Taking into account the lack of detailed soil surveys in several forested areas, some studies use generalized maps (1:200,000) even for small areas (Patriche et al. 2006), as these are the only soil information sources in such situations. The information regarding land use are extracted either from fine scale sources (1:10,000, orthophotoimages, LANDSAT, SPOT satellite images) or from medium (1:25,000, 1:50,000) and small (Corine Land Cover) scale maps.

Regarding the quantification of soil erosion factors, the studies applying USLE–ROMSEM model follow either the classic computation approach, or attempt to substitute some factors by formulas specific to other models (RUSLE, USPED).

Thus, for computing slope length factor (*L*), Anghel and Todică (2008) use the formula proposed by Desmet and Govers (1996), Bilaşco et al. (2009), Ştefănescu et al. (2011) and Roşca et al. (2012) use the Mitasova et al. (1996) formula, while Arghiuş and Arghiuş (2011) apply Moore et al. (1993) procedure. Studies applying the formula from the Romanian methodology, depart from the spatial representation of flow length as the pixel's side or diagonal, according to flow orientation (Biali and Popovici 2003; Patriche 2005; Dumitru et al. 2010), or quantify this factor in GIS using, for instance, Slope Length module from SAGA–GIS (Patriche et al. 2012).

Similarly, the quantification of slope factor (*S*) follows either the Romanian methodology (Moţoc et al. 1975, 1979; ICPA 1987), or makes use of other formulas, such as the one proposed by Moore et al. (1993), applied by Arghiuş and Arghiuş (2011), or the WEPP equation, applied by Dumitru et al. (2010). Regarding the manners of quantifying crop and crop management factor (*C*), apart from the studies using the coefficients specified by the Romanian methodology (Biali and Popovici 2003; Patriche 2005; Dumitru et al. 2010; Ştefănescu et al. 2011), some studies (Patriche et al. 2006, 2012; Prefac 2008) apply the formulas proposed by

Table 17.1 GIS applications in Romania designed for estimation of soil surface erosion[a]

No.	Authors/model	Study area, scale	Model's features
1	Biali and Popovici (2003) USLE–ROMSEM	Small basins from Tutova hills – Area: 39.8, 46.9 km^2 – Resolution: 25 × 25 m – Local scale	Input data – DEM from 1:5000 topographic maps, soil map, land use map at scale 1:10,000 Erosion factors – *R*—ICPA (1987) – *K*—ICPA (1987) – *L*—25 m (N–S, E–W flow), $25\sqrt{2}$ m (NW–SE, NE–SW flow) – *S*—Moţoc et al. (1979) – *C*—Moţoc et al. (1979) Results – Mean basin erosion: 12.64, 9.5 t ha^{-1} $year^{-1}$
2	Patriche (2005) USLE–ROMSEM	Central Moldavian Plateau – Area: 930 km^2 – Resolution: 100 × 100 m – Regional scale	Input data – Topographic maps at scale 1:50,000, soil map at scale 1:200,000, SPOT and LANDSAT satellite images Erosion factors: – *R*—ICPA (1987) – *K*—ICPA (1987) – *L*—100 m (N–S, E–W flow), $100\sqrt{2}$ m (NW–SE, NE–SW) – *S*—Moţoc et al. (1979) – *C*—Moţoc et al. (1979) Results – Mean erosion: 4.57 t ha^{-1} $year^{-1}$
3	Patriche et al. (2006) USLE–ROMSEM/RUSLE	Small basins tributary to Zăbala river – Area: 1.54, 2.72 km^2 – Resolution: 10 × 10 m – Local scale Steril deposits from Călimani mountains – Area: 3.8 km^2 – Resolution: 5 × 5 m – Local scale	Input data – DEM 10 × 10 m – Soil map at scale 1:200,000 – CLC 2000 – LANDSAT image Erosion factors – *R*—ICPA (1987)/Van der Knijff et al. (2000) – *K*—ICPA (1987)/unique value – *LS* factor—Moţoc et al. (1975, 1979), Moore et al. (1993), Desmet and Govers (1996) – *C* factor—De Jong et al. (1998)/unique value Results – Mean basins' erosion assessed by different methods: from 13 to 65 t ha^{-1} $year^{-1}$

(continued)

Table 17.1 (continued)

No.	Authors/model	Study area, scale	Model's features
4	Anghel and Todică (2008) USLE–ROMSEM	Motru mining area – Area: 150 km^2 – Resolution: 10 × 10 m – Regional scale Sucevita basin – Area: 204 km^2 – Resolution: 10 × 10 m – Regional scale	Input data – Orthophotoimages, topographic maps at scale 1:25,000, CLC 1992, 2000, LANDSAT images Erosion factors – *R*—Stănescu et al. (1969) – *K*—ICPA (1987) – *L*—Desmet and Govers (1996) – *S*—Moţoc and Sevastel (2002) – *C*—Moţoc and Sevastel (2002) Results Modal erosion class: 0–1 t ha^{-1} year^{-1}, (65.2 % in Motru area, 90.51 % in Sucevița basin)
5	Prefac (2008) USLE–ROMSEM	Râmna hydrographic basin Area: 419 km^2 Resolution: 30 × 30 m – Regional scale	Input data – Soil map at scale 1:200,000, CLC 2000, LANDSAT image Erosion factors – *R*—ICPA (1987) – *K*—ICPA (1987) – *LS*—Moţoc et al. (1975, 1979) (slope length derived in SAGA-GIS) – *C*—NDVI (De Jong et al. 1998) Results – Mean erosion: 1.85 t ha^{-1} an^{-1} (2.86 t ha^{-1} an^{-1}—Subcarpathians, 0.44 t ha^{-1} an^{-1}—plain area)
6	Cârdei (2009), Cârdei et al. (2009) USLE—vector representation	Slope profiles in Valea Călugărească area – Local scale	Erosion factors – Vector representation of rainfall erosivity, topographic factor, slope factor, vegetation cover, soil conservation practices rainfall intensity, duration of rainfall events
7	Bilaşco et al. (2009) USLE–ROMSEM	Someşan Plateau – Area: 2625 km^2 – Resolution: 20 × 20 m – Regional scale	Input data – Topographic maps at scale 1:25,000, soil map at scale 1:200,000, CLC 2000 Erosion factors – *R*—Stănescu et al. (1969) – *K*—Moţoc et al. (1975) – *LS*—Mitasova et al. (1996) – *C*—Moţoc et al. (1975) Results – Modal erosion class: 0–0.5 t ha^{-1} an^{-1} (79.8 % of study area)

(continued)

Table 17.1 (continued)

No.	Authors/model	Study area, scale	Model's features
8	Popa (2010) WEPP	Slope profiles at Perieni – Local scale Small basin – Area: 0.29 km^2 – Local scale	Input data – Erosive rains from 1989 to 1993 period – Simulation for fallow and cultivated plots Results R^2 between measured and simulated values —0.347 to 0.993 (for runoff), 0.546 to 0.943 (for erosion)
9	Dumitru et al. (2010) USLE–ROMSEM, WEPP equations, PESERA	Adamclisi Commune – Area: 137.6 km^2 – Resolution: 30 × 30 m – Regional scale (1:200,000)	Input data – 30 × 30 m DEM, soil map at scales 1:200,000 and 1:10,000, land use map at scale 1:10,000 Erosion factors – *R*—Moţoc et al. (1975, 1979) – *K*—ICPA (1987) – *L*—30 m (N–S, E–W flow), $30\sqrt{2}$ m (NW–SE, NE–SW flow) – *S*—WEPP equations – *C*—Moţoc et al. (1975, 1979) Results – Modal erosion class: 0–2 t ha^{-1} year^{-1} (98.14 %)
10	Ştefănescu et al. (2011) USLE–ROMSEM	Roşia Montana – Area: 52.29 km^2 – Resolution: 10 × 10 m – Regional scale	Input data – Topographic maps at scale 1:25,000, soil map at scale 1:200,000, orthophoto images, CLC 2000 Erosion factors – *R*—Stănescu et al. (1969) – *K*—ICPA (1987) – *LS*—Mitasova et al. (1996) – *C*—Moţoc et al. (1975, 1979) Results – Modal erosion class: 1.1–8 t ha^{-1} an^{-1} (50.13 %)
11	Arghiuş and Arghiuş (2011) USLE–ROMSEM	Codrului Ridge and Piedmont – Area: 963 km^2 – Resolution: 10 × 10 m – Regional scale	Input data – 10 × 10 m DEM, CLC 2000, orthophotoimages Erosion factors – *R*—Moţoc and Sevastel (2002) – *K*—ICPA (1987) – *L*—Moore et al. (1993) – *S*—Moţoc and Sevastel (2002) – *C*—Moţoc and Sevastel (2002) Results – Mean erosion rate: 0.575 t ha^{-1} year^{-1}

(continued)

Table 17.1 (continued)

No.	Authors/model	Study area, scale	Model's features
12	Patriche et al. (2012) USLE–ROMSEM	Dobrovăț basin – Area: 186 km^2 – Resolution: 20 × 20 m – Regional scale	Input data – Topographic maps at scale 1:5.000, soil map at scale 1:5,000, LANDSAT image Erosion factors – *R*—ICPA (1987) – *K*—ICPA (1987) – *LS*—Moțoc et al. (1975, 1979) (slope length derived in SAGA-GIS) – *C*—NDVI (Van der Knijff et al. 2000) Results – Mean erosion rate: 5.4 t ha^{-1} year^{-1}
13	Roşca et al. (2012) USLE, RUSLE, USPED	Vasluieț basin (middle and lower) – Area: 320 km^2 – Resolution: 10 × 10 m – Regional scale	Input data – Topographic maps at scale 1:5,000, soil maps at scale 1:10,000, orthophotoimages, LANDSAT image Erosion factors – *R*—ICPA (1987) – *K*—ICPA (1987) – *L*—Moțoc et al. (1975), Mitasova et al. (1996) – *S*—Moțoc et al. (1975) – *C*—Moțoc and Sevastel (2002), Van der Knijff et al. (2000) Results – Mean erosion rates: 7.78–8.16 t ha^{-1} year^{-1} (USLE), 19.24–22.24 t ha^{-1} year^{-1} (RUSLE 3D), 14.6 t ha^{-1} year^{-1} (USPED + RUSLE)
14	Domniță (2012) Hydrological model	Several basins from Apuseni mountains – Areas: from 20 to 139 km^2 – Local and regional scales	Input data – DEM – Soil maps – Land use maps – Rainfall events Outputs – Flow velocity – Runoff – Flow concentration time – Runoff coefficients – Discharge calculations – Hydrographs

[a]*R* rainfall erosivity, *K* soil erodibility, *L* slope length factor, *S* slope factor, *C* crop and crop management factor

Van der Knijff et al. (2000), De Jong et al. (1998) based on NDVI values derived from LANDSAT satellite images.

Quantification and mapping of rainfall erosivity and soil erodibility generally follows the Romanian methodology.

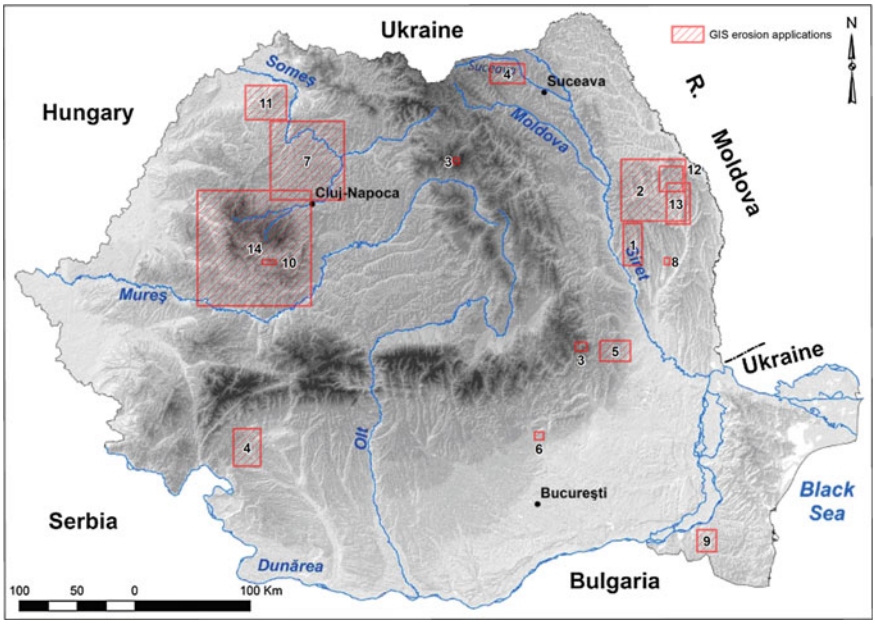

Fig. 17.1 Location of soil erosion studies specified in Table 17.1 (*numbers* on map correspond to *number* from the first table column)

The estimates of surface erosion may vary significantly depending on the applied model. Patriche et al. (2006) compares the results achieved by USLE–ROMSEM and RUSLE, using several ways of quantifying the factors. The models are applied on 2 small hydrographic basins form the Subcarpathians (Hanganu and Hurjui), for which validation data were available. The 9 variants of applied models generate mean erosion rates between 13 and 43.6 t ha^{-1} $year^{-1}$, compared to a measured rate of 28.8 t ha^{-1} $year^{-1}$ for Hanganu basin and mean erosion rates between 19.6 and 65.6 t ha^{-1} $year^{-1}$, compared to a measured average of 38.1 t ha^{-1} $year^{-1}$ for Hurjui basin. The best results are produced by USLE–ROMSEM model, in the case of Hanganu basin, and by RUSLE model, in the case of Hurjui basin (Fig. 17.2).

Another study, carried out by Dumitru et al. (2010) for the Adamclisi commune (Dobrogea), compares the results produced by USLE–ROMSEM, WEPP and PESERA (Kirkby et al. 2004) models, the last one being a physical model applied at European scale. The authors found that the highest estimates of surface erosion were generated by USLE–ROMSEM model, with a maximum value of 14.924 t ha^{-1} $year^{-1}$, followed by WEPP model, with a maximum value of 3.922 t ha^{-1} $year^{-1}$ and PESERA model which produced unrealistic values, less than 0.4 t ha^{-1} $year^{-1}$ (Fig. 17.3).

The study carried out by Roşca et al. (2012) in the middle and lower Vasluieț basin (Central Moldavian Plateau) compares the performances of 5 models (2 variants of USLE–ROMSEM, 2 variants of RUSLE and USPED model), showing that

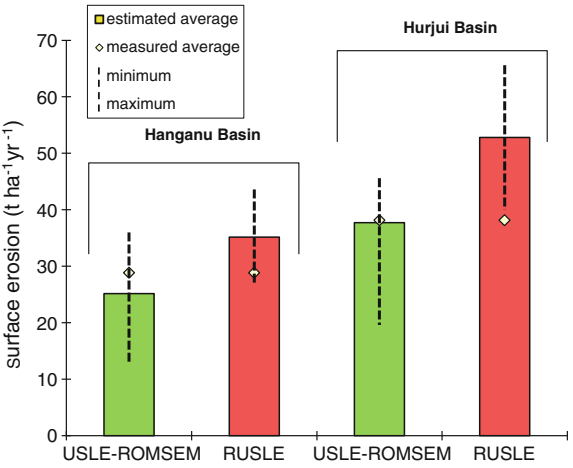

Fig. 17.2 Measured and estimated erosion using different models on 2 hydrographic basins from the Subcarpathians (*Source data* Patriche et al. 2006)

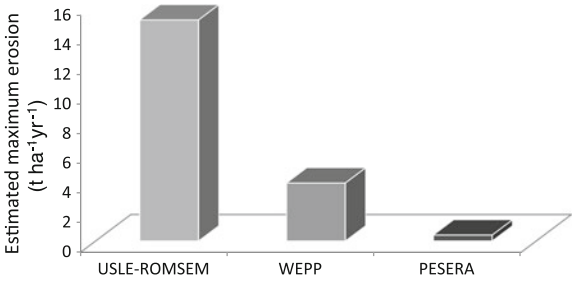

Fig. 17.3 Maximum erosion estimated by different models in Adamclisi commune (*Source data* Dumitru et al. 2010)

USLE–ROMSEM model generates lower erosion values compared to the others. Evaluating the results in relation to other studies, the authors conclude that USLE–ROMSEM model is better suited for surface erosion estimation in the study area (Fig. 17.4).

Summarizing these aspects, the research regarding soil erosion in Romania, extending over more than 70 years, have evolved from small-scale qualitative assessments to fine scale quantitative evaluations in relation with the progress in spatial analysis techniques implemented in GIS and the development of erosion-oriented software packages. Most of the GIS applications aim to implement the USLE model adapted by Moţoc et al. (1975, 1979) for the specific environmental settings of Romania. Model validation is most often an expert-knowledge confirmation of results, due to the lack of measured erosion data for hydrographic basins or other geographical units, which represent a weak point of these applications.

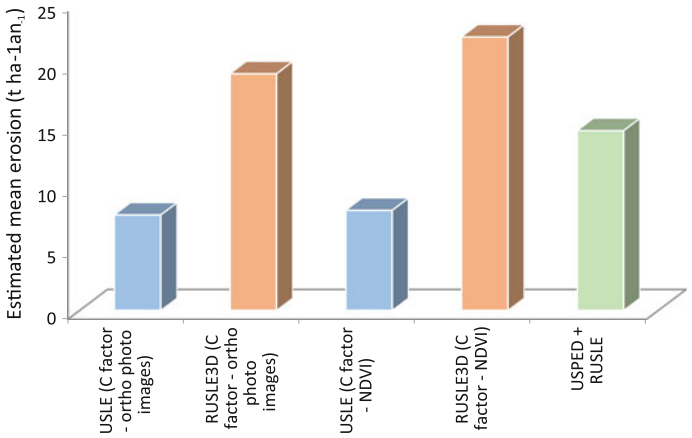

Fig. 17.4 Mean surface erosion values estimated by different models in the middle and lower Vasluieț basin (*Source data* Roșca et al. 2012)

USLE/RUSLE Versus ROMSEM

The universal soil loss equation, under the form of either USLE or RUSLE, is probably the most commonly applied erosion model, from local and regional scales to national (Panagos et al. 2014) and even continental scales (Van der Knijff et al. 2000; Grimm et al. 2002). For the Romanian territory as well, most of the applications use ROMSEM model derived from USLE. For this reason and given that there are important methodological differences between the models, we chose to present comparatively the various quantification manners for erosion factors.

USLE (Wischmeier and Smith 1978) and RUSLE (Renard et al. 1991, 1997) have the same mathematical expression:

$$E = R \times K \times L \times S \times C \times P \tag{17.1}$$

- E: mean annual erosion rate (t ha^{-1} year^{-1});
- R: rainfall erosivity factor (MJ mm ha^{-1} h^{-1} year^{-1});
- K: soil erodibility factor (t ha h ha^{-1} MJ^{-1} mm^{-1});
- L: slope length factor;
- S: slope factor;
- C: crop and crop management factor;
- P: soil conservation practice factor.

The differences consist in the manner the factors are being quantified. For instance, RUSLE introduced a correction for precipitations falling on quasi-horizontal surfaces, the algorithms for computation of slope and slope length factors were modified, a temporal dimension was added to soil erodibility etc.

The erosion estimation leaving out the *C* and *P* factors is called potential erosion, while the effective erosion takes into account all control factors.

Within the Romanian version of USLE (Moţoc et al. 1975, 1979), there are substantial differences in the way the erosion factors are conceived and quantified. Consequently, they cannot be substituted by corresponding factors defined in the international scientific literature. For instance, the values of rainfall erosivity factor are less than one, representing the average annual soil loss per unit of rainfall aggressiveness [as defined by Stănescu et al. (1969)], while in the original USLE this factor has values of hundreds, as it expresses the product of kinetic energy of a rainfall event and its maximum 30 min intensity. The Romanian version of USLE was adopted by ICPA (1987), becoming the standard procedure for erosion risk assessment on agricultural lands.

The erosion control factors are briefly presented as follows.

Rainfall erosivity (*R*) is the capacity of rain events to produce erosion and it depends mainly on rain intensity and duration. Mathematically, rainfall erosivity is the annual sum of products between kinetic energy of erosion capable rainfalls and their maximum 30 min intensity (I_{30}):

$$e = 0.29\left[1 - 0.72e^{(-0.05i)}\right] \text{ (Brown and Foster 1987)} \tag{17.2}$$

- e—rainfall kinetic energy per precipitation unit (MJ ha^{-1} mm^{-1});
- i—rainfall intensity (mm h^{-1}).

$$R = \sum EI_{30} \tag{17.3}$$

- R—annual rainfall erosivity (MJ mm ha^{-1} h^{-1} year^{-1});
- E—rainfall kinetic energy (MJ ha^{-1});
- I_{30}—rainfall maximum intensity during a 30-min period (mm h^{-1}).

The direct computation of rainfall erosivity is quite difficult, because rainfall intensity is not commonly recorded by meteorological stations. Consequently, various indirect methods were proposed as alternatives for rainfall erosivity estimation, based on statistical relationships between this factor and other parameters, easier to measure (e.g. mean annual precipitations, mean precipitations of the warm season, maximum daily or hourly precipitation etc.) (Table 17.5).

Recently Meusburger et al. (2012), applied Brown and Foster (1987) equations for computation and derivation of spatial distribution of *R* factor for Switzerland. An automated algorithm was implemented in C programming language, which can be used to apply the model with other input data with the same temporal resolution. For Europe, Van der Knijff et al. (2000) applied relation (17.4), for the northern half

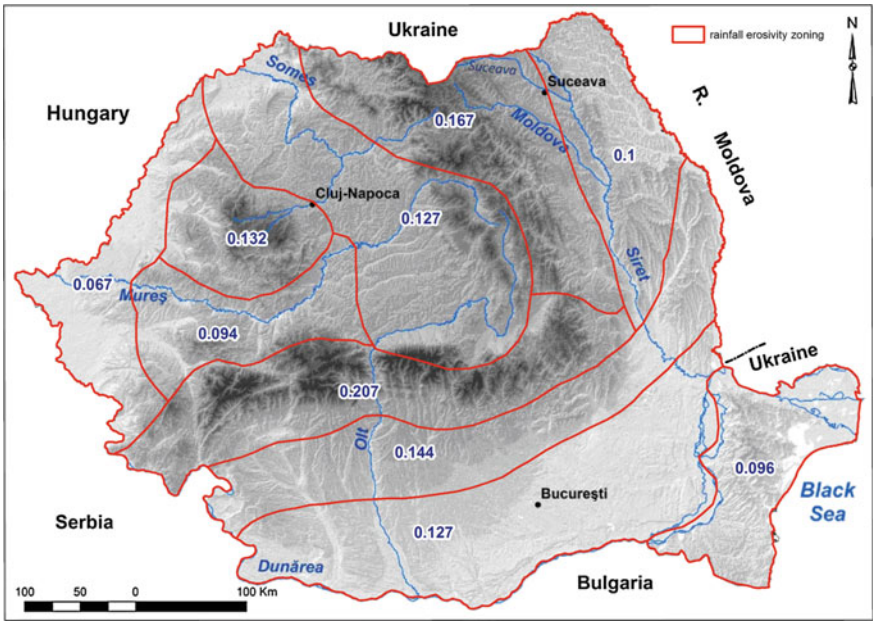

Fig. 17.5 Rainfall erosivity zoning for Romania (Reproduced from ICPA 1987)

of the continent, and relation (17.5) for the southern half, along with fuzzy techniques for rendering the transition from North to South.

In Romania, rainfall erosivity is expressed differently, representing the mean annual soil loss per unit of rainfall aggressiveness (ICPA 1987). This index represents the product of rainfall amount and 15 min maximum rainfall intensity (Stănescu et al. 1969). The values of rainfall erosivity vary between 0.064, for the Western Plain and 0.207, for the Southern Carpathians and partially, for the Getic and Curvature Subcarpathians (Fig. 17.5).

Soil erodibility (*K*) represents the mean annual soil loss per unit of rainfall erosivity (t ha h ha^{-1} MJ^{-1} mm^{-1}). This parameter expresses soil susceptibility for erosion and it depends mainly on its textural characteristics and on other factors as well, such as soil structure, permeability, organic matter content. Generally, soil erodibility increases from light (sandy) to heavy (clay) textures, with a maximum for loamy textures. Though less cohesive, sandy soils present lower erodibility values due to their high permeability which allows a great fraction of the water to infiltrate the soil without producing erosion. As texture it becomes finer, the higher clay content decreases infiltration and enhances runoff, leading to more intense erosion processes. On the other hand, the increase of clay content induces an increase in soil cohesiveness, through formation of hydrostable structures, leading to a decrease in soil erodibility values, beginning with loam-clay and clay textures (Table 17.2).

Table 17.2 Mean erodibility values for different textural classes (Van der Knijff et al. 2000)

Dominant surface textural class	Clay (%)	Silt (%)	Sand (%)	*K*
No texture (e.g. hystosoils)	–	–	–	–
Coarse (clay <18 % and sand >65 %)	9	8	83	0.0115
Medium (18 % < clay < 35 % and sand >15 %, or clay <18 % and 15 % < sand < 65 %)	27	15	58	0.0311
Medium fine (clay <35 % and sand <15 %)	18	74	8	0.0438
Fine (35 % < clay < 60 %)	48	48	4	0.0339
Very fine (clay >60 %)	80	20	0	0.0170

Soil erodibility can be assessed using different formulas or nomographs (Wischmeier and Smith 1978) based on granulometry, organic matter content, soil structure, and permeability. Computation formulas for soil erodibility were proposed by Römkens et al. (1986) and revised by Renard et al. (1997) and by Torri et al. (1997) (Table 17.5). It is to be noted that the particle size classes given in these formulas correspond to the American granulometric system, which differs from the Romanian one. Thus, the sandy fraction in the American system is comprised in the 0.05–2 mm interval, while in Romania it corresponds to the 0.02–2 mm interval.

In ROMSEM (Moţoc et al. 1975, 1979), soil erodibility is a dimensionless factor and it is assessed based on a series of qualitative soil parameters: surface erosion degree, cohesion and structuring degree of soil mass, soil profile development degree (Table 17.3). According to ICPA (1987) standards, erodibility results from soil type/subtype, texture and surface erosion degree.

The different magnitude orders of erodibility values from ROMSEM and other USLE models is noticeable. According to the Romanian methodology, the

Table 17.3 Soil erodibility assessment based on erosion state and some physical properties (Moţoc et al. 1975)

Soil characteristics	Erodibility value
Very highly or excessively eroded soils, with very small cohesivity and no structure	1.2
Highly or very highly eroded soils, with small cohesivity and weak structure	1.0
Highly or very highly eroded soils with medium cohesivity, or weakly and moderately eroded soils with small cohesivity	0.8
Highly or very highly eroded soils, with high cohesivity, well structured and highly developed profile	0.7
Weakly or moderately eroded soils, with medium cohesivity, highly developed profile and loose parent material	0.7
Weakly or moderately eroded soils, with high cohesivity, very good structure, highly developed profile and loose parent material	0.6

erodibility values are dimensionless and vary between 0.6 and 1.2, representing correction coefficients for soil erosion. For instance, a value of 1 indicates that soil physical properties are not capable of reducing the erosion process, a value of 0.6 indicates that erosion is reduced by 40 % through the effect of physical soil properties. Moreover, a value of 1.2 indicates that soil inner properties enhance erosion by 20 %. In the original and other USLE/RUSLE models, erodibility has a measurement unit (t ha h ha^{-1} MJ^{-1} mm^{-1}) with maximum values most commonly around 0.04–0.05.

Slope length (λ) represents the plan projection of the distance form runoff formation to runoff concentration or to the beginning of sediment deposition. In USLE, *slope length* (*L*) *factor* is quantified as the standardized length of slope (or slope segment), raised to a power (*m*) varying between 0.2 and 0.6 (Table 17.5, Formula 17.15). In ROMSEM (Moţoc et al. 1975, 1979), *L* factor is expressed as slope length raised to the power 0.3 (Table 17.5, Formula 17.19). In RUSLE (Renard et al. 1997), the exponent *m* is determined with Formulas 17.16 and 17.17 (Table 17.5) proposed by Foster et al. (1977) and McCool et al. (1989).

In order to achieve continuous spatial distributions of *L* factor in GIS environment, the linear slope length (λ) was substituted by the specific contributing area (A_s) (Moore and Burch 1986; Desmet and Govers 1996; Mitasova et al. 1996), resulting from the multiplication of flow accumulation (equal with the number of drained upslope pixels) with the pixel side (resolution). Van der Knijff et al. (2000) used Moore et al. (1993) formula for deriving *L* factor at European scale (Table 17.5, Formula 17.18).

For *slope factor* (*S*), USLE uses Formula 17.20, while ROMSEM one of the 17.21 or 17.20 Formulas (Table 17.5). RUSLE uses different formulas for slopes higher and lower than 9 % (McCool et al. 1987) (Table 17.5, Formulas 17.23 and 17.24). Moore et al. (1993) proposed a relation for quantifying slope factor regardless of slope angle class (Table 17.5, Formula 17.25). The *LS* factor resulting from combining this formula with *L* factor based on specific contributing area (Table 17.5, Formula 17.18) is also known as sediment transport capacity index.

Crop and crop management factor (*C*) expresses the erosion protection of vegetation, which manifests through the interception of a part of rain water, thus reducing runoff, the attenuation of raindrops impact on soil, the effect of soil structuring and root development, the absorption of soil water by roots. *C* factor is dimensionless, expressing the influence of vegetation on soil erosion by means of coefficients with values ranging from approximately 0, when vegetation reduces almost completely the potential erosion, and 1 for bare soils. In Romania, according to the methodology proposed by Moţoc et al. (1975, 1979, 2010), the *C* factor values vary between 0.001 for natural pastures and closed forests with litter, 1 for corn in monoculture and 1.6 for bare field (Table 17.4).

In RUSLE, the computation of *C* factor is quite complex, as it results from the multiplication of 5 subfactors related to prior land use, canopy and surface cover, surface roughness and soil moisture.

An alternative consists in identification of unique values for the *C* factor for different land use categories. Numerous studies, attempting to estimate soil erosion

Table 17.4 Mean values for *C* factor (Moţoc et al. 2010)

Crop and crop management	*C* factor
Bare field or fallow	1.6
Corn in monoculture	1.0
Corn in rotation	0.8
Potatoes and sugar beets	0.6
Sunflower	1.1
Spring grain	0.2
Winter grain	0.14
Perennial grasses in first year	0.2
Perennial grasses after second year	0.014
Established meadow	0.01
Slightly degraded meadow	0.2
Moderately degraded meadow	0.4
Highly degraded meadow	0.8
Young wine plantations under 3 years	0.8
Wine plantations in bearing	0.7
Young fruit plantations with soil as fallow	0.8
Fruit plantation in bearing with soil as fallow	0.6
Fruit plantations with alternating row intervals in sod	0.25
Naturally established meadow	0.001
Established wood with litter	0.001

at small and medium scale (Šúri et al. 2002—Slovakia; Cebecauer and Hofierka 2008—Slovakia; Kouli et al. 2009—Crete Island; Bathrellos et al. 2010—Evia Island, Greece; Bosco and de Rigo 2013—Europe), start from Corine Land Cover land use classification (EEA) and define coefficients for different land use classes. However, their values differ quite a lot from one author to another and therefore, their choice must rely on effective erosion validation.

A simpler solution is to derive the *C* factor from satellite images, by means of relations based on the normalized difference vegetation index (NDVI). Such formulas were proposed by Van der Knijff et al. (2000) and applied for the European territory, by De Jong (1994) and De Jong et al. (1998) (Table 17.5, Formulas 17.26 and 17.27). Except for the advantage of speed and simplicity of calculations, the use of satellite images allows the temporal derivation of *C* factor, making it possible to analyse the time evolution of this parameter. The main problem is that NDVI and *C* factor values are corresponding to the moment of image acquisition. Therefore, the derivation of *C* factor must rely on sets of images acquired in different days for the year.

Soil conservation practice factor (*P*) expresses the efficiency of soil conservation practices by means of correction coefficients (≤ 1), indicating the relative diminution of mean annual soil loss compared with upslope-downslope tillage ($P = 1$).

Table 17.5 Methods for quantifying the erosion factors from USLE/RUSLE/ROMSEM

No.	Authors/region	Formulas
Rainfall erosivity		
1	Rogler and Schwertmann (1981)/Bavaria (Germany)	$R = 10\ (-1.48 + 1.48\ N_s)$ (17.4) N_s—mean precipitation amount (mm) of warm season (May–October)
2	Zanchi (cited by Van der Knijff et al. 2000)/Toscana (Italy)	$R = a\ P_{year}$ (17.5) P_{year}—mean annual precipitations (mm) a—coefficient ranging from 1.1 to 1.5
3	Diodato (2004)/Italy (Mediterranean area)	$EI_{30} = 12.142\ (abc)^{0.6446}$ (17.6) a, b and c—mean annual precipitations, annual maximum daily precipitation and annual maximum hourly precipitation
4	Rousseva and Stefanova (2006)/Bulgaria	$EI_{30} = \alpha\ (nP)^{1.81}$ (17.7) P—mean erosive rainfall for a certain meteorological station α—meteorological station specific coefficient n—mean annual number of erosive rainfalls
5	Renard and Freimund (1994)/SUA	$R = (0.07397\ F^{1.847})/17.2$, for $F < 55$ mm (17.8) $R = (95.77 - 6.081\ F + 0.477\ F^2)/17.2$, for $F \geq 55$ mm (17.9) F—Fournier coefficient (Arnoldus 1980), derived from mean monthly precipitations (p_i): $F_i = p_i^2/(\sum p_i/12)$ (17.10)
Soil erodibility		
6	Römkens et al. (1986) revised by Renard et al. (1997)	$K = 0.0034 + 0.0405 \cdot \exp\left[-0.5 \cdot \left(\frac{\log D_g + 1.659}{0.7101}\right)^2\right]$ (17.11) K—soil erodibility (t ha h ha^{-1} MJ^{-1} mm^{-1}) D_g: geometric mean weight diameter of soil particles (mm) $D_g = \exp\left[\sum f_i \cdot \ln\left(\frac{d_i + d_{i-1}}{2}\right)\right]$ (17.12) d_i and d_{i-1} are maximum and minimum diameters of i particle size class and f_i is the mass fraction of i class

(continued)

Table 17.5 (continued)

No.	Authors/region	Formulas
7	Torri et al. (1997)	$K = 0.0293 \cdot \left(0.65 - D_G + 0.24D_G^2\right) \exp\left[-0.0021\frac{\mathrm{OM}}{f_{\mathrm{clay}}} - 0.00037\left(\frac{\mathrm{OM}}{f_{\mathrm{clay}}}\right)^2 - 4.02f_{\mathrm{clay}} + 1.72f_{\mathrm{clay}}^2\right]$ (17.13) $D_G = -3.5f_{\mathrm{clay}} - 2.0f_{\mathrm{silt}} - 0.5f_{\mathrm{sand}}$ (17.14) K—soil erodibility (t ha h ha^{-1} MJ^{-1} mm^{-1}) OM—organic matter content (%) f_{sand}—sand fraction (0.05–2 mm) f_{silt}—silt fraction (0.002–0.05 mm) f_{clay}—clay fraction (< 0.002 mm)
Slope length factor		
8	Wischmeier and Smith (1978), Renard et al. (1997)	$L = (\lambda/22.13)^m$ (17.15) λ—slope length; m—exponent ranging from 0.2 to 0.6. $m = \beta/(1 + \beta)$ (16) (Foster et al. 1977) (17.16) $\beta = (\sin\theta/0.0896)/[3(\sin\theta)^{0.8} + 0.56]$ (17.17) (McCool et al. 1989)
9	Moore et al. (1993)	$L = 1.4\ (A_s/22.13)^{0.4}$ (17.18) A_s—specific contributing area
10	Moţoc et al. (1975, 1979)/Romania	$L = \lambda^{0.3}$ (17.19) λ—slope length
Slope factor		
11	Wischmeier and Smith (1978)	$S = 65.4\ \sin^2\theta + 4.56\ \sin\theta + 0.0654$ (17.20) θ—slope angle
12	Moţoc et al. (1975, 1979)/Romania	$S = \theta^{1.5}$ (17.21) $S = 1.36 + 0.97\ \theta + 0.138\ \theta^2$ (17.22)

(continued)

Table 17.5 (continued)

No.	Authors/region	Formulas
13	McCool et al. (1987)	$S = 10.8 \sin \theta + 0.03$ for $\theta < 9$ % (17.23) $S = 16.8 \sin \theta - 0.50$ for $\theta \geq 9$ % (17.24)
14	Moore et al. (1993)	$S = (\sin \theta / 0.0896)^{1.3}$ (17.25)
Crop and crop management factor		
15	Van der Knijff et al. (2000)	$C = \exp\left[-\alpha \cdot \frac{\text{NDVI}}{(\beta - \text{NDVI})}\right]$ (17.26) NDVI—normalized difference vegetation index α, β—coefficients
16	De Jong (1994), De Jong et al. (1998)	$C = 0.431 - 0.805$ NDVI (17.27)

Table 17.6 *P* factor values (Moţoc et al. 1975)

Slope class (%)	Conservation practice			
	Contouring system	Stripcropping system or buffer grass strips	Terraces	Upslope-downslope tillage
0–5	0.5	–	0.15	1.0
5–10	0.6	0.30		
10–15	0.7	0.35		
15–20	0.8	0.40		
20–25	0.9	0.45		
>25	0.95	0.50		

The values of these coefficients, according to Moţoc et al. (1975, 1979), are given in Table 17.6. Their differentiation is made according to the type of soil conservation practice and slope class. It is to be noticed that the maximum efficiency is related to slope terracing ($P = 0.15$). The stripcropping system and the buffer grass strips present an intermediate efficiency ($P = 0.3$–0.5), while the lowest efficiency corresponds to the contouring system ($P = 0.5$–0.95).

The final stage in soil erosion spatial modelling according to USLE/RUSLE methodology consists in multiplying the GIS layers representing the control factors in order to derive the potential erosion (without considering the effect of vegetation and support practices) and the effective erosion. Generally, the effective erosion values are grouped in erosion risk classes. Table 17.7 presents the limits of such classes as defined by the Romanian methodology.

Summarizing the above aspects regarding soil erosion factors, the different manners of quantification used in USLE, RUSLE and ROMSEM models are distinguished. Various formulas were proposed for simplifying rainfall erosivity calculations for computation of soil erodibility, for deriving the *LS* factor in GIS environment and for computing the *C* factor from satellite images. The different design of ROMSEM model does not allow the application of such formulas, especially when it comes to rainfall erosivity and soil erodibility.

Table 17.7 Erosion risk classes for arable lands without conservation practices (ICPA 1987)

Class	Estimated soil loss (t ha^{-1} $year^{-1}$)
No risk	≤ 1
Small	2–8
Medium	9–16
High	17–30
Very high	≥ 31

Example of ROMSEM Application

The ROMSEM model (Moţoc et al. 1975, 1979; ICPA 1987) was applied in Dobrovăţ hydrographic basin from the Central Moldavian Plateau (Fig. 17.6). The basin has an area of 186 km^2, with altitudes ranging from 122 to 409 m. The surface lithology is dominated by clay facies. The relief is characterized by cuestas and structural plateaus formed on oolitic limestone. The soil cover is mainly represented by Luvisols, in the northern part, where forests dominate land use, and by Chernozems, in the southern half, where agricultural lands have a greater extent.

For this region, a 20 m resolution digital elevation model (DEM) was produced (Pîrnău 2011), on the basis of which slope angle and slope length were computed in SAGA–GIS 2.0.8 software. These layers were further used to compute slope factor and slope length factor, according to the Romanian methodology. The integrated spatial distribution of *LS* factor is displayed in Fig. 17.7a.

Soil types and subtypes were digitized from 1:10,000 scale soil maps (Pîrnău 2011), produced and provided by Iaşi County Office for Soil Survey. In the attribute table of soil vector layer, numerical codes of different magnitude were assigned to parameters required for soil erodibility computation, namely for surface erosion degree, textural classes and soil type/subtype. The codes were further combined in a new column, resulting unique combinations of erosion degree—texture—soil type/subtype. Erodibility values were then assigned to these combinations, according to the Romanian methodology, and the vector layer was converted into raster, resulting the spatial distribution of erodibility factor (Fig. 17.7b).

The *C* factor was computed based on NDVI derived from a Landsat multi-spectral image, using the relation (17.26) proposed by Van der Knijff et al.

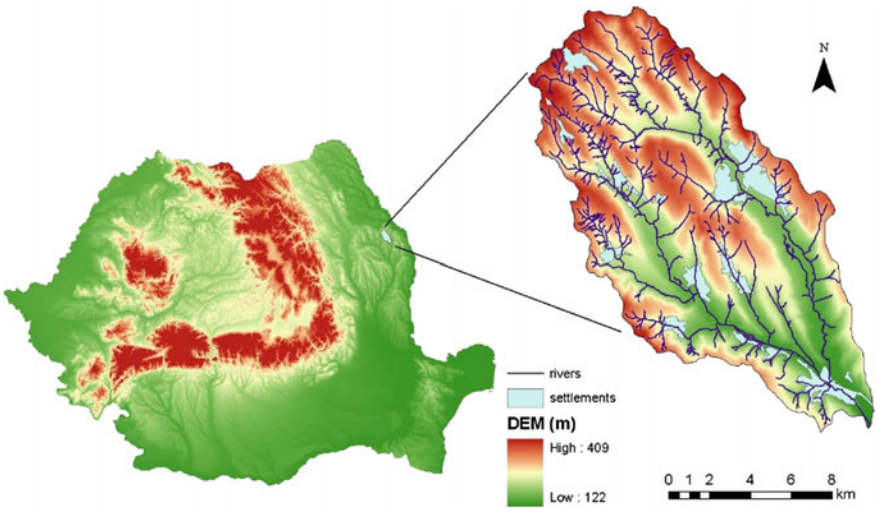

Fig. 17.6 Geographical position of Dobrovăţ basin within Romania

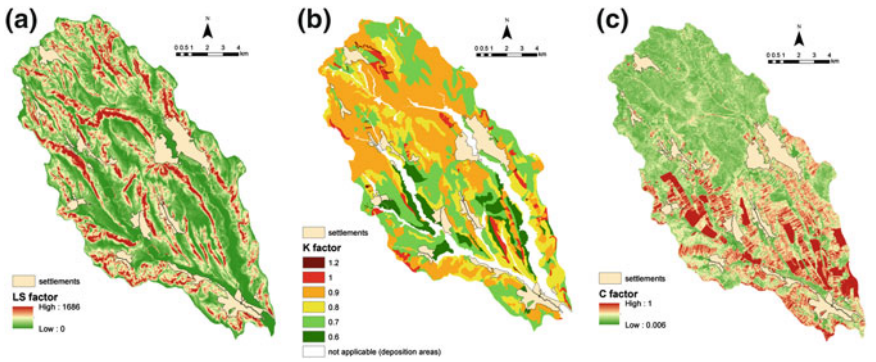

Fig. 17.7 Erosion control factors. **a** Slope and slope length factor. **b** Soil erodibility factor. **c** Crop and crop management factor

(2000) (Fig. 17.7c). Rainfall erosivity was extracted from the georeferenced zoning displayed in Fig. 17.2. Two erosivity values cover the basin: 0.100, for most of the area and 0.144, for the southeastern part.

The raster layers representing the control factors for surface erosion were combined in order to achieve the spatial distribution of potential and effective erosion. The 2 layers were further classified, according to the Romanian methodology (Table 17.5), into 5 erosion risk classes (Fig. 17.8).

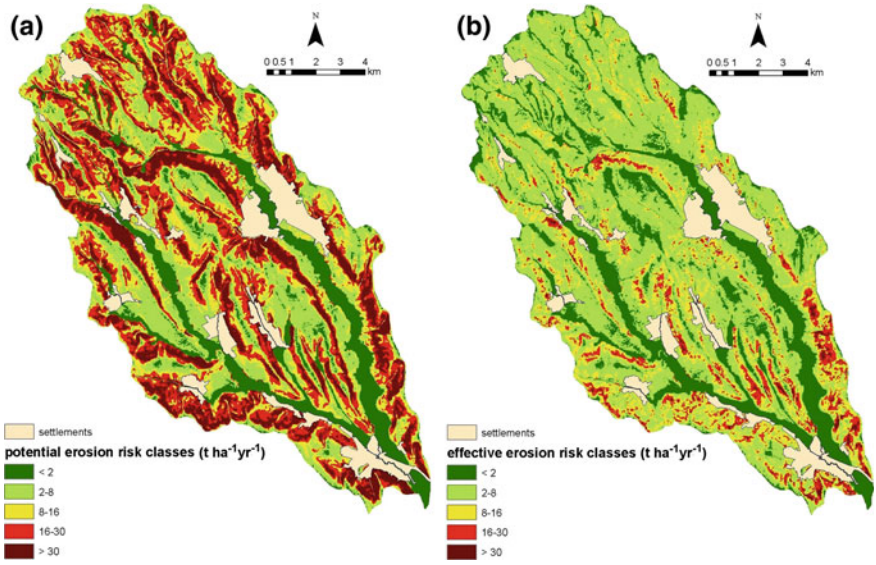

Fig. 17.8 Potential **a** and effective **b** erosion classes

The results show that the mean potential erosion for the whole basin is 15.6 t ha^{-1} $year^{-1}$. The integration of vegetation effect decreases the effective erosion values down to a mean of 5.4 t ha^{-1} $year^{-1}$. An area of 13.4 km^2, representing 7.3 % of the basin, presents high and very high erosion risk. The agricultural lands are affected by a mean erosion rate of 4.9 t ha^{-1} $year^{-1}$, the values ranging from 0 to 67 t ha^{-1} $year^{-1}$. Experimental data measured at Podu Iloaiei agricultural research station in similar environmental settings (Ailincăi et al. 2012) show that mean annual soil loss is about 5 t ha^{-1} $year^{-1}$ on corn and wheat fields, which dominate land use structure in Dobrovăț basin. This value is in agreement with the mean erosion rate estimated on arable lands by application of ROMSEM model. For bare soils and slope angles of 16 %, the experimental data indicate a mean soil loss value of 18.24 t ha^{-1} $year^{-1}$. In Dobrovăț basin, the estimated potential erosion by ROMSEM model, which corresponds to soil loss on bare fields, has a mean value of 23.27 t ha^{-1} $year^{-1}$ for the slope angle interval of 15–17 %. These comparisons with measured data validate, in our opinion, the ROMSEM model results.

Conclusions

Presently, there is a wide variety of models designed for soil erosion assessment, with local or spatial character, some simpler, others more complex. The choice of a certain model must rely on the study purpose and scale, on the availability of input data, on the desired accuracy. Models' validation constitute an important step, but sometimes difficult to achieve because of insufficient experimental data. Many times, the validation of models is carried out through expert knowledge.

USLE and RUSLE are the erosion models most commonly applied. The scales of applications range from local and regional, to national and even continental. Their main advantages are the relative conceptual simplicity and ease of application, the demand of less input data of lower complexity, compared to the physical models. On the other hand, the results may be less accurate, especially when evaluations are carried out at small scales. Even in these situations, they present certain importance, constituting a first approximation of erosion risk and revealing the high risk areas which demand supplementary, more detailed evaluations.

The factors from USLE/RUSLE may be quantified by multiple alternative methods. Numerous relations were proposed for simplifying rainfall erosivity computation. Various relations were suggested for achieving soil erodibility, as well as erodibility values for textural classes. Efforts were made for achieving *L* factor three-dimensionally, in GIS environment. Diverse coefficients were proposed for crop and crop management factor, as well as relations based on satellite images. The alternative, simpler methods facilitate model application, but increase the uncertainty of results. For this reason, the final validation step is very important.

In Romania, the USLE model adapted by Moţoc et al. (1975, 1979), ICPA (1987) differs substantially from the original model: rainfall erosivity is expressed as annual soil loss per unit of rainfall aggressiveness; soil erodibility is a

dimensionless factor with values between 0.6 and 1.2; slope length is not standardized; *C* factor may take values up to 1.6 for bare soil. All these differences do not commonly allow the substitution of a certain factor by relations proposed abroad, excepting *C* factor, up to a certain extent. A consequence of these differences is that they hamper the comparison of the control exerted by erosion factors derived according to ROMSEM model, on the one hand and USLE, RUSLE models, on the other hand. Yet, the results concerning potential and effective erosion can be compared with results achieved by application of other models.

References

Ailincăi C, Jităreanu G, Bucur D, Ailincăi D (2012) Soil erosion and conservation measures in Moldavian Plateau. Cerc Agron Moldova XLV(4):29–42

Anghel T, Todică S (2008) Quantitative assessment of soil erosion using GIS empirical methods. A comparative study between the Motru mining area and the Sucevița catchment. Ann Univ Oradea Geogr Ser XVIII:95–102

Arghiuș C, Arghiuș V (2011) The quantitative estimation of the soil erosion using USLE type ROMSEM model. Case-study- the Codrului ridge and piedmont (Romania). Carpath J Earth Env 6(2):59–66

Arnoldus HM (1980) An approximation of the rainfall factor in the universal soil loss equation. In: De Boodt M, Gabriels D (eds) Assessment of erosion. Wiley, Chichester, pp 127–132

Bathrellos GD, Skilodimou HD, Chousianitis KG (2010) Soil erosion assessment in southern Evia Island using USLE and GIS. In: Proceedings of the 12th international congress, Patras, Greece, May 2010. Bull Geol Soc Greece XLIII(3):1572–1581

Biali G, Popovici N (2003) Tehnici SIG în monitoringul degradării erozionale. Gh. Asachi, Iași (in Romania)

Bilașco Ș, Horvath C, Cocean P et al (2009) Implementation of the USLE model using GIS techniques. Case study the Someşean Plateau. Carpath J Earth Env 4(2):123–132

Bosco C, de Rigo D (2013) Land cover and soil erodibility within the e-RUSLEModel. Sci Top Focus 1, MRI-11b13. doi:10.6084/m9.figshare.856670

Brown LC, Foster GR (1987) Storm erosivity using idealized intensity distributions. Trans ASAE 30:378–386

Cârdei P (2009) New forms and directions in mathematical modeling of pluvial erosion. WSEAS Trans Environ Dev 9(5):607–618

Cârdei P, Herea V, Muraru V, Sfaru R (2009) Vector representation for the soil erosion model USLE, a point of view. Bull Univ Agric Sci Agric 66(1–2):46–53

Cebecauer T, Hofierka J (2008) The consequences of land-cover changes on soil erosion distribution in Slovakia. Geomorphology 98:187–198

Cook HL (1936) The nature and controlling variables of water erosion process. Soil Sci Am Soc Proc 1:60–64

De Jong SM (1994) Applications of reflective remote sensing for land degradation studies in a mediterranean environment. Ned Geogr Stud 177:1994

De Jong SM, Brouwer LC, Riezebos HT (1998) Erosion hazard assessment in the Peyne catchment, France. Working paper DeMon-2 project. Department of Physical Geography, Utrecht University

Desmet PJJ, Govers G (1996) A GIS-procedure for automatically calculating the USLE LS-factor on topographically complex landscape units. J Soil Water Conserv 51(5):427–433

Diodato N (2004) Estimating RUSLE's rainfall factor in the part of Italy with a Mediterranean rainfall regime. Hydrol Earth Syst Sci 8(1):103–107

Domniţa M (2012) Runoff modeling using GIS. Application in torrential basins in the Apuseni mountains. Dissertation, "Babeş-Bolyai" University of Cluj-Napoca, Vrije Universiteit Brussel
Dumitru S, Mocanu V, Eftene M, Coteţ V (2010) The assessment of soil erosion process in a test area at NUTS4 level. Res J Agric Sci 42(3):122–130
EEA, Corine Land Cover, European Environment Agency. http://www.eea.europa.eu/publications/COR0-landcover. Accessed 23 Feb 2015
Florea N, Orleanu C, Ghitulescu N et al (1977) Harta eroziunii solurilor R.S. România la scara 1:500,000. In: Folosirea Raţională a Terenurilor Erodate. Ministerul Agriculturii şi Industriei Alimentare şi SCCES Perieni, Bucureşti (in Romanian)
Foster GR, Meyer LD, Onstad CA (1977) A runoff erosivity factor and variable slope length exponents for soil loss estimates. Trans ASAE 20:683–687
Grimm M, Jones R, Montanarella L (2002) Soil erosion risk in Europe. European Soil Bureau, Institute for Environment and Sustainability, JRC Ispra, EUR19939EN
ICPA (1987) Metodologia elaborării studiilor pedologice. Partea a III-a – Indicatorii ecopedologici, ICPA, Bucuresti (in Romanian)
Ioniţă I, Rădoane M, Sevastel M (2006) Chapter 1.13 Romania. In: Boardman J, Poesen J (eds) Soil erosion in Europe. Wiley, Chichester, pp 155–166
Kirkby MJ, Jones RJA, Irvine B et al (2004) Pan-European soil erosion risk assessment: the PESERA map, version 1 October 2003, explanation of special publication Ispra 2004 No. 73 (S.P.I.04.73). European soil bureau research report No. 16, EUR 21176, Office for Official Publications of the European Communities, Luxembourg
Kouli M, Soupios P, Vallianatos F (2009) Soil erosion prediction using the revised universal soil loss equation (RUSLE) in a GIS framework, Chania, Northwestern Crete, Greece. Environ Geol 57:483–497. doi:10.1007/s00254-008-1318-9
Laflen JM, Lane LJ, Foster GR (1991) WEPP: a new generation of erosion prediction technology. J Soil Water Conserv 46:34–38
McCool DK, Brown LC, Foster GR et al (1987) Revised slope steepness factor for the universal soil loss equation. Trans ASAE 30:1387–1396
McCool DK, Foster GR, Mutchler CK et al (1989) Revised slope length factor for the universal soil loss equation. Trans ASAE 32:1571–1576
Merritt WS, Letcher RA, Jakeman AJ (2003) A review of erosion and sediment transport models. Environ Modell Softw 18:761–799
Meusburger K, Steel A, Panagos P et al (2012) Spatial and temporal variability of rainfall erosivity factor for Switzerland. Hydrol Earth Syst Sci 16:167–177. doi:10.5194/hess-16-167-2012
Mitasova H, Hofierka J, Zlocha M et al (1996) Modeling topographic potential for erosion and deposition using GIS. Int J Geogr Inf Syst 10:629–642
Moore ID, Burch GJ (1986) Modeling erosion and deposition: topographic effects. Trans ASAE 29:1624–1640
Moore ID, Turner AK, Wilson JP et al (1993) GIS and land-surface-subsurface process modeling. In: Goodchild MF, Parks BO, Steyaert LT (eds) Environmental modeling with GIS. Oxford University Press, New York, pp 196–230
Morgan RPC (2010) Model development: a user's perspective. In: Morgan RPC, Nearing M (eds) Handbook of erosion modelling. Wiley
Motoc M (1983) Ritmul mediu de degradare erozională a solului in R. S. Romania. In: Buletinul Informativ al ASAS, vol 13. Academy of Agricultural and Forestry Sciences "Gheorghe Ionescu-Sisesti", Bucureşti, pp 47–65 (in Romanian)
Moţoc M, Sevastel M (2002) Evaluarea factorilor care determină riscul eroziunii hidrice în suprafaţă. Editura Bren, Bucureşti (in Romanian)
Moţoc M, Munteanu S, Băloiu V et al (1975) Eroziunea solului si metodele de combatere. Edit. Ceres, Bucureşti (in Romanian)
Moţoc M, Stanescu P, Taloescu I (1979) Metode de estimare a eroziunii totale si efluente pe bazine hidrografice mici. ICPA, Bucureşti (in Romanian)
Moţoc M, Ioniţă I, Nistor D et al (2010) Soil erosion control in Romania. State of the art. In: Nistor D (ed) Sustainable utilization of soil and water resources on sloping land—research

results—2nd edn. Academy of Agricultural and Forestry Sciences "Gheorghe Ionescu-Sisesti", Research and Development Center for Soil Erosion Control Perieni, Bucharest, pp 26–47
Munteanu I, Untaru G, Parichi M et al (2000) Harta terenurilor Romaniei la sc. 1:1,000,000 privind riscul si gradul de manifestare a proceselor de eroziune, alunecari, prabusiri si inundatii. Protecţia mediului in Agricultură, Helicon, Timişoara, pp 43–54 (in Romanian)
Panagos P, Meusburger K, Van Liedekerke M et al (2014) Assessing soil erosion in Europe based on data collected through a European network. Soil Sci Plant Nutr 60:15–29. doi:10.1080/00380768.2013.835701
Patriche CV (2005) Podişul Central Moldovenesc dintre râurile Vaslui şi Stavnic – studiu de geografie fizică. Edit. "Terra Nostra", Iaşi (in Romanian)
Patriche CV, Căpăţână V, Stoica DL (2006) Aspects regarding soil erosion spatial modeling using the USLE/RUSLE within GIS. Geogr Tech 2:87–97
Patriche CV, Pîrnău RG, Roşca B et al (2012) Assessment of soil erosion and its impact on humus spatial and temporal dynamics. Study case: Dobrovăţ basin (eastern Romania). Bull UASVM Agric 69(1):185–194
Pîrnău RG (2011) Utilizarea terenului şi calitatea solurilor agricole în bazinul hidrografic Dobrovăţ. Dissertation, Universitatea Alexandru Ioan Cuza University, Iaşi (in Romanian)
Popa N (2010) Soil erosion models used in Romania. In: Nistor D (ed) Sustainable utilization of soil and water resources on sloping land—research results—2nd edn. Academy of Agricultural and Forestry Sciences "Gheorghe Ionescu-Sisesti", Research and Development Center for Soil Erosion Control Perieni, Bucharest, pp 288–294
Prefac Z (2008) Dinamica versanţilor din bazinul hidrografic al Râmnei. Dissertation, Universitatea din Bucureşti (in Romanian)
Renard KG, Freimund JR (1994) Using monthly precipitation data to estimate the R factor in the revised USLE. J Hydrol 157:287–306
Renard RG, Foster GR, Weesies GA et al (1991) RUSLE: revised universal soil loss equation. J Soil Water Conserv 46(1):30–33
Renard RG, Foster GR, Weesies GA et al (1997) Predicting soil erosion by water: a guide to conservation planning with the revised universal soil loss equation (RUSLE). Agriculture Handbook no. 703, USDA-ARS
Rogler H, Schwertmann U (1981) Erosivität der Niederschläge und Isoerodentenkarte Bayerns. Zeitschrift für Kulturtechnik und Flurbereinigung 22:99–112
Römkens MJM, Prasad SN, Poesen JWA (1986) Soil erodibility and properties. In: Proceedings of the 13th congress of the international soil science society, vol 5. Hamburg, Germany, pp 492–504
Roşca B, Vasiliniuc I, Topşa G (2012) Models for estimating soil erosion in the middle and lower Vasluieţ basin. Bull UASVM Agric 69(1):163–172
Rousseva S, Stefanova V (2006) Assessment and mapping of soil erodibility and rainfall erosivity in Bulgaria. In: Proceedings of the conference on water observation and information system for decision support "BALWOIS 2006". Ohrid, Republic of Macedonia, A-152
Stănescu P, Taloiescu I, Drăgan L (1969) Contribuţii la stabilirea unor indicatori de estimare a erozivităţii pluviale. Analele ICIFP Pedol 2(36):361–369 (in Romanian)
Ştefănescu L, Constantin V, Surd V et al (2011) Assessment of soil erosion potential by the USLE method in Roşia Montană mining area and associated Natech events. Carpath J Earth Environ Sci 6(1):35–42
Šúri M, Cebecauer T, Hofierka J, Fulajtár E (2002) Soil erosion assessment of Slovakia at a regional scale using GIS. Ecology (Bratislava) 21(4):404–422
Torri D, Poesen J, Borselli L (1997) Predictability and uncertainty of the soil erodibility factor using a global data set. Catena 31(1–2):1–22
USDA-ARS (2008) Draft scientific documentation revised universal soil loss equation version 2. http://www.ars.usda.gov/Research/docs.htm?docid=6028. Accessed 23 Feb 2015
Van der Knijff JM, Jones RJA, Montanarella L (2000) Soil erosion risk assessment in Europe. European Soil Bureau, Joint Research Centre, Space Applications Institute
Van Rompaey A, Verstraeten G, Van Oost K et al (2001) Modelling mean annual sediment yield using a distributed approach. Earth Surf Proc Land 26(11):1221–1236

Vătău A, Teodorescu V, Ionescu V (1993a) Harta erodabilității solurilor la sc. 1:500,000. Soil erodibility map of Romania at a scale 1:500,000. DTM, București (in Romanian)
Vătău A, Teodorescu V, Ionescu V (1993b) Harta coeficientului de scurgere standard la sc. 1:500,000. Standard soil loss map of Romania at a scale 1:500,000. DTM, Bucuresti
Williams JR (1975) Sediment-yield prediction with universal equation using runoff energy factor. In: Proceedings of the sediment-yield workshop, USDA Sedimentation Lab., Oxford, Mississippi, 28–30 Nov 1972, ARS-S-40, 1975
Wischmeier WH, Smith DD (1978) Predicting rainfall erosion losses: a guide to conservation planning. Agriculture Handbook No. 537, USDA

Part V
Rivers

Chapter 18
Geomorphological Evolution and Longitudinal Profiles

Maria Rădoane, Ionuț Cristea, Dan Dumitriu and Ioana Perșoiu

Abstract The contribution of Romanian geomorphology to the study of longitudinal profiles revolved mainly around the following question: how can the shape of long profiles be interpreted in order to identify the evolutionary traits of landforms? The approaches to providing an answer to this question can be ranked into following categories: longitudinal profiles and the knick-points and knickzones approach; tectonic and lithologic control on the evolution of the drainage network; longitudinal profiles concavity related to river age and channel bed material grain size. A range of new methods for determining river gradients, as well as modern facilities for processing large databases were employed in this study, assisting us in demonstrating that tectonics prevailed over lithology (as well as other secondary factors) in generating knickzones along longitudinal profiles. Furthermore, the differential uplift of major Carpathian structural units (e.g., the Carpathian flysch ot the peri-Carpathian molasse) was detected in the distribution of stream gradient index. Tectonic movements established the general evolution pattern of the drainage network and prompted rivers to constantly adapt in order to reach the equilibrium shape of longitudinal profiles. Regardless of age, the shape of longitudinal profiles continually adjusted to ensure that geomorphological work is performed by rivers under conditions of high variability of tectonic movements and geomorphic time.

Keywords Long profile concavity · Knick-points · Knickzones · Tectonics · Lithology · Romanian Carpathians

M. Rădoane (✉) · I. Cristea · I. Perșoiu
Stefan cel Mare University, Universității 13, 720229 Suceava, Romania
e-mail: radoane@usm.ro; mariaradoane@gmail.com

D. Dumitriu
Alexandru Ioan Cuza University, Carol I Av. 11, 700506 Iași, Romania

M. Rădoane and A. Vespremeanu-Stroe (eds.), *Landform Dynamics and Evolution in Romania*, Springer Geography,
DOI 10.1007/978-3-319-32589-7_18

Longitudinal Profiles and the Knick-Points and Knickzones Approach

Longitudinal profiles are the third adjustable dimension of alluvial channel morphology (following cross-sections and reaches) (Richards 1982) or the third holarchic unit of a fluvial system (Ichim et al. 1989). The time required for the adjustment of the longitudinal profile shape is considerable, similar to cyclic periods (Schumm and Lichty 1965), resulting in an optimal shape whereby the energy expenditure for water and sediment transport is minimized. The inclusion of this topic in the chapter dedicated to rivers and their landform shaping capacity is motivated by the sensitivity of longitudinal profiles to major changes in the fluvial system and their ability to preserve these changes mainly in the shape of profile curves. The plotting of these profiles shows altitude against distance downstream. The resulting form is a curve, more or less regular, the concavity of which increases toward the headwater area. This is their most obvious and persistent feature regardless of the climatic conditions, the length of the river or the rock cut by the riverbed. The attention there is focussed on stream profile concavity, partly because it is assumed to be "…so common as to be almost universal" [Rubey (1933), quoted by Wheeler (1979)]. So it is only natural that this largely generalized observation be a fascinating subject for research of geologists, geomorphologists, and geographers everywhere.

While there is no specific approach aimed at analyzing longitudinal profiles, Romanian geographers' studies on transverse valleys (Orghidan 1969) and connecting valley shoulders and terrace levels [in a synthesis by Posea et al. (1974)] were commonly illustrated using long profile graphs. Several attempts were made to correlate the ages of Carpathian denudation surfaces with consecutive levels of longitudinal profiles pertaining to rivers located at the base of the mountains (such as the tributaries of Strei river within Haţeg Depression—Grumăzescu 1975). Without overtly mentioning the shape of longitudinal profile, the authors researching the connection of terrace levels identified several distortions in the long profiles generated by tectonic and neotectonic movements (Niculescu 1963; Necea et al. 2005); moreover, in the case of a long Carpathian river such as Bistriţa, Donisă (1968) observed that the alternation of alluvial deposition and valley deepening stages was not a synchronous process, hence the difficulty in determining terrace ages by employing the altitude criterion.

The study of longitudinal profiles was associated to the confluence topic (Ichim 1979) in order to deduce whether the spatial distribution of junction points between same order rivers, on one hand, and of relative altitude of thresholds, on the other, have any significance as references in the evolution of the valley system. By processing a large population of first to fourth-order valleys in the Strahler system across a 2000 km^2 area in Stânişoara Mts we confirmed that two levels of slope discontinuity with a certain homogeneity can be identified (Ichim 1979). In attempting to explain the geomorphological significance of slope gradient changes the author disregarded lithological influence, as the frequent sequences of strata

characteristic for the flysch are unlikely the cause for such homogenous levels in drainage basins as different in terms of the geology. According to the author, the two levels resulted from phases of maximum intensity of slope processes, colluviation of hillslope base, and silting of valley bottoms, therefore reducing longitudinal profile gradients. The author believed these phases most likely coincided with Pleistocene climate changes; however, this statement was not substantiated by evidence other than morphological.

Tectonic and Lithologic Control on the Evolution of the Drainage Network

Further research on the significance of knickzones took an important leap with the refinement of identifying thresholds in the longitudinal profile (k_{sn}—normalized steepness index cf Whipple et al. 2007). This index, computed for each river reach, allows for the highly accurate identification of all types of slope gradient discontinuities along the river within a numerous family of rivers. Various applications of this work method[1] were designed in order to distinguish the role played by tectonics in drainage network organization across large areas, such as Putna basin in the Carpathian Curvature region (Cristea 2011), the eastern area of the Eastern

[1]The methodology is employed mainly in the analysis of rivers deepened in the bedrock and is based on the assumption that if a river crosses a uniformly lifted region with lithologically homogeneous substrate, it will have some characteristic traits. In the case of a mature fluvial morphological system in a state of erosional equilibrium, longitudinal profiles are concave at the top and lacking irregularities overall (Hack 1973). However, inverse relationships will occur in the logarithmic space, in the ratio between local gradient and river length (Hack 1957) or the ratio between local gradient and upstream basin area. The linear regression of the local thalweg gradient (slope—S, in %) and its drainage area (area—A, in km^2) can be used to determine the river concavity index (θ) and the steepness index (k_s):

$$S = k_s \cdot A^{-\theta} \tag{18.1}$$

Due to the close interdependence between the two parameters, the standardization of this index is recommended for further comparative studies of k_s values, by relating it to a reference concavity (θ_{ref}), using the same law:

$$S = k_{sn} \cdot A^{-\theta ref} \tag{18.2}$$

The normalized steepness index—k_{sn} is, in fact, a measurement of river reach gradient, adapted to a certain expected relation between the local gradient and the drained area. The value of the reference concavity is established according to the average concavity determined for the study area, but often the 0.45 value is employed. Finally, the values of the new index for each river reach can be compared, with highest values indicating threshold occurrence.

Carpathians and southern sector of the Southern Carpathians (Molin et al. 2012) and several rivers in the Transylvanian basin (Ter Borgh 2013).

Longitudinal profile analysis in Putna drainage basin (upper sector) can be regarded as an exemplar for applying knickzone methodology in a region of high tectonic intensity such as the Carpathian Curvature. The entire region consists of folded sediments pertaining to the Eastern Carpathian nappes (i.e., Tarcău and Marginal Folds) and the western flank of the Carpathian avantfosse. The mountain unit formations include Cretaceous and Paleogene sequences of conglomerates, sandstones, limestones, marls, and clays. The Subcarpathian nappe comprises mainly of Miocene sandstones, conglomerates, marls, and clays (Fig. 18.1a). From the tectonic perspective, the latest uplift occurring during the Pliocene-Quaternary, greatly influenced the direction and the morphological features of the drainage

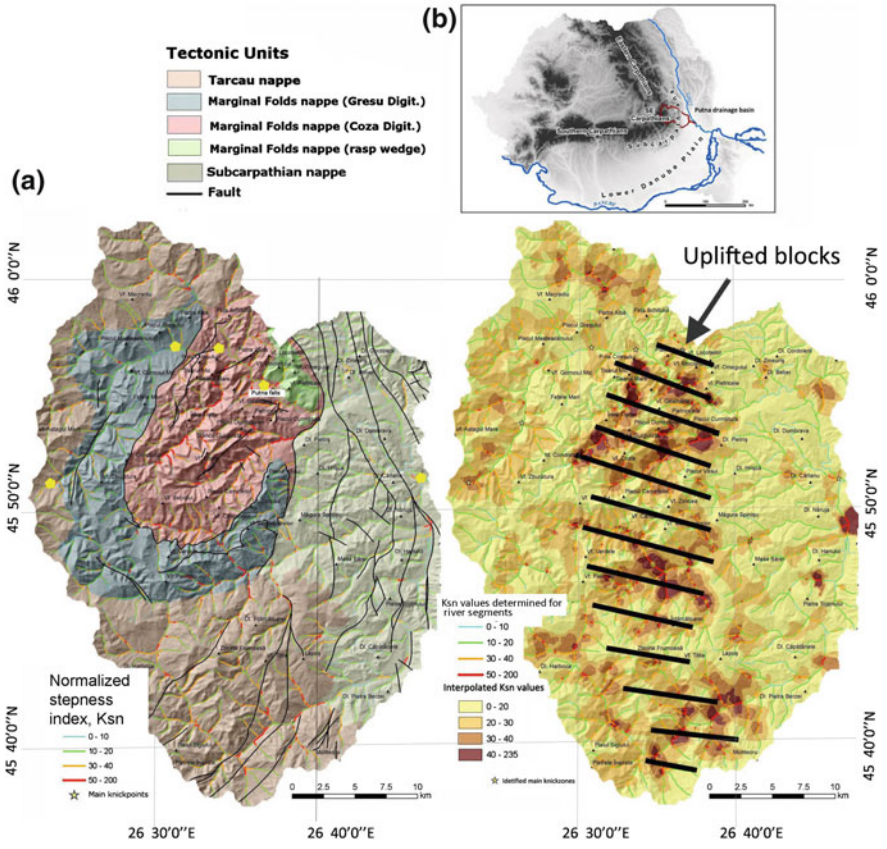

Fig. 18.1 Applying knickzone methodology in a region of high tectonic intensity such as the Carpathian Curvature, *upper* drainage basin of the Putna river. **a** Map of geological structural units and distribution of river reaches with various k_{sn} values. **b** The effects of tectonic uplift on the shape of longitudinal profiles, regardless of the lithological composition of the substrate, resulted from k_{sn} values interpolation

network within this area (Fielitz and Seghedi 2005; Necea 2010), and resulted in river-channel deepening in the bedrock. This phenomenon occurred in the 3–4 m terrace level, as well.

The geographical distribution of normalized steepness index values is shown in Fig. 18.1b. The interpretation of these values was carried out taking into account the main geo-structural units traversed by rivers and tectonic or lithologic anomalies in order to highlight the role of each factor in shaping longitudinal profiles in Putna upper basin.

The occurrence of reaches with slope anomalies ($k_{sn} > 50$) is not necessarily related to the lithological traits of a certain nappe within the basin; instead, they appear to be clustered within a much broader area, located between 26.5° and 26.68° E, and another one between 26.75° and 26.78° E (Fig. 18.2), overlying the eastern margin of the mountain unit, and the edge of the folded molasse, respectively, whereby the occurrence can solely be explained by tectonics (Fig. 18.1a). In terms of the distribution against latitude (Fig. 18.1b), slope anomalies indicate the occurrence of differential uplift of the block structure which left its imprint, to a large extent, on the current structure of the drainage network. Relatively recent hydrographical changes appear to have played a significant role by augmenting the length of the river, as well as the subsequent increase in the drainage basin area, by approx. 900 km^2. Unsurprisingly, the largest cluster of knickpoints, both in terms of magnitude and frequency, overlies the Cretaceous outcrop in Digitation of Coza, from the half-window of Vrancea. According to Necea (2010), Cretaceous deposits were uncovered during the Late Pleistocene, as exhumation rates reached unprecedented values, of up to 3.2 ± 0.3 mm/year.

The influence of lithology on steepness index values is relevant, but not definitive. For instance, according to the 1:100 000 geological map, the most important slope distortion in the longitudinal profile of river Putna (i.e. Putna Waterfall area) occurs on a Kliwa sandstone outcrop. However, it is also located along the aforementioned tectonic-structural alignment on the outskirts of the Carpathian flysch, which is believed to have an even stronger influence. Moreover, by correlating the main lithofacies in the region with k_{sn} values it can be noted there are no significant differences. In general, slope gradients are similar, despite the rather dissimilar lithology. However, under certain conditions, harder lithofacies can contribute to generating and preserving major slope ruptures, as indicated by the maximum values of the k_{sn} index (e.g., the effects of Piatra Geamănă conglomerates-upstream of the confluence with Mărului stream; within the reach located in the vicinity of the homonym peak—downstream of Putna waterfall—or Bârseşti conglomerates (outcropping in the molasse area located north of the homonym village or nearby Valea Sării-all of which are marked by a yellow star in Fig. 18.1a).

As with the study by Ichim (1979), it can be concluded that overall, albeit lithology can have a certain local influence on longitudinal profiles of rivers in upper Putna basin, given the extent of the stratigraphic diversity of Carpathian flysch, it fails to account for the regional traits. Therefore, the recent tectonic evolution of the SE Carpathians, i.e. the differential peripheral uplift of the flysch or

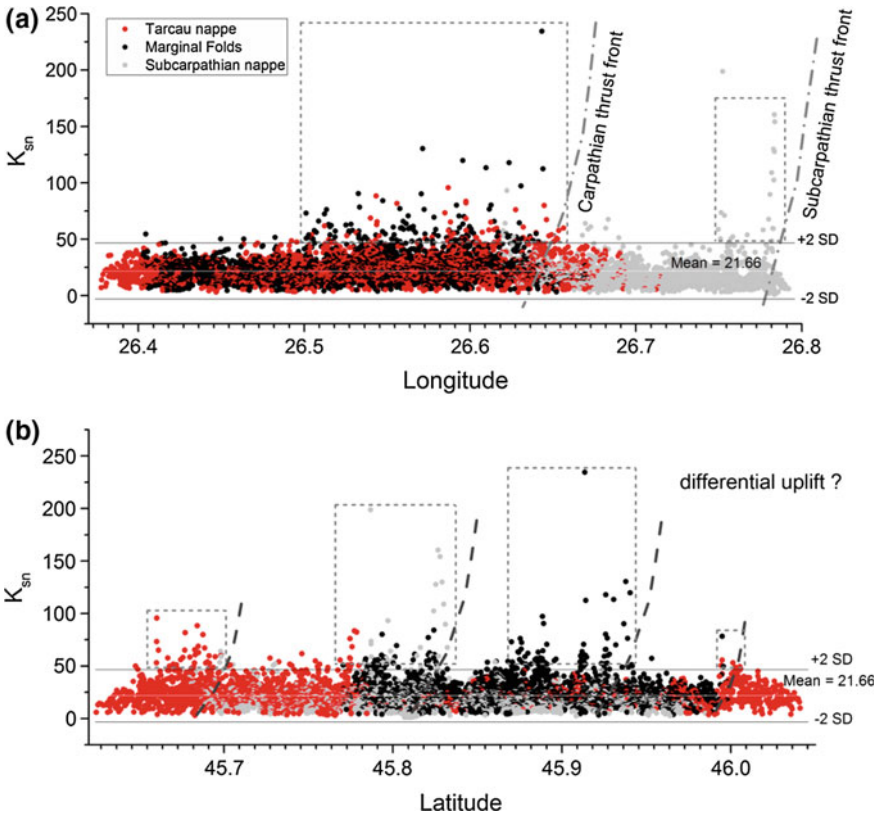

Fig. 18.2 Distribution of the normalized steepness index in Putna drainage basin. **a** Longitude distribution. k_{sn} deviation above the 0.45 threshold value indicates the role played by tectonics in controlling the shape of longitudinal profiles. **b** Latitude distribution. k_{sn} deviation indicates the presence of several tectonic blocks uplifted differently

the molasse in the vicinity of Caşin-Bisoca fault line, likely had a major influence on the shape of the longitudinal profile.

A successful overview of all observations indicating how longitudinal profiles should be "read" in order to capture the distribution of knickzones is provided by Hack (1973), who was primarily interested in finding and explaining the shape of equilibrium profiles in rivers. To determine whether a river is in a dynamic equilibrium state, he introduced a calculation method employing the relation between river slope gradient and length, based on which knick-points and knickzones can be determined along longitudinal profiles regarded as anomalous reaches. The distortions in the natural concavity of longitudinal profiles can be quantized by

applying the *stream gradient index*, also known as *SL index* (slope versus length) or *Hack index.*[2]

In the case of the 13 Carpathian rivers (Table 18.1 and Fig. 18.3) the relation between SL_{total} and the concavity index, Ca, is positive (Fig. 18.4a). Moreover, the value of SL_{total} increases southward in the Eastern Carpathians and westward in the Southern Carpathians, whereby the peak values occur in Argeş and Dâmboviţa rivers.

The following types of anomalous reaches are present in the investigated rivers: (1) the earliest distortions occur in the immediate vicinity of the headwaters (ranging from 2 to 5 km from the springs), typically above 1000 m a.s.l.; (2) in rivers from the northern and central sectors of the Eastern Carpathians the main anomaly occurs in the mid-course, at 300–600 m a.s.l. (Molin et al. 2012, refer to 500–650 m—page 4), commonly overlying the Tarcău Nappe; (3) in rivers from the southern rim of the Southern Carpathians the same anomalous zone is present in the transition area to the Subcarpathians; (4) distortions were observed in both the transition areas from the mountains to the piedmont, and from the piedmont to the plain. Most anomalies were documented in the longitudinal profiles either of rivers from the northern sector of the Eastern Carpathians (i.e., Moldova and Suceava) (first category), rivers located on both flanks of Trotuş fault line (second category), or rivers located west of the Intramoesic fault line (Fig. 18.4a).

Based on these observations provided by a study area significantly broader than Putna drainage basin, we can further infer that tectonic activity is the main cause for inherited anomalies of longitudinal profiles. Recent studies on the structural evolution of the Eastern and Curvature Carpathians and their foreland (Mațenco et al. 2003; Fielitz and Seghedi 2005) indicated the shape (and particularly the planform) of the drainage network is closely linked to tectonic activity along the main fault lines (shown in Fig. 18.3). The tectonics of Tarcău Nappe had the most extensive influence on the distortion of longitudinal profiles of eastern Carpathian rivers, whereas the other causes discussed in the literature (Seeber and Gomitz 1983) are secondary.

[2]The stream gradient index (SL) is computed using the equation:

$$SL = \Delta H \times L/\Delta L \tag{18.3}$$

where ΔH is the difference in elevation between two points located along the river, ΔL is the length of the reach delimited by the two points, and L is the cumulative length of the river up to the respective points. The SL index can be calculated for the entire length of the river, in which case it becomes SL_{total}, taking into account the difference in elevation between the headwaters and river mouth and the natural logarithm of the total length of the river, as in Eq. 18.4:

$$SL_{total} = \Delta H/\mathrm{In}L \tag{18.4}$$

Seeber and Gomitz (1983) believe that when $SL_{section}$ divided by SL_{total} yields a result below 2, there are no anomalies. Conversely, when the result ranges from 2 to 10, the profile exhibits second-order anomalies, whereas a result equal to or above 10 indicates first-order anomalies. This classification implies that first-order distortions indicate the occurrence of very steep slopes, second-order indicates steep slopes, whereas values under 2 describe graded profiles.

Table 18.1 Data on the studied streams

River, junction with	Drainage basin A (km^2)	Network order Ω	Relief ratio RR (m/km)	Average discharge Q (m^3/s)	Suspended load Q_s (kg/s)	Concavity index, Ca[a]	Median diameter of bed material (mm)
Suceava, Siret	2616	8	7.88	14.1	5.90	0.494	52.4
Moldova, Siret	4299	8	8.19	26.2	14.70	0.431	37.5
Bistriţa, Siret	6974	8	7.44	52.0	8.30	0.503	NA
Trotuş, Siret	4456	8	8.95	33.0	38.45	0.488	88.6
Putna, Siret	2480	7	11.0	13.4	91.80	0.651	83.1
Bârlad, Siret	7395	7	4.84	9.01	NA	0.686	0.28
Buzău, Siret	5264	8	6.44	25.7	80.30	0.765	66.9
Ialomiţa, Danube	10,430	8	5.94	45.7	95.00	0.672	32.1
Siret, Danube	42,274	9	4.17	254.0	221.00	0.634	11.1
Teleajen, Prahova	1656	7	14.4	9.35	NA	0.866	NA
Dimbovita, Arges	2837	7	10.5	13.3	21.30	0.685	NA
Argeş, Danube	12,590	8	7.28	49.7	45.20	0.765	NA
Olteţ, Olt	2474	7	11.02	8.6	39.40	0.781	70.9
Jiu, Danube	10,070	8	5.20	86.8	114.00	0.800	NA

NA not available

[a]The concavity of the profile was determined as a ratio of the measured areas on the profile graphic, Ca = *A*1/*A*2, where *A*1 is the numerically integrated area between the curve of the profile and a straight line uniting its ends and *A*2 is the triangular area created by that straight line, the horizontal axis traversing the head of the profile. The concavity index Ca allows the following interpretation: if its value is close to 0.0, the form of the profile is close to a straight line; if its value is close to 1.0, the profile is L-shaped

The latter include outcrops of very resilient rocks, increasing coarse sediment inputs, changes in the base level, or the effects of confluence points.

As regards the theory according to which "The longitudinal profiles of rivers draining the southern Carpathians are close to the equilibrium shape, in agreement with the older emersion of the chain. The longitudinal profiles of the rivers draining the eastern and southeastern Carpathians are in a transient state of disequilibrium as a consequence of a more recent emersion of the chain and of the Pliocene–Pleistocene tectonic activity in the Bend Zone" (Molin et al. 2012, p. 57) our opinion differs

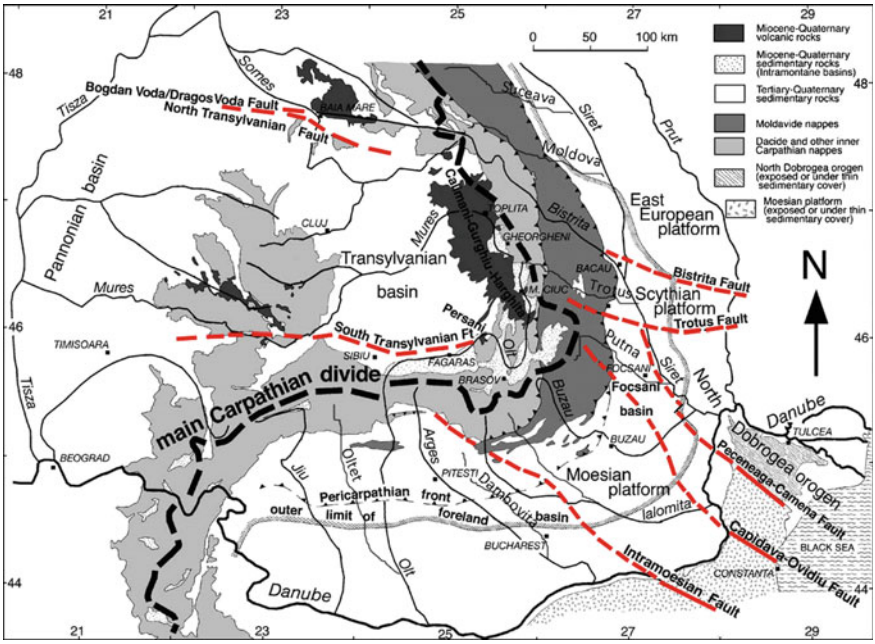

Fig. 18.3 Geological sketch map of the Eastern and Southern Carpathians of Romania and surrounding areas with major river courses and the first order drainage divide of the Carpathians (modified by Fielitz and Seghedi (2005) after Săndulescu et al. 1978; Săndulescu 1984; Maţenco et al. 2003)

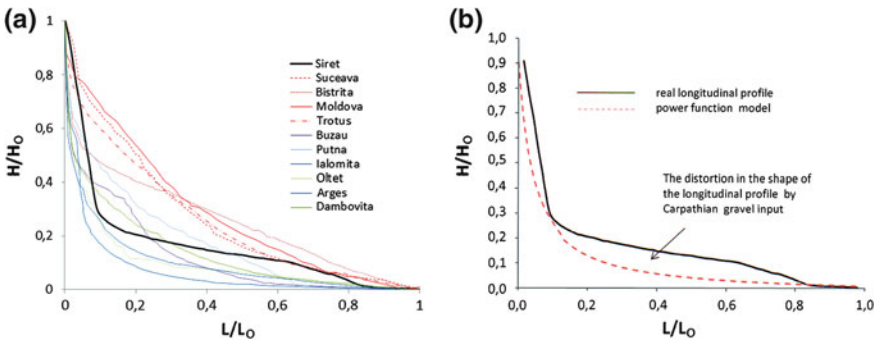

Fig. 18.4 Forms of Carpathian longitudinal profiles. **a** Rivers from the north of Eastern Carpathians (Suceava, Moldova, Bistrita, Trotus) have a longitudinal profile of low concavity and rivers from the south of Carpathians (Putna, Buzau, Ialomita) have a longitudinal profile of high concavity. In *black* is shown the longitudinal profile of Siret River. **b** Real longitudinal profile versus power function model of the Siret river (other discussions in the text)

slightly. The argument in the next section of this chapter based on the same Carpathian long profiles shows that a landform such as a longitudinal profile may be in a state of dynamic equilibrium even during intense tectonic activity.

Longitudinal Profiles Concavity Related to River Age and Channel Bed Material Grain Size

The radial-divergent structure of the drainage network outside of the Carpathians, and the rather similar size and order according to Strahler's system (at least on the eastern flank of the Eastern Carpathians) sparked some interest for explaining the shape of longitudinal profiles in relation to river age and bed material grain size. Moreover, long profiles were a pretext to gain more insight in the consistency of classical theories regarding landform evolution, such as cyclic relief versus dynamic equilibrium (Rădoane et al. 2003). The 13 rivers selected (Fig. 18.3 and Table 18.1) for the case study yielded several general observations regarding river behavior within a cyclic timeframe. The most relevant conclusions are presented further on.

Longitudinal profiles reach an advanced state of high concavity and evenness (*grade* type profile) after evolving for millions of years (i.e., cyclic time, acc. Schumm and Lichty 1965), and are typical for rivers with ancient drainage along the same channel. Conversely, a low flexure of the longitudinal profile indicates a young and vigorous river undergoing a deepening process and evolving toward the equilibrium profile (*grade*). At least, this is Davis' (1899) concept regarding the geographical cycle of landform modeling:

"…the graded condition of a river would be first attained at the mouth, and would then advance retrogressively upstream. When the trunk streams are graded, early maturity is reached; when the smaller headwaters and side streams are also graded, maturity is far advanced; and when even the wet-weather rills are graded, old age is attained" (p. 489).

Thus, we expected that longitudinal profiles of rivers analyzed in this study had evolved accordingly to some extent. However, after reviewing the literature on the age of the drainage network in the Eastern Carpathians, we concluded the following: (1) The northern rivers (Suceava, Moldova and Bistriţa) have carried on along the same channels since as early as the Lower Sarmatian (i.e., approx. 13.5 million years ago); (2) The age of next river to the south, Trotuş, is fragmented, and not fully elucidated as yet (Dumitriu 2007), albeit it is commonly accepted that the river is older in the upper course and increasingly younger toward the lower course (Meotian in Comăneşti depression and Pliocene downstream of Tg. Ocna; 10 and 5.4 million years, respectively); (3) Further south, rivers Putna, Buzău, Prahova, and Ialomiţa have undergone the most significant changes, particularly due to Valachian uplift movements, such that the ages along their current channels range from Upper Pliocene to Pleistocene (i.e., approx. 2.5 million years); (4) Siret river is a special case, by pertaining to the Carpathian type in terms of the bed deposits

and being considerably younger than its tributaries, as the age of its channel is closely linked to the coarse sediment of Carpathian origin, resulting in prominent Villafranchian accumulations of alluvium in Colinele Tutovei.

To sum up, older rivers from the study area pertaining to the Eastern Carpathians have less evolved longitudinal profiles (senso geographical cycle theory), whereas the profiles of younger rivers from the Curvature region are more concave (thus more evolved, according to the same theory).

In order to better understand this (at least theoretical) paradox, longitudinal profile curves were further investigated with multiple means of analysis. In Fig. 18.4a the mature rivers are compared with a network order (Strahler system) of 7, 8, and 9. Also, for plotting and calculations of the parameters of the longitudinal profile form "unit" profiles were used. "Unit" profile were obtained from the ratio: H/H_o ratio of altitude, where H is the stream altitude at the point of measurement, H_o is the stream altitude from the river mouth at the headwaters; L/L_o ratio of distance, where L is the stream distance from the river mouth at the point of measurement, L_o is the stream distance from the river mouth at the headwaters. A wide range of longitudinal profile forms for Eastern and Southern Carpathian rivers (in this case) can be seen (Fig. 18.4a) from profiles slightly flexured to profiles strongly curved. Siret River has a longitudinal profile is deformed in lower course (Ichim and Rădoane 1990). Although this river flows mostly over a plateau, it has all the features of a Carpathian river, because of the granulometric and petrographic nature of the deposits from the riverbed (Fig. 18.5). The large amount of coarse sediments brought by the right bank tributaries from the Carpathians caused much aggradation of the riverbed and consequently, distorted the longitudinal profile (Fig. 18.4b) (to see also Chap. 28).

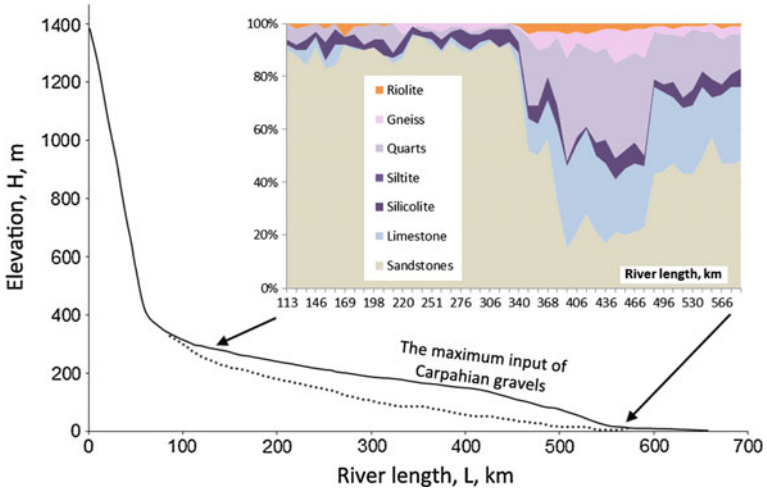

Fig. 18.5 Changes in the petrographic distribution of channel sediments along the Siret river. The maximum of input of Carpathian gravels occurs between 320 and 500 km and it is caused by bed material of crystalline and volcanic rocks more resistant to abrasion

Exponential, logarithmic, and power functions modeling are able to indicate which factor exerts the strongest influence on the longitudinal profile form. These functions were selected from a larger set of equations as the best predictors of longitudinal profile. Thus, if *the grain size of bed material is fairly uniform and the water discharge and sediment load increase at a significant rate along the river*, the longitudinal profile tends to achieve a highly concave shape and is adjusted by a *power function* (Snow and Slingerland 1987). Within our study area, Siret river (Figs. 18.4b and 18.6) approximates these conditions, whereby 80 % of the channel length overlies a relatively uniform lithological region. The power function model curve highlights this protuberance (Fig. 18.4b) so that we may assume that the power function provides the nearest adjustment to the initial shape of Siret longitudinal profile.

Rivers with *bed deposits comprising of coarse materials* (i.e., boulders and gravel) are typically dominated by transport processes, such that their longitudinal profiles range from slightly concave to almost straight, and thus are modeled by a *linear and exponential function*. In our study, rivers north of Trotuş (Figs. 18.6 and 18.7a) illustrate this type, whereby transport slope gradients are high and bed deposits are coarse along the entire length of the channel.

For rivers whereby the *bed material grain size decreases sharply*, from boulders and gravel in the upper course to fine sand in the lower course, the *logarithmic function* provides the best model for deriving the longitudinal profile curve. This is typical especially for rivers located south of Trotuş (Figs. 18.6 and 18.7a).

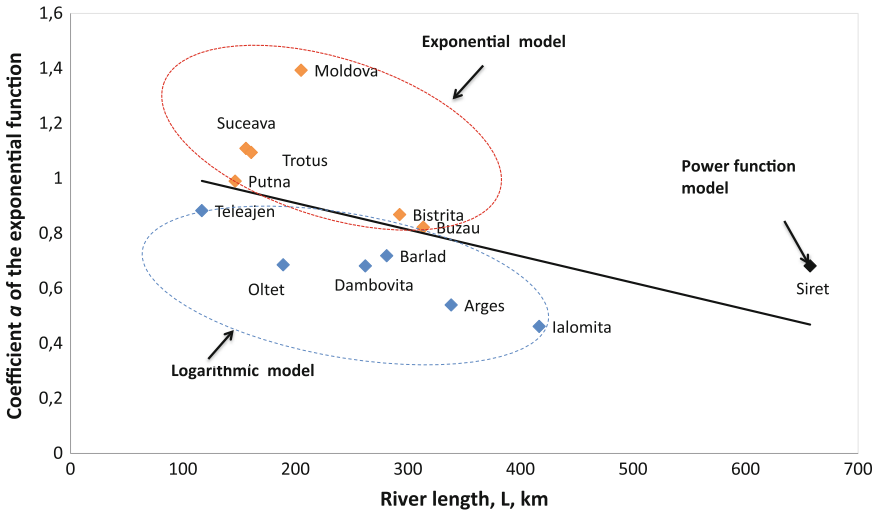

Fig. 18.6 River ranking according to the mathematical model best describing the longitudinal profile curve. Coefficient *a* of the exponential function was chosen to have a single criterion of comparison. In *red* cluster are grouped those rivers for which exponential model is closest to fit real longitudinal curve and in *blue* cluster, those rivers for which logarithmic model is closest. Siret river is singular in terms of mathematical function. Other discussions in the text

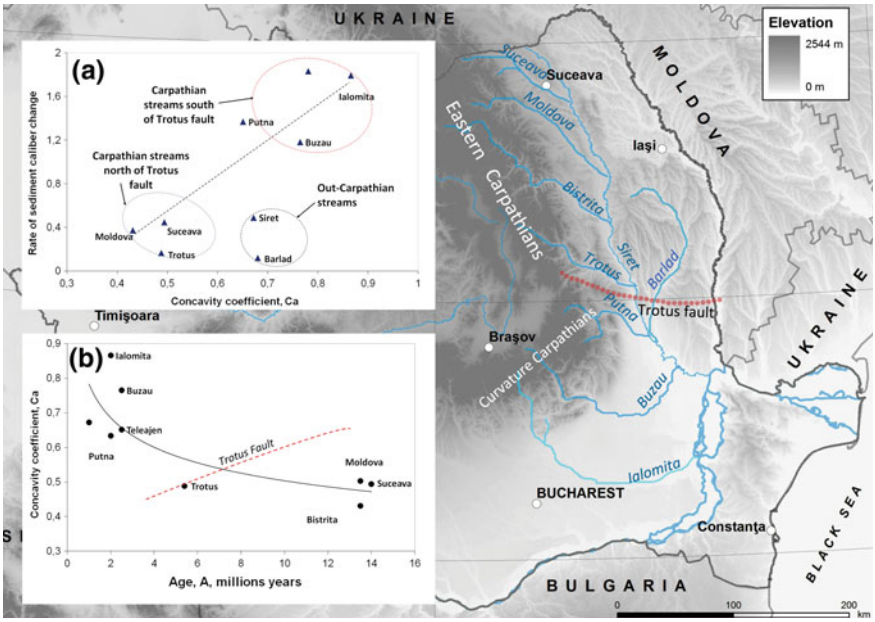

Fig. 18.7 The effect of Trotus fault in discrimination of longitudinal profile shape. **a** Relationship between the rate of bed material size change (coefficient *b* of the power function for the D50 change along the river) to the longitudinal profile concavity coefficient. **b** Relation between longitudinal profile concavity and drainage network age in the Eastern Carpathians (see further discussions in the text)

The conclusions regarding the relation between longitudinal profiles and the ages of Eastern Carpathian rivers are synthesized in Fig. 18.7b. By correlating the two parameters (i.e., profile concavity and river age), the result appears to be somewhat reversed compared to established evolution models.

From Davis' (1899) model to Snow and Slingerland's (1987) numerical simulation, models show that the younger the river, the more its longitudinal profile resembles a straight line; conversely, the older the river, the higher the concavity in its upper part, whereas the lower part asymptotically approaches the base level. In other words, longitudinal profiles evolve from a linear-exponential shape in the primary stage towards a shape modeled by the power function, specific to equilibrium or grade longitudinal profiles, as denominated by Davis.

However, it appears that Carpathian rivers do not "comply" with this general trend. Our previous arguments and the synthetic diagram shown in Fig. 18.7 suggest that age has had little influence, if any, on the shape of longitudinal profiles of rivers draining the external flank of the Carpathians. Rivers located north of Trotuş valley, whereby the documented ages range from 12 to 13 million years along the same courses (thereby granting sufficient time for an erosion cycle, according to Davis), appear to have the least evolved longitudinal profiles (i.e., low concavity, high slope gradient). Instead, rivers located south of Trotuş (Putna, Buzău, Prahova, Ialomiţa),

whose courses were subjected to major changes, interruptions, uplifting or subsidence, and have only maintained their current course for the past 2.5 million years, have achieved highly concave longitudinal profiles, thus reaching an evolved state.

We believe the phenomenon we observed in Eastern Carpathian rivers is a good illustration of the dynamic equilibrium theory, based on which (Hack 1960) discontinued the supremacy of cyclic theories of landform evolution. The dynamic equilibrium theory states that in order to exist, a landform need not undergo the three stages of evolution—youth, maturity, old age; a landform will maintain those characteristics which ensure a state of equilibrium in the exchange of mass and energy with another landform.

"The landscape and the processes molding it are considered a part of an open system in a steady state of balance in which every slope and every form is adjusted to very other. Changes in topographic form take place as equilibrium conditions change, but it is not necessary to assume that the kind of evolutionary changes envisaged by Davis ever occur" (Hack 1960, p. 81).

In accordance with this theory, we make the following statements regarding the case study: (1) The equilibrium profile of a river may also be a low concavity, high slope gradient profile, defined by a linear-exponential theoretical curve; (2) The linear-exponential equilibrium profile is also definitive for equilibrium between erosion and accumulation, and thus for transport, which has been, with little variation, the main characteristic of rivers north of Trotuş for over 12 million years; (3) Tectonic activity during this long timespan had a significant contribution to shaping longitudinal profiles in their current form, not only by generating knick-zones (as previously discussed), but also by influencing the general shape of profile curvature. Thus, Trotuş fault line generated discernible differences in drainage network geometry in the northern sector (i.e., south-east orientation) compared to the south (predominant eastern orientation). Longitudinal profiles of northern rivers were forced to constantly adjust to tectonic uplift movements (which is also the case at present, at uplift rates above 2 mm/year—Zugrăvescu et al. 1998). Similarly, southern rivers adjusted to tectonic uplift in their upper courses, whereas the lower courses were affected by negative movements.

It is likely that tectonic uplifting north of Trotuş fault line may have exceeded rivers' capacity to generate high concavity equilibrium profiles. However, this does not imply that current profiles are not equilibrium profiles; in fact, the curves to which these rivers (Suceava, Moldova, Bistriţa, partially Trotuş) evolved represent a form of equilibrium achieved during the past 12–13 million years (from the Middle Miocene) in order to counteract the effects of tectonic movements and climate changes. Moreover, it is the optimal manner of performing the function of transport of landform decay products.

Equilibrium profiles of rivers located south of Trotuş fault line were also greatly influenced by the complex tectonic activity along fault lines from the southeastern foreland and platform sectors during the Upper Pliocene–Quaternary (Fig. 18.6b). However, in this instance subsidence prevailed (by −3 mm/year—Zugrăvescu et al. 1998) in the lower courses, whereas uplifting (by as much as +5 mm/year) was

dominant in the upper basins. Despite the relatively young age of the drainage network, crustal movements led to adjustments of longitudinal profiles by increasing river concavity. As in the previous case, the longitudinal profiles of these rivers are equilibrium profiles, best defined by the logarithmic function model, whereby the bed material, comprising of all grain sizes ranging from blocks and boulders, to gravel, sand and very fine sand, has a gradual distribution. Moreover, the profile shape is optimal for achieving the transport function of river channels.

Conclusions

The study of longitudinal profiles by Romanian geomorphologists aimed at identifying the overall shape of grade longitudinal profiles and exploring the causes for situations when high concavity was not achieved. The most prominent fault lines in Eastern Romania are likely responsible for the shapes of river longitudinal profiles and the evolution of the drainage network. A range of new methods for determining river gradients, as well as modern facilities for processing large data bases were employed in this study, assisting us in demonstrating that tectonics prevailed over lithology (as well as other secondary factors) in generating knickzones along longitudinal profiles. Furthermore, the differential uplift of major Carpathian structural units (e.g., the Carpathian flysch ot the peri-Carpathian molasse) was detected in the distribution of stream gradient index. Tectonic movements established the general evolution pattern of the drainage network and prompted rivers to constantly adapt in order to reach the equilibrium shape of longitudinal profiles. Regardless of age, the shape of longitudinal profiles continually adjusted to ensure that geomorphological work is performed by rivers under conditions of high variability of tectonic movements and geomorphic time.

Acknowledgments The research leading to these results also has received partial funding from the Exploratory Research Projects PN-II-ID-PCE-2011-3-0057, "Reconstruction of Romanian river-channel changes in the past 11,700 years: The role of climatic conditions and human impact".

References

Cristea I (2011) Valea Putnei Vrâncene. Studiu geomorfologic. Ph.D thesis, "Ştefan cel Mare" University, Suceava (in Romanian)

Davis WM (1899) The geographical cycle. Geogr J 14(5):481–504

Donisă I (1968) Geomorfologia Văii Bistriţei. Romanian Academy Press, Bucureşti (in Romanian)

Dumitriu D (2007) Sistemul aluviunilor din bazinul râului Trotuş. "Ştefan cel Mare" University Press, Suceava (in Romanian)

Fielitz W, Seghedi I (2005) Late Miocene-Quaternary volcanism, tectonics and drainage system evolution in the East Carpathians, Romania. Tectonophysics 410:111–136

Grumăzescu C (1975) Depresiunea Hațegului. Studiu geomorfologic. Romanian Academy Press, București (in Romanian)
Hack JT (1957) Studies of longitudinal stream-profiles in Virginia and Maryland: US geological survey professional paper 294B, pp 45–97
Hack JT (1960) Interpretation of erosional topography in humid temperate regions. Am J Sci 258A:89–97
Hack JT (1973) Stream-profiles analysis and stream-gradient index. J Res US Geol Surv 1:421–429
Ichim I (1979) Munții Stânișoara. Studiu geomorfologic. Romanian Academy Press, București (in Romanian)
Ichim I, Rădoane M (1990) Channel sediment variability along a river: a case study of the Siret River, Romania. Earth Surf Proc Land 15:211–225
Ichim I, Bătucă D, Rădoane M, Duma D (1989) Morfologia și dinamica albiilor de râu. Technical Press, București (in Romanian)
Mațenco L, Bertotti G, Cloetingh S, Tarapoanca M, Leever K (2003) Pliocene to active tectonics in the aftermath of the continental collision in the SE Carpathians corner: inferences from seismic, kinematic, geomorphological and remote sensing studies. In: Geophysical research abstracts, Nice
Molin P, Fubelli G, Nocentini M, Sperini S, Ignat P, Grecu F, Dramis F (2012) Interaction of mantle dynamics, crustal tectonics, and surface processes in the topography of the Romanian Carpathians: a geomorphological approach. Glob Planet Change 90–91:58–72
Necea D (2010) High-resolution morpho-tectonic profiling across an orogen: tectonic-controlled geomorphology and multiple dating approach in the SE Carpathians. Ph.D thesis, VU University, Amsterdam
Necea D, Fielitz W, Mațenco L (2005) Late Pliocene-Quaternary tectonics in the frontal part of the SE Carpathians: insights from tectonic geomorphology. Tectonophysics 410:137–156
Niculescu G (1963) Terasele Teleajenului în zona Subcarpaților cu privire specială asupra mișcărilor tectonice cuaternare. In: Probleme de Geografie, vol IX. București (in Romanian)
Orghidan N (1969) Văile transversale din România. Academy Press, România (in Romanian)
Posea G, Popescu N, Ielenicz M (1974) Relieful României. Scientific and Encyclopedic Press, București (in Romanian)
Rădoane M, Rădoane N, Dumitriu D (2003) Geomorphological evolution of longitudinal river profiles in the Carpathians. Geomorphology 50:293–306
Richards K (1982) Rivers: form and process in alluvial channels. Methuen, London and New York
Rubey WW (1933) Equilibrium conditions in debris-laden streams. Am Geophys Union Trans, 497–505
Săndulescu M (1984) Geotectonica României. Technical Press, București (in Romanian)
Săndulescu M, Krautner H, Borcos M, Nastaseanu S, Patrulius D, Stefanescu M, Ghenea C, Lupu M, Savu H, Bercia I, Marinescu F (1978) Atlasul geologic, sheet 1. Romania 1.1000000. Inst Geol Geofiz. Bucharest (in Romanian)
Schumm SA, Lichty RW (1965) Time, space and causality in geomorphology. Am J Sci 263:110–119
Seeber L, Gomitz V (1983) River profiles along the Himalayan arc as indicators of active tectonics. Tectonophysics 92:335–367
Snow RS, Slingerland RL (1987) Mathematical modelling of graded river profiles. J Geol 95:15–33
Ter Borgh MM (2013) Connections between sedimentary basins during continental collision: how tectonic, surface and sedimentary processes shaped the Paratethys. Ph.D thesis, Utrecht Studies in Earth Sciences, 45, Utrecht University, Utrecht
Wheeler DA (1979) The overall shape of longitudinal profiles of streams. In: Pitty AF (ed) Geographical approaches to fluvial processes. GeoAbstracts, Norwich, pp 241–260
Whipple K, Wobus C, Crosby B, Kirby E, Sheenan D (2007) New tools for quantitative geomorphology: extracting and interpretation of stream profiles from digital topographic data. GSA annual meeting, Denver, Colorado
Zugrăvescu D, Polonic G, Horomnea M, Dragomir V (1998) Recent vertical crustal movements on the Romanian territory, the major tectonic compartments and their relative dynamics. Rev Roum Geophys 42:3–14

Chapter 19
River Behavior During Pleniglacial–Late Glacial

Ioana Perşoiu, Maria Rădoane and Petru Urdea

Abstract Recent investigations in the area, based on absolute chronologies, support a first attempt to answer how the rivers from this part of Southeastern Europe adjusted to direct and indirect effects of climate changes during the Last Glacial, and how important are the local/regional controls in their reactions. In general, during the Pleniglacial, the rivers were characterized by coarse gravel braided pattern, with the first notable changes during Late Glacial, when they could transform in large-scale meandering channels. A regional exception is recorded along the rivers draining the Western Romanian/Eastern Hungary, where the dominant pattern is the large-scale meandering channel, with local developments of braided/anabranched reaches. The vertical development of fluvial features does reflect the local/regional tectonic settings (different rates of subsidence and uplifts). They vary from few meters amplitude, in the areas affected by subsidence or in tectonically stable regions, to 30–40 m, or even higher, in the uplifting areas. The timing of terrace/floodplain formations remains a matter of debate, as more temporal and spatial data are necessary. Drainage basin characteristics, i.e., dimension and elevation, where identified as local controls which can impose a higher/lower sensitivity of fluvial systems to climate changes, reflected in different river adjustments, even if they are in the same areas. The sea-level oscillation of the Black Sea had a local effect, affecting only the lower reach of Danube River and the surrounding rivers.

Keywords Eastern Europe · Last Glacial · Fluvial processes · Climate change · Tectonics

I. Perşoiu (✉) · M. Rădoane
Departament of Geography, "Ştefan cel Mare" University,
Universităţii 13, Suceava 720229, Romania
e-mail: ioanapersoiu@gmail.com

M. Rădoane
e-mail: radoane@usm.ro

P. Urdea
Departament of Geography, West University of Timişoara,
Blvd. V. Parvan 4, Timişoara 300223, Romania
e-mail: petru.urdea@e-uvt.ro

M. Rădoane and A. Vespremeanu-Stroe (eds.), *Landform Dynamics and Evolution in Romania*, Springer Geography,
DOI 10.1007/978-3-319-32589-7_19

Introduction

The rivers draining Romania (the Southeastern Carpathians and the surrounding hinterland) are generally small, with relatively medium to small size drainage basins (less than 10,000 km^2) and discharges generally in the order of tens of m^3/s; with some exceptions: the lower course of the Danube (6500 m^3/s), Siret (44,835 km^2, 706 km long, 220 m^3/s), Mureş (28,310 km^2, 761 km long, 184 m^3/s), Olt (24,050 km^2, 615 km long, 190 m^3/s) and Someş (15,015 km^2, 388 km long, 120 m^3/s).

Most of the Romanian rivers are transitional ones, crossing more than one relief unit, thus presenting a series of particularities in terms of morphology (e.g., high variability in the form of the longitudinal profiles; with frequent occurrence of variable sized structurally and/or tectonically imposed knickpoints; high variability in lateral development and preservation of valley bottom and fluvial terraces—both along the same river and between rivers; frequent changes of channel typology along the river courses).

Earlier geomorphologic and sedimentologic studies, synthesized by Posea et al. (1974), Posea (2002), established some common features along the main courses of these rivers, i.e., the presence of a coarse gravel sheet in the lower part of the floodplains alluvial fill, covered by fine sediments (sands and clays) probably Holocene in age; generalized and correlated (in time) terrace levels in the perimeter of Transylvanian Depression and Moldavian Platform. However, several differences were observed, mainly attributed to different rates of neotectonic uplifts and subsidences (with ranges between −4 and +6 mm/year, Zugrăvescu et al. 1998). Generally, rivers in uplifted and tectonically stable areas have narrow (few km wide), deeply incised (hundred of meters) well-conserved valleys, with strath-terraces, and in some cases display a complex history of multiple episodes of valley fill and entrenchment. On contrary, rivers in subsidence areas (e.g., eastern edge of Pannonian Basin, lower Danube plain) have progressively borrowed terraces with thick sediment layers and floodplains transformed into large alluvial plains with frequent channel changes.

Previous studies (prior to the 2000s) concerning fluvial behavior in the last glacial—interglacial were lacking absolute age controls on the timing of the inferred changes. However, few recent studies (e.g., Giosan et al. 2006; Popescu et al. 2004; Benecke et al. 2013; Howard et al. 2004; Macklin et al. 2010; Perşoiu 2010; Nádor et al. 2007, 2011; Thamó-Bozsó et al. 2007; Sipos 2012; Necea et al. 2013), give the first chronologic framework concerning the fluvial dynamics during this period. They are targeting rivers in mountainous (Someşul Cald River, Apuseni Mountain; Putna River in the Southeastern Carpathians), hilly (Someşul Mic, Arieş and Pârtoţ rivers in NW Transylvania; Siret River in the NE Moldova) and plain areas (Mureş/Maros, Crişul Repede/Sebes-Körös, Crişul Negru/Fekete-Körös,

Crişul Alb/Fehér–Körös, Barcău/Berettyó, Ier/Ér, Crasna/Krászna and Someş/Szamos Rivers in the eastern part of Pannonian Basin, west of Romania; Teleorman and Danube rivers in the southern part of Romania), as well as the lower course of the Danube (Brăila Island, present-day Danube Delta and the former course of Danube River in the continental self of the Black Sea) (Fig. 19.1).

The time interval covered by the cited studies is mainly Middle Pleniglacial–Late Glacial (MIS 3, MIS 2; ca. 59,000–11,700 years BP). Few exceptions, along the rivers draining the SE Carpathians, highlight fluvial features estimated to be Eemian–Early Pleniglacial (MIS 5, MIS4) in age. Figure 19.2 proposes a chronological synthesis of the fluvial morphologies presented in the following section.

The final objective is to obtain a regional perspective on the Pleniglacial–Late Glacial fluvial behavior, and to discuss the importance of natural controls (e.g., climate, tectonism, eustatic oscillations of the Black Sea, drainage basin characteristics), based on these recent findings.

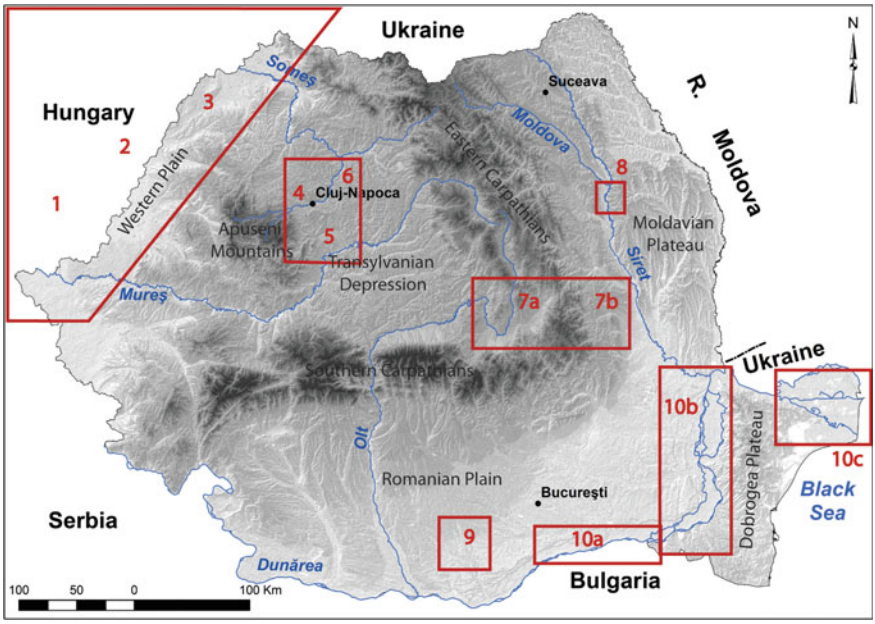

Fig. 19.1 Location of the cited study areas: *Western Romanian Plain (Great Hungarian Plain)*: *1* Mureş/Maros River, *2* Criş/Körös Rivers, *3* Someş/Szamos; *NW Transylvanian Depression*: *4* Someşul Mic River, *5* Arieş River, *6* Săcălaia drainage basin (Pârtoţ River); *SE Carpathians: 7a* lt River (Braşov Depression); *7b* Zăbrăuţ, Şuşiţa, Putna, Milcov, Zăbala and Naruja Rivers (Sub Carpathians of Curvature); *Moldavian Plateau*: *8* Siret River; *Romanian Plain*: *9* Teleorman River; the lower reach of Danube River: *10a* Danube River between Giurgiu and Oltenita; *10b* Brăila Island; *10c* Danube Delta and the Black Sea continental platform

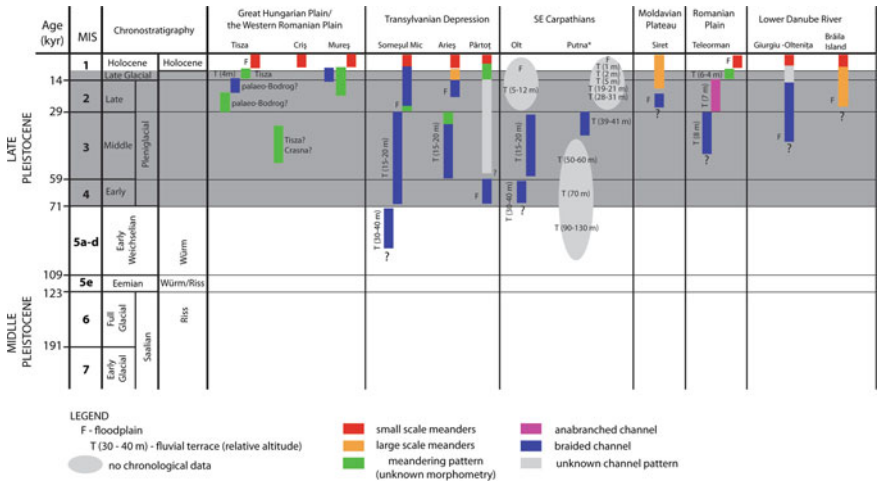

Fig. 19.2 The ages of the lower fluvial features, as reflected by the recent studies on Late Quaternary fluvial evolution: **a** *Western Romanian Plain/Great Hungarian Plain*: Posea (1997), Timár et al. (2005), Nádor et al. (2007, 2011), Kiss et al. (2014); **b** *Transylvanian Depression*: Pendea et al. (2009), Feurdean et al. (2015), Perşoiu (2010), Perşoiu and Feurdean (2013), Perşoiu and Rădoane (in prep.), Perşoiu and Perşoiu (in prep.), **c** *SE Charpatian* (Olt River in the Brasov Depression; Putna and the surrounding rivers in the Subcapathians): Necea et al. (2013); **d** *Moldavian Plateau*: Rădoane et al. (2015); **e** *Romanian Plain*: Howard et al. (2004), Macklin et al. (2010), **f** *the lower Danube*: Benecke et al. (2013)

Regional Synthesis on Pleniglacial–Late Glacial Fluvial History

Western Romanian Plain (Great Hungarian Plain)

The Western Romanian Plain, part of the Northeastern and Eastern Great Hungarian Plain (GHP)/Nagy Alföld, is drained by tributaries of Tisza River (Someş/Syamos, Barcău/Berettyó, Crasna/Krászna, Crişul Repede/Sebes-Körös, Crişul Negru/Fekete-Körös, Crişul Alb/Fehér–Körös, Mureş/Maros), with catchment areas in the Apuseni Mountains and the northern Eastern Carpathians. The Late Quaternary fluvial history is recorded in the lowest fluvial morphologies of the area (ca. 4–6 m vertical amplitude), i.e., the first fluvial terrace, the higher and the lower floodplain levels (Posea 1997). The morphological particularity of the area, presented in a first synthesis study by Manciulea (1938), is given by the presence of large alluvial fans developed along the lower reaches of the main rivers, the generalized meandering pattern of the present-day drainage systems, the presence of numerous fluvial morphological relicts, reflecting the existence of different channel typologies in the past (braided, anabranching, meandering), and of extended humid areas, especially before the hydrological interventions in the nineteenth and twentieth centuries.

Generally, the evolution of the lower reaches of Someş/Szamos, Criş /Körös—Barcău/Berettyó, Mureş/Maros, Timiş-Bega, and Caraş-Nera rivers is closely linked with the tectonic structure of the Pannonian basement. The "chessboard" faulted type structure of this region, individualized since the Miocene, consists in blocks affected by differentiated vertical movements (Săndulescu and Visarion 1977; Maţenco and Radivojević 2012). The blocks with negative vertical movement correspond to tectonic depressions (grabens and half-graben types), and where associated with intermittent subsidences, including during the Late Quaternary. These particular areas played a decisive role in the location, individualization and evolution of the low, divagation plains. Examples from the eastern part of the Great Hungarian Plain/Western Romanian Plain are the so-named "tectono-morphological evolutionary couplings" of Curtici-Békés, Makó, Szeged, Tomnatec Depressions with Criş/Körös and Mureş/Maros rivers systems, Srpska Crnja and Pančevo Depressions with Timiş/Tamiš-Bega/Begej rivers systems, and Zagajica Depression—Caraş/Karaš-Nera rivers systems.

The complexity of the fluvial behavior in this perimeter and further to the west is well known mainly by the most recent studies realized on the eastern part of the GHP, covering the last ca. 48,000 years history of the median and lower courses of Tisza, Ier/Ér, Crişul Repede/Sebes-Körös, Crişul Negru/Fekete-Körös, Crişul Alb/Fehér–Körös, Mureş/Maros and Someş/Szamos Rivers (e.g., Timár et al. 2005; Thamó-Bozsó et al. 2007; Kasse et al. 2010; Nádor et al. 2007, 2011; Kiss et al. 2014; Robu et al. 2015) (Fig. 19.3.). The image is not yet complete, but some moments and causes of large-scale fluvial adjustments can be already distinguished.

The tectonic influences on rivers' behavior are reflected mainly in the history of spatial position of the main rivers: Danube, Tisza and Bodrog and their tributaries. In Early Weichselian the south Tisza Graben was the most intensive subsidence area from the Great Hungarian Plain, becoming the confluence area of the three main rivers draining GHP: Danube River, coming from the Virsereg Gorge, Tisza River from the Eastern part of the alluvial plain, and Bodrog River from the north (Gábris and Nádor 2007; Kiss et al. 2014; Starkel et al. 2015).

In the eastern part of the GHP, a new drainage configuration took place around Late Pleniglacial–Late Glacial, when tectonic subsidence along the Érmellék region (the floodplain of Ier/Ér River) became active, forcing Tisza River to move further to the east, along the present-day Ier/Ér floodplain, and in the perimeter of Körös (Cris) Plain. (Nádor et al. 2007). After Thamó-Bozsó et al. (2007), the Érmellék region was tectonically active even earlier, in Middle Pleniglacial.

Between 14,000 and 20,000 years ago (or 16,000–18,000 years ago, after Timár et al. 2005), Tisza River experimented an abrupt avulsion to the west, of ca. 70 km, under the influence of rapid subsidence of Bodrog and Bereg Plain, replacing the older Bodrog River (Timár et al. 2005; Nádor et al. 2007; Kiss et al. 2014). In a larger context (at the level of the entire GHP), this is the period when the major drainage network has established the present-day configuration (Nádor et al. 2007).

Morphological proofs of fluvial adjustments to Late Quaternary climatic conditions are offered by the numerous fluvial relicts (e.g., large-scale palaeomeanders or fragments of braided rivers, different channel alignments) dispersed on the

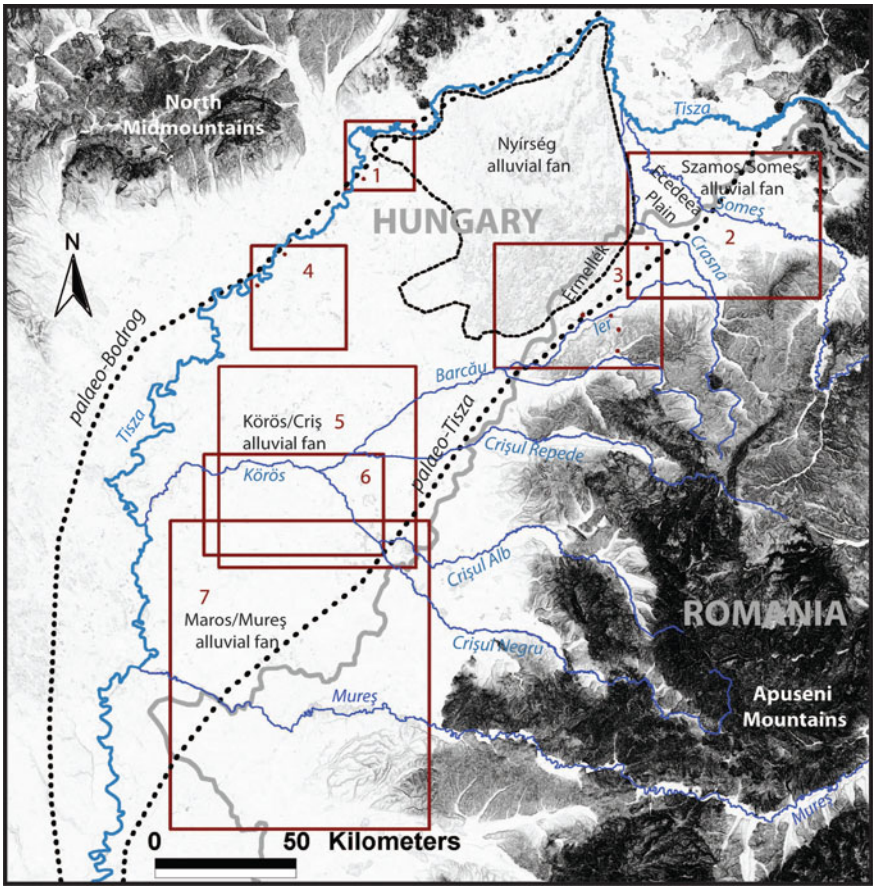

Fig. 19.3 Location of recent studies in the eastern part of Great Hungarian Plain, partly covering the Western Romanian Plain: *1* Timár et al. 2005; *2* Robu et al. (2015); *3* Thamó-Bozsó et al. (2007); *4* Kasse et al. (2010); *5* Nádor et al. (2007); *6* Nádor et al. (2011); *7* Kiss et al. (2012, 2014). Positions of palaeo-Bodrog and palaeo-Tisza after Timár et al. (2005) and Nádor et al. (2007)

surface of the alluvial fans of Someş/Szamos, Körös/Criş and Mureş/Maros Rivers, and along the middle reach of Tisza River.

During Late Pleniglacial (MIS2), the palaeo Bodrog river (?), the precursor of Tisza or Sajo fluvial systems, recorded a meandering (47,000–20,000 yrs ago) and then a braided (ca. 18,000–14,000 yrs ago) phase. During this time, the vegetation was first dominated by herbs (steppe) and later by open coniferous forest, supporting a high sediment supply to the river. This pattern was interrupted by a climatically induced shift to large meandering system or by the tectonically induced avulsion of Tisza River in the area, in the final phase of the Late Pleniglacial or Late Pleniglacial–Late Glacial transition (Kasse et al. 2010; Cserkész-Nagy et al. 2012).

After Kasse et al. 2007, this last channel metamorphosis was related mainly to the climate warming, associated with the development of coniferous forests, decreased snow-melt discharges and an increase in evaporation, while after Timár et al. (2005), the event was mainly conditioned by the more rapid subsidence in the Bodrogköz–Polgár area than in the central part of the GHP.

In the Érmellék region, a large meandering river, larger than the present-day Ier/Ér River, was active at least from ca. 46,000–39,000 years (MIS3, Middle Pleniglacial), and date the active tectonic phase in this area. Similar mineralogic composition of sediments as in the recent Barcău/Berettyó, Ier/Ér and Crişul Repede/Sebes-Körös rivers, and partly the modern Tisza River, suggest that this old river had the drainage basin in the northern part of the Apuseni Mountain (Thamó-Bozsó et al. 2007). After Timár et al. 2005 and Nádor et al. 2007, this large meandering river correspond to the old Tisza River, before its large-scale avulsion, ca. 70 km to the west.

On the other hand, a series of observations as: (a) the mention that the large-scale meanders along the floodplain of Ier/Ér are comparable in size with the present-day meanders of Tisza River (Nádor et al. 2007); (b) the arguments used by Posea (1997) that Crasna/Krászna River had flowed along Ier/Ér River trough Körös/Criş basin at the level of T 4–6 m fluvial terrace and the floodplain, before the activation of tectonic subsidence in the Ecedeea Plain; (c) the comparable sizes of these palaeomeanders with the similar palaeomeanders in the vicinity of the present-day Crasna/Krászna River; and (d) the location of catchments area of Crasna/Krászna River in the Apuseni Mountains; are arguments that the river draining the Érmellék region during Late Pleniglacial could be Crasna/Krászna River, instead of Tisa/Tisza River.

From this perspective, according to Posea (1997), tectonic activation of subsidence in the Ecedeea Plain caused Crasna/Krászna avulsion to the north. The recognizable large-scale meanders along the present-day Crasna/Krászna River support the maintenance of the meandering pattern after the river spatial reconfiguration. No absolute ages along Crasna/Krászna River are yet available to support a more detailed discussion on the moment of this flow reorganization. Nevertheless, according to Nádor et al. 2007, the large-scale meandering river entering from Érmellék region in the northeast part of the Körös/Criş basin, is at least 14,000–18,000 years old, suggesting that the moment of flow reorganization occurred after that moment.

On the surface of Körös/Criş alluvial fan, 10,000–15,000 years old braided channels, indicating palaeo-low directions from the southeast, suggests that a braided river was active during the Late Glacial in the area, most probability after the avulsion of the large meandering river from the northwest (Nádor et al. 2007). The authors, based on heavy mineral analysis and floodbasin sedimentary sequences from the area, suggest that this braided river was probably a precursor of the Crişul Negru/Fekete-Körös and Crişul Alb/Fehér–Körös Rivers, and was related (high sediment supply) with neotectonic uplift of the southern margin of the Körös/Criş Basin.

However, Kiss et al. (2012, 2014), analyzing the spatial distributions of palaeochannels on Mureş/Maros alluvial fan (Fig. 19.4), suggest that this huge

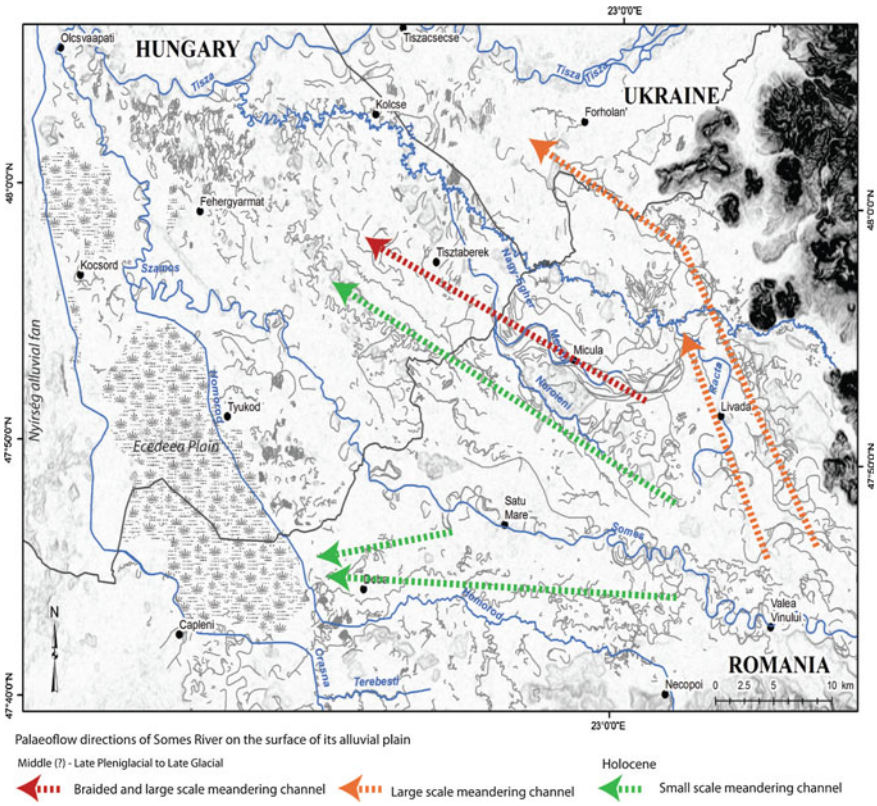

Fig. 19.4 Late Quaternary palaeodrainage directions and fluvial relicts on the surface of Somes alluvial plain (adapted after Posea et al. 1997; Robu et al. 2015)

braided channel, coeval with the large meandering ones, correspond to the old Mureş/Maros River flowing to the subsidence area of Körös Basin (Curtici-Békés tectonic block, Maţenco and Radivojević 2012) during the second half of the Oldest Dryas and the Bölling interstadial, a humid period which could explain large bankfull (ca. 1970 m^3/s) and solid discharges.

These channel patterns were preceded by large meandering channels of the same river, active during ca. 18,700–13,300 years ago, an interval which corresponds with Ságvár–Lascaux interglacial, a humid and warm period, when in the area the forest steppe transited to closed forest. Discharge reconstructions for the large palaeomeanders founded in the perimeter of Mureş/Maros alluvial fan (2062 and 1426 m^3/s) suggest 3–8 times higher discharges than the ones of the present-day Mureş/Maros River (Kiss et al. 2012, 2014). Similar patterns are reported along the median course of Tisza River (Timár et al. 2005; Kasse et al. 2010) and in the perimeter of Someş/Szamos and Crasna/Krászna alluvial fans (Robu et al. 2015).

The Younger Dryas cooling is not reflected clearly in the fluvial records. The pollen diagrams do not show significant changes, suggesting the maintenance of coniferous forest with some deciduous elements, while the absolute ages of the channel infills indicate the continuity of the large-scale meanders along Tisza River (Kasse et al. 2010). During this period, Mureş/Maros River experimented a meandering—braided pattern, with a progressive decreasing of discharge as the climate became warmer and arid (Kiss et al. 2014).

The glacial–postglacial transition is marked by a dramatic shift from boreal to deciduous forests in the region (Kasse et al. 2010). In the case of Tisza River, this vegetation change and the related decrease of solid discharge and changes in the flow regime (e.g. decreasing of snow-melt runoff) is reflected in channel incision, up to 4 m deep, and channel change from large meanders to small-scale meanders (Kasse et al. 2010). The modern small-scale meandering rivers in the Körös/Criş basin seam to be no older than 10 kys (Thamó-Bozsó et al. 2007). This age suggests local fluvial reconfiguration during Early Holocene, after Mureş/Maros River had abandoned its northern courses for some southern directions, under the influence of activated subsidence along the Tomnatec and Srpska Crnja tectonic blocks. In the perimeter of the Mureş/Maros alluvial fan, the first Holocene (ca. 7100 years BP) direction of Mureş/Maros River was along the present-day Galaţca River. It was followed by now completely abandoned course around 6100 years BP, and a last position along the present-day Aranca River around 1600 years BP, before stabilizing the present-day course (Kiss et al. 2012, 2014).

As a general trend, decrease of meanders is reported along all the rivers draining the western part of GHP. No data are yet available to discuss the temporal synchronies or delays of these channel metamorphosis to climate and vegetation changes at the start of the Holocene. During the Holocene, studies on Mureş/Maros and Someş/Samos alluvial fans do suggest lateral avulsions and discrete spatial changes in channel behavior (Kiss et al. 2014; Posea 1997; Robu et al. 2015; Perşoiu and Rădoane, Chap. 20, this volume).

In synthesis, during the last ca. 48,000 yrs, in the Eastern and Northeastern part of the Great Hungarian Plain, which include also the morphological unit known in the Romanian literature as the Western Romanian Plain, the rivers were mainly meandering. However, this meandering pattern coexisted with braided and anabranching channels/branches, along the same channel/palaeodischarge direction and during different periods of time (Fig. 19.4). This complex fluvial behavior was caused both by climate changes and local/regional tectonics.

A major characteristic of the rivers is the maintenance of their large dimensions during the cold period, and a drastic reduction of their morphologies at the beginning of the Holocene, when the periglacial environment was replaced by a temperate one.

The particularity of the area is given by the frequent channel repositioning, trough local avulsions on the surface of the alluvial fans surfaces, or larger avulsions, at regional scale, imposed by temporal activations of tectonically active areas (subsidences or uplifts) from the central and marginal parts of the GHP.

Transylvanian Depression

The main rivers draining Transylvanian Depression, e.g., Someşul Mare, Someşul Mic, Someş, Arieş, Mureş, Târnava Mare, Târnava Mică, Olt, are characterized by large valleys, few to 20 km wide and 150–160 m high. Along them are developed 6–8 strath-terraces, with appropriate altitudes, and well-developed floodplains. Based on the existing regional synthesis (e.g., Posea et al. 1974), the Late Quaternary fluvial history of the area is reflected in the last three fluvial terraces and the present-day floodplain, marking ca. 30–40 m fluvial vertical incision. Recent studies performed in the NW part of Transylvanian Depression, mainly along Someşul Mic and Arieş Rivers, give some new insights on the age and structure of the most recent fluvial features: Pendea et al. 2009; Perşoiu 2010; Perşoiu and Rădoane, in prep; Perşoiu and Perşoiu, in prep).

The 30–40 m terrace is the most developed and visible fluvial terrace, and was used as reference morphology for spatial and temporal correlation between the large valleys (Posea et al. 1974). The Pleniglacial ages of the loess like sequence on top of the 30–40 m fluvial terrace along Someşul Mic River (Pendea et al. 2009) place the fluvial terrace formation in Early Weichselian (MIS 5). The fluvial sequence consists in coarse grained materials, suggesting their deposition by a braided channel.

The 15–22 m fluvial terrace is more fragmentary conserved, but continue to be easily recognizable. The upper part of the alluvial sequences along Someşul Mic and Arieş Rivers were dated to ca. 40,000–37,000 yrs, showing that they are synchronous, and deposited at least during Middle Pleniglacial (MIS3). The sedimentary contexts suggest that both the rivers had coarse grained braided channels. In the case of Someşul Mic River (Fig. 19.5), this channel typology was maintained until the river incised, abandoning this level. On contrary, Arieş River probably experimented a meandering phase before the large vertical incision, as suggested by the palaeomeander relicts on the surface of the fluvial terrace and the fine sediments imposed erosivelly on top of the coarse braided materials. (Perşoiu and Rădoane, in prep; Perşoiu and Perşoiu, in prep).

No intermediate fluvial terrace was identified between the 15–20 m one and the present-day floodplain of Someşul Mic River. The elevations of the two morphological units, and the medium thickness of valley bottom alluvial sequences, of ca. 5 m, attest a vertical incision of ca. 20–25 m. Before or during the Last Glacial Maximum, Someşul Mic River returned to a braided phase, with accumulation of boulders and cobbles in the floodplain perimeter. A similar behavior is reported along Arieş River, as the top age of coarse gravel materials (ca. 18,000 years old) from the floodplain perimeter indicate.

During Late Glacial, the two rivers show a more complex fluvial history. Along Someşul Mic River, the coarse gravel braided pattern was maintained until the edge of the Holocene, with no significant channel typology changes during the known stadials and interstadials. On contrary, Arieş River has changed from braided to meandering most probably during Bolling—Allerod Interstadial, as there where not

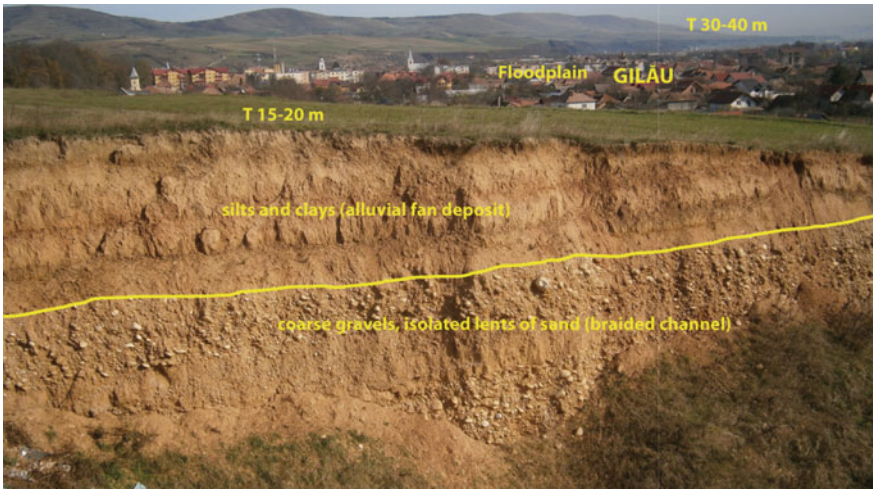

Fig. 19.5 Someşul Mic River at Gilău. A coarse gravel braided channel was active during the Middle Pleniglacialş after incision and terrace formation, a local torrent deposited fine materials on top of the fluvial alluvia (after Perşoiu and Perşoiu, in prep.)

found evidences of the existance of a braided pattern during the cold and dry Younger Dryas.

The Lateglacial—Holocene climatic transition is reflected in the Someşul Mic River's fluvial archives by a transitory phase, when a slightly incised wandering or anastomosing channel was active on the surface of the floodplain, replaced shortly after by a deeply incised, narrow meandering channel. The moment of the last important change occurred probably when the deciduous forests became dominant at lower and medium altitudes, ca. 10,300 yrs ago (Perşoiu and Rădoane, Chap. 20, this volume). Along Arieş River, the transition was probably more continuous, with the already existing meandering channel adjusting to the new temperate conditions.

Another characteristic of the Transylvanian Depression is the presence of large valleys along the small tributaries, with lower number of terraces frequently covered by thick hillslope materials, large floodplains, and misfitted channels draining humid areas and lakes in the floodplain perimeters.

Their Late Quaternary evolution and correlation with the behavior of the larger rivers are not well understood. Recent investigations completed in Săcălaia drainage Basin (Feurdean et al. 2015; Perşoiu and Feurdean, 2013) give some first informations on this topic. The thickness of floodplain sediments is ca. 11 m upstream from Ştiucilor Lake, and ca. 6 m downstream from this lake. In the bottom are present cobbles and pebbles, covered by 1–2 m thick sequence of fine and medium sands, followed by 5–10 m thick fine silty—clayey materials. The alluvial and lacustrine sediments suggest that the vertical aggradation was the main process on the surface of this floodplain.

In the first phase, when coarser sediments were deposited, the floodplain was a drained one, with a defined river channel. It was followed by a more humid phase, when the floodplain became partly drained or started to evolve under lacustrine conditions. The age of sandy materials indicate that the first phase was active at least ca. 55,000 yrs ago (Feurdean et al. 2015), and was maintained until Late Glacial, before the start of Bolling- Allerod Interstadial (Perşoiu and Feurdean 2013). At this time the floodplain was drained by a braiding or meandering channel, without significant changes in the pattern of sedimentation.

The first important change occurred in Bolling—Allerod interstadial and maintained until Mid Holocene, when the floodplain evolve as a humid, partly drained one, most probably by a meandering channel, with a low sedimentation rate. After 4700 years BP, the sedimentation rate increased dramatically, as a consequence of climatic deterioration and human impact (Perşoiu and Feurdean 2013). Also, Ştiucilor Lake has formed, and the upstream floodplain became lacustrine or partly drained, evolving under the direct influence of the lake water level oscillation.

Discussion

The reconstruction of the Middle Pleniglacial—Holocene fluvial behavior of Someşul Mic and Arieş Rivers suggest that the main rivers draining Transylvanian Depression do have synchronous behaviors in terms of large phases of aggradations and incisions related with large-scale climatic changes. However, local specific conditions can alter the general response, with differences in the types and moments of fluvial adjustment to the same climatic changes. Additional complexity in the resulted regional picture is given by the local development of an intermediate, 8–12 m high fluvial terrace, not yet investigated by modern technics (e.g. fluvial architecture, absolute ages).

Also, the identified distinct phases of Middle Pleniglacial—Holocene floodplain history in the Săcălaia drainage basin are expected to be similar along the small-scale rivers from the low table of Transylvanian Depression, most probable with differences in their rates, depended on local geological conditions, dimension of the drainage basins, human history in the area.

This generalized perspective highlights that the medium and small-scale rivers seams to have different reactions to climate changes from the last ca. 55,000 years, with distinct morphological and sedimentological resulting units.

Such an example is the amplitude of fluvial response of the two categories of rivers, even if they are located in the same area (the NW part of the Transylvanian Depression), to the climatic change from the warmer Middle Pleniglacial to colder Late Pleniglacial. The larger rivers, as Someşul Mic and Arieş, had recorded strong vertical incisions and fluvial terrace detachments, while the same moment do not have a clear morphological or sedimentary mark along the smaller Pârtoţ River (Săcălaia drainage basin), as it evolved at the level of the already formed floodplain.

The two types of fluvial adjustments to large-scale climatic changes during the last glacial do show that, apparently, the medium size rivers are more sensitive/responsive to these climate variations than the smaller ones. This finding is surprising, being well known that the rivers with smaller drainage basins are, generally, more receptive to climatic changes than the larger ones.

This differential behavior could be a consequence of the drainage basin characteristics. The medium size rivers have the catchment areas in the surrounding mountains, which give 1000–2000 m vertical amplitude for the fluvial systems. As today, complex vertical vegetation belts were present in the drainage basin perimeters. The main vegetation structures were cold steppe, forest steppe and coniferous forests, receptive to climate changes mainly by vertical belt migrations. The altitudinal vegetation adjustments to climate changes influenced the flow discharges, which further forced the rivers to readjust their morphologies to the new climatic conditions. On the other side, the drainage basins of the small-scale rivers are located mainly at mid altitudes, usually containing the lowest vegetation belts. Therefore, the vertical migration of vegetation was less expressive in these areas than in the former one, so the impact of vegetation changes on flow discharge is expected to be less important.

SE Carpathians *(Curvature Carpathians)*

The intramontane basin Brasov is drained by the upper reach of Olt River, and the few other small tributaries with catchments areas in the surrounding mountaneous areas (e.g. Râul Negru, Bârsa, Homorod). A number of six fluvial strath and fill—terraces documents fluvial incision of ca. 100 m, starting with Middle Pleistocene (Necea et al. 2013).

The Pleniglacial history in the area starts with the T 30–40 m fluvial terrace, estimated to be formed during the Eemian/Early Weichselian–Early Pleniglacial (MIS 5, MIS 4), with a minimum age of ca. 59,000 years. Around this moment occurred also the last tectonically induced change of the Olt River's flow direction, from a northward course along the Bârsa—Baraolt Basin, to the present-day configuration. This flow direction change is documented by the large-scale development of the 15–20 m altitude fill-terrace in Sfântu Gheorge sub-basin and the eastern edge of Transylvanian Depression, while the older terraces have restricted occurrence or are even missing (as for example the 30–40 m fill-terrace) in the two areas (Necea et al. 2013).

The coarse gravel sediments of the 30–40 m and 15–20 m high fill-terrace of the Olt River, close to Arini and Sfântu Gheorge (Necea et al. 2013; personal observations), suggest that at the level of the two terraces, the river had a braided pattern.

After Necea et al. 2013 (and cited authors), the following fill-terrace, 5–12 m high, is recognized only along Homorod River, a tributary of Olt River in the Bârsa—Baraolt basin. No absolute ages are available for this particular fluvial terrace, while de relative ages suggest its formation around 40,000–20,000(?) years.

On the eastern flank of the SE Carpathians, the upper and median reaches of Zăbrăuţ, Şuşiţa, Putna, Milcov, Zăbala, and Naruja developed a number of 11 fluvial terraces, most of them strath-terraces, marking 240 m fluvial incision (Fig. 19.6). The absolute and relative ages of them suggest their formation starting with upper Middle Pleistocene, mainly from Upper Pleistocene to Holocene. Their genesis was attributed to local tectonics, with phases of incision during intensive tectonic uplifts and fluvial lateral erosion during tectonic relative stability (Necea et al. 2013).

After the authors, the 39–41 m high strath-terrace was abandoned between 29,000 and 16,000 years ago. Based on this dated interval, the terrace has formed in Middle Pleniglacial (MIS 3). However, considering the high number of terraces attributed to ca. 97–29/16 kyr (T 50–60 m; T 70 m and T 90–130 m), is not excluded that MIS 3 and 4 include also the formation of one or more of these superior terraces. The presence of 1–3 m thick gravel layer under the dated loess sequences along the 39–41 m terrace suggests that, at the moment of its formation, the rivers were braided.

Fig. 19.6 Putna Valley downstream from the confluence with Zăbala Valley, a representative example of phases of incision during intensive tectonic uplifts and fluvial lateral erosion during tectonic relative stability. Upper level of valley shoulders was maintained at 90–135 m, below that a succession of 5 fluvial terraces was developed. These terraces have a mixed structure or in bedrock (CrIstea 2011)

The existing age control on fluvial terraces in the area give a minimum 50–60 m fluvial incision during the last 73,000 yrs, from which the last 40 m correspond to six terrace levels (T 28–31 m; T 19–21 m; T 9–11 m; T 5 m; T 2 m and T 1 m) formed during Late Glacial—Holocene.

The spatial distribution of the lower terraces, paired versus unpaired, large-scale development versus restricted appearance along the rivers, do suggest, in the authors opinion, spatial migration of fluvial incision due to migration of uplift center from the orogen (Subcapathian nappes) trough the foredeep basin (Focşani Basin).

Moldavian Plateau

The existing synthesis (e.g., Posea et al. 1974; Posea 2002) on fluvial systems draining the eastern part of Romania (Moldavian Plateau) indicate that the Late Quaternary fluvial evolution in the area is reflected in the well-developed remnants of the last three terraces (T 30–35/40–50 m; T 20–25/30 m; T 10–15 m) and relatively large floodplains along the main rivers (Siret, Prut, Bahlui, Bârlad, Bistriţa).

A very recent study performed along Siret River, downstream from the confluence with Moldova River (Rădoane et al. 2015) give a first absolute chronological control on the topic. The upper part of the generalized coarse gravel layer in the base of the floodplain fill-terraces was dated to ~20,000 years (Fig. 19.7), suggesting that Siret River had a coarse gravel braided channel during Late Pleniglacial (MIS 2), at least during the LGM.

Also, on the top of the floodplain terraces (T 5–7 m; T 4 m, T 2–3 m) were identified three generations of palaeomeanders. Their morphometries suggests 1.2–1.5 times higher bankfull discharges than along the present-day meandering channel. After the same authors, these palaeodischarge values indicate Middle to Late Holocene age of these fluvial relicts. The absolute ages of the fossil trunks fixed in the fine sediments of the three floodplain terraces, less then 3000 years old, confirm their relative young ages.

This information indicated that between ca. 20,000–6000 years, vertical accretion was the dominant process in the floodplain perimeter, with a deposition of a minimum 7 m sedimentary layer. After then, the lateral and vertical erosion processes became dominant, with the detachment of the three floodplain fill-terraces.

The presence of crossbeded sandy layers on top of the coarse gravel layer suggests a dramatic change of the fluvial style. Their internal structures indicate mainly in-channel deposition in meandering channel(s). No data are yet available to support a more detailed discussion on the moment of channel metamorphosis and the spatial and temporal river adjustment to climate changes before LGM and during Late Glacial–Early Holocene.

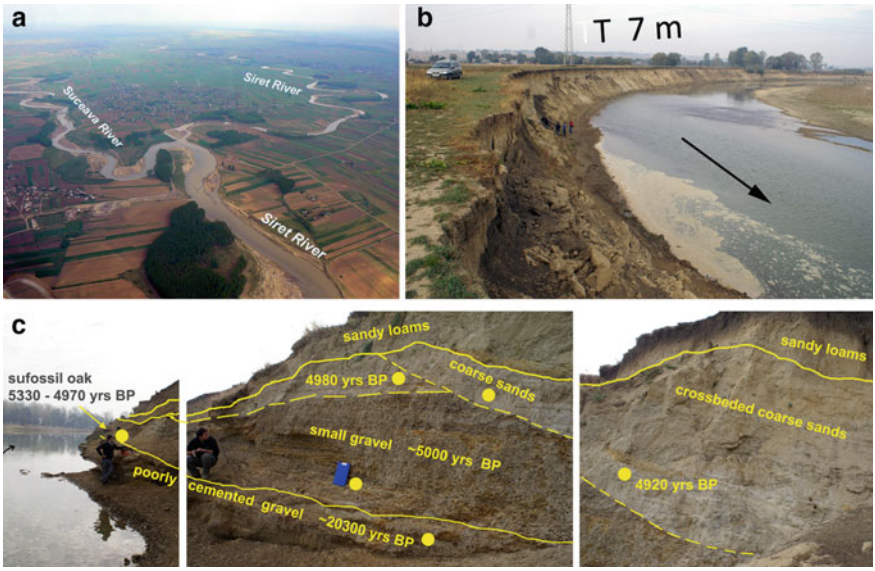

Fig. 19.7 The floodplain structure of Siret River, downstream the confluence with Suceava River : **a** Confluence Suceava River to Siret River; **b** cross section in fluvial terrace of 7 m; **c** the floodplain structure showing a braided channel phase which comprises the lower coarse deposits; and a sinuous and meandering phase, when bed material of decreasing grain size accumulated in the form of gravel lobes (in *meander chute-bars*) overlain by overbank sediments deposited by floods (adapted after Rădoane et al. 2015)

Romanian Plain, the Lower Course of Danube River

The main collector in the area is Danube River, marking the southern and eastern geographical limit of the Romanian Plain. Along the Romanian territory, its course is alluvial and meandering, except the area of Porţile de Fier Gorge, where the rock is present in the channel bed, and the channel reach known as the Great Island of Brăila, where it has an anabranching pattern.

The main tributaries in this perimeter, Jiu, Olt, Argeş, Dâmboviţa, and Ialomiţa, are medium scale rivers, with drainage basins located in the northern mountainous areas (Southern and Eastern Carpathians). The smaller size rivers, tributaries of the larger ones or even direct tributaries of Danube River, have catchment areas located mainly in the hilly areas (e.g., Motru, Olteţ, Cotmeana, Teleorman, Colentina, Moştiştea).

The fluvial terraces are well developed, with numbers that decrease from west to east, as the waters of the "Black Sea" lake (modern day western Black Sea region) gradually movement to the east during the Quaternary: five fluvial terraces along Danube, Jiu, and Olt Rivers, one to three terraces along Argeş, Dâmboviţa Rivers and other secondary rivers from the eastern part of the area (e.g., Olteţ, Desnăţui, Vedea, Teleorman, Ialomiţa, Buzău) (Posea et al. 1974). According to the

authors, the main cause of fluvial terraces formation in the area was the Black Sea eustatic oscillation, with tectonics playing a secondary role, more important in the western part of the Romanian Plain and Getic Piedmont.

The floodplains follow the same pattern: narrower, from 100 m to 7 km width, in the western part, while through the east they became large, more than 10 km width, with complex morphologies (e.g., well-developed levees, meandering belts, sometimes floodplain terraces).

The Late Quaternary evolution of fluvial discharge in this perimeter is a matter of debate, as the most accepted idea is that the rivers here evolved mainly under the influence of eustatic oscillation, of no more then few tens of meters vertical amplitude, while the role of recent tectonics and climatic changes played only secondary roles (Posea et al. 1974). Recent studies along Teleorman River (Howard et al. 2004; Macklin et al. 2010), the lower course of Danube River, downstream from Giurgiu to Danube Delta (Ghenea and Mihăilescu 1991; Giosan et al. 2006; Benecke et al. 2013) and on the western continental platform of the Black Sea (Popescu et al. 2004; Lericolais et al. 2010) give some new insights on this topic.

The oldest dated alluvial sequence in the area is located along Teleorman River, at the level of the 8 m fluvial terrace. The sedimentary facieses indicate the existence of a coarse gravel braided channel around 36,800 years ago, which place the flowing of the river at this level in Middle Pleniglacial (MIS3), before LGM. This fluvial environment was then replaced by an anabranching channel, slightly incised in the surface of the fluvial terrace, a phase maintained through LGM and early Late Glacial (Macklin et al. 2010).

For the same interval of time, the facies composition and absolute ages of the sedimentary sequences along the lower course of Danube River, before entering in the perimeter of Brăila Island, suggest that the river already flowed on the present-day floodplain, as a coarse gravel braided channel (Benecke et al. 2013). According to the authors, this channel type was active at least between ca. 32,000–15,000 years ago.

A significant change is reported during Bolling–Allerod Interstadial and Younger Dryas stadial, both in the case of Teleorman River and the lower course of Danube. In the first case, the anabranching channel has metamorphosed in large-scale meandering one, with up to 5 times larger meanders than the present ones, during the warmer Bolling–Allerod Interstadial. A slight vertical incision, of ca. 1 m deep, and maintenance of this pattern was reported for Younger Dryas stadial. In the case of Danube, the floodplain sediments became finer, indicating a decreasing energy of flow, with no distinctive reactivations during the Younger Dryas. No indications on channel typology functional at that time are available.

The last important change occurred at the start of the Holocene. Along Teleorman River, the channel has transformed into small-scale meandering one and incised up to 3 m, occupying the present-day floodplain level. The moment of this metamorphosis is unknown, as no older sediments then ca. 4000 years were found

in the floodplain perimeter. On contrary, along Danube River the change seems to be related with the moment of Black Sea connection with the Mediterranean Sea, ca. 9500–9000 years ago, when the water level of the Black Sea dramatically increased and the lower reach of Danube River started to evolve under limnic or partly drained floodplain conditions (Perşoiu and Rădoane, Chap. 20, this volume).

Further downstream, in Brăila Island area, even if the available descriptions of sedimentary sequences do not have absolute age control (Ghenea and Mihăilescu 1991), the studies in the near vicinity (Popescu et al. 2004; Lericolais et al. 2010) give some indications which can be tentatively putted in an absolute chronological framework (Starkel et al. 2015).

In the central and southern part of Brăila Island, the thick coarse alluvia without significant facies changes, together with the evidences of avulsion in the central Brăila Island (Ghenea and Mihăilescu 1991) and on the inner shelf of Black Sea (Popescu et al. 2004), suggest the maintenance of a meandering/anabrancing channel type during the entire interval of time before the moment when the Black Sea became connected to the Mediterranean Sea. Based on the available age controls, this behavior was active at least during LGM and was maintained until Early Holocene, ca. 9500–9000 years ago.

On contrary, the northern part of Brăila Island seems to have a more complex history, being the only identified reach directly influenced by the eustatic oscillation of the Black Sea, before its connection with the Mediterranean Sea. The records in the area starts with the layer of coarse alluvia (sands and gravels) present at ca. −50 m depth (Ghenea and Mihăilescu 1991), which mark an intensified erosion and floodplain aggradation during the Neoeuxinian phase, when the Black Sea level dramatically lowered. This eustatic phase most probably correspond with the water level decrease at ca. −120 m below the present one, during LGM (Lericolais et al. 2010). The following fine fluvial-lacustrine facieses, located at a depth of −40 m, occurred during Late Glacial, when the Black Sea level rose up to ca. −40 m (Lericolais et al. 2010), and the northern Brăila Island functioned as a gulf of the Black Sea (Ghenea and Mihăilescu 1991). During Younger Dryas, when the sea-level regression was bellow −100 m, a new coarse alluvial sequence indicate that Danube river has advanced again in the area, flowing further on the surface of the continental shelf, down to −90 m water depth (Popescu et al. 2004; Lericolais et al. 2010).

After the Black Sea was reconnected to the Mediterranean Sea, 10–25 m thick layers of sands and clays were deposited by periodic floods, peats, marshes, and shallow lakes. Danube River has maintained its meandering pattern, as the sequences of pebbles and coarse sands in the Brăila Island perimeter indicate (Ghenea and Mihăilescu 1991). Danube Delta started to form after ca. 5200 cal BP, when the Black Sea level became stable in the area, within −2 m and +1.5 m of the current level (Giosan et al. 2006).

Discussion

The two case studies from the eastern part of Romanian Plain show a complex fluvial history during the last ca. 40,000 years, where climate changes and local tectonics seems to play a more important role than eustatic oscillation of the Black Sea.

The lower course of Danube River evolved the entire period in the perimeter of its already existing floodplain, and the dominant processes were in-channel and overbank vertical aggradation. The influence of sea-level fluctuations were recognized only in the northern part of Brăila Island and the western continental shelf of the Black Sea, consisting in the lengthening of the meandering/anabranching river channel during regressions, and abandonments of the channel(s), and prodelta and delta formations during transgression periods. The main change occurred in Early Holocene, when the river has generalized its meandering pattern and a series of lakes, marshes, and secondary/abandoned channels developed on the perimeter of the floodplain. Apparently, this change is related with the moment of reconnection of the Black Sea to the Mediterranean Sea, and the associated rapid transgression (Benecke et al. 2013). An alternative explanation about the main cause of this generalized Early Holocene fluvial transformation could be the associated vegetation development to warmer climate, responsible for an increased lateral stability of the channel and dramatic reduction of liquid and solid discharges.

The avulsion of the Danube River in the central part of Brăila Island (Ghenea and Mihăilescu 1991), the existence of anabranched channels on the continental self, and the apparent presence in the area of the southern paleo-branch on the Peceneaga—Camena fault, a major crustal fault between the North Dobrogea Orogen and the Moesian Platform (Popescu et al. 2004), are indicators that the channel typology and behavior downstream from Hârsova was probably influenced by local tectonics too (Starkel et al. 2015). Moreover, the coexistence of meandering/anabranching channels with further upstream braided ones, can be interpreted in terms of regional tectonism, as the lower meandering channel with anabranched reaches are superimposed on the subsidence area formed at the contact between Moesian Platform and the North Dobrogea (subsidence rates −1 to 3 mm/year, after Zugrăvescu et al. 1998; Starkel et al. 2015).

By contrary, Teleorman River show a high sensitivity to Late Quaternary climate changes, without identifiable influences of local/regional tectonics and eustatic oscillations. The higher sensitivity of this river, comparative with the lower course of Danube River, is most probably a consequence of its small dimensions (160 km channel length, with a drainage area of ca. 830 km^2), which make it more receptive and responsive to climatically induced changes in vegetation composition and flow regimes.

The Role of Natural Controls on Pleniglacial–Late Glacial Fluvial Adjustments

The available new information of Late Quaternary fluvial evolution highlights once again the complexity of this subject, especially when the discussion is transferred to a more regional view, at the entire Romanian territory. The main challenge is to distinguish and estimate the importance of natural controls (climate, tectonism, eustatic oscillation, drainage pattern characteristics), their reflection in a regional pattern (e.g., aggradation, incision, channel typology, spatial behavior), after the isolation of local particularities.

The most evident finding, in a Northwest–Southeast transect (Fig. 19.8), is given by the amplitude of fluvial features covering the last ca. 71,000 years.

In the perimeter of the Western Romanian Plain, affected by a generalized subsidence trough the west, the fluvial history during the last ca. 45,000 yrs seems to be recorded in the 4–6 m amplitude fluvial morphological units (one fluvial terrace, the upper floodplain and the lower floodplain, after Posea 1997). Further east, in the Transylvanian Depression this interval of time is recorded starting with the detachment of the T 30–40 m fluvial strath-terrace (MIS5/MIS 4 transition?). In the Brasov Depression, the T 30–40 m cut and fill-terrace was estimated as minimum 59,000 years old, being formed at least during Early Pleniglacial (MIS4). The two areas are affected by a continuous tectonic uplift, at a smaller rate than the values recorded in the surrounding mountains (ca. 0–1 mm/year, after Zugrăvescu et al. 1998). In the perimeter of SE Carpathians, the most tectonically active region from Romanian, with an uplift rate estimated to ca. 5–6 mm/yrs (Zugrăvescu et al. 1998), frequently affected by earthquakes, the fluvial terraces reflect a minimum 50–60 m vertical incision, with the last 40 m during Late Pleniglacial–Holocene (MIS 2 and MIS1). In the Moldavian Plateau, knows as a tectonically stable region, with large alluvial fans developed along the eastern edge of the Eastern Carpathians, the last 7 m high alluvial features, all of them developed in the floodplain perimeter, reveal the most recent fluvial history, starting with LGM. Based on regional syntheses (e.g., Posea et al. 1974), which remark the morphological similarities between the Moldavian and Transylvanian rivers, it is not excluded that the Pleniglacial history of the Moldavian rivers to be reflected also in the last 30–40 m high relief along the valleys. In the SE part of the Romanian Plain, the last 36,000 years (MIS 3, MIS 2 and MIS 1) are recorded in the last ca. 6 m vertical amplitude fluvial morphologies, while further downstream, along the lower course of Danube River, the same period is included in the floodplain history.

The highlighted regional differences in the vertical amplitude of the Pleniglacial–Holocene fluvial features are direct reflections of the large-scale Late Quaternary tectonic pattern on the Romanian territory. On this general pattern, the local tectonic uplifts and subsidences, continuous or marked by periodic earthquakes, with temporal/periodic (re)activations, can impose the particularity of the fluvial behavior in some specific regions, as: local/regional avulsions (Great Hungarian Plain/the Western Romanian Plain, the lower reach of Danube River—Brăila

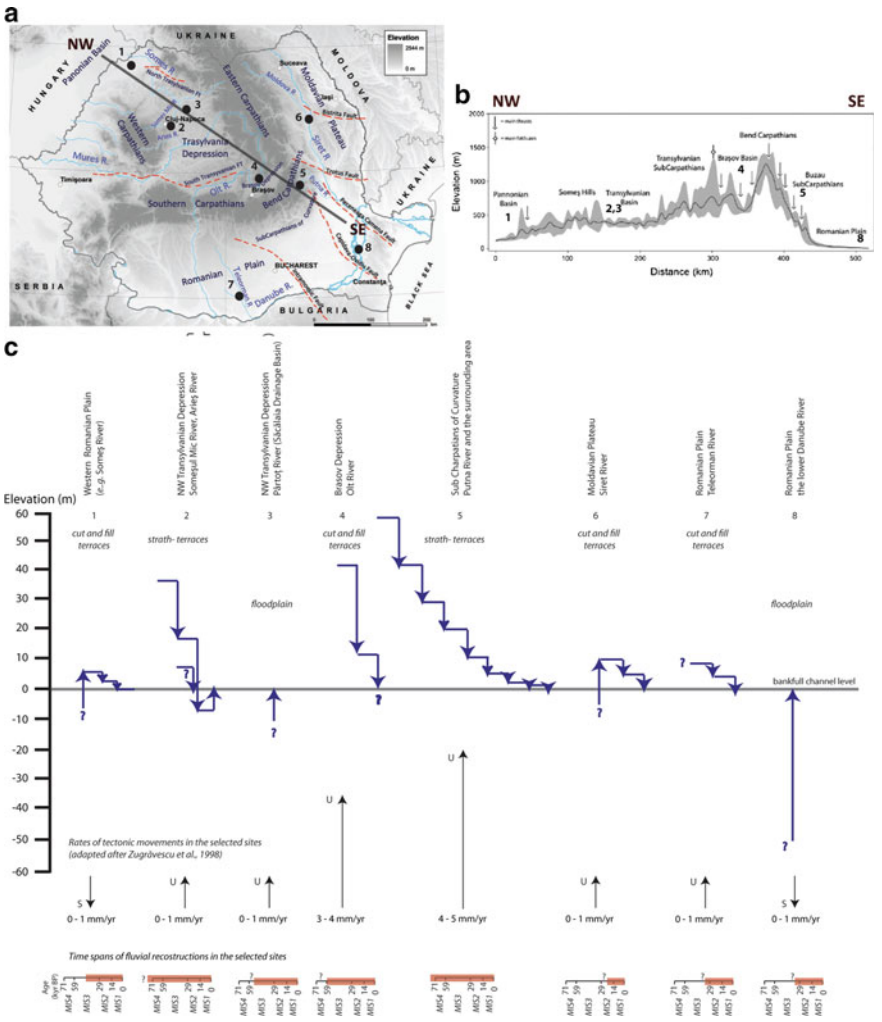

Fig. 19.8 The amplitude of the fluvial features covering the last ca. 71,000 years BP, as reflected by the recent studies on Late Quaternary fluvial behavior. **a** Location of sites discussed in the text; main faults dividing several tectonic units (adapted after Fielitz and Seghedi 2005); **b** NW–SE transect along the Romanian territory, extending from the Panonian basin to the Romanian Plain; main thrusts and fold axis are shown (adapted after Molin et al. 2012). **c** Vertical development of fluvial terraces and floodplains in relation with the neotectonic rates in the selected sites

Island), higher vertical range and increased number of the fluvial terraces (eastern part of SE Carpathians), increased thickness of sediments (lower reach of Danube River—Brăila Island, subsidence rate of −1 to −3 mm/year), coexistence of different channel types along the same river or in the same area (Great Hungarian Plain/the Western Romanian Plain—the Mureş/Maros, Criş/Körös aluvial fans).

Detailed Pleniglacial palaeoclimate and palaeoenvironmental reconstruction are not yet available on the Romanian territory. However, a series of recent studies (Feurdean and Tanţău, Chap. 4, this volume and the references therein) covering mainly the NW part of Romania, show similar Last Glacial Maximum—Holocene climatic patterns as known in the Western Europe The same mentioned studies indicate Romania as a glacial refugial area for tree species, suggesting bidirectional vertical migrations of vegetation belts to climate changes (e.g., migration of coniferous species both at lower and upper altitudes during warmer phases). This pattern was dramatically changed only during Early Holocene, when deciduous species arrived from the west, imposed the new vertical arrangement of vegetation, maintained thereafter. The second order climate changes, recorded during the Holocene, are recorded only in a one-directional migration of tree species (e.g., presence of coniferous species at mid altitudes after 8200 years). At a more regional scale, loess deposits from Central and Eastern Europe do suggest that MIS 3 has a drier and probably colder climate that during the Last Glacial Maximum (Feurdean et al. 2014). The same synthesis concluded that the climate changes during MIS 3 and MIS 2 in this part of Europe were more or less synchronous with the ones from North Atlantic region, and less dramatic in terms of magnitude. The vegetation was sensitive to these changes, but with a decreasing magnitude of adjustments from the north to the south, in a European transect. In this context, boreal forests where maintained in the area, including the coldest phases of the last glacial. This observation is in accordance with Pendea et al. 2009, which indicate, in the NW part of Transylvanian Depression, the oscillations of boreal forest steppe to periglacial steppe during the Pleniglacial.

In this context, the estimation of the importance of climate in the fluvial adjustments along the Romanian rivers, should consider both the direct/indirect effects of large-scale climate changes on flow regime (from warmer to colder and vice versa, and the associated changes on permafrost and vegetation structure/composition).

The role of the short phases of climatic transition (according to Knox 1983; Vandenberghe 2003, few tens to hundred years of geomorphological instability, during the reaction of vegetation to the new climatic conditions) is not yet understandable, as the available data do not clearly link the moments of fluvial changes (e.g., channel vertical incision and terrace detachment) with them.

However, the presented fluvial records do suggest high fluvial sensitivity to millennial scale climate changes, during the last 71,000 years. The coarse gravel braided patterns reported along rivers as Someşul Mic, Arieş, Olt, Siret, Teleorman, Danube, indicate that this type of channel was generalized during the Pleniglacial, with some temporal/spatial deviations (e.g., Tisza, Mureş/Maros, Teleorman, Crasna/Krászna) imposed by local geological/geomorphological conditions. Similar regional trend can be extracted from the numerous cases (taking into account the existing studies) which report large-scale meandering patterns during the Bolling–Allerod Interstadial (e.g., Tisza, Mureş/Maros, Arieş, Teleorman), followed by generalized metamorphosis in small-scale meandering channels, during the Early Holocene, when the climate became temperate.

The difference in fluvial reaction to millennial scale climate changes between the medium- and small-scale rivers from the NW part of Transylvanian Depression could be explained by the dimension and location of the catchment areas (in the mountainous areas vs. in the hill domain). During climatic transitions, the vegetation adjustments in larger drainage basins were more ample than in the smaller ones (where only one vegetation belt was present), therefore a higher instability of slopes and channels is expected, which is translated by the end in a higher receptivity of these rivers to large-scale climate changes.

An opposite example, where the smaller river is more sensitive to climate changes than the larger one, is given by Teleorman River and the lower reach of Danube. In this case, the very large drainage basin of the Danube River is responsible for the attenuation of the climatic signal, and only the most important changes are expected to be recorded in large-scale fluvial adjustment, as the detachment of the last fluvial terrace and formation of the present-day valley bottom.

The role of eustatic oscillation on fluvial behavior seems to play a second role, with direct effects recognizable only along the lowest reach of Danube River, in the Braila Island, in the perimeter of the present-day Danube Delta and the continental platform of the Black Sea.

At a more regional scale, the highlighted patterns in Pleniglacial–Late Glacial fluvial behavior along the Romanian rivers, are in accordance with the ones mentioned by Starkel et al. 2015, for the fluvial systems from Central and Eastern Europe. According to the authors, the main controls on Pleniglacial fluvial behavior are the climatic and vegetation fluctuations, while local conditions as tectonism, sea-level oscillation, meltwater supply or wind activity during dry periods (to mention only the controls acting in the perimeter of Romania and surrounding areas), act as secondary controls, reflected in the particularity of fluvial responses.

Conclusions

The Pleniglacial–Late Glacial fluvial history of the Romanian rivers can be partly reconstructed based on a series of recent studies on the morphology, sedimentology and absolute chronology of floodplains and lower fluvial terraces located mainly at mid and low altitudes.

The large-scale climate changes and vegetation adjustments are identified as the main controls on fluvial behavior. However, some drainage basin characteristics (e.g. surface and location of the catchment area, the relief ratio) are probably responsible for an increased fluvial sensitivity to climate changes, or, by contrary, for a more conservative behavior.

Commonly, the rivers had predominantly coarse gravel braided channels during the cold Pleniglacial. The first important change in the fluvial style was recorded during Late Glacial, when many rivers abandoned the braided style for large-scale meandering channels (3–8 times larger then the present-day ones), and the second

one occurred in Early Holocene, when the rivers maintained their meandering pattern, but drastically reduced their dimensions.

The role of tectonics is mainly reflected in the vertical amplitude of the fluvial features, from maximum 7 m amplitudes in relatively stable or subsiding areas, to minimum 50–60 m vertical amplitudes in the areas with high tectonic uplifts. Local-scale tectonics is responsible for specific fluvial reactions, sometimes giving the particularity of the area, as in the case of the eastern part of the Great Hungarian Plain/the Western Romanian Plain, or the eastern part of the SE Carpathians.

The less important role is played by the Black Sea level oscillation, reduced only to the lowest reach of the Danube River and surrounding areas, even if it recorded large amplitudes in the past (e.g., −120 m sea level drop during LGM).

On this general framework, a series of particularities in the perimeter of the drainage basin or even at a more local scale, are responsible for a series of differences in the fluvial response, as the coexistence of the involved processes (e.g., avulsion, occurrence and amplitude of vertical incision, aggradation, channel type metamorphosis), or high sensitivity and reaction time to climate change *versus* a more conservator behavior. These findings highlight the potential of Romanian fluvial archives to have an important contribution on the present-day debate on how the European rivers do adjusted their forms and behavior to Late Quaternary climate changes, and how local conditions can alter these signals.

Acknowledgments The research was supported by two grants of the Romanian Ministry of Education (UEFISCDI), project number PN-II-RUPD-2012-3-0547 and project number PN-II-ID-PCE-2011-3-0057.

References

Benecke N, Hansen S, Nowacki D, Reingruber A, Ritchie K, Wunderlich J (2013) Pietrele in the Lower Danube region: integrating archaeological, faunal and environmental investigations. Documenta Praehistorica XL, 175–193

Cristea I (2011) Putna Valley from Vrancea area. Geomorphological study (in Romanian), "Ştefan cel Mare" University, Suceava, Romania (unpublished PhD study)

Cserkész-Nagy Á, Thamó-Bozsó E, Tóth T, Sztanó O (2012) Reconstruction of a Pleistocene meandering river in East Hungary by VHR seismic images, and its climatic implications. Geomorphology 153–154:205–218

Feurdean A, Perşoiu A, Tantau I, Stevens T, Magyari EK, Onac BP, Markovic S, Andric M, Connor S, Farcas S, Gałka M, Gaudeny T, Hoek W, Kolaczek P, Kune P, Lamentowicz M, Marinova E, Michczynska DJ, Perşoiu I, Płociennik M, Słowinski M, Stancikaite M, Sumegi P, Svensson A, Tamas T, Timar A, Tonkov S, Toth M, Veski S, Willis KJ, Zernitskaya V (2014) Climate variability and associated vegetation response throughout Central and Eastern Europe (CEE) between 60 and 8 ka. Quatern Sci Rev 106:206–224

Feurdean A, Marinova E, Nielsen AB, Liakka J, Veres D, Hutchinson SM, Braun M, Timar-Gabo A, Astalos C, Mosburgger V, Hickler T (2015) Origin of the forest steppe and exceptional grassland diversity in Transylvania (central-eastern Europe). J Biogeogr 42(5):951–962

Fielitz W, Seghedi I (2005) Late Miocene-Quaternary volcanism, tectonics and drainage system evolution in the East Carpathians, Romania. Tectonophysics 410:111–136

Gábris G, Nádor A (2007) Long-term fluvial archives in Hungary: response of the Danube and Tisza rivers to tectonic movements and climatic changes during the Quaternary: a review and new synthesis. Quatern Sci Rev 26:2758–2782

Ghenea C, Mihăilescu N (1991) Palaeogeography of the Lower Danube Valley during the last 15000 years. In: Starkel L, Gregory KJ, Thornes JB (eds) Temperate oalaeohydrology. Wiley, New York, pp 343–363

Giosan L, Donnelly JP, Constantinescu S, Filip F, Ovejanu I, Vespremeanu-Stroe A, Vespremeanu E, Duller GAT (2006) Young Danube delta documents stable Black Sea level since the middle Holocene: Morphodynamic, paleogeographic, ad archaeological interpretations. Geol Soc Am 34(9):757–760

Howard AJ, Macklin MG, Bailey DW, Mills S, Andreescu R (2004) Late-glacial and Holocene river development in the Teleorman Valley on the southern Romanian Plain. J Quat Sci 19 (3):271–280

Kasse C, Bohncke SJP, Vandenberghe J, Gy Gábris (2010) Fluvial style changes during the last glacial-interglacial transition in the middle Tisza valley (Hungary). Proc Geol Assoc 121: 180–194

Kiss T, Urdea P, Sipos G, Sümeghy B, Katona O, Tóth O, Onaca A, Ardelean F, Timofte F, Ardelean C (2012) Trecutul râului/ The past of the river. In: Sipos G (ed) Trecutul, prezentul, viitorul râului Mureş/past, present, future of the Maros/Mureş River. Edit. Universităţii de Vest, Timişoara, pp 33–64

Kiss T, Sümeghy B, Sipos G (2014) Late Quaternary paleodrainage reconstruction of the Maros River alluvial fan. Geomorphology 204:49–60

Knox JC (1983) Responses of river system. In: Wright Jr. HE (ed) Late Quaternary environments of United States, The Holocene, University of Minnesota Press, Minneapolis, pp 26–41

Lericolais G, Giuchard F, Morigi C, Minereau A, Popescu I, Radan S (2010) A post Younger Dryas Black Sea regression identified from sequence stratigraphy correlated to core analysis and dating. Quat Int 255:199–209

Macklin MG, Bailey DW, Howard AJ, Mills S, Robinson RAJ, Mirea P, Thissen L (2010) River Dynamics and the Neolithic of the Lower Danube Catchment. In: The lower Danube in the prehistory: landscape changes and human-environment interactions. Proceedings of the international conference Alexandria, 3–5 Nov 2010

Manciulea S (1938) Tisa Plain (in Romanian), Bul Soc Reg Rom de Geografie LVII:66–150

Matenco L, Radivojević D (2012) On the formation and evolution of the Pannonian Basin: constraints derived from the structure of the junction area between the Carpathians and Dinarides. Tectonics 31(6):1–31

Molin P, Fubelli G, Nocentini M, Sperini S, Ignat P, Grecu F, Dramis F (2012) Interaction of mantle dynamics, crustal tectonics, and surface processes in the topography of the Romanian Carpathians: Aa geomorphological approach. Glob Planet Change 90–91:58–72

Nádor A, Thamó-Bozsó E, Magyari Á, Babinszki E (2007) Fluvial responses to tectonics and climate change during the Late Weichselian in the eastern part of the Pannonian Basin (Hungary). Sed Geol 202:174–192

Nádor A, Sinha R, Magyari A, Tandon SK, Zs Medzihradszky, Babinszki E, Thamó-Bozsó E, Unger Z, Singh A (2011) Late Quaternary (Weichselian) alluvial history and neotectonic control on fluvial landscape development in the southern Körös plain, Hungary. Palaeogeogr Palaeoclimatol Palaeoecol 299:1–14

Necea D, Fielitz W, Kadereit A, Andriessen PAM, Dinu C (2013) Middle Pleistocene to Holocene fluvial terrace development and uplift-driven valley incision in the SE Carpathians, Romania. Tectonophysics 602:332–354

Pendea IF, Gray JT, Ghaleb B, Tanţău I, Bădărău AS, Nicorici C (2009) Episodic build-up of alluvial fan deposits during the Weichselian Pleniglacial in the western Transylvanian Basin, Romania and their paleoenvironmental significance. Quat Int 198(1–2):98–112

Perşoiu I (2010) Recostruction of Holocene geomorphological evolution of Someşu Mic Valley (in Romanian). Unpublished PhD thesis "A. I. Cuza" University, Iasi, Romania

Perşoiu I, Feurdean A (2013) Late Quaternary floodplain evolution in the low tableland of Transylvanian Depression, Romania. In: IAG—international conference on geomorphology, Paris, France

Perşoiu I, Perşoiu A (in prep.) Variable fluvial response to Late Quaternary climate changes in NW Romania

Perşoiu I, Rădoane M (in prep.) Late Quaternary evolution of Someşul Mic River, Romania

Popescu I, Lericolais G, Panin N, Normand A, Dinu C, Le Drezen E (2004) The Danube Submarine Canyon (Black Sea): morphology and sedimentary processes. Mar Geol 206:249–265

Posea G, Popescu N, Ielenicz M (1974) Relief of Romania (in Romanian). Scientific Press, Bucureşti

Posea G (1997) The Western Romanian plain (in Romanian). Editura Fundaţiei România de Mâine, Bucureşti

Posea G (2002) Geomorphology of Romania (in Romanian). Editura Fundaţiei România de Mâine, Bucureşti

Rădoane M, Nechita C, Chiriloaei F, Rădoane N, Popa I, Roibu C, Robu D (2015) Late Holocene fluvial activities and relations with subfossil trunks: case study Moldova and Siret Rivers, Romania. Geomorphology 239:142–159

Robu D, Niga B, Perşoiu I (2015) Investigation of fluvial landforms in the north-eastern Pannonian Basin, using cartographic materials from the XIX–XXI Centuries. EGU General Assembly 2015, Geophysical Research Abstracts, Vol. 17, EGU2015-13448

Săndulescu M, Visarion M (1977) Considerations sur la structure tectonique du soubassement de la depression de Transylvanie. Dari de seama ale sedintelor, Inst Geo Geofiz LXIV:153–173

Sipos G (ed) (2012) Trecutul, prezentul, viitorul râului Mureş/past, present, future of the Maros/Mureş River. Edit. Universităţii de Vest, Timişoara, 212 p

Starkel L, Michczyńska DJ, Gębica P, Kiss P, Panin A, Perşoiu I (2015) Climatic fluctuations reflected in the evolution of fluvial systems of Central-Eastern Europe (60–8 ka cal BP). Quat Int 388:97–118

Thamó-Bozsó E, Magyari A, Nagy A, Unger Z, Kercsmár Z (2007) OSL dates and heavy mineral analysis of Upper Quaternary sediments from the valleys of the Ér and Berettyó Rivers. Geochronometria 28:17–23

Timár G, Sümegi P, Horváth F (2005) Late Quaternary dynamics of the Tisza River: evidence of climatic and tectonic controls. Tectonophysics 410:97–110

Vandenberghe J (2003) Climate forcing of fluvial system development: an evolution of ideas. Quat Sci Rev 22:2053–2060

Zugrăvescu D, Polonic G, Horomcea M, Dragomir V (1998) Recent vertical crustal movements on the Romanian territory, major tectonic compartments and their relative dynamics. Revue Romaine de Geophysique 42:3–14

Chapter 20
Fluvial Activity During the Holocene

Ioana Perşoiu and Maria Rădoane

Abstract Recent palaeohydrologic studies along rivers draining Romanian territory and the eastern Hungary give new insights on the Holocene fluvial evolution, in terms of the main causes for river dynamics, the involved processes and mechanism, and the associated sedimentological and morphological features. The climate change from glacial to interglacial conditions is the main cause for large-scale channel metamorphosis, from braided/large-scale meanders to small-scale meanders, and from vertical aggradation process to vertical incision. The process was not a uniform one, as the moment of transformation did occur well after the onset of the Holocene, most probably closely related with the moments of large-scale vegetation adjustments, then to climate amelioration itself. Thereafter, the rivers show a higher sensitivity to second-order climatic variations (including short abrupt climatic changes: $10–10^2$ years) and to local conditions (e.g., local tectonics). The more frequent data from Late Holocene do illustrate a good correlation between the fluvial processes along the investigated rivers and their floodplains/low alluvial plains, and the succession of warm/dry and cold/wet periods. Also, they point to an increase of fluvial processes during this time, when the climate generally became colder and wetter and the vegetation became more opened along the rivers. The human impact plays a secondary role, becoming more important only during the last centuries. The floodplains and the low alluvial plains, interpreted previously mainly as Holocene morphologies and sedimentary units, have, in fact, a more complex history, in terms of genesis, ages, and evolution.

Keywords Eastern Europe · Holocene · Hydrological events · Paleochannels · Fluvial adjustments

I. Perşoiu (✉) · M. Rădoane
Stefan Cel Mare University, Universităţii 13, 720229 Suceava, Romania
e-mail: ioanapersoiu@gmail.com

M. Rădoane
e-mail: radoane@usm.ro

M. Rădoane and A. Vespremeanu-Stroe (eds.), *Landform Dynamics and Evolution in Romania*, Springer Geography,
DOI 10.1007/978-3-319-32589-7_20

Introduction

The now accepted models on Late Quaternary evolution of Romanian rivers are still dominated by long-held traditional view that aggradation (braided rivers, coarse gravel sediments) occur during glacials, while incision and erosion of sediments (meandering rivers) during interglacials (e.g., Posea et al. 1974; Geografia Romaniei—Vol III 1987; Ficheux 1996; Pop 2001; Posea 2002).

From this perspective, the floodplains and alluvial plains are generally attributed to the Holocene, with a decrease in age from the mountainous regions to the lower plains. Therefore, the floodplains at the higher altitudes formed starting with Late Glacial (e.g., Someşul Cald, Apuseni Mountains), while in the hilly and plain domains, they where created during the Holocene, with the final phase being recorded during Late Holocene, in the most lower areas (e.g., the alluvial plain of Someş River, the alluvial plain of Crişul Negru River, the floodplain of the lower Danube). This long profile discrepancy in the floodplain age is attributed to the Late Glacial—Holocene oscillations of the two main regional base levels: the Black Sea, for the rivers draining the southeast and eastern part of Romania, and the Pannonian Basin, for the rivers draining the northwestern and western parts of the country.

The sedimentological evidences along the medium and lower courses of the Romanian rivers do suggest the existence of a generalized sequence, with coarse alluvia (boulders, cobbles, coarse sands) in the lower part of the sedimentary sequence, covered by finer materials (finer sands and clays) in the top. These sedimentary sequences differ highly in their thickness, between 1–2 m and more than 20–40 m thick, interpreted as reflections of local conditions of evolution (e.g., drainage basin relief, tectonism, sea level oscillation, vertical aggradations induced by human activity). It is generally accepted that the coarser layer was deposited during a colder and wetter climate (Early–Mid Holocene), while the upper finer materials during the drier Late Holocene, when more abundant vegetation occupied the drainage basins and when the last important sea level increase has occurred. The upper finer materials, consisting in fine sands, clays, and silts, frequently with one–two archeological levels, are interpreted as results of an increased rate of vertical aggradation in the floodplain areas, during the last centuries, induced by human activities.

The main morphological features in the perimeters of the low alluvial plains and the well developed (hundred of meters—few km wide) floodplains are (i) *the lower floodplains* (1–3 m high), frequently flooded, containing a series of fluvial features associated with the present day active channels, predominantly meandering: levees, point bars, palaeomeanders or abandoned courses; and (ii) *the upper floodplains* (3–8 m high), with one–two discreet levels, less affected by flood events. The detachment of the floodplain terraces are attributed to Late Holocene climate changes: the rivers have incised, as the climate became drier and, in consequence, the solid and liquid discharges have decreased (Posea et al. 1974).

A series of recent studies on Late Quaternary fluvial evolution of some rivers draining the Romanian territory: Someş, Mureş, Crişuri, Someşul Cald, Someşul Mic, Arieş, Putna, Şuşiţa, Milcov, Zăbala, Moldova, Siret, Teleorman, the lower

Fig. 20.1 Location of the cited study areas: (*1*, *2*, *3*) *Western Romanian Plain (Great Hungarian Plain)*: *1* Someş/Szamos River, *2* Criş/Koros Rivers, *3* Mureş/Maros River; (*4*, *5*, *6*, *7*) *Transylvanian Depression*: *4* Someşul Mic River, *5* Pârtoţ River, *6* Someşul Cald River, *7* Aries River; (*8*, *9*) *Moldavian Plateau*: *8* Moldova River, *9* Siret River; (*10*) *SE Carpathians*: Putna, Şuşiţa, Milcov and Zăbala Rivers; (*11*, *12*) *Romanian Plain*: *11* Teleorman River, *12* the lower reach of Danube River (between Giurgiu and Oltenita)

Danube (Howard et al. 2004; Macklin et al. 2010; Benecke et al. 2013; Nádor et al. 2007. 2011; Kiss et al. 2014; Necea et al. 2013; Chiriloaie et al. 2012; Rădoane et al. 2015; Perşoiu 2010; Perşoiu and Rădoane, in prep.; Perşoiu and Perşoiu, in prep.) (see Fig. 20.1), additionally supported by indirect information from palaeoenvironmental and climatic studies (Perşoiu, Chap. 3, this volume; Feurdean and Tanţău, Chap. 4, this volume, and the cited papers), give new insides on the Holocene fluvial processes and mechanisms, and the controls behind them (both natural and human induced).

The aim of this chapter is to present the new results on the topic, as they are reflected by the cited studies, and to highlight the way these recent findings are integrated in a more regional (European) model of the Holocene fluvial behavior. The following discussion is centered on (a) the involved fluvial processes and mechanisms, and the causes behind them; and (b) the sedimentological and morphological features generated during this time span. The fluvial history described here starts with the short transition phase, at the end of Younger Dryas Stadial, and continues with Holocene, with details covering millennial–centennial time scales.

Fluvial Processes and Mechanisms

The Late Glacial–Holocene Transition

The Late Glacial–Holocene transition, when the climatic and environmental conditions had changed from periglacial to temperate ones, is associated with dramatic changes in the fluvial behaviors, in terms of channel metamorphosis, and the associated vertical and lateral aggradational processes. The amplitude and moments of these fluvial changes, and their climatic and environmental conditioning, are well known at continental scale (e.g., Starkel 1983; Starkel and Thornes 1991; Kasse et al. 2010; Janssens et al. 2012). The general model indicates a first important change during Bolling–Allerod Interstadial, when the rivers have transformed from wide, coarse gravel to fine materials, braided channels to large-scale meandering ones (few times larger than the present ones), with a possible returning to braided pattern during the Younger Dryas Stadial. The second phase was recorded in Early Holocene, when small scale meandering channels, usually associated with vertical incision, started to impose the dominant fluvial landscape (Fig. 20.2).

However, a series of studies from Germany (Erkens et al. 2011), Poland (Starkel 2002a, 2007), Hungary (Nádor et al. 2011) highlight the idea that, even if a generalized fluvial change occurred when the climate became temperate, as a widespread decrease of liquid and solid discharges (under the direct and indirect effects of climate conditions), the fluvial reaction pattern is far from a synchronous one, both in terms of space and time. The complexity of fluvial response to the new climatic and environmental conditions depends on other natural controls, at local, drainage basin scale, or even a more regional scale. Therefore, the amplitude of

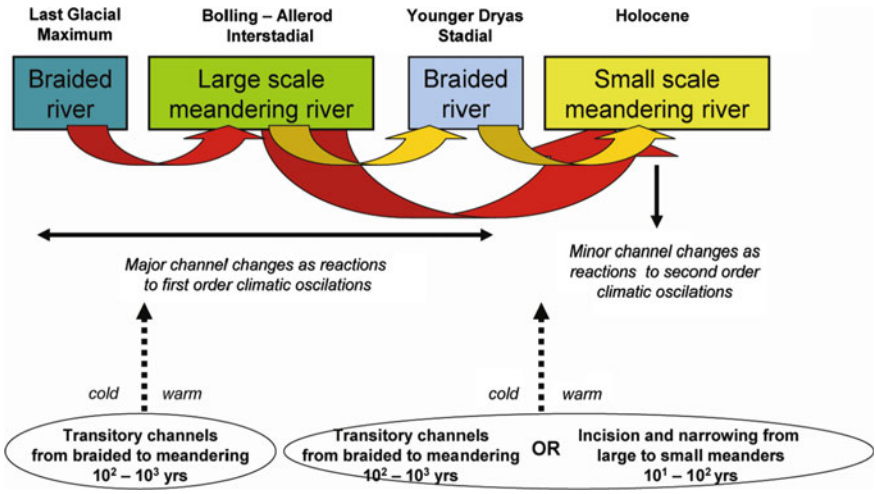

Fig. 20.2 General model of fluvial adjustments to Late quaternary climate changes, in NW and Central Europe

changes and the moments of their occurrence are highly variable, if rivers from different areas are compared between them. Between the causes of these discrepancies were identified the rivers dimensions (the smaller ones seems to be more sensitive than the larger ones), the position and dimension of drainage basins (large/small basins; low/high amplitude of relief), local/regional scale tectonism (e.g., Pannonian Basin), the moments of large scale vegetation changes.

The most recent studies on rivers located in Romania and in its close vicinity (Fig. 20.1), do confirm the general model of a generalized channel metamorphosis in small-scale meandering one. The picture is far from complete, as the available data from the transition period are scarce.

For example, the information along Someşul Cald—Someşul Mic Rivers (Perşoiu 2010; Perşoiu and Rădoane, in prep.) suggest that the channel metamorphosis in small-scale meandering one occurred with a delay of at least 1000 years after the onset of the Holocene, and most probably was preceded by an intermediate phase of a wandering/anabranching channel pattern. Moreover, local morphological and geological conditions could be responsible for a complex long-profile river answer to climate changes. Therefore, on the surface of the relict alluvial fan of Someşul Mic River at the entrance in the hilly domain, a coarse gravel braided pattern was maintained during the entire Late Glacial and, most probably, during the first thousand years of Early Holocene, and was followed by a short, few hundred years long, transition phase to small-scale meandering channel (Fig. 20.3).

The second recognizable pattern of river transformation is reported along Crişul Repede/Sebes-Körös, Crişul Negru/Fekete-Körös, Crişul Alb/Fehér–Körös (Nádor et al. 2007), Mureş/Maros River (Kiss et al. 2014), Someş/Szamos River (Posea 1997), Teleorman (Howard et al. 2004; Macklin et al. 2010), where large-scale meandering channels, even older than Bolling–Allerod Interstadial were progressively replaced by small-scale meandering ones, without a transitory phase as in the previous-mentioned cases. Here too, the moments of changes are not synchronous between them and do not necessarily correspond with the onset of the Holocene.

Discussions

The delays in rivers adjustment to the new climatic conditions covering few hundred/ thousand of years after the start of the Holocene are comparative, at least in pattern, if not completely in time, with the ones reported elsewhere in the Western and Central Europe (e.g., Starkel 2002a, 2007; Nádor et al. 2011; Erkens et al. 2011).

These delays in the fluvial adjustments to climate amelioration cannot be triggered to the reaction time of the existing vegetation, estimated to be no longer than few decades (Knox 1983). The palaeohydrological studies performed in Central Europe (e.g., Starkel 2002a) have demonstrated that the last large-scale rivers metamorphosis occurred around 10,000 years BP, with at least a 1000 years delay compared to rivers from Western Europe, and the cause for this behavior could be the delay in the deciduous species expansion eastwards (e.g., Notebaert and Verstraeten 2010).

In the NW part of Romania, the large-scale vegetation changes started at ca. 10,700 years BP, with the arrival of *Quercus, Tilia, Acer, Fraxinus excelsior,*

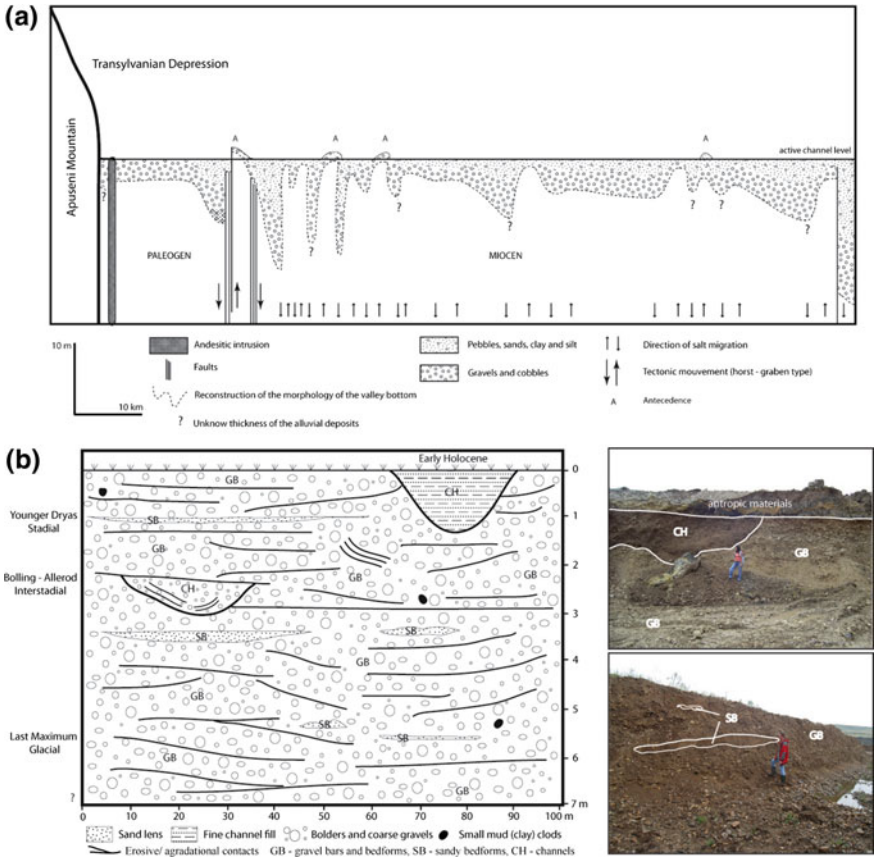

Fig. 20.3 The floodplain of Someşul Mic River: **a** the reconstructed longitudinal profile of the valley bottom, between Gilău and Dej (modified after Perşoiu and Rădoane 2011); **b** coarse boulders and gravels deposited by the Late Glacial braided river, followed by the transitory meandering/wandering channel, slightly incised in the previous sediments, active during the first centuries—millennia of the Early Holocene (adapted after Perşoiu 2010, Perşoiu and Rădoane in prep.)

Corylus avellana species in the area (Feurdean and Tanţău, Chap. 4, this volume). The second important age reference is ca. 10,300 years BP, when the deciduous species became dominant at mid-altitudes and the new vertical vegetation distribution (maintained until present) was established. Because there are no indicators about a consistent migration lag of vegetation species between the northwestern part of Transylvanian Depression and the western flank of Eastern Carpathians, the two highlighted moments can be generalized at least for the Western and Central part of Romania.

In this context, the mentioned delays in fluvial response to the new temperate conditions seem to be more related to the moments of large-scale vegetation

adjustments, than to climate amelioration itself. As a result, the main cause for a generalized fluvial metamorphosis was a dramatic decrease of solid discharge, mainly at mid–low altitudes. From this perspective, the different moments of change were tightly related to the internal equilibrium of each fluvial system. Local controls, as tectonics, size and morphology of the drainage basin, etc., played an important role in this process, by amplifying, delaying, or even imposing the nature of fluvial response (i.e., regional avulsion, maintenance of vertical aggradations, or braided patterns at lower rates).

The Holocene

The models of Holocene evolution of Tisza/Tisa River in Hungary (Kasse et al. 2010), Siret and Teleorman Rivers in Romania (Rădoane et al. 2015; Howard et al. 2004; Macklin et al. 2010), indicates the existence of a significant channel vertical incisions 4–7 m in amplitude during this period of time. However there are no clear evidences when these incisions have started. The main question is if they occurred at the Holocene onset, or later on, during Mid Holocene. For example, along Teleorman River the Holocene fluvial sediments, present in the lower floodplain, are no more than ca. 4000 years old. In the case of Siret River, the ages of the fossil trunks fixed in the fluvial sediments suggest that the last three floodplain terraces were formed also during the last few thousand years. On the other hand, the absolute ages available along Someşul Cald, Someşul Mic, and Arieş Rivers suggest an Early Holocene channel vertical incision (Perşoiu and Rădoane, in prep.; Perşoiu and Perşoiu, in prep.).

A more complex picture is given by the planform fluvial palaeo-morphologies in the floodplain perimeters. The histories of Someşul Mic River and of the rivers draining the Western Plain highlight the role of local controls in spatial and temporal distribution of general channel behavior.

In the case of Someşul Mic River, the local structural and tectonical geology (downstream/lateral uplifts and subsidences, imposed by diapirism and small-scale fault systems) were found responsible for a series of channel planform behavior, as long-profile succession of sinuous, meandering, anabranching channel reaches, preferential directions of channel avulsions, or the existence of some stable channel reaches (antecedence). This pattern was maintained during the entire Holocene, probably with lower rates in the past, when the floodplain was more forested, as suggested by the numerous fossil trunks dated around 7800 years BP, both along Someşul Mic River and elsewhere in Europe (Perşoiu 2010; Rădoane et al. 2015; Friedrich et al. 2004; Starkel et al. 2012) and, in consequence, the channel banks were more protected from lateral erosion (Perşoiu 2010; Perşoiu and Rădoane, in prep.).

The Holocene evolution of the lower courses of Someş/Szamos and Mureş/Maros Rivers, shows relatively large-scale regional avulsions (if compared with the ones occurred along the more narrow floodplains along the most Romanian Rivers), with important repositioning of active channels (Fig. 20.4). The lower course of

Fig. 20.4 The Holocene positions (*gray-shaded areas*)of the lower reaches of Someş/Szamos, Mureş/Maros and Criş/Körös, in the perimeter of their alluvial plains (adapted after Posea et al. 1997; Robu et al. 2015; Kiss et al. 2014; Nádor et al. 2007, 2011)

Someş/Szamos River initially was directed along the present day Noroieni River, than was the one flowing along the Homorod-Balcaia system, which was abandoned ca. 5000 years ago for the present day course (Posea 1997). The Holocene history of the lower reach of Mureş/Maros River is recorded in three distinct palaeoflow directions in the perimeter of its alluvial fan, along which different channel types coexisted (braided, meandering). The present day position was

established ca. 2000 years ago, during the Roman Period, when the last large-scale avulsion occurred (Kiss et al. 2014). The causes for these avulsions are not yet well understood. Local slope variations imposed by tectonics are frequently identified as the possible main cause for them, but the role of climate deteriorations and even human impact are also discussed.

The three highlighted case studies, both along a narrow floodplain and on large alluvial plains, do suggest that the rivers are probably more sensitive to local controls when they evolve under temperate conditions.

In a more detailed outlook, a series of fluvial events and trends identified along the investigated rivers suggest an increase in fluvial activity during Late Holocene, following a particular moment, i.e., ca. 4700 years BP (Perşoiu 2010; Perşoiu and Rădoane, in prep.; Feurdean et al. 2015; Posea 1997; Howard et al. 2004; Rădoane et al. 2015):

- local channel planform repositioning in the floodplain of Someşul Cald River at 4700 year BP (location: Apuseni Mountains);
- an increase in bedload granulometry in the palaeochannels of Someşul Mic River (Jucu site), from pebbles and sands to cobbles in sandy matrix, dated post 4700 years BP and maintained until present day (location: Transylvanian Depression);
- the development of Stiucii Lake and accelerated increase of floodplain vertical aggradation along Pârtoţ River, a small tributary of Someşul Mic River (location: Transylvanian Depression);
- the occurrence of the last significant avulsion of the lower course of Someş River at ca. 5000 years ago, position maintained thereafter (location: the Western Plain);
- no older fluvial sediments than ca. 4000 years BP in the floodplain perimeter of Teleorman River, suggesting an intensive phase of erosion quite before this period of time (location: Romanian Plain);
- a rising incidence of exceptional hydrological events after 4700–4000 years BP, both along Siret and Moldova River, as suggested by the increasing frequency of fossil trunks in fluvial sediments, and the reconstructed growth and felling periods (annual resolution) on them (location: Moldavian Plateau, Fig. 20.5);
- a general granulometric increase of the in-channel sediments along Moldova River, during Late Holocene. The available data suggest that the moment of change occurred around 3300–3000 years BP, and consisted in the replacement of fine materials (pebbles, sands), with coarser ones, with median diameters between 36 and 17 mm (location: Moldavian Plateau).

The palaeoclimatic reconstruction based on ice from Scărişoara cave, Perşoiu, Chap. 3 this volume) indicate that the moment 4700 years BP represent the most important abrupt climatic oscillation (lasting for a few hundred years) during the entire Holocene, and is part of a generalized climatic deterioration during Late Holocene. Also, at ca. 5000 years BP, the *Fagus* forest became the dominant forest

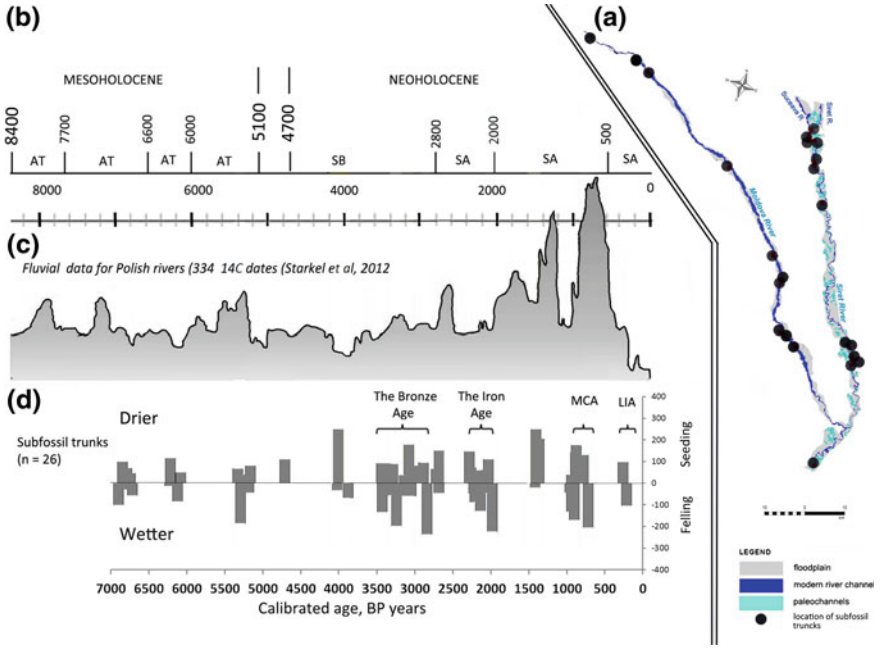

Fig. 20.5 Subfossil trunks as indicators of exceptional hydrologic events. **a** Location of the subfossil trunks along the Moldova and Siret Rivers; **b** Chrono-stratigraphy of the Meso and Neo Holocene; **c** The correlation between these periods and the probability density function diagram of fluvial data from Polish rivers. Curve was constructed using the option 'Sum' in the OxCal program (Bronk Ramsey et al. 2007) and the IntCal09 calibration curve (Reimer et al. 2009) (cf. Starkel et al. 2012); **d** Assessment of wet (resulting in flood events) and dry periods based on dendrochronologic sequences from 26 dated subfossil trunks along the Rivers Siret and Moldova (*HCO* Holocene Climatic Optimum; *LBA* Late Bronze Age; *MWP* Medieval Warm Period; *MCA* Medieval Climatic Anomaly; *LIA* Little Ice Age) (modified after Rădoane et al. 2015)

at mid-altitudes, configuration maintained thereafter (Feurdean and Tanţău, Chap 4 this volume). The large-scale *Fagus* expansion during the last millennia seems to be sustained by the late Holocene general climatic deterioration, and represent one of the most important (and the last one of such amplitude) vertical vegetation configuration during the entire Holocene; And last but not least, at this time was reported the massive migration of Indo-European populations in the area, with a profound modification of society and land use (Glodariu 1997). However, the palaeoenvironmental reconstructions do not show a significant human impact on vegetation at this particular time, the first signs of a considerable impacts being reported few centuries–millennia thereafter (Feurdean et al. 2013).

All these apparently dispersed information, not yet very well constrained chronologically, do suggest that the main causes for an increase in Late Holocene

fluvial activity seems to be the general climatic deterioration, and vegetation reconfiguration at mid-altitudes, responsible for an increase in solid discharge.

During the Late Holocene, more or less the last 4000 years, the more detailed sedimentological, dendrological, and chronological data along Someşul Mic, Moldova and Siret Rivers, suggest high river sensibilities to well-known second-order climatic variations, as the warm Roman Period, the cold and wet Dark Age Period, the Medieval Warm Period, Little Ice Age, or the present day warm period.

The evidences along Someşul Mic River place preferentially the palaeosols and meanders development in the floodplain perimeters during the warm periods, with only isolated flow events (meander cut-offs, floods), while from the cold and wet phases dominates the sedimentological and morphological structures indicating channel planform changes, associated with an increase in overflow frequency (Perşoiu 2010).

Intervals of time with intense fluvial activity along Moldova and Siret Rivers where induced based on distinct phases of felling trees, mainly between 3500 and 2900, 2200 and 2075, 1000 and 800 years BP, and were interspersed with the less-humid ones, as the late Medieval Warm Period or ca. 1400 years BP.

In terms of fluvial processes that governed the channel reaction to Late Holocene climate changes, the two rivers had two different patterns. Along Siret River, the channel was maintained as sinuous–meandering, while in the floodplain perimeter, the deposition of ca. 7 m thick alluvial materials, mainly by lateral accretion and overbank sedimentation, was followed by channel incision, with the detachment of two distinct alluvial terraces (below 4 m high and 5–7 m high). During this time, the flow discharge was 1.2–1.5 times more than the present one, as the hydrologic reconstructions based on palaeomeanders from the two terraces suggest. In the case of Moldova River, the braided pattern was maintained during the last ca. 3000 years, associated with the deposition of ca. 4 m thick coarse gravel sediments along the valley. The exception from this general pattern is the inferior reach of the river, close to the confluence with Siret River, where the channel has changed couple of times between braided and wandering types.

Recent investigations on small lakes (in Romanian named *tău* and *iezer*) (Florescu 2015), have proved that the land use change after 4000 years BP, mainly through deforestation and extension of pastures, had significant impact on sediment budgets in their catchments areas. However, along the investigated floodplains there are no clear evidences in support of large-scale human impact on liquid and solid discharges. Overall, the role of humans in the fluvial processes, both along the channel and the floodplains/alluvial plains, appears as secondary, with a minimum impact at least at the beginning of this phase. All these findings are in accordance with the ones reported elsewhere in Europe, where cycles in river activities where more closely linked to climate change than to a local anthropogenic activity (Starkel 2002a, b; Macklin et al. 2005; Thorndycraft and Benito 2006; Starkel et al. 2006, 2012) (see Figs. 20.5b and 20.6).

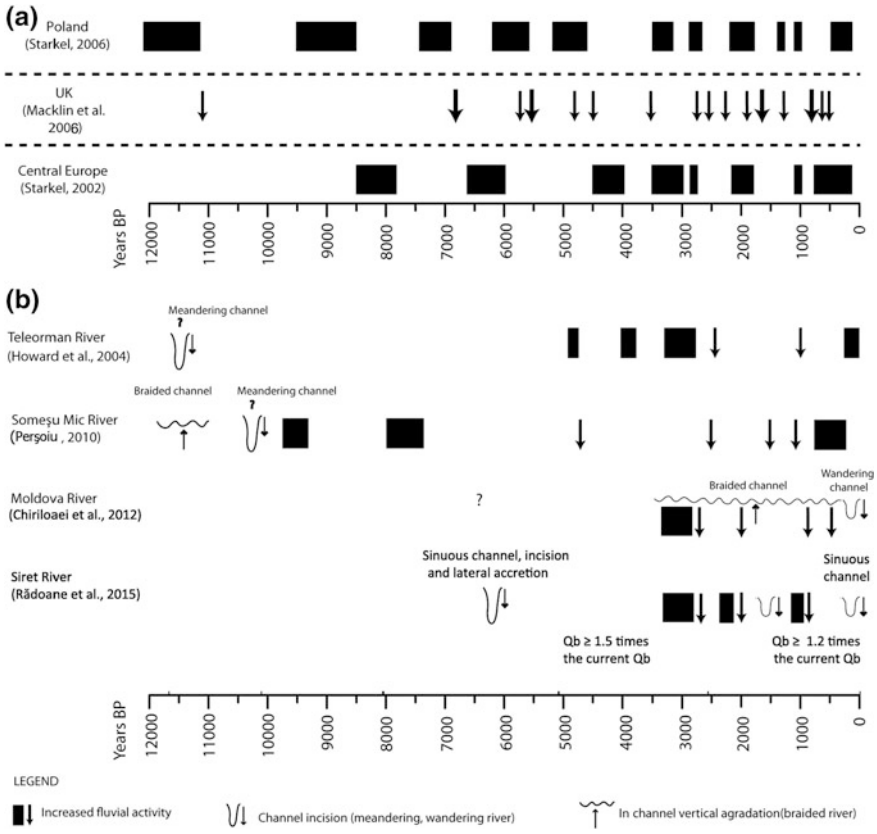

Fig. 20.6 Temporal correlation of periods with increased fluvial activity: **a** in Europe: UK (Macklin et al. 2006), Poland (Starkel 2006) and Central Europe (Starkel 2002b); and **b** Romania: Teleorman River (Howard et al. 2004), Someşu Mic River (Perşoiu 2010), Moldova River (Chiriloaei et al. 2012), Siret River (Rădoane et al. 2015)

The Holocene Fluvial Sedimentological and Morphological Features

The cited studies in this paper do indicate, also, that the floodplains, developed both in mountainous areas and lower altitudes, are highly diverse in respect of their ages (Fig. 20.7), genesis, the nature of fluvial morphologies and sediment assemblages. This diversity is caused by local controls, as drainage basin characteristic, local geological and morphological conditions, etc., while the first- and second-order climate changes, and the associated vegetation adjustments (both latitudinal and altitudinal), give the general framework for the fluvial evolution. These ideas are highlighted in the following examples.

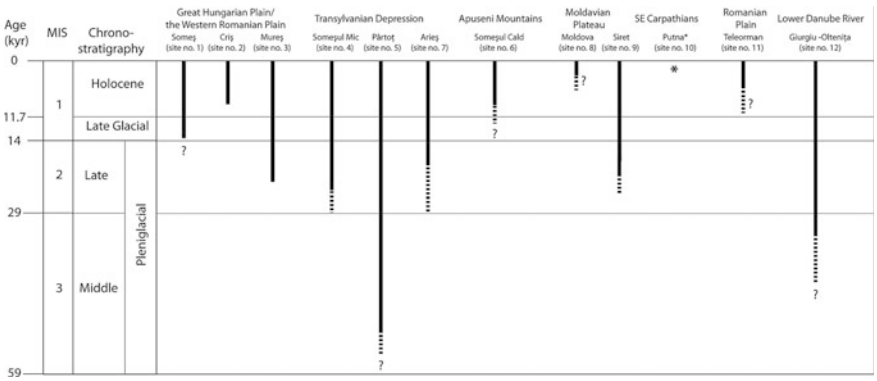

Fig. 20.7 The ages of the lower alluvial plains and floodplains, as reflected by recent studies on Late Quaternary fluvial evolution: Someş (Posea 1997; Timár et al. 2005); Criş (Nádor et al. 2007, 2011); Mureş (Kiss et al. 2014), Someşul Mic, Someşul Cald (Perşoiu 2010; Perşoiu and Rădoane, in prep.); Pârtoţ (Feurdean et al. 2015); Aries (Perşoiu and Perşoiu, *in prep.*); Moldova (Chiriloaie et al. 2012); Siret (Rădoane et al. 2015); Putna (Necea et al. 2013); Teleorman (Howard et al. 2004; Macklin et al. 2010); lower Danube (Benecke et al. 2013)

Along the medium and lower courses of Someşul Mic and Arieş, the absolute ages of the 15–20 m high fluvial terrace, and of the floodplain sediments, do suggest that the two valley bottoms where (Jucu, Fundătura) formed around 30,000 years ago. This phase of intensive incision was followed, during the next ca. 20,000 years, by a dominant vertical aggradation process, the result being ca. 5 m thick layer of boulders and cobbles in sandy matrix. The Holocene history of the two floodplains is restricted to narrow channels and relatively isolated palaeochannels, generally subordinated, morphological, and sedimentological, to the previous, periglacial, morphologies, and sedimentary structures. Generally, the in-channel sediments are coarse, dominated by cobbles and pebbles, with isolated sandy lens, while the finer sediments, as clay, sandy-clay or silts reflect channel fills and overbank deposits.

However, this image is complicated by local conditions. For example, along Someşul Mic River where identified two areas where the old sediments were removed through an intense lateral channel activity. These exceptions are related to the diapiric alignments intersecting Someşul Mic River and its floodplain, responsible for an increased channel sensibility to lateral avulsion and meandering.

The upper reach of Someşul Cald River, located in the mountainous area, has a relatively well-developed floodplain, also dominated by coarse gravel sediments and frequent peatbogs, Holocene in age. The data available in this area suggest that the floodplains here where also formed in periglacial conditions, at least Younger Dryas in age.

Pârtot Valley, a small tributary of Someşul Mic River in the hilly area do show a complete different image. Here, the valley bottom was formed before 50,000 years ago, and the vertical aggradation process dominated thereafter. A massive layer of sand was deposited in periglacial conditions, and was replaced by clays starting with Bolling Allerod Interstadial, with a dramatic increase of sedimentation rate

during Late Holocene, most probably related to the local history of the lake developed in the floodplain perimeter (Feurdean et al. 2015).

Further to the west, the Holocene history of Someş/Szamos, Criş/Körös, and Mureş/Maros alluvial plains reflect the general narrowing of channels, a slight incision in the previous alluvial surface (the upper alluvial plain, Posea 1997) and frequent channel avulsions, which completely changed the drainage patterns in the areas. The sediments are dominantly fine, and reflect channel-fill and overbank deposition mainly. However, along the main rivers, for example, along Someş River, the in-channel sediments can be coarse (cobbles, pebbles, and sands), with a general downstream decrease. Therefore, the relation between different alluvial architectures and textures seems to be more complex, comparative with the general assumption that the coarser layer was formed in periglacial conditions, and was covered by the finer one during (Late) Holocene.

The Holocene history of the floodplains along Siret and Moldova Rivers was not similar, as the two rivers had different patterns, at least in terms of spatial behavior (Chiriloaei et al. 2012; Rădoane et al. 2015).

Moldova River is a coarse gravel braided channel, with the main source of sediments in the mountainous area and from the tributaries. Its floodplain is 3–6 m wide and the thickness of sediments along it has between 4 and 18 m. The massive character of the coarse alluvial sediments overlying the fossil trunks suggests continuous in-channel vertical aggradation (i.e., a braided stream environment) during the previous three millennia and a lack of significant channel shifting during flood events. In the recent decades, the active belt has narrowed with ca. 79 % (<1.2 km wide 100 years before), while the channel has incised, maintaining, however, its alluvial character.

In the case Siret river, the floodplain development and channel evolution can be divided into two main phases: (i) a braided channel phase dated at ~20,000 years, when the River Siret transported large amounts of coarse material (e.g., coarse gravel), which comprises the lower floodplain terrace deposits; and (ii) a sinuous and meandering phase, when bed material of decreasing grain size accumulated in the form of gravel lobes (in meander chute-bars) overlain by overbank sediments deposited by floods (Fig. 20.8b).

The lateral accretion deposits, which consist primarily of gravel, were not deposited as a single alluvial sheet. Moreover, they are shaped as a set of gravel lobes that developed upstream, as suggested in Fig. 20.8b, thus indicating the lateral accumulation of bed material in point bars. It was estimated that the river required 700–1000 years to migrate from one side of the floodplain to the other, and to remove the alluvial material (mostly gravel) from the concave banks and deposit it in the convex banks (commonly in scroll bar lobes) until the river reached the opposite side of the floodplain, and another millennium to return to the prior position. This relatively simple pattern of floodplain material processing is favored by the semiconfined style of the Siret River floodplain (35–40 %). The generation of palaeomeanders located below the surface of the terrace 5–7 m (Fig. 20.8a) was shaped by a streamflow discharge that is 1.5 times the current bankfull discharge, and most likely occurred ca. 5000 years BP (‘the last one coincides with the

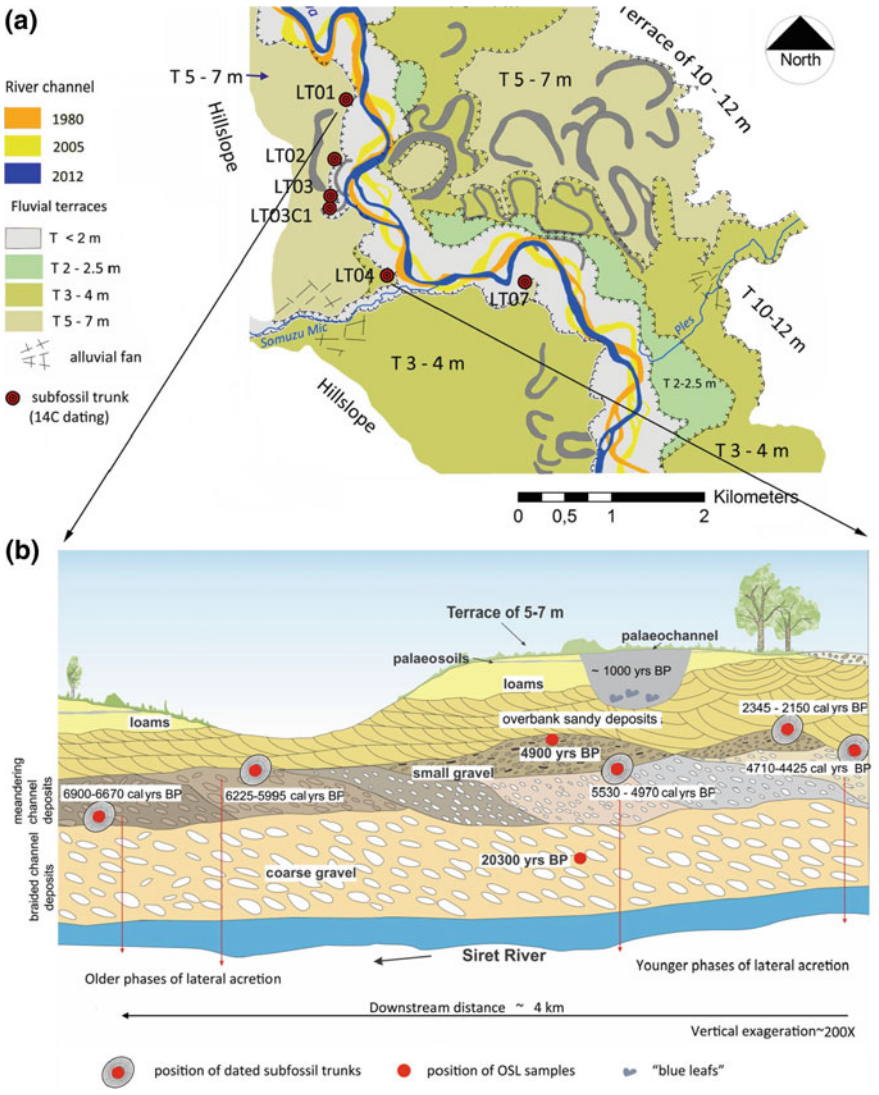

Fig. 20.8 Floodplain of Siret River downstream from Suceava confluence: **a** Geomorphological sketch of subfossil trunk sampling sites, paleochannel traces and floodplain terraces; **b** Cross section through coarse channel deposits in a Holocene fluvial terrace (modified after Rădoane et al. 2015)

abandonment of many palaeochannels at the transition from Atlantic to Subboreal', cf. Starkel et al. 2012). The next generation of meanders was shaped by an average stream flow discharge that is 1.2 times the present bankfull discharge, occurred during the strong fluvial activity of the Medieval Period (ca.1000–900 years BP)

('Last distinct phase of fluvial activity connected both with cooling and with increased human activity started from 1000 cal YBP', cf. Starkel et al. 2012).

Along the upper reaches of Şuşiţa, Putna, Milcov, and Zăbala Rivers, draining the Subcarpathian nappes and Focşani Basin, were identified three distinct fluvial terraces and the present day floodplain (T 9–11 m; T 5 m; T 2 m and T 1 m) as formed during the Holocene. The spatial distribution of the lower terraces, paired versus unpaired, large-scale development versus restricted appearance along the rivers are interpreted as reflections of spatial migration in fluvial incision, due to migration of uplift center from the orogen (Subcapathian nappes) through the foredeep basin (Focşani Basin) (Necea et al. 2013).

The two study sites located in the south, in the perimeter of the Romanian Plain highlight different scenarios on morphological and sedimentological Holocene fluvial relicts.

The young ages of sediments in the lower floodplain of Teleorman River, ca. 4000 years old, together with the ages of the next two fluvial terraces, which goes back from ca. 36,800 years BP to Younger Dryas Stadial, do support the idea that the Holocene history of Teleorman River (at least in the study area) is reduced to the lower floodplain, drained by a very dynamic river, capable to remove the Early–Mid Holocene morphologies and sedimentary structures (Howard et al. 2004).

On the other hand, the sediments investigated in the floodplain of lower Danube near Giurgiu do suggest that the floodplain predated Late Pleniglacial. Vertical aggradation, with coarse gravels (at least between 32,000 and 15,000 years BP) and finer sediments (starting with Bolling–Allerod Interstadial), was the dominant process in periglacial conditions, and apparently maintained during the first millennia in Early Holocene. After ca. 9500 years ago, when the sea level of Black Sea dramatically increased, due to connection with the Mediterranean Sea (Lericolais et al. 2010), the sediments became very fine (clays), deposited mainly in limnic or partly drained floodplain conditions (Benecke et al. 2013).

All these findings disproves some of generally accepted assumptions on floodplain age, sedimentological structure, morphology, and evolution along Romanian rivers (Introduction), highlighting the local diversity in fluvial response at the same climatic and environmental stimulus.

Conclusion

Fluvial processes and mechanisms

The Late Glacial–Holocene transition, when the periglacial conditions where replaced by the temperate ones, is reflected in fluvial records by large-scale channel metamorphosis from predominantly braided/large-scale meanders to small-scale meanders, and replacement of the dominant vertical aggradation process by channel vertical incision. These findings are in good agreement with the ones found elsewhere in Europe, in the previous periglacial areas and along the channel reaches located at mid-altitudes.

However, the fluvial reaction pattern is far from a uniform one if considered the mechanisms of changes (e.g., the existence of a transitory phase when the channel has changed from braided to meandering one), and also in space and time, both along the same river or between two different rivers. There are evidences that the fluvial changes occurred after the onset of the Holocene, most probably after the large-scale migration of deciduous species from the west. Local controls are also responsible for a series of particularities in the fluvial behavior at this particular moment.

Thereafter, the rivers show a higher sensitivity to second-order climatic variations (including short abrupt climatic changes: $10–10^2$ years) and to local conditions (e.g., local tectonics), if compared with the one during the previous periglacial period.

The more frequent data from Late Holocene do illustrate a good correlation between the fluvial processes along the investigated rivers and their floodplains/low alluvial plains, and the succession of warm/dry and cold/wet periods: meandering, soil processes during warm phases versus avulsions, and channel abandonment increased frequency of floods during the wet ones. Also, they point to an increase of fluvial processes during this time, comparative with Early–Mid Holocene, when the climate generally became colder and wetter and the vegetation became more open along the rivers. The human impact during this time plays a secondary role, becoming more important only during the last centuries.

Fluvial sedimentological and morphological features

The floodplains and the low alluvial plains, interpreted previously mainly as Holocene morphologies and sedimentary units, have, in fact, a more complex history, in terms of genesis, ages, and evolution.

In the perimeter of the Western Romanian Plain, the fluvial history goes back at least 45,000 years (Chap. 19, this volume). Additional to the generalized channel adjustments as response to major climatic changes (i.e., glacial–interglacial), local tectonic conditions seems to be the main cause for spatial readjustments of flows, including during the Holocene.

Along the mid and low reaches of the investigated rivers, the valley bottoms where formed during Middle Pleniglacial, Late Pleniglacial (e.g., Pârtoţ, Someşul Mic, Arieş, Siret), or even during the Holocene (e.g., Teleorman). Indeed, the coarser sediments from the floodplain perimeters where deposited mainly in periglacial conditions. However, coarse in-channel materials were deposited also during the Holocene (in the present day too), and are in complex facies association with the previous ones and with finer alluvium (in-channel sediments, palaeochannel fills, overbank deposits) superimposed on them.

The information from mountain areas highlight too the different fluvial reaction to similar stimulus, caused mainly by the local conditions of evolution. This is exemplified by the upper reach of Somesul Cald River, evolving in tectonically stable settings, where the floodplain age goes back to at least Late Glacial, and the upper Putna River and the rivers from the vicinity, highly affected by tectonic uplifts, where the Holocene fluvial history is reflected in three strath-terraces and a very recent floodplain.

Acknowledgments The research was supported by two grants of the Romanian Ministry of Education (UEFISCDI), project number PN-II-RUPD-2012-3-0547 and project number PN-II-ID-PCE-2011-3-0057. We are grateful to Delia Robu for her help in drawing the figures.

References

Benecke N, Hansen S, Nowacki D, Reingruber A, Ritchie K, Wunderlich J (2013) Pietrele in the lower danube region: integrating archaeological, faunal and environmental investigations. Documenta Praehistorica, p 175–193

Chiriloaei F, Rădoane M, Perşoiu I, Popa I (2012) Late Holocene history of the Moldova River Valley. Romania, Catena 93:64–77

Erkens G, Hoffmann T, Gerlach R, Klostermann J (2011) Complex fluvial response to Late glacial and Holocene allogenic forcing in the Lower Rhine Valley (Germany). Quat Sci Rev 30: 611–627

Feurdean A, Parr CL, Tanţău I, Fărcaş S, Marinova E, Perşoiu I (2013) Biodiversity variability across elevations in the Carpathians: parallel change with landscape openness and land use. Holocene 23(6):869–881

Feurdean A, Marinova E, Nielsen AB, Liakka J, Veres D, Hutchinson SM, Braun M, Timar-Gabo A, Astalos C, Mosburgger V, Hickler T (2015) Origin of the forest steppe and exceptional grassland diversity in Transylvania (central-eastern Europe). J Biogeogr 42(5):951–962

Ficheux R (1996) Les monts Apuseni (Bihor)—Vallées et aplanissements. Romanian Academy Press, Cluj Napoca

Florescu G (2015) Cercetari paleolimnologice in nordul Carpatilor Orientali. Unpublished PhD thesis. Ştefan cel Mare University, Suceava, Romania

Friedrich M, Remmele S, Kromer B, Hofmann J, Spurk M, Kaiser KF, Orcel C, Küppers M (2004) The 12,460-year hohenheim oak and pine tree-ring chronology from Central Europe—a unique annual record for radiocarbon calibration and paleoenvironment reconstructions. Radiocarbon 46(3):1111–1122

Geografia României, III, Carpathians and Transylvanian Depression (in Romanian) (1987) Romanian Academy Press, Bucureşti

Glodariu I (1997) Societatea umană din teritoriul intracarpatic în epoca veche, din Istoria României.Transilvania, Vol. I, Cluj Napoca, p 63–114 (Ed.)

Howard AJ, Macklin MG, Bailey DW, Mills S, Andreescu R (2004) Late-glacial and Holocene river development in the Teleorman Valley on the southern Romanian Plain. J Quat Sci 19 (3):271–280

Janssens MM, Kasse C, Bohncke SJP, Greaves H, Cohen KM, Wallinga J, Hoek WZ (2012) Climate-driven fluvial development and valley abandonment at the last glacial-interglacial transition (Oude IJssel-Rhine, Germany), Neth J Geosci—Geologie en Mijnbouw 91(1/2): 37–62

Knox JC (1983) Responses of river system. In: Wright HE Jr (ed) Late quaternary environments of United States, The Holocene, University of Minnesota Press, Minneapolis, p 26–41

Kasse C, Bohncke SJP, Vandenberghe J, Gábris Gy (2010). Fluvial style changes during the last glacial–interglacial transition in the middle Tisza valley (Hungary). In: Proceedings of the Geologists' Association 121, p 180–194

Kiss T, Sümeghy B, Gy Sipos (2014) Late quaternary paleodrainage reconstruction of the Maros River alluvial fan. Geomorphology 204:49–60

Lericolais G, Giuchard F, Morigi C, Minereau A, Popescu I, Radan S (2010) A post Younger Dryas Black Sea regression identified from sequence stratigraphy correlated to core analysis and dating. Quat Int 255:199–209

Macklin MG, Johnstone E, Lewin J (2005) Pervasive and long-term forcing of Holocene river instability and flooding in Great Britain by centennial-scale climate change, The Holocene 15 (7):937–943

Macklin MG, Benito G, Gregory KJ, Johnstone E, Lewin J, Michczynska Soja R, Starkel L, Thorndycraft VR (2006) Past hydrological events reflected in the Holocene fluvial record of Europe. Catena 66:145–154

Macklin MG, Bailey DW, Howard AJ, Mills S, Robinson RAJ, Mirea P, Thissen L (2010) River dynamics and the neolithic of the lower Danube catchment. In: Proceedings of the international conference on the lower Danube in the prehistory: landscape changes and human-environment interactions, Alexandria, 3–5 Nov 2010

Nádor A, Thamó-Bozsó E, Magyari Á, Babinszki E (2007) Fluvial responses to tectonics and climate change during the Late Weichselian in the eastern part of the Pannonian Basin (Hungary). Sediment Geol 202:174–192

Nádor A, Sinha R, Magyari A, Tandon SK, Zs Medzihradszky, Babinszki E, Thamó-Bozsó E, Unger Z, Singh A (2011) Late Quaternary (Weichselian) alluvial history and neotectonic control on fluvial landscape development in the southern Körös plain, Hungary. Palaeogeogr Palaeoclimatol Palaeoecol 299:1–14

Necea D, Fielitz W, Kadereit A, Andriessen PAM, Dinu C (2013) Middle Pleistocene to Holocene fluvial terrace development and uplift-driven valley incision in the SE Carpathians, Romania. Tectonophysics 602:332–354

Notebaert B, Verstraeten G (2010) Sensitivity of West and Central European river systems to environmental changes during the Holocene: a review. Earth-Sci Rev 103:163–182

Perşoiu I (2010) Recostruction of Holocene geomorphological evolution of Someşu Mic Valley (in Romanian). Unpublished PhD thesis A. I. Cuza University, Iasi, Romania

Perşoiu I, Rădoane M (2011) Spatial and temporal controls on historical channel responses—study of an atypical case: Someşu Mic River, Romania. Earth Surf Land Process 36:1391–1409

Perşoiu I, Perşoiu A (*in prep*). Variable fluvial response to Late quaternary climate changes in NW Romania

Perşoiu I, Rădoane M (*in prep*). Late quaternary evolution of Someşul Mic River, Romania

Posea G, Popescu N, Ielenicz M (1974) Relief of Romania (in Romanian). Scientific Press, Bucureşti

Posea G (1997) The western Romanian plain (in Romanian). Editura Fundaţiei România de Mâine, Bucureşti

Posea G (2002) Geomorphology of Romania (in Romanian). Editura Fundaţiei România de Mâine, Bucureşti

Pop GP (2001) Transylvanian Depression (in Romanian), "Presa Universitară Clujeană" Press, Cluj Napoca

Ramsey CB (2007) Radiocarbon Calibration and Analysis of Stratigraphy: the OxCal Program 4.0.5. http://c14.arch.ox.ac.uk/embed.php?File=oxcal.html2007

Rădoane M, Nechita C, Chiriloaei F, Rădoane N, Popa I, Roibu C, Robu D (2015) Late Holocene fluvial activities and relations with subfossil trunks: case study Moldova and Siret Rivers, Romania. Geomorphology 239:142–159

Reimer PJ, Baillie MGL, Bard E, Bayliss A, Beck JW, Blackwell PG, Bronk Ramsey C, Buck CE, Burr GS, Edwards RL, Friedrich M, Grootes PM, Guilderson TP, Hajdas I, Heaton TJ, Hogg AG, Hughen KA, Kaiser KF, Kromer B, McCormac FG, Manning SW, Reimer RW, Richards DA, Southon JR, Talamo S, Turney CSM, van der Plicht J, Weyhenmeyer CE (2009) IntCal09 and Marine09 radiocarbon age calibration curves, 0–50,000 years cal BP. Radiocarbon 51(4):1111–1150

Robu D, Niga B, Perşoiu I (2015) Investigation of fluvial landforms in the north-eastern Pannonian Basin, using cartographic materials from the XIX–XXI Centuries. In: EGU General Assembly 2015, Geophysical Research Abstracts, 17, EGU2015-13448

Starkel L (1983) The reflection of hydrologic changes in the fluvial environment of the temperate zone during the last 15,000 years. In: Gregory KJ (ed) Background to paleohydrology. Wiley, New York, pp 213–235

Starkel L (2002a) Younger Dryas-Preboreal transition documented in the fluvial environment of Polish rivers. Glob Planet Change 35:157–167

Starkel L (2002b) Change in the frequency of extreme events as the indicator of climatic change in the Holocene (in fluvial systems). Quat Int 91:25–32

Starkel L, Thornes JB (1991) Temperate palaeohydrology—fluvial processes in the temperate zones during the last 15,000 years, Wiley, NY

Starkel L, Soja R, Michczynska D (2006) Past hydrological events reflected in Holocene history of Polish rivers. Catena 66:24–33

Starkel L (2007) The diversity of fluvial system response to the Holocene hydrological changes using Vistula River catchment as an example, Annales societatis geologorum poloniae, 77:193–205

Starkel L, Michczyńska D, Krąpiec M, Margielewski W, Nalepka D, Pazdur A (2012) Progress in the Holocene chrono-climatostratigraphy of Polish territory. Geochronometria 40(1):1–21 (Versita Central European Science Journals)

Timár G, Sümegi P, Horváth F (2005) Late quaternary dynamics of the Tisza River: evidence of climatic and tectonic controls. Tectonophysics 410:97–110

Thorndycraft VR, Benito G (2006) The Holocene fluvial chronology of Spain: evidence from a newly compiled radiocarbon database. Quaternary Sci Rev 25:223–234

Chapter 21
Styles of Channel Adjustments in the Last 150 Years

Maria Rădoane, Ioana Perșoiu, Francisca Chiriloaei, Ionuț Cristea and Delia Robu

Abstract By analysis of representative case studies employing a unitary method, we determined a general trend of active channel narrowing in Romanian rivers (ranging from 30 to 76 % between 1860 and 2010), very similar to other European rivers. The narrowing tendency was not a linear process throughout the past century; around 1980 the greatest variability in the active channel width was documented, particularly in terms of narrowing, whereas post-2000 a tendency toward recovery of the active channel width became noticeable, as both the sinuosity and braiding indices display the same behavior. In the vertical plan, the rivers occurring in a quasi-natural state are dominated by channel bed incision throughout their entire length, increasing in downstream direction. Within the upper basin where the main channel receives numerous tributaries originating in the mountain sector which deliver coarse sediment to the main river, aggradation may occur sporadically. Higher incision rates were documented in the lower course of rivers. It was determined that incision was prevalent among the processes acting on the channel bed sections under investigation (representing 62 % of the altered area and changing bed level between −0.25 and −2.70 m), with aggradation accounting for the remaining 38 % (causing changes ranging from +0.15 to +1.25 m). The magnitude of the processes (incision or aggradation) for sections with an MQI <0.3 was four times higher than for sections with a moderate or good MQI (>0.3). The variable that exhibited the strongest response to climate conditions was water

M. Rădoane (✉) · I. Perșoiu · F. Chiriloaei · I. Cristea · D. Robu
Stefan cel Mare University, Universității 13, 720229 Suceava, Romania
e-mail: radoane@usm.ro; mariaradoane@gmail.com

I. Perșoiu
e-mail: ioanapersoiu@gmail.com

F. Chiriloaei
e-mail: francisca@usm.ro

I. Cristea
e-mail: icristea@atlas.usv.ro

D. Robu
e-mail: deliarobu@gmail.com

M. Rădoane and A. Vespremeanu-Stroe (eds.), *Landform Dynamics and Evolution in Romania*, Springer Geography,
DOI 10.1007/978-3-319-32589-7_21

discharge (Qw), whereas the sediment load (Qs) was highly responsive to both climatic signals and anthropogenic factors. The sediment load has been instrumental in the adjustments of the channel beds by maintaining a balance between the two controlling factors, nature and man.

Keywords Channel planform adjustments · Channel bed level · Narrowing · Incision · Climate and human controls

Introduction

Topics such as the analysis of historical behavior of river channels throughout Romania and the assessment of their degree of alteration were solely tackled in a limited number of case studies (Diaconu et al. 1962; Hâncu 1976; Panin 1976; Bondar et al. 1980; Bondar 2001; Ichim et al. 1989; Ichim and Rădoane 1990; Pascu 1999; Amăriucăi 2000; Rădoane and Rădoane 2005; Rădoane et al. 2003, 2008a, b, c; Feier and Rădoane 2007). However, in the recent years, studies on the degree and styles of changes in river channels during the past 100–150 years have become more common (Dumitriu 2007; Ioana-Toroimac et al. 2010; Perşoiu 2010; Rădoane et al. 2010, 2013a; Cristea 2011; Floroiu 2011; Perşoiu and Rădoane 2011; Zaharia et al. 2011; Chiriloaei 2012; Chiriloaei et al. 2012; Armaş et al. 2012; Sipos 2012), thus providing sufficient data regarding these phenomena.

The selection of the 150 years threshold for evaluating river change at the reach scale (according to the definition by Brierley and Fryirs 2005) was motivated by the data sources required for assessing these changes (namely, instrumental records, historical documents, maps, aerial photos, or, more seldom, sediment archives, dating, etc.). In Romania, the earliest cartographic sources employed to rigorously analyze river channel planform change date back to as late as 1764 (for the Transylvanian area) and 1894–1902 (for the rest of the territory), whereas the instrumental records necessary for the assessment of vertical changes do not go beyond the 1950s (Rădoane et al. 2013a, b).

In Europe, the assessment period for river channel planform change based solely on cartographic data can range up to 200–250 years (Surian et al. 2009; Hohensinner et al. 2014). Thus, in the vast majority of such analyses the authors considered two main causes for channel change: climate changes related to the end of the Little Ice Age (LIA) and global warming, on one hand, and anthropogenic impacts, on the other. In several European rivers a general tendency toward incision was reported during the past 150 years, ensued by channel narrowing and lateral stability (e.g. Liébault and Piégay 2002; Rinaldi 2003; Surian and Rinaldi 2003; Wyżga 2008). Subsequent to analyzing the alleged anthropogenic causes for these changes, a number of authors (Gurnell 1997; Winterbottom 2000; Liébault and Piégay 2001, 2002; Rinaldi 2003; Surian and Cisotto 2007; Wyżga 2008; Zawiejska and Wyżga 2010; Škarpich et al. 2013) showed that mutations in the type and distribution of riparian vegetation, land use/land cover changes, gravel

mining, and local or large-scale hydraulic works altered the water discharge and sediment loads, as well as the local power of rivers, thus resulting in changes in river morphology and behavior.

Romanian rivers were subjected to significant changes similar to those reported throughout Europe (Petts et al. 1989; Rinaldi 2003; Wyżga 2008): *Disturbances within the drainage basins*, particularly pre-1950, when massive deforestation occurred in the Eastern-Carpathian river basins (as is the case with Putna River in Vrancea, whereby the erosion rate was as high as 10,000–30,000 t/km^2/year, compared to the national average value of 206 t/km^2/year). Post-1950, steps were taken to reduce soil erosion by means of large-scale reforestation and erosion control works, such that after 1980 the amount of sediments reaching the channel network decreased. *Gravel mining* peaked in Romania during the communist era, as large-scale construction sites were opened (1970–1989). Albeit post-1989 gravel mining diminished considerably, it increased again with the economical relaunch of the 2000s. *Dams* (of which 260 were built on the main Romanian rivers) control over 13 billion cubic meters of water (amounting to one-third of the total discharge through the stream network), and in an average period of 15 years, the reservoirs have had depositions about 200 million m^3 of sediments. *Riverbank protection structures and levees* were built throughout the twentieth century, mainly along rivers crossing urban areas. From 1950 to 1990, in the broader context of hydropower construction works, 771 km of levees were erected on the largest Romanian rivers, whereas approximately 16,000 km (out of a total of 76,000 km) of river channels were rectified, especially following the catastrophic 1970–1975 flood events. The sum of these interventions on the geomorphological fluvial systems has resulted in significant changes in alluvium delivery rates, in riverbed deposits variability, as well as in the regimen of the present dynamic of channels. It is therefore natural to expect that the response of river channels be similar to those reported in other European regions.

Our approach on analyzing the evolution of river channels during the past 60–150 years is structured as follows: (1) reconstructing channel planform configuration changes; (2) reconstructing channel bed level changes; (3) revealing the correlations between channel adjustments and various anthropogenic interventions, as well as between the former and present climate variability, respectively; (4) a comparative approach to the evolution of Romanian river channels against channels from other European regions.

Reconstructing Fluvial Changes in Terms of Channel Planform Adjustments

Six reaches were selected for carrying out measurements and investigations in order to determine their channel planform behavior (Fig. 21.1; Table 21.1) according to a unitary methodological protocol (Rădoane et al. 2013a). These reaches cover the entire typological range of channels, whereas the study period varies between

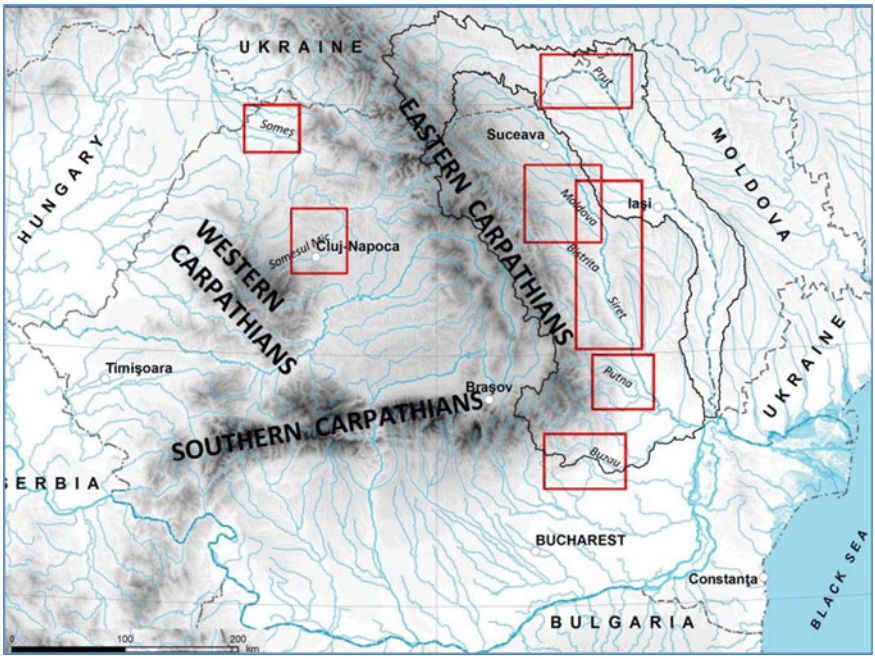

Fig. 21.1 Location map of the investigated rivers; *red lines* mark the study sites

145 years (for NW Romania) and 100 years (for ESE Romania). The degree of anthropogenic intervention in controlling fluvial processes in our study area was evaluated based on the Morphological Quality Index (MQI) (cf. Rinaldi et al. 2013). This index assesses (based on expert judgement) the extent of the river length characterized by a high degree of artificiality, and, conversely, the extent to which it remains in nearly natural conditions. The resulting scores are included in Table 21.1 and show the degrees (ranging from 0—natural to 1—high modified) of human intervention for river reaches included in the study. The approximate year when the degree of artificiality of channels increased significantly is indicated in brackets, under the MQI values (corresponding to dam construction—Someșul Mic, Siret, Buzău, gravel mining—Moldova, Siret, Buzău, extensive reforestation—Putna).

The results regarding the behavior of river channels were summarized using three morphological parameters (Fig. 21.2), namely: the active channel width (Abw, m), the sinuosity index (SI), and the braiding index (BI). These parameters are relatively easily determined and are highly sensitive to alterations in the streamflow discharge and sediment load regime.

The active channel width (Fig. 21.2) (also known as the low floodplain where the river migrates unimpeded) is in direct relation to the type and size of the river. The morphometric parameter may range within a certain variation margin. Several researchers established a direct relationship between the width of the active belt and the floodplain width as follows: the floodplain width is approximately tenfold the

Table 21.1 General data on the Romanian rivers (for the reaches under investigation) regarding their present and historical evolution

River	Drainage basin area, A (km^2)	River length, L (km)	Channel types	Reach length, Lr (km)	Mean annual discharge, Q (m^3/s)	Suspended sediment load, mean annual, Qs (g/s)	Bed material, D50 (mm)	Morphological Quality Index (MQI)	Years of historic maps and of aerial images
Someş	15,155	345	Meandering	70	116.2	135.6	4.9… 1.28	0.45 (1980)	1860, 1890, 1977, 2008
Someşu Mic	3595	176.8[a]	42 underreachs, sinuous-meandering-anabranched)	105	22.5	9.5	16…1	0.74 (1977)	1860, 1884, 1956, 1970, 1977, 2005
Moldova	4316	213	9 underreachs (braiding to wandering)	110	35.1	43.2	36…16	0.45 (1970)	1910, 1960, 1980, 2005
Siret	44,591	690	Meandering–sinuous	158	76.9	62.1	11.2… 25.9	0.53 (1970)	1900, 1960, 1980, 2004
Prut	28,463	865	Meandering	97	78.0	55.1	15…7	0.35 (1980)	1915, 1980,2004
Putna	2518	160.3	6 sunderreachs (sinuous-halfconfinned, wandering, braiding, meandering)	136	16.1	91.8	8.0… 0.08	0.24 (1960)	1900, 1955, 1968,1980, 2004
Buzău	5238	303.4	Wandering	35	27.7	63.7	55.4… 8.2	0.55	1900, 1960, 1980, 2004

Additional explanations are provided in the text

[a]Length calculated from Someşu Cald headwaters

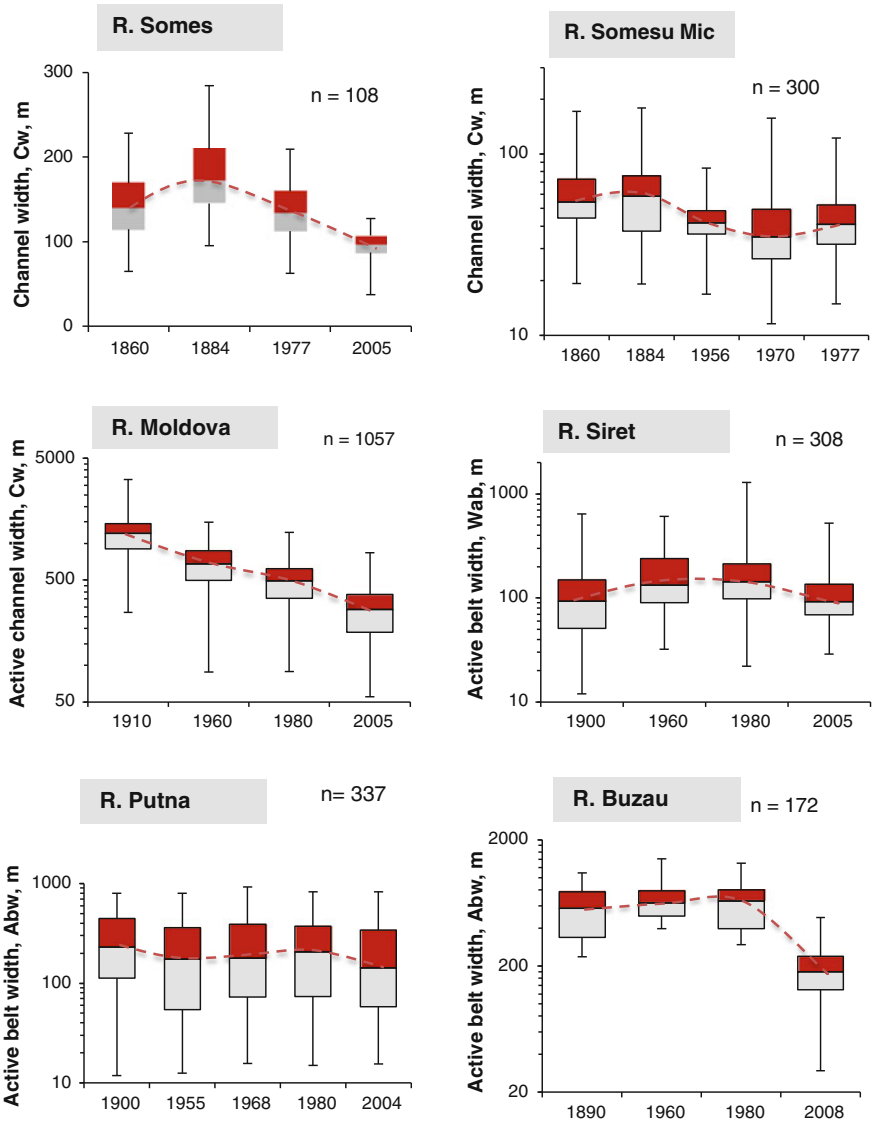

Fig. 21.2 Active channel width changes that affected the studied river reaches during the last 100–150 years; *boxes* represent inner and outer quartiles; *vertical lines* represent inner and outer tenths; *n*—number of width measurements

width of the active belt (Bridge and Leeder 1979) and even up to 20 times the width of the active belt (Bridge 2003). Whereas the trends of active channel width variability are not uniform in the six rivers under investigation, a general tendency is easily discernible: *a decrease in the active channel width during the last 100–150 years.*

The degree of active channel narrowing is variable; the highest value was documented for the braided channel of Moldova River (on average 76 % along the 110 km—long investigated reach), followed by the wandering channel of Buzău River (73 %). Whereas the two rivers are comparable in terms of their degree of artificiality, Buzău further underwent anthropogenic interventions due to dam construction (i.e., Cândești dam, responsible for the leap in channel narrowing documented post-1980). Someșul Mic River, characterized by a predominantly anabranching channel (also comprising bedrock reaches and mixed reaches) has a narrowing rate below 30 % (with the highest values recorded from 1884 to 1956). A similar value is typical for the meandering–sinuous channel of Siret River.

If we further take into account Someș River, whereby the channel is typically meandering with a moderate degree of artificiality and the narrowing rate amounts to 45 %, it becomes apparent that the sinuous–meandering type of channel shows significantly higher "resistance" to alterations induced by control factors compared to the braided–wandering type. Meandering channels respond to decreasing streamflow discharge and sediment load values by creating a new generation of meanders with smaller radii within the previous generation (documented by Kiss and Blanka 2012 for Hernád River, tributary of the Tisza), without substantial changes in the active channel width.

Putna River is known, along with smaller rivers from the Carpathian Curvature area, for the high sediment transport rates occurring in the piedmont geomorphological domain (Rădoane et al. 2008a; Cristea 2011); the average narrowing amounts to 39 % throughout the investigated reach, whereby various types of channel alternate as follows from upstream to downstream: from a rectilinear semi-confined type of channel to unitary–sinuous, wandering–braided, and eventually meandering when Putna River reaches Siret lowlands.

An additional observation concerning the behavior or rivers under investigation during the aforementioned time frame regards the nonuniformity of trends. Regardless of the channel type and the physical environment of the river, *the 1980s decade stands out in terms of the highest rate of channel narrowing*. Following this period, a tendency toward *active channel recovery* of its previous state (prior to 1960) was documented. The recovery signal was strong enough to manifest itself in all selected rivers (albeit to various extents), regardless of the degree of human intervention. As will be shown in the following section on the dynamics of channel bed levels, the 1980s decade was the most propitious for river channel narrowing and incision.

The ***sinuosity index*** (SI) and ***the braiding index*** (BI) parameters are commonly employed to rank river channels according to their typology (cf. Leopold and Wolman 1957; Schumm 1985; Rinaldi et al. 2013), and their sensitivity to factors controlling the type of channel (particularly at the decadal and centennial scale).

The values of these parameters in the investigated river channels indicate no significant leaps, albeit a trend in channel adjustments over time is discernible. The diagrams in Fig. 21.3 include the results yielded by measurements in the shape of box plots. The average values of the sinuosity index show that none of the studied rivers can be fully ranked as meandering (i.e., SI > 1.5) (perhaps with the exception

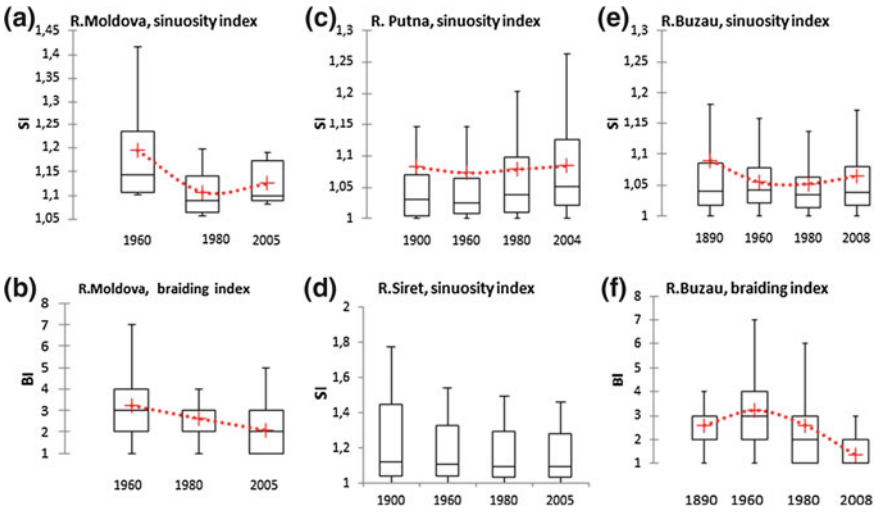

Fig. 21.3 Changes in the sinuosity and braiding indices occurring in various time frames during the past century on some Romanian rivers: Change of sinuosity index (**a**) and braiding index (**b**) of Moldova R between 1960 and 2005. **c** Evolution of sinuosity index of the Putna R between 1900 and 2004. **d** Evolution of sinuosity index of the Siret R between 1900 and 2005. Change of sinuosity index (**e**) and braiding index (**f**) of Buzau R between 1890 and 2008. The *red line* connects the average values of the two indices (Si and BI)

of short reaches pertaining to Siret River and Prut River, upstream Stânca-Costești Reservoir—Fig. 21.1). However, within the variation limits ranging from 1.0 to 1.5, these rivers showed a common tendency: *higher values around 1900 ensued by SI recovery toward 2005*. The sinuosity curve displays a negative flexure (near the 1 value) around 1980.

The sinuosity index competes with the braiding index which could only be determined for two rivers (Moldova and Buzău). Whereas an overall decrease in the degree of channel braiding was documented, a slight BI recovery occurred during the 1970s decade.

The change of the channel type due to active channel narrowing over a period of 100–150 years is not an isolated case for Romanian rivers. Similar behaviors were reported in rivers from various European regions whereby similar studies were conducted. By comparing results obtained for 15 Carpathian rivers (from Romania, Poland, and the Czech Republic) with those yielded for several Alpine rivers (from France and Italy) (Fig. 21.4) we determined that the degree of narrowing is greater in the case of the 38 investigated Alpine rivers, whereby the distribution of values is statistically far more uniform compared to the Carpathian lot. The latter have a considerably broader variation margin (ranging between 18 and 84 %), whereas the average is below the value obtained for Alpine rivers. The explanation can either rely on statistical arguments (i.e., the smaller sample size), or, more plausibly, at least in the case of Romanian rivers, on the delay of massive human intervention compared to Central and Western Europe, such that as late as the mid-twentieth

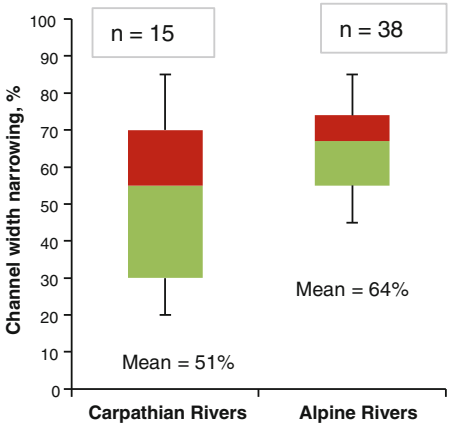

Fig. 21.4 Comparison of river channel narrowing (%) over last 100 year between Carpathian rivers and Alpine rivers. Created based on: Wyżga (1993), Marston et al. (1995), Rinaldi and Simon (1998), Wyżga (2001), Kondolf et al. (2002), Lach and Wyżga (2002), Rinaldi (2003), Surian and Rinaldi (2003), Surian et al. (2009), Zawiejska and Wyżga (2010), Ioana-Toroimac et al. (2010), Škarpich et al. (2013)

century the streamflow discharge and sediment loads in Romanian Carpathian rivers had not been significantly altered. Further discussion on this topic will ensue the analysis of channel bed incision and/or aggradation.

To conclude, based on the analysis of representative case studies employing a unitary method, we determined a general trend of active channel narrowing in Romanian rivers (ranging from 30 to 76 % between 1860 and 2010), similar to other European rivers but less intense. The narrowing tendency was not a linear process throughout the past century; around 1980 the greatest variability in the active channel width was documented, particularly in terms of narrowing, whereas post-2000 a tendency toward recovery of the active channel width became noticeable, as both the sinuosity and braiding indices display the same behavior. Considering that massive anthropogenic interventions on Romanian rivers occurred with a considerable delay as compared to rivers from other European regions, we firmly believe that the climate factored significantly into this behavior.

Channel Bed-Level Adjustments During the Past 50 Years

In order to analyze the vertical behavior of channel bed levels we selected 8 rivers pertaining to Siret drainage basin (with an area of 44,591 km^2) and Prut basin (an area of 28,463 km^2) (Fig. 21.5). The rivers were monitored in several cross sections of which 48 were selected for the analysis of channel bed adjustments. The sampled cross sections are representative for gravel-bed Carpathian rivers, whereas sand beds occur only in the lower courses of Siret, Buzău and Putna Rivers, as well as on

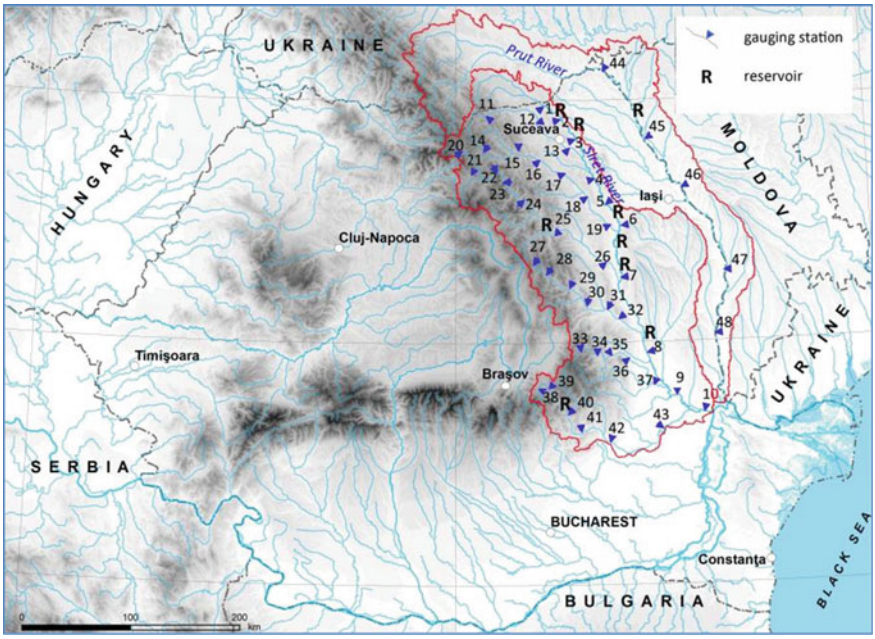

Fig. 21.5 Location of the 48 analyzed cross sections on the investigated rivers (Siret, Suceava, Moldova, Bistrița, Trotuș, Putna, Buzău and Prut)

Prut River downstream of Stânca-Costești reservoir.[1] The acquired database provided us with both an overview on the spatial variability of river channels vertical behavior, and on its temporal variability. The following two sections are focused on this analysis.

Spatial Trends of Channel Bed-Level Adjustments

The spatial trends in the behavior of channel beds from 1960 to 2010 are easier to discern by using graphical representations as depicted in Figs. 21.6, 21.7 and 21.8.

[1]The database comprised of measurements on the stream discharge (mean annual and annual maximum values), measurements of suspended sediment loads and minimum annual water stages in the warm season (April to September) and cold season (December to March), respectively. It was determined that of the two periods, the lowest values were recorded during the cold season. The annual minimum water levels were compared starting from the same reference plan. The minimum water level time series were available from 1960 to 2012 for 6 rivers out of 8 (with the exception of Buzău river, where a complete data series is available only for 10 years), whereas for the annual discharge and suspended sediment load we obtained complete data series from 1950 to 2010 for all 7 rivers included in the study.

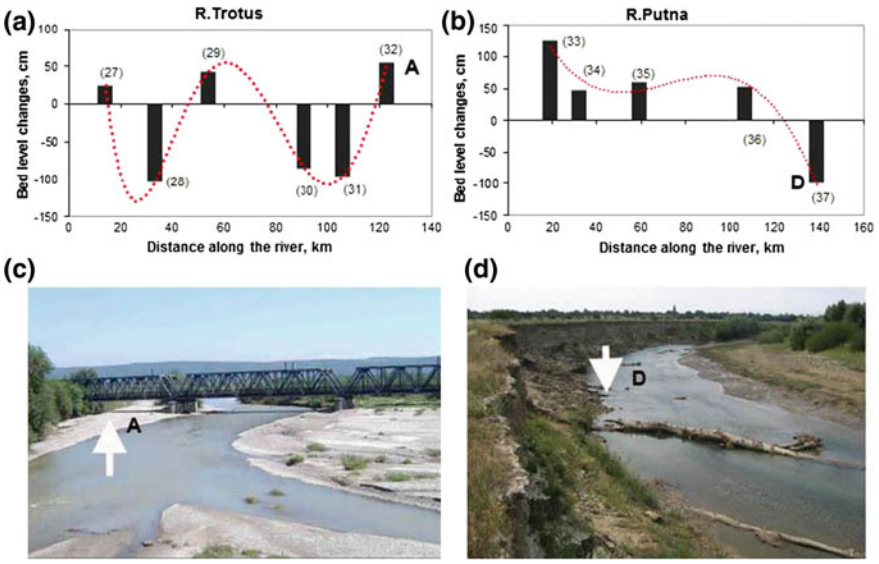

Fig. 21.6 Generalized trends of bed level changes along the Trotuș (**a**) and Putna Rivers (**b**). (*27*) … (*37*)—number of each cross section cf. with Fig. 21.5. The red line is an attempt to show a poly trend line: **c** Trotuș River 10 km upstream of the confluence with Siret River, where the railway bridge pillars were buried caused by aggradation of the bed (*photo* N. Rădoane). **d** Putna River in the lower reach where channel bed degradation is prevalent (*photo* I. Cristea). Other explanations in text

Each column shows the maximum absolute value of the bed level change (in cm) during the considered time period at gauging stations along the river (whereby the position is designated by the distance from the headwaters to the respective streamgage in km). The rivers were ranked into three main categories according to the degree of human intervention in order to have a measure of the anthropogenic factor in this dynamic.

River group A (**with a low artificiality**). This group includes Trotuș, Putna (Fig. 21.6) and Bistrița Rivers (the latter upstream of the Izvoru Muntelui Reservoir, L = 167 km), which have undergone the least amount of direct human intervention (whereas indirect interferences included mainly changes in the forest land cover within the drainage basins). These rivers are singular within the study area, as they have undergone processes of both aggradation (Fig. 21.6c, d) and degradation of the channel bed during the same time frame along the same river. In the absence of any direct or major human interventions, these rivers adjusted by means of aggradation–degradation in relation to a slightly positive trend of the stream discharge and sediment load along the river. This river is dominated by aggradation throughout all four Carpathian (no. 33) and Subcarpathian (34, 35, 36) reaches. The most prolific Romanian region in terms of sediment yield (along with the Buzau basin) (to see Chaps. 27 and 28) has been on an upward trend during the past 50 years. The increase in forested area in the Putna basin by over 7 % during

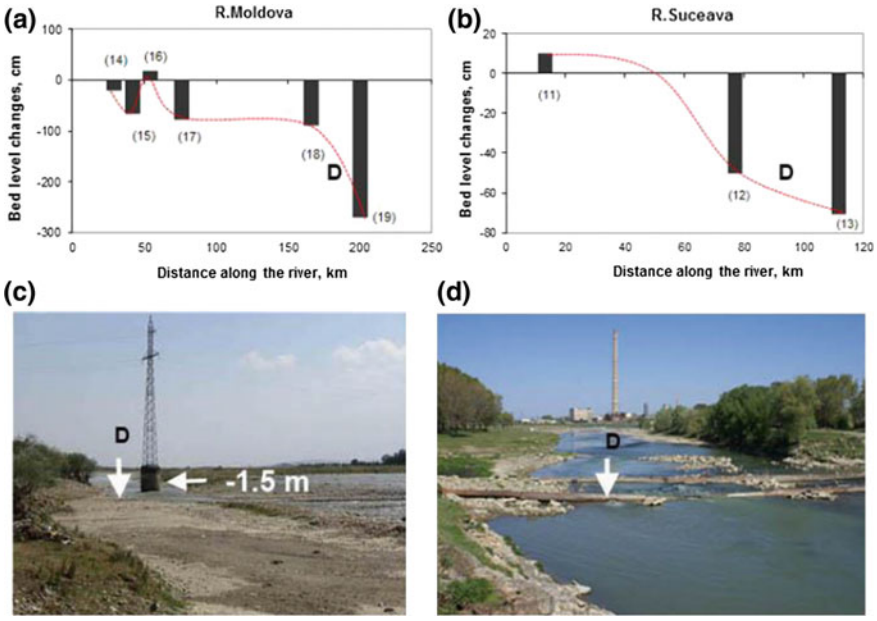

Fig. 21.7 Generalized trends of bed level changes along the Moldova (**a**) and Suceava Rivers (**b**). (*11*) … (*17*)—number of each cross section cf. with Fig. 21.5: **c** Moldova River 95 km upstream of the confluence with Siret River, incision of 1.5 m. **d** Suceava River in the lower reach where channel bed degradation exhumated the two pipes initially buried −1 m below the riverbed (*photos* N. Rădoane). Other explanations in text

the last century has not been able to significantly reduce the amount of sediment transferred from the hillslopes to the channel bed. The majority of this stock of sediment is then deposited in the outer Carpathian Piedmont area, such that toward the confluence with the Siret River the Putna acquires sufficient energy to have generated a 1-m-deep incision between 1960 and 2010.

River group B (**with a moderate artificiality**). Suceava and Moldova Rivers were included in this class due to the moderate direct interventions their channels have been subjected to, mainly by gravel mining in their mid- and lower courses. This group also includes Buzău River; however, the short data series available, comprising bed-level measurements over a period of just 10 years, does not allow for a comprehensive discussion in this regard. Rivers included in group B are defined by generalized incision of the bed, as the discharge and sediment load carried by the rivers slightly increased. Both gravel mining and the lowering of the base level of Siret River contributed to enhancing the state of degradation of the channel beds, whereby the highest values are reached at the junctions with Siret (Chaps. 13 and 19, cf. Fig. 21.5).

River group C (**with a high artificiality**). This class includes Bistrița (the last 125 km), Prut and Siret (Fig. 21.8) Rivers, which are defined by ample changes in terms of the water discharge and sediment load. Due to the number of consecutive

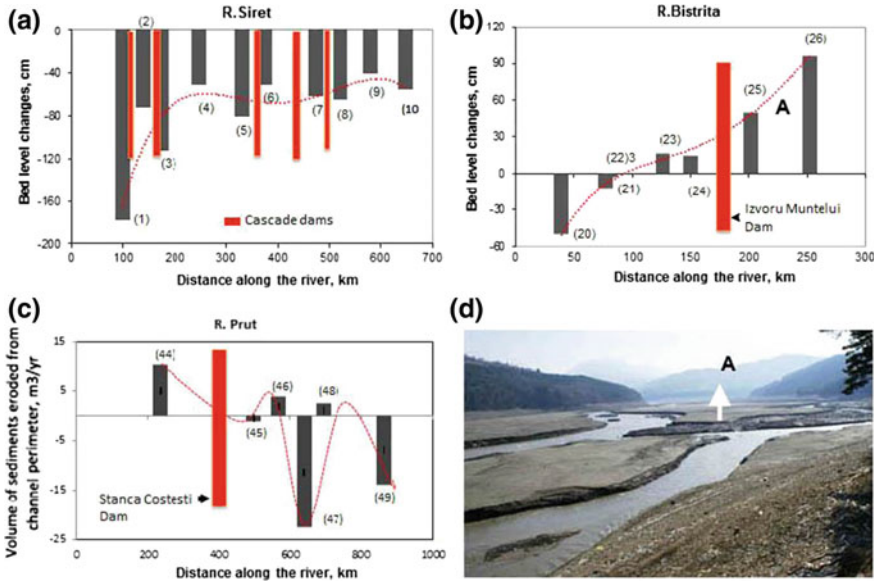

Fig. 21.8 Generalized trends of bed level changes along the Siret (**a**) Bistrița (**b**) and Prut (**c**) Rivers controlled by dams. (*1*) … (*48*)—number of each cross section cf. with Fig. 21.5. **d** Channel bed aggradation on Bistrița River upstream of Izvoru Muntelui Reservoir (*photo* N. Rădoane). Other explanations in text

dams built along Siret River, the sediment load was altered to a large extent (80 %), thus incision was generalized throughout its entire 600-km length. In a similar manner, the sediment load rate diminished by as much as 95 % on Prut River due to the presence of Stânca-Costești reservoir, thus resulting in downstream channel bed incision along 476 km. Downstream from the IzvoruMuntelui Reservoir, the river (L = 125 km) is completely transformed by the construction of a channel that receives the entire water discharge of the upstream river. The natural channel of the river receives just 9 % of the initial discharge. Consequently, aggradation is prevalent as a result of the state of underfitness of the channel to the new water discharge conditions. Therefore, in section no. 26 (Frunzeni), the channel bed level has risen by 96 cm between 1960 and 2010.

Finally, we may conclude that: (1) rivers occurring in a quasi-natural state are dominated by channel bed incision throughout their entire length, increasing in downstream direction; (2) within the upper basin where the main channel receives numerous tributaries originating in the mountain sector which deliver coarse sediment to the main river, aggradation may occur sporadically; (3) higher incision rates documented in the lower courses of rivers ranked in classes A and B are further boosted by gravel mining in these reaches, albeit we are unable to establish the extent of this influence; (4) dams are by far the cause for the amplest changes in channel bed levels.

Decadal Trends of Channel Bed Level Adjustments

Based on an important database on channel bed behavior in the last 50 years in eastern Romania, Rădoane et al. (2013a, b) identified some distinct trends. They concern two categories of considered rivers (in quasi-natural state vs. highly artificial channels) for that a decadal behavior of channel bed levels was determined. To capture as much of these changes as possible, we divided the Qw, Qs, and BL data series into 10-year subseries, and the linear regression trend was calculated for each of the subseries. The regression coefficient (indicating the direction and intensity of the relations between the three variables and time) was used as a synthetic index to extract the trends from the large amount of data available. We preferred this simple method for data series analysis because it is a simple tool for comparing the variations in the data series throughout the 50-year time frame. The results are presented in the form of several diagrams (Figs. 21.9 and 21.10) which serve to compare rivers with low human intervention to those affected by high anthropogenic interference and their respective responses to water and sediment transfer.

In the first case (Fig. 21.9a) the 23 cross sections which characterize reaches with MQI >0.3 (close to natural state cf Rinaldi et al. 2013) indicate an average state which discriminates between 1970 and 1980 and 1980 and 1990 decades (whereby incision was the main process) and the following ones, i.e., 1990 and 2000 and 2000 and 2010 (with a slight tendency of aggradation). In this case, the largest scattering around the average was recorded in the 1970–1980 decade, when some of the greatest floods occurred in Romania; the response of the channel beds consisted either in excessive aggradation (Suceava, section no. 11, Putna, section no. 34), or abrupt incision (Moldova, section no. 17, Trotuş, section no. 28). Incision was characteristic for the majority of reaches during this time frame (1970–1990), albeit its values show great variability. During the following decades (the 90s and the 00s) aggradation prevailed in most instances resulting in slight channel bed-level recovery.

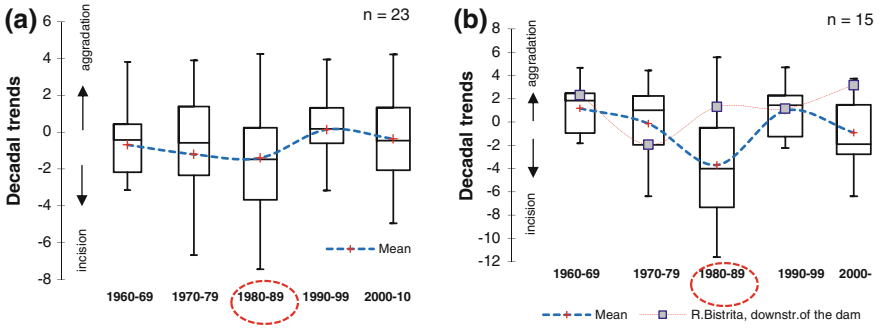

Fig. 21.9 Decadal trends for river bed level in the Siret drainage basin: **a** River channel cross sections under quasi-natural conditions (MQI > 0.3). **b** River channel cross sections with a high degree of artificiality (MQI < 0.3) (modified after Rădoane et al. 2013a). The regression coefficient (indicating the direction and intensity of the relations between the BL and time) was used as a synthetic index for decadal trends

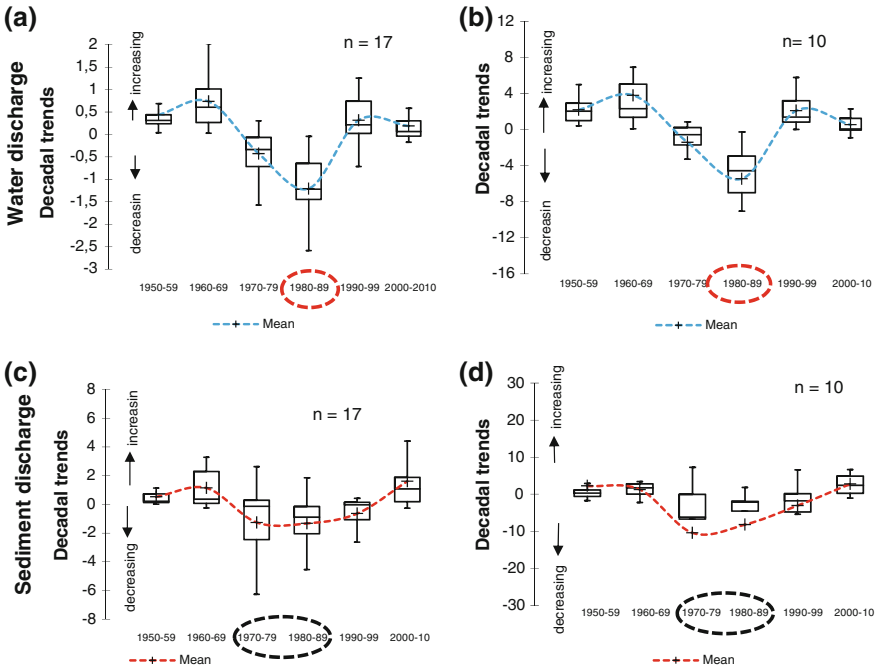

Fig. 21.10 Decadal trends for water discharge (Qw) of rivers under quasi-natural conditions (**a**), and under artificiality conditions (**b**); Decadal trends for sediment load (Qs) under quasi-natural conditions (**b**), and under artificiality conditions (**d**). Decades with a negative trend are shown to highlight the positive trend decades (modified Radoane et al. 2013a). The regression coefficient (indicating the direction and intensity of the relations between the Q, Qs, and time) was used as a synthetic index for decadal trends

In the second case (Fig. 21.9b), with the notable exception of under adapted channel of Bistrița River downstream of Izvoru Muntelui Reservoir, all other channels, despite their varying degree of artificiality, exhibit a decadal behavior within the same tendency interval. In this respect, the 1980–1989 decade is also the most dynamic in terms of channel bed-level adjustment rates; this interval was marked in both categories of rivers in order to highlight that regardless of the conditions under which rivers evolve, there is a distinct temporal signal in the type of adjustment of the channel bed.

The causes for this situation reside in the variability of the two control factors, Qw and Qs, which are the modeling forces within the river channel domain. Therefore, we conducted the same type of statistical analysis for both parameters (Qw—streamflow discharge and Qs—sediment load) for the aforementioned categories of rivers (Fig. 21.10). The decadal behavior of the two variables is similar among each other, as well as in relation to the channel bed-level adjustments. During the 1980s decade, a downward trend in the streamflow discharge was documented which coincided with a decrease in precipitation amounts in the study

area. Moreover, this resulted in a reduction of the sediment load; thus, both variables were subjected to persistent climatic control.

Without making a too bold statement, it is rather easy to observe a common trait in the decadal variations of the three variables under discussion: Qw, Qs and BL; albeit, it is more apparent for the former two (Qw and Qs) and less sharp in the case of BL, which we consider to be natural in the latter case. The Qw → Qs → BL cascade of processes becomes increasingly complicated due to the external disruptors of the climatic signal (such as drainage basin geology and topography, intensity of geomorphological processes, land use/land cover, etc.). Although the general pattern of decadal variability is quasi-similar in all three variables, we observed that it can be highly disturbed in the sections controlled by anthropogenic factors.

Regardless of the degree of artificiality, the general trend was toward recovery of the previous state of the channel bed level post-2000. Moreover, human interventions no longer had the ampleness of those from previous decades. Gravel mining (directly altering the channel bed level) decreased to 64 % of the total sediment yield of Siret basin, whereas just one dam became functional on Siret River, such that the fluvial system had sufficient resources to attempt balancing its dynamic state (see Fig. 21.8), although it was not able to match its state prior to 1970.

To conclude, the mirror analysis of the decadal behavior of river channel beds (under quasi-natural conditions versus anthropogenically altered) pertaining to Siret basin yields the following:

- the majority of the sections under quasi-natural conditions have been dominated by degradation of the channel beds during the '70–'79 and '80–'89 decades, whereas after 1999 incision diminished and slight aggradation was initiated in some instances;
- within the river reaches controlled by anthropogenic interventions, Qs is the variable which has the strongest influence in terms of bed-level changes, as well. The time frame when no less than 5 reservoirs became operational on Siret River, thus filtering the sediment load, occured during a decade when the streamflow discharge was on a climate-induced downtrend. In some instances, the rate of decrease in the Qs was as high as 10 times the rate of reduction in Qw, therefore resulting in the incision of the bed. Moreover, it was the signal conveyed by the Qs variability which generated the tendency of recovery (sensu Wolman and Gerson 1978) in some river sections where the channel bed was undergoing relented incision or even slight aggradation.

Climate Versus Anthropogenic in the Evolution of River Channels

The results obtained so far in Siret, Prut, and Someș drainage basins greatly enhance the understanding of the circumstances under which the changes in the streamflow discharge and sediment loads, whether natural or human-induced,

contribute to the onset of a certain type of response in the channel bed. Furthermore, the results presented in this chapter provide new data regarding present fluvial processes in a previously understudied European region and contribute to gaining more insight into this phenomenon on a regional scale.

For the analysis of climate variability within the study area, we selected a data set of observations on precipitation that we were able to use to generate water discharge and further resulted in the calculation of bankfull discharge (which has maximum geomorphological effectiveness in riverbed modeling). Thus, it was identified 29 meteorological and rainfall stations whose records cover the entire 1950–2010 period. The periods with the highest amounts of rainfall were 1969–1975 and 2006–2008, whereas the driest were 1961–1966, 1983–1986, and 1994–1998. These phases are quasioverlapping throughout the entire study area with slight differences in amplitude. The slope coefficient (b) from the linear regression was employed to demarcate trend categories: positive ($b > 0.5$), relatively stationary ($0.5 < b > -0.5$), and negative ($b < -0.5$). Data were interpolated using the Residual Kriging method (Fig. 21.11). Overall, north of the Trotus River, the trend in the precipitation series is positive, albeit with low sensitivity in terms of the slope coefficient of the regression line. In the southeastern part of the study area, the trend throughout the 60 years of precipitation records has been negative. The situation illustrated in Fig. 21.11 is confirmed by other studies for the geographical area of Romania (Stefan et al. 2004; Ionita et al. 2012) and has been linked to large-scale atmospheric circulation patterns. In particular, it has been shown that the North Atlantic Oscillation is the dominant atmospheric phenomenon that controls a large part of the interannual to decadal variability in precipitation and river flows in Europe and the Middle East (Hurrell 1995).

The general trends in precipitation are expected to be mirrored by the water discharge. The available database comprises the water discharge (Qw) and suspended sediment load (Qs) data series in the form of mean annual values for the 1950–2010 period. Of the 43 investigated reaches, we determined the trends of the Qw and Qs variables for the reaches with a low degree of artificiality. Close to rainfall trends, the trend coefficients for Qw and Qs are grouped into two distinct parts, i.e., the northern sector, exhibiting a general tendency of increases in the amount of water and sediments, and the southern sector, where overall decreases in water discharge and sediment load were documented. In general, the suspended sediment load coefficients were consistently higher than the water discharge coefficients. By relating these data with the previously determined trends in annual rainfall, we may conclude that the climatic signal is strong in the responses of water discharge and suspended sediment load in the seven rivers.

Among the most aggressive human interventions, the significant reduction in forested areas is often cited. Whereas in the early eighteenth century the land cover of the Romanian territory included no less than 40 % forests, during the elapsed time this category has decreased to 27 % (considerably lower compared to the European average, 34 %). Between 1990 and 2006, deforestation has strongly prevailed compared to afforestation in the drainage basins included in our study area, so that each basin lost between 0.9 and 4.3 % of its total forested area

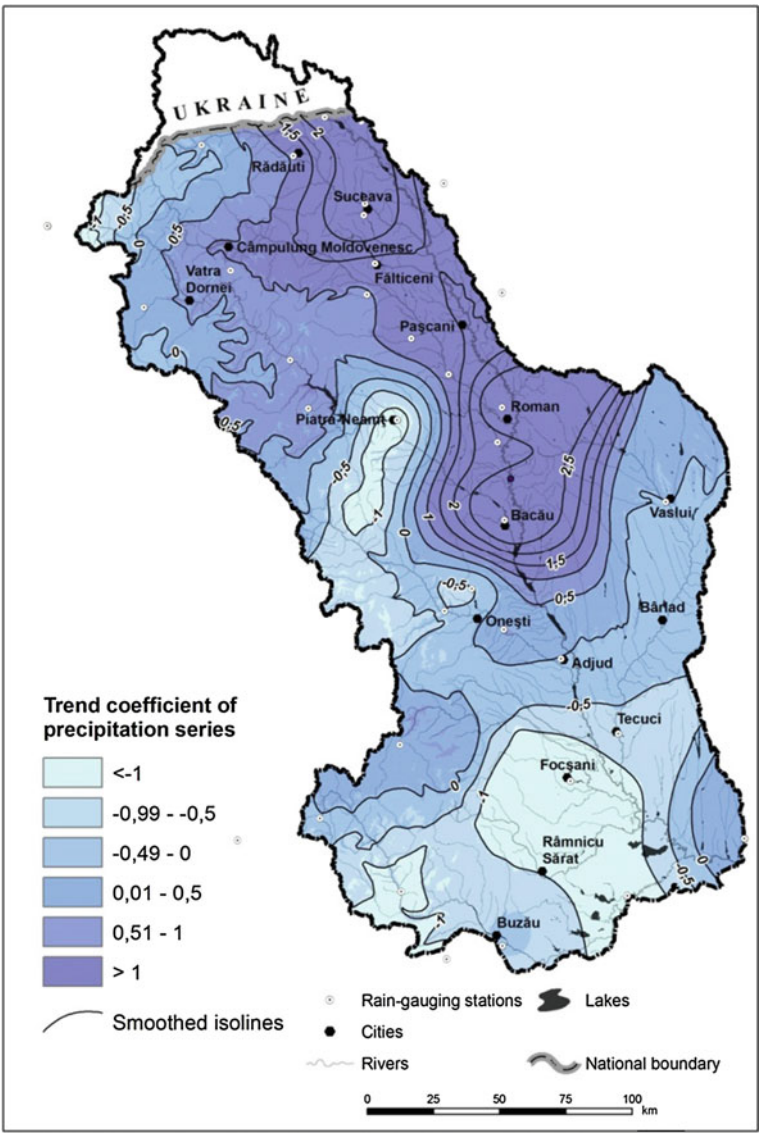

Fig. 21.11 Illustration representing the trend in annual precipitation between 1950 and 2010 at 29 rainfall stations within the Siret basin (modified after Radoane et al. 2013a). The *b* coefficient of the linear regressions for the precipitation series was used to draw the isolines (other explanations are in the text)

(Fig. 21.12). The sole exceptions were the Putna River basin, which gained an additional 3.6 % of forest area during the past 16 years, and the Buzau basin, where the forested area remained almost unchanged over the same time period.

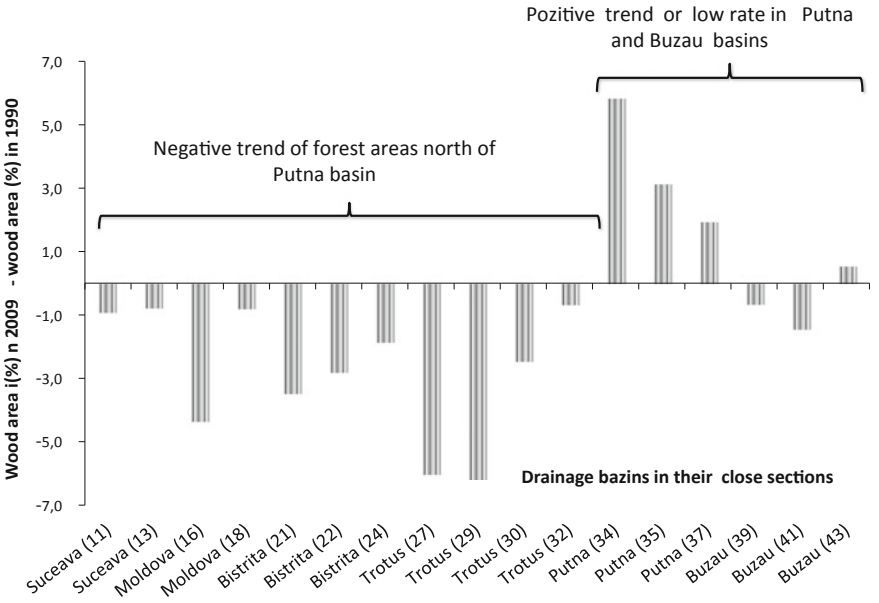

Fig. 21.12 Changes in the forested areas within the East-Carpathian river basins (the *numbers in brackets* indicate the position of the cross section according to Fig. 21.5)

To conclude, the rivers of the Siret River basin, representing a range of intensities of anthropogenic interference, exhibit sensitivity in the responses of water discharge and sediment load to climatic signals (particularly the variations in annual rainfall), albeit with low statistical significance. The sole human intervention that is significant in terms of the change in the amount of sediment transported by a river is the construction of cascading dams on two of the seven rivers, whereas other types of interventions (e.g., land use and land cover changes, levees and groins, gravel mining, etc.) are overwhelmed by the strong influence of the climatic signal on the variability of Qw and Qs.

The argument presented by Schumm (1977) in his conceptual approach to river metamorphosis was confirmed by our observations. Therefore, we added our own conclusions inferred from the results of the present study, to Schumm's conceptual scheme (1977) (Table 21.2). Our contribution regards the nuances of the relations between Qw and Qs and the response of the channel bed by either incision or restoration (i.e., recovery of the bed level prior to the onset of incision), separated according to the type of control: quasi-natural and anthropogenic.

By correlating the response of the bed level with the size of Qw and Qs, we observed that on a medium timescale, the most significant regulator of the two variables is the change in the sediment load (Qs). For example, a decrease by one unit of Qw (Qw−1) resulted in a reduction of Qs by 2 (Qs−2) to 3 times as high (Qs−3) (which occurred in the 1980–1990 decade, when the onset of channel bed incision and channel narrowing were the prevailing processes). During the

Table 21.2 Geomorphic impacts of changes in streamflow discharge and sediment load on river channels leading adjustments in channel bed morphology

(a) Schumm (1977)

Change	River bed morphology	Change	River bed morphology
Qs+Qw	Aggradation, channel instability, wider and shallower channel	Qs+Qw−	Aggradation
Qs−Qw	Incision, channel instability, narrower and deeper channel	Qs+Qw+	Processes increased in intensity
Qw+Qs	Incision, channel instability, wider and deeper channel	Qs−Qw−	Processes decreased in intensity
Qw−Qs	Aggradation, channel instability, narrower and shallower channel	Qs−Qw+	Incision, channel instability, deeper, wider? channel

(b) Rădoane et al. (2013a)

Quasi-natural control		Human control	
Change	River bed morphology	Change	River bed morphology
Qw+1 Qs+1.5… +2	Incision BL=−	Qw+1 Qs+0.3	Incision BL=−
Qw−1 Qs−3	Incision BL−	Qw−1 Qs −3…−7	Incision BL−
Qw+1 Qs+2…+4	Channel bed recovery BL+=	Qw+1 Qs+1… +2	Channel bed recovery BL=+

Qw+1: increase of the streamflow discharge by 1 unit; Qs+1.5…+2: increase of the sediment load by 1.5…2 times as much the water discharge; Qw−1: decrease in the streamflow discharge by 1 unit; Qs−3: decrease in the sediment load by 3 times as much Qw; BL=−: stability or incision of the bed level; BL=+−: stability or aggradation of the bed level

following decades, an increase of Qw by 1 unit (Qw+1) led to an increment of Qs by 1 (Qs+1) to 4 (Qs+4) times as high, which promptly resulted in a tendency of recovery of the channel bed level by aggradation and slight broadening.

The movement of the suspended and dragged sediments within the fluvial systems is not a simple enough process such that it may be controlled solely by the climatic factor. The positive or negative leaps of the sediment load show the high degree of sensitivity of this variable to both climate changes (through the signal transmitted via Qw) and to the anthropogenic interventions particularly. The sensitivity of Qs has been documented in all investigated rivers, regardless of their degree of artificiality; however, it is more apparent in rivers where the human control is prevalent. The sole river showing no response to the climatic signal is Bistrița River downstream of the Izvoru Muntelui Reservoir, whereby the channel bed has undergone significant aggradation (by nearly 1 m), whereas all the anthropogenically controlled sections were undergoing incision (1980–1989, to see Fig. 21.8b).

The results concerning the behavior of investigated rivers are summarized in Fig. 21.13 and may be regarded as a representative trend for Romanian rivers during the past 100–150 years. During this time frame nearly all types of channels were subjected to transformations, which can be ranked into two main types for

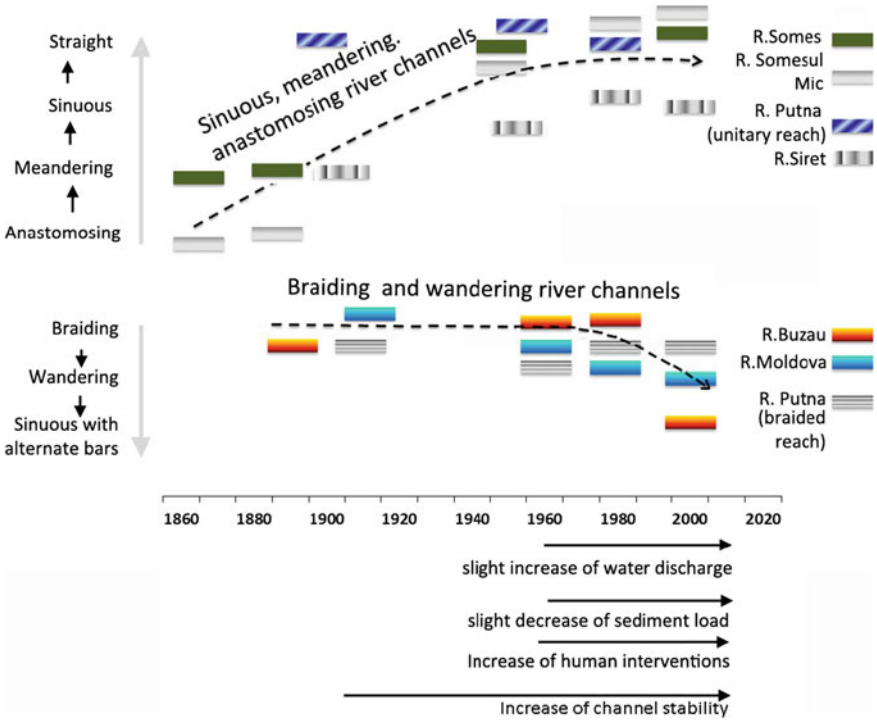

Fig. 21.13 The characterization of the behavioral trend and channel typology metamorphosis specific to Romanian rivers during the last 150 years. **a** Sinuous and anastomosing river channels tend to become straight, and one meandering tend to become sinuous. **b** Braiding river channels tend to become wandering, and ones wandering tend to become sinuous with alternating bars

rivers under investigation: meandering and anabranching channels became sinuous, with a slight tendency of recovery (i.e., meandering) after the 1980s, whereas braided channels were converted to wandering and sinuous channels with alternating bars. This entire range of phenomena was enhanced by the increasing extent of human intervention, particularly after 1970, when channels became more stable (as fluvial processes focused on incision to the detriment of lateral erosion).

Between rivers exemplified in Fig. 21.13, Moldova distinguishes with one of the most important river channel adjustments to climate change and human impact in the last hundred years. Geomorphologists described this river as a one difficult controlled by dams or other works because of the dynamics of sediment at the exit of the Carpathian area. For this reason, the degree of artificiality was kept relatively low. This was until the 1980s when important reserves of gravel in an intense pace began to be exploited. Changes in river channel planform are visible by a succession of cartographical imagery showing significant decadal changes in terms of the decrease in the number of branches and channel narrowing (Fig. 21.14a).

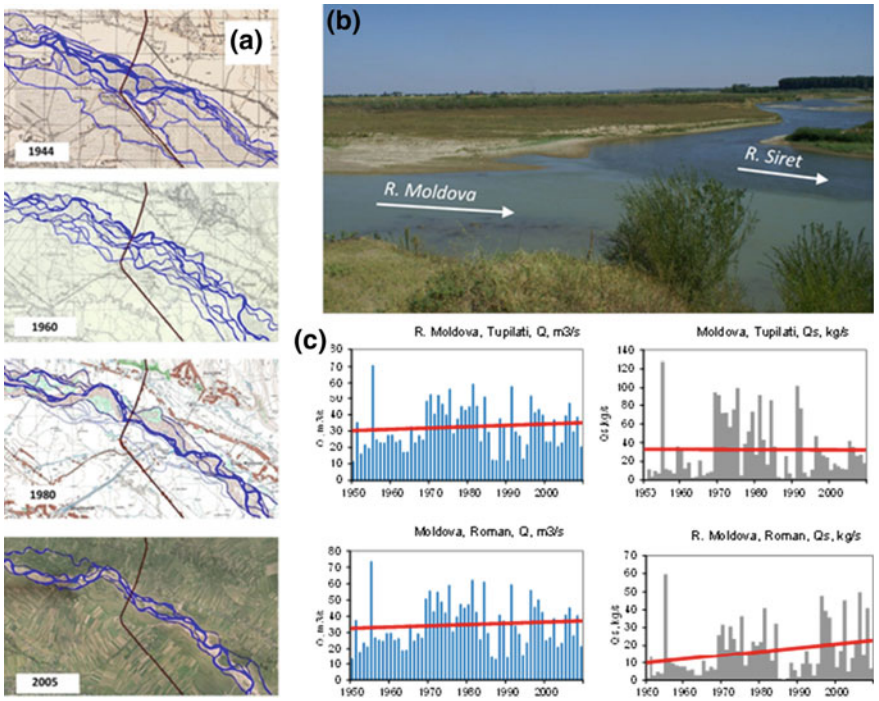

Fig. 21.14 Changes in river channel planform of Moldova River: **a** Succession of cartographic imagery of reaches no. 2 and 3 of Moldova channel between 1944 and 2005, showing the decrease of the number of branches and the invasion with vegetation of old isles. **b** Junction between Moldova and Siret Rivers. The sediment load of the river originates from the gravel plants. **c** The multinannual variation of streamflow discharge and suspended sediment load in the extra-Carpathian sector of Moldova (the tendency of increase in suspended sediment load in the closing section of the river is a result of sediment remobilization by intensive gravel mining, particularly post-1995)

Channel adjustment mechanisms, at least post-1950, occurred in relation to an increase in streamflow discharge and decreasing suspended sediment load (Fig. 21.14c). Intensive extraction of coarse sediment in the 101 gravel plants distributed along the extra-Carpathian course of the river contributed to a large extent to channel narrowing and incision. Moreover, anthropogenic intervention within the channel led to an increment in suspended sediment load toward the junction with Siret River, thereby explaining the increasing suspended sediment load values, particularly after 1995 (Fig. 21.14c). In the image showing the junction of the two rivers (Fig. 21.13b), the high suspended sediment load of Moldova River is apparent; considering the absence of flood events within its drainage basin, this image is conclusive for the anthropogenic effect in sediment remobilization.

Comparative Approach to the Evolution of Romanian River Channels and Channels from Other European Regions

The results obtained thus far by studying Romanian rivers are certainly not singular in the literature, but they are the outcome of the first approach in terms of level of analysis for the geographical area of Romania. Table 21.3 summarizes several studies from various regions in Europe spanning over the last century, including Romanian ones. The data suggests extensive interest in assessing the magnitude and particularly the causality of changes. The aspects which we would like to highlight in particular include: the magnitude of channel adjustments, the temporal trends of channel changes and the causes cited for these changes.

In terms of the *magnitude of channel adjustments*, it was determined that rivers in Italy have undergone the most substantial changes in size parameters (incision up to 10 m in depth and channel narrowing up to 80 %) (Surian and Rinaldi 2003; Surian et al. 2009). Similar or somewhat lower incision rates and channel narrowing have been documented in rivers from other regions, such as the French Alps, southeastern France, Scotland, and the Polish Carpathians. However, river metamorphosis in recent times was not confined to the European territory and was also documented in China, South America, and the USA (James 1997; Stover and Montgomery 2001; Li et al. 2007).

Compared to the magnitude of these changes in river channels during the twentieth century, it should be noted that adjustments are less extensive in Romania in terms of incision depths (62 % of examined cases, ranging from 0.5 to 3 m), whereas in the remaining 38 % of reaches aggradation was the dominant process (with magnitudes ranging from 0.15 to 1.25 m). Furthermore, channel narrowing was less extensive compared to Alpine rivers (see Fig. 21.4).

Albeit incision and channel narrowing have been the norm in fluvial geomorphology throughout the European continent in the past century, the rivers pertaining to Siret and Prut drainage basins exhibit a relatively low amount of incision. In our opinion, the reason resides in the considerably higher sediment transport rate from the source area to delivery area compared to other European regions. The values depicting the sediment output within Siret basin are telling: 277 t/km^2/year, against 206 t/km^2/year for the rest of the Romanian territory and 166 t/km^2/year for the Bulgarian territory (Gergov 1996). According to the spatial pattern established by Vanmaercke et al. (2011) for Europe, the sediment output measured in Siret basin falls into the European mountain and mediterranean type, which ranks highest in the classification (over 200 t/km^2/year, with peak values of 30,000 t/km^2/year in drainage basins from Spain, Italy and Turkey). Within the Romanian territory, the largest sediment yield measured based on the suspended sediment loads in the closing sections of rivers were in the Carpathian Bend area, i.e., Putna, Râmna, Râmnic, and Buzău Rivers basins (over 3500 t/km^2/year).

Regarding the *temporal trends of the channel bed changes*, channel adjustments such as incision and narrowing began in the early twentieth century, but reports on the occurrence of these processes throughout Europe became more numerous

Table 21.3 Data on the recent channel changes in some European rivers over the last 100 years: (−) incision; (+) aggradation (Rădoane et al. 2013a, b, with additions)

River	Country	A (km^2)	Q (m^3/s)	Studied river length (km)	Incision (m)		Narrowing, %
					Twentieth century	Last 30–40 years	
Mszanka	Poland	175	52	19.5		−1.2…−2.0	
Porębianka				15.4			
Raba			12.1		−3.0	−1.5	40
Dunajec		6804	85.5	250	−3.1	−0.7	45
Polish Carpathian rivers	Poland				−1.3…−2.8	>−3	
Moravka	Slovakia			13.5		−8	71
Malnant	France	15.9		7.1	−1.5…−7	−2.4	Narrowing
Roubion		600	1.8	75		−1.06	67
Eygues		1150		102		−1.51…−3.04	54–77
Mountain and piedmont rivers, SE France		63…17,600				−1.31 ± 0.6	55
Arno	Italy	8830	97.4	198	Up to −9		38–50
Tagliamento		2580	109.0	178		−1.5…−3.0	58
Piave		3899	132.0	222		−1.0… −2.0	69
Brenta		1567	71.0	174		−2.5…−5.0	58
Trebia		1070	24.0	116			62
Vara		572	23.0	62			85

(continued)

Table 21.3 (continued)

River	Country	A (km^2)	Q (m^3/s)	Studied river length (km)	Incision (m)		Narrowing, %
					Twentieth century	Last 30–40 years	
12 rivers	*N* and Central Italy	572–3899	8–132	53–222	−8…−10		80
Tagus	Spain	24,788	64.0	1181			37
Jarama		11,597	38.0				32
Tay	Scotland	4690	160.0				34
Tummel							
Prut	Romania	28,463	85.3	631		−1.13…+0.86	
Someşu Mic		3733	22.6	169		−1…−3	30 (1870–1956)
Prahova		3750	8.1	18		−3…−5	56–65 (1900–2006)
Moldova		4316	35.3	110		−0.25…−2.70	79 (1910–2005)
Siret		36,123	211.0	657		−0.44…−1.77	30
Suceava		2330	17.1	156		+0.15…−0.70	
Bistriţa		6388	62.7	292		−0.50…+1.00	
Trotuş		4077	34.6	161		+0.60…−1.03	
Putna		2518	16.1	136		+1.25…−1.00	39
Buzău		5238	27.7	35			73
Someş		15,155	116.2	70			45

during the past 30–40 years. The most detailed analysis on river changes during the past 100 years was carried out in Italy (Surian et al. 2009). The authors were able to delimit three stages: stage I lasting until 1950, stage II between 1950 and early 1990, and stage III post-1990. Prior to 1900, channels underwent little change in terms of the magnitude of morphological parameters (channel width and depth) due to the lack of a dominant process. However, beginning with the first stage described by the authors, channel narrowing was established as the prevailing process (likely, combined with channel bed incision). During the second stage (approximately 1950–1990), the incision and narrowing rates augmented. The third stage (the last 15–20 years) was defined by a decrease in the adjustment rates by incision and narrowing and the onset of a tendency toward restoration of the previous configuration and recovery of the bed level, according to Surian et al. (2009).

Our observations match the pattern described by Surian et al. (2009), as it was determined that the most ample changes in channel beds occurred during the 1980–1990 decade in Italy, France, Poland, as well as in Romania.

The topic which we further documented regards the attempt to assess the role of the climatic factor versus the anthropogenic factor in controlling these changes. The significant number of reaches considered for this analysis, with various degrees of artificiality, contributes to increasing the level of confidence in the results. Thus, *climatic variability has ingrained the general pattern of evolution of the channel beds, over which the human influence left its own strong mark*. The variable which acted as an arbitrator was the sediment load. The scale and complexity of anthropogenic interventions (e.g., Bistrița River downstream of Izvoru Muntelui reservoir) left the river too few degrees of freedom. Conversely, in the cases of Siret, with its five small cascading dams, and Prut downstream of Stânca-Costești reservoir, both rivers were granted enough freedom to rebuild their sediment loads, mostly from their own beds, but also from the inputs of tributaries.

In Western Europe the human impact on rivers has gained some degree of refinement to it (as rivers are controlled by fine works of art, gravel mining is banned or severely reduced, extensive work has been done to reduce the input of sediment to channel beds, etc.), such that the following statement is justified:

"Channel adjustments were driven mainly by human actions, but the role of large floods was also notable in some cases. Besides the direct effect of channelization on channel morphology, the major effect of human actions was on sediment regime" (p. 94, Surian et al. 2009).

However, Romania is far from establishing a sustainable form of human control over rivers (Rădoane et al. 2013b). Nevertheless, the onset of the "globalization" phenomenon of morphological changes in river channels is undisputable, at least after 1960 onwards (based on the available reliable database which attests to this).

Acknowledgments The research leading to these results also has received partial funding from the Exploratory Research Projects PN-II-ID-PCE-2011-3, "Reconstruction of Romanian river channel changes in the last 11,700 years: The role of climatic conditions and human impact." This work was also partially supported by a grant of the Romanian National Authority for Scientific

Research and Innovation, CNCS–UEFISCDI, project number PN-II-RU-TE-2014-4-0855 "Reconstruction of Late Holocene History of Romanian rivers based on geomorphological and dendrochronological interpretation of subfossil trunks."

References

Ackers P, Charlton FG (1971) The slope and resistance of small meandering channels. In: Proceedings of the Institute of Civil Engineers Supplementary Paper 73625-5. Institute of Civil Engineers: London, pp 349–370

Amăriucăi M (2000) Șesul Moldovei extracarpatice dintre Păltinoasa și Roman. Studiu geomorfologic și hidrologic. Carson Press, Iași (in Romanian)

Armaș I, Gogoașe-Nistoran DE, Osaci-Costache G, Brașoveanu L (2012) Morphodynamic evolution patterns of Subcarpathian Prahova River (Romania). Catena 100:83–99

Bertoldi W, Zanoni L, Tubino M (2009) Planform dynamics of braided streams. Earth Surf Proc Land 34(4):547–557

Bondar C, State I, Dediu R, Supuran I, Vaşlaban G, Nicolau G (1980) Data on the Danube channel bed level in arranged regime between Baziaş and Ceatal Izmail. INHGA, București, Studii și cercetări de hidrologie, XLVIII (in Romanian)

Bondar C (2001) The physical degradation of the Danube River bed in the inferior sector. J Environ Prot Ecol 2(3):724–732

Bridge JS, Leeder MR (1979) A simulation model of alluvial stratigraphy. Sedimentology 26:617–644

Bridge JS (2003) Rivers and floodplains. Blackwell Publishing, Oxford

Brierley GJ, Fryirs KA (2005) Geomorphology and river management: applications to the river styles framework. Blackwell Publications, Oxford

Chiriloaei F (2012) Analiza cantitativă a modificărilor albiei râului Moldova în sectorul extracarpatic. PhD thesis, Alexandru Ioan Cuza University, Iași, (in Romanian)

Chiriloaei F, Rădoane M, Perșoiu I, Popa I (2012) Late Holocene history of the Moldova River Valley, Romania. Catena 93:64–77

Church M, Jones D (1982) Channel bars in gravel-bed rivers. In: Hey RD, Bathurst JC, Thorne CR (eds) Gravel-Bed Rivers. Wiley, Chichester, pp 291–324

Cristea I (2011) Studiul geomorfologic al văii Putna Vrânceană. PhD thesis, Ștefan cel Mare University, Suceava (in Romanian)

Diaconu C, Ciobanu S, Avădanei A, Motea I, Stănescu S (1962) Despre stabilitatea albiilor râurilor României. Studii de hidrologie III. Romanian Waters National Administration, București, pp 53–63 (in Romanian)

Dumitriu D (2007) Sistemul aluviunilor din bazinul râului Trotuș. Universității Suceava Press, Suceava (in Romanian)

Feier I, Rădoane M (2007) Dinamica în plan orizontal a albiei minore a râului Someșu Mic înainte de lucrările hidrotehnice majore (1870–1968). Analele Universității Suceava, Seria Geografie 16:13–26 (in Romanian)

Floroiu I (2011) Tipuri de albie pe cursul inferior al râului Buzău. Studii și cercetări de geografie și protecție a mediului 10(1):91–98

Gergov G (1996) Suspended sediment load of Bulgarian Rivers. GeoJournal 40(4):387–396

Gurnell AM (1997) Channel change on the River Dee, 1946–1992, from the analysis of air photographs. Regul Rivers Res Manage 13:13–26

Hâncu S (1976) Regularizarea albiilor de râu. Ceres Press, București

Hohensinner S, Jungwirth M, Muhar S, Schmutz S (2014) Importance of multi-dimensional morphodynamics for habitat evolution: Danube River 1715–2006. Geomorphology 215:3–19

Hurrell JW (1995) Decadal trends in the North Atlantic Oscillation: regional temperatures and precipitation. Science 269:676–679

Ichim I (1979) Munţii Stânişoarei. Studiu geomorfologic. Editura Academiei, Bucureşti (in Romanian)
Ichim I, Bătucă D, Rădoane M, Duma, D (1989) Morfologia şi dinamica albiilor de râu. Technical Press, Bucureşti (in Romanian)
Ichim I, Rădoane M (1990) Channel sediment variability along a river: a case study of the Siret River, Romania. Earth Surf Proc Land 15:211–225
Ioana-Toroimac G, Dobre R, Grecu F, Zaharia L (2010) A 2D active-channel's evolution of the Upper Prahova River (Romania) during the last 150 years. Geomorphol-Relief Processus Environ 3:275–286
Ionita M, Lohmann G, Rimbu N, Chelcea S, Dima M (2012) Interannual to decadal summer drought variability over Europe and its relationship to global sea surface temperature. Clim Dyn 38(1–2):363–377
James LA (1997) Channel incision on the lower American River, California, from streamflow gage records. Water Resour Res 33:485–490
Kiss T, Blanka V (2012) River channel response to climate and human induced hydrological changes: case study on the meandering Hernad River, Hungary. Geomorphology 175–176:115–125
Kondolf GM, Piégay H, Landon N (2002) Channel response to increased and decreased bedload supply from land use change: contrasts between two catchments. Geomorphology 45:35–51
Lach J, Wyżga B (2002) Channel incision and flow increase of the upper Wisłoka River, Southern Poland, subsequent to the reafforestation of its catchment. Earth Surf Proc Land 27:445–462
Leopold LB, Wolman MG (1957) River channel patterns: braided, meandering and straight. US Geol Surv Prof Pap 282–B:39–85
Li L, Lu X, Chen Z (2007) River channel change during the last 50 years in the middle Yangtze River, the Jianli reach. Geomorphology 85:185–196
Liébault F, Piégay H (2001) Assessment of channel changes due to long-term bedload supply decrease, Roubion River, France. Geomorphology 36:167–186
Liébault F, Piégay H (2002) Causes of 20th century channel narrowing in mountain and piedmont rivers of southeastern France. Earth Surf Proc Land 27:425–444
Marston RA, Girel J, Pautou G, Piegay H, Bravard JP, Arneson C (1995) Channel metamorphosis, floodplain disturbance and vegetation development: Ain River, France. Geomorphology 13:121–131
Nanson GC, Knighton AD (1996) Anabranching rivers: their cause, character and classification. Earth Surf Proc Land 21:217–239
Panin N (1976) Aspecte privind procesele fluviale şi marine în Delta Dunării. Anuarul Institutului de Geologie şi Geofizică, Bucureşti 50:149–165 (in Romanian)
Pascu M (1999) Cercetări privind influenţa regularizării radicale a albiilor de râuri asupra stabilităţii unor construcţii aferente şi a mediului înconjurător–cu referire la bazinul hidrografic al râului Prahova. PhD thesis, Universitatea Tehnică „Gh. Asachi", Iaşi (in Romanian)
Perşoiu I (2010) Reconstituirea evoluţiei geomorfologice a văii Someşul Mic în Holocen. PhD thesis "A. I. Cuza" University, Iaşi (in Romanian)
Perşoiu I, Rădoane M (2011) Spatial and temporal controls on historical channel responses—study of an atypical case: Someşu Mic River, Romania. Earth Surf Land Proc 36(10):1391–1409
Petts GE, Moller H, Roux AL (eds) (1989) Historical change of large Alluvial Rivers: Western Europe. Wiley, Chichester
Rao AR (1980) Stochastic analysis of thresholds in hydrologic time series. In: Coates DR, Vitek JD (eds) Thresholds in geomorphology. Allen and Unwin, London, pp 179–208
Rădoane M, Rădoane N (2005) Dams, sediment sources and reservoir silting in Romania. Geomorphology 71:217–226
Rădoane M, Rădoane N, Dumitriu D (2003) Geomorphological evolution of longitudinal river profiles in the Carpathians. Geomorphology 50:293–306
Rădoane M, Rădoane N, Cristea I, Perşoiu I, Burdulea A (2008a) Quantitative analysis in the fluvial geomorphology. Geographia tehnica, Cluj-Napoca 1:100–111

Rădoane M, Rădoane N, Cristea I, Oprea-Gancevici D (2008b) Contemporary changes of the Prut River channel, Romanian border. Revista de Geomorfologie 10:57–71
Rădoane M, Rădoane N, Dumitriu D, Miclăuş C (2008c) Downstream variation in bed sediment size along the East Carpathians Rivers: evidence of the role of sediment sources. Earth Surf Proc Land 33:674–694
Rădoane M, Pandi G, Rădoane N (2010) Contemporary bed elevation changes from the Eastern Carpathians. Carpathian J Earth Environ Sci 5:49–60
Rădoane M, Obreja F, Cristea I, Mihailă D (2013a) Changes in the channel-bed level of the eastern Carpathian Rivers: climatic vs. human control over the last 50 years. Geomorphology 193:91–111
Rădoane M, Perşoiu I, Cristea I, Chiriloaei F (2013b) River channel plan channel planform change based on successive cartographic data. A methodological form change based on successive cartographic data. Revista de Geomorfologie 15:69–88
Rinaldi M (2003) Recent channel adjustments in alluvial rivers of Tuscany, Central Italy. Earth Surf Proc Land 28:587–608
Rinaldi M, Simon A (1998) Bed-level adjustments in the Arno river, Central Italy. Geomorphology 22:57–71
Rinaldi M, Surian N, Comiti F, Busserttini M (2013) A method for the assessment and analysis of the hydromorphological condition of Italian streams: the morphological quality index (MQI). Geomorphology 180–181:96–108
Schumm SA (1977) The fluvial system. Willey, Chichester
Schumm SA (1985) Pattern of alluvial rivers. Ann Rev Earth Planet Sci 13:5–27
Sipos G (ed) (2012) Past, Present, Future of the Maros/Mures River. Szegedi Tudományegyetem, West University Press, Timişoara
Škarpich V, Hradecký J, Dušek R (2013) Complex transformation of the geomorphic regime of channels in the forefield of the Moravskoslezské Beskydy Mts.: case study of the Morávka river (Czech Republic). Catena 111:25–40
Stefan S, Ghioca M, Rimbu N, Boroneat C (2004) Study of meteorological and hydrological drought in southern Romania from observational data. Int J Climatol 24:871–881
Stover SC, Montgomery DR (2001) Channel change and flooding, Skokomish River, Washington. J Hydrol 243:272–286
Surian N, Rinaldi M (2003) Morphological response to river engineering and management in alluvial channels in Italy. Geomorphology 50:307–326
Surian N, Cisotto A (2007) Channel adjustments, bedload transport and sediment sources in a gravel-bed river, Brenta River, Italy. Earth Surf Proc Land 32:1641–1656
Surian N, Rinaldi M, Pellegrini L, Audisio C, Maraga F, Teruggi L, Turitto O, Ziliani L (2009) Channel adjustments in northern and central Italy over the last 200 years. In: James LA, Rathburn SL, Whittecar GR (eds) Management and restoration of fluvial systems with broad historical changes and human impacts, vol 451. Geological society of America special paper, pp 83–95
Vanmaercke M, Poesen J, Verstraeten G, de Vente J, Ocakoglu F (2011) Sediment yield in Europe: spatial patterns and scale dependency. Geomorphology 130:142–161
Winterbottom SJ (2000) Medium and short-term channel planform changes on the rivers Tay and Tummel, Scotland. Geomorphology 34:195–208
Wolman MG, Gerson R (1978) Relative scales of time and effectiveness of climate in watershed geomorphology. Earth Surf Land Proc 3:189–308
Wyżga B (1993) River response to channel regulation: case study of the Raba River, Carpathians, Poland. Earth Surf Proc Land 18:541–556
Wyżga B (2001) A geomorphologist's criticism of the engineering approach to channelization of gravel-bed rivers: case study of the Raba River, Polish Carpathians. Environ Manage 28:341–358

Wyżga B (2008) A review on channel incision in the Polish Carpathian rivers during the 20th century. In: Habersack H, Piégay H, Rinaldi M (eds) Gravel-Bed Rivers VI: from process understanding to river restoration. Developments in earth surface processes. Elsevier, Amsterdam, pp 525–555

Zaharia L, Grecu F, Ioana-Toroimac G, Neculau G (2011) Sediment transport and river channel dynamics in Romania-Variability and Control Factors. In: Manning AJ (ed) Sediment Transport in Aquatic Environments. InTech, pp 293–316

Zawiejska J, Wyżga B (2010) Twentieth-century channel change on the Dunajec River, Southern Poland: Patterns, causes and controls. Geomorphology 117(3–4):234–246

Part VI
Black Sea Coast and Danube Delta

Chapter 22
The Evolution of Danube Delta After Black Sea Reconnection to World Ocean

Alfred Vespremeanu-Stroe, Luminiţa Preoteasa, Florin Zăinescu and Florin Tătui

Abstract This chapter presents synthetically the latest progresses made on Danube Delta evolution based on new cores, sedimentological and morphological analyses which together with the newly obtained absolute ages (AMS ^{14}C and OSL) shed a new light upon the delta formation in both its evolutionary phases (chronology) and the growth patterns. It is the first proposed reconstruction of the fluvial delta which succeeds to date delta front advancement (Old Danube lobe: 8/7.5–5.5 ka) into Danube Bay and the formation of the initial spit. Contrary to the former views, for the first time, it is proven that the early stage of delta plain formation preceded with more than a millennium both the inception of the initial spit and the relative stabilization of the sea level. Moreover, the fluvial delta morphology is reinterpreted to show that most of the present landscape is the recent result of fluvial aggradations which followed after the initial topography (former delta plain) was drowned through the concurrent action of subsidence and sea level rise. With regard to the maritime delta, we bring new arguments into the debate concerning the southern delta (composed by lagoons and sandy barriers built by longshore circulation versus deltaic lobes construction and reworking) which demonstrate that a southern distributary (Dunavăţ, derived from Sf. Gheorghe) had an intense activity and formed open-coast lobes during 2.6–1.3 ka. Moreover, the evolution of each of the six open-coast lobes belonging to maritime delta is systematically presented in relation with Danube flow changes with a focus on their chronology, progradation rates and spatial extension. New evidences have been also produced to document the changes induced by the solid discharge reduction on the Danube since the mid-twentieth century, which recently fostered the shifting of the active lobes from asymmetric to deflected (Sf. Gheorghe) or from fluvial dominated to wave influenced (Chilia).

Keywords Deltaic lobe · River deltas · Delta front · Sea-level rise · Neotectonics · Lobe switching

A. Vespremeanu-Stroe (✉) · L. Preoteasa · F. Zăinescu · F. Tătui
Faculty of Geography, University of Bucharest, 1st N. Bălcescu Blv., sector 1, 010041 Bucharest, Romania
e-mail: fredi@geo.unibuc.ro

M. Rădoane and A. Vespremeanu-Stroe (eds.), *Landform Dynamics and Evolution in Romania*, Springer Geography,
DOI 10.1007/978-3-319-32589-7_22

Introduction

Deltas are complex and unique natural systems due to the large number of interacting forces with inherent fluctuations which alternatively share the leading role in the ongoing morphodynamics at different spatial and temporal scales. The activity of concurrent controlling factors often sort out locally into the prevalence of different morphodynamic processes which lead to the coexistence within a river delta of divergent morphological patterns and related features such as wave- and river-influenced lobes, symmetrical and asymmetrical lobes, erosive and accumulative coasts, subsiding and uplifting areas.

The Danube Delta is a world heritage natural reserve, famous worldwide for the numerous pristine fluvial, marine, and coastal landscapes such as gallery-like natural channels, lakes, fluvial levees, aeolian dunefields, beach ridge plains, barrier islands and spits, lagoons and barriers, beach-dune systems, a preserved testimony of complex delta evolution. Natural deltaic landscape diversity is therefore proof of a long term, continuously evolving system through alternation and interdependence of each controlling factor.

Danube Delta genesis and evolution was the subject of numerous debates and hypotheses during the last century and a half and continues to be a focus of contention as novel and complementary investigation techniques are now available to produce data to numerous interdisciplinary studies in this research field, contributing to the enrichment and continuous refinement of the state of the art of our understanding of this dynamic natural system. Moreover, it has recently became a representative reference in global studies pertaining to either pattern formation (Ashton and Murray 2005; Jerolmack and Swenson 2007; Ashton and Giosan 2011), controlling factors and conditions (Bhattacharya and Giosan 2003; Li et al. 2011; Anthony 2015) or present day dynamics under the influence of global changes (Syvitski et al. 2009) due to its queer evolution and highly diverse morphology.

Taking into consideration the progress in knowledge made so far and the existing empirical data, this chapter is devoted to a refined interpretation of the Danube Delta genesis and evolution based on both existing and novel data. The results of our recent studies on this topic (Vespremeanu-Stroe et al. 2013; Preoteasa et al. 2016; Vespremeanu-Stroe et al. submitted) contributed with almost half of the currently existing absolute ages from the Danube Delta (Fig. 22.1) which, together with the new stratigraphic profiles and accurate mapping of the fluvial and marine shaped morphologies, significantly improved the knowledge on the deltaic systems evolution.

The herein proposed evolutionary model of the Danube Delta differs from the previous more than 30 theories in that it arguments for the first time the advancement of the delta front in the Danube Bay following the Black Sea–Mediterranean reconnection, reconstructs the initial spit formation and reassesses its influence on Danube Delta evolution and presents a detailed chronology of all the maritime lobes with newly produced ages which allowed a more accurate

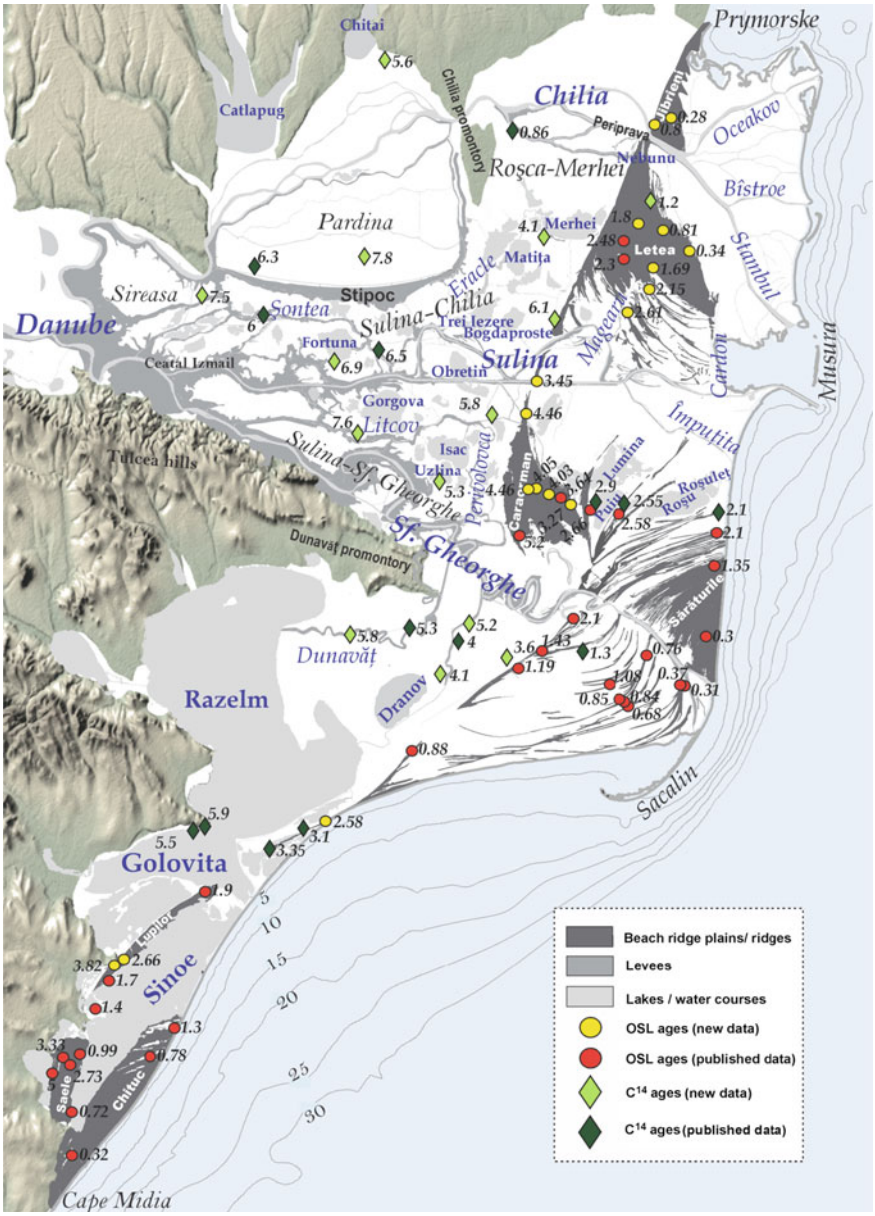

Fig. 22.1 The map of Danube Delta. Position of the OSL and AMS ages used in the paper. All values are expressed in ka (modified after Vespremeanu-Stroe et al. submitted)

interpretation of their morphological evolution. Moreover, it presents new evidences and new interpretation on the southern (maritime) delta (e.g., Razelm–Sinoe lagoon complex), and a novel, comprehensible cartographic representation of Danube Delta evolution at different key moments.

A Short History of the Theories Concerning Danube Delta Genesis and Evolution

The main issues dealt with by most of the theories referring to the Danube Delta genesis and evolution were: (i) the predeltaic shoreline configuration (e.g., maritime golf, lagoon), (ii) the initial spit: its postulated existence and morphological configuration and evolution (Antipa 1914; Zenkovich 1956; Panin et al. 1983; Carozza et al. 2012), (iii) Danube's distributaries: number, paleochannel route, chronology, and discharge variability (de Martonne 1931; Mihăilescu 1947), (iv) deltaic lobes chronology, evolution and/or transformation (i.e., golf, lagoon, fluvial dominated, wave influenced): Brătescu (1921); de Martonne 1931; Zenkovich 1956; Panin (1983, 1989); Giosan et al. (2006); Vespremeanu-Stroe et al. (2013); Preoteasa et al. (2016).

The elaboration of the first (and most of the) theories regarding the Danube Delta genesis and evolution started with the assessment of the accommodation space configuration. One of the first proponents of an initial maritime gulf associated to a subsiding region where Danube Delta started to be built was Murgoci (1912), followed by Antipa (1914) who asserted that the gulf was latter enclosed by a sand barrier stretching from Jibrieni (N) to Histria (S), being subsequently perched by six Danube's distributaries (the northernmost and southernmost were placed nearby Periprava, respectively in front of Histria). Brătescu (1921) considered that a series of coastal barriers have been formed between Jibrieni and Histria after the individualization of Sulina and Chilia channels, whereas the major role in coastal sand barriers formation was played by Sulina fluvial current which contributed to Răducu, Ceamurlia, and Caraorman barriers formation at the intersection with the maritime currents, whereas Letea ridge plain lately formed by coastal sediments accumulations as successive ridges from south to north, updrift of Sulina arm mouth.

In 1931, de Martonne supports the hypothesis of fluvial dominated Danube Delta formation into a former lagoon, enclosed by sand ridges in the nearby of the Caraorman meridian. In the aftermath of the French geographer's work, Zenkovich (1956) stated that the former gulf was transformed into a lagoon being crossed form North to South by a continuous, 60 km long sandy barrier, coincident with the western side of the actual Jibrieni, Letea, and Caraorman ridge plains (Fig. 22.1), entirely built by allochtonous (non-Danubian) sediments transported by the longshore currents, hypothesis which was also endorsed by Coteţ (1960) and Banu and Rudescu (1965). Another hypothesis was launched by Popp (1965) claiming that Chilia and Stipoc were peninsulas, while Letea, Caraorman, and Sărăturile were islands within the initial gulf, in which Letea and Caraorman served as connection

points for sand barriers built by longshore currents, whereas Sărăturile remained isolated.

The evolutionary pattern proposed by Zenkovich (1956) served as a model for producing the first absolute chronology of the Danube Delta by Panin et al. (1983). The ages of 11,700–9800 years BP were obtained for the initial spit Letea–Caraorman (or the "backbone" of the Danube Delta) and assumed as the inception age of the delta (Panin 1983, 1989; Panin et al. 1983). In a referential study of Stanley and Warne (1994), based on the assessment of absolute chronologies of deltas formed all around the word, the authors conclude upon the modern deltas development within a confined time span, from about 8500 to 6000 years ago in relation with the deceleration of the sea level rise. Recently, Giosan et al. (2006) produced a new absolute chronological framework for the maritime delta (mainly based on radiocarbon ages) interpreted by authors as attesting Danube Delta inception $\sim$5200 years ago, about 5 ka years later than previously proposed by Panin et al. (1983). There have been also several attempts to ascribe Danube Delta formation to the sea level regressions and transgressions, some of them related to the Quaternary glaciations (Slanar 1945; Pfenenstiel 1950 cited by Ştefănescu 1982), others with regional Black Sea level fluctuations, respectively to a presumed Phanagorian regression (Coteţ 1960; Popp 1965; Banu and Rudescu 1965). Recent evidences prove the lack of regressions (i.e., Phanagorian) during mid- and late Holocene (Giosan et al. 2006 for the eastern part of Danube Delta; Brückner et al. 2010 for Taman Peninsula; Vespremeanu-Stroe et al. 2013 for the southern Danube Delta).

Danube Delta has been built around various (as number) and alternating (as power) distributaries. Tracking the history of Danube's distributaries formation and transformations is the uttermost undertaking in the constant application to paleoenvironmental reconstruction. With few exceptions (Brătescu 1921; Vâlsan 1934; Popp 1965), most of the references argued in favor of Sf. Gheorghe distributary as having the leading role into the deltaic evolution as it was the first one developed within the Danube Delta system and the largest Danube's discharge conveyor most of the time since delta inception. The first theory centered upon the primacy of Sf. Gheorghe distributary was proposed by de Martonne (1931) which claims the Sf. Gheorghe arm transported the largest Danube's discharge until it reached the (SW) geographical coordinates of present-day Caraorman ridge plain, after which it changed in favor of Sulina which rapidly build a protruding lobe, outstretching the present-day limits of the Sulina coast. Then, most of Danube discharge was claimed again by Sf. Gheorghe branch, the sediments of which were transported by longshore currents in the downdrift direction isolating the Razelm, Zmeica and Sinoe lakes, and finally switched to present-day Chilia channel (de Martonne 1931). The primacy of Sf. Gheorghe arm amongst the other distributaries in the Danube Delta chronology was then accepted by most of the authors.

Zenkovich (1956) ascribed the beach ridge plains formation updrift of the river mouths (due to the groin effect played by river mouth for the longshore sediment transport) and revised the chronological hierarchy of the deltaic lobes from the eastern (maritime) delta: (1) Old Sf. Gheorghe, (2) Sulina (which he supposed that it would have been more extended seaward than the present state), (3) modern Sf.

Gheorghe and (4) lastly modern Chilia lobe. As concerning the southern delta, he proposed that it was formed through successive downdrift barriers formation closing several lagoons, without the direct influence of any Danube distributary (Zenkovich 1956). His theory is still very influential on most of the new morphogenetic studies which took over the Zenkovich evolutionary model without significant changes (Giosan et al. 2005, 2006, 2012; Romanescu 2009; Bony et al. 2015). Original perspectives for the southern Danube Delta are brought by Panin (1983, 2003) and Vespremeanu-Stroe et al. (2013) which propose the existence of open-coast lobes built by the southernmost branch of the Danube (Dunavăţ); the latter also invokes neotectonics as one of the main controlling factors in southern delta shaping.

Most the scenarios have been elaborated on marine deltaic lobes, particularly on those which are still visible, whereas just a few mentions or general remarks exist about the evolution of the fluvial compartment of the Danube Delta. This is partly because of the specific fluvial deltaic processes such as avulsions, bifurcations, meanderings and floods which, together with specific deltaic subsidence, complicate the morphology and stratigraphy by generating sedimentary gaps, truncations or amalgamated sedimentation within the stratigraphic structure, rendering the paleoreconstruction process very difficult. The present day puzzle-like aspect of the fluvial delta morphology is difficult to be interpreted as a continuous process, the chronological proxies being either reworked or sparse, and the different depths at which the one and the same layer has been intercepted proving difficult to be interpreted without a wider context and multiple approaches necessary to replicate the existing data and to test the hypotheses. However, the researches undertaken since the mid of the nineteenth century and the ongoing methodological and technical progress led to numerous relevant and reliable data collections, available now for accurate interpretations. The new geochronological framework shed a new light on the existing data and their significance partially or totally changed in some cases, whereas the previous evolutionary scenarios have been proved as more or less spurious.

The Fluvial Delta Evolution

Since Antipa (1914), the structure of the Danube Delta has been divided into two compartments: the fluvial and the maritime delta as a result of the degree of open-coast wave influence. These two distinct morphosedimentary units are separated by a coastal barrier spit named the Jibrieni–Caraorman barrier or *the initial-spit*.

The reconstruction of the fluvial delta evolution is based on an overall 11 cores of 6–9 m depths (8 new cores and three recently published in Carozza et al. 2013; Filip and Giosan 2014) which were absolute dated (Fig. 22.2) and then correlated to the deep drills (of 25–50 m depths) undertaken in the 50′ and 60′ (described in Popp 1961; Liteanu and Pricăjan 1963). The cores were described in detailed through sedimentological analyses which, together with the new-obtained absolute ages (AMS), allowed to relate the stratigraphic units of the delta plain with the

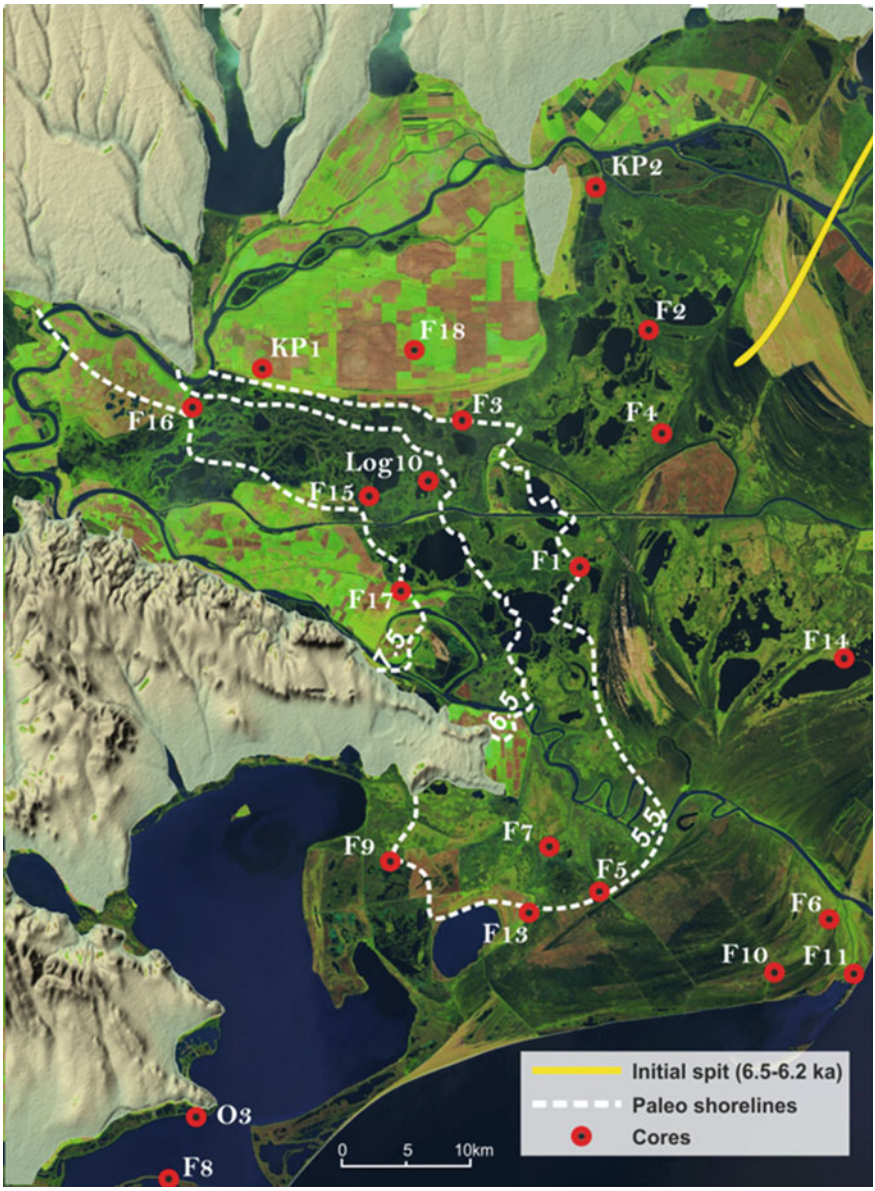

Fig. 22.2 Fluvial delta evolution between 7.5 and 5.5 ka. Please notice the three different stages in fluvial delta development, the configuration of the initial spit and the position of the new cores used in the paper

morphogenetic processes and to reconstruct the main building phases of the current deltaic landscape which prove to be: (i) the early delta front advancement into the Danube Bay, and (ii) the late delta stage of fluvial aggradation.

The Initial Spit (6.7/6.5–5.8 ka)

In the absence of robust evidences supported by chronological data or morphological analysis, all the evolutionary models (since Antipa 1914 up to recent studies of Panin 2003; Giosan et al. 2006, 2013; Carozza et al. 2013) were inspired by the nowadays noticeable river-dominated morphology to hypothesize that early Danube Delta formed from its very inception into a lagoon closed by the "initial spit."

Nevertheless, our new data suggest that most of the surficial delta plain features (belonging to fluvial delta) are much younger than the sedimentary layouts associated with delta progradation into the Danube Bay, so that its current morphology cannot be indicative for the early Danube Delta evolution. Moreover, the new-obtained ages corresponding to modern delta front advancement in the Danube Bay (after Black Sea reconnection to the Mediterannean waters and to the World Ocean ca. 9400 years ago; Soulet et al. 2011) state an age of 8.0–7.5 ka for the earliest stage of delta formation (Figs. 22.2 and 22.3) which seems to contradict the existence of the initial spit at that time, as long as the oldest spits built in similar isostatic conditions started to form ca. 6500 years ago, following the sea level rise deceleration (Buynevich et al. 2015; Del Rio et al. 2015).

For the reconstruction of the initial spit formation and dynamics we collected several samples both from the present sandy barrier (i.e., the remnants of the initial spit) and close behind it (the former lagoon), which produced ages younger than 6.1 ka; the latter is indicative for an initial stage of the spit-platform elongation which was approaching the mid-sector of the Danube Bay. The north-south gradual decrease of the ages, from older than 5.2 ka in the south Caraorman, 4.46 ka in north Caraorman, 3.5 ka at Ceamurlia and 2.6–1.2/0.8 ka in Letea, to 0.8 ka in the western Jibrieni beach ridge plain (b.r.p.) (Figs. 22.1 and 22.2), indicates a long-term behavior of the spit, characterized by backward migration through overwash processes during severe onshore storms. This means that the initial spit evolved in a similar manner with the Danube Delta present-day barrier spits: Sacalin, Musura, Bistroe, and Oceakov (Vespremeanu-Stroe and Preoteasa 2015).

Taking into account the specific morphodynamics of the initial spit, it was not possible to date the former spit roots because they were eroded long time ago. Therefore, the reconstruction of the spit formation was based on both F4 core stratigraphy (which intercepted a 6.1 ka old horizon of fine quartos sands corresponding to the distal tip of the spit-platform) and geometric estimates of the subaqeous spit-platform development, of which the mean elongation rate (of 61 ± 9 m/year) was assessed using longshore sediment transport (LST) magnitudes recorded in Caraorman and Letea b.r.p. (Vespremeanu-Stroe et al. 2016) and the average water depths indicated by the predeltaic loess deposits (Ghenea and

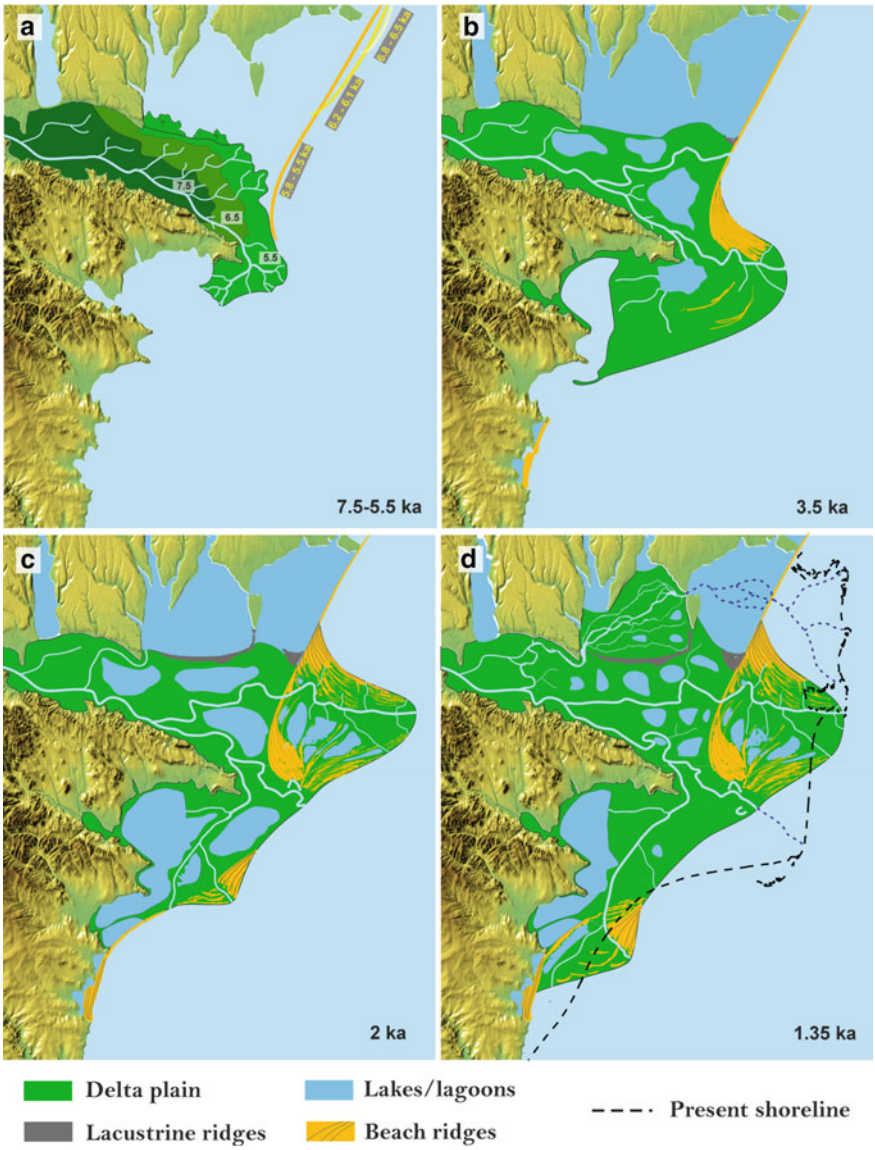

Fig. 22.3 Successive stages of the Danube Delta evolution: early delta front advancement into the Danube Bay: 7.5–5.5 ka (**a**); the maximum extension of the old Sf. Gheorghe lobe: 3.5 ka (**b**); Sulina and Old Dunavăţ lobes at 2 ka (**c**); delta coast position at 1.35 ka (**d**) (modified after Vespremeanu-Stroe et al. submitted)

Mihăilescu 1991). Finally, a time span of 480–650 years resulted, necessary for the spit to reach the F4 core position (Răducu beach ridge) that supports an age of spit inception of 6.75–6.5 ka years BP (Vespremeanu-Stroe et al. submitted).

Further southward, the spit-platform developed in deeper waters (with mean depths of 10–23 m according to isopachs of marine flooding surface estimated by Ghenea and Mihăilescu 1991 and Giosan et al. 2012), which slowed down the spit advance (to ca. 35–50 m/year) and lasted for 200–300 years till the spit joined the Danube Delta coast, respectively to the Old Danube lobe which at that time just started to develop the first open-coast lobe (the Old Sf. Gheorghe lobe) (Fig. 22.2). All in all, the very recent study of (Vespremeanu-Stroe et al. submitted) indicates that the spit started to form 6.7–6.5 ka, about 1000–1300 years after the Danube Delta began to advance in the Danube Bay. Around 5.8 ka ago, the spit merged to the Old Danube lobe and transformed into a sandy barrier which completely closed the Danube Bay.

Morphological Evidences

Even if the present configuration of the fluvial delta was recently shaped as already mentioned, the accurate determination of the present-day morphology may deliver important information about its evolution.

First of all, two main morphological complexes are distinguishable: (i) Danube's main distributaries constrained by their high and wide levees systems (up to 5 km) for Sf. Gheorghe and Sulina (Fig. 22.4) but significantly narrower (<2 km) for Chilia branch (except for the sector close to the delta apex), and (ii) large low-lying areas (depressions) spanning in-between the distributaries levees at 2–3.5 m below the Danube levees systems; they generally comprise a scattered web of lakes (ca. 140) into extensive reed marshes. The distinct configurations of the three main distributaries suggest different evolutionary patterns, ages, and environmental conditions. Therefore, the meandered Sf. Gheorghe branch shows by far the largest levees and, over time, fed four open-coast lobes from a total of six in the entire maritime delta or derived large secondary branches (Sulina, Litcov, Dunavăţ). All these facts indicate it recorded the longest fluvial activity. Sulina has a regular aspect (quasi-linear for most of the course) with only two large meanders before crossing the first beach ridge (Ceamurlia, part of the initial spit), whilst the northern branch of Chilia looks completely different, developing two large but complex braided systems (Chilia 1 and Chilia 2 lobes, corresponding to Pardina and Roşca–Merhei depressions). Its numerous secondary branches have narrow levees whilst some of them have none (Fig. 22.4). Additionally, the two major interdistributary depressions (Sulina-Sf. Gheorghe and Chilia–Sulina), covered by a network of anabranching channels, swamps and lakes, show discordant levee indices (ratio of levee surface area to total area of the depression) of 0.36 for Sulina-Sf. Gheorghe and 0.2 for Chilia–Sulina, which altogether recommends modern Chilia and the northern delta as the youngest branch and deltaic sector, respectively. These morphological evidences of the relative chronology are also supported by sedimentological data as presented below.

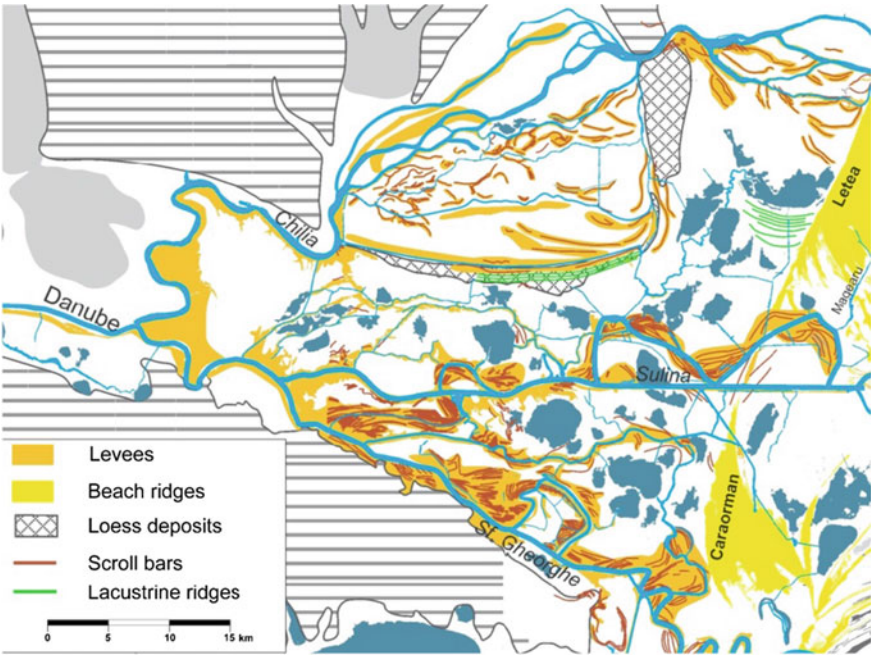

Fig. 22.4 Map of the river-built levees, lacustrine ridges and beach ridges from the fluvial delta and adjacent regions

Early Delta Stage of Coastal Progradation into Danube Bay (8/7.5–5.5 ka)

This stage was reconstructed based on the ages obtained from marine silts and sands intercepted on the cores that belong to delta front facies. Ages as old as 7.4 and 7.5 ka (F16 and F17 cores) support a 7.5 ka coastline placed close behind (westward) their position (Fig. 22.2), which defines the time interval when the first floodplains expanded over the current position of Danube Delta with a marked preferancy for the southern part, along the southern Danube distributary of Sf. Gheorghe, respectively (Fig. 22.3a). This indicates that earliest delta shape was southward skewed proving that Sf. Gheorghe is the oldest Danube branch and the only one which remained active during this long timespan, despite numerous avulsions or climatic and anthropically induced changes in the Danube watershed (Kaplan et al. 2009) which induced dramatic discharge fluctuations (Vespremeanu-Stroe et al. submitted).

The reconstructed 6.5 ka coastline (Fig. 22.3) shows an impetuos expansion of the delta front even during moderate sea-level rise (of 1.5–2 m during the 7.5–6.5 ka interval). At that time, delta plain extended to ca. ½ of the Danube Bay forming a large river-dominated lobe, herein called Old Danube lobe, but preserved

a marked asymmetry between the northern and southern compartments due to river flow preferences toward the deepest part of the Danube Bay that are in the south, as indicated by isopach of predeltaic sediments (Ghenea and Mihăilescu 1991; Giosan et al. 2012). At this moment, the initial spit is in the early stage of formation and starts to close the northern unit of the initial Danube Bay that will remain an open-water space for several millenia, until modern Chilia activation, respectively (2.0–1.7 ka; Filip and Giosan 2014; Vespremeanu-Stroe et al. submitted).

Concluding, the reconstructed old coastlines indicate that the first deltaic lobe (Old Danube lobe) was built relatively early (7.5–5.5 ka), in the southern and central parts of the current fluvial delta, whilst the distal northern part preserved as large open-water bodies: lacustrine for Pardina and marine or lagoonal (after 6.5 ka) for Roşca–Merhei. Contrary to the previous opinions, we argue that the initial spit had no influence upon the very early delta formation (as it did not exist), but since 6.5 ka it started to gradually close the northern Bay affecting the sediment deposition into the newly formed lagoon (Vespremeanu-Stroe et al. submitted).

Late Delta Stage of Fluvial Aggradation (5.5 ka—Present)

The concurrent action of the continuous, yet slow sea level rise (2–2.5 m: 7.5–5.5 ka; 0.5–1 m: 5.5–3.5 ka; Vespremeanu-Stroe et al. 2013), and the low–moderate subsidence (0.4–0.6 mm/year; Vespremeanu-Stroe et al. submitted) submerged most of the delta plain created during early stages and transformed it into large shallow lakes and extensive reed marshes. Following these slow but significant changes, a second stage of delta plain construction, defined by fluvial and peat aggradation, developed during the last 5.5 ka. The peat deposition was both extensive and intense during 5.5–3.5 ka. In most places, the freshwater peat overtops the marine deposits (foreshore sands) and rarely thin layers of fluvial sediments. The basal peat is found at 5–6.5 m depth with small differences imposed by the local site (delta plain) elevation and sea level during its formation. Taking into account that peat is a very precise sea level indicator (the reed survives at mean water depths of 0…−1 m) this means that local water level rised with ca. 4–5 m during the last 5500 years.

The largest peat deposits (>1 m thick) have a filamentous structure (derived from reed) and started to form roughly at the same time: 5–5.3 ka. The age similarities of the basal peat highlight a generalized reduction of the fluvial flux toward inner delta plain and the relative stabilization of the sea level, although a low rise continued till ca. 3500 years ago.

The present-day aspect of the interdistributary depressions with a very dense channel network indicate that after partial submerge of the Old Danube lobe delta plain, the newly formed shallow lakes and the subsiding depressions accommodating reed marshes (Fig. 22.3b, c) recalled for new episodes of fluvial aggradation through numerous but minor avulsions of the secondary channels and overbank

flooding. The restart of the siliciclastic deposition was undertaken around 4–3 ka as indicated by top age of the massive peat deposits.

A detailed view of the fluvial history during the late delta stage of fluvial aggradation is difficult to obtain due to rapid changes occured in subsiding areas which preserve subaerially only the recent landforms. The delta front ages demonstrate that Sf. Gheorghe branch had a continuous fluvial activity over the last 8000–7500 years, but all other distributaries are younger. Thus, in the northern part of the current Sulina-Sf. Gheorghe interdistributary depression a proto-Sulina branch and its secondary distributaries built the northern unit of the Old Danube lobe during 7.5–5.5 ka. After that, it drastically diminished its discharge and abandoned the southern distributaries, but probably maintained a weak activity only in the northern part of the Old Danube lobe (*Fortuna–Bogdaproste* area) where peat deposits are missing instead of fluvial sediments. These northern paleochannels probably fed not only the local floodplains but also the lacustrine system of Pardina which, for a very long timespan, existed as open-water areas (Vespremeanu-Stroe et al. submitted).

Within Sulina-Sf. Gheorghe depression, Litcov channel has massive levees but only in the upstream part and considerably narrower downwards. The pronounced switch between the two sectors corresponds to a turning point where the paleodistributary course changed its flow direction to the North and continued to build levees for a long period. This is indicative of a high and prolonged flow on the Litcov upstream channel which recommends it as probably the oldest distributary derived from Sf. Gheorghe branch during the late delta stage (post-5500 BP). After Litcov changed its route on a northward position following an avulsion, the new course corresponded to the modern Sulina, so that current Litcov channel is likely to maintain one of the initial courses of (*Paleo-*)Sulina. The avulsion moment was not dated yet, but it may have occurred well before 3.5 ka when the Sulina pierced the initial spit.

After a long time lag following Old Danube lobe advancement into Danube Bay, the modern Chilia started to fill the Pardina basin which, at that time, was a shallow lake surrounded by loess deposits (Filip and Giosan 2014). In the south part of the Pardina basin, a lacustrine strandplain (Stipoc) was built of fine sands overlying a submerged loess platform (Panin 1972; Ghenea and Mihăilescu 1991; Filip and Giosan 2014). As documented by several cores, the main stratigraphy of Pardina shows fluvial sands and silts down to 2–2.5 m depth (with basal ages of 1.5–1.76 ka (F18, KP1; Fig. 22.5) which overlay very uniform fine silts and clays (with mean size of 3–20 μm) lacking interstratified coarser textures which prove their lacustrine (or lagoonal) origin.

After Chilia filled partially the Pardina lake, it started to build the most recent inner deltaic lobe (Chilia 2) of the fluvial delta into Roşca–Merhei depression which at that time was a shallow lagoon as supported by F2 and KP2 cores (Fig. 22.5). Here, the brackish sandy silts underlying fluvial sands are found at depths of 1.8–2.5 m only. The current Chilia 2 lobe presents typical bayhead delta morphology with multiple distributaries bifurcating primarily at its apex, near Chilia loess plateau, which was considered to have started to grow 800 years ago and

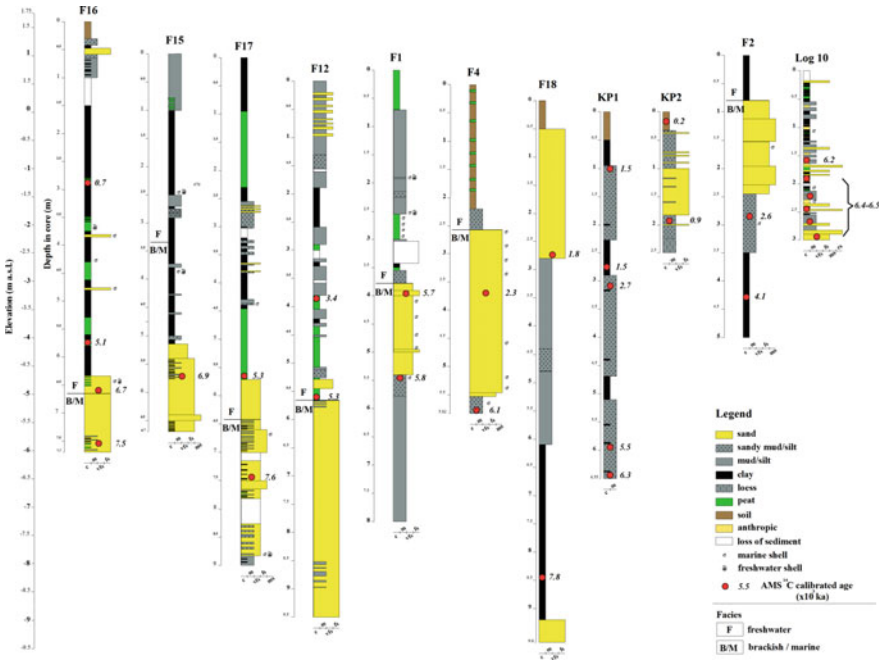

Fig. 22.5 The stratigraphy of the fluvial delta (after Vespremeanu-Stroe et al. submitted)

spanning until at least 300 years ago when Chilia pierced the sandy coastal barrier (Filip and Giosan 2014). Contrary, our three ages from western Jibrieni (0.79 ka) and from the first ridges of Letea mainly composed of Danubian sediments (0.81 and 1.2 ka) all belonging to the early stage of the modern Chilia open-coast lobe, indicate a completely different moment of the Chilia open-sea mouth (and delta) formation, respectively at about 900 years ago, supporting an older inception of Chilia 2 and Chilia 3 lobes than previously estimated (Giosan et al. 2012; Filip and Giosan 2014).

The Maritime Delta Evolution

Danube Delta entered under the influence of waves and nearshore currents during the last six millennia (6000–5500 years ago), following more than 2000 years (8.0/7.5–5.5 ka) of Old Danube lobe advancement into the Danube Bay as a fluvial dominated bayhead delta, in conditions of limited fetch specific to an open bay (before 6.5 ka) or to a lagoon (semi-) closed by coastal barriers (6.5–5.7 ka). Six large open-coast deltaic lobes alternatively developed in association with the three main distributaries: Sf. Gheorghe (S), Sulina (central) and Chilia (N). Four of the wave-influenced deltaic lobes: Old Sf. Gheorghe, Old Dunavăţ, New Dunavăţ and

Modern Sf. Gheorghe have been built in relation with the Sf. Gheorghe branch, whereas the other two, (Sulina and Chilia III lobes) are related to Sulina and Chilia distributaries, all of them making up the eastern and the southern territories of the actual delta.

Built within a strong southward longshore transport system, the wave-influenced deltaic lobes followed a very general development pattern of which the morphodynamic feedbacks at the river mouth stand out as holding the leading role. The sediment dynamics at the river open-coast mouth may achieve a river-dominated morphology during the first stage (of a few centuries maximum) in conditions of high sediment discharge and a relative short coastline, but along with the coast lengthening the lobe attained a wave-influenced morphology which further development occurred through the cyclic progress of the following stages: (i) subaqueous mouth bar (deltaic platform) building, (ii) barrier island emergence or spit emergence, and (iii) transformation into a barrier spit frequently with several secondary spits on the downdrift lobeside; in parallel, on the updrift lobeside the coast has a continuous progradation with variable intensities through beach face accretion. These processes derived from the prevalence of the northern waves especially during energetic conditions, which promoted an asymmetric development to each of the wave-influenced lobes consisting in two morphosedimentological units represented by: a *beach ridge plain* (b.r.p.; updrift lobeside) resulting from prograding beaches usually capped by thin aeolian deposits, and a *barrier-marsh plain* (downdrift), made up of isolated beach ridges (derived from former barrier islands and spits) which were encased into the muddy deltaic plain due to fluvial silting and bioaccumulation (Preoteasa et al. 2016).

Tracking the maritime delta evolution required both coring of the delta plain (for the downdrift units of the lobes) and OSL datings of the visible sandy features. Beach ridges are ubiquitous features of wave-influenced lobes and facilitate precise reconstruction of the shoreline evolution, therefore they are regarded as accurate chronological benchmarks analogous to the tree rings growth (Tamura 2012). Where absolute (e.g., radiocarbon or OSL) age of a beach ridge is available, this is the ideal proxy to trace the paleoshoreline configuration. The lack of major anthropic transformations on the beach ridges in the Danube Delta facilitated the reconstruction of lobes histories and their maximum extension. Therefore, shoreline dynamics could be confidently reconstructed for Sf. Gheorghe and Sulina lobes, based on the existing beach ridges, whereas the recent evolution of the young Chilia lobe can be tracked mainly from historical maps. It was rather difficult to reconstruct the southern delta development (Dunavăţ lobes) where neotectonics and large reworking processes removed most of the previous shoreline sequences but the previous efforts (Vespremeanu-Stroe et al. 2013) facilitated the getting of an integral reconstruction.

In the following sections, each open-coast lobe will be discussed in chronological order.

Old Sf. Gheorghe Lobe (SG1: 6/5.5–3.5 ka)

The first open-coast deltaic lobe which morphology was influenced by the prevalent northeastern waves, developed at the mouth of the Sf. Gheorghe arm; it is commonly denominated Old Sf. Gheorghe lobe (SG1). Like all the wave-influenced deltaic lobes of the Danube Delta, its evolution was ruled out by the complex interactions between the marine and fluvial controlling factors which acted to trap updrift of the river mouth a part of the longshore drift, creating the Caraorman b.r.p, the oldest (5.5–3.2 kyear) ridge plain preserved within the actual deltaic territory. Shoreline progradation rates varied significantly during Caraorman formation (from 2.8 to 4.4 m/year; Fig. 22.6a), whereas the surface growth rates remained constantly at 6.2–6.5 km^2/100 years, in accordance with the steady longshore sediment fluxes (Vespremeanu-Stroe et al. 2016).

SG1 open-coast lobe started to form around 6000–5700 years ago when Sf. Gheorghe distributary overpassed Dunavăţ Promontory and exit the bay. At the updrift, the initial spit connected to the fluvial lobe which, after that prograded once with the river mouth advancement, built a series of subparallel beach ridges which finally shaped the current Caraorman b.r.p. The SG1 shoreline achieved the maximum extension around 3500 BP (Fig. 22.3c) through mean progradation rates of

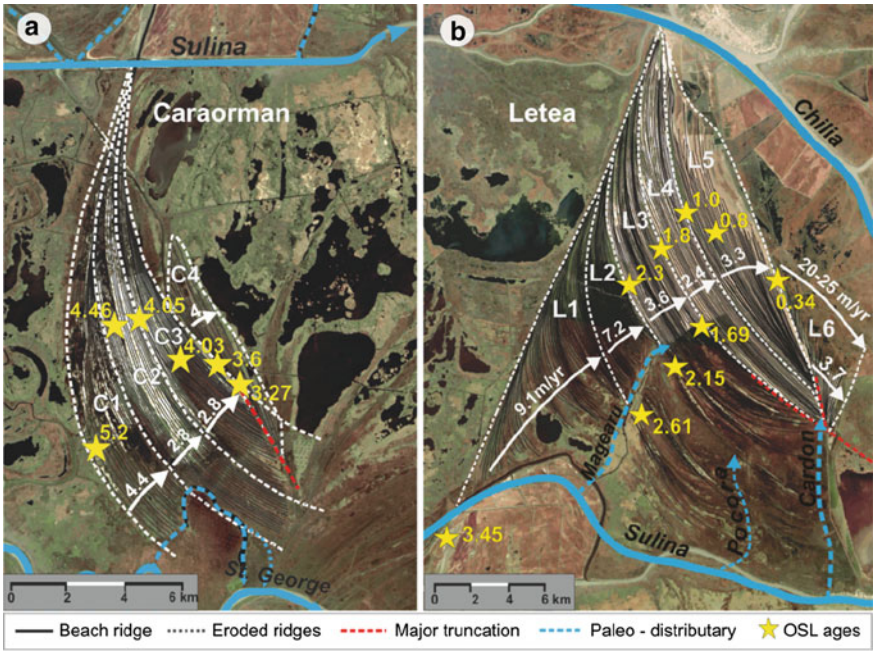

Fig. 22.6 Configuration of Caraorman (**a**) and Letea (**b**) beach ridge plains. Please see the OSL ages and progradation rates specific to the individualized ridgesets (reproduced from Vespremeanu-Stroe et al. 2016)

8–9 m/year near the river mouth, gradually decreasing sideways both updrift and downdrift (Fig. 22.7).

The geochronologic, stratigraphic and paleontologic evidences recently produced by Bony et al. (2015) near Doloşman cape (O2 core; Fig. 22.1) (location of Orgame ancient city foundation), show that a transition from open-coast to semi-enclosed environment occurred at 3.5 ka (marine to lagoon) and another change (from mesohaline to oligohaline lagoon) during 2.2–2.0 ka. This indicates that the northern part of the Goloviţa Lake evolved directly from coastal shoreface

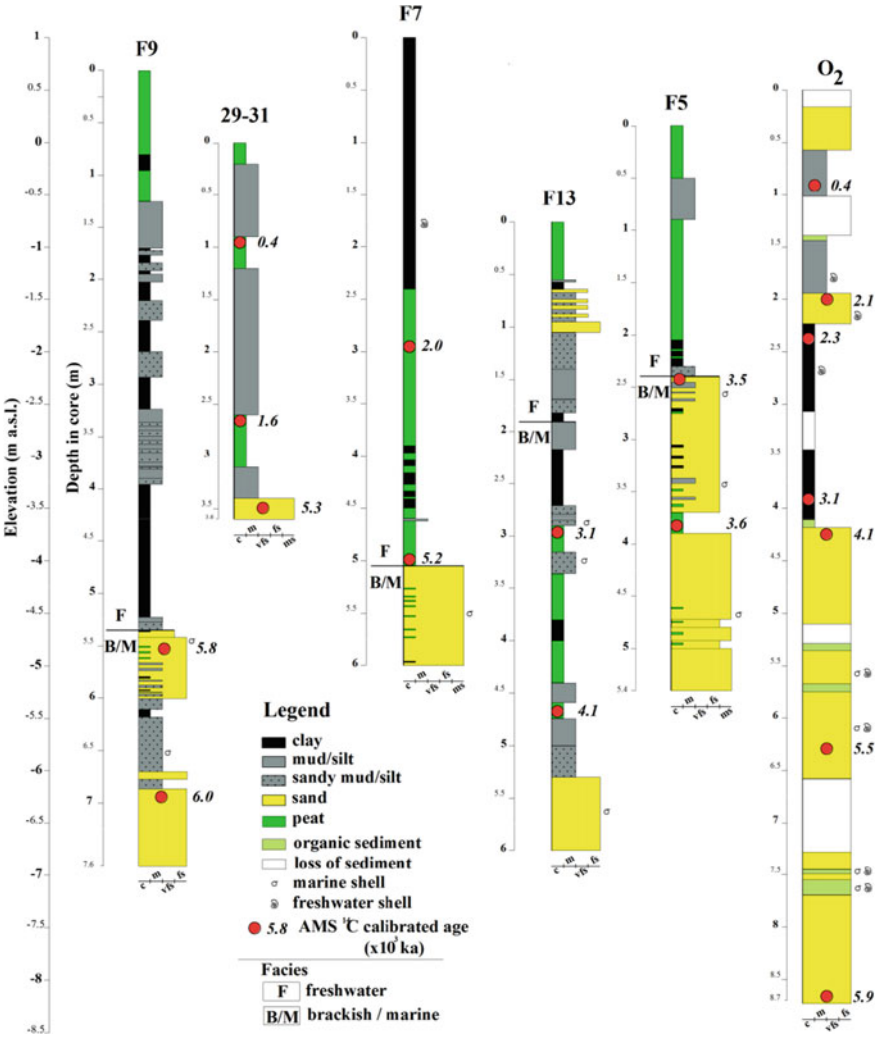

Fig. 22.7 Stratigraphy of old Sf. Gheorghe (SG1) deltaic lobe and adjacent southern region (after Vespremeanu-Stroe et al. submitted)

to a lagoon environment enclosed by a barrier which allowed the water transfer through inlets and around the barrier distal tip. Most probably, Razelm–Goloviţa lagoon system has been separated by the sea through a series of spits.

Today, the morphology of the downdrift lobe side is only partially indicative of the original configuration as intensive subsidence movements related to both neotectonics and sediments compaction affected the deltaic territory southward of Sf. Gheorghe arm (Polonic et al. 1999; Vespremeanu-Stroe et al. 2013). Stratigraphic investigations revealed characteristics of a subsided barrier-marsh plain that was afterwards covered with surficial layers of peat, silts and clays, conferring the monotonous aspect of the marshy delta plain, developed between Sf. Gheorghe branch and Razelm Lagoon (Fig. 22.7). It consists mainly of a marshy delta plain at the north currently overlaying the presumed drowned former barrier-marsh plain, a large lagoon system (Razelm–Goloviţa) in the west and a few narrow and NE-SW elongated, partially submerged beach ridges in the south.

Sulina Lobe (3.5–2.0/1.35 ka)

The Sulina branch breached the initial spit 3.5 ka ago empowered by an avulsion during an episode of avulsion which captured most of the Sf. Gheorghe discharge, and started to build a new open-coast lobe. Based on absolute chronology, high resolution stratigraphical investigations and morphological interpretations, very recent studies distinguished three different stages of Sulina lobe development: (i) an initial moderate expansion (3.5–3.3 kyear: 10–15 m/year), followed by (ii) a long-lasting fast expansion (3.3–2 ka: 20–27 m/year) and (iii) the lobe decay phase with the progradation restricted only to the southernmost secondary branch (Împuţita: 2.0–1.35 ka), followed by a generalized erosion afterwards (post 1.35 ka) (Vespremeanu et al. submitted). During the first stage (3.5–3.3 ka), the relatively weak river flow permitted a significant part of the allochtonous sediments carried by longshore currents to bypass the river mouth enabling sand accumulation downdrift which joined the eastern part of Caraorman b.r.p. After the 3.3 ka moment, Sulina branch experiences its fast advancement rate, which characterized most of its active existence. During this fast progradation stage (3.3–2 ka), the surface growth rates of the lobe exhibit a threefold increase, reaching up to 42 km^2/100 years (3.3–2.6 ka) and 68 km^2/100 years (2.6–2 ka), reflecting the strengthening of the discharge on the Sulina branch and the inception of Letea b.r.p. development, which stands out as the largest ridge plain in the Danube Delta (Figs. 22.6b and 22.8).

Sulina lobe entered in a decline phase ca. 2000 years ago when the new evolution pattern started exhibiting massive erosion of the lobe front and slow progradation along its flanks. At the updrift side, Letea plain is fed by the northern LST-borne allochthonous sediments, while the downdrift distal sector of the lobe is supplied with sediments resulted from the reworking of the lobe protuberance and through the direct discharge of Împuţita, which was the last active distributary of

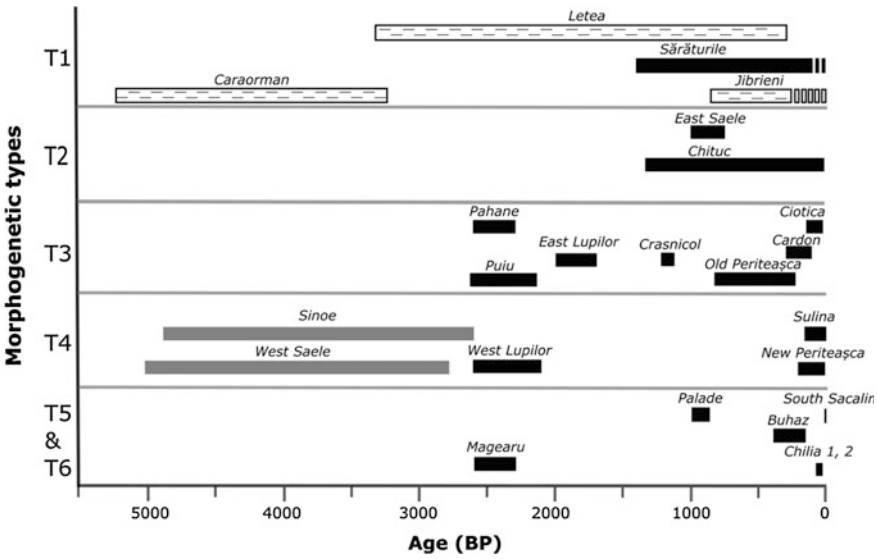

Fig. 22.8 The morphochronological template of Danube Delta beach ridge plains (from Vespremeanu-Stroe et al. 2016)

Sulina (Preoteasa et al. 2016). As a result, a barrier-marsh plain which prograded at mean rates of 5–6 m/year developed downdrift of Împuţita mouth during 2–1.35 ka. Letea plain is composed of non-Danubian quartz rich sands down to a depth of 18–20 m (Liteanu and Pricăjan 1963), whereas on the downdrift side of the lobe barrier-marsh plains developed as a result of the cyclic recurrence of barrier islands and spits which trapped riverborne sands and silts, and to a lesser proportion allochthonous sediments which succeeded to bypass the river mouths (Vespremeanu et al. submitted).

Although presently carrying 19 % of the Danube's waters due to channel regulation works (started since the mid-nineteenth century) that doubled its discharge in the early twentieth century compared to mid-nineteenth century, Sulina distributary certainly had a much greater percentage of Danube's flow at the time of lobe development. This convergence acting over the large timespan of Sulina activity (more than 2000 years) created a complex lobe in morphological terms in which large beach ridge plains with massive dunes and barrier-marsh plains containing loosely spaced barriers and large lakes coexist. The northern updrift half hosts complexes of large parabolic dunes which are not a common presence in river deltas whilst the downdrift part of the lobe is occupied by numerous lakes of various size, with surfaces ranging from 1 to 20 km^2 that are remnants of former large lagoons which became enclosed by barriers and spits.

In accordance with the natural continuation of the existing beach ridges formed each side of the Sulina arm mouth, the maximal extension of the mouth (2000 years ago) was located 6–7 km offshore, as was earlier assumed by Brătescu (1921) and

Vâlsan (1934). The subsequent erosion of Sulina fed the downdrift Sărăturile b.r. p. which is formally part of the Modern Sf. Gheorghe lobe.

Dunavăţ Lobes (2.6–2 ka / 2–1.3 ka)

The southern delta evolution was disputed between the two main morphogenetic theories: (i) the result of deltaic lobes construction and reworking (Antipa 1914; Panin 1983, 2003), versus (ii) built by LST-driven sandy barriers (Brătescu 1921; Vâlsan 1934; de Martonne 1931; Zenkovich 1956; Mihăilescu 1947; Coteţ 1960; Giosan et al. 2005, 2006, 2012; Bony et al. 2015). Our recent studies focused on the reconstruction of the Histria coastal region evolution brought new data proving the southern delta was initially developed by Dunavăţ branch and explain the current puzzle-like morphology through the combined action of neotectonics and wave reworking following lobe switching (Vespremeanu-Stroe et al. 2013; Preoteasa et al. 2013).

For reconstructing the early phase of Dunavăţ distributary one has to track the Old Sf. Gheorghe (SG1) lobe delta plain transformations following its abandonment at ca. 3500 BP. The downdrift plain of the abandoned SG1 lobe started to subside differentially the initial topography (lower rates in north and significantly higher in the south). At the present, the upper stratigraphy of the delta plain, the surficial layer overlying marine sands, respectively, looks very similar with that of the fluvial delta, namely of the Old Danube Lobe, indicating a common evolutionary pattern specific to a late stage of fluvial aggradation which followed the early delta front advancement (Vespremeanu-Stroe et al. submitted). Therefore, excepting the F9 core which intercepted the levees of Dunavăţ branch, all the other cores undertaken in the marshy delta plain (between Sf. Gheorghe branch and Razelm Lake) contain a massive peat layer accommodated on the upper delta front (foreshore) sands (Fig. 22.7) at 3–5.5 m indicating the lack of fluvial sediments flux toward inner delta and the "drowning" of the early delta plain.

Fluvial aggradation has initiated at very different times, as indicated by the age of the peat top layer or that of the siliciclastic sediments overlying peat: between 3.3–3.0 ka (F13 and F5) and 2–1.7 ka (F7 and F31). This is also in accordance with the sedimentation rates assessed by Bony et al. (2015) in the Goloviţa Lake (O2 core) which record the highest mean values in the 3.1–2.35 ka interval (2.4 mm/year), which should be interpreted as response to an active intern (intralagoon) distributary discharging sediments not far of Doloşman Cape (<10 km). All these data contradict the former theory of a lacustrine lobe developed since 2.0–1.8 ka by Dunavăţ into Razelm–Goloviţa Lakes (Giosan et al. 2006) and argue for a continuous but moderate fluvial aggradation at least for the last 3000 years, occurring in several local phases.

A new open-coast lobe (Old Dunavăţ: D1) starts building in front of the current Periteaşca b.r.p. around 2.6 ka in conformity with the OSL ages of Pahane (2.58 ka) and Lupilor Old (2.66 ka) beach ridges (Fig. 22.3c). Nowadays, only a sector of the downdrift unit remained visible from D1 lobe because the rest was

reworked by waves after its abandonment or subsided. However, the quick restart of the progradation in front of Lupilor barrier, around 2000–1900 years BP (Vespremeanu-Stroe et al. 2013), advocates for a switch of the Dunavăţ on a new southern route and the inception of a new open-coast lobe (New Dunavăţ: D2) at ca. 16–20 km south of D1 lobe. Accordingly, the Old Dunavăţ lobe lasted between 2.6–2.0 ka, being afterwards abandoned syncronously with the Sulina lobe, during the period of major avulsions from Danube Delta (2100–1900 years BP). Taking into account the significantly faster progradation of the New Dunavăţ lobe (in comparison with D1), it means that the new course of Dunavăţ benefited of a larger flow after lobe switching. The OSL ages sampled from sandy ridges belonging to early to late (*I1, C1* samples) stages of the New Dunavăţ lobe, set its age to 2.0–1.3 ka BP (Fig. 22.3d) and establish it was younger and more active than previously considered by Panin (1983, 2003).

Modern Sf. Gheorghe Lobe (2.1/1.4 ka—Present)

The next phase of progradation in the front of the old Sf. Gheorghe lobe (abandoned ca 3.5 ka) will start about 1400 years later (2.1 ka), triggered by the gradual reactivation of the Sf. Gheorghe modern course.

After the abandonment of the Sulina lobe triggered by the fluvial discharge switch in favor of Sf. Gheorghe (with most of the flow still redirected on Dunavăţ), the river mouth started to advance slowly at mean rates of 2–4 m/year with a gradual increase during 1.5–1.2 ka, as a result of the successive avulsions which redistributed more water and sediment captured from the neighboring branches of Împuţita and Dunavăţ. Since that moment (since 1.2 ka) till the early twentieth century, the river mouth advanced seawards rather uniformly, with a mean rate of 10 m/year.

Like any other maritime lobe developed within the unidirectional wave climate of the Danube Delta, the modern Sf. Gheorghe lobe has been built asymmetrically on each side of the homonymous arm mouth. Morphological and sedimentological analyses together with a newly obtained chronology throw light on the multiple ridgeset (10) structure of Sf. Gheorghe lobe (Fig. 22.9), each of them (except for the first one) following a common evolutionary pattern reflected by the cyclic succession of the recurring stages: (i) subaqueous deposition and the outgrowth of the mouth bar; (ii) barrier island emergence, and (iii) transformation into a barrier spit (with several secondary spits) that later become encased into the muddy deltaic plain as narrow sandy ridges, building out on the downdrift side of the lobe as a barrier-marsh plain (Preoteasa et al. 2016).

Updrift of the river mouth, the groin effect exerted by the mouth bar and fluvial currents for the longshore carried sediments results in gently decreasing depths and intermediate to dissipative beaches, the constant progradation of which generates successive beach and foredune ridges composing the Sărăturile ridge plain. Downdrift of the river mouth, the alternation between the exposed and

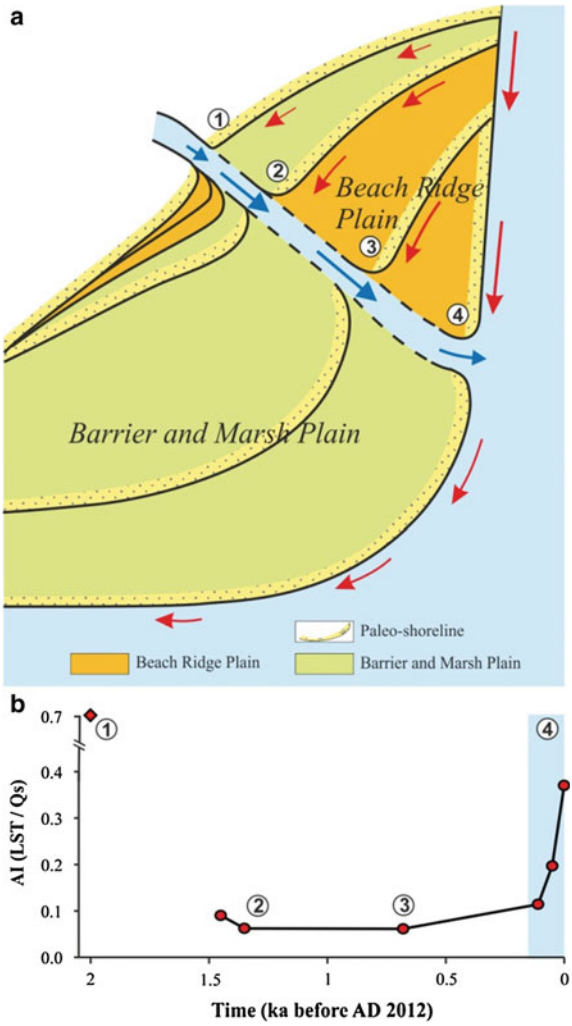

Fig. 22.9 **a** Schematic illustration of the modern Sf. Gheorghe (SG2) lobe morphology under alternatively changing longshore and fluvial sediment transport; **b** Sedimentary index—*Si* (defined as the ratio of longshore sediment transport—*LST* and Danube sediment discharge—*Qs*) evolution. Please notice the correspondence between figures **a** and **b** of the four (1–4) stages in lobe evolution: stage 1 corresponds to the early stage S1 and stages 2–4 describe the cyclic evolution of the lobe (S2–S10 stages in Fig. 22.10). Reproduced from Preoteasa et al. (2016)

sheltered-state environments relative to the prevalent northeastern waves determined by the cyclic arm mouth bar and updrift ridge formation, led to the emplacement of alternating facies of sandy ridges separated by surficial marshy depressions into a barrier-marsh plain. The evolutionary model of the modern Sf. Gheorghe deltaic lobe was primarily controlled by the ratio between waves and river-born sediment (Si) which variations influence the mouth bar development (position and volume) that in turn, proved to have a key role in determining the timing of each evolutionary phase and the morphology of barrier-marsh plain ridgesets. The Si maintained constantly low values ($Si \leq 0.1$) through the lobe development, allowing a constant evolution (Fig. 22.10). Although the size and lifespan of each ridgeset increased exponentially with every new cycle (the latest

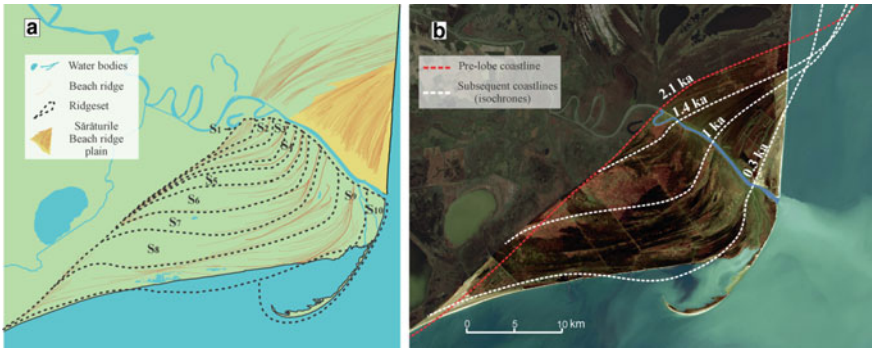

Fig. 22.10 The evolution of the modern Sf. Gheorghe (SG2) lobe. **a** Map of beach ridges and of ridgesets (S1–S10) within the barrier-marsh plain (*downdrift*) and beach ridge plains (*updrift*) (from Preoteasa et al. 2016). **b** Reconstruction of the successive coastlines. 2013 Landsat image in the background

cycles lasting 4–5 times longer than the first ones: 200–440 years versus 50–80 years), due to the constant lengthening of the associated coastline and rapidly increasing nearshore depths, the preservation of low Si and constant river mouth advancing rates enabled a uniform development pattern of the lobe. The recent evolution of the river mouth suggests significant changes as a consequence of human-induced depletion of sediments supplied by the Danube flow (which decreased threefold during twentieth century), and is mainly expressed by the complete cessation of the updrift coastal progradation and of river mouth long-term seaward expansion in favor of downdrift migration. This is indicative of the transition of the Sf. Gheorghe mouth from an asymmetric to a deflected wave-influenced delta morphology, whose current developments mark a significant change in the multicentennial cyclic evolutionary pattern (Preoteasa et al. 2016).

Modern Chilia Lobe (0.9 ka—Present)

The youngest lobe in the Danube Delta currently develops under the combined influence of the river and waves at the mouth of Chilia arm, occupying 8 % of the present day Danube Delta surface. It is the third deltaic lobe built by Chilia distributary in the Danube Delta following two inner lobes formed in lacustrine–lagoon conditions in its way to the Black Sea and the first of them which encountered an open-coast regime. The study of Vespremeanu-Stroe et al. (submitted) distinguished three phases in the contemporary Chilia III lobe development since its inception: (i) wave-dominated river mouth (0.9–0.25 ka); (ii) fluvial dominated development (1750–1950 AD); (iii) wave-influenced lobe under anthropogenic pressure (1950—present).

Recent studies report the inception of the Chilia open-coast lobe around 0.3 ka (Mikhailova and Levashova 2001; Filip and Giosan 2014) after Sf. Gheorghe discharge decreased in favor of Chilia arm or much earlier ~0.9 ka (Vespremeanu-Stroe et al. submitted).

According to the new absolute chronology, recorded both updrift (West Jibrieni: 0.79 ka) and downdrift (Eastern Letea: 0.81 ka, 1.2 ka) of the Chilia branch, the initial phase (with a *wave-dominated development*) started ca. 0.9 ka and lasted until ca. 1750 AD when increase in the Chilia sediment load triggered the rapid expansion of the lobe (Vespremeanu-Stroe et al. submitted). The downdrift accumulation zone is composed of low quasi planar beach ridges made up of sediments with a higher content of feldspar and mica indicating the riverine source of sediments, which aligned westward by the latest deposited beach ridges from the Letea b.r.p., part of the Sulina lobe formation. The evolutionary pattern of the Letea ridges is reversed from downdrift diverging to updrift diverging at 0.9 ka indicating an updrift avulsion of the river mouth (Fig. 22.6b). The slightly concave shoreline represents a legacy of the initial embayment plan view shape. The surface growth rates of the Jibrieni plain (2.3 km^2/100 years) indicate significant sediment bypass over the mouth whilst the overall (7 km^2/100 years) reflects a lesser contribution of fluvial sediments in the building of the lobe.

As a consequence of a low discharging river mouth under asymmetric wave influence during this stage, successive deflections of the river mouth occurred where spits were anchored by the northern side (sometimes breached) leaving encased lakes such as the Nebunu in the northern tip of the Letea b.r.p.

The next phase (*fluvial dominated development)* lasted from ca. 1750 to 1950 AD and is morphologically characterized by a fractal branching distributary network created by the bifurcation caused by river mouth bar formation. The rapid advancement of secondary distributary mouths which number increased from 12 in 1856 to 20 in 1898 and up to 30 in 1935–1944, created an indented shoreline as indicated by the historical maps. Oceakov, Bistroe and Stambul preserved as the largest branches which, by their positions and orientations fostered the radial growth of the lobe since 1750 at a mean constant rate of about 100 m/year, although growth in surface increased from 134 km^2/100 years (mid-nineteenth century) to 196 km^2/100 years (the 1900s) and then to 306 km^2/100 years (the 1950s). The lobe development unfolded under the increasing contribution of the fluvial discharge, by the infilling of the previous Chilia 2 lobe (Roşca–Merhei and Lisky–Prymorske basins) growing proportion of water and sediment flow over Chilia channel (to ca. 70 % of the Danube's discharge) and sediment supply increase by the anthropogenic deforestation in the lower Danube watershed (Kaplan et al. 2009; Giosan et al. 2012; Filip and Giosan 2014).

Since the middle of the twentieth century, the Chilia arm underwent a rapid discharge decrease, from 72 % (of the Danube's flow) in 1910 to 54.3 % in 1991–2000 (Gâştescu 2009) whilst sediment retention by dams built further upstream induced severe sediment depletion causing the clogging of the most river mouths which number dropped from 30 in 1944, to only 10 currently active. Therefore,

during the anthropogenic period (1950—present) the changes of the hydrological regime fostered the shoreline to become wave-shaped building the first generations of barriers and spits (Oceakov, Bistroe and Musura–Stambul) at the mouths of the largest secondary channels of Chilia arm, while the previously protruding arm mouths entered into a receding stage like in the case of Oceakov arm which retreating rates reached of up to 50 m/year. Presently, progradation is observed only close and in-between the Bistroe and Stambul mouths and at the Jibrieni spits in the north, where beach ridge plains prograde at rates close to 10 m/year.

Beach Ridge Plains

Beach ridge plains (b.r.p.) are a common feature of the wave-influenced deltaic lobes, that are created by juxtaposition of successive berms on the prograding sandy coasts with different shapes and sizes depending on the accretionary mechanisms and the accommodation space (Vespremeanu-Stroe et al. 2016).

The Danube Delta b.r.p. are all part of the maritime delta, and started forming around 5.5 ka after the relative stabilization of the sea level. They developed at different moments in association with the prograding coasts with rich sediment source that remains trapped in the nearshore and gets redistributed to the foreshore and backshore by waves and wind.

The different possibilities to maintain a prograding coast imply a variety of conditions favorable for b.r.p. genesis and evolution (Fig. 22.8) in the Danube Delta which is reflected in the six main types of ridge plains accommodated on: (i) the updrift side of asymmetric wave-influenced deltaic lobes; (ii) littoral cell end positioned at delta-mainland boundary; (iii) downdrift shoreline convergence zone of a rapid prograding lobe; (iv) progradation of embayed coasts; (v) prograding barrier spits associated with river mouths; (vi) prograding interdistributary barriers (Vespremeanu-Stroe et al. accepted). The first type (updrift side of asymmetric wave-influenced deltaic lobes) originates at the interactions between the fluvial currents from the Danube's distributaries and the longshore currents which generate hydraulic and morphologic groin effects (Komar 1973; Giosan 2007) restricting sediment bypass downcoast and creating progradational conditions for the updrift side. These conditions favored the construction of 2/3 of all Danube Delta b.r.p., which correspond to the updrift side of lobes Sf. Gheorghe (Caraorman and Sărăturile), Sulina (Letea) and Chilia (Jibrieni). Type 2 occurs at the littoral cell end, at the contact with the mainland shoreline and is responsible for the construction of the Chituc–East Saele b.r.p. (1.4 ka—present). Accumulative conditions of the type 3 occur at the distal downdrift part of lobes where wave sheltering created by the deltaic lobe protuberance fosters the local counterdrift (oriented northeastward) toward the mouth and creates a "cul-de-sac" for sediments (Anthony 2015). Cardon, Puiu West, Puiu East, Crasnicol, Old Periteaşca, Ciotica, Pahane and Lupilor East have a rotational clockwise pattern and usually fade into deltaic barrier-marsh plain or delta plain muds. Type 4 b.r.p. develop in regions of LST

convergence (New Periteaşca) or where the alongshore wave energy gradient decreases favoring accumulation (Saele West, Sinoe, Sulina). The downdrift distal ends of spits or near river mouths can exhibit conditions that generate the emergence of type 5 b.r.p. These occur in the modern Sf. Gheorghe lobe as Palade, Buhaz and Sacalin South or on the prograding barrier spits successively formed downdrift of Magearu branch. The interdistributary prograding barriers of the contemporaneous lobe of Chilia are part of type 6 b.r.p. (Bistroe and Stambulul Vechi) which reflects the early stage of development with an elongated and narrow shape.

The two biggest b.r.p. in the Danube Delta are Caraorman (5.5–3.2 ka) and Letea (3.5–0.1 ka) and now occupy a central position in the deltaic plain, developing over millennial timescales. They are composed of smaller ridgesets with specific morphometric characteristics and progradation rates characterized by fast progradation of the initial and last sets, and slow progradation of the central sets. The first case (fast progradation) imposes narrow beach ridges, covered by thin (<1 m) aeolian deposits versus higher foredune ridges (developed on the slowly prograding ridgesets) which were later reworked into complex dunefields with large parabolic dunes (Caraorman) and parabolic dune complexes (Letea). This decrease in progradation rates is attributed to the increase in volume of the accommodation space caused by the seaward migration of the river mouth which blocks the LST and lengthens the littoral cell (Caraorman), while the activation/deactivation of secondary branches (via avulsions or bifurcations) significantly alters the b.r.p. progradation rates (Vespremeanu-Stroe et al. 2016).

Conclusions

We propose a revised and complete evolutionary model of the Danube delta which tries to elucidate the old fluvial delta development and brings new insights into the maritime delta lobe switching and large-scale coastal dynamics. We used morphological and morphometric analyses, stratigraphic evidence and geochronology, integrated with the concepts of coastal development under a storm asymmetric climate, variable sea level rise, LST supply and river mouth dynamics principles. The fluvial delta construction comprises two major phases: (i) the early delta front advancement into the Danube Bay and (ii) the late delta stage of fluvial aggradation. The first phase lasted from 8/7.5 to 5.5 ka and corresponds to the Old Danube lobe, when almost 2/3 of the current fluvial delta was built, characterised by a temporal lag between the southern (Sf. Gheorghe) and central unit (proto-Sulina). We suggest that the initial spit started to influence the delta formation only since 6.5 ka, when it gradually closed the northern Bay, affecting sediment deposition into the new-formed lagoon. The second phase developed during the last 5.5 ka and it was characterised by fluvial and peat aggradation.

Since 5.5 ka, the Danube has sprouted into six open-coast lobes with distinctive surfaces and progradation rates as a result of the various degrees of wave and fluvial influence as indicated by the plan shape morphological features (beach ridge plains,

barrier-marsh plains, mud plains). The lobe dynamics of Sulina, Sfântu Gheorghe, and Chilia share a common evolutionary pattern which consists in a first stage of slower development and higher wave influence, a second stage of increasing sediment deposition and a final stage (of decay) in which either authigenic or human-induced changes cause a shift in the development pattern, which increases wave influence and leads to adjustment and finally abandonment.

Concerning the southern Danube Delta, the present work brings new data proving that this compartment was initially developed by Dunavăţ branch (two lobes) and explains the current puzzle-like morphology through the combined action of subsidence, neotectonics and wave reworking following lobe switching.

Acknowledgments Research activities were undertaken in the frame of Sfântu Gheorghe Marine and Fluvial Research Station, Faculty of Geography, University of Bucharest. We are grateful to all our colleagues participating to field campaigns: Cristi Ţepurică, Liliana Croitoru, Florin Voicu and Diana Hanganu. We are highly indebt to our colleague Dr. Sabin Rotaru who helped us in field campaigns, data analysis and stratigraphy columns drawing. We thank Dr. Marius Stoica for guidance in microfaunal sample analysis. This work has been carried out thanks to the support of the project number PNII-RU-TE-2011-3-0293 awarded to AVS and PN-II-RU-TE-2014-4-2527 awarded to LP, funded by the Romanian National Authority for Scientific Research (CNCS-UEFISCDI).

References

Anthony EJ (2015) Wave influence in the construction, shaping and destruction of river deltas: a review. Mar Geol 361:53–78

Antipa G (1914) Câteva probleme ştiinţifice şi economice privitoare la Delta Dunării. An. Acad. Rom., Mem. Sect. St. 2(36):61–135 (in Romanian)

Ashton AD, Giosan L (2011) Wave-angle control of delta evolution. Geophys Res Lett 38: L13405. doi:10.1029/2011GL047630

Ashton AD, Murray AB (2005) Delta simulations using a one-line model coupled with overwash. Coastal Dynamics '05, Barcelona, Spain

Banu AC, Rudescu L (1965) Delta Dunării, Bucureşti (in Romanian)

Bhattacharya JP, Giosan L (2003) Wave-influenced deltas: geomorphological implications for facies reconstruction. Sedimentology 50(1):187–210

Bony G, Morhange C, Marriner N, Baralis A, Kaniewski D, Rossignol I, Lungu V (2015) History and influence of the Danube Delta lobes on the evolution of the ancient harbour of Orgame (Dobrogea, Romania). J Archaeol Sci 61:186–203

Brătescu C (1921) Contribuţii la studiul deltei dunărene. Evoluţia morfologică şi cronologică a ei. BSRG 30:35–56 (in Romanian)

Brückner H, Kelterbaum D, Marunchak O, Porotov A, Vött A (2010) The Holocene sea level history since 7500 BP—lessons from the eastern Mediterranean, the Black and Azov seas. Quatern Int 225(2):160–179

Buynevich IV, Bitinas A, Pupienis D (2015) Aeolian sand invasion: georadar signatures from the Curonian Spit dunes, Lithuania. In: Randazzo G, Cooper JAG, Jackson D (eds) Sand and gravel spits. Springer, pp 67–78

Carozza JM, Micu C, Mihail F, Carozza L (2012) Landscape change and archaeological settlements in the lower Danube valley and delta from early Neolithic to Chalcolithic time: a review. Quatern Int 261:21–31

Carozza JM, Carozza L, Radu V, Leveque F, Micu M, Burens-Carozza A, Opreanu G, Haită C, Danu D (2013) Apres le deluge: evolution geomorphologique du delta du Danube après la reconnexion Mer Noire-Mer Mediterannee et ses implications sur le peuplement eneolitique-chalcolitique. Quaternaire, Centre National de la Recherche Scientifique 24 (4):503–512

Coteţ PV (1960) Evoluţia morfohidrografică a deltei Dunării. Probleme de geografie VII (in Romanian)

de Martonne E (1931) Europe Centrale, II. Paris, pp 786–787

Del Rio L, Benavente J, Gracia FJ, Alonso C, Rodriguez-Polo S (2015) Anthropogenic influence on spit dynamics at various timescales: case study in the Bay of Cadiz (Spain). In: Randazzo G, Cooper JAG, Jackson D (eds) Sand and gravel spits. Springer, pp 123–138

Filip F, Giosan L (2014) Evolution of Chilia lobes of the Danube Delta: reorganization of deltaic processes under cultural pressure. Anthropocene 5:65–70

Gâştescu P (2009) The Danube Delta biosphere reserve. Geography, biodiversity, protection, management. Rev Roum Géogr/Rom J Geogr 53(2):139–152

Ghenea C, Mihăilescu N (1991) Palaeogeography of the lower Danube Valley and Danube Delta during the last 15000 years. In: Starkel L, Gregory KJ, Thornes JB (eds) Temperate palaeohydrology; fluvial processes in the temperate zone during the last 15000 years. Wiley, New York, p 548

Giosan L (2007) Morphodynamic feedbacks on deltaic coasts: lessons from the wave-dominated Danube Delta. In: Proceedings of coastal sediments, pp 828–841

Giosan L, Vespremeanu E, Donnelly JP, Bhattacharya J, Buonaiuto F (2005) River delta morphodynamics: examples from the Danube Delta. In: Giosan L, Bhattacharya J (eds) River deltas: concepts, models, case studies. SEPM Special Publication 83, pp 391–410

Giosan L, Donnelly JP, Constantinescu Ş, Filip F, Ovejanu I, Vespremeanu-Stroe A, Vespremeanu E, Duller GAT (2006) Young Danube Delta documents stable Black Sea level since the middle Holocene: morphodynamic, paleogeographic, and archaeological implications. Geology 34(9):757–760

Giosan L, Coolen M, Kaplan JO, Constantinescu S, Filip F, Filipova-Marinova M, Kettner AJ, Thom N (2012) Early anthropogenic transformation of the Danube-Black Sea system. Sci. Rep. 2:1–6

Giosan L, Constantinescu Ş, Filip F, Deng B (2013) Maintenance of large deltas through channelization: nature vs. humans in the Danube delta. Anthropocene 1:35–45

Jerolmack DJ, Swenson JB (2007) Scaling relationships and evolution of distributary networks on wave-influenced deltas. Geophys Res Lett 34(23):L23402

Kaplan JO, Krumhardt KM, Zimmerman NE (2009) The prehistoric and preindustrial deforestation of Europe. Quatern Sci Rev 28:3016–3034

Komar PD (1973) Computer models of delta growth due to sediment input from rivers and longshore transport: Geological Society of America. Bulletin 84:2217–2226

Li W, Bhattacharya JP, Yingmin W (2011) Delta asymmetry: concepts, characteristics and depositional models. Petroleum Science 8:278–289

Liteanu E, Pricăjan A (1963) Alcătuirea geologică a Deltei Dunării: Hidrobiologia 4:57–82 (in Romanian)

Mihăilescu V (1947) Geografia României. Facultatea de Ştiinţe, Bucureşti (in Romanian)

Mikhailova MV, Levashova EA (2001) Sediment balance in the Danube river mouth. Water Resour 28:180–184

Panin N (1972) Histoire Quaternaire du Delta du Danube. Essai d'interpretation des facies des depots deltaiques. Cercetări Marine 4:5–15

Panin N (1983) Black Sea coast line changes in the last 10,000 years. A new attempt at identifying the Danube mouth as described by the ancients. Dacia 27:175–184

Panin N (1989) Danube Delta. Genesis, evolution and sedimentology. Revue Roumaine de Geologie, Geophysique, Geographie 33:25–36

Panin N (2003) The Danube delta geomorphology and Holocene evolution: a synthesis. Géomorphologie 4:247–262

Panin N, Panin S, Herz N, Noakes JE (1983) Radiocarbon dating of the Danube delta deposits. Quatern Res 19:249–255

Polonic G, Zugrăvescu D, Horomnea M, Dragomir V (1999) Crustal vertical recent movements and the geodynamic compartments of Romanian Territory, Istanbul, Turkey. In: 2nd Balkan Geophysical Congress. Book of Abstracts 300–301

Popp N (1961) Caracterizarea litologică a pământurilor Deltei Dunării pe baza datelor de foraj. Meteorologia, hidrologia şi gospodărirea apelor 4:126–139

Popp N (1965) Geneza şi evoluţia Deltei Dunării în general şi a stufăriilor în special. In: Monografia stufului din Delta Dunării, pp 13–23 (in Romanian)

Preoteasa L, Vespremeanu-Stroe A, Hanganu D, Katona O, Timar-Gabor A (2013) Coastal changes from open coast to present lagoon system in Histria region (Danube Delta). In: Conley DC, Masselink G, Russell PE, O'Hare TJ (eds) Proceedings of the 12th international coastal symposium (Plymouth, England), J Coast Res SI 65:564–569

Preoteasa L, Vespremeanu-Stroe A, Tatui F, Zăinescu F, Gabor-Timar A, Cârdan I (2016) The evolution of an asymmetric deltaic lobe (Sf. Gheorghe, Danube) in association with cyclic development of the river-mouth bar: long-term pattern and present adaptations to human-induced sediment depletion. Geomorphology 253:59–73

Romanescu G (2009) The geomorphological evolution of the Razim-Sinoie barrier spit during the historical periods. Pontica 42:493–517

Slanar H (1945) Zur Kartographie und Morphologie des Donaudeltas. Mitteilungen der geogr. Gesselschaft 1–12. Wien

Soulet G, Menot G, Lericolais G, Bard E (2011) A revised calendar age for the last reconnection of the Black Sea to the global ocean. Quatern Sci Rev 30(9–10):1019–1026

Stanley DJ, Warne A (1994) Worldwide initiation of Holocene marine deltas by deceleration of sea-level rise. Science 265(5169):228–231

Ştefănescu CM (1982) La formation et l'evolution du delta du Danube. Comite des Traveaux Histoiques et Scientifiques, Biblioteque Nationale, Paris

Syvitski JPM, Kettner AJ, Overeem I, Hutton EWH, Hannon MT, Brakenridge GR, Day J, Vorosmarty C, Saito Y, Giosan L, Nicholls RJ (2009) Sinking deltas due to human activities. Nat Geosci 2:681–686

Tamura T (2012) Beach ridges and prograded beach deposits as palaeoenvironment records. Earth Sci Rev 114:279–297

Vâlsan G (1934) Nouvelle hypothèse sur le Delta du Danube: Warsaw. Congrès International de Géographie, Comptes Rendus II:342–355

Vespremeanu-Stroe A, Preoteasa L (2015) Morphology and the cyclic evolution of Danube Delta spits. In: Randazzo G, Cooper JAG, Jackson D (eds) Sand and gravel spits. Springer, pp 327–339

Vespremeanu-Stroe A, Preoteasa L, Hanganu D, Brown T, Bîrzescu I, Toms P, Timar-Gabor A (2013) The impact of the Late Holocene coastal changes on the rise and decay of the ancient city of Histria (Southern Danube Delta). Quatern Int 293:245–256

Vespremeanu-Stroe A, Preoteasa L, Zăinescu F, Rotaru S, Croitoru L, Timar-Gabor A (2016) Formation of the Danube Delta bech ridge plains and signatures in morphology. Quatern Int

Vespremeanu-Stroe A et al. (submitted) Holocene evolution of the Danube delta: an integral reconstruction and a revised chronology. Marine Geology

Zenkovich VP (1956) Zagadka Dunaiskoi Delty. Priroda 45:86–90

Chapter 23
Danube Delta Coastline Evolution (1856–2010)

Alfred Vespremeanu-Stroe, Florin Tătui, Ștefan Constantinescu and Florin Zăinescu

Abstract Danube Delta coastline evolution showed a significant variability in the past 150 years related to different driving forces which change the leading role between them depending on the temporal and spatial scales taken into consideration. At long time scales (centuries), coastline dynamics is mainly driven by the dramatic decrease of Danube sediment discharge after 1950. This is pointed out by the significantly higher shoreline migration rates and area changes between 1856 and 1961/1979 in comparison with the subsequent period, especially along the accumulative sectors. As a consequence, since mid-twentieth century, Chilia lobe started the transition from fluvial-dominated morphology to wave-influenced aspect and behaviour. At multi-decadal scale, shoreline dynamics is ultimately driven by climate variability, related to North Atlantic Oscillation (NAO), which controls the storminess variations along the Danube Delta coast. From this point of view, there is a marked difference between the 1961–1979 time interval, characterised by dominantly negative NAO phase, which determined active storminess, inducing high shoreline mobility, and the 1979–2006 period, which showed less dynamic coastlines (on both prograding and erosive sectors) as a result of the lower storminess imposed by the dominance of positive NAO phase. At inter-annual scale, waterline morphodynamics is influenced by storm regime and river floods.

Keywords Delta coast erosion/progradation · Longshore sediment transport · Coastal storms · North Atlantic Oscillation · River mouth

A. Vespremeanu-Stroe · F. Tătui (✉) · Ş. Constantinescu · F. Zăinescu
Faculty of Geography, University of Bucharest, 1st N. Bălcescu Blv., sector 1, 010041 Bucharest, Romania
e-mail: florin.tatui@geo.unibuc.ro

M. Rădoane and A. Vespremeanu-Stroe (eds.), *Landform Dynamics and Evolution in Romania*, Springer Geography,
DOI 10.1007/978-3-319-32589-7_23

Introduction

Shoreline evolution is variable over a wide range of different temporal and spatial scales. This dynamic behaviour is caused by the very rapid adjustments of form and process that can undergo on sandy coasts. Along this type of coastal environment, periods of accretion and erosion are generally associated to low- and high-energy wave conditions, but they also exhibit strong site-specific variations depending on the time- and spatial scales taken into consideration.

On wave-dominated deltaic coasts, the medium- and long-term coastline evolution is controlled by the combined effects of wave climate (and the wave-driven nearshore circulation) and terrestrial sedimentary input represented by the delta-forming river solid discharge (Coleman and Wright 1975; Bhattacharya and Giosan 2003). These deltaic coasts crucially depend on sustained sediment supplies in order to maintain their shoreline position and to balance subsidence and erosion. Because of the general decreasing trend in river sediment supply, many of the world's river deltas are becoming vulnerable to accelerated erosion and subsidence and more exposed to flooding and sea-level rise (Ericson et al. 2006; Syvitski et al. 2009).

Despite the fact that the first measurements of Danube suspended sediment transport at river mouths date back to the beginning of the twentieth century (Almazov et al. 1963), there were only general theoretical data about bed load, very important for the construction of littoral deposits. These difficulties related to scarce in situ measurements, corroborated with a lack of good quality and reliable data of wave climate, nearshore currents and related sediment transport, made up very difficult the early analysis of deltaic coast (Gâştescu and Driga 1984; Vespremeanu and Ştefănescu 1988) and Danube river mouths (Vespremeanu 1983, 1984; Vespremeanu et al. 1986) morphodynamics and evolution.

After 1990, new information and data were obtained about Danube Delta coastal morpho- and hydrodynamics (Giosan 1998; Giosan et al. 1999; Stănică 2003; Vespremeanu-Stroe 2004, 2007) and state-of-the-art GIS shoreline detection and analysis techniques were employed based on historical maps, satellite images, aerial photos and GPS surveys, facilitating new types of analysis of shoreline behaviour at different timescales. Recent studies came up with new approaches of waterline dynamics at multi-annual and decadal time-scales as a result of climate variability (Vespremeanu et al. 2004; Vespremeanu-Stroe et al. 2007) and human activities (Ungureanu and Stănică 2000; Stănică et al. 2007) or of future projections of shoreline position (Stănică and Panin 2009) along the Danube Delta coast.

Our goal is to make a review of the recent findings related to Danube Delta shoreline dynamics and evolution in the past 150 years, emphasising the different factors which have driven the evolution at different timescales (from multi-annual to multi-decadal and centennial).

The multi-decadal waterline dynamics was analysed along 162 km of low-lying beaches superposed on the Romanian Danube Delta coast, from Musura Bay to Cape Midia (Fig. 23.1). In addition, Chilia deltaic shoreline, which covers

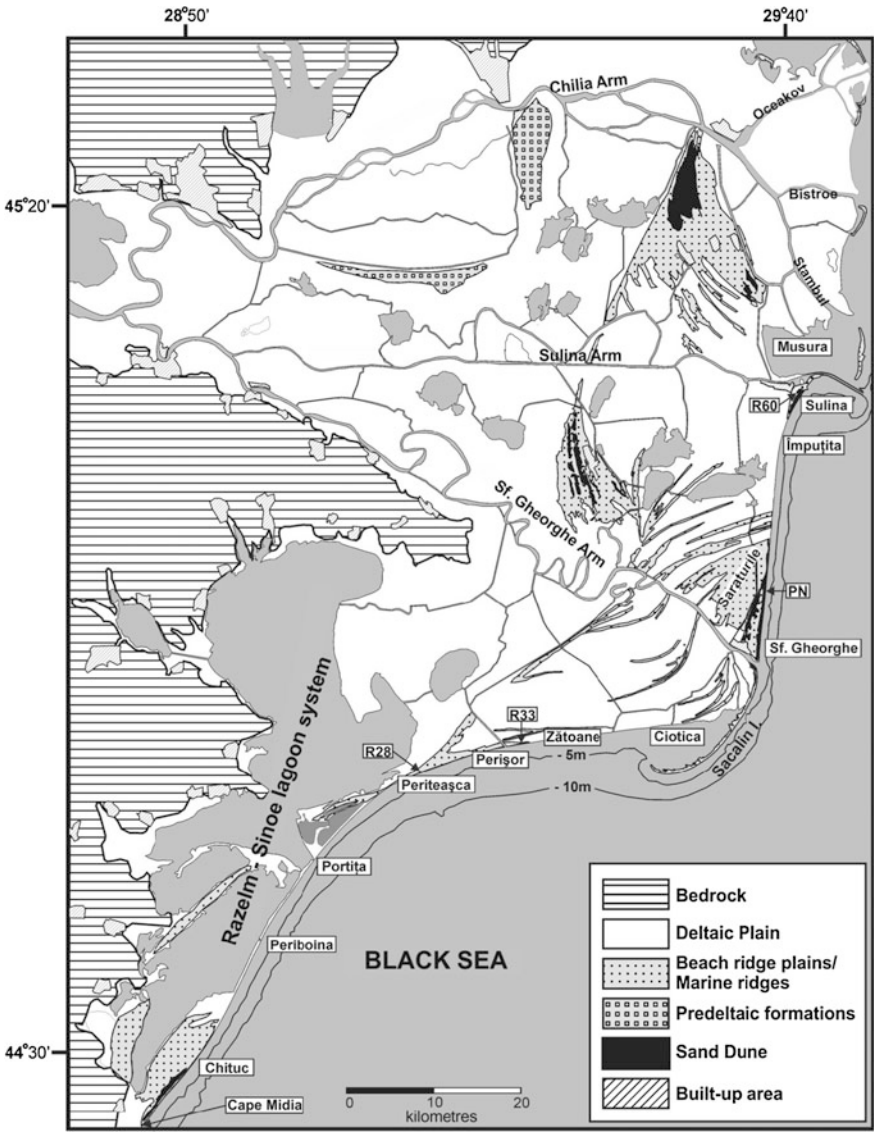

Fig. 23.1 Danube Delta coast. Please see in *black rectangles* the position of the coastal sectors and of the benchmarks used in the paper

Ukrainian Danube Delta coast, was taken into consideration while analysing coastline evolution in the past 150 years (Fig. 23.1). The Romanian Danube Delta coast consists of five littoral cells, most of them being dominated by erosion. Both the stable and prograding sectors have subaerial beaches with seasonally controlled morphology, displaying 15–25 m widths at the beginning of the spring and

30–50 m at the end of the summer due to the seasonal differences in wave climate and sea-level oscillations dependent on the Danube discharge (Vespremeanu-Stroe and Preoteasa 2007). The retreating sectors are characterised by narrow beaches, sometimes backed by washover fans. The wave climate is medium-energy, with a significant wave height of 1.4 m and a corresponding period of 5.5 s in deep water. During regular storms, offshore significant wave height increase to 2–4 m, peaking at 7 m during extreme storms. Waves from the north-eastern directions are dominant in terms of both magnitude and frequency.

Along the tideless and wave-dominated Danube delta coast, the longshore sediment transport (LST) was found to be the primary control on shoreline mobility (Giosan et al. 1999) due to the strong asymmetry in wave attack relative to shoreline orientation. Recent LST estimates for the Danube delta coast highlight the major role played by high-energy events. Thus, the LST computations for 1991–2000 interval point to an average amount of 1.25×10^6 m^3/year of sediment mobilised alongshore by storms, which is 62 % of the total LST; more important is the resultant LST during storms, which is responsible for 78 % of the net southward LST due to the high frequency of northern and north-eastern storms (Vespremeanu-Stroe 2004).

Coastline Evolution in the past 150 Years

Existence of reliable good-quality maps of Danube Delta coast since mid-nineteenth century, together with satellite images, aerial photos and GPS surveys available after 1990, made possible the extraction of numerous shorelines which were comparatively analysed by means of GIS techniques (Digital Shoreline Analysis System-DSAS; Thieler et al. 2009).

Shoreline evolution in the past 150 years (Fig. 23.2a) displays a variability of coastal environments along the Danube Delta coast, whose behaviour was dominated by either erosion or accumulation. Prograding sectors are relied to the presence of: (i) active deltaic lobes (Chilia and Sf. Gheorghe secondary delta), which get most of the Danube discharge, (ii) engineering structures (jetties and harbour dykes), which induce accumulation updrift (Midia Harbour) or in their shadow, immediately downdrift (Sulina jetty) due to wave diffraction and (iii) natural river mouths (Sf. Gheorghe), whose mouth bar and fluvial plume create a groyne effect for the LST, inducing accumulation on the updrift beaches. The mean shoreline progradation rates along these sectors are comprised between 10 and 25 m/year for Sulina beach and Sf. Gheorghe secondary delta, and 40–70 m/year, for Chilia secondary delta. Erosive sectors are related to beaches superposed on the long-term retreating deltaic lobes following their abandonment, which let protuberant coasts exposed to wave reworking (Sulina), whose erosion was intensified by the lack of longshore supplied sediments due to river jetties construction. The most erosive sectors overlay on the divergence zones of nearshore currents, placed at the boundary of two littoral cells, and on the updrift sectors of long-lasting littoral cells

(i.e. central part of Sulina-Sf. Gheorghe coast, Zătoane and Portița Periboina sectors). In all cases, the mean shoreline retreating rates register values of maximum 20 m/year.

There is a marked difference in shoreline migration rates during the 1856–1961/1979 interval and the subsequent period (Fig. 23.2a), with significantly higher values during the first time interval, especially along the accumulative sectors; this is mainly attributable to the drastic decrease of Danube solid load. In the past century, Danube Delta became increasingly starved of sediments due to their entrapment in dam reservoirs, especially after 1950, when many dams were built in the lower Danube watershed (e.g. approximately 50 % of the dams built in Romania in the twentieth century were constructed between 1960 and 1980 and 45 % after 1980; Rădoane and Rădoane 2005). This is shown by the threefold decrease of suspended sediment discharge from 1365 kg/s at the beginning of the twentieth century to 640 kg/s at present (see Fig. 24.2 in Constantinescu, Chap. 24 this volume).

Along Chilia lobe coastline, the progradation rates decreased dramatically (with more than 75 %, from 50–80 m/year between 1856 and 1979 to 10–20 m/year afterwards), many sectors becoming slow prograding, stable or even erosive (Fig. 23.2a). The coastal area change rates (Fig. 23.3) show a more intense diminishing (approximately 90 %) of accumulated surfaces between the two time intervals, from 110 km^2/year to 9 km^2/year, with respect to a mean value of 83 km^2/year for the past 150 years. This situation is the result of the increased dominance of wave-related processes which carry the sands alongshore and the silts and clays offshore in the detriment of fluvial processes (weakened by the lower Danube sediment discharge), marking this way the recent and present transition of this secondary delta from a fluvial-dominated deltaic lobe to a wave-dominated one. In this respect, many barrier islands developed after 1980 at the mouths of Chilia distributaries: Oceakov, Bistroe, Stambul (Vespremeanu-Stroe and Preoteasa 2015). The progradation rates registered along the Sf. Gheorghe secondary delta showed small variations (Fig. 23.2a), while the accumulated surface rates remained constant (near the value of 15 km^2/year, Fig. 23.3) in the past 150 years, indicating the relative stability of this sector at long-term scales.

The erosive sectors present a much lower variability in terms of both shoreline retreating and erosional surface rates between the two analysed time intervals. Along Sulina–Sf. Gheorghe coast, the erosional surface rates decreased slightly from 25 km^2/year, between 1856 and 1961, to 20 km^2/year afterwards (Fig. 23.3), a part of the strong erosion characterising the central part of this sector being compensated by the strong accumulation occurred in the second half of the twentieth century in the vicinity of Sulina jetties (Fig. 23.2a). Along Ciotica—Perișor coastline, the erosional surface rates increased from 19 km^2/year to 29 km^2/year, demonstrating the long-term erosive character of this coastal sector. Perișor–Portița sector changed its behaviour from slightly eroding to slightly prograding in the past 150 years (Fig. 23.3), probably due to the pronounced accumulative behaviour of the Periteașca beach in the past 50 years.

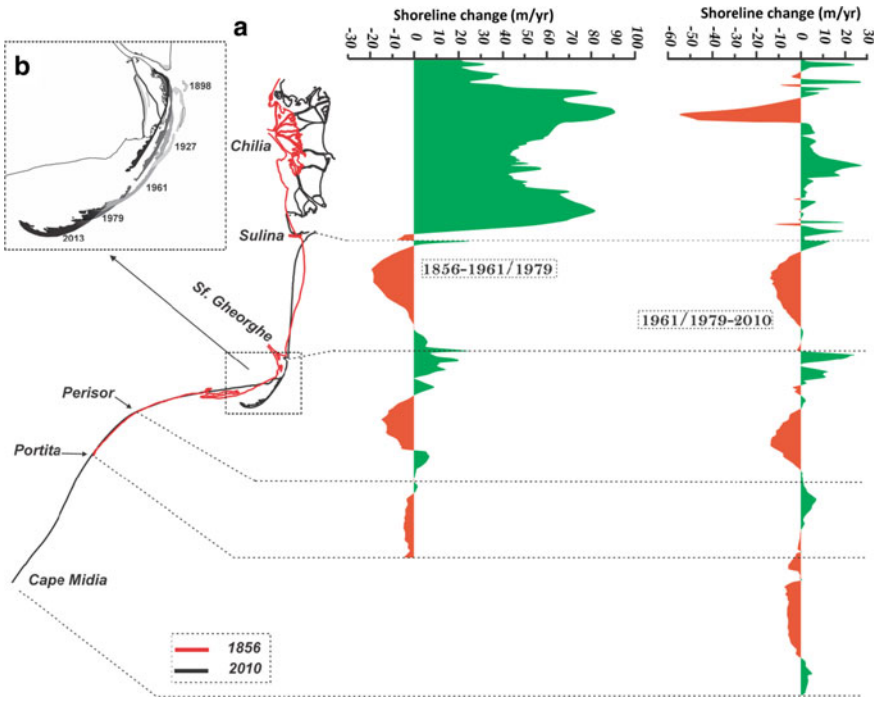

Fig. 23.2 **a** Shoreline changes between 1856 and 2010. Please see the position of the 1856 and 2010 shorelines and the different shoreline behaviour between 1856–1961/1979 and 1961/1979–2010 time intervals; **b** The successive positions of the Sacalin barrier spit between 1898 and 2013 (reproduced from Vespremeanu-Stroe and Preoteasa 2015)

Due to its different and more complex shoreline behaviour, Sacalin Spit was treated separately (Fig. 23.2b). It appeared in 1897 as an emerged breaker bar after a major flood. In the past century, it suffered continuous elongation (towards South) and backward migration due to the combined effects of LST and overwash processes during storms. The high shoreline mobility of the narrow and low Sacalin barrier is mainly driven by coastal storms and associated processes: longshore and cross-shore sediment transport, overtopping, washover fan building and sediment transport during breaching. Episodically, it experiences large elongation (up to 500 m/year) and retreat rates (up to 80 m/year), the latter related to extreme storms.

All in one, we can formulate that, at long time-scales (>50 years), shoreline behaviour along Danube Delta coast is highly influenced by the river sediment load changes as a result of human activities, rather than by storminess variability, the latter having a more pronounced effect on coastline migration at multi-annual and decadal time-scales, as will be further explained.

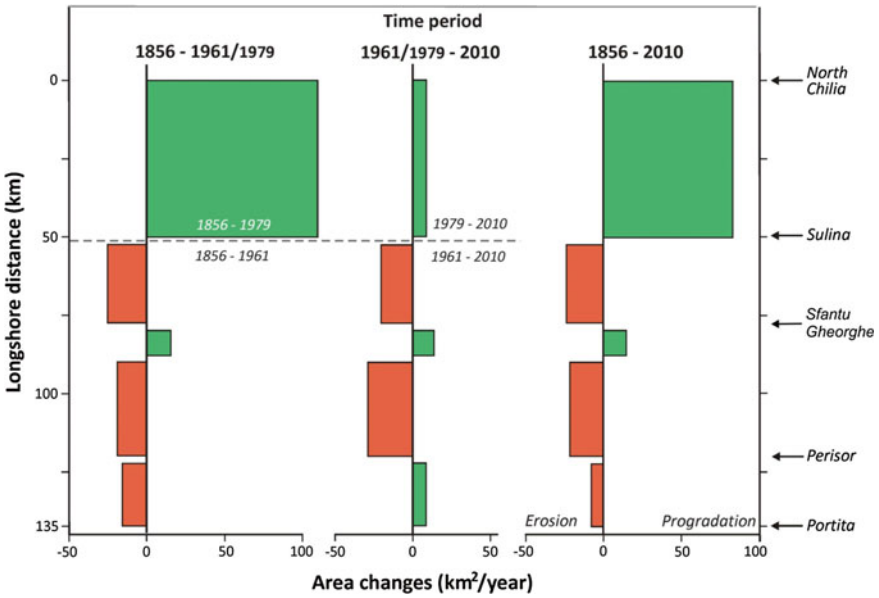

Fig. 23.3 The evolution of area change rates between 1856 and 2010 along Chilia–Portița sector. Please see the different rates between 1856–1961/1979 and 1961/1979–2010 time intervals

Climate Variability Imprint on Multi-decadal Shoreline Dynamics

Present Romanian Danube Delta shoreline configuration shows that, from a total length of approximately 162 km, more than half (90 km–55.6 %) is affected by erosion, while 48 km (29.6 %) is characterised by accumulative processes (advancing) and 24 km (14.8 %) is in dynamic equilibrium (relative stability). For the past five decades, the dominance of erosional processes can be mainly identified on Împuțita-PN (20 km length), central Sacalin Spit (17 km), Ciotica–Perișor (15.5 km), Portița and Periboina–Chituc (20 km) sectors. Progradational processes are characterising mostly Musura Bay (7 km), Sulina (south of the jetties-4 km), Southern Sacalin Spit (3 km), Periteașca (10 km) and Chituc–Cape Midia (10 km) coastlines, while relatively stable shorelines border, among others, Sulina (2 km), Sf. Gheorghe (5 km), Ciotica (1.5 km) and North Portița (5 km) beaches.

Generally, the erosive coasts represent the updrift and central sectors of the littoral cells. The prograding sectors superpose on various types of coastal environments, governed by different driving factors: (i) secondary deltas built by Danube distributaries (i.e. Chilia and Sf. Gheorghe); (ii) the downdrift areas (South Sacalin Island, Chituc–Cape Midia) of the littoral cells; (iii) stretches of coast (Periteaşca) where the LST is convergent due to abrupt changes in coastline orientation and (iv) up- and downdrift of engineering structures (Sulina). Both the

prograding and retreating coasts preserve their nineteenth century position and spatial distribution, despite a slight southward alongshore migration recorded in the second half of the twentieth century. Four coastal sectors that were defined as stable (the shoreline changes were small and non-directional) for the 1961 to present time period were either prograding (Musura–Sulina, Sf. Gheorghe) or retreating (Ciotica, South Periteaşca) prior to 1961 (Vespremeanu-Stroe et al. 2007).

At multi-annual scale, shoreline morphodynamics is highly influenced by storm regime and river floods. The obliquely onshore storms are the most effective in modelling shoreline behaviour. During energetic events, the storm-induced extreme waves and water-level conditions are key drivers in shoreline evolution. Shoreline response to these conditions is affected by the storm characteristics (intensity, direction and duration) and by pre-existing beach and dune morphologies. For example, the strongest storm cluster (December 1997–January 1998) registered in the last half century on the Danube Delta coast yielded a pronounced morphological impact on the deltaic coast, most of the low-lying coastal sectors being overwashed-up by the waves, which overtopped the highest units of the sub–aerial coast and formed extensive wash-over fans. Along Sulina–Sf. Gheorghe coastline, the storm-induced shoreline recession was comprised between 10–20 m along the stable and accumulative sectors and 25–50 m on the erosive beaches, up to ten times higher than normal conditions (Tătui et al. 2014). Despite the high intensity of the storm cluster and the associated high rates of shoreline retreat, the beach-dune system recovered completely relatively fast, in a time-interval between 1.5 and 4 years along the stable and accumulative sectors, respectively. The Danube river mouth areas are strongly controlled by fluvial deposition, especially during floods, when supplementary quantities of sediment are supplying the beaches, conducting to shoreline progradation, as it was the case of Sf. Gheorghe beach following the historical floods from 2005 to 2006.

Even seen relatively uniform at centennial time-scale (as previously presented), Romanian Danube Delta coast presents, at multi-decadal scale, a temporal variability of the coastal processes intensity after 1960, marked by rapid erosion/accumulation in the first two decades and an attenuation of shoreline dynamics afterwards. Based on topographical and GPS surveys, maps, aerial photos and satellite images analysed by GIS techniques and on wind data and Hurrell's North Atlantic Oscillation (NAO) index data (Hurrell 1995), Vespremeanu-Stroe et al. (2007) documented the relation between climate variability (represented by NAO) and shoreline dynamics via storm regime on the Danube Delta coast.

NAO is the dominant mode of winter climate variability in the North Atlantic region, defined as a meridional oscillation in atmospheric mass between the subtropical high and the polar low (Hurrell et al. 2001; Hurrell 2003) and expressed by an index computed as the difference in the sea-level air pressure between the Icelandic low and the Azores high (van Loon and Rogers 1978). The analysis of wind distribution on the Romanian territory (Vespremeanu-Stroe et al. 2012) showed that a negative correlation is observed between NAO index and the wind characteristics (mean speed, frequency and intensity of the stormic events) at multi-annual and multi-decadal scales, with higher values in the extra-Carpathian

areas. Moreover, Vespremeanu-Stroe and Tătui (2005, 2011), Vespremeanu-Stroe et al. (2007) demonstrated that, on the Danube delta coast, there is a strong NAO signal in the wind regime expressed by the high correlations established between the NAO index and the storm frequency at Sulina ($r = -0.76$) and Sfântu Gheorghe ($r = -0.77$) meteorological stations. From this point of view, we can distinguish two periods with different storm characteristics in the past 50 years: a very active interval between 1961 and 1979, which coincides with predominantly negative NAO phase, and a relatively quiet period, with low variability, between 1980 and 2000s, which overlaps a strongly positive NAO phase.

The inter-annual shoreline behaviour along the accretionary Sulina and Periteaşca beaches (represented by R60 and R28 benchmarks) and the retreating Zătoane sector (represented by R33 benchmark) is negatively correlated with NAO phases (Fig. 23.4). Shoreline evolution along these sectors shows an accentuated advance/retreat in the 1960s and 1970s followed by an obvious shift towards less dynamic beaches after 1980, in accordance with the transition of NAO index from dominantly negative to dominantly positive values for the same time intervals (Fig. 23.4).

The same shift in shoreline behaviour can be followed along the whole Danube Delta coast, with significant differences in coastal processes intensity between 1961–1979 and 1980–2006 time intervals. The interdistributary Sulina–Sf. Gheorghe coast (Fig. 23.5a, b) experienced maximum erosion rates of 24 m/year between 1961 and 1979, which diminished considerably to 10 m/year after 1980 (Table 23.1).

The average retreat rates for the erosive sectors of the Danube Delta coast decreased from 55 % along the Sulina–Sf. Gheorghe coast (from 14 m/year to 6.3 m/year) to approximately 65 % along Zătoane beach (from 14.7 to 4.9 m/year) and Portiţa–Chituc sector (from 8.3 to 3 m/year) between the two time intervals (Fig. 23.5c). By contrast, the prograding sectors were more variable in their

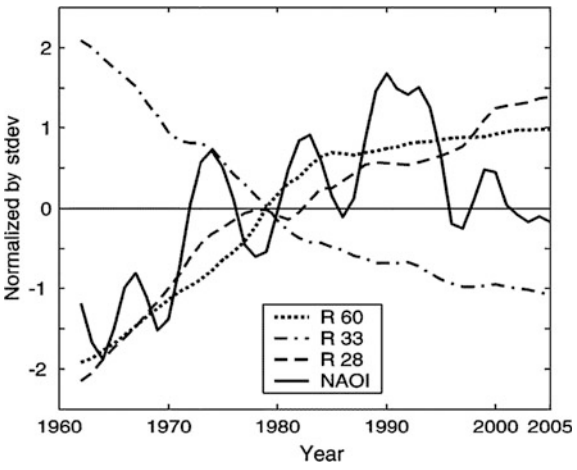

Fig. 23.4 Time evolution of shoreline mobility at R60, R33 and R28 benchmarks and Hurrel's NAO index (reproduced from Vespremeanu-Stroe et al. 2007)

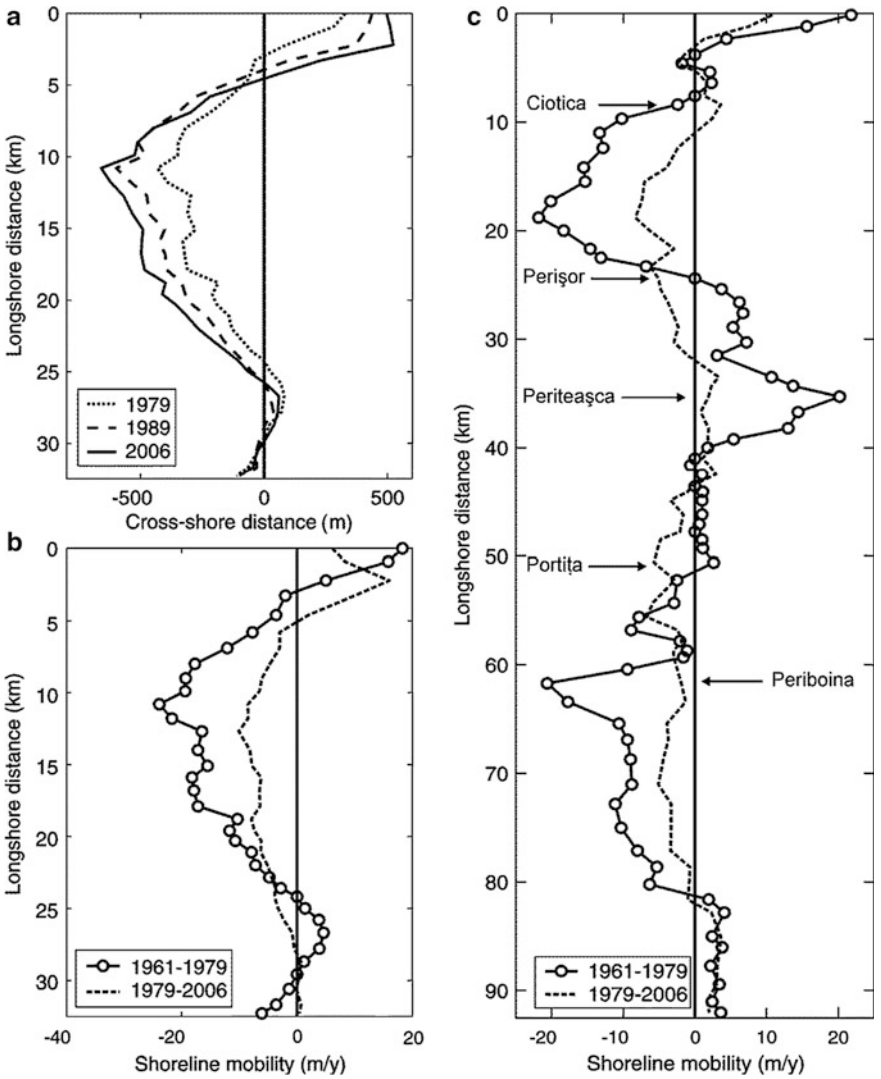

Fig. 23.5 Shoreline evolution between 1961 and 2006. **a**, **b** Sulina (0 km)—Sf. Gheorghe (32 km) sector; **c** Turetki (0 km)—Cape Midia (92 km) sector. In *panel A*, the "0" line represents the shoreline reference position in 1961, while in *panels B and C*, the "0" line indicates no changes in shoreline position, dividing the retreating (−) and accretionary (+) coastal sectors (reproduced from Vespremeanu-Stroe et al. 2007)

shoreline behaviour. On the marshy coasts of Musura and Sf. Gheorghe secondary deltas, which are protected by barriers and/or extensive flat nearshore zones, the advance rate decreased by 80 %, whereas on the open prograding beaches the decrease varied between 20 % along the Chituc–Cape Midia shore, 35 % at Sulina and 61 % at Periteaşca (Vespremeanu-Stroe et al. 2007).

Table 23.1 Mean and maximum shoreline migration rates for the erosional and accretional sectors of Danube delta coast between 1961 and 2006 (reproduced from Vespremeanu-Stroe et al. 2007)

Coastal sectors		Time interval			
		1961–1979		1979–2006	
		Mean value (m/year)	Max. value (m/year)	Mean value (m/year)	Max. value (m/year)
Erosional sectors	E1 (Impuțita–North Saraturile)	−14.0	−24.0	−6.3	−10.1
	E2 (Sacalin I.)	−23	−37.2	−17.7	−26.9
	E3 (Zătoane)	−14.7	−21.8	−4.9	−8.2
	E4 (Portița–North Chituc)	−8.3	−20.5	−3.0	−6.7
Accretional sectors	A1 (Musura–secondary delta)	52.8	91.6	10.4	15.6
	A2 (Sulina)	12.4	15.8	8.1	10.8
	A3 (Sf. Gheorghe–secondary delta)	16.9	21.8	3.7	6.6
	A4 (Periteașca)	6.0	20.2	2.3	4.8
	A5 (South Chituc)	2.8	4.1	2.3	3.5

The comparative analysis of shoreline positions indicates that coastal areas affected by accelerated erosion did not extend their length during the 1961–1979 more energetic interval, as it would have been expected, but expanded alongshore with more than 13 km during the less active 1979–2006 interval. This is explained by the fact that the intensification of erosive processes connected to stormy active periods must be analysed in close connection to the increase of the accretional processes intensity, as these processes develop simultaneously and compensate each other within the same littoral cells. Thus, the coastal sectors with intense erosion do not necessarily extend their surface during stormy periods due to the sediment volume conservation within the coastal system, which only affects the speed of shoreline retreat (Vespremeanu-Stroe and Tătui 2011). Instead, a slight alongshore migration (southward, in accordance with the direction of the net LST) of erosive sectors was observed in the last five decades.

Conclusions

More than half (∼55 %) of the present Romanian Danube Delta shoreline is affected by erosion. The present coastline configuration is the result of the long-term evolution of this deltaic coast. In the past 150 years of evolution, Danube Delta coastline experienced significant morphodynamic variability related to

different driving forces which changed the leading role between them depending on the considered temporal and spatial scales.

The waterline evolution in the past 150 years was significantly influenced by the threefold decrease of Danube sediment discharge in the last century, especially after 1950, as a result of numerous dams built in its watershed. An evident difference in shoreline migration and correspondent area changes rates was observed during the 1856–1961/1979 interval and the subsequent period, with significantly higher values during the first time interval, especially along the accumulative sectors. For example, along Chilia lobe coastline, the progradation rates decreased with more than 75 % and the corresponding area change rates diminished with approximately 90 %, favouring the wave-related processes and marking the transition of this lobe from a fluvial-dominated to a wave-dominated one. Along erosive sectors, there was significantly lower variability in terms of both shoreline retreating and erosional surface rates between the two time intervals.

Shoreline changes and storminess are well-connected at multi-annual time scale, whereas the multi-decadal coastline evolution is ultimately controlled by the NAO phases via storm regime. Storm frequency and intensity on the Danube Delta coast are widely controlled by NAO variability, experiencing negative correlations ($r = -0.76$). Storm activity is dependent on local climatic variability and decisively influences the dynamics and evolution of coastal landscapes. Hence, the multi-decadal NAO control on the coastal processes intensity via coastal storms: NAO phases dictate the frequency and intensity of the coastal storms that further influence the magnitude and rhythm of erosional and accretional coastal processes. Different shoreline dynamics patterns can be distinguished from this point of view in the last five decades: (i) high mobility during 1961–1979 interval with high retreating and advancing rates and (ii) low mobility afterwards (1979–2006). The shoreline advanced fastest along the coast of active lobes (Chilia and Sf. Gheorghe), while the divergence zones in the LST system experienced the highest rates of retreat ($\sim$20 m/year and $\sim$10 m/year in the first/second time interval). During the second interval, the decrease of shoreline changes rates was similar for the erosive beaches (55–66 %) and non-uniform for the accretionary coasts (20–61 % for open beaches and 80 % for the sheltered secondary deltas). Moreover, there was a slight alongshore southward migration of these sectors in accordance with the direction of the net LST.

Acknowledgements Research activities were undertaken in the frame of Sfântu Gheorghe Marine and Fluvial Research Station, Faculty of Geography, University of Bucharest.

References

Almazov A, Bondar C, Diaconu C, Ghederim V, Mihailov V, Miţă P, Nichiforov I, Rai I, Rodionov N, Stănescu S, Stănescu V, Vaghin V (1963) Zona de vărsare a Dunării–Monografia hidrologică. Bucharest (in Romanian)

Bhattacharya JP, Giosan L (2003) Wave–influenced deltas: geomorphological implications for facies reconstructions. Sedimentology 50:187–210

Coleman JM, Wright LD (1975) Modern river deltas; variability of processes and sand bodies. In: Broussard ML (ed) Deltas, models for exploration. Houston Geological Society, pp 99–149
Ericson J, Vorosmarty CJ, Dingman SL, Ward LG, Meybeck M (2006) Effective sea-level rise in deltas: Causes of change and human dimension implications. Global Planet Change 50:63–82
Gâştescu P, Driga B (1984) Long-term evolution of the Black Sea Coast in front of the Danube Delta between Sulina and Sf. Gheorghe arms. RRGGG Géographie 28:73–78
Giosan L (1998) Long-term sediment dynamics on Danube delta coast. In: Dronkers J, Scheffers MBAM (eds) Physics of estuaries and coastal seas, pp 365–376
Giosan L, Bokuniewicz H, Panin N, Postolache I (1999) Longshore sediment transport pattern along the Romanian Danube Delta Coast. J Coastal Res 15(4):859–871
Hurrell JW (1995) Decadal trends in the North Atlantic Oscillation regional temperatures and precipitation. Science 269:676–679
Hurrell JW (2003) Climate: North Atlantic and Arctic Oscillation (NAO/AO). In: Holton JR, Pyle J, Curry J (eds) Encyclopaedia of atmospheric sciences. Academic Press, Boulder
Hurrell JW, Kushnir Y, Visbeck M (2001) The North Atlantic Oscillation. Science 291 (5504):603–605
Rădoane M, Rădoane N (2005) Dams, sediment sources and reservoir silting in Romania. Geomorphology 71:112–125
Stănică A (2003) Coastal dynamics between Sulina and Sf. Gheorghe–Black Sea coastal zone in front of the Danube Delta, Romania. Unpublished PhD Thesis, University of Bucharest (in Romanian)
Stănică A, Dan S, Ungureanu VG (2007) Coastal changes at the Sulina mouth of the Danube River as a result of human activities. Mar Pollut Bull 55:555–563
Stănică A, Panin N (2009) Present evolution and future predictions for the deltaic coastal zone between the Sulina and Sf. Gheorghe Danube river mouths (Romania). Geomorphology 107 (1–2):41–46
Syvitski JPM, Kettner AJ, Overeem I, Hutton EWH, Hannon MT, Brakenridge GR, Day J, Vorosmarty C, Saito Y, Giosan L, Nicholls RJ (2009) Sinking deltas due to human activities. Nat Geosci 2:681–686
Tătui F, Vespremeanu-Stroe A, Preoteasa L (2014) Alongshore variations in beach-dune system response to major storm events on the Danube Delta coast. J Coastal Res 70:693–699
Thieler ER, Himmelstoss EA, Zichichi JL, Ergul A (2009) Digital shoreline analysis system (DSAS) version 4.0—an ArcGIS extension for calculating shoreline change. U.S. Geological Survey Open–File Report 2008–1278
Ungureanu GV, Stănică A (2000) Impact of human activities on the evolution of the Romanian Black Sea beaches. Lakes Reservoirs Res Manage 5:111–115
van Loon H, Rogers JC (1978) The seesaw in winter temperatures between Greenland and northern Europe: part I. General description. Mon Weather Rev 106:296–310
Vespremeanu E (1983) The geomorphological evolution of the Sf. Gheorghe arm mouth in the last 200 years. RRGGG—Géographie 27:61–68
Vespremeanu E (1984) The geomorphological evolution of the Kilia secondary delta (Danube Delta, north-western Black Sea). Analele Universităţii Bucureşti–Geografie XXXIII:83–90
Vespremeanu E, Suciu I, Oancea G (1986) The geomorphological evolution of the Sulina mouth in the last 200 years. Analele Universităţii Bucureşti-Geografie XLI:84–89
Vespremeanu E, Ştefănescu D (1988) Present-day geomorphological processes on the Romanian delta and lagoon littoral of the Black Sea. Analele Universităţii Bucureşti–Geografie XXXVII:85–91
Vespremeanu E, Vespremeanu-Stroe A, Constantinescu Ş (2004) Evoluţia ţărmului deltei Dunării în ultimii 40 ani. Studii şi cercetări de oceanografie costieră 1:15–30 (in Romanian)
Vespremeanu-Stroe A (2004) Transportul de sedimente în lungul ţărmului şi regimul valurilor pe coasta Deltei Dunarii. Studii şi Cercetări de Oceanografie Costieră 1:67–82 (in Romanian)
Vespremeanu-Stroe A (2007) Danube Delta coast. Geomorphological study. PhD Thesis, University of Bucharest, Ed. Universitară, Bucharest (in Romanian)

Vespremeanu-Stroe A, Preoteasa L (2007) Beach–dune interactions on the dry–temperate Danube delta coast. Geomorphology 86:267–282

Vespremeanu-Stroe A, Preoteasa L (2015) Morphology and the cyclic evolution of Danube Delta Spits. In: Randazzo G, Jackson DWT, Cooper JAG (eds) Sand and gravel spits. Springer International Publishing, p 327–339

Vespremeanu-Stroe A, Tătui F (2005) The influence of North Atlantic Oscillation on Romanian Black Sea coast wind regime. Analele Univ Buc Seria Geografie LIV:17–25

Vespremeanu-Stroe A, Tătui F (2011) North-Atlantic Oscillation signature on coastal dynamics and climate variability of the Romanian Black Sea Coast. Carpathian J Earth Environ Sci 6 (1):308–316

Vespremeanu-Stroe A, Constantinescu Ş, Tătui F, Giosan L (2007) Multi-decadal evolution and North Atlantic Oscillation influences on the dynamics of the Danube delta shoreline. J Coastal Res 50:157–162

Vespremeanu-Stroe A, Cheval S, Tătui F (2012) The wind regime of Romania—characteristics, trends and North Atlantic Oscillation influences. Forum Geografic X I(2):118–126

Chapter 24
Soft Cliffs Retreat Under the Shadow of Three Ports on the Southern Romanian Coast

Ștefan Constantinescu

Abstract The soft rocky coast between Cape Midia and Vama Veche was investigated based on cartographic documents. Shoreline evolution was computed for the past century focusing on two different periods: in cvasi–natural regime/low anthropic pressure (before 1960; 1910–1960) and under strong human influence (after 1980). Two decades of transition (1960–1980) were characterized by the construction of new defence structures, new resorts, and other industrial facilities that transformed completely the coast. Lithological formations (limestone, clay, and loess) cause the unstable nature of these cliffs. The highest erosion values occur on Mangalia beach and 2 Mai coast, with more than 4 m/year. In cvasi–natural regime, progradation represents 62.5 % and the retreat area only 37.5 % of the entire coast. The balance was tilted quickly in just two decades (1960–1980), when the erosion sectors affected 50.8 % of the coastline. Coast responded to these anthropogenic pressures by a pulsating behavior, with higher amplitude of oscillations after 1980 and with a spread of erosion processes that affect now 67.3 % of the coast. Construction of the three ports, Midia, Constanța, and Mangalia, imposed a new scenario by changing the distribution/settling of sediments coming from the Danube and generating a positive feedback. Intense retreating rhythms correspond to the negative phase of the NAO from 1961 to 1972. In the next decades, a period with a positive NAO index, the magnitude of erosive processes on the deltaic coast was smaller. In the case of cliff coast, this process has not reflected in shoreline dynamic and erosion rates became higher, as a direct effect to anthropogenic impact. After a strong intervention, the ability to withstand disturbances induced by human influence should be considered in a larger context, which cannot exclude the upstream Danube valley, the most important source of sediment, not only for the deltaic coast, but also for the cliff one. Accelerated anthropogenic pressure on the environment, involving dams on rivers and extending coastal structures, will generate negative effects in the future, in a difficult context imposed by the climate change.

Ș. Constantinescu (✉)
Faculty of Geography, University of Bucharest, 1st N. Bălcescu Blv., Sector 1, 010041 Bucharest, Romania
e-mail: stefan.t.constantinescu@gmail.com

M. Rădoane and A. Vespremeanu-Stroe (eds.), *Landform Dynamics and Evolution in Romania*, Springer Geography,
DOI 10.1007/978-3-319-32589-7_24

Keywords Sea-cliff · Erosion · Black Sea · Shore platform · Danube · NAO

Introduction

Rocky coasts are the legacy of marine and subaerial processes that have been operating for thousands of years (Trenhaile 1987). This affirmation should be completed in the present with another critical point that creates a new form of legacy: anthropogenic influence. If modern rocky coastal morphology is partially inherited (Woodroffe 2002) expressing a synthesis of all processes that interacted in time, an artificial aspect tends to developed very quickly under human footprint. A new baseline for physical processes was imposed in the past decades for the next generations who will be responsible for coastal preservation in a difficult context designed by the climate change scenario. We must not forget that rocky coast affected by erosion represents an irreversible process and there is no way to restore such coast once it has been eroded (Sunamura 1992).

Western coast of the Black Sea (Fig. 24.1) was opened to trade routes since ancient times, toward cities like Histria, Tomis (Constanța), or Callatis (Mangalia). Human pressure had been maintaining for more than two millennia within reasonable limits, without affecting the general circulation of sediments alongshore. From the second half of the twentieth century, new ports defence structures had to change the coast configuration in an unprecedented manner, generating disturbances and a positive feedback. Coastal system suffered a sudden change of state that switched from a natural self-controlled behavior to a human controlled regime. In that context, cliffs experience a pulsatile morphodynamic, as a result of new ports facilities, new defence structures. and new resorts for tourists.

The purpose of this material is to present the morphodynamics of this coast in the past century from two different perspectives: in natural regime (before 1960) and under strong anthropogenic influence (after 1980). Two decades of transitions were recorded between 1960 and 1980, when the new defence structures, new resorts and other industrial facilities transformed completely the coast.

General Background

Deficit of sediment represents a major global concern and the principal cause is the presence of dams that altered 48 % of all river flow worldwide (Grill et al. 2015). Danube is not an exception, with a reduction of 60 % of sediments toward the natural conditions (McCarney-Castle et al. 2012; Fig. 24.2). In the past decades, the southern cliffed coast expressed a direct response to the sediment reduction from the Danube. Keeping the sediments, especially the sand, on a rocky shore is a challenging job in the context of accelerated sea-level rise.

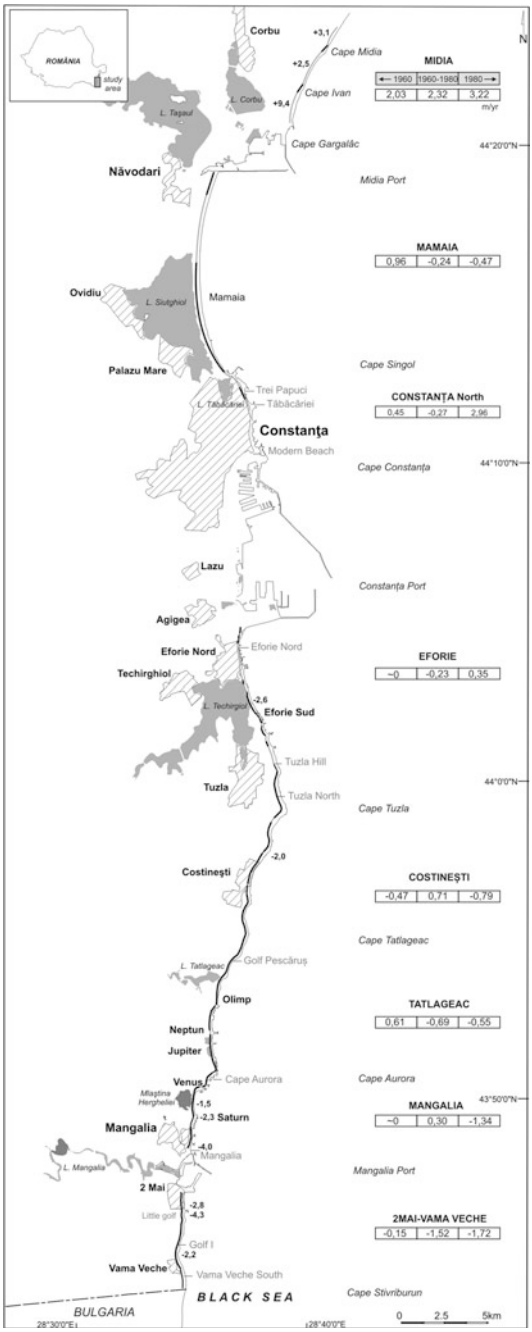

Fig. 24.1 Sea-cliff coast between Cape Midia and Vama Veche. *Bold line* along the coast, expresses erosion areas, after 1980; *gray line* corresponds to accretion areas. *Numbers in boxes* represent the average rhythms of erosion (−) and accretion (+) in meters/year for each coastal subdivision. Maximum rhythms are marked closed to the water line with bold numbers. Cliff profiles from Fig. 24.3 are illustrated with a *gray line* and written with the same color

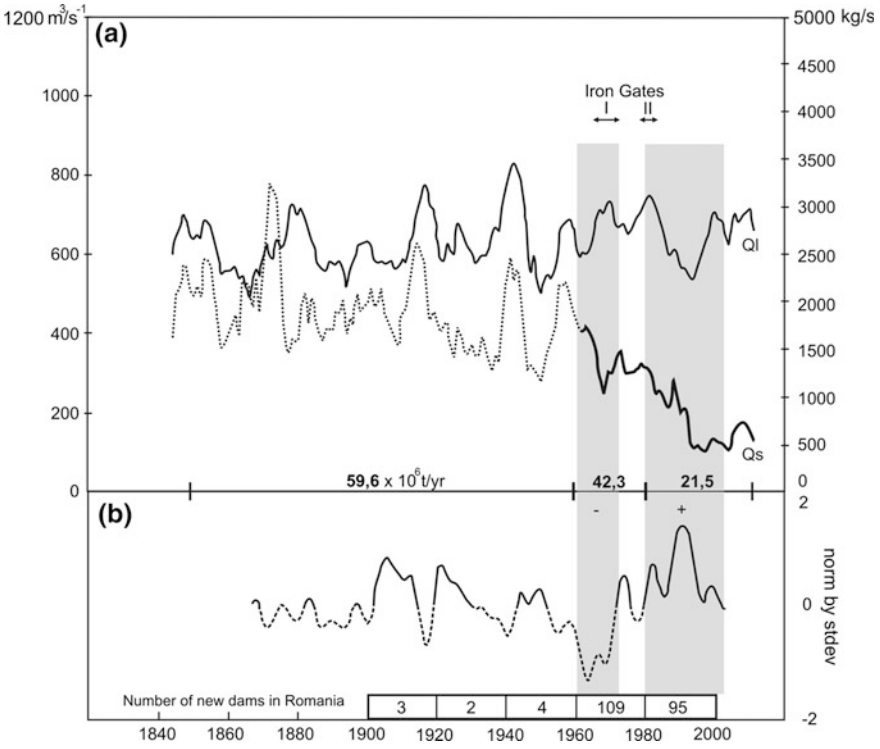

Fig. 24.2 **a** Five years average distribution of Danube liquid discharge (Ql) and sediment load (Qs) at the entrance of Danube Delta (Ceatal Izmail). *Bold numbers* represent the average sediment discharge calculated for time intervals. **b** The mean winter (December–March) NAO index expressed like points line (negative phases) or continuous line (positive phases). Gray columns correlate the NAO values with the Danube's discharge for different types of phases (data from EEA 2008). The number of new dams in Romania is presented in the base (Rădoane and Rădoane 2005)

New recent studies proved that global mean sea level (GMSL) rose at a rate of 3.0 ± 0.7 mm per year between 1993 and 2010, consistent with prior estimates from tide gauge records (Hay et al. 2015). This new value implies that future coastal protection projects should be revised. Tourism requests in every season new sources of sand in order to rebuild the beaches, an ongoing concern of any hotel manager. But this perspective is strictly local and the problem of sediments could not be dislocated from this general context. In this case, the soft cliffed coast depends directly from what happened upstream on the Danube valley. Sediment retention, an important concern in every delta that is in course to drown (Giosan et al. 2014), represents the same problem for the touristic beaches, downstream the deltaic coast.

The construction of the biggest port in Black Sea (Constanța) and of two others, north (Midia) and south (Mangalia), has changed completely the pattern of

longshore sediment transport (LST), generating a current deviation offshore. In that way, the main source of feeding southern beaches was lost.

Coastal barrier lakes and lagoons interrupt the distribution of sea-cliffs, developed in loess at the top (10–20 m), in an intermediary reddish-green clay stratum and limestone in base. Within the top layer there are several fossil soils strata (Conea 1970). Limestone does not always rise above sea level and high rates of erosion will correspond to those sectors. Direct contact between clay strata and the sea will cause a red water aspect (2 Mai, Pescăruș Bay). This lithological predisposition will favor landslides and subsurface seepage as active processes in subaerial cliff erosion.

Offshore waves have a significant mean height between 0.8 and 0.95 m (Bondar 1998; Giosan et al. 1999). The microtidal regime of the Black Sea, with values between 7 and 11 cm (Bondar et al. 1973), does not influence erosive processes. The presence of coastal groins and defence structures contribute to wave refraction, causing local variations in their proximity. Winter storms lead to a loss of the beach sediments offshore with medium and long-term effects. Sea level rise is another factor contributing to the increase of erosion. At Constanța, the average value from 1933 to 2000 was 1.28 mm/year (Malciu and Diaconu 2000).

Sedimentary source for the northern sector (Cap Midia–Cap Singol) comes mainly from the Danube. South of Constanța port, fluvial input is reduced, consisting predominantly in sediments resulted from shellfish or from cliff and limestone substrate erosion. Average diameter of beach sediments increases from north (0.22 mm at Mamaia) to the south (0.58 mm at Vama Veche). Submerged sediments have a uniform average value (0.17 mm) higher only at Vama Veche (0.26 mm), where a reflective beach develops (Halcrow 2012).

Cape Midia in North is composed from greenschist (Proterosoic), much newer layers forming Cape Ivan and Cape Gargalâc: limestone from Bathonian and Callovian (medium Jurasic). South of Mamaia barrier, from Cape Singol to Agigea, Sarmatian limestone in two stripes appears. The external one, exposed to the sea, is from Bessarabian (inferior Sarmatian) and the internal one belongs to Kersonian (superior Sarmatian). South of Agigea to Vama Veche, only Kersonian limestone is presented.

Morphodynamics Hidden in Maps

First maps which expressed the cliffs morphology date from the nineteenth century and provides only a local image. The most numerous studies were related to the coast of Constanța, but without a cartographic projection or coordinate system (de Marigny 1830; Spratt 1856; Hartley 1881). Lack of information about authors occurs in the case of cartographic products derived from military surveys: Constanța plan of 1831, Austrian map of Constanța in 1857. The cartographic base was represented by the following sets of maps: *Planurile Directoare de Tragere* (S.G.A. 1913–1924) and topographic maps from 1959 to 1961 and 1978 to 1980

(D.T.M. 1960/1980). For the last interval, aerial images and GPS measurements fixed under the national landmarks network were used. The maps were georeferenced using common landmarks verified in the field by GPS measurements. Cartographical data were then transformed using the same projection, namely Stereo 70, national cartographic projection of Romania.

We analyzed the evolving patterns of shoreline change along the cliffed coast using cross-shore profiles separated at a distance of 200 m. Automatic extraction of rates was performed using the Digital Shoreline Analysis System (Thieler et al. 2009).

Morphology of the Coast

In the case of inactive cliffs (Eforie Nord, Neptun, Mangalia, etc.) subaerial processes define the morphology (Fig. 24.3). Creeping, slope wash, and rotational landslides appear on gentle slopes while on steeper cliffs, sliding and toppling is the most common. The presence of clay in the base of strata favors groundwater to induce slides like on Eforie and Tuzla coast. Wave energy is not so important as lithology in the case of these cliffs and the retreat is episodic, usually between November and April, when the storm events are frequent.

One case of cliffs that become bluffs is when a protective beach or artificial structures in the base exist (Bird 2000). Coastal bluffs are the main characteristics for the Romanian cliffs, especially in the touristic resorts like Eforie, Costineşti, and Neptun or in the case of important cities (Constanţa, Mangalia). In natural conditions, debris of material appears at the toe of slopes, which in time could be removed by the waves. If the debris persists longer, the erosion is halted for a while (sometimes several months or even years). Before anthropogenic intervention, the general tendency of cliffs was to present almost a vertical top profile in loess and a natural talus in the half or third part of the slope. When the distance to the waterline exceeds 10–15 m, in a context of tide amplitude of few centimeters, the talus received waves attack only during winter storms. For that reason in many cases the

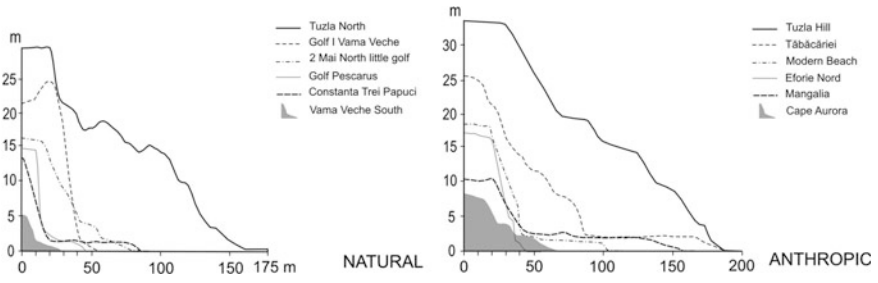

Fig. 24.3 Different types of cliff morphology in natural (*left*) and anthropogenic influence

talus was vegetated, even with shrub species. When subaerial processes prevail, the upper part of the profile changes to a more gentle aspect.

The highest cliffs appear in Constanța (38 m) followed by Eforie and Costinești (more than 30 m). If at Midia the average altitude is 9.31 m, from Cape Singol the coast becomes higher with maximum values in Constanța–Eforie, followed by a decreasing behavior until Mangalia Port (7.1 m). After this point, in 2 Mai–Vama Veche the medium altitude increases at 14 m (Fig. 24.4). This tendency is better illustrated in the medium cliff break aspect which, for the entire cliffed coast, presents an average value of 12.2 m. The emersed shore (between cliff break and water line) has an average altitude of only 5.2 m. For each sector an average value was computed (−7.2 m) corresponding to the submerged shore, between the water line and −12 m depth. Declivity is one of the most important factors in generating

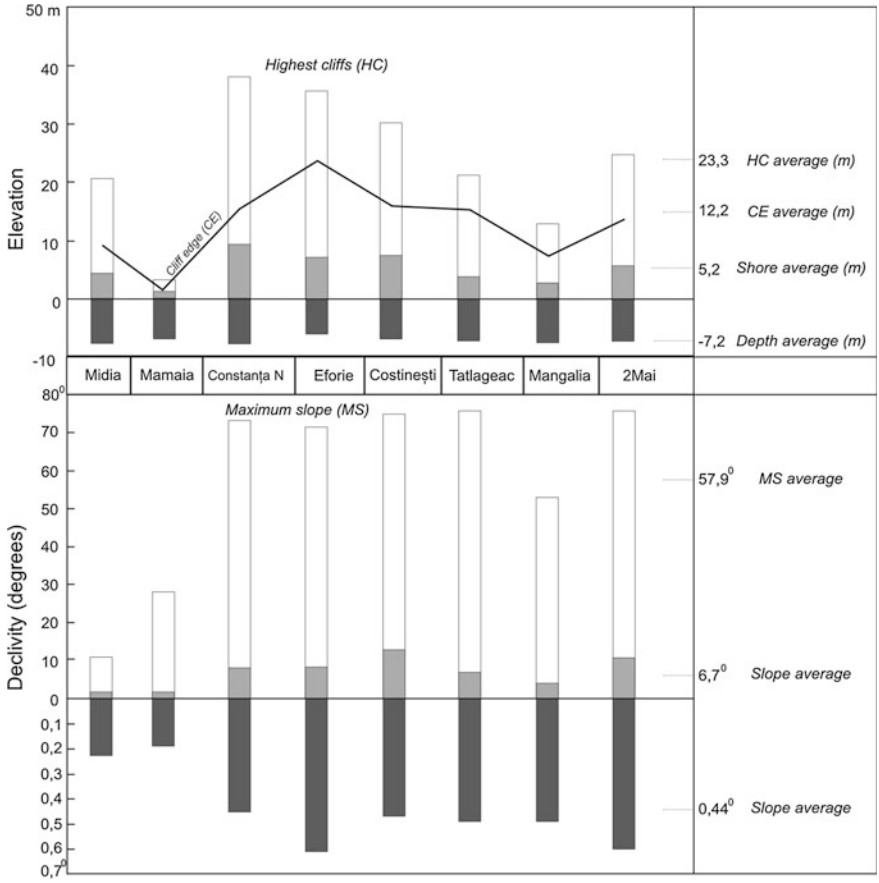

Fig. 24.4 Principal morphometric parameters for the cliffed shore: elevation and declivity with medium values corresponding to each coastal unit. *Lighter* and *dark gray boxes* express the emerged and the submerged shore respectively

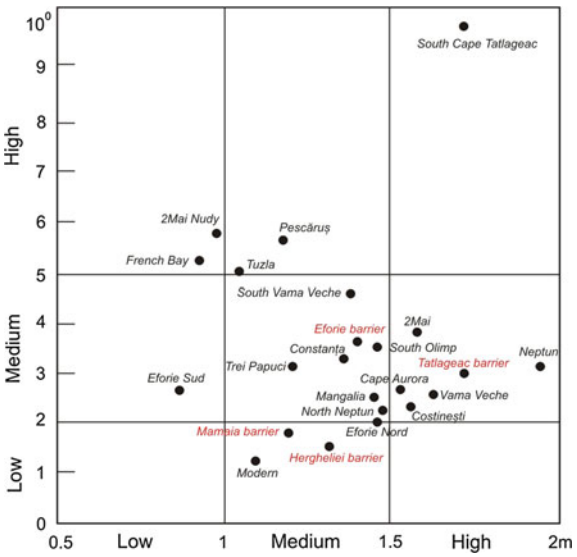

Fig. 24.5 Correlation between altitude (OX, meters) and declivity (OY, degrees) for the main beaches along the coast. Three different classes were identified for each parameter: low, medium, and high values. Beaches installed on littoral barriers are written in *red*

gravitational processes, thus its regional distribution was investigated (Fig. 24.5). Maximum slopes correspond to Constanța-Tatlageac area (Costinești: 12.68°, Eforie: 8.34°) with a gently aspect in Midia (1.54°), where cliffs are inactive. The medium declivity value for the entire emerged shore is 6.7° and only 0.44° for the submerged shore. The maximum potential energy is found in Eforie (42.2 m) and 2 Mai (31.9 m) units, with the highest values of underwater slopes (0.6°). The most uniform and smallest declivity gradient is on the littoral barrier of Mamaia (0.19°) and Midia (0.23°) units, both receiving the largest amount of sediments coming from the Danube. These morphometric parameters were important in the natural conditions of the coast prior to 1960, generating differences in the energy involved into gravitational and marine processes. After strong human intervention, presence of groins and port defence structures imposed new critical points for the coastal system. Cliff stabilization, especially in Constanța, Eforie, and Mangalia minimalized the marine erosion against the coastal slope, subaerial processes being predominant.

Sloping structures placed at the toe of cliffs constitute obstacles in the front of marine energy. These revetments preserve the shoreline and protect the cliff in the first years, but soon after, the depth at the base becomes higher, all the sands will be vanished to offshore and the structure will collapse. Different types of material were used create the protective structures: rock armor, tetrapod, or even cement walls (Cape Tuzla, Costinești, Cape Aurora etc.; Figure 24.6). Slumping is the most important process for natural cliffs with vertical profiles (2 Mai, Vama Veche, Pescăruș) and landslides dominate gentle slopes (Eforie Sud, Tuzla, and Costinești, before human intervention) favored by the presence of clay layer in the base.

Fig. 24.6 Intense erosion in the northern sector of Costineşti (−2 m/year). Bunkers from the Second World War were installed initially at the cliff base. New restoration projects were made in the Past years involving sea walls and rock armor in the cliff base, but the anthropogenic pressure increased on the tableland

A storm ledge appears at the base of the cliffs, in many cases being caused by the marine shells, or sometimes being cut into limestone (Cape Ivan) or clay (2 Mai) with a bench aspect. Unfortunately, many of these forms were covered by the coastal protection structures in the recent years. Notches on the Romanian cliffed coast can be classified in two categories depending on lithology (Constantinescu 2012): (i) those encountered in limestone, which have a flat roof and dimensions imposed by the rock elevation; (ii) notches formed in soft rocks (clay and loess) which present a roof with slopes usually greater than 45°. Depending on the shore platform extension, three different cases can be individualized: (i) a short extent of shore platform will determine an installation of niches apron mean sea level; (ii) a sloping aspect of shore platforms to the sea will create a storming notch at 1–3 m above the mean sea level; (iii) when shore platform has a gentle slope and a width more than five meters, the energy of waves will be dissipated on them; the notches will have an aspect similar with those created by broken waves (Sunamura 1992), with small dimensions and a sloping roof. At Agigea, there is a structural shore platform developed on a horizontal layer of limestone with the outer edge under the erosive action of waves. The height is uniform between 4 and 5 m above the medium sea level. In the base spectacular notches with a flat roof appear.

The beach has a protective role for the cliff, diminishing the wave action. Only in the case of important storms (especially in winter) the coastal slope could be

attacked by the waves. Beaches are developed in bays (Midia, French Bay, Vama Veche, etc.) along a littoral barrier (Mamaia, Eforie, Tatlageac, Hergheliei) or like a narrow stripe in the base of cliffs (Costineşti, Tatlageac, 2 Mai–Vama Veche). Every resort has artificial beaches developed between groins that need supplementary nourishment every year. Southern beaches have an average altitude of 1.37 m and a medium slope of 3.48°. An interesting relation between average height and declivity determines different morphometric categories (Fig. 24.5):

- low altitude beaches (below 1 m) tend to present, in most cases, high gradients (above 5°) and are characteristic to the base of cliffs like in French Bay and 2 Mai small golf, being strongly erosive; otherwise, these low altitude beaches present medium declivities (2–5°) (Eforie Sud);
- medium altitude beaches (1–1.5 m) generate all kinds of categories: in most cases, medium declivity (2–5°) like Eforie barrier, Mangalia, or south Vama Veche, followed by low declivity class (Hergheliei and Mamaia barriers, Eforie Nord and Modern Beach); sometimes, like in the case of active cliffs with high altitude, beaches with high declivity appear at cliff toe (Pescăruş and Tuzla);
- high altitude beaches (above 1.5 m) have in most situations medium gradients (2 Mai, Vama Veche, Cape Aurora, Neptun, Costineşti) followed by higher values (above 5°), as in sectors with shell deposits which appear in the base of cliffs (South Cape Tatlageac).

Morphodynamics Under Anthropogenic Footprint

In the present, nearly three-fourth of the southern coast is affected by erosion, the highest rhythms (Fig. 24.7) being recorded at 2 Mai Military Unit (−4.3 m/year; Fig. 24.8) and Mangalia (−4.0 m/year). Other strong erosive coasts are Eforie littoral barrier (−2.6 m/year), Saturn beach (−2.3 m/year), Vama Veche (−2.2 m/year), or Hergheliei littoral barrier (−1.5 m/year). The accumulation processes characterized Cape Midia coast, the only one that received directly fluvial sediments, being north of any port defence structures (+3.2 m/year).

In natural regime, before 1960, progradation represented 62.5 % from the entire cliffed coast and the retreat area only 37.5 % (Fig. 24.7). The balance was tilted quickly in just two decades (1960–1980), when the erosion sectors affected 50.8 %. Coast responded to these anthropogenic pressures by a pulsating behavior (Fig. 24.7) with higher amplitude of oscillations after 1980 and with a spread of erosion processes that now affects 67.3 % of the entire area. Erosion of Mamaia barrier extends to the north, with values of −2 m/year. Beach nourishment project, which was brought in the 1980s, in the southern part of the resort, prove to be inefficient, as well as the construction of six breakwaters (1988–1990). This interval corresponds to the maximum erosion on the deltaic shore, when maximum rhythms of −24 m/year were recorded south of Sulina (Vespremeanu-Stroe et al. 2007).

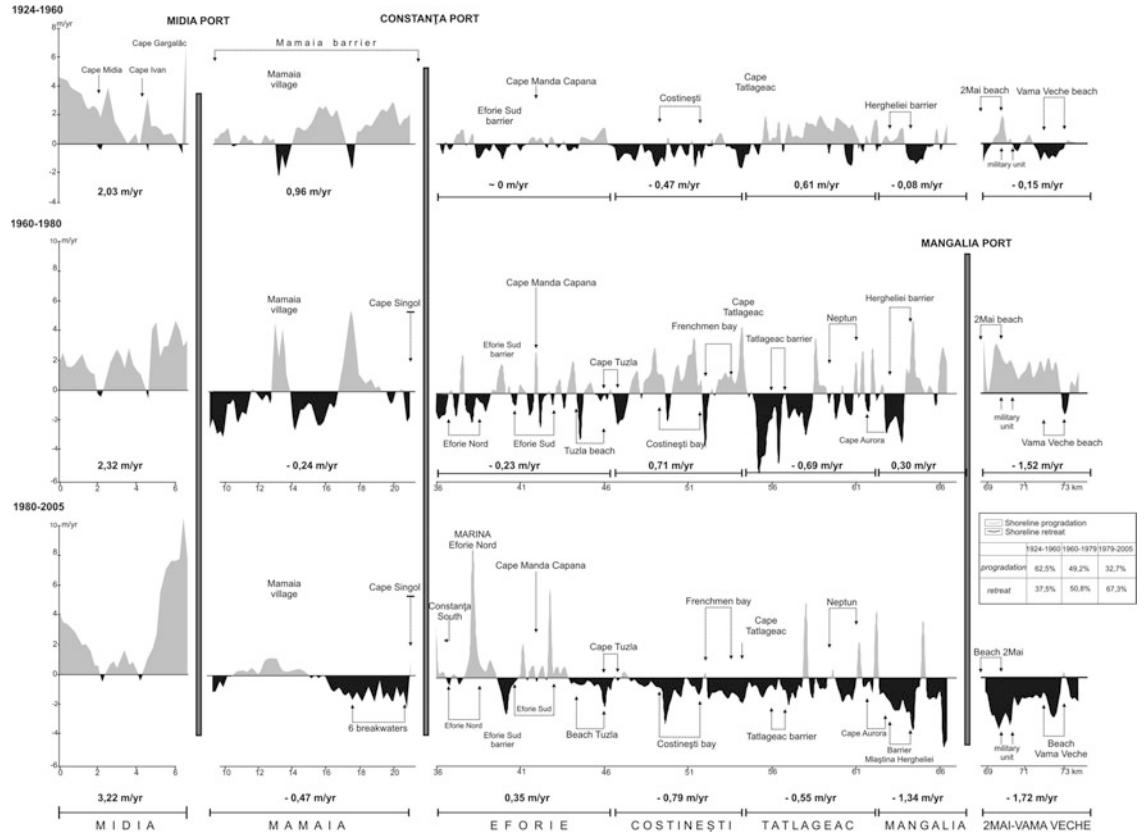

Fig. 24.7 Rhythms of erosion and accretion calculated for each coastal unit in three periods: before 1960, 1960–1980, and after 1980. Accretion areas are illustrated in *gray* while the erosion is expressed in *black*. *Bold numbers* (m/year) corresponds to the average value of the coastal unit for each time interval

Fig. 24.8 The most intense erosion spot, along the Romanian cliffed coast, at 2 Mai-Vama Veche military unit (−4.3 m/year). The *black arrow* on 2001 photo marks the position of a building hidden between the trees. Ten years after, the house still stands on the cliff edge, but soon the building collapsed into the sea. The limestone layer is bellowing the water line, so the contact is direct between the sea and clay/loess strata, with a reddish color of water. A bunker from the WW2 (2001), served as foundation for the new restaurant from the small golf (on the *right* of the images)

The efficiency of new protection structures seems to be useful only at local scale and only for a short period, the principal issue being the deficit of sediments that come from the Danube. At a regional scale, some important issues were highlighted: the regime of the central and southern part of Mamaia barrier changed from accumulative (0.96 m/year) to erosive (−0.47 m/year); new coastal groins and seawalls caused local accumulation (Eforie North Eforie South, Neptune, etc.), but only for two decades, thereafter retreating processes occurring; from Cape Tuzla to Vama Veche, erosion becomes a dominant process, amplified after 1980, at an average rhythm of −1.1 m/year; south mole of Mangalia port initially caused mild accumulation (1960–1980), after which erosion extended southwards, with a medium rhythm of −1.72 m/year; a series of recreational beaches (Mamaia, Eforie, Neptune, Cap Aurora etc.) require new amounts of sand every spring, but with no overall quantification of the contribution. Purpose is strictly seasonal without complying an unified beach nourishment plan.

Intense retreat rhythms correspond to the negative phase of the NAO, from 1961 to 1972, but also associated with adverse effects of port building (Fig. 24.2b). Construction of inadequate defence structures without geomorphological and hydrodynamic criteria in establishing their position, amplified these effects at local scale. Between 1979 and 2000, a period with a positive NAO index, the low incidence of winter storms reduce the magnitude of erosive processes on the deltaic

coast (Vespremeanu-Stroe et al. 2007). The correlation with the NAO index is negative, but anthropogenic intervention exceeded the influence of natural factors, becoming the responsible agent in coastal morphodynamics.

Conclusions

In the present, almost 70 % of the cliffed coast is affected by erosion, the most exposed areas being south of Constanța port. Construction of the three ports has generated a divergent drift to offshore, favoring erosion. The coast is withdrawing and some restoration projects proved to be inefficient (French Bay, south of Costinești), generating a positive feedback typical situation. New hard rock protection structures (Cape Tuzla, Costineşti, Eforie etc.) will shelter the cliff from erosion with a reversed response from a bathymetrical perspective, meaning increasing the depth and a permanent sediment loss.

New restoration works are necessary; some are in progress, involving beach nourishment and rehabilitation of the old defending structures. When seeking economic benefits on short term, without considering the secondary effects against coastal morphodynamics, repercussions will be visible on long term. Accelerated anthropogenic pressure on the environment in the past decades, involving dams on rivers and extending coastal structures, will generate negative effects for the new century, in a difficult context imposed by the climate change.

Searching long-term sustainable solutions is a difficult task. A concept like *resilience* (Wildavsky 1988) applied in the case of coastal systems could be a solution. After a strong intervention in those areas, the ability to withstand disturbances induced by human influence should be considered in a larger context, which cannot exclude the deltaic coast and the upstream Danube valley (Constantinescu et al. 2015). Will the system be able *to jump back*, to return to its former shape after a deformation (Comfort et al. 2010) and to recalibrate the sand fluxes along the coast? The answer should be sought in another kind of approach, when it will be necessary to work *with* water not *against* water, like in the case of Sand Motor experiment developed on the Dutch coast. In the shadow of three ports hides not only the problem of erosion, but also our short-time perspective about the coastal system.

References

Bird ECF (2000) Coastal geomorphology: an introduction. Wiley, Chichester

Bondar C (1998) Hydromorphological relation characterizing the Danube river mouth and the coastal zone in front of the Danube Delta. GeoEcoMarina 3:99–102

Bondar C, Roventa V, State I (1973) Marea Neagră în zona litoralului românesc. Monografie hidrologică, Institutul de Meteorologie și Hidrologie, București

Comfort LK, Boin A, Demchak CC (eds) (2010) Designing resilience: preparing for extreme events. University of Pittsburgh Press, Pittsburgh

Conea A (1970) Formaţiuni cuaternare în Dobrogea (loessuri şi paleoloessuri). Editura Academiei RSR, Bucureşti

Constantinescu Ş (2012) Analiza geomorfologică a ţărmului cu faleză dintre Capul Midia şi Vama Veche. Ph.D. thesis, Ed. Universitară, Bucureşti

Constantinescu Ş, Achim D, Rus I, Giosan L (2015) Embanking the lower Danube: from natural to engineered floodplains and back. In: Hudson PF, Middelkoop H (eds) Geomorphic approaches to integrated floodplain management of lowland fluvial systems in North America and Europe. Springer, New York, NY, pp 265–288

de Marigny, T (1830) Plan aproximatif du Danube depuis ses ambouchures dans la Mer Noire jusqu a Galats. Scale 1:350,000, 41 × 34 cm, Publisher Alexandre Braun, Odessa

Direcţia Topografică Militară (D.T.M.) (1960/1980) Harta topografică. Scale 1:25,000. Proiecţia cilindrică transversală conformă Gauss-Kruger, Sistem de coordonate 1942, Bucureşti

European Environment Agency, European Commission, World Health Organization (eds) (2008) Impacts of Europe's changing climate: 2008 indicator-based assessment: joint EEA-JRC-WHO report. European Environment Agency, Office for Official Publications of the European Communities [distributor], Copenhagen, Luxembourg

Giosan L, Bokuniewicz HJ, Panin N, Postolache I (1999) Longshore sediment transport pattern along the Romanian Danube delta coast. J Coastal Res 15(4):859–871

Giosan L, Syvitski J, Constantinescu S, Day J (2014) Climate change: protect the world's deltas. Nature 516:31–33. doi:10.1038/516031a

Grill G, Lehner B, Lumsdon AE et al (2015) An index-based framework for assessing patterns and trends in river fragmentation and flow regulation by global dams at multiple scales. Environ Res Lett 10:015001. doi:10.1088/1748-9326/10/1/015001

Halcrow (2012) Raport Diagnostic al Zonei Costiere, A.N. Apele Române Administraţia Bazinală de Apă Dobrogea – Litoral, http://mmediu.ro, last accessed 26 iunie 2013

Hartley C (1881) Kustenjeh Anchorage. Surveyed under the direction of Sir C.A. Hartley CE, Sup. Eng. to the Danubian Commission 1881, Scale 1:12,000, 68.5 × 40.4 cm, United Kingdom Hydrographic Office (UKHO), London

Hay CC, Morrow E, Kopp RE, Mitrovica JX (2015) Probabilistic reanalysis of twentieth-century sea-level rise. Nature 517:481–484. doi:10.1038/nature14093

Malciu V, Diaconu V (2000) Long-term trend of sea level at the Romanian littoral, IOC Workshop Report No. 171, Annex III

McCarney-Castle K, Voulgaris G, Kettner AJ, Giosan L (2012) Simulating fluvial fluxes in the Danube watershed: the "Little Ice Age" versus modern day. The Holocene 22:91–105. doi:10.1177/0959683611409778

Rădoane M, Rădoane N (2005) Dams, sediment sources and reservoir silting in Romania. Geomorphology 71:112–125. doi:10.1016/j.geomorph.2004.04.010

Serviciul Geografic al Armatei (S.G.A.) (1913–1924) Planurile Directoare de Tragere, Scale 1: 20,000. Sheets: 5638, 5639, 5640, 5642, 5643, 5644. Bucureşti

Spratt TAB (1856) Sketch of the routes from Kustenjeh to Chernavoda and Rassova with the Karasu Lakes by Capt T. Spratt R.N. C.B. 24 July 1854. Made during a reconnaissance in company with Lieut. Col. the Hon. A. Gordon and Lieut. Col. J. Desaint de l'Etat Major. Single sheet. Col. lith. Scale: 1:99 500, 102 × 50 cm, United Kingdom Hydrographic Office (UKHO), London

Sunamura T (1992) Geomorphology of rocky coasts. Wiley, Chichester

Thieler ER, Himmelstoss EA, Zichichi JL, Ergul A (2009) Digital Shoreline Analysis System (DSAS) version 4.0—an ArcGIS extension for calculating shoreline change: U.S. Geological Survey Open-File Report 2008–1278

Trenhaile AS (1987) The geomorphology of rock coasts. Clarendon Press, Oxford University Press, Oxford [Oxfordshire], New York

Vespremeanu-Stroe A, Constantinescu Ș, Tătui F, Giosan L (2007) Morphodynamics of the Danube delta coast: multi-decadal evolution and North Atlantic Oscillation Influences. In: Proceedings of international coastal symposium, Australia. J Coast Res SI 50, 157–162

Wildavsky AB (1988) Searching for safety. Studies in social philosophy and policy. Transaction Books, New Brunswick

Woodroffe CD (2002) Coasts: form, process, and evolution. Cambridge University Press, Cambridge

Chapter 25
Foredunes Dynamics on the Danube Delta Coast

Luminița Preoteasa and Alfred Vespremeanu-Stroe

Abstract This chapter is devoted to the foredunes developed on the dry temperate Danube delta coast with a focus on the Sf. Gheorghe beach (Sărăturile ridge plain) at the updrift of the Sf. Gheorghe mouth. It presents the medium term (e.g. 17 years) beach–foredune dynamics and foredune morphology together with the alongshore variability pattern as influenced by dune superposition over three different shoreline modal states: erosive, stable, and accretionary. The morphology of the foredunes (from different coastal sectors) is briefly described, highlighting the imprints of the site-specific characteristics of the controlling factors (e.g., shoreline dynamics, beach width, vegetation cover, nearshore configuration) on foredunes shape, size, and behavior. The role of extreme events (e.g., severe storms and Danube floods) and fair weather conditions is discussed along with the geomorphological evolution of the beach–foredune system derived from seasonal topographic surveys and cartographical data analyses.

Keywords Accretion · Alongshore pattern · Vegetation density · Scarp recovery · Equilibrium slope · Danube delta

Introduction

Foredune systems are significant coastal landforms both geomorphologically and ecologically (Ollerhead et al. 2013), valued for their recreational amenities and for their role as natural coastal defense structure (Saye et al. 2005). Beaches and foredunes form one of the most dynamic coastal subsystems, which driving forces act to continuously attune them to the ongoing variations of the environmental factors. The understanding of the foredune tendency to reach and maintain an equilibrium profile requires addressing the question of the "ideal configuration"

L. Preoteasa (✉) · A. Vespremeanu-Stroe
Faculty of Geography, University of Bucharest, 1st N. Bălcescu Blv.,
010041 Sector 1, Bucharest, Romania
e-mail: preluminita@yahoo.com

M. Rădoane and A. Vespremeanu-Stroe (eds.), *Landform Dynamics and Evolution in Romania*, Springer Geography,
DOI 10.1007/978-3-319-32589-7_25

concept which refers to a (*cross-shore*) morphology experiencing minimum of changes during the high energy events engaging wind and wave sediment reworking. The ideal cross-shore profile would imply an adaptation to both: (i) *storm wave run up*, which energy is most efficiently dissipated across a gently sloping seaward flank, and to (ii) *medium and high winds* during which minimum erosion or deposition take place especially when low wind speed fluctuations, which also correspond to a uniform and smooth morphology with gently sloping flanks. But for this equilibrium profile to be achieved it is necessary, continuous sediment flux provided, that the two majors controlling factors—accommodation space and vegetation—to work in favor of the configuration above described. This would involve a permanent sediment sorting mechanisms acting so that to preserve both cross-shore and alongshore morphology.

As components of the complex dynamic coastal system, foredunes dynamics is often studied within the framework of beach/foredune interaction (Psuty 1988; Sherman and Bauer 1993; Sherman and Lyons 1994; Hesp 2002, 2013; Bauer and Davidson-Arnott 2003; Arens 2007; Vespremeanu-Stroe and Preoteasa 2007; Milne et al. 2012; Houser and Ellis 2013) or within the broader context of the active coastal system (e.g., from the longshore bars to the back of the foredunes: Short and Hesp 1982; Ruessink et al. 2003; Aagaard et al. 2004, 2007) providing significant information on sediment transport within the system or on spatial and temporal sediment budget variations. However, the role of nearshore processes and morphological change is considered as a flexible and dynamic constraint on the supply and transport of sediment between submerse beach, berms, and fordunes (Houser 2009). Yet, information on sediment budgets does not provide knowledge as to how the sediment is distributed in the dune system (Bochev van der Burgh et al. 2011).

Along the Romanian coast, foredunes formed at places where sufficient sediment supply, significant onshore or alongshore winds and enough accommodation space were available to promote the exchange of sediment between the nearshore and foreshore (beach) and the backshore (dunes) by wind. Although of relatively smaller volume than the Late Holocene dunes systems currently situated at about 30 km inland (e.g., Caraorman and Letea dunefields), the present-day foredunes are common features along the Danube Delta coast, where both Danubian and allochtonous sediments converge to produce a vigorous alongshore sediment flux.

This chapter is about the foredunes developed along Sărăturile ridge plain, on the updrift flank of the modern Sf. Gheorghe lobe. This particular foredune system has been chosen as study site for the monitoring of sand dune dynamics as it is considered the most representative foredune system along the Romanian coast in terms of size, age (activity duration), natural state, growth, and evolutionary pattern (Preoteasa 2008). As the morphological changes within the beach–foredunes system are continuous and cumulative (Masselink and Gehrels 2014), studies integrating multiple scale dynamics are compelling for understanding their specific behavior and the role they play in the larger scale, integrating morphological feature evolution. In addition, the current state of the foredunes developed on Musura and Sacalin barrier islands will also be briefly presented.

This chapter presents medium-term (i.e., 17 year) beach–foredune dynamics on both cross-shore profiles and 3D polygons (of thousands of m^2) and the pattern of alongshore variability in foredunes dynamics and morphology as influenced by their superposition over three different beach sectors in terms of geometry and morphodynamics, ranging from erosive sectors with narrow beaches (≤ 15 m) of intermediate type to stable and slightly prograding with wide beaches (40–50 m) of intermediate to dissipative type (Vespremeanu-Stroe 2007). In addition to the seasonal energetics and vegetation density, the foredunes are highly sensitive to storm winds and waves, high or low water levels occurrence, and to local or far-field human intervention; such variations of the controlling factors which have forced the recent foredunes evolution will be referenced and their impact will be assessed.

Regional Setting

The Danube delta coast, located on the western side of the Black Sea area, stretches along a total length of 200 km from the Primorskoe promontory (Ukraine) at the N to Midia Cape (Romania) at the S (Fig. 25.1). The general physiographical features distinguish a northern sector of 55 km corresponding to Chilia fluvial dominated deltaic lobe, where the shoreline is made up of sandy beaches, barriers, spits, and islands and rarely of muddy benches with reed. The former support small foredunes; the largest eolian features develop mainly on Musura Island. The next 33 km (southward) belong to Sulina—Sf. Gheorghe interdistributary coast with two main foredune sites, one developed along ca. 3 km downdrift of the Sulina jetties, the other along ≈8 km north of Sf. Gheorghe mouth (Sf. Gheorghe beach, the southern half of Sărăturile strandplain coast). Further downdrift, perennial foredune structures developed locally on Sacalin Island and South Chituc ridge plain.

The well-developed foredunes formed particularly along the Sf. Gheorghe beach which became stable since early twentieth century, after a long interval of rapid progradation (7–10 m/year for 650–1930 AD, Preoteasa et al. 2016). It develops along a coast which aspect (of 96°) determines the prevalence of incident waves from northeast and a resultant southward sediment transport system with mean rates of $0.98 - 1 \times 10^6$ m^3/year (Dan et al. 2009; Vespremeanu-Stroe 2007). The wave climate along the Danube Delta is medium energy with a mean offshore significant wave height of 1.43 m, increasing to 2–4 m during regular storm events; the maximum wave height exceeds 6 m during extreme storms. The monthly multiannual analysis of the LST shows a highly skewed distribution with ca. 60 % occurring during winter, and 8 % during summer (Vespremeanu-Stroe 2004).

Danube Delta currently evolves within a temperate dry climate, with average precipitation about 340–380 mm/year. The mean multiannual temperature is 11 °C with sharp differences between seasons (January: −1 … −0.2 °C; August: 21.8–22.3 °C). The mean wind speed on Danube Delta coast is 6.95 m/s, with a higher speed of the northern winds (7.5 m/s) than of the southern winds (5.6 m/s; data from Sulina

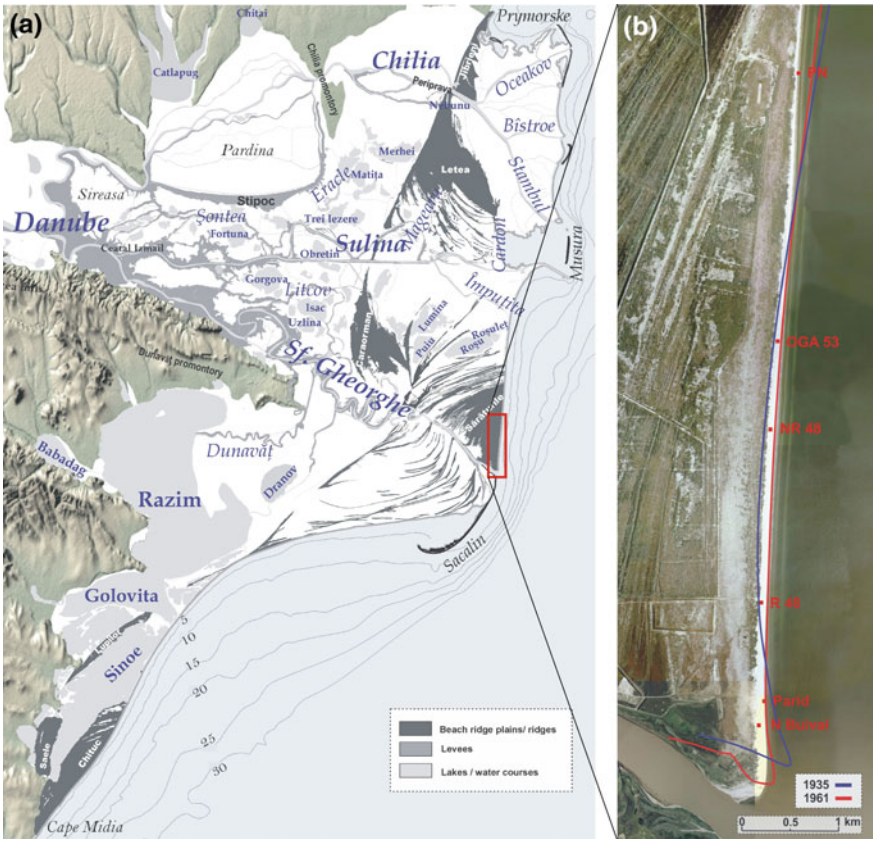

Fig. 25.1 Danube Delta map (**a**) with the box showing the foredunes study site on Sărăturile ridge plain. Sărăturile coast (*right*) with the three different mophodynamic sectors roughly delineated between the benchmarks as follows: **a** erosive sector stretching about 2 km updrift and downdrift of PN; **b** stable sector between OGA 53 and Parid, and **c** slightly accumulative sector between Parid and Sf. Gheorghe mouth

meteorological station: 1961–2000). 74 % of winds with sand transport potential (≥ 6 m/s) are coming from the northern sector (ENE–WNW). The present wind climate is macroenergetic on the coast (e.g., 63–75 [vu] at Sf. Gheorghe and Sulina meteorological stations) according to Bullard's (1997) adjustments to Fryberger's technique (Fryberger 1979). High rates of potential transport, of about 83 % of the total annual aeolian drift occur during the cold active season (October–April). The directional variability of the sand-transporting winds is small, resulting in a southward aeolian drift, with a resultant drift direction of N 197° at Sulina and N 182.4° at Sf. Gheorghe stations (Preoteasa and Vespremeanu-Stroe 2004).

The storm regime along the Danube Delta is marked by the dominance of the northern storms (71 % of the total number of storms and 87 % of the severe storms are from northern sector). Foredunes are severely impacted by extreme storms in

which cases storm surges overpass 0.7 m (maximum water level >1.5 m), the waves are extremely high (Hs > 5 m) and are commonly driven by wind speeds higher than 25 m/s. During the last 50 years, 12 category IV onshore storms have been recorded and 5 category V onshore storms (a 10-year return period). The strongest storm (SSI = 1031) registered during the last half century occurred in January 1998 and had the highest total morphological impact (SIP = 633). It was a category V storm with a total duration of 157 h. The wind blew onshore (RWD = 35°) with maximum speeds of 28 ms^{-1}, inducing a theoretical maximum Hs of 7.4 m (corresponding peak period of 9.2 s) and a storm surge of almost 1 m. It was the second event of a storm cluster as it was preceded by another extreme storm (15–18 December 1997): category V (SSI = 768, SIP = 329), D = 82 h, RWD = 19°, maximum wind speed of 28 ms^{-1} and Hsmax = 6.8 m, with a similar storm surge of 1 m (Tătui et al. 2011).

The low-energy storms (category I: Vmax < 15 m/s, Hs $\leq$ 2.5 m) are generally constructive, while medium energy storms (category II–III: Vmax < 25 ms^{-1}, Hs: 2.5–5 m) are predominantly conservative for the foredunes. Their impact becomes sensible when they occur as storm clusters, in which case the high frequency (17 storms per year or 60 % of the total) imposes cumulative morphological changes which contribute the most in creating an equilibrium profile of the subaerial beach.

The local sea level is also engaged in beach width and hence the beach–dune system dynamics; this is particularly sensitive to the eastern winds and to seasonal Danube discharge which is higher during April–July interval, while the lowest levels correspond to September–October interval. Recent estimates show that St. Gheorghe solid discharge is about 0.80×10^6 m^3/year (Panin and Jipa 2002), comparable with the local LST.

The mean grain size of both submerged and subaerial sand varies alongshore, under the influence of the longshore currents, becoming finer downdrift, from 200 to 190 μm within the boundaries of our study site. Sediment mean size influences the mean slope of the nearshore barred—beach—foredunes profile which decreases accordingly, from 0.45° to 0.36°.

The species composing the vegetation cover on the foredunes (*Eringyum* sp., *Salsola* sp., *Saueda* sp., *Elymus* sp., *Convulvulus* sp., *Petasites* sp.) are sensitive to both water availability and continuous sand flux.

In the context of the temperate dry climate, low density vegetation cover of primarily psammophyte species and the sediment load coming from the Danube and from the nearshore currents, comparatively small to medium size foredune currently form only at the distal part of a littoral cell, over constrained accommodation space (e.g., updrift of the river mouths), or naturally or anthropogenic sheltered sectors (e.g., downdrift of Sulina jetties).

Foredune Morphology Along the Deltaic Coast

In this chapter the morphology of the foredunes from different sectors along the deltaic coastline is briefly presented, with the highlight of the imprints of the local characteristics of the controlling factors (i.e., shoreline dynamics or beach width) on foredunes shape and size.

The beach–dune systems along the Danube Delta coast are highly patchy due to the rare combination of the few sediment depocenters exposed to resultant wind direction, sediment entrapment prone areals (e.g., rough surface associated with dense vegetation or rugged topographic surface, the presence of protruding features acting like a groin for the sand flux). The contemporary foredunes are comparatively small, no higher than 3–4 m a.s.l, with widths ranging from 2 to 3 m up to 80–100 m (e.g., close by the river mouth, at the updrift side) and lengths ranging from several tens of meters (Musura and Sacalin barrier islands) to several (up to 7) kilometers (Sărăturile, Chituc). They usually present gentle fronting slopes and steep backing slopes. Few exceptions are recorded on the erosive coasts where the stoss slope is steep due to frequent episodes of dune toe washed by waves and to wind pressure exerted on the entire foredune ridge.

An important contribution to foredunes development and a major factor conferring diversity of both intra- and inter-sites foredune morphology is the vegetation cover (e.g., spatial dispersion, density, seasonal variability) (Hesp 2002). Medium- to long-term foredune dynamics is also subject to the influence of the shoreline dynamics and orientation, beach width, and nearshore geometry and related fetch characteristics within the specific unidirectional wind climate. Further below the foredunes from Musura barrier island, Sulina beach, Sărăturile beach, and Sacalin Island will be characterized in terms of their specific morphology.

Foredunes Developed on Barrier Islands and Spits

One of the main morphological signatures of the barrier island dynamics is the alongshore succession of washover fans which were built at a backward position by reference to the former (pre-storm) waterline and small, ephemeral secondary spits at the downdrift. The washover fans are ideal places for foredune emplacement as, by their nature, they provide extensive low-lying, vegetation-free, quasi-planar (and implicit low roughness) deposits of uncohesive sediments making available not only large sand surfaces to be winnowed and to form dunes, but also furnishing the ground for readily installation of vegetation. Its subsequent growth contributes to surface roughness increment and hence more efficient conditions for sand trapping and dunes stabilization. Thus, most of the foredunes are currently clustered on the northern sector (of both islands) which is the most stable of the barrier island (connected to the mouth).

Musura Island

Musura is a barrier island of about 6 km long, which developed downdrift of a vigorous river mouth—Stambulul Vechi mouth—as many other barrier islands did in the past, as part of the cyclic growth pattern of the open-coast deltaic lobes (Vespremeanu-Stroe and Preoteasa 2015). It is a young barrier which started to emerge in the late 1980s as a series of drift-aligned islets which merged and extended southward with a mean rate of 176 m/year (1996–2013 (Fig. 25.2a);

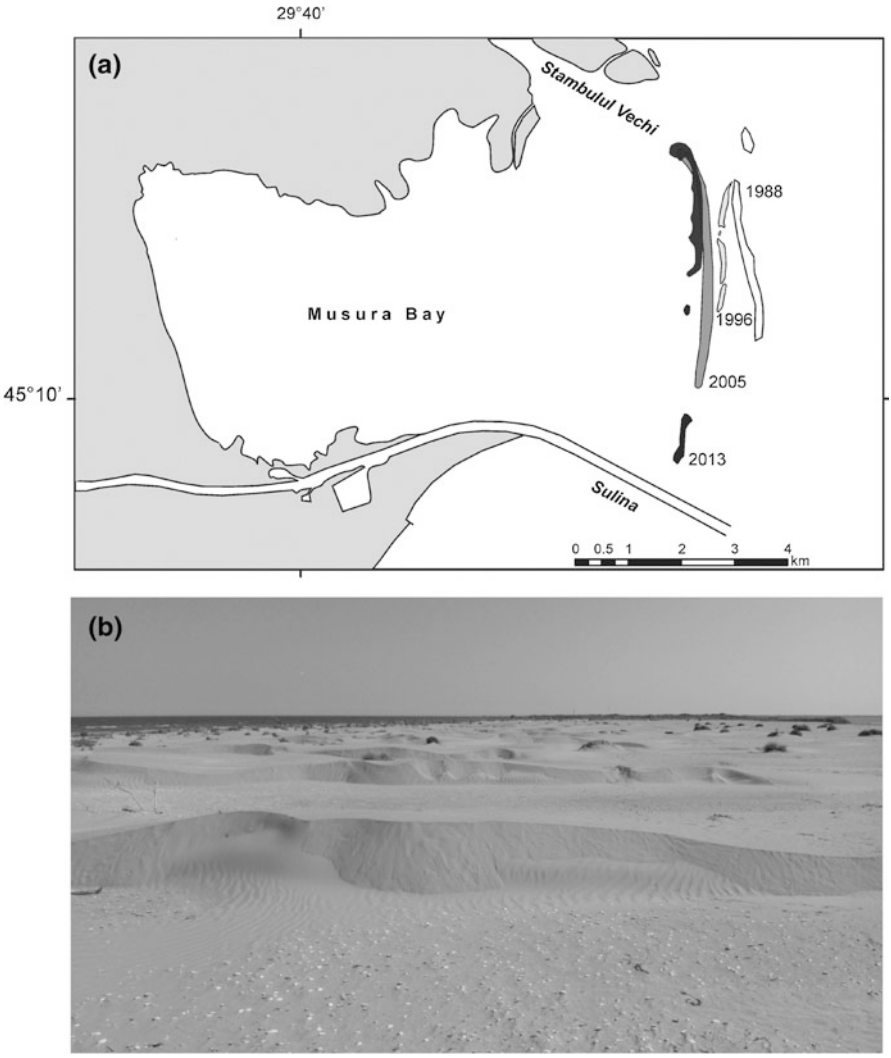

Fig. 25.2 Musura barrier island evolution (**a**); mobile transverse dunes formed on the central part of the bearrier (**b**)

presently, the southern end slowed down its downdrift elongation, reaching to just 200 m near the Sulina arm jetties where a future welding is probable in natural conditions. Until recently, the island migrated landward at rates of 35–50 m/year (1988–2005), mainly under the pressure of storms, to achieve the present-day equilibrium with the lateral shoreline sectors, retreated at much lower rates of 2–5 m/year (Vespremeanu-Stroe and Preoteasa 2015). During the last 10 years, the northern sector became stable whereas the middle and southern sectors retreated at much lower rates of 2–5 m/year (Vespremeanu-Stroe and Preoteasa 2015).

The oldest foredunes here started to develop after Danube high waters recorded in 2010 and are currently covered by vegetation (especially with *Tamarix* sp.). They stand as short ridges (300–500 m), narrow (5–10 m), and small (1.5–2 m) sand accumulations anchored by psammophytic herbaceous and woody vegetation.

On the middle sector of the island there are only small (no higher than 1 m), highly mobile dunes accommodated on washover fans built during February 2012 storm. Most of them are transverse mobile dunes with lengths of 10–25 m and widths of 3–5 m. The dunes are rapidly changing their position and morphometrics depending on the wind conditions, but their crests are usually E–W and SE–NW aligned, respectively, perpendicular on the prevalent northern and northeastern winds (Fig. 25.2b).

Sacalin Spit

The largest foredune systems along the Sacalin spit are associated with its most stable alongshore sectors. Stable foredunes development at the northern tip of the barrier island has been initiated after 1942 when this sector merged with the mainland (Vespremeanu-Stroe 2007). Freshwater proximity and steady sediment supply favors the rapid spreading of a large variety of plant species enabling rapid sand accumulations and surface aggradation. Barrier island juxtaposition to the mainland together with the rapid vegetation growth since the early 1970s led to the gradual stabilization of this sector together with the surface roughness increment, encouraging the slow aggradation at one hand, while exposing it to the hydrodynamic effects of the mouth dynamics, fluvial sediment fluctuations and to the NE prevalent wind direction at the other hand. These factors regularly combine to deliver sediment to the beach–foredune system via proximal longshore bar emergence and welding to the subaerial beach (e.g., every 1–3 years). These sediment pulses together with the high roughness surface, often resulted in a constrained sediment flux, forced to rapid localized sand accumulation, essentially as precipitation ridges. Alternatively, due to their advanced position, they are more susceptible to increased waves energy. A more balanced long-term foredunes development is usually achieved by the change of the foredune position to a more sheltered, backward place. This generally occurs when and where former foredunes are breached by the storm waves and sand is further landward splayed as washover fans, where enough space is available. These sand features are subsequently reworked by wind and foredunes are readily initiated.

The most prominent foredune systems on Sacalin spit is also the oldest emplaced at the northern edge, in the 1980s, along the westward recurved tip mainly under the influence of the NE waves diffraction processes at the downdrift tip of the mouth bar. The northward directed countercurrents also diffract around the northern tip of the spit, entering on the Sf. Gheorghe mouth. Thus they contribute to maintain the stability of the northern edge of the Sacalin spit constantly forced by the southward deflected river mouth, by ongoing sediment delivery and relative large beach width, excepting the high local water level intervals associated with the high Danube discharge or NE winds. The relatively large beach width specific to the calm weather conditions are fully exposed to the prevalent NE winds contributing to a WNW–ESE alignment (i.e., obliquely onshore positioned relative to the Sacalin spit northern sector overall orientation) of the best developed foredunes system from Sacalin spit. It measures about 200 m long, 20 m width, and splitting downdrift (westward) in two different ridges of 2.5 m height, covered by *Tamarix* sp.

Fordunes Developed on Beach Ridge Plains

The morphodynamic feedbacks between river and waves (including the hydraulic and morphologic groin effect) maintain a multiple cell system contributing to the local retention of sand (Giosan 2007; Anthony 2015) which may be then arranged in successive shore parallel beach ridges. Beach face accretion and berm construction during fair weather conditions are the common processes generating large and medium size BRPs in the Danube Delta. In places, shoreline progradation is dependent upon bar welding processes building wide and low berms (e.g., *Sacalin South*). Yet, the ultimate force conferring the definite "ridge" aspect of the prograding coasts in the Danube Delta is related to aeolian processes which create either unitary foredune crests where shoereline is relatively stable (e.g., central and southern sectors of Sărăturile BRP) or thin eolian sand sheets (incipient/embryo foredunes) tens of centimeters higher than adjacent berms (and washover fans if they are present) where shoreline advancement occurs at fast pace (Sulina beach) (Vespremeanu-Stroe et al. accepted).

Sulina Beach

Despite their small size, perennial foredunes developed along almost 3 km downdrift of the Sulina mouth jetties. The size and the good conservation potential of these dunes are associated with the rapid shoreline advancement rates which at one hand work to limit the time needed for bigger sand volumes accumulation and at the other hand work to build wider beaches which keep them at distance from waves. The shoreline evolution rate of this sector computed for the last four decades was of 2–8 m/year (Vespremeanu-Stroe 2007), the fastest progradation rate recorded along the deltaic coasts excepting the secondary deltas. In the last decade the shoreline

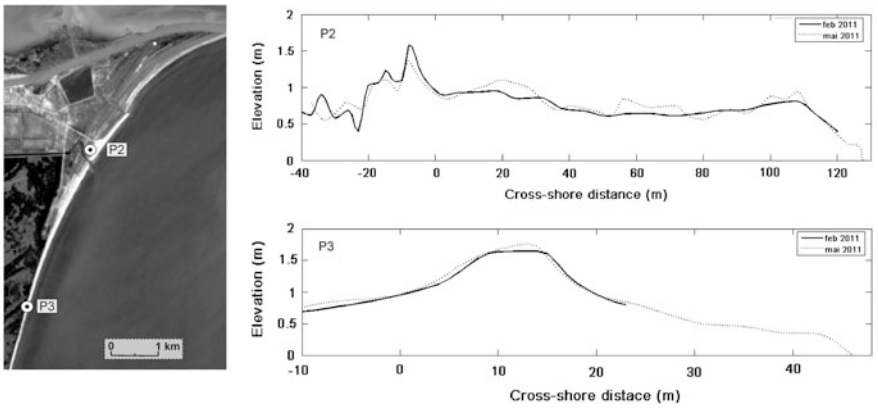

Fig. 25.3 Sulina coast (*left*) and foredunes morphometric characteristics (*right*)

progradation rates decreased to ca. 50 % (1–4 m/year), reflecting the achievement of the plan view equilibrium with the nearshore wave climate adapted to the recent extension of the Sulina jetties and to the southern dike (emplaced in 1981).

The rapid shoreline progradation episodes were accompanied by the construction of several dune ridges separated by an *interdune area.* The foredune ridges formed at a 120 m distance from the waterline, 5–40 m wide, and 1.5 m height and are covered by *Tamarix* sp. (Fig. 25.3a). The dunes from the second ridge (landward), situated at more than 150 m from the shoreline are 2.5 m high, stabilized by the *Tamarix, Hippophae,* and *Salix* sp. Further southward, along a dynamic equilibrium sector, the shoreline evolution rate between 1962 and 2000 was of 2–4 m/year, foredunes preserve relatively similar sand volumes and size if compared with those situated closer by the jetties, whereas their position from the shoreline varies between 20 and 40 m (Fig. 25.3b).

Sărăturile Ridge Plain

The foredunes along Sărăturile coast achieved the present configuration gradually since the 1970s under the influence of the new colonized wooden species (*Tamarix* sp., *Salix* sp.) which temporarily coincide with the founding of a large experimental forest planted in 1963 to the North of Sf. Gheorghe village. According to air photographs inspection (1970 series), GPR profiles and the locals' testimonies, before the allochtonous wooden vegetation dispersal, sand dunes on Sărăturile coast displayed as smaller foredunes, both in width and height. Due to their small dimensions and lack of any significant obstacles, the storm winds carried sand behind the foredune, at large distances (up to 400 m), and formed vegetation-free, highly mobile dunes, usually represented by hummocky or barchanoid types at the back of the foredunes. The quasi-continuous line of woody vegetation settled in the 1970s on the landward limit of the foredunes stopped the sand flux between the

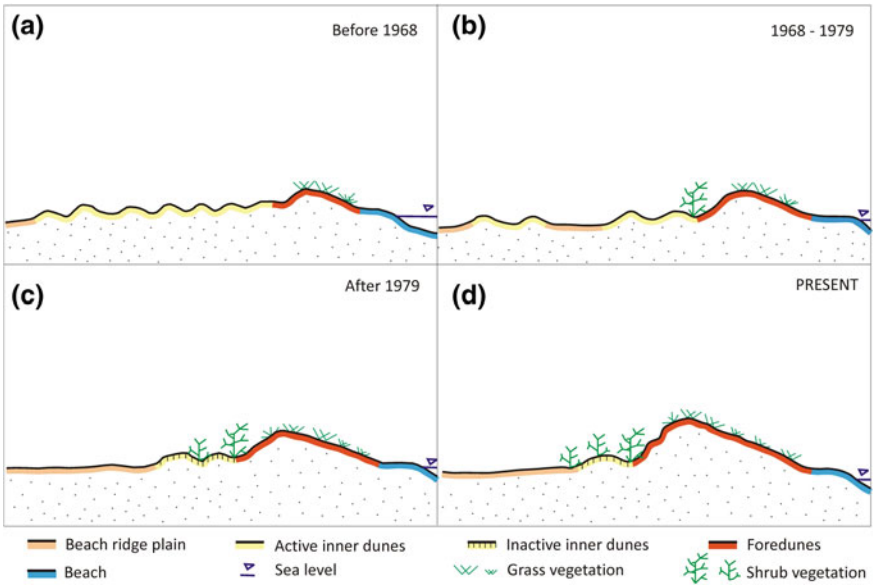

Fig. 25.4 The model of foredunes evolution along Sărăturile coast in relation with sediment flux transformations (between foredune and beach /back-dune) induced by vegetation cover changes

beach–foredune system and the white/mobile sand dunes formed behind it which allowed the alongshore gradual sand accumulation increase in front of vegetation alignment and the foredune volume growth (Fig. 25.4).

Nowadays, Sărăturile coast comprises three alongshore sectors with different morphodynamic state, each of them being characterized (from North to South) by erosive (ca. 7 km), stable (~5 km), and accumulative processes (~1 km) in accordance with the alongshore changing characteristics of the sediment transport. Here, foredune emplacement relative to the average shoreline position is particularly dictated by the last extreme storm which ultimately acts to regulate the coastline evolution at larger temporal and spatial scales through washover fans formation (Photo 25.1).

Washover fans constitute favorable settings for foredunes development as they provide local sand supply necessary for foredune inception and, by their backward position relative to the waterline, a more sheltered environment for dunes preservation.

Because of the gradual alongshore changes of the foredunes morphometrics and dynamics, the case analyzed and discussed at each benchmark is considered as representative for each morphodynamic sector which, by their systemic nature, cannot be reasonably framed within clearly marked spatial boundaries. Thus, due to the alongshore gradual changes or/and propagation of morphometric and morphodynamic characteristics we choose to loosely delineate three distinctive shoreline sectors (Fig. 25.4).

The erosive beach (northern sector—PN)

The northern sector of Sărăturile beach—for which representative cross-shore profiles have been monitored at PN benchmark (Fig. 25.1b)—extending roughly between 6–8 km updrift of the Sf. Gheorghe mouth is slightly protected by the presence of two small longshore bars with a mean volume of 38–40 m^3/m for the outer bar and of 15 m^3/m for the inner bar; they develop across the narrowest cross-shore migration zone (280–300 m), wherein they migrate at the most rapid rates (40–43 m/year) and during the shortest return period (∼2.8 years) along the entire study area (Tătui 2015).

Here, foredunes form, grow, disappear, and then rebuild as long as they have to cope with moderate erosion. The foredune monitored at PN benchmark colonized a beach with medium-term (1990–2014) shoreline retreat rate of 2.6 m/year. However, it is interesting to note that this shoreline mobility rate is close by the critical rate of foredune maintenance, as long as to the north, where the erosion accelerates, the foredunes are generally missing. The erosion intensity along PN beach is much lesser than that recorded along the updrift sector spanning over ca. 15 km long, where long term (i.e., centennial) erosive trend inherited from Sulina deltaic lobe recession, to which medium-term (i.e., multi-decadal) erosion generated by the new plan view equilibrium shape achieved after Sulina jetties construction and chronic sediment depletion associated to the far-field anthropogenic interventions (e.g., upstream dams, dykes) concur to a mean shoreline retreat rate of 14 m/year (1961–1979), respectively, 6.3 m/year (1979–2003) (Vespremeanu-Stroe 2007) which do not allow the minimum time and accommodation space for foredune growth. Nevertheless, during periods lacking severe storms the embryo dunes locally coalesce into incipient foredunes which resist till next high storm surge.

Developed along a shoreline sector subject to erosional processes propagating from the updrift, the foredunes display the lowest morphometric parameters and the highest morphodynamics along the study area. Beach width is highly variable, measuring in average 15–20 m, while the mean foredune volume ranges from 14 to 35 m^3/m, and shows a declining trend since 2006 (Fig. 25.5a, a1). Most probably, the present-day foredune belt initiated from sand winnowed on the washover fans which were emplaced during the most aggressive northeastern storm from the last 50 years (21–27 January 1998, Zăinescu and Vespremeanu-Stroe, Chap. 34, this volume). In this sector the alongshore continuity of the foredunes is in sometimes interrupted by storm waves in places where washover fans form, becoming at their turn appropriate settings (e.g., sediment availability, sheltered position) for subsequent foredunes initiation. Where withstanding as continuous foredunes belt, the constantly retreating shoreline forces them to migrate landward. The specific morphodynamics in this case is mainly controlled by the general configuration of the accommodation space which is principally imposed by the vegetation cover density and its spatial dispersal pattern, as well as the preexisting topography (e.g., remnant knobs interspersed within the wooden vegetation at the back of the foredunes).

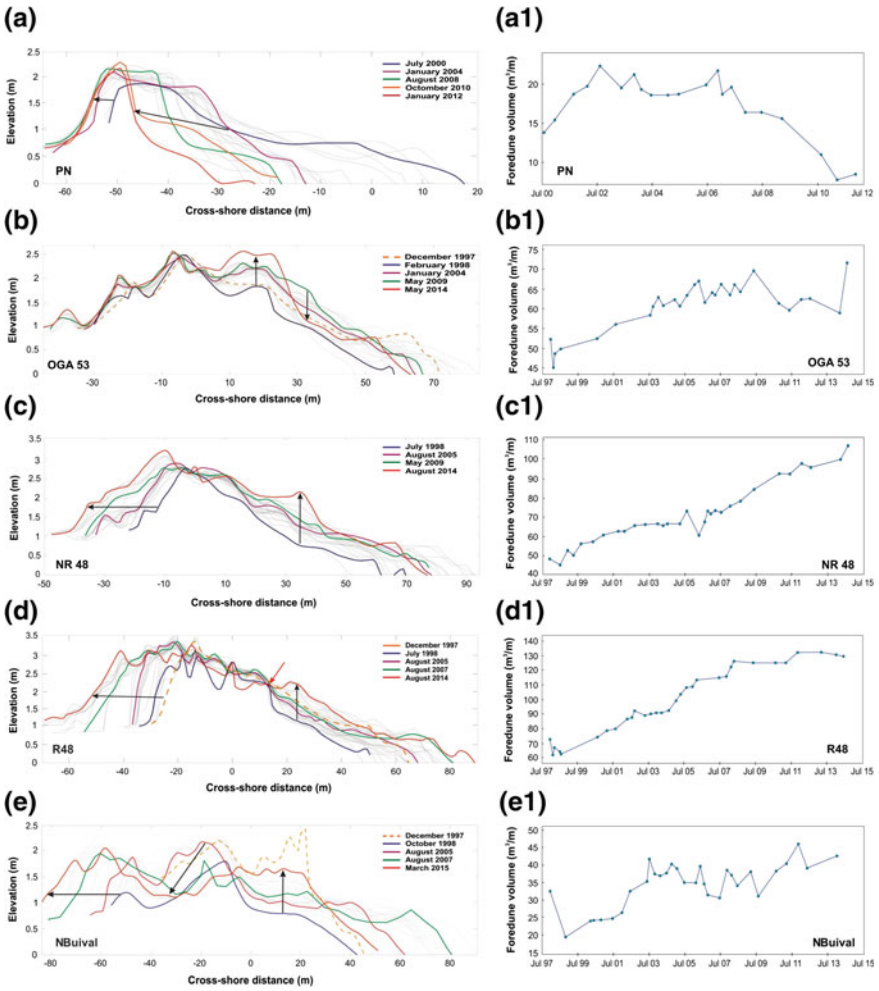

Fig. 25.5 Foredunes dynamics over medium-term scale (e.g., 2002–2012 for PN benchmark and 1998–2013 for OGA 53, NR48, R48, and NBuival) along Sărăturile shoreline represented as morphologic profiles changes on the *left column* and as sand volume evolution on the *right column*

Stable beach (central sector; N OGA 53—Parid)

Downdrift of the previously discussed sector, along the next 4 km (Fig. 25.1b), the coast become stable since early twentieth century when the long-term progradation pattern ($\sim$10 m/year for 650–1940 AD) ceased as a consequence of the changes of the Sf. Gheorghe river mouth evolutionary pattern in relation with human-induced depletion of sediment supplied by the Danube flow (Preoteasa et al. 2016). The upper shoreface has a gentle slope which dissipates wave energy more efficiently than on the other sectors. It accommodates three longshore bars which

regularly develop across a wide zone which may be reaching 400 m (at the downdrift part of this sector), with alongshore constant mean volume of the distal bar of 40–42 m^3/m and slightly smaller inner bar: 38–40 m^3/m, slower bars migration rates (30–35 m/year) and longer return period (4.5–5 years) (Tătui 2015).

The foredunes exhibit the greatest consistency from the entire study area, with volumes that range alongshore between 60 and 130 m^3/m, while the crest elevation maintains at 3–3.5 m a.s.l. The beach width varies seasonally between 25 and 40 m, allowing sufficient space for the obliquely onshore and alongshore winds to readily achieve a high transport potential and to provide sand for building the most robust and highest foredunes sector. Morphologically, this sector is characterized by a robust and unitary, continuous alongshore foredunes ridge, with long and gentle slopes (1.5° to 3° for the fronting slope and 5° to 10° for the backing slope which locally, at the contact with the dense vegetation can reach the equilibrium slope, of about 30°) and wide well-rounded crest. These features describe a seaward aerodynamic cross-shore profile of the dunes enabled by the sparse, mainly herbaceous vegetation cover and the high aeolian flux within fordune system that was computed at about 30–50 % of that on the beach (Vespremeanu-Stroe and Preoteasa 2007). Correspondingly, the intense eolian activity creates conditions for overimposed transversal sand accumulations and circular blowouts formation on the foredunes crest. They generally evolve toward trough blowouts or through merging two or more neighboring blowouts generate alongshore elongated depressions.

Accretionary beach (the southern sector—N Buival)

The adjacent river mouth coast, spanning along 1.1 km (best described by N Buival benchmark, (Fig. 25.1b, Photo 25.1) registered a slight accretion of 1.3 m/year during 2000–2010 interval and maintained a stable position since then.

Here, in condition of fair weather, part of the southward drifting longshore sediments (which encounter perpendicularly the mouth bar) are transported onshore on the subaerial beach (berms), whereas most of them are collected by upper shoreface until the next severe storm capable to rework sediments and to force sediment bypass beyond the mouth bar. The largest shoreface sand volumes along the interdistributary Sulina—Sf. Gheorghe coast are encountered along this sector characterized by the widest bar zone (of 550–600 m), with three sandbars, of ca. 60 m^3/m the outer bar and 25 m^3/m the inner bar, display the slowest migration rates (25 m/year) and the longest return period (5.4 years) from the study area (Tătui 2015).

The foredunes are widest in this sector, reaching up to 100 m, favored by the new accommodation space (washover fans) created through foredunes overwash during January 1998 extreme storm; contrary, the height is low (ca. 2 m a.s.l.) and gradually decreases toward the river mouth. Despite the large foredune widths their volumes are significantly lower in comparison with the stable coast ranging between 25 and 50 m^3/m.

Hence, the net distinctive morphological feature when compared to the updrift foredune belt is the fragmentary aspect set by the presence of oblique and shore

Photo 25.1 Foredune alignment over ca. 3 km updrift of Sf. Gheorghe mouth. Noteworthy, the foredunes emplaced on a position previously occupied by washover fans formed during January 1998 storm (courtesy of Mihaela Marin)

parallel blowouts and deflation lags which almost divide the foredunes into two alignments. The blowouts here are controlled mainly by the NE winds and subsequently by the air currents topographic distortion which contributes to the morphological diversity of this foredunes sector ranging in size from small hummocks such as embryo dunes and remnant knobs to precipitation ridges or deflation lags either superimposed or intertwined in shore parallel ridges. These diverse morphological features constantly respond to a steady sediment flux supplied by both the beach and the foredunes as allowed by the low density vegetation cover. Due to its position relative to the Sf. Gheorghe mouth bar and to the peculiar morphodynamics imposed by the continuous sediment input and constantly adjusting accommodation space, this sector is particularly exposed to the storm surge. Therefore, the major morphological changes within the beach–foredune system are subject to the alternating storm waves and calm intervals. During storm conditions the fronting slope of the foredunes is regularly scarped or locally or completely breached, accompanied by washover fans and remnant knobs shaping during extreme wave events. Otherwise, during fair weather conditions the foredunes are constantly smoothed by the vigorous sedimentary flux associated to low roughness conditions (i.e., fine, uncohesive sands; low vegetation cover, low dune elevation, gentle slopes). Thus, the foredunes here, located at about 25–40 m landward from the waterline, have been almost obliterated by the extreme storm waves in January 1998 (Fig. 25.6), which left behind vast washover fans and remnant knobs.

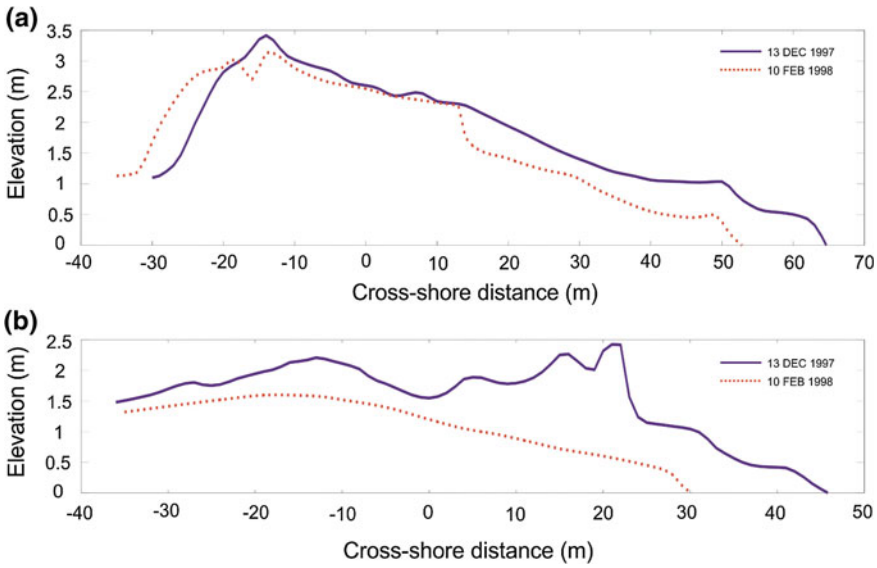

Fig. 25.6 January 1998 storm impact on foredunes at R48 and NBuival benchmarks (modified from Tătui et al. 2013)

Immediately after that event, they started to rebuild at a backward position through aggradation as a double foredune alignment, in the middle of which an elongated blowout, controlled by the NE winds, separates a massive, quasi-continuous foredune alignment about 30 m wide and 1.5–2 m high at the upper part of the beach from a smaller foredune alignment (precipitation ridge) formed 20 m backward from the previous, at the contact with the wooden vegetation.

Foredune Evolution on Danube Delta Coast

Foredunes dynamics and evolution has been seasonally monitored over the last 17 years (1997–2014) at 7 benchmarks (excepting PN benchmark where measurements have been undertaken for 12 years) along the southern Sărăturile coast (8 km), of which the most representative 5 cross-shore profiles dynamics for each morphodynamic pattern encountered along Sărăturile shoreline will be further discussed.

The Erosive Beach (Northern Sector: PN—OGA53)

The general trend of beach–foredune dynamics at PN, monitored over 12 years (e.g., 2000–2012) is representative for the beach–foredune system situated between 6 and 8 km updrift of Sf. Gheorghe mouth (Fig. 25.4). It is expressed by the net landward recession, with narrow beaches and foredune narrowing and heightening as major accompanying morphological changes. During this time lag, the shoreline retreated ca. 35 m, the foredunes stoss (seaward) slope moved landward ca. 30 m, while the lee slope migrated ca. 5 m and accreted 0.5 m (Fig. 25.5a). The major discrepancies between the two slopes (since 2007; after 7 years of similar dynamic trend) set contrasting evolutionary trends of foredune volume and height (Fig. 25.5a, a1) highlighting the mechanism which acts to keep in place the foredunes under the threat of shoreline erosion. In fact, where enough free vegetation or sparse vegetation room at the back of the foredunes, their volume and shape (foredune width and height) may be preserved while landward migrating, whereas if dense (especially woody) vegetation interferes in their backward migration, the foredunes are forced to accrete while scarped and narrowed due to storm waves.

Its morphometry renders this foredune system highly vulnerable to the entire range of storm waves which, depending on their intensity, either collide with the fronting slope generating or often maintaining an alongshore continuous scarp or, where very narrow, breach them locally producing small size washover fans (regular or moderate–severe storms) or overwash them completely or even overtop them yielding wide, often alongshore contiguous washover fans (during extreme storms).

The Stable Beach (Central Sector: OGA 53—Parid)

Analyses of the successive topographical surveys from this sector, spanning roughly between 1 and 6 km updrift of Sf. Gheorghe mouth (Fig. 25.1b) reveals a seasonal morphodynamic pattern, with reversible changes of the shoreline position of about ±15 m. Foredunes fronting slope aggrades during calm weather interval (especially during July–November) under the impetus of the spring time high waters and related heightening of the berms, while beach lowers and foredunes are scarped during colder, more energetic interval (November–April). All these seasonal morphological changes result in a net foredune aggradation over longer time span when no major storms occur. The overall foredunes aggradation during the 1997–2014 period occurred at different rates at the 3 benchmarks along this metastable sector, respectively (from North to South) 1.65 m^3/m/year at OGA 53, 3.3 m^3/m/year at NR48 and 3.4 m^3/m/year at R 48 (Fig. 25.5b1–d1). Transversal (cross-shore) topographic profiles surveyed between 1997 and 2014 at the 3 benchmarks show a common dynamic pattern of foredune–beach system overall defined by: (i) large sand deposition on foredune slopes, (ii) small oscillations of the

foredune crest height, (iii) significant seasonal variations of the beach width (imposed by shoreline advances and retreats) which exert further control on sediment availability for dune growth, and (iv) a marked seasonality of foredune volume changes defined by major aggradation during late spring—fall (May–November) and slight erosion during December–April interval (Fig. 25.5b–d). The aggradation during the first interval is favored by wide beaches and a higher density of vegetation cover which may be more efficient the windborne sands entrapment, whilst the narrower beaches and frequent storms during the latter interval usually lead to foredune erosion.

As foredunes aggrade, reaching at 3–4 m height a.s.l., a common morphodynamic response (feedback) sets during high winds (storms), respective blowouts initiation on the crest flanks which in short time (2–4 years) merge into larger blowouts, most of them elongated on a NNE–SSW axis. As long as they occupy preferentially the former crest position, the foredune crest is pushed back on a landward position or sometimes split into two crests. Foredune crest is usually the most eroded sector of the foredune due to maximum flow acceleration development which act to increase the potential for erosion (Hesp 2002).

Unlike the other sectors of the Sf. Gheorghe shore, the direct impact of the storm waves is minimal here, with only small scarps locally produced on the seaward slope of the foredunes. Our topographic datasets at the three above mentioned benchmarks documents the main specific morphodynamic situations locally encountered along this coastal sector. The northern case of OGA 53 benchmark is a good example of foredune developed on a sector where cross-shore dynamics is locally constrained either by vegetation and remnant knobs at the back of the actual foredunes or by a sheltered position in respect to the front line of neighboring vegetation. Previous studies reporting foredune changes monitored over 1998–2007 interval show an accumulative foredune trend at a rate of 2.6 m^3/m that subsequently decreased to ca. 0.7 m^3/m (2006–2014) yielding a mean rate of 1.65 m^3/m for the overall monitored interval (1997–2014). The low amplitude, yet wiggled foredune sand volume growth curve at OGA 53 (Fig. 25.5c1) reflects their high sensitivity to multiple factors such as seasonal beach width oscillations or storm occurrence, but the marked lows were recorded in 2005, 2006, 2010 and 2012–2013 years, from which the first three correspond to high water levels associated with the extraordinary Danube floods (with estimated return periods longer than 10 years, cf. Preoteasa et al. 2016). Therefore, the reduced mean width of the subaerial beach during Danube floods affected at greater extent the sectors with narrow or medium beach widths than those with commonly larger beaches (i.e., N Buival case).

Successive changes of the beach–foredune system depict the general pattern of foredune development since the seaward slope scarping to the aggradation of a new foredune crests (on a seaward position) and subsequent foredune profile transformation into a double crested ridge. Generally, foredunes scarp recovery occurs during fair weather conditions when wide beaches provide sufficient dry sediment to be delivered at the scarp foot. The prevalent oblique onshore winds yield a vigorous sediment flux over the seaward slope. The airflow currents lose their

transport capacity at the top of the seaward slope after they experienced flow acceleration over the slope and efficient sediment loading. Rapid sediment deposition takes place on the landward slope due to flow separation typically occurring at the lee of the slope change (Hesp 2002). The intense sand flux within foredune system results in an extensive aggradation (uniformly distributed over most of the seaward slope) and maintains milder fronting slopes with an aerodynamic profile which ease sand bulk translation from the upper berm to the foredune crest and efficiently dissipate the wave run-up energy in case of large storm surge. In addition, an increased sand deposition rate provides suitable conditions for psammophytic plant species proliferation (e.g., *Eryngium* sp., *Saueda* sp., *Cakile* sp.) and surface roughness increase resulting in efficient sand accumulation. Thus, during the frequent low to medium onshore winds (5.5–13 m/s) an intensive sand accumulation occurs in the lower or medium sector of the stoss slope, at 10–20 m from the dune toe, promoting the formation of a secondary foredune crest; on the prograding sectors or where wide beaches, this secondary crest may result in foredune crest deduplication. This process is reinforced through blowout initiation at the foredune crest and air flow channelization which excavates sand and dispatches it circularly at the outer edges of saucer blowouts or of trough blowouts obliquely and alongshore aligned. This sediment dynamics finally result in the landward displacement of the main foredune crest.

Elsewhere, high sand transport rates may result in comparable sand deposition and foredune aggradation simultaneously on both sides of the foredune and over the upper beach. This is particularly the case at NR 48 and R48 benchmarks where a continuous growth of the foredune volume recorded during the last two decades. The only sector of the cross-shore profile which preserved its former shape and size is the main foredune crest (Fig. 25.5c). The quasi-continuous aggadation is mainly assigned to a steady wide beach and to the large sediment volumes stored within the nearshore bars which confer the efficient protection of this shoreline sector against storm waves attack. Additionally, NR48 foredune sector is affected by the barrier effect of the back-dune dense woody vegetation which promotes the entrapment of all the onshore wind-borne sands and which protects the foredunes from the offshore wind transport.

Another particular case is represented by the foredunes development at R 48 benchmark where the steady volume growth is generated by the large amounts of sand trapped at the lee slope, at the contact between the steep foredunes slope (25° to 33°) and the high dense wooden vegetation (e.g., *Hipophae* sp., *Salix* sp.) which functions like an efficient omnidirectional sand trap. About 90 % of the sand accumulation across the R 48 beach–foredune system was found out to occur on the lee slope (Vespremeanu-Stroe and Preoteasa 2007). The overall dune crest elevation changes amplitude is about 0.5 m; instead, larger and localized elevation changes related to rapid sand accumulation around seasonal shrubs must be distinguished from the global elevation changes. Sand aggradation here cannot overpass 3–3.5 m a.s.l, whereas a large sediment volume accumulates at the lee of the foredunes determining their rapid widening through landward migration of the lee slope.

However, local factors should be taken into account when inspecting the foredunes aggradation and their contribution should be carefully distinguished. It is important to mention the acceleration of a recent morphological change affecting most part of the foredunes: the initiation of circular and/or elongated blowouts at the foredune crest and their subsequent coalescence. This is the case of a blowout evolving immediately (ca. 5 m) updrift of the monitored profile, initiated right on the foredune crest which accounts for the larger sediment delivery and massive lee slope aggradation during the last five years. However, blowouts were observed to have been initiated within the widest and highest foredunes sectors along Sărăturile coast and they must be related to a feedback mechanism acting to adjust the foredunes morphometry to the local sedimentary fluxes and energetic conditions. Otherwise, the foredunes from this sector are rarely affected by the storm waves, remaining rather sensitive to high waters (local sea level) as it was the case in 2006 and 2010 (Fig. 25.5c1).

Accretionary Beach (the Southern Sector: Parid—Cape Buival)

The southern half of this short sector (1.1 km) is relative young (<80 years), being created by the southward migration (with a mean rate of ca. 8 m/year) of the Sf. Gheorghe mouth initiated in early 20th century once with transition of the river mouth from an asymmetric to a deflected wave-influenced delta morphology (Preoteasa et al. 2016). Moreover, it exhibits a very dynamic shoreline behavior at medium-term scale, with periods of erosion and accretion (which are missing on the rest of Sf. Gheorghe beach), being connected to mouth bar changes of various causes, i.e., during Danube floods, storms, meanders cutoff, or self-organization processes.

Constant but low sediment inputs during intervals of fair weather conditions participated to shoreline advance in average of 1–3 m/year. However, the sand volumes stored in nearshore bars and foredunes are smaller in comparison with the adjacent central sector of Sf. Gheorghe beach (stable position). Thus, the average beach width maintained to high values of 40–45 m during last decade (2004–2014), whilst foredune sand volume equals 30–50 m^3/m depending on the cross-shore position. This is the sector where the biggest subaerial beaches (berms) have been recorded in July–September 2007 (ca. 80 m) as a result of the sediment transfer from the upper shoreface in connection with the big flood occurred in 2006 and to the following long lasting fair weather conditions favorable for beach face accretion. Otherwise, despite the large widths of the berms (which normally translate into long beach fetch supplying the wind transport capacity) the continuous foredune development lasted until March 2005, when the volume stabilized at about 40 m^3/m (Fig. 25.5e, e1). Shortly after, a group of regular storms occurred in the spring and fall of 2006 pushed the seaward slope crest slightly backward (about 10 m until August 2007) but, more importantly, they moved most of the sands from the initial (2005) fordune crest to a secondary landward crest which significantly raised during that period (Fig. 25.7).

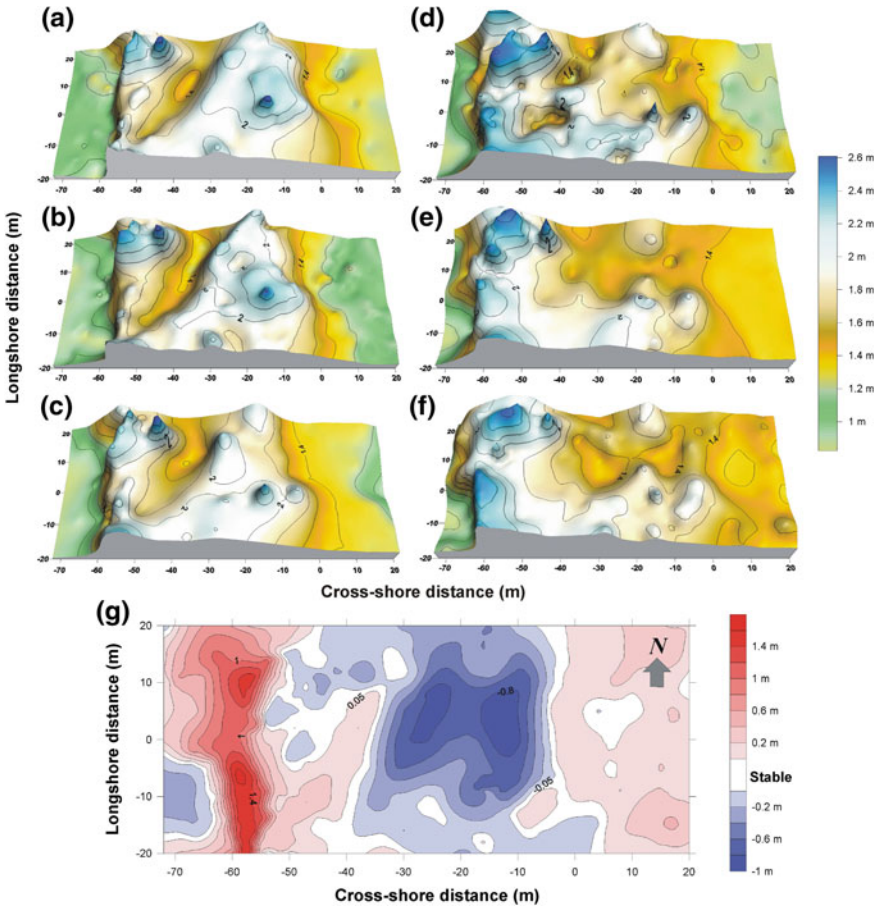

Fig. 25.7 Successive DEMs of the foredunes at NBuival benchmak: **a** March 2005; **b** August 2005; **c** January 2006, **d** July 2006; **e** March 2007, **f** August 2007, **g** surface changes occured during March 2005 and August 2007 (Preoteasa 2008)

The historical flood recorded in spring 2006 and the associated higher local sea levels enabled the successive low and moderate storms to completely flood the beach forcing the wind fetch to develop entirely on the foredune and to trigger their overall remobilization. After that, a new foredune crest started to rebuild on an advanced seaward position comparable with that recorded before the historical January 1998 storm. This advanced position was supported by the low-intensity storms specific to the recent years (post–2006) which transported the sands for short distances. Maintenance of a robust sediment flux within the foredunes contributes to blowouts preservation and constant delivery of sand to the backward foredunes which crests are no higher than 1.7–2 m, but still migrate landward. In the present, due to the antagonist migration of the two crests (landward for the back-crest and

seaward for the new crest) the foredunes stretch across 115 m width, despite their modest sand volume.

The rapid foredunes morpodynamics together with the wiggling sand volume of the foredunes reveal the mechanisms which keep this highly sensitive system to multiple external forcings to a dynamic equilibrium profile.

Sacalin Barrier Island

A series of interacting controlling factors such as the direction of prevalent waves propagation and subsequent wave transforming processes in relation with the mouth bar morphology, inter- and intra-annual sediment flux variability, local sea level oscillations dichotomically act on foredune development: they enable frequent nearshore bar welding to the subaerial beach contributing to significant rapid beach enlargement, fetch enhancement, and readily foredune development on a seaward position. After the storm from January 1998, several sparse, small size foredune ridges developed along several sectors of the spit. The most prominent foredunes have been built on the northern sector, at the location of a washover fan formed at 200 m downdrift of the river mouth, during the January 1998 event, besieging wooden vegetation species (*Tamarix* sp., *Hipophae* sp.). The backward position together with the sheltered environment provided by the neighboring vegetation led to rapid development of a small, yet stable precipitation ridge. It is relatively narrow (30–40 m), developed along 100 m, with the crest no higher than 3 m a.s.l. It initially formed as a narrow (15 m wide) and low (3.25 m high) foredune belt within a sinuous, alongshore developed sector protected at three sides (updrift, landward, and dowdrift) by dense wooden vegetation. Starting from the spring 2005, a rapid sand accumulation initiated at about 15 m in front of this precipitation ridge, in row with the most advanced positioned vegetation shrubs bordering this accumulative sector. Since then, the sediment deposition took place mainly within the newly formed, more advanced foredunes or even in front of it (Fig. 25.8) interfering with the sediment flux which previously reached the foredune ridge behind it. As the landward positioned foredune ridge become isolated from the sediment flux, it still preserves its position, shape, and dimensions owing to the efficient protection of the vegetation cover.

The successive cross-shore profiles show the great stability of landward foredune ridge whilst the rapid development of the recently formed fronting sand ridge at one hand and the large beach width variations and the associated frequent bar welding at the other hand. The largest sand accumulation recorded in May 2011 is probably related to the widest beaches during the monitored interval. However, the advanced position of the frontal ridge exposed it to the storm waves attack which provoked their erosion, inclusively the loss of the benchmark. During the fieldwork campaign in summer 2014, only the oldest foredune ridge existed, protected by the wooden vegetation cover with waves reaching near the dune foot on fair weather conditions.

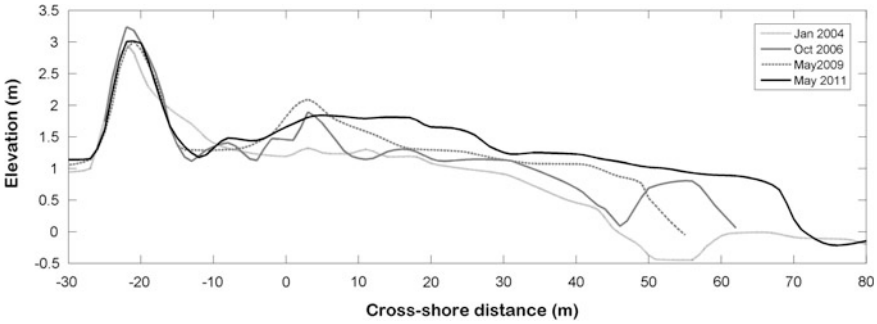

Fig. 25.8 Beach–foredunes system dynamics on Sacalin Spit (*Northern tip*)

Conclusions

Foredune arrangement (e.g., location, size, activity duration, morphology) along Danube Delta coastline reflects both inherited and present-day coastal dynamics. The beach–dune systems along the Danube Delta coast are rather sparse due to the rare combination of the few sediment depocenters exposed to resultant wind direction or sediment entrapment prone areas (e.g., rough surface associated with dense vegetation or rugged topographic surface, the presence of a protruding features acting like a groin for traveling sediments).

The alongshore differences of the foredune volumes represent the legacy of prevalent northerly sediment transport which controls the longshore sediment dispersal pattern. Yet, the prevalent unidirectional component of the circulatory system conceals important site-specific influences to depositional processes and foredune volume variations along the study site. One of these important emerging contributions is the particular configuration resulted from the foredune transgression and the recently emplaced (post 1970) local wooden vegetation which is conducive for efficient sand trapping controlling foredunes morphometry and position relative to the shoreline.

The November–April (active season) interval specific dynamics is mainly driven by high energetic wind and wave climate, low vegetation cover density, and sometimes high local waters influenced by nearby fluvial discharge, all generating narrower and lower beaches which are readily swept by the waves to reach the fordunes and to produce local or alongshore contiguous scarps. High wind speeds and low vegetation cover of the foredune yield larger sedimentary fluxes on the foredunes, often generating crest erosion, blowout initiation over the foredune crest, and accretion on the lee slope together which enable landward dune migration. Yet the net accumulative trend of the foredunes is negatively impacted mainly during storm events which may trigger foredunes scarping or overwash. As low and medium energy storms affect the Sărăturile foredunes sectors partially and locally, the severe storms could result in fully overtopping just of the foredune (especially on the sector situated immediately updrift of the Sf. Gheorghe mouth: NBuival

sector). If at short timescale the effects of such event are negative in terms of sediment loss, when considered at longer time scales it turns to be rather an important impetus in foredunes development along the Danube Delta coastline in that, in time, they often create specific accommodation space as washover fans which, by their spatial extension, sediment volume and sheltered position relative to the water line are prerequisite in foredunes initiation and preservation over longer time spans.

During May–October (fair weather period) the low wind and wave energy together with the lower local water levels enable wider and higher beaches. Larger volumes of dry sand within the beach and foredunes are available for the wind to transport especially to the dune toe and stoss slope. During May–October the frequent low-to-medium onshore winds (5.5–13 m/s) enable an intensive sand accumulation in the lower or medium sector of the stoss slope.

Thus, foredune equilibrium profile is set in accordance with the temperate dry climate (via specific sediment input and vegetation cover characteristics) and relatively low marine energetic conditions (e.g., limited fetch, microtidal environment), respectively, with the scarce sediment transport system, low roughness (e.g., low foredune elevation, milder slopes, low density vegetation cover), and high sediment transport conditions over the beach and foredunes.

Acknowledgments Since 2002 the research activities were undertaken in the frame of Sfântu Gheorghe Marine and Fluvial Research Station (Faculty of Geography, University of Bucharest). The authors are indebted to all the colleagues and students who participated to data collection during the numerous fieldwork campaigns. Special thanks to our colleagues Florin Zăinescu, Florin Tătui, and Alin Păroiu for helping us with data processing and for the useful discussions. The measurements were supported by different CNCS-UEFISCDI (National Authorithy for Scientific Research) grants awarded to LP (2916/31 GR/2006) and AVS (PN-II-RU-TE-2011-3-0293).

References

Aagaard T, Davidson-Arnott RGD, Greenwood B, Nielsen J (2004) Sediment supply from shoreface to dunes: linking sediment transport measurements and longterm morphological evolution. Geomorphology 60:205–224

Aagaard T, Orford J, Murray AS (2007) Environmental controls on coastal dune formation; Skallingen Spit, Denmark. Geomorphology 83(1–2):29–47

Anthony EJ (2015) Wave influence in the construction, shaping and destruction of river deltas: a review. Mar Geol 361:53–78

Arens SM (2007) Transport rates and volume changes in a coastal foredune on a Dutch Wadden island. J Coast Conserv 3:49–56

Bauer BO, Davidson-Arnott RGD (2003) A general framework for modeling sediment supply to coastal dunes including wind angle, beach geometry, and fetch effects. Geomorphology 49(1–2):89–108

Bullard JE (1997) A note on the use of the Fryberger method for evaluating potential sand transport by wind. J Sediment Res 67:499–501

Dan S, Stive MJ, Walstra DJR, Panin N (2009) Wave climate, coastal sediment budget and shoreline changes for the Danube Delta. Mar Geol 262(1–4):39–49

Fryberger SG (1979) Dune forms and wind regime. In: McKee ED (ed) A study of global sand seas, pp 137–169
Giosan L (2007) Morphodynamic feedbacks on deltaic coasts: lessons from the wave-dominated Danube delta. Coastal Sediments '07, p. 828–841
Hesp H (2002) Foredunes and blowouts: initiation, geomorphology and dynamics. Geomorphology 48(1–3):245–268
Hesp PA (2013) A 34 year record of foredune morphodynamics at Dark Point, NSW, Australia. In: Conley DC, Masselink G, Russell PE, O'Hare TJ (eds) Proceedings 12th International Coastal Symposium (Plymouth, England), J Coastal Res SI 65:1295-1300
Houser C (2009) Synchronisation of transport and supply in beach-dune interaction. Prog Phys Geogr 33(6):733–746
Houser C, Ellis J (2013) Beach and dune Interaction. In: Shroder John F (ed) Treatise on geomorphology, vol 10. Academic Press, San Diego, pp 267–288
Masselink G, Gehrels R (2014) Coastal environments and global changes. p 448
Milne FD, Dong P, Davidson M (2012) Natural variability and anthropogenic effects on the morphodynamicsof beach-dune system at Montrose Bay, Scotland. J Coastal Res 28(2):375–388
Ollerhead J, Davidson-Arnott R, Walker IJ, Mathew S (2013) Annual to decadal morphodynamics of the foredune system at Greenwich Dunes, Prince Edward Island, Canada. Earth Surf Proc Land 38(3):284–298
Panin N, Jipa D (2002) Danube River sediment input and its interaction with the north-western Black Sea. Estuar Coast Shelf Sci 54:551–562
Preoteasa L, Vespremeanu-Stroe A (2004) Analiza potențialului de transport eolian în Delta Dunării, St. și cerc. de oceanografie costieră, vol 1, pp 47–66
Preoteasa L (2008) Relieful eolian din Delta Dunării—studiu de geomorfologie. Editura Universitară, București (in Romanian)
Preoteasa L, Vespremeanu-Stroe A, Tătui F, Zăinescu F, Timar-Gabor A, Cârdan I (2016) The evolution of an asymmetric deltaic lobe (Sf. Gheorghe, Danube) in association with cyclic development of the river mouth bar: long-term pattern and present adaptation to human induced sediment depletion. Geomorphology 253:59–73
Psuty NP (1988) Sediment budget and dune/beach interaction. J Coastal Res SI 3:1–4
Ruessink BG, Wijnberg KM, Holman RA, Kuriyama Y, van Enckevort IMJ (2003) Intersite comparison of interannual nearshore bar behavior. J Geophys Res 108:5–12
Saye SE, van de Wal D, Pye K, Blott SJ (2005) Beach-dune morphological relationships and erosion/accretion: an investigation at five sites in England and Wales using LIDAR data. Geomorphology 72(1–4):128–155
Sherman DJ, Bauer BO (1993) Dynamics of beach-dune system. Prog Phys Geogr 17(4):413–447
Sherman DJ, Lyons W (1994) Beach–state controls on aeolian sand delivery to coastal dunes. Phys Geogr 15(4):381–395
Short AD, Hesp PA (1982) Wave, beach and dune interactions in southeastern Australia. Mar Geol 48:259–284
Tătui F (2015) Longshore bars behavior along the Danube delta coast. Editura Ars Docendi, București (in Romanian)
Tătui F, Vespremeanu-Stroe A, Preoteasa L (2011) Intra-site differencies in earshore bar behavior on a nontidal beach (Sulina-Sf. Gheorghe, Danube delta coast). J Coastal Res SI 64:840–844
Tătui F, Vespremeanu-Stroe A, Preoteasa L (2013) The correlated behavior of sandbars and foredunes on a nontidal coast (Danube Delta, Romania). J Coastal Res SI 65:1874–1879
van der Burgh B, Wijnberg KM, Hulscher SJMH (2011) Decadal-scale morphologic variability of managed coastal dunes. Coast Eng 58(9):927–936
Vespremeanu-Stroe A (2004) Transportul de sedimente în lungul țărmului și regimul valurilor pe coasta Deltei Dunării, St. și cerc. de oceanografie costieră, vol 1, pp 67-82
Vespremeanu-Stroe A (2007) Țărmul Deltei Dunării—studiu de geomorfologie. Edit Universitară, București (in Romanian)

Vespremeanu-Stroe A, Preoteasa L (2007) Beach–dune interactions on the dry–temperate Danube delta coast. Geomorphology 86:267–282

Vespremeanu-Stroe A, Preoteasa L (2015) Mophology and the cyclic evolution of Danube delta spits. In: Randazzo G, Jackson D, Cooper JAG (eds) Sand and gravel spits. Springer, p 327–339

Zăinescu F, Vespremeanu-Stroe A, Valchev N, Tătui F (submitted) Storm climate on the Danube Delta coast

Chapter 26
Evolution and Morphodynamics of Danube Delta Shoreface

Florin Tătui and Alfred Vespremeanu-Stroe

Abstract The present Danube Delta shoreface morphology (in terms of longshore variability of cross-shore profile shape and slope) and behaviour (sediment distribution and transport, depth changes) reside from the co-existence of different types of accretionary, stable and erosive sectors. This configuration is the result of various controlling factors: the long-term evolution of the delta and of each deltaic lobe, the up/downdrift distance to the river mouths, the position of each sector into a specific littoral cell (expressed in sediment availability), the angle made by shoreline with the incident waves and the presence of engineering structures. Shoreface evolution in the past 150 years is highly influenced by the Danube river sediment supply changes, as a consequence of human pressure, and, secondary, is a function of the climatic forcing (storminess) variability, while the inter-annual shoreface morphodynamics is mainly linked to wave energy fluctuations and river floods. The upper shoreface variability is controlled by the multi-annual nearshore sandbars net offshore migration. Intra-site differences in the cross-shore bar behaviour characteristics (both spatially and temporally), expressed by different bar behaviour on the sediment-rich accretionary sectors in comparison with the erosive ones, are the result of the coast(line) evolution and of the morphodynamic state of the beach. Their variability in terms of morphometric (sandbar volumes), geometric (time-averaged widths and depths of the bar zone) and morphodynamic parameters (offshore migration rates and cycle return periods) is related to the complex feed-backs between three key environmental factors: (i) shoreface morphology (i.e. nearshore slope), (ii) alongshore sediment availability and (iii) surf-zone hydrodynamics.

Keywords River suspended sediment discharge · Floods · Storminess · Nearshore sandbars · Longshore transport · Danube delta

F. Tătui (✉) · A. Vespremeanu-Stroe
Faculty of Geography, University of Bucharest, 1st N. Bălcescu Blv.,
010041 Sector 1, Bucharest, Romania
e-mail: florin.tatui@geo.unibuc.ro; florin.tatui@yahoo.com

M. Rădoane and A. Vespremeanu-Stroe (eds.), *Landform Dynamics and Evolution in Romania*, Springer Geography,
DOI 10.1007/978-3-319-32589-7_26

Introduction

The shoreface represents the boundary between the beach and the inner continental shelf (from run-up limit to wave base) that is permanently approaching equilibrium under changing dynamic conditions: waves, wind and currents (Niedoroda et al. 1985; Cowell et al. 1999; Short and Jackson 2013). Its extremely complex behaviour and harsh environment, which limits the possibilities of investigation (wave breaking, strong nearshore currents and underwater processes which are not directly visible), make the shoreface the poorest understood part of the coastal zone. Acting as a filter, source, sink and/or barrier of sediment from/to the active zone (the area in which the littoral processes take place), the shoreface plays a dominant role in sediment transport processes between the beach and the inner shelf (Finkl 2004), having a significant long-term contribution to the coastal sediment budget and shoreline movement (Hinton and Nicholls 2007) and being also a vital element in determining coastal response to external forcing (Backstrom et al. 2008). Understanding present and long-term shoreface morphodynamics is particularly important for forecasting coastal response to predicted sea-level rise, increasing storminess and human pressure on coastal environment.

Shoreface morphodynamics is a matter of large-scale coastal behaviour, applying to timescales of decades and distances of tens of km (Cowell and Thom 1994). We should though make a distinction between the upper shoreface, which is evolving at spatial scales of 0.05–1 km and temporal scales from events/seasons to years, and the lower shoreface, which is evolving at spatial scales of more km (tens of km) and temporal scales from decades to centuries/millennia (Cowell and Thom 1994). These marked discrepancies are mainly induced by the different processes acting on the two twin-environments (wave breaking and nearshore currents on the upper shoreface versus wave shoaling, wave asymmetry and gravity currents on the lower shoreface) and, secondary, by the same processes which develop with different intensities (i.e. down- and upwelling currents, sediment settling from river plumes). We will also make this distinction in the present chapter, choosing to discuss the lower shoreface (between 5 and 20 m depth) evolution on the whole Danube Delta coast (Fig. 26.1a) at multi-decadal and centennial scales and the upper shoreface (from shoreline to 5 m depth) morphodynamics on the Sulina–Sfântu Gheorghe coast at seasonal and multi-annual timescales.

Shoreface dynamics has been investigated worldwide on many wave-dominated non-deltaic coastal environments ranging from straight sandy coastlines (Niedoroda et al. 1984; Wright 1995; Stive and de Vriend 1995; van de Meene and van Rijn 2000) and geologically constrained ones (Roy et al. 1994; Hequette and Hill 1993; Hequette et al. 2001) to steep, high-energy embayments (Backstrom et al. 2007, 2009a, b). Compared to other long, straight and gentle shorefaces, relatively little is known about shoreface morphodynamics of deltaic coasts. On the wave-dominated deltaic coasts, as is the case of most Danube Delta beaches, the transversal shoreface profile can change from concave to linear and convex, or inversely, under

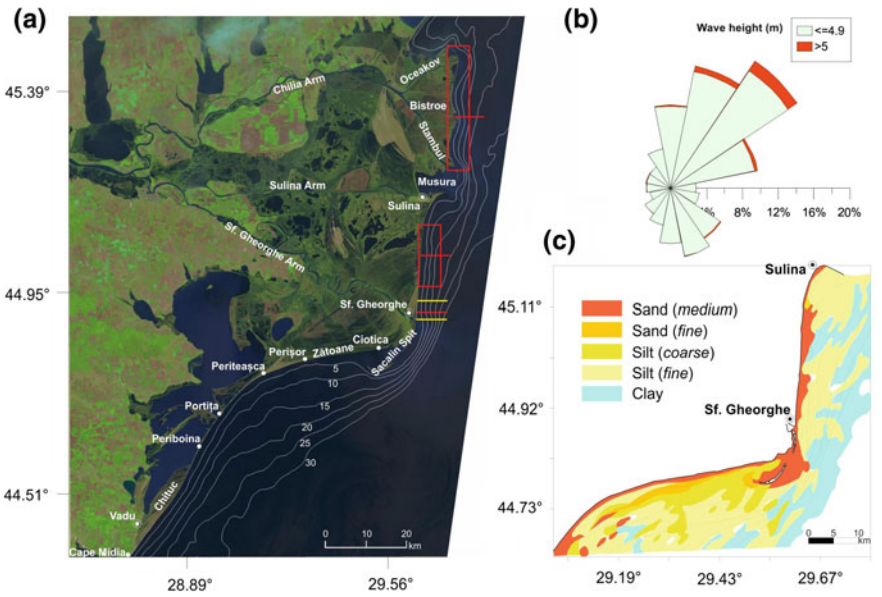

Fig. 26.1 **a** Danube Delta coast (*Landsat image from May 2013*). Please notice the extent of the cross-shore profiles (*red and yellow lines*) and the areas (*red boxes*) used for different analysis in the paper (*see explanation in text*); **b** directional frequency distribution of mean wave height (H_0) at 18 km offshore SE of Sf. Gheorghe river mouth (1949–2013) from NCEP wave hindcast; **c** sedimentology map of Sulina–Portița coastal sector (modified after *Sedimentology and bathymetric map of the Black Sea continental shelf—Sulina sheet*, realized by GEOECOMAR in 1995)

the wave influence, but also of the fluvial currents and river-borne sediments which circulate and settle down to delta front and prodelta.

The first, albeit scarce, Romanian research studies of Danube Delta submerged relief and fluvial-marine interactions started earlier in the twentieth century with concern to the bathymetry changes resulted from the European Commission of the Danube maps (since 1856) comparison (Brătescu 1923), followed by a 50 years gap, after which they were mainly focused on applied engineering analysis (Jianu and Şelariu 1970; Bondar et al. 1973, 1980) devoid of any fundamental approach of submerged littoral processes. In the 1980s and early 1990s, we register some progresses in the understanding of deltaic submerged relief through theoretical studies of the beach profile (Vespremeanu 1987; Vespremeanu and Ştefănescu 1988; Postolache et al. 1992), analysis of delta front evolution and nearshore gradients to 12–15 m depth (Bondar et al. 1984; Vespremeanu 1984), sediment budgets distribution (Panin 1989; Mikhailova and Levashova 2001) and longshore sediment transport—LST (Bondar and Harabagiu 1992; Panin et al. 1979–1979; Shuisky 1984, 1985; Gâştescu and Driga 1986). More in-depth analytical studies came up in the past 20 years, based on LST numerical modelling (Giosan et al. 1999; Vespremeanu-Stroe 2004, 2007; Dan et al. 2009) or extensive measurements of

nearshore topography and sandbars behaviour (Stănică and Ungureanu 2006; Vespremeanu-Stroe et al. 2007a; Tătui et al. 2011; Tătui 2015; Tătui et al. 2016).

Despite the recent years increasing amount of information related to Danube Delta coastal evolution and dynamics, its shoreface remained poorly understood. The aim of this chapter is to raise the curtain on Danube Delta shoreface evolution and morphodynamics over the medium (multi-annual) and large timescales (decades to centuries) and to be a starting point for future in-depth research studies related to the behaviour of this complex coastal feature.

Present-Day Danube Delta Shoreface Characteristics

We analysed shoreface characteristics, dynamics and evolution along the Danube Delta coast, taking into consideration both Romanian and Ukrainian sectors (Fig. 26.1a). It is situated in the North-Western Black Sea basin, where some of the largest European rivers (Danube, Dnieper and Dniester) flow into the sea, conducing to the largest width of the Black Sea continental shelf (over 200 km wide). With a length of 2870 km, a drainage basin of over 817,000 km^2, an average water discharge of about 190 km^3/year and sediment discharge of 25–35 Mt/year (out of which 4–6 Mt/year is sandy material), the Danube River is the largest and the most important water and sediment supplier of the Black Sea basin (Panin and Jipa 2002). It flows into the sea through three main distributaries: Chilia, which transports approximately 58 % of the water and sediment discharge; Sulina, the major waterway—19 %; and Sf. Gheorghe—23 % (Bondar and Panin 2001).

The Danube Delta coast is a low-lying area interrupted by river mouths and, sometimes, by engineering structures (Sulina jetties and Midia harbour). Since it is virtually tideless (maximum spring tide range of 0.12 m—Bondar and Panin 2001), wind waves and swell are the only drivers of water motion in the nearshore zone. Danube Delta coast is medium-wave energy with the exception of Musura, Sacalin Lagoon and Ciotica—Zătoane sectors, which are characterised by low-energy conditions (Vespremeanu-Stroe 2007). The average offshore significant wave height H_s is 1.43 m with the corresponding mean period T_0 of 5.5 s. Wave height increases to 2–4 m during regular storm events, with maximum offshore significant heights up to 7 m during extreme storms. Waves from the north-eastern directions are dominant in terms of both magnitude and frequency (30 % of all waves are coming from N to NE directions), followed by southern waves (13 % of all waves)—Fig. 26.1b. They approach the shoreline at oblique angles, inducing strong longshore currents which are, on most sectors, southward oriented and transport net volumes of sediments up to 1×10^6 m^3/year (Vespremeanu-Stroe 2004, 2007; Dan et al. 2009).

The shoreface limits on Danube Delta coast take into consideration its deltaic character. The onshore extension is given by the position of the waterline (Schwartz 2005), while the transition between the upper and the lower shoreface is represented by the seaward limit of the bar zone, which is situated, in most cases, at distances of 250–550 m from the shoreline, in water depths from 3 to 4.5 m (Tătui 2015).

Generally, the outer limit of the lower shoreface is defined by the wave base (Short 1999), but, in this case of deltaic coast, where the fluvial processes are very important, we have decided to lower the limit under this threshold and to define the transition from the lower shoreface to the inner continental shelf in water depths of 15–20 m, which corresponds, most of the time, with the position of the delta front.

Nearshore currents (both longshore and cross-shore—onshore/offshore) are inducing significant changes in the morphology and behaviour of the upper shoreface. Analysing recent behavioural differences of nearshore sandbars along Sulina–Sf. Gheorghe coastal sector, Tătui (2015) modelled wave and current conditions on the upper shoreface during storm events and showed that the values of wave height, longshore and undertow currents speed and associated longshore and cross-shore sediment transport rates are decreasing from the erosional to the stable and accumulative sectors. This translates into higher net offshore sandbar movement and shorter cycle return periods along the erosional deltaic sectors in comparison with the accumulative ones (Tătui et al. 2016). Cross-shore sediment transport between the upper and the lower shoreface is relatively small along the Danube Delta coast (e.g. values of 0.05×10^6 m^3/year along the stable Sf. Gheorghe beach and maximum values of 0.17×10^6 m^3/year along the erosive sector of Sulina–Sf. Gheorghe coast), characteristic to some episodes of outer bar decay and disappearance. Hence, the big importance of longshore sediment transport, which is responsible for alongshore sediment redistribution, sediment availability degree and, possibly, for the accumulation of sediments and sediment by-passing at Danube river mouths below depth of closure (due to the supposed presence of longshore baroclinic jets associated with coastal upwelling and downwelling) and lower importance of strong undertow currents, associated with the severe and extreme storms, and of gravity currents.

The fluvial offshore extended currents and, especially, the buoyant plumes, which transport fluvial sediments at large distances, are also very important for settling suspended sediments on both upper and lower shoreface. The buoyant plumes extend from river mouths to considerable distances offshore function of river discharge and wind speed and direction. On the lower shoreface, the coastal currents generated by winds and geostrophic gradients are usually longshore oriented and also the main responsible for coastal setup/setdown, driving significant seaward/landward near-bottom cross-shore flows in situations with down/upwelling. In this area, transport due to wave motions is less important than on the upper shoreface and sediment transport rates are significantly smaller as wave stirring of sediment is weaker.

From sedimentology point of view, Danube Delta shoreface shows significant variability (Fig. 26.1c). The Sulina–Sf. Gheorghe coastal sector is characterised by the presence of sands down to 5–7 m water depths, continued with silts and clays at higher water depths. A relative different situation occurs on other sectors (most of them affected by erosion), where the extension of sands is present down to larger water depths (7–10 m; Fig. 26.1c) due to a more extensive bed return flow.

The sedimentological research study conducted by Dimitriu et al. (2008) along Sf. Gheorghe–Cape Midia coastal area during 2005 and 2006 showed that shoreface

surficial sediments fill in a wide spectrum of grain size classes, from medium and very fine sand, silt, very fine silt to coarse clay. The very fine to medium sands are present especially on the upper shoreface to approximately 10 m depth, having the largest extension in front of Sacalin Spit. The width of these sandy deposits is up to 2500 m south of Portița and up to 4500 m in front of Chituc beach ridge plain (Dimitriu et al. 2008). Silt sediments are present on the eastern side of the coastal sector placed south of Zătoane at more than 8–10 m water depths, partially bordering the sandy dominated areas. Significant extension of silt area (approximately 8000 m) is present in front of Portiţa, while silts are present up to 20 m depth and even more in Vadu/Cape Midia sector (Dimitriu et al. 2008). The shell deposits are discontinuous, with parallel displacement to the shoreline, bordering the sandy deposits. They have the largest extension from Portița to Periboina and in front of Chituc beach ridge plain.

The present Danube Delta shoreface configuration is the result of (i) the long-term evolution of the delta and of each deltaic lobe, (ii) the up/downdrift distance to the river mouths, (iii) the position of each sector into a specific littoral cell (expressed in sediment availability) and the angle made with the incident waves, and (iv) the presence of engineering structures. All these factors conduced to the co-existence of different types of constructive, stable and erosive sectors. Some of the accretionary sectors, as in front of Chilia river mouths or downdrift of Sf. Gheorghe mouth, are related to Danube river mouths influence, some of them simply represent the downdrift end of a littoral cell (Chituc), which impose relatively high rates of sediment supply (large availability of sediment volumes), and some are the result of longshore sediment transport convergence (Periteașca) or the result of engineering structures, as is the case of Sulina jetties, which interrupt the dominant southward directed longshore drift, altering nearshore circulation and inducing high accumulation rates updrift (in the Musura Bay) or immediately downdrift (Sulina beach), whilst an increasing coastal erosion occurs for large areas downdrift (ca. 20 km in the central part of Sulina–Sf. Gheorghe interdistributary coast). The erosive sectors represent the updrift part of littoral cells (Zătoane, Portița) or are starved in sediments due to the presence of jetties which determine a divergence zone for the nearshore circulation (central part of Sulina–Sf. Gheorghe sector).

Accordingly to these facts, the shoreface morphology differs substantially on different sectors of Danube Delta coast, depending on their medium-term behaviour. The shape of the shoreface profile on constructive (progradational) sectors differs from that of the erosive (transgressive) sectors. The former ones result in a convex or linear shoreface profile, while on erosive coasts slightly concave shoreface profile develops (Fig. 26.2).

Shoreface slope records significant cross-shore variability which further fosters distinct behaviours of the nearshore bars via nearshore currents regime. On the upper shoreface, the nearshore slope varies from 0.1° to 0.4°, along the accumulative and stable sectors, to 0.4°–0.6°, on the erosive sectors. These values have direct implications on sandbars number and the extent of bar zone, with more sandbars and a wider bar zone along the constructive sectors in comparison with the

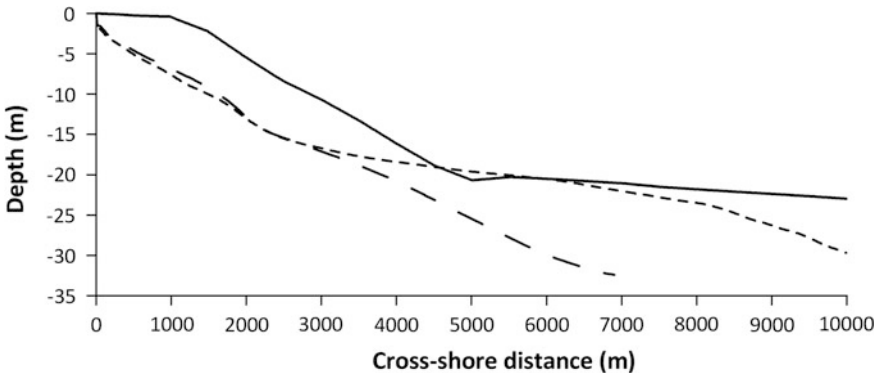

Fig. 26.2 Representative shoreface profiles for accumulative (Chilia—*solid line*), erosive (central Sulina–Sf. Gheorghe—*dotted line*) and stable (Sf. Gheorghe beach—*dashed line*) sectors extracted from Danube Delta coast DEM (2008). The position of profiles is marked by *red lines* in Fig. 26.1a. *Please see the difference between convex, concave and, respectively, linear configuration of the profiles*

erosive ones. The overall average slope of the lower shoreface increases from 0.1° to 0.3° along the constructive sectors to 0.2°–0.4° on erosive ones, with maximum values of over 0.6°. The steeper lower shoreface along the erosive sectors causes higher speed of the undertow on the upper shoreface, which, combined with high bar amplitudes, lead to breaking wave reformation between sandbars and, accordingly, to faster offshore bar movement.

Depth of closure values computed by Dan (2013) show a large variability along the Danube Delta coast, ranging from 5 to 7 m along Ciotica–Portița area to 7–10 m along Sulina–Sf. Gheorghe beach and 10–12 m in front of Sacalin Spit. The smaller values are caused by the sheltering against northern wave directions due to the Sulina jetties and Sacalin Spit, while the maximum values are mainly due to the full exposure to both dominant wave directions (Dan et al. 2009). The same alongshore variability is registered by the delta front edge position. It ranges from 8 to 12 m depth along accumulative sectors to more than 15 m depth on the erosive coasts, the differences being related to the specificity of accumulation processes driven mainly by the distance to Danube river mouths.

The main morphological feature of the upper shoreface along Danube Delta coast is the existence of net offshore migrating breaker sandbars. The bar system is a sort of time-and space-varying energy filter, dissipating most of the wave energy during storms and permitting waves to cross undisturbed towards the shoreline in calmer periods (Pruszak et al. 2011). Their number is variable (from one to four individual entities) on Danube Delta coast, function of nearshore slope (increasing number of sandbars with decreasing slope) and different environmental characteristics of each coastal sector (wave energy, sediment supply). They have mainly 2D morphology as, in most of the cases, are represented by longshore sandbars, parallel with the shoreline, quasi-linear in shape, with no apparent 3D morphology. These sandbars develop and move from the shoreline to almost 600 m offshore and

corresponding water depths of almost 5 m. An exceptional case is represented by the sandbars developed in certain areas in front of the Sacalin Barrier Spit where 5–8 individual bars can be identified up to 1000–1200 m from the shoreline and 8 m water depths most probably due to the presence of strong fluvial currents and their channels dug into subaqueous delta platform (part of the river mouth bar) which are deflected to the south; therefore, these bars are the result of fluvial influence and not breaker bars.

On Sulina–Sf. Gheorghe coastal sector, bar characteristics are not consistent alongshore (Fig. 26.3) and considerable variability exists for the sandbar position

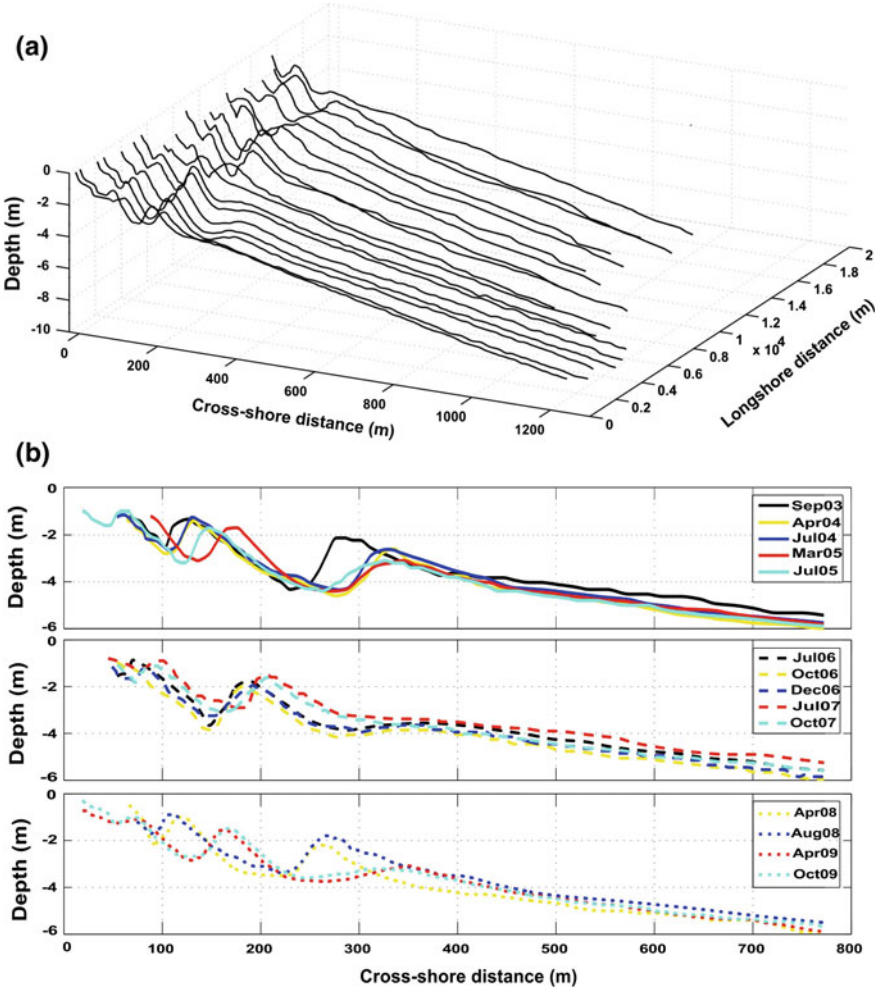

Fig. 26.3 **a** 3D representation of the cross-shore profiles on Sulina–Sf. Gheorghe beach (October 2009; *zero in alongshore direction represents the position of Sf. Gheorghe mouth*); **b** sandbars morphology and cross-shore dynamics on Sf. Gheorghe beach

and morphology (expressed by morphometric parameters: bar crest depth, sandbar height, width, and volume) between different sectors of the coast (Tătui et al. 2011; Tătui 2015; Tătui et al. 2016). The inner bar zone is comprised between 20–40 and 110–130 m from the shoreline. Inner sandbar average position is 70 m from the shoreline, with a corresponding water depth of 1.05 m. It has an averaged alongshore height of 0.6 m, width of 40 m and volume of 15 m^3/m. The mean cross-shore position of the middle bar is 160 m from the shoreline (the middle bar zone extends from 110–130 to 225–250 m), correspondent to water depth of 1.55 m; its average height is 0.95 m, with a mean width of 70 m and volume of 30 m^3/m. The outer bar moves between 225–250 and 300–550 m from the shoreline in water depths of 2–2.9 m. It has a mean height of 0.75 m, width of 95 m and volume of 40 m^3/m.

Long-Term Shoreface Evolution (the last 150 Years)

The present shoreface morphology is the result of the long-term evolution of the Danube Delta coast. At multi-decadal and centennial timescales, the shoreface sediment volume changes are linked to Danube sediment supply changes, storminess variability, longshore sediment transport distribution and impact of engineering structures. Based on comparative analysis (profile to profile and DEM volume changes) of historical and modern maps (since 1856) and bathymetrical measurements (2008 and 2014) extending along both Romanian and Ukrainian sectors to water depths of 20 m, we are focusing on the last one and a half century of coastal evolution, which was dominated by increasing human influence on the Danube river watershed and, accordingly, on the coastal morphodynamics.

The Danube Delta shoreface evolution in the past 150 years (Fig. 26.4) shows distinct patterns of sedimentation and erosion rates between different time intervals. The presence of active deltaic lobes (Chilia) or developing barrier islands (Sacalin) induced significant increase of shoreface volumes in the past century, while decreasing volumes are related mainly to retreating coasts belonging to the abandoned deltaic lobes (Sulina, Dunavăţ).

The sedimentation in front of Chilia secondary delta was very active until 1935, reaching values of 20 m of accumulation ($\sim$0.4 m/year) between 1871/1897 and 1935, and constantly decreased afterwards (making place to slight erosion in the nearshore) due to the decreasing fluvial influence and increasing intensity of nearshore processes (wave energy, wave-induced currents), which prepare the gradual transition of this deltaic lobe from a fluvial-dominated morphology to a wave-influenced one.

The erosion largely extended over the Sulina–Sf. Gheorghe coastal sector until the first half of the twentieth century as a remnant of the Sulina deltaic lobe retreat, in the natural tendency of the coastline to equilibrate with the dominant wave direction. The erosion sector re-arranged afterwards and the vertical erosion rates increased especially after 1970s to maximum values of $\sim$0.3 m/year due to the

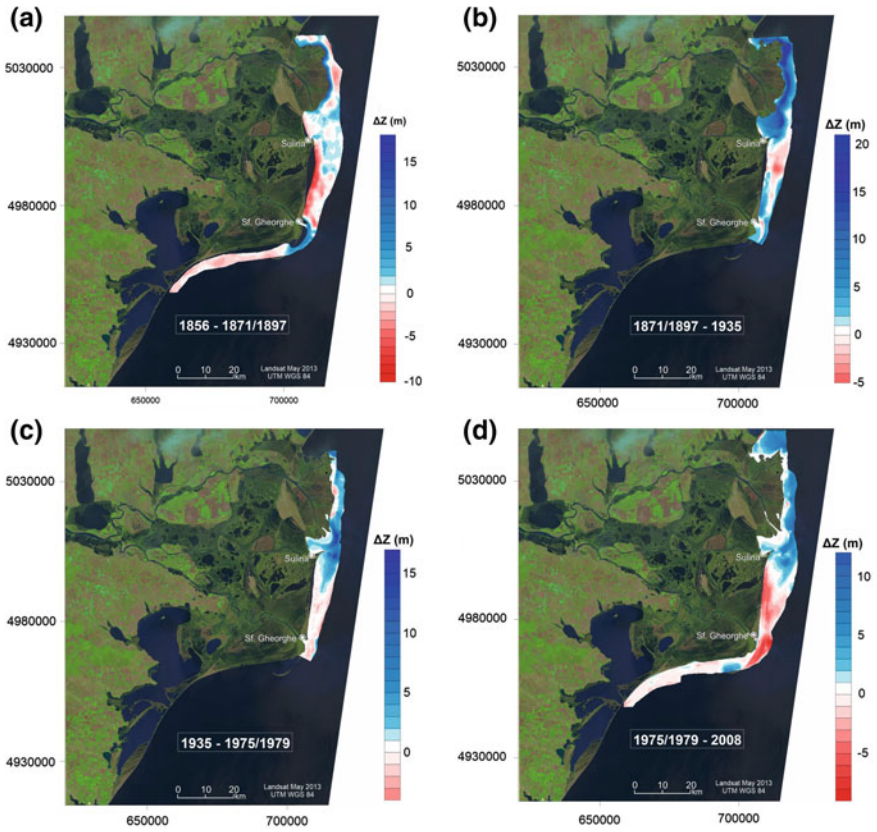

Fig. 26.4 Evolution (depth changes) of Danube Delta shoreface for different time-intervals: **a** 1856–1871/1897; **b** 1871/1897–1935; **c** 1935–1975/1979; **d** 1975/1979–2008

construction of Sulina jetties. Established in the second half of the nineteenth century by the European Commission of the Danube in order to facilitate navigation at the entrance of the Sulina Channel, the present 9 km long parallel jetties were progressively lengthened during the twentieth century (especially in the period 1921–1937 and after 1989), blocking the net southward longshore sediment transport and inducing severe erosion downdrift.

In order to separate the shoreface behaviour of constructive versus erosive sectors in the overall evolution of the Danube Delta shoreface, we have analysed the long-term evolution of one representative sector for each category: the prograding Chilia secondary delta shoreface and the central part of the erosive Sulina–Sf. Gheorghe coast (Fig. 26.5).

Figure 26.5a, b present the evolution of one selected profile for each sector (their position is marked in Fig. 26.1a), while Fig. 26.5c, d show the evolution of shoreface volumes versus intensity of coastal processes along each sector. Shoreface volumes were calculated for each available DEM based on a mobile

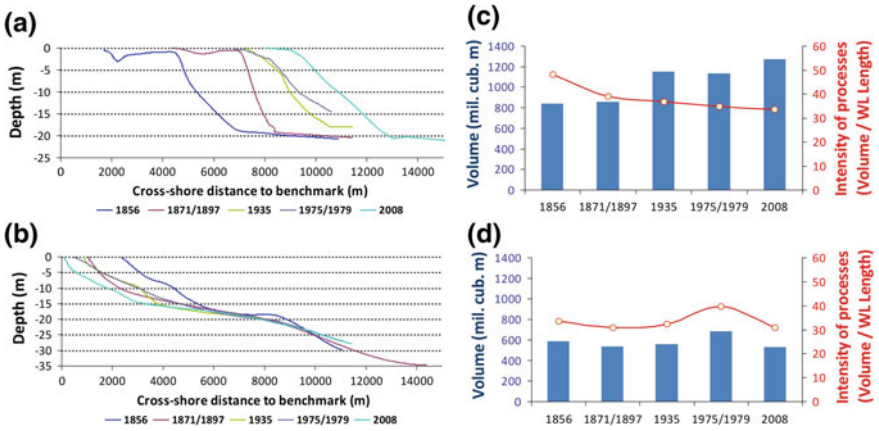

Fig. 26.5 Evolution of the prograding Chilia secondary delta shoreface(*upper panel*) and of the central part of the erosive Sulina–Sf. Gheorghe coast (*lower panel*) in the last 150 years: **a**, **b** Shoreface cross-shore profiles (*please see their position in* Fig. 26.1a); **c**, **d** Shoreface volumes versus intensity of coastal processes (*please see explanation in text regarding how were the values computed*)

window (the longshore extent is marked in Fig. 26.1a) covering 5 km from the shoreline. The intensity of coastal processes is explained by a non-dimensional value obtained from the ratio of shoreface volume (computed as mentioned above) and the corresponding waterline length (expressed in km) inside each mobile window and could be considered an indirect indicator of the changes of state of the coastal system at a certain time.

The Chilia secondary delta shoreface advanced constantly between 1856 and 2008, with the exception of 1935–1975/1979 interval, when the central sector, correspondent to Bistroe distributary, started to erode and to develop wave-driven features. Therefore, the accumulation occurred mainly on the lower shoreface and on the upper shoreface placed North (Oceakov) and South (Stambulul Vechi)—Fig. 26.5. The sedimentary volumes deposited on the shoreface increased step by step from approximately 900×10^6 m^3 in 1856 and 1871/1897 to almost 1200×10^6 m^3 in 1935 and 1975/1979 and approximately 1300×10^6 m^3 in 2008. In the same time, the intensity of coastal processes in front of this deltaic lobe decreased slowly in the past century, indicating that Chilia branches could hardly sustain the continuous development of the lobe (indicated by the slow increase of sediment volumes deposited on fast increasing shoreline lengths/lobe perimeter), marking the recent transition from a fluvial-dominated to a wave-dominated one, as already mentioned.

The Sulina–Sf. Gheorghe erosive sector was characterised by continuous erosion of the upper shoreface, while, on the lower shoreface, erosion was interrupted by slight accumulation (between 1871/1897 and 1935) and stability (between 1935 and 1975/1979). The shoreface sedimentary volumes were relatively constant in the past 150 years (of about 550×10^6 m^3), with a slight increase in 1975 (Fig. 26.5).

In contrast to the accretional sector, the intensity of coastal processes on this erosive sector shows the same variability as sedimentary volumes, indicating similar erosional patterns along the erosive areas in the past 150 years.

The overall shoreface rates of change, computed based on the shoreface volume changes reported to the common area of successive bathymetrical maps, show net accumulation for all time intervals, but with considerable variability (Fig. 26.6). The mean values increased considerably from almost 6.5 cm/year between 1856 and 1871/1897 to almost 8 cm/year between 1871/1897 and 1935. After that, the net shoreface rates of change decreased dramatically, reaching ~1.5 cm/year for the 1975/1979–2008 interval. This significant decrease, especially in the past three decades, could be explained by the drastic change of status of the Danube river suspended sediment discharge (Q_s), as a result of the construction of dams in its watershed, which retain most of the solid discharge. The threefold decrease of the Danube sediment discharge (Fig. 26.6) in the last century marks the transition from a (quasi-) natural behaviour characteristic for 1840–1955 time interval, during which Q_s registered an average value of 1895 kg/s, to a moderate modified one (1955–1985, Q_s = 1,365 kg/s), climaxing with a strongly modified status (1985—Present, Q_s = 640 kg/s).

Taking into consideration storminess influence on Danube Delta shoreface evolution in the past 150 years, due to the lack of reliable measured wind data for the second half of the nineteenth century and first half of the twentieth century, we were not able, for the moment, to correlate directly the shoreface behaviour with storminess between 1850 and 1950. Based on the fact that after 1960 there is a good

Fig. 26.6 Shoreface rates of change (columns) versus Danube's suspended sediment discharge (black line with grey bullets) for different time intervals in the past 150 years

correlation ($r = -0.76$) between the North Atlantic Oscillation Index (NAOI) and the multi-decadal winter coastal storm frequency with direct imprint on the Danube delta coastal morphodynamics (Vespremeanu-Stroe et al. 2007b; Vespremeanu-Stroe and Tătui 2011) and assuming that the same correlation was valid before, we could obtain some indirect information about the storminess characteristics in that period by analysing the distribution of the NAOI values between 1850 and present (Cropper et al. 2015). Between 1850 and 1900, the NAOI was predominantly negative, indicating a possible energetic interval, characterised by higher intensity and frequency of coastal storms. This could explain the larger extent of erosion and smaller shoreface rate of change values registered between 1856 and 1871/1897 along the Danube Delta coast, despite the high values of sediment discharge. The small erosion intensity from 1871/1897 and 1935 could be linked to the positive NAO phases in this time interval, which probably induced a lower storminess; this situation, corroborated with relatively high Danube sediment discharge, determined very high sedimentation and positive rates of change along the shoreface. The first half of the 1935–1975/1979 time interval was characterised by predominantly positive NAOI values (associated with low storminess), while the second half had negative NAOI values (associated with high storminess). Hence, it is very difficult to dissociate storminess imprint on shoreface evolution for this period. After 1980, storminess frequency and intensity decreased, confirmed by the predominantly positive NAOI values, inducing small shoreface erosion along the sectors which were not affected by engineering structures (e.g. Ciotica–Portița).

Concluding, we may assert that the long-term (decades to centuries) shoreface morphodynamic variability and evolution are linked mainly to Danube river sediment supply changes, as a consequence of human pressure, and, secondary, to the climatic forcing (storminess) variability, whose signal is more evident in the multi-annual behaviour of this deltaic coast. Moreover, the changes of the longshore circulation caused by engineering works have a significant imprint on the multi-decadal shoreface behaviour, especially for the downdrift areas.

Inter-annual Shoreface Morphodynamics and Sandbar Behaviour

Danube Delta coast bathymetrical surveys from 2008 and 2014, together with the seasonal and annual bathymetries (2003–2014) of the upper and lower shoreface (study area covers the southern half of the Sulina–Sf. Gheorghe coast: 16 km long), recent high resolution satellite images, ortophotos and GPS surveys were used in explaining recent inter- and multi-annual shoreface morphodynamics. As we will present, this behaviour is linked to storminess and river floods.

Depth changes computed between 2008 and 2014 (Fig. 26.7) along Sulina–Sacalin coast show extensive accumulation and stability across the shoreface. They highlight the presence of two littoral cells and, respectively of two accumulative areas (depocenters): one in the shadow of Sulina jetties (the 5-km long Sulina

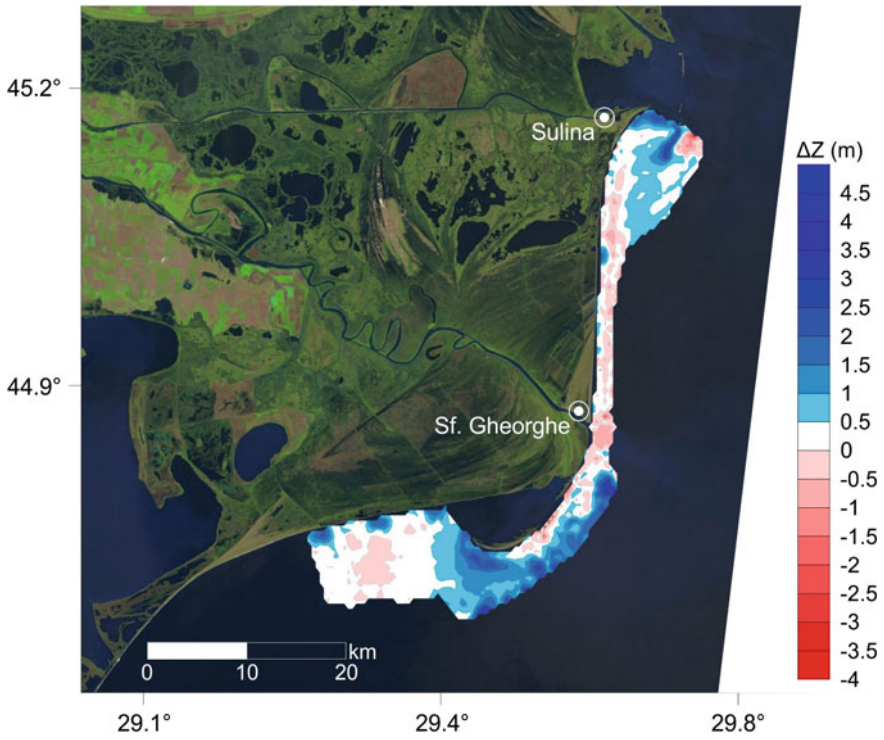

Fig. 26.7 Depth changes along Sulina–Sacalin coast (2008–2014) superposed on a Landsat image from May 2013

beach), caused by wave diffraction-related currents, which induce sediment settling downsouth of the jetties, and one related to the distal unit of the Sacalin Spit, which represents the sink area of this littoral cell, getting much of the sediments eroded both between Sulina and Sf. Gheorghe and in front of the spit or part of the sediments transported by the Sf. Gheorghe arm. The southern sector of Sacalin Spit gained, between 2008 and 2014, from the shoreline to depth of closure (8 m according to Dan 2013), approximately 2.8×10^6 m^3/year of sandy sediments coming from north of Sf. Gheorghe arm ($\sim 1 \times 10^6$ m^3/year), from the erosion of the northern and central Sacalin spit ($\sim 1 \times 10^6$ m^3/year) and from sandy sediments brought by the Danube ($\sim 0.8 \times 10^6$ m^3/year). This deposition was higher between 2008 and 2012 and lower afterwards due to the appearance in 2012 of a 3.5 km breach in the central part of the spit which determined almost 1×10^6 m^3/year of these sands to be used for spit recovery between 2012 and 2014. The volume of fine sediments accumulated between 2008 and 2014 in front of the Sacalin Spit from 8 to 20 m depths amounts $\sim 7.3 \times 10^6$ m^3/year, which exceeds with almost 4×10^6 m^3/year the amount of fine sediments transported by the Sf. Gheorghe arm. The origin of these sediments is difficult to be accounted for, but possible sources could be (i) lower shoreface erosion of Sulina–Sf. Gheorghe and

Ciotica–Zătoane sectors, (ii) a part of the buoyant plumes related to Sulina and Chilia arms, and (iii) the onshore transport of sediments from the upper continental shelf. The erosional rates along the Sulina–Sf. Gheorghe sector for 2008–2014 time interval are significantly lower than the computed rates between 1975/1979 and 2008 due to a remarkably low storminess occurring since 2006 to present (Zăinescu et al. submitted).

The shoreface slopes (from shoreline to 20 m depth), computed between 2008 and 2014 for the study area covering 16 km from Sf. Gheorghe mouth to the north, show small seasonal differences, with higher values after the stormy winter season and lower values after the calm summer season. The same change level (~10 %) can be observed when computing the volumes of the shoreface profile (to 20 m depth), the values being higher after the calm season, due to gain of sediments on the entire shoreface profile, and lower after winter season, due to increased erosion in all shoreface compartments.

Accumulative and erosive sectors have different shoreface morphodynamics, with higher slopes (0.45°–0.6°) and smaller volumes (~20–30,000 m^3/m) on the erosive shorefaces in comparison with the constructive ones (0.25°–0.35° and 30–35,000 m^3/m, respectively). Despite these differences, based on the analysed data, there is no clear trend regarding multi-annual shoreface slopes and volumes on either accumulative or erosive sectors.

As a result of the distance from Danube river mouths, which modulates the accumulation patterns of sediments transported by river plumes during floods, the Danube Delta shoreface experiences different morphodynamic behaviour. The areas situated in the proximity of river mouths show a fully active shoreface (Fig. 26.8),

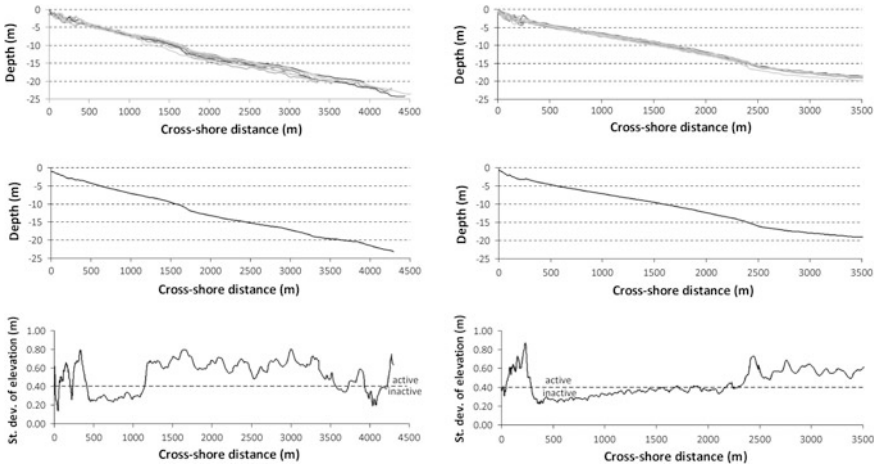

Fig. 26.8 Cross-shore distribution of profile envelope (*upper panel*), mean profile (*middle panel*) and standard deviation of elevation (*lower panel*) measured between 2003 and 2014 for two locations: one in the proximity of Sf. Gheorghe mouth (*left*) and one in the central Sf. Gheorghe coast (*right*). The position of profiles is marked by *yellow lines* in Fig. 26.1a

where the morphodynamic activity occurs across almost the entire shoreface. The morphodynamic behaviour changes with the increasing distance from these sedimentary sources, the shoreface becoming seaward partially active (Fig. 26.8), characterised by closure on the outer limit of the upper shoreface and re-opening on the middle/lower shoreface (at 12–16 m depths, seaward of the delta front maximum slope position) related to a possible onshore supply of sediment from the upper continental shelf and to sediment settling down from buoyant plumes. These data show that the middle and lower shoreface is morphologically active in many instances, with the activity increasing with timescale.

The high variability of the upper shoreface profile (down to 5 m depth, respectively up to 400–500 m from the shoreline) is caused by the multi-annual nearshore sandbars movement (Fig. 26.9). A general presentation of this behaviour on various Danube Delta coastal sectors is found in Tătui (2015), while a comprehensive analysis of the multi-annual sandbar behaviour along the Sulina–Sf. Gheorghe coast is presented in Tătui et al. (2011) and Tătui et al. (2016) using Complex Empirical Orthogonal Function (CEOF) analysis. Along this coastal area, the bar behaviour is found to be temporally and spatially different, exhibiting

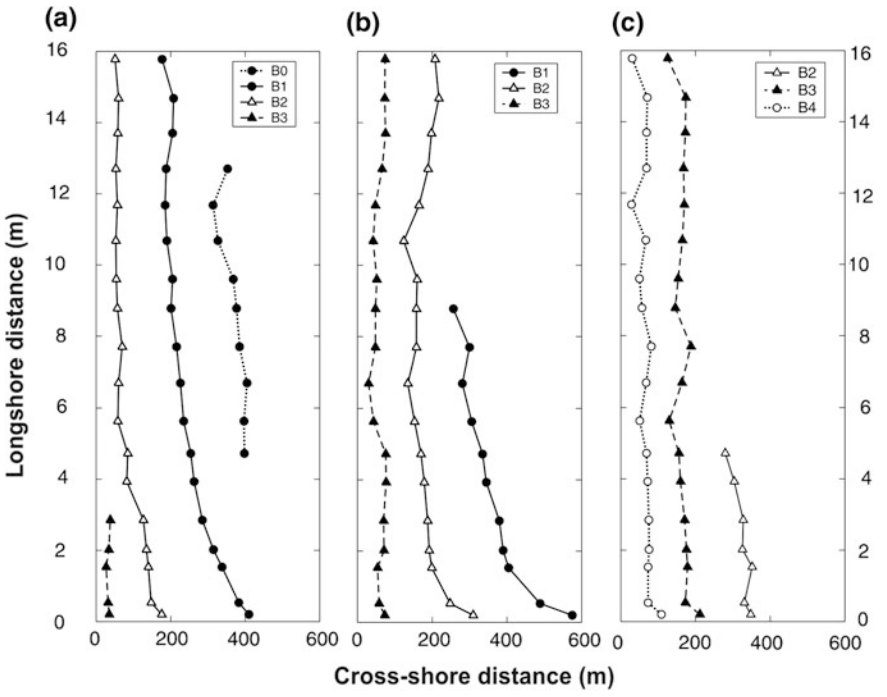

Fig. 26.9 Longshore distribution of individual bar (B0–B4) crests in **a** September 2003, **b** July 2006 and **c** October 2009 along Sulina–Sf. Gheorghe beach (*zero in alongshore direction represents the position of Sf. Gheorghe mouth*). Please pay attention to the longshore differences in sandbar net offshore migration rates and associated cycle return periods

considerable intra-site variability. They have a seasonal behaviour (Fig. 26.3b), with a pronounced offshore movement during winter (due to intense storm activity) and a moderate/slight onshore movement in summer, during fair weather conditions (Vespremeanu-Stroe et al. 2007a). Sometimes, in the summer, along the accumulative and stable sectors, during long-lasting calm periods with sandbars onshore movement, the inner bar is connecting to the sub-aerial beach, contributing to its enlargement and, hence, to the increase of the aeolian fetch and sediment supply for the foredunes. At annual scale, these sandbars exhibit a net offshore migration with various rates (Fig. 26.9), depending on environmental characteristics of each sector (mainly nearshore slope and wave climate), describing a multi-annual cycle. This net offshore migration cycle is characterised by three stages: bar formation close to the shoreline, net offshore migration through the surf zone and bar decay and eventually disappearance at the limit between the upper and the lower shoreface.

Along the accumulative sector, located in the vicinity of Sf. Gheorghe mouth, sandbars register the smallest offshore migration rates (20–30 m/year) and, hence, the largest cycle return periods (~5.5 years). On the central stable sector, the sandbars move offshore with rates of 30–37 m/year, having cycle return periods of ~4.5–5 years, while the northern erosive sector is characterised by the highest migration rates (40–50 m/year) and shortest cycle return periods (~2.8 years).

On the southern sector, the sandbars dynamics is highly influenced by mouth bar behaviour, as they are attached to the subaqueous northern wing of the Sf. Gheorghe mouth bar, which acts during calm periods as a '*sediment trap*' and causes steeper waves at the contact with the fluvial current, inducing higher sediment budgets and enlarging the low-sloping upper shoreface in this area. This intra-site variability of sandbar behaviour is primarily determined by the complex feed-backs between nearshore slope and morphology (due to the shoreline evolution of the delta and the exceptional presence of the Sf. Gheorghe mouth bar), sediment availability (as a result of the long-term evolution of the coast and of the position of each sector into the littoral cell) and surf zone hydrodynamics (alongshore distribution of wave patterns, longshore and cross-shore currents and sediment transport).

Conclusions

The present Danube Delta shoreface morphology (in terms of cross-shore profile shape and slope and longshore variability), sedimentology and behaviour differ substantially on different sectors (accretionary, stable and erosive) of Danube Delta coast, depending on their medium-term behaviour. This behaviour is the result of the long-term evolution of the delta and of each deltaic lobe, the up/downdrift distance to the river mouths, the position of each sector into a specific littoral cell (expressed in sediment availability) and the presence of engineering structures.

At multi-decadal and centennial timescales, the shoreface sediment volume variability is mainly linked to the Danube river sediment supply changes, and,

secondary, to changes in storminess and LST distribution as a result of engineering structures. The presence of active deltaic lobes (Chilia) or developing barrier islands (Sacalin) induced significant increase of shoreface volumes in the last century, while decreasing volumes are related mainly to retreating deltaic lobes (Sulina). The construction of Sulina jetties accentuated the erosion by blocking the longshore circulation and inducing severe erosion downdrift. In the last three decades, the significant decrease of Danube sediment input determined an important reduction of shoreface volumes. The inter-annual shoreface morphodynamics is related to the distance from the Danube river mouths, which modulates the accumulation patterns of sediments transported by river plumes during floods and determines the variable position of the delta front slope, and to storm pattern changes.

The upper shoreface is characterised by the presence of net offshore migrating breaker sandbars. The intra-site differences in their spatial and temporal sandbar behaviour are the result of sensible differences of environmental characteristics, especially nearshore slope and wave regime, with substantially different bar morphology, geometry and migration patterns (bar morphodynamics) on the sediment-rich accretional sectors than on the erosive sectors.

Our results should provide a better understanding of coastal processes along the Danube Delta coast, necessary for sustainable coastal management and planning.

Acknowledgements Research activities were undertaken in the frame of Sfântu Gheorghe Marine and Fluvial Research Station, Faculty of Geography, University of Bucharest. We thank our colleague Dr. Ştefan Constantinescu who kindly provided us old maps and associated bathymetrical grids for the Danube Delta coast. FT was supported by the strategic grant POSDRU/159/1.5/S/133391.

References

Backstrom J, Jackson DWT, Cooper JAG (2007) Shoreface dynamics of two high-energy beaches in Northern Ireland. J Coastal Res SI 50:594–598

Backstrom J, Jackson DWT, Cooper JAG, Malvárez GC (2008) Storm-driven shoreface morphodynamics on a low-wave energy delta: the role of nearshore topography and shoreline orientation. J Coastal Res 24(6):1379–1387

Backstrom J, Jackson DWT, Cooper JAG (2009a) Shoreface morphodynamics of a high-energy, steep and geologically constrained shoreline segment in Northern Ireland. Mar Geol 257: 94–106

Backstrom J, Jackson DWT, Cooper JAG (2009b) Contemporary morphodynamics of a high-energy headland-embayment shoreface. Cont Shelf Res 29:1361–1372

Bondar C, Harabagiu E (1992) Regimul depunerilor de aluviuni la gura canalului Sulina. Studii de Hidraulică XXXIII:131–141 (in Romanian)

Bondar C, Panin N (2001) The Danube Delta hydrologic database and modelling. Geo-Eco-Marina 5–6:5–52

Bondar C, State I, Roventa V (1973) Marea Neagră în zona litoralului românesc al Mării Negre. Monografie hidrologică. Bucharest, 516 p (in Romanian)

Bondar C, State I, Cernea D, Minescu F (1980) Aplicarea metodei energetice îmbunătățite la studiul proceselor dinamicii țărmului românesc al Mării Negre. Studii de Hidrologie XLVIII:169–190) (in Romanian)

Bondar C, State I, Buta C (1984) Caracteristicile evoluției versantului submarin al Deltei în perioada 1830–1970. Studii şi Cercetări Hidrologice 52:181–197 (in Romanian)
Brătescu C (1923) Danube Delta. Chronologic and morphologic genesis and evolution. BSRRG XLIV: 3–39 (in Romanian)
Cowell PJ, Thom BG (1994) Morphodynamics of coastal evolution. In: Carter RWG, Woodroffe CD (eds) Coastal evolution. Late quaternary shoreline morphodynamics. Cambridge University Press, Cambridge, pp 33–86
Cowell PJ, Hanslow DJ, Meleo J (1999) The shoreface. In: Short AD (ed) Handbook of beach and shoreface morphodynamics. Wiley, Chichester, pp 39–71
Cropper T, Hanna E, Valente MA, Jonsson T (2015) A daily Azores–Iceland North Atlantic Oscillation index back to 1850. Geosci Data J 2:12–24
Dan S (2013) Coastal dynamics of the Danube Delta. PhD thesis, Delft University of Technology, 159 pp
Dan S, Stive M, Walstra D, Panin N (2009) Wave climate, coastal sediment budget and shoreline changes for the Danube Delta. Mar Geol 26:39–49
Dimitriu RG, Oaie G, Szobotka S, Sava C, Rădan SC, Fulga C, Opreanu G (2008) Cartarea hidro-geomorfologică a zonei litorale Sfântu Gheorghe–Vadu. Prime rezultate ale cercetării integrate geofizice-geoecologice (2005–2006). Geo-Eco-Marina 14:75–80 (in Romanian)
Finkl CW (2004) Leaky valves in littoral sediment budgets: loss of nearshore sand to deep offshore zones via chutes in barrier-reef systems, Southeast coast of Florida, USA. J Coastal Res 20:605–611
Gâştescu P, Driga B (1986) Morphohydrographical changes of Romanian accumulation Black Sea coast. RRGGG–Geogr 30:29–30
Giosan L, Bokuniewicz H, Panin N, Postolache I (1999) Longshore sediment transport pattern along the Romanian Danube Delta coast. J Coastal Res 15(4):859–871
Hequette A, Hill PR (1993) Storm-generated currents and offshore sediment transport on a sandy shoreface, Tibjak Beach, Canadian Beaufort Sea. Mar Geol 113:283–304
Hequette A, Desrosiers M, Hill PR, Forbes DL (2001) The influence of coastal morphology on shoreface sediment transport under storm-combined flows, Canadian Beaufort Sea. J Coastal Res 17:507–516
Hinton CL, Nicholls RJ (2007) Shoreface morphodynamics along the Holland Coast. In: Balson PS, Collins MB (eds) Coastal and shelf sediment transport. Geological Society, London, Special Publications, 274, pp 93–101
Jianu M, Şelariu O (1970) Processus morphologiques dans la zone terminale du bras Sf. Gheorghe du Danube. Hydrology of Deltas: Proceedings of the Bucharest Symposium, IASH-UNESCO, pp 120–127
Mikhailova M, Levashova EA (2001) Sediment balance in the Danube River Mouth. Water Resour 28(2):180–184 (Translated from Vodnye Resursy 28(2):203–207)
Niedoroda AW, Swift DJP, Hopkins TS, Ma C (1984) Shoreface morphodynamics on wave-dominated coasts. Mar Geol 60:331–354
Niedoroda AW, Swift DJP, Hopkins TS (1985) The shoreface. In: Davis RA (ed) Coastal sedimentary environments. Springer, New York, pp 533–624
Panin N (1989) Danube Delta: genesis, evolution and sedimentology. RRGGG–Geol 33:25–36
Panin N, Jipa D (2002) Danube River sediment input and its interaction with the north-western Black Sea. Estuar Coast Shelf Sci 54:551–562
Panin N, Fârnoagă D, Caraivan G, Dinu C, Gaiță C, Panin S et al (1979–1994) Monitoringul geoecologic al sistemului Dunăre-Deltă-Litoral-MareaNeagră, 15 volumes, Institutul Geologic al României, Centrul Român de Geologie şi Geoecologie Marină, Bucharest (in Romanian)
Postolache I, Diaconeasa D, Şelariu O (1992) Caracteristici morfohidrografice în domeniul pantei submarine. Studii de Hidraulică XXXIII:159–169 (in Romanian)
Pruszak Z, Ostrowski R, Schönhofer J (2011) Variability and correlations of shoreline and dunes on the southern Baltic coast (CRS Lubiatowo, Poland). Oceanologia 53(1):97–120

Roy PS, Cowell PJ, Ferland MA, Thom BG (1994) Wave dominated coasts. In: Carter RWG, Woodroffe CD (eds) Coastal evolution. Late quaternary shoreline morphodynamics. Cambridge University Press, Cambridge, pp. 121–186

Schwartz ML (ed) (2005) Encyclopedia of coastal sciences. Encyclopedia of Earth Sciences Series. Springer, 1197 pp

Short AD (1999) Handbook of beach and shoreface morphodynamics. Wiley, Chichester, 379 pp

Short AD, Jackson DWT (2013) Beach morphodynamics. In: Shroder J. (Editor in Chief), Sherman DJ (eds) Treatise on geomorphology, vol 10, Academic Press, San Diego, Coastal Geomorphology, pp 106–129

Shuisky YD (1984) Dynamics of Kiliya delta coastline of the Danube river. Trans Sov Oceanogr Inst 172:50–60

Shuisky YD (1985) Sources of sedimentary material in shore zone of the western Black Sea. Geol J 45(4):127–139 (in Russian)

Stănică A, Ungureanu GV (2006) Morfodinamica reliefului submers pe tărmul Sulina-Sfântu Gheorghe. Studii si cercetări de oceanografie costieră, 2 (in Romanian)

Stive MJF, de Vriend HJ (1995) Modelling shoreface profile evolution. Mar Geol 126:235–248

Tătui F (2015) Nearshore sandbars behaviour on Danube delta coast. PhD Thesis, University of Bucharest, Ed. Ars Docendi, Bucharest, 156 pp (in Romanian)

Tătui F, Vespremeanu-Stroe A, Ruessink BG (2011) Intra-site differences in nearshore bar behavior on a nontidal beach (Sulina-Sf. Gheorghe, Danube Delta coast). J Coastal Res 64:840–844

Tătui F, Vespremeanu-Stroe A, Ruessink BG (2016). Alongshore variability of cross-shore bar behavior on a nontidal beach. Earth Surface Processes and Landforms. doi:10.1002/esp.3974

van de Meene JWH, van Rijn LC (2000) The shoreface-connected ridges along the central Dutch coast—part 1: field observations. Cont Shelf Res 20:2295–2323

Vespremeanu E (1984) Morphological and morphodynamic aspects of the submarine relief in front of the Danube Delta (in the north-west of the Black Sea). RRGGG–Geographie 28:79–84

Vespremeanu E (1987) Probleme de geomorfologie marină. Editura Universității București, 117 pp (in Romanian)

Vespremeanu E, Ştefănescu D (1988) Present-day geomorphological processes on the Romanian delta and lagoon litoral of the Black Sea. Analele Universității București 37:85–91

Vespremeanu-Stroe A (2004) Transportul de sedimente în lungul țărmului și regimul valurilor pe coasta Deltei Dunării. Studii şi Cercetări de Oceanografie Costieră 1:67–82 (in Romanian)

Vespremeanu-Stroe A (2007) Danube Delta coast. Geomorphological study. PhD Thesis, University of Bucharest, Ed. Universitară, Bucharest, 226 pp (in Romanian)

Vespremeanu-Stroe A, Tătui F (2011) North-Atlantic Oscillation signature on coastal dynamics and climate variability of the Romanian Black Sea Coast. Carpathian J Earth Environ Sci 6 (1):308–316

Vespremeanu-Stroe A, Constantinescu Ş, Tătui F (2007a) The multianual behaviour of nearshore bars on a microtidal coast. Rev Geomorfol 9:107–123 (in Romanian)

Vespremeanu-Stroe A, Constantinescu Ş, Tătui F, Giosan L (2007b) Multi-decadal evolution and North Atlantic Oscillation influences on the dynamics of the Danube delta shoreline. J Coastal Res 50:157–162

Wright LD (1995) Morphodynamics of inner continental shelves. CRC Press, Boca Raton, 241 pp

Zăinescu F, Vespremeanu-Stroe A, Tătui F, Valchev N submitted. Storm climate on the Danube Delta coast: evidences of recent storminess change and links with large-scale teleconnection patterns. Natural Hazards

Part VII
Dynamics of the Sediment System

Chapter 27
Sediment Sources and Delivery

Dan Dumitriu, Maria Rădoane and Nicolae Rădoane

Abstract This section is dedicated to the contribution of geomorphic processes in dislocation, setting in motion and removal of rock particles from the drainage system in Romania. The total volume of eroded material amounts to ca. 126 Mt/year for the entire territory of Romania. Sediments are dislodged by means of various processes including sheet erosion or rill and gully erosion, as well as mass movements (landslides, collapse, mudflows, creep, etc.). The arable lands yield approximately 80 % of the total soil loss in Romania, slightly above the European mean value of 70 %. The contribution of slope processes (sheet and rill erosion, gully erosion, landslides) was estimated at about 67 % and of fluvial processes at about 33 %. The ratio of the two major domains (slopes and river beds) in terms of sediment source contribution was 90:10 according to estimates from the 1980s. In our days, our own evaluations indicate a more balanced ratio, i.e., 67:33. We believe the tendency of adjustment of the relationship between the two sediment source domains is factual and strongly dependent on the changes of controls during the past three decades. The VII and VIII order drainage network (Strahler's system) from Romania discharges into the Danube sediments which may account for less than 1 % of the amount of sediment yielded by the hillslopes and river beds from the investigated area. At Ceatal (before the Danube enters the deltaic sector), the river transfers on average an annual volume of 20.5 Mt of sediments (from 1985 to 2006). Between 1840 and 1970 the mean amount of alluvium carried by the Danube was 57.3 Mt/year. The difference is accounted for by the sediment storage in the river basin which represents over 37.5 %. The largest sediment storage occurs in reservoirs, and the value determined by us is very similar to the global value (36.6 %).

D. Dumitriu
Alexandru Ioan Cuza University, Carol I Av 11, 700506 Iași, Romania
e-mail: dndumitriu@yahoo.com

M. Rădoane (✉) · N. Rădoane
Ștefan cel Mare University, Universității 13, 720229 Suceava, Romania
e-mail: radoane@usm.ro; mariaradoane@gmail.com

N. Rădoane
e-mail: nicolrad@yahoo.com

M. Rădoane and A. Vespremeanu-Stroe (eds.), *Landform Dynamics and Evolution in Romania*, Springer Geography,
DOI 10.1007/978-3-319-32589-7_27

Keywords Sediment system · Controlling factors · Geomorphological processes · Sediment yield · Sediment delivery ratio

Introduction

Sediment transfer from sources to delivery is a key topic of dynamic geomorphology. The rate at which this process occurs can change dramatically, which is commonly a signal of major landform adjustments. In this section dedicated to sediment sources and delivery we aim to document the contribution of geomorphic processes in dislocation, setting in motion and removal of rock particles from the drainage system in Romania. This sample objective was addressed through case studies from various Romanian regions whereby individual investigations were conducted during the past decades.

Deciphering sediment dynamics was a necessity in the early 1980s when hundreds of dams became operational and their reservoirs turned into retainers of upstream landform erosion products. The need to find answers as to where these sediments originate and whether it is possible to control sediment transfer rates has brought forward new approaches in Romanian geomorphology. Thus, the newly created concept of *sediment system* was introduced in Romania by Ichim (1986, 1988, 1992), Ichim and Rădoane (1987). The sediment system approach was interdisciplinary and major results yielded by these investigations were showcased in the national symposia on "Sediment sources and delivery" (1986, 1988, 1990, 1992). Hence, the results presented in this section are the product of this concept applied to various drainage basins across the Romanian territory, and particularly to basins with relevant hydropower production potential.

The sediment system concept was defined as part of a fluvial geomorphic system and is structured on four levels: (i) controls; (ii) geomorphic processes; (iii) sediment sources (in terms of processes and areas of origin) and sinks (natural and anthropogenic); (iv) sediment delivery (Fig. 27.1).

The sediment system pertaining to the Romanian territory, of which the autochthonous drainage network tributary to the Danube accounts for over 97.8 %, was approached based on this concept. Neither the space nor the available data are sufficient to tackle all four levels of the sediment system structure; however, in this chapter we will focus on at least two levels, i.e., sediment sources and sediment delivery ratio. As regards the sediment sinks, in the absence of factual data, these can be estimated based on the difference of the two levels mentioned above.

Studies on the sediment system or targeted only at certain levels of the system have been carried out in a large variety of drainage basins differing in terms of size, geological substrate, main landforms, land use, etc., which are illustrated in Fig. 27.2, with the synthetic data on the results of research summarized in Table 27.1. The total area of investigated drainage basins amounts to ca. 40,000 km^2.

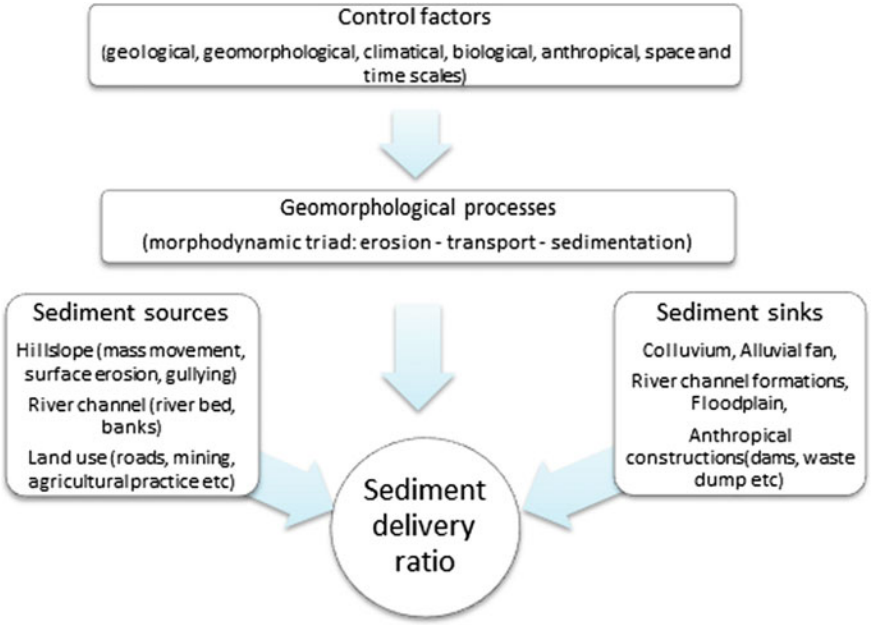

Fig. 27.1 Levels of organization of the sediment system (redesigned after Ichim 1986)

Fig. 27.2 Location of study areas investigated by the authors of this section on the topic of sediment systems in Romania

Table 27.1 Data on the sediment systems from drainage basins indicated in Fig. 27.1

River	A (km^2)	River length (km)	Hillslope field			River channel field			Sources
			S (%)	G (%)	MM (%)	ICEC (%)	BL (%)	SY (t/km^2/ year)	
1. Pângărați (Bistrița)	18	7	23	11	26	43	120	184	Rădoane (2002)
2. Oanțu (Bistrița)	38	15	16	10	30	44	90	255	Rădoane (2002)
3. Trotuş	4350	160	15	40	10	35	9.1	276.8	Dumitriu (2007)
4. Bârlad	7395	281	64	30	2	4	8	131	Rădoane and Rădoane (2007)
5. Jijia	5722	275	64	13	2	21	10	307	”
6. Bahlueț	558	50	55	35	4	6	NA	326	Rădoane and Rădoane (2001)
7. Putna	2518	160.3	70			30	12	3846	Ichim et al. (1998)
8. Buzău	5240	303.4	4.2–70			30	31	811	Rădoane et al. (1997)
9. Bâsca Chiojdului	345	42	45			55	37	1715	Rădoane et al. (1997)
10. Argeş	2837	339	58			42	76 % from SY	1074	Ichim et al. (1994a)
11. Topolog	543	100	58			42	36	147	Rădoane and Rădoane (2007)
12. Four small catchments	1… 54.3	–	88			12	614… 186	10445… 4800	Rădoane et al. (1992)
13. Olteț (Olt)	2470	186	60			40	9–11	667	Rădoane and Rădoane (2007)
14. Jiu	2474	416	15			15 (70)	5	169	Radoane et al. (1995b)
15. Bonțu (Someşu Mic)	18.14		20	NA	60	20	15	280	Rădoane et al. (2014)
16. Bistrița	4200		45			55	20	76	Rădoane (2004)

A drainage basin area; *S* sheet erosion; *G* gully erosion; *MM* mass movement; *ICEC* in-channel erosion contribution; *SSL* suspended sediment load; *BL* Bedload; *SY* sediment yield; *NA* non available

The research methods employed in these studies consisted primarily of field geomorphological mapping, inventorizing sediment-generating geomorphic processes, estimating the amounts of displaced rock, and assessing the sediment delivery ratio according to the order of the drainage basins and the sum of controls responsible for sediment transfer. In the early stage of research (1980), many of the large Romanian reservoirs were already functional or were being designed or built in these drainage basins, such that studies were focused mainly on producing forecasts on the evolution of reservoir silting in the respective basins.

The following sections of this chapter address a brief analysis of the types of sediment-yielding processes which can provide a clearer perspective on transformations occurring in this field.

Sediment Sources in Relation with Sediment–Yielding Processes

The analysis of sediment sources requires the identification of the entire range of processes transferring alluvium from the slopes to the stream channels. Sediments are dislodged by means of various processes including sheet erosion or rill and gully erosion, as well as mass movements (landslides, collapse, mudflows, creep, etc.). The entire amount of sediments displaced from the hillslopes is not transferred to the river channels, as a large share is stored for certain duration at different levels of the slope or at the contact with the channel.

For the Romanian territory Moţoc (1984) determined that the total volume of eroded material yielded by all the aforementioned processes amounts to ca. 126 Mt/year (Table 27.2). During the three decades that passed since this evaluation the factors controlling sediment-producing processes have altered their action due to both climatic variability and multiple human interventions in the sediment system.

Table 27.2 Sediment delivery ratio in relation to the type of erosion on the Romanian territory (Moţoc 1984)

Process	Gross erosion		Sediment delivery ratio (%)	Delivered sediments	
	(Mt/year)	(%)		(Mt/year)	(%)
Sheet erosion	61.8	49.0	26	16.1	36.2
Gully erosion	29.8	23.6	46	13.7	31.0
Mass movement	15.0	12.0	35	5.3	11.6
Gully erosion and landslides in forested areas	6.8	5.4	40	2.7	5.9
Riverbank and in-channel erosion	12.6	10.0	54	6.8	15.3
Total	126.0	100.0	35	44.1	100.0

By comparing our results shown in Table 27.1 with the estimates listed in Table 27.2 we determined that some sediment-yielding processes (i.e., gully erosion and mass movements) have similar contributions, with few differences between the two sets of data. However, the contribution of riverbank and in-channel erosion to the sediment supply is as high as 33 % compared to 10 % as estimated by Moțoc (1984). The contribution of bedload as a sediment source has increased steadily during the last 20 years due to the general trend of channel incision throughout most of the Romanian drainage network (Rădoane et al. 2013), whereas the share of sheet erosion is at least 10 % lower according to our assessment compared to the data in Table 27.1; the latter is, to a large extent, an effect of land restitution after 1991 which resulted in a large share of agricultural land turning fallow (cf. Popa, Chap. 15, this volume).

Sheet Erosion as Sediment Sources

The assessment of sheet erosion rates for various land use classes was introduced in Romania in the 1950s and employed experimental plots for determinations (Arghiriade 1977; Gaşpar et al. 1982; Rădoane 2002; Ailincăi et al. 2012; Popa et al. 2013). The data provided by these studies were used to generate Fig. 27.3 based on which the following general conclusions were inferred:

(i) both the layer of runoff water and the specific erosion rates depend to a significant degree on the land use/land cover (LULC) (Vanacker et al. 2007);
(ii) on lands protected by vegetation (i.e., pastureland, meadows), sheet erosion rates are very low, ranging from 0.003 to 1.4 t/ha/year. On degraded grasslands, the sheet erosion rates increase with the degree of usage;
(iii) in deciduous forests with good consistency (0.8–1) and thick layers of litter, both the runoff and sheet erosion are very low, under 0.2 t/ha/year. Higher values are typical for spruce forests where litter is largely missing, in which case sheet erosion rates can be as high as 7 t/ha/year;
(iv) the highest sheet erosion rates were documented in non-vegetated plots (25.6–68.6 t/ha/year). Such lands are infrequent in mountain areas, and therefore sheet erosion is generally rather low compared to hills and plateaus;
(v) on arable land used for various crops sheet erosion ranged between 0.12 t/ha/year in the case of plots with perennial grasses and 20.8 t/ha/year in plots cultivated with sunflower. The obtained results on the potential erosion (conditioned by geomorphological, soil and climate factors) have shown that on the fields uncovered by vegetation from the Moldavian Plateau, the mean soil losses due to erosion were 18.17 t/ha/year (Bucur et al. 2011), whereas the maximum value is as high as 42.37 t/ha/year (Popa et al. 2013).

Like any other geomorphic process, sheet erosion is highly variable in time and across space. Within the Romanian territory, Ioniță (2011) distinguished five stages

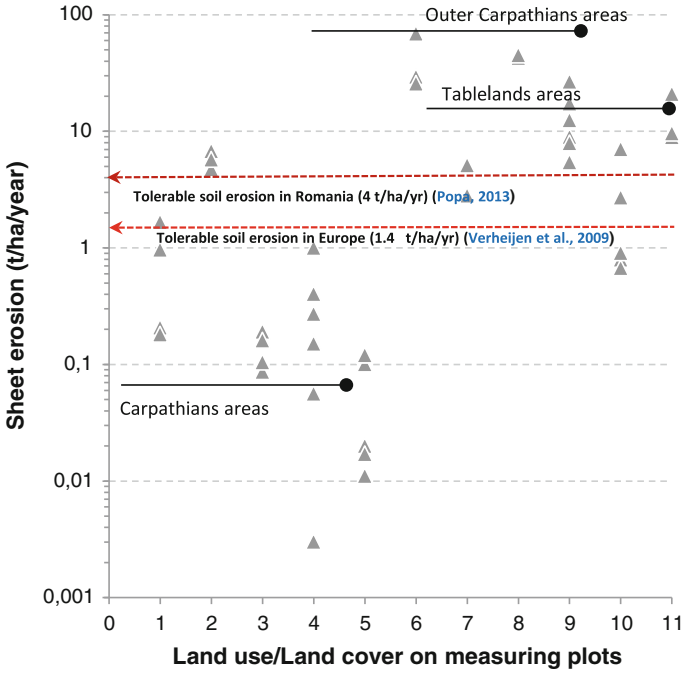

Fig. 27.3 Centralized data on erosion rates by measuring plots in Romania (summarized from data provided by Arghiriade 1977; Gaşpar et al. 1982; Rădoane 2002; Ioniţă et al. 2006; Ailincăi et al. 2012; Popa et al. 2013). *1* Spruce forest; *2* Spruce forest without litter; *3* Beech forest; *4* Meadow–land; *5* Pastureland; *6* Non-vegetated land; *7* Orchard; *8* Dead-fallow land; *9* Corn; *10* Wheat; *11* Sunflower

of amplification or reduction in sheet erosion as a result of human intervention: (1) a *preparing stage* for future land degradation (1829–1899) when the most dynamic change of the native landscape was recorded. Following the Treaty of Adrianople (1829) the Romanian Principalities liberalized the timber and grain trade which resulted in large scale forest clearing for agricultural purposes; (2) a *transitory stage* (1900–1920) associated with the extension of the cultivated land up to 48 % of the total area; (3) the *climax stage* (1921–1970) defined by both the traditional up and down hill farming and the peak rate of land degradation during the 1960s; (4) a *decreasing tendency* of land degradation (1971–1990) as a result of the extension of conservation practices and of the rainfall pattern; (5) the *present-day* revival of land degradation associated to the Act no. 18/1991 when up and down hill farming under small plots is on the screen again. Under these circumstances, the rate of land division increased and it is higher than before World War II (Ioniţă et al. 2006). While in 1940 the number of plots amounted to 22 million, in 2004 there were no less than 48 million small plots in Romania (Ambăruş 2007). On the other hand, large and very large farms (50–100 ha and over 100 ha) with a trading profile

represent only 0.3 % (Bălteanu and Popovici 2010). Another law, no. 1/2000, was promulgated and is focusing on the forestland division for private ownership.

By comparing the values listed in Table 27.2 with the tolerable value of soil erosion in Europe, i.e., of 1.4 t/ha/year (Verheijen et al. 2009) (whereas according to Bucur et al. 2011; Sevastel 2012; Popa et al. 2013, the value for Romania is 4–6 t/ha/year) it appears that large areas of the investigated basins (with the exception of those located in the plateaus) fall within normal limits in terms of sheet erosion. However, to date the effects generated by changes in the land use/land cover (i.e., the excessive division of property, down hill farming, the destruction of erosion control works, forest clearing) or by climate changes (mainly the increasing rainfall intensity) on soil erosion in Romania were not quantized.

The amount of material supplied to the river channels through sheet erosion ranges from 5 to 20 % (Lu et al. 2003; Belyaev et al. 2005; Wilkinson and McElroy 2007). Dumitriu (2007) calculated the sheet erosion rate in Trotuş drainage basin based on the correlation between the measurements on sheet erosion on plots located under similar conditions (in terms of climate, runoff, soil, etc.) to those from the basin and the detailed geomorphological mapping of sheet erosion in relation to the slope classes, land use classes and the types of hillslope surface. Thus, it was estimated that sheet erosion provides 136 t/km^2/year (or ca. 1.4 t/ha/year) of the total annual sediment yield in Trotuş drainage basin, which accounts for approximately 20 %. The sediment delivery ratio through this type of process was estimated at ca. 10.2 %. The same algorithm was employed by Rădoane et al. (2014) to assess the sheet erosion in Bonţu drainage basin (upstream of Ştiucii Lake), which accounts for 16.5 % of the gross erosion (568 t/km^2/year).

Furthermore, the assessment of sheet erosion in Trotuş basin using the SedNet (*Sed*iment River *Net*work) model was attempted (Prosser et al. 2001; Wilkinson et al. 2004). The model is based on physical processes estimating the annual sediment yield and its components (mean annual stream flow discharge and sediment load; sheet erosion; gully erosion; river bank erosion; hillslope delivery ratio–HSDR) and provides good results for basins larger than 3000 km^2.

Using the SedNet model it was determined that sheet erosion in Trotuş basin accounts for ca. 15 % of the total effective hillslope erosion, with a mean value of approximately 1.75 t/ha/year. The sheet erosion in the entire Trotuş basin was estimated at 77,925 t/year. In the majority of the 146 catchments generated by the SedNet model (38.89 %) the rate of sheet erosion ranges between 100 and 500 t/year, whereas the percentage of catchments with rates between 500 and 1000 t/year is ca. 25.4 %. In 21.43 % cases the annual sheet erosion rate exceeds 1000 t/year. Only in 14.29 % instances the estimated rates are below 100 t/year (Fig. 27.4).

To conclude, arable lands yield approximately 80 % of the total soil loss in Romania, slightly above the European mean value of 70 %. The mean calculated value of sheet and rill erosion in Europe is around 1.2 t/ha/year for the entire area and ~3.6 t/ha/year for arable land (Cerdan et al. 2010). In Romania, the mean estimated value of sheet and rill erosion is ca. 4.2 t/ha/year (Ioniță et al. 2006).

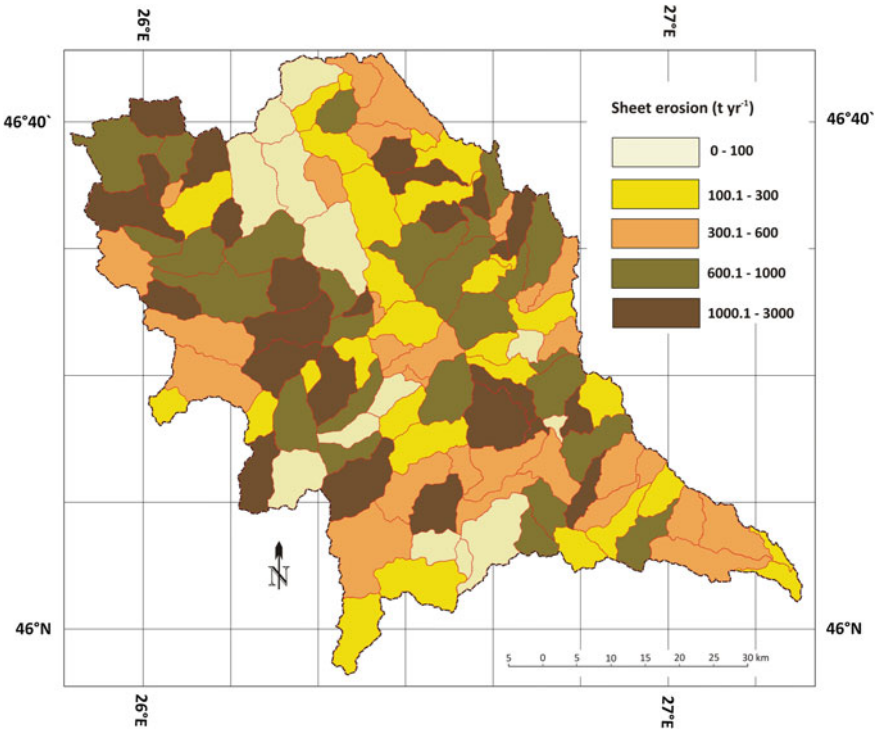

Fig. 27.4 Sheet erosion in catchments from Trotuş drainage basin calculated using the SedNet model

Gully Erosion Processes as Sediment Sources

Regarded as sources of alluvium, gully erosion processes can account for 10 % up to as high as 95 % of the total sediment yield in a drainage basin (Poesen et al. 2003). The effectiveness of these processes in terms of land degradation and evacuation over short periods of time of large amounts of material originating in the fertile layer of soil has caught the attention of Romanian researchers: Moţoc et al. (1979), Mihai et al. (1979), Moţoc (1982, 1984), Gaşpar and Cristescu (1987); Rădoane (1980, 2002); Radoane et al. (1995a, 1999); Ioniţă (1999); (see also Chap. 16, this volume).

Based on the data on sediment sources provided by these studies we were able to draw some general conclusions regarding a large portion of the Romanian territory, as follows:

(i) The greatest density of gullies occurs in the plateaus on lands with gradients between 10 and 15 degrees, used mainly as pasturelands. However, gullies are present on all lands which are subjected to inappropriate exploitation, regardless of the landform where they occur (Rădoane et al. 1999);

(ii) The volume of soil and rock dislodged by gullying processes in the area located between Siret and Prut Rivers was estimated at 274 million m^3 or 411 Mt. The most active period of gullying from the Moldavian Plateau varies between 25 and 50 years. Hence, in this region of Romania the contribution of gully erosion to the sediment budget ranges from 3.3 to 6.5 t/ha/year;

(iii) In the mountain areas gully erosion can be significant if the anthropogenic impact is exacerbated (by overgrazing, down hill roads, logging transport tracks, etc.). In Pângărați and Oanțu catchments, whereby the road density is 2 km/km^2, of which 80 % are forest roads, 20–30 % of the total evacuated sediments are produced solely by road degradation (Rădoane 2002). In some oil extraction areas from Trotuș basin, the density of the downslope road network is as high as 2.5–6.5 km/km^2 (Surdeanu et al. 1988; Dumitriu 2007), whereas the drainage network density is just 1082 km/km^2.

The aggregate length of gullies from Trotuș drainage basin in 2006 was ca. 622 km, while the mean density of gullies was 0.14 km/km^2. Approx. 95.7 % of the drainage basin area falls into the lowest density class, below 1 km/km^2; 2.6 % of the basin area ranges between 1 and 2 km/km^2; the areas with gully densities above 2 km/km^2 account for 1.7 % of the basin area (Dumitriu et al. 2010).

The gully erosion assessed using the SedNet model in the same basin has a share of 40 % of the sediment yield, i.e. ca. 47.5 t/km^2/year. In nearly 50 % of the catchments generated by the SedNet model the gully erosion rates range between 100 and 1000 t/year (Fig. 27.5). Exceptional values, above 10,000 t/year, occur in Comăneşti Depression and on the left hillside of Trotuș valley downstream of Căiuți (where gully erosion accounts for over 90 % of the effective erosion of hillslopes).

To conclude, gully erosion processes can provide on average up to 31 % of the alluvia reaching the drainage network. The contribution of these processes as sediment sources is roughly 0.7 t/ha/year, or, in absolute values, 13.8 Mt of the total amount of 44.6 Mt of sediments carried annually by rivers (Moţoc et al. 1992).

Mass Movement Processes as Sediment Sources

Landslides mobilize considerable amounts of slope deposits, thus ranking among the major sediment-supplying processes, particularly in the Subcarpathian and plateau regions, as well as in the flysch highland area (Surdeanu 1986; Bălteanu et al. 2010). When regarded as sediment sources, one of the most significant elements of a landslide resides in the coupling or the connectivity between the slope and the fluvial system (Harvey 2001; Peart et al. 2005; McCabe et al. 2013; Jurchescu 2014). This aspect was observed in the inventory of the landslides from the study areas illustrated in Fig. 27.1. The conclusions concerning the contribution of mass movements in providing sediments are summarized as follows:

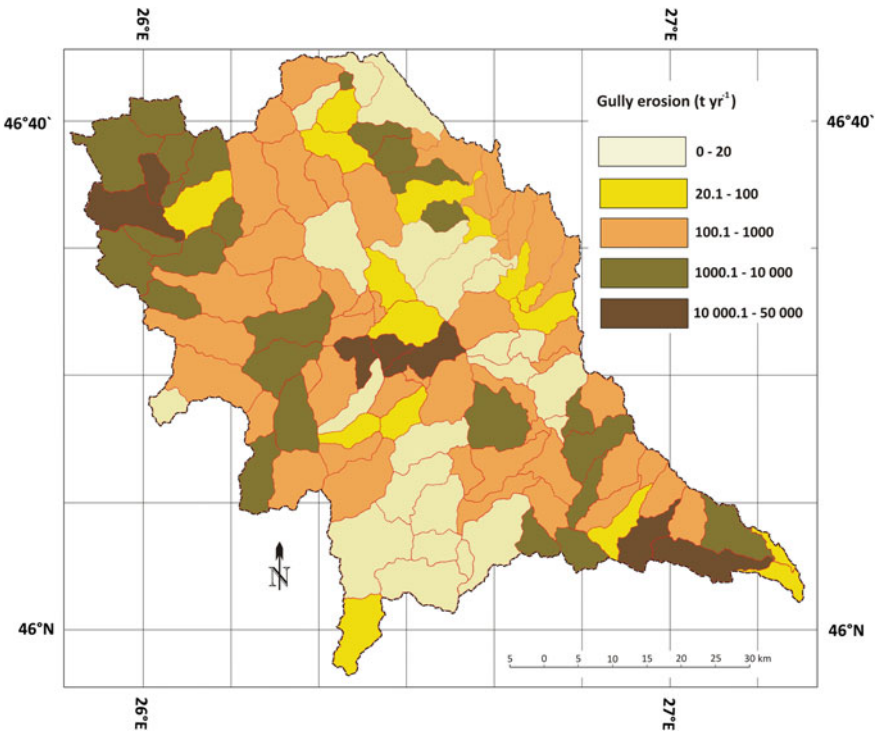

Fig. 27.5 Gully erosion as a sediment source in Trotuş drainage basin calculated using the SedNet model

(i) The percentage of the material supplied to river beds by landsliding varies depending on the characteristics of reaches whereby the transfer occurs (confined, partly confined or laterally unconfined sensu Brierley and Fryirs (2005); the nature of sectioned deposits; the land use/land cover). Thus, on Bâsca Mare River, (Varlaam–Bâsca Rozilei reach) landslides contribute ca. 78 % to the sediment yield. On the middle sector of Buzău River (Cislău–Cândeşti reach) whereby the valley widens considerably and the contact with the hillslopes is reduced to a few sectors, the mean sediment input of mass movement processes was estimated at ca. 4.2 %. However, if we accept the idea that at recurrence intervals of 10–12 years these can be reactivated at average velocities of at least 1 m/month, the volume transferred to the river bed can increase up to 30 % of the total amount of sediment carried by Buzău River (Ichim et al. 1990);

(ii) According to estimates, at present, mass movement processes play a decisive role in providing alluvium to the Subcarpathian river reaches, such that in the years with peaking relapse of the process the amount of material evacuated by mass movement accounts for 30 % up to 65 % of the total material supplied to river beds. For instance, in the Subcarpathian sector of Putna

River, landslides with average velocities of 1 m/month and recurrence intervals of 10–12 years have a transfer potential of ca. 65 % of the mean total sediment yield, which was estimated at ca. 3,567,000 t/year (Ichim et al. 1998).

(iii) In the case of rivers from the central and northern sectors of the Eastern Carpathians located north of Putna basin, mass movements have a lower contribution compared to the other categories of processes by which sediments are transferred to river beds, both due to the reduction of the Subcarpathian area northward, and the increase in the percentage of forested land. Against this background, it was determined that mass movement processes only account approx. 10 % of the total sediment yield in Trotuş drainage basin (Dumitriu 2007).

(iv) In the plateaus, the contribution of mass movement processes to the sediment yield is considerably lower due to low connectivity with the river channels. According to the survey carried out during a 21 years period in the Moldavian Plateau by Pujină (1998), it appears that only 2 % of the amount of material mobilized by landslides is eventually evacuated into the 2nd to 4th order drainage network (Strahler's system). In Bonţu basin located in the Transylvanian Plateau Rădoane et al. (2014) found that whereas landslides dislocate approx. 2745 t/km^2/year (which accounts for 80 % of the gross erosion), they only contribute to the sediment yield with less than 2 % due to the phenomenon known as drainage network sedimentation.

To conclude, forwarding a realistic mean value regarding the input of landslides to the total sediment yield at the scale of a broad territory is not a facile task. The variation margin in the basins comprised in our study was large, ranging between 2 % (in basins located in the plateaus) and 60 % (for catchments from the Subcarpathians and the flysch mountains). Albeit, Moţoc (1984) suggested a mean percentage of 12 %, which is likely a realistic figure.

Fluvial Processes as Sediment Sources

River bed sediments are provided by two major types of processes, i.e., riverbank erosion and bed erosion. We will not focus on bed processes in this section, as they are discussed in two separate chapters in this volume (e.g., see Chap. 21 for the dynamics of river bed and bank processes or Chap. 28 for bed deposits and the role of rivers in processing the sediment influx); however, we retain some conclusions regarding the assessments on the contribution of river beds as sediment sources

(i) The contribution of fluvial processes to the sediment budget in a drainage basin becomes relevant from the third order drainage network onwards. Starting from this level of the river network, the valleys acquire the typical

elements of fluvial relief under the temperate climate whereby Romanian rivers evolve (Ichim and Rădoane 1984);

(ii) Lateral erosion varied within a broad margin, from several cm/year (in the case of small stream channels deepened in cohesive rocks) up to 27–35 m/year (in alluvial beds of large wandering or braided rivers). Investigations on lateral erosion on Trotuș River determined that the lateral erosion rate differs depending on the landform traversed by the river (or, moreover, indicates the increase of the drainage basin size), as well as on the period of occurrence of major floods (1960–1980 and 2005–2010) (Fig. 27.6).

(iii) Bed erosion has a significant contribution as sediment source, as the dominant bed process documented in the majority of rivers (ca. 60 % in Eastern Romania, cf. Rădoane et al. 2010) is channel deepening. Along most river beds lies a mobile layer of sediments under 50 cm thick; however, in some instances this layer can exceed 100–150 cm in thickness along river reaches undergoing massive human intervention such as gravel mining.

Finally, we can conclude that the average ratio of 33 % pertaining to river beds as sediment sources determined by our investigations (Table 27.1) is supported by the reality of Romanian rivers.

Sediment Sources According to Area of Origin

The significant amount of suspended sediment evacuated from a drainage system, particularly during large flood events, has prompted us to find an answer to the question whether the domains from the upstream drainage basin which have the

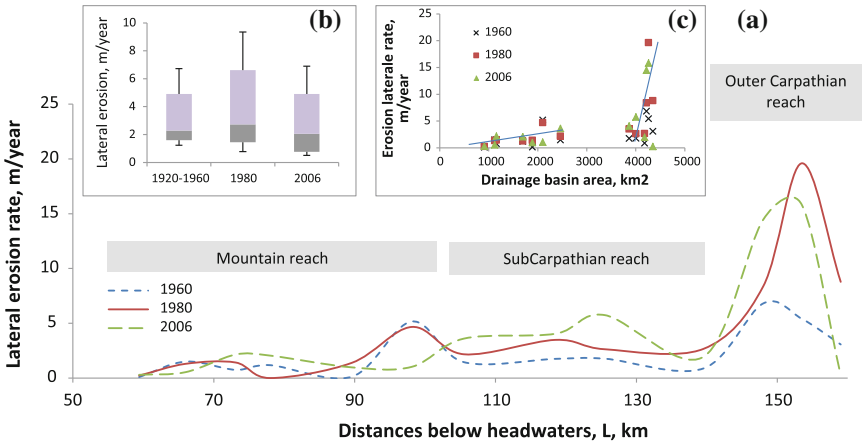

Fig. 27.6 Lateral erosion as sediment source along the Trotuș River. **a** Lateral erosion rate on Trotuș River along 100 km of the river length from 1920 to 2006; Variation of lateral erosion rates depending on the main relief units traversed by the river valley; **b** Temporal variation of lateral erosion rates represented as boxplots; **c** Variation of lateral erosion rates depending on the size of the drainage basin

greatest contributions in providing these sediments are the hillslopes or the river beds? The more accurate the answer, the higher will be the effectiveness of sediment transfer control measures. Our interest targeted mainly the evacuated suspended sediment originating particularly in the erosion of the topsoil horizon. Our analysis of case studies presented in Table 27.1 resulted in some concrete data; we hereby illustrate the situation of two drainage basins (Olteț and Topolog) originating in the Southern Carpathians, with elongated shapes overlying diverse landforms and geological units.

By applying the method introduced by Grimshaw and Lewin (1980) the area of suspended sediment origin was deduced based on the eq. $Qs = f(Q)$. This relation acquires different forms depending on the season and the size of transported material, resulting in high dispersion which can suggest the following aspects:

(i) the top of the plot indicates the summer discharge when the stream flow discharge and solid load are high and alluvium originates mainly in the catchment;
(ii) the bottom of the plot commonly indicates the autumn–winter discharge, when alluvium derives mostly from the river bed.

In the case of Olteț River, the *Qs*–*Q* correlation plot between 1990 and 1991 (Fig. 27.7a) indicates the occurrence of a threshold at Q = 4–10 m^3/s, depending on which the two types of sources according to the dominant areas of origin were distinguished, i.e., the catchment domain or the river bed domain. As regards Topolog River (Fig. 27.7b), at stream flow discharge values above 1–3 m^3/s the catchment may contribute to the total volume of sediments evacuated from the basin with fine alluvium. Below this threshold value, the fine sediments discharged by the river originate mainly in the channel banks.

On an average, over the duration of a year, the bed of Olteț River supplies ca. 40 % of the suspended sediment, whereas the catchment provides the remaining

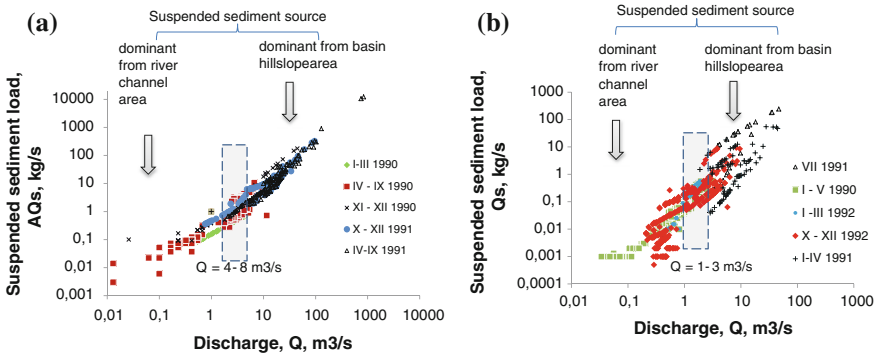

Fig. 27.7 Identifying suspended sediment sources using the hydrograph method in two drainage basins. **a** Olteț, tributary of Drăgașani reservoir (on Olt River). **b** Topolog, tributary of Băbeni reservoir (on Argeș River). Basin location is indicated in Fig. 27.2

60 %. The seasonal variation is significant, as during the summer the input of the catchment may be as high as 80–90 % of the amount of alluvium, while the contribution of the river bed (although quantitatively relevant) is much lower; in the autumn and winter the input of the catchment slopes decreases such that the bed supplies 70–80 % of the alluvium, particularly the banks. Extreme events, and floods, in particular, leave a strong mark on the scale of the slope/bed ratio: for example, in 1990, when precipitation and consequently the stream flow discharge were low, 72.3 % of the total volume of measured suspended sediments of 75,402 t came from the river bed; in 1991, when precipitation were abundant and the maximum discharge amounted to 1190 m^3/s, only 9.7 % of the total volume of suspended alluvium originated in the bed; in 1992 precipitation were diminished and the peak discharge was as low as 29 m^3/s, 37.9 % of the total 18,309 t of suspended sediment, coming from the bed.

In Topolog River, the variability of correlations is higher due to the numerous human interventions altering the discharge. However, results indicate percentages similar to Olteț River as follows: on Milcoiu reach, the slopes provide 58 % of the suspended sediment, and the remaining 42 % are delivered by the channel bed. During the years when precipitation and streamflow discharge are high, the contribution of slopes is considerably higher (e.g., in 1991 the catchment provided 79 % of the suspended alluvium), whereas in drier years the bed becomes the main source of sediments (for example, in 1990 the bed yielded 51 % of the total suspended alluvium).

On Trotuș River, Dumitriu (2007) employed a research methodology combining direct field measurements and the SedNet model. Thus, within the drainage basin the input of the slopes amounts to ca. 65 % while the river beds supply 35 % to the sediment yield.

The data cited in the Romanian literature regarding the ratio of contribution of the two domains (river beds versus hillslopes) to the sediment yield refer particularly to small basins/catchments (under 50 km^2) derived from field experimental research. Thus, in Colinele Tutovei, river beds account for 26–75 % of the sediment sources (Moţoc et al. 1979); in the Subcarpathians the share of river bed domain increases from 55 up to 85 % (Gaşpar and Untaru 1979). In small catchments from the flysch mountains the river beds contribute ca. 32 % (Rădoane 1986); in Nandra basin (Getic Piedmont) the input of the beds is approx. 65 % of the total amount of sediment evacuated from the basin (Bălteanu and Teodorescu 1985). Overall, it was observed that as the basin size increases, the contribution of river bed domain as a sediment source augments as well.

At the conclusion of this review, we return once more to the results presented in Tables 27.1 and 27.2 in order to infer a comparative average state of global estimates for the Romanian territory. Based on the assessment made by Moțoc (1984) the ratio of the two major domains (hillslopes and river beds) in terms of sediment source contribution is 90:10. Instead, our evaluations indicate a more balanced ratio, i.e., 67:33. We believe that the tendency of adjustment of the relationship between the two sediment source domains is factual and strongly dependent on the changes of controls during the past three decades.

Sediment Yield

The earliest investigations focusing on the sediment yield of Romanian rivers (i.e., the sediments evacuated through the drainage network) were carried out by Diaconu (1964, 1971). His study from 1971 provides the first overview of the sediment yield and transport throughout the Romanian territory; within this analysis a large volume of data on the suspended solid load measured in 202 drainage basins from 1952 to 1967 was processed, based on which the earliest maps depicting the nationwide spatial distribution of the sediment yield in t/ha/year were produced. For the Romanian territory, the calculated mean specific suspended sediment load was 1.88 t/ha/year, which corresponds to a volume of 44.5 Mt of solid materials discharged by rivers (Fig. 27.8).

Mociornița and Birtu (1987) updated the map of specific sediment yield with data from 1950 to 1984; furthermore, additional data was provided on the influence of major flood events from 1970, 1972, 1975, and 1979, on the sediment yield, as well as on the role of reservoirs in the sediment system. The authors established that with the exception of the Danube, Romanian rivers transfer on average ca. 1550 kg/s/year of suspended alluvium, which translates to an annual sediment yield of 48.9 Mt. The specific sediment yield amounted to 2.06 t/ha/year. The largest amount of suspended sediment was transported by rivers crossing the Subcarpathian region, whereby the mean values of the specific sediment yield are

Fig. 27.8 Map of suspended sediment yield in t/ha/year (redesigned after Diaconu 1971). Basins Olteț and Topolog illustrated in Fig. 27.7 are highlighted on the map

above 10 t/ha/year, up to a maximum value exceeding 20–25 t/ha/year in the Curvature Subcarpathians.

We attempted to update the map of sediment yield in Siret drainage basin with data regarding the suspended solid load until as recently as 2010 (Obreja 2013) and other data resulting from our own investigations on the drainage basins from this region. Based on the series of maps illustrating this process between 1971 and 2010 (Fig. 27.9), we were able to outline several observations.

The area where the highest rates of sediment yield were constantly documented is the Curvature piedmont; the Mociornița and Birtu (1987) edition of the map can be disregarded due to the erroneous depiction of sediment yield isopleths. A second area with increasing sediment yield is located in the middle sector of Bârlad basin whereby the rate has increased from 5–10 to 10–15 t/ha/year, ranking into the upper class. The last edition of the map (2010) was based on a dense network of measurement points (shown on the map) and an advanced interpolation technique (which took into account land erodability). We regard this exercise as suggestive for the evolution of sediment yield values and aerials throughout the Romanian territory in relation to the mutations in land use/land cover and climate changes during the last 50 years (Rădoane et al. 2013).

By processing a complex database acquired from various sources (measurements in hydrometric cross-section from the national network ensured by the *Romanian Waters Administration*, indirect estimations on the account of sediment stock from some reservoirs, personal measurements on small basins) two controls were selected as criteria for the analysis of the sediment yield across a broad territory such as Romania. The two criteria are the *lithological composition of the substrate* generating alluvium and the *size of drainage basins* which provide a selection of the volume of sediments transferred from the source area to the delivery area. This control is well shaped in the relations presented in Fig. 27.10 and which were determined based on measurements performed in 336 drainage basins from Romania.

Results confirm that, overall, the sediment yield is inversely proportional to the drainage basin area according to a general regression slope $b = -0.239$. However,

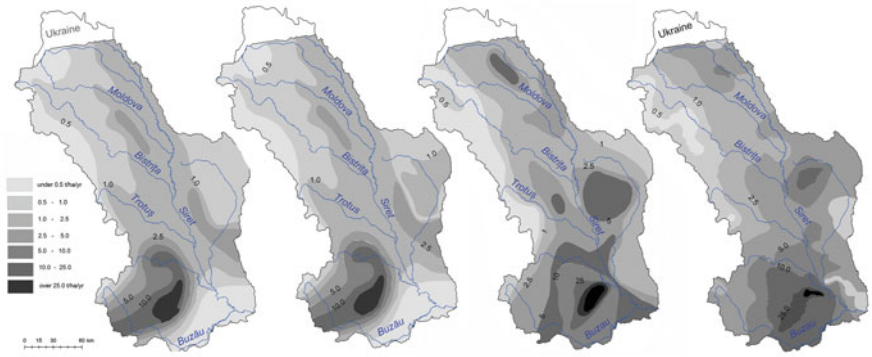

Fig. 27.9 Evolution of knowledge on the specific suspended sediment yield in Siret drainage basin

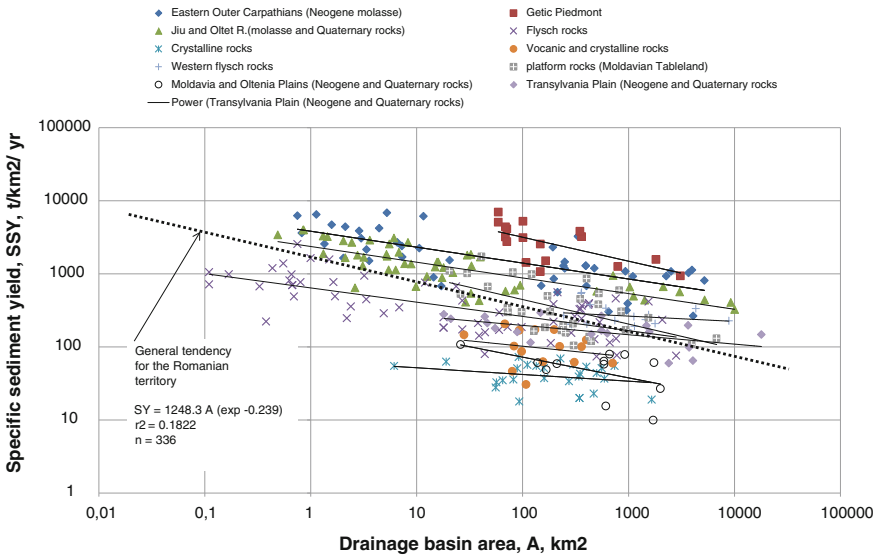

Fig. 27.10 Regional distribution of the specific sediment yield (estimated based on the transfer of suspended sediment by rivers by Rădoane and Rădoane 2005, updated)

against the background of this negative trend a multitude of particular situations arise whereby the lithological substrate exerts significant control. The variation slope of the sediment yield with the lowest decline (regression slope = −0.092) was documented in basins overlying crystalline and volcanic rocks where SY was below 100 t/km^2/year. Conversely, in the drainage basins overlying friable deposits in the Getic Piedmont where SY varies between 1000 and 10,000 t/km^2/year according to a steeper slope (b = −1.102) depending on the basin size. The basins located in the molasse and piedmont area of the Carpathian Curvature falls in the same category (see also Figs. 27.8 and 27.9).

Against the regional context analysed by Vanmaercke et al. (2011), the Romanian territory ranks among the continental and alpine areas with the Carpathian region, and the mediterranean and steppe area with the regions located on friable rocks with energetic potential.

Sediment Delivery Ratio (SDR)

The studies conducted thus far, particularly in eastern Romania (Moldavian Plateau, Moldavian Subcarpathians, and Eastern Carpathians) and the Getic Subcarpathians and Piedmont allow for an assessment of the sediment delivery ratio (i.e., the percentage of the total amount of alluvium from the source area evacuated from the drainage system) throughout the national territory. Several factors influence the

sediment delivery ratio, and their interactions are extremely complex (Walling 1983; Richards 2002). Therefore, an empirical method is used for a SDR regionalization.

One of the most well-established relationships is the one between the SDR and the catchment area as a power function (Fig. 27.11). The SDR may range from 0 to 1 or 0 to 100 %, but the correlation slope between the SDR and the catchment area differs according to the location of the catchment on the Globe. Its values may range from −0.01 to −0.7 (according to Walling 1983; Ferro and Minacapilli 1995; Lu et al. 2006).

We selected and synthesized a number of results obtained for the Romanian territory (Rădoane and Ichim 1987; Rădoane and Rădoane 2001; Dumitriu 2007) (Fig. 27.11). The diagram indicates that the SDR varies greatly even within areas smaller than the national territory: the variation in the slope (−0.232) is smaller for the Carpathian and Subcarpathian catchments (SDR1) and greater (−0.33) for the plateau and higher plain catchments (SDR2). This phenomenon is linked to the energetic potential and the sediment evacuation capacity. If the area is approximately 10 km^2, the correlation curves have very similar slope gradients; for example, as the catchment area increases, the rhythm of the variation changes noticeably. In the catchments in the plateau and higher plain areas, the SDR drops under 5 %. In the Carpathian and Subcarpathian areas, the evacuation of sediment in catchments over 2000 km^2 constantly ranges above 20 %.

The evacuation of sediment from a drainage system is dependent on the capacity of the outflow and the organization of the drainage network (Richards 2002). Our empirical approach included exploring the effects of the drainage network order (Strahler's system) (Rădoane and Ichim 1987). The slope-channel coupling phenomenon for sediment displacement and evacuation played an important role for the drainage network.

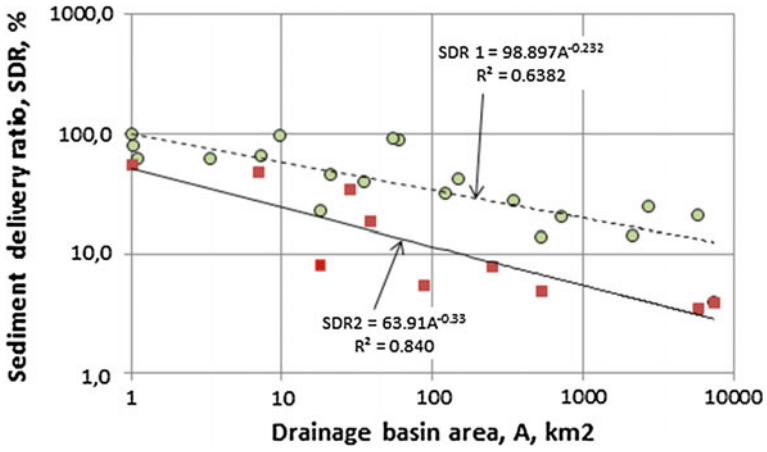

Fig. 27.11 The sediment delivery ratio curve as a function of the catchment size in the Carpathian and Sucarpathian area (SDR1) compared to the plateau and higher plain areas (SDR2) in Romania

By using a vastly enhanced database with new entries (Table 27.3), we re-computed the relationship between the SDR and the drainage network order in the same regional context across Romania. We can better understand the rank of our study area regarding sediment dynamics.

By plotting the data (Fig. 27.12), we were able to find subtle differences in the changes in the SDR throughout a given area. In drainage networks with an order (Strahler's system) below VII, the variability in the SDR is described by sinusoidal bends, either concave or flared. The shape of the SDR curves is strongly related to the landform hosting the catchment. Moreover, the catchments from the higher plains and plateaus rank among a very sinuous group of curves whose shape is generated by the rapid decline in the sediment load from 2nd to 3rd order elements of the drainage system. Conversely, all other catchments from the Subcarpathian and piedmont areas rank among the flared-type curves because the sediment load remains significant in higher order drainage networks. In the mountain area, the SDR curve is largely concave, with the inflexion point occurring in the lower order drainage network and the curve becoming asymptotic in higher order networks.

In the mountain catchments, the SDR curves have higher concavity in 1st, 2nd, 3rd, and 4th order networks, after which the variation slope ranges approximately 20 %. Although the transport capacity of the drainage network is high because of the relatively low amount of sediments, the balance is maintained between the sediment supply and evacuation.

The largest amount of sediment displaced by the drainage network occurs in the Subcarpathian and piedmont catchments (the connectivity to sediment sources is maximal); however, the evacuation of sediments is also high, reaching almost 50 % in the 6th and 7th order networks. The SDR curves are elongated and irregular, with large variations depending on the drainage network order.

The variability of the SDR curves shown in Fig. 27.12 is maximal in the case of the Jiu drainage network. We documented an extremely high sediment load resulting from the coal ore washing (Rădoane et al. 1995a, b), such that the delivery ratio reached 95 % regardless of the river order (Strahler's system). Under natural conditions, such an SDR curve is not achievable; however, anthropogenic interference (e.g., through mining activities) can also result in this outcome.

To conclude, we estimate that the VII and VIII order drainage network (Strahler's system) from Romania discharges into the Danube, sediments which may account for less than 1 % of the amount of alluvium yielded by the hillslopes and river beds from the investigated area. At Ceatal (before the Danube enters the deltaic sector), the river transfers on average an annual volume of 20.5 Mt of sediments (from 1985 to 2006). Between 1840 and 1970 the mean amount of alluvium carried by the Danube was 57.3 Mt/year (Bondar 2008). The difference is accounted for by the sediment storage in the river basin which represents over 37.5 %. The largest sediment storage occurs in reservoirs, and the value determined by us is very similar to the global value (36.6 %) estimated by Syvitski et al. (2005). One of the highly effective rivers in terms of sediment transfer is Siret River (see also Fig. 27.1 and Chap. 28, this volume) which evacuates annually $\sim$10 Mt

Table 27.3 The sediment delivery ratio (%) related to the drainage network order (Strahler's system) in several key areas in Romania

Region	Drainage network order (Strahler's system)							Source
	I	II	III	IV	V	VI	VII	
Catchments in the flysch mountains	100.0	65.2	42.2	33.2	26.1	20.0	–	Rădoane and Ichim(1987), Rădoane (2002), Dumitriu (2007)
Catchments in the Eastern Sucarpathians and Curvature Sucarpathians (Neogene molasses rocks)	–	100.0	80.9	61.6	45.6	30.0	25.0	Rădoane and Ichim(1987), Rădoane (2002), Dumitriu (2007)
Jijia river catchment (Moldavian Plateau)	100.0	49.5	34.6	19.0	12.0	5.5	3.5	Ioniță (2000), Rădoane and Rădoane (2001)
Bârlad river catchment (Moldavian Plateau)	100.0	52.0	31.1	17.0	8.0	4.9	4.0	Ioniță (2000), Rădoane and Rădoane (2001)
Olteț river catchment (Getic Subcarpathians and Piedmont)	100.0	82.0	66.0	34.0	30.0	23.0	18.6	Ichim et al. (1994b), Rădoane and Rădoane (2003)
Topolog river catchment (Getic Subcarpathians and Piedmont)	100.0	55.0	34.0	28.0	25.0	20.0		Rădoane and Rădoane (2007)
Jiu river catchment, effects of mining	100.0	99.0	97.0	96.5	96.0	95.5	95.0	Radoane et al. (1995a, b)
Small catchments on the right side hillslope of Olt river, downstream of Rm. Vâlcea (Getic Subcarpathians and Piedmont)	100.0	81.0	62.0	46.0	40.0			Rădoane et al. (1992)
Arges river catchment, upstream of Oiești reservoir (Getic Subcarpathians and Piedmont)	100.0	82.0	70.0	60.0	55.0	50.0	42.3	Ichim et al. (1994a)
Bonțu river catchment, upstream of Știucii Lake (Transylvanian Plain)	100.0	85.0	15.0	6.24				Rădoane et al. (2014)

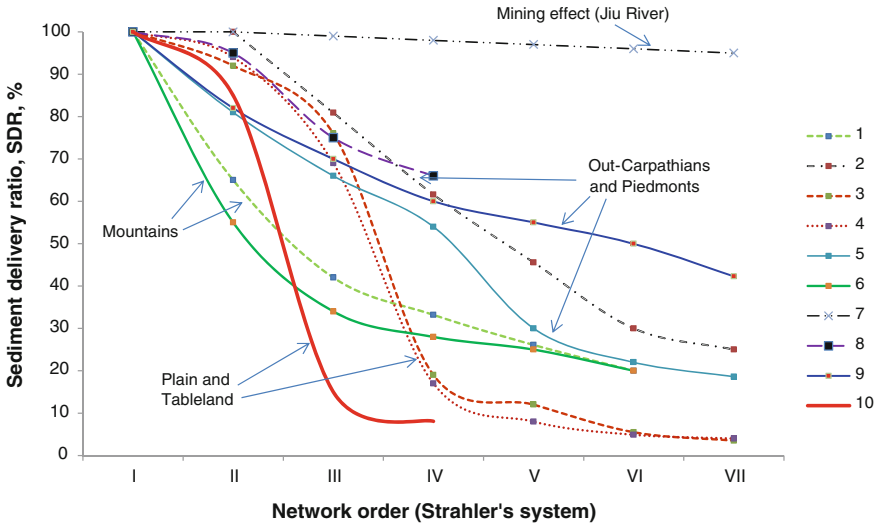

Fig. 27.12 Relationship between the sediment delivery ratio and the drainage network order (Strahler's system) in several Romanian regions: *1* Small catchments from the flysch mountain area; *2* Catchments from the Moldavian and Curvature Subcarpathians; *3* Jijia drainage basin (Moldavian Tableland); *4* Bârlad drainage basin (Moldavian Tableland); *5* Olteț drainage basin (piedmont area); *6* Topolog drainage basin; *7* Jiu drainage basin (mining effect); *8* Small catchments, Olt River left side (piedmont area); *9* Argeș River, upstream of Oiești Reservoir; *10* Bonțu drainage basin (upstream of Știucii Lake, Transylvania Plain)

of alluvium into the Danube, despite the fact that several reservoirs are functional in the upper Siret basin.

Conclusions

Sediment transfer from sources to delivery is a key topic of dynamic geomorphology. The rate at which this process occurs can change dramatically which is commonly a signal of major landform adjustments. The arable lands yield approx. 80 % of the total soil loss in Romania, slightly above the European mean value of 70 %. The mean calculated value of sheet and rill erosion in Europe is around 1.2 t/ha/year for the entire area and ~3.6 t/ha/year for arable land. In Romania the mean estimated value of sheet and rill erosion is ca. 4.2 t/ha/year.

Regarding the input of landslides to the total sediment yield at the scale of a broad territory this is not a facile task. The variation margin in the basins comprised in our study was large, ranging between 2 % (in basins located in the plateaus) and 60 % (for catchments from the Subcarpathians and the flysch mountains). Albeit, Moțoc (1984) suggested a mean percentage of 12 %, which is likely a realistic figure.

About the fluvial field, we can conclude that the average ratio of 33 % pertaining to river beds as sediment sources determined by our investigations is supported by the reality of Romanian rivers. Based on the assessment made by Moțoc (1984) the ratio of the two major domains (slopes and river beds) in terms of sediment source contribution was 90:10. Instead, our own evaluations indicate a more balanced ratio, i.e., 67:33. We believe the tendency of adjustment of the relationship between the two sediment source domains is factual and strongly dependent on the changes of controls during the past three decades.

The VII and VIII order drainage network (Strahler's system) from Romania discharges into the Danube sediments which may account for less than 1 % of the amount of alluvium yielded by the hillslopes and river beds from the investigated area. At Ceatal (before the Danube enters the deltaic sector), the river transfers on average an annual volume of 20.5 Mt of sediments (from 1985 to 2006). Between 1840 and 1970 the mean amount of alluvium carried by the Danube was 57.3 Mt/year. The difference is accounted for by the sediment storage in the river basin which represents over 37.5 %. The largest sediment storage occurs in reservoirs, and the value determined by us is very similar to the global value (36.6 %).

Acknowledgements This research is part of a project funded by the Fund for Scientific Research, Romania (research project PN-II-ID-PCE-2011-3-0057 and PN-II-RUTE-2017-4-0855).

References

Ailincăi C, Jităreanu G, Bucur D, Ailincăi D (2012) Eroziunea solului și măsuri de conservare în Podișul Moldovei. Cercetări Agronomice în Moldova 45(152):29–42 (in Romanian)

Ambăruș D (2007) Cercetări privind evoluția proceselor erozionale și a amenajărilor pentru atenuarea lor, funcție de dinamica categoriilor de folosință de pe terenurile în pantă. Ph. D thesis, University "Gh. Asachi", Iași (in Romanian)

Arghiriade C (1977) Rolul hidrologic al pădurii. Ceres Press, București (in Romanian)

Bălteanu D, Popovici EA (2010) Land use changes and land degradation in post-socialist Romania. Rev Roum Géogr 54(2):95–105

Bălteanu D, Teodorescu V (1985) Element for sediment budget of small catchment, the Getic Piedmont, Romania. Rev Roum Géol Géophys Géogr 29:73–78

Bălteanu D, Chendeș V, Sima M, Enciu P (2010) A country–wide spatial assessment of landslide susceptibility in Romania. Geomorphology 124:102–112

Belyaev VR, Wallbrink PJ, Golosov VN, Murray AS, Sidorchuk AY (2005) A comparison of methods for evaluating soil redistribution in the severely eroded Stavropol region, southern European Russia. Geomorphology 65:173–193

Bondar C (2008) Hydro morphological balance of the Danube river channel on the sector between Bazias (km 1072.2) and Danube Delta Inlet (km 80.5). Paper presented at the international expert conference on 'the safety of navigation and environmental security in a transboundary context in the Black Sea Basin', Odessa

Brierley GJ, Fryirs KA (2005) Geomorphology and river management: applications of the river style framework. Blackwell Publications, Oxford

Bucur D, Jităreanu G, Ailincăi C (2011) Soil erosion control on arable lands from north–east Romania. In: Godone D, Stanchi S (eds) Soil erosion issues in agriculture, pp 295–314

Cerdan O, Govers G, Le Bissonnais Y, Van Oost K, Poesen J, Saby N, Gobin A, Vacca A, Quinton J, Auerswald K, Klik A, Kwaad F, Raclot D, Ioniţă I, Rejman J, Rousseva S, Muxart T, Roxo MJ, Dostal T (2010) Rates and spatial variations of soil erosion in Europe: a study based on erosion plot data. Geomorphology 122:167–177

Diaconu C (1964) Rezultate noi în studiul scurgerii de aluviuni în suspensie a râurilor R.P.R. Studii de Hidrologie 11:81–223 (in Romanian)

Diaconu C (1971) Probleme ale scurgerii de aluviuni pe râurile României. Studii de Hidrologie 31:5–213 (in Romanian)

Dumitriu D (2007) Sistemul aluviunilor din bazinul râului Trotuş. Universităţii Suceava Press, Suceava (in Romanian)

Dumitriu D, Condorachi D, Miclăuş C, Niculiţă M (2010) Modele de evaluare a bugetului de aluviuni în relaţie cu impactul antropic dintr-un bazin hidrografic. Studiu de caz: bazinul râului Trotuş. Technical report PNCD II–Idei, 146/2007 (in Romanian)

Ferro V, Minacapilli M (1995) Sediment delivery processes at basin scale. Hydrol Sci J 40:703–717

Gaşpar R, Cristescu C (1987) Cercetări asupra scurgerii şi transportului de aluviuni în bazine hidrografice torenţiale mici parţial amenajate. ICAS, Bucureşti (in Romanian)

Gaşpar R, Untaru E (1979) Contribuţii la studiul transportului de aluviuni a bazinelor torenţiale parţial împădurite. ASAS Informative Bull 8:22–30 (in Romanian)

Gaşpar R, Untaru R, Roman F, Cristescu C (1982) Cercetări hidrologice în bazine hidrografice torenţiale mici. ICAS, Bucureşti (in Romanian)

Grimshaw DL, Lewin J (1980) Source identification for suspended sediment. J Hydrol 47:151–162

Harvey AM (2001) Coupling between hillslopes and channels in upland fluvial systems: implications for landscape sensitivity, illustrated from the Howgill Fells, northwest England. Catena 42:225–250

Ichim I (1986) Sistemul aluviunilor. In: Ichim I, Rădoane M, Rădoane N (eds) Lucrările Simpozionului "Proveniența și efluența aluviunilor", Piatra Neamt I, pp 1–31 (in Romanian)

Ichim I (1988) Semnificaţia mărimii suprafeţei bazinului hidrografic în dinamica proceselor fluviale. Hidrotehnica 33:17–28 (in Romanian)

Ichim I (1992) Probleme ale cunoaşterii sistemului aluvionar din Romania. Lucrările celui de-al IV lea Simpozion "Proveniența și efluența aluviunilor", Piatra Neamţ, pp 1–7 (in Romanian)

Ichim I, Rădoane M (1984) Cercetări privind sursele de aluviuni şi energia potenţială de eroziune cu exemplificări din regiunea Vrancei. Hidrotehnica 29:183–187 (in Romanian)

Ichim I, Rădoane M (1987) A multivariate statistical analysis sediment yield and prediction in Romania. Catena Suplements 10:137–146

Ichim I, Rădoane M, Rădoane N, Surdeanu V (1990) Proveniența și efluența aluviunilor râului Buzău. Abordare geomorfologică. In: Ichim I, Rădoane M, Rădoane N (eds) Lucrările Simpozionului "Proveniența și efluența aluviunilor", Piatra Neamt III, pp 71–93 (in Romanian)

Ichim I, Rădoane M, Rădoane N, Catană C (1994a) Sediment balance in the Argeş drainage basin (Vidraru Dam–Oeşti Reservoir). Rev Roum G.G.G. 38:105–110

Ichim I, Rădoane M, Rădoane N, Grasu C, Cochior C (1994b) Bugetul de aluviuni al bazinului râului Olteţ. In: Lucrările Sesiunii Ştiinţifice Anuale, Institutul de Geografie, Bucureşti, pp 139–144

Ichim I, Rădoane M, Rădoane N, Grasu C, Miclăuş C (1998) Dinamica sedimentelor. Aplicaţie la râul Putna-Vrancea, Tehnică, Bucureşti (in Romanian)

Ioniţă I (2000) Formarea și evoluția ravenelor din Podișul Bârladului. Carson Press, Iași (in Romanian)

Ioniţă I (2011) The human impact on soil erosion and gulling in the Moldavian Plateau, Romania. Land Anal 7:71–73

Ioniţă I (1999) Studiul geomorfologic al degradărilor de teren din bazinul mijlociu al văii Bârladului. Ph.D thesis, University "Al. I. Cuza", Iaşi (in Romanian)

Ioniţă I, Rădoane M, Mircea S (2006) Soil erosion in Romania. In: Boardman J, Poesen J (eds) Soil erosion in Europe. Willey, England, pp 155–167

Jurchescu M (2014) Analysing connectivity through landslide-channel geomorphic coupling in a large drainage system of Southern Romania. Paper presented at the EGU General Assembly, 27 April–2 May, Vienna

Lu H, Moran CJ, Prosser IP, Raupach MR, Olley J, Petheram C (2003) Hillslope erosion and sediment delivery: a basin wide estimation. Technical report 15/03. CSIRO Land and Water, Canberra

Lu H, Moran CJ, Prosser IP (2006) Modelling sediment delivery ratio over the Murray Darling basin. Environ Model Softw 21:1297–1308

McCabe M, Fuller IC, McColl ST (2013) Shallow landsliding and catchment connectivity within the Houpoto Forest, New Zealand. GeoScience: a working paper series in physical geography. School of People, Environment and Planning. Massey University, Auckland

Mihai Gh, Taloescu I, Neguț N (1979) Influența lucrărilor transversale asupra evoluției ravenelor formate pe alternanțe de orizonturi permeabile și impermeabile. Buletinul ASAS 8:17–28 (in Romanian)

Mociorniță C, Birtu E (1987) Câteva aspecte ale transportului de aluviuni în România. Hidrotehnica 32(7):241–245 (in Romanian)

Moțoc M (1984) Participarea proceselor de eroziune și a folosințelor terenului la diferențierea transportului de aluviuni în suspensie pe râurile din România. Buletinul ASAS 13:25–33 (in Romanian)

Moțoc M (1982) Ritmul mediu de degradare erozionala a solului din Romania. Buletinul ASAS 11:47–65 (in Romanian)

Moțoc M, Ioniță I, Nistor D, Vătău A (1992) Soil erosion control in Romania. The Bulletin of Regional Environmental Centre, Budapest

Moțoc M, Stănescu P, Taloiescu I (1979) Metode de estimare a eroziunii totale și a eroziunii efluente pe bazine hidrografice mici. Buletinul ASAS 8:20–30 (in Romanian)

Obreja F (2013) Studiul transportului de aluviuni în bazinul hidrografic Siret. Ph.D. thesis, University of Suceava, Suceava (in Romanian)

Peart MR, Ng KY, Zhang DD (2005) Landslides and sediment delivery to a drainage system: some observations from Hong Kong. J Asian Earth Sci 25:821–836

Poesen J, Nachtergale J, Vertstraeten G, Valentin C (2003) Gully erosion and environmental change. Importance and research needs. Catena 50:91–134

Popa N, Nistor D, Filiche E, Petrovici G (2013). Studies on runoff and erosion rates in Eastern Romania. In: Proceedings of the 1st CIGR inter–regional conference on land and water challenges, Bari

Prosser IP, Rustomji P, Young B, Moran C, Hughes A (2001) Constructing river basin sediment budgets for the national land and water resources audit, 15(01). CSIRO land and water technical report, Canberra, p 34

Pujină L (1998) Cercetări privind efluența aluvionară de pe terenurile agricole afectate de procese complexe de alunecare din podișul Bârladului și valorificarea economică superioară a acestora. Ph.D thesis, University "Gh. Asachi", Iași (in Romanian)

Rădoane N (1980) Contribuții la cunoașterea unor procese torențiale din bazinul râului Pângărați în perioada 1976–1979. Stud Cercet G.G.G. 27:53–63 (in Romanian)

Rădoane N (1986) Efectul antropic în provenienta și efluența aluviunilor din bazine hidrografice mici. In: Ichim I, Rădoane M, Rădoane N (eds) Lucrările Simpozionului "Proveniența și efluența aluviunilor", Piatra Neamț I, pp 189–205 (in Romanian)

Rădoane N (2002) Geomorfologia bazinelor hidrografice mici. Universitătii Suceava Press, Suceava (in Romanian)

Rădoane M (2004) Dinamica reliefului în zona lacului Izvorul Muntelui. Universitătii Suceava Press, Suceava (in Romanian)

Rădoane M, Ichim I (1987) Probleme ale scurgerii aluviunilor pe râurile din România. Hidrotehnica 32:44–49 (in Romanian)

Rădoane M, Rădoane N (2001) Eroziunea terenurilor și transportul de aluviuni în sistemele hidrografice Jijia și Bârlad. Revista de Geomorfologie 3:73–86 (in Romanian)

Rădoane N, Rădoane M (2003) Cercetări geomorfologice pentru evaluarea rolului albiei râului Olteţ ca sursă de aluviuni. Anal. Univ. "Ştefan cel Mare" 10:27–35 (in Romanian)
Rădoane M, Rădoane N (2005) Dams, sediment sources and reservoir silting in Romania. Geomorphology 71:112–125
Rădoane M, Rădoane N (2007) Geomorfologie aplicată. Universităţii Suceava Press, Suceava (in Romanian)
Rădoane M, Ichim I, Rădoane N, Miclăuş C, Grasu C (1992) Bugetul de aluviuni în bazine hidrografice mici din Valea Oltului. In: Ichim I, Rădoane M, Rădoane N (eds) Lucrările Simpozionului "Proveniența și efluența aluviunilor", Piatra Neamț IV (supl.), pp 189–205 (in Romanian)
Rădoane M, Ichim I, Rădoane N (1995a) Gully distribution and development in Moldavia, Romania. Catena 24:127–146
Rădoane N, Rădoane M, Ichim I, Miclăuş C (1995b) Influenţele mineritului asupra tranzitului de aluviuni pe râul Jiu, amonte de Sadu. Studii și cercetări G.G.G. 42:63–72 (in Romanian)
Rădoane N, Rădoane M, Ichim I, Grasu C, Miclăuş C (1997) Sursele de aluviuni și transportul aluvionar în Bazinul hidrografic Bâsca Chiojdului. Anal Univ "Ştefan cel Mare" 6:33–44 (in Romanian)
Rădoane M, Rădoane N, Ichim I, Surdeanu V (1999) Ravenele. Forme, procese, evoluţie. Presa Universitară, Cluj–Napoca (in Romanian)
Rădoane M, Pandi G, Rădoane N (2010) Contemporary bed elevation changes from the Eastern Carpathians. Carpathian J Earth Environ Sci 5:49–60
Rădoane M, Obreja F, Cristea I, Mihăilă D (2013) Changes in the channel–bed level of the Eastern Carpathian rivers: climatic vs. human control over the last 50 years. Geomorphology 193:91–111
Rădoane N, Zamoşteanu A, Rădoane M (2014) Sediment budget of the Ştiucii Lake catchment (Transylvania Plain). Carpathian J Earth Environ Sci 9(4):31–46
Richards K (2002) Drainage basin structure, sediment delivery and the response to environmental change. In: Jones SJ, Frostick LE (eds) Sediment flux to basins: causes, controls and consequences. The Geological Society of London, Special Publication 5(191):149–160
Sevastel M (2012) Some aspects concerning evaluation of the alluvia sources from agricultural watersheds. Anal Univ Oradea, Protecţia Mediului 19:878–885
Surdeanu V (1986) Alunecările de teren ca surse de aluviuni. In: Ichim I, Rădoane M, Rădoane N (eds) Lucrările Simpozionului "Proveniența și efluența aluviunilor", Piatra Neamt I, pp 229–237
Surdeanu V, Rădoane N, Catana C (1988) Alunecarea de teren de la Taşbuga (Carpaţii Orientali). Lucrările Staţiunii "Stejarul" Piatra Neamţ, 9:39–52 (in Romanian)
Syvitski JPM, Vörösmarty CV, Kettner AJ, Green P (2005) Impact of humans on the flux of terrestrial sediment to the global coastal ocean. Science 308:376–380
Vanacker V, Von Blanckenburg F, Govers G, Molina A, Poesen J, Deckers J, Kubik P (2007) Restoring dense vegetation can slow mountain erosion to near natural benchmark levels. Geology 35:303–306
Vanmaercke M, Poesen J, Verstraeten G, de Vente J, Ocakoglu F (2011) Sediment yield in Europe: spatial patterns and scale dependency. Geomorphology 130:142–161
Verheijen FGA, Jones RJA, Rickson RJ, Smith CJ (2009) Tolerable versus actual soil erosion rates in Europe. Earth Sci Rev 94:23–38
Walling DE (1983) The sediment delivery problem. J Hydrol 65:209–237
Wilkinson BH, McElroy BJ (2007) The impact of humans on continental erosion and sedimentation. Geol Soc Am Bull 119:140–156
Wilkinson S, Henderson A, Chen Y (2004) SedNet user guide. Client report for the cooperative research centre for catchment hydrology. CSIRO Land and Water, Canberra

Chapter 28
River Channel Sediments

Maria Rădoane, Nicolae Rădoane, Dan Dumitriu and Crina Miclăuș

Abstract In this section, we will discuss the spatial pattern of bed material distribution along the river network as the link between sediment sources and sediment delivery. The variety of controls (i.e., drainage basin size and features, sediment source distribution and effectiveness, longitudinal profile shape, major anthropogenic interventions, etc.) will be related to the characteristics of riverbed deposits. In this context of sediment dynamics along the two rivers, we propose a spatial analysis of channel material grain size and grain size distribution form, by addressing downstream fining and downstream coarsening, as well as riverbed material distribution bimodality, form variability and grain petrography of fluvial sediments. Finally, sediment budgets are discussed for two major rivers representative for Romania (Siret and Prut) which highlight the role of sediment sources and human impact.

Keywords Channel deposits · Grain sizes · Bimodality · Gravel morphometry · Gravel petrography · River sediment budget

Introduction

The interest in riverbed deposits has steadily augmented as rivers were subjected to an increasing degree of anthropogenic intervention (particularly by dam and reservoir construction) which interfered with the natural flow of sediments along

M. Rădoane (✉) · N. Rădoane
Ștefan cel Mare University, Universității 13, 720229 Suceava, Romania
e-mail: radoane@usm.ro; mariaradoane@gmail.com

N. Rădoane
e-mail: nicolrad@yahoo.com

D. Dumitriu · C. Miclăuș
Alexandu Ioan Cuza University, Carol I Av 11, 700506 Iași, Romania
e-mail: dnddumitriu@yahoo.com

C. Miclăuș
e-mail: crina_miclaus@yahoo.co.uk

M. Rădoane and A. Vespremeanu-Stroe (eds.), *Landform Dynamics and Evolution in Romania*, Springer Geography,
DOI 10.1007/978-3-319-32589-7_28

river channels, aside from covering a large part of the alluvial material. Prior to 1990, the construction materials industry required annually large amounts of sands and sorted gravel, up to nearly 80 million m^3 (Călinoiu et al. 1988). Further on, after a brief period of decline, the required amount of gravel increased again, and also the pressure exerted on river channels and floodplain land. The quality requirements and restrictions imposed for Quaternary sand and gravel mining result in a confinement of the mining area almost exclusively to the middle and lower sectors of major river channels. For example, in Siret drainage basin 230 gravel pits yield approximately 2 million m^3 of gravel and sand, thus contributing to a large degree to the transformation of river channels. It is in this context that research interests in fluvial sediments have developed (Ichim and Rădoane 1990; Ichim et al. 1998; Dumitriu 2007; Rădoane et al. 2008), and the results will be highlighted in this chapter.

In addition to the practical and economical aspects of channel deposits, a large amount of data on this topic was yielded by scientific approaches of a more theoretical nature (including downstream fining, competition between abrasion and hydraulic sorting of riverbed material, bimodality of bed deposits, sediment particle shape and petrography and long profile distribution etc.). In a remarkable study on the evolution of ideas in this field, Gomez et al. (2001) showed that Leonardo da Vinci produced the first comment on the progressive reduction in the size of fluvial sediments (i.e., downstream fining) in *Codex Hammer* (1504–1506). The study also includes the first comments on the causes of the processes of reduction of bed material size, mainly by particle abrasion and hydraulic sorting. The phenomena has been widely investigated considering the numerous complications involved in this mechanism, such as the equal mobility condition (Parker et al. 1982; Wilcock 1992; Gasparini et al. 2004), the role of the local base level (Ferguson et al. 1996) or the riverbed aggradation (Seal et al. 1997; Gomez et al. 2001), river basin concavity (Gasparini et al. 2004), lateral input of sediments (Knighton 1980, 1982, 1999; Ichim and Rădoane 1990; Rice and Church 1998; Rice 1999) and human interventions (Surian 2002).

Based on the experience provided by a plethora of highly refined studies on particle size variability along a single river or river reach (Brierley and Hickin 1985; Parker 1991; Werrity 1992; Paola and Seal 1995; Ferguson et al. 1996; Rice and Church 1998 and many others), we envisaged a spatial approach of riverbed material variability along several rivers pertaining to large fluvial systems ($A > 40{,}000$ km^2). However, achieving this objective has not been an easy task, as volumetric sampling in gravel-bed channels proved to be somewhat of a challenge for those who venture into the study of this phenomenon (for instance, in the upper sectors of investigated Carpathian rivers the weight of samples sieved in situ exceeded 1000 kg, which entailed significant effort for the research team). Nonetheless, these efforts were justified by the amount of data yielded by riverbed deposits on the drainage basin and sediment sources, the effectiveness of transport processes, the hydraulic parameters adjustment mechanisms, etc. In short, "rivers are gutters down which flow the ruins of continents" (Leopold et al. 1964, p. 97).

To sum up, in this chapter we will discuss the spatial pattern of bed material distribution along the 2000 km—long river network comprising of Siret and Prut drainage basins as the link between sediment sources and sediment delivery. The variety of controls (i.e., drainage basin size and features, sediment source distribution and effectiveness, longitudinal profile shape, major anthropogenic interventions etc.) will be related to the characteristics of riverbed deposits.

East-Carpathian Rivers' Sediment Sources and Transfer Rates

The gravels forming Carpathian riverbeds originate in areas with different lithologies within the drainage basins. The distribution of lithological units in the two major drainage basins (i.e., Siret and Prut) indicates the varying layout of source rock units. In the case of Siret River the general geological arrangement is composed of an array of north-oriented strips unfolding eastward; these strips pertain to the Neogene volcanic and sedimentary-volcanic regions of the Eastern Carpathians (the NW extremity), the Mesozoic crystalline and Cretaceous–Paleogene flysch regions (the middle sector), and the Neogene molasse and the Moldavian Platform in the eastern halves of both basins. As regards Prut River, albeit a Carpathian river, the friable rocks pertaining to the Moldavian Platform account for 86 % of its drainage basin. The coarser riverbed material identified by our measurements up to the confluence with Stânca–Costeşti Reservoir originates in the crystalline (1.05 % of the entire basin area) and flysch domains (amounting to 12.72 % of the drainage basin).

In time, (from the Sarmatian to present-day, see also Chap. 18, this volume) the Carpathian tributaries were the agents through which large amounts of material were transferred and deposited along the border of the Carpathian area in the shape of an ample piedmont, known as the Moldavian Piedmont (Martiniuc 1948). Subsequent tectonic movements and the formation of the Subcarpathians strongly interfered with the piedmont as a landform; however, it did not disturb its geological composition. The remains of the piedmont dispersed on top of interfluves, which are visible in the shape of numerous outcrops, allowed for an accurate reconstruction of its extent, genesis and relation to source rivers. Although destroyed by tectonics and erosion and further incorporated into other landforms, the activity of geomorphic processes, and particularly of fluvial processes, demonstrates that the Moldavian Piedmont is in fact functional, has been and is still being constructed, at least during the Holocene stage of our reference timeframe (Ichim and Rădoane 1990; Rădoane et al. 2008).

The suspended sediment load (Fig. 28.1) determined based on direct measurements at gauging stations from Siret and Prut drainage basins demonstrates the manner in which these fine materials are distributed along rivers. Albeit, we have no direct gauging data on the coarse sediment transfer, the estimates based on calculus

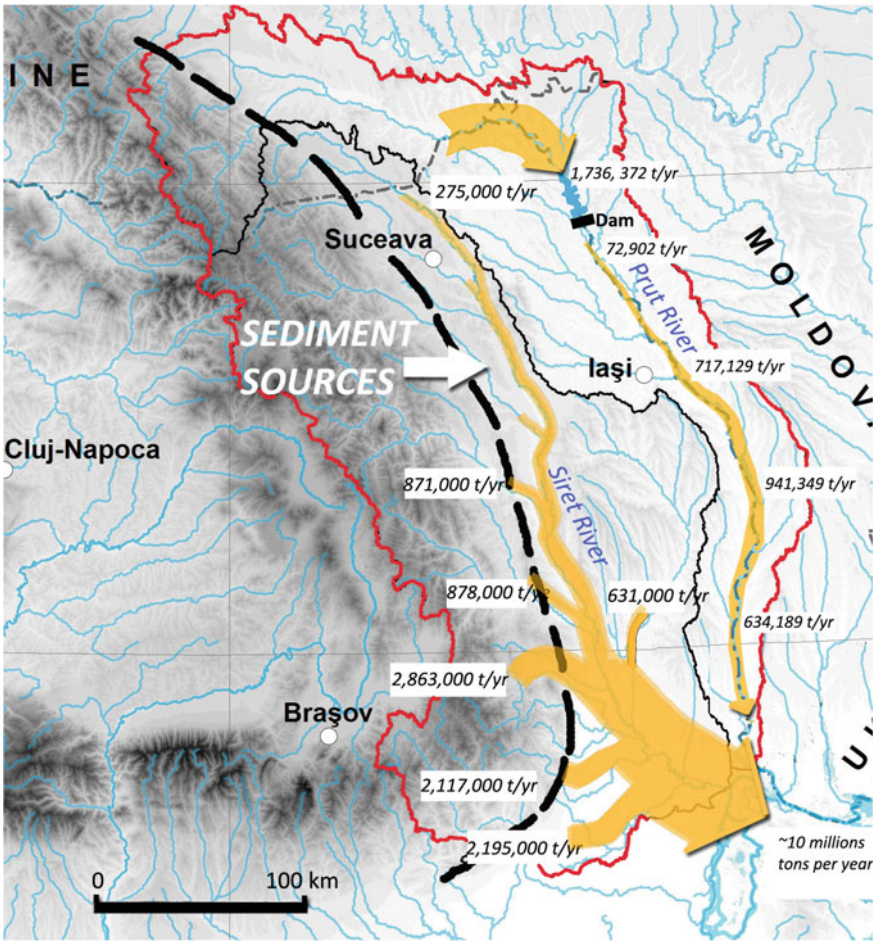

Fig. 28.1 Suspended sediment loads along Siret and Prut Rivers

equations (Diaconu and Şerban 1994) indicate that this parameter ranged from under 10 % to over 35 % of the total suspended sediment load.

The source of suspended sediments is mainly soil erosion within the catchment; once the eroded material reaches the channel, it exerts a significant degree of control on the grain size distribution of bed material. On Siret River the contribution of lateral tributaries increases southward as their sediment yields augment (the last right-side tributaries, Putna, Râmnicu Sărat, and Buzău, each unload in Siret River over 2 million tons of fine sediment per year). On Prut River, Stânca–Costeşti reservoir retains completely the coarse sediment load, and over 94 % of the suspended load. In the absence of lateral tributaries which could make major sediment contributions, restoring the suspended sediment stock occurs almost exclusively from its own channel.

In this context of sediment dynamics along the two rivers, we propose a spatial analysis of *channel material grain size* and *grain size distribution form*, by addressing downstream fining and downstream coarsening, as well as riverbed material distribution bimodality, form variability and grain petrography of fluvial sediments.

Granulometric Spectrum of Rivers from Siret and Prut Drainage Basins

Our investigations on riverbed material variability in rivers from Siret and Prut drainage basins intended primarily to verify the exponential model of size reduction along the river according to the so-called "Sternberg law" which states that bed sediment grain size decreases in proportion to the work performed against friction along the river. Figure 28.2 illustrates this variation for several large rivers in Siret drainage basin, and Prut basin, separately. Their lengths range from 150 to 950 km. According to this parameter, the median diameter, D_{50}, decreases exponentially overall; however, in certain river reaches the exponential decrease is disrupted, to

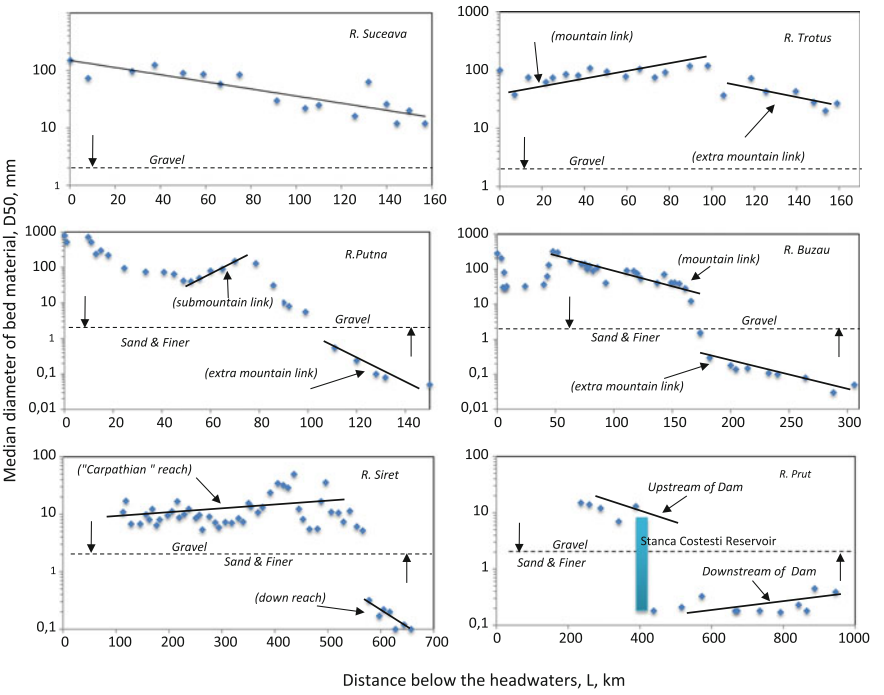

Fig. 28.2 Variation of median diameter of riverbed material in several rivers pertaining to Siret and Prut drainage basins (Rădoane et al. 2008, modified and completed). Discussion in text

such an extent that on Trotuș and Siret Rivers the sediment grain size increases along most of their lengths. The situation is different in the case of Prut River whereby the channel material variation is interrupted by Stânca–Costești Reservoir, upstream of which the decrease in grain size is exponential, whereas downstream the sediments tend to become coarser along the river. In Table 28.1 are highlighted the river reaches where either the exponential decrease or increase in riverbed sediment grain size occurs, as well as the model determination coefficient and the "fining" and "coarsening" coefficients of bed material. The only rivers closely fitting the exponential model throughout their entire lengths are Suceava and Moldova.

The main reason why the Sternberg model was not validated in the other rivers lies in the contribution of tributaries providing massive inputs of coarse alluvia to

Table 28.1 Fining and coarsening coefficients for riverbed deposits of rivers pertaining to Siret and Prut drainage basins

River	Length of sedimentary link (km)	Determination coefficient of the exponential equations $D_{50} = f(L)$ (R^2)	Fining coefficient	Coarsening coefficient
Suceava	157	0.753	−0.0143	
Moldova	202	0.739	−0.0102	
Trotuș (total)	159	0.349	−0.0061	
Trotuș (mountain area)	98	0.480		0.0056
Trotuș (Sub- and extra-Carpathian)	61	0.590	−0.0147	
Putna (total)	150	0.793	−0.0565	
Putna (mountain area)	99	0.736	−0.0381	
Putna (Subcarpathian)	27			0.0371
Putna (extra-Carpathian)	51	0.882	−0.0615	
Buzău (total)	306	0.908	−0.0288	
Buzău (mountain area)	166	0.800	−0.0185	
Buzău (extra-Carpathian)	140	0.887	−0.0155	
Siret «Carpathian»	566	0.028		0.0007
Siret extra-Carpathian	159	0.778	−0.0141	
Prut (upstream of reservoir)	400	0.814	−0.0058	
Prut (downstream of reservoir)	550	0.472		0.0015

the respective rivers, which far exceeded their processing capacities. Rivers from the northern sector of the study area, i.e., Suceava, Moldova, and upper Prut, have basins whereby suspended sediment yields are lower compared to the southern sector; thereby their tributaries carry smaller fine sediment loads. Thus, collectors achieve an exponential decrease of riverbed material with close fining coefficient values, particularly in the case of Suceava and Moldova (-0.0143 km^{1} and -0.0102 km^{-1}, respectively).

Conversely, on rivers from the southern sector of the study area (Trotuş, Putna, Buzău), whereby the drainage basins overlie regions with high sediment yields, the size variability of bed material increases. The mountain reach of Trotuş River is a representative case for high aggressiveness of tributaries in relation to the collector, which results in increasing bed material grain size along over 100 km of the river length. The same occurs on a shorter reach of Putna River, as well as on Buzău River in the gorge sector. However, the case which elicited a plethora of citations in the literature is no other than Siret River, where the phenomenon of riverbed sediment grain size increase (thus reversing the classic negative exponential model) was documented along 566 km, i.e., 80 % of the river length, albeit Siret does not cross a similarly long mountain area. Moreover, it was the highly vigorous geomorphic activity of its Carpathian affluents which led to such a performance.

The leap in sediment grain size mentioned previously and illustrated in Fig. 28.2 occur from 341 to 438 km on Prut River. This 81 km-long sector also includes Stânca–Costeşti reservoir (44 km long). The grain size leap from gravel to sands due to the low supply of particles ranging from 2 to 8 mm in diameter is a common trait documented along rivers; however, the explanation for this phenomenon remains a highly debated problem. In this particular instance, the natural leap in grain size is "hidden" by Stânca–Costeşti Reservoir and the remaining 37 km downstream of the reservoir due to the occurrence of the "hydraulic pavement" phenomenon. The particle size analysis of riverbed material revealed that 37 km downstream of the dam the bed is composed of fine sands, below 0.2 mm in terms of median diameter, maintaining the same size characteristics (or even lower) until 865 km from the headwater.

The exponential model applied to the D_{50} variation along the channel sector between 438 km and the junction with the Danube (946 km) shows a slight increase tendency. This phenomenon was also documented in other sand bed rivers, such as Bârlad, where the bed sediment grain size increases accordingly along the 220 km-long river channel (Rădoane and Rădoane 2006). This is related to the effectiveness of sorting sandy sediments during transport, whereby finer particles are removed whereas the coarser grains are relented into the bed. The hydrodynamic environment is also accurately outlined by the Trask sorting coefficient (*So*) of riverbed material, indicating that as the coefficient value is closer to 1, the particle size is more uniform and thus the hydrodynamic environment more active. The most effective sorting of bed material along Prut River was documented between 404 and 657 km; along the narrowest sector of the drainage basin (734–842 km), the coefficient value is as high as 1.05.

In the latter area, the sediment input from the basin through lateral tributaries is negligible, such that the river processes and sorts almost exclusively the bed material originating upstream or remobilized from its own bed. Near the junction with the Danube the sorting decreases, in our opinion, due to the significant influx of sediments carried by tributaries from Fălciului Hills, whereby the geology comprises of the Bălăbăneşti–Tuluceşti layers, of fluvial–lacustrine origin (Sficlea 1980).

Field observations and numerical simulations of downstream fining (Parker 1991; Hoey and Ferguson 1994) revealed that a sharp concavity in the longitudinal profile can drive a faster reduction of riverbed material, which was confirmed in our case (Chap. 18, this volume). The shift from the coarsening sector to the fining sector occurs through a «granulometric leap» or threshold, ranging from 7 km on Trotuş River, to 10 km on Siret, 22 km on Buzău and 30 km on Putna. As regards Prut River, we have already shown that in this particular case the leap coincides with Stânca–Costeşti Reservoir. The distance over which this leap occurs is very short, as reported in the literature (Ashworth and Ferguson 1989; Sambrook Smith and Ferguson 1995; Ferguson et al. 1996), and scientists have shown great interest in attempting to explain it (Yatsu 1955; Ibbeken 1983; Sambrook Smith and Ferguson 1995; Sambrook Smith 1996; Rice 1998; Constantine et al. 2003; Gasparini et al. 2004). Recent research and lab experiments (Venditti et al. 2010) demonstrated that gravel-sand transition is steep because gravels tend to form a front which has a counterpart in the terrain morphology. In the cases illustrated in this study the gravel fronts on Siret, Putna and Buzău Rivers correspond to the morphological contact between the Lower Siret Plain and Lower Piedmont Plain. As the slope gradient decreases abruptly in the morphological contact area, it is likely that gravel-sand transition is strongly controlled by sorting processes (according to the aforementioned authors). With the reduction of the shear stress, coarser particles are deposited whereas finer ones are transported selectively. Resuming on older statement of Ferguson (2003), as sand makes up a greater portion of the bed surface, transport rates of both sand, and to a lesser extent gravel, increase. This increases the downstream sand supply relative to gravel. The shift occurs where a critical sand coverage on the gravel bed occurs. So where there is a strong downstream gradient in the sand coverage, the transition will be abrupt" (Venditti et al. 2010, p. 8). Consequently, the content of riverbed deposits in the gravel-sand transition area is highly bimodal, which we will tackle in the next section of this chapter.

Spatial Pattern of Riverbed Deposit Bimodality

Riverbed deposits of gravel bed rivers have a particular feature which distinguishes them from other types of deposits, namely bimodality, which is defined by the existence of two modes (peaks) in the grain size distribution, separated by a shortage in the small gravel category (i.e., the 1–8 mm). There is still ample debate over this phenomenon, summarized by Sambrook Smith and Ferguson (1995),

Sambrook Smith (1996), Venditti et al. (2010), which led us to the conclusion that no agreement has been reached on a single universally accepted explanation regarding the phenomenon in its entirety. The authors list three possible causes, supported by relevant studies: (i) the effect of base level (which appears to have the highest likelihood of being met in a consistent and variable number of rivers), (ii) the lateral input of fine alluvia (which requires major sediment sources), and (iii) the attrition/abrasion of riverbed material (effective particularly in large rivers).

Our research (Rădoane et al. 2008) pointed out that the lateral influx of fine sediments (listed second among the causes cited above) is the main explanation for the bimodality of grain size distributions on gravel-bed rivers pertaining to Siret drainage basin. In our view, solving this problem meant finding an answer to a number of questions, such as: What is the necessary amount of sand in riverbed sediment that is needed for bimodality to appear? What is the source of the sand in the second mode? Does it originate mostly from the riverbed sediments by abrasion of larger particles or is it from the hillside basin (by soil erosion and transportation)? Why is it that we could not identify a modal class of the coarse sand type or small gravel type (0.5–8 mm) in any of the samples? Is it indeed a lack of material or is it more likely a unimodal grain size distribution which overlaps with another unimodal grain size distribution whose source is foreign to the proper river channel?

A comprehensive database comprising nearly 200 sampling points along the main east-Carpathian rivers was a very useful tool in finding answers to those questions (Fig. 28.3a, b). In case Prut river, Stanca Costesti Dam has separated the two types of grain size distribution of bed material (Fig. 28.3c, d). Most probably the dam was located in the area of "the granulometric jump" between gravel to sands.

Thus, we were interested in obtaining a series of general or particular conclusions for either whole river lengths or certain river segments, and learning of any differences that may appear between the Carpathian tributaries or the tributaries and the main river, the Siret, which is strongly controlled by its Carpathian tributaries. Table 28.2 provides a synthesis of our observations of the grain size distributions. Wilcock (1993) found a threshold value of $B = 1.7$ for the bimodality index, which separates a modal sediment ($B \leq 1.7$) from another modal sediment ($B \geq 1.7$). In our study, we found a threshold value of $B = 2.0$, which is very close to the one determined by Wilcock.

In brief, the results yielded by our analysis can be summarized as follows:

(i) Bimodality is best distinguished for the Siret's riverbed material, where the 4 mm (−2 *phi*) to 0.5 mm (1 *phi*) fraction is less than 4 % of the global sample. In this case, the sand fraction is 26.9 % on average (but there are sampling points where the sand fraction can be up to 45–55 %). Carpathian rivers affluent to the Siret River feature a less pronounced bimodality, which is spread over a larger spectrum of diameters. Actually, the sand fraction percentage in the global samples is 10 % on average for northern rivers and up to 20 % for the southern rivers in the studied area. For the northern rivers, the difference between the sand fractions and the fraction class separating the modes is very small (which implies a less evident bimodality), whereas for

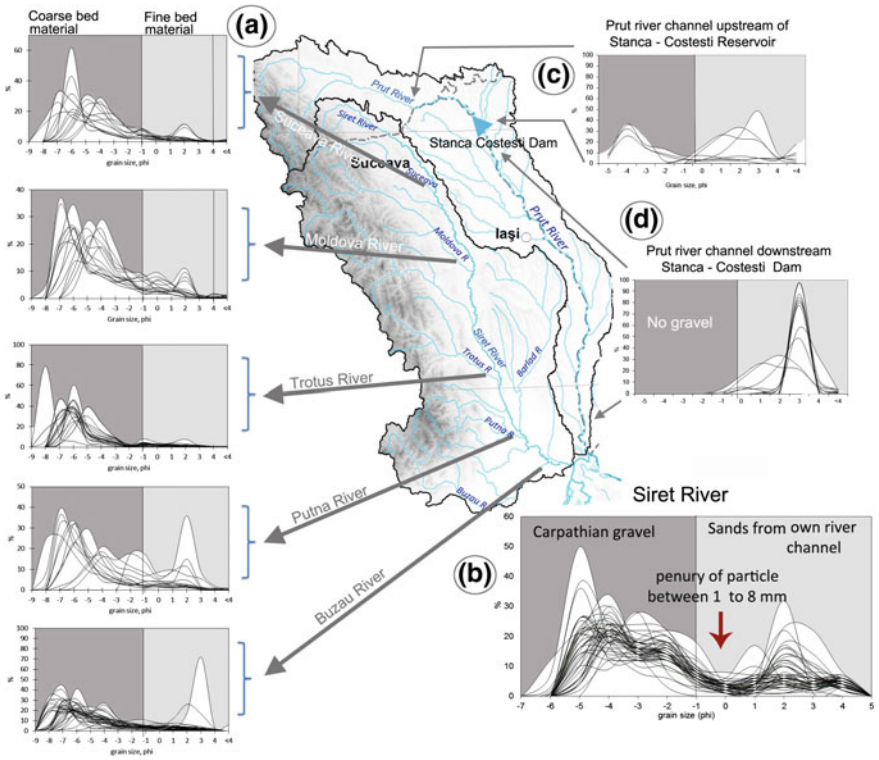

Fig. 28.3 Spatial pattern of the channel deposit distribution: **a** Histograms representing the grain size distributions for the global samples taken at certain points along the rivers. Competition between coarse bed material to fine bed material is shown. **b** Histograms of the grain size distributions of bed material along the Siret River. Penury of the particles in interval 1–8 mm determines bimodality of med material. Source of bed material is indicated. **c** Bed material bimodality of the Prut River upstream Stânca–Costești Reservoir. **d** Bed material unimodality downstream Stânca–Costești Dam

the rivers in the southern part of the studied area this difference increases, which leads to more pronounced bimodality of the riverbed material (Table 28.2).

(ii) From the previous discussions we can draw the conclusion that *the bimodality appears to be limited to the Carpathian rivers and tributaries to the Siret, and very pronounced for the Siret River itself.* For the first rivers with lengths between 150 and 300 km, we were expecting an increasing bimodality along their course, as occurs with other rivers in various geographic environments, such as those in Italy (Ibbeken and Schleyer 1991), Japan (Kodama 1992, 1994), Canada (Shaw and Kellerhals 1982) and Scotland (Sambrook Smith 1996). However, statistics on a total of 190 global samples (Table 28.2) demonstrate that unimodal distributions prevail for all Carpathian rivers that are tributary to the Siret. Bimodality is present

Table 28.2 A synthesis of the bimodality degrees of the fluvial bed sediments, together with average data on the proportion of the parent material and on the proportions of 0.5–4, 1–8 mm and under 1 mm fractions in the fluvial bed material (Rădoane et al. 2008)

River	Sampled points along the river ($\sim L$, km)	Unimodal distributions ($B < 2.0$)		Bimodal distributions ($B > 2.0$)		Parental material (molasse rocks and quaternary rocks)	Weight of 0.5–4 mm fractions in the bed material	Weight of 1–8 mm fractions in the bed material	Sand weight (under 1 mm) in the bed material
		N	$\bar{B}$	N	$\bar{B}$ ($B_{min} \div B_{max}$)	(%)			
Surface samples									
Suceava	16 (172 km)	14 ($\sim$152 km)	0.553	2 ($\sim$20 km)	6.14 (B: 4.43 ÷ 7.84)	64.6	6.21	9.04	4.89
Moldova	18 (205 km)	13 ($\sim$150 km)	0.446	5 ($\sim$55 km)	4.888 (B: 3.48 ÷ 6.47)	21.2	9.86	12.54	6.96
Trotuș	21 (149 km)	20 ($\sim$140 km)	0.703	1 ($\sim$7 km)	8.00	24.6	1.41	1.59	1.26
Putna	11 (95 km)	8 ($\sim$68 km)	0.614	3 ($\sim$27 km)	4.27 (B: 2.63 ÷ 6.60)	36.6	6.19	5.57	4.62
Buzău	33 (214 km)	26 ($\sim$164 km)	0.539	7 ($\sim$50 km)	5.31 (B: 2.04 ÷ 9.05)	21.6	6.27	7.43	7.23
Subsurface samples									
Suceava	16 (172 km)	4 ($\sim$40 km)	0.469	12 ($\sim$132 km)	4.22 (B: 2.01 ÷ 6.36)	64.6	12.61	20.66	11.61
Moldova	18 (205 km)	3 ($\sim$35 km)	0.283	15 ($\sim$170 km)	3.53 (B: 2.16 ÷ 5.06)	21.2	13.89	24.74	13.10
Trotuș	21 (149 km)	4 ($\sim$28 km)	0.740	17 ($\sim$121 km)	3.63 (B: 2.01 ÷ 5.31)	24.6	11.58	14.22	11.74
Putna	11 (95 km)	2 ($\sim$16 km)	0.866	9 ($\sim$79 km)	4.80 (B: 2.33 ÷ 10.80)	36.6	9.81	17.44	12.10
Buzău	33 (214 km)	10 ($\sim$70 km)	0.470	23 ($\sim$144 km)	5.22 (B: 2.31 ÷ 8.32)	21.6	9.24	15.39	17.12
Global samples									
Suceava	16 (172 km)	13 ($\sim$112 km)	0.479	3 ($\sim$60 km)	4.77 (B: 3.0 ÷ 5.84)	64.6	7.59	13.10	7.39
Moldova	18 (205 km)	9 ($\sim$90 km)	0.471	9 ($\sim$90 km)	4.13 (B: 3.50 ÷ 4.68)	21.2	10.83	17.62	9.38
Trotuș	21 (149 km)	17 ($\sim$121 km)	0.564	4 ($\sim$28 km)	4.89 (B: 3.31 ÷ 7.17)	24.6	5.56	6.84	5.44

(continued)

Table 28.2 (continued)

River	Sampled points along the river ($\sim L$, km)	Unimodal distributions ($B < 2.0$)		Bimodal distributions ($B > 2.0$)		Parental material (molasse rocks and quaternary rocks)	Weight of 0.5–4 mm fractions in the bed material	Weight of 1–8 mm fractions in the bed material	Sand weight (under 1 mm) in the bed material
		N	$\bar{B}$	N	$\bar{B}$ ($B_{min} \div B_{max}$)	(%)			
Putna	17 (146 km)	6 ($\sim$52 km)	0.610	11 ($\sim$94 km)	5.44 (B: 2.38 $\div$ 11.90)	36.6	7.27	12.66	16.58
Buzău	41 (293 km)	20 ($\sim$143 km)	0.459	21 ($\sim$150 km)	6.47 (B: 2.04 $\div$ 19.0)	21.6	6.54	10.96	13.84
Siret	53 (725 km)	6 ($\sim$80 km)	0.636	47 ($\sim$ 645 km)	7.11 (B: 3.04 $\div$ 9.40)		3.81	21.94	26.94

on river segments shorter than those that feature unimodality (Table 28.2 also displays the length of the river segment for which riverbed material is unimodal or bimodal); on the last 40 km of the Suceava, Moldova and Trotuş bimodality appears at only four sampling points. Only the Putna and Buzău rivers present bimodality along river lengths of less than 100 km in the medium-inferior part of the rivers. In contrast, for the Siret riverbed, material bimodality is quasi-general. In this case, the riverbed material presents a low bimodality or it is unimodal for very short river segments that are immediately downstream of the confluence spot.

(iii) *The bimodality of riverbed materials is related to the quality of the parent material*, which is also the source of the riverbed sand and the source of the second mode. In order to demonstrate this assertion we related the distribution of the parent material (i.e., the area percentage of friable rocks upstream of each riverbed material sampling point—Fig. 28.4c) to the bimodality index distribution within the same diagram (Fig. 28.4a, b). Friable rocks (molasse and platform deposits) are capable of supplying large amounts of fine alluvium to riverbeds, particularly when the relief energy further endorses it.

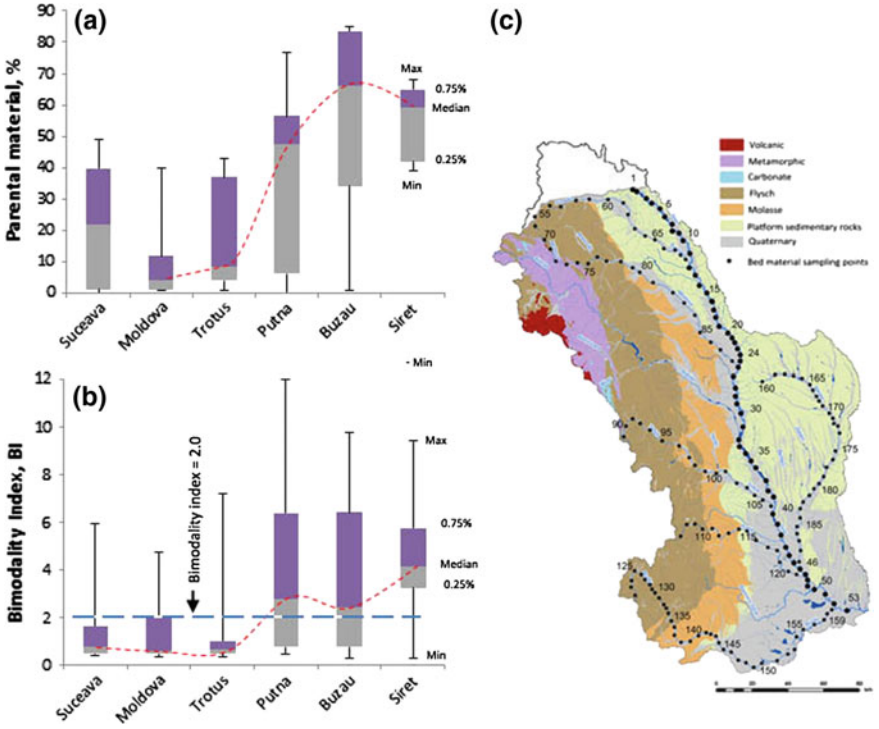

Fig. 28.4 Distribution of parent material in investigated river basins (**a**) and effects on the distribution of bed material bimodality index (**b**). Distribution of main types of rocks in Siret drainage basin and bed material sampling points (**c**)

As shown in Fig. 28.1, the amounts of fine material discharged by the main tributaries of Siret River increase southward, following approximately the trend line illustrated in Fig. 28.4a. The bimodality index of riverbed material exceeds the 2.0 threshold value particularly from the confluence with Putna River onwards. On Suceava, Moldova and Trotuș, the sand percentage in the aggregate sample is below 9 %, and thus the bimodality index was rarely above the 2.0 threshold value. Conversely, in Putna and Buzău drainage basins, where the transfer rates of fine alluvium from the basin to the river are extremely high, over 20 t/ha/year, the average sand percentage is 14 % (albeit in some reaches it exceeds 30–35 %), thus generating the second mode.

(iv) An explanation for bimodality may reside in the transfer rate of fine alluvium from the source area to the riverbed. The large amounts of alluvia composed of silt and sand, through their sheer volume eventually overpower the unimodal distributions of existing riverbed material, well sorted and distributed according to Sternberg's law. Basically, the latter is overlapped by a new unimodal sand peak distribution originating in the catchment and reaching the riverbed through the suspended load. This idea is illustrated in Fig. 28.5, showing several gauging points along Buzău River. The gravel mode undergoes continuous downstream fining along the river and eventually fades completely at the contact with Lower Siret Plain. The second mode (i.e., sand mode) begins to emerge in the bed material distribution as early as the mountain area, becoming dominant on exit from the molasse area and the high piedmont plain. The intersection of the two modes occurs in the 1–8 mm fraction range, appearing as if there is a shortage in this fraction of bed material. In fact, these fractions would be found in higher amounts than sand if the parental material would not provide fine alluvia to the riverbed. Thus, sand fractions are stored and their presence has been revealed by a distinct distribution peaking on 1–2 *phi* with a slight left asymmetry. Therefore, the bimodality of riverbed material distribution results from an overlay of unimodal distributions of sand originating in the basin and the unimodal distributions of gravel processed by the river through abrasion and hydraulic sorting (Fig. 28.5a, b).

(v) In this conceptual model we have drawn for the Carpathian tributaries, the case of Siret River appears somewhat reversed. We have shown earlier (Table 28.2 and Fig. 28.3) that the riverbed material is characterized by a strong bimodality along most of its length. The difference is that the gravel mode has an allochthonous source whereas the sand mode is owned by the river itself. If, for the Carpathian tributaries, the gravel mode is affected by a downstream fining, which clearly indicates the autochthonous source of their processing and sorting, the Siret would be mostly fit for transportation of fine particles, but it needs to face an 'avalanche' of gravel with increasing sizes along the river from its lateral inputs. Simply put, an alien coarse grain size distribution overlaps over a relatively fine riverbed grain size distribution of

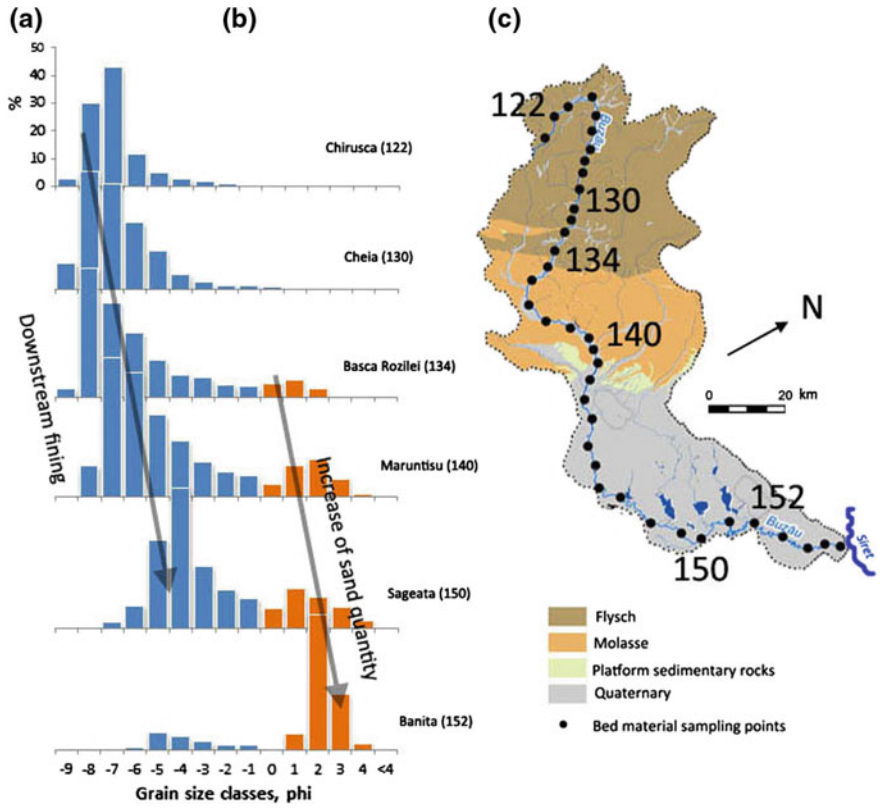

Fig. 28.5 Bimodality along Buzău River. **a** Gravel mode distribution along the river. **b** Sand mode distribution along the river. **c** Buzău drainage basin: surface geology and bed material sampling points along the river

the Siret itself. Evidently, a very strong penury of the diameters within the 0.5–4 mm range appears between the two distributions. This is due, in our conceptual model, to the fact that the tails of the gravel mode and the sands mode overlap in this sector.

To sum up, "sedimentary links" (cf. Rice 1998, 1999) manifest not only in terms of downstream fining, but also in driving bimodality. Along Siret River, between two Carpathian junctions, riverbed material bimodality is highest upstream of the confluence and barely noticeable immediately downstream of such a confluence. The massive influx of gravel generates unimodality just downstream of the confluence; however, this will diminish rapidly due to a large input of autochthonous sand (20–30 % of the aggregate sample) which is notable particularly upstream of junctions. Therefore, in the absence of these Carpathian tributaries, Siret River would transport mainly fine sediments.

The distortion of the longitudinal profile shape (Ichim and Rădoane 1990; Rădoane et al. 2003; Rădoane et al., Chap. 18, this volume) is determined by the "front" of a pebble sheet which is continuously accumulating since the Sarmatian (Martiniuc 1948). This front corresponds to the formation limit of the Moldavian Piedmont. At present, this piedmont was highly fragmented by the tributaries of Siret River, but the gravel accumulation mechanism is still active. This front is similar to the one described earlier according to the experimental research conducted by Venditti et al. (2010). There is evidence that the main paths of the principal Carpathian tributaries started developing in the Lower and Middle Sarmatien and are more recent (Upper Quaternary) in the south. Paradoxically the Siret is "younger" from the point of view of its Carpathian tributaries. The main rivers north of the Trotuş, formed in the Sarmatian, and flowed into the Sarmatic Sea which covered the present territory of the Moldavian Tableland. The sea retreated to the southeast and the torrential character of the rivers induced the formation of huge fluviodeltaic fans of gravels and sands. The river that now collects these tributaries formed itself on a surface that had remained immersed. South of the Trotuş, the formation of fluviodeltaic fans and later of large alluvial fans continued up to the Quaternary, when the Romanian Plain was covered by a lake that occupied the whole area of the Lower Siret. Consequently, the Siret is younger and younger from north to south and developed itself at the Moldavian Piedmont border. All these points suggest the continuity of piedmont gravel sheet formation to the present. Thus, the limit of the massive presence of gravels in the riverbed beyond the mountains may be regarded as the extra-Carpathian limit of the present gravel sheet formation. Morphologically, this corresponds to the discontinuity of the Siret longitudinal profile. Taking into account all these features, we consider that a natural geomorphological paradox is expressed by Siret, which is a river situated beyond the Carpathians on the greatest part of its length, but from the point of view of its sedimentary facies, its longitudinal profile, and its stream bed dynamics, is a Carpathian river for almost 85 % of its total length (Ichim and Rădoane 1990).

Morphometric Variability of Riverbed Material

The shape of riverbed sedimentary particles, as well as the grain size and petrographic composition are an indisputable source of data on the sediment source, transport and deposition environments (Pettijohn 1949; Ichim et al. 1998). For the gravel shape analysis we collected over 30,000 boulders from the beds of several Romanian rivers. The established granulometric classes were 16–32 and 32–64 mm, and the petrography of measured clasts was uniform along the entire river length, in order to have a common assessment standard for each river; thus, we

selected siliceous sandstone clasts on Suceava River, limestone on Moldova, Tarcău and Kliwa sandstones on Trotuș, and Kliwa sandstone on Putna. The morphometric parameters we determined (i.e., roundness, flattening, asymmetry, etc.) are detailed in the papers investigating this topic in depth: Miclăuș et al. (1995), Ichim et al. (1998), Dumitriu (2007).

Particles shape is strongly controlled by the transport distance from the source to the river mouth, which equates the shaping power of the river water loaded with fine sediments. The behavior of all morphometric indices of gravel was assessed in relation to the river length and the results are summarized below.

The abrasion or roundness of gravel does not occur uniformly along the river; moreover, in all analyzed cases, gravel roundness along the river best resembles a parabola shape (Fig. 28.6). The optimal value of abrasion is not achieved at the river mouth, as might be expected, but somewhere in the middle to lower river course. While this trend is common to other rivers described in the literature (Krumbein 1941; Plumley 1948; Dal Cin 1967; Richards 1982), the cause for this phenomenon is still little understood. Dumitriu (2007) observed that the decrease in sediment grain roundness is controlled by the competition between river hydrodynamics and the input of new sediments through lateral tributaries which manifests over short distances on Trotuș River. However, the overall trend remains unchanged (parabolic) and is still poorly explained to date.

Gravel *flatness* varies according to a concave parabola in all investigated rivers (Suceava, Moldova, Trotuș-for *phi* ranging between 32 and 64 mm, Putna) and all

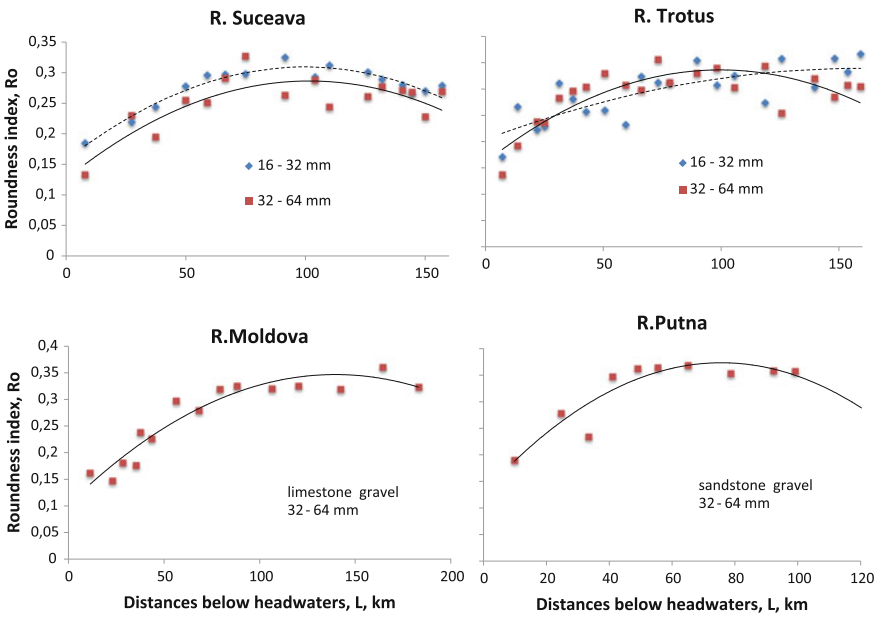

Fig. 28.6 Variation of gravel morphometric parameters along four Carpathian rivers

categories of rocks (limestone and various types of sandstones). The same type of variation was documented in Piave, Italy, on quartz and andesite (Dal Cin 1967), prompting the following explanation: flatness is a good indicator of hydroclimatic conditions. In the upper course, very flat gravel clasts are very likely to break perpendicular to the *ab* plane due to stream flow aggressiveness. In the middle course the power of the river flow diminishes, therefore gravel tends to remain for a longer time on the riverbed, undergoing abrasion by the sand load transported at relatively low levels. Thus far, the explanations regarding gravel flattening are reasonable enough but are hardly convincing as regards the increase in flattening in the lower river course. Dal Cin (1967) believes the explanation resides in the high frequency of saltation in the lower course which appears to impact particularly on gravel flattening.

Gravel sphericity ranges from 0 to 1.0 and measures the ratio between the maximum projected area of a particle and the area of a sphere of equal volume (Sneed and Folk 1958). This morphometric index is highly dependent on lithology. The variation of sphericity for limestone clasts (on Moldova River) has a hyperbolic shape, therefore showing a rapid increase in sphericity in the headwater area, ensued by relatively constant values until the river mouth. In the case of Putna River, the variation of sphericity for Kliwa sandstone particles along the river is defined by a quadratic polynomial function (convex parabola). However, on Trotuș the variability becomes more complex due to the input of numerous tributaries from the Carpathian area supplying coarse alluvia to the main riverbed. Sphericity is related to qualitative shape classes (i.e., spheres, blades, discs and sticks), thus it influences sorting processes, mobilization control and sediment transport. Disc-shaped clasts have low sphericity, are imbricated and hard to mobilize, but once entrained in transport—particularly in suspended form—they are transferred much farther than the sedimentation velocity allows (Lane and Carlson 1954).

The conclusions of these particular analyses of gravel morphometric indices are centered on the concept of "optimal shape" of Carpathian riverbed gravels. The assessment of the optimal shape of sandstone gravel was carried out based on the 10 descriptive classes of Sneed and Folk (1958). Thus, the investigated fluvial domain (i.e., east Carpathian rivers) is best described, with nuances depending very little on lithology, by the compact-blade and blade-shape gravels from the 16–32 and 32–64 mm classes.

The generalization of gravel shape variation tendencies on Suceava, Moldova and Putna Rivers shows that the middle–lower courses (i.e., exiting the mountains and entering the Subcarpathians) provide the best conditions for achieving optimal gravel shape, namely highest roundness, lowest flatness. Along this sector the gravel class (2–64 mm) is largely prevalent (over 80 %) within the riverbed material, which substantiates the presence of the largest gravel mines located along riverbeds.

Petrographic Variability of Gravel

We tackled the petrographic composition of riverbed material on investigated rivers, applied exclusively to the 16–32 and 32–64 granulometric classes, in order to acquire additional data on the relationship between source area and bed deposits, on the degree of gravel attrition in relation to lithology and the competition between various types of rocks during longitudinal fluvial transfer. As expected, the lithology of bed material is indicative of the petrographic composition of the source area, but the percentages differ. The source area of gravel from investigated riverbeds comprises of all types of rocks (igneous, metamorphic and sedimentary). The distribution of these lithological units' features bands-oriented from north to south and succeeding from west to east (Fig. 28.7).

Siret River, with its allochthonous gravel, stands out again due to the strong control exerted by its Carpathian tributaries on petrography. Thus, the following petrographic sectors have been distinguished along Siret: *calcareous,* between Moldova and Bistrița Rivers; *quartzose* downstream of the confluence with Bistrița River; and *sandstone–calcareous* downstream of the junction with Trotuș (Ichim and Rădoane 1990). Downstream of the confluence with Bistrița the influx of gravel consisting of resistant rocks (metamorphic, volcanic and calcareous) completely changes the petrographic spectrum of the riverbed deposits. While sandstones

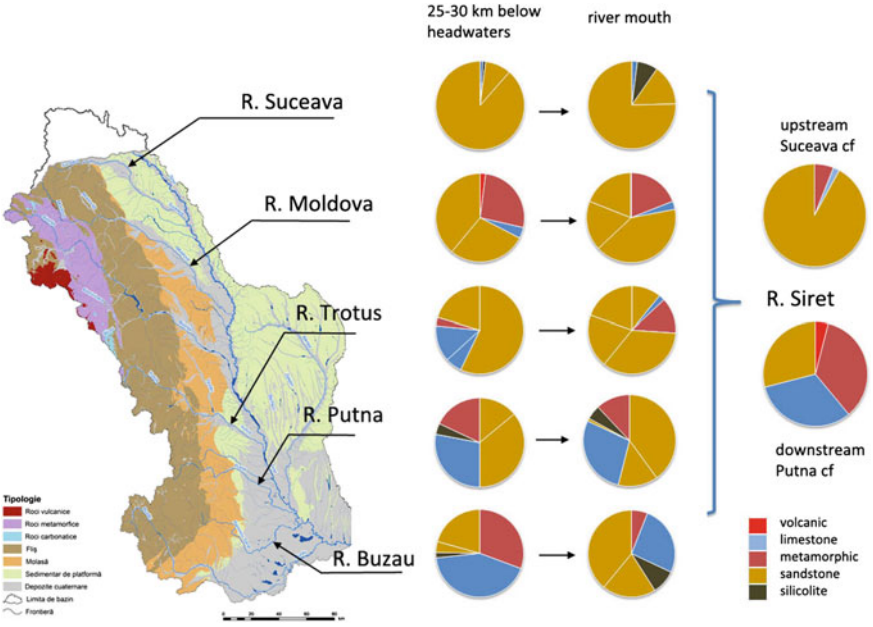

Fig. 28.7 Comparative diagrams of petrographic distribution of gravel in the headwaters area and the river mouths of rivers from Siret drainage basin

account for as much as 90 % of the petrographic composition of bed material on Siret River on its entering the Romanian territory, in the lower course their percentage decreases to 29 %. The accelerated attrition of this type of rock has contributed to the increase in the load of fine material transported by the river or deposited in various storing units (mainly scroll bars, islands, natural levees, etc.).

Discussions and Conclusions

The analysis of riverbed sediments and suspended sediment flow through the drainage network in Siret and Prut drainage basins enabled us to quantize them in the shape of a sediment budget (Fig. 28.8).

An impressive database comprising of data on the two drainage basins built over a long period of time by our research team has allowed for an assessment of the sediment sources, storage and delivery. We estimated the budget during the same timeframe for both drainage networks (1960–2010) in order to have a global comparative view on budget elements. Both networks are subjected to a wide range of controls, both natural and anthropogenic interventions, particularly in the shape of dams. However, the two main rivers differ greatly in terms of sediment sources and storage: whereas Siret is almost entirely supplied with sediments by its Carpathian tributaries (over 90 %), Prut River (draining Woody Carpathians) provides itself with the largest sediment input (over 53 %) and its tributaries have a low contribution. The greatest amounts of sediments entering the fluvial system are stored in reservoirs built on the main rivers. On both Siret and Prut, the channel beds underwent degradation downstream of the main reservoirs and sediment remobilization in the wetted perimeter (particularly on Prut River), such that the sediment delivery has comparative values. It is, however, higher on Siret when the

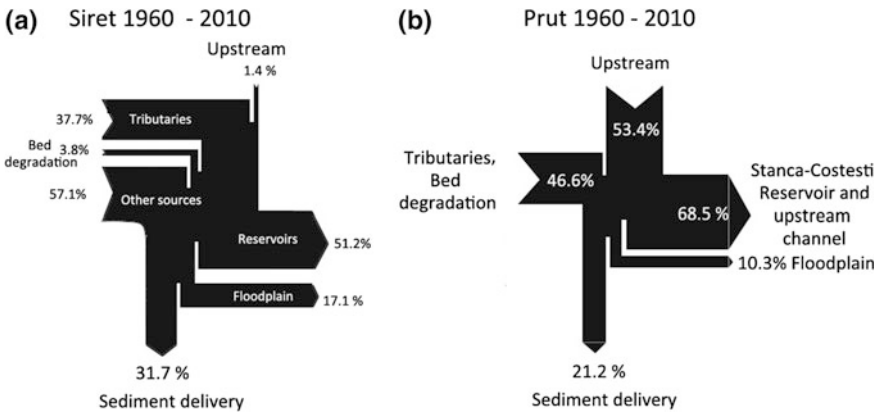

Fig. 28.8 Sediment budget for gravel and sand for the Siret (**a**) and Prut (**b**) Rivers (period 1960–2010)

sources become very effective in the lower sector of the river, and slightly lower on Prut when the inputs through lateral tributaries are scarce. It should be noted that in both drainage networks the anthropogenic impact on sediment redistribution (both fine and coarse) has been significant, and there is great potential for future changes in river channels.

Acknowledgements This research is part of two projects funded by the Fund for Scientific Research, Romania (research project PN-II-ID-PCE-2011-3-0057 and PN II-RUTE-2017-4-0855).

References

Ashworth PJ, Ferguson RI (1989) Size-selective entrainment of bed-load in gravel bed streams. Water Resour Res 25(4):627–634

Brierley GJ, Hickin EJ (1985) The downstream gradation of particle sizes in the Squamish River, British Columbia. Earth Surf Proc Land 10:597–606

Călinoiu M, Paraschivescu G, Ungureanu C (1988) Influenţa factorilor antropici asupra formării şi valorificării acumulărilor de nisipuri şi pietrişuri în R.S. România. Lucrările celui de–al II–lea Simpozion "Provenienţa şi Efluenţa Aluviunilor", Piatra Neamţ (in Romanian)

Constantine CR, Mount JF, Florsheim JL (2003) The effects of longitudinal differences in gravel mobility on the downstream fining pattern in the Consumnes River, California. J Geol 111:233–241

Dal Cin R (1967) Le Ghiaie del Piave. Morfometria, granulometria, disposizione e natura dei ciottoli, Mem. del Museo Tridentino, XVI, 3 (in Italian)

Diaconu C, Şerban P (1994) Sinteze şi regionalizări hidrologice. Technical Press, Bucureşti (in Romanian)

Dumitriu D (2007) Sistemul aluviunilor din bazinul râului Trotuş. University of Suceava Press, Suceava (in Romanian)

Ferguson RI (2003) Emergence of abrupt gravel to sand transitions along rivers through sorting process. Geology 31:159–162

Ferguson R, Hoey T, Wathen S, Werritty A (1996) Field evidence for rapid downstream fining of river gravels through selective transport. Geology 24(2):179–182

Gasparini NM, Tucker GE, Bras RL (2004) Network-scale dynamics of grain-size sorting: implications for downstream fining, stream-profile concavity and drainage basin morphology. Earth Surf Proc Land 29:401–532

Gomez B, Rosser BJ, Peacock DH, Murray Hicks D (2001) Downstream fining in a rapidly aggrading gravel bed river. Water Resour Res 37(6):1813–1823

Hoey TB, Ferguson R (1994) Numerical simulation of downstream fining by selective transport in gravel bed rivers: model development and illustration. Water Resour Res 30(7):2251–2260

Ibbeken H (1983) Jointed source rock and fluvial gravel controlled by Rosin's law: a grain-size study in Calabria, South Italy. J Sedimentol Petrol 53(4):1213–1231

Ibbeken H, Schleyer R (1991) Source and sediment. A case study of provenance and mass balance at an active plate margin (Calabria, Southern Italy). Springer, Berlin

Ichim I, Rădoane M (1990) Channel sediment variability along a river: a case study of the Siret River, Romania. Earth Surf Proc Land 15:211–225

Ichim I, Rădoane M, Rădoane N, Grasu C, Miclăuş C (1998) Dinamica sedimentelor. Aplicaţie la râul Putna, Technical Press (in Romanian)

Knighton AD (1980) Longitudinal changes in the size and sorting of stream-bed material in four English rivers. Bull Geol Soc Am 91:483–502

Knighton AD (1982) Longitudinal changes in the size and shape of stream bed material: evidence of variable transport conditions. Catena 9:25–34
Knighton AD (1999) The gravel–sand transition in a disturbed catchment. Geomorphology 27:325–341
Kodama Y (1992) Effect of abrasion on downstream gravel–size reduction in the Watarase river, Japan: field work and laboratory experiments. Environmental research center papers, 15, Tsukuba
Kodama Y (1994) Downstream changes in the lithology and grain size of fluvial gravels, the Watarase River, Japan: evidence of the role of abrasion in downstream fining. J Sed Res A 64 (1):68–75
Krumbein WC (1941) Measurement and geological significance of shape of rock fragments. J Sediment Petrol 11:64–72
Lane EW, Carlson EJ (1954) Some observations on the effect of particle shape on the movement of coarse sediments. Trans Am Geophys Union 35(3):453–462
Leopold LB, Wolman MG, Miller JP (1964) Fluvial processes in geomorphology. Freeman and Co, San Francisco
Martiniuc C (1948) Contribution à la connaissance du Sarmatien entre Siret et Carpathes. Analele Stiintifice ale Universității din Iași (Sci Nat), XXI, Iași (in French)
Miclăuș C, Rădoane M, Ichim I, Rădoane N, Grasu C (1995) Analiza geostatistică a faciesului actual al albiei râului Moldova. Analele Univ. "Al.I.Cuza", Iași (in Romanian)
Paola C, Seal R (1995) Grain size patchiness as a cause of selective deposition and downstream fining. Water Resour Res 31:1395–1407
Parker G (1991) Selective sorting and abrasion of river gravel, II; Applications. J Hydraul Eng 28:529–544
Parker G, Klingerman PC, McLean DG (1982) Bedload and size distribution in paved gravel bed streams. J Hydraul Eng Div, Am Soc Chem Eng 108:544–571
Pettijohn FJ (1949) Sedimentary rocks. Harper and Brothers, New York
Plumley WJ (1948) Black hills terrace gravel: a study in sediment transport. J Geol 56:526–577
Rădoane M, Rădoane N (2006) Rolul intervențiilor antropice și al schimbărilor climatice în evoluția recentă a albiei Râului Bârlad (Podișul Moldovei). Studii și cercetări de geografie 53–55:117–136 (in Romanian)
Rădoane M, Rădoane N, Dumitriu D (2003) Geomorphological evolution of longitudinal river profiles in the Carpathians. Geomorphology 50:293–306
Rădoane M, Rădoane N, Dumitriu D, Miclăuș C (2008) Downstream variation in bed sediment size along the East Carpathians Rivers: evidence of the role of sediment sources. Earth Surf Land Process 33(5):674–694
Rice S (1998) Which tributaries disrupt downstream fining along gravel-bed rivers? Geomorphology 22:39–56
Rice S (1999) The nature and controls on downstream fining within sedimentary link. J Sediment Res 69A:32–39
Rice S, Church M (1998) Grain size along two gravel-bed rivers: statistical variation, spatial patterns and sedimentary links. Earth Surf Process Land 23:345–363
Richards K (1982) Rivers. Form and process in alluvial channels. Methuen, Londra
Sambrook Smith GH (1996) Bimodal fluvial bed sediments: origin, spatial extent and processes. Prog Phys Geogr 20(4):402–417
Sambrook Smith GH, Ferguson RI (1995) The gravel–sand transition along river channels. J Sediment Res A 65(2):423–430
Seal R, Paola C, Parker G, Southard JB, Wilcock PR (1997) Experiments on downstream fining of gravel: I. Narrow-channel runs. J Hydraul Eng Div, Am Soc Chem Eng 123:874–884
Sficlea V (1980) Podișul Covurlui, In: "Cercetări în Geografia României", Editura Științifică și Enciclopedică, București (in Romanian)
Shaw J, Kellerhals R (1982) The composition of recent alluvial gravels in Alberta Riverbeds. Alberta Res Counc Bull, 41

Sneed ED, Folk RL (1958) Pebbles in the lower Colorado River, Texas: a study in particle morphogenesis. J Geol 66:114–150

Surian N (2002) Downstream variation in grain size along an Alpine River, analysis of controls and processes. Geomorphology 43:137–149

Venditti JG, Dietrich WE, Nelson PA, Wydzga MA, Fadde J, Sklar I (2010) Mobilization of coarse surface layers in gravel bedded rivers by finer gravel bed load. Water Resour Res 46: W07506. doi:10.1029/2009WR008329

Werrity A (1992) Downstream fining in a gravel bed river in Southern Poland: lithological control and the role of abrasion. In: Billi P, Hey RD, Thorne CR, Tacconi P (eds) Dynamics of gravel-bed rivers. Wiley, Chichester, pp 333–350

Wilcock PR (1992) Experimental investigation of the effects of mixture properties on transport dynamics. In: Billi P, Hey RD, Thorne CR, Tacconi P (eds) Dynamics of gravel-bed rivers. Wiley, Chichester, pp 109–130

Wilcock PR (1993) Critical shear stress of natural sediments. J Hydraul Eng Div, Am Soc Chem Eng 119(4):491–505

Yatsu E (1955) On the longitudinal profile of the graded river. Trans Am Geophys Union 36: 655–663

Chapter 29
The Lower Danube Loess, New Age Constraints from Luminescence Dating, Magnetic Proxies and Isochronous Tephra Markers

Alida Timar-Gabor, Cristian Panaiotu, Daniel Vereș, Cristian Necula and Daniela Constantin

Abstract Loess and loess-derivative deposits currently form some of the most ubiquitous sedimentary landforms in Europe, including important parts of Romania. Loess-palaeosol sequences (LPS) are continental archives of Quaternary paleoclimates since these deposits are a direct product of geomorphic processes driven by past climate variability. Understanding these processes needs data input provided by absolute chronologies. Loess is generally considered an ideal material for the

A. Timar-Gabor (✉) · D. Vereș · D. Constantin
Faculty of Environmental Science and Engineering,
Babeș-Bolyai University, Fântânele 30, 400294 Cluj-Napoca, Romania
e-mail: alida.timar@ubbcluj.ro; alida_timar@yahoo.com

D. Vereș
e-mail: danveres@hasdeu.ubbcluj.ro

D. Constantin
e-mail: daniela.constantin1@gmail.com

A. Timar-Gabor · D. Constantin
Interdisciplinary Research Institute, Bio-Nano-Science
of Babeș-Bolyai University, Treboniu Laurian 42,
400271 Cluj-Napoca, Romania

C. Panaiotu · C. Necula
Faculty of Physics, University of Bucharest, N. Balcescu 1,
010041 Bucharest, Romania
e-mail: cristian.panaiotu@g.unibuc.ro

C. Necula
e-mail: c3necula@yahoo.com

D. Vereș
Institute of Speleology, Romanian Academy,
Clinicilor 5, 400006 Cluj-Napoca, Romania

D. Constantin
Faculty of Biology and Geology, Babeș-Bolyai University,
Mihail Kogalniceanu 1, 400084 Cluj-Napoca, Romania

M. Rădoane and A. Vespremeanu-Stroe (eds.), *Landform Dynamics and Evolution in Romania*, Springer Geography,
DOI 10.1007/978-3-319-32589-7_29

application of luminescence dating. In this chapter, we present a review of the latest methodological advances in constraining the chronology of several key Romanian LPS alongside the dating of several loess-alluvial deposits that harbour tephra layers. Luminescence chronologies as well as time-depth models based on magnetic susceptibility variations assign the topmost loess layer to the last glacial cycle that comprises, according to the north European stratigraphic terminology, the Weichselian glaciation (Marine Isotope Stage (MIS) 4 and MIS 2 phases). The uppermost palaeosol is assigned to MIS5 especially to the Eemian interglacial (MIS5e), an equivalent to the north European stratigraphy, and to the Riss–Würm interglacial in the Alpine stratigraphy. As proved by the high-resolution chronologies, the sedimentation rates of loess varied during the last glacial both within a specific loess section, as well as between different loess sections, the major controlling factor being the topographic context. The luminescence chronologies discussed here improved and expanded the long-held stratigraphy of Romanian loess constructed decades ago by using relative methods, suggesting that a re-evaluation of the regional chronostratigraphic inferences in a high-resolution absolute dating approach has to be conducted.

Keywords Loess · Quaternary paleoclimates · Luminescence chronologies · Magnetic susceptibility · Palaeosol · Lower Danube

Introduction

Loess and loess-derivative deposits currently form some of the most ubiquitous sedimentary landforms in Europe, including important parts of Romania (Haase et al. 2007; Jipa 2014). Located mainly south of the Scandinavian ice sheet margin, what is referred to as the European loess belt represents the most extensive continental palaeoclimate archive. These extensive loess deposits archive important palaeoclimate information since they are a direct product of geomorphic processes driven by past climate variability. In places, such sedimentary archives are recording a history of environmental change that spans over several glacial-interglacial cycles. In most areas, such deposits comprise in fact a suite of fossil palaeosols interbedded within packages of clastic sediments, the proper loess, a well-sorted, silty, loamy, calcareous and porous sediment. The generally accepted notion is that loess is linked with aeolian accumulation of particles eroded during arid and cold periods that limited vegetation development and enhanced the physical weathering of exposed terrains. Upon sedimentation, these deposits underwent significant pedosedimentary and biogeochemical changes. By analogy to the development of the current topsoil, Holocene in age, palaeosols are related to past interglacial periods that favoured the development of vegetation and intense pedogenesis.

Although, this simplistic assumption of wet-warm interglacials with pedological development and cold–dry glacials with accumulation of clastic materials is

currently being challenged (Zech et al. 2013), a significant body of research has shown that LPS provide unique archives for understanding past environmental and climate change in the terrestrial realm. In some places, such as in central–eastern Europe and the Chinese Loess Plateau, such deposits include tens to hundreds of meters of sediments, allowing for high-resolution multidisciplinary investigations. More recently, investigations of several European key sections showed that loess deposits, given a proper analytical resolution, might also preserve a record of wind activity superimposed on millennial-scale climate changes, comparable to the information extracted from other archives, particularly polar ice cores (see, e.g. Rousseau et al. 2002, 2011; Kadereit and Wagner 2014). Indeed, much attention is currently being directed on understanding the impact of rapid climate change events within glacials and interglacials such as the Dansgaard–Oeschger (DO) cycles and oceanic cold events (Heinrich events) upon the European continental environments. DO cycles, or Greenland interstadials and stadials (GIS/GS, Svensson et al. 2006, 2008) denote a series of abrupt climate change events recorded in polar ice cores and traced over most of the globe in various records including speleothems, lacustrine, or marine deposits (see, e.g. Wang et al. 2001). Greenland interstadials are regarded as warm and/or humid spells, some lasting millennia, whereas the stadials were characterized by a return to cold conditions that limited biological activity and enhanced physical erosion (Wolff et al. 2009). Heinrich events on the other hand represent events of extreme cold conditions in the ocean realm, related to episodic surges of ice from the main North Atlantic ice sheets (Hemming 2004). Their impact on the terrestrial environments has been extreme, with cold and dry climates that drove an expansion of steppe elements at the expense of woodland species (Fletcher et al. 2010). These rapid climate changes had a profound impact on wind strength and patterns of atmospheric circulation, precipitation distribution, and landscape-scale physical weathering; these processes also played the major role in the genesis of fine-grained detrital sediments such as loess.

Indeed, whereas the orbital pacing can be recognized in the nature of LPS accumulation, the imprint of centennial–to–millennial climate variations is less evident because significant regional differences in palaeoclimate led to a different response of the terrestrial environment to such thresholds, both longitudinal and latitudinal, particularly to what concerns the distribution of precipitation and vegetation cover. And this is readily exemplified by the occurrence of embryonic soil horizons within some LPS profiles. The issue of whether these horizons represent a clear response to the millennial-scale climate variability in terms of brief episodes of environmental conditions allowing for the initiation of pedogenesis is still debated. Moreover, loess internal physical and chemical processes active during sedimentation and formation likely result in the smoothing of the palaeoclimate signal archived. As such, one must bear in mind that the particularity of loess formation implies a rather episodic character of build-up, and therefore some terrestrial records are invariably fragmentary and/or usually characterized by varying sedimentation rates (Fitzsimmons and Hambach 2014). Therefore, securing a reliable chronological framework for LPS of interest is of paramount importance in palaeoclimatic research involving such sedimentary archives.

Despite the fact that the LPS in southeastern Europe are regarded as the most complete and continuous on the continent, this region is currently underreported in terms of absolute chronologies available when compared to the more westerly European loess sections.

In this chapter, we present a review of the latest methodological advances in better constraining the chronological frame of several key Romanian LPS (Mircea–Vodă, Mostiştea and Costineşti) alongside the dating of several loess-alluvial deposits that harbour tephra layers.

The Dating Approach of the Romanian Loess-Palaeosols Sequences

The chronologies obtained for loess deposits can be either relative or absolute. Physico-chemical properties of the sediment magnetic, remanence-acquiring minerals, allowed the vast development of the palaeomagnetic and magnetic susceptibility variation records of loess-palaeosol sequences, with direct implications on correlating records and providing chronological control through tuning or comparing with, for example, polar ice or marine isotopic event stratigraphy. Amino acid geochronology estimates the ages of loess-palaeosol deposits by analysing the extent of racemization in amino acids preserved within carbonate fossils (Novothny et al. 2009). Although limited by method constraints, radiocarbon dating has also been applied widely in loess research, traditionally for dating plant material, animal bones or charred remains. Novel palaeoclimate proxies include biomarkers (plant leaf wax *n*-alkane lipids, carboxylic acids or alcohols) that can be dated using radiocarbon (Zech et al. 2011). However, the method of choice to obtain absolute chronologies by dating mineral particles within loess is currently the optically stimulated luminescence (OSL) applied on quartz and feldspar of different grain sizes (Wintle 2008). This method outdates the thermoluminescence dating technique (TL).

Loess research in Romania has a long tradition (Rădan 2012 and references therein), with notable contributions brought by Conea (1969). More recent loess research includes investigations of its origin and significance in sedimentological terms (Buggle et al. 2008; Jipa 2014), pedostratigraphic considerations, and multi-method dating (Panaiotu et al. 2001; Bălescu et al. 2003; Timar et al. 2010; Fitzsimmons et al. 2012; Vereș et al. 2012; Constantin et al. 2014, among others).

Mircea–Vodă site (Figs. 29.1, 29.2a) is located in the Dobrogea plateau (SE Romania), approximately 15 km east of Danube valley. It is a typical loess plateau section over 26 m thick, comprising six well-developed palaeosols intercalated within six loess layers. Costineşti section (Figs. 29.1, 29.2b) is a cliff-exposure along the Black Sea shore (Dobrogea, SE Romania), north of Costineşti comprising five well-developed loess-palaeosols intercalated within five loess layers. The Mostiştea lake section (Figs. 29.1, 29.2c) is a cliff exposure in the Danube Plain

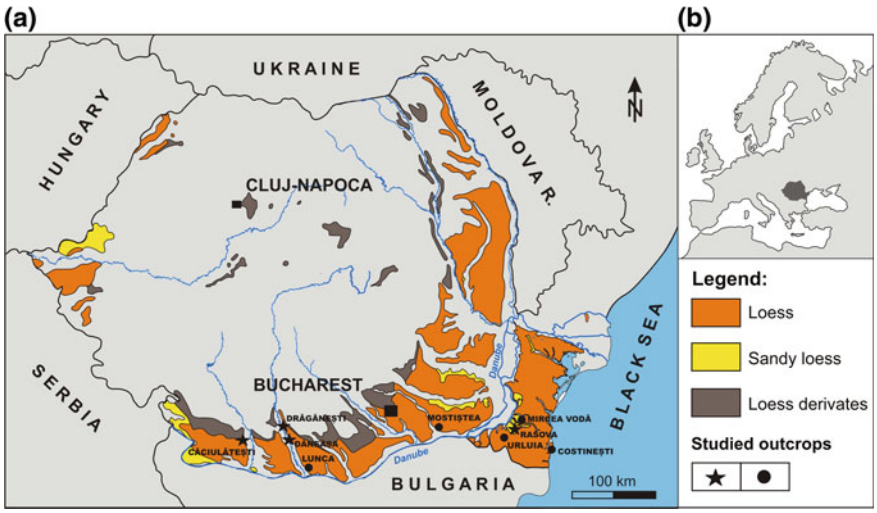

Fig. 29.1 **a** Loess distribution in Romania. High-resolution luminiscence chronologies are shown with filled circles. Filled stars indicate loess where occurrences of the Campanian Ignimbrite/Y-5 tephra have been described. **b** Map of Europe with the Romanian territory highlighted

Fig. 29.2 Overview of Mircea–Vodă (**a**), Costineşti (**b**) and Mostiştea (**c**) loess outcrops numbered among the most representative loess sections in Romania. Please note the *dark yellow stripes* of loess that intercalate the *reddish* fossil soils

(SE Romania) developed over 22 m in thickness and showing four loess-palaeosol layers and the Holocene topsoil.

As discussed below, the chronostratigraphic framework established for the Romanian LPS generally agrees with the results of similar investigations carried out on Serbian, Hungarian or Ukrainian loess. Yet, the available data in this region are integrated in disparate stratigraphic frameworks that in turn are correlated to the well-established Chinese loess stratigraphy (Markovic et al. 2015). According to this nomenclature, loess layers and palaeosols are indicated with the letters L and S, respectively, and consecutive numbers are assigned starting from the top of the unit (S0 and L1) downwards.

Pedostratigraphical observations and magnetic proxies generally assign the topmost loess layer to the Last Glacial cycle that comprises, according to the north European stratigraphic terminology, the Weichselian glaciation (71–14 ka, Lisiecki and Raymo 2005) which encompasses the cold MIS (Marine Isotope Stage) 4 and MIS 2 phases, interbedded in some instances with a weakly developed palaeosol that likely reflects milder climates during MIS3. The uppermost palaeosol is assigned to MIS5 (130–70 ka, Lisiecki and Raymo 2005), especially to the Eemian interglacial (MIS5e, 115–132, Shackleton et al. 2003), an equivalent to the north European stratigraphy, and to the Riss–Würm interglacial in the Alpine stratigraphy.

Magnetic Susceptibility and Magnetic Time Depth Model

Loess–palaeosol sequences contain a magnetic record of palaeoclimate changes throughout the Quaternary period (Maher and Thomson 1999). The sediment's magnetic properties depend on (a) the magnetic mineral content and characteristics of the source material, and (b) post-depositional weathering/soil formation processes (Evans and Heller 2003 and references therein). The magnetic enhancement seen in palaeosols, characteristic for Chinese and Russian steppe loess type sequences, is currently explained by pedogenesis (Maher 2011), whereby the in situ production of new ultrafine magnetic minerals occurs during soil formation. An opposite magneto-climatic relationship was found in some Alaskan and Siberian sequences with high magnetic susceptibility (χ) values in loess and low χ values in palaeosols. This behavior is explained by the so-called wind-vigour model where by stronger winds increase the input of heavier magnetic minerals during glacials, while during warmer interglacial periods aeolian activity is weak, and hence, the transport of dust particles rich in iron-oxides is reduced (Maher 2011).

A number of studies over the last 15 years have shown that the loess/palaeosol sequences from the lower Danube basin and Dobrogea have recorded in detail global and regional climate oscillations over the last 800 ka, with their magnetic properties similar to LPS from China, denoting strong magnetic enhancement of palaeosols produced by pedogenesis (Jordanova and Petersen 1999; Panaiotu et al. 2001; Fitzsimmons et al. 2012).

Several features from the magnetic susceptibility curve of LPS from the lower Danube and Dobrogea can be used as markers to correlate LPS both at regional and/or global scale (Panaiotu et al. 2001; Fitzsimmons et al. 2012). Best examples are the second palaeosol (S2) and the third palaeosol (S3) (Fig. 29.3). The S2 is a double palaeosol followed by an incipient soil in the overlying loess. This feature can be identified both in sections from the middle and lower Danube basin and in the classical Chinese LPS, and correlated with MIS 7. Palaeosol S3 can be used as regional marker because it has the strongest magnetic susceptibility on all sections, marking probably a significantly different environmental forcing during MIS 9 with respect to the two palaeosols S1 and S2.

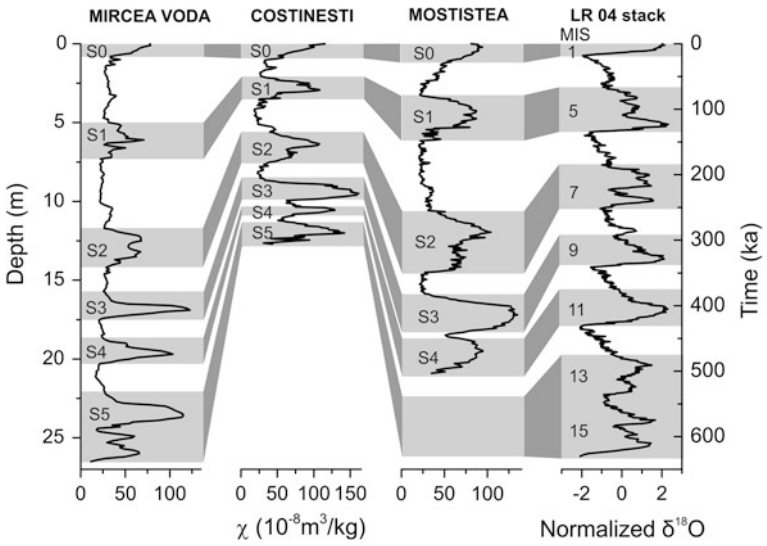

Fig. 29.3 Correlation of the magnetic susceptibility records of loess profiles from Mircea–Vodă (Timar et al. 2010), Costineşti and Mostiştea (Panaiotu et al. 2001) with the stack of 57 globally distributed benthic $\delta^{18}O$ records (Lisiecki and Raymo 2005). *Grey bands mark* palaesols (S1 to S5) and the recent soil (S0) whereas *white bands* indicate loess layers

Such characteristics of the magnetic properties of LPS have been synthesized in a relative geochronological framework, recently applied to the main loess profiles in the middle and lower Danube basin and Dobrogea (Fitzsimmons et al. 2012 and references therein). This geochronological framework is based on the correlation of the magnetic susceptibility records of LPS to a target curve, usually an astronomically tuned $\delta^{18}O$ record. Palaeosols with enhanced susceptibility (Fig. 29.3) are correlated to specific interglacials (odd-numbered marine isotope stages) and loess with reduced magnetic susceptibility to cold stages (even-numbered marine isotope stages). The method involves some form of visual matching of top and bottom of palaeosols to the boundaries of marine isotope stages in the target curve, which can be arbitrary and poorly constrained. Between these hard tie points, the sedimentation rate is assumed constant (e.g. Buggle et al. 2009), which is probably a very crude approximation.

To avoid the shortcomings from this visual matching, Necula and Panaiotu (2008) used for the first time the Match protocol on a LPS (Lisiecki and Lisiecki 2002), utilizing dynamic programming to find the optimal fit between magnetic susceptibility and the target curve. A time series for magnetic susceptibility can be generated using the Match–2.3 software and the stacked benthic $\delta^{18}O$ records as the target curve (Lisiecki and Raymo 2005). This method was applied for the LPS from Mostiştea, Costineşti, and Mircea–Vodă (Timar et al. 2010; Vasiliniuc et al. 2011, 2012; Constantin et al. 2014). All palaeosols are associated with corresponding odd-numbered marine isotope stages and loess layers with even-numbered stages

(Fig. 29.3) in agreement with accepted stratigraphy for the middle and lower Danube basin and Dobrogea loess (e.g. Fitzsimmons et al. 2012). Since this method produces a continuum time depth model, it can be tested against independent dating, such as luminescence. This comparison (Timar-Gabor et al. 2011; Vasiliniuc et al. 2011, 2012; Constantin et al. 2014) has proved that this magnetic time-model provides a basic, but realistic, time frame for the LPS. Based on these magnetic time depth models, the beginning of loess accumulation in the two investigated sections from Dobrogea is around 600 ka, the start of MIS 15 (Constantin et al. 2014) and around 430 ka at Mostiştea (Necula and Panaiotu 2008). Because OSL and IRSL dating methods cannot cover such old ages without further method development, this method is the only one that can provide a time frame for the LPS until the first palaeomagnetic marker at the Brunhes–Matuyama boundary (773 ka).

New Constraints from Optically Stimulated Luminescence (OSL) Dating

The Method

Luminescence dating is at present, the most applied method in establishing absolute chronologies for loess, which is generally assumed to be an ideal material for developing, testing, and applying luminescence techniques. The optically stimulated luminescence is a radiometric dating method that has the potential of covering age intervals spanning from 10^2 to 10^6 years. It relies on the properties of some mineral grains such as quartz, feldspars, calcite, etc., to store energy resulted from exposure to the environmental radiation field during their burial within deposits, and release it in the form of light upon stimulation with heat (thermoluminescence —TL) or with light (optically stimulated luminescence—OSL) ensuring that the latent luminescence signal is zeroed or reset. Such materials are called dosimeters and their use in retrospective dosimetry (dating) is based on the functional relationship between the burial time that is the amount of stored energy, and the intensity of the luminescence emitted when exposed to light or heat. The OSL age reflects the time elapsed since the last exposure to light of the buried mineral. In a rough manner, it represents the ratio between the total dose of radiation absorbed during mineral burial (the laboratory-determined equivalent dose) and the rate at which the radiation dose was delivered (annual dose). The annual dose is calculated in these studies based on the specific activities of natural isotopes from ^{238}U, ^{235}U, ^{232}Th series and ^{40}K determined by high-resolution gamma spectrometry. The annual dose cumulates contributions from alpha, beta, gamma, and cosmic radiation fields. The factors that influence the size of the annual dose are the water content of the sediment, depth, altitude and latitude, as well as the nature of the bedrock and dated sediments.

Literature data on LPS dating using quartz documents an upper age limit of between 50 and 100 ka (Wintle and Murray 2006; Timar et al. 2010; Timar-Gabor et al. 2011; Timar-Gabor and Wintle 2013) and low accuracy and precision for samples older than Eemian, caused by high dose rate in loess and the fact that the natural luminescence signal of quartz approaches saturation. As such, at all locations, we will focus on luminescence dating of the uppermost loess-palaeosol couplet, and the top of the second loess unit.

Although quartz luminescence studies (Wintle 2008) from worldwide failed to provide reliable dating of loess deposited during the Saal Glacial (that precedes the Eemian interglacial and equivalent of MIS 6), one loess sample from the top of L2 was collected from each of the three sections. The feldspar IRSL signal is, by contrast, subject to fading of the signal through time, resulting in the need to substantially correct the age estimates. The recent development of the post–IR IRSL protocol appears to access a more stable signal, thereby, providing more reliable ages, potentially extending the dating range beyond that of quartz, to up to 300 ka (Buylaert et al. 2012).

OSL Chronologies on Romanian Loess

The timing of the environmental changes recorded in the L1 loess from Mircea–Vodă (Fig. 29.4a) was dated using fine (4–11 μm) and coarse (63–90 μm) quartz by applying the single-aliquot regenerative dose (SAR) protocol and polymineral fine grains (4–11 μm) by using several protocols (conventional IRSL, post–IR–OSL and post–IR IRSL) (Timar-Gabor et al. 2011; Vasiliniuc et al. 2012, 2013a, b). Due to intense bioturbation and rootlets that hampered the sampling procedure in the topmost part of the L1 loess layer at Costineşti and Mostiştea, loess samples have been collected from the transition to the modern soil S0 only at Mircea–Vodă. Thus, nine samples were collected from L1 and one sample from the top of L2. At Mostiştea, nineteen samples were extracted starting from 0.5 m below the modern soil, at closely spaced depth intervals (10–25 cm), from L1 (12 samples), S1 (5 samples) and one sample from the top of the L2. At Costineşti, high-resolution (10 cm) sample collection has been performed starting from 30 cm below the S0 soil for L1 (10 samples) and S1 (3 samples).

The topmost loess sample from Mircea–Vodă yields a 4–11 μm quartz OSL age of 8.7 ± 1.3 ka (Timar et al. 2010) and a post–IR OSL age of 10 ± 1.5 ka on the polymineral fine grains (Vasiliniuc et al. 2013a) that indicate that loess deposition has continued well into the Holocene. A similar time lag has been confirmed by quartz OSL ages of 11.3 ± 1.0 ka reported in Constantin et al. (2015) for a loess sample at 28 cm below the lower boundary of the modern soil in the Lunca loess-palaeosol section (western part of the Romanian Plain, Fig. 29.1). Yet, Fitzsimmons and Hambach (2014) dated the onset of pedogenesis of modern soil in the Urluia section in Dobrogea at 11 ± 1.1 ka (Fig. 29.1). These results are contradictory, and more sites from a wider region and different topography need to be further investigated. However, such results are part of a contrasting regional

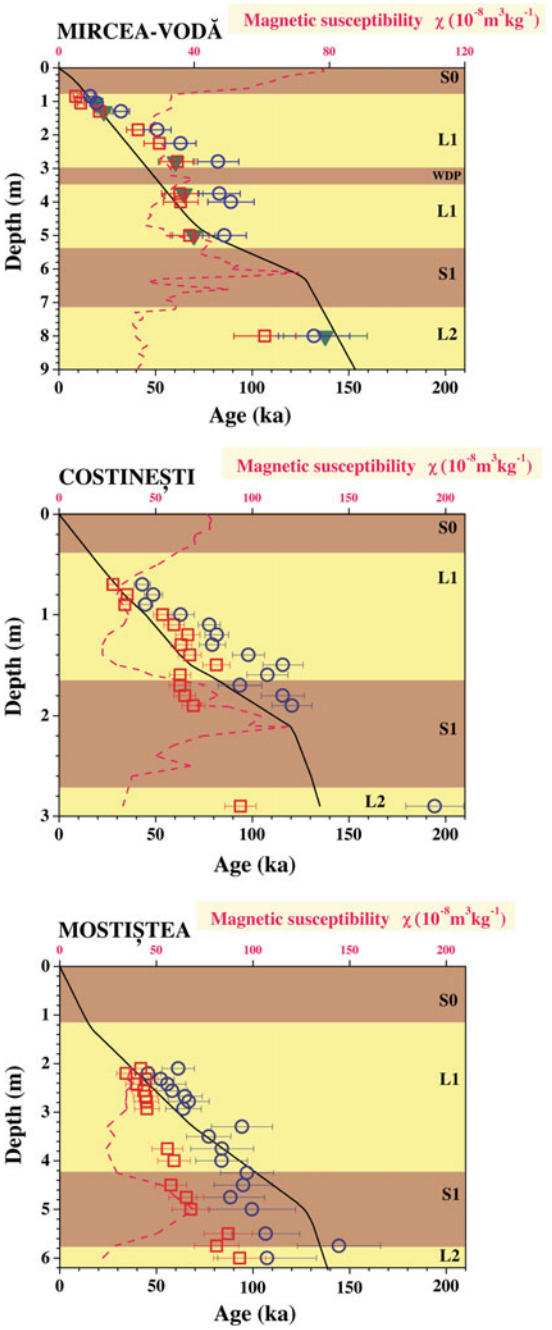

Fig. 29.4 Luminescence chronologies established for the Mircea–Vodă (Timar-Gabor et al. 2011; Vasiliniuc et al. 2012), Mostiștea (Vasiliniuc et al. 2011) and Costinești (Constantin et al. 2014; Timar-Gabor and Wintle 2013) loess sections over the Last Glacial Cycle. OSL ages using fine (4–11 μm) and coarse (63–90 μm) quartz are given with *open squares* and *open circles,* respectively, while the uncorrected post–IR IR225 polymineral fine grains ages are indicated with *filled triangles*. Luminescence ages are compared with a magnetic age-depth model (*black solid line*) and the magnetic susceptibility variations along the profile are represented by *pink-dashed lines*. *Error bars* show 1σ total uncertainty. WDP stands for the weakly developed palaeosol in L1 loess unit

framework reported from Vojvodina (Serbia) and Hungarian loess (Marković et al. 2014 and references therein) that document a possible lag for the terrestrial sediments, compared to marine or ice sediments, in recording the environmental response to climate change associated with the transition from Late Glacial to Holocene.

The quartz OSL chronologies of the three Romanian key sections indicate that deposition of the uppermost loess unit occurred during MIS 2–4 (Fig. 29.4a–c). Despite noticeable variations in the magnetic susceptibility curve along the L1 loess at Costineşti and Mostiştea sections, the loess accumulation was continuous and uninterrupted by pedogenesis. However, for Mircea-Vodă section, magnetic susceptibility trends and quartz OSL ages (Timar et al. 2010), polymineral fine grains IRSL ages (Vasiliniuc et al. 2013b) and post–$IR_{50}IR_{225}$ ages (Vasiliniuc et al. 2012) assigned the formation of a weakly developed palaeosol during MIS 3. The obtained luminescence chronologies in Romania are in agreement with the magnetic age-depth models developed over the Last Glacial period (Fig. 29.4) and can be well correlated to those from Serbia (Schmidt et al. 2010; Stevens et al. 2011) or Hungary (Schatz et al. 2012). The quartz SAR–OSL ages (Fig. 29.4) confirm the chronostratigraphic position of S1 palaeosols from Mircea–Vodă, Mostiştea and Costineşti, in that it formed during MIS 5 (132–71 ka; Lisiecki and Raymo 2005). This warm and humid interglacial period was proceeded by the major glacial advance known as the Saalian glacial or MIS 6 (191–132 ka; Lisiecki and Raymo 2005). Even though, this period is generally perceived as beyond the reach of quartz SAR–OSL luminescence dating, coarse quartz extracted from samples collected from the top of the L2 layer indicating loess deposition at around 132 ± 18 ka (Timar-Gabor et al. 2011) and ~194 ± 15 ka (Constantin et al. 2014) at Mircea–Vodă and Costineşti (Fig. 29.4). The obtained OSL chronologies as well as the magnetic age-depth model indicate that the long-held stratigraphic framework for the Quaternary deposits in this region established by Conea (1969, 1972) needs re-evaluation. According to it, the two uppermost palaeosol horizons were interpreted as interstadials of the last glacial while only the following third palaeosol is assumed to have formed during the Last Interglacial.

Several studies acknowledge situations where variability and hiatuses characterize the dust accumulation during glacial periods (Stevens et al. 2007; Buylaert et al. 2008; Roberts 2008). Development of absolute chronologies at high-resolution allows the identification of such discontinuities and calculation of reliable sedimentation rates for loess. The quartz OSL-based chronologies of the L1 unit at Mostiştea and Mircea–Vodă revealed that loess sedimentation, although continuous, occurred at different magnitudes within the same unit, as well as at different sites. Thus, the dust deposited during MIS 2 at a slower rate in Mostiştea and Mircea–Vodă (2.9 cm ka^{-1}; Vasiliniuc et al. 2011 and 3.5 cm ka^{-1}; Timar-Gabor et al. 2011) than in MIS 4 at 7.3 and 25 cm ka^{-1}, respectively. Similar amplitude of climatic variability during cold stadials of the last glacial period have been recorded in loess sections from the western Romanian Plain at Lunca (Constantin et al. 2015), as well as in Vojvodina (Schmidt et al. 2010). Yet, exceptional high accumulation rates for MIS 2 (Last Glacial Maximum), amounting

to 6–8 m within several thousand years (up to 2.4 m ka^{-1}) have been reported by Fitzsimmons and Hambach (2014) at Urluia (Dobrogea), near Mircea–Vodă. The major factor that influenced such a high depositional rate is considered to be the underlying topography, with loess being deposited in a dome-like structure. Loess deposition comparable to that at Urluia occurred in Serbian loess sites of Surduk (Antoine et al. 2009) and Belotinac (Basarin et al. 2011) as well as at Süttő, in Hungary (Novothny et al. 2011). The balance of evidence inclines towards the MIS 2 as the most substantial deposition phase across the Danube basin (Fitzsimmons and Hambach 2014). Such a basin-wide variable depositional context highlights the role that absolute chronologies play in establishing a consistent stratigraphic framework for the Danubian loess.

The glacial periods of MIS 10, MIS 8, and MIS 6 are classified as a part of the big polycyclic Saalian (Riss) glaciation (Kukla 2005). In the study of Vasiliniuc et al. (2012) post IR–IR_{225} ages for L2, L3 and L4 the (uncorrected for fading) ages obtained by applying post IR–IR_{225} on polymineral fine grains yielded ages of 156 ± 24 ka, 269 ± 46 ka and 415 ± 83 ka, respectively. The ages are in good agreement with the palaeomagnetic time depth model and assign these units to MIS6, MIS 8 and MIS 10. The obtained chronologies sustained the previously reported broad IRSL dating using alkali feldspars (Bălescu et al. 2003, 2010) on loess sections from Dobrogea (Mircea–Vodă and Tuzla).

Point Age Control—The Campanian Ignimbrite/Y5 Tephra

Tephrochronology is a widespread method for linking and dating various records, and in synchronizing/comparing palaeoclimate events (Lowe 2011). The method is based on mineralogical examination, as well as on the geochemical fingerprinting of glass shards or minerals using an electron microprobe or similar analytical tools, including laser ablation mass spectrometry or the ion microprobe. Dating can be performed either directly on the volcanic products, such as through argon–argon dating, or more commonly, through the close contact dating (radiocarbon, luminescence, varve chronology, etc.) of sediments embedding tephras. When a genetic linking is established with the source volcanic field, and a reliable age control is also available, tephra layers provide marker horizons of exceptional value in comparing records and in constraining other chronological data, including luminescence ages (Constantin et al. 2012; Vereș et al. 2012; Anechitei-Deacu et al. 2013).

Here, we present a synopsis of latest advances in developing a tephrostratigraphic framework for the Lower Danube region, reviewing the chemical and chronological data on volcanic ash layers embedded in Pleistocene terrestrial sedimentary successions in southwestern Romania (Constantin et al. 2012; Vereș et al. 2012) (Fig. 29.5), alongside several occurrences within Dobrogea (Fitzsimmons et al. 2013; Anechitei-Deacu et al. 2013). For all these tephra layers, analyses of major oxide concentrations of glass shards yielded phonolite/trachyte compositions highly

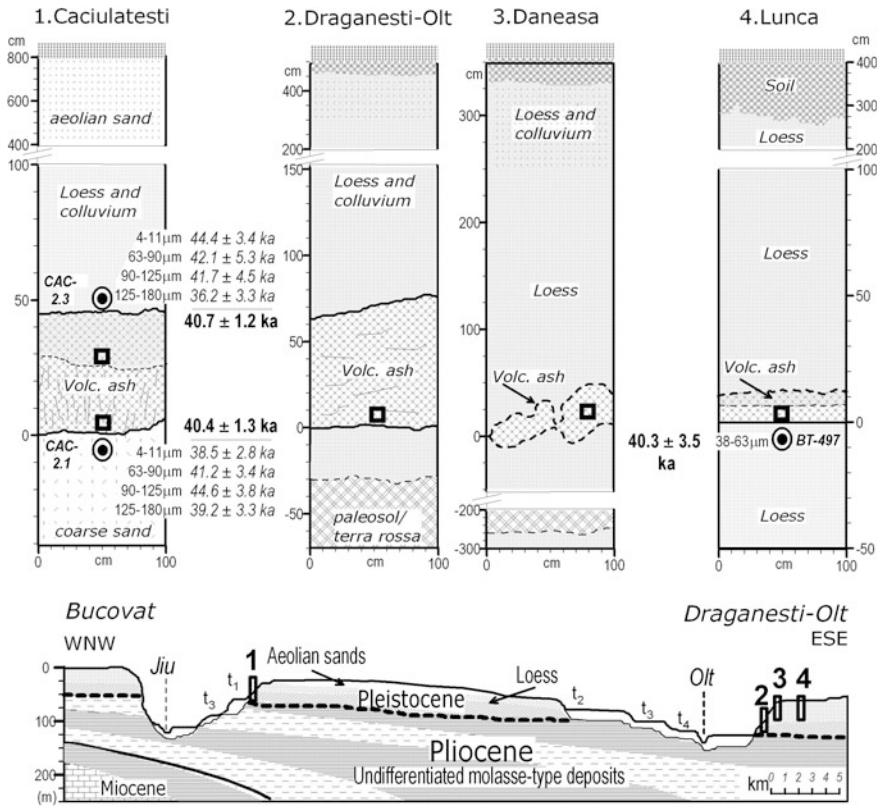

Fig. 29.5 Schematic representation of the sedimentary profiles studied in the Jiu–Olt valleys including the outlines of volcanic *ash* occurrences. The base of the *ash* layers is taken as 0 cm on the profiles (note that profiles are at different scales). *Circles* represent the stratigraphic position and related optical ages of the luminescence ages. The *lower panel* presents a schematic representation of the Pliocene–Pleistocene sedimentary infill of the Dacic Basin between the lower Jiu (Bucovăț village) and Olt (town of Drăgănești–Olt) river valleys alongside details on surface morphology (modified after Liteanu and Bandrabur 1960). The *dashed line* shows the supposed limit between Pliocene–Pleistocene sediments and the relative locations of the profiles investigated in this study are shown by the *numbered rectangles* (*1* Căciulătești; *2* Drăgănești–Olt; *3* Dăneasa; *4* Lunca). Note that the profiles of Drăgănești–Olt and Dăneasa are located circa 2 km apart, while the site of Lunca is located circa 25 km to the south. Modified from Vereș et al. (2012)

consistent between the different ash occurrences, but also with the Campanian Ignimbrite/Y5 (hereafter CI) tephra. Therefore, all the tephra occurrences discussed are geochemically assigned to CI tephra originating in the Phlegrean fields of southern Italy, in one of the most explosive volcanic eruptions in Europe during the Late Quaternary (Fedele et al. 2003). It is absolutely dated by $^{40}Ar/^{39}Ar$ method to 39.28 ± 0.11 ka (De Vivo et al. 2001), and the fine ash component of this eruption has been identified widely in lacustrine, marine, loess, and cave sediments, extending from central Mediterranean to North Africa and the Volga Plain.

Jiu Valley: The sedimentary profile investigated is a ravine cut outcrop at Căciulăteşti (N–43′56′3″; E–23°56′6″) in the upper terrace (T1) deposits of Jiu River (Fig. 29.5). It consists of around 50 cm thick tephra that rests upon consolidated sands mixed with thin layers of fluvial gravels (Bandrabur 1971). The tephra is covered by 4 m of loess and colluvium, with the whole suite overlain by 7–10 m of loose aeolian sands forming dunes, likely Holocene to present in age. Here, the SAR–OSL protocol was applied in dating a suite of selected grain-sized quartz separated from the embedding fluvial sands and loess, yielding composite ages of 40.7 ± 1.2 and 40.3 ± 1.3 ka, respectively (Constantin et al. 2012), matching both the age of the CI, but also significantly refining the local chronostratigraphic framework (Vereş et al. 2012).

Olt valley: at the sites of Drăgăneşti–Olt (N–44°09′36″; E–24°32′49″) and Dăneasa (N–44°09′6″; E–24°33′8″) a grey-yellowish ash layer is embedded in an approximately 5–10 m thick succession of discontinuous loess-palaeosol and colluviums resting upon tens of metres of sands, marls and gravels, regionally known as the Frăteşti beds, supposedly Pleistocene in age (Liteanu and Bandrabur 1960). The ash layer is in places significantly thick (up to 75 cm) and homogenous. To the south, at the site of Lunca (N–43°5′41″; E–24°46′17″), the CI is embedded in typical loess. Although its thickness is more tapered here, the CI ash is traceable laterally over a large span that opens new perspectives for investigating other profiles in the region. The OSL dating at Lunca yielded an age of 40.3 ± 3.5 ka (Vereş et al. 2012), confirming the results of glass chemical fingerprinting that showed the ash as yet another regional occurrence of the CI. It also allowed direct stratigraphic comparisons between the sedimentary successions of Drăgăneşti–Olt/Dăneasa situated at the limit between loess and alluvial sedimentation of the Dacic Basin, and the proper LPS succession of Lunca, in the Danube Plain.

Danube valley: at the Valea cu Pietre location within Rasova village (Fig. 29.1) there is a truncated loess profile hosting circa 20 cm thick ash layer. The multi-method luminescence investigations applied here included the SAR–OSL dating on aliquots of fine (4–11 μm) and medium-grained (63–90 μm) quartz, as well as single grain analyses on 125–180 μm quartz on samples from the embedding sediments (Anechitei-Deacu et al. 2013). Fine-grained (4–11 μm) quartz SAR–OSL analyses yielded ages of 44.4 ± 4.5 ka below the ash, and 41.4 ± 4.2 ka above the ash layer. Single grain analysis demonstrates, however that coarse material from these samples exhibited low sensitivity and responded poorly to internal checks of the SAR protocol, in contrast with the behavior of the finer sediment.

Dobrogea—Urluia quarry site is a substantial exposure of loess-palaeosols and limestone basement rocks located on the Dobrogea loess (Fitzsimmons et al. 2013), approximately 15 km south of the Danube, within a zone of particularly thick loess deposits (Jipa 2014). An unexpectedly thick tephra deposit reaching up to 110 cm in height has been found within the uppermost loess level (circa 14 m thick) that represents the last full glacial cycle. Chemical fingerprinting of glass shards confirmed that this occurrence is related to the CI ash fall. The OSL dating results of two loess profiles embedding the tephra also confirm the chronological linking of

this ash occurrence to the CI (Fitzsimmons et al. 2013). Here, the ash fallout might have sealed a palaeovalley draining through the loess field (from where the exceptional thickness), but nevertheless, given its consistent thickness and widespread occurrence in Dobrogea (it has been visually identified in several other locations between the Danube valley and Urluia), it will certainly play a strong role in providing a securely dated framework for MIS 3 loess deposits in the region.

Based on our observations, it appears that in all analyzed locations as well as on other sites undergoing investigations (southeast Romania) the widespread CI tephra is a primary deposit, with a consistent fine ash deposit that blanketed the topography both thickly and rapidly, with potentially catastrophic impacts on local ecosystems, including Palaeolithic humans (Fitzsimmons et al. 2013). Thus, it currently forms the most important, absolutely dated stratigraphic marker horizon, that in our case allows direct comparison in both chronological and palaeoclimatic terms between the Romanian loess records and various palaeoclimate archives from the Mediterranean–Black Sea area. The event also coincided with the onset of the extremely cold climatic phase Heinrich Event 4; it is has been assumed that their combined effect may have exacerbated the severity of the climate through linked feedbacks across the North Atlantic region (Fitzsimmons et al. 2013).

Concluding Remarks

The study of terrestrial records in Romania that archive past climate information are highly desirable for a deeper understanding of the effects past global climate change had on the continental interiors of Europe. Here, we presented a synopsis of the latest dating efforts for providing master records in the loess fields of the Lower Danube.

We have shown that recent applications of luminescence dating on several key LPS from Romania clearly opened new perspectives for loess research in this region, considerably advancing the understanding of mechanisms related to loess deposition and the chronological span covered. Thus, the luminescence chronologies discussed here—although still site-specific—improved and expanded the long-held stratigraphy of Romanian loess constructed by Conea (1970), suggesting that a re-evaluation of the regional chronostratigraphic inferences in a multi-method high-resolution dating approach must be attempted. For example, the loess magnetic time series constrained by luminescence results, have shown that the environmental response to the climate shifts up to the penultimate glacial supercycle (Saal or Riss) was archived in the four uppermost loess layers and the intercalated well-developed fossil soils.

As proved by the high-resolution chronologies, the sedimentation rates of loess varied during the last glacial (Weichselian) both within a specific loess section, as well as between loess sections from the same region, the major factor being the topographic context—in order to offset such events, a better spatial coverage with the emergence of new LPS profiles is desirable. Even more, and although additional

absolute dating is required, emerging OSL ages indicate a delayed start of the Holocene soil formation in loess sections from southeastern Romania, as well as in Serbia. This observation brings important implications in what concerns the synchronicity of change with respect with leads/lags in the climate system modulated by past regional hydroclimatic differences. Therefore, the improved site-specific chronologies, if continually refined, should allow for more secure regional correlations with other archives, particularly when aided by the presence of well-defined isochronous marker horizons, such as tephra layers. To illustrate this, we discussed several occurrences of the Campanian Ignimbrite/Y5 tephra layer in loess/terrestrial deposits from the Lower Danube region, and the implications arising in securely correlating records and assessing the reliability of luminescence dating of various terrestrial deposits. However, for an outstanding use of such marker horizons as chronostratigraphic tools, refining (both in chronological and sedimentological terms) the regional stratigraphic contexts and improved spatial coverage of sites is also a necessity. This is even more important as current efforts within our community aim at building a comprehensive pan-European loess stratigraphic framework for Middle and Late Pleistocene, including the Danube basin stratigraphy correlated to the well-established Chinese loess stratigraphy.

Hopefully, following a similar approach as discussed in this contribution, including high-resolution sampling and combination of quartz and feldspar luminescence dating methods applied on multiple grain sizes would yield consistent results leading to more site-specific chronologies with reduced uncertainties that would allow attaining the necessary precision for achieving fine correlations even on centennial–to–millennial time scale changes.

Acknowledgments AT-G, DV and DC acknowledge the financial support from a grant of the Romanian National Authority for Scientific Research CNCS-UEFISCDI, PN-II-RU-TE-2011-3-0062, nr. 73/05.10.2011. Also DC acknowledges the financial support of the Sectorial Operational Programme for Human Resources Development 2007–2013, co-financed by the European Social Fund under the project POSDRU/159/1.5/S/133391-"Doctoral and postdoctoral excellence programmes for training highly qualified human resources for research in the fields of Life Sciences, Environment and earth". DV acknowledges support from grant PN-II-ID-PCE-2012-4-0530 of the Romanian National Authority for Scientific Research CNCS-UEFISCDI and grant GTC_34029/2013 from Babeş-Bolyai University.

References

Anechitei-Deacu V, Timar-Gabor A, Fitzsimmons KE, Veres D, Hambach U (2013) Multi-method luminescence investigations on quartz grains of different sizes extracted from a loess section in Southeast Romania interbedding the Campanian Ignimbrite ash layer. Geochronometria 14(1):1–14

Antoine P, Rousseau DD, Fuchs M, Hatte C, Gauthier C, Markovic SB, Jovanovic M, Gaudenyi T, Moine O, Rossignol J (2009) High-resolution record of the last climatic cycle in the southern Carpathian Basin (Surduk, Vojvodina, Serbia). Quat Int 198:19–36

Bălescu S, Lamothe M, Mercier N, Huot S, Bălteanu D, Billard A, Hus J (2003) Luminescence chronology of Pleistocene loess deposits from Romania: testing methods of age correction for anomalous fading in alkali feldspars. Quat Sci Rev 22:967–973

Bălescu S, Lamothe M, Panaiotu C, Panaiotu CG (2010) La chronologie IRSL des sequences loessiques de L'Est de la Roumanie. Quat 21:115–126

Bandrabur T (1971) Geologia Câmpiei Dunărene dintre Jiu și Olt. Studii Tehnice și Economice J9, 7e146 (in Romanian)

Basarin B, Vandenberghe DAG, Markovič M, Catto N, Hambach U, Vasiliniuc V, Derese C, Roncevic S, Vasiljevic DA, Rajic L (2011) The Belotinac section (Southern Serbia) at the southern limit of the European loess belt: initial results. Quat Int 240:128–138

Buggle B, Glaser B, Zoller L, Hambach U, Marković SB, Glaser I, Gerasimenko N (2008) Geochemical characterisation and origin of South-eastern and Eastern European loesses (Serbia, Romania, Ukraine). Quat Sci Rev 27:1058–1075

Buggle B, Hambach U, Glaser B, Gerasimenko N, Marković SB, Glaser I, Zoller L (2009) Stratigraphy, and spatial and temporal paleoclimatic trends in Southeastern/Eastern European loess–paleosol sequences. Quat Int 196:86–106

Buylaert JP, Murray AS, Vandenberghe D, Vriend M, De Corte F, Van den haute P (2008) Optical dating of Chinese loess using sand-sized quartz: establishing a time frame for late Pleistocene climate changes in the western part of the Chinese loess plateau. Quat Geochronol 3:99–113

Conea A (1969) Profils de loess en Roumanie. La stratigraphie des loess d'Europe. In: Fink J (ed) Bulletin de l'Association française pour l'étude du Quaternaire. Suppl. INQUA: 127–134

Conea A (1972) Guidebook to excursion of the INQUA Loess symposium in Romania, 11–15 Sept 1972. Geological Institute Bucharest

Constantin D, Timar-Gabor A, Vereș D, Begy R, Cosma C (2012) SAR-OSL dating of different grain-sized quartz from a sedimentary section in southern Romania interbedding the Campanian Ignimbrite/Y5 ash layer. Quat Geochronol 10:81–86

Constantin D, Begy R, Vasiliniuc S, Panaiotu C, Necula C, Codrea V, Timar-Gabor A (2014) High-resolution OSL dating of the Costineşti section (Dobrogea, SE Romania) using fine and coarse quartz. Quat Int 334–335:20–29

Constantin D, Camenita A, Panaiotu C, Necula C, Codrea V, Timar-Gabor A (2015) Fine and coarse-quartz SAR-OSL dating of Last Glacial loess in Southern Romania. Quat Int 357:33–43

De Vivo B, Rolandi G, Gans PB, Calvert A, Bohrson WA, Spera FJ, Belkin HE (2001) New constraints on the pyroclastic eruptive history of the Campanian volcanic Plain (Italy). J Miner Petrol Sci 73:47–65

Evans ME, Heller F (2003) Environmental magnetism. Principles and applications of enviromagnetics. Academic Press, Amsterdam

Fedele FG, Giaccio B, Isaia R, Orsi G (2003) The Campanian ignimbrite eruption, Heinrich event 4, and Palaeolithic change in Europe: a high-resolution investigation. In Volcanism and the earth's atmosphere. Geophys Monogr 139:301–325

Fitzsimmons KE, Hambach U (2014) Loess accumulation during the last glacial maximum: evidence from Urluia, southeastern Romania. Quat Int 334–335:74–85

Fitzsimmons KE, Marković SB, Hambach U (2012) Pleistocene environmental dynamics recorded in the loess of the middle and lower Danube basin. Quat Sci Rev 41:104–118

Fitzsimmons KE, Hambach U, Vereș D, Iovita R (2013) The Campanian ignimbrite eruption: new data on volcanic ash dispersal and its potential impact on human evolution. PLoS ONE 8: e65839

Fletcher WJ, Sanchez Goni MF, Allen JRM, Cheddadi R, Combourieu-Nebout N, Huntley B, Lawson I, Londeix L, Magrih D, Margarif V, Müller UC, Naughton F, Novenko E, Roucoux K, Tzedakis PC (2010) Millennial-scale variability during the last glacial in vegetation records from Europe. Quat Sci Rev 2010:2839–2864

Haase D, Fink J, Haase G, Ruske R, Pécsi M, Richter H, Altermann M, Jäger K-D (2007) Loess in Europe—its spatial distribution based on a European Loess Map, scale 1:2,500,000. Quat Sci Rev 26:1301–1312

Hemming SR (2004) Heinrich events: massive late Pleistocene detritus layers of the North Atlantic and their global climate imprint. Rev Geophys 42:RG1005. doi:10.1029/2003RG000128
Jipa DC (2014) The conceptual sedimentary model of the Lower Danube loess basin: sedimentogenetic implications. Qua Int 351:14–24
Jordanova D, Petersen N (1999) Paleoclimatic record from a loess soil profile in northeastern Bulgaria-II. Correlation with global climatic events during the Pleistocene. Geophys J Int 138:533–540
Kadereit A, Wagner GA (2014) Geochronological reconsiderations for the Eastern European key loess section at Stayky in Ukraine. Clim Past 10:783–796
Kukla G (2005) Saalian supercycle, Mindel/Riss interglacial and Milankovitch dating. Qua Sci Rev 24:1573–1583
Lisiecki LE, Lisiecki PA (2002) Application of dynamic programming to the correlation of paleoclimate records. Paleoceanography (17):1049. doi:10.1029/2001PA000733
Lisiecki LE, Raymo ME (2005) A Pliocene-Pleistocene stack of 57 globally distributed benthic $\delta^{18}O$ records. Paleoceanography 20:PA1003. doi:10.1029/2004PA001071
Liteanu E, Bandrabur T (1960) Géologie de la Plaine Gétique Méridionale d'entre leJiu et l'Olt, vol. 29/30. Annuaire du Comité Géologique, pp 171–182
Lowe DJ (2011) Tephrochronology and its application: a review. Quat Geochronol 6:107–153
Maher BA (2011) The magnetic properties of quaternary aeolian dusts and sediments, and their palaeoclimatic significance. Aeolian Res 3:87–144
Maher BA, Thompson R (1999) Quaternary climates, environments and magnetism. Cambridge University Press, Cambridge
Marković SB, Timar-Gabor A, Stevens T, Hambach U, Popov D, Tomić N, Obrecht I, Jovanović M, Lemhkhul F, Kels H, Markovic R, Gavrilov M (2014) Environmental dynamics and luminescence chronology from the Orlovat loess–palaeosol sequence (Vojvodina, northern Serbia). J Quat Sci 29:189–199
Marković SB, Stevens T, Kukla GJ, Hambach U, Fitzsimmons KE, Gibbard P, Buggle B, Zech M, Guo Z, Hao Q, O'Hara Dhand K, Smalley I, Újvári G, Sümegi P, Timar-Gabor A, Veres D, Sirocko F, Jary Z, Svensson A, Jović V, Kovács J, Zvirčev Z, Vasiljević DA (2015) The Danube loess stratigraphy—new steps towards a pan-European loess stratigraphic model. Earth-Sci Rev 148:228–258
Necula C, Panaiotu C (2008) Application of dynamic programming to the dating of a loess paleosol sequence. Rom Rep Phys 60:157–171
Novothny A, Frechen M, Horvath E, Bradák B, Oches EA, McCoy WD, Stevens T (2009) Luminescence and amino acid racemization chronology of the loess-paleosol sequence at Sutto, Hungary. Quat Int 198:62–76
Panaiotu CG, Panaiotu EC, Grama A, Necula C (2001) Paleoclimatic record from a loess-paleosol profile in Southeastern Romania. Phys Chem Earth (A) 26(11–12):893–898
Rădan SC (2012) Towards a synopsis of dating the loess from the Romanian Plain and Dobrogea: authors and methods through time. Geo-Eco-Marina 18:153–172
Roberts HM (2008) The development and application of luminescence dating to loess deposits: a perspective on the past, present and future. Boreas 37:483–507
Rousseau D-D, Antoine P, Hatté C, Lang A, Zoller L, Fontugne M, Ben Othman D, Luck JM, Moine O, Labonne M, Bentaleb I, Jolly D (2002) Abrupt millennial climatic changes from Nussloch (Germany) Upper Weichselian Eolian records during the last glaciation. Rapid Commun Quat Sci Rev 21(14–15):1577–1582
Rousseau D-D, Antoine P, Gerasimenko N, Sima A, Fuchs M, Hatté C, Moine O, Zoeller L (2011) North Atlantic abrupt climatic events of the last glacial period recorded in Ukrainian loess deposits. Clim Past 7:221–234
Schatz A-K, Buylaert J-P, Murray A, Stevens T, Scholten T (2012) Establishing a luminescence chronology for a palaeosol-loess profile at Tokaj (Hungary): a comparison of quartz OSL and polymineral IRSL signals. Quat Geochronol 10:68–74

Schmidt ED, Machalett B, Marković SB, Tsukamoto S, Frechen M (2010) Luminescence chronology of the upper part of the Stari Slankamen loess sequence (Vojvodina, Serbia). Quat Geochronol 5:137–142

Stevens T, Thomas DSG, Armitage SJ, Lunn HR, Lu H (2007) Reinterpreting climate proxy records from late Quaternary Chinese loess: a detailed OSL investigation. Earth-Sci Rev 80:111–136

Stevens T, Marković SB, Zech M, Hambach U, Sümegi P (2011) Dust deposition and climate in the Carpathian Basin over an independently dated last glacial–interglacial cycle. Quat Sci Rev 30:662–681

Svensson A, Andersen KK, Bigler B, Clausen HB, Dahl-Jensen D, Davies SM, Johnsen SJ, Muscheler R, Rasmussen SO, Röthlisberger R, Peder Steffensen J, Vinther BM (2006) The Greenland ice core chronology 2005, 15–42 ka. Part 2: comparison to other records. Quat Sci Rev 25:3258–3267

Svensson A, Andersen KK, Bigler M, Clausen HB, Dahl-Jensen D, Davies SM, Johnsen SJ, Muscheler R, Parrenin F, Rasmussen SO, Röthlisberger R, Seierstad I, Steffensen JP, Vinther BM (2008) A 60 000 year Greenland stratigraphic ice core chronology. Clim Past 4:47–57

Timar A, Vandenberghe D, Panaiotu EC, Panaiotu CG, Necula C, Cosma C, Van den haute P (2010) Optical dating of Romanian loess using fine-grained quartz. Quat Geochronol 5:143–148

Timar-Gabor A, Wintle AG (2013) On natural and laboratory generated dose response curves for quartz of different grain sizes from Romanian loess. Quat Geochronol 18:34–40

Timar-Gabor A, Vandenberghe DAG, Vasiliniuc S, Panaoitu CE, Panaiotu CG, Dimofte D, Cosma C (2011) Optical dating of Romanian loess: a comparison between silt-sized and sand-sized quartz. Quat Int 240:62–70

Vasiliniuc Ş, Timar-Gabor A, Vandenberghe DAG, Panaiotu CG, Begy CS, Cosma C (2011) A high resolution optical dating study of the Mostiştea loess-palaeosol sequence (SE Romania) using sand-sized quartz. Geochronometria 38:34–41

Vasiliniuc Ş, Vandenberghe DAG, Timar-Gabor A, Panaiotu CG, Cosma C, van den Haute P (2012) Testing the potential of elevated temperature post-IR IRSL signals for dating Romanian loess. Quat Geochronol 10:75–80

Vasiliniuc Ş, Vandenberghe DAG, Timar-Gabor A, Cosma C, van den Haute P (2013a) Combined IRSL and post-IR OSL dating of Romanian loess using single aliquots of polymineral fine grains. Quat Int 293:15–21

Vasiliniuc Ş, Vandenberghe DAG, Timar-Gabor A, van den Haute P (2013b) Conventional IRSL dating of Romanian loess using single aliquots of polymineral fine grains. Radiat Meas 48:60–67

Vereş D, Lane CS, Timar-Gabor A, Hambach U, Constantin D, Szakács A, Fülling A, Onac BP (2012) The Campanian ignimbrite/Y5 tephra layer—a regional stratigraphic marker for Isotope Stage 3 deposits in the Lower Danube region, Romania. Quat Int 293:22–33

Wang YJ, Cheng H, Edwards RL, An ZS, Wu JY, Shen C-C, Dorale JA (2001) A high resolution absolute-dated Late Pleistocene Monsoon record from Hulu Cave, China. Science 294:2345–2348

Wintle AG (2008) Luminescence dating where it has been and where it is going. Boreas 37:471–482

Wintle AG, Murray AS (2006) A review of quartz optically stimulated luminescence characteristics and their relevance in single-aliquot regeneration dating protocols. Radiat Meas 41:369–391

Wolff EW, Fischer H, Rothlisberger R (2009) Glacial terminations as southern warmings without northern control. Nat Geosci 2:206–209

Zech M, Zech R, Buggle B, Zoeller L (2011) Novel methodological approaches in loess research—interrogating biomarkers and compound-specific stable isotopes, Eiszeitalter und Gegenwart. Quat Sci J 60:170–187

Chapter 30
Lakes, Lacustrine Sediments, and Palaeoenvironmental Reconstructions

Marcel Mîndrescu, Gabriela Florescu, Ionela Grădinaru and Aritina Haliuc

Abstract Acting as sensitive and accurate barometers, lake and peat sediment records enable us to acquire an increasingly broader perspective on the mechanisms behind climatic and environmental changes. Over the past two decades, the rising number and amount of data yielded by palaeolimnological studies for the Central–Eastern Europe, in general, and Romania, in particular, allowed for the construction of a wide network of well-dated records which enabled comparison with the hallmark palaeoclimatic event stratigraphy of the North–Atlantic area and Western Europe. More specifically, the combined use of biological indicators with physical and geochemical data resulted in a multi-proxy approach for a variety of sites extending from the Transylvanian lowlands to the uplands of the Romanian Carpathians and spanning throughout the Holocene to the Pleniglacial. This section introduces a brief synthesis of the most outstanding results delivered by various investigations on Romanian lake and peat archives. Among these, lakes and peat bogs which came into existence during deglaciation, including both glacial lakes located in higher elevation mountain areas and lakes formed at lower elevations due to landslides subsequent to permafrost thaw are prevalent, and were preferred for such studies due to their long lifespan and location in mountain areas which have exhibited increased sensitivity to centennial and millennial-scale climate changes. The potential of lacustrine sediments for inferring past dynamics of climate and

M. Mîndrescu (✉) · G. Florescu · I. Grădinaru · A. Haliuc
Cirques and Lakes Research Group, Ștefan Cel Mare University, Universității 13, 720229 Suceava, Romania
e-mail: marcel.mindrescu@gmail.com

G. Florescu
e-mail: gabriella.florescu@yahoo.com

I. Grădinaru
e-mail: ionela.gradinaru@gmail.com

A. Haliuc
e-mail: aritinahaliuc@gmail.com

M. Rădoane and A. Vespremeanu-Stroe (eds.), *Landform Dynamics and Evolution in Romania*, Springer Geography,
DOI 10.1007/978-3-319-32589-7_30

environmental conditions prompts us to highlight the necessity for expanding the spatiotemporal coverage of such studies in Romania in an attempt to create a relatively unitary perspective on regional palaeoenvironmental evolution.

Keywords Lakes · Genesis · Ages · Sedimentation rates · Climatic signals · Human impact

Introduction

The earliest investigation on lacustrine sediments in Romania was carried out by de Martonne and Murgoci (1900) at Cîlcescu Lake in Parâng Mts (Southern Carpathians) whereby the nature and apparent characteristics of the sediment core were observed. Unfortunately, during the following century these early attempts at establishing lake sediment analysis as a topic of study in Romania were not ensued by similar efforts until recent times. Only in the past two decades did research in the field of lacustrine sediment analysis resume timidly and was performed mainly by biologists who focused to a considerable degree on vegetation history and study topics such as changes in vegetation structure and composition, tree line dynamics, land use changes, evolution of fire activity, etc. Such approaches were prevalent in the lacustrine sediment research conducted in the aforementioned timeframe in Romania and have produced valuable data which could be employed for further assessments of climate and environmental changes. Furthermore, researchers turned their attention to subjects such as calculating precise sedimentation rates (particularly for the last 200 years) based on absolute age data acquired from radiocarbon dating and radioactive isotope dating (^{210}Pb, ^{137}Cs) or determining recent pollution history. During recent years more complex investigations have been undertaken focusing on multi-proxy approaches (geochemistry, biological proxies). Results yielded by various geochemical and physical analyses produced data on the nature, origin and transfer of sediments comprised in lacustrine archives which are dependent on a number of variables intimately connected to geomorphology (relief, geology, catchment size, site elevation, regional climate extreme events, etc.).

Romanian Lakes

Romania is a middle-sized European country whose territory comprises of a large variety of landforms, ranging from littoral to alpine glacial relief. Accordingly, this territory is endowed with an equally diverse range of lakes located in all major landforms (plains, hills and mountains). While during the mid-20th century the estimated number of lakes was 3450 (of which 1150 anthropogenic, 27 %) amounting to 2600 km^2 total water body area, in 2010 it had augmented to as high as 3650 (of which 2147 man-made, 59 %) amounting to 4620 km^2 (Gâștescu

2010). This overall increase resulted from the multiplication of man-made lakes in an attempt to compensate for the extinction of natural water bodies mainly by draining and altering the natural evolution of the majority of lakes from the Danube Delta.

As regards the classification of Romanian lakes according to genetic typology, the Atlasul (1972–1979) lists *11 types of natural lakes*—i.e., floodplain and deltaic lakes; fluvial lakes; fluvio-marine limans and lagoons; dune lakes; loess lakes; natural dam lakes; karst lakes in salt; karst lakes in limestone; karst lakes in gypsum; volcanic crater lakes; nivation lakes; lakes formed on structural benches (many of which are in fact accommodated by gravitational faults resulting from RSFs); and glacial lakes; and *6 types of man-made lakes* classified depending on their use, as fish farms; multiple purpose lakes (hydropower and water supply); bent lakes; salt mine lakes; temporary lakes employed for flood control (polder-type); and ponds.

Romanian lakes are altogether understudied to date, both in terms of number of surveyed sites and proxies used. The earliest and one of the main approaches in lacustrine investigation focused on mapping lacustrine bathymetry and determining morphometric variables of lakes. As such, bathymetric sketches were made for all glacial lakes (with the exception of small ones) in the Transylvanian Alps (Southern Carpathians) and Rodna Mts, Eastern Carpathians (Pişota 1968, 1971). The dataset built by Pişota (1968, 1971) was the starting point for further scientific work in the field of limnology, such as creating the lacustrine index and database comprising all glacial lakes in the Romanian Carpathians (Mîndrescu et al. 2016a). To date, a large share of Romanian lakes have been mapped, providing basic data for detailed studies on lacustrine sediments. We participated in this effort by mapping and creating bathymetrical sketches for previously uncharted lakes (Mîndrescu 2001, 2003; Mîndrescu et al. 2013) or upgrading existing ones subsequent to anthropogenic interventions on lakes (Vespremeanu-Stroe et al. 2008; Mîndrescu et al. 2010b e.g., lake Ştiol, Rodna Mts).

Lake Genesis

The range of active genetic processes leading to lake formation may be ranked into three major classes according to the type of erosion/accumulation—*glacial, fluvial and maritime*, to which a passive genetic process—*dissolution of soluble rocks* (limestone, dolomite, gypsum, salt, etc.) is added. An additional type of naturally occurring water body consists of natural dam lakes emerging from landsliding processes, which are typical for highland landform evolution in Romania. The majorities of lacustrine bodies pertaining to the latter type are located in the outer Carpathian hills and plateaus, such as the Transylvanian Depression or Buzău Subcarpathians (e.g., Porumbenii Mari, Manta) and are usually small ephemeral lacustrine bodies. However, albeit fewer in number, landslide-dammed lakes formed in the higher Carpathian uplands (particularly in the flysch range) have

considerably longer lifespans (e.g., lake Bolătău–Feredeu in the Northern Carpathians, Mîndrescu et al. 2016b).

Altogether, the vast majority of lakes formed as a result of fluvial activity (e.g., the 800 lakes located in the Danube floodplain and delta alone) according to the assessment made prior to the great drainage projects (Gâştescu 2010), followed by glacial lakes. These two genetic types are largely distributed in relation to major landforms as follows: fluvial lakes in the lowlands (plains) and glacial lakes in the highlands (alpine areas). Albeit the most numerous and prominent fluvial lakes are the ones located within the Danube floodplain and deltaic area, lakes formed along the main inland rivers are also quite common. Conversely, at present glacial lakes and glacial peat bogs amount to 270 items (Mîndrescu et al. 2016a); their distribution is uneven throughout the Romanian Carpathians, with the majority located in the Southern Carpathians in highlands exceeding 2200 m above sea level (a.s.l.) in the western sector and 2400 a.s.l. in the eastern sector, whereas a small number are found in the Northern Romanian Carpathians (Rodna and Maramureş Mts). Glacial lakes are often accompanied by sackung lakes (Mîndrescu and Cristea 2011) which emerge in both glaciated environments (whereby the basins are carved in the in situ rock) and non-glaciated areas (mainly in superficial deposits).

In contrast, the least number of lakes pertains to the crater genetic type, consisting solely of three items located in Harghita Mts (Eastern Carpathians): Sfânta Ana Lake, and Mohoş and Luci peat bogs. While the Romanian Carpathians enfold the longest volcanic range in Europe, the reason for the small number of crater lakes could reside in the advanced aging of these volcanoes which resulted in the destruction of typical volcanic structures (craters, throat, etc.).

Hence, whereas lakes in Romania are relatively diverse in terms of genetic typology, they are neither as numerous nor as large as may be expected; therefore, only a relatively small share of all lakes have suitably long lifespan such that their sedimentary archives could be employed for palaeoenvironmental studies.

An Overview on Lacustrine Sites Investigated to Date

Palaeolimnological research focused thus far on 42 open lake and peat bog sites (Fig. 30.1 and Table 30.1) located throughout the Romanian territory which yielded a large amount of data regarding topics such as past climate changes, vegetation history and dynamics, past land use changes, pollution history and human impact, sedimentation rates, etc.

Site Elevation and Latitudinal Location

The locations of investigated sites range in terms of elevation from 240 to 2250 m a.s.l., albeit the majority (29) are above 1000 m a.s.l. Around 70 % are spread in the

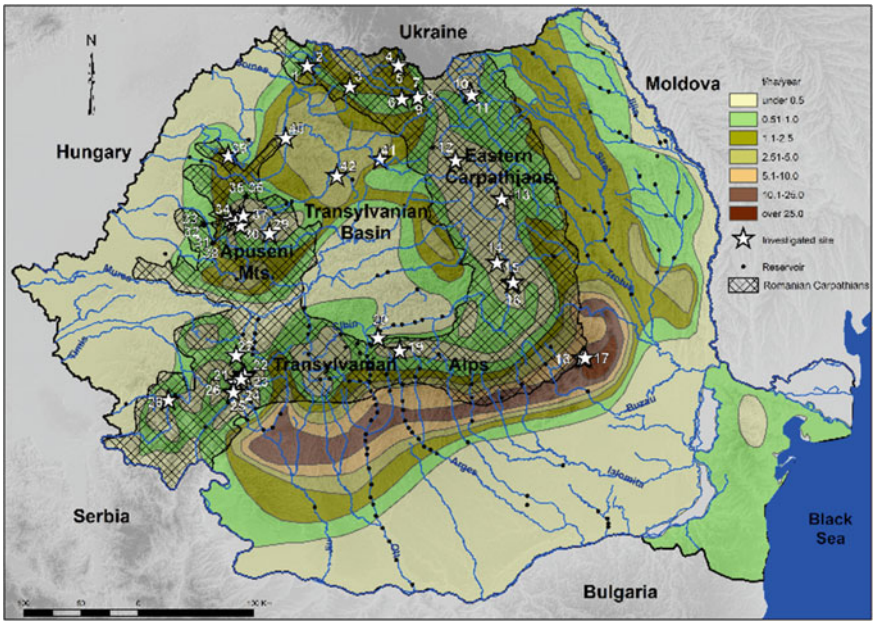

Fig. 30.1 Location of studied lake sites in relation to the specific sediment yield. The site numbers correspond to the ones listed in Table 30.1 (modified after Rădoane and Rădoane 2005; Mociornița and Brateș 1987; Diaconu 1971)

northern half of the Romanian territory, in the Northern Carpathians, Apuseni Mts, and the northern Transylvanian Depression. This particular distribution of sites preferred for palaeolimnological studies is linked to the magnitude of the vegetational response which follows an S–N latitudinal and elevational trend (Feurdean et al. 2014). Extra-Carpathian lowlands (i.e., plains, plateaus and Subcarpathians <800 m a.s.l.) are particularly underrepresented in the growing network of investigated lacustrine and peat bog sites which is likely the effect of prevailing dry conditions during the Late Glacial at low altitudes (Feurdean et al. 2007a). However, recent findings indicate that major climatic events are well expressed not only in the upland areas, as previously thought, but also in the lowland regions of Romania, where the magnitude of climate shifts is expected to be lower (Lascu et al. 2014).

Site Type and Origin

Peat bogs were prevalent (ca. 60 % of all investigated sediment archives) in terms of research interest due to the increased stability of peat bog deposition environment compared to lacustrine environments (i.e., absence of wind-induced

Table 30.1 Lacustrine sites investigated in Romania dated based on absolute date measurements (^{14}C, ^{210}Pb, etc.)

No.	Site name	Geographic location	General information (elevation, area, maximum water depth, thickness of sediment sequence, age yrs cal BP)	Type of investigated site	Estimated age (yrs cal BP)	SR[c] (mm/year)	Proxies	References
1	Preluca Ţiganului	Eastern Carpathians—Gutâiului Mts western slope 47° 48′ 83″ N 23° 31′ 91″ E	Elev. = 830 m a.s.l. Site area = 2.374 ha CA[a] = 29 ha St[b] = 10 m (hiatus) Age = 14.400 at 9.88 m	Peat bog Located in rock slope failure (sackung) Rock type = volcanic breccia	LG–H: 0–14400	0.69	Lithostratigraphy, pollen, plant macrofossil, mineral magnetic analyses (SIRM), organic matter content via LOI, charcoal, petrographic analyses (clay mineralogy and grain size measurement)	Wohlfarth et al. (2001) Björkman et al. (2002, 2003) Feurdean and Bennike (2004) Feurdean (2005) Feurdean and Astalos (2005) Feurdean et al. (2007a, b, 2008)
2	Steregoiu	Eastern Carpathians—Gutâiului Mts slope 47° 48′ 48″ N 23° 32′ 41″ E	Elev. = 930 m a.s.l. Site area = 0.59 ha CA = 12.55 ha St = 5.92(hiatus) Age = 14.000 at 5.30 m	Peat bog Located in rock slope failure Rock type = volcanic breccia	LG–H: 0–14000	0.38	Lithostratigraphy, pollen, plant macrofossils	Björkman et al. (2002) Fărcaş et al. (2006) Feurdean and Bennike (2004) Feurdean and Astalos (2005) Feurdean et al. (2007a, 2008)

(continued)

Table 30.1 (continued)

No.	Site name	Geographic location	General information (elevation, area, maximum water depth, thickness of sediment sequence, age yrs cal BP)	Type of investigated site	Estimated age (yrs cal BP)	SR[c] (mm/year)	Proxies	References
3	Vărătec (Fenyves-tetö)	Eastern Carpathians—Lăpuşului Mts 47° 39′ 43.63″ N 24° 02′ 21.77″ E	Elev. = 1340 m a.s.l. Site area = 1.2 ha CA = 2.84 ha St = 4.0 (hiatus) Age = 9102 at 3.81 m	Peat bog located in rock slope failure Rock type = volcanic breccia	H: 0–approx. 9790 (older but no 14C dates)	0.42	Lithostratigraphy, geochemistry, testate amoebae, humification	Schnitchen et al. (2003, 2006)
4	Tăul Mare Bardău	Eastern Carpathians—Maramureş Mts 47° 50′ 08.89″ N 24° 35′ 42.62″ E	Elev. = 1615 m a.s.l. Site area = 0.84 ha CA = 5.34 ha St = 3.80 m Age = 7030 at 3.79 m	Peat bog Located in glacial cirque Rock type = conglomerates	H: 0–7030	0.54	Lithostratigraphy, pollen, carbon isotopic composition of bulk peat, sedimentation rates (SR) using ^{210}Pb, ^{226}Ra, ^{137}Cs and ^{241}Am	Fărcaş et al. (2013) Cristea et al. (2014) Hutchinson et al. (2015)
5	Cristina	Eastern Carpathians—Maramureş Mts 47° 50′ 09.08″ N 24° 37′ 08.18″ E	Elev. = 1573 m a.s.l. Area = 0.12 ha CA = 21.05 ha St = 3.01 m Age = 8000 at 3.01 m	Peat bog with pool Located in glacial cirque Sampled in peat Rock type = conglomerates	H: 2300–8000	0.38	Lithostratigraphy, pollen	Fărcaş et al. (2013)
6	Buhăescu Mare	Eastern Carpathians—Rodna Mts, northern slope	Elev. = 1918 m a.s.l. Pool area = 0.1 ha Peat bog area = 1.44 ha CA = 15.75	Peat bog with pool Located in glacial cirque Sampled in pool area	H: 0–10000	0.09	Lithostratigraphy, pollen, stomata, plant macrofossils, magnetic	Geantă et al. (2014) Hutchinson et al. (2015)

(continued)

Table 30.1 (continued)

No.	Site name	Geographic location	General information (elevation, area, maximum water depth, thickness of sediment sequence, age yrs cal BP)	Type of investigated site	Estimated age (yrs cal BP)	SR[c] (mm/year)	Proxies	References
		47° 34′ 21.51″ N 23° 38′ 31.12″ E	St = 1.25 m (hiatus) Water depth = 0.5 m Age = 9928 at 0.86 m	Rock type = crystalline schist			susceptibility, charcoal, organic carbon content (LOI), elemental geochemistry, grain size, sedimentation rates (SR) using ^{210}Pb, ^{226}Ra, ^{137}Cs and ^{241}Am	
7	Gărgălău	Eastern Carpathians—Rodna Mts, northern slope 47^0 34′ 25.65″ N 24^0 48′ 10.23″ E	Elev. = 1812 m a.s.l. Site area = 1.62 ha CA = 16.21 ha St = 1.50 m Age = 11200 at 1.50 m	Peat bog Located in glacial cirques Rock type = crystalline schist	H: 160–11200	0.13	Pollen and spore analysis, AMS radiocarbon dates	Tanţău et al. (2014)
8	Știol[d]	Eastern Carpathians—Rodna Mts, northern slope 47° 34′ 30″ N 24° 48′ 55″ E	Elev. = 1670 m a.s.l. Site area = 0.059 ha (lake) CA = 153 ha St = 1.30 m Water depth = 2 m Age = 100 at 0.14 m	Glacial lake Located in glacial cirque Rock type = crystalline schist	H: 0–130	1.40	Sedimentation rates (SR) based on mineral magnetic properties and ^{210}Pb, ^{226}Ra, ^{137}Cs and ^{241}Am, pollution history	Hutchinson et al. (2015) Mîndrescu et al. (2010b) Akinyemi et al. (2013)

(continued)

Table 30.1 (continued)

No.	Site name	Geographic location	General information (elevation, area, maximum water depth, thickness of sediment sequence, age yrs cal BP)	Type of investigated site	Estimated age (yrs cal BP)	SR[c] (mm/year)	Proxies	References
9	Poiana Ştiol	Eastern Carpathians—Rodna Mts, northern slope 47° 35′ 14″ N 24° 48′ 99″ E	Elev. = 1540 m a.s.l. St = 3.20 m Site area = 0.6 ha CA = 10 ha Age = 10.380 at 2.93 m	Peat bog Located in a cirque floor sinkhole Rock type = crystalline limestone	H: 0–11000	0.28	Lithostratigraphy, pollen	Tanţău et al. (2011a) Tanţău and Fărcaş (2004) Tanţău (2006) Fărcaş et al. (2006)
10	Bolătău–Feredeu	Eastern Carpathians—Feredeului Mts 47° 37′ 21″ N 25° 25′ 54″ E	Elev. = 1137 m a.s.l Site area = 0. 23 ha CA = 29.57 St = 4.01 m Water depth = 5.4 Age = 4419 at 3.06 m	Lake Landslide-dammed, located on the slope near the wathershed Rock type = flysch	H: 6800–7000	0.69	AMS radiocarbon, 137Cs dates and isotopic geochemistry	Mîndrescu et al. (2016b) Németh et al. (2014) Mîndrescu et al. (2013)
11	Iezer–Feredeu	Eastern Carpathians—Feredeului Mts 47° 36′ 13″ N 25° 26′ 58″ E	Elev. = 920 m a.s.l. Site area = 0.75 ha CA = 355 ha St = 4.11 m Water depth = 4.47 m Age = 1035 at 3.86 m	Lake Landslide-dammed located on the bottom of valley Rock type = flysch	H: 0 to >1035–1176 cal AD	3.73	Cladocera, elemental geochemistry, lithostratigraphy, magnetic properties, grain size	Mîndrescu et al. (2013, 2010a, c)

(continued)

Table 30.1 (continued)

No.	Site name	Geographic location	General information (elevation, area, maximum water depth, thickness of sediment sequence, age yrs cal BP)	Type of investigated site	Estimated age (yrs cal BP)	SR[c] (mm/year)	Proxies	References
12	Iezerul Călimani	Eastern Carpathians—Călimani Mts 47° 19′ 40″ N 25° 16′ 25″ E.	Elev. = 1650 m a.s.l St = 5.0 m Site area = 0,255 ha Water depth = 0.7 m Age = 14800 at 4.60 m	Lake with peat bog Located in rock slope failure (enhanced by nivation) Rock type = volcanic breccia	LG–H: 0–17730	0.31	Lithostratigraphy, pollen	Fărcaş et al. (1999, 2003, 2006) Fărcaş and Tanţău (2002) Feurdean et al. (2007b)
13	Lacu Roşu	Eastern Carpathians—Hăghimaş Mts 46^{0} 47′ 0″ N 25^{0} 47′ 0″ E	Elev. = 983 m a.s.l. Site area = 11.65 ha CA = 3880 ha St ≈ 3 m Water depth = 9.6 m Age = 160 at 0.60 m	Lake Landslide-dammed located on the bottom of valley Rock type = limestone	H: 0–150	11.70	Estimation of sedimentation rate, 210Pb and 137Cs, geochemistry	Begy et al. (2009, 2014) Pandi (2004)
14	Luci	Eastern Carpathians—Harghita Mts 46° 17′ 52.46″ N 25° 43′ 03.24″ E	Elev. = 1080 m a.s.l. Site area = 120 ha CA = 1065 ha St = 7.50 m (hiatus) Age = 14700 at 7.22 m	Peat bog Located in former volcanic crater Rock type = andesite	LG–H: 0–14900	0.49	Lithostratigraphy, pollen,	Tanţău et al. (2003c, 2014) Tanţău (2006) Fărcaş et al. (2006) Feurdean et al. (2007b)

(continued)

Table 30.1 (continued)

No.	Site name	Geographic location	General information (elevation, area, maximum water depth, thickness of sediment sequence, age yrs cal BP)	Type of investigated site	Estimated age (yrs cal BP)	SR[c] (mm/year)	Proxies	References
15	Sfânta Ana	Eastern Carpathians—Harghita Mts 46° 07′ 35″ N 25° 53′ 18″ E	Elev. = 950 m a.s.l. St = 11.7 m (2010) Water depth = 6 m (2000) Site area = 19.7 ha (2000) CA = 202 ha Age = 26056.5 at 10.62 m	Lake Located in whole volcanic crater Fed exclusively by meltwater and runoff Rock type = andesite	LG–H: 0–27000 (assumed to be older, ~40 k)	0.04	Lithostratigraphy, pollen, macrofossil, diatom, cladocera, geochemistry, testate amoebae, cysts, sedimentation rates (SR) using ^{210}Pb, ^{226}Ra, ^{137}Cs and ^{241}Am	Magyari et al. (2006, 2009c, 2014a, b) Buczkó and Magyari (2007) Hutchinson et al. (2015) Begy et al. (2011)
16	Mohoş	Eastern Carpathians—Harghita Mts 46° 08′ 0.52″ N 25° 54′ 13.26″ E	Elev. = 1040 m a.s.l. Site area = 80 ha St = 10.65 m CA = 230 ha Age = 9750 at 10.05 m	Peat bog with Sphagnum Located in a former volcanic crater Rock type = andesite	LG–H: 0–13890	0.10	Lithostratigraphy, pollen	Tanţău et al. (2003a, b, 2006) Tanţău (2006) Fărcaş et al. (2003, 2006) Feurdean et al. (2007b)
17	Lacul Negru–Bisoca	Curvature Subcarpathians, Buzău sector 45° 32′ 58.98″ N 26° 40′ 07.54″ E	Elev. = 910 m a.s.l. Site area = 2 ha CA = 10 ha St = 7.0 m (hiatus) Age = 11060 at 6.66 m	Peat bog with Sphagnum Located in a landslide basin near watershed Rock type = molasse	H: 0–11000	0.60	Lithostratigraphy, pollen	Tanţău et al. (2003a) Tanţău (2006) Fărcaş et al. (2006)

(continued)

Table 30.1 (continued)

No.	Site name	Geographic location	General information (elevation, area, maximum water depth, thickness of sediment sequence, age yrs cal BP)	Type of investigated site	Estimated age (yrs cal BP)	SR[c] (mm/year)	Proxies	References
18	Lacul cu Mușchi–Bisoca	Curvature Subcarpathians, Buzău sector 45° 33′ 02.36″ N 26° 40′ 21.89″ E	Elev. = 930 m a.s.l. Site area = 0.6 ha CA = 4.5 ha	Peat bog with Sphagnum Located in a landslide basin near watershed Rock type = molasse	Not specified	–	Lithostratigraphy, pollen	Tanțău et al. (2003a) Tanțău (2006)
19	Avrig 1 Avrig 2 (2 cores)	Transylvanian Basin—Făgăraș Depression 45° 43″ N 24° 23″ E	Elev. = 400 m a.s.l. St Avrig 1 = 8.06 m St Avrig 2 = 11.9 m Site area = 10 ha Age Avrig 1 = 13880 at 7.2 m	Peat bog with Sphagnum Located on fluvial terrace of river Olt Rock type = platform deposits	Avrig 1: LG–H: 0–17200 Avrig 2: H: 0–4800	0.52	Lithostratigraphy, pollen	Tanțău et al. (2006, 2011b) Feurdean et al. (2007b)
20	Capra	Transylvanian Alps—Făgăraș Mts, southern slope 45° 36′ 04.75″ N 24° 37′ 44.11″ E	Elev. = 2249 m a.s.l. Site area = 1.88 ha CA = 29.7 ha Water depth = 13.1 m St = 0.6 m Age = 170 at 0.185 m	Lake Located in glacial cirque Rock type = crystalline schist	H: 1840–2008 AD	1.09	Sedimentation rates (SR) using ^{210}Pb, ^{226}Ra, ^{137}Cs and ^{241}Am, pollution history	Hutchinson et al. (2015) Akinyemi et al. (2013)
21	Galeș	Transylvanian Alps—Retezat Mts, northern slope 45° 23′ 09.69″ N 22° 54′ 38.51″ E	Elev. = 1973 m a.s.l. Site area = 3.68 ha CA = 177.5 ha Water depth = 20 m St = 3.28	Lake Located in glacial cirque Rock type = granite Age = 13540 at 2.80 m	LG–H: 0–15124	0.30	Pollen, macrofossils, conifer stomata, diatoms, Cladocera, chironomids, chrysophyte stomatocyst	Buczkó et al. (2013) Magyari et al. (2009a, b) Soróczki-Pintér et al. (2014)

(continued)

Table 30.1 (continued)

No.	Site name	Geographic location	General information (elevation, area, maximum water depth, thickness of sediment sequence, age yrs cal BP)	Type of investigated site	Estimated age (yrs cal BP)	SR[c] (mm/year)	Proxies	References
22	Tăul dintre Brazi	Transylvanian Alps—Retezat Mts, northern slope 45° 23′ 49.58″ N 22° 54′ 11.43″ E	Elev. = 1730 m a.s.l. Site area = 0.11 ha CA = 5.28 ha Water depth = 1.1 m St = 4.9 m Age = 13620 at 5.78 m	Lake Located on the bottom of a glacial valley Rock type = granite	LG–H: 0–15750	0.21	Lithostratigraphy, elemental geochemistry, organic matter content via LOI, pollen, macrofossils, conifer stomata, diatoms, ostracode, chironomids, ancient DNA	Magyari et al. (2009a, b, 2011, 2013) Buczkó et al. (2009, 2012b) Tóth et al. (2012) Iepure et al. (2011)
23	Bucura	Transylvanian Alps—Retezat Mts, southern slope 45° 21′ 38.58″ N 22° 52′ 34.15″ E	Elev. = 2040 m a.s.l. Site area = 10 ha CA = 201.4 ha Water depth = 17.5	Lake Located in a complex glacial cirque Rock type = granite	Not published	–	Pollen, macrofossils, cladocera, chironomids	Buczkó et al. (2013)
24	Lia	Transylvanian Alps—Retezat Mts, southern slope 45° 21′ 08.73″ N 22° 52′ 44.24″ E	Elev. = 1910 m a.s.l Site area = 1.3 ha CA = 431.9 Water depth = 4.3 m St = 7.62 Age = 14200 at 7.62	Lake Located in glacial cirque Rock type = granite	LG–H: 14200	0.54	Diatoms (siliceous algae), pollen, macrofossils, cladocera, chironomids	Buczkó et al. (2013)

(continued)

Table 30.1 (continued)

No.	Site name	Geographic location	General information (elevation, area, maximum water depth, thickness of sediment sequence, age yrs cal BP)	Type of investigated site	Estimated age (yrs cal BP)	SR[c] (mm/year)	Proxies	References
25	Tăul Negru	Transylvanian Alps—Retezat Mts, northern slope 45° 21′ 34.24″ N 22° 49′ 44.46″ E	Elev. = 2005 m Site area = 4.6 ha Water depth = 24.8 m St = 0.43 m Age = 140 at 0.095 m	Lake Located in glacial cirque Rock type = granite	H: 1860–2000	0.68	Sedimentation rates (SR) using ^{210}Pb, ^{226}Ra, ^{137}Cs and ^{241}Am, atmospheric contamination and ecological changes	Hutchinson et al. (2015) Rose et al. (2009)
26	Tăul Zănoguţii	Transylvanian Alps—Retezat Mts, western slope 45° 20′ 03.35″ N 22° 48′ 18.02″ E	Elev. = 1855 m a.s.l. St = 4.80 (5.65) m (hiatus) CA = 54.1 Site area = 0.21 ha Age = 11140 at 4.70 m	Lake Located in glacial cirque Rock type = granites	LG–H: 0–14800	0.42	Lithostratigraphy, pollen, diatoms, green algae	Fărcaş et al. (1999, 2003, 2006) Feurdean et al. (2007b)
27	Semenic (Zănoaga Roşie)	Western Carpathians—Banat Mts Semenic range 45° 08′ 23″ N 21° 59′ 00″ E	Elev. = 1400 m a.s.l. St = 1.6 m	Peat bog Located in rock slope failure (on summit) Rock type = crystalline schist	LG–H: 0–7620	0.21	Lithostratigraphy, pollen, plant macrofossil	Rösch and Fischer (2000 Fărcaş et al. (2003, 2005, 2006)

(continued)

Table 30.1 (continued)

No.	Site name	Geographic location	General information (elevation, area, maximum water depth, thickness of sediment sequence, age yrs cal BP)	Type of investigated site	Estimated age (yrs cal BP)	SR[c] (mm/year)	Proxies	References
28	Peşteana	Western Carpathians—Banat Mts Poiana Ruscă range 45° 32′ 37.42″ N 22° 48′ 28.62″ E	Elev. = 508 m a.s.l. Site area = 1.5 ha CA = 6.5 ha St = 5.10/max. 5.80 m (hiatus)	Peat bog with pool Located in a landslide basin Rock type = crystalline schist	LG–H: ca. 0–17000	0.30	Lithostratigraphy, pollen, testate amoebae	Fărcaş et al. (2006)
29	Căpăţâna	Western Carpathians—Apuseni Mts 46° 30′ 20.88″ N 23° 09′ 5.53″ E	Elev. = 1220 m a.s.l. St = 5.35 m	Peat bog, infilled sinkhole Located on plateau Rock type = limestone	H: ca. 0–7000	0.76	Lithostratigraphy, pollen, testate amoebae	Fărcaş et al. (2003, 2006)
30	Molhaşul Mare	Western Carpathians—Apuseni Mts 46° 35′ 24″ N 22° 45′ 51″ E	Elev. = 1224 m a.s.l. Site area = 8 ha St = 5.7 m	Peat bog, infilled sinkhole Located on plateau Rock type = limestone	H: 0–5700	1.00	Lithostratigraphy, pollen, charcoal	Feurdean and Willis (2008a, b) Feurdean et al. (2009)
31	Călineasa	Western Carpathians—Apuseni Mts 46° 33′ 03, 550″ N 22° 47′ 26, 94″ E	Elev. = 1360 m a.s.l. Site area = 1 ha St = 2.24 m	Peat bog, infilled sinkhole Located on plateau Rock type = limestone	H: 0–5100	0.44	Lithostratigraphy, pollen, charcoal, magnetic susceptibility, LOI	Feurdean and Willis (2008b)

(continued)

Table 30.1 (continued)

No.	Site name	Geographic location	General information (elevation, area, maximum water depth, thickness of sediment sequence, age yrs cal BP)	Type of investigated site	Estimated age (yrs cal BP)	SR[c] (mm/year)	Proxies	References
32	Padiş–Sondori	Western Carpathians—Apuseni Mts 46° 35′ 44, 86″ N 22° 44′ 00, 96″ E	Elev. = 1290 m a.s.l. Site area = 1 ha St = 0.76 m	Peat bog, infilled sinkhole Located on plateau Rock type = limestone	H: 0–6000	0.13	Lithostratigraphy, pollen, charcoal	Feurdean and Willis (2008b) Feurdean et al. (2009)
33	Padiş	Western Carpathians—Apuseni Mts 46° 35′ 53.2″ N 22° 43′ 58.4″ E	Elev. = 1240 m a.s.l. St = 0.9 m	Peat bog, infilled sinkhole Located on plateau Rock type = limestone	H: ca. 0–5300	0.17	Lithostratigraphy, pollen, magnetic susceptibility, LOI	Bodnariuc et al. (2002) Jalut et al. (2003) Fărcaş et al. (2003, 2006)
34	Bergerie	Western Carpathians—Apuseni Mts 46° 37′ 23.1″ N 22° 40′ 56.4″ E	Elev. = 1400 m a.s.l. St = 2.3 m	Peat bog with Sphagnum, infilled sinkhole Located on plateau Rock type = limestone	H: ca. 0–7900	0.29	Lithostratigraphy, pollen	Bodnariuc et al. (2002) Jalut et al. (2003) Fărcaş et al. (2006)
35	Ic Ponor I (core 1)	Western Carpathians—Apuseni Mts 46° 37′ 46″ N 22° 48′ 24″ E	Elev. = 1040 m a.s.l. St = 2.95 m (hiatus) Area = 7 ha	Peat bog, infilled sinkhole Located on plateau Rock type = limestone	H: ca. 0–10100	0.29	Lithostratigraphy, pollen	Bodnariuc et al. (2002) Jalut et al. (2003) Fărcaş et al. (2003, 2006)

(continued)

Table 30.1 (continued)

No.	Site name	Geographic location	General information (elevation, area, maximum water depth, thickness of sediment sequence, age yrs cal BP)	Type of investigated site	Estimated age (yrs cal BP)	SR[c] (mm/year)	Proxies	References
36	Ic Ponor II (core 2)	Western Carpathians—Apuseni Mts 46° 37′ 46″ N 22° 48′ 24″ E	Elev. = 1020 m a.s.l. St = 1.65 m (hiatus)	Peat bog, infilled sinkhole Located on plateau Rock type = limestone	H: ca. 0–9900	0.16	Lithostratigraphy, pollen	Bodnariuc et al. (2002) Jalut et al. (2003) Fărcaş et al. (2003, 2006)
37	Pietrele Onachii	Western Carpathians—Apuseni Mts 46° 38′ 33″ N 22° 50′ 43″ E	Elev. = 1055 m a.s.l. Site area = 3.5 ha St = 1.85 m	Forested peat bog, infilled sinkhole located on plateau Rock type = limestone	H: 0–5500	0.34	Lithostratigraphy, pollen, charcoal	Feurdean and Willis (2008b)
38	Cimetière	Western Carpathians—Apuseni Mts Coordinates not specified	Elev. = 1280 m a.s.l. St = 1.30 m	Peat bog, infilled sinkhole Located on plateau Rock type = limestone	H: 0–8800	0.15	Lithostratigraphy, pollen	Bodnariuc et al. (2002)
39	Mlaştina de la Iaz	Western Carpathians—Apuseni Mts 47° 06′ 30″ N 22° 39′ 40″ E	Elev. = 300 m Site area = 0.35 ha St = 5.40 m (hiatus) Age = 7000 at 5.20 m	Peat bog (forested) Located into a landslide basin Rock type = crystalline schist	H: 0–7000 (8380 maximum but not used)	0.74	Lithostratigraphy and pollen	Grindean et al. (2014)
40	Turbuţa	Transylvanian Basin, northwestern part 47° 15′ 26.5″ N 23° 18′ 42.9″ E	Elev. = 275 m a.s.l. Site area = 1.5 ha St = 1.9 m (hiatus)	Paleolake landslide dammed Rock type = sedimentary platform deposits	LG–H: 5000–13100	0.14	Lithostratigraphy, pollen, micro-charcoal, total carbon analyses	Feurdean et al. (2007a)

(continued)

Table 30.1 (continued)

No.	Site name	Geographic location	General information (elevation, area, maximum water depth, thickness of sediment sequence, age yrs cal BP)	Type of investigated site	Estimated age (yrs cal BP)	SR[c] (mm/year)	Proxies	References
41	Măgheruş	Transylvanian Basin, northern part, in Măgheruş Valley 24° 23′ 47.21″ E 47° 05′ 56.43″ N	Elev. = 345 m a.s.l. Site area = 0.6 CA = 1939 ha St = 1.39 Age = 15495 at 1.265 m	Paleolake landslide-dammed Located on valley bottom Rock type = sedimentary platform deposits	LG: 11000–17000 (max. 17894)	0.08	Radiocarbon dating, mineral magnetic analyses, loss on ignition, organic macrofossils (sclerotia of Cenococcum geophillum)	Lascu et al. (2014)
42	Ştiucii	Transylvanian Basin, northern part 46° 58′ 044″ N 23° 54′ 106″ E	Elev. = 239 m a.s.l. Study area = 38 ha St = 7.27 m	Lake Mixed origin: salt karst and landslide-dammed Rock type = sedimentary platform deposits	H: 0–12000	0.61	Lithostratigraphy, pollen, micro and macrocharcoal, organic matter content via LOI, magnetic susceptibility, elemental geochemistry; sedimentation rates (SR) using ^{210}Pb, ^{226}Ra, ^{137}Cs and ^{241}Am	Hutchinson et al. (2015) Feurdean et al. (2015)

[a]Catchment area
[b]Sediment thickness
[c]Sedimentation rate (estimation)
[d]Data corresponds to old glacial lake prior to human intervention

disturbances, waves, bioturbation, sediment re-deposition, etc.), as well as to the affinity of pollutants for organic fragments. However, not all proxies can be successfully applied to peat sediments.

In the majority of studied lakes the water depth is above 4 m, which according to Smol (2009) ranks as suitable for paleolimnological studies due to the absence of wind interference or bioturbation. Whereas investigated peat bogs formed mainly in karst sinkholes on limestone or in landslide basins, most of the open lakes are either glacial or landslide-dammed. Two sites are remnants of palaeolakes whereby the lacustrine sediments are buried under the topsoil horizon (i.e., Măgheruș and Turbuța).

As regards the type of parent rock hosting peat bogs and lakes, the sites from Apuseni Mts formed on limestone, while glacial lakes from Retezat Mts (Southern Carpathians) formed on granite and volcanic crater lakes and peat bogs on andesite. The sites from the Northern Carpathians occur either on volcanic breccia (Gutâi–Lăpuș Mts) or crystalline rocks (Rodna Mts), as is also the case with the lakes from Semenic and Poiana Ruscă Mts.

Sediment Thickness and Ages

The length of sedimentary sequences collected from Romanian lacustrine and peat bog sites ranges between 0.76 and 11.7 m, with the longest core extracted from Sfânta Ana crater lake. In over 2/3 of sites the thickness of sediment profile exceeds 3 m which is sufficient to ensure adequate resolution for Holocene climate reconstructions. With very few exceptions, the ages of investigated sites vary between 5.1 and 17.9 ka (Măgheruș). The oldest site documented thus far is Sfânta Ana (26 ka, Eastern Carpathians), whereas the youngest is landslide-dammed lake Iezer–Feredeu (1.035 ka, Northern Carpathians), albeit its 4 m-thick laminated sediment profile is comparable to older sedimentary archives. The sites from Apuseni Mts cover the Late Holocene, while sackung (Tăul dintre Brazi, Iezerul Călimani) and crater lakes and peat bogs (Sfânta Ana) and palaeolakes (Măgheruș, Turbuța) span throughout the entire Holocene and the Late Glacial to various extents. Considering that in most instances the clay samples from the base of the sequences contain small amounts of pollen, based on which the actual onset of sedimentation cannot be dated, the determined ages are likely underestimated.

Lacustrine/Peat Bog Sedimentation Rates

The earliest estimates on sedimentation rates and sediment sources were made for the landslide-dammed Lacu Roșu Lake, in the Eastern Carpathians (Bojoi 1968). 40 years later the sedimentation rate at Lacu Roșu was assessed again using radiometric dating techniques (^{210}Pb and ^{137}Cs), yielding a mean sedimentation

accumulation rate (SAR) of 0.87 ± 0.17 g/cm^2 year (11.70 mm/year) which would indicate that the lake will be 80 % silted in 81 ± 30 years if the current rate is maintained (Begy et al. 2014). ^{137}Cs originating from both sources (Chernobyl, 1986 and nuclear weapon tests from 1963) was determined; the first peak appears at the depth of 23 cm whereas the second was observed at 42 cm (Begy et al. 2009).

At Iezer–Feredeu Lake, a landslide-dammed lake located in the Northern Carpathians, the average estimated sedimentation rate (SR) amounted to 3.73 mm/year during its 1035 years cal BP lifespan (Mîndrescu et al. 2013). Iezer–Feredeu greatly differs from Lacu Roşu in terms of mean SR values, mainly due to size differences between their catchments: Lacu Roşu has a catchment (3880 ha) more than 10 times the size of Iezer catchment (355 ha).

In the vicinity of the Iezer–Feredeu lies Bolătău–Feredeu Lake, with similar origins as the former but considerably older according to the latest findings, i.e. 6.8–7 k years BP (Mîndrescu et al. 2016b). Its mean calculated sedimentation rate is 0.70 mm/year during the past 4500 years BP. The sediment accumulation rate assessed solely for the last millenium is ca. 0.1 mm/year, almost 4 times lower compared to Iezer Lake, both of which were estimated based on radiocarbon dating of the profile bottom. As the two lakes evolved under very similar topographic (elevation, relief), geological and vegetation cover conditions, the sole difference between the two lies in the size of the catchments—30 ha in the case of Bolătău vs 355 at Iezer, demonstrating the importance of catchment size in relation to the magnitude of sediment accumulation. The two ^{137}Cs isotope peaks were determined at 6.5 and 12 cm depth (Mîndrescu et al. 2016b). Compared to Lacu Roşu, whereby similar data is available, it should be noted that during the past 50 years the mean rates were constant in both lakes but very different in terms of value: 8.5 mm/year in Lacu Roşu and 2.4 mm/year in Bolătău–Feredeu.

A similarly high sedimentation rate was documented in Ştiol glacial lake, Rodna Mts, which was modified through human intervention (disabled lake) by building a dam in a strict scientific reserve. Between the creation of the dam (October 2002) and the sediment sampling in July 2006, an approximately 25 mm thick sediment layer has accumulated on the bed of the lake. The rate of sedimentation in this period may therefore be calculated as 6.25 mm/year and it would appear that sedimentation has increased at least 16 times since the creation of the dam (Mîndrescu et al. 2010b). For a period of over 170 years, at Ştiol Lake the age depth model shows low and slightly increasing trend in the rate of sedimentation from 1840 to 1965, followed by two clear episodes of increased sediment accumulation; one around 1965 (from 0.04 to 0.06 g/cm^2/year) and the second and more marked one after 2003, from 0.06 to 0.09 g/cm^2/year (Hutchinson et al. 2015).

Sedimentation rates in natural lakes and peat bogs are paralleled to the same parameters determined for reservoirs. Relevant contributions to the study of lacustrine sedimentation in reservoirs were made by Rădoane and Rădoane (2005) whose approach focused on the silting degree and silting rates of 138 reservoirs. It was estimated that the areas producing the largest amounts of sediments which consequently result in high lacustrine sedimentation rates are the Southern and Curvature Subcarpathians whereby many of the reservoirs are located (Fig. 30.1).

The study determined that Romania ranks among the countries with high reservoir sedimentation rates (min. 6—max. 3208 $m^3\ km^{-2}\ year^{-1}$). Moreover, the total sedimentation rate (21.670 $hm^3\ year^{-1}$) ranges among the highest in Europe (Verstraeten et al. 2006). The magnitude of sedimentation in reservoirs is also high in the Moldavian Plateau (Eastern Romania) as a result of intensive soil erosion, ranging from 15 to 115 mm/year, particularly in Tutova Hills, whereby the rates determined based on ^{137}Cs determinations are commonly above 60 mm/year (Ioniță et al. 2000). Overall, sedimentation rates in natural lacustrine sites are significantly lower compared to their counterparts in reservoirs due to a variety of factors of which the most relevant are the size of the catchment (considerably greater in reservoirs) and the type of water and sediment supply.

Altogether, based on the data provided by all reviewed studies, the *long-term sedimentation rates* were computed for 40 natural open lake and peat bog sites which have been investigated during the past decades, the majority of which were obtained based on radiocarbon dates, and to a lesser extent ^{210}Pb dates (in the cases of Ştiol, Capra and Lacu Roşu Lakes) (see Table 30.1 and Fig. 30.1). According to our review, the mean values range from 0.04 (Sfânta Ana Lake) to 11.7 mm/year (Lacu Roşu); the intermediate mean sedimentation rates are ranked in 4 classes, as follows: (1) *SR under* 0.21 mm/year, typical for the two volcanic crater water bodies, Sfânta Ana Lake and Mohoş peatbog, as well as some glacial lakes (e.g. Buhăescu Mare in Rodna Mts) and plateau lakes fed by very small-sized catchments, such as Tăul dintre Brazi or Padiş–Sondori; (2) *SR between* 0.28 and 0.49 mm/year, documented in glacial lakes such as Cristina Lake (Maramureş Mts), sackung lakes and large peatbogs (Luci, Harghita Mts); (3) *SR between* 0.52 and 0.76 mm/year, typical for the majority of glacial lakes, as well as landslide-dammed Bolătău–Feredeu Lake; (4) *SR above* 1 mm/year, characteristic for glacial Ştiol Lake from Rodna Mts and Capra Lake from Făgăraş Mts (whereby the sedimentation rates were determined for the past 160 years), Molhaşul Mare peatbog (mid-Holocene age), as well as landslide-dammed lakes Iezer–Feredeu (3.73 mm/year for the past 1.150 kyr) and Lacu Roşu.

An Integrated Late Pleniglacial–Holocene Palaeoenvironmental Perspective Based on Geochemical and Biological Lake Sediment Proxies

Understanding the mechanisms and impacts of past climate changes on the environment in terms of magnitude and temporal—spatial patterns has become a milestone in the context of the recent global projections (IPCC 2014). The need for palaeoclimatic and palaeoenvironmental reconstructions covering a large period of time and particularly based on quantitative or at least semiquantitative information is strongly felt, especially in areas where such aspects have not been thoroughly investigated. In this respect, due to their pronounced sensitivity to climatic and

environmental changes, lake and peat sediments are regarded as valuable archives as they record important information concerning processes and events manifested at various spatial and temporal scales.

One such region where palaeoclimatic data sets are particularly scarce is the Central–Eastern Europe. Here, several lacustrine and peat archives, some of which are located in the Romanian Carpathians, have become very valuable sources of information regarding the reconstruction of regional climatic and environmental history. Albeit Romania is a climatically sensitive area influenced by Atlantic, Mediterranean and Siberian air masses (Lascu et al. 2014), and therefore has the potential to record climatic shifts and test potential synchronicities with other sites across Europe, very few dated lacustrine sequences are available from this region. Overall, quantitative and semi-quantitative palaeoclimate reconstructions are extremely rare in Romania (Feurdean et al. 2008, 2012a; Tóth et al. 2012), whereas qualitative information is more abundant.

For the existing dated Romanian records the most widely employed proxies are biological, more specifically pollen and plant macrofossil analyses, with a special focus on the Late Glacial and Early Holocene periods where abrupt and short climatic events triggered important environmental changes (Magyari et al. 2013; Buczkó et al. 2012b; Tanţău et al. 2009; Feurdean et al. 2014). Nonetheless, even the main short-term Holocene climatic shifts documented in the North Atlantic Area (Blockley et al. 2012) have been shown to impact on the Romanian territory (e.g., Feurdean and Willis 2008b; Magyari et al. 2009b).

We hereby showcase the most significant short-term climatic events recorded in lake and peat sedimentary archives on the Romanian territory within the framework of a regional comparison (Fig. 30.2). These climatic oscillations are further related to the Intimate event stratigraphy (Blockley et al. 2012) from 26,000 to 8000 cal yr BP, whereas the 8000 cal BP to present period is roughly related to the regional climatic changes documented by Mayewski et al. (2004) and Magny and Haas (2004). Among the reviewed sites, the longest timeframe covered by a lacustrine sedimentary sequence was reconstructed in Eastern Romania at Sfânta Ana Lake (946 m a.s.l.), extending back to the Pleniglacial (26,000 cal yr BP). Palaeoclimatic reconstructions based mainly on pollen analyses are abundant in NW and Western Romania, both in terms of number and consistency, whereas in the SW Romanian Carpathians the proxies employed for lacustrine sediment investigations are rather diverse.

Sensitivity to Climatic Signals

Within the investigated studies, mid-elevation sites (730–1100 m a.s.l) were found to be the most sensitive to climate change during the Late Glacial and Early Holocene (Feurdean et al. 2012b). Less prominent climatic shifts were recorded only at mid-altitude sites (Feurdean et al. 2007b; Magyari et al. 2013), which might be explained by the fact that at higher elevations the terrain was covered by ice until

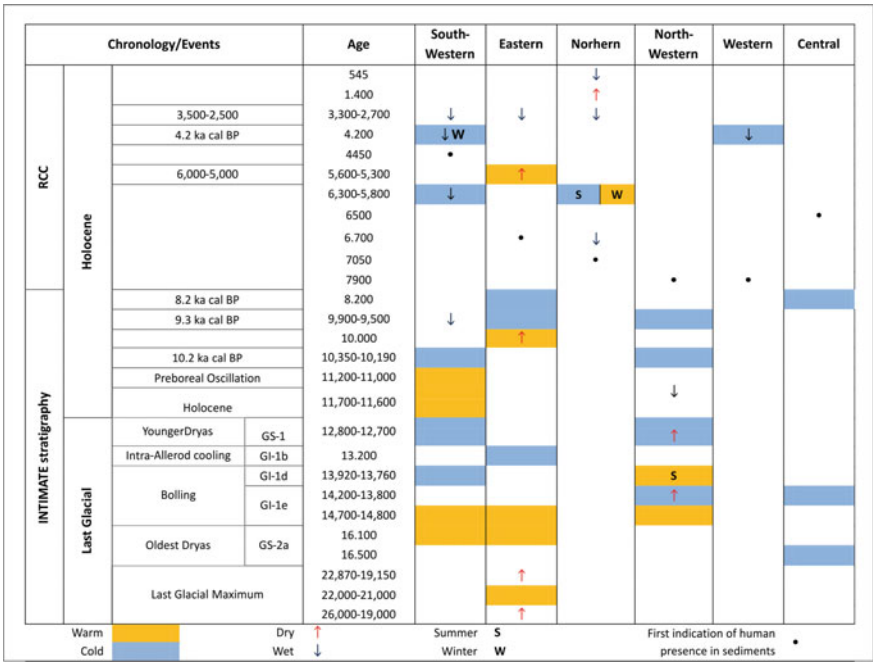

Fig. 30.2 Summary of inferred climatic changes between 26,000 and 550 cal y BP at reviewed sites from Romania

warming conditions were established (Early Holocene) which imprinted a prolonged cooling effect on the surrounding environment. Furthermore, lowlands are generally underrepresented on the map of Romanian palaeoclimate reconstructions. Although climate changes are expected to be recorded at a lower magnitude at lowland sites (Feurdean et al. 2014), palaeoclimatic archives located in the Transylvanian Basin (i.e., lakes Măgheruş, Avrig, Turbuţa, Ştiucii) recorded prominent climatic events which occurred in the North Atlantic area and propagated towards the Central–Eastern Europe.

26–19 ka cal BP. During the Late Glacial Maximum (26,000–19,000 cal yr BP) the geochemical proxies employed for the oldest lacustrine sequence in Romania (Sfânta Ana Lake) located in the Eastern Romanian Carpathians indicate a general low lake productivity accompanied by an increase in the aeolian input (Magyari et al. 2014a). This suggests enhanced climatic aridity, limited vegetation cover, unconsolidated soils and high wind speed (Kasse 2002). Two short climatic fluctuations, from 23,500 to 23,000 cal yr BP, and 22,000–21,000, respectively, were associated with the millenial-scale stadial/interstadial climatic fluctuations in marine isotope stage 2: GI–2.1-GI–2.2. From 22,870 to 19,150 cal yr BP, enhanced regional continentality and persistent drought were inferred from tree diversity and increased fire activity (Magyari et al. 2014a).

18–12 ka cal BP. During this interval the northerly shift in the summer westerly jet from the Mediterranean Sea region (Strandberg et al. 2011; Huntley et al. 2013 cited by Magyari et al. 2014a) coupled with increased summer insolation (Berger and Loutre 1991 cited by Magyari et al. 2014a) impacted the ecosystems in two phases: the first interval (19–16.1 ka) was dominated by changes in summer insolation, whereas during the second one (16.1–12 ka) warming and precipitation increase prevailed. However, these changes manifested to various extents throughout the Carpathians, while the lowlands were shown to exhibit lower sensitivity. Thus, in Southern Transylvania a clear response of the vegetation to the Oldest Dryas cold phase—16.65 kyr cal BP was documented (Avrig record—Tanţău et al. 2006), whereas in Northern Transylvania (Măgheruş record—Lascu et al. 2014) the physical and chemical proxies indicate warmer and wetter conditions during Bølling–Allerød (or Greenland Interstadial 1, GI–1) followed by the cooler and drier Late Glacial Stadial (Younger Dryas/Greenland Stadial 1, GS–1).

In the SW Carpathians, the contribution of winter precipitation inferred from diatom silica oxygen isotope variations ($\delta^{18}O_{DIAT}$) was generally higher during the Late Glacial (until 12.3 kyr cal BP) (Buczkó et al. 2012a, b; Magyari et al. 2013). The prolonged cold and most likely wet conditions sustained in-wash processes, inhibited lake productivity and provided suitable conditions for steppe-tundra vegetation development (Korponai et al. 2011). In the Eastern Carpathians, from 18,000 to 16,100 cal yr BP, the presence of warmer climate species indicates an enhanced effect of summer insolation on vegetation composition (Magyari et al. 2014a). At 16,100 cal yr BP increased lake productivity and high levels of clastic input suggest a coupled effect of warm and highly moist conditions.

A detailed qualitative reconstruction of Late Quaternary climate and environment in the western sector of the Northern Carpathians based on multi-proxy analyses (Feurdean and Bennike 2004) showed that prior to 14.7 kyr cal BP (the Pleniglacial), cold and dry conditions prevailed, ensued by a short phase with more stable environmental conditions. A pollen-based quantitative temperature reconstruction (Feurdean et al. 2008) showed a 2 °C increase in annual temperatures, which reached 4 °C at 14.8 kyr cal BP. This event is equivalent to the GS–2/GI–1e transition in the Greenland ice core isotope record, which shows an increase in temperature amplitude (Blockley et al. 2012). During this period, in the Northern, Eastern and Southwestern Carpathians, the temperature increase was documented in winter temperatures, whereas summer temperatures remained unchanged.

In the SW Carpathians, an episode of slight warming occurred around 14,920 cal yr BP, inferred exclusively from geochemical proxies, which was related to the GI–1e event in the NGRIP (Braun et al. 2013). The transition from cold to warm conditions, i.e., Oldest Dryas/Bølling, is marked here at 14,700 cal yr BP by an increase in chironomid-inferred mean July air temperature by 2.8 °C (Tóth et al. 2012), while geochemical proxies (Braun et al. 2013), macrofossils, and stomata (Magyari et al. 2011; Korponai et al. 2011) show a delay of almost 500 years, at ~14250 cal yr BP. The warming period—Bølling (GI–1e)—was documented in the Eastern Carpathians in the Sfanta Ana Lake record at around 14,700 cal yr BP

in the shape of a pronounced increase in temperature which resulted in vegetation growth and catchment slope stability.

In the western part of the Northern Carpathians a cooler and drier climatic phase was documented from around 14.1 to 13.8 kyr cal BP followed by an increase in air temperature and moisture availability. In the SW Carpathians from 13,920 to 13,760 cal yr BP the geochemical proxies point towards a weak cold episode, probably matching the GI–1d short-event from NGRIP, followed by short-term warmer conditions between 13,760 and 12,950 cal yr BP (Buczkó et al. 2009, 2012a, b). During Bølling/Allerød interstadial the chironomid-reconstructed air temperatures of the warmest month are placed around 8.1–8.7 °C (for comparison, present day temperature is 11.2 °C), lower compared to other records across Europe (Tóth et al. 2012). This was explained by stronger oceanic influences in the Southern Carpathians coupled with a down-slope cooling effect coming from the perennial ice-covered peaks, which might have affected the warm season (Tóth et al. 2012).

In the western sector of the Northern Romanian Carpathians, between 13.8 and 12.7 kyr cal BP an increase in summer temperature close to present day values (13–17 °C) was noticed. However, winter and annual temperatures (−6 to −12 °C and 0.5–6 °C, respectively), as well as annual precipitation (550–700 mm) were lower (Feurdean et al. 2008). Higher summer temperatures are also indicated by enhanced fire activity in the area (Feurdean et al. 2012a). This LG warming is also evident in the Southern Carpathians, and related to the previous observations, it indicates the prevalence of stronger inter-seasonal variability and enhanced continental conditions (Feurdean et al. 2008; Braun et al. 2013; Buczkó et al. 2009, 2012a, b; Magyari et al. 2011).

In the Eastern Carpathians around 13,200 cal yr BP the geochemical proxies reveal a lake level drop which appears to reflect the intra-Allerød cooling event (GI–1b). In the Luci pollen record (Harghita Mts), the climatic shifts (14,700 and 13,200 cal yr BP) are weakly expressed, albeit this site appears to have been more sensitive to the changes which occurred during the Allerød (13,800 cal yr BP) (Tanţău et al. 2014).

The magnitude of climate changes for the 14.7–8 ka cal BP interval was much lower compared to the Western Europe, with more oceanic influences (Feurdean et al. 2014); the onset of the LG cold intervals was accompanied by marked decrease in precipitation values and most likely increased continentality; low fire activity characterized the LG; short climatic fluctuations around 13.9, 13.6 and 13.2 ka cal BP were generally reflected in vegetation composition changes (Tanţău et al. 2006, 2014; Feurdean et al. 2007a, b, 2012a, b; Magyari et al. 2013).

12.8–11.7 ka cal BP. The decline in temperatures during *Younger Dryas* (12.8–11.7 ka cal BP) was recorded across the entire Romanian Carpathian Region and manifested more strongly during winter. The marked decrease in precipitation associated to the cooling indicates a progressive transition towards more continental or seasonally variable climatic conditions (Feurdean et al. 2014).

In the SW Carpathians abrupt climate shifts occurred throughout the Late Glacial and at the onset of the Holocene (Iepure et al. 2011; Korponai et al. 2011).

However, a strong regional vegetation response was recorded during the YD cooling at 12.8 kyr cal BP, which involved deforestation and spread of steppe-tundra and snowbed vegetation (Magyari et al. 2011). Although the chironomid-inferred temperatures do not show a marked decrease at the onset of the Younger Dryas (less than 1 °C), the diatom-based reconstructions suggest that the cooling associated with YD mainly occurred during the winter season. The ecosystem changes recorded in the Southern Carpathians during Younger Dryas were most likely caused by strong seasonal changes which implied longer and likely colder winters with slightly altered July temperatures and increased precipitation (Iepure et al. 2011; Buczkó et al. 2012a; Magyari et al. 2013; Tóth et al. 2012). Similarly, recurrent cold, dry YD conditions (12.9–11.5 kyr cal BP) were also recorded in the western part of the Northern Carpathians whereby the onset of Younger Dryas was characterized by a 2 °C increase in mean summer temperature (pollen-based reconstruction) and a marked decrease of ca. 9 °C in mean winter temperature, concomitant with a 250 mm decrease in annual precipitation (Feurdean et al. 2008). Diminished peat surface moisture and lake levels in the former area (Feurdean et al. 2013b; Schnitchen et al. 2003, 2006), SW Carpathians (Magyari et al. 2009b; Buczkó et al. 2012a, b), along with the diatom/chironomid-inferred cold conditions in the SW Carpathians (Buczkó et al. 2012a; Magyari et al. 2013; Tóth et al. 2012) and the augmenting landscape openness in Southern (Tanţău et al. 2006) and Northern Transylvania (Feurdean et al. 2007a, b), as well as in the western sector of the Northern Carpathians (Björkman et al. 2002, 2003) and Eastern Carpathians (Tanţău 2006; Tanţău et al. 2003a) also support these findings.

Between 12,450 and 11,400 cal yr BP, a decrease in the duration of the winter ice-cover season was inferred in the SW Carpathians (Buczkó et al. 2009, 2012a, b; Braun et al. 2013) which is synchronous with the warming phase detected in the Eastern Carpathians at ∼12,500 cal yr BP (Magyari et al. 2014a).

Farther north, pollen-related findings showed that glaciation was not as severe in Călimani Mts compared to Retezat Mts (Fărcaş et al. 1999). The regional persistence of broad-leaved temperate forest (at 46° N) during the LGM, coupled with charcoal data suggest a continuous, regional and extra-local presence of wood biomass and its frequent burning, likely as a result of increased continentality, with relative warm and dry summers.

11.7–8 ka cal BP. Similar to other regions in Europe, climate warming at the YD—Holocene transition resulted in enhanced vegetation competition and diversity. This major and abrupt climate shift triggered a visible response in vegetation at both lowland and upland sites (Fărcaş et al. 1999, 2006; Björkman et al. 2002, 2003; Tanţău et al. 2003a, c, 2006; Feurdean 2005; Tanţău 2006; Feurdean et al. 2007a, b), which demonstrates that all elevations were comparably vulnerable. During the Early Holocene (11.7–8 ka cal BP) high summer insolation led to an increase in summer temperature and thus influenced seasonality. Biomass burning reached maximum values due to fire-prone conditions and biomass availability.

In the Eastern Carpathians the YD—Holocene transition (11,700 cal yr BP) appeared most evident at Luci and Bisoca peat bogs (Harghita Mts and Buzăului Subcarpathians, respectively), where vegetation reconstructions from peat sediments reveals the role of the YD cooling conditions in limiting the vegetation development; the fast replacement of open vegetation by forests at the LG/Holocene transition was interpreted as a response to the Early Holocene warming (Tanţău et al. 2009, 2014). At lowland sites, after the YD cold event the Avrig sediment record indicates that vegetation responded rather slowly to the Early Holocene warming.

In the SW Carpathians the onset of the Holocene warming is marked in geochemical proxies, at ∼11,600 cal yr BP. Evolution of July temperatures is reflected in the chironomid record by a two steps increase during from 11,500 to 10,830 cal yr BP, first by 0.6 °C and second, by 2.7 °C.

During this period the palaeoenvironmental records from the western sector of the Northern Carpathians revealed moister conditions; overall, the pollen-based quantitative reconstruction of winter, summer and annual temperatures, as well as precipitation (Feurdean et al. 2008) enabled the identification of two main climatic intervals: (i) 11.7–11.2 kyr cal BP—characterized by less stable climate with a decrease in seasonality and reduction in continentality; (ii) 11.2–8.3 kyr cal BP—during which generally stable climatic conditions prevailed, albeit it was interrupted by minor fluctuations occurring around 10.2 kyr cal BP (i.e., a drop of 100 mm in precipitation amount) and 8350–8000 cal yr BP (a decrease by ∼1.5–2 °C in mean annual temperatures and 200 mm reduction in precipitation). This last cooling event appears to reflect the 8.2 ka event centennial-scale cold phase also documented in other regions.

Charcoal records revealed lower fire activity between 12 and 10.7 kyr cal BP in the lowland of northern Transylvania due to a shortage in fuel availability against the background of arid and strongly seasonal climatic conditions, i.e.,higher summer temperature (4 °C above current mean temperature) and lower precipitation (by 33 %) compared to the present (Feurdean et al. 2013b).

In the SW Carpathians, the warming tendency (Magyari et al. 2011; Braun et al. 2013) was interrupted by a short-lived cold event, between 11.2 and 11 kyr cal BP, which determined an increase in the duration of ice-cover (Buczkó et al. 2012b) and a drop in July temperatures by ∼1 °C (Tóth et al. 2012). The event was associated with the Preboreal Oscillation which occurred at ∼11,250 cal yr BP as defined in the GRIP $\delta^{18}O$ isotope record (Rasmussen et al. 2006). Between 10.6 and 10.3 kyr cal BP, the chironomid record coupled with the presence of fir pollen grains suggested that summer mean temperatures were ∼2.8 °C higher than present temperatures (Tóth et al. 2012; Magyari et al. 2013). A short-term cooling was detected at 10,350–10,190 cal yr BP, when mean summer temperatures decreased by ∼1 °C (Tóth et al. 2012) and the water table dropped suddenly (Magyari et al. 2013). This event was also reported in other parts of the Carpathians between 10,000–10,500 cal yr BP (e.g., Tămaş et al. 2005; Feurdean et al. 2008; Tanţău et al. 2009, 2014) and lowland Transylvania (Feurdean et al. 2007a), Western Europe (Lang

et al. 2010) and most likely corresponds with the 10.2 ka event identified in Greenland ice cores (Björck et al. 2001).

Between 9900 and 9500 cal BP, higher lake levels accompanied by decreasing lake productivity and changes in sediment geochemistry, vegetation and fossil organisms (Buczkó et al. 2012a; Magyari et al. 2009b, 2011; Soróczki-Pintér et al. 2014), appear to reflect the shift towards drier conditions from ~9200 cal yr BP. This is also evident in the Eastern Carpathians (Tanţău et al. 2009, 2014) and can be further linked with the 9.3 ka widespread climatic anomaly which might have been triggered by meltwater input into the North Atlantic.

The 8.2 ka cooling anomaly detected in the Greenland ice core isotope record, characterized by lower temperatures, minima in ice accumulation rates and windy conditions (Alley et al. 1997; Wiersma and Renssen 2006; Renssen et al. 2001 cited by Buczkó et al. 2012b) was also recorded in the Eastern (Tanţău et al. 2009, 2014) and Southern Carpathians, but manifested weakly by a slow rise in the lake level and increased storminess between 8400 and 8200 cal yr BP (Buczkó et al. 2012a; Magyari et al. 2009a, b). In other regions of the Carpathians this particular timeframe was either showcased by the lowest water levels at Sfânta Ana Lake (Magyari et al. 2009c), decreased mire surface wetness and dry summer conditions with cold winters (Schnitchen et al. 2006; Feurdean et al. 2008), or was not reflected at all in other temperature-proxy records such as speleothems (Tămaş et al. 2005; Constantin et al. 2007). Some small change towards a drier climate was noticed around the same timing in lowland Transylvania (Turbuța peat bog) (Feurdean et al. 2007a).

8.2–3 ka cal BP. Between 8000 and 3000 cal yr BP, in the western sector of the Northern Carpathians, coldest month and annual temperatures were lower compared to current conditions, whereas summer temperatures and precipitation showed increased values, comparable to the present; however, more stable conditions prevailed compared to the Early Holocene, but were interrupted by a number of short-term climate oscillations (Schnitchen et al. 2006; Feurdean et al. 2008). A dry event is identified around 6740 cal yr BP in Tăul Mare Bardău (Maramureş Mts) sediment record (Cristea et al. 2014). In the lowlands, a cooler and wetter climate was inferred between 7100 and 3300 cal yr BP which favored woodland extension and reduced biomass burning (Feurdean et al. 2012a).

In the SW Carpathians, diatom records reflect a short-lived event between 6300 and 5800 cal yr BP, characterized by summer cooling, a decrease in winter ice-cover season and an augmenting size of the water body, probably as a result of cooler and moister conditions (Buczkó et al. 2013; Magyari et al. 2009a, b). The event is synchronous with a short climatic change recorded in the SE Europe and the Northern Mediterranean Region known as 6000–5000 cal yr BP cold anomaly (Mayewski et al. 2004) characterized by cooler summers and warmer winters (Cheddadi et al. 1996 cited by Tanţău et al. 2011a). This anomaly was also identified, albeit with an even greater amplitude, in the Eastern Carpathians, at Sfânta Ana Lake (Buczkó et al. 2012a) and Poiana Ştiol peat bog (Tanţău and Fărcaş 2004;

Tanţău et al. 2011a), in Buzău Subcarpathians (Tanţău et al. 2009) and Southern Transylvania—Făgăraş Depression (Tanţău et al. 2006, 2011b).

Furthermore, at 4200 cal yr BP a significant decrease in $\delta^{14}O_{DIAT}$ signals another climatic change, characterized by increased winter precipitation and/or cooler winters (Magyari et al. 2013), which was aligned to the 4200–3800 RCC (Mayewski et al. 2004). This event was also detected in Apuseni Mts whereby the pollen record revealed a short-term abrupt cooling and wet event which started around 5500 cal yr BP, reaching maximum at 4200 cal yr BP (Feurdean and Willis 2008b). It was also recorded in the stalagmite oxygen ($\delta^{18}O$) and carbon ($\delta^{13}C$) isotopes (Onac et al. 2002), tree-ring records (Kern and Popa 2007) and supported by proxy-based evidence (pollen and testate amoebae) in NW Romania (Schnitchen et al. 2006; Feurdean et al. 2008).

3 ka cal BP to Present. In the Northern Carpathians the last 3000 cal yr BP were characterized by warm winters (0–1 °C mean temperature of the coldest month) and elevated annual temperatures (7–8 °C); precipitation decreased by about 100 mm.

After 3200 cal yr BP, diatom assemblages reflect a sudden increase in water level in the SW Carpathians which culminated around 2800 cal yr BP (Buczkó et al. 2012b; Magyari et al. 2013). This shift towards wetter conditions is also reflected in the Eastern Carpathians at Sfânta Ana Lake (whereby it is part of a major environmental change which occurred between 3300 and 2700 cal yr BP, Buczkó et al. 2012b), the Northern Carpathians (Cristea et al. 2014), speleothem $\delta^{18}O$ (showing gradual decrease) and other proxies in the Carpathians (Magyari et al. 2013; Schnitchen et al. 2006, etc.). In the eastern part of the Northern Carpathians (flysch mountains), a succession of different environmental conditions spanning the last 4000 years is reflected in sedimentation changes and limnogeological evolution documented for Bolătău Lake (Németh et al. 2014).

A dry event occurred at 1430 cal yr BP in the Northern Carpathians, ensued by another wet event at 545 cal yr BP, strongly related to a decrease/increase in precipitation availability (Cristea et al. 2014). Based on pollen stratigraphy from Iaz peat bog, cold and dry conditions were inferred in NW Transylvania between 1600 and 1300 cal yr BP (Grindean et al. 2014), followed by warmer conditions between 1300 and 1100 cal yr BP (Grindean et al. 2014; Feurdean et al. 2012a).

During the last 2500 years, in Buhăescu Mare Lake (Rodna Mts) and Tăul Mare Bardău peat bog (Maramureş Mts) the warm–cold oscillations known as RWP, DACP, MWP and LIA were also detected by multi-proxy analyses (Cristea et al. 2014; Geantă et al. 2014). Little Ice Age cold event was also traced in the lowlands in Avrig record (Tanţău et al. 2011b) at ca. 600–700 cal yr BP. Over the past millennia, drier conditions may be inferred in the Eastern Carpathians from lake eutrophication and gradual shallowing, and in NW Romania from the testate amoebae record (Schnitchen et al. 2003, 2006).

Human Impact

The earliest human impact appears within the palynological records around 8000–7000 cal yr BP in the Central, Western and North–Western Romanian regions when landscape spatial heterogeneity increased. However, in Eastern Romania human presence is documented as late as ca. 4000 cal yr BP, which would suggest, when corroborated with archeological data, that the Eastern region was outside the major human movement tracks. This finding leaves room for more interpretation about how human settlements developed within the Romanian territory and how/whether this is related to climate.

In the lowlands, human impact markedly altered burning trends from about 5500 cal yr BP onward, whereas in the mountain regions its earliest influence was felt later, around 3500 cal yr BP. It appears that prior to ca. 2500 cal yr BP the disturbances were mostly natural (Feurdean et al. 2010) and only after this date the human impact became more prominent. Recent research revealed a strong link between major land use strategies of prehistoric societies (the use of fire as a tool to clear forests and extend alpine pastures) and changes in vegetation diversity (Feurdean et al. 2013a).

The most recent and alarming human impact on the environment was also traced in Romanian Carpathians by means of multi-pollutant chemical and biological analyses (Begy et al. 2009, 2011; Rose et al. 2009). Thus, the past 250 years received special attention due to the significant changes occurring in lake ecosystems during this timeframe (e.g., acidification, high productivity) driven mainly by anthropogenic activities undertaken near or within the catchments. The Lacul Negru sediment record showed that the earliest atmospheric contamination occurred in 16th century with the inception of industrial activities, followed by an important increase in the 18th century, when the release of atmospheric pollutants was associated with coal combustion activities. Over the last ~300 years, the changes experienced by lake ecosystems are assigned to the enhanced human impact and subsequent land use changes. Moreover, strong recent human impact has been locally highlighted in the eastern part of the Northern Carpathians based on the study of physical and geochemical properties of recent sediments at Iezer–Feredeu Lake (Mîndrescu et al. 2013).

Furthermore, ^{210}Pb and ^{137}Cs radioisotope analyses revealed that Sfânta Ana Lake is experiencing an intense process of eutrophication (Begy et al. 2011). The reconstructed sedimentation rate revealed two distinct periods in the evolution of Lacu Roşu: ~1800–1989, characterized by a regular sedimentation rate when catchment deforestation was within a normal margin, and post-1989, when the high demand for wood led to increased woodfelling and triggered land use changes and augmented sedimentation rates (Begy et al. 2009).

Conclusions

Albeit palaeolimnological research is a new field of scientific investigation in Romania (no more than ca. 15 years), it has already produced a network of sites located at different elevations, in diverse physical environments and undergoing various degrees of anthropogenic influence, which has the potential to reveal local and regional differences in the environmental response to climate fluctuations and anthropogenic stressors. To date investigations focused mainly on lacustrine and peat bog sites older than 5 ka located above 1000 m a.s.l. in the northern half of the Romanian territory (Northern Carpathians and Apuseni Mts). The mean thickness of investigated sedimentary sequences is commonly above 3 m, but in a small number of instances the sediment profiles were as thick as 10–12 m. Sedimentation hiatuses occur in a well-marked number of cases. Lacustrine deposits accumulated during variable timeframes ranging typically from 5 to 15 ka, although in exceptional cases the absolute ages of lake sediments are as high as 19–26 ka, spanning throughout the Holocene and Late Glacial to the Late Pleniglacial. Based on this data the sedimentation rates for natural lakes and peat bogs have been estimated, which range within a rather broad interval, although they are not nearly as high as rates of accumulation in man-made reservoirs.

As regards the climatic and palaeoenvironmental data inferred from various multi-proxy analyses applied to sedimentary records from Romanian lakes and peat bogs, biological and geochemical records along with historical and archaeological data and the use of model-data comparison demonstrate that during the Late Pleniglacial—Late Glacial and the early Holocene the climate was mainly driven by natural forces, whereas during the second part of the Holocene it was influenced by mixed natural-anthropogenic factors. During the Holocene a strongly divergent pattern in biomass burning in the lowlands as opposed to the highlands suggests that forests in the Romanian Carpathians were cleared much later than in the rest of Europe (Feurdean et al. 2012a). Further on, as we approach the present times, particularly over the last millennium, human activities appear to shape the environment to an ever increasing extent.

Despite chronological uncertainties, the scarcity in quantitative information and the variety of investigation methods employed, the reconstruction is relatively unitary throughout the Romanian territory. However, new high resolution data is required to fill in gaps (particularly for uncharted areas such as the lowlands) along with novel integrated interpretations of existing information, for building more accurate climatic and environmental prediction models, and ultimately for implementing sustainable local management.

Acknowledgments Authors acknowledge the project PN-II-RU-TE-2012-3-0386 (UEFISCDI Romania). AH acknowledges support through the project "SOCERT. Knowledge society, dynamism through research" contract number POSDRU/159/1.5/S/132406; this project is co-financed by European Social Fund through Sectoral Operational Programme for Human Resources

Development 2007-2013. Investing in people! GF acknowledges support through the project "Sustainable performance in doctoral and post-doctoral research PERFORM-Contract no. POSDRU/159/1.5/S/138963", project co-funded from European Social Fund through Sectorial Operational Program Human Resources 2007–2013.

References

Akinyemi OF, Hutchinson SM, Mîndrescu M, Rothwell JJ (2013) Lake sediment records of atmospheric pollution in the Romanian Carpathians. Quatern Int 293:105–113

Atlasul RSR (1972–1979) Ed. Academiei, București

Begy R et al (2009) Recent changes in Red Lake (Romania) sedimentation rate determined from depth profile of 210Pb and 137Cs radioisotopes. J Environ Radioact 100:644–648

Begy R-C, Timar-Gabor A, Somlai J, Cosma C (2011) A sedimentation study of St. Ana Lake (Romania) applying the ^{210}Pb and ^{137}Cs dating methods. Geochronometria 38(2):93–100

Begy R-C, Simon H, Reizer E (2014) Efficiency testing of Red Lake protection dam on Roșu stream by ^{210}Pb method. J Radioanal Nucl Chem. doi:10.1007/s10967-014-3684-y

Björck S, Muscheler R, Kromer B et al (2001) High-resolution analyses of an early Holocene climate event may imply decreased solar forcing as an important climate trigger. Geology 29:1107V1111

Björkman L, Feurdean A, Cinthio K, Wohlfarth B, Possnert G (2002) Lateglacial and early Holocene vegetation development in the Gutaiului Mountains, NW Romania. Quatern Sci Rev 21:1039–1059

Björkman L, Feurdean A, Wohlfarth B (2003) Lateglacial and Holocene forest dynamics at Steregoiu in the Gutâiului Mountains, NW Romania. Rev Palaeobot Palynol 124:79–111

Blockley SP, Lane CS, Hardiman M et al (2012) Synchronisation of palaeoenvironmental records over the last 60,000 years, and an extended INTIMATE event stratigraphy to 48,000 b2k. Quatern Sci Rev 36:2–10

Bodnariuc A, Bouchette A, Dedoubat JJ et al (2002) Holocene vegetational history of the Apuseni Mountains, central Romania. Quatern Sci Rev 21(12):1465–1488

Bojoi I (1968) Contribuții la sedimentologia Lacului Roșu. Lucrările Stațiunii de Cercetări Biologice, Geologice și Geografice Stejaru, Piatra Neamț 1:87–105 (in Romanian)

Braun M, Hubay K, Magyari E et al (2013) Using linear discriminant analysis (LDA) of bulk lake sediment geochemical data to reconstruct lateglacial climate changes in the South Carpathian Mountains. Quatern Int 293:114–122

Buczkó K, Magyari E (2007) The Holocene diatom flora of Lake Saint Anna (Eastern Carpathians, Europe). Algol Stud 124(1):1–28

Buczkó K, Magyari E, Soróczki-Pintér É, Hubay K, Braun M, Bálint M (2009) Diatom-based evidence for abrupt climate changes during the Late Glacial in the Southern Carpathian Mountains. Cent Eur Geol 52(3):249–268

Buczkó K, Magyari E, Hübener T et al (2012a) Responses of diatoms to the Younger Dryas climatic reversal in a South Carpathian mountain lake (Romania). J Paleolimnol 48(2):417–431

Buczkó K, Magyari EK, Braun M, Bálint M (2012b) Diatom-inferred lateglacial and Holocene climatic variability in the South Carpathian Mountains (Romania). Quatern Int 293:123–135

Buczkó K, Wojtal AZ, Magyari EK (2013) Late quaternary Nupela taxa of Retezat Mts (S. Carpathians), with description of *Nupela pocsii* sp. nov. (Bacillariophyceae). Pol Bot J 58 (2):427–436

Constantin S, Bojar A-V, Lauritzen S-E, Lundberg J (2007) Holocene and Late Pleistocene climate in the sub-Mediterranean continental environment: a speleothem record from Poleva Cave Southern Carpathians, Romania. Palaeogeogr Palaeoclimatol Palaeoecol 243:322–338

Cristea C, Cuna SM, Fărcaş S et al (2014) Carbon isotope composition as an indicator of climatic changes during the middle and late Holocene in a peat bog from the Maramureş Mountains (Romania). Holocene 24(1):15–23

de Martonne E, Murgoci GM (1900) Sondage et analyse des boues du Lac Gâlcescu. Comptes rendus de l'Académie des Sciences. Sect Hydrol 932–935

Diaconu C (1971) Probleme ale scurgerii aluviunilor pe râurile din România. Studii de Hidrologie 30. INMH (in Romanian)

Fărcaş S, Tanţău I (2002) L'évolution de la végétation tardi-et postglaciare de Monts Călimani dans le context de celle de Roumanie. Contribuţii Botanice 37:265–274

Fărcaş S, de Beaulieu JL, Reille M et al (1999) First 14C datings of Late Glacial and Holocene pollen sequences from Romanian Carpathes. Comptes Rendus de l'Académie des Sciences-Series III-Sciences de la Vie 322(9):799–807

Fărcaş S, Lupşe V, Tanţău I, Bodnariuc A (2003) Reflectarea procesului de antropizare în diagramele sporo-polinice din Munţii Apuseni [Reflection of human impact in pollen diagrams from Apuseni Mountains]. In: Petrescu I (ed) Mediul—Cercetare, protecţie şi gestiune p 231–236 (in Romanian)

Fărcaş S, Tanţău I, Ursu T, Goszlar T (2005) L'analyse palynologique de la séquence tourbeuse de Zănoaga Roşie III (Monts Semenicului). Contrib Bot XL:317–328

Fărcaş SI, Tanţău I, Ursu TM et al (2006) The study of the Late- and Postglacial dynamics of the vegetation from Peşteana, Poiana Ruscă Mountains. Contribuţii Botanice 41:109–118

Fărcaş S, Tanţău I, Mîndrescu M, Hurdu B (2013) Holocene vegetation history in the Maramureş mountains (Northern Romanian Carpathians). Quatern Int 293:92–104

Feurdean A (2005) Holocene forest dynamics in northwestern Romania. Holocene 15(3):435–446

Feurdean A, Astalos C (2005) The impact of human activities in the Gutâiului Mountains, Romania. Stud UBB Geol 50(1):63–72

Feurdean A, Bennike O (2004) Late Quaternary palaeoecological and palaeoclimatological reconstruction in the Gutâiului Mountains, northwest Romania. J Quat Sci 19(8):809–827

Feurdean A, Willis KJ (2008a) The usefulness of a long-term perspective in assessing current forest conservation management in the Apuseni Natural Park, Romania. For Ecol Manage 256:421–430

Feurdean A, Willis KJ (2008b) Long-term variability of Abies alba in NW Romania: implications for its conservation management. Divers Distrib 14(6):1004–1017

Feurdean A, Mosbrugger V, Onac BP, Polyak V, Vereş D (2007a) Younger Dryas to mid-Holocene environmental history of the lowlands of NW Transylvania, Romania. Quatern Res 68(3):364–378

Feurdean A, Wohlfarth B, Björkman L et al (2007b) The influence of refugial population on Lateglacial and early Holocene vegetational changes in Romania. Rev Palaeobot Palynol 145 (3):305–320

Feurdean A, Klotz S, Mosbrugger V, Wohlfarth B (2008) Pollen-based quantitative reconstructions of Holocene climate variability in NW Romania. Palaeogeogr Palaeoclimatol Palaeoecol 260(3):494–504

Feurdean AN, Willis KJ, Astaloş C (2009) Legacy of the past land-use changes and management on the 'natural' upland forest composition in the Apuseni Natural Park, Romania. Holocene 19 (6):967–981

Feurdean A, Willis KJ, Parr CL, Tanţău I, Fărcaş S (2010) Post-glacial patterns in vegetation dynamics in Romania: homogenization or differentiation? J Biogeogr 37(11):2197–2208

Feurdean A, Spessa A, Magyari EK, Willis KJ, Veres D, Hickler T (2012a) Trends in biomass burning in the Carpathian region over the last 15,000 years. Quatern Sci Rev 45:111–125

Feurdean A, Tămaş T, Tanţău I, Fărcaş S (2012b) Elevational variation in regional vegetation responses to late-glacial climate changes in the Carpathians. J Biogeogr 39(2):258–271

Feurdean A, Parr CL, Tanţău I et al (2013a) Biodiversity variability across elevations in the Carpathians: parallel change with landscape openness and land use. Holocene 23(6):869–881

Feurdean A, Liakka J, Vannière B et al (2013b) 12,000-Years of fire regime drivers in the lowlands of Transylvania (Central-Eastern Europe): a data-model approach. Quatern Sci Rev 81:48–61

Feurdean A, Perşoiu A, Tanţău I et al (2014) Climate variability and associated vegetation response throughout Central and Eastern Europe (CEE) between 60 and 8 ka. Quatern Sci Rev 106:206–224

Feurdean A, Marinova E, Nielsen AB et al (2015) Origin of the forest steppe and exceptional grassland diversity in Transylvania (central-eastern Europe). J Biogeogr. doi:10.1111/jbi.12468

Gâștescu P (2010) The lakes in Romania. An actual synthesis. Lakes Reservoirs Ponds 4(1):5–23

Geantă A, Gałka M, Tanţău I, Hutchinson SM, Mîndrescu M, Feurdean A (2014) High mountain region of the Northern Romanian Carpathians responded sensitively to Holocene climate and land use changes: a multi-proxy analysis. Holocene 24:944–956

Grindean R, Tanţău I, Fărcaş S, Panait A (2014) Middle to Late Holocene vegetation shifts in the NW Transylvanian lowlands (Romania). Stud UBB Geol 59(1):29–37

Hutchinson SM, Akinyemi FO, Mîndrescu M, Begy R, Feurdean A (2015) Recent sediment accumulation rates in contrasting lakes in the Carpathians (Romania): impacts of shifts in socio-economic regime. Reg Environ Change. doi:10.1007/s10113-015-0764-7

Iepure S, Namiotko T, Magyari EK (2011) Ostracod preservation and response to Late Glacial and Early Holocene climate changes in a sub-alpine belt lake of the southern Romanian Carpathians. Joannea Geol Paläontol 11:91–94

Ioniță I, Mărgineanu RM, Hurjui C (2000) Assessment of the reservoir sedimentation rates from 137Cs measurements in the Moldavian Plateau. Acta geol Hisp 35(3–4):357–367

IPCC, Climate change (2014) Impacts, adaptation and vulnerability. http://ipcc-wg2.gov/AR5/. Accessed 11 Oct 2014

Jalut G, Bodnariuc A, Bouchette A, Dedoubat JJ, Otto T, Fontugne M (2003) Holocene vegetation and human impact in the Apuseni Mountains, Central Romania. In: Tonkov S (ed) Aspects of Palynology and palaeoecology (Festschrift in honour of Elissaveta Bozilova). Pensoft Publishers, Sofia-Moscow, pp 137–170

Kasse CK (2002) Sandy aeolian deposits and environments and their relation to climate during the Last Glacial Maximum and Lateglacial in northwest and central Europe. Prog Phys Geogr 26 (4):507–532

Kern Z, Popa I (2007) Climate-growth relationship of tree species from a mixed stand of Apuseni Mts., Romania. Dendrochronologia 24(2):109–115

Korponai J, Magyari EK, Buczkó K et al (2011) Cladocera response to Late Glacial to Early Holocene climate change in a South Carpathian mountain lake. Hydrobiologia 676(1):223–235

Lang B, Bedford A, Brooks S et al (2010) Early-Holocene temperature variability inferred from chironomid assemblages at Hawes Water, northwest England. Holocene 20(6):943–954

Lascu I, Wohlfarth B, Onac BP, Björck S, Kromer B (2014) A Late Glacial paleolake record from an up-dammed river valley in northern Transylvania, Romania. Quatern Int. doi:10.1016/j.quaint.2014.11.041

Magny M, Haas JN (2004) A major widespread climatic change around 5300 cal yr BP at the time of the Alpine Iceman. J Quat Sci 19(5):423–430

Magyari EK, Buczkó K, Jakab G et al (2006) Holocene palaeohydrology and environmental history in the South Harghita Mountains, Romania. Földtani Közlöny 136:249–284

Magyari E, Jakab G, Braun M, Buczkó K, Bálint M (2009a) High-resolution study of Late Glacial and Early Holocene tree line changes in the Southern Carpathian Mountains. European Geoscience Union General Assembly 2009, Vienna Geophysical Research Abstracts 11. EGU2009, p 10549

Magyari EK, Braun M, Buczkó K et al (2009b) Radiocarbon chronology of glacial lake sediments in the Retezat Mts (South Carpathians, Romania): a window to Late Glacial and Holocene climatic and paleoenvironmental changes. Cent Eur Geol 52(3):225–248

Magyari EK, Buczkó K, Jakab G, Braun M, Pál Z, Karátson D (2009c) Palaeolimnology of the last crater lake in the Eastern Carpathian Mountains—a multiproxy study of Holocene hydrological changes. Hydrobiologia. doi:10.1007/s10750-009-9801-1

Magyari EK, Major Á, Bálint M et al (2011) Population dynamics and genetic changes of Picea abies in the South Carpathians revealed by pollen and ancient DNA analyses. BMC Evol Biol 11(1):66

Magyari EK, Demény A, Buczkó K et al (2013) A 13,600-year diatom oxygen isotope record from the South Carpathians (Romania): reflection of winter conditions and possible links with North Atlantic circulation changes. Quatern Int 293:136–149

Magyari EK, Vereş D, Wennrich V et al (2014a) Vegetation and environmental responses to climate forcing during the Last Glacial Maximum and deglaciation in the East Carpathians: attenuated response to maximum cooling and increased biomass burning. Quatern Sci Rev 106:278–298

Magyari EK, Kuneš P, Jakab G et al (2014b) Late Pleniglacial vegetation in eastern-central Europe: are there modern analogues in Siberia? Quatern Sci Rev 95:60–79

Mayewski PA, Rohling EE, Curt Stager J et al (2004) Holocene climate variability. Quatern Res 62(3):243–255

Mîndrescu M (2001) Vinderel Lake (Maramureş Mts). Morphohydrological aspects. Ann Univ Suceava Geogr Sect X:137–148

Mîndrescu M (2003) The Livia Lake (Northern Maramureş Range). Hydrological and morphological aspects. Ann Univ Suceava Geogr Sect XII:49–55

Mîndrescu M, Cristea AI (2011) Rock mass failures and antislope scarps in the Northern Romanian Carpathians. Paper presented at the Carpatho-Balkan-Dinaric Conference on Geomorphology, Ostravice, Czech Republic, 17–20 October 2011

Mîndrescu M, Iosep I, Cristea IA, Forgaci D, Popescu D-A (2010a) Lacurile Iezer şi Bolătău (Obcina Feredeului)—cele mai vechi lacuri de baraj natural formate prin alunecare din România. Volumul conferinţei "Resursele de apă din România. Vulnerabilitate la presiunile antropice" Târgovişte, 11–13 iunie 2010 (in Romanian)

Mîndrescu M, Cristea IA, Hutchinson SM (2010b) Bathymetric and sedimentological changes of glacial lake Ştiol, Rodna Masiff. Carpathian J Earth and Environ Sci 5(1):57–65

Mîndrescu M, Cristea IA, Florescu G (2010c) Water quality and ecology of the Iezer and Bolătău lakes. Lakes, reservoirs, and ponds. Romanian. J Limnol 4(1–2):117–130

Mîndrescu M, Cristea AI, Hutchinson SM, Florescu G, Feurdean A (2013) Interdisciplinary investigations of the first reported laminated lacustrine sediments in Romania. Quatern Int 293:219–230

Mîndrescu M, Zamosteanu A, Cristea IA (2016a) Glacial lakes and peat bogs in the Romanian Carpathians. Ed. Universit. Suceava, Romania

Mîndrescu M, Németh A, Grădinaru I, Bihari Á, Németh T, Fekete J, Bozsó G, Kern Z (2016b) Bolătău sediment record–chronology, microsedimentology and potential for a high resolution multimillennial palaeoenvironmental proxy archive. Quat Geochronol 32:11–20

Mociornița C, Brateş E (1987) Unele aspecte privind scurgerea de aluviuni în suspensie în Romania. Hidrotehnica 32(7):11–19 (in Romanian)

Németh A, Mindrescu M, Grădinaru I et al (2014) 550 years in sedimentological record from a varved type lake (Bolătău, Bukovina, NE Romania)—changing storm frequency and climate fluctuation. Late Pleistocene and Holocene climatic variability in the Carpathian-Balkan region (CBW2014). Abstracts volume. Georeview special issue. doi:10.4316/GEOREVIEW.2014.0.0.187

Onac BP, Constantin S, Lundberg J, Lauritzen SE (2002) Isotopic climate record in a Holocene stalagmite from Urşilor Cave (Romania). J Quat Sci 17(4):319–327

Pandi G (2004) A Gyilkos-Tó. Hidrogeográfiai tanulmány. Ed. Casa Cărţii de Ştiinţă, Cluj

Pişota I (1968) Lacurile glaciare din Munţii Rodnei. Anal Univ Bucureşti (Şt. nat) Geol Geogr 12 (2):113–124 (in Romanian)

Pişota I (1971) Lacurile glaciare din Carpaţii Meridionali. Ed. Acad. Române, Bucureşti (in Romanian)

Rădoane M, Rădoane N (2005) Dams, sediment sources and reservoir silting in Romania. Geomorphology 71:112–125

Rasmussen SO, Andersen KK, Svensson AM et al (2006) A new Greenland ice core chronology for the last glacial termination. JGeophys Res: Atmos (1984–2012): 111(D6)

Rösch M, Fischer E (2000) A radiocarbon dated Holocene pollen profile from the Banat mountains (Southwestern Carpathians, Romania). Flora (Jena) 195(3):277–286

Rose NL, Cogălniceanu D, Appleby PG et al (2009) Atmospheric contamination and ecological changes inferred from the sediment record of Lacul Negru in the Retezat National Park, Romania. Advanc Limnol 62:319–350

Schnitchen C, Magyari E, Tóthmérész B, Grigorszky I, Braun M (2003) Micropaleontological observations on a Sphagnum bog in East Carpathian region—testate amoebae (Rhizopoda: Testacea) and their potential use for reconstruction of micro- and macroclimatic changes. Hydrobiologia 506–509:45–49

Schnitchen C, Charman DJ, Magyari EK et al (2006) Reconstructing hydrological variability from testate amoebae analysis in Carpathian peatlands. J Paleolimnol 36:1–17

Smol JP (2009) Pollution of lakes and rivers: a paleoenvironmental perspective. Wiley

Soróczki-Pintér É, Pla-Rabes S, Magyari EK, Stenger-Kovács CS, Buczk K (2014) Late Quaternary Chrysophycean stomatocysts in a Southern Carpathian mountain lake, including the description of new forms (Romania). Phytotaxa 170(3):169–186

Tămaş T, Onac BP, Bojar A-V (2005) Lateglacial-Middle Holocene stable isotope records in two coeval stalagmites from the Bihor Mountains, NW Romania. Geol Q 49(2):185–194

Tanţău I (2006) Histoire de la végétation tardiglaciaire et holocéne dans les Carpates Orientales (Roumanie). Ed. Presa Universitară Clujeană, Cluj-Napoca

Tanţău I, Fărcaş S (2004) Chronologie de l'histoire de la végétation holocène de Monts Rodnei (Carpates Orientales). Contrib Bot 39:241–250

Tanţău I, Reille M, de Beaulieu JL et al (2003b). Vegetation history in the Eastern Romanian Carpathians: pollen analysis of two sequences from the Mohoş crater. Veg Hist Archaeobot 12 (2):113–125

Tanţău I, Fărcaş S, Reille M, de Beaulieu JL (2003c) L'analyse palinologique de la sequence de Luci: nouvelles donnees concernant l'histoire de la végétation tardiglaciaire et holocène de Monts Harghitei. Contrib Bot 38:155–161

Tanţău I, Reille M, de Beaulieu JL, Fărcaş S (2006) Late Glacial and Holocene vegetation history in the southern part of Transylvania (Romania): pollen analysis of two sequences from Avrig. J Quat Sci 21(1):49–61

Tanţău I, Reille M, de Beaulieu JL, Fărcaş S, Brewer S (2009) Holocene vegetation history in Romanian Subcarpathians. Quatern Res 72(2):164–173

Tanţău I, Feurdean A, de Beaulieu JL, Reille M, Fărcaş S (2011a) Holocene vegetation history in the upper forest belt of the Eastern Romanian Carpathians. Palaeogeogr Palaeoclimatol Palaeoecol 309(3):281–290

Tanţău I, Fărcaş S, Beldean C, Geantă A, Ştefănescu L (2011b) Late Holocene paleoenvironments and human impact in Făgăraş Depression (southern Transylvania, Romania). Carpathian J Earth Environ Sci 6(1):171–178

Tanţău I, Feurdean A, de Beaulieu JL, Reille M, Fărcaş S (2014) Vegetation sensitivity to climate changes and human impact in the Harghita Mountains (Eastern Romanian Carpathians) over the past 15,000 years. J Quat Sci 29(2):141–152

Tanţău I, Reille M, Fărcaş, S, De Beaulieu JL (2003a) Aspects de l'histoire de la végétation tardiglaciaire et Holocène dans la région des Subcarpates de la Courbure (Subcarpates de Buzău). Stud UBB Geol 48(2):15–26

Tóth M, Magyari EK, Brooks SJ, Braun M, Buczkó K, Bálint M, Heiri O (2012) A chironomid-based reconstruction of late glacial summer temperatures in the southern Carpathians (Romania). Quatern Res 77(1):122–131

Verstraeten G, Bazzoffi P, Lajczak A, Radoane M, Rey F, Poesen J, de Vente J (2006) Soil erosion in Europe. In: Boardman J, Poesen J (eds) Reservoir and pond sedimentation in Europe. Wiley, p 759–774

Vespremeanu-Stroe A, Urdea P, Tătui F, Constantinescu Ş, Preoteasa L, Vasile M, Popescu R (2008) Date noi privind morfologia lacurilor glaciare din Carpaţii Meridionali. Rev Geomorfol 10:73–87 (in Romanian)

Wohlfarth B, Hannon G, Feurdean A, Ghergari L, Onac BP, Possnert G (2001) Reconstruction of climatic and environmental changes in NW Romania during the early part of the last deglaciation ($\sim$15000–13600 cal yr BP). Quatern Sci Rev 20(18):1897–1914

Part VIII
Geomorphologic Hazards

Chapter 31
Snow Avalanche Activity in Southern Carpathians (Romanian Carpathians)

Mircea Voiculescu

Abstract Snow avalanches represent an undeniable reality in the Romanian Carpathians both as a geomorphic process and as a type of hazard, and cause damage to transportation routes or tourism infrastructure and losses of human lives. In this context, the past snow avalanche activity is poorly evaluated, even if these mountains are known for the high occurrence of snow avalanches. The scientific analysis of snow avalanches using dendrogeomorphologic approach is recent in the Romanian Carpathians. The first results were obtained in the Făgăraș Massif and the Bucegi Mountains, located in the eastern part of the Southern Carpathians (Romanian Carpathians). The present contribution aims to analyse the snow avalanche chronology using dendrogeomorphologic approach, to reconstruct temporal patterns of past snow avalanches (magnitude, return period, synchronicity), and to examine the relationships between winter types with major snow avalanche events. We performed a dendrogeomorphic analysis based on 182 *Picea abies* in Făgăraș Massif and 99 *Picea abies* 77 *Larix decidua Mill* in Bucegi Mountains. We sampled trees in three snow avalanche tracks in Făgăraș massif and in three snow avalanche tracks in Bucegi Mountains and obtained 392 and 352 samples, respectively. Our results from tree ring records yielded 19 and 17 snow avalanche winters in the 1968–2011 chronology and 94 snow avalanche winters in the 1852–2013 chronology in the Făgăraș Massif and 32 avalanche winters in the 1954–2011 chronology, 27 avalanche winters in the 1962–2012 chronology and 30 avalanche winters in the 1964–2011 chronology in Bucegi Mountains, respectively. We identified three avalanche types: small avalanches with Avalanche Activity Index (AAI) between 10 and 20 %, large avalanches with AAI between 21 and 30 % and very large avalanches with AAI > 31 %. We also obtained a similar return period ranging from 13 to 14.9 years in the Făgăraș Massif and from 13.1 to 15.2 years in the Bucegi Mountains. Eight avalanche events were synchronous in two or three stands in the Făgăraș Massif and five avalanche events in the Bucegi Mountains.

M. Voiculescu (✉)
West University of Timişoara, V. Pârvan 4, 300223 Timişoara, Timiş, Romania
e-mail: mircea.voiculescu@e-uvt.ro

M. Rădoane and A. Vespremeanu-Stroe (eds.), *Landform Dynamics and Evolution in Romania*, Springer Geography,
DOI 10.1007/978-3-319-32589-7_31

To determine the relationship between snow avalanches and winter temperatures, we use the Winter Standardized Index (WSI) between 1979 and 2012 for the Bâlea Lac weather station in the Făgăraş Massif and between 1961 and 2011 for the Vf. Omu and Sinaia weather stations in Bucegi Mountains. We obtained a correlation between these parameters and our dendrogeomorphological results; the probability of major snow avalanche occurrence was highest during cold and normal winters in Făgăraş Massif and cold in Bucegi Mountains.

Keywords Snow avalanches · Dendrogeomorphic approach · Magnitude · Return period · Synchronicity · Romanian carpathians

Introduction

Snow avalanches are common denudational processes in the mountains, with well-defined glacial areas to be found in the Pyrenees, the Alps, the Himalayas and the Andes. Snow avalanches generally occur at the contact of alpine with subalpine areas (McClung and Schaerer 2006; Strunk 1997) on surfaces known as open slopes (unconfined), gullies or avalanche tracks (confined). They also occur in forests, where tree density, size and the distribution of forest and the patterns of local topography influence the probability of avalanche releases (Bebi et al. 2001; Schneebeli and Bebi 2004; Teich et al. 2012; Viglietti et al. 2010).

Avalanches should be understood in the larger context of the study of snow, which is the primary agent acting on the overall and detailed morphology, especially in alpine-type mountain areas (Francou 1993a, b). Snow avalanches are one of the major forms of snow moving (Schönenberger et al. 2005), whether "*as rapid gravity drainage, on the slopes along the length of their path from starting zone to runout zone*" (Ammann 2003, p. 83), or "as *rapid downslope movements resulting from the failure of an unstable snow cover*" (Luckman 1977, p. 31). It is generally considered that the large majority of avalanches are 'clean' (Rapp 1960): such avalanches do not contain dendritic material in their composition and snow is redistributed at the base of the track or slope. On the other hand, there is another type of avalanche, "*a mass of snow moving downslope, which may also contain ice, soil, rocks, or other debris*" (Fredston and Fesler 1984, quoted by Butler 1998, p. 213). The geomorphological effect of these avalanches is indirect and is found either in the supply of glacier with snow or in snowmelt runoff patterns (Luckman 1978).

Snow avalanches are major natural hazards that affect inhabited areas (settlements, housing, roads or skiing infrastructure) (Fuchs et al. 2004, 2005; Fuchs and Bründl 2005; Jamieson and Stethem 2002; Stethem et al. 2003), causing loss of human lives (Höller 2007, 2009; Jamieson and Stethem 2002).

Avalanches always happen during the dormant season of the trees' growth, and the evidence of damage is reflected in the growth rings of trees in the season after the event (Luckman 2010). The study of the growth of tree rings allows for the reconstruction of the event's chronology, highlighting its magnitude and frequency,

which is the study subject of dendrogeomorphology (Luckman 2010). Dendrogeomorphology is generally based on two fundamental elements (Corona et al. 2012): (i) the trees of the temperate climate form a tree ring every year; and (ii) trees affected by some geomorphological processes (avalanches, creep, rockfalls, landslides, debris flow) will record the event in their tree rings as characteristic growth disturbances.

Thus, the use of tree rings of resinous and deciduous trees for the reconstruction of event chronologies, for dating and for assessing the magnitude, frequency and return period of avalanches has been developed over many decades, enjoying considerable success.

The first applications of dendrogeomorphology to avalanche analysis date to the 1960s and 1970s (Butler 1979; Ives et al. 1976; Carrara 1979; Potter 1969; Schaerer 1972; Smith 1973); it obtained pioneering results in the reconstruction of avalanches in the US. Later, in the 1980s and 1990s, and especially in the 2000s, research was conducted mainly in the mountains of the Western US (Bryant et al. 1989; Butler and Malanson 1985b; Jenkins and Hebertson 1994; Hebertson and Jenkins 2003; Patten and Knight 1994; Rayback 1998; Reardon et al. 2008) and in the mountains of Canada, in British Columbia and Quebec (Boucher et al. 2003; Dubé et al. 2004; Germain et al. 2005, 2009; Larocque et al. 2001). Attention was paid to establishing of snow avalanche chronologies, supplementing existing statistics and improving sampling techniques and the relationship between snow avalanche activity and climatic conditions.

In Europe, the first studies started before 2000, gathering momentum thereafter. Attention was focused mainly on assessing the magnitude, frequency and return period of snow avalanches in mountainous areas in Iceland (Decaulne and Sæmundsson 2008; Decaulne et al. 2012) and Norway (Decaulne et al. 2014), in the Spanish Pyrenees (Molina et al. 2004; Muntán et al. 2004, 2009), Alps (Casteller et al. 2007; Corona et al. 2010, 2012; Garavaglia and Pelfini, 2011; Stoffel et al. 2006; Stoffel and Hitz 2008; Szymczak et al. 2010) and the Carpathian Mountains (Malik and Owczarek 2009; Tumajer and Treml 2015).

Research has also been conducted on other continents: South America (Casteller et al. 2008; Mundo et al. 2007) and Asia (Kajimoto et al. 2004; Köse et al. 2010; Laxton and Smith 2009). In this context, most studies have been conducted on various coniferous species that have very well-defined annual tree rings and show disturbances such as reaction wood or traumatic resin ducts.

Snow avalanches are undoubtedly an attribute of the Romanian Carpathians, with the Southern Carpathians, in particular, being subject to avalanches as one of the most relevant geomorphic processes and mountain hazards, affecting human life and causing damage to forests, tourism infrastructure and transport and communications.

The main goals of our study are: (i) to present the first synthetic results obtained on snow avalanche activity in several areas of the Carpathians using the dendrogeomorphic approach, (ii) to supplement the existing database on recorded snow avalanches and (iii) to reconstruct the spatio-temporal patterns of snow avalanche activity.

Study Area

A Review of Snow Avalanches Research in the Făgăraș Massif and the Bucegi Mountains

The scientific study of avalanches in the Romanian Carpathians is recent, occurring mostly after 2000. In its first stage, attention was paid to the morphometric characteristics of snow avalanche tracks (Voiculescu 2004) and to the potential of snow avalanche activity in the Făgăraș Massif (Voiculescu et al. 2011). Researchers then approached the management of snow avalanches in the Bucegi and Făgăraș mountain ranges (Voiculescu 2009; Voiculescu and Popescu 2011); avalanches that disturb the mountain environment (Voiculescu and Ardelean 2012); reconstruction of the huge snow avalanche in the Urlătoarea valley in Bucegi Mountains from February 1969 (Voiculescu 2010) and the relief incidence and types of human activities involving accidents (Voiculescu 2014). Lately, avalanche research has received particular attention, due to the use of the dendrogeomorphology method with good results in several areas of the Făgăraș Massif and the Bucegi Mountains. Some studies on the chronology, magnitude, frequency and return period have used the signal events recorded in the structure of trees (Chiroiu et al. 2015a, b; Voiculescu et al. 2013; Voiculescu and Onaca 2013, 2014).

The management of snow avalanches had two critical moments (Voiculescu 2009). The first was the creation of the Mountain Rescuer Public Services (MRPS) by Government Decision 140/1968. This has the role of accident prevention, surveying, coordinating and organising mountain rescues in the event of snow avalanches and damaging events caused by snow avalanches. The second moment was the creation of the Programme of Nivometeorology within the National Administration of Meteorology (PN–NAM) in partnership with Météo France, the Centre d'Études Neige–Grenoble, during the 2003–2004 winter season. The main purpose of the programme is to study snow and its future evolution as well as avalanche-triggering conditions. The PN–NAM has one nivometeorological laboratory in the Făgăraș Massif at Bâlea Lac weather station (2040 m a.s.l.) and two nivometeorological laboratories in the Bucegi Mountains, one at the Vf. Omu weather station (2505 m a.s.l.) and the other at the Sinaia weather station (1500 m a.s.l.).

Formation and Motion of Snow Avalanches

The spatial distribution of snow avalanches and their characteristics depend on the interaction between morphometric factors (elevation, slope inclination and exhibition) and climatic variables (solar radiation, temperature, type and amount of accumulated snow and wind) (Luckman 2010; McClung and Schaerer 2006; McClung 2001; Schweizer et al. 2003). These elements have played a critical role in triggering snow avalanches and their dynamics, which can be used in evaluating

their magnitude and frequency (Butler 1986; Butler and Malanson 1985b; McClung and Schaerer 2006). According to the analyses of the PN–NAM and also personal observations, the snow avalanches in the Făgăraş Massif and Bucegi Mountains manifest themselves in the same way as those considered in the avalanche research literature.

Considering the average altitude of the Romanian Carpathians and according to the geographical classification of Vanni (1965), there are two types of snow avalanches: medium-high mountain and valley floor avalanches, each with a local character (Voiculescu 2009). In the first case, snow avalanches occur within the glacial cirques or in the upper part of the glacial valleys, at elevations higher than 2220–2300 m. In the second case, snow avalanches occur in the lower part of the glacial valleys below an altitude of 2000 m and at the contact between the alpine level and the timberline at 1500–1600 m, or in the forest. Therefore, topographic sites are open slopes and very steep, at 25°–45° and over 45°, as listed in the literature (Luckman 1977; McClung and Schaerer 2006), and deep gullies or multiple gullies, large gullies and steeper slopes (Luckman 1977; McClung and Schaerer 2006) are found in the Bâlea glacial area, in particular (Voiculescu et al. 2011; Voiculescu 2014).

The Romanian Carpathians alpine area has not a great spatial extension. The lower half of the alpine slopes and valley bottoms are covered with trees and shrubs. According to Butler and Sawyer (2008) and Corona et al. (2012), this provides a good opportunity to use the dendrogeomorphologic method to evaluate snow avalanches with a good annual, decadal and centennial resolution.

In our case, the quantitative analysis of snow avalanches using a geomorphic process was based on the following assumptions: (i) effectiveness of the dendrogeomorphologic method, (ii) total lack of research in Romania, (iii) method validation by means of specific elements of analysis (historical records, nivometeorologic data) and (iv) integration of our studies with international studies.

Considering its position, the Făgăraş Massif is under the action of humid air masses from the Atlantic Ocean and also of air masses from the Arctic with low temperatures and large and persistent snow depth, while the Bucegi Mountains come under the continental influence of the Siberian anticyclone, which brings cold polar air inflows with very low temperatures (−30 °C), strong winds and snowstorms. Sometimes Mediterranean cyclones occur in the area, bringing wet, warm air and abundant snow with considerable snow depths.

Snow Avalanche Accidents

Snow avalanches are the most dangerous natural hazard and risk phenomenon, if we consider the number of fatalities and injuries/burials recorded each year, and the revalued recent winter tourism potential through a series of specific activities (off-piste skiers, back-country skiers and climbers). Although Romania is part of the International Commission for Alpine Rescue (ICAR) of Europe, avalanche statistics

are incomplete and difficult to use and should be considered with caution. The Făgăraș Massif is the only mountainous area that has a well-established statistical basis. To document the number of casualties recorded in the two investigated mountainous areas, we used MRPS and PN–NAM database statistics (National Administration of Meteorology, 2004–2005, 2005–2006, 2007–2008, 2008–2009) and some websites, archival material (newspapers), mass media, eyewitness statements and our field observations (commemorative plaques and crosses). Between the months November–June for the years 1963–2015, in the Făgăraș Massif, 76 fatalities and 50 burials/injuries (62 fatalities and 50 injuries on the northern slope and 14 fatalities on the southern slope) were recorded. Of these, 40 fatalities and 42 burials/injuries in the Bâlea glacial area were recorded, or an average value of 1.07 fatalities per year (0.51 per year in the Făgăraș Massif and 0.56 per year in the Bâlea glacial area, and of 0.70 burials/injuries per year, 0.11 per year in Făgăraș Massif and 0.59 per year in the Bâlea glacial area) (Voiculescu 2014).

In the Bucegi Mountains, 20 fatalities (of which 75 % occurred in the Vf. Omu high glacial area) and 74 burials/injuries (of which, 78.3 % occurred in the Vf. Omu high glacial area) were recorded.

Site Selection and Location

The sampling sites were chosen taking into account the events recorded by PN–NAM and MRPS and then based on the clear evidence of physical injury to the trees. The investigated areas from the Făgăraș Massif are in the Bâlea and Arpaș glacial areas (Fig. 31.1).

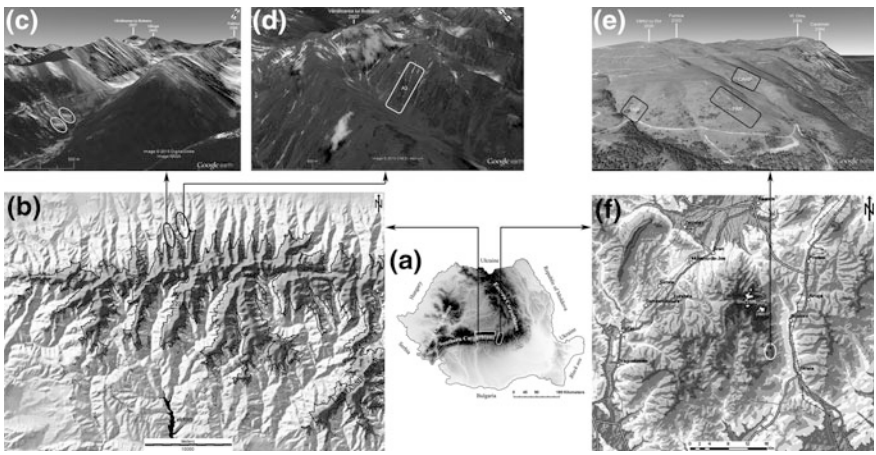

Fig. 31.1 Location in Southern Carpathians (**a**) of the study areas in the Făgăraș Massif (**b**) and Bucegi Mountains (**f**): Google Earth satellite image showing the TRC1 and TRC2 snow avalanche paths (**c**) and A3 snow avalanche path (**d**) and CARP, PAR and TAR snow avalanche paths (**e**)

In the Bâlea glacial area, we investigated two stands, located on the bedrock that contains three lobes on the western slope of the glacial valley between 1280 and 1550 m a.s.l., below the Transfăgărăşan highway. The bedrock is covered by slope deposits that are primarily composed of metamorphic rocks (crystalline schists, sericite-chlorite schist and paragneiss). Slope inclination has high values, ranging from 30° to 35° and from 35° to 45°. The middle part of the sector is covered by young trees, while a large part of the valley bottom is covered by trees, mainly *Picea abies.* Geomorphologically, the area is dominated by erosion, rockfall, spills and rock slides during the summer and by snow avalanches during the winter. The dynamics of this slope was accentuated by the construction of Transfăgărăşan highway between 1970 and 1974.

In the Arpaş glacial area, a large avalanche located on the eastern slope of the glacial valley track was investigated. In the starting zone, this avalanche intersects the shoulder of the glacial valley (Chiroiu et al. 2015a). The top track is covered by herbs and shrubs (*Sorbus aucuparia* and *Rubus idaeus*) and small trees (*Alnus viridis, Pinus mugo*), and the middle part and the valley bottom, by conifers (*Picea abies*). The main processes dominating the area are snow avalanches, debris flows and rockfalls (Chiroiu et al. 2015b).

The investigated area of the Bucegi Mountains is located between 1550 and 2000 m a.s.l. in the southern half of the Bucegi Mountains, in the Sinaia ski area, one of the most important skiing areas in Romania (see Fig. 31.1). Tourism infrastructure and skiing activities have grown considerably, especially in the last 10–15 years. Therefore, the incidence of snow avalanches has increased. The slope inclination is high, ranging from 35° to 40° on the upper part and from 25° to 30° on the bottom part. In the ski area, we sampled three stands. The slope is covered mainly by grass and here and there by small trees or shrubs (*Alnus viridis, Vaccinium myrtillus* and *Vaccinium vitis-idaea).* In the complex, there are cuesta front floors, which act as springboards for avalanches triggered at the highest altitudes of the ski area. The characteristics of snow avalanche tracks are shown in Table 31.1.

As the northern slope of the Făgăraș Massif is dominated by humid air masses from the Atlantic Ocean and by Arctic air masses, Scandinavian anticyclones bring early and late snowfalls and low temperatures. The Bucegi Mountains come under the continental influence of Siberian anticyclones that bring cold polar air invasions with very low temperatures (−30 °C), strong winds and snowstorms, although sometimes, Mediterranean cyclones occur in the area, bringing wet, warm air and abundant snow with considerable snow depths. According to Corona et al. (2012), there is a relationship between snow avalanches and winter temperatures.

The relationship between the annual number of days with snowfall (n_s) and the annual number of days with rainfall (n_r) are good indicators of the prevalence of solid/liquid precipitation. This indicator is directly conditioned by elevation and less by local influences. The value of this indicator is 1.5 at the highest peaks of the Bucegi Mountains, 0.80 at the timberline (at Sinaia weather station) and 1.7 at the lower parts of the alpine zone of Făgăraș Massif (at Bâlea Lac weather station). In

Table 31.1 Characteristics of investigated snow avalanche path

Snow avalanche path code	Elevation (m a.s.l.)		Vertical drop	Starting from a		Confined/ unconfined	Slope (°)	Aspect	Accessibility	Man-made infrastructure
	Max. (starting zone)	Min. (runout zone)		Point	Line					
TRC1	1500 (forestry zone)	1300 (forestry zone)	200	+		Unconfined	30°–35°	Eastern	Yes	No
TRC2	1510 (forestry zone)	(subalpine zone)	210	+		Unconfined	30°–35°	Eastern	Yes	No
A3	1900 (subalpine zone)	(subalpine zone)	570		+	Confined	35°–45°	Western	Partially	No
CARP	2000 (subalpine zone)	1670 (subalpine zone)	330		+	Unconfined	35°–40°	Eastern	Yes	Yes[a]
PAR	1880 (subalpine zone)	1700 (subalpine zone)	180		+	Both	30°–35°	Southeastern	Yes	No
TAR	1870 (subalpine zone)	1660 (subalpine zone)	210		+	Both	30°–35°	Southeastern	Yes	Yes[b]

[a]Signaled piste
[b]Display panels

this context, during the winter season, when there is snow avalanche activity (1 November–31 May), precipitation fall mostly as snow.

Vf. Omu weather station recorded 134 days with snowfall, Sinaia weather station, 91, at Bâlea Lac weather station, 133.5. At the higher elevations, the length of the snowfall season varied from 237 to 362 days (average 326), whilst at the timberline, at Sinaia weather station, the season varied from 181 to 276 days (average 238). The number of days with snow cover is 184.4 at Vf. Omu weather station, 148.3 at Sinaia weather station and 224 at Bâlea Lac weather station. Therefore, the cold season is long, between 8 and 10 months at the higher elevations and 5 months at timberline, with permanent snow cover at higher elevations. The characteristics of the climate are illustrated in Table 31.2.

Tree Ring Analysis of Snow Avalanches in Southern Carpathians

Impact of Snow Avalanche Activity

Most external deformations (tilting, scars, broken branches, topping and uprooting) are caused by snow avalanches, but could also be caused by other geoprocesses, i.e. rockfalls or debris flows (Decaulne et al. 2014; Stoffel et al. 2013). The impact of snow avalanches on trees is represented by reaction wood, callus tissue or scars and abrupt growth decrease. Therefore, the sampling strategy has several stages: field research (geomorphic mapping must be carried), selecting and visual investigation on trees affected by avalanches, coding samples, recording the geographical coordinates of trees, measuring the diameter and height of trees from which the sample was taken and, finally, processing of samples (Casteller et al. 2011; Corona et al. 2013; Decaulne et al. 2012, 2013, 2014; Germain et al. 2009).

It is considered that the optimal number of sampled trees depends on the nature of the investigation, trees age and the period of the recorded events (Luckman 2010). Therefore, different opinions were elicited in the literature: Burrows and Burrows (1976), Luckman and Frazer (2001) and Stoffel et al. (2006) note that a single tree can be used to highlight an old avalanche, Hebertson and Jenkins (2003) recommend a minimum of 20 trees per stand, Butler and Sawyer (2008) suggest that 10 trees are sufficient but that 100 trees would be an ideal number. Recently, Germain et al. (2010) mention a minimum of 40 trees sampled for a single snow avalanche track and Decaulne et al. (2012) confirm that a minimum of 20 trees per stand should be used.

We sampled 358 trees, 182 in the Făgăraș Massif and 176 in the Bucegi Mountains, obtaining 744 samples in total, 392 samples in the Făgăraș Massif and 352 in the Bucegi Mountains. Sampling was carried out with a Haglöf increment borer (with a diameter of 5.15 mm and 30 or 40 cm long, according to the shape of the stem) (Table 31.3).

Table 31.2 Climatic characteristics of Vf. Omu, Sinaia (Bucegi Mountains) and Bâlea (Făgăraş Massif) weather stations

Weather station alt—m	Geographical coordinates		Vegetation belt	Climatic influence	Snow avalanche type	Air temperature (0 °C)		Total precipitation (mm)		Snow depth (cm)	
	Lat.	Long.				Annual	[a]	Annual	[a]	Annual	[a]
Vf. Omu-2505	45°27′	25°27′	Alpine	E	continental	−2.5	−9.7	995.7	184.8	34.5	55.4
Bâlea Lake-2070	45°36′	24°37′	Subalpine	N/NW	maritime	0.2	−7.3	1213.7	225.7	66.1	112.5
Sinaia-1500	45°23′	25°30′	Timberline	E	continental	3.7	−4.5	1057.4	191.8	25.9	46.6

[a]Winter season (01 November–31 April or 31 May)

Table 31.3 Samples from *Picea abies* and *Larix decidua Mill.* trees in the stands from Făgăraș Massif and Bucegi Mountains

Snow avalanche stand code	Sector	Number of trees sampled	Number of samples
TRC1		35 (*Picea abies*)	70
TRC2		42 (*Picea abies*)	84
TOTAL BÂLEA		77	154
A3	Centre Border Opposite slope	25 (*Picea abies*) 71 (*Picea abies*) 9 (*Picea abies*)	50 170 18
TOTAL A3		105	238
TOTAL FĂGĂRAȘ			392
CARP	Centre Border	50 (15 *Picea abies*, 37 *Larix decidua Mill.*) 12 (3 *Picea abies*, 9 *Larix decidua Mill.*)	100 24
PAR	Centre Border	10 (*Picea abies*, 7 *Larix decidua Mill.*) 61 (39 *Picea abies*, 22 *Larix decidua Mill.*)	20 122
TAR	Centre Border	10 (*Picea abies*) 33 (31 *Picea abies*, 2 *Larix decidua Mill.*)	20 66
TOTAL BUCEGI		176	352
TOTAL		358	744

Amongst the most common types of growth disturbances, we found and analysed the following: reaction wood (Braam et al. 1987); scars that mark the passage of snow avalanches charged with a mixture of boulders, tree or plant material (Alestalo 1971; Shroder 1980; McClung and Schaerer 2006); traumatic resin ducts (Bollschweiler et al. 2008; Stoffel et al. 2005); and callus tissue resulting from destruction of the cambium (Stoffel et al. 2005; Bollschweiler et al. 2008). For traumatic resin ducts and callus tissue, we established the exact location of injury within the annual growth tree ring to distinguish between snow avalanches and other geomorphological processes (e.g. rockfalls). To eliminate other causes of injury, we considered only traumatic resin ducts located at the beginning of the growth cycle.

According to the limitation factor principle and the choice of site, we built a reference chronology to separate the influence of climatic signal influence to other possible geomorphological processes (Corona et al. 2012; Decaulne et al. 2013, 2014) (e.g. rockfall, creep).

Snow Avalanche Chronology

All the growth disturbances attributed to snow avalanches were used to construct an event–response histogram and to calculate the snow Avalanche Activity Index (*AAI*) with values from 0 to 100 %) for each year *t* based on the percentage of tree responses (*R*) in relation to living trees during year *t* (Corona et al. 2010, 2012; Decaulne et al. 2012; Germain et al. 2009) (31.1):

$$\mathrm{AAI}_t = \left(\sum_{i=1}^{n} R_\mathrm{t}\right) \Big/ \left(\sum_{i=1}^{n} N_\mathrm{t}\right) \times 100 \tag{31.1}$$

where R_t is the response of a tree to an event in year *t* and N_t is the number of living trees during that year.

The frequency (*f*) or return period of GD is another element for snow avalanche analysis, which is calculated for each tree (*T*) using the following formula (Corona et al. 2010; Decaulne et al. 2012) (31.2). Based on these calculations, we determined the individual *GD* frequency for each tree (1/frequency):

$$\mathrm{t} = \frac{\left(\sum_{i=T}^{n} \mathrm{GD}\right)}{\left(\sum_{i=T}^{n} \mathrm{yr}\right)} \tag{31.2}$$

where GD represents the number of growth disturbances for each tree whilst yr the total number of years tree *T* was alive.

Age of Sampled Trees

The age of sample trees is an important element in dendrogeomorphology. Luckman (2010) notes that two trees that are about 200 years old are more important for the history of snow avalanches in a given area than 30 trees that are 50 years old. However, depending on the characteristics of the investigated stand, both young and old trees are acceptable (Decaulne et al. 2012, 2013, 2014).

In our areas, tree age groups were variable, depending on the natural state of the forest and the impact of human activities on the investigated mountain area (building of the Transfăgărăşan highway and ski activities). The highest value in Bâlea glacial area is covered by an age group of between 10 and 20 years and between 20 and 30 years. Thus, 88 % of the trees are younger than 30 years. We can conclude that most of the trees date from after the construction of the Transfăgărăşan highway. In stand A3 (cf. Fig. 31.1), where the forest is mature, the age groups under 30 and between 61–100 years and 101–150 years have similar percentages of between 21 and 22 %. The highest percentage is in the 31–60 years

range group (30 %) and the lowest share of the age group is over 150 years old (6 %).

In the Bucegi Mountains, the situation is similar. In the CARP stand, the youngest tree was 9 years old and the oldest 56 years, giving an average of 23.5 years. In the PAR stand, the tree age was between 7 and 51 years, with an average of 21.8 years, while in the TAR stand, the youngest tree was 9 years old and the oldest, 52 years, with an average of 25 years. The 11–20 years age group had the highest percentage of growth disturbances (45.2 % in the CARP stand; 54 and 46 % in the PAR and TAR stands, respectively). The 21–30 age group had a significant representation (27.4 % in the CARP stand, 19 % in the PAR stand and 26 % in the TAR stand), as did the 31–40 group (11.3 in the CARP stand, 10 % in the PAR stand and 13 % in the TAR stand) (Voiculescu and Onaca 2013, 2014). These values attest to the existence of young forests permanently affected by snow avalanches.

Tree Ring Analysis of Snow Avalanches

The growth disturbances registered in tree rings were divided into four major categories (Table 31.4). In all sample stands, reaction wood had the largest percentage, followed by traumatic resin ducts, abrupt growth changes and callus tissue and scars.

In the TRC2 and TRC1 stands, for 43 snow avalanche winters in the 1967–2011 chronology, we identified trees registering one or more growth disturbances in 12 of the years, and for 32 snow avalanche winters in the 1963–2011 chronology, one or more growth disturbances were registered in 18 of the years. The differences are caused by the sliding surface morphology, the topography characteristics and the frequency of snow avalanches on TRC2. In the A3 stand, a 161-years chronology was identified, with 97 years being registered as having one or more growth disturbances (Chiroiu et al. 2015a).

In the Bucegi Mountains, in the CARP stand, 57 snow avalanche winters in the 1954–2012 chronology with one or more growth disturbances were identified; in the PAR stand, 49 snow avalanche winters in the 1962–2012 chronology with one or more growth disturbances were identified; and in the TAR stand, 47 snow avalanche winters in the 1964–2011 chronology with one or more growth disturbances were identified (Voiculescu and Onaca 2013, 2014). The sliding surfaces are herbaceous and the topography is marked by the presence of the cuesta front that provides dendritic material for the snow avalanche.

The oldest disturbance in the Bâlea valley stands was recorded in 1968 and the most recent, in 2008. In the Arpaș stand, the oldest disturbance was recorded in 1852 and the most recent, in 2012. In the Bucegi Mountains, the oldest disturbances were recorded in 1954 (CARP stand), 1969 (PAR) and 1964 (TAR), and the most recent in 2010 (CARP stand) 2012 (PAR stand) and 2010 (TAR stand) (Fig. 31.2).

Table 31.4 Tree ring indicators of snow avalanche events recorded at TRC1, TRC2, A3 and CARP, PAR and TAR

Stands	Reaction wood		Traumatic resin ducts		Abrupt growth changes		Callus tissue and scars	
TRC1	1995, 1996, 1997, 2001, 2003, 2005, 2008	33.4 %	1997, 2005, 2006, 2008	19 %	1996, 1997, 1998, 1999, 2003	23.8 %	2005, 2006, 2007, 2008, 2009	23.8 %
TRC2	1968, 1971, 1973, 1976, 1987, 1988, 1999, 2000, 2001, 2002, 2003, 2004, 2005, 2006, 2007, 2008	47 %	1996, 2000, 2002, 2003, 2004, 2005, 2006, 2007, 2008	26.5 %	1976, 1997, 2006	8.9 %	1976, 1997, 2002, 2003, 2005, 2006	17.6 %
A3	1852, 1856, 1880, 1881, 1882, 1888, 1892, 1905, 1908, 1909, 1917, 1923, 1929, 1930, 1933, 1936, 1951, 1952, 1954, 1955, 1956, 1958, 1959, 1960, 1962, 1963, 1965, 1967, 1969, 1970, 1973, 1975, 1976, 1980, 1981, 1982, 1984, 1988, 1992, 1993, 1995, 1996, 1997, 1998, 2000, 2002, 2003, 2005, 2006, 2007, 2009, 2010, 2011, 2012	33.7 %	1876, 1895, 1898, 1905, 1906, 1907, 1908, 1910, 1912, 1916, 1918, 1919, 1912, 1923, 1926, 1929, 1930, 1932, 1936, 1940, 1943, 1944, 1946, 1947, 1949, 1952, 1953, 1955, 1956, 1963, 1968, 1970, 1972, 1974, 1979, 1981, 1983, 1984, 1987, 1989, 1993, 1995, 1996, 1998, 1999, 2002, 2005, 2006, 2008, 2009	31.3 %	1859, 1866, 1868, 1885, 1888, 1895, 1897, 1898, 1905, 1907, 1916, 1917, 1923, 1927, 1929, 1931, 1939, 1942, 1944, 1947, 1948, 1950, 1952, 1954, 1956, 1962, 1963, 1966, 1967, 1971, 1975, 1976, 1978, 1981, 1984, 1987, 1988, 1989, 1990, 1992, 1993, 1996, 1997, 1998, 1999, 2002, 2003, 2005, 2007, 2009, 2010	31.9 %	1988, 2003, 2006, 2007, 2008	3.1 %
CARP	1954, 1960, 1970, 1974, 1977, 1980, 1982, 1985, 1986, 1987, 1989, 1990, 1991, 1992, 1995, 1998, 1999, 2002, 2003, 2004, 2005, 2006, 2007	50 %	1988, 1994, 1996, 2000, 2001, 2002, 2004, 2005, 2007, 2008, 2009, 2010	26.1 %	1970, 1982, 1989, 1994, 2006, 2008	13 %	1989, 2003, 2007, 2008, 2009	10.9 %

(continued)

Table 31.4 (continued)

Stands	Reaction wood		Traumatic resin ducts		Abrupt growth changes		Callus tissue and scars	
PAR	1976, 1977, 1979, 1984, 1985, 1996, 1998, 2001, 2002, 2003, 2005, 2006, 2007, 2008, 2009	38.5 %	1985, 1991, 1999, 2000, 2002, 2003, 2006, 2007, 2008, 2009, 2010, 2011	30.7 %	1985, 1987, 1993, 1995, 1998, 2001	15.4 %	1969, 2001, 2002, 2005, 2010, 2012	15.4 %
TAR	1965, 1972, 1974, 1979, 1981, 1982, 1984, 1985, 1988, 1989, 1991, 1992, 1993, 1995, 1997, 1998, 1999, 2000, 2001, 2002, 2003, 2005, 2006, 2008	53.4 %	1964, 1967, 1983, 1987, 1992, 1993, 1997, 2001, 2003, 2005, 2006, 2007, 2008, 2009, 2010	33.3 %	1975, 1981, 1988, 1997, 2003	11.1 %	1992	2.2 %

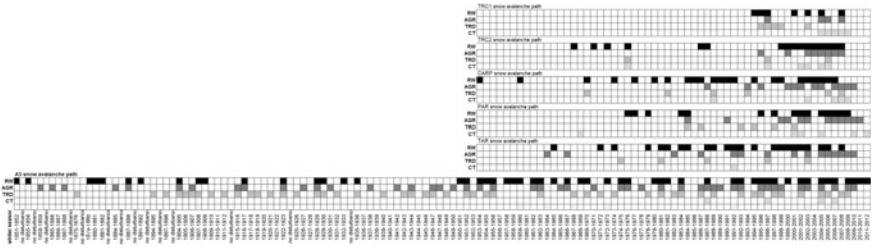

Fig. 31.2 Snow avalanche activity associated with the chronological distribution of different damage types: *RW* is reaction wood; *AGR* is abrupt growth changes; *TRD* is traumatic resin ducts and *CT* is callus tissue

Magnitude and Frequency of Snow Avalanches

Annual distribution of the major events in the investigated stands is represented by the AAI. Choosing the minimum necessary threshold for evidence of a snow avalanche is still a crucial question of dendrogeomorphology (Luckman 2010). Some researchers (Butler and Sawyer 2008; Butler et al. 2010; Germain et al. 2010; Reardon et al. 2008) show that the recording of avalanches must be present in at least two trees for 10, 20 or even 40 % of sampled trees containing records for the year.

In accordance with Decaulne et al. (2012, 2013, 2014); Germain et al. (2010); Reardon et al. (2008), and in order to evaluate the snow avalanche magnitude, we used the minimum threshold of 10 %, intermediate thresholds of 20 % and maximum thresholds of 40 % (Bryant et al. 1989; Butler and Malanson 1985a; Butler et al. 1987).

In the Bâlea glacial valley, the situation was as follows: in the TRC1 stand, 23 snow avalanche events were found between 1968 and 2011, from which seven events (30.4 %) had AAI > 10 %, two events (8.6 %) had AAI > 20 % and only one event (4.3 %) had AAI > 40 %. In the TRC2 stand, 21 snow avalanche events were found between 1968 and 2011, from which six events (28.5 %) had AAI > 10 %, two events (9.5 %) had AAI > 20 % and other two events (9.5 %) had AAI > 40 %. In the A3 stand, 99 snow avalanche events were found between 1852 and 2012 (Chiroiu et al. 2015a), from which 11 events (11.1) had AAI > 10 %, and only one event (1 %) had AAI > 20 % (Fig. 31.3).

In the Sinaia ski area, the situation is as follows (Voiculescu and Onaca 2013, 2014): in the CARP stand, 34 snow avalanche events were found between 1954 and 2011, in which five events (14.7 %) had AAI > 10 %, two events (5.8 %) had AAI > 20 % and another two events (5.8 %) had AAI > 40 %; in the PAR stand, 27 snow avalanche events were found between 1963 and 2012, of which four events (14.8 %) had AAI > 10 %, three events (11.1 %) had AAI > 20 % and other two events (7.4 %) had AAI > 30 %; in the TAR stand, 32 snow avalanche events were found between 1963 and 2011, of which nine events (28.1 %) had AAI > 10 %, four events (12.5 %) had AAI > 20 % and only one event (3.1 %) had AAI > 30 % (see Fig. 31.3).

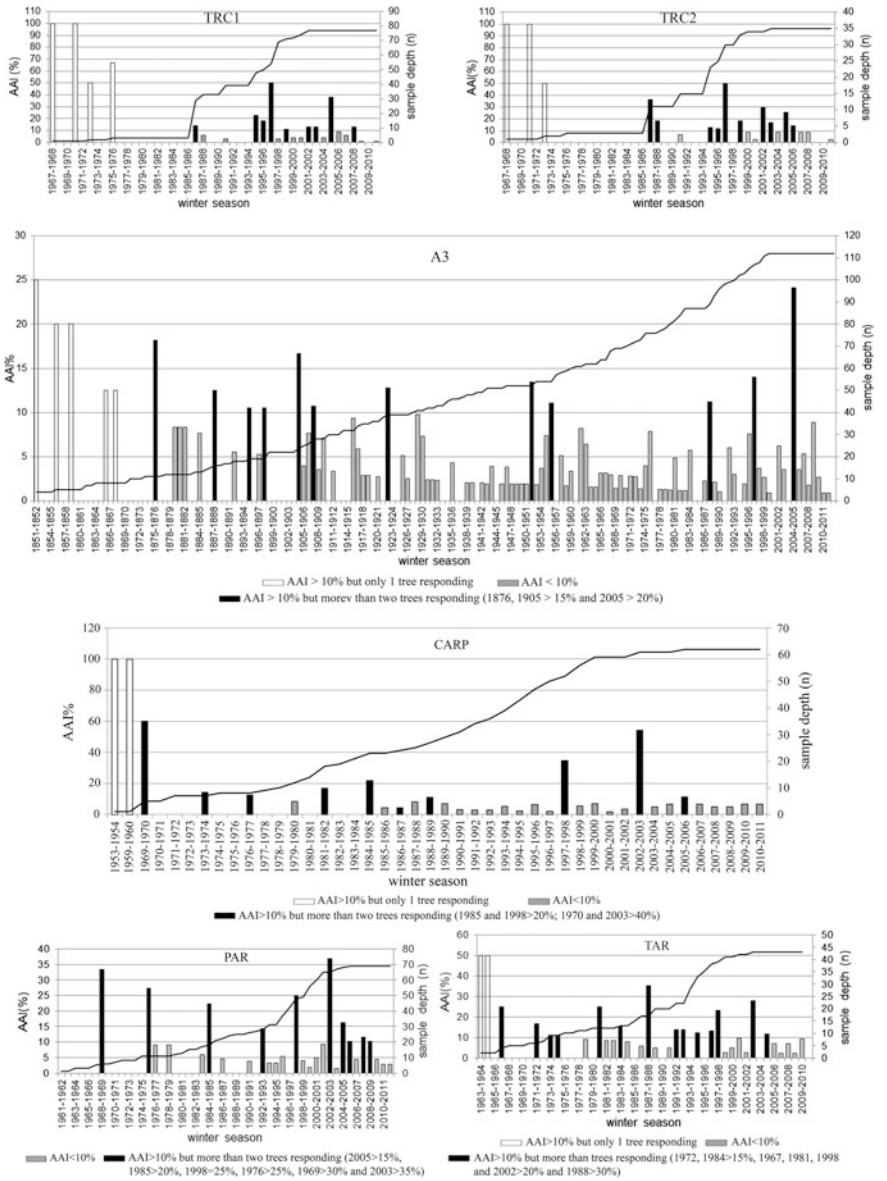

Fig. 31.3 Event–response histogram showing snow avalanche-induced growth responses from the 35 sampled trees of TRC1 42 sampled trees of TRC2 and 105 sampled trees of A3 in Făgăraș Massif and 62 sampled trees of CARP, 69 sampled trees of PAR and 39 sampled trees of TAR in Bucegi Mountains combined to the percentage of living trees/year

Table 31.5 Return period

Stands	Snow avalanche chronology	Return period
TRC1	1968–2011 (43 ani)	14.9
TRC2	1968–2011 (43 ani)	13.0
A3	1852–2013 (161)	13.4
CARP	1954–2011 (57)	13.1
PAR	1964–2012 (48)	13.7
TAR	1964–2011 (47)	15.2

The frequency and distribution of trees with growth disturbances following the snow avalanche impact helped us to reconstruct the past events. Thus, we were able to calculate the return period of snow avalanches (Table 31.5).

In the investigated stands, the values of the return period were similar: 13–14.9 years in the Făgăraș Massif and 13.1–15.2 years in the Bucegi Mountains (Voiculescu and Onaca 2013, 2014). In the lower part of the transport zone and in the runout zone, flexible species (e.g. alder and juniper) and fragmented soil were found in snow avalanche stands in the Făgăraș Massif, with pioneer species (e.g. spruce and larch), young trees similar to the adjacent forest in avalanche stands from the Bucegi Mountains. According to Weir (2002), these vegetative and soil indicators show a frequency of between 10 and 20 years.

The spatial extent of past events in the investigated stands highlighted three types of snow avalanche activity.

In the TRC1 and TRC2 stands, the small avalanches (AAI > 10 %) that affected the central and upper stands had sub-decadal return periods. The large avalanches (AAI > 20 %) had a return period of between 10 and 23 years and covered the northern half of the TRC1 stand and the north-central part of the TRC2 stand. The major snow avalanches (AAI > 30 %) had a return period between 30 and 50 years and affected the central and western periphery of the stands to the Bâlea valley. In the A3 stand, the small snow avalanches were specific to the central part of the track, large avalanches affected the periphery and the major avalanches were on the edges of the track and in the adjacent forest (Chiroiu et al. 2015a).

In the CARP stand, the small avalanches had sub-decadal return periods specific to the upper sector of the stand. The large avalanches that had a return period between 10 and 26 years generally cover 50 % of the stand. The major snow avalanches had a return period of between 26 and 34 years and affected the bottom stand and the trees on the opposite side (Voiculescu and Onaca 2013).

In the PAR stand, the small avalanches had a sub-decadal return period, being present mainly in the central part of the stand. The large snow avalanches covered more than 50 % of the stand, except for the extreme southeast part. The major snow avalanches had a return period of between 30 and 40 years, and sometimes over 40 years, affecting all stands due to their expansion space (Voiculescu and Onaca 2014).

In the TAR stand, the small snow avalanches with a sub-decadal return period were present in the central part of the stand. The large snow avalanches with a

return period of between 10 and 20 years and between 20 and 30 covered up to 30 % of the stand. These avalanches affected the periphery of the stand, but not to any great distance. The major snow avalanches with a return period of between 30 and 40 years, affected, as in the previous case, all stands due to their expansion space (Voiculescu and Onaca 2014).

Snow Avalanche Synchronicity

In accordance with Casteller et al. (2011, p. 74), we found snow avalanche synchronicity in the investigated stands, defined as the event recorded in two or three stands in the same winter season. Thus, in the Făgăraș Massif, the snow avalanche events of the 1987–1988, 1994–1995, 1995–1996, 1996–1997, 1998–1999, 2001–2002, 2002–2003 and 2004–2005 winter seasons were synchronous in two or three stands. In the Bucegi Mountains, we found five seasons with synchronous events in two or three stands and two winter seasons where the avalanche events had AAI $\geq$ 20 % and were synchronous in all investigated stands (Voiculescu and Onaca 2013, 2014). The same situation was found in the Făgăraș Massif in the 1996–1997 and 2004–2005 winter seasons, with one exception when snow avalanches had AAI > 20 % (Table 31.6).

Snow Avalanche Activity and Climate Relationships

To determine the relationship between snow avalanche activities and climate, we used the Winter Standardized Index (WSI) (Micu 2009) and we calculated thermal severity of winters between 1961 and 2011 for the Vf. Omu and Sinaia weather stations, and between 1979 and 2013 (Table 31.7) for using the following formula (31.3):

$$\mathrm{WSI} = t_i - t_{\mathrm{mean}}/\sigma \tag{31.3}$$

where t_i is the winter temperature mean (°C), t_{mean} is the multiannual temperature winter mean (°C) and σ is the standard deviation.

In the Făgăraș Massif, the main events occurred over six normal winters (54.5 %), four warm to very warm winters (36.4 %) and in one cold winter (9.1 %). Among the medium avalanches, one occurred in the TRC1 stand and another in a cold winter in TRC2. Among the major avalanches, one occurred in a cold winter (2004–2005) in TRC1 and four in normal winters (1986–1987, 1996–1997, 2001–2002, 2004–2005) (Fig. 31.4).

In the Bucegi Mountains at altitudes above 2000 m a.s.l., 10 cold winters and very cold winters were found (40 %). Normal winters had a similar incidence (40 %), while warm and very warm winters accounted for 20 %. In the areas located below 2000 m altitude, 32 % of the winters were cold or very cold, 44 % of

Table 31.6 Synchronicity for 3 stands în Făgăraş Massif and for 3 stands în Bucegi Mountains

Bucegi Mountains (stands) winter season	CARP return period-13.1 years (according to Voiculescu and Onaca 2013, 2014)		PAR return period-13.7 years (according to Voiculescu and Onaca 2013, 2014)		TAR return period-15.2 years (according to Voiculescu and Onaca 2013, 2014)	
	AAI > 10 %	AAI > 20 %	AAI > 10 %	AAI > 20 %	AAI > 10 %	AAI > 20 %
1973–1974	17 %/3/17				11.1 %/9/11	
1975–1976				25 %/3/11	11.1 %/3/10	
1984–1985	10 %/5/19			20 %/4/18		
1997–1998		25 %/27/44		25 %/12/46		20 %/9/36
2002–2003		50 %/40/51		35 %/24/63		25 %/12/39

Făgăraş massif (stands) winter season	TRC1 return period-14.9 years (present study)		TRC2 return period-13 years (present study)		A3 return period-3.3–6, 5 years (according to Chiroiu et al. 2015a)	
	AAI > 10 %	AAI > 20 %	AAI > 10 %	AAI > 20 %	AAI > 10 %	AAI > 20 %
1987–1988	18.2 %/3/11				11.2 %/10/89	
1994–1995		23 %/11/48	13 %/3/23			
1995–1996	18 %/9/50		12 %/3/23			
1996–1997		50 %/27/54		50 %/15/30	14 %/57/107	
1998–1999	11 %/8/71		18 %/6/33			
2001–2002	13 %/10/77			29.4 %/10/34		
2002–2003	13 %/10/77		17.1 %/6/35			
2004–2005		38 %/29/77		25.7 %/9/35		24.1 %/27/112

Table 31.7 Winter severity classification grid

Winter type	Mean temperature winter (°C)	Winter Standardized Index values
Very warm	>0.5	>1.5
Warm	−1.3,…,0.5	0.5–1.5
Normal	−3.1,…,1.3	0.5,…,0.5
Cold	−4.9,…−3.1	−1.5,…−0.5
Very cold	<−4.9	<−1.5

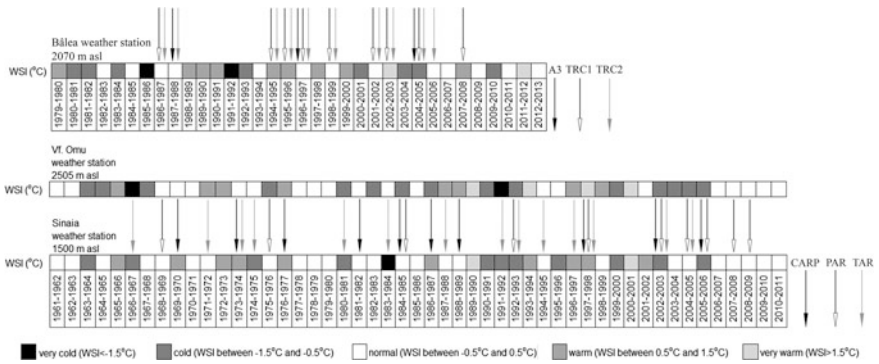

Fig. 31.4 Relationship between Winter Standardized Index and snow avalanche events

winters were normal and 25 % of winters were warm. Of the major avalanches (AAI > 30 %), two occurred in normal winters (1968–1969 in the TAR stand and 1987–1988 in the PAR stand) and one (2002–2003) in a cold winter in all stands. Of the medium snow avalanches (AAI > 20 %), three occurred in cold winters (1966–1967, 1980–1981, 2002–2003), two in normal winters (1975–1976, 1984–1985) and one in a warm winter (1997–1998) (Voiculescu and Onaca 2013, 2014) (see Fig. 31.4).

Final Remarks

We believe that the dendrogeomorphologic method is a very good tool for establishing a clear chronology of snow avalanches and for identifying the critical parameters of this geomorphological process and natural hazard, such as frequency, magnitude and return period. Furthermore, given that avalanche activity in the Romanian Carpathians is poorly documented, with historical records incomplete or present for the short term only, the method is an extremely important information source for undocumented periods.

Our results are extremely important, highlighting for the first time in the Romanian Carpathians some elements of the analysis of snow avalanches, whose

evaluation so far has been speculative. First, we determined the chronology of snow avalanches, unrecorded in any document or database for the Romanian Carpathians. Second, we determined the magnitude and acceptable thresholds of AAI, and the three main types of snow avalanche: small (AAI > 10 %), large (AAI > 20 %) and very large or major (AAI > 30 or 40 %).

The results indicate a sustained activity of avalanches in the second half of the 1990s and largely in the 2000s, in all stands in the Făgăraş Massif. We also found a sustained activity of snow avalanches in the 1980s and early 2000s in the CARP stand, quite active in the 1990s but very active in the 2000s in the PAR stand, and active in the 1980s, very active in the 1990s and more active in the early 2000s in the TAR stand.

Using the dendrogeomorphologic method, we confirmed in the TAR stand the large snow avalanche of the 1980–1981 winter season, which had an AAI = 25 %, resulting in the deaths of two skiers (marked with a commemorative cross) and the snow avalanche from the 1983–1984 winter season that had a AAI > 15 % resulting in the deaths of two skiers. In the PAR stand, we confirmed a large snow avalanche (AAI > 20 %) that resulted in the death of one skier.

The members of Sinaia MRPS have told us that in this area three consecutive snow avalanches occurred, all being dangerous for the activity of skiers. I also confirmed in the CARP stand the accidents with three injuries/burials in small snow avalanches in the 2005–2006 winter season and the small snow avalanches for the PAR stand in the same winter season. Those cases are recorded by the PN–NAM statistics (2006).

Although snow avalanches from the Romanian Carpathians are in medium-high mountains (Voiculescu 2009), they manifest themselves in similar conditions to those of alpine mountain areas, synchronicity being a good example of support. This element is remarkable if we consider that many of the avalanche events had $20 \geq \text{AAI} \geq 30$ or exceeded 40 or even 50 %. If we compare the synchronicity values of the investigated areas with those obtained in other mountainous areas, we notice that it is slightly higher than in Montana (2.1–11 years) obtained by Reardon et al. (2008) or than in the French Alps (2.5–12 years), as obtained by Corona et al. (2010), and lower (20 years) than that obtained by Casteller et al. (2007) in the Swiss Alps or the values obtained by Decaulne et al. (2012) in northern Iceland (9–16 years) and Decaulne et al. (2013, 2014) in Norway, 6–16 years and 15–20 years. It is also interesting to note that we identified synchronistic events in five out of six stands of two neighbouring mountain areas (Făgăraş and Bucegi) in the 2002–2003 winter season in the CARP, PAR and TAR stands (with 25 % > AAI > 50 %), in the TRC1 and TRC2 stands (with 13 % > AAI > 17.1 %) and in the 2004–2005 winter season in the PAR and TAR stands (with 10 % > AAI > 20 %), and in TRC1, TRC2 and F3 (with 24.1 % > AAI > 38 %). This was due to similar snowfall conditions, snow depth and WSI, confirmed by Micu (2009), for the eastern half of Southern Carpathians and local suitability terrain factors (Chiroiu et al. 2015a, b; Voiculescu et al. 2013; Voiculescu and Onaca 2013, 2014).

The dendrogeomorphologic method, which is in its infancy in Romania, is the only tool to reconstruct past snow avalanches in areas where woody plants are available and to complete missing data. This method is also very relevant for land-use planning and for the identification of danger zones and for ski and tourism activity and those working in mountain areas.

References

Alestalo J (1971) Dendrochronological interpretation of geomorphic processes. Fennia 105:1–139
Ammann W (2003) Les avalanches. Evénements extrêmes et changements climatiques. Organe consultatif sur les changements climatiques (OcCC), Berne, pp 83–86
Bebi P, Kienast F, Schönenberger W (2001) Assessing structures in mountain forests as a basis for investigating the forests' dynamics and protective function. For Ecol Manag 145:3–14
Bollschweiler M, Stoffel M, Schneuwly DM, Bourqui K (2008) Traumatic resin ducts in Larix decidua trees impacted by debris flows. Tree Physiol 28:255–263
Boucher D, Filion L, Hétu B (2003) Reconstitution dendrochronologique et fréquence des grosses avalanches de neige dans un couloir subalpin du mont Hog's Back, Gaspésie centrale (Québec). Géog Phys Quatern 57:159–168
Braam RR, Weiss EJJ, Burrough PA (1987) Spatial and temporal analysis of mass movement using dendrochronology. Catena 14(6):573–584
Bryant CL, Butler DR, Vitek JD (1989) A statistical analysis of tree-ring dating in conjunction with snow avalanches: comparison of on-path versus off-path responses. Environ Geol Water Sci 14(1):53–59
Burrows CJ, Burrows VL (1976) Procedure for the study of snow avalanche chronology using growth layers of woody plants. University of Colorado, Institute of Arctic and Alpine, Research Occasional Paper. 23–54
Butler DR (1979) Snow avalanche path terrain and vegetation, Glacier National Park, Montana. Arct Antarct Alp Res 11:17–32
Butler DR (1986) Snow avalanche hazards in Glacier National Park, Montana: Meteorologic and climatologic aspects. Phys Geogr 7(1):72–87
Butler DR (1998) Teaching natural hazards: the use of snow avalanches in demonstrating and addressing geographic topics and principles. J Geogr 87(6):212–225
Butler DP, Malanson GP (1985a) A reconstruction of snow-avalanche characteristics in Montana, USA, using vegetative indicators. J Glaciol 31:185–187
Butler DR, Malanson GP (1985b) A history of high-magnitude snow avalanches, Southern Glacier National Park, Montana, U.S.A. Mt Res Dev 5(2):175–182
Butler DR, Sawyer CF (2008) Dendrogeomorphology and high-magnitude snow avalanches: a review and case study. Nat Hazards Earth Syst Sci 8:303–309
Butler DR, Malanson GP, Oelfke JG (1987) Tree-ring analysis and natural hazard chronologies: minimum sample sizes and index values. Prof Geogr 39(1):41–47
Butler DR, Sawyer CF, Maas JA (2010) Tree-ring dating of snow avalanches in Glacier National Park, Montana, USA. In: Stoffel M, Bollschweiler M, Butler DR, Luckman BH (eds) Tree rings and natural hazards, a state-of-the-art. Springer, Heidelberg, pp 33–44
Carrara PE (1979) The determination of snow avalanche frequency through tree-ring analysis and historical records at Ophir, Colorado. Geol Soc Am Bull 90:773–780
Casteller A, Stöckli V, Villalba R, Mayer AC (2007) An evaluation of dendroecological indicators of snow avalanches in the Swiss Alps. Arct Antarct Alp Res 39:218–228
Casteller A, Christen M, Villalba R, Martínez-Stöckli HV, Leiva JC, Bartelt P (2008) Validating numerical simulations of snow avalanches using dendrochronology: the Cerro Ventana event in Northern Patagonia, Argentina. Nat Hazards Earth Syst Sci 8:433–443

Casteller A, Villalba R, Araneo D, Stöckli V (2011) Reconstructing temporal patterns of snow avalanches at Lago del Desierto, southern Patagonian Andes. Cold Region Sci Technol 67:68–78

Chiroiu P, Stoffel M, Onaca A, Urdea P (2015a) Testing dendrogeomorphic approaches and thresholds to reconstruct snow avalanche activity in the Făgăraș Mountains (Romanian Carpathians). Quat Geochronol 27:1–10

Chiroiu P, Ardelean AC, Onaca A, Voiculescu M, Ardelean F (2015b) Assessing the anthropogenic impact on geomorphic processes using tree-rings: a case study in the Făgăraș Mountains (Romanian Carpathians). Carpathian J Earth Environ Sci 11(1):27–36

Corona C, Rovera G, Lopez SJ, Stoffel M, Perentine P (2010) Spatio-temporal reconstruction of snow avalanche activity using tree-rings: Pierres Jean Jeanne avalanche talus, Massif de l'Oisans, France. Catena 83:107–118

Corona C, Saez JP, Stoffel M, Bonnefoy M, Richard D, Astrade L, Berger F (2012) How much of the real avalanche activity can be captured with tree-rings? An evaluation of classic dendrogeomorphic approaches and comparison with historical archives. Cold Region Sci Technol 74–75:31–42

Corona C, Lopez Saez J, Stoffel M, Rovéra G, Edouard J-P, Berger F (2013) Seven centuries of avalanche activity at Echalp (Queyras massif, southern French Alps) as inferred from tree rings. The Holocene 23:292–304

Decaulne A, Sæmundsson Þ (2008) Dendrogeomorphology as a tool to unravel snow avalanche activity; preliminary results from the Fnjóskadalur test site, Northern Iceland. Norsk Geografisk Tidsskrift-Norwegia. J Geogr 62:55–65

Decaulne A, Eggertsson Ó, Sæmundsson Þ (2012) A first dendrogeomorphologic approach of snow avalanche magnitude frequency in Northern Iceland. Geomorphology 167–168:35–44

Decaulne A, Eggertsson Ó, Laute K, Beylich AA (2013) Dendrogeomorphologic approach for snow-avalanche activity reconstruction in a maritime cold environment (upper Erdalen, Norway). Zeitschrift für Geomorphologie 57:55–68

Decaulne A, Eggertsson Ó, Laute K, Beylich AA (2014) 100-year extreme snow-avalanche record based on tree-ring research in upper Bødalen, inner Nordfjord, Western Norway. Geomorphology 218:3–15

Dubé S, Filion L, Hétu B (2004) Tree-ring reconstruction of high-magnitude snow avalanches in the northern Gaspé Peninsula, Québec, Canada. Arct Antarct Alp Res 36:555–564

Francou B (1993a) Hautes montagnes, passion d'explorations. MASSON

Francou B (1993b) Une représentation factorielle des cryospheres d'altitude dans le monde. Géomorphologie et aménagement de la montagne, Centre de géomorphologie, Caen, pp 75–87

Fuchs S, Bründl M (2005) Damage potential and losses resulting from snow avalanches in settlements of the Canton of Grisons Switzerland. Nat Hazards 34:53–69

Fuchs S, Bründl M, Stötter J (2004) Development of avalanche risk between 1950 and 2000 in the Municipality of Davos, Switzerland. Nat Hazards Earth Syst Sci 4:263–275

Fuchs S, Keiler M, Zischg A, Bründl M (2005) The long-term development of avalanche risk in settlements considering the temporal variability of damage potential. Natural Hazards and Earth System Sciences 5:893–901

Garavaglia V, Pelfini M (2011) The role of border areas for dendrochronological investigations on catastrophic snow avalanches: a case study from the Italian Alps. Catena 87:209–215

Germain D, Filion L, Hétu B (2005) Snow avalanche activity after fire and logging disturbances, northern Gaspé Peninsula, Quebec, Canada. Can J Earth Sci 42:2103–2116

Germain D, Filion L, Hétu B (2009) Snow avalanche regime and climatic conditions in the Chic-Choc Range, eastern Canada. Clim Change 92:141–167

Germain D, Hétu B, Filion L (2010) Tree-ring based reconstruction of past snow avalanche events and risk assessment in Northern Gaspé Peninsula (Québec, Canada). In: Stoffel M, Bollschweiler M, Butler DR, Luckman BH (eds) Tree rings and natural hazards, a state-of-the-art. Springer, Heidelberg, pp 51–73

Hebertson EG, Jenkins MJ (2003) Historic climate factors associated with major avalanche years on the Wasatch Plateau, Utah. Cold Reg Sci Technol 37:315–332

Höller P (2007) Avalanche hazards and mitigation in Austria: a review. Nat Hazards 43:81–101
Höller P (2009) Avalanche cycles in Austria: an analysis of the major events in the last 50 years. Nat Hazards 48:399–424
Ives JD, Mears AI, Carrara PE, Bovis MJ (1976) Natural hazards in Mountain Colorado. Ann Assoc Am Geogr 66:129–144
Jamieson B, Stethem C (2002) Snow avalanche hazards and management in Canada: challenges and progress. Nat Hazards 26:35–53
Jenkins MJ, Hebertson EG (1994) Using vegetative analysis to determine the extent and frequency of avalanches in Little Cotonwood Canyon, Utah. In: Proceedings of the international snow science workshop (Snowbird Utah, 30 Oct–3 Nov 1994). American Avalanche Institute, Wilson, WI, pp 91–103
Kajimoto T, Daimaru H, Okamoto T, Otani T, Onodera H (2004) Effects of snow avalanche disturbance on regeneration of subalpine Abies mariesii forest, northern Japan. Arct Antarct Alp Res 36:436–445
Köse N, Aydın A, Akkemik Ü, Yurtseven H, Güner T (2010) Using tree-ring signals and numerical model to identify the snow avalanche tracks in Kastamonu, Turkey. Nat Hazards Earth Syst Sci 54:435–449
Larocque S, Hétu H, Filion L (2001) Geomorphic and dendroecological impacts of slushflows in central Gaspé peninsula (Québec, Canada). Geogr Ann 83A:191–201
Laxton SC, Smith DJ (2009) Dendrochronological reconstruction of snow avalanche activity in the Lahul Himalaya, Northern India. Nat Hazards 49:459–467
Luckman BH (1977) The geomorphic activity of snow avalanches. Geogr Ann 59A(1–2):31–48
Luckman BH (1978) Geomorphic work of snow avalanches in the Canadian Rocky Mountains. Arct Alp Res 10(2):261–276
Luckman BH (2010) Dendrogeomorphology and snow avalanche research. In: Stoffel M, Bollschweiler M, Butler DR, Luckman BH (eds) Tree-rings and natural hazards: a state-of-the-art. Springer, Heidelberg, New York, pp 27–35
Luckman BH, Frazer GW (2001) Dendrogeomorphic investigations of snow avalanche tracks in the Canadian Rockies. In: Unpublished poster presented at the international conference on the future of dendrochronology, Davos
Malik I, Owczarek P (2009) Dendrochronological records of debris flow and avalanche activity in a mid-mountain forest zone (Eastern Sudetes—Central Europe). Geochronometria 34:57–66
McClung DM (2001) Characteristics of terrain, snow supply and forest cover for avalanche initiation caused by logging. Ann Glaciol 32:223–229
McClung DM, Schaerer P (2006) The Avalanche handbook. The Mountaineers, Seattle, USA
Micu D (2009) Snow pack in the Romanian Carpathians under changing climatic conditions. Meteorol Atmos Phys 105:1–16
Molina R, Muntán E, Andreu L, Furdada G, Oller P, Gutiérrez E, Martìnez P, Vilaplana JM (2004) Using vegetation to characterize the avalanche of Canal del Roc Roig, Vall de Núria, eastern Pyrenees, Spain. Ann Glaciol 38:159–165
Mundo IA, Barrera MD, Roig FA (2007) Testing the utility of Nothofagus pumilio for datinga snow avalanche in Tierra del Fuego, Argentina. Dendrochronologia 25:19–28
Muntán E, Andreu L, Oller P, Gutiérrez E, Martinez P (2004) Dendrochronological study of the Canal del Roc Roig avalanche path: first results of the Aludex project in the Pyrenees. Ann Glaciol 38:173–179
Muntán E, Garcia C, Oller P, Marti G, Garcia A, Gutierrez E (2009) Reconstructing snow avalanches in the Southeastern Pyrenees. Natural Hazards and Earth System Sciences 9:1599–1612
Patten RS, Knight DM (1994) Snowavalanches and vegetation pattern in Cascade Canyon, Grand Teton National Park, Wyoming, USA. Arct Alp Res 26:35–41
Potter N (1969) Tree-ring dating of snow avalanche tracks and the geomorphic activity of avalanches, northern Absaroka Mountains, Wyoming, Boulder. CO. Geol. Soc. Am. Spec. Pap. 123:141–165

Rapp A (1960) Recent development of mountain slopes in Karkevagge and surroundings, northern Scandinavia. Geogr Ann 42:73–200

Rayback SA (1998) A dendrogeomorphological analysis of snow avalanches in the Colorado Front Range, USA. Phys Geogr 19:502–512

Reardon BA, Pederson GT, Caruso CJ, Fagre DB (2008) Spatial reconstructions and comparisons of historic snow avalanche frequency and extent using tree-rings in Glacier National Park, Montana, U.S.A. Arct Antarct Alp Res 40(1):148–160

Schaerer P (1972) Terrain and vegetation of snow avalanche sites at Rogers Pass, British Columbia. In: Slaymaker O, McPherson HJ (eds) Mountain geomorphology: geomorphological processes in the Canadian Cordillera. Tantalus Research Ltd. Edition, Vancouver B.C., pp 215–222

Schneebeli M, Bebi P (2004) Snow and avalanche control. In: Burley J, Evans J, Youngquist JA (eds) Encyclopedia of forest sciences. Elsevier, Oxford, pp 397–402

Schönenberger W, Noack A, Thee P (2005) Effect of timber removal from windthrow slopes on the risk of snow avalanches and rockfall. For Ecol Manag 213:197–208

Schweizer J, Jamieson B, Schneebeli M (2003) Snow avalanche formation. Rev Geophys 41:2–25

Shroder JF (1980) Dendrogeomorphology: review and new techniques of tree-ring dating. Prog Phys Geogr 4:161–188

Smith L (1973) Indication of snow avalanche periodicity through interpretation of vegetation patterns in the North Cascades, Washington. Methods of Avalanche control on Washington mountain highways—third annual report. Washington State Highway Commission Department of Highways, Olympia, WA, pp 55–101

Stethem C, Jamieson B, Liverman D, Germain D, Walker S (2003) Snow avalanche hazard in Canada—a review. Nat Hazards 28:487–515

Stoffel M, Hitz OM (2008) Snow avalanche and rockfall impacts leave different anatomical signatures in tree rings of Larix decidua. Tree Physiol 28(11):1713–1720

Stoffel M, Schneuwly D, Bollschweiler M, Lièvre I, Delaloye R, Myint M, Monbaron M (2005) Analyzing rockfall activity (1600–2002) in a protection forest—a case study using dendrogeomorphology. Geomorphology 68:224–241

Stoffel M, Bollschweiler M, Hassler GR (2006) Differentiating events on a cone influenced by debris-flow and snow avalanche activity—a dendrogeomorphological approach. Earth Surf Proc Land 31:1424–1437

Stoffel M, Butler DR, Corona C (2013) Mass movements and tree rings: a guide to dendrogeomorphic field sampling and dating. Geomorphology 200:106–120

Strunk H (1997) Dating of geomorphological processes using dendrogeomorphological methods. Catena 31:137–151

Szymczak S, Bollschweiler M, Stoffel M, Dikau R (2010) Debris-flow activity and snow avalanches in a steep watershed of the Valais Alps (Switzerland): dendrogeomorphic event reconstruction and identification of triggers. Geomorphology 116:107–114

Teich M, Marty C, Gollut C, Grêt-Regamey A, Bebi P (2012) Snow and weather conditions associated with avalanche releases in forests: Rare situations with decreasing trends during the last 41 years. Cold Reg Sci Technol 83–84:77–88

Tumajer J, Treml V (2015) Reconstruction ability of dendrochronology in dating avalanche events in the Giant Mountains, Czech Republic. Dendrochronologia 34:1–9

Vanni M (1965) Pour une classification géographique des avalanches. In: International symposium on scientific aspects of snow and ice avalanches. Report and discussions. Davos, pp 397–407

Viglietti D, Letey S, Motta R, Maggioni M, Freppaz M (2010) Snow avalanche release in forest ecosystems: a case study in the Aosta Valley Region (NW-Italy). Cold Reg Sci Technol 64 (2):167–173

Voiculescu M (2004) Types of Avalanches and their morphogenetical impact in Făgăraş Masiff-Southern Carpathians (Romania). Geomorphologia Slovaca, Číslo 1, ročník 4, Bratislava, pp 72–81

Voiculescu M (2009) Snow avalanche hazards in the Făgăraş massif (Southern Carpathians): Romanian Carpathians—Management and perspectives. Nat Hazards 51(3):459–475

Voiculescu M (2010) L'utilisation de la method dendrochronologique pour la reconstitution de la grande avalanche de neige du fevrier 1969 de Monts Bucegi - Carpates Meridionales, Roumanie. In: Surdeanu V, Stoffel M, Pop O (eds) Dendrogeomorphologie et dendroclimatologie– methodes de reconstitution des milieux geomorphologiques et climatiques des regions montagneuses. Presa Universitară Clujeană, pp 125–149

Voiculescu M (2014) Patterns of the dynamics of human-triggered snow avalanches at the Făgăraş massif (Southern Carpathians), Romanian Carpathians. Area 46(3):328–336

Voiculescu M, Ardelean F (2012) Snow avalanche—disturbance of high mountain environment. Case study—the Doamnei glacial valley the Făgăraş massif-Southern Carpathians, Romanian Carpathians. Carpathian J Earth Environ Sci 7(1):95–108

Voiculescu M, Onaca A (2013) Snow avalanche assessment in the Sinaia ski area (Bucegi Mountains, Southern Carpathians) using the dendrogeomorphology method. Area 45(1):109–122

Voiculescu M, Onaca A (2014) Spatio-temporal reconstruction of snow avalanche activity using dendrogeomorphological approach in Bucegi Mountains Romanian Carpathians. Cold Reg Sci Technol 104–105:63–75

Voiculescu M, Popescu F (2011) The management of Snow avalanches in the Ski Areas in Southern Carpathians. Case study: Făgăraş massif and Bucegi Mountains. In: Zhelezov G (ed) Sustainable Development in Mountain Regions: Southeastern Europe. Springer, New York, pp 103–120

Voiculescu M, Ardelean F, Onaca A, Török-Oance M (2011) Analysis of snow avalanche potential in Bâlea glacial area – Făgăraş massif, (Southern Carpathians - Romanian Carpathians). Zeitschrift für Geomorphologie 55(3):291–316

Voiculescu M, Onaca A, Chiroiu P (2013) L'analyse de la dynamique forestière et de l'impact mécanique des avalanches de neige sur les arbres en utilisant la méthode dendrochronologique. Étude de la vallée glaciaire Bâlea – Massif Făgăraş (Carpates Méridionales, Roumanie). In: Decaulne et al (eds) Arbres & dynamiques. Maison des Sciences de l'homme, Presses Universitaires Blaise Pascal, Clermont Ferrand, p 89–105

Weir P (2002) Snow avalanche. Management in forested terrain. Ministry of Forestry, Forest Science Program, British Columbia

Chapter 32
Mass Movements

Mihai Micu, Marta Jurchescu, Ionuț Șandric, Mihai Ciprian Mărgărint, Zenaida Chițu, Dana Micu, Roxana Ciurean, Viorel Ilinca and Mirela Vasile

Abstract Romania represents one of Europe's most active landslide hotspots. The importance of studying these phenomena is both fundamental (establishing the morphogenetic and morphodynamic frameworks) and applied (quantifying and predicting the potential losses inflicted by such processes). The analysis of agents–processes–forms can be directed toward predictive assessments through susceptibility–hazard–risk studies. The complexity of landslides conditioning factors as well as the available data in terms of quantity (multi-temporal and typological more or less complete landslide inventories) and quality (point and polygon-based inventories, uncertainties induced by the correlation between the used method and the working scale) are imposing local-to-regional and regional-to-national approaches, aiming to highlight, in a predictive manner (based either on heuristic, statistic, or probabilistic

M. Micu (✉) · M. Jurchescu · D. Micu
Institute of Geography, Romanian Academy, Dimitrie Racoviță 12,
023993 Bucharest, sector 2, Romania
e-mail: mikkutu@yahoo.com

I. Șandric
Faculty of Geography, University of Bucharest, N. Bălcescu 1,
010041 Bucharest, sector 1, Romania

Z. Chiţu
National Institute of Hydrology and Water Management, Bucureşti-Ploieşti 97,
013686 Bucharest, Romania

R. Ciurean
Department of Geography and Regional Research, University of Vienna,
Universitaetsstr. 7, 1010 Vienna, Austria

M.C. Mărgărint
Departament of Geography, Alexandru Ioan Cuza University of Iași,
Carol I Av 11, 700506 Iași, Romania

V. Ilinca
Geological Institute of Romania, Caransebeș 1, sector 1, Bucharest, Romania

M. Vasile
Research Institute of the University of Bucharest, M. Kogălniceanu 36-46, 050107 sector 5,
Bucharest, Romania

M. Rădoane and A. Vespremeanu-Stroe (eds.), *Landform Dynamics and Evolution in Romania*, Springer Geography,
DOI 10.1007/978-3-319-32589-7_32

predictions) the spatial and temporal sequences more or less prone to future processes, as well as the potential consequences and their mitigation strategies.

Keywords Landslides · Damages · Inventory · Susceptibility · Hazards · Risks · Romania

Mass Movements Assessment: From Process to Risk

A large spectrum of predisposing, preparing, and triggering factors is asserting Romania as one of Europe's most prone areas in terms of slope mass movements. The wide variety of processes and associated forms is directly conditioned by the morphostructural and lithological heterogeneities which are controlling the relief's main topographic features, whereas the intensity and duration of human settlements are mainly conditioning the different stages of landslide activity, the latter being highlighted as preparing factors for the occurrence of first time failures or reactivations. Spring rain showers which are often overlapping the snowmelt in the mountainous, high hilly or tableland areas, alongside torrential summer rainfalls or long-lasting autumn rains are the main triggers of a large variety of mass movements. The already mentioned variety is increased by the country's high seismicity induced especially by the Vrancea seismic region.

In response to the wide variety of mass movements, their consequences can extend from environmental damages (e.g., land degradation induced by shallow slides or flows) to large monetary losses caused to transport infrastructure or buildings. The last century's history provides several examples (Fig. 32.1) of major mass movement events (a selection is given in Table 32.1), in which both natural and human-induced causes led to significant damages to human settlements, life lines, and transport network.

The practical valences (especially applied, but also fundamental) of mass movement assessments involve a wide range of stakeholders, either executive, end users, or experts. At national level, there are several ministries involved in mass movements management, either through structural (funds and logistics for emergency situations interventions) or nonstructural (territorial development plans, including landslide hazard and risk maps, environmental permits, environmental agreements/consents, and environmental authorizations) measures.

Lately, the concern of scientists is slightly moving from fundamental toward applied landslide studies. Hyogo Framework for Actions (2005–2015) contributed significantly to the development of the conceptual framework of landslide risk management, while Horizon 2020 aims at transforming technological achievements into viable commercial products. From this point of view, both proactive and reactive sequences (Fig. 32.2) should focus on developing proper hardware–software applications, aiming to support vulnerability and risk reduction: Early Warning Systems (both local and regional; EWS) or Decision Support System (mainly regional; DSS). A DSS application has been developed within

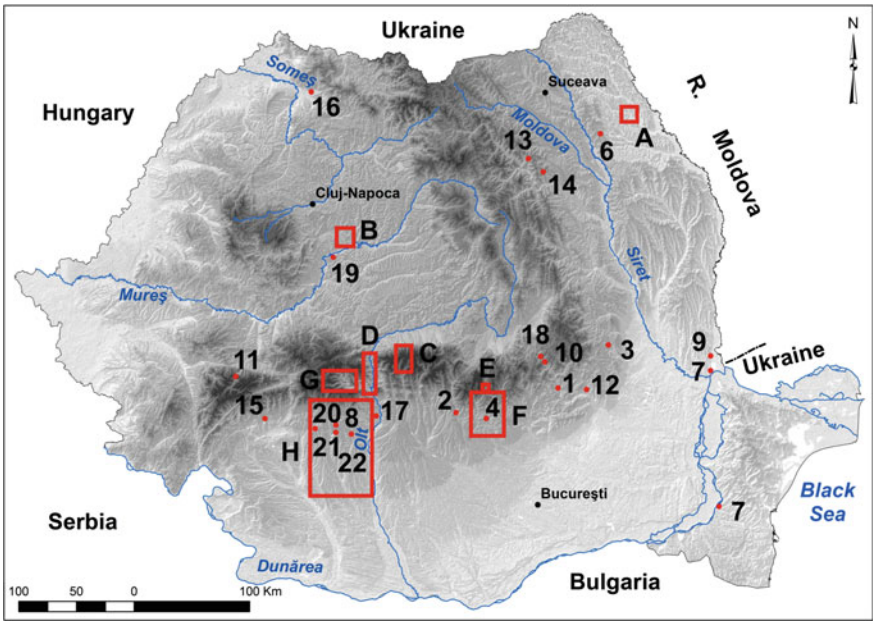

Fig. 32.1 The position of described case studies within Romania: 1–22 major damaging landslides (see Table 32.1); *A* Moldavian plateau case study, *B* Transylvanian depression case study, *C* Transfăgărăşan road case study, *D* Olt valley case study, *E* Breaza case study, *F* Ialomiţa Subcarpathians case study, *G* Lotru valley case study, *H* Olteţ river basin case study

FP7 CHANGES (Van Westen et al. 2014), which is currently under functional implementation in the Buzău County.

Considering the robust signals of climate and environmental change, as well as the numerous uncertainties associated to the identification, assessment, and management of landslide risks, the Horizon 2020 Program will support a new framework, in which the results of interactions between the stakeholders (from both private and public sectors) involved in landslide risk management, should be transformed from technological achievements into viable commercial products.

Either passive (functioning only inside a specific legal framework) or active (provide supplementary solutions outside the legal constrains), especially the DSS developed a lot during the last years. Created in such a way, DSS are able to support authorities in different stages of landslide risk management (prevention, preparedness, response, recovery, Fig. 32.2): prevention plans (nonstructural measurements; *Emergency Preparedness System*, *Territorial Planning*); structure intervention preparedness measurements (warning/alarming; *Early Warning System*); response coordination and control (intervention management—*Intervention Coordination System*); post-disaster recovery coordination (critical infrastructure rehabilitation, property reconstruction; *Damage Functions*, *Damage Curves*, *Long-term Planning System*).

Table 32.1 Examples of some of the most important landslides and their associated damages

No.	Location	Process	Period	Causes	Damages	Source
Predominantly natural factors						
1	Chirleşti (Buzău mountains)	Earth flow	1953, 2006, 2010	Precipitation	10 houses destroyed in 1953, 1 house destroyed in 2006, two houses destroyed in 2010	Bălteanu and Micu (2012)
2	Malu cu Flori (Ialomiţa Subcarpathians)	Rock slide	1972, 1979, 2010	Precipitation, snow melt	Above 50 ha of orchards, one county road, 20 houses endangered	Ialomiţa County inspectorate for emergency situations (IES) report 2010
3	Lacul lui Baban (Vrancea Subcarpathians)	Complex (earth and rock slide, earth flow)	1971	Snow melt, precipitation	Village of Constandoiu partially destroyed (relocated afterwards)	Sandu (1999)
4	Vârfuri (Ialomiţa Subcarpathians)	Rock slide	February 1980	Snow melt, precipitation	130 houses destroyed or heavily damaged	Dâmboviţa County IES report 2012
5	Zemeş (Tazlău Subcarpathians)	Rock slide	June 1992	Precipitation	47 oil drilling rigs and the connecting pipes destroyed	Bacău County inspectorate for emergency situations report 1992
6	Pârcovaci (Suceava tableland)	Rock slide	December 1996	Snow melt, precipitation	95 houses destroyed or heavily damaged	Dinu and Cioacă (1997)
7	Seimeni, Galaţi (Danube terraces)	Lateral rock spread	Quasi-continuous	Lateral erosion and high underground water level	Hundreds of houses endangered	Cazacu and Drăghici (2011)

(continued)

Table 32.1 (continued)

No.	Location	Process	Period	Causes	Damages	Source
8	Lăpuşata (Getic Piedmont)	Rock slide	November 2004	Precipitation	6 houses destroyed	Vâlcea County IES report 2004
9	Tulucești (Tutova hills)	Rock slide	February 2013	Precipitation, snow melt	Destroyed railway	Galați County IES report 2013
10	Siriu, D.N.10 (Buzău mountains)	Complex (rock slide, debris flow)	Yearly since 2005	Precipitation, snow melt	National road (D.N. 10) constantly closing	Buzău County IES report 2005–2013
11	Râul Mare (Retezat mountains)	Complex (flash flood, debris flow)	July 1999	Precipitation	13 dead, 21 injured	Hunedoara County IES report 1999
12	Răteşti (Buzău Subcarpathians)	Rock slide	June 2014	Precipitation	Mid eighteenth century Monastery severely damaged (quasi-destroyed)	Buzău County IES report 2014
13	Pătru Vodă (Stânisoarei Mts)	Hillslope deposit slide	June 1991	Precipitation	5 houses destroyed	Ichim (1970)
14	Cuiejdel (Stânișoarei Mts)	Hillslope deposit slide	June 1991	Precipitation	A new natural dam lake has appeared; volume = 907,000 m^3	Rădoane (2003)
Predominantly human factors						
15	Certej (Metaliferi mountains)	Tailing dam collapse	October 1971	Maintenance/exploitation problems	89 dead, 76 injured	Sima (2011)
16	Baia Mare and Baia Borşa (Western hills)	Tailing dam collapse	January and March 2000	Maintenance/exploitation problems; fast snowmelt and precipitation	Severe heavy metal pollution	Sima (2011)

(continued)

Table 32.1 (continued)

No.	Location	Process	Period	Causes	Damages	Source
17	Ocnele Mari (Vâlcea Subcarpathians)	Complex (salt mine sealing collapse, landslide)	2001, 2002, 2004	Maintenance/exploitation problems	More than 100 households destroyed (rebuilt in another location) or severely damaged	Vâlcea County IES report 2001–2004
18	Siriu (Buzău mountains)	Rock slide	April 2006	Reservoir inflow–outflow variations due to precipitation	Large reservoir siltation; hydropower plant affected	Micu and Bălteanu (2013)
19	Ocna Mureş (Târnave tableland)	Salt mine sealing collapse	December 2010	Maintenance/exploitation problems; precipitation	1 supermarket, households and roads swallowed by the sink hole	Mureş County IES report 2010
20	Mateeşti (Panga North coal sterile, Getic Subcarpathians)	Earth slide-earth flow on spoil dump	2005, February–March 2008, March 2009, 2010	Dump creation/maintenance problems, precipitation	8 houses buried, 16 people evacuated, threat of damming the nearby river in February 2008	Boengiu et al. (2008)
21	Seciurile (Getic Subcarpathians)	Complex (collapse, landslides)	May 8, 2006	Mining activities (and maintenance)	200 houses destroyed	Boengiu et al. (2008, 2013)
22	Alunu–Valea Lacului (Getic Subcarpathians)	Earth slide-earth flow	November 2004	Dump maintenance problems, local springs, precipitation	12 houses affected, county road affected on 400 m, interruption of electricity supply	Vâlcea County IES report 2004

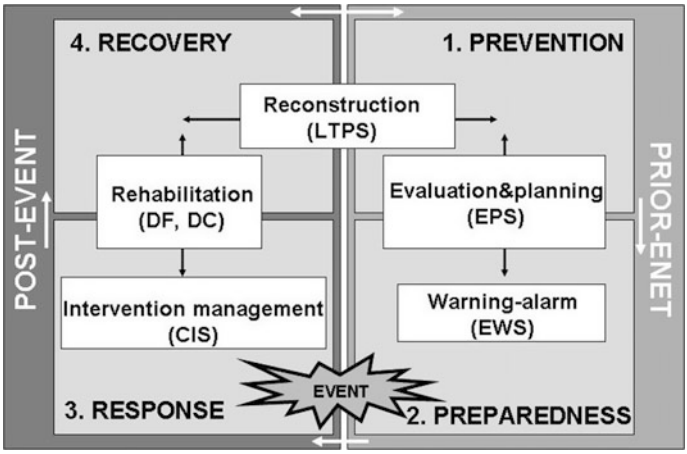

Fig. 32.2 The conceptual framework of support functions within a landslide risk study (*EPS* Emergency preparedness system, *EWS* Early warning system, *CIS* Coordination intervention system, *DF* Damage functions, *DC* Damage curves, *LTPS* Long-term planning system)

Data and Methodological Approaches

The continuous technological advances, largely enhanced during the last two decades, contributed to the development of more focused methodologies for mass movement analysis. Still, there is a continuous struggle to develop common methodologies from a data-rich to a data-scarce environment, with a great concern for the reduction of associated uncertainties. The use of new Earth Observation data products, coming from both active and passive remote sensing (e.g., the free data from SENTINEL satellites family) encourages the knowledge through innovative research and technological development meant to assist minimization and mitigation damage caused by landslides (Scaioni et al. 2014). It should be stressed that, data harmonization should be applied in all the steps of risk assessment chain, by means of data format, database structure, methodological approach and sometimes even in terms of terminology. In order to improve risk perception and preparedness for the reduction (or recovery) of reconstruction costs, landslide risk studies should provide reliable solutions derived from a proper hazard assessments deriving at their turn from accurate susceptibility mapping.

Necessary Data for Landslide Inventory

The basis for all the above-mentioned outcomes is a suitable landslide inventory. The existing inventories contain a large amount of information about the landslide events for a given area. This information mainly relates to location, size, type,

activity status, date of occurrence, or last reactivation and can be completed by additional information regarding landslide geometry, geology, hydrogeology, land cover/use, triggering factors, casualties and damage, remedial measures. Integrated in a GIS environment, with a set of unique identification codes for each landslide event, these inventories are currently known as LDBs (Landslide Databases, Van Den Eeckhaut and Hervás 2012a), and by cartographic plotting they could become Landslide Inventory Maps. During the last years, there is a growing awareness in using new tools and techniques for obtaining more accurate maps of landslides (Guzzetti et al. 2012). This trend is also easy to state for the Romanian landslide literature. Regional (up to county size) inventories have been carried out by specialized institutions (Van Den Eeckhaut and Hervás 2012b), while others, mainly based on topographical map (1:50,000), focused on catchments' or geometrical shape samples inventories, have been carried out by academic teams mainly through the interpretation of remote sense imagery. These maps have been used as milestones to assess landslide susceptibility (e.g., Constantin et al. 2011; Armaş 2012; Grozavu et al. 2013; Mărgărint et al. 2013a, b; Mărgărint and Niculiţă 2015; Şandric 2009, 2011) and/or landslide hazard (e.g., Micu 2011).

Data and Methodologies Used in Landslide Susceptibility Assessment

Throughout an extremely vast literature (describing data requirements, methodological approaches and modeling techniques), landslide susceptibility is defining the probability (in general based on pixel analysis) of occurrence/initiation in space of a certain type of landslide. Some studies have used geomorphic features represented by basins, slope sectors, unique condition units to calculate the landslides susceptibility (Cascini 2008). Recently (Martha 2010; Şandric 2010), new approaches that involve landslide inventories derived out of object-based image analysis have been developed and tested. Since the mid-1990s, in the Romanian literature (Rădoane et al. 1995) there is an increasing number of studies focusing on landslide susceptibility, using either qualitative (expert knowledge), semiquantitative (expert knowledge combined with weighted overlay) or quantitative approaches (e.g., statistic, probabilistic, deterministic). Expert knowledge-related methods consist in general in a weighted overlay of various factors considered by an expert to have an important contribution for the landslide occurrences (Mihai 2005). Bălteanu et al. (2010) asserted that the weight allocation for each factor is rather subjective, since it reflects the opinion of one specialist or of a small group of specialists. Data used for these landslide susceptibility studies is frequently represented by derivatives from digital elevation models, lithology, land use, and land cover. The statistical methods used in landslide susceptibility studies make use of (bivariate and multivariate) statistical analyses and theories like logistic regression, discriminant analysis, probability theory, etc. The methods are applied on spatial

data structures—raster or vector—to calculate the probable location for landslides occurrence. They are less subjective to weights allocation for each factor and they are data driven. Being data-driven makes them highly subjective to the quality of landslides inventory leading to high uncertainties when the landslides inventory is not adjusted for each statistical method. In order to use these methods it is imperative to have a landslide inventory or at least the location (either as points or polygons) of present and past landslide events (e.g. Şandric 2005, 2008; Şandric and Chiţu 2009; Bălteanu and Micu 2009; Micu and Bălteanu 2009; Chiţu et al. 2009, 2014; Mihai et al. 2009; Chiţu 2010; Constantin et al. 2011; Armaş 2011, 2012; Mărgarint et al. 2011; Grozavu et al. 2012). Deterministic (geotechnical) methods use engineering laws to calculate a "*safety factor,*" which represents a ratio between the material shear strength and the required shear force to maintain the material on the slope. However, this approach requires expensive field data collection that makes them less accessible for studies at regional scales (Nicorici et al. 2012).

Data and Methodologies Used in Landslide Hazard Estimation

Landslide hazard is defined as "*the probability of occurrence within a specified period of time and within a given area of a potentially damaging phenomenon*" (Varnes 1984). This definition was enlarged by Guzzetti et al. (1999), in order to allow the integration of the landslide magnitude. The foundation of a quantitative hazard assessment is therefore given by a frequency–magnitude relationship (Corominas and Moya 2008). There are two main categories of methods widely known for assessing landslide frequency: (i) direct methods, related to temporal landslide records, and (ii) indirect methods, based upon the statistical analysis of the triggering threshold.

Landslide hazard assessments, that comply with all three components comprised in the definition of hazard (location, time and size), are only a few worldwide. One major reason for this situation is the lack or incompleteness of historical landslide records, which has hindered from both directly determining landslide frequency and establishing quantitative relationships between landslide occurrences and characteristics of the triggering events (e.g., earthquakes, rainfall) (Van Westen et al. 2006). In Romania, landslide hazard analyses are at their very beginning. Nevertheless, there have been a few earlier concerns for correlating landslides to the main triggers (rainfall, earthquakes).

Indirect frequency assessments rely on some precursor studies which provided first insights into the landslide–triggers relation (e.g. Bălteanu 1983). A first approximation of the cyclic behavior of the general landslide phenomenon in

Romania was established by Surdeanu (1996, 1998) and Surdeanu et al. (2009) at 30–35 years. This was done on the basis of detecting wet periods and years with rainfall excess which also corresponded to periods of landslide reactivations in the Eastern Carpathians flysch mountains. Further rainfall analyses (e.g. Dragotă et al. 2008; Micu 2008; Bălteanu and Micu 2009; Chiţu 2010; Micu et al. 2010) translated monthly and annual rainfall amounts into landslide-triggering favorability classes. Based on event or historical landslide databases, the above works and other (Ilinca 2010, 2014) propose preliminary climatic thresholds for different landslide types in study case areas. A first quantitative hazard mapping in Romania is provided by Şandric (2008) in an area of the Curvature Subcarpathians. By simulating daily time series of water amounts reaching the soil and applying a dynamic Bayesian analysis with error propagation, the author produces continuous maps of conditional probabilities of landslide occurrence depending on the water input. Further on, landslide hazard scenarios were proposed by Jurchescu (2012) at various timescales (annual, monthly, daily) in the Getic Subcarpathian and Piedmont hills, based on past landslides-generating rainfall events for which temporal probabilities were defined.

Direct estimations on the magnitude–frequency behavior of landslides in Romania have been provided in earlier years in form of denudation rates. Annual denudation rates and associated return periods were computed, based on field observations over certain time intervals, for either single processes/experimental sites or for small catchments dominated by one landslide type (slides, rockfalls) (Bălteanu 1983; Surdeanu 1998; Rădoane and Rădoane 2007). The latter study actually assessed the rate of sediment transfer from landslides to the riverbed, focusing on river-coupled landslides. The rates, spatially assigned to the mapped landslides, were computed considering: type of mass movement, activity, velocities, and depth of landslide deposits. Mean recurrence intervals were included for the episodic processes. Recently, probabilistic analyses on a historic landslide database covering the 1970–2005 period was achieved (Chiţu 2010). Landslide hazard scenarios were mapped at a 1 km^2 grid unit for different return periods (5, 10, and 20 years). For debris flows or rockfalls, direct magnitude–frequency relationships have been established by either analyzing series of recorded events or by dendrogeomorphological dating of processes (Ilinca 2010, 2014; Pop et al. 2010; Surdeanu et al. 2010).

At the site level, past investigations include estimations of movement rates (Bălteanu 1983) and inquiries on the relations among meteoric water—soil moisture—landslide dynamics (Surdeanu 1998). A much more consistent step toward landslide hazard computation has been undertaken through the application of deterministic models (Micu 2008; Constantin et al. 2010; Chiţu 2010). Although referring to triggering mechanisms (soil moisture, pore water pressure, critical location of groundwater table), or magnitude/intensity characteristics (runout, material depth, duration, 3D extension, or velocity), the analyses did not yet assess the hazard since no temporal probabilities were provided for the movements.

A representative example of data requirements issues, as well as the influence of these challenges on the subsequent selection of analysis methods is represented by the study of rockfall hazards. In most of the high-risk areas, rockfalls should be investigated through various means: from the visual observation of a site and its integration into a rockfall hazard rating system of different complexity, to hazard evaluations by modeling the mechanical and climatic forcings as well as the runout areas. At country level, simultaneous homogeneity and adaptability of the evaluation methods for hazard and risk assessment are required; Romania lacks this kind of studies and approach at scientific and administrative level. A first approach of rockfall hazard evaluation is reported for DN 7A which follows the Lotru Valley, Jieț Valley and connects the Brezoi and Petroşani localities, by Ilinca et al. (2008) and Ilinca (2009, 2010), on the basis of a 6-year inventory, using Rockfall Hazard Rating System and GIS modelling.

Data and Methodologies Used in Landslide Risk Analysis

The combined information on hazard and its consequences (vulnerability and value of elements at risk) is used to derive qualitative and (semi) quantitative risk analysis, including the total losses due to different hazards with different return periods and magnitudes (Devoli et al. 2007; Van Westen et al. 2008; Van Den Eeckhaut et al. 2010 among many others).

In Romania, availability, access, and reliability of data information represents a central issue in the state-of-the art landslide risk assessment research. In terms of official, existent data, providers vary depending on the scale of investigation from national institutes (e.g., National Institute of Statistics) to local administration technical offices; however, the often lack of know-how and supportive administrative and legislative frameworks reduces the functional collaboration between experts and stakeholders. At a regional scale (Vrancea seismic region), a good example of risk analysis and data requirements was provided by FP 7 ECLISE (http://www.eclise-project.eu/): in order to obtain the map of vulnerability index, several criteria of assessing the vulnerability have been taken into consideration, like *physical* (represented by households and communication networks—roads, railroads—in terms of density), *social* (population density at NUTS5 level), *environmental* (protected areas: existence and classification), while the lack at NUTS5 level of conclusive economical data did not allow the evaluation of economic vulnerability. An interesting attempt to assess vulnerability at a regional level is offered by Stângă and Grozavu (2012), taking into account five categories with several variables and indicators, meant to quantify the vulnerability: rural habitat, demographic features, agriculture, environmental quality, and emergency situations. At a larger scale (Nehoiu catchment, Buzău Carpathians), Godfrey et al. (2015) provided a detailed analysis on the data requirements for buildings physical vulnerability assessment to hydrometeorological hazards.

Landslide Inventory and Its Place Within Risk Analysis

The landslides inventory represents the key for a successful forthcoming susceptibility, hazard, and risk assessment. The choice of the risk methodological approach should reside not only on the quantity of the available data within the inventory, but on their quality. Especially for regions prone to a wide variety of landslides (like the Subcarpathians, the Moldavian or the Transylvanian Tablelands, the Eastern Flysch Carpathians), a typologically based inventory should contain enough morphological, morphometrical, or morphodynamic data in order to allow the development of properly representative maps. The Romanian legislation (LG 124/1995, Ord. MLPAT 62/N/1995/1998, LG 575/2001, HGR 382 and 447/2003, Norm. GT-019-98) states the procedure of obtaining landslide characterization data files, but does not offer proper guidelines on their use within landslide hazard or risk maps. The rather often lack of landslide precise positioning within the legally asked specific inventory sheets is a weakness in the inventory development. The use of the same name (usually, just the hamlet or the village name) does not allow a proper positioning or delays a lot the time sequence between the eventual conversion of that particular point into polygon.

Landslide Inventory: Results Within Large Homogeneous Morphostructural Units

Several case sites or regions of Romania are developing landslide inventories using either personal criteria or internationally agreed guidelines. International projects like FP6 SAFELAND, FP7 CHANGES, and FP7 ECLISE offered the framework inside which local (Jaedicke et al. 2014) and county-level (Jurchescu et al. 2012; IGAR 2014; Zumpano et al. 2014) inventories were used for susceptibility, hazard, or risk assessments.

Such a landslide inventory at a regional scale was prepared for the Moldavian Plateau (a detailed description and statistical analysis of the polygon-based landslide inventory is provided in Chap. 12, this volume). In this homocline region, the landslides are spread mainly along the fronts of cuestas, with slope angle generally comprised between 8° and 15°. Landslide occurrence is strongly influenced by different lithological formations: consolidated rocks like sandstones, limestone and volcanic tuffs, alternating with clays, sands, and marls. The largest landslides occur along the slopes which present hard rock at the upper part, and during their long evolution they have created impressive mono- or poly-amphitheater-like landforms, locally called "*hârtoape*". In most of the cases they are affected by recent reactivations, embedded in the mass of old landslides. In clayey formations a large number of superficial landslides occur, most of them featuring a translational character.

Due to this complexity of landslides (in terms of type, age, size, or activity), two types of inventories were carried out: point- and polygon-based. The point-based inventory was achieved by interpretation of ortophotos at a 1:5000 scale and GoogleEarth imagery, while for polygon-based inventory LIDAR DEM imagery has also been used. The assignment of points for obtaining landslide inventories is still in discussion in the scientific literature. Depending on the purpose of the inventory, some different ways are reported: using centroid points (Simon et al. 2013), assigning points to each main scarp (Petschko et al. 2014), semi-automatically assigning points for depletion areas using geomorphometric variables (e.g., mass balance index, Mărgărint et al. 2013a, b) or multiple other techniques for sampling landslide data (Regmi et al. 2013).

The point-based inventory (more than 9500 points) for the Moldavian Plateau was obtained using the following rules: (i) the clearly individualized landslides bodies, even those smallest than 1 ha, were represented by one point; (ii) the landslides covering more than one slope aspect were represented by separate points; (iii) in case of cuesta scarps, entirely covered by landslides, one point was assigned to each landslide crown situated at more than 500 m apart; (iv) for complex landslides (given by high density of the channel network) the second and the third rules were combined (Fig. 32.3).

Other important inventories at regional level were obtained within European CHANGES and ECLISE FP7 projects. Based on archive data (Institute of Geography, Romanian Academy), detailed geomorphological field mapping, local authorities databases (Buzău and Vrancea County Inspectorates for Emergency Situations) and digital stereographic photo interpretation using color aerial orthophotos, a dataset of more than 3500 landslides was set up for the Vrancea Seismic Region. The results were used in landslide susceptibility, hazard and risk assessments (IGAR 2014; Damen et al. 2014; Riedmann et al. 2014).

Fig. 32.3 Polygon-based versus point-based landslide inventory. LIDAR DEM image **a** and associated satellite GoogleEarth image **b**. Sample from the northern part of the Moldavian Plateau

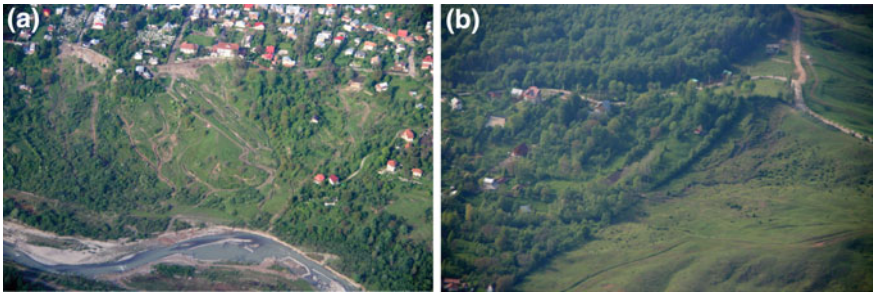

Fig. 32.4 Airborne oblique pictures in the Ialomiţa Subcarpathians (*Photos* **a** and **b** I. Şandric)

At national level, an ongoing inventory is being established within an EUR-OPA project entitled "*Pan–European and nation–wide landslide susceptibility assessment*" (2012–2016; coordinator CERG Strasbourg). Compiling literature–available data, regional inventories provided via institutional agreements or by the authors of some PhD theses, the project was able to compile a national inventory of almost 30,000 landslides, comprising 95 % slides, 3 % flows, and 2 % falls (Micu et al. 2014a, b).

Landslides inventories at very large scale (1:200–1:5000) were made by Şandric and Chiţu (2009) in the area of Prahova and Ialomiţa Subcarpathians. Very high-resolution oblique pictures (Fig. 32.4) were taken during several flights (Cessna F172H airplane, Canon 400D, 18–250 mm lens). The aerial photos provide, from different viewpoints, a large scale perspective over natural landscape processes and helped classifying the landslides according to the type of movement. Some of the photos were used to create anaglyph images, bringing a 3D perspective to the image interpretation process. The vertical photos were successfully georeferenced with a standard error of approximately 10 m and used in a GIS for mapping the location of the landslides units (Şandric 2009; Chiţu 2010).

Landslide Inventory: Results at a Catchment Level

Identification of landslide processes and their spatial pattern has also been carried out at the level of catchments and drainage basins. Such is the case of the historical landslide inventory of the Olteţ River basin located in southern Romania (Jurchescu 2012; an extract of it is depicted in Fig. 32.5).

Given that the extent of the study area exceeds 2400 km^2, the inventory was compiled for a small scale of 1:200,000, which imposed a slightly more detailed scale for the acquisition of the data. Therefore, the inventory was obtained through interpretation of topographic maps and satellite imagery, while geomorphologic field reconnaissance and historical data were only used to verify some findings. The reason

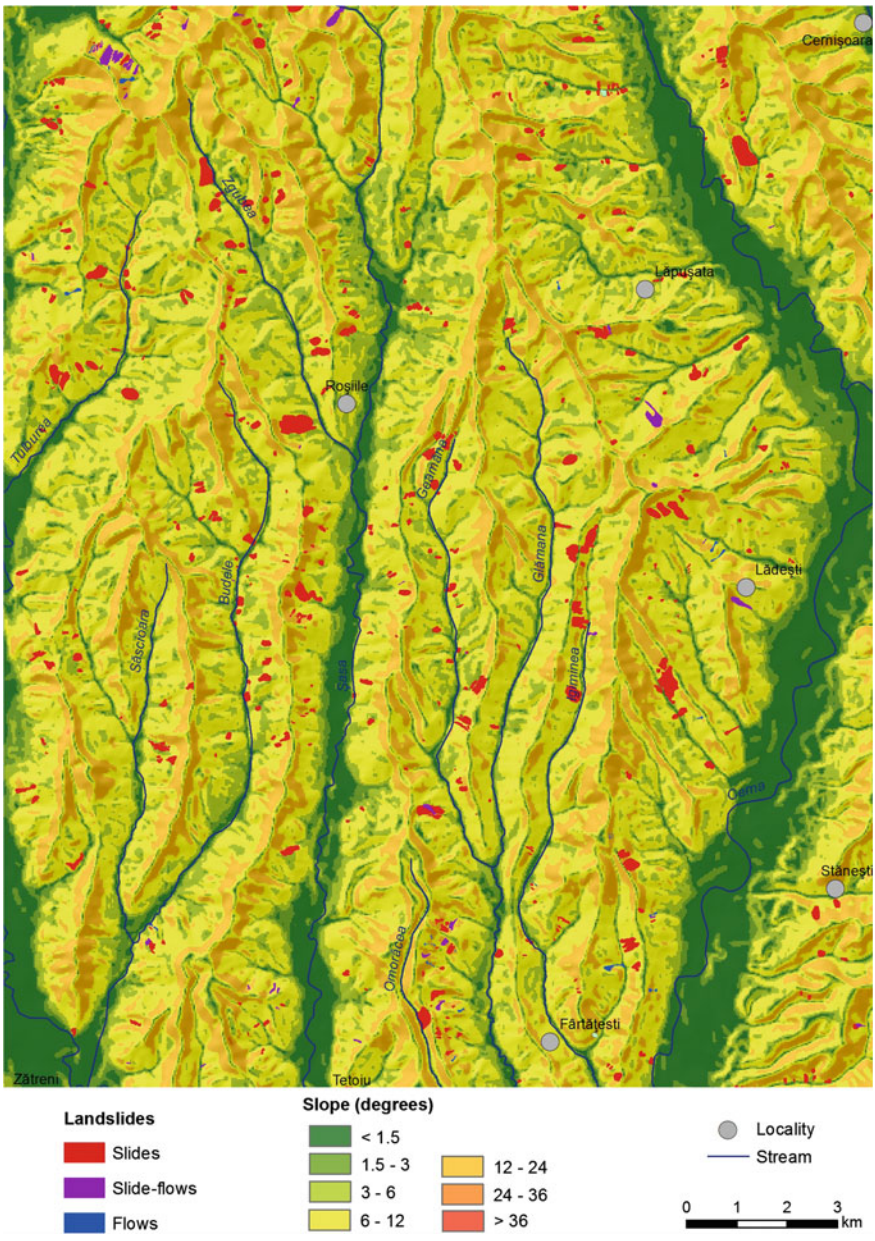

Fig. 32.5 Detail from the landslide distribution map of the high piedmont sector of the Olteț basin (an extract from the map of Jurchescu 2012)

for this was ensuring homogeneity in the inventorying process by using data that cover the entire study area. Points were used for representing this small-scale inventory. Besides the spatial distribution, the map of landslide processes also comprises their

typology according to the classification of Dikau et al. (1996). An index ranking the confidence in mapping (MCI) as high, medium or low, was assigned to each landslide, following the example given by Thiery et al. (2007). The total inventory consists of more than 2100 landslides; 35 % of the total number of landslides was determined with a high, 47 % with a medium and 18 % with a low MCI. The main types of mass movements are slides and flows, typically encountered in the hilly sectors of the basin corresponding to the Getic Subcarpathians and the higher Getic Piedmont. A medium-scale inventory (1:50,000–1:25,000) was performed for these sectors of the basin, by analyzing high-resolution aerial photography and satellite imagery, integrated with local field survey results and other historic information. At this scale, landslides could be represented using polygon geometry, but a division of landslides into depletion and runout zones was considered inappropriate. Characteristics referring to typology, state of activity, and depth of the sliding surface were stored in a GIS. Shallow slides are commonly found to be grouped, affecting steep slopes within low-order catchments. Deep-seated slides are located on the slopes of both main and secondary streams and have a large development on the cuesta scarp slopes. The greatest part of the landslide-affected area occupies moderate slope angle surfaces of 6–12° (66 %) (Fig. 32.5). Specific for the spatial distribution of landslides is the tendency to form clusters of multiple landslides where individual bodies are often hard to distinguish. These occur more frequently on clay and marl deposits containing sand intercalations. A high density of landslides is also found in the coal mining fields (of the Berbeşti mining basin): on the artificial slopes of sterile heaps and quarries, on the nearby destabilized slopes, as well as induced by the presence of underground galleries.

Landslide Susceptibility Assessment

In order to provide an overview on the typical morphostructural units of Romania suitable for such an analysis, several examples of landslide susceptibility analyses will be presented in detail: Curvature Subcarpathians, Moldavian and Transylvanian Tablelands, Getic Piedmont, High Carpathians (Fig. 32.1).

Expert Knowledge and Statistical Analysis in Landslide Susceptibility Assessment: A Case Study in the Curvature Subcarpathians

Expert knowledge is a qualitative approach for landslide susceptibility assessment which integrates in an interpretative way the role of landslide predisposing factors (in 2007, Thiery provides a detailed description on its application in terms of subjectivism degree, benefits, and constrains).

The Ialomiţa Subcarpathians are localized in the western part of Curvature Subcarpathians, between the Ialomiţa and Prahova valleys. This specific area exhibits a wide range of lithological formations and an extremely complex structure. The lithological formations range from lower Cretaceous—lower Miocene formations in flysch facies to molasse formations (Miocene and Pliocene molasse) and Quaternary deposits (Damian 2003). These formations, except for Pliocene and Quaternary, are involved in a complex structure characterized by nape systems, the folding of post-nappe covers, the diapirism phenomena and the vertical faults (Ştefănescu 1995). The high temporal frequency of landslides (1997, 1998, 2005, 2006, 2010, 2012 and 2014) leads to the consideration that these processes play a major role in the evolution of this area's landscape, where the most frequent processes are: slumps, earth flows, mud flows, and complex movements.

The expert knowledge approach was applied for landslide susceptibility mapping in the Ialomiţa Subcarpathians (Fig. 32.6) using Weighted Overlay—a tool implemented in ArcGIS, which offers the possibility of assigning, for each

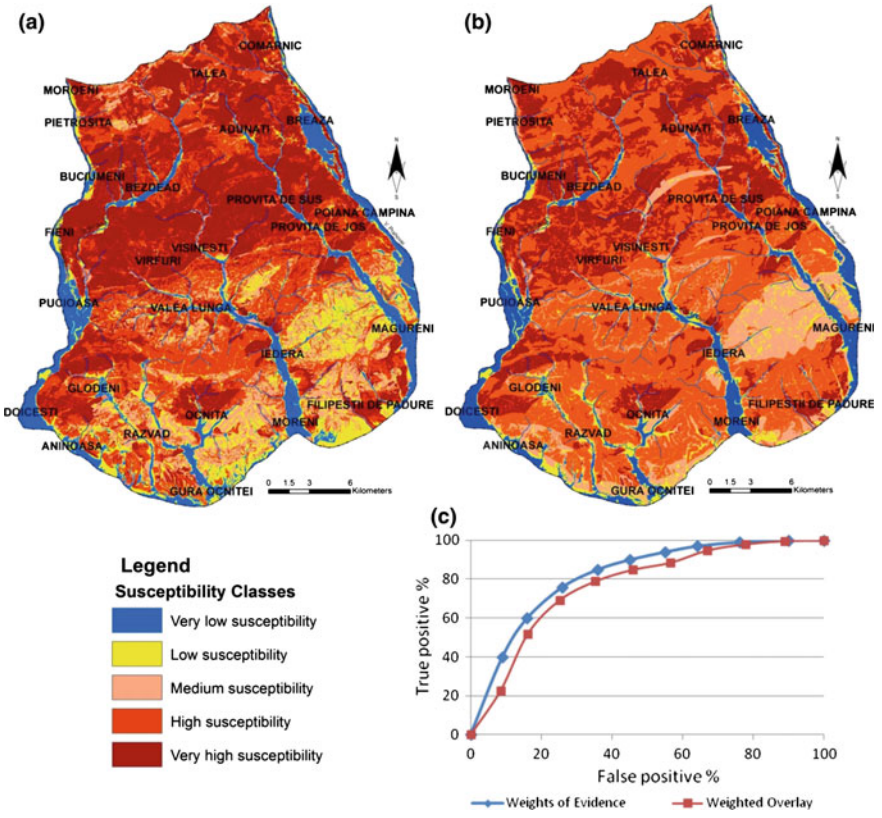

Fig. 32.6 Susceptibility maps. **a** Landslide susceptibility map using weights of evidence. **b** Landslide susceptibility map using weighted overlay. **c** ROC curves for WoE and WO

predisposing factor class, a weight value between 1 and 5 based only on the investigator's experience. For this study the following input data have been used: a 20 m cell-sized DEM, lithology, faults density, drainage density, land use, land cover, mapped landslides. Also, several terrain parameters were derived from the DEM such as: slope gradient, slope aspect, profile curvature, and plan curvature. Because most of the environmental factors introduce redundant information, only three factors were kept: lithology, slope and land use. The two maps reveal the same high landslide susceptibility classes located around the communes of Provița, Vișinești, Iedera, Vârfuri, Bezdead, Glodeni and the town of Breaza, while the difference between the two maps is induced by the overestimation of the medium landslide susceptibility areas in the map carried out by weighted overlay.

In order to show the utility of the expert knowledge approach, we compared the susceptibility maps obtained with the help of the mentioned method and *Weights of Evidence* (bivariate statistical analysis). After validating the two maps using the ROC curves, the map relying on the expert's knowledge has a value of 0.76, close to the one prepared using the probabilistic method—0.82. The ROC values of the two maps encouraged the authors to consider that, in the presence of the detailed landslide inventory, expert knowledge-based approach can be used either for rapid delineation of landslide-prone areas saving time and money, or complementary with statistical methods in order to improve probabilistic estimates. The disadvantage of the expert judgment method is that it could be used only in the area where the investigator has knowledge about hillslope behavior.

Landslide Susceptibility Assessment in Tableland Regions: Case Studies from the Transylvanian and Moldavian Plateaus

Using quantitative methods for landslide susceptibility assessment it is possible to obtain good results, reflected by high values of Area under the Receiver Operating Characteristic (AUROC). For four equal-square-shaped sectors (225 km^2) situated in the extra- and intra-Carpathian chain, one of the common methods was applied, i.e., binary logistic regression (Mărgărint et al. 2013a, b). The same predictors (elevation, slope angle, slope aspect, slope height, profile, plan and mean curvature, lithology, distance from the drainage network, land use) and the same materials for data acquisition were used for all sectors (in the inventory extraction and logistic regression). For all sectors, the AUC values are higher than 0.88 for the training samples and higher than 0.85 for the validation samples. Figure 32.7 shows the landslide susceptibility maps for an intra-Carpathic sector—Căpuşu de Câmpie, located in the central part of the Transylvanian Depression and for an extra-Carpathic sector—Şipote, located in the northern part of the Moldavian Plateau (Mărgărint et al. 2013a, b).

The homocline structure, lithology, and geomorphometrical variables show an obvious spatial repetition for landslide occurrence and clustering patterns,

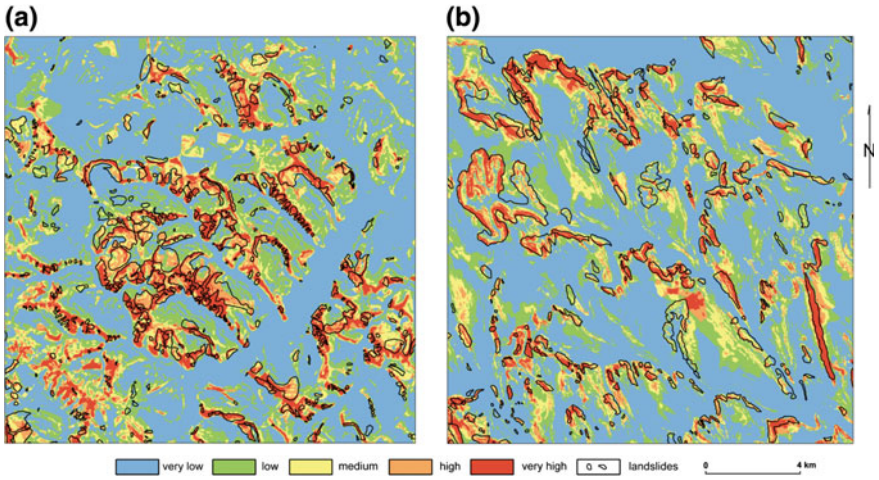

Fig. 32.7 Classified landslide susceptibility maps. **a** Căpuşu de Câmpie sector. **b** Şipote sector

especially for the Moldavian Plateau (see Mărgărint and Niculiţă Chap. 12, this volume), and similar results have also been reported for the LR and AHP susceptibility models (Mărgarint and Niculita 2014).

Landslide Susceptibility Assessment in Large Drainage Basins: The Case Study of the Olteţ River Basin

In a study of applied geomorphology, meant to support regional planning by identifying areas most potentially subject to landslides and prioritizing these for more in-depth studies, Jurchescu (2012) and Jurchescu et al. (in prep.b) analyzed landslide susceptibility within a top–down framework. The study area was the Olteţ drainage basin extending over four landform types, namely: the Southern Carpathians, the Getic Subcarpathians, the Getic Plateau (Getic Piedmont), and the Romanian Plain.

The first stage in this approach was a heuristic susceptibility estimation for the entire extent of the basin at a regional scale. Based on the obtained preliminary results, the most affected sector, identified as pertaining to the Subcarpathian and high Piedmont hills, was selected for a more detailed analysis, at a medium scale (1:50,000–1:25,000) using data at a correspondingly higher resolution (30 m). At this scale, a quantitative estimation of susceptibility was performed, through a logistic regression analysis (Jurchescu 2012; Jurchescu et al. 2014b, in prep.b).

Information on the considered causal factors (elevation, slope angle, slope aspect, plan and profile curvatures, lithology, land cover, distance to rivers, and distance to anthropic landforms) was extracted using: a DEM derived from topographic maps and updated with the anthropic landforms, a lithological map, and a land cover map obtained as a result of a supervised classification of a LANDSAT 7 ETM+ Surface Reflectance product (GLFC and GSFC 2011). The multivariate analysis was combined, in this case, with a simple bivariate one. The latter was used as a data preprocessing stage. It served for transforming all classified parameters, in such a way that they expressed the degree of favorability to landslide occurrence, using, at the same time, a unitary scale from 0 to 100. The new transformed factors played the role of explanatory variables in the regression. In order to avoid over- or underestimation of the observed data, an equal number of pixels were sampled from both landslide-affected and landslide-free subareas. Only the central pixel of each landslide body was selected, while in the random extraction of cells from the landslide-free area those adjacent to landslide bodies were avoided due to their uncertain nature. The total sample was randomly split into training (80 % of the total sample) and validation (20 %) datasets, each of them preserving the equal ratio between landslide and non-landslide records. The actual analysis was performed with the stepwise forward logistic regression, using the likelihood ratio for testing the significance of the predictors. Coefficients were determined through the maximum likelihood method. The *Natural Breaks* algorithm (Jenks 1967) was used to distinguish among several classes in the final probability map.

An extract of the classified, medium-seated landslide susceptibility map, corresponding to the high part of the piedmont sector between the Olteţ and Cerna Rivers, is provided in Fig. 32.8. From the predictors introduced into the analysis, the only one rejected by the likelihood ratio test was the one based on the distance to the anthropic relief. The most significant explanatory variables are the transformed variables of land cover and slope angle.

Success and prediction rates with values above 78 % prove a good agreement with the landslide datasets, while the area under the ROC curve, of 0.856, indicates a good accuracy of the model. The susceptibility ranges between 0.011 and 0.998. Of the total area investigated, 28 % belongs to very low susceptibility, 31 % to low susceptibility, 20 % to medium susceptibility, 11 % to high susceptibility and 11 % to very high susceptibility.

From the perspective of sediment transfer dynamics, the question was raised whether the estimation of susceptibility to specific geomorphic processes at a catchment scale could be exploited for the spatial identification of potential sediment sources in the basin (Jurchescu 2012). In the specific case of the Olteţ basin, the presence of a reservoir at river outlet emphasizes the importance of estimating sediment budgets, the first stage of which would consist in studying sediment sources.

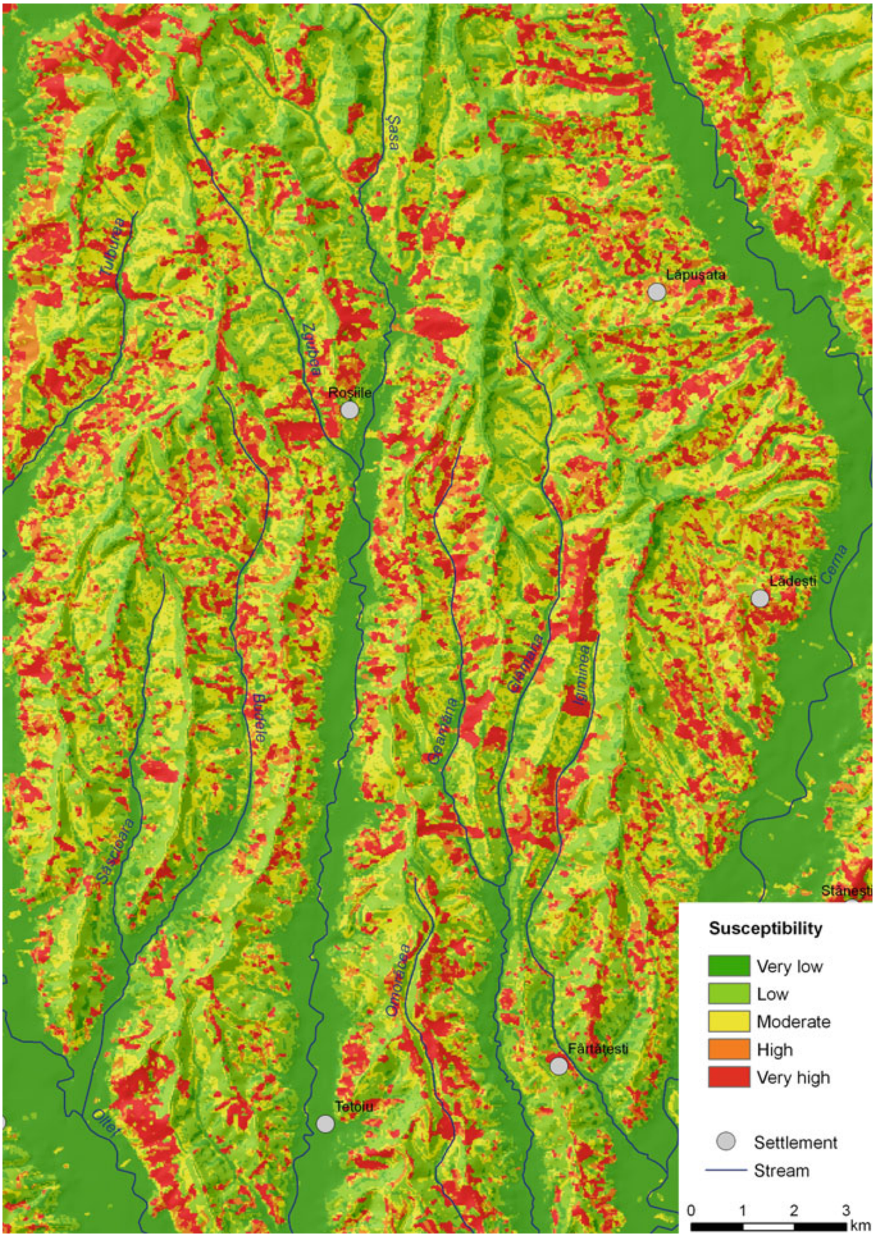

Fig. 32.8 Detail from the medium-seated landslide susceptibility map (Jurchescu 2012), corresponding to the high piedmont sector of the Olteţ drainage basin

Rockfall Susceptibility Estimation in the Carpathian Mountains

Rockfalls are geomorphic processes that frequently occur in the mountain areas of Romania, especially in the Southern Carpathians and to a lesser extent in the Flysch Carpathians and Apuseni Mountains. The extent of these processes is a consequence of both geological constitution and geomorphic aspects. As the studies are very few, as well as the systematic inventories (while susceptibility maps are missing so far), we will here refer to only three representative mountain road sectors which are yearly affected by this kind of processes, that is, the Olt Gorges, Lotru Valley and the Transfăgărăşan Road, corresponding to National Roads (DN) DN 7, DN 7A and DN 7C, respectively, within the Southern Carpathians.

The occurrence of rockfalls on the roads along the Olt and Lotru valleys is related primarily to the geologic and geomorphic contexts. Both valleys are cut into metamorphic rocks like gneisses, micaschists, and amphibolites. The events from the Olt Gorges and Lotru Valley are both lithologically and structural–tectonically controlled. Apart from these controls, the human influence is very important as many valley parts of the slopes are cut in order to make road embankments. Most of the rockfalls (regardless of their magnitude) reach the road embankments because of the short distance between slope and the road. In these circumstances, even small runouts can easily reach the road.

Although rock slopes are developed only in few lithostratigraphic units, rock properties can greatly vary due to the local conditions, related to microtectonics and alteration degree. For example, *Rock Mass Quality* (*Q*) estimated for 17 investigated rock slopes near the Brădişor Reservoir have values that range from 0.17 to 1.33, which makes 35 % to have poor quality and 65 % very poor quality (Ilinca 2010). The area with the highest rock fall frequency in the Lotru Valley is located exactly near the Brădişor Reservoir, where rockfalls occur due to the intense tectonized metamorphic rocks related to the Cozia (Lotru) Fault. Many block detachments frequently happen along joints and schistosity planes, but also along slickensides developed approximately parallel with the slope face (Ilinca 2012).

The Transfăgărăşan Road has also been developed through intense slope cutting, which produced several sectors with large vertical and overhanging rockwalls, especially above 1400 m. In this case, overlaying very steep topography, both exposure of hard jointed rock and the severe high mountain climate can easily enhance the detachment of boulders. Recent measurements of joints patterns and characteristics on the south-oriented portion of the road, in the area of the Bâlea–Capra tunnel indicates a density of 10 fissures per meter, their thickness varying from less than 0.05 to 24 mm (Fig. 32.9).

A high frequency of very small fissures can be noticed, but this does not necessarily certify a high potential production of small-size boulders, as the fissures are most probably newly formed. Taking into account the distribution of these

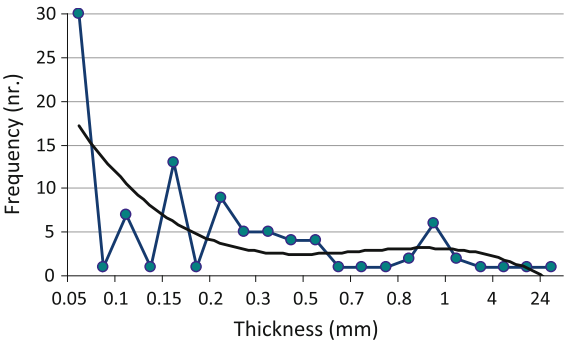

Fig. 32.9 Thickness of rock fissures in rockwalls near the Bâlea–Capra tunnel, in the alpine sector of the Transfăgărăşan road

discontinuities and their frequency, it is possible to say that the size range of the material engaged in rockfalls is expected to correspond mostly to mean size boulders, but it does not exclude neither centimeter-sized nor large-sized rock fragments.

Landslide Hazard Assessment

Triggering Factors and Thresholds

Generally, rainfall is the most common trigger of landslides (Crozier 1986; Corominas 2001), but the response of the landslide system in relation to geotechnical, hydrological, and climatological conditions is not direct but rather complex, due to the nonlinear character of the rock/soil water system (Crozier 1997; Van Asch 1997; Schmidt and Dikau 2004). Prediction of landslide-triggering thresholds is a key issue in the landslide hazard research. A literature review reveals no unique rainfall-related thresholds, neither from the point of view of exceptional or antecedent cumulative rainfalls, nor from intensity–duration relationships (as widely discussed in a number of works in the last two decades, e.g. Aleotti and Chowdhury 1999; Dai and Lee 2003; Aleotti 2004; Flentje and Chowdhury 2002; Flentje et al. 2005; Walker 2007; Bunce 2008; Pujină 1998; Thiebes 2012).

In Romania, except for precipitation, an important landslide-triggering factor is represented by the earthquakes. Vrancea Seismic Region is responsible for the major seismic effects all throughout half of Romania's territory, potentially affecting more than one-third of its total population, while the effects are exceeding the natural borders, reaching Moldova, Ukraine, Bulgaria, and Greece. The region generates 3–4 intermediate (90–200 km hypocenter depth) earthquakes over magnitude 7 per century, causing severe damages and inflicting casualties. Since 1700, 14 earthquakes with magnitudes above 7 (among which seven above 7.5 and three of 7.7–7.9) were registered, while the last century was marked by four major events, measuring 7.10 M_w (1908, 1986), 7.40 M_w (1977), and 7.70 M_w (1940). The losses

registered in 1940 exceeded 1000 victims and 4000 injured people, while those of 1977, overpassing 2 billion USD, were represented by 1570 victims, above 11,000 injured and more than 35,000 collapsed buildings (Lungu et al. 2007). In the Curvature Carpathians, the immediate or delayed effects of earthquakes are comprising disturbances in piping process (especially on salt breccia formations), groundwater level disturbances, spring emergences, fissures, mud volcanos, and also landslide occurrence (in form of rock slumps, rock-block slides, rockfalls, or rock avalanches). The landslides can be co-seismic (rockfalls, rock avalanches) or post-seismic (rock-block slides, debris flows). The main conditioning factors for earthquake-triggered landslides are: (i) slope lithology–structure relationship (tectonic and lithologic contacts in the immediate vicinity, parallel bedding); (ii) slope orientation (the south, south-east or south-west facets are already covered by low strength, weakly cemented, or weathered deposits); (iii) cover deposits layout and thickness (weathered deposits, with high water saturation either due to precipitation or existing springs). Unfortunately, the lack of regional analyses focusing on Arias Intensity made a proper assessment of earthquake-induced landslide susceptibility difficult to achieve. Recent studies (Micu et al. 2014a, b) proved that under propitious conditions (strike-slip vicinity, south-west facing slope covered with weathered slope deposits, positioned in front of the main seismic wave propagation direction, slope in accordance with the structural orientation) landslides may be triggered (accidentally, not widespread) by earthquakes with magnitude above 4.

Triggering Thresholds and Recurrence Intervals

In Romania, soil degradation and specifically rainfall-triggered landslides of various types and forms were described and recognized as a nationwide problem since over 80 years ago (Macovei and Botez 1923). In the absence of detailed historic landslide data, only few attempts were made toward identifying landslide-triggering rainfall thresholds. This often meant establishing a relationship with the particular triggering events shortly after the production of landslides. Most studies of landslide-triggering rainfall have been carried out on a temporal analysis basis, usually applied to single sites or areas to small extent, while only few attempted a spatial analysis approach, targeting larger areas widely prone to landsliding. In general, the Romanian scientific community widely recognizes that landslides are mainly triggered by heavy rainfalls or rainfalls associated to snowmelt events, but there are only a few contributions focusing on the investigation of landslide–rainfall/snowmelt triggering mechanisms in this country. The high complexity of landslide-triggering mechanisms is also emphasized by Bălteanu (1980), showing that the influence of rainfall on landslide failures is highly dependent on the landslide typology, kinematics and lithology (in terms of bedrock and regolith) involved.

In order to outline rainfall–landslide relationships, two approaches have been followed: (i) an overview of landslide-triggering precipitation thresholds for the Eastern and Curvature Carpathians of Romania and (ii) a definition of thresholds for

landslide occurrence in the sectors of the Getic Subcarpathians and Getic Piedmont encompassed by the Olteț basin.

Analyzing the high positive deviation behavior in the precipitation regime in Romania, Dragotă (2006) showed that in general, the intense and prolonged rainfall events often caused considerable floods, flash floods, and slope instability events (e.g., landslides, mudflows), as well as great economic damages and casualties. The author documented damages produced by some major heavy rainfall episodes in Romania and showed that those registered in April–May 1970 and July 1975, caused 70,000 ha of landslide-affected lands, particularly in the mountainous and hilly regions of the Vaslui, Iaşi, Vrancea, Buzău, Suceava, Cluj and Alba counties. Dragotă (2006) also identified the wettest decades of the twentieth century, in which the heavy rainfall events, concentrated mostly in early summer less in the autumn–winter interval, determined great economic damages at national level due to severe flooding and widespread landslide-affected areas. These decades were 1910–1919, 1932–1941, 1966–1975, and 1986–1996. The heavy rainfalls of the years 1969, 1970, 1975, 1995, and 1997 are frequently mentioned as potential triggers in most studies, documenting landsliding activity in various regions of Romania. Furthermore, the years 2005 and 2010 were distinguished among the costliest wet years of the twenty first century (at least in the Curvature Region of Romania) in terms of the effects of some recent major landslide events, as reported by the Vrancea and Buzău Inspectorates for Emergency Situations, Micu et al. (2013) and discussed in the local media. Bălteanu (1983) applied both temporal and spatial analysis approaches in the study of mass movement processes in the Buzău Subcarpathians (the Curvature Subcarpathians). The author documented the triggering conditions of shallow landslide events in the Valea Viei catchment (the Curvature Subcarpathians), linking their failure, reactivation or their transformation into a mudflow-like process, to the occurrence of heavy rainfall (July 1969), as well as to the rain-on-snow events (April 1970). Moreover, the analysis of the behavior of some medium-seated (e.g., Dealul Mănăstirea, Dealul Viei, Begu) and deep-seated landslide events (e.g., Tega, Valea Fântânii), identified the torrential rainfall associated with strong slope undercutting and the long spans of heavy rainfalls among the main factors involved in the immediate failure of deep-seated landslides. However, no critical thresholds of rainfall amounts (or intensities) were established in this study.

Several works in the Romanian literature contributed to the analysis of landslide–rainfall relationships, by proposing thresholds for the initiation of some significant landslide failures, derived from the in situ measurements on short antecedent intervals of up to two months prior to the occurrence of slope processes. Documenting the characteristics of land degradation in Romania, Surdeanu (1998) provided a valuable review of some of the main contributions to the study of the seasonal landslide-triggering thresholds in the Romanian Carpathians and Subcarpathians in relation to landslide typology, with a focus on the Moldavian and Curvature sectors (Table 32.2).

Empirical thresholds, based on the analysis of the antecedent precipitation over the February–September 2005 interval, in relation to the occurrence of some

Table 32.2 Landslide–rainfall triggering thresholds in Romania (updated from Surdeanu 1998)

Triggering thresholds	The Moldavian Carpathians		The Curvature Carpathians and Subcarpathians	
	Shallow and medium-seated landslides	Deep-seated landslides	Shallow and medium-seated landslides	Deep-seated landslides
Wet interval	February–March 1998	April–June, 1969	May 4–8, 2005	May 5–7, 2005
Threshold	10 mm/24-h	400 mm/April (twice the monthly average)	50 mm/12-h	57 mm/48-h
Case study	Bistriţa valley	Varlaam, Buba, Huiduman	Nehoiu, Bonţu Mare	Bisoca
Reference	Dinu and Cioacă (1997)	Surdeanu (1998)	Micu et al. (2013)	Micu et al. (2013)
Wet interval	June–July 1969, 1970	August 27–28, 1969	July 2, 1975	July 14, 1969
Threshold	45–56 mm/24-h	47–74 mm/24-h	177 mm/24-h	201 mm/June (twice the monthly average)
Case study	Izvorul Muntelui	Rugineşti, Pângăraţi	Pănătău	Gârboi
Reference	Surdeanu (1996)	Ichim (1970, 1972)	Bălteanu and Constantin (1998)	Bălteanu (1970)
Wet interval	November–December 1996	September 1970	September 19–21, 2005	September 23–24, 1972
Threshold	15–20 % of the annual precipitation	35–55 mm/24-h	93 mm/3 consecutive days	62 mm/48-h
Case study	Izvorul Muntelui	Pângăraţi	Muscel, Valea Viei	Valea Viei
Reference	Surdeanu (1998)	Ichim and Bojoi (1970)	Dragotă et al. (2008)	Bălteanu (1970)
Wet interval			All throughout the year	All throughout the year
Threshold			35 mm/24-h	100 mm/24-h
Case study			Breaza	Breaza
Reference			Şandric (2008)	Şandric (2008)

shallow landslide events in the Muscel catchment (the Buzău Subcarpathians), were also proposed by Dragotă et al. (2008). The antecedent precipitation conditions were investigated using the daily precipitation measurements of Pătârlagele weather station (289 m a.s.l.) and linked to the occurrence of four major shallow landslide events (February 21–23, May 6–12, July 12–16, and August 19–21) reported by the

Buzău Inspectorate for Emergency Situations. The findings of the study showed that the surveyed slope processes occurred in similar antecedent wet conditions such as: precipitation amounts cumulated over 24 h of at least 25 mm; antecedent precipitation amounts over three consecutive days prior the events of 50–100 mm; precipitation amounts cumulated over at least three nonconsecutive rainfall days of 32–41 mm; and antecedent precipitation amounts over 10 days prior the event of 36–122 mm. These thresholds were established for landslide events acting mostly as reactivations, which affected areas of 0.3 up to 5 ha.

The deep-seated landslides–rainfall coupling is rather complex and becomes relevant in relation to long-term rainfalls (Terranova et al. 2007). Most studies investigating the effects of heavy rainfall events or exceptional wet intervals on the occurrence or recurrence of deep-seated landslides were based on the antecedent daily rainfall approach, developed by Crozier and Eyles (1980), which can be regarded as a proxy of antecedent soil moisture. Wieczorek (1987) recognized the important role of antecedent rainfalls in the initiation of landslides and debris flows, but also the difficulty in quantifying its influence. Later, Chowdhury and Flentje (2004) proposed the approach of antecedent rainfall percentage exceedance time (ARPET). Micu and Bălteanu (2013) asserted that dormant and relict landslides covering large areas present a high reactivation potential. Micu et al. (2013) provided some preliminary results on the empirical relationships between precipitation and the occurrence of three recent deep-seated failures occurred in the Buzău Carpathians and Subcarpathians (part of the Curvature Region—an area highly prone to mass movement processes due to its geological, lithological, climatic settings). The investigations focused solely on daily precipitation provided by the local rain gauges operating in the network of the Romanian Waters. The main physicogeographic settings of landslides and the precipitation preparing–triggering conditions are summarized in Table 32.3 and Fig. 32.10.

The study showed no obvious quantitative similarities in respect to the cumulated antecedent precipitation between the three slope failure events. However, precipitation amounts (summing 60 to more than 250 mm) over up to two months prior the landslide displacements, with return periods from 10 to 35 years (e.g., Bâsca Mare–Viforâta landslide), as well as high precipitation amounts (above 50 mm) cumulated over three consecutive days before the final slope failure (e.g., Bisoca landslide), were found relevant enough to highlight the preparedness–triggering role of precipitation.

Later, Micu et al. (2014a, b) investigated into more details the rainfall–landslide coupling for the most recent deep-seated landslide failure (Bâsca Mare–Viforâta). Naum and Michalevich (1956) reported for the first time the destructive effects of this landslide, which caused significant traffic disruptions in the neighbor area in the extremely wet year of 1953. In July 2013, a partial reactivation of an older part of the landslide (completely forested) took place, destroying 7 ha of forest, 90 m of forest road, and blocking completely the thalweg of Bâsca Mare River. The mass movement lasted 4 days, exposing the settlements located 500 m downstream the pounded water to a significant flood risk. The analysis of rainfall conditions was based on the antecedent rainfall approach applied for a period of 180 days prior the

Table 32.3 Main settings and antecedent precipitation conditions for three deep-seated landslides occurred in the Buzău Carpathians and Subcarpathians in the 2000–2013 interval

	Deep-seated landslide events (Failure date)		
	Mordana (June 20, 2000)	Bisoca (May 7, 2005)	Bâsca Mare–Viforâta (July 15, 2013)
Generalized physiogeographic settings of landslide	Complex, rotational rock slide and debris flow Scarp and body: rill–gully flow; both drainage and sedimentation; active piping in salt breccia	Simple, translational rock slide along structural surface Surface: 12.5 ha, 500,000 m^3; river blockage (advancing development)	Complex, quasi-total reactivation; rotational rock slide then rock/debris slide
Wet spells over the A180 days	Maximum length: 7 days Number of wet spells prior to the event (7 resulting in 146.5 mm)	Maximum length: 5 days Number of wet spells prior to the event (13 resulting in 270.3 mm)	Maximum length: 3 days Number of wet spells prior to the event (14 resulting in 301.9 mm)
Potential preparing precipitation thresholds	A52–58 days = 26.6 mm (RP of 2.4 years)	A7 days = 58.3 mm (RP of 37.2 years) A10 days = 61.3 mm (RP of 21.0 years) A15 days = 71.5 mm (RP of 15.1 years) A20 days = 82.4 mm (RP of 10.7 years)	A25 days = 137.2 mm (RP of 27.8 years) A30 days = 143.3 mm (RP of 18.6 years) R60 days = 262.1 mm (RP of 33.2 years)
Potential triggering precipitation thresholds	A6 days = 51.6 mm (RP of 30.4 years)	A3 days = 56.5 mm (RP of 105.9 years)	A20 days = 111.5 mm (RP of 23.7 years)

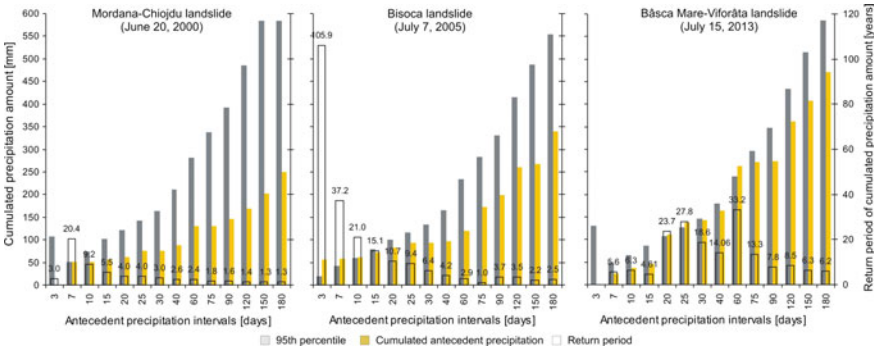

Fig. 32.10 Cumulated precipitation amounts over a 180 days antecedent period prior the failure of three recent deep-seated landslides in the Curvature Carpathians and Subcarpathians, relative to the corresponding level of the 95th percentile and the associated return periods

landslide failure. The findings of this study outlined the preparing–triggering role of heavy rainfalls but also of the joint action between rainfall showers and earthquakes in the reactivation of the Bâsca Mare–Viforâta deep-seated landslide. The positive precipitation deviations (up to 119 %) in the 6 months prior to the Viforâta–Bâsca Mare event appeared to have a great contribution to the preparedness of the landslide reactivation (Fig. 32.11). The precipitation conditions characterizing the 180 days antecedent interval is illustrated in the same figure and could be summarized as: a high occurrence probability (80.5 %) of heavy precipitation events (>10 mm/day) over the entire antecedent interval; high cumulated antecedent rainfall amounts of 111–143 mm (over 20–30 days) and 260 mm (over 60 days) exceeding the corresponding thresholds of the 95th percentile and having return periods of 19–29 years and slightly over 30 years, respectively; a high 24-h rainfall amount in day four prior to the event, with a return period of 32.5 years. The results also indicated that the cumulative rainfall amounts over 15 days and shorter antecedent intervals (of up to 46 mm and return periods below 7 years) are weakly connected to the Viforâta–Bâsca Mare landslide reactivation. The spring snow melting processes were found in general to have a low contribution to the reactivation of the landslide.

In the *Olteț basin*, rainfall thresholds have been investigated particularly in the sectors corresponding to the central parts of the Getic Subcarpathians and the Getic Piedmont (Jurchescu 2012; Jurchescu et al. 2013, 2014a, b, in prep.a). Nevertheless, in the conducted analyses, an enlargement was brought to what is commonly understood by threshold, i.e., "a minimum or maximum level of some quantity needed for a process to take place or a state to change" (White et al. 1996), whereas "a minimum threshold defines the lowest level below which a process does not occur" (Guzzetti et al. 2007). Rather than focusing on the identification of the minimum thresholds of single landslide processes, the authors proposed to investigate thresholds for *multiple–occurrence landslide events* (*MOLEs*) *of different magnitudes*. The data, compiled from official sources, like newspapers and reports of the local authorities, are characterized by incompleteness since restricted to landslides which caused damage. The limited landslide records covered the period 1998–2010. Still, within these limitations, the records were interpreted as a proxy for the unknown real data series. For each landslide entry, attached information included, among other characteristics, the date and location with the maximum precision provided by the source. Climatic information was assigned to each landslide record after firstly deciding the areas characteristic for each gauging station according to the Thiessen polygons and applying a relative correction to the rainfall data in order to account for snow accumulation as well as snowmelt, relevant for the winter and spring landslides. Hence, rainfall series were transformed into a series approximating water inputs into slopes.

Magnitude is strictly linked to the temporal component, and even more in case of MOLEs, leading to what is known as frequency–magnitude relationships. It is argued that at coarse resolutions (e.g., one year, one month), landslides are of the multiple–occurrence kind (temporal cluster of landslides), the severity of which can

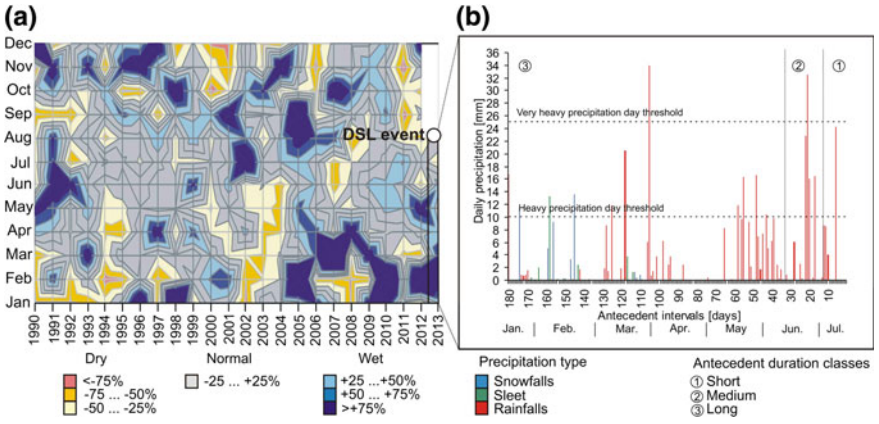

Fig. 32.11 Precipitation deviations over the operating period of the Varlaam rain gauge **a** and the evolution of daily precipitation type over the 180 days antecedent interval prior the Bâsca Mare–Viforâta landslide event (*DSL event* deep-seated landslide event) (after Micu et al. 2014a, b)

be expressed using specific measures [as mentioned by Crozier and Glade (1999), Crozier (2005), Rossi et al. (2010)].

The most widely employed method in expressing rainfall thresholds is the complementary use of two parameters. The most popular example is the intensity–duration (ID) threshold. In Romania, the application of such thresholds is limited by both the amount of historical landslide data available and its precision. In the case of the Olteț basin, the highest certainty found in the available data could be narrowed down to a monthly temporal resolution. Therefore, Jurchescu (2012) and Jurchescu et al. (2013, in prep.a) sought to adapt the tools used worldwide for identifying rainfall thresholds at a fine temporal scale (i.e., daily, hourly) to the coarser monthly scale. By interpreting monthly landslide events as MOLEs, it was argued that, in case of such multiple occurrence events, the analysis should be conducted after firstly differentiating among groups of maximum homogeneity, and one of the means to separate such groups would be magnitude. The number of landslides reported per month (L mo^{-1}) was one of the measures selected to express the magnitude of the events (in this case considered an a priori *magnitude*). Supported by these prerequisites, the studies propose the existence of several thresholds—for each of the different categories of magnitude of the MOLEs, thresholds for which the corresponding exceeding probabilities could be calculated.

Empirical rainfall thresholds are considered, of the types distinguished by Guzzetti et al. (2007): (i) *thresholds that use measurements of rainfall events* and (ii) *thresholds that consider antecedent conditions.* From the first category, the ID thresholds have been adapted to a monthly level by considering the monthly mean daily intensity (I_{mo}) and the monthly number of rainy days (D_{mo}) (Fig. 32.12). The minimum (usually 5 % probability of landslide expectancy) and maximum (usually 95 % probability) thresholds, widely plotted for, in general, single landslides,

between which several curves can point to different probabilities of the failure taking place (e.g. Crozier 1997; Glade 2000; Aleotti 2004; Crozier 2005), could be established, in case of monthly multiple landslide occurrences, separately for each particular magnitude. In Fig. 32.12a, the normalized monthly scaled ID data are plotted for all magnitude events. Lines were drawn visually in order to show how the minimum threshold evolves depending on the event's intensity. By introducing this magnitude differentiation, it was proved that what could have seemed a high dispersion in the population sample reveals in fact a relative order considering the high limitations which exist in the data. In Fig. 32.12b, the events of 2 L mo^{-1} were isolated in order to derive a minimum threshold for events of such intensity. The resulted equation is:

$$\mathrm{NI_{mo}} = 4.55 D_{\mathrm{mo}}^{-0.54} - 0.61 \tag{32.1}$$

where $\mathrm{NI_{mo}}$ = normalized monthly mean daily intensity and D_{mo} = monthly number of rainy days.

This threshold shows that with increasing number of rainy days per month, the minimum mean daily intensity necessary to trigger landslide events of a certain magnitude decreases.

From the category of thresholds that consider antecedent conditions, through the same transferring mechanism from hourly to monthly level, thresholds commonly defined as relations between antecedent rainfall and critical rainfall (Aleotti 2004) were translated into relations between antecedent monthly rainfall and rainfall of the event-month. Results are given in Fig. 32.13 using normalized variables. Similarly to Fig. 32.12, lines drawn arbitrarily in Fig. 32.13a reveal that the

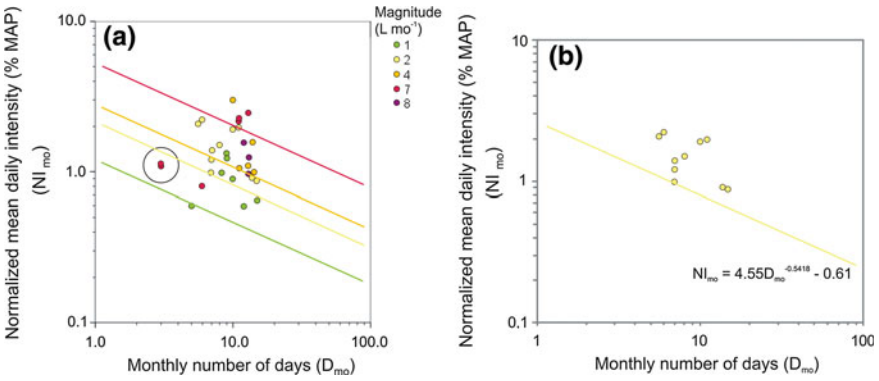

Fig. 32.12 **a** Rainfall events that have resulted in monthly multiple landslide occurrences of different magnitudes (number of landslides per month, L mo^{-1}) in the hilly area of the Olteț basin (1998–2010), for which the normalized monthly mean daily intensity ($\mathrm{NI_{mo}}$) and the monthly number of rainy days (D_{mo}) have been computed. *Lines* drawn manually indicate the minimum thresholds for different magnitude events. The *circle* delimits landslide cases considered outliers in relation to rainfall, pointing to another triggering factor. **b** Normalized $\mathrm{ID_{mo}}$ threshold for the occurrence of landslide events of magnitude 2 L mo^{-1} (Jurchescu et al. 2013)

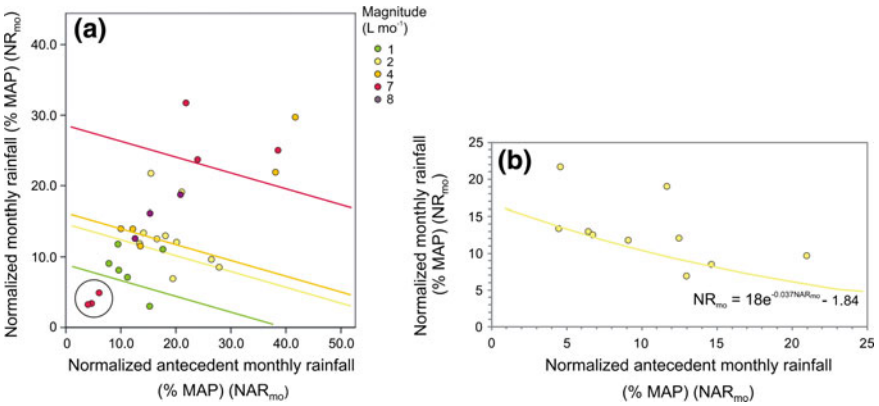

Fig. 32.13 **a** Rainfall events that have resulted in monthly multiple landslide occurrences of different magnitudes (number of landslides per month, L mo^{-1}) in the hilly area of the Olteț basin (1998–2010), for which the normalized monthly rainfall amounts (NR_{mo}) and the normalized antecedent one month rainfall (NAR_{mo}) have been computed. *Lines* drawn manually indicate the minimum thresholds for different magnitude events. The *circle* delimits landslide cases considered outliers in relation to rainfall, pointing to another triggering factor. **b** Rainfall threshold for the occurrence of landslide events of magnitude 2 L mo^{-1} (Jurchescu et al. 2013)

minimum amounts of rainfall needed to trigger an event vary with the magnitude expressed as the number of landslides. In Fig. 32.13b, the events of minimum 2 L mo^{-1} were separated to allow for computing the minimum threshold function. The equation was expressed as follows:

$$NR_{mo} = 18e^{-0.04NAR_{mo}} - 1.84 \quad (32.2)$$

where NR_{mo} = normalized rainfall of the event-month (%) and NAR_{mo} = normalized antecedent one month rainfall (%).

These findings of Jurchescu et al. (2013, in prep.a) are in agreement with conclusions formulated by Crozier (2005), Guzzetti et al. (2007) and Rossi et al. (2010).

The correlation—at different time resolutions (annual, monthly, daily)—between the temporal distribution of landslide events and the rainfall regime has also been addressed for particular cases of slope instability in the region, in view of producing landslide hazard scenarios (Jurchescu 2012; Jurchescu et al. 2014a, b, in prep.b, c). For these occasions, the specific relation between magnitude and frequency of the rainfall trigger was identified, based mainly on the general methodology developed by D'Ecclesiis et al. (1991) and Zêzere et al. (2004a, b). According to their assumptions, the triggering threshold is defined as the extreme couple amount–duration resulting from a statistical processing.

The goal at an annual scale consisted in determining critical annual rainfall necessary to explain landslide annual events and estimating the corresponding return period (RP) (Jurchescu 2012; Jurchescu et al. 2014a, b, in prep.b). Annual

multiple occurrence landslide events were found to correlate well with the ascending curves of the cumulated deviation of effective rainfall from the mean, as well as with years following at least another year with effective precipitation above mean. A comparative analysis of the intensities of MOLEs characteristic to the years 2005 and 2006, expressed in terms of reported damage, indicated a highly superior value for 2006 relative to 2005. The higher intensity of the 2006 event corresponds climatically to effective precipitation lower than in 2005, having values slightly above or even below mean (depending on the gauging station). However, looking at the effective rainfall of previous years, 2006 is highlighted as being the third consecutive year exceeding the climatic normal.

A rough estimation of the recurrence interval of wetness conditions necessary to produce an important annual MOLE was derived at a coarse temporal scale from the analysis of long-term variation in annual rainfall, as revealed by the polynomial curves. Thus, a cycle of landslide-abundant years mainly coincides with a cycle of rainfall excess and has a rough return period of 20 years. 2010—a recent year of precipitation and temperature extremes both in Romania and the Danube basin (Micu et al. 2013)—produced a large number of landslides in the Olteţ basin (over three damaging movements in most of the high susceptible municipalities). The temporal probability of the 2010-trigger was composed of: (i) the probability of a wet cycle (1/20) and (ii) the probability of a 2010-type of situation appearing within a wet cycle (1/4).

At a monthly scale, the analysis of landslide-triggering thresholds and its frequency zoomed into 2010 in order to identify the situation specific to the months April–May 2010 which had an important impact in terms of caused damage (Jurchescu 2012; Jurchescu et al. in prep.b). Eight reactivated landslides that resulted in damage were reported, mostly medium and deep-seated. The parameter chosen to best express the triggering effect of precipitation was represented by cumulative effective rainfall, based on its preliminary good correlation with monthly landslide events. Thus, for this particular scenario, the total rainfall over the October 2009–May 2010 interval (i.e., considering an antecedent period of 6 months) exceeded 490 mm in the north (Polovragi gauging station, 53 years RP) and 360 mm in the south (Târgu Logreşti gauging station, 89 years RP) (Jurchescu et al. 2014b).

Finally, the landslide cases (medium and deep-seated) reactivated between March 10 and 13, 2006 on the territory of a municipality in the Getic Subcarpathian hills were analyzed at a daily timescale in correlation with the rainfall–snowmelt pattern generating it. The threshold was calculated in terms of total water supplied to the slopes. Since limited daily data was available (i.e., only on rainfall and temperature but not on snow cover), a correction was applied to adjust the raw rainfall series when snow-related phenomena were present (Jurchescu et al. 2014a, in prep.c). The results showed that a relevant water amount of 60–68 mm accumulated over a short-lasting period of 7–8 days (i.e., ,considering 4 antecedent days), having a return period of 25–26 years. This amount–duration threshold and its corresponding return period are portrayed in Fig. 32.14. Nevertheless, a longer antecedent period of 120 days prior to the event could not be neglected either,

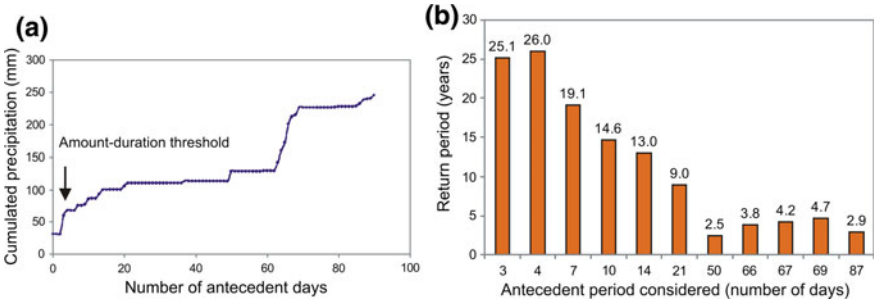

Fig. 32.14 **a** Identification of the water input threshold triggering the multiple landslide events of March 10–13, 2006 in the Alunu municipality of the Olteț basin. **b** The return period of 26 years corresponding to this water threshold in comparison to those of several other cumulated water amounts (Jurchescu et al. 2014a)

leading to a total amount of water reaching the soil of more than 377 mm (antecedent and event water input) which corresponds to a return period of 5 years (Jurchescu et al. 2014a).

The above-detailed results may lead to the obtaining of landslide hazard maps. Such an example is given by the landslides hazard map for the municipality of Breaza (Fig. 32.15), which represents different states of probability for deep-seated landslides. Bayes theory was used to calculate the posterior probability for such a landslide to occur according to different precipitations values (Şandric 2008). From left to right, the occurence probability of a deep-seated landslide of high magnitude is increasing (from yellow to red) alongside the precipitation that reaches the terrain surface. A precipitation step of 20 mm/24 h is shown in the left medallion, further on leading to 100 mm/24 h on the last medallion from the right (Şandric 2008).

Complementary to the geomechanical control and predisposition, the climate is considered as well both preparing and triggering factor within a rock fall hazard assessment. With increasing altitude, seasonal frost enlarges its duration and magnitude and is expected to impact more on rock fracturing by both macrogelivation and ice segregation. Such a situation occurred in April 2012 on the Transfăgărăşan Road, when two rock fall events followed the ending of the seasonal freezing (Fig. 32.16). On April 16, the fall of two boulders summing 560 m^3 was recorded near Arefu village, at an altitude of 1250 m, while several days later a similar event occurred close to the highest sector of the road, at approximately 1950 m elevation (close to the Bâlea Lake touristic station). This delay could reflect the thermal behavior of rock, which reacts to the differences in air between the two altitudinal floors. Thawing of interstitial and inter-joints ice as well as meltwater enhanced the enlargement of joint spaces and led to rock detachment. Continuous measurements of rock temperature that were performed at the time in the Bâlea glacial cirque show that there is also a delay between the end of the long interval of subzero temperatures and the two rockfalls. During the 2 weeks preceding the event, a sequence of diurnal freeze-thaw oscillations were observed in rock,

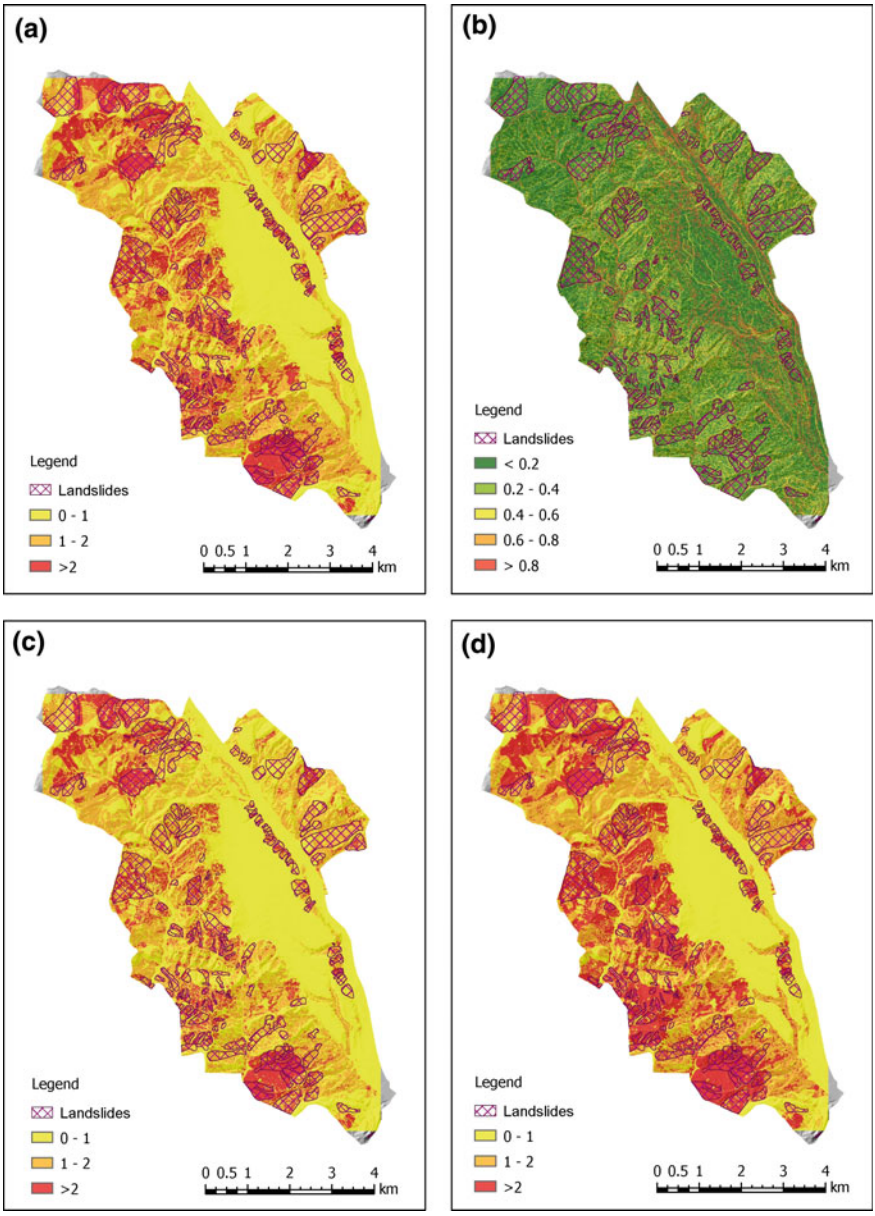

Fig. 32.15 Landslide hazard maps for the region of the town Breaza

summing 260 positive hours degrees. Moreover, with only four days before the event, rock temperature showed a significant increase, covering 136 positive hours degrees (Fig. 32.16). This thermal evolution sustains the implication of seasonal thawing and of associated processes in the triggering of the two rockfalls.

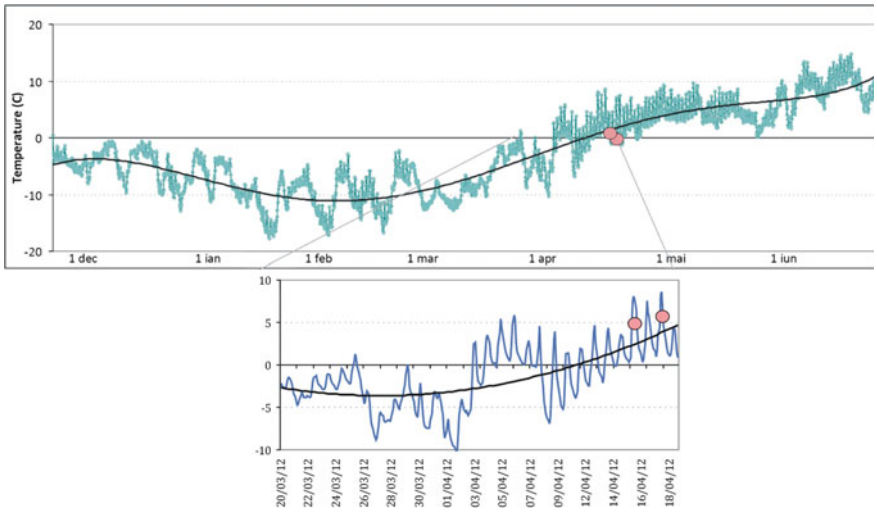

Fig. 32.16 Seasonal frost in 2011–2012 and thermal evolution of rock surface in the Bâlea glacial cirque before the triggering of two rockfalls on the Transfăgărăşan road in April 2012 (*pink dots* represent the days of events occurrence)

During summer months, rockfalls are induced by intense short duration rainfalls when their occurrence is associated with debris flows. According to the rockfall inventory for the period 2004–2009, the highest frequency of rockfall events in the Olt and Lotru Valleys is related with transition seasons, January–March and October–November, respectively, which may differ as duration depending on the altitude (Fig. 32.17). The occurrence is again highly connected to the exit from the seasonal freeze-thaw cycle and with the snow melting interval, and it sustains our

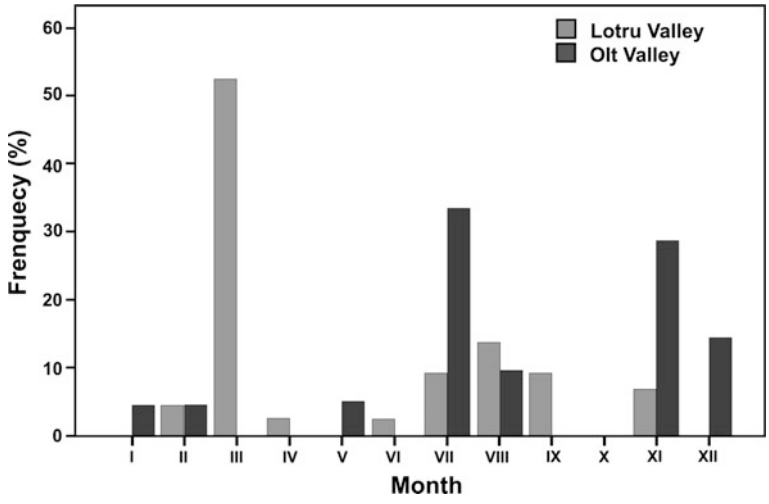

Fig. 32.17 Monthly frequency of rockfalls in Olt and Lotru valleys (Ilinca 2009)

previous example by validating it in a different location and using higher number of events. In July–September a high frequency is also recorded, associated with heavy rainfall from this particular period of the year (Ilinca 2010).

When evaluating frequency and intensity in relation to consequent damages of rockfalls on the roads, it is estimated that the Olt Gorge is by far the Romanian Carpathians mountain corridor the most affected by rockfall events, as it borders one of the most used roads in Romania—National Road 7/European Road 81. Tens to hundreds of rockfalls occur yearly although the official records are much smaller. This difference is due to the monitoring and registering system of the road administrator (Romanian National Company of Motorways and National Roads) that only record the major events that affect the traffic. For example, the rockfall events with small magnitude (often below 1 m^3) that do not reach the road are usually not included in the official records (Ilinca 2010). In the last decades, major rockfall events occurred, but by far the most catastrophic rockfall had been occur on December 28, 2005 in the northern part of the Olt Gorge. The event involved 10,000 m^3 of rocks and debris detached from the slope, which blocked both the European Road 81 and the railway; the road remained closed for two weeks (Ilinca 2009). Another major event took place at 207 km, where 1000 m^3 of large rocks blocked the road. The consequences of rockfalls in the above-described transport corridor implied 6 injured persons, 7 damaged cars and damages as well for the roads and railways between the years 2002 and 2012 (Ilinca and Varariu 2013). In the last years there infrastructure works have been made along E81 road, consisting mainly in fitting flexible ring net barriers in order to prevent and minimize the rockfalls effects.

The Transfăgărăşan Road (DN 7C) is only functional between July and October, because of the expensive maintenance during winter. Nevertheless, this also prevents additional direct and indirect damages attributed to high magnitude rockfalls occurring in transition seasons, but cannot prevent the occurrence of such events in summer, when they are associated to heavy precipitations. Between 2008 and 2013 only, a cumulated mass of more than 12,000 m^3 following rockfalls had to be removed from the road.

Landslide Risk Analysis

Exposure, Vulnerability, and Risk Assessment to Landslides

In order to estimate the probability of damage to individuals, population, property and the environment due to the occurrence of landslides, the risk must be analyzed using a stepwise procedure: hazard identification, hazard assessment, inventory of elements at risk and exposure, vulnerability assessment, and risk estimation (Fell et al. 2005; Van Westen et al. 2006). As hazard identification and assessment have been discussed previously, in this section exposure, vulnerability, and risk

assessment are shortly analyzed and then different recent methodological approaches and solutions developed or applied nationally are examined. Lastly, issues regarding uncertainty analysis in vulnerability and risk assessment are considered.

Exposure

Exposure is defined as the totality of people, property, systems, or other elements present in hazard zones that are thereby subject to potential losses (UN-ISDR 2004). In contrast to physical vulnerability, which represents the proportion of the total value of the element likely to be impacted by a landslides with a given magnitude and intensity, exposure shows only which elements are present and thus susceptible of being adversely affected. A comprehensive exposure analysis takes into account not only the extent of the landslide and its frequency but also the spatial and temporal probability that an element at risk (static or dynamic) is within the landslide path. In practice, the calculation of exposure depends mostly on the scale of analysis and landslide type and it can vary from individual elements (buildings and people inside buildings exposed to rockfalls, Corominas et al. 2005; Corominas and Mavrouli 2011; Agliardi et al. 2009), pixel level (people, linear infrastructure and buildings exposed to debris flow and shallow landslides, Jaiswal et al. 2011; Zêzere et al. 2008), up to municipal level (Pellicani et al. 2014). Fell et al. (2005) and Corominas et al. (2014) propose different approaches for computing exposure of static and dynamic elements at risk taking into account multiple scenarios.

Relatively numerous studies evaluate exposure by spatially overlaying a set of elements at risk with landslide susceptibility zones, the result being considered as an intermediate step toward a complete risk assessment. In Romania, Mărgărint et al. (2013a, b) generated an exposure map for Huşi town (north-east Romania) using a statistical model (logistic regression) to calculate the spatial probability of landslide occurrence, and urban planning maps for extracting the built-up areas and linear infrastructure. Although the susceptibility is not dynamically analyzed, the authors show the multi-temporal expansion of the urban area toward the areas with high and very high susceptibility.

Information on elements at risk can be collected using various techniques according to the scope, scale of analysis, and resource availability. Mihai and Săvulescu (2006) combined field mapping, GPS measurements, photodocumentation, desktop mapping, and aerial image interpretation for developing a geomorphic hazards and assets database in a GIS environment (with detailed information about street and urban utilities network, buildings, engineering works, critical facilities), for Predeal town. The authors recognize the sources of error stemming from input data, measurements and mapping of the elements at risk as well as landslide and erosional processes. For regional or national scale analyses, the elements at risk can be categorized or clustered in wards, districts, municipalities or counties, and the data is mostly collected from censuses and national or regional authorities.

Lastly, it is worth noting that although within the disaster risk community (as opposed to global environmental change; see Turner et al. 2003) exposure is considered to be a separate component of the risk equation, the location of an element at risk with respect to a landslide body is used as physical vulnerability indicator due to the fact that often the interposing objects between the landslide process and the element at risk (which can influence the spatial probability of the former) are not included in the hazard modeling (Godfrey et al. 2015).

Vulnerability

Vulnerability is a term with many different connotations depending mostly on the research orientation. Two main schools and directions are preeminent in the literature: (1) the engineering (natural science) perspective, where vulnerability is "the degree of loss to a given element or set of elements at risk resulting from the occurrence of a hazard of a given magnitude in a given area, expressed as a percentage of loss (between 0: no damage, to 1: total damage)" (Varnes 1984); (2) the social perspective, where vulnerability is related with the variation in exposure (Wisner et al. 2004) or in the capacity of people to cope with the hazard (Adger 2000; Cutter et al. 2003). Blaikie et al. (1994) define vulnerability as the "characteristics of a person or group in terms of their capacity to anticipate, cope with, resist against, and recover from the impact of natural hazards." In the former approach, the role of the community in altering the outcomes of hazard impact are lessened or neglected, whereas in the latter, the human system plays a central role (Brooks 2003). Birkmann (2006) give a comprehensive overview of the conceptual models and main perspectives from which it is generally addressed.

The number of theoretical and practical studies dealing with natural hazard vulnerability has increased in the last decades in Romania both for social as well as physical assessments (for a short overview see Tanislav et al. 2009; Sorocovschi 2007; Stângă and Rusu 2006); however, not many are specifically looking at landslide hazards and even fewer are reported in the international literature. Socioeconomic vulnerability to landslides has been evaluated for the Slănic Prahova municipality (south-east Romania) using a model that includes indicators characterizing the demographic, social, and economic setting as well as indicators representing the degree of preparedness, effectiveness of the response and capacity to recover (Eidsvig et al. 2014). The results showed that, in comparison with other five case studies in Europe, Slănic town scored high for all components except the demographic and social ones, with particularly high scores on the economic as well as the preparedness response and recovery components. Although the results are reasonable compared with field observations, the method can be improved by using disaster impact data and by increasing the number of case studies.

Another indicator-based approach was proposed by Stângă and Grozavu (2012) for the Tutova Hills rural region. The model takes into account five categories of variables (rural habitat, demographic features, agriculture, environmental quality and emergency situations), from which a set of indicators have been mathematically

expressed and standardized in order to calculate a general vulnerability index (GVI). The selected indicators are: total population, age groups structure, weight of arable land on slopes, weight of land under forestry, and distance from the nearest town. The GVI was calculated based on the geometric mean of the above-mentioned indicators. For further use in risk assessment and mitigation, the authors suggest the integration of hazard information in the model.

Functional vulnerability of road infrastructure has been assessed at regional scale in the Buzău County (south-east Romania) in a study performed within the FP7 IncREO Project (Increasing Resilience through Earth Observation, InCREO, 2014). The scope was to evaluate the villages' propensity of being isolated by simulating the effect of a blockade for segments of rural roads connecting settlements with more than 1000 inhabitants. The resulting vulnerability map differentiates between villages completely isolated and those which are served by alternative connecting road infrastructure (case in which the detour distance is indicated).

Physical vulnerability of buildings to landslides (and floods) was assessed at local scale in the Nehoiu Valley (Buzău County, south-east Romania) using an indicator based approach (Godfrey et al. 2015). The methodology integrated multi-criteria spatial evaluation and expert knowledge for obtaining a vulnerability index (VI) used to calibrate transferred vulnerability curves relevant for the investigated area. Although the model is particularly useful in areas where no or limited information exists, it relies heavily on the quality and availability of vulnerability curves, and the expert knowledge input. In order to improve the model, the authors acknowledge the need to include more damage information for the validation of the results.

For future quantitative assessments, the results obtained hitherto in modeling seismic vulnerability (e.g., fragility curves, parameterization of vulnerability, elements at risk characterization, inventories, etc.) (Enulescu 2007; Lungu et al. 2007; Sandi et al. 2008; Perrault et al. 2013), can potentially be adapted and used for landslide vulnerability assessment.

Risk

In the everyday use of language the term "risk" emphasizes the chance or possibility of an outcome, as for example "the risk of an accident," whereas in technical settings it's meaning is focused on the consequences (in terms of "potential losses") due to a particular cause, in space and time. The UN International Strategy for Disaster Reduction (UN-ISDR 2009) defines risk as being "*the combination of the probability of an event and its negative consequences*" (see also ISO/IEC Guide 73). Landslide risk assessment represents a methodology used to determine the nature and extent of risk by analyzing the potential hazards (i.e., mass movements) and evaluating internal or external vulnerabilities of exposed element at risk that together could result in loss of life, injury, economic loss, services disruption and/or environmental damage.

In qualitative or semiquantitative assessments, risk is simply defined as a function of hazard, vulnerability, and the amount of elements at risk, whereas in quantitative studies the above-mentioned components are associated with a spatial or temporal probability. Several studies give an overview of the various methods of landslide risk assessment and their applicability at different spatial scales (Dai et al. 2002; Fell et al. 2005; Van Westen et al. 2006; Corominas et al. 2014).

Systematic research on mass movement processes in Romania started as early as the twentieth century; however, only recently studies concentrated on developing qualitative and (semi) quantitative methodologies for assessing the hazard and its probability of damage. The main body of work focuses on susceptibility and hazard assessment meanwhile there is still a great need for vulnerability, exposure, and especially risk assessments. Nevertheless, some results are reported in the literature at local, regional as well as European level. Landslide risk for individual buildings in Cornu locality (Prahova Subcarpathians) was assessed in a recent study by Armaş (2014). The spatial probability of landslides was calculated using a bivariate Landslide Susceptibility Index (LSI), their frequency was assessed based on historic records and local interviews, and vulnerability of buildings was defined as damage percentage evaluated subjectively as a function of building size and construction type. Finally, the risk was calculated by multiplying the spatial probability of landslides with vulnerability value for each building and summing up the losses for the selected 10-year return period. The present study proposes a semiquantitative methodology for risk assessment, given the challenge (among other) of collecting data on landslide intensity and consequent damages used to compute the buildings' vulnerability.

A similar approach for assessing landslide risk was proposed by Micu (2011) for settlements located in the Muscel Basin (Curvature Subcarpathians); the risk was estimated qualitatively as a function of hazard (bivariate statistical analysis of spatial probability and frequency–magnitude relationship analysis) and vulnerability (expressed as potential damage level); the latter was estimated based on expert knowledge using a set of indicators relevant for the exposed buildings, roads, electricity network, and land use types (presence/absence of insurance or subventions, material of construction, maintenance). Starting with the example of the analyzed case study, the author discussed the appropriate methodology versus scale of analysis, as well as the challenges faced in the implementation of a complete risk management process in the Romanian context.

Although the creation and implementation of "*landslide risk maps*" at local scale (practically, susceptibility maps) is legally binding (Law no. 575/2001 on the approval of national territory planning, Section V—Natural risk areas), a nationwide landslide risk assessment is still missing due to multiple reasons among which the lack of available and readily accessible data, the complexity of the analyzed physical processes and of their interactions with the human environment are notable. First steps in the direction of improving this state-of-the art have been made by Bălteanu et al. (2010) who aimed at creating a nationwide spatial assessment of landslide susceptibility (as a preliminary phase for hazard and risk

studies), emphasizing Romania's position on the European landslide hazard and risk "hotspots" map (Jaedicke et al. 2014).

Uncertainties Within Landslide Susceptibility–Risk Studies

Within any landslide hazard or risk study, there are inherent uncertainties, more or less addressed in the literature. They might arise (as aleatory or epistemic) at all stages (from process evaluation to risk analysis) and they have the potential to propagate all throughout the evaluation.

Dealing with Uncertainty in Susceptibility and Hazard Assessments

In landslide susceptibility and hazard assessment, the uncertainty can be defined as the degree in lack of information about a certain measured value (Karssenberg 2002), which can be for example the location of a landslide, the classification used for landslide typology or the evolution of a landslide as a geomorphic process, etc. Usually, the uncertainty is expressed in values between 0 and 1 and, in general it is associated with the probability (Karssenberg 2002).

Uncertainty sources in landslides susceptibility analyses are very diverse: location of data collected in the field, classification systems for land use and land cover, numeric and graphic data available at different scales, mapping errors, etc. Uncertainty also propagates from one factor to another (Goodchild 1980; Fisher 1998; Heuvelink 1998; Karssenberg 2002) in the process of landslides modeling. For example: a certain digital elevation model is used to generate slope and the generated slope is used for landslides susceptibility mapping. The same example applies to any other derivatives from digital elevation models and any other products obtained with data based on digital elevation models, like evapotranspiration based on solar radiation, etc. (Karssenberg 2002). The uncertainty from these will further propagate in the final susceptibility map. Nominal and categorical data is also subjective to uncertainties, but in this case the uncertainty is related to the boundaries between neighboring polygons and to the proper identification of the polygon. For example the identification of the correct location of the lithological unit or the identification of the correct location of the land cover type, etc. (Karssenberg 2002). In Fig. 32.18 a landslides susceptibility map with uncertainty propagation is presented for the town of Breaza (Curvature Subcarpathians). The map presents not only a fixed probability value, but a range of values containing the minimum, maximum, average and the standard deviation for the probability values. In this case study only one uncertainty source has been taken into consideration, i.e., the digital elevation model. A DEM with a spatial resolution of 2.5 m was

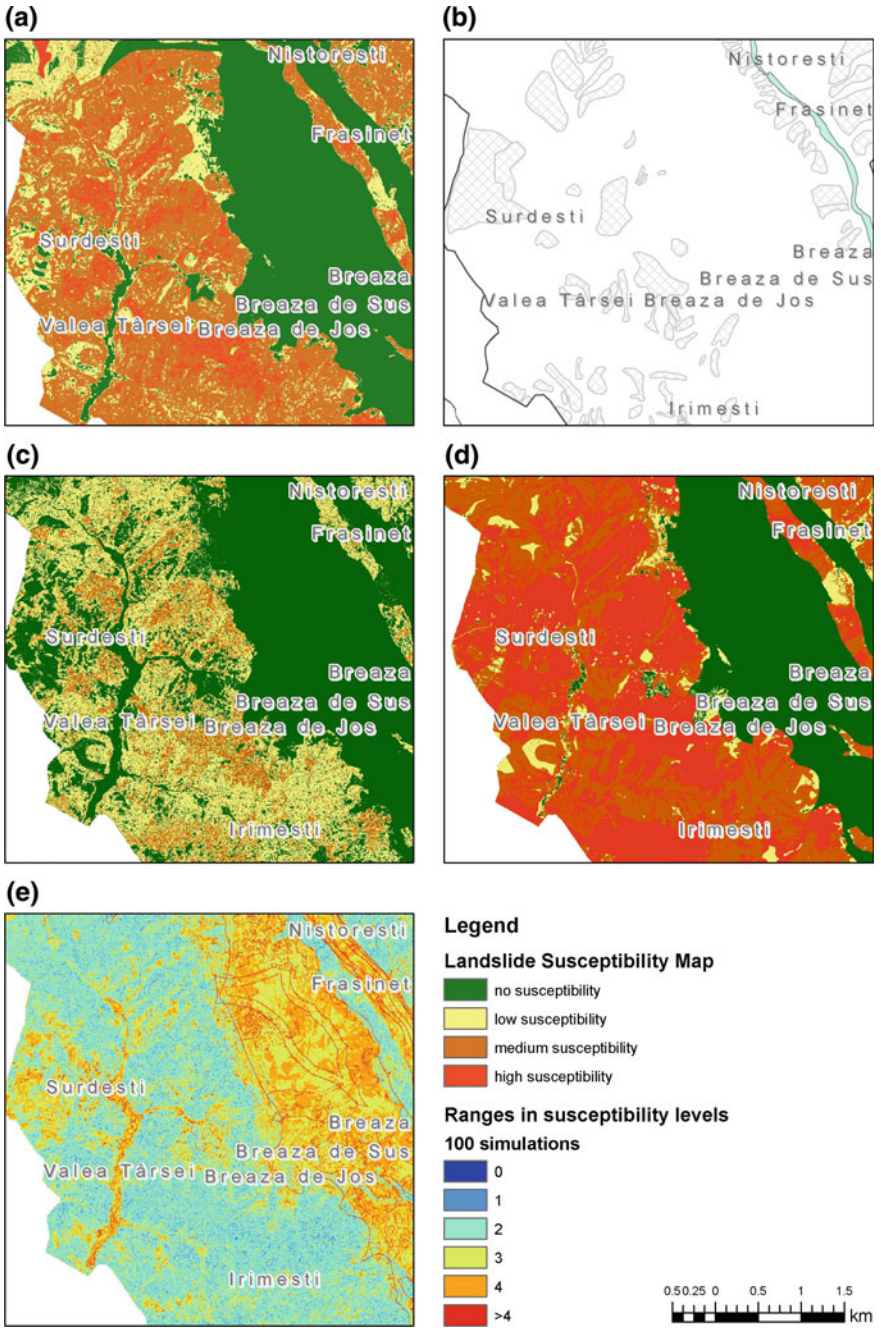

Fig. 32.18 Landslide susceptibility maps, Breaza town, Curvature Carpathians. **a** Mean susceptibility. **b** Present day landslides. **c** Minimum susceptibility. **d** Maximum susceptibility. **e** Standard deviation of susceptibility per pixel

available and in the mean time, a set of elevation points equally distributed on the entire area were measured (DGPS). Based on the elevation points, the accuracy of the DEM was calculated. The error was assessed based on the Kolmogorov–Smirnov test for normal distribution and for a p value higher than 0.05, the distribution was considered normal (Şandric 2008). Using the standard deviation of 3.67 and a mean value 4.74, noise has been generated and added to the existent DEM dataset. A number of 300 simulations were performed, thus 300 new DEMs have been obtained (Şandric 2008). For each new DEM, all the terrain parameters like slope, curvature, topographic wetness index, etc., were calculated. For each simulation a new susceptibility map was created based on the parameters derived from the newly generated DEM. In the final step the minimum, maximum, average and the standard deviation for each pixel have been calculated leading to the final susceptibility maps with uncertainty propagation (Şandric 2008).

Figure 32.18 (Şandric 2015, submitted) presents not just one landslide susceptibility map, but a set of maps with the lower and upper boundaries of the *per-pixel* susceptibility. This type of maps is offering to the decision-makers additional information (compared with just one static susceptibility map) on the range in which the probability for landslides occurrences is varying, providing an insight into the different areas' extents that could be potentially affected by landslides in the future.

Dealing with Uncertainty in Vulnerability and Risk Assessment

As the development of robust landslide risk management policies and decision-making frameworks relies heavily "on a better understanding and on great sophistication, transparency and rigor in the application of science" (Dai et al. 2002), experts dedicate more time and resources to the investigation of uncertainty and its consequent effects. However, uncertainty in risk analysis is not a new field of investigation and a great body of work has been dedicated to tackle this issue (as an illustration, see Rowe 1994; Rougier et al. 2013; Flage et al. 2014). In a statistical sense, uncertainty can be defined as the difference between the measured value of some quantity and its actual "true" value. Two types of uncertainty are generally considered in landslide risk assessment: aleatory uncertainty which originates from "real" variability or randomness in the known (or observable) processes or phenomena; and epistemic uncertainty which is presumed to be caused by our limited knowledge about fundamental processes or lack of data (Paté-Cornell 1996; Nadim et al. 2005; Corominas et al. 2014).

Uncertainty can be rooted in a number of stages in the risk analysis process, including—but not bounded to: lack of–, limited or unreliable landslide inventories, unidentified or unknown interactions between and variability (spatial and temporal) of triggering and preparatory geo-factors, resolution of DEM, estimation of

temporal probability, runout model calibration, calculation of landslide intensity, lack of-, limited- or unreliable information on elements at risk (distribution, value, characteristics, etc.), lack of-, limited or unreliable past damage information, model assumptions and simplifications, interpretation of results (map classifications, etc.), and expert knowledge elicitation in all process stages. Thus, uncertainty can generally be associated with input data/data, model/procedure and output (Bell and Glade 2004; Glade 2003; Eidsvig et al. 2014).

Depending on the available time/resources and scope of analysis, uncertainty can be modeled or quantified using a number of methods, including: Bayesian analysis —a standard procedure for quantifying input/data analysis (Lee et al. 2002), stochastic models (Monte Carlo simulations, First Order Second Moment) (Uzielli et al. 2008; Mavrouli 2014; Tate 2012), scenario analysis (Mazzorana et al. 2009; Li et al. 2010) and expert elicitation (Winter et al. 2014).

Uncertainty analysis in the Romanian literature is mostly applied in hazard assessments and few contributions are recorded so far in vulnerability or risk assessments. According to the European Commission Guidelines (EC 2010), "*risk analysis should take into account uncertainties which need to be understood in order to communicate the output results effectively.*" Indeed, the most important goal in developing tools for measuring uncertainty is their use in conveying a more transparent, clear and reliable risk analysis output that can be successfully applied in decision-making processes and risk reduction strategies.

Conclusions

The fundamental and applied importance of mass movements studies in Romania have been recognized since the beginning of the twentieth century. Numerous studies indicate the proneness of the Romanian territory to different types of mass movements, as well as areas with different probability of future landslide occurrence in both space and time. Landslide risk assessment represents an important topic in applied geomorphic studies. As one of Europe's most active landslide hotspots, Romania still lacks an appropriate legislative framework for landslide risk assessment and management. Moreover, the data required for such studies, even though largely available, is scattered among a wide range of stakeholders and the lack of harmonized approaches (in terms of language, storage, handling protocols or guidelines, etc.) delays time-effective approaches. The development of proper spatial decision support systems aiming at landslide risk reduction will definitely contribute to the optimization of the organizational framework, establishing the stakeholders' proper levels of implication in hazard identification, risk analysis, risks prioritization and, as a consequence, the adaptation of authorities' response.

An overall literature analysis outlines an increasing number of studies focusing on landslide susceptibility. Areas like the Curvature Subcarpathians, Getic Subcarpathians and Piedmont or the Moldavian plateau are well described through qualitative, semiquantitative and quantitative approaches. The high overall potential

of the Carpathians in terms of rockfalls or debris flows is not very well described, deterministic runout models lacking almost entirely. There are progresses made during the last years (studies focusing mainly on trans-Carpathian roads), but regional approaches are still needed. Especially in complex environments, like the one of the Subcarpathian hills, expert judgment is often used in combination with bivariate or multivariate statistical analysis in order to train and validate susceptibility models, aiming to allow a proper regional generalization. Larger and more comprehensive landslide inventories are developed as a support for susceptibility analysis, and by comprising information related to the occurrence moment, some empirical or more detailed assumptions concerning certain triggering thresholds may be validated. Landslide hazard assessment involves scenarios at different return periods, and beyond any doubt one should assume that within the following 10–50–100 years, at least the climate and the land use classes may suffer (more or less important) changes. Starting with this assumption, dynamic risk assessment (based on the above-mentioned changes) should be compared with static risk studies (assuming no changes).

An assessment of the degree of damage that may result from the occurrence of landslides of a given type and intensity in the future cannot be performed in the absence of reliable, up to date and accessible historical damage inventory. This implies that for each recorder hazard event, the inventory must contain at least information about the intensity (or/and magnitude) of the process and a measure of its resulting consequences (e.g., casualties, number of buildings destroyed, monetary losses, etc.). In Romania, it is often the case that if such information exist it is: (a) incomplete, (b) aggregated at regional or municipal level with no information about the spatial distribution of losses or afflictions, or (c) inaccessible. Considering the Romanian social, economic, politic and institutional context, physical vulnerability assessments must be complemented with studies dealing with other vulnerability dimensions in order to reflect fully the propensity to damage. This is especially true for local scale studies where communities are compelled to use alternative methods of coping with the threat than those offered by the administrative and legislative framework. Overall, it can be noted that there is a lack of landslide vulnerability studies in comparison with susceptibility and hazard at local, regional, as well as local scales.

Landslide exposure studies in Romania are scarce. However, given they are less ambitious in scope (in comparison with risk) and therefore less data demanding, they can be easier applied at regional as well as local scale. A qualitative exposure analysis can satisfactorily give information about the expected losses in the case of a landslide event (in numbers, monetary terms, etc.) by using the spatial probability of landslides and elements at risk information. Subsequently, this information can be improved by assigning temporal probability and intensity values to the landslide events. Thus, reliable exposure maps represent a valid tool for landslide risk management, especially because they easily allow for changes (e.g., in urban development and inflation) to be incorporated in the study.

Uncertainty analysis generally relates to quantitative (probabilistic) landslide risk assessments. The challenges faced when performing such a task were

acknowledges (non-exhaustively) in this chapter and are subject of much scientific debate. However, prior to the selection of the most appropriate methodology, experts must identify the scope and usefulness of such analysis in relation to the end users. For the former, uncertainty (including sensitivity) analysis is mandatory for conveying methodological soundness and transparency followed by the acceptance of research findings. For the latter, uncertainty analysis can support the decision-making processes, given the clear communication of scientific results and their limitations, as well as to investigate into future challenges like environmental and demographic changes.

It is important to recognize the substantial potential for the development of landslide hazard and risk studies, however, the Romanian legislative and institutional framework hinder the immediate use and implementation of risk information in spatial planning and decision-making. The top-down approach used in disaster risk management impedes the implementation of potential advancements at local scale (e.g., results of research projects, institutional initiatives, involvement of communities, etc.) case in which the efficient use of scientific results is diminished.

A synthesis of the uncertainties that might arise within any landslide risk study emphasizes that consecutively, landslide susceptibility, hazard and risk assessments suffer from the uncertainties of the original input data which are propagating within the analysis leading to a (relative) final map. There are still questions that have to be addressed (Micu et al. 2015 in prep.): which is the best way to quantify the uncertainties within the input data; are the uncertainties changing from a data-rich to a data-scarce environment; in which way do they propagate inside hazard or risk scenarios; how can they be quantified and visualized within the final map?

All together, there is a stressed need for the development of a modern risk culture. Risk management, risk communication or governance should be developed within the cooperation of a broad spectrum of stakeholders, including executives, experts and moreover end users, as emphasized within international governance or applicative research frameworks like the former EU's FPs, HyogoFA or Horizon 2020.

Acknowledgments Part of the results presented within this chapter were supported by the European Project FP-7 CHANGES (Grant Agreement No. 263953) and by the grants financed by the Romanian Ministry of Education, CNCS–UEFISCDI, project numbers PN II-RU-PD-2010-118, PN II-RU-PD-2013-3-0624 and TD 293.

References

Adger N (2000) Institutional adaptation to environmental risk under the transition in Vietnam. Ann Assoc Am Geogr 90(4):738–758

Agliardi F, Crosta G, Frattini P (2009) Integrating rockfall risk assessment and countermeasure design by modeling rechniques. NHESS 9:1059–1073

Aleotti P (2004) A warning system for rainfall-induced shallow failures. Eng Geol 73:247–265

Aleotti P, Chowdhury RN (1999) Landslide hazard assessment: summary review and new perspectives. Bull Eng Geol Environ 58:21–44

Armaş I (2011) Weights of evidence method for landslide susceptibility mapping. Prahova Subcarpathians, Romania. Nat Hazards 60:937–950
Armaş I (2012) An analytic multicriteria hierarchical approach to assess landslide vulnerability, case study: Cornu village, Subcarpathian Prahova Valley/Romania. Z für Geomorphol 55: 209–229
Armaş I (2014) Diagnosis of landslide risk for individual buildings: insights from Prahova Subcarpathians, Romania. Environ Earth Sci 71:4637–4646
Bălteanu D (1970) Morfodinamica porniturilor de teren pe Valea Apostului (Munţii Buzăului). SCGGG-Geogr XVII:2 (in Romanian)
Bălteanu D (1980) Măsurători asupra unor procese de creep în perimetrul în perimetrul Staţiunii de Cercetări Geografice Pătârlagele. SCGGG-Geogr XVII (in Romanian)
Bălteanu D (1983) Experimentul de teren în geomorfologie. Edit. Academiei Române, Bucureşti (in Romanian)
Bălteanu D, Constantin M (1998) Valley damming by landslides in the Buzău Subcarpathians. Analele Universităţii din Oradea, Ser. Geografie-Geomorfologie VIII(A):33–38
Bălteanu D, Micu M (2009) Landslide investigation: from morphodynamic mapping to hazard assessment. A case study in the Romanian Subcarpathians, muscel catchment. In: Malet J-Ph, Remaitre A, Bogaard T (eds) Landslide processes. From geomorphologic mapping to dynamic modelling. CERG Editions, Strasbourg, pp 235–241
Bălteanu D, Micu M (2012) Morphodynamics of the Chirleşti mudflow (Buzău mountains). Rom J Geogr 56(2)
Bălteanu D, Chendeş V, Sima M, Enciu P (2010) A country-wide spatial assessment of landslide susceptibility in Romania. Geomorphology, Special Issue "Recent advances in landslide investigation" 124(3–4):102–112
Bell R, Glade T (2004) Landslide risk analysis for Bíldudalur, NW-Iceland. Nat Hazard Earth Syst Sci 4:1–15
Birkmann J (2006) Indicators and criteria for measuring vulnerability: theoretical basis and requirements. In: Birkmann J (ed) Measuring vulnerability to natural hazards towards disaster resilient societies. United Nations University, Tokyo, pp 55–77
Blaikie P, Cannon T, Davis I, Wisner B (1994) At risk—natural hazards, people's vulnerability, and disasters. Routledge, London
Boengiu S, Licurici M, Marinescu E (2008) Landscape changes induced by the mining activity at the contact between the Olteţ Piedmont and Gorj Subcarpathians. GIS applications. Bull Geol Soc Greece XLII(II):74–81
Boengiu S, Török-Oance M, Vîlcea C (2013) Deep-seated landslides of Seciurile (Getic Piedmont, Romania) and its implication for the settlement. In: Margottini C, Canuti P, Sassa K (eds) Landslide science and practice. Social and economic impact and policies, vol 7. Springer, Berlin-Heidelberg, pp 113–119
Brooks N (2003) Vulnerability, risk and adaptation: a conceptual framework. http://www.gsdrc.org/go/display&type=Document&id=3979, pp 1–20. Accessed 7 Nov 2014
Bunce CM (2008) Risk estimation for railways exposed to landslides. PhD thesis, University of Alberta, Edmonton, Canada
Cascini L (2008) Applicability of landslide susceptibility and hazard zoning at different scales. Eng Geol 102:164–177
Cazacu GB, Draghici G (2011) Identificarea şi determinarea hazardelor naturale – alunecarea de la Seimeni. Revista Română de inginerie civilă 2 (in Romanian)
Chitu Z, Sandric I, Mihai B, Savulescu I (2009) Evaluate Landslide Susceptibility using Statistical Multivariate Methods: A case-study in the Prahova Subcarpathians, Romania, In: Malet JP, Remaitre A, Borgaard T (Eds) Landslide Processes:From Geological Mapping to Dynamic Modelling, Editions du CERG, Strasbourg, pp. 265–270
Chiţu Z (2010) Predicţia spaţio-temporală a hazardului la alunecări de teren utilizând tehnici S.I.G. Studiu de caz arealul subcarpatic dintre Valea Prahovei şi Valea Ialomiţei. Manuscript PhD thesis, University of Bucharest (in Romanian)

Chiţu Z, Istrate A, Adler MJ, Şandric I, Olariu B, Mihai B (2014) Comparative study of the methods for assessing landslide susceptibility in Ialomiţa Subcarpathians, Romania. In: Engineering geology for society and territory, IAEG XII congress volumes. Springer, ISBN 978-3-319-10303-7

Chowdhury R, Flentje P (2004) Uncertainties in rainfall-induced landslide hazard. Q J Eng GeolHydrogeol 35:61–70

Constantin M, Trandafir AC, Jurchescu MC, Ciupitu D (2010) Morphology and environmental impact of the Colţi-Aluniş landslide (Curvature Carpathians), Romania. Environ Earth Sci 59(7):1569–1578

Constantin M, Bednarik M, Jurchescu MC, Vlaicu M (2011) Landslide susceptibility assessment using bivariate statistical analysis and the index of entropy in the Sibiciu Basin (Romania). Environ Earth Sci 63:397–406

Corominas J (2001) Landslides and climate. In: Proceedings of the 8th international symposium on landslides, vol 4. Cardiff (Galles), pp 1–33

Corominas J, Mavrouli O (2011) Quantitative risk assessment for buildings due to rockfalls: some achievements and challenges. In: International Journee de Recontre sur les Danger Naturel 2011, Lausanne, Switzerland, 17–18 Feb 2011

Corominas J, Moya J (2008) A review of assessing landslide frequency for hazard zoning purposes. Eng Geol 102:193–213

Corominas J, Copons R, Moya J, Vilaplana J, Altimir J, Amigo J (2005) Quantitative assessment of the residual risk in rockfall protected area. Landslides 2:343–357

Corominas J, van Westen CJ, Frattini P, Cascini L, Malet J-P, Fotopoulou S (2014) Recommendations for the quantitative analysis of landslide risk. Bull Eng Geol Environ 73(2):209–263

Crozier MJ (1986) Climatic triggering of landslide episodes. In: Landslides: causes, consequences and environment. Croom Helm, pp 169–192

Crozier MJ (1997) The climate-landslide couple: a southern hemisphere perspective. In: Matthews JA, Brunsden D, Frenzel B, Gläser B, Weiß MM (eds) Rapid mass-movement as a source of climatic evidence for the Holocene, vol 19. Gustav Fischer, Stuttgart, pp 333–354

Crozier MJ (2005) Multiple-occurrence regional landslide events in New Zealand: Hazard management issues. Landslides 2:247–256

Crozier MJ, Eyles RJ (1980) Assessing the probability of rapid mass movement. In: Proceedings of the third Australia and New Zealand conference on geomechanics. New Zealand Institute of Engineers, pp 247–251

Crozier MJ, Glade T (1999) Frequency and magnitude of landsliding: fundamental research issues. Z für Geomorphol, NF Suppl Bd 115:141–155

Cutter SL, Boruff BJ, Shirley WL (2003) Social vulnerability to environmental hazards. Soc Sci Q 84(2):242–261

Dai FC, Lee CF (2003) A spatiotemporal probabilistic modeling of storm-induced shallow landsliding using aerial photographs and logistic regression. Earth Surf Proc Land 28(5): 527–545

Dai F, Lee C, Ngai Y (2002) Landslide risk assessment and management: an overview. Eng Geol 64(1):65–87

Damen M, Micu M, Zumpano V, Van Westen CJ, Sijmons K, Balteanu D (2014) Landslide mapping and interpretation: implications for landslide susceptibility analysis in discontinuous data environment. In: Proceedings of the international conference analysis and management of changing risks for natural hazards, pp 177–186

Damian R (2003) Controlul structural-geologic si morfologic in stabilitatea versantilor subcarpatici; conditii climatice si hidrologice. In: Armaş I, Damian R, Şandric I, Osaci–Costache G (eds) Vulnerabilitatea versanţilor la alunecări de teren în sectorul subcarpatic al Văii Prahova. Editura Fundaţiei România de Mâine, Bucureşti (in Romanian)

D'Ecclesiis G, Grassi D, Merenda L, Polemio M, Sdao F (1991) Evoluzione geomorfologica di un'area suburbana di Castronuovo S. In: Andrea PZ (ed) Incidenza delle piogge su alcuni movimenti di massa, Geologia Applicata e Idrogeologia, vol XXVI. Bari, pp 141–163

Devoli G, Strauch W, Chave G, Hoeg K (2007) A landslide database for Nicaragua: a tool for landslide hazard management. Landslides 4:163–176

Dikau R, Brunsden D, Schrott L, Ibsen M-L (1996) Landslides recognition, identification, movement and causes. Wiley, NewYork

Dinu M, Cioacă A (1997) Precipitation-induced landslides in the Moldavian Plateau (1996–1997). RRG, 41, Bucureşti

Dragotă CS (2006) Precipitaţiile excedentare din România. Edit. Academiei Române (in Romanian)

Dragotă C, Micu M, Micu D (2008) The relevance of pluvial regime for landslide genesis and evolution. Case study: Muscel basin (Buzău Subcarpathians, Romania). In: Present environment and sustainable development, vol 2. Edit. Universităţii "Al. I. Cuza", Iaşi, pp 242–257

EC (2010) Commission staff working paper: risk assessment and mapping guidelines for disaster management, SEC

Eidsvig U, McLean A, Vangelsten B, Kalsnes B, Ciurean RL, Argyroudis S, Winters M, Mavrouli O (2014) Assessment of socioeconomic vulnerability to landslides using an indicator-based approach: methodology and case studies. Bull Geol Eng Environ 73:307–324

Enulescu C (2007) Date statistice privind construcţiile de locuinţe în Europa şi America de Nord. Construcţii 2:61–65 (in Romanian)

Fell R, Ho K, Lacasse S, Leroi E (2005) A framework for landslide risk assessment and management, state of the art paper 3. In: Proceeding of the international conference on landslide risk management, Vancouver, Canada, 31 May–2 June 2005

Fisher P (1998) Improved modeling of elevation error with geostatistics. GeoInformatica 2(3):215–233

Flage R, Aven T, Zio E, Baraldi T (2014) Concerns, challenges and directions of development for the issue of representing uncertainty in risk assessment. Risk Anal 34(7):1196–1207

Flentje P, Chowdhury RN (2002) Frequency of landsliding as part of risk assessment. In: Australian geomechanics news, vol 37(2). Australian Geomechanics Society, Institution of Engineers, Australia, pp 157–167

Flentje PN, Chowdhury RN, Tobin P, Brizga V (2005) Towards real-time landslide risk management in an urban area. In: Hungr O, Fell R, Couture R, Eberhardt E (eds) International conference on landslide risk management. Taylor & Francis Ltd., Vancouver, Canada, pp 741–751

Glade T (2000) Modelling landslide triggering rainfall thresholds at a range of complexities. In: Bromhead E, Dixon N, Ibsen M-L (eds) Landslides in research, theory and practice. Thomas Telford, Cardiff, pp 633–640

Glade T (2003) Vulnerability assessment in landslide risk analysis. Die Erde 134(2):121–138

Godfrey A, Ciurean RL, van Westen CJ, Kingma NC, Glade T (2015) Assessing vulnerability of buildings to hydro-meteorological hazards using an expert-based approach—an application in Nehoiu Valley, Romania. Int J Disaster Risk Reduction 13:229–241

Goodchild MF (1980) Fractals and the accuracy of geographical measures. J Int Assoc Math Geol 12(2):85–98

Grozavu A, Mărgărint MC, Patriche CV (2012) Landslide susceptibility assessment in the Brăieşti-Sineşti sector of Iaşi Cuesta. Carpath J Earth Environ Sci 7(39–46):201

Grozavu A, Pleşcan S, Patriche CV, Mărgărint MC, Roşca B (2013) Landslide susceptibility assessment: GIS application to a complex mountainous environment. In: Kozac J et al (eds) The Carpathians: integrating nature and society towards sustainability. Springer, pp 31–44

Guzzetti F, Carrara A, Cardinali M, Reichenbach P (1999) Landslide hazard evaluation: an aid to a sustainable development. Geomorphology 31:181–216

Guzzetti F, Peruccacci S, Rossi M (2007) Rainfall thresholds for the initiation of landslides in central and southern Europe. Meteorol Atmos Phys 98:239–267

Guzzetti F, Mondini AC, Cardinali M, Fiorucci F, Santangelo M, Chang KT (2012) Landslide inventory maps: new tools for an old problem. Earth-Sci Rev 112:42–66

Heuvelink GBM (1998) Error propagation in environmental modelling with GIS. In: Research monographs in geographic information systems. Taylor & Francis, London

Ichim I (1970) Quelques aspects concernat le rôle des processus de mouvement de mase dans la modelage des versants des montagnes de flysch comprises entre les valles du Cuejdiu et du Nemţişoru. Lucrările Staţiunii de Cercetări Biologice, Geologice şi Geografice "Stejarul" 3:126–133. Pângăraţi

Ichim I (1972) Le role des processus de mouvement de masse dans le modelage des monts du flysch (Carpathes Orientales). Acta geographica Debrecina X:209–223

Ichim I, Bojoi I (1970) Accelerarea modelării reliefului din bazinele hidrografice Pângăraţi şi Oanţu ca urmare a ploii torenţiale din ziua de 28 Aug 1968. Lucrările Staţiunii de Cercetări Biologice, Geologice şi Geografice "Stejarul" 3:105–115. Pângăraţi (in Romanian)

Ilinca V (2009) Rockfall hazard assessment. Case study: Lotru Valley and Olt Gorge. Rev Geomorfol 11:101–108

Ilinca V (2010) Valea Lotrului. Studiu de geomorfolgie aplicată. PhD thesis, University of Bucharest (in Romanian)

Ilinca V (2012) Evaluarea la scară mare a hazardului la căderi de roci. Studiu de caz: un sector din drumul naţional 7A. In: National symposium on geomorphology, Craiova, 19–21 May 2012 (in Romanian)

Ilinca V (2014) Characteristics of debris flows from the lower part of the Lotru River basin (South Carpathians, Romania). Landslides 11:505–512

Ilinca V, Vararіu G (2013) Rockfalls assessment along Olt Gorge in the sector between Brezoi and Călimăneşti. In: National symposium on geomorphology, Suceava, 30 May–1 June, Abstract pp 46–47

Ilinca V, Chiţu Z, Şandric I, Mihai B, Săvulescu I (2008) Rockfall hazard assessment. A case study from Vâlcea County (Romania). In: Geophysical research abstracts, EGU, eISSN:1607–7962

Institute of Geography of the Romanian Academy (2014) WP5. WATER. D5.2. Report on climate change signals in the Vrancea Seismic Region, ECLISE enabling climate information services for Europe, FP7-ENV-20101, 112 p. http://www.ecliseproject.eu/content/mm_files/do_857/D5.2_RSV_final_report.pdf. Accessed 20 Mar 2015

ISU Bacău: http://www.isubacau.ro/. Accessed on 10 Mar 2012

ISU Buzău: http://www.isubuzau.ro/. Accessed on 12 Feb 2014

ISU Dâmboviţa: http://www.isudb.ro/. Accessed on 14 Feb 2014

ISU Galaţi http://www.isujgalati.ro/. Accessed on 20 Jan 2014

ISU Hunedoara: http://isujhunedoara.ro/. Accessed on 12 Mar 2015

ISU Ialomiţa: http://www.isujialomita.eu/. Accessed on 28 Oct 2014

ISU Mureş: http://www.isumures.ro/. Accessed on 28 Oct 2014

ISU Vâlcea: http://www.isuvl.ro/. Accessed on 3 Apr 2014

Jaedicke et al (2014) Identification of landslide hazard and risk 'hotspots' in Europe. 73(2): 325–339

Jaiswal P, van Westen CJ, Jetten V (2011) Quantitative estimation of landslide risk from rapid debris slides on natural slopes in the Nilgiri hills, India. NHESS 11:1723–1743

Jenks GF (1967) The data model concept in statistical mapping. Int Yearbook Cartogr 7:186–190

Jurchescu M (2012) Bazinul morfohidrografic al Olteţului. Studiu de geomorfologie aplicată. Manuscript PhD thesis, University of Bucharest (in Romanian)

Jurchescu M, Bălteanu D, Micu M, Chendeş V, Sima M, Zumpano V (2012) Landslide susceptibility assessment in the Southern part of Vrancea-Buzau Seismic Region. In: Geophysical research abstracts, vol 14. EGU General Assembly 2012, EGU2012–5698

Jurchescu M, Dragotă C, Marinică I, Grecu F (2013) Reconsidering rainfall thresholds for landslide occurrence events under scarce data constraints. Examples from a hilly area in South-Western Romania. In: Geomorphologia Slovaca et Bohemica, vol 13(1). Bratislava, p 34

Jurchescu M, Dragota C, Borcan M (2014a) Landslide hazard scenario assessment at a large spatio-temporal scale: the case of a municipality in the getic Subcarpathians, Romania. In: Geophysical research abstracts, vol 16. EGU General Assembly 2014, EGU2014–14733

Jurchescu M, Dragotă C, Marinică I (2014b) Dezvoltarea la scară medie a unui scenario de hazard legat de alucecările de teren – studiu de caz în bazinul Olteţului. Paper presented at the XXXth

national symposium on geomorphology, University of Bucharest, Orşova, 29–31 May 2014 (in Romanian)
Karssenberg D (2002) Building dynamic spatial environmental models. PhD thesis, Utrecht University, the Netherlands
Lee CF, Ye H, Yeung MR, Shan X, Chen G (2002) A GIS-based methodology for natural terrain landslide susceptibility mapping in Hong Kong. Episodes 24:150–159
Li Z, Nadim F, Huang H, Uzielli M, Lacasse S (2010) Quantitative vulnerability estimation for scenario-based landslide hazards. Landslides 7:125–134
Lungu D, Arion C, Aldea A, Văcăreanu R (2007) Seismic hazard, vulnerability and risk for Vrancea events. In: International symposium on strong Vrancea earthquakes and risk mitigation, Bucharest, Romania, 4–6 Oct 2007
Macovei G, Botez G (1923) Comunicare asupra fenomeneor de alunecări şi prăbuşiri de teren din judeţul Râmnicul Sărat. D.S. ale Inst. Geol. Român (1914–1915), Bucureşti (in Romanian)
Mărgarint MC, Niculita M (2014) Comparison and validation of logistic regression and analytic hierarchy process models of landslide susceptibility in monoclinic regions. A case study in Moldavian Plateau, NE Romania. In: EGU2014–6371, Geophys research abstracts, vol. 16
Mărgărint MC, Niculiţă M (2015) Landslide type and spatial pattern in Moldavian Plateau. In: Rădoane M, Vespremeanu-Stroe A (2015) Landform dynamics and evolution in Romania. Springer
Mărgarint MC, Grozavu A, Patriche CV, Tomasciuc AMI, Urdea R, Ungurianu I (2011) Évaluation des risques de glissements de terrain par la méthode de la régression logistique: application à deux zones basses de Roumanie. Dynam Environ 28:41–50
Mărgărint MC, Grozavu A, Patriche CV (2013a) Assessing the spatial variability of coefficients of landslide predictors in different regions of Romania using logistic regression. Nat Hazards Earth Syst Sci 13:3339–3355
Mărgărint M, Juravle D, Grozavu A, Patriche C, Pohrib M, Stângă I (2013b) Large landslide risk assessment in hilly areas. A case study of Huși town region (north-east of Romania). Ital J Eng Geol Environ Book Ser 6:275–286
Martha TR (2010) Characterising spectral, spatial and morphometric properties of landslides for semi-automatic detection using object-oriented methods. Geomorphology 116(1–2):24–36
Mavrouli O (2014) Vulnerability assessment for reinforced concrete buildings exposed to landslides. Bull Eng Geol Environ 73:265–289
Mazzorana B, Zischg A, Largiader A, Hubl J (2009) Hazard index maps for woody material recruitment and transport in alpine catchments. Nat Hazards Earth Syst Sci 9:197–209
Micu M (2008) Evaluarea hazardului legat de alunecări de teren în Subcarpaţii dintre Buzău şi Teleajen. Manuscript PhD thesis, Institute of Geography, Bucharest (in Romanian)
Micu M (2011) Landslide assessment: from field mapping to risk management. A case - study in the Buzău Subcarpathians, Forum geografic. Studiişi cercetări de geografie şi protecţia mediului Volume 10, Issue 1/ June 2011, doi: 10.5775/fg.2067-4635.2011.021
Micu M, Bălteanu D (2009) Landslide hazard assessment in the Bend Carpathians and Subcarpathians, Romania. Z Geomorphol 53(Supplement 3):49–64
Micu M, Bălteanu D (2013) A deep-seated landslide dam in the Siriu Reservoir, Bend Carpathians —Romania. Landslides 10(3):323–329
Micu M, Chendeş V, Sima M, Bălteanu D, Micu D, Dragotă C (2010) A multi-hazard assessment in the Bend Carpathians of Romania. In: Glade T, Casagli N, Malet JP (eds) Mountain risks: bringing science to the society. CERG Editions, Strasbourg
Micu M, Bălteanu D, Micu D, Zarea R, Ruţă R (2013) 2010-landslides in the Romanian Curvature Carpathians. In: Loczy D (ed) Extreme weather and geomorphology. Springer, pp 251–265. doi:10.1007/978-94-007-6301-2
Micu M, Jurchescu M, Micu D, Zarea R, Zumpano V, Bălteanu D (2014a) A morphogenetic insight into a multi-hazard analysis: Bâsca Mare landslide dam. Landslides. doi:10.1007/s10346-014-0519-4

Micu M, Malet JP, Bălteanu D, Mărgărint C, Niculiţă M, Jurchescu M, Chitu Z, Şandric I, Simota, C, Mathieu A (2014b) Typologically-differentiated landslide susceptibility assessment for Romania. In: Geophysical research abstracts, vol 16, EGU2014–13315

Micu M, Bălteanu D, Zumpano V, Kucsicsa G, Popovici A, Jurchescu M, Micu D (2015) Landslide hazard assessment in the Curvature Carpathians and Subcarpathians of Romania: between necessity and uncertainties (in prep.)

Mihai B (2005) Timiş mountains (Curvature Carpathians): geomorphic potential and mountain landscape planning. Edit. Universităţii din Bucureşti

Mihai B, Săvulescu I (2006) Data collection and analysis for the GIS large scale geomorphic hazard and risk mapping in mountain towns and resorts. A case study in Predeal town, Curvature Carpathians. Rev Geomorfol 8:85–93

Mihai B, Şandric I, Săvulescu I, Chiţu Z (2009) Detailed mapping of landslide susceptibility for urban planning purposes in Carpathian and Subcarpathian towns of Romania. In: Gartner G, Ortag F (eds) Cartography in central and eastern Europe. Lecture notes in geoinformation and cartography. Springer, Heidelberg/Berlin, pp 417–429

Nadim F, Einstein H, Roberds W (2005) Probabilistic stability analysis for individual slopes in soil and rock, state of the art paper 3. In: Proceedings of the international conference of landslide risk assessment, Vancouver, Canada, 31 May–2 June 2005

Naum T, Michalevich V (1956) Contribuţii la cunoaşterea degradărilor de teren din Carpaţii de la Curbură. An Univ CI Parhon 9:213–241 (in Romanian)

Nicorici C, Gray J, Imbroane AM, Barbosu, M (2012) GIS susceptibility maps for shallow landslides: a case study in Transylvania, Romania. Carpath J Earth Environ Sci 7:83–92

Paté-Cornell ME (1996) Uncertainty in risk analysis: six levels of treatment. Reliab Eng Syst Saf 54:95–111

Pellicani R, van Westen CJ, Spilotro G (2014) Assessing landslide exposure in areas with limited landslide information. Landslides 11(3):463–480

Perrault M, Geuguen P, Aldea A, Demetriu S (2013) Using experimental data to reduce the single-building sigma of fragility curves: case study of the BRD tower in Bucharest, Romania. Earthquake Eng Eng Vib 12:643–658

Petschko H, Brenning A, Bell R, Goetz J, Glade T (2014) Assessing the quality of landslide susceptibility maps—case study Lower Austria. Nat Hazards Earth Syst Sci 14:95–118

Pop O, Surdeanu V, Irimuş IA, Guitton M (2010) Distribution spatiale des coulées de debris contemporaines dans le Massif du Căliman (Roumanie). Studia Universitatis Babeş-Bolyai, Geographia, Cluj-Napoca 55(1):33–44

Pujină D (1998) Cercetări asupra unor procese de alunecare a terenurilor agricole din Podişul Bârladului şi contribuţii privind tehnica de amenajare a acestora. Manuscript PhD thesis, "Gh. Asachi", Iaşi University (in Romanian)

Rădoane N (2003) A new natural dam lake in the catchment of Bistriţei Moldoveneşti – Lake Cuejdel. Studii şi Cercetări de Geografie, Tom XLIX-L:211–216

Rădoane M, Rădoane N (2007) Applied geomorphology. Edit. Universităţii din Suceava, Suceava

Rădoane M, Rădoane N, Ichim I (1995) Folosirea metodei cubului matricial în evaluarea susceptibilităţii la alunecări de teren. Caz studiu: judeţul Neamţ. Studii şi cercetări de geografie, t 40:111–118 (in Romanian)

Regmi NR, Giardino JR, McDonald EV, Vitek JD (2013) A comparison of logistic regression-based models of susceptibility to landslides in western Colorado, USA. Landslides 11:247–262

Riedmann M, Bindrich M, Damen M, Van Westen CJ, Micu M (2014) Generating a landslide inventory map using stereo photo interpretation and radar interferometry techniques, a case study from the Buzău area, Romania. In: Proceedings of the international conference analysis and management of changing risks for natural hazards, pp 571–577

Rossi M, Witt A, Guzzetti F, Malamud BD, Peruccacci S (2010) Analysis of historical landslide time series in the Emilia-Romagna region, Northern Italy. Earth Surf Process Landforms 35(10):1123–1137

Rougier J, Sparks S, Hill LJ (2013) Risk and uncertainty assessment for natural hazards. In: Rougier J, Sparks S, Hill L (eds). Cambridge Unversity Press

Rowe W (1994) Understanding uncertainty. Risk Anal 14(95):743–750
Sandi H, Pomonis A, Francis S, Georgescu E, Mohindra R, Borcia I (2008) Seismic vulnerability assessment. Methodological elements and applications to the case of Romania. Construcţii 2:5–17
Şandric I (2005) Aplicaţii ale teoriei probabilitatilor condiţionate în geomorfologie. Analele Universităţii Bucureşti 54:83–97 (in Romanian)
Şandric I (2008) Sistem informaţional geografic temporal pentru analiza hazardelor naturale. O abordare bayesiană cu propagare a erorilor. Manuscript PhD thesis, University of Bucharest (in Romanian)
Şandric I (2009) Landslide inventory for the administrative area of Breaza, Curvature Subcarpathians, România. J Maps 5(1):75–86
Şandric I (2010) Object-oriented methods for landslides detection using high resolution imagery, morphometric properties and meteorological data. In: International archives of the photogrammetry, remote sensing and spatial information sciences—ISPRS archives. International Society for Photogrammetry and Remote Sensing, pp 486–491
Şandric I (2011) Landslide susceptibility for the administrative area of Breaza, Prahova County, Curvature Subcarpathians, România. J Maps 7(1):552–563
Şandric I (2015) Analysis of uncertainty propagation from GIS data into landslides susceptibility assessment. Geomorphology (Submitted)
Şandric I, Chiţu Z (2009) Landslide inventory for the administrative area of Breaza, Curvature Subcarpathians, Romania. J Maps 7:75–86. doi:10.4113/jom.2009.1051
Sandu M (1999) Alunecarea de la Lacul lui Baban. Stadiu de evoluţie. Revista Geografică, t. V, Bucureşti (in Romanian)
Scaioni A, Longoni L, Melillo V, Papini M (2014) Remote sensing for landslide investigations: an overview of recent achievements and perspectives. Remote Sens 6–10:9600–9652
Schmidt J, Dikau R (2004) Modelling historical climate variability and slope stability. Geomorphology 60:433–447
Sima M (2011) Mining and river pollution in Metaliferi mountains. Applications in the Crisul Alb and Certej river basins. Edit. Academiei Române, Bucureşti
Simon N, Crozier M, de Roiste M, Rafek AG (2013) Point based assessment: selecting the best way to represent landslide polygon as point frequency in landslide investigation. Electron J Geotech Eng 18:775–784
Sorocovschi V (2007) Vulnerabilitatea, componentă a riscului. Concept, variabile de control, tipuri şi modele de evaluare. In: Riscuri şi catastrofe, VI, Casa Cărţii de Ştiinţă, Cluj-Napoca, pp 58–69 (in Romanian)
Stângă I, Grozavu A (2012) Quantifying human vulnerability in rural areas—case study of Tutova hills (Eastern Romania). NHESS 12:1987–2001
Stângă I, Rusu C (2006) The concepts of vulnerability and resilience used in natural risk analysis. Buletinul Societătii de Geografie din România 12:129–142
Ştefănescu M (1995) Stratigraphy and structure of Cretaceous and Paleogene flysch deposits between Prahova and Ialomiţa valleys. Rom J Tectonics Reg Geol. Institutul Geologic al României, Bucureşti
Surdeanu V (1996) La repartition des glissements de terrain dans le Carpates Orientales (zone du flysch). Geografia Fisica e Dinamica Quaternaria 19(2):265–271
Surdeanu V (1998) Geografia terenurilor degradate. I. Landslides. Edit. Presa Universitară Clujeană, Cluj-Napoca (in Romanian)
Surdeanu V, Rus I, Irimuş IA, Petrea D, Cocean P (2009) Rainfall influence on landslide dynamics (Carpathian Flysch Area, Romania). Geografia Fisica e Dinamica Quaternaria 32(1):89–94
Surdeanu V, Pop O, Chiaburu M, Dulgheru M, Anghel T (2010) La dendrogéomorphologie appliquée a l'étude des processus géomorphologiques des zones minières dans le Massif du Calimani (Carpates Orientales, Roumanie). In: Surdeanu V, Stoffel M, Pop O (eds) Dendrogéomorphologie et dendroclimatologie—méthodes de reconstitution des milieux géomorphologiques et climatiques des régions montagneuses. Presa Universitară Clujeană, Cluj-Napoca, pp 107–124

Tanislav D, Costache A, Murătoreanu G (2009) Vulnerability to natural hazards in Romania. Forum Geografic, Studii si cercetări de geografie şi protectia mediului 8(8):131–138
Tate E (2012) Uncertainty analysis for a social vulnerability index. Ann Assoc Am Geogr 10:1–18
Terranova O, Antronico L, Gulla G (2007) Landslide triggering scenarios in homogeneous geological contexts: the area surrounding Acri (Calabria, Italy). Geomorphology 87(4):250–267
Thiebes B (2012) Landslide analysis and early warning systems. Local and regional case study in the Swabian Alb, Germany. Springer Theses. Springer, Berlin Heidelberg
Thiery MY, Malet J-P, Sterlacchini S, Puissant A, Maquaire O (2007) Landslide susceptibility assessment by bivariate methods at large scales: application to a complex mountainous environment. Geomorphology 9(1–2):38–59
Turner B, Kasperson R, Matson R, McCarthy J, Corell L, Christensen R (2003) A framework for vulnerability analysis in sustainability science. In: Proceedings of the national academy of sciences of the US
UN-ISDR (2004) Living with risk: a global reviews of disaster reduction initiatives, vol 1. United Nations, New York and Geneva
UN-ISDR (2009) Terminology on Disaster Risk Reduction, United Nations, New York and Geneva
Uzielli M, Nadim F, Lacasse S, Kaynia AM (2008) A conceptual framework for quantitative estimation of physical vulnerability to landslides. Eng Geol 102(3–4):251–256
Van Asch TWJ (1997) The temporal activity of landslides and its climatological signals. In: Matthews JA, Brunsden D, Frenzel B, Gläser B, Weiß MM (eds) Rapid mass movement as a source of climatic evidence for the holocene. Palaeoclimate research, vol 19. Gustav Fischer, Stuttgart, pp 7–16
Van Den Eeckhaut M, Hervás J (2012a) State of the art of national landslide database in Europe and their potential for assessing landslide susceptibility, hazard and risk. Geomorphology 139–140:545–558
Van Den Eeckhaut M, Hervás J (2012b) Landslide inventories in Europe and policy recommendations for their interoperability and harmonization. A JRC contribution to the EU-FP7 safeland project. Luxembourg Publications Office of the European Union
Van Den Eeckhaut M, Poesen J, Vandekerckhove L, Van Gils M, Van Rompaey A (2010) Human-environment interactions in residential areas susceptible to landsliding: the Flemish Ardennes case study. Area 42(3):339–358
Van Westen CJ, van Asch T, Soeters R (2006) Landslide hazard and risk zonation—why is it still so difficult? Bull Eng Geol Environ 65(167):184
Van Westen CJ, Castellanos E, Kuriakose SL (2008) Spatial data for landslide susceptibility, hazard, and vulnerability assessement: an overview. Eng Geol 102:112–131
Van Westen CJ, Bakker WH, Andrejchenko V, Zhang K, Berlin J, Cristal I, Olyazadeh R (2014) Roskchanges: a spatial decision support system for analyzing changing hydro-meteorological risk. In: Proceedings of the international conference analysis and management of changing risks for natural hazards, Padua, Italy, 18–19 Nov 2014
Varnes DJ (1984) Landslide hazard zonation, a review of principles and practice. IAEG Commission on Landslides, UNESCO, Paris
Walker BF (2007) Rainfall data analysis and relation to the incidence of landsliding at Newport. Aus Geomech 42(1)
White ID, Mottershead DN, Harrison JJ (1996) Environmental systems, 2nd edn. Chapman & Hall, London
Wieczorek GF (1987) Effect of rainfall intensity and duration on debris flows in central Santa Cruz Mountains. In: Costa JE, Wieczorek GF (eds) Debris flow/avalanches: process, recognition, and mitigation. Geological Society of America. Reviews in engineering geology, vol 7, pp 93–104
Winter M, Smith J, Fotopoulou S, Pitilakis K, Mavrouli O, Corominas J, Argyroudis S (2014) An expert judgment approach to determining the physical vulnerability of roads to debris flow. Bull Eng Geol Environ 73(2):291–305

Wisner B, Blaikie P, Cannon T, Davis I (2004) Natural hazards, people's vulnerability and disasters, 2nd edn. Routledge, London, New York

Zêzere JL, Reis E, Garcia R, Oliveira S, Rodrigues ML, Vieira G, Ferreira AB (2004a) Integration of spatial and temporal data for the definition of different landslide hazard scenarios in the area north of Lisbon (Portugal). Nat Hazards Earth Syst Sci 4:133–146

Zêzere JL, Rodrigues ML, Reis E, Garcia R, Oliveira S, Vieira G, Ferreira AB (2004b) Spatial and temporal data management for the probabilistic landslide hazard assessment considering landslide typology. In: Lacerda E, Fontoura S (eds) Landslides: evaluation and stabilization. Taylor & Francis Group, London, pp 117–123

Zêzere J, Garcia R, Oliviera S, Reis E (2008) Probabilistic landslide risk analysis considering direct costs in the area north of Lisbon (Portugal). Geomorphology 94:4467–4495

Zumpano V, Hussin H, Reichenbach P, Bălteanu D, Micu M, Sterlacchini S (2014) A landslide susceptibility analysis for Buzău County, Romania. Revue Roumaine de Geographie/Rom J Geogr 58(1)

Chapter 33
Floods and Flash-Floods Related to River Channel Dynamics

Florina Grecu, Liliana Zaharia, Gabriela Ioana-Toroimac and Iuliana Armaș

Abstract Floods and flash-floods are a major factor in hydrogeomorphological river dynamics. This chapter has two main aims: (i) to analyse the characteristics of floods in Romania, based on their origin, frequency and magnitude; (ii) to present case studies on the relation between river channel dynamics and floods. In most cases, in Romania, floods occur in spring and summer (up to 3/4 of the total number of floods) and have mostly pluvial origins. Rivers from the External Curvature (Carpathians, Subcarpathians and Romanian Plain) suffered historical floods in 2005, reflected by a slight extension of the river channel (for example, Putna and Buzău watercourses). Rivers from Banat Plain also recorded floods in 2005; a high volume of water created breaches in dikes and the long stagnation of water determined morphological modifications of the floodplain. The Danube River registered historical floods in 2006; due to the morphometry of the floodplain, the river overflowed the banks and the dikes, covering the floodplain between Rast and Bistreț towards the homonym lake. The flash-flood from Ilișua River basin in June 2006 generated some modifications in the river channel morphology due to fine materials accumulation, with a thickness of 0.2–1.5 m, and coarser ones, which created bars with heights of 0.5–1 m; materials came from landslides and bank collapse. The interactions between hydrological phenomena and morphological processes may have consequences with ephemeral character, reversible on short-term, but also on long-term, with a potential impact on the environment and on the society. This analysis underlines the applied character of hydrogeomorphology.

Keywords Floods · Flash-floods · Hydrogeomorphological dynamics · River channels · Romania

F. Grecu (✉) · L. Zaharia · G. Ioana-Toroimac · I. Armaș
Faculty of Geography, University of Bucharest, N. Bălcescu 1,
010041 Bucharest, sector 1, Romania
e-mail: grecu@geo.unibuc.ro; florinagrecu@yahoo.com

M. Rădoane and A. Vespremeanu-Stroe (eds.), *Landform Dynamics and Evolution in Romania*, Springer Geography,
DOI 10.1007/978-3-319-32589-7_33

Introduction

Floods and flash-floods are a major factor in hydrogeomorphological dynamics. During flash-floods, given the large liquid and solid volumes transported by rivers, the erosion and accumulation processes intensify, generating important modifications, generally fast, of the river channel and floodplain (in flooding conditions). As natural hazards, flash-floods and floods are most often the effect of heavy rains, therefore they are considered hydro-meteorological hazards (UNISDR 2009) and are being analysed closely connected to these (Grecu 2009). The intense dynamics of the environment in the last decades has led to the appearance of other floods' study methods as well, besides the hydrological or landscape-related ones (Demers et al. 2014). The hydrogeomorphological researches have appeared and developed in close connection to the fluvial geomorphology ones. They respond to the contemporary interdisciplinary research requests in explaining the long-term evolution of the rivers within hydrographic basins. The notion of hydrogeomorphology, introduced by Scheidegger in 1972 (Cyril et al. 2013), partially synonym with the one of fluvial geomorphology, is also used as a research method in studies on floods, being developed in this direction (Schumm 1985; Masson et al. 1996; Kondolf and Piégay 2003; Arnaud-Fassetta and Fort 2004; Arnaud-Fassetta et al. 2005; Habersack et al. 2008; Malavoi and Bravard 2010; Ballais et al. 2011; Swanson et al. 2011 etc.). The concept includes the interdependency relations between water (loaded or not with sediments) and the relief of the river channels, the erosion and accumulation processes and forms, favourable or not to the flooding of the periodically emerged lands. These relationships coexist in a double sense: water contributes to the shaping of the channel, which is extremely dynamic during flash-floods, while the channel, through its morphometric characteristics and micro-relief, influences the dynamics of the water, its erosion, transport and accumulation capacities.

The main elements that must be followed in the interdisciplinary analysis of river channel dynamics are:

- *the fluvial relief* (*geomorphology*): the channel and the floodplain, erosion processes and landforms (lateral and vertical), accumulation forms (islands, sand barriers), channel pattern, the width of the channel and of the floodplain, the slope on the longitudinal profile, the cross profile;
- *the river flow* (*hydrology*) *and the generating factors*: the water discharge, the sediment load, the water levels, the flow velocity; characteristics of the precipitations as the main source of water supply (quantity, duration and intensity, previous precipitations);
- *factors that influence the dynamics of the river channel*: natural (geologic, geomorphologic, hydroclimatic, bio-pedo-geographic) and anthropic ones (engineering works, land use, exploitation of alluviums within the river channel etc.).

In Romania, the experience in researches on fluvial geomorphology and river channel dynamics have imposed hydrogeomorphology as a research method

especially in the last two–three decades, in studies elaborated by Ichim et al. (1989, 1998), Rădoane et al. (1991, 2003, 2008, 2013), Grecu (1992), Grecu et al. (2008, 2010, 2012a, b, 2013), Bojoi et al. (1998), Dumitriu (2007), Arghiuş (2008), Goţiu and Surdeanu (2008), Pandi and Sorocovschi (2009), Ioana-Toroimac (2009), Ioana-Toroimac and Grecu (2013), Ioana-Toroimac et al. (2010, 2013), Gogoaşe Nistoran et al. (2011), Zaharia et al. (2011), Perşoiu and Rădoane (2011), Armaş et al. (2012), György (2012), Stângă (2012), etc., as well as in recent PhD theses. The present climatic changes and the anthropic activities within the river channels give hydrogeomorphology the necessary applied character.

Characteristics of the Floods in Romania and Hydrogeomorphological Interrelations

The genetic, morphometric and morphographic characteristics of the rivers and of the fluvial relief are determined by the geological and geomorphological specific of the Romanian territory (Posea 2002; Bălteanu et al. 2012), by the role of the main baric centres and by the presence of the Danube and of the Black Sea. If the genesis of the hydrographic network is influenced by the morphostructure and the tectonics of the main relief (Molin et al. 2012), the morphography of the river channels is the result of the synergic action of the climatic, morphological, hydrological and bio-pedo-geographic factors upon the lithology in various conditions specific to the Carpathians, Subcarpathians, plateaus and plains.

The Origin, Frequency and Magnitude of Floods in Romania

Flash-floods in Romania can have pluvial, snow melting or mixed origins and can occur in any period of the year. On the rivers with small and medium hydrographic basins, floods have mostly pluvial origins, being generated by heavy rains and having fast manifestation (from a few hours to 1–2 days), with high impact on river channels. In the case of large hydrographic basins, the determinant role is owned by the long-duration rains and by snow melting. These floods are slower (from a few weeks to 1–2 months) and the large water and sediments volumes act upon the river channel for a longer time, inducing slower changes of its morphology and morphometry. In most cases, annual floods in Romania have pluvial origins. There are, though, some regional differences, imposed by climatic and orographic particularities. Thus, in the north and north-west parts of the country, the rate of pluvial origins among annual floods reaches 47–50 % (of all the considered years), while in the south and south-east the rate increases to over 75 % (Stanciu 2004). The annual floods originated exclusively by snow melting have a low frequency (3–4 % in the west and 0–2 % in the rest of the country). Those with mixed origins represent

25–30 % in the south and east parts of the country and 10–15 % in the south-west (Diaconu 1971; Diaconu and Şerban 1994).

In Romania, floods occur most frequently in spring (30–46 % of the total floods in a year) and in summer (25–40 %), while in winter and autumn their number is smaller (5–29 and 8–20 %, respectively) (Diaconu 1971; Stanciu 2004). The frequency of floods (with peaks that overpass at least two times the mean multiannual discharge) is higher on mountainous rivers (6–7 per year), and decrease by half on rivers from plain areas (about 3 floods annually) (Diaconu and Şerban 1994).

Among the largest floods and flash-floods that occurred in Romania in the twentieth century, the most serious social and economic damages had the ones in (Fig. 33.1): May 1912 (in the south-western part of the country—Banat region), April and July 1932 (in Crişuri and Mureş basins), July 1940 (in Ialomiţa basin), July 1941 (in Argeş—Vedea basins), July 1969 (on the Upper Siret River), May 1970 (in Someş—Tisa, Mureş, Crişuri, and upper Siret basins), October 1972 (in Jiu basin), July 1975 (in Olt, Argeş—Vedea, and Ialomiţa—Buzău basins), August 1979 (in Prut basin) and December 1995–January 1996 (in Someş basin and in other basins from Banat) (Mustăţea 2005; Mihailovici et al. 2006a; Şerbu et al. 2009; ANAR-INHGA 2011).

The beginning of the twenty-first century is marked by floods and flash-floods of high magnitude and low frequency, both with large spatial extension and with regional and local character. Outstanding was the year 2005, when seven flooding

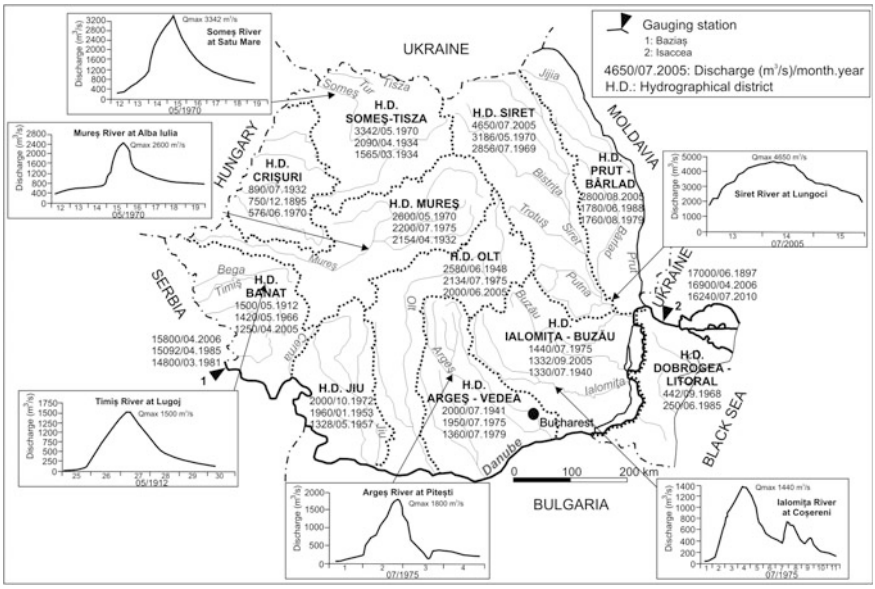

Fig. 33.1 The highest flood peaks recorded in Romania within hydrographical districts, and on the Danube River (according to: Mihailovici 2006; Mustăţea 2005; Şerban et al. 2006; Gâştescu and Ţuchiu 2012)

episodes affected the entire country, the most important occurring in April, July and September. 2005 is one of the years with the highest values of precipitations and discharges since the beginning of the systematic recordings in Romania (Mihailovici et al. 2006a). After 2005, large floods and flash-floods occurred in April–May 2006 (on the Danube), in July 2008 (in Siret and Prut basins), in June–July 2010 (in the upper basins of Prut and Siret, and on the Danube), in September 2013 (on rivers from the southern Moldavian Plateau) and in March–May 2014 (in the southern part of Argeş—Vedea hydrographic district). In Romania, the areas affected by historical floods with significant damages are situated along the Danube and the main rivers from the hydrographic districts of Someş, Mureş, Vedea, Argeş, Ialomiţa, Siret, and Prut (Fig. 33.2).

Hydrogeomorphological Inter-conditionings

Previous studies on river channel dynamics have shown that major floods determine adjustments on the longitudinal and cross profiles of the river channels through fast changes in the *aggradations–degradation* cycles.

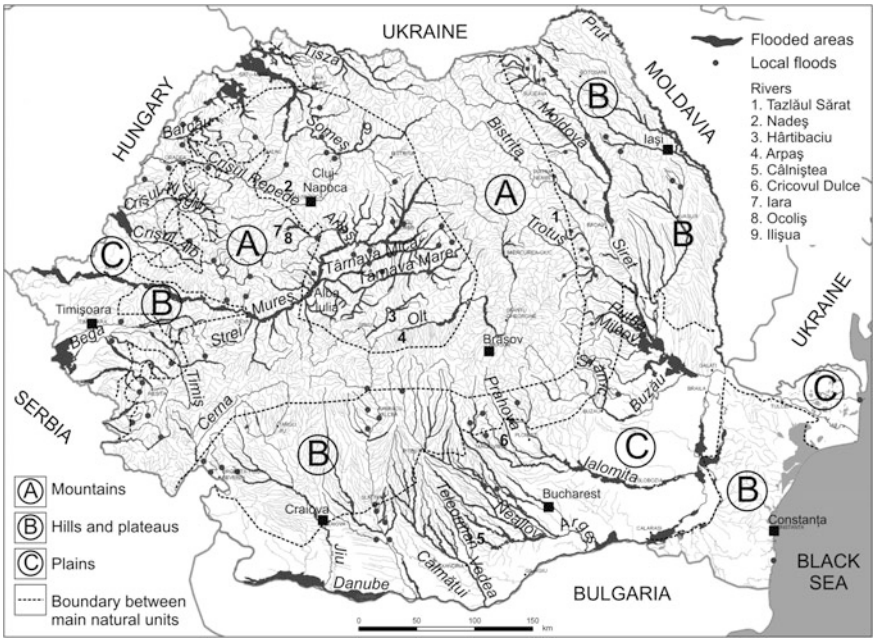

Fig. 33.2 Areas affected by significant historic floods in Romania (modified from ANAR 2014)

Consequent to the floods from 1970 and 1975, in the *Eastern Carpathians and Moldavian Subcarpathians*, the riverbed has incised by: 50 cm on Bistriţa River (at Frumosu), 80 cm on Trotuş River (at Ghimeş–Făget), 80 cm on Tazlăul Sărat River (at Lucăceşti) and 80–100 cm on Putna River (at Tulnici) (Rădoane et al. 1991). The migration of the aggradation–degradation cycles towards downstream, at the exterior of the Carpathians, with speeds that reach or overpass 8–10 km/year, contributes to the heightening of the riverbeds, which favours the accumulation processes and the flooding of the floodplain (Ichim and Rădoane 1990). The analysis of Trotuș riverbed elevation showed an alternation of aggradation and degradation phases, but also significant linear trends: a degradation trend between 1961 and 2007 in the mountain sector (at Ghimeș–Făget) and in the subcarpathian one (at Tg. Ocna), and an aggradation trend between 1963 and 2005 in the lower sector (at Vrânceni) as a consequence of the accumulation of sediments eroded upstream (Zaharia et al. 2011). Intense degradations of the riverbed of Trotuș River were noticed in the years with high floods (1969, 1970, 1972, 1979, 1988, 1991 and 2005) (Fig. 33.3a).

In the case of Milcov River, located at the external curvature of the *Carpathians, Subcarpathians and plain unit* (*glacis and lowland*), the river channel has frequently adjusted due to floods. During the event from July 2005 (12–18th), in the area of Odobeşti town, the river channel (braiding in this sector) has been strongly affected by lateral erosion. Downstream, the slope is low (0.65 m/km), and the channel becomes sinuous and afterwards meandering, prevailing channel deposition processes. In these conditions, at Goleşti, as a consequence of the July 2005 flood (maximum discharge of 724 m^3/s), fine sediments were deposited on a 1.2 m thickness (Săcrieru 2008).

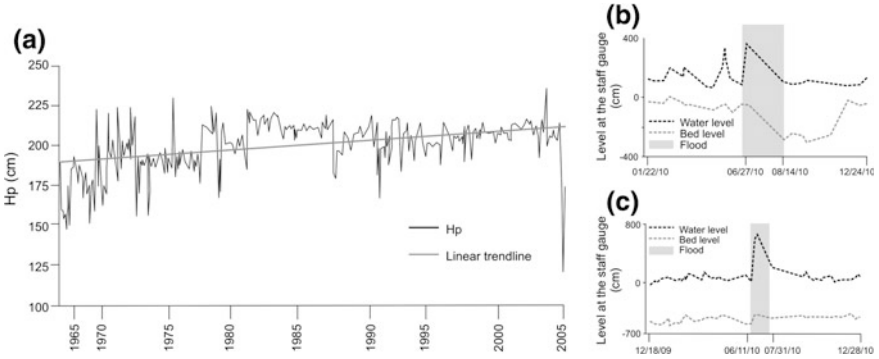

Fig. 33.3 **a** Vertical dynamics of Trotuş river channel at Vrânceni gauging station between 1963 and 2005 (H_p the difference between the water stage—measured from the "0" elevation of the staff gauge—and the maximum water depth; modified from Zaharia et al. 2011). **b**, **c** Siret riverbed dynamics in relation to the water level at Lespezi (**b**) and at Lungoci (**c**) during the June–July 2010 flood (modified after Obreja 2012)

In the *Moldavian Plateau and the Lower Siret Plain*, the analysis of Siret river bed dynamics during the June–July 2010 flood indicated aggradations ranging from 15 to 100 cm and degradations from 65 to 200 cm, in different flow phases. Thus, at Lespezi gauging station, the thalweg suffered a degradation of 200 cm (Fig. 33.3b). At Lungoci (the last gauging station upstream the confluence with the Danube), the thalweg experienced an aggradation of 100 cm during the increasing time of the flood and a degradation of 50 cm during the decreasing phase (Fig. 33.3c) (Obreja 2012).

In the *Transylvanian Depression,* river channel dynamic processes may be correlated as well to floods and flash-floods. Thus, on Nadeş River (tributary of Someşul Mic River in the north-western part of the Transylvanian Depression), at Aghireşu and Mera gauging stations, channel incised by 24–82 cm in 1970–1973 and 1978–1979, due to large floods during these years (Pandi and Sorocovschi 2009).

The rivers from Hârtibaciu catchment registered high discharges in 1975 (when Hârtibaciu reached 210 m^3/s at Cornăţel, the mean multiannual discharge being of only 6.86 m^3/s), 1981, 2005 (maximum discharge of 102 m^3/s). Several factors are responsible for Hârtibaciu floods: heavy rains, low slope of the river (locally, under 1 m/km) and the small dimensions of the torrential channel; the floods transform the floodplain into a swamp (Grecu 1992).

In 1975, Târnava Mare River recorded high-magnitude floods (900 m^3/s at Mediaş and 851 m^3/s at Blaj) which impacted on the channel (Vodă 2007). On the Arpaşul Mare River, the historic flood of 10–11 June, 2011 (return period of 100 years) determined the erosion and the retraction of the right bank on about 8 m at Arpaşu de Sus gauging station, followed by a sediment accumulation of about 1.4 m thickness (Petrea and Man 2011).

For the rivers from the *Haţeg Depression*, bank erosion estimation indicates important differences between the values obtained at mean discharges and at the bankfull stage. Thus, in the case of Strei River, the erosion coefficient is 0.037 at mean discharges (8.66 m^3/s) and over ten times higher 0.367 at the bankfull stage (405.39 m^3/s) (Goţiu and Surdeanu 2008).

River Channels Particularities—Control Factors of Floods and Flash-Floods

Among morphometric particularities, the concavity coefficient of the longitudinal profile of river channels constitutes a floods' control factor. At small concavities and low slope, the flow has slow velocities, and the floods have local manifestation

depending on the torrential character of the precipitations. On large rivers, which cross various landforms, the concavity is specific to the upper course, where the high concavity favours solid transport and the river incision (Hack 1957; Larue 2014).

On Romania's territory, the high vulnerability to floods is characteristic to some areas in *subsidence plains*, where the river channels frequently modify their flow direction, when showing large and low-height floodplains, like in the case of Lower Siret, Someş, Crişuri and Timiş rivers. The *confluence* sectors of the rivers within these areas (e.g. Siret, Putna, Buzău and its tributaries, Prut, Danube, Someş, Barcău, Crişul Repede, Crişul Negru, Crişul Alb, Timiş etc.) are frequently subject to flooding, even when the large water volume comes from few tributaries. *The tight channels, deepened in soft rocks,* autochthonous to the plains (e.g. Vedea, Teleorman, Neajlov, Câlniştea rivers according to Grecu et al. 2012a or to the hills and plateaus like Hârtibaciu River—Grecu 1992; rivers from the Transylvanian Plain—Sorocovschi 2005, and from the Moldavian Plain—Bojoi et al. 1998), are susceptible to flash-floods and floods due to low longitudinal slopes. On these rivers, the pulsating aggradation–degradation cycles have low intensities, which does not allow the recirculation of high quantities of sediments. In the Moldavian Plain, 294 confluences have been investigated from this point of view: 61 % corresponding to some concavities along the collecting valley, 11 % to some convexities, and 27 % to a rectilinear profile (Bojoi et al. 1998). If the impermeable character of the geological substrate is also considered, one can conclude that the floods from the Moldavian Plain are favoured not only by the precipitations, but also by the relief and, more precisely, by the geometry of confluences.

The morphological and morphometric characteristics of the floodplains of the large rivers from the Romanian Plain, the Banato–Crişană Plain and the Danube's floodplain make these sectors extremely vulnerable to floods. The width of the floodplain, the relative altitude, the relations with the terraces and with the slopes (the slope processes and microforms), the anthropogenic works (channelization or diking), the presence of wetlands, the characteristics of floodplain deposits (e.g. the impermeability due to the reddish clay, the reduced thickness of the Quaternary floodplain deposits from the Banato–Crişană Plain—Posea 2002) influence the magnitude and extension of floods. The meandering process, corresponding especially to low slopes, manifests itself in tight connection with the dimension of the floodplains. In the Romanian Plain, the meandering process is one of the particularities of the river channels present dynamics, beside the important renewals of the draining network (Grecu 2010). Câlniştea River (tributary of Neajlov), autochthonous of the Romanian Plain, presents an intense meandering process. The diachronic analysis of the meanders shows the decrease of meanders length, of their amplitude and of the sinuosity along the investigated sector (from 2.89 to 2.45), which indicates a slight equilibrium tendency and a straightening process (Grecu et al. 2012a).

Case Studies on the Relation Between River Channel Dynamics and Floods

Rivers from the Region of the External Curvature (Carpathians, Subcarpathians, Plain)

The diachronic analysis of the braided channel width of some representative rivers from the Curvature region (Carpathians, Subcarpathians and plain), conducted in relation with the frequency and magnitude of floods, highlighted the morphogenetic role of the major floods upon the river channel dynamics.

On Buzău and Putna rivers, originating from the Carpathians, crossing the Subcarpathians and flowing into Siret River in the plain, the largest floods recorded at Banița and respectively Boțârlău gauging stations, occurred in 1970, 1972, 1975, 1988, 1991 and 2005 (Fig. 33.4a, b). Most of the important floods occurred in the 1970s (with peaks higher than the mean of the maximum annual discharges of 1970–2010): 8 floods on Buzău and 10 floods on Putna (Fig. 33.4c, d). During the same period (1970–1979), the maximum discharges corresponding to the annual floods had the highest average: 853 m^3/s on Buzău and 645 m^3/s on Putna, which reflects the high magnitude of floods in the 1970s. In the 1980–1989 and 1990–2000 decades, the average of the annual flood peaks decreased significantly for both rivers and increased again in the 2000–2010 decade, along with the number of floods with high magnitude (Fig. 33.4c, d). While on the Putna River, the highest discharge (1598 m^3/s) occurred during July 2005 flood, on the Buzău River the maximum discharge was recorded during the flood of July 1975 (2200 m^3/s). In 2005, the floods on Buzău River have been attenuated by the reservoir dams (from Siriu and Cândești), thus the maximum discharge was of 925 m^3/s.

The diachronic analysis (based on the comparison of the width of the braided channels measured on cross profiles on topographic maps of 1980, on orthophotoplans of 2005, on Google Earth images of 2008, 2009 and 2010) and the hydrological study (based on monthly and annual maximum discharge series from the period 1970–2010 at the gauging stations Boțârlău on Putna River and Baniţa on Buzău River) have shown that, for the analysed river sectors (40 km on Putna River upstream Boțârlău and 90 km on Buzău River upstream Baniţa, respectively), the largest widths of the braided channels correspond to the year 1980, which coincides to the fact that in the 1970s both rivers presented frequent and high-magnitude floods. Between 1980 and 2005, the braided channels have narrowed by 22 % on Putna River and by 67 % on Buzău River, which can also be explained by the lower frequencies and magnitudes of the floods during this period. In the case of Buzău River, the more intense narrowing (compared to Putna) is also the result of sediment transport diminishing as a consequence of the construction of the two dams and reservoirs. The high flood of 2005 has determined the increase of the width of the active braided channels (Fig. 33.4e, f), more evident in the case of Putna River, with a natural flow regime. Between 2005 and 2008/9, a slight extension of the river channels took place (21 % on Putna and 12 % on Buzău),

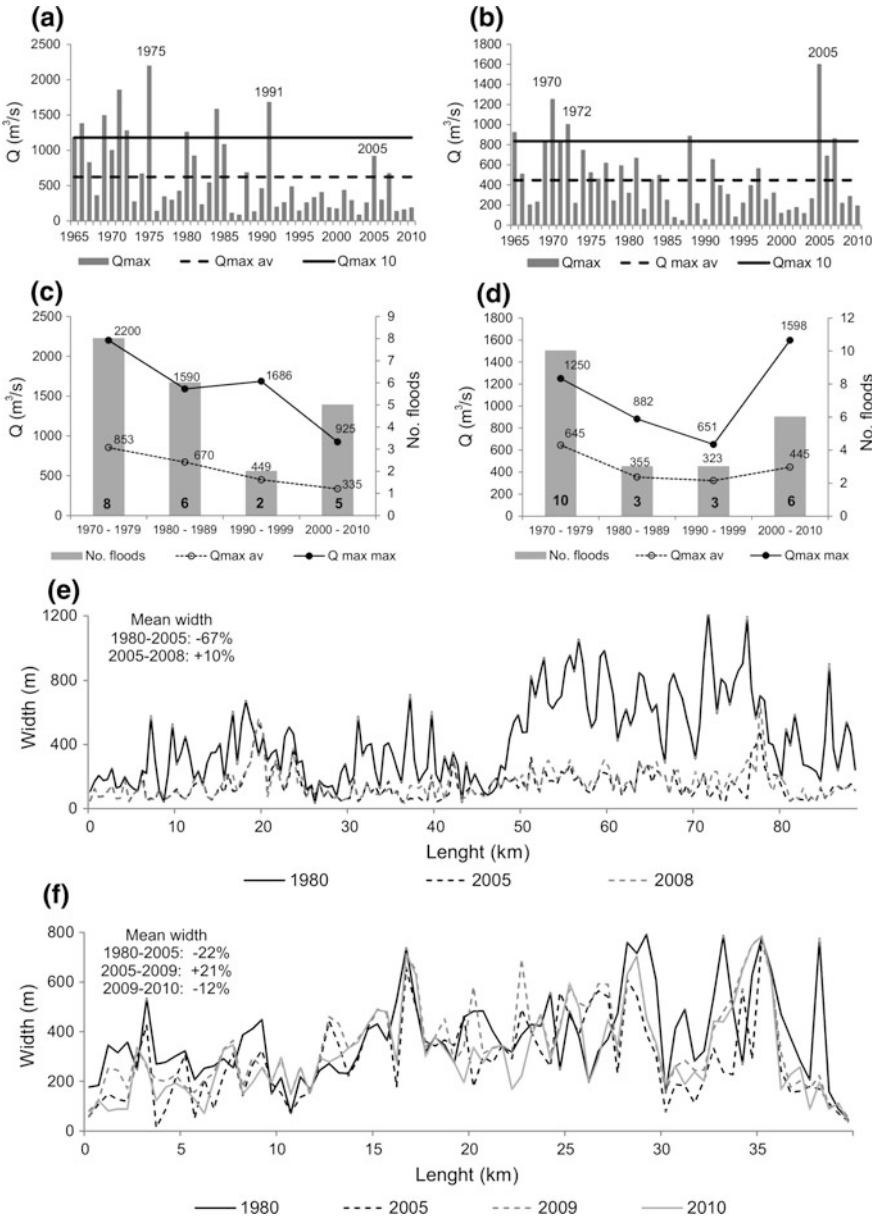

Fig. 33.4 Variations of maximum discharges of annual floods (Qmax) during 1965–2010 compared with their average (Qmax av) and with the 10 years return period maximum discharge (Qmax 10) for Buzău River at Baniţa gauging station **a** and Putna River at Boţârlău gauging station **b**. Decadal variations of the number of floods with peaks higher than Qmax av, of the average maximum discharges (Qmax av) and of the highest discharges (Qmax max) on Buzău River at Baniţa gauging station **c** and on Putna River at Boţârlău gauging station **d**. Variations of braided channel's width of Buzău river upstream Baniţa **e** and of Putna River upstream Boţârlău **f**

which might reflect the morphogenetic role of the 2005 flood. In the case of Putna River, between 2009 and 2010, the width of the active braided channels decreased by 12 %, in the context of floods with low peaks (Fig. 33.4b).

Recent studies concerning the lateral dynamics of the river channels from the contact between the Curvature Subcarpathians and the Romanian Plain have shown the narrowing of the active braided channels in the 1980–2005 time period. Consequently, the mean width of the Prahova River channel diminished by 44 %, the one of Milcov River by 43 %, and the one of Cricovul Dulce River by 18 %. This process can be attributed to lower frequencies and magnitudes of the floods during this period, but also to gravel extractions from riverbeds and to the protection works against floods (Ioana-Toroimac and Grecu 2013; Ioana-Toroimac et al. 2013; Grecu et al. 2012b, 2013, 2014).

The mapping of the Subcarpathian river channels (Prahova, Slănic, Putna) on large-scale topographic maps and plans dating from 1893 to 1997 shows the changes of the channel dynamics for the three rivers in an interval of about 100 years (Table 33.1) (Grecu et al. 2008). The sinuosity and braiding processes have decreased during the analysed time interval, the indices varying from one river to another. Based on the obtained values, one can estimate that rivers' tendency is to slightly redress their channels on the middle sector (in the Curvature Subcarpathians).

Rivers from the Central Sector of the Romanian Plain

The central sector of the Romanian Plain (between the rivers Olt to the west and Argeş to the east) is drained by watercourses belonging to three main hydrographic basins: Călmăţui (in Teleorman County), Vedea (with the tributary Teleorman River) and Neajlov (sub-basin of Argeş River). Călmăţui, Neajlov and Vedea rivers have longitudinal profiles with low declivities: between 2 and 2.5 % in the upper sectors (due to the lithology constituted mainly by gravels) and below 1–2 % in the lower sectors. The low slope and the soft lithological substratum favours lateral erosion, intense meandering and rivers' overflowing at high floods.

Table 33.1 Variations of sinuosity and braiding indices over 100 years on Prahova, Slănic and Putna rivers, on the subcarpathian course

Parameters	Prahova		Slănic		Putna	
	1893	1980	1899–1901	1970–1971	1893–1895	1980
Sinuosity index (K_s) $K_s = Lr/Ldr$	1.113	1.117	1.703	1.661	1.714	1.655
Braiding index (K_d) $K_d = L_s/L_r$	2.140	1.740	1.274	1.092	2.265	1.566

Lr sinuous length; *Ldr* straight length; L_s the sum of arms' lengths; L_r the length of the main arm

The greatest floods occurred on the three rivers in 1970, 1972, 1975, 1979, 1995 and 2005 (Fig. 33.5a). These events generated inundations, with important material damages and influenced the morphological and morphometric characteristics of the river channels. On Vedea River (at Alexandria), the highest discharges occurred during the floods of October 1972 (949 m^3/s), July 2005 (834 m^3/s), July 1975 (544 m^3/s), and July 1970 (463 m^3/s), the mean multiannual discharge being of 11 m^3/s. The Teleorman River (at the Teleormanu gauging station) has recorded the highest discharges during the floods of October 1972 (278 m^3/s), July 2005 (196 m^3/s), March 1969 (168 m^3/s) and March 1984 (160 m^3/s) (its mean multiannual discharge being of 3.2 m^3/s). On Neajlov River, the maximum discharges exceeded 300 m^3/s and even 400 m^3/s during the floods of March 1973 (430 m^3/s), March 1984 (392 m^3/s), July 1975 (385 m^3/s), July 1970 (340 m^3/s) and October 1972 (301 m^3/s), its mean multiannual discharge being of 8.8 m^3/s (Grecu et al. 2012a).

Channels' adjustments during floods are triggered by high discharges and water velocity, but also by sediment load. For example, if the mean annual suspended sediments discharge of Vedea River at Alexandria is 12.3 kg/s, during the major

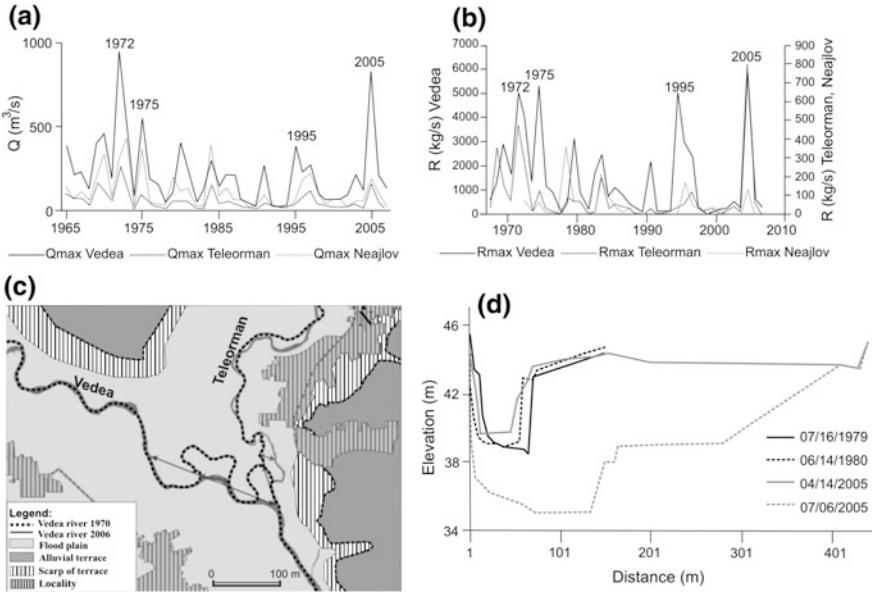

Fig. 33.5 **a** Variations of annual flood peaks (Qmax) registered between 1965 and 2010 on Vedea (at Alexandria), Teleorman (at Teleormanu) and Neajlov (at Călugăreni) rivers (based on data from Romanian Waters National Administration A.N.A.R.). **b** Variations of maximum annual suspended sediment discharges (Rmax) recorded between 1965 and 2010 on Vedea (at Alexandria), Teleorman (at Teleormanu) and Neajlov (at Călugăreni) rivers (based on data from A.N.A.R.). **c** Lateral dynamics of Vedea and Teleorman river channels in the neighbourhood of their confluence, between 1970 and 2006 (from Grecu et al. 2012a). **d** Vertical dynamics of Vedea river channel at Alexandria gauging station (based on data from A.N.A.R.)

floods (of 1972, 1975, 1995 and 2005), it surpassed 5000 kg/s (the maximum reached 5838 kg/s during the July 2005 flood) (Fig. 33.5b). Teleorman River (at Teleormanu gauging station), which has a mean annual suspended sediments discharge of only 1.44 kg/s, reached 796 kg/s during the July 2005 flood, and the Neajlov River, during the 1979 flood, reached a maximum suspended sediments discharge of 359 kg/s (the mean multiannual suspended sediments discharge being of only 1.12 kg/s) (Grecu et al. 2012a).

The diachronic analysis at the confluence of Vedea River with Teleorman, its most important tributary, indicates a pronounced dynamics, because of the contribution in water and sediments of the Teleorman River, important especially during floods. Between 1970 and 2006, Vedea river channel reduced its length by 2.5 km in the analysed sector. This shortage is due, first, to the natural rectification of the riverbed (by meanders' cutting and downstream migration), and, second, to human interventions. The Teleorman river channel downsized by 1.1 km, and it changed the confluence area (Fig. 33.5c). The Vedea meander from upstream the confluence with Teleorman shortened by 600 m, and the alluvial fan of both rivers deviated the confluence with 0.83 km (Grecu et al. 2012a).

In 2005, an year characterised by high-magnitude floods and inundations, which affected the whole country (Zaharia et al. 2006) due to heavy precipitations, which surpassed the mean multiannual value by 163 % in May and by 332 % in September at Alexandria, high discharges were registered on Vedea River, which exceeded by 500 % the mean monthly values of 1961–2006 between June and September. Impressive exceeding was recorded in July (725 %), August (911 %) and September (1308 %). The suspended sediment discharge recorded exceptional values, as well, mostly in July, August and September, when it surpassed the mean monthly values by 988, 2248 and 2971 % (Grecu et al. 2010). The morphodynamic role of the major 2005 flood is shown by comparing the cross-river channel profiles from Alexandria gauging station on Vedea River, between 1979 and 2005 (Fig. 33.5d).

Transylvanian Depression

In the Transylvanian Depression, large-scale floods were recorded in May 1970, June 1975, March 1981, December 1995 and in June 1998, 2005 (Sorocovschi 2005; Arghiuş 2008).

Mureş River is one of the longest rivers in Romania (with a length of 716 km and a basin area of 27,830 km^2). It springs from the Eastern Carpathians (Hăşmaşul Mare), flows on east-west general direction, and it confluences with Tisza River in Hungary. Due to the large extension of the catchment, the dynamic factors act differently in space and time. On the whole basin, the biggest floods took place in May 1970 and July 1975, when at Alba Iulia (in the middle sector), discharges of 2600 and 2144 m^3/s respectively were recorded. In the lower sector, at Arad, the highest discharge was recorded during the 1975 flood (2200 m^3/s), followed by the

1970 flood (2150 m^3/s) (Mustăţea 2005). In the Mureş corridor, from the South–Western Transylvanian Depression, the riverbed has a low slope and sandy bedrock. The analysis of the vertical dynamics in relation with the flow showed that, in the years with high discharges, when floods occurred, a sharper modification of the thalweg was also triggered (mostly incision). The most important periods with these modifications are between 1974 and 1982 at Alba Iulia and between 2004 and 2008 at Acmariu (Pandi and Horváth 2013). During high flow periods, the vertical dynamics of the riverbed was generally moderated (for example 1989–1996). The general tendency of incision in the bedrock, during the last decades, can be put on the account of anthropogenic improvements (mostly reservoir dams), built on Mureş River and its tributaries (mainly on Târnave rivers, with rich sediment loads). On the entire analysed period, the degradation of Mureş riverbed was of approx. 300 cm at Alba Iulia (between 1971 and 2010), and of approx. 40 cm at Acmariu (between 1977 and 2010). Based on the diachronical analysis of the lateral dynamics on a meandering sector, downstream Ocna Mureş (near Rădeşti village), the natural cut-off of two meanders was identified on images of 1978 and 2005, as a consequence of the major floods of 1975 and 2005. On the considered sector, the river length reduced from 8.406 km (in 1911) to 6.905 km (in 2005), and the sinuosity index from 2.4 to 2 (Pandi and Horváth 2013).

In *Arieș basin* (sub-basin of Mureş River, situated in the east of Western Carpathians and in the west of Transylvanian Depression), river channels of Arieş and its tributaries (for example Iara, Ocoliş), suffered changes due to the major floods of March 1981, December 1995 and July 2005. Consequently, after the 1981 March flood, when the Arieş River reached, at most of the gauging stations, the highest discharges of the 1978–2005 period (126 m^3/s at Câmpeni, 180 m^3/s at Buru), its riverbed degraded at Câmpeni by 0.7–0.9 m and by 0.5–1 m at Buru (at the exit from the Carpathians), mostly in the vicinity of the right bank. After the 2005 flood, on Iara River, at Iara gauging station, the riverbed degraded in the central sector by 35–45 cm, while, towards the banks, accumulation processes took place. In the case of Ocoliş River, the riverbed aggradated by 30–40 cm (Arghiuş 2008).

Rivers from the Banat Plain

Situated in the western part of the country, the Banat Plain corresponds to a tectonic basin, which has altitudes of less than 100 m in the subsiding plain of Timiş, low river slopes, large floodplains and numerous abandoned meanders (Posea 1995; Grecu 2010). The plain is drained by a dense stream network, among which the most important are Mureş, Timiş, Bega and their tributaries, which spring from the Carpathians. The high density of the hydrographic network, the low slopes of the riverbeds in the plain sector, the reduced depth of the groundwater, the presence of the red clay, all favour the floods and marshes. To reduce the amplitude of these phenomena, since the first half of the eighteenth century, large engineering works (damming, channelling, draining etc.) were made in the region, most of which are

still functional today. Among the major flash-floods and floods in the Banat Plain, the most important were those of May 1912, June 1966 and April 2005 (Fig. 33.1).

Due to abundant precipitations (over 150–200 mm) fallen in successive episodes in April 2005 (from 13th to 16th, 17th to 19th, 21st to 22nd and 26th to 27th), the second interval cumulating up to 100 mm and being the most important (Zaharia et al. 2006), four flood waves occurred on the main rivers (Bega and Timiş). The most important was the one after the second rainy interval, with peak discharges with return periods of 10–100 years. In some places, the water submerged even the protection dikes, and, on April 18th, under the pressure of water, the dike located on the right bank of Timiş gave up downstream Şag village; a volume of 350×10^6 m^3 of water flooded 21,200 ha (17,500 ha in Romania and 3700 ha in Serbia) in the low subsidence plain between Timiş and Bega, where it stagnated for several weeks, forming the so called "Sea of Banat". The water excess was eliminated by pumping, the action taking two months (Stănescu and Dobrot 2005). The high water volume spilled during the flash-flood and its velocity intensified the vertical and lateral geomorphological processes in the river channel, and the force with which the water entered the floodplain, through the dam breaches, as well as its long stagnation determined morphological modifications in the floodplain.

The Danube River on Romanian Territory

The second longest river of Europe (after Volga), the Danube flows on the Romanian territory on its last sector of 1075 km long (38 % of its total length of 2780 km), before reaching the Black Sea through the Danube Delta. The river forms the natural border between Romania and Serbia, Bulgaria, Moldova and Ukraine on about 800 km and drains approximately 98 % of the Romanian territory. After crossing the Carpathians through the Iron Gates defile, the Danube reaches the Romanian Plain, separating it from the Prebalkanic Plateau in the south, and the Dobrogea Plateau in the east. Upstream Călăraşi, the thalweg exceeds 0 m absolute elevation, while downstream the elevation falls below 0 m and even down to −30 m absolute elevation. According to the thalweg position, the water depth varies from 4 to 10–11 m (Institutul de Geografie 1969).

The analysis of river channel cross profiles' variations between 1993 and 2012 reveals two sectors with different characteristics situated approximately west and east of Giurgiu town. On the western sector, the erosion process took place in the vicinity of the right bank, while the accumulation one on the left bank. The maximum depth, recorded in 1993, remained on the centre of the channel at Corabia and on the right side at Zimnicea (Fig. 33.6a and Table 33.2). At Giurgiu, the cross profile becomes asymmetric, with the maximum depth near the left bank during the analysed period (Fig. 33.6a). Downstream, at Chiciu, the asymmetry changes and the maximum depth is observed near the right bank, recorded in 2003.

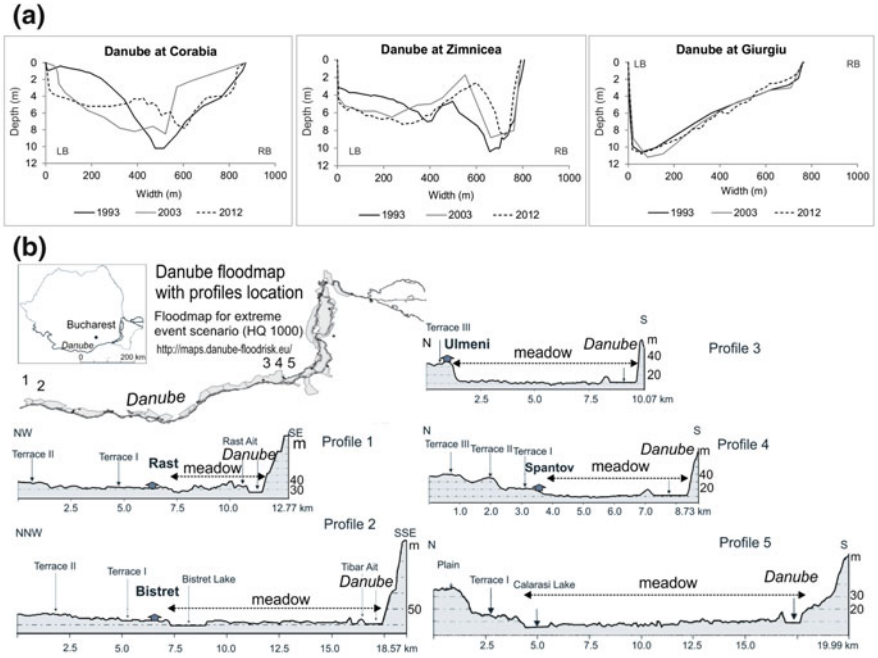

Fig. 33.6 **a** Variations of Danube's cross profile at Corabia, Zimnicea and Giurgiu gauging stations (based on data from A.N.A.R.). **b** Cross profiles on Danube valley (from SRTM)

Table 33.2 Morphometric elements of the cross profiles through the Danube river channel

Gauging station[a]	Cross-section area (m^2)			Width (m)			Mean depth (area/width) (m)			Maximum depth (m)		
	1993	2003	2012	1993	2003	2012	1993	2003	2012	1993	2003	2012
Corabia	3085	3781	4097	872	872	869	4.3	4.3	4.7	10.2	8.2	7.8
Turnu Măgurele	4166	4433	4739	651	651	651	6.4	6.8	7.2	9.8	9.8	9.9
Zimnicea	4617	4322	4369	807	792	794	5.7	5.4	5.5	10.4	8.8	8.5
Giurgiu	4648	4832	4739	761	760	766	6.1	6.3	6.1	10.6	11.2	10.8
Chiciu	4273	4337	4082	744	744	748	5.7	5.8	5.4	8.2	10	9.4

All the values are calculated at low water level

[a]The location of gauging stations is shown in Fig. 33.7a

Along the Romanian sector of the Danube, the river channel has a variable width, from less than 1 km to over 10 km (the maximum width is about 30 km in the ramification sector between Călăraşi and Brăila), while the relative altitude decreases along the river (upstream of Oltenița it exceeds 3 m at the mean level of the Danube). The river channel is delimited by terraces, the number of which decreases from west to east. The inferior terrace (t1) stretches along the river between Baziaş and Brăila; its mean altitude varies between 5–6 m and 12–13 m; it

is inhabited and the towns and villages extend also in the floodplain, being vulnerable to floods (Grecu et al. 2007).

The current morphohydrology of the river channel was strongly modified by the engineering works (dams, dikes, draining etc.), with impacts on the liquid and solid discharge and on the fluvial dynamics. In Danube's floodplain, diking works started in 1904, and the maximum diked area was reached in 1987—431,700 ha (representing 75 % of Romanian Danube's floodplain, which extend on 573,000 ha), in 53 closed perimeters, with a total length of the dikes of 1158 km. Drainage works were achieved on 418,000 ha and the irrigation ones on 225,000 ha (Stanciu et al. 2010; Vişinescu and Bularda 2008). The diking works along the Romanian sector of the Danube determined the rise of the water level, by 0.6 m upstream and 1.2 m downstream (Vişinescu and Bularda 2008), which allows a faster propagation of floods.

The morphometry and relief of the floodplain represent favourable or restrictive factors in the natural or anthropic dynamics of the floods. The morphological cross profiles of the Danube valley, combined with the floods of 2006, emphasise the significance of the width and relative altitude of the river channel. Between Rast and Bistreţ, where the floodplain exceeds 11 km in width, the river overflowed the banks and the dikes, covering the floodplain as far as the Bistreţ Lake. At Spanţov and Ulmeni, the floodplain has only 3 and 6 km respectively in width, therefore a large volume of water was spilled on small areas (profiles 3 and 4 on Fig. 33.6b).

Danube River has a mean multiannual discharge at the entrance in the country (at Baziaş gauging station) of 5352 m^3/s; this value increases before reaching the delta (at Isaccea) to 6450 m^3/s (1931–1944, from A.N.A.R.). Between 1840 and 2010, the minimum discharges of the Danube decreased to less than 1300 m^3/s, while the maximum ones surpassed 15,000 m^3/s (Şerban et al. 2006; Sălăjan et al. 2011; Zaharia and Ioana-Toroimac 2013). The Danube floods are specific to spring and summer. Due to the very large basin area (over 800,000 km^2), the floods are slow, with durations ranging from a few weeks to 1–2 months. These are generally caused by high spring precipitations, associated with water from snow melting. The biggest floods from the systematic measurements period (which started in 1838, at Orşova) occurred in 1895, 1987, 1970, 2006, 2010, when the Danube discharges exceeded 15,000 m^3/s on some sectors (Şerban et al. 2006; Sălăjan et al. 2011) (Table 33.3).

During the flood of spring 2006, the Danube registered, at the entrance in the country (at Baziaş), the highest discharge from the measuring period: 15,800 m^3/s on April 15th. The peak discharges of this flood had values higher than those with a return period of 100 years at several stations along the Romanian Danube (Fig. 33.7b). The Danube level exceeded in most of the sections the projected levels of dikes, of 20 years return period (in some cases with over 100 cm) and of 100 years (with more than 40–60 cm) (Fig. 33.7b, c), and the water overflowed the floodplain. Due to the long duration of the flood, which lasted over 2 months (Fig. 33.7a), the pressure exerted by the water generated, directly, 7 natural breaches in the dikes, which inundated 57,501 ha, and, indirectly, 2 controlled breaches and 15,643 ha (Mihailovici et al. 2006b). Therefore, 20 % of the diked areas were flooded (Vişinescu and Bularda 2008). The flash-flood and the associated floods determined some modifications of the river channel and of Danube floodplain.

Table 33.3 Maximum levels and discharges of the Danube during the floods of 1970, 1981, 2006 and 2010 (from Şerban et al. 2006; Anghel et al. 2010; Teodor et al. 2010)

Nº	Gauging station[a]	Maximum levels (m)				Maximum discharges (m^3/s)			
		1970	1981	2006	2010	1970	1981	2006	2010
1	Baziaş					13,710	14,800	15,800	12,070
2	Gruia	823	862	899	760	13,900	14,700	15,800	12,430
3	Calafat	776	802	861	710	14,300	14,100	15,495	
4	Bechet	784	787	845	735	13,830	14,250	15,825	
5	Corabia	756	745	801	665	13,630	14,300	15,730	
6	Turnu Măgurele	710	701	790	691	14,940	14,400	16,500	
7	Giurgiu	795	772	822	727	14,930	15,000	16,500	14,200
8	Oltenița	772	763	809	722	14,640	14,600	16,422	
9	Călărași	703	711	737	692	15,800	14,800	15,760	
10	Brăila	637	619	699	713	15,000	13,700	14,670	14,990
11	Galați	595	580	661	678			14,420	16,220
12	Isaccea	507	490	524	537	18,000	14,500	14,325	16,240

[a]The location of the gauging stations is shown in Fig. 33.7a

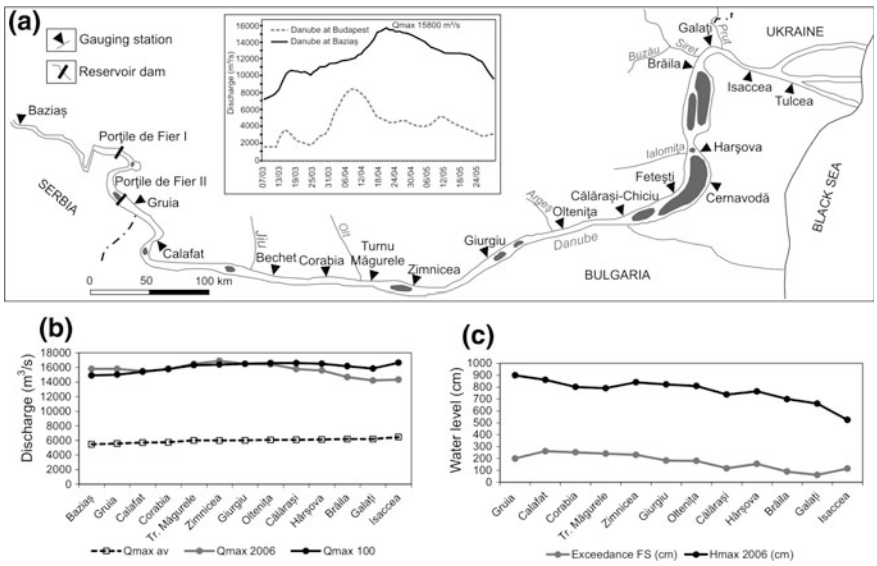

Fig. 33.7 **a** Gauging stations' location on the Danube and the flood of spring 2006 (hydrograph modified from Baciu et al. 2006). **b** Maximum discharges of the Danube recorded during spring 2006 flood (Qmax 2006) compared with maximum discharges with a return period of 100 years (Qmax 100) and with mean maximum discharges (Qmax av). **c** Maximum water levels of the Danube recorded at the stuff gauge during spring 2006 flood (Hmax 2006) and the exceedance of the flooding stage (FS) (from Baciu et al. 2006)

The sediment load has an important role in the river channel dynamics. Between 1956 and 1995, the suspended sediment load had a mean value of 657 kg/s at Baziaş and 1230 kg/s at Ceatal Izmail (Bondar et al. 1996). During the 1981 flood, which lasted 47 days, the sediment volume transported by the Danube represented 11.3–30 % of the mean volume of the same year. During the 2006 flood, which lasted 75 days, the sediment volume represented 24.8–51 % of the mean volume of the same year, with values oscillating between 6.9×10^6 t at Baziaş and 8.55×10^6 t at Isaccea (Teodor et al. 2010).

Flash-Floods and Their Morphodynamic Role

In the mountain and hilly regions, the flash-floods, generally at local scale and, generated by heavy rains with convective origins in summer, are of high importance for channel dynamics. These are specific to rivers draining small-size catchments (up to hundreds of km^2), with high slopes, dense relief fragmentation, low forestation and large impermeable areas. The force of these floods is amplified by the materials that are eroded and transported; sometimes they become muddy flows with strong mechanical impact on the river channel.

The flash-flood from Ilişua River basin. On June 20th 2006, the Ilişua River basin, located on the western side of the Eastern Carpathians (basin area 350 km^2, mean altitude approx. 500 m, slope 15%), received heavy rains that exceeded 110 l/m^2, with an intensity of over 251/m^2/h (Şerban et al. 2010; Hognogi et al. 2011). The heavy rains generated flash-floods, with human loses (11 dead), material damages, and hydrogeomorphological impact. On the Ilişua River (52 km in length), the flood wave reached 4.5 m in height from the thalweg, flooding the lower part of the valley. The peak discharge estimated for a mean section was of 280 m^3/s, corresponding to a probability of 0.7–0.8 % (Hognogi et al. 2011). At Târlişua, the maximum estimated discharge was 249 m^3/s, and the rising time of only 10 min (Şerban et al. 2010). The flood caused changes in the morphology of the river channel and floodplain. Important volumes of sediments were dislocated from the upper course and deposited in the middle and inferior sectors, causing riverbed's aggradation. At Cristeştii Ciceului station, the suspended sediment discharge reached 21,500 kg/s, which reflects the impressive erosive and transportation force of the flood. Consequently, the river channel has widened by 2–3 m and up to 10–12 m in some places, abandoned old channels and created new ones (within the floodplain), cut loops, incised or aggradated the riverbed (Purdel 2011). In the confluence sectors, the sediments brought by the tributaries were deposited as alluvial fans in the river channel and the floodplain of Ilişua River. The flood and inundation generated some modifications in the river channel morphology due to fine material accumulation (mud, sand and clay) with a thickness of 0.2–1.5 m and even coarser materials (gravel), that created mounds and bars with heights of 0.5–1 m (Purdel 2011). River channel morphology was also adjusted by landslides and bank collapse.

Conclusions

Flash-floods and floods occurring on rivers in Romania had different magnitudes and characteristics, both spatially and in time, with significant effects on the morphology of river channels and floodplains due to erosion and accumulation processes. During floods, the interactions between morphological processes and hydrological ones may have an ephemeral character, reversible on short-term, but influencing the long-term evolution of the river. One can observe that vertical variations of river channels may reach tens and even hundreds of centimetres, whereas lateral variations have the tendency to redress the river channels towards a previous equilibrium.

The hydrogeomorphological processes due to floods have negative socio-economical and environmental impact. The impact on the population and the environment can be considered of mean magnitude, except for the overflowing of the Danube and the flash-floods. The settlements from floodplains, the transport infrastructure and the engineering works are vulnerable to flash-floods and floods. This spotlights the highly applied character of hydrogeomorphology.

References

Administraţia Naţională Apele Romane (ANAR) (2014) Zone afectate de inundaţii istorice semnificative. http://www.rowater.ro/EPRI%20%20Harti%20zone%20afectate%20de%20inundatii/PFRA_Romania.jpg. Accessed Nov 2012 (in Romanian)

Administratia Naţională Apele Romane – Institutul National de Hidrologie şi Gospodărire a Apelor (ANAR-INHGA) (2011) Sinteza studiilor de fundamentare a schemelor directoare de amenajare şi management ale bazinelor hidrografice. http://www.mmdiu.ro/protectia_mediului/evaluare_impact_planuri/2012-03-15_evaluare_impact_planuri_planamenajarebazinehidro2011.pdf. Accessed Nov 2012 (in Romanian)

Anghel E, Frimescu L, Baciu O, Simota M, Gheorghe C (2010) Caracterizarea viiturilor excepţionale din 2010. In: Abstracts of the Conferinţa Ştiinţifică Jubilară a Institutului Naţional de Hidrologie şi Gospodarire a Apelor, Bucharest, Sept 2010, pp 178–190 (in Romanian)

Arghiuş V (2008) Studiul viiturilor de pe cursurile de apă din estul Munţilor Apuseni şi riscurile associate. Editura Casa Cărţii de Ştiinţă, Cluj-Napoca (in Romanian)

Armaş I, Nistoran Gogoaşe D, Osaci-Costache G, Braşoveanu L (2012) Morphodynamic evolution patterns of Subcarpathian Prahova Valley (Romania). Catena 100:83–99. doi:10.1016/j.catena.2012.07.007

Arnaud-Fassetta G, Fort M (2004) La part respective des facteurs hydroclimatiques et anthropiques dans l'évolution récente (1956-2000) de la bande active du Haut Guil, Queyras, Alpes françaises du Sud. Méditerranée 1–2:143–156

Arnaud-Fassetta G, Cossart E, Fort M (2005) Hydro-geomorphic hazards an impact of man-made structures during the catastrophic flood of June 2000 in the Upper Guil catchment (Queyras, Southern French Alps). Geomorphology 66:41–67. doi:10.1016/j.geomorph.2004.03.014

Baciu O, Anghel E, Frimescu L, Corbuş C, Ciobotaru D, Mătreaţa M, Simota M (2006) Elaborarea prognozelor hidrologice pe Dunăre în perioada viiturii din intervalul aprilie-mai 2006. Hidrotehnica 51(5):21–30 (in Romanian)

Ballais J-L, Chave S, Dupont N, Masson E, Penven M-J (2011) La méthode hydrogéomorphologique de détermination des zones inondables. Physio-Géo 5. doi:10.4000/physio-geo.3307

Bălteanu D, Jurchescu M, Surdeanu V, Ionita I, Goran C, Urdea P, Rădoane M, Rădoane N, Sima M (2012) Recent landform evolution in the Romanian Carpathians and pericarpathians regions. In: Lócyz D et al (eds) Recent landform evolution: the Carpatho-Balkan-Dinaric region. Springer Science+Business Media M.V., pp 249–286

Bojoi I, Apetrei M, Vârlan M (1998) Geomorfometria luncilor. Model de analiză în bazinul superior al Jijiei. Editura Academiei Române, Bucureşti (in Romanian)

Bondar C, State I, Buta C, Harabagiu E (1996) Date privind bilanţul scurgerii de aluviuni în suspensie şi procesele morfologice de albie pe sectorul românesc al Dunării în perioada anilor 1956–1995. Sesiunea de comunicări ştiinţifice I.N.M.H., Manuscript, Bucureşti (in Romanian)

Cyril F, Douvient J, Delahaye D (2013) Introduction du numéro thématique: "Hydro-géomorphologie quantitative". Geomorphologie: relief, processus, environnement 1:3–6

Demers S, Olsen T, Buffin-Bélanger T, Marchand J-P, Biron PM, Morneau F (2014) L'hydrogéomorphologie appliquée à la gestion de l'aléa d'inondation en climat tempéré froid: l'exemple de la rivière Matane (Québec). Physio-Géo 8:67–88

Diaconu C (1971) Râurile României. Monografie hidrologică. Institutul de Meteorologie şi Hidrologie, Bucureşti (in Romanian)

Diaconu C, Şerban P (1994) Sinteze şi regionalizări hidrologice. Editura Tehnică, Bucureşti (in Romanian)

Dumitriu D (2007) Sistemul aluviunilor din bazinul râului Trotuş. Editura Universităţii Suceava, Suceava (in Romanian)

Gâştescu P, Ţuchiu E (2012) The Danube river in the lower sector in two hydrological hypostases —high and low waters. Riscuri şi catastrofe XI(10, 1):165–182

Gogoaşe Nistoran D, Armaş I, Ionescu C (2011) Inundation maps for extreme flood events at the mouth of the Danube River. Int J Geosci 2:68–74

Goţiu D, Surdeanu V (2008) Hazardele naturale şi riscurile associate din Ţara Haţegului. Presa Universitară Clujeană, Cluj-Napoca (in Romanian)

Grecu F (1992) Bazinul Hîrtibaciului, Elemente de morfohidrografie. Editura Academiei, Bucureşti (in Romanian)

Grecu F (2009) Hazarde şi riscuri naturale. Editura Universitară, Bucureşti (in Romanian)

Grecu F (2010) Geografia câmpiilor României. Editura Universităţii din Bucureşti, Bucureşti (in Romanian)

Grecu F, Zaharia L, Ioana-Toroimac G, Dobre R (2007) Risque meteo-hydrologique dans la vallée du Danube roumain. Le cas des inondations d'avril – mai 2006. In: Ben Boubaker H (ed) Actes du XXeme Colloque de l'Association Internationale de Climatologie, Tunis-Carthage, 3–8 Sep 2007, pp 277–282

Grecu F, Osaci-Costache G, Ioana-Toroimac G (2008) Dynamics tendency of some minor riverbeds in the Curvature Subcarpathians. Paper presented at the 13th Belgium-France-Italy-Romania geomorphological meeting, Porto Heli, Greece, 18–21 June 2008

Grecu F, Zaharia L, Ghiţă C, Vacaru L (2010) The dynamic factors of hydrogeomorphic vulnerability in the central sector of the Romanian plain. Metal Int XV(9):139–148

Grecu F, Zaharia L, Ghiţă C, Comănescu L, Cîrciumaru E, Albu M (2012a) Sisteme hidrogeomorfologice din Câmpia Română. Hazard – Vulnerabilitate – Risc. Editura Universităţii din Bucureşti, Bucureşti (in Romanian)

Grecu F, Molin P, Dobre R, Ioana-Toroimac G, Fubelli G, Dramis F (2012b) River channel dynamics in the contact area between Romanian Plain and Curvture Subcarpathians (Romania). Paper presented at the 16th joint geomorphological meeting, morphoevolution of tectonically active belts, Rome, 5–12 July 2012

Grecu F, Ioana-Toroimac G, Zaharia L (2013) River channel recent dynamics in relation to floods in the Curvature Carpathians (Romania). Paper presented at the 7th conference IAG, Paris, 27–31 Aug 2013

Grecu F, Ioana-Toroimac G, Molin P, Dramis F (2014) River channel dynamics in the contact area between Romanian Plain and Curvature Subcarpathians. Rev Geomorfol 16:5–12
György Sipos (2012) Past, present, future of the Maros/Mureş River. FUTUMAR. Timişoara
Habersack H, Piégay H, Rinaldi M (eds) (2008) Gravel-bed rivers VI: from process understanding to river restoration. Elsevier, Amsterdam, pp 525–555
Hack JT (1957) Studies in longitudinal stream profiles in Virginia and Maryland. US geological survey professional paper (249-B), pp 45–97
Hognogi G, Nicula G, Cocean G (2011) Flash floods in the Ilişua basin. Aerul şi apa componente ale mediului, pp 465–472
Ichim I, Rădoane M (1990) Channel sediment variability along a river: Siret river case study (Romania). Earth Surf Land Process 15:211–225
Ichim I, Bătucă D, Rădoane M, Duma D (1989) Morfologia şi dinamica albiilor de râu. Editura Tehnică, Bucureşti (in Romanian)
Ichim I, Rădoane M, Rădoane N, Grasu C, Miclăuş C (1998) Dinamica sedimentelor. Aplicaţie la râul Putna – Vrancea. Editura Tehnică, Bucureşti (in Romanian)
Institutul de Geografie (1969) Geografia văii Dunării româneşti. Editura Academiei, Bucureşti (in Romanian)
Ioana-Toroimac G (2009) La dynamique hydrogeomorphologique de la riviere Prahova (Roumanie). Doctoral thesis, UST Lille and University of Bucharest. https://ori-nuxeo.univ-lille1.fr/nuxeo/site/esupversions/f9686450-07f1-4411-98a5-972b3357e9c2. Accessed on Sept 2014
Ioana-Toroimac G, Grecu F (2013) Abandoned borrow pits—an issue of landscape management. Case study: Buzău River's floodplain (Romania). Paper presented at the 7 conference IAG, Paris, 27–31 Aug 2013
Ioana-Toroimac G, Dobre R, Grecu F, Zaharia L (2010) Évolution 2D de la bande active de la Haute Prahova (Roumanie) durant les 150 dernières années. Géomorphologie: relief, processus, environnement 3:275–286
Ioana-Toroimac G, Zaharia L, Grecu F (2013) Braided channel's adjustments and hydroclimatic variability. Case study: Slănic River (Buzău watershed). In: Papers of INHGA—scientific conference, Bucharest, 23–26 Sept 2013, pp 67–74
Kondolf GM, Piégay H (eds) (2003) Tools in fluvial geomorphology. Wiley, Chichester
Larue J-P (2014) Profils longitudinaux et ruptures de pente: enseignements géomorphologiques en Bretagne du sud. Physio-Géo 8. doi:10.4000/physio-geo.3798
Malavoi JR, Bravard JP (2010) Eléments d'hydromorphologie fluviale. http://www.onema.fr/hydromorphologie-fluviale. Accessed on Sept 2014
Masson M, Garry G, Ballais J-L (1996) Cartographie des zones inondables. Approche Hydrogéomorphologique. Edition Villes et territoires, Paris
Mihailovici M (2006) Convieţuind cu viiturile. Paper presented at the world water day conference, Bucharest, Romania, 23 Mar 2006 (in Romanian)
Mihailovici JM, Gabor O, Rândaşu S, Asman I (2006a) 2005 floods in Romania. Hidrotehnica 51(6):26–35
Mihailovici J, Gabor O, Pătru Ş, Rândaşu S (2006b) Soluţii propuse pentru reamenajarea fluviului Dunărea pe sectorul românesc. Hidrotehnica 51(5):9–20 (in Romanian)
Molin P, Fubelli G, Nocentini M, Sperini S, Ignat P, Grecu F, Dramis F (2012) Interaction of mantle dynamics, crustal tectonics and surface processes in the topography of the Romanian Carpathians: a geomorphological approach. Glob Planet Change 90–91:58–72
Mustăţea A (2005) Viituri excepţionale pe teritoriul României. Geneză şi efecte. Editat de I.N.H.G. A., Bucureşti (in Romanian)
Obreja F (2012) The sediment transport of the Siret River during the floods from 2010. Forum geografic. Studii şi cercetări de geografie şi protecţia mediului XI(1):90–99. doi:10.5775/fg.2067-4635.2012.064.i
Pandi G, Horváth C (2013) Mureş River middle course riverbed dynamics between the Arieş and Strei confluences. Aerul şi apa componente ale mediului:49–56

Pandi G, Sorocovschi V (2009) Dinamica verticală a albiei râurilor în Dealurile Clujului şi Dejului. Riscuri şi catastrofe VIII(7):218–226 (in Romanian)
Perşoiu I, Rădoane M (2011) Spatial and temporal controls on historical channel response. Study of an atypical case: Someşul Mic River, Romania. Earth Surf Land Process 36(10):1391–1409
Petrea NM, Man N (2011) Characteristics of the flood wave from June 2011 on Arpaşu Mare River at Arpaşu de Sus gauging station. In: Papers – Conferinţa Ştiinţifică anuală Institutul Naţional de Hidrologie şi Gospodărire a Apelor, Bucharest, 1–3 Nov 2011, pp 284–294. http://inhgacercetare.ro/doc/inhga_2011/2-24_287-294_Petrea-Man_INHGA%202011.pdf. Accessed on Sept 2014
Posea G (1995) Câmpia de Vest a României. Editura Fundaţiei România de Mâine, Bucureşti (in Romanian)
Posea G (2002) Geomorfologia Romaniei. Editura Fundaţiei România de Mâine, Bucureşti (in Romanian)
Purdel A (2011) Analiză asupra modificărilor geomorfologice majore produse de viitura excepţională de pe râul Ilişua din data de 20.06.2006. In: Papers of Conferinţa Ştiinţifică Anuală a Institutului Naţional de Hidrologie şi Gospodărire a Apelor, Bucharest, 1–3 Nov 2011, pp 295–302. http://inhgacercetare.ro/doc/inhga_2011/2-25_295-302_Purdel_INHGA%202011.pdf. Accessed on Sept 2014 (in Romanian)
Rădoane M, Ichim I, Pandi G (1991) Tendinţe actuale în dinamica patului albiilor de râu din Carpaţii de Curbură. Studii şi cercetări de geografie, XXXVIII:21–31 (in Romanian)
Rădoane M, Rădoane N, Dumitriu D (2003) Geomorphological evolution of longitudinal river profiles in the Carpathians. Geomorphology 50:293–306
Rădoane M, Rădoane N, Cristea I, Oprea-Gancevici D (2008) Evaluarea modificărilor contemporane ale albiei râului Prut pe graniţa romanească. Rev Geomorfol 10:57–73 (in Romanian)
Rădoane M, Perşoiu I, Cristea I, Chiriloaei F (2013) River channel planform changes based on successive cartographic data. A methodological approach. Rev Geomorfol 15:69–88
Săcrieru R (2008) Bazinul morfohidrografic Milcov. Studiu geomorfologic. Teza doctorat, Universitatea din Bucureşti, Bucureşti (in Romanian)
Sălăjan L, Frâncu A, Druţă A (2011) Aspecte ale viiturilor pe Dunăre din anul 2010. Paper presented at the Sesiunea anuală de comunicări Institutul Naţional de Hidrologie şi Gospodărire a Apelor, Conferinţa Ştiinţifică Jubiliară, Bucharest, 1–3 Nov 2011
Schumm SA (1985) Patterns of alluvial rivers. Annu Rev Earth Planet Sci 13:5–27
Şerban P, Gălie A, Buţă C (2006) Analiza viiturilor produse pe Dunăre în perioada aprilie – mai 2006. Hidrotehnica 51(5):3–8 (in Romanian)
Şerban P, Selagea G, Máthé H, Hognogi EG (2010) Efecte produse de viitura din 20.06.2006 în bazinul râului Ilişua (bazinul Someşul Mare). Aerul şi apa componente ale mediului:156–165
Şerbu M, Obreja F, Olariu P (2009) Viiturile din anul 2008 în bazinul superior al Siretului. Cauze, efecte, evaluare. Hidrotehnica 54(12):38–44 (in Romanian)
Sorocovschi V (2005) Câmpia Transilvaniei. Studiu hidrogeografic. Ed. Casa Cărţii de Ştiinţă, Cluj-Napoca (in Romanian)
Stanciu P (2004) Caracteristicile viiturilor şi secetelor. Hidrotehnica 49(2–3):27–33 (in Romanian)
Stanciu P, Oprişan E, Tecuci I (2010) Elemente de strategie în gestionarea integrată a Apelor fluviului Dunărea. Paper presented at the Conferinţa Ştiinţifică Jubiliară, Institutul Naţional de Hidrologie şi Gospodărire a Apelor, Bucharest, 28–30 septembrie 2010 (in Romanian)
Stănescu V, Dobrot R (2005) Viitura din perioada 14–30 aprilie 2005 in bazinul hidrografic Timiş – Bega. Hidrotehnica 50(7–8):3–16
Stângă IC (2012) Bazinul Tutovei. Riscurile naturale şi vulnerabilitatea teritoriului. Editura Univ. "Alexandru Ioan Cuza", Iaşi (in Romanian)
Swanson BJ, Meyer GA, Coonrod JE (2011) Historical channel narrowing along the Rio Grande near Albuquerque, New Mexico in response to peak discharge reductions and engineering: magnitude and uncertainty of change from air photo measurements. Earth Surf Land Process 36:885–900

Teodor S, Rădulescu C, Ciucă R (2010) Tranzit aluvionar comparativ pe sectorul romanesc al Dunării, rezultat pe perioada celor mai mari viituri din ultimele trei decenii. Paper presented at the Conferinţa Ştiinţifică Jubiliară, Institutul Naţional de Hidrologie şi Gospodărire a Apelor, Bucharest, 28–30 septembrie 2010 (in Romanian)

UNISDR (2009) Terminology on disaster risk reduction. United Nations Geneva http://www.unisdr.org/files/7817_UNISDRTerminologyEnglish.pdf. Accessed on Sept 2014

Vişinescu I, Bularda M (2008) Modificări severe în regimul hidrologic al Dunării şi impactul acestora asupra agriculturii în lunca îndiguită. Analele INCDA Fundulea LXXVI:101–112 (in Romanian)

Vodă M (2007) Bazinul Târnave. Amenajări şi scurgere lichidă. Editura Casa Cărţii de Ştiinţă, Cluj-Napoca (in Romanian)

Zaharia L, Ioana-Toroimac G (2013) Romanian Danube River management: Impacts and perspectives. In: Arnaud-Fassetta G, Masson E, Reynard E (eds) European continental hydrosystems under changing water policy. Friedrich Pfeil Verlag, München, pp 159–170

Zaharia L, Beltrando G, Nedelcu G, Boroneant C, Ioana-Toroimac G (2006) Les inondations de 2005 en Roumanie. In: Beltrando G, Madelin M, Quénol H (eds) Actes du XIXème Colloque International de Climatologie, Epernay (Franţa), 6–9 Septembre 2006, pp 557–562

Zaharia L, Grecu F, Ioana-Toroimac G, Chirilă G (2011) Sediment transport and river channel dynamics in Romania—variability and control factors. In: Manning AJ (ed) Sediment transport in aquatic environments. TECH, Rijeka, pp 293–316

Chapter 34
Storm Climate and Morphological Imprints on the Danube Delta Coast

Florin Zăinescu and Alfred Vespremeanu-Stroe

Abstract Coastal storms hitting the Danube Delta coast are recurring high-energy events (of high winds and waves), which in most cases are the result of Mediterranean (extratropical) cyclones following different trans-Balkan routes. By using long-term wind (1962–2012) and wave (1949–2013) data, we investigated the climatology of storms and their impact on the deltaic coast. There are on average 30 storms/year occurring with a distinct seasonality, from which ca. 3 events/year correspond to severe storms (wind speed $v \geq 20$ m/s; significant wave height $H_s \geq 4$ m) usually registered during the winter months. Storminess shows a significant multidecadal variability with certain periods of increased activity as during the late '60s, the '70s and the '90s, and less active in the '80s or 2000s especially since 2006. These periods correlate well with the variations in the teleconnection patterns over Europe (NAO, EA, EARW, SCAND with −0.76, −0.55, 0.56, 0.55 as correlation coefficients). A 5-category scale of storms has been established using wind speed thresholds and associated wave heights that define morphological changes on the coast. The extreme storm of January 1998 is the only category V event for which data on topographic change is recorded, suggesting significant sediment losses and an extremely variable longshore response dictated by shoreline exposure to storm waves and pre-storm site morphology. Moreover, the large prevalence of the northern waves during storms created an apparent unidirectional (southward) development of the coastal features—islands, spits, and beach barriers, subaqueous deltaic platforms, depocenters—and finally ended up by conferring an asymmetric architecture to each of the five open-coast lobes with completely distinct features updrift (sandy strandplains) and downdrift (barrier-marsh plains and deltaic mud plains) of the river mouth.

F. Zăinescu (✉) · A. Vespremeanu-Stroe
Faculty of Geography, University of Bucharest, 1st N. Bălcescu Blv., sector 1, 010041 Bucharest, Romania
e-mail: florinzainescu@yahoo.com

A. Vespremeanu-Stroe
e-mail: fredi@geo.unibuc.ro

M. Rădoane and A. Vespremeanu-Stroe (eds.), *Landform Dynamics and Evolution in Romania*, Springer Geography,
DOI 10.1007/978-3-319-32589-7_34

Keywords Storms · North Atlantic Oscillation · Climate change · Beach hazards · Coastal erosion · Black Sea

Introduction

The atmosphere can interact directly with the coastal environment through the transport of wind-blown sand, but most wind energy is transferred to the coasts via wave propagation and dissipation nearshore. Wind waves are mainly a function of wind speed and secondary of wind duration and fetch length. Waves can arrive from hundreds of kilometers, the energy of which it gets converted into nearshore currents and sediment dynamics, when reaching the shore. Thus, the wind energy gathered by sea surface on thousands to hundreds of thousands of km^2 is then consumed on just a few tens or hundreds of kilometers of coasts whose dynamics is supported by the wave breaking associated processes. Moreover, most of this energy transfer is accomplished unevenly in only several high magnitude coastal storms that preferentially occur in one season. Onshore storms are the single-most important element in remobilizing the sediments and shaping the deltaic coast through the intensity of winds, waves, longshore currents, and storm surge (temporary rise in local sea level associated with the wave setup during storms) (Vespremeanu-Stroe 2007).

On the Danube Delta coast, severe storms are the result of the passage of Mediterranean (extratropical) cyclones, which follow different tracks over the Pontic region (Black Sea, Aegean Sea, Balkans, Anatolia) and make up over 80 % of the regular storm cases on the Romanian coast (Maheras et al. 2009). Similar to other types of extratropical cyclones, the Mediterranean depressions are low pressure systems formed by baroclinic instability processes with typical scales of 1000 km and lifespan of the order of 1 week. In reality, coastal storms occurrence is more complex, because the low intensity (regular) storms can arise from different atmospheric circulation conditions. In this regard, Maheras et al. (2009) identifies five anticyclonic and seven cyclonic circulation types, with only a few cyclonic circulation types determining the majority of storm events, and attributes the most extreme cases to a high pressure gradient along the Romanian Black Sea coast.

Storms pose significant hazards that can damage ecosystems and threat population. Extreme storms can cause flooding, dune destruction, barrier disintegration (Ferreira et al. 2009; Masselink and Sytze 2014) and important land loss on deltas, whereas frequent but low intensity events lower the beach elevation, widen the surf zone and determine high rates of sediment transport. At the same time, storms are a major risk factor for navigation, being able to cause shipwrecks, and for economic activities such as tourism and offshore oil rigs (Chiotoroiu and Ciuchea 2009). This situation is exacerbated in recent decades by the rising effects of anthropogenic climate change and sea level rise. Therefore, a thorough understanding of past storminess and short-term and long-term response of the coast to these events is highly important.

There are a few studies focusing on the western Black Sea coast which linked the medium-term (decadal) coastal evolution with storminess (Vespremeanu-Stroe et al. 2007), established thresholds and presented cases of storm impacts on the coast (Trifonova et al. 2012), or analyzed the storm climatology (Valchev et al. 2012; Zăinescu et al. submitted). This chapter aims: (i) to present a record of coastal wind and wave climatology for the Danube Delta, (ii) to interpret the change in storminess in the past decades in relation with the major modes of atmospheric variability, (iii) to briefly assess the morphological impact of the greatest storm recorded in the last 50 years (the case of the January 1998 extreme storm) and (iv) to illustrate the influences of wind and wave climate in shaping the geomorphology of the Danube Delta coast.

Regional Setting

The Danube Delta coast stretches on ca. 190 km in the northwestern part of the Black Sea basin (Fig. 34.1). The coast prograded over the last millennia through the three main distributaries (Sf. Gheorghe, Sulina, and Chilia) as a result of a rich fluvial sedimentary input of ca. 31×10^6 m^3/year [1840–2013, according to National Institute of Hydrology and Water Management (NIHWM) data]. It presents a highly diverse morphological construction, as a result of the interactions between river and waves in the virtual absence of tides. A variety of coastal configurations arises at the intersection of longshore currents and river mouths, with numerous barrier islands and spits—Sacalin, Musura, Oceakov, Bîstroe—and extremely fast eroding and accreting sectors. Although the coasts generally show N–S orientations, thus highly influenced by the NE waves, the E–W sector of Periteaşca–Ciotica is sheltered from the northern waves and receives most of the energy from the southern direction. Along the Danube Delta, beaches commonly display widths of 10-50 m and are controlled by the seasonal differences in storm activity and sea level, via Danube flow with common high widths in late summer—early fall months and low widths in the winter and early spring (Vespremeanu-Stroe and Preoteasa 2007). Stable sectors are frequently backed by 2–3.5 m high and 50–100 m wide foredunes, whereas retreating sectors consist of low lying sandy barriers vulnerable to overwashing. Beaches are fronted by multiple nearshore bars (1–3) displaying a multiannual offshore migratory trend (Tătui et al. 2014).

Storms show a bimodal distribution with a high frequency and intensity of northern winds (80 %) and less intense and less frequent southern winds (Fig. 34.1b). The land-locked Black Sea basin is protected from ocean swell and relies on local winds blowing over the available fetch to produce usually short, steep waves with short periods of 5–7 s. The wave climate in this case is a function of the fetch and depth of the sea combined with the prevailing winds, and exhibits considerable marine energy (H_s = 1.43 m) and a moderate to high sedimentary transport exerted by the longshore currents ($0.5–1 \times 10^6$ m^3/year) mainly depending on the shoreline aspect (Vespremeanu-Stroe 2004). The storm wave rose

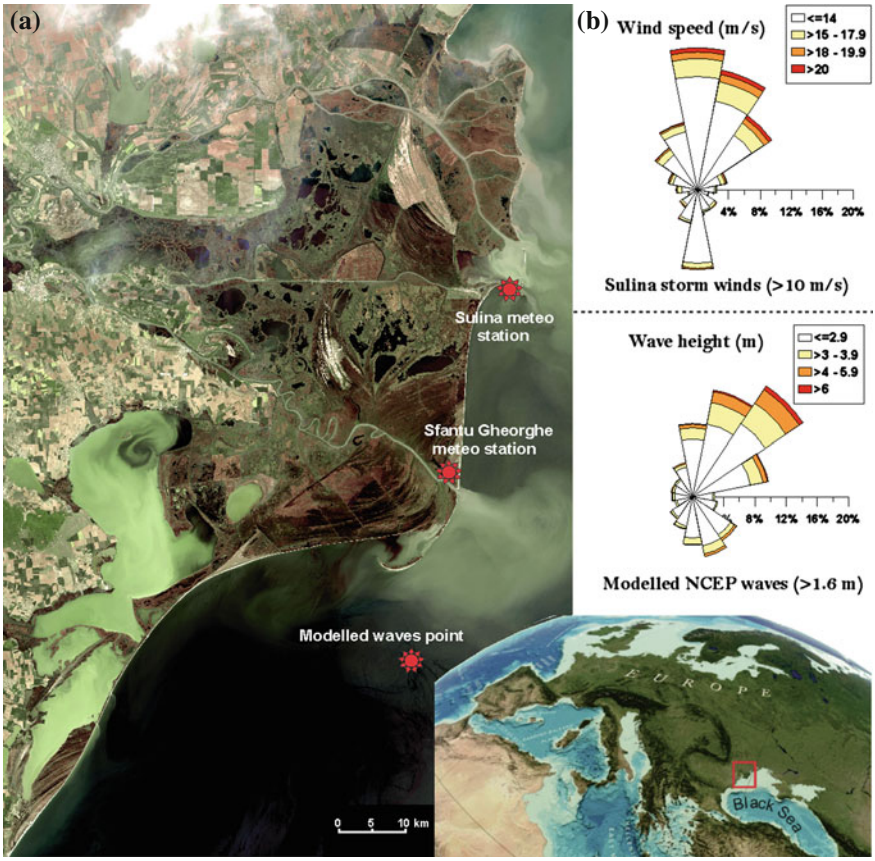

Fig. 34.1 Study site. **a** The Danube Delta coast and the location of weather stations and wave modelling point. **b** Wind and wave storm roses based on data from Zăinescu et al. submitted

shows a high occurrence of northeastern waves which also give the highest occurrence of extreme waves. These are the most erosive waves for the Danube Delta coast due to their high frequency and energy.

Methods

The current study analyzes wind and wave data previously reported in Zăinescu et al. (submitted). The wind dataset spans from 1962 to 2012 and consists of wind speed and wind direction measurements at the Sulina meteorological station (Fig. 34.1). The meteorological station is ideally located on the Sulina mouth jetties

Fig. 34.2 The Sulina meteorological station. The main building sits on top of the Sulina branch jetties. The wind measurement equipment is placed on *top* of the construction. *Photo* from the Sulina channel

(Fig. 34.2), at ca. 1.5 km away from the coastline, benefiting from the low roughness of the sea surface. Only recently (1980s) a few willows began to grow on the eastern side, but these are smaller (4–7 m) than the instrument height (10 m) and flank a direction where the strong winds are very uncommon. Hence, Sulina station may be regarded as a reliable long-term source of wind data. We also used a second wind dataset from the Sfântu Gheorghe meteo station, which is placed at ca. 1.5 km from the beach; and although its position is not sheltered by obstacles, the overall high roughness (the vicinity of the Sfântu Gheorghe village and a nearby forest plantation) make the wind speed values significantly lower than on the beach. Long-term data from nearshore wave buoys is missing for the Romanian coastal zone. In this regard, wave modeling can overcome this paucity of information. The modeled dataset spans 65 years, from 1949 to 2013, and is outputted hourly to a point in front of the Sfântu Gheorghe distributary mouth, at 18 km distance from the shore (Fig. 34.1), based on the NCEP/NCAR pressure reanalysis (Kalnay et al. 1996). A full description of wave data hindcast methodology is provided in Zăinescu et al. submitted.

A statistical analysis of storms imposes the necessity of setting a threshold of wind speed and wave height in order to identify a population of storm events. Storm thresholds depend on the local climatic and morphological conditions and have been established for the western Black Sea or Romanian coasts between 10 m/s and 15 m/s for at least 12 or 24 h (Vespremeanu 1987; Chiotoroiu 1999; Bocheva et al.

2007; Valchev et al. 2012). Here, we used a main wind threshold of minimum sustained wind speed of 10 m/s for 24 h, while for gathering data about shorter storms we used a less frequent threshold defined by a wind speed value of 10 m/s for at least 12 h, which includes a minimum period of 3 h with wind speeds reaching 15 m/s. The corresponding wave height threshold is of 1.6 m. A storm season was defined to start on the 1st of August and end on the 31st of July. The storm climate and its reception by the coast were assessed using the proxies of storm severity index (SSI), storm impact potential (SIP), and storminess index (SI) developed in Zăinescu et al. (submitted):

$$\mathrm{SSI} = \sum (V^3 T)/10^3 \tag{34.1}$$

where V = wind speed (m/s), T = Total duration of a certain wind speed (h).

$$\mathrm{SIP} = \sum (V^3 T \sin \alpha)/10^3 \tag{34.2}$$

where α = the angle between the wind direction and shoreline orientation.

The morphologic index (SIP) integrates both the wind speed and the wind angle and thus corresponds to the potential morphological impact of a storm. The sine of this angle has maximum values for angles around 90° (perpendicular) and decreases to 0 when reaching parallel to shore directions. Offshore wind directions are excluded. A value of 0.1 and not 0 is attributed to longshore wind directions (0°).

The Storminess index (SI) results from averaging wind data (normalized values of Sulina and Sfântu Gheorghe SSI) with wave data (normalized values of wave power).

$$\mathrm{SI} = S1 + S2 + \cdots + Sn \tag{34.3}$$

where Sn = normalized storm proxy for the parameter "n"; n = number of storm proxies available for a specific year.

The wave energy of a storm (wave energy flux) was computed by the equations provided by USACE (1984) and described by Moritz and Moritz (2006).

Monthly North Atlanic Oscillation (NAO), East Atlantic West Russia (EAWR), East Atlantic (EA), and Scandinavia pattern (SCAND) data were obtained from the Climate prediction Centre of the National Oceanic and Atmospheric Administration web site (http://www.cpc.ncep.noaa.gov/data/teledoc/telecontents.shtml) and correlated with storminess. Although DJFM (winter) values of NAOI are often cited in the literature, we used seasonal NAOI averages coinciding with a storm season (August–July) as we found no significant differences in correlations between the DJFM index and the seasonal one.

A 5-category scale of storms has been established on increasing thresholds of wind speed. Category I and II storms make up 90 % of all events, occurring at a rate

of 17 events (I) to nine events (II) per season. These storms reach a 10 and 15 m/s wind speed threshold for 24 and 15 h and waves do not usually pass 4 m. The category III and IV storms are severe, occur less often (∼9 % of cases), and reach 20 and 24 m/s, respectively for at least 6 h. An average season experiences 2–3 severe storms with offshore waves that may reach 7 m in height. The last category (V) corresponds to the most extreme cases when winds reach speeds of 28 m/s for at least 2 h. Only seven storms reaching these criteria have been identified, when offshore waves reached 7–10 m during storm peak.

Results

Seasonality and Multidecadal Variability

Storms are high magnitude wind and wave events which exhibit large seasonal, interannual, and multidecadal variability in the North–Atlantic and European regions (Valchev et al. 2012; Lionello et al. 2012; Clarke and Rendell 2009; Keim et al. 2004). This variability often reflects the seasonal occurrence of extratropical cyclones, which are more frequent during winter, whereas in some intervals (years) the storm tracks prefer meridionally diverted routes (more northern over the western Atlantic or southern routes over the Mediterranean) determined by mean air pressure differences in the North Atlantic between Azores high and Iceland low baric centers.

Seasonal variability shows the high frequency of storms in October–March interval if we consider the occurrence of all storm waves during a time span of 64 years, using the wave height threshold of 1.6 m (Fig. 34.3). Taking into account all waves (both fair-weather and storm conditions) the mean height varies considerably intra-annually, between 1.6 m in winter and a minimum of 0.65 m in the summer. Moreover, most of the wave energy is received by the shore in just a very short period (especially during severe and extreme storms) if consider that big waves (>4 m high), bringing half of the annual wave power to the shore, are encountered in 1 % of the time, mainly in the wintertime. The highest number of stormy days records in the 6–months active interval of October–March when ∼70 % of the storms occur, even more evident for severe and extreme storms (Category III–V: 84 %). This period has on average 40 stormy days with the highest probability of extreme storms occurrence (Category V) during December and January—1.35 extreme storm days/month.

During the winter months, especially in late January–February when seawater temperature reaches a minimum, coastal storms can encounter a frozen sea state and a sheltered beach behind ice feet (a rampart-like ice feature) which severely lessen

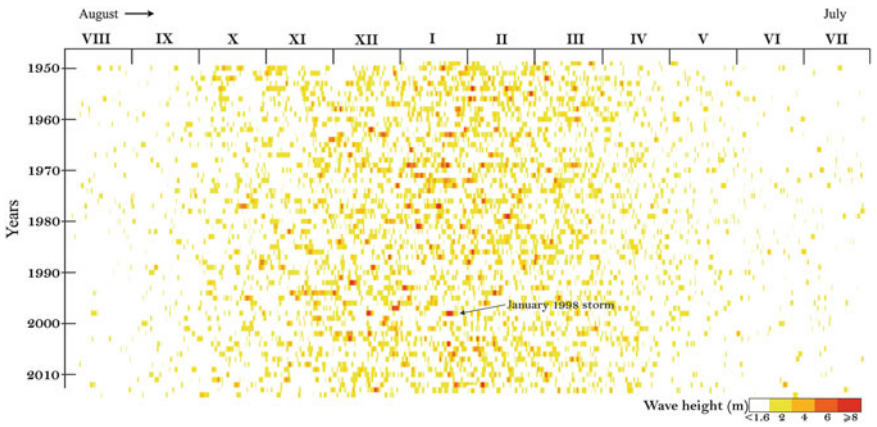

Fig. 34.3 Temporal distribution of storm waves (1949–2013). Each cell represents 3 h intervals. Horizontal scale (I–XII) represents calendar months (January–December)

their impact. Sea surface can freeze in exceptional cases hundreds of meters offshore and even more than one kilometer due to the low salinity of Danube Delta coastal waters. The big frozen events are associated with cold air mass intrusion lasting for several weeks such as in January–February 1958, February 2003, or February 2012. The storms producing in January and February have a chance of 35–40 % to encounter ice feet on the beach which normally means a minor morphological impact (Zăinescu et al. submitted).

At a medium-term (decadal) timescale large storminess amplitudes are noticeable when analyzing the seasonal SSI or wave power (Fig. 34.4).

The highest clustering of severe storms recorded during 1967–1973, including two extreme events in 1969 and 1973 (Fig. 34.5), which displayed wind speeds and offshore waves that reached 28 m/s and 10 m, respectively. Total wave power and

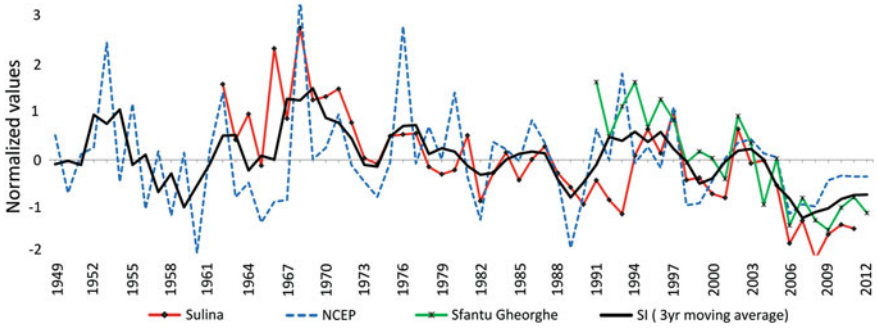

Fig. 34.4 Time series of SI (storminess index) and SSI (counted for Sulina and Sfântu Gheorghe) for the Danube Delta coast (from Zăinescu et al. submitted)

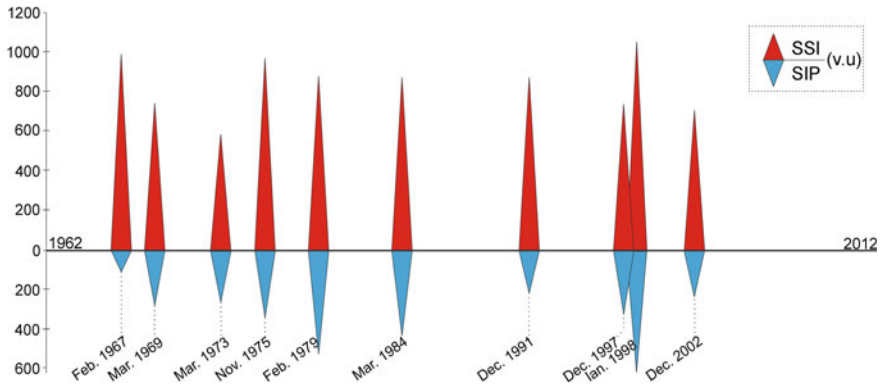

Fig. 34.5 Top 10 storms (5-year return period) based on SSI. Note the difference between the SSI and the corresponding SIP values attributable to different wind directions (from Vespremeanu-Stroe et al. 2014)

duration of big waves (higher than 4 m) is greatest during this interval. In terms of intensity, 1991–1998 interval is the second energetic interval with two extreme storms occurring in the same winter—extreme storm cluster of December 1997–January 1998—which caused massive impact on the Danube Delta coast. These storms reached waves of 8–10 m, lasted 4–7 days and were exceptionally aggressive due to strong onshore NE winds (25–30 m/s). In respect to their close temporal occurrence, the two extreme storms can be considered a cluster and it is the only example of this kind in the last 50 years.

Three periods of moderate storminess have been identified: 1958–1966, 1974–1981, and 1999–2005. During these intervals, storms were less frequent but extreme events still occurred. One of them, occurred in February 1979, is the second strongest storms. Storm waves lasted for 8 days and reached 10 m in height at which time the Sf. Gheorghe village was flooded causing the collapse of numerous buildings. This storm was also reported on the Bulgarian coast and caused prolonged flooding, infrastructure damage, and erosion (Andreeva et al. 2011).

Quiescent intervals, or periods of low storminess occurred in 1958–1966, 1982–1990 and 2006–2013. Only a single case of one-year return period storm occurred in the last interval in February 2012, which indicates a major decrease in storm magnitude and frequency in both wave and wind parameters. The stormy, moderate, and quiescent periods appear to succeed one after other at intervals of 7–9 years. This was first noted by Valchev et al. (2012) for the Bulgarian Black Sea coast. In terms of wind direction, all severe and extreme storms show northern and northeasterly wind and wave characteristics.

Links with Large-Scale Teleconnection Patterns

Teleconnections are interactions between widely separated parts of the ocean and the atmosphere occurring at different time scales (Orfila et al. 2005). Anomalies often persist for several consecutive years influencing the multidecadal climate variability and induce spatial and temporal scale correlations (Kiladis and Diaz 1989). The most known teleconnection is the El Niño Southern Oscillation (ENSO) which develops anomalies over the equatorial Pacific (Philander 1990). The second well known teleconnection is the NAO which is the dominant mode of climatic variability in temperate northern hemisphere (Hurrell 1995). The NAO is related to the Icelandic low and Azores high pressure centers that cause storms to prefer routes over Northern and Western Europe when difference in pressure is greatest, whereas storm tracks shift to southeastern Europe in the opposite situation (Hurrell 1995; Tsimplis and Shaw 2008). Other teleconnection patterns interplay with the NAO and influence the European climate (Moore et al. 2013). The EA is a prominent mode of low frequency variability over the North Atlantic that has an effect on the position of the North Atlantic storm tracks and jet streams (Seierstad et al. 2007; Woollings and Blackburn 2012). The East Atlantic/Western Russia (EAWR) is defined by two main anomaly centers located over the Caspian Sea and Western Europe. During the negative EAWR phases, wetter than normal weather conditions are observed over a large part of the Mediterranean region, whereas during positive phases drier conditions prevail (Barnston and Livezey 1987). The EAWR has previously been found to have a strong influence on the climatic conditions over the Central and Southern Europe (Ioniţă 2014). The SCAND is defined by a center over Scandinavia and weaker centers of opposite sign over Western Europe and Eastern Russia. The positive phase of this pattern reflects major blocking anticyclones over Scandinavia and western Russia, while the negative phase is associated with negative height anomalies in these regions. Variability in storminess is affected by these large-scale circulation patterns (Hurrell 1995; Lozano and Swail 2002; Caires and Sterl 2005; Wang et al. 2011; Vespremeanu-Stroe and Tătui 2011; Ioniţă 2014) with varying degrees of correlation around Europe (Matulla et al. 2007; Almeida et al. 2011). Moreover, storminess can vary due to changes in sea surface temperature (Graham and Diaz 2001). It is also highly probable that anthropogenic influence affected extratropical circulation during the latter half of the twentieth century (Gillett et al. 2003; Hegerl et al. 2007), which in turn affects storminess, but the WASA Group (1998), using long records of station data, suggest that observed changes in storminess in Northern Europe over the latter part of the twentieth century fall well within the limits of variability observed in the past.

On the Danube Delta coast, negative values of NAO are associated with increased storminess, whereas positive values correspond to years of low or moderate storminess (Vespremeanu-Stroe et al. 2007; Vespremeanu-Stroe and Tătui 2011). The NAO correlates very well with SI ($r = -0.76$ for 1962–2005), but this decreased or even reversed since 2006, when a very low episode of storminess occurred (Fig. 34.6). The EA, EAWR and SCAND exhibit moderate correlations

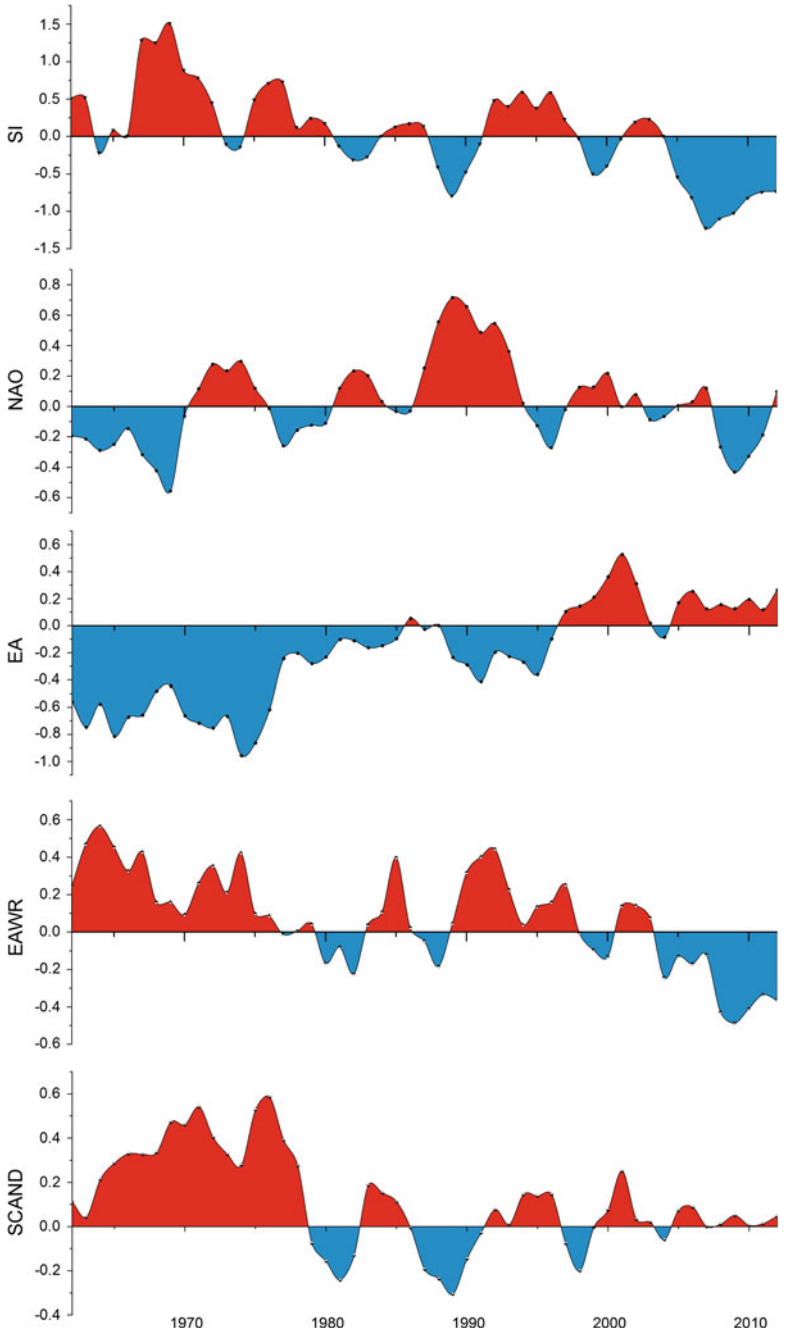

Fig. 34.6 Normalized SI (storminess index) time series plotted with major European teleconnection patterns (NAO, EA, EAWR, SCAND). All values are 3-year moving averages (from Zăinescu et al. submitted)

($r = -0.55$, 0.56, 0.55, respectively, significant at $p < 0.01$) for all the study period, suggesting a synergetic effect along the NAO on the northwestern Black Sea coast storminess.

It appears that on the Danube Delta coast, the NAO interacts with other teleconnection patterns (EA, EAWR, and SCAND) and cannot account by itself for all the variation in storminess, especially in the last 10 years. The EA and EAWR explain well the recent decreasing storm frequency and intensity and their long-term increasing/decreasing trends may hint to a future of lower storminess (Zăinescu et al. submitted).

Storm Impact on the Coast

For the low Atlantic coast of Europe, various researchers have pursued the task of understanding the response of shores to storms (Cooper et al. 2004; Regnauld et al. 2004; Ciavola et al. 2007; Anthony 2013). Several thresholds to discriminate the significant morphological changes were proposed based on significant wave height (H_s) (Pessanha and Pires 1981; Haerens et al. 2012; Del Rio et al. 2012; Almeida et al. 2012). Morton (2002) identifies the most important factors in storm impact: maximum wind speed and direction, timing of storms, tidal range, type, and density of vegetation. In essence, storm response depends on the combined actions of waves and wind on a raised water level (storm surge), depending on the wind direction relative to the coast (Haerens et al. 2012), and the pre-storm morphology of the coast on the other hand (Hequette et al. 2001; Backstrom et al. 2008). The first successful coupling between processes and morphology was conceptualized by Sallenger (2000) who established four levels of impact of storms on barrier islands as a function of maximum vertical extent of waves (wave runup) and the maximum dune crest elevation. The first level is the "swash" regime which implies a temporary sand transport from the beach to an offshore location. During the "collision" regime, runup is higher than the dune toe elevation and waves impact the dunes creating scarps, leading to sediment loss. When the wave runup surpasses the dunes, the overwash regime sets in, and water laden with sediments can pass landwards, creating washover fans or sheets. The most extreme case occurs in very rare storms when the increase in sea level surpasses the dune crest, remaining completely submerged and causing the most intense erosion and sand remobilization.

On the Danube Delta coast, during regular storms (Category I and II; V ≥ 10 and 15 m/s; H_s: 1.6–4 m), swash regime dominates, transporting beach sediments offshore, but concomitantly wind-borne sands are usually transported from the upper beach to the foredunes (depending on the wind direction) contributing to volume increase in foredunes; this kind of aeolian accretion is specific only to

category I storms, while during second category wave and wind erosion prevail. Otherwise, during storm decay when their height decreases, waves leave behind an incipient high berm closer to the dune toe which can be later reworked and used as source of sand for the dunes.

During severe storms (Category III and IV; V ≥ 20 and 24 m/s; H_s: 4–7 m), swash and collision regimes usually dominate and impose significant beach erosion and medium foredune sediment loss through scarping and loss of sediment to the beach and offshore. The wind usually erodes the dune stoss slope, moving the

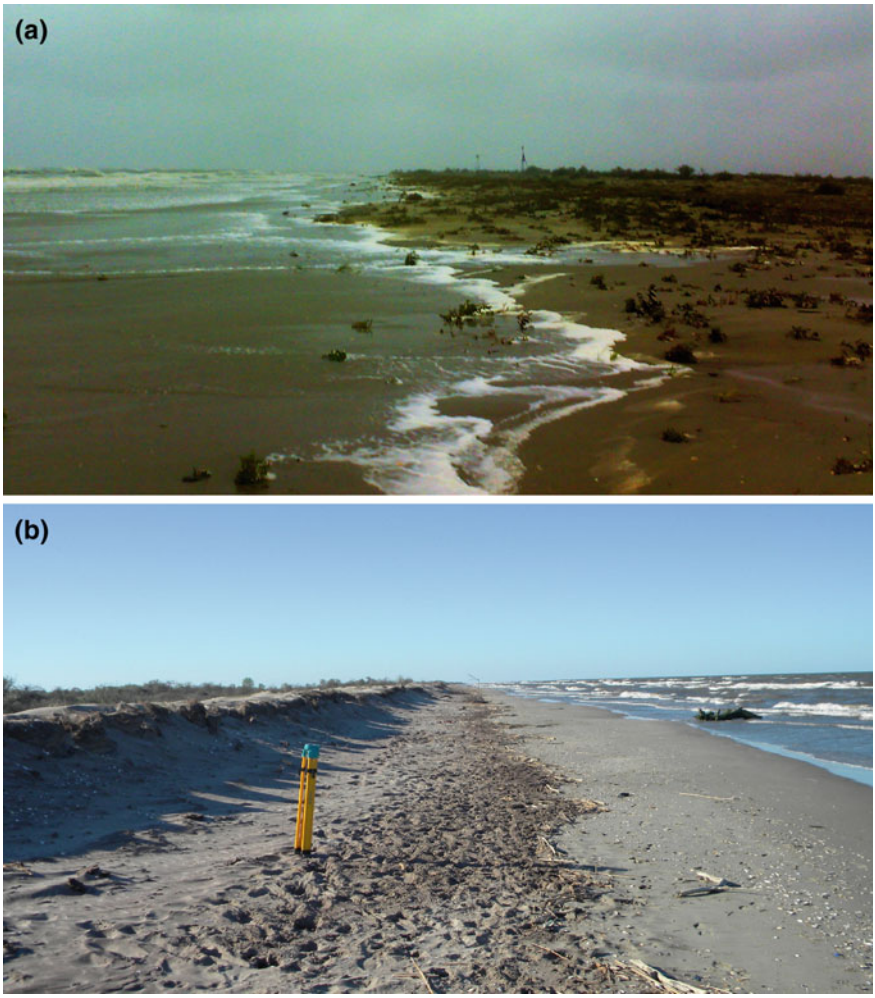

Fig. 34.7 Effects of the October 2013 storm (category III, duration of 75 h, H_s: ~4 m, V_{max}: 20–21 m/s). **a** Minor overwashing of topographic lows between the dunes North of Sf. Gheorghe distributary during the storm. **b** Minor scarping of dunes on the slightly erosive coastal sector of Sărăturile ridge plain (photo by Florin Tătui)

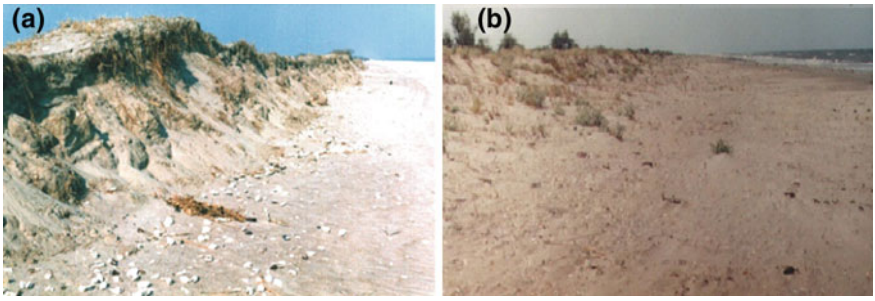

Fig. 34.8 Dune scarping North of Sf. Gheorghe beach during January 1998 (**a**) and recovery August 2002 (**b**) (from Vespremeanu-Stroe 2007)

sediment to the dune crest or beyond, to the landward slope. A lesser overwash regime may occur on topographic lows in the foredunes. Figure 34.7 shows the effects during and after the October 23 Category III storm, which caused minor overwash of low sectors of dunes and scarping. Erosive effects are attributed to NE winds and waves.

Extreme storms (Category V: $V_{max} \geq 28$ m/s, $H_s \geq 7$ m) are erosive for all beach-dune systems and exhibit extensive overwash and collision regimes (Fig. 34.9). During the last 50 years, only 7-category V storms have been registered corresponding to an average 7-year return period. A documented case of extreme storm on the Danube Delta is the 21–27 January 1998 event, when significant morphological changes occurred along the coast (Vespremeanu-Stroe 2007; Tătui et al. 2014). This storm yielded the highest SSI ($\sim$1000) together with the highest impact potential (SIP = 633). It lasted for 157 h, during which winds blew mainly from the NE at a maximum speed of 28 m/s and waves were close to 8 m, which produced a maximum storm surge of 1 m (Fig. 34.8; Tătui et al. 2014). It is highly probable that impact was exacerbated due to the occurrence in the previous month (15–18 December 1997) of another aggressive Northeastern (an extreme Category V storm) with high scorings of SSI (768) and SIP (329), highlighting the importance of storm clustering.

Analysis of the changes induced by this event on the Sf. Gheorghe—Sulina coast shows that most sectors were overwashed and extensive washover sheets and fans developed (Fig. 34.10). One large washover fan occurred between the R48 and NB profile lines, which penetrated landwards over 300 m and breached the developing foredunes. Kilometer long terrace-like washover sheets appeared in the north, skewed to Southwest due to inheritance of storm waves direction (Northeastern), where fordunes were thin (5–20 m; most of them were obliterated) and the shoreline has a general retreating behavior (up to 14 m/year in some sectors). Here, the maximum extension of ca. 150 m was favored by the inter-swale topographic lows of the Sărăturile beach ridge plain. The pre-storm (October/December 1997)

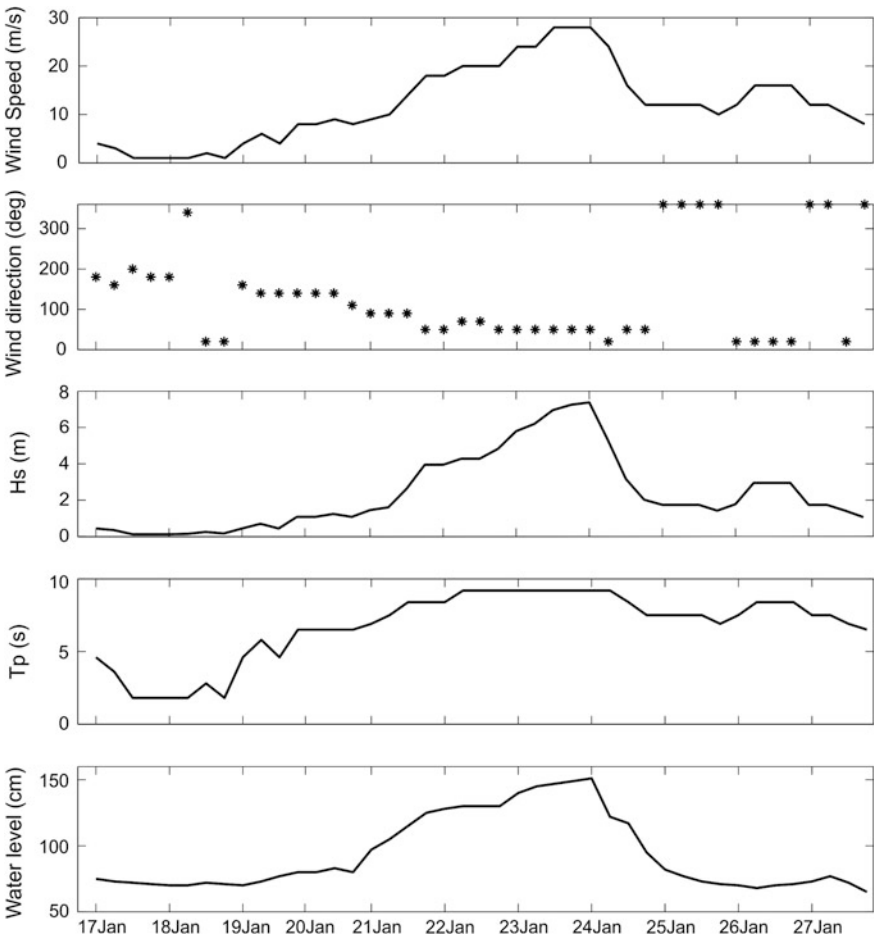

Fig. 34.9 Parameters of the January 1998 storm: wind speed, wind direction, significant wave height (H_s), peak period (Tp), and water level (the latter is measured at Sf. Gheorghe gauge; 57 cm is the mean multiannual level; from Tătui et al. 2014)

and post-storm (February 1998) measurements on three cross-shore profiles show that storm induced a landward shoreline displacement from 10 to 50 m (Fig. 34.10a) decreasing southwards, which is up to 8 times more than on an average year. But in average, for the Împuţita—North Sărăturile erosive sector, the mean coastline retreat of 30–40 m reported by the next summer (August 1998) measurements (Vespremeanu-Stroe 2007) is equivalent to 4–6 years of common erosion.

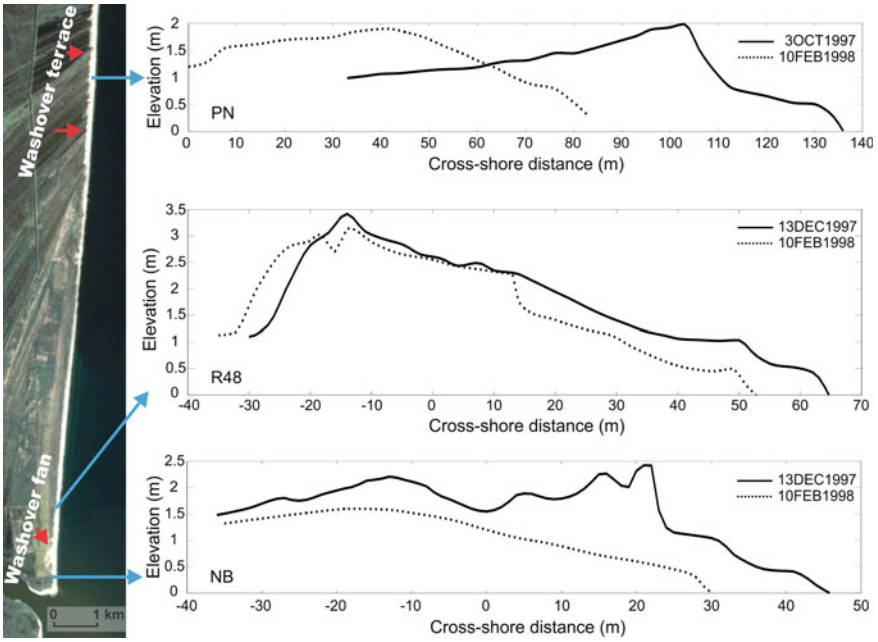

Fig. 34.10 Morphological signatures of the extreme storm of January 1998. Pan sharpened Landsat image is from September 1999. Modified from Tătui et al. (2014)

The high fordunes on the central Sf. Gheorghe beach (i.e., R48 benchmark; Fig. 34.10b) experienced collision regime and lost 15–20 m^3/m of sand through scarping, but stored enough sediment to buffer the effects of waves. Besides the large foredune height and widths, the main controlling factor which diminished the storm impact, the sand loss volume, respectively, is the gently sloping aspect of the stoss foredune flank (1–2°) which efficiently dissipated the wave swash. Therefore, this coastal sector exhibited the lowest exposure (vulnerability) to extreme events for decades. Other sectors experienced overwashing and significant losses occurred near the river mouth (Sf. Gheorghe arm) at the NB profile, where 40–50 m^3/m of sand were removed in association with overwash processes (Fig. 34.10c). A major role in the storm impact magnitude and alongshore variability of response appears to be the difference in beach and foredune width, heights and volumes which are further determined by the long-term shoreline dynamics (erosion/accretion processes).

Long-Term Imprints on Morphology

A river delta advances as long as a significant part of fluvial sediments remain trapped near the river mouth, which means that sediments carried by the river must be higher than the capacity of longshore and coastal currents to redistribute these sediments. When lobes develop and protrude into the sea, they are increasingly exposed to marine agents, and even if the overall wave climatology has remained constant, the nearshore wave climate changes. The magnitude of the longshore transport, which in turn is a function of wave height and direction relative to the shore, is crucial in determining the development of a deltaic lobe. The prevailing wave direction may have a significant influence on lobe abandonment processes that redistribute the sediments downdrift, sometimes forming either sand waves or downdrift migrating spits (Nienhuis et al. 2013).

Cumulative response of storm events manifests at decadal scales as the main source of variability in the coastal processes. Vespremeanu-Stroe et al. (2007) found that in time both accretion and erosion change the intensity, and these changes are linked to storminess variability. Nevertheless, over the longer timescale of centuries and millennia, storminess variability tends to fade out and only the mean characteristics of waves and wind leave an imprint on the deltaic morphology. Asymmetry in the wave climate creates lobes with contrasting updrift and downdrift morphologies (Bhattacharya and Giosan 2003). This can be easily identified in the lobes of Sfântu Gheorghe (both old and modern) and Sulina where beach ridge plains develop updrift of the river mouths whilst barrier-marsh plains and deltaic mud plains develop downdrift thanks to rich fluvial supply (Preoteasa et al. 2016). Moreover, this asymmetry can also be noticed on the modern Chilia lobe, which preferentially develops to the south.

Conclusions

In this study, the storm conditions and storm history of the Danube Delta coast since the mid-twentieth century have been evaluated using a wide range of parameters (i.e., maximum wind speed, resultant wind direction, wave energy) which were synthetically expressed by three new proposed indices: SSI (storm severity index; energetic index), SIP (storm impact potential; morphological index), and SI (storminess index). A description of the impact of regular (Category I–II), severe (Category III–IV), and extreme (Category V) storms has been established.

The seasonality of storms is reflected in the difference of storm occurrence between the active (October–March) and the quiescent (April–September) seasons of 6 months each. In the active season ca. 70 % of all storms, 84 % of the severe, and 100 % of the extreme storms occur. Long-term storminess oscillations were

established based on all three indices (combining wind and wave data) which indicate different periods of increased storminess (1967–1973, 1991–1998), moderate (1958–1966, 1974–1981, and 1999–2005) and relatively quiescent (1958–1966, 1982–1990, and 2006–2013), which were related to variations in the major atmospheric teleconnections over Europe (especially to NAO and EAWR), suggesting complex interactions.

The primary factor modulating the short-term (days to seasons) and medium-term (years to decades) evolution rhythms of the deltaic coast is the climatic variability expressed by variations in storm frequency and intensity. Over centuries and millennia, the storminess fluctuations fade but storms, together with river discharge, remain the most important shaping processes. The actual physiognomy of the Danube Delta is doubtless marked by the strong asymmetry of the wave-driven longshore currents during storms which imposed for each of the five open-coast lobes an asymmetric wave-influenced morphology with completely distinct features updrift (sandy standplains) and downdrift (barrier-marsh plains and deltaic mud plains) of the river mouth.

Acknowledgments Research activities were undertaken in the frame of Sfântu Gheorghe Marine and Fluvial Research Station, Faculty of Geography, University of Bucharest. The authors are grateful to Nikolay Valchev from the Bulgarian Academy of Sciences, Institute of Oceanology for providing the wave data and to our colleagues Florin Tătui and Luminița Preoteasa for their helpful suggestions offered during the study. This work was funded by the Romanian National Authority for Scientific Research, CNCS—UEFISCDI under PN-II-RU-TE-2011-3-0293 and PN-II-CT-RO-FR-2014-2-0062 grants and by CCCDI – UEFISCDI project number 792, within PNCDI III.

References

Almeida LP, Ferreira O, Vousdoukas MI, Dodet G (2011) Historical variation and trends in storminess along the Portuguese South Coast. Nat Hazards Earth Sys Sci 11:2407–2417

Almeida LP, Vousdoukas MV, Ferreira Ó, Rodrigues BA, Matias A (2012) Thresholds for storm impacts on an exposed sandy coastal area in Southern Portugal. Geomorphology 143:3–12

Andreeva N, Valchev N, Trifonova E, Eftimova P, Kirilova D, Georgieva M (2011) Literary review of historical storm events in the western Black Sea. Proc. Union Scientists Varna Mar Sci, p 105–112 (in Bulgarian)

Anthony EJ (2013) Storms, shoreface morphodynamics, sand supply, and the accretion and erosion of coastal dune barriers in the Southern North Sea. Geomorphology 199:8–21

Backstrom JT, Jackson DWT, Cooper JAG, Malvarez GC (2008) Storm-driven shoreface morphodynamics on a low-wave energy delta: the role of nearshore topography and shoreline orientation. J Coast Res 24:1379–1387

Barnston AG, Livezey RE (1987) Classification, seasonality and persistence of low-frequency atmospheric circulation patterns. Monthly Weather Rev 115(6):1083–1126

Bhattacharya JP, Giosan L (2003) Wave-influenced deltas: geomorphological implications for facies reconstruction. Sedimentology 50(1):187–210

Bocheva L, Georgiev C, Simeonov P (2007) A climatic study of severe storms over Bulgaria produced by Mediterranean cyclones in 1990-2001 period. Atmos Res 83:284–293

Caires S, Sterl A (2005) 100-year return value estimates for wind speed and significant wave height from the ERA-40 data. J Clim 18(7):1032–1048

Chiotoroiu B (1999) Les tempêtes dans le basin occidental de la mer Noire. Presses Universitaires du Septentrion, Lille

Chiotoroiu B, Ciuchea V (2009) Severe weather conditions and maritime accidents along the Romanian Black sea coast. In: Proceedings of the XIII international scientific and technical conference on marine traffic engineering—MTE 09, Malmo, Sweden, p 35–39

Ciavola P, Armaroli C, Chiggiato J, Valentini A, Deserti M, Perini L, Luciani P (2007) Impact of storms along the coastline of Emilia-Romagna: the morphological signature on the Ravenna coastline (Italy). J Coast Res 50:540–544 (Special Issue)

Clarke ML, Rendell HM (2009) The impact of North Atlantic storminess on Western European coasts: a review. Quat Int 195(1–2):34–41

Cooper JAG, Jackson DWT, Navas F, McKenna J, Malvarez G (2004) Identifying storm impacts on an embayed, high-energy coastline: examples from Western Ireland. Mar Geol 210:261–280

Del Rio L, Plomaritis TA, Benavente J, Valladares M, Ribera P (2012) Establishing storm thresholds for the Spanish Gulf of Cadiz coast. Geomorphology 143–144:13–23

Ferreira O, Ciavola P, Armaroli C, Balouin Y, Benavente J, Del Rıo L, Deserti M, Esteves LS, Furmanczyk K, Haerens P, Matias A, Perini L, Taborda R, Terefenko P, Trifonova E, Trouw K, Valchev N, Van Dongeren A, Van Koningsveld M, Williams JJ (2009) Coastal storm risk assessment in Europe: examples from 9 study sites. J Coastal Res. SI 56 (II), 1632–1636

Gillett NP, Graf HF, Osborn TJ (2003) Climate change and the North Atlantic Oscillation. In: Hurrell JW, Kushnir Y, Ottersen G, Visbeck M (eds) The North Atlantic Oscillation: climatic significance and environmental impact. Am Geophys Union, Washington DC, pp 193–209

Graham NE, Diaz HF (2001) Evidence for intensification of North Pacific winter cyclones since 1948. Bull Am Meteorol Soc 82(9):1869–1893

Haerens P, Bolle A, Trouw K, Houthuys R (2012) Definition of storm thresholds for significant morphological change of the sandy beaches along the Belgian coastline. Geomorphology 143–144:107–117

Hegerl GC, Zwiers FW, Braconnot P, Gillett NP, Luo Y, Marengo Orsini J, Nicholls N, Penner JE, Stott PA (2007) Understanding and attributing climate change. In: Solomon S, Qin D, Manning M, Chen Z, Marquis M, Averyt KB, Tignor M, Miller HL (eds) Climate OUT change 2007: the physical basis. Contribution of working group I to the fourth assessment report of the intergovernmental panel on climate change. Cambridge University Press, Cambridge, UK, and New York, p 663–745

Hequette A, Desrosiers M, Hill PR, Forbes DL (2001) The influence of coastal morphology on shoreface sediment transport under storm-combined flows, Canadian Beaufort Sea. J Coast Res 17:507–516

Hurrell JW (1995) Decadal trends in the North Atlantic Oscillation: regional temperature and precipitation. Science 269:676–679

Ioniță M (2014) The impact of the East Atlantic/Western Russia pattern on the hydroclimatology of Europe from mid-winter to late spring. Climate 2(4):296–309

Kalnay E, Kanamitsu M, Kistler R, Collins W, Deaven D, Gandin L, Joseph D et al (1996) The NCEP/NCAR 40-year reanalysis project. Bull Am Meteorol Soc 77(3):437–471

Keim BD, Muller RA, Stone GW (2004) Spatial and temporal variability of coastal storms in the North Atlantic Basin. Mar Geol 210(1):7–15

Kiladis GN, Diaz H (1989) Global climatic anomalies associated with extremes in the Southern Oscillation. J Clim 2:1069–1090

Lionello P, Cavaleri L, Nissen KM, Pino C, Raicich F, Ulbrich U (2012) Severe marine storms in the Northern Adriatic: characteristics and trends. Phys Chem Earth Parts A/B/C 40:93–105
Lozano I, Swail V (2002) The link between wave height variability in the North Atlantic and the storm track activity in the last four decades. Atmos Ocean 40(4):377–388
Maheras P, Tolika K, Chiotoroiu B (2009) Atmospheric circulation types associated with storms on the Romanian Black Sea coast. Application of a new automated scheme. Studia Universitatis "Vasile Goldiş", Seria Ştiinţele Vieţii 19(1):193–198
Masselink G, van Heteren S (2014) Response of wave-dominated and mixed-energy barriers to storms. Mar Geol 352:321–347
Matulla C, Schöner W, Alexandersson H, von Storch H, Wang XL (2007) European storminess: late nineteenth century to present. Clim Dyn. doi:10.1007/s00382-007-0333-y
Moore GWK, Renfrew IA, Pickart RS (2013) Multidecadal mobility of the North Atlantic oscillation. J Clim 26(8):2453–2466
Moritz H, Moritz H (2006) Evaluating extreme storm power and potential implications to coastal infrastructure damage. In: 9th International workshop on wave hindcasting and forecasting, Victoria
Morton RA (2002) Factors controlling storm impacts on coastal barriers and beaches—a preliminary basis for near real-time forecasting. J Coast Res 18:486–501
Nienhuis JH, Ashton AD, Roos PC, Hulscher SJ, Giosan L (2013) Wave reworking of abandoned deltas. Geophys Res Lett 40(22):5899–5903
Orfila A, Álvarez A, Tintoré J, Jordi A, Basterretxea G (2005) Climate teleconnections at monthly time scales in the Ligurian Sea inferred from satellite data. Prog Oceanogr 66(2):157–170
Pessanha L, Pires O (1981) Elementos sobre o clima de agitacao marıtima na costa Sul do Algarve. Report Instituto de Meteorologia
Philander SG (1990) El Nino, La Nina and the southern oscillation. Academic Press, New York
Preoteasa L, Vespremeanu-Stroe AI, Tătui F, Zăinescu F, Timar-Gabor A, Cârdan I (2016) The evolution of an asymmetric deltaic lobe (Sf. Gheorghe, Danube) in association with cyclic development of the river mouth bar: long-term pattern and present adaptation to human induced sediment depletion. Geomorphology 253:59–73
Regnauld H, Pirazzoli PA, Morvan G, Ruz MH (2004) Impacts of storms and evolution of the coastline in western France. Mar Geol 210:325–337
Sallenger AH (2000) Storm impact scale for barrier islands. J Coast Res 16:890–895
Seierstad IA, Stephenson DB, Kvamsto NG (2007) How useful are teleconnection patterns for explaining variability in extratropical storminess? Tellus 59A:170–181
Tătui F, Vespremeanu-Stroe A, Preoteasa L (2014) Alongshore variations in beach-dune system response to major storm events on the Danube Delta coast. J Coast Res, SI70:693–699
Trifonova E, Valchev N, Andreeva N, Eftimova P (2012) Critical storm thresholds for morphological changes in the western Black Sea coastal zone. Geomorphology 143–144: 81–94
Tsimplis MN, Shaw AGP (2008) The forcing of mean sea level variability around Europe. Glob Planet Change 63:196–202
USACE (1984) Shore protection manual. Coast Eng Res Center, Fort Belvoir
Valchev N, Trifonova EV, Andreeva NK (2012) Past and recent trends in the western Black Sea storminess. Nat Hazards Earth Syst Sci 12:961–977
Vespremeanu E (1987) Probleme de geomorfologie marină (Edit). Universităţii din Bucureşti, Bucharest (in Romanian)
Vespremeanu-Stroe A (2004) Transportul de sedimente în lungul ţărmului şi regimul valurilor pe coasta Deltei Dunării. Studii şi cercetări de oceanografie costieră 1:67–82 (in Romanian)
Vespremeanu-Stroe A (2007) Ţărmul Deltei Dunării. Studiu de geomorfologie. PhD thesis, Universitatea din Bucureşti (in Romanian)
Vespremeanu-Stroe A, Preoteasa L (2007) Beach–dune interactions on the dry–temperate Danube Delta coast. Geomorphology 86(3):267–282

Vespremeanu-Stroe A, Tătui F (2011) North-Atlantic oscillation signature on coastal dynamics and climate variability of the Romanian Black Sea coast. Carpathian J Earth Environ Sci 6 (1):309–316

Vespremeanu-Stroe A, Constantinescu Ş, Tătui F, Giosan L (2007) Multi-decadal evolution and North Atlantic Oscillation influences on the dynamics of the Danube Delta shoreline. J Coast Res 50:157–162

Vespremeanu-Stroe A, Preoteasa L, Tătui F (2014) Oceanografie fizică. Editura Ars Docendi, Bucuresti, p 172

Vespremeanu-Stroe A, Preoteasa L, Zăinescu F, Rotaru S, Croitoru L, Timar-Gabor A. Formation of the Danube Delta beach ridge plains and signatures in morphology. Quat Int (accepted)

Wang XL, Wan H, Zwiers FW, Swail VR, Compo GP, Allan RJ, Vose RS, Jourdain S, Yin X (2011) Trends and low-frequency variability of storminess over western Europe, 1878–2007. Clim Dyn 37(11–12):2355–2371

WASA Group (Waves and Storms in the North Atlantic) (1998) Changing waves and storms in the northeast Atlantic? Bull Am Meteorol Soc 79(5):741–760

Woollings T, Blackburn M (2012) The North Atlantic jet stream under climate change and its relation to the NAO and EA patterns. J Clim 25(3):886–902

Zăinescu F, Vespremeanu-Stroe A, Valchev N, Tătui F. Storm climate on the Danube Delta coast: evidence of recent storminess change and links with large-scale teleconnection patterns (submitted)